UNIVERSITY OF CALIFORNIA
SCRIPPS INSTITUTION OF OCEANOGRAPHY

CONTRIBUTIONS

1957

This volume contains contributions from the Scripps Institution of Oceanography which appeared during 1957 in publications other than *Bulletins of the Scripps Institution of Oceanography.*

NOV 195[illegible]
LIBRARY
POFI
FISH & WILDLIFE
SERVICE

THE LIBRARY
UNIVERSITY OF CALIFORNIA
SCRIPPS INSTITUTION OF OCEANOGRAPHY
LA JOLLA, CALIFORNIA
July 1958

PERIODICAL
Calif. Univ.
S.I.O.
Contributions
1957

DATE	ISSUED TO
JUN 30 1960	

PERIODICAL

Calif. Univ. S.I.O.
Contributions

1957

LIBRARY
BUR. OF COMM. FISH.
HON. BIOL. LAB.

UNIVERSITY OF CALIFORNIA
SCRIPPS INSTITUTION OF OCEANOGRAPHY

CONTRIBUTIONS

1957

This volume contains contributions from the Scripps Institution of Oceanography which appeared during 1957 in publications other than *Bulletins of the Scripps Institution of Oceanography.*

THE LIBRARY
UNIVERSITY OF CALIFORNIA
SCRIPPS INSTITUTION OF OCEANOGRAPHY
LA JOLLA, CALIFORNIA
July 1958

2152^{60}

PHOTOLITHOPRINTED BY CUSHING - MALLOY, INC.
ANN ARBOR, MICHIGAN, UNITED STATES OF AMERICA
1958

IN MEMORIAM

Harald Ulrik Sverdrup (1888–1957)

On 21 August 1957, Harald Ulrik Sverdrup died in Oslo from a heart attack, only two days after the death in Stockholm, also by heart failure, of his close friend Carl-Gustaf Rossby. The era of the explorer-scientist from the countries of the large Coriolis force is drawing to an end.

Sverdrup came from a family of churchmen. His maternal grandfather, Ole Vollan, was a parish-verger in Bergen's cathedral and one of the political leaders in the liberal party; his paternal grandfather, a minister of the church, had five sons who became ministers and three daughters who married ministers. His father was professor of theology at the University of Oslo when Sverdrup enrolled there as student in "Physical Oceanography and Astronomy". His early interest was in astronomy, but this changed when he received one of the renowned Carnegie assistantships to Professor V. Bjerknes. During the next six years he published twenty papers, largely in dynamic meteorology. His doctoral dissertation, *Der nordatlantische Passat*, represents the first attempt towards energy and momentum budgets of the North Atlantic trade winds. The use here of mathematics as a tool for quantitative description rather than deductive reasoning is typical also of his later work.

At the age of 29, Sverdrup took charge of the scientific work on Roald Amundsen's North Polar expedition, with additional duties as navigator and part-time cook. The expedition ship *Maud* left Norway in July 1918, planning to come home in three years. Sverdrup did not return to Norway until December 1925. Winter after winter the ship was frozen fast, and the goal to duplicate the drift of the *Fram* (with his relative, Otto Sverdrup, as Captain) was never realized. Nevertheless, the collected observations represent one of the few significant records of the Arctic. These include astronomic and meteorologic observations, measurements of tides, currents, the physical properties of sea-water and of sea-ice, studies in marine geology, aurora polaris, gravity, magnetism, atmospheric electricity, even some observations concerning animal and bird life on the drift ice. At one time Sverdrup left the ship to spend eight months as a lone white man with the nomadic Chukchi tribe of north-eastern Siberia, an experience he later reported in a delightful popular book.* The most significant of the *Maud* papers, *Dynamics of Tides on the North Siberian Shelf*, was completed for publication during the last winter in the Arctic, without adequate literature and without the benefit of discussion. Only sea-going oceanographers can appreciate this feat. Yet, the achievement of which Sverdrup was most proud is not scientific: after seven years on the *Maud* he parted friends with all his shipmates.

Upon his return, Sverdrup succeeded V. Bjerknes in the Chair of Meteorology at the Geophysical Institute in Bergen, Norway. In 1931, he became research professor at the Christian Michelsen Institute in Bergen. The two appointments enabled him to devote most of his efforts from 1925 to 1935 towards a general account of the expedition and to publish fifty papers on the diverse observations. During this decade he also spent two half-year periods in Washington to participate in the analysis of oceanographic data collected on the seventh cruise of the *Carnegie*. In 1928 he married Gudrun Bronn Vaumund. In 1931 he took charge of the scientific work on the Wilkins Ellsworth North Polar Expedition aboard the submarine *Nautilus*, and in 1934 Sverdrup spent two months with the glaciologist H. W. Ahlmann in the high-lying snow fields of Spitzbergen and published the first quantitative heat budget of glaciers. These ten years (1925–1935) following the *Maud* expedition were the most productive of a productive scientific career.

In 1936 Sverdrup accepted, for a limited period, the Directorship of the Scripps Institution of Oceanography, at La Jolla, California, and accordingly took leave of absence from the Michelsen Institute for three years. But the war intervened and he did not permanently return to Norway until 1948. The Scripps Institution then had thirty employees in all and no sea-going vessel. Sverdrup

*An English translation by Sverdrup entitled *Reindeer Hair in Your Soup* has unfortunately not been published.

persuaded Mr. Robert Scripps to donate the schooner *E. W. Scripps* and initiated a study of the Gulf of California and of the waters off southern California. At the outbreak of the war, the *E. W. Scripps* was diverted to Navy studies, and again the Institution was left landlocked. Sverdrup laboured hard in an attempt to remedy this situation. Near the end of his tenure an opportunity arose of financial support for work in California waters to study environmental factors related to the fluctuation in the population of the California sardine and of other pelagic fishes. Sverdrup seized this opportunity with both hands and initiated the Marine Life Research Program, a program active at Scripps today.

The twelve years in California presented Sverdrup with the first opportunity to teach, an activity he enjoyed and did exceedingly well. His effectiveness as a teacher came largely as a result of his modesty and warm personal interest in human beings. He made colleagues of his students rather than subordinates. Among his students and younger collaborators were Roger Revelle, Richard Fleming, Robert Arthur, Don Pritchard, Robert Reid, Gifford Ewing and myself. By the end of the war, the need for more trained physical oceanographers had become evident, and Sverdrup organized the first systematic course in oceanography given in the United States. This was attended by several dozen officers of the armed forces. All of us will remember how Sverdrup entertained us at his home with stories of the Chukchi tribe and demonstrations of his physical fitness (e.g., standing on his head at the age of sixty).

During the pre-war years Sverdrup devoted much effort to write, in collaboration with Martin Johnson and Richard Fleming, a comprehensive 1100-page volume, *The Oceans, their Physics, Chemistry and Marine Biology.* I consider Chapter 15 of *The Oceans . . .* , entitled " The Water Masses and Currents of the Oceans", as Sverdrup's outstanding scientific achievement. At the outbreak of the war, Sverdrup worked on problems dealing with underwater sound. Later he developed current charts for life rafts and methods for predicting sea and swell for amphibious landings. He was glad for the opportunity to throw his great energy and knowledge behind the war effort. The invasion of his native land and the death of one of his brothers while engaged on a Commando raid had brought great sorrow to him. After the war he favoured co-operation with scientists from all countries, including the U.S.S.R., as a contribution towards world peace. Ironically he was called a red stooge in a California paper and a pawn of American imperialism in a communist paper of Norway, both articles appearing at about the same time. He was undisturbed by these attacks; he had lived according to his convictions and, in his own words, " that was that". I feel that these unhappy incidents must be recorded; they shed as much light on the man as his scientific contributions. Palmén in a recent letter characterized him as a "sällsynt gedigen person". This means something like "an out of the ordinary sterling person", but the Swedish expression is far more precise and striking.

In 1948, at the age of sixty, Sverdrup returned to Norway, He greatly admired Nansen's decision to drop all scientific research at this time of life and had told me he would do the same. He did. And, like Nansen, he embarked upon new activities which were as important and interesting as his earlier ones, As Director of the Norsk Polar Institutt, he was engaged at the time of his death in organizing that institute's activity during the International Geophysical Year. He was President of the International Council for the Exploration of the Sea and preparing for the fall meeting in Bergen. He was in charge of Norwegian activities for improving fisheries in India. He was Prorector of the University of Oslo and Director of the Summer School for foreign students at the University. He was also Chairman of a committee for re-organizing the Norwegian educational system; a task to which he had held for many years in spite of difficulties and disappointments.

A small stroke in spring gave warning that he was taxing himself too hard. Like Rossby, he chose to ignore the warning and to serve full strength till the hour of his death.

W. H. Munk

UNIVERSITY OF CALIFORNIA
SCRIPPS INSTITUTION OF OCEANOGRAPHY
CONTRIBUTIONS, NEW SERIES
1957

Contrib. Number — Page Number

900 REVELLE, ROGER and HANS E. SUESS. Carbon dioxide exchange between atmosphere and ocean and the question of an increase of atmospheric CO_2 during the past decades. Tellus, v.9, no.1, 1957. pp.18-27 1

901 REVELLE, ROGER and M. B. SCHAEFER. General considerations concerning the ocean as a receptacle for artificially radioactive materials. In "The Effects of Atomic Radiation on Oceanography and Fisheries", Pub. no. 551, National Academy of Sciences-National Research Council, 1957. pp.1-25 13

901a KRUMHOLZ, LOUIS A., E. D. GOLDBERG and HOWARD BOROUGHS. Ecological factors involved in the uptake, accumulation and loss of radionuclides by aquatic organisms. In "The Effects of Atomic Radiation on Oceanography and Fisheries", Pub. no. 551, National Academy of Sciences-National Research Council, 1957. pp.69-79 39

902 CRAIG, HARMON. Isotopic tracer techniques for measurement of physical processes in the sea and the atmosphere. In "The Effects of Atomic Radiation on Oceanography and Fisheries", Pub. no. 551, National Academy of Sciences-National Research Council, 1957. pp.103-120 51

902a CRAIG, HARMON. Disposal of radioactive wastes in the ocean: the fission product spectrum in the sea as a function of time and mixing characteristics. In "The Effects of Atomic Radiation on Oceanography and Fisheries", Pub. no. 551, National Academy of Sciences-National Research Council, 1957. pp.34-42 69

903 WOOSTER, WARREN S. and BOSTWICK H. KETCHUM. Transport and dispersal of radioactive elements in the sea. In "The Effects of Atomic Radiation on Oceanography and Fisheries", Pub. no. 551, National Academy of Sciences-National Research Council, 1957. pp.43-51 79

903a SCHAEFER, MILNER B. Large scale biological experiments using radioactive tracers. In "The Effects of Atomic Radiation on Oceanography and Fisheries", Pub. no. 551, National Academy of Sciences-National Research Council, 1957. pp.133-137 89

904 FOLSOM, THEODORE R. and JOHN H. HARLEY. Comparison of some natural radiations received by selected organisms. In "The Effects of Atomic Radiation of Oceanography and Fisheries", Pub. no. 551, National Academy of Sciences-National Research Council, 1957. pp.28-33 95

Contrib. Number | Page Number

905 FOLSOM, THEODORE R. and ALLYN C. VINE. On the tagging of water masses for the study of physical processes in the oceans. In "The Effects of Atomic Radiation on Oceanography and Fisheries", Pub. no. 551, National Academy of Sciences-National Research Council, 1957. pp.121-132 103

906 LIEBERMANN, LEONARD. Air bubbles in water. Journal of Applied Physics, v.28, no.2, 1957. pp.205-211 115

907 RUSNAK, GENE A. A fabric and petrologic study of the Pleasantview sandstone. Journal of Sedimentary Petrology, v.27, no.1, 1957. pp.41-55 123

908 KANWISHER, JOHN and ALFRED EBELING. Composition of the swim-bladder gas in bathypelagic fishes. Deep-Sea Research, v.4, no.3, 1957. pp.211-217 139

909 KNAUSS, JOHN A. An observation of an oceanic front. Tellus, vol.9, no.2, 1957. pp.234-237 147

910 BODEN, BRIAN P. and ELIZABETH M. KAMPA. Records of bioluminescence in the ocean. Pacific Science, v.11, no.2, 1957. pp.229-235 153

911 SWEENEY, BEATRICE M. and J. WOODLAND HASTINGS. Characteristics of the diurnal rhythm of luminescense in *Gonyaulax polyedra*. Journal of Cellular and Comparative Physiology, v.49, no.1, 1957. pp.115-128 161

912 HASTINGS, J. WOODLAND and BEATRICE M. SWEENEY. The luminescent reaction in extracts of the marine dinoflagellate, Gonyaulax polyedra. Journal of Cellular and Comparative Physiology, v.49, no.2, 1957. pp.209-225 175

913 ZOBELL, CLAUDE E. and RICHARD Y. MORITA. Barophilic bacteria in some deep sea sediments. Journal of Bacteriology, v.73, no.4, 1957. pp.563-568 193

914 RUSNAK, GENE A. The orientation of sand grains under conditions of "unidirectional" fluid flow. 1. theory and experiment. Journal of Geology, v.65, no.4, 1957. pp.384-409 199

915 KNAUSS, JOHN A. and J. L. REID. The effect of cable design on the accuracy of the GEK. American Geophysical Union, Transaction, v.38, no.3, 1957. pp.320-325 229

916a HEDGPETH, JOEL W. Introduction. GSA Memoir 67, Treatise on Marine Ecology and Paleoecology: v.1, Ecology. pp.1-16 . . . . *

916b HEDGPETH, JOEL W. Classification of marine environments. GSA Memoir 67, Treatise on Marine Ecology and Paleoecology: v.1, Ecology. pp.17-28 . . . . *

916c HEDGPETH, JOEL W. Concepts of marine ecology. GSA Memoir 67, Treatise on Marine Ecology and Paleoecology: v.1, Ecology. pp.29-52 . . . . *

* Not available for exchange.

Contrib. Number		Page Number
916d	HEDGPETH, JOEL W., GUNNAR THORSON, and GORDON GUNTER. Obtaining ecological data in the sea. GSA Memoir 67, Treatise on Marine Ecology and Paleoecology: v.1, Ecology. pp.53-86	*
916e	HOLMES, ROBERT W. Solar radiation, submarine daylight, and photosynthesis. GSA Memoir 67, Treatise on Marine Ecology and Paleoecology: v.1, Ecology. pp.109-128	*
916f	REVELLE, ROGER and RHODES FAIRBRIDGE. Carbonates and carbon dioxide. GSA Memoir 67, Treatise on Marine Ecology and Paleoecology: v.1, Ecology. pp.239-296	*
916g	GOLDBERG, EDWARD D. Biochemistry of trace metals. GSA Memoir 67, Treatise on Marine Ecology and Paleoecology: v.1, Ecology. pp.345-358	*
916h	HEDGPETH, JOEL W. Marine biogeography. GSA Memoir 67, Treatise on Marine Ecology and Paleoecology: v.1, Ecology. pp.359-382	*
916i	FOX, DENIS L. Particulate organic detritus. GSA Memoir 67, Treatise on Marine Ecology and Paleoecology: v.1, Ecology. pp.383-390	*
916j	JOHNSON, MARTIN W. Plankton. GSA Memoir 67, Treatise on Marine Ecology and Paleoecology: v.1, Ecology. pp.443-460	*
916k	HEDGPETH, JOEL W. Sandy beaches. GSA Memoir 67, Treatise on Marine Ecology and Paleoecology: v.1, Ecology. pp.587-608	*
916l	LIMBAUGH, CONRAD and FRANCIS P. SHEPARD. Submarine canyons. GSA Memoir 67, Treatise on Marine Ecology and Paleoecology: v.1, Ecology. pp.633-639	*
916m	HEDGPETH, JOEL W. Estuaries and lagoons, II., biological aspects. GSA Memoir 67, Treatise on Marine Ecology and Paleoecology: v.1, Ecology. pp.693-729	*
916n	COE, WESLEY R. Fluctuations in littoral populations. GSA Memoir 67, Treatise on Marine Ecology and Paleoecology: v.1, Ecology. pp.935-940	*
916o	MENZIES, ROBERT J. Annotated bibliography: marine borers. GSA Memoir 67, Treatise on Marine Ecology and Paleoecology: v.1, Ecology. pp.1029-1034	*
916p	ZOBELL, CLAUDE E. Annotated bibliography: marine bacteria. Memoir 67, Treatise on Marine Ecology and Paleoecology: v.1, Ecology. pp.1035-1040	*
916q	JOHNSON, MARTIN W. Annotated bibliography: Copepods. GSA Memoir 67, Treatise on Marine Ecology and Paleoecology: v.1, Ecology. pp.1165-1170	*

---

* Not available for exchange.

Contrib. Number | Page Number

917 **ROBINSON, MARGARET.** Sea temperature in the Gulf of Alaska and in the northeast Pacific Ocean, 1941-1952. BULLETIN OF THE SCRIPPS INSTITUTION OF OCEANOGRAPHY OF THE UNIVERSITY OF CALIFORNIA, v.7, no.1, 1957. pp.1-98 . . . . *

918 **NORTH, WHEELER J.** Sensitivity to light in the sea anemone *Metridium senile* (L.) II. Studies of reaction time variability and the effects of changes in light intensity and temperature. Journal of General Physiology, v.40, no.5, 1957. pp.715-733 237

919 **FOX, DENIS L.** The pigments of fishes. In "The Physiology of Fishes", Brown, Margaret Elizabeth, Ed. New York, Academic Press, 1957. pp.367-385 257

920 **DALES, R. PHILLIPS.** Pelagic polychaetes of the Pacific Ocean. BULLETIN OF THE SCRIPPS INSTITUTION OF OCEANOGRAPHY OF THE UNIVERSITY OF CALIFORNIA, v.7, no.2, 1957. pp.99-168 . . . . *

921 **DUNTLEY, SEIBERT Q., ALMERIAN R. BIOLEAU, and RUDOLPH W. PREISENDORFER.** Image transmission by the Troposphere I. Optical Society of America, Journal (ICO Symposium issue), v.47, no.6, 1957. pp.499-506 277

922 **ORTON, GRACE L.** The bearing of larval evolution on some problems in frog classification. Systematic Zoology, v.6, no.2, 1957. pp.79-86 285

923 **SHEPARD, FRANCIS P.** Northward continuation of San Andreas Fault. Seismological Society of America, Bulletin, v.47, no.3, 1957. pp.263-266 293

924 **MCALLISTER, RAYMOND F.** Photography of submerged vertical structures. American Geophysical Union, Trans., v.38, no.3, 1957. pp.314-319 298

925 **BRADSHAW, JOHN S.** Laboratory studies on the rate of growth of the foraminifer, "*Streblus beccarii* (Linné) var. *tepida* (Cushman)". Journal of Paleontology, v.31, no.6, 1957. pp.1138-1147 305

926 **ZOBELL, CLAUDE E. and RICHARD MORITA.** Deep sea bacteria. Galathea Expedition Reports. *Publication delayed.* . . . . *

927 **MORITA, RICHARD.** Effect of hydrostatic pressure on succinic, formic, and malic dehydrogenases in *Escherichia coli*. Journal of Bacteriology, v.74, no.2, 1957. pp.251-255 317

928 **JOHNSON, MARTIN W.** The copepod *Choniosphaera cancrorum*, parasitizing a new host, the green crab *Carcinides maenas*. Journal of Parasitology, v.43, no.4, 1957. pp.470-473 323

929 **RAITT, RUSSELL W.** Seismic-refraction studies of Eniwetok Atoll. U.S.G.S. Professional Paper 260-S, 1957. pp.685-698 327

930 **REVELLE, ROGER and K. O. EMERY.** Chemical erosion of beach rock and exposed reef rock. U.S.G.S. Professional Paper 260-T, 1957. pp.699-709 345

* Not available for exchange.

Contrib. Number | Page Number

931 MENZIES, ROBERT J. The marine borer family Limnoriidae (Crustacea, Isopoda). Part I: northern and central America: systematics, distribution, and ecology. Bulletin of Marine Science of the Gulf and Caribbean, v.7, no.2, 1957. pp.101-200 373

932 SHEPARD, FRANCIS P. and GENE A. RUSNAK. Texas bay sediments. Institute of Marine Science, v.3, no.2, 1957. pp.5-13 473

933 TYLER, JOHN E. Monochromatic measurement of the volume scattering of natural waters. Optical Society of America, Journal, v.47, no.8, 1957. pp.745-747 483

934 ANDERSON, VICTOR C. Dielectric recorder. Review of Scientific Instruments, v.28, no.7, 1957. pp.504-509 487

935 PHLEGER, FRED B and ROBERT R. LANKFORD. Seasonal occurences of living benthonic foraminifera in some Texas bays. Cushman Foundation for Foraminiferal Research, Contributions, v.8, part 3, 1957. pp.93-105. 493

936 BURSTYN, H. L. At the sign of the Quadrant. Mystic, Connecticut, Mystic Seaport, 1957. 119 p. . . . . *

937 EBELING, ALFRED W. The dentition of eastern Pacific mullets, with special reference to adaptation and taxonomy. Copiea, no.3, 1957. pp.173-185 507

938 ARRHENIUS, G., M. N. BRAMLETTE, and E. PICCIOTTO. Localization of radioactive and stable heavy nuclides in ocean sediments. Nature, v.180, no.4576, 1957. pp.85-86 527

939 HASTINGS, J. WOODLAND and BEATRICE SWEENEY. On the mechanism of temperature independence in a biological clock. National Academy of Sciences, Proceedings, v.43, no.9, 1957. pp.804-811 531

940 COE, WESLEY R. Fluctuations in populations of littoral marine invertebrates. Journal of Marine Research, v.15, no.3, 1956. pp.212-232 539

941 SPIESS, FRED N. Acceleration measurements in the deep ocean. Journal of Marine Research, v.16, no. 1, 1957. pp.23-33. . . . . *

942 HOLMES, ROBERT W., MILNER B. SCHAEFER and BELL M. SHIMADA. Primary production, chlorophyll, and zooplankton volumes in the tropical eastern Pacific. Inter-American Tropical Tuna Commission, Bulletin, v.2, no.4, 1957. pp.127-169 561

943 TOKIOKA, TAKASI. Two new appendicularians from the eastern Pacific, with notes on the morphology of *Fritillaria aequatorialis* and *Tectillaria fertilis*. American Microscopical Soc., Trans., v.76, no.4, 1957. pp.359-365 605

944 RUSNAK, GENE A. Reply to the "discussion" of a fabric and petrologic study of the Pleasantview sandstone. Journal of Sedimentary Petrology, v.27, no.3, 1957. pp.346-350 613

---

* Not available for exchange.

Contrib. Number		Page Number
945	LANKFORD, ROBERT R. and JOSEPH R. CURRAY. Mid-Tertiary rock outcrop on continental shelf, northwest Gulf of Mexico. Geological Note; American Assoc. of Petroleum Geologists, Bulletin, v.41, no.9, 1957. pp.2113-2117	619
946	EL WARDANI, SAYED A. On the geochemistry of germanium. Geochimica et Cosmochimica Acta, v.13, no.1, 1957. pp.5-19	625
947	INMAN, DOUGLAS L. Wave-generated ripples in nearshore sands. U.S. Army, Corps of Engineers, Beach Erosion Board Technical Memorandum no.100. Oct. 1957. pp.1-42	641
948	GROVES, GORDON W. Day to day variation of sea level. Meteorological Monographs, v.2, no.10, 1957. pp.32-45	713
949	BODEN, BRIAN P. and EDWARD BRINTON. The euphausiid crustaceans *Thysanopoda aequalis* Hansen and *Thysanopoda subaequalis* Boden, their taxonomy and distribution in the Pacific. Limnology and Oceanography, v.2, no.4, 1957. pp.337-341	729
950	MUNK, WALTER, M. J. TUCKER, and F. E. SNODGRASS. Remarks on the ocean wave spectrum. Naval Hydrodynamics, Symposium. National Academy of Sciences-National Research Council Publication 515, 1957. pp.45-60	735
951	PREISENDORFER, RUDOLPH W. Exact reflectance under a cardioidal luminance distribution. Royal Meteorological Society, Quarterly Journal, v.83, no.358, 1957. pp.540-543	753
952	GOLDBERG, E. D. and GUSTAF ARRHENIUS. Chemistry of Pacific pelagic sediments. Geochimica et Cosmochimica Acta, v.13, 1958. pp.153-212	757
953	PREISENDORFER, RUDOLPH W. A mathematical foundation for radiative transfer theory. Journal of Mathematics and Mechanics, v.6, no.6, 1957. pp.685-730	819
954	BRAMLETTE, M. N. Significance of coccolithophorids in calcium-carbonate deposition. Geological Society of America, Bulletin, v.69, no.1, 1958. pp.121-126	865
955	MUNK, WALTER and F. E. SNODGRASS. Measurements of southern swell at Guadalupe Island. Deep-Sea Research, v.4, no.4, 1957. pp.272-286	871
956	MOORE, DAVID G. and P. C. SCRUTON. Minor internal structures of some recent unconsolidated sediments. American Assoc. of Petroleum Geologists, Bulletin, v.41, no.12, 1957. pp.2723-2751	889
957	POOLE, DAVID M. Size analysis of sand by a sedimentation technique. Journal of Sedimentary Petrology, v.27, no.4, 1957. pp.460-468	919
958	WISNER, ROBERT L. Is the spear of istiophorid fishes used in feeding? Pacific Science, v.12, no.1, 1958. pp.60-70	929

Contrib. Number		Page Number
959	CRAIG, HARMON. Geochemical kinetics of radiocarbon and tritium distribution, and the production rate of natural tritium. Conference on Nuclear Processes in Geologic Settings, 3d, Proc. NAS-NRC Publication. *Publication delayed.*	*
960	RODEN, GUNNAR. Oceanographic and meteorological aspects of the Gulf of California. Pacific Science, v.12, no.1, 1958. pp.21-45	941
961	MAZIA, DANIEL. SH compounds in mitosis. I. the action of mercaptoethanol on the eggs of the sand dollar *Dendraster excentricus*. Experimental Cell Research. *Publication delayed.*	*
962	Ó HEOCHA, COLM. Comparative biochemical studies of the phycobilins. Archives of Biochemistry and Biophysics, v.73, no.1, 1958. pp.207-219	967
963	YOSHIDA, KOZO and HAN-LEE MAO. A theory of upwelling of large horizontal extent. Journal of Marine Research, v.16, no. 1, 1957. pp.40-54.	*
964	ELSASSER, WALTER and WALTER MUNK. Geomagnetic drift and rotation of the earth. In "Beno Gutenberg Testimonial." London, Pergamon Press Ltd. *Publication delayed.*	*
965	LASKER, REUBEN and R. W. HOLMES. Variability in retention of marine phytoplankton by membrane filters. Nature, v.180, no.4597, 1957. pp.1295-1296.	981
966	REVELLE, ROGER. International cooperation in the marine sciences. Science, v.126, no.3287, 1957. pp.1319-1323	985

* Not available for exchange.

UNIVERSITY OF CALIFORNIA
SCRIPPS INSTITUTION OF OCEANOGRAPHY
CONTRIBUTIONS, NEW SERIES
1957

AUTHOR INDEX

	Contrib. Number	Page Number
ANDERSON, VICTOR C.		
Dielectric recorder	934	487
ARRHENIUS, GUSTAF		
(and M. N. Bramlette and E. Picciotto) Localization of radioactive and stable heavy nuclides in ocean sediments.	938	527
(with E. D. Goldberg) Chemistry of Pacific pelagic sediments.	952	753
BODEN, BRIAN P.		
(and Elizabeth M. Kampa) Records of bioluminescence in the ocean.	910	153
(and Edward Brinton) The euphausiid crustaceans *Thysanopoda aequalis* Hansen and *Thysanopoda subaequalis* Boden, their Taxonomy and distribution in the Pacific.	949	729
BOILEAU, ALMERIAN R.		
(and R. W. Preisendorfer with S. Q. Duntley) Image transmission by the Troposphere I.	921	277
BOROUGHS, HOWARD		
(and Edward D. Goldberg, with Louis A. Krumholz) Ecological factors involved in the uptake, accumulation and loss of radionuclides by aquatic organisms.	901a	39
BRADSHAW, JOHN S.		
Laboratory studies on the rate of growth of the foraminifer, "*Streblus beccarii* (Linné) var. *tepida* (Cushman)".	925	305
BRAMLETTE, M. N.		
(and E. Picciotto, with Gustaf Arrhenius) Localization of radioactive and stable heavy nuclides in ocean sediments.	938	527
Significance of coccolithophorids in calcium-carbonate deposition.	954	865
BURSTYN, H. L.		
At the Sign of the Quadrant.	936	*
BRINTON, EDWARD		
(with Brian P. Boden) The euphausiid crustaceans *Thysanopoda aequalis* Hansen and *Thysanopoda subaequalis* Boden, their taxonomy and distribution in the Pacific.	949	729

* Not available for exchange.

	Contrib. Number	Page Number
COE, WESLEY R.		
Fluctuations in littoral populations.	916n	*
Fluctuations in population of littoral marine invertebrates.	940	539
CRAIG, HARMON.		
Isotopic tracer techniques for measurement of physical processes in the sea and the atmosphere.	902	51
Disposal of radioactive wastes in the ocean: the fission product spectrum in the sea as a function of time and mixing characteristics.	902a	69
Geochemical kinetics of radiocarbon and tritium distribution and the production rate of natural tritium.	959	*
CURRAY, JOSEPH R.		
(with Robert R. Lankford) Mid-Tertiary rock outcrop on continental shelf, northwest Gulf of Mexico	945	619
DALES, R. PHILLIPS		
Pelagic polychaetes of the Pacific Ocean.	920	*
DUNTLEY, SEIBERT Q.		
(and Almerian R. Boileau and Rudolph W. Preisendorfer) Image transmission by the Troposphere I.	921	277
EBELING, ALFRED		
(with John Kanwisher) Composition of the swim-bladder gas in bathypelagic fishes.	908	139
The dentition of eastern Pacific mullets, with special reference to adaptation and taxonomy.	937	507
ELSASSER, WALTER		
(and Walter Munk) Geomagnetic drift and rotation of the earth.	964	*
EL WARDANI, SAYED A.		
On the geochemistry of germanium.	946	625
EMERY, K. O.		
(with Roger Revelle) Chemical erosion of beach rock and exposed reef rock.	930	345
FAIRBRIDGE, RHODES		
(with Roger Revelle) Carbonates and carbon dioxide.	916f	*
FOLSOM, THEODORE R.		
(and John H. Harley) Comparison of some natural radiations received by selected organisms.	904	95
(and Allyn C. Vine) On the tagging of water masses for the study of physical processes in the oceans.	905	103
FOX, DENIS L.		
The pigments of fishes.	919	257
Particulate organic detritus.	916i	*
GOLDBERG, EDWARD D.		
(and Howard Boroughs, with Louis A. Krumholz) Ecological factors involved in the uptake, accumulation and loss of radionuclides by aquatic organisms.	901a	39

* Not available for exchange.

	Contrib. Number	Page Number
GOLDBERG, EDWARD D. (continued)		
Biochemistry of trace metals.	916g	*
(and Gustaf Arrhenius) Chemistry of Pacific pelagic sediments.	952	757
GROVES, GORDON W.		
Day to day variation of sea level.	948	713
GUNTER, GORDON		
(and Gunnar Thorson, with Joel W. Hedgpeth) Obtaining ecological data in the sea.	916d	*
HARLEY, JOHN H.		
(with Theodore R. Folsom) Comparison of some natural radiations received by selected organisms.	904	95
HASTINGS, J. WOODLAND		
(and Beatrice M. Sweeney) Characteristics of the diurnal rhythm of luminescense in *Gonyaulax polyedra.*	911	161
(and Beatrice M. Sweeney) The luminescent reaction in extracts of the marine dinoflagellate, *Gonyaulax polyedra.*	912	175
(and Beatrice M. Sweeney) On the mechanism of temperature independence in a biological clock.	939	531
HEDGPETH, JOEL W.		
Introduction.	916a	*
Classification of marine environments.	916b	*
Concepts of marine ecology.	916c	*
(and Gunnar Thorson and Gordon Gunter) Obtaining ecological data in the sea.	916d	*
Marine biogeography.	916h	*
Sandy beaches.	916k	*
Estuaries and lagoons, II., biological aspects.	916m	*
HOLMES, ROBERT W.		
Solar radiation, submarine daylight and photosynthesis.	916e	*
(and Milner B. Schaefer and Bell M. Shimada) Primary production, chlorophyll, and zooplankton volumes in the tropical eastern Pacific.	942	561
(with Reuben Lasker) Variability in retention of marine phytoplankton by membrane filters.	965	981
INMAN, DOUGLAS L.		
Wave-generated ripples in nearshore sands.	947	641
JOHNSON, MARTIN W.		
Plankton.	916j	*
Copepods.	916q	*
The copepod *Choniosphaera cancrorum,* parasitizing a new host, the green crab *Carcinides maenas.*	928	323
KAMPA, ELIZABETH M.		
(with Brian P. Boden) Records of bioluminescence in the ocean.	910	153

* Not available for exchange.

	Contrib. Number	Page Number
KANWISHER, JOHN		
(and Alfred Ebeling) Composition of the swim-bladder gas in bathypelagic fishes.	908	139
KETCHUM, BOSTWICK H.		
(with Warren S. Wooster) Transport and dispersal of radioactive elements in the sea.	903	79
KNAUSS, JOHN A.		
An observation of an oceanic front.	909	147
(and Joseph L. Reid) The effects of cable design on the accuracy of the GEK.	915	229
KRUMHOLZ, LOUIS A.		
(and E. D. Goldberg and Howard Boroughs) Ecological factors involved in the uptake, accumulation and loss of radionuclides by aquatic organisms.	901a	39
LANKFORD, ROBERT R.		
(with Fred B Phleger) Seasonal occurrences of living benthonic foraminifera in some Texas bays.	935	493
(and Joseph R. Curray) Mid-Tertiary rock outcrop on continental shelf, northwest Gulf of Mexico.	945	619
LASKER, REUBEN		
(and R. W. Holmes) Variability in retention of marine phytoplankton by membrane filters.	965	981
LIEBERMANN, LEONARD		
Air bubbles in water.	906	115
LIMBAUGH, CONRAD		
(and Francis P. Shepard) Submarine canyons.	916*l*	*
MCALLISTER, RAYMOND F.		
Photography of submerged vertical structures.	924	298
MAO, HAN-LEE		
(with Kozo Yoshida) A theory of upwelling of large horizontal extent.	963	*
MAZIA, DANIEL		
SH compounds in mitosis. I. The action of mercaptoethanol on the eggs of the sand dollar *Dendraster excentricus*.	961	*
MENZIES, ROBERT J.		
Annotated bibliography: marine borers.	916o	*
The marine borer family Limnoriidae (Crustacea, Isopoda). Part I: northern and central America: systematics, distribution and ecology.	931	373
MOORE, DAVID G.		
(and Phillip C. Scruton) Minor internal structures of some recent unconsolidated sediments.	956	889
MORITA, RICHARD Y.		
(with Claude E. ZoBell) Barophilic bacteria in some deep sea sediments.	913	193

* Not available for exchange.

	Contrib. Number	Page Number
MORITA, RICHARD Y. (continued)		
(with Claude E. ZoBell) Deep sea bacteria.	926	*
Effect of hydrostatic pressure on succinic, formic, and malic dehydrogenases in *Escherichia coli*.	927	317
MUNK, WALTER		
(and M. J. Tucker and F. E. Snodgrass) Remarks on the ocean wave spectrum.	950	735
(and F. E. Snodgrass) Measurements of southern swell at Guadalupe Island.	955	871
(and Walter Elsasser) Geomagnetic drift and rotation of the earth.	964	*
NORTH, WHEELER J.		
Sensitivity to light in the sea anemone *Metridium senile* (L.) II. Studies of reaction time variability and the effects of changes in light intensity and temperature.	918	237
Ó HEOCHA, COLM		
Comparative biochemical studies of the phycobilins.	962	967
ORTON, GRACE L.		
The bearing of larval evolution on some problems in frog classification.	922	285
PHLEGER, FRED B		
(and Robert R. Lankford) Seasonal occurrences of living benthonic foraminifera in some Texas bays.	935	493
PICCIOTTO, E.		
(and M. N. Bramlette, with Gustaf Arrhenius) Localization of radioactive and stable heavy nuclides in ocean sediments.	938	527
POOLE, DAVID M.		
Size analysis of sand by a sedimentation technique.	957	919
PREISENDORFER, RUDOLPH W.		
(and A. R. Boileau, with S. Q. Duntley) Image transmission by the Troposphere I.	921	277
Exact reflectance under a cardioidal luminance distribution.	951	753
A mathematical foundation for radiative transfer theory.	953	819
RAITT, RUSSELL W.		
Seismic-refraction studies of Eniwetok Atoll.	929	327
REID, JOSEPH L.		
(with John Knauss) The effects of cable design on the accuracy of the GEK.	915	229
REVELLE, ROGER		
(and Hans E. Suess) Carbon dioxide exchange between atmosphere and ocean and the question of an increase of atmospheric CO_2 during the past decades.	900	1
(and M. B. Schaefer) General considerations concerning the ocean as a receptacle for artificially radioactive materials.	901	13
(and Rhodes Fairbridge) Carbonates and carbon dioxide.	916f	

---

* Not available for exchange.

	Contrib. Number	Page Number
REVELLE, ROGER (continued)		
(and K. O. Emery) Chemical erosion of beach rock and exposed reef rock.	930	345
International cooperation in the marine sciences.	966	985
ROBINSON, MARGARET		
Sea temperature in the Gulf of Alaska and in the northeast Pacific Ocean, 1941-1952.	917	*
RODEN, GUNNAR		
Oceanographic and meteorological aspects of the Gulf of California.	960	941
RUSNAK, GENE A.		
A fabric and petrologic study of the Pleasantview sandstone.	907	123
The orientation of sand grains under conditions of "unidirectional" fluid flow. 1. theory and experiment.	914	199
(with Francis P. Shepard) Texas bay sediments.	932	473
Reply to the "discussion" of a fabric and petrologic study of the Pleasantview sandstone.	944	613
SCHAEFER, MILNER B.		
(with Roger Revelle) General considerations concerning the ocean as a receptacle for artificially radioactive materials.	901	13
Large scale biological experiments using radioactive tracers.	903a	89
(and B. M. Shimada, with R. W. Holmes) Primary production, chlorophyll, and zooplankton volumes in the tropical eastern Pacific.	942	561
SCRUTON, PHILLIP C.		
(with David G. Moore) Minor internal structures of some recent unconsolidated sediments.	956	889
SHEPARD, FRANCIS P.		
(with Conrad Limbaugh) Submarine canyons.	916*l*	
Northward continuation of San Andreas Fault.	923	293
(and Gene A. Rusnak) Texas bay sediments.	932	473
SHIMADA, BELL M.		
(and M. B. Schaefer, with R. W. Holmes) Primary production, chlorophyll, and zooplankton volumes in the tropical eastern Pacific.	942	561
SNODGRASS, FRANK E.		
(and M. J. Tucker, with Walter Munk) Remarks on the ocean wave spectrum.	950	735
(with Walter Munk) Measurements of southern swell at Guadalupe Island.	955	871
SPIESS, FRED N.		
Acceleration measurements in the deep ocean.	941	*
SUESS, HANS		
(with Roger Revelle) Carbon dioxide exchange between atmosphere and ocean and the question of an increase of atmospheric CO_2 during the past decades.	900	1

* Not available for exchange.

	Contrib. Number	Page Number
SWEENEY, BEATRICE M.		
(and J. Woodland Hastings) Characteristics of the diurnal rhythm of luminescense in *Gonyaulax polyedra.*	911	161
(with J. Woodland Hastings) The luminescent reaction in extracts of the marine dinoflagellate, *Gonyaulax polyedra.*	912	175
(and J. Woodland Hastings) On the mechanism of temperature independence in a biological clock.	939	531
THORSON, GUNNAR		
(and Gordon Gunter, with Joel W. Hedgpeth) Obtaining ecological data in the sea.	916d	*
TOKIOKA, TAKASI		
Two new appendicularians from the eastern Pacific, with notes on the morphology of *Fritillaria aequatorialis* and *Tectillaria fertilis.*	943	605
TUCKER, M. J.		
(and F. E. Snodgrass, with Walter Munk) Remarks on the ocean wave spectrum.	950	735
TYLER, JOHN E.		
Monochromatic measurement of the volume scattering of natural waters.	933	483
VINE, ALLYN C.		
(with Theodore R. Folsom) On the tagging of water masses for the study of physical processes in the oceans.	905	103
WISNER, ROBERT L.		
Is the spear of istiophorid fishes used in feeding?	958	929
WOOSTER, WARREN S.		
(and Bostwick H. Ketchum) Transport and dispersal of radioactive elements in the sea.	903	79
YOSHIDA, KOZO		
(and Han-Lee Mao) A theory of upwelling of large horizontal extent.	963	*
ZOBELL, CLAUDE E.		
(and Richard Morita) Barophilic bacteria in some deep sea sediments.	913	193
Annotated bibliography: marine bacteria.	916p	*
(and Richard Morita) Deep sea bacteria.	926	*

* Not available for exchange.

Särtryck ur Tellus nr 1. 1957

Carbon Dioxide Exchange Between Atmosphere and Ocean and the Question of an Increase of Atmospheric CO_2 during the Past Decades

By ROGER REVELLE and HANS E. SUESS, Scripps Institution of Oceanography, University of California, La Jolla, California

(Manuscript received September 4, 1956)

Abstract

From a comparison of C^{14}/C^{12} and C^{13}/C^{12} ratios in wood and in marine material and from a slight decrease of the C^{14} concentration in terrestrial plants over the past 50 years it can be concluded that the average lifetime of a CO_2 molecule in the atmosphere before it is dissolved into the sea is of the order of 10 years. This means that most of the CO_2 released by artificial fuel combustion since the beginning of the industrial revolution must have been absorbed by the oceans. The increase of atmospheric CO_2 from this cause is at present small but may become significant during future decades if industrial fuel combustion continues to rise exponentially.

Present data on the total amount of CO_2 in the atmosphere, on the rates and mechanisms of exchange, and on possible fluctuations in terrestrial and marine organic carbon, are inadequate for accurate measurement of future changes in atmospheric CO_2. An opportunity exists during the International Geophysical Year to obtain much of the necessary information.

Introduction

In the middle of the 19th century appreciable amounts of carbon dioxide began to be added to the atmosphere through the combustion of fossil fuels. The rate of combustion has continually increased so that at the present time the annual increment from this source is nearly 0.4 % of the total atmospheric carbon dioxide. By 1960 the amount added during the past century will be more than 15 %.

CALLENDAR (1938, 1940, 1949) believed that nearly all the carbon dioxide produced by fossil fuel combustion has remained in the atmosphere, and he suggested that the increase in atmospheric carbon dioxide may account for the observed slight rise of average temperature in northern latitudes during recent decades. He thus revived the hypothesis of T. C. CHAMBERLIN (1899) and S. ARRHENIUS (1903) that climatic changes may be related to fluctuations in the carbon dioxide content of the air. These authors supposed that an increase of carbon dioxide in the upper atmosphere would lower the mean level of back radiation in the infrared and thereby increase the average temperature near the earth's surface.

Subsequently, other authors have questioned Callendar's conclusions on two grounds. First, comparison of measurements made in the 19th century and in recent years do not demonstrate that there has been a significant increase in

---

Contribution from the Scripps Institution of Oceanography, New Series, No. 900. This paper represents in part results of research carried out by the University of California under contract with the Office of Naval Research.

(2)

Reproduced by Permission

Table 1. CO_2 added to atmosphere by consumption of fossil fuels

Decade	Average amount added per decade Measured		Cumulative total added			
	10^{18} gms	% Atm CO_2	10^{18} gms	% Atm CO_2	10^{18} gms	% Atm CO_2
1860—69	0.0054	0.23	0.0054	0.23		
1870—79	0.0085	0.36	0.0139	0.59		
1880—89	0.0128	0.54	0.0267	1.13		
1890—99	0.0185	0.79	0.0452	1.92		
1900—09	0.0299	1.27	0.0751	3.19		
1910—19	0.0405	1.72	0.1156	4.91		
1920—29	0.0470	2.00	0.1626	6.91		
1930—39	0.0497	2.11	0.2123	9.02		
1940—49	0.0636	2.71	0.2759	11.73		
	Forecast					
	Assuming fossil fuels are used to meet future requirements of fuel and power as estimated by UN (1955)				Assuming fossil fuel consumption remains constant at estimated 1955 rate	
1950—59	0.091	3.9	0.367	15.6	0.367	15.6
1960—69	0.128	5.4	0.495	21.0	0.458	19.5
1970—79	0.176	7.5	0.671	28.5	0.549	23.4
1980—89	0.247	10.5	0.918	39.0	0.640	27.2
1990—99	0.340	14.5	1.258	53.5	0.731	31.1
2000—09	0.472	20.0	1.730	73.5	0.822	35.0

atmospheric CO_2 (Slocum, 1955; Fonselius *et al.* 1956). Most of the excess CO_2 from fuel combustion may have been transferred to the ocean, a possibility suggested by S. Arrhenius (1903). Second, a few percent increase in the CO_2 content of the air, even if it has occurred, might not produce an observable increase in average air temperature near the ground in the face of fluctuations due to other causes. So little is known about the thermodynamics of the atmosphere that it is not certain whether or how a change in infrared back radiation from the upper air would affect the temperature near the surface. Calculations by Plass (1956) indicate that a 10 % increase in atmospheric carbon dioxide would increase the average temperature by 0.36° C. But, amplifying or feed-back processes may exist such that a slight change in the character of the back radiation might have a more pronounced effect. Possible examples are a decrease in albedo of the earth due to melting of ice caps or a rise in water vapor content of the atmosphere (with accompanying increased infrared absorption near the surface) due to increased evaporation with rising temperature.

During the next few decades the rate of combustion of fossil fuels will continue to increase, if the fuel and power requirements of our world-wide industrial civilization continue to rise exponentially, and if these needs are met only to a limited degree by development of atomic power. Estimates by the UN (1955) indicate that during the first decade of the 21st century fossil fuel combustion could produce an amount of carbon dioxide equal to 20 % of that now in the atmosphere (Table 1).[1] This is probably two orders of magnitude greater than the usual rate of carbon dioxide production from volcanoes, which on the average must be equal to the rate at which silicates are weathered to carbonates (Table 2). Thus human beings are now carrying out a large scale geophysical experiment of a kind that could not have happened in the past nor be reproduced in the future. Within a few centuries we are returning to the atmosphere and oceans the concentrated organic carbon stored in sedimentary rocks over hundreds of millions of years. This experiment, if adequately documented, may yield a far-reaching insight into the processes determining weather and climate. It therefore becomes of prime importance to attempt to determine the way in which carbon dioxide is partitioned between the atmosphere, the oceans, the biosphere and the lithosphere.

---

[1] World production of CO_2 from the use of limestone for cement, fluxing stone and in other ways was about 1 % of the total from fossil fuel combustion in 1950.

The carbon dioxide content of the atmosphere and ocean is presumably regulated over geologic times by the tendency toward thermodynamic equilibrium between silicates and carbonates and their respective free acids, silica and carbon dioxide (UREY, 1952). The atmosphere contains and probably has contained during geologic times considerably more CO_2 than the equilibrium concentration (HUTCHINSON, 1954), although uncertainties in the thermodynamic data are too great for an accurate quantitative comparison. Equilibrium is approached through rock weathering and marine sedimentation. Estimated rates of these processes give a very long time constant of the order of magnitude of 100,000 years. Rapid changes in the amount of carbon dioxide produced by volcanoes, in the state of the biosphere, or as in our case, in the rate of combustion of fossil fuels, may therefore cause considerable departures from average conditions.

Table 2. Estimated present annual rates of some processes involving atmospheric and oceanic carbon dioxide, in part after HUTCHINSON (1954)

	10^{18} gms	In units of atm $CO_2(A_0)$
Consumption of fossil fuels—CO_2 produced.	0.0091	0.0039
Bicarbonate and carbonate added to ocean by rivers (as CO_2)[1] . .	0.00103	0.0004
Photosynthesis on land —CO_2 consumed	0.073 ± 0.018	0.031
Photosynthesis in ocean —CO_2 consumed	0.46 ± 0.3	0.20

[1] According to CONWAY (1942) and HUTCHINSON (1954) 87 % of the river borne bicarbonate and carbonate comes from weathering of carbonate rocks, the remainder from weathering of silicates.

The answer to the question whether or not the combustion of coal, petroleum and natural gas has increased the carbon dioxide concentration in the atmosphere depends in part upon the rate at which an excess amount of CO_2 in the atmosphere is absorbed by the oceans. The exchange rate of isotopically labeled CO_2 between atmosphere and ocean, which, in principle, could be deduced from C^{14} measurements, is not identical with the rate of absorption, but is related to it.

Notations and geochemical constants

In our discussion of exchange and absorption rates we shall use the following notations:

S_0: Total carbon of the marine carbon reservoir at equilibrium condition, at time zero.
A_0: Atmospheric CO_2 carbon at time zero.
i: Annual amount of industrial CO_2 added to the atmosphere.
t: Time in years.
$s = S_t - S_0$: Amount of CO_2 derived from industrial fuel combustion in the sea at time t.
$r = it - s$: Amount of CO_2 derived from industrial fuel combustion in the atmosphere at time t.
r^*: Observed decrease in C^{14} activity.
$\tau(\text{atm})$: Average lifetime of a CO_2 molecule in the atmosphere, before it becomes dissolved in the sea.
$\tau(\text{sea})$: Average lifetime of carbon in the sea, before it becomes atmospheric CO_2.
$k_1 = 1/\tau(\text{atm})$: Rate of CO_2 transfer per year from the atmosphere to the sea.
$k_2 = 1/\tau(\text{sea})$: Rate of CO_2 transfer per year from the sea to the atmosphere.
P_{CO_2}: Partial CO_2 pressure in the atmosphere.

Table 3 gives the amount of carbon, expressed in CO_2 equivalents, in the various geochemical reservoirs on the surface of the Earth.

The symbols S^* and A^* shall be used for denoting respective "effective" reservoirs.

Rate of CO_2 exchange between sea and atmosphere

Two types of C^{14} measurements independently allow calculation of the exchange rate

Table 3. Amount of carbon, computed as CO_2, in sedimentary rocks, hydrosphere, atmosphere and biosphere from data given by RUBEY (1951), HUTCHINSON (1954), and SVERDRUP et al. (1942)

	Total on Earth: 10^{18} gms	In units of A_0
Carbonate in sediments...	67,000	28,500
Organic carbon in sediments	25,000	10,600
CO_2 in the atmosphere (A_0)	2.35	1
Living matter on land[1]....	0.3	0.12
Dead organic matter on land..................	2.6	1.1
$CO_2+H_2CO_3$ in ocean[2]....	0.8	0.3
CO_2 as HCO_3^- in ocean[2] ..	114.7	48.7
CO_2 as $CO_3^{=}$ in ocean[2]	14.2	6.0
Total inorganic carbon in ocean................	129.7	55.0
Dead organic matter in ocean................	10	4.4
Living organic matter in ocean................	0.03	0.01
Total carbon in ocean (S_0)	140	59.4

[1] Living organic matter on land estimated from assays of standing timber in the world's forests. 30 % of land surface is relatively thick forest, averaging about 5,000 board feet/acre of commercial size timber or 0.26 gm CO_2/cm^2 of forest. Assuming that total living matter in forests is twice the amount of timber, and that other components of the biosphere are $^1/_3$ of total gives 0.34×10^{18} gm CO_2 in land biosphere.

[2] Carbon dioxide components in sea water are assumed to be in equilibrium with a CO_2 partial pressure of 3×10^{-4} atmospheres; chlorinity: 20 ‰; temperature: 10° C; alkalinity: 2.46×10^{-3} meq/L. Under these conditions pH = 8.18. Volume of the Ocean = 1.37×10^{24} cm^3. This is probably an underestimate, because the water below the thermocline contains CO_2 produced by oxidation of organic matter, and the average temperature of the ocean is somewhat less than 10° C.

through the sea-air interface, if assumptions are made with respect to mixing rates of the water masses in the oceans: (*a*) the apparent C^{14} age of marine materials and (*b*) the effects of industrial coal combustion on the C^{14} concentration in the atmosphere (SUESS 1953). Experimental data on these two subjects are inadequate for rigorous quantitative interpretation but are sufficiently accurate to allow estimates of the order of magnitude of the rate constant for the exchange.

Considering the combined marine and atmospheric carbon reservoir as a closed system in equilibrium, the following relation holds by definition:

$$\frac{\tau\ (\text{sea})}{\tau\ (\text{atm})} = \frac{k_1}{k_2} = \frac{S_0}{A_0}\ . \qquad (1)$$

τ (sea), the average lifetime of a carbon atom as a member of the marine reservoir, is equal to the average apparent C^{14} age of marine material.

An apparent C^{14} age of marine material is obtained by comparison of the C^{14} activity with that of a wood standard corrected for isotopic fractionation effects in nature or in the laboratory by mass spectrometric measurement of the C^{13}/C^{12} ratios. In marine carbonate the C^{13}/C^{12} ratio is about 2.5 % higher than in land plants (NIER and GULBRANSEN, 1939 and CRAIG 1953, 1954). Because of the double mass difference the effect for C^{14} should be twice as large as that for C^{13}, if the isotopic distribution is established sufficiently rapidly so that radioactive decay of C^{14} can be neglected. If, after normalizing to equal C^{13}/C^{12} ratios, a lower C^{14} concentration is found than that of the wood standard, then this difference is attributed here to the effect of radioactivity, and is expressed as apparent age. A detailed study of the expected relationship between the isotopic fractionation factors for C^{13} and C^{14} in the bio-geochemical cycle of carbon has been made by CRAIG (1954).

Assuming from the then available C^{14} measurements that shell and wood have the same specific C^{14} activity, CRAIG (1954) attributed this unexpected result to slow transfer of CO_2 across the ocean-atmosphere interface resulting in a radiocarbon age of 400 years for surface ocean bicarbonate. Since then, more precise C^{14} measurements, supplemented by mass spectroscopic C^{13} determinations, have been published by SUESS (1954, 1955) and by RAFTER (1955) (see also HAYES ET AL., 1955). The standard error of about 0.5 % corresponds to an uncertainty in the age values of about 40 years. The apparent ages calculated from the published measurements are as follows:

Atlantic: (SUESS, 1954).

Mercenaria mercenaria	Shells	440 yrs.
Nantucket sound (from under 45 ft of water)	Flesh	540 yrs.
Sargassum weed from sea surface, 36°24′ N, 69°37′ W		320 yrs.

New Zealand area: (Rafter, 1955).

Pauna Shells	350 yrs.
Limpet shells	360 yrs.
Cockle shells	280 yrs.
Pauna flesh	290 yrs.
Limpet flesh	140 yrs.
Seaweed	250 yrs.
Seawater (East Cape area)	370 yrs.

The average of the ages given here is 430 yrs. for the Atlantic samples and 290 yrs. for the New Zealand samples. The difference of 140 yrs. is due to the fact that the ages of the first group were calculated using wood grown in the 19th century as standard, whereas contemporaneous wood was used as standard for the New Zealand samples.[1]

Assuming that these apparent ages for marine surface materials are representative for the average age of marine carbon, or in other words, that mixing times of the oceans are short compared to the ages measured, an apparent age of about 400 years for marine carbon corresponds, according to Eq. (1), to an exchange time τ (atm) of about 7 years.

This *lower* limit for the exchange time of CO_2 between the atmosphere and the sea can now be compared with computations of this quantity from the observed effect of industrial fuel combustion on the specific C^{14} activity of wood. This second way, however, will lead to an *upper* limit for the exchange time if rapid mixing in the oceans is assumed.

At present 9.1×10^{15} grams of C^{14} free CO_2, or a fraction of 3.9×10^{-3} of the atmospheric CO_2, is added per year to the atmosphere by artificial burning of fossil fuels. The total amount added during the 100 years prior to 1950 corresponds to about 12 % of the atmospheric carbon reservoir.

Neglecting any effect of the industrial CO_2 on the rate constants k_1 and k_2 one obtains:

$$\frac{ds}{dt} = k_1 (it - s) - k_2 s \tag{2}$$

and integrated:

$$s = it \frac{k_1}{k_1 + k_2} - i \frac{k_1}{(k_1 + k_2)^2} \left(1 - e^{-(k_1 + k_2)t}\right) \tag{3}$$

for the amount of industrial CO_2 in the sea at the time t. As $k_1 \approx 60\ k_2$, we may neglect k_2 as small compared to k_1. We then obtain:

$$s = it - \frac{i}{k_1} \left(1 - e^{-k_1 t}\right) \tag{4}$$

or

$$r = it - s = \frac{i}{k_1} \left(1 - e^{-k_1 t}\right) \tag{5}$$

Expressing i, s, and r in units of the atmospheric CO_2, we obtain with $i = 0.25$ % (corresponding to the value during the 1940's) and $t = 40$ years, the following values of r for exchange times $\tau\ (\text{atm}) = \frac{1}{k_1}$ as listed:

Table 4

$1/k_1 = \tau$(atm) years	r %
5	1.2
10	2.5
20	4.4
30	5.5
40	6.3
100	8.3
∞	10.0

Empirical values for the decrease in the specific C^{14} activity r^* were obtained by comparing C^{14} activities of wood samples grown in the 19th century with those grown more recently, taking into account isotope fractionation effects by C^{13} measurements and correcting for the C^{14} decay by normalizing to equal age (Suess 1955).

With the assumption that the total atmospheric carbon reservoir is only negligibly greater than the amount of CO_2 in the atmosphere, r^* will be equal to r.

Table 5

Tree	Years of growth from annual rings	r^* %
Spruce, Alaska.....	1945—1950	1.77
White Pine, Massachusetts	1936—1946	3.40
	1946—1953	2.90
Incense Cedar, California	1940—1944	1.85
	1950—1953	1.05
Cedrela, Peru	1943—1946	0.05
	1948—1953	1.05

---

[1] See Fergusson and Rafter. These authors have now found that 110 years should be added to all of their previous age determinations to correct for the difference of the standards.

It might be tempting to assume that the effects found in the samples investigated and their individual variations are due to local contamination of air masses by industrial CO_2 and that the world-wide decrease in the C^{14} activity of wood is practically zero. This, however, implies a too fast exchange rate and is inconsistent with the lower limit of τ (atm) given above. By coincidence, it so happens that taking the average of the r^* values listed, 1.73 %, an exchange time τ (atm) of 7 years is obtained as an upper limit, identical with the lower limit obtained previously from the C^{14} age of marine surface material. An exchange time of 7 years, however, makes it necessary to assume unexpectedly short mixing times for the ocean.[1]

By reconsidering the relative size of the marine and atmospheric carbon reservoirs, and the assumptions necessary for treating the combined reservoirs as a closed system, we may approximate more closely to the conditions prevailing in nature. First, it seems possible that some of the organic matter and carbonate present in soils may have to be added to the carbon that constitutes the atmospheric carbon reservoir. Practically nothing is known about the C^{14} age of soils and it may be that some of the soil carbon, partly through bacterial action, is in more rapid isotopic exchange with atmospheric CO_2 than the data on plant assimilation and biological oxidation indicate. The total amount of carbon in soils may be equal to, or larger by as much as a factor of two than that in the CO_2 of the atmosphere. Rapid exchange with such carbon would decrease the change in C^{14} activity resulting from industrial fuel combustion by a factor equal to the ratio of the total "effective" atmospheric carbon reservoir to the atmospheric CO_2. However, the overturn time of the atmospheric CO_2 through the terrestrial biological cycle and the soil is probably at least several decades and it therefore seems improbable that a mechanism exists that might account for an atmospheric reservoir of more than 1.5 times the CO_2 in the atmosphere.

Nevertheless, it is interesting, in order to demonstrate how the uncertainty in the size of the atmospheric carbon reservoir affects our results, to introduce "effective" reservoirs A^* and S^*, so that $A^* > A$, because of exchange with soil carbon, and $S^* < S$, because of incomplete mixing in the oceans. A^* and S^* are defined in such a way that Eq. (1) becomes

$$\frac{k_1}{k_2} = \frac{S^*}{A^*} \qquad (1\ a)$$

For Eq. (5):

$$r^* = \frac{A}{A^*}\,\frac{i}{k_1}\,(1 - e^{-k_1 t}) \qquad (5\ a)$$

is to be substituted.

Then the relationships of the three unknown quantities k_1, S^* and A^* according to the two equations (1 a) and (5 a) are shown graphically in figure 1.

With an average age of surface sea carbon of 400 years, i.e., $k_2 = 1/400$, one finds, even with an improbably large A^* equal to 3 A, that S^* is only 10 to 30 % smaller than S, so that the resulting mixing times of the oceans cannot be larger than a few 100 years.

The overturn time for the marine carbon through rock weathering and precipitation can be estimated to be of the order of 100,000 years (table 3). During an average lifetime of sea carbon of 400 years an amount corresponding to 0.3 % of the marine reservoir will be added to the oceans through rock weathering in the form of C^{14} free carbon and be precipitated after isotopic equilibration. On the average, this will cause the C^{14} age of sea carbon to appear about 35 years older. Locally, and especially along shores, the effect may well be considerably greater, so that the ages measured so far may, on the average, be too great by as much as 100 years. In figure 1, solutions are shown for $1/k_2 = 300$ years, indicating a value of S^*/S of about $^2/_3$ for acceptable values of A^*.[1]

A possibility that the addition of C^{14} free CO_2 to the atmosphere from volcanic eruptions in the 19th century may obscure the

---

[1] In a separate paper in this issue, H. Craig evaluates the exchange time by considering present data on the C-14 production rate by cosmic rays, and obtains a value of 7 ± 3 years. He further finds that a more detailed model of ocean mixing gives the same value. An earlier estimate of 20 to 50 years (Suess 1953) was based on C-14 measurements of woods grown in an area of industrial contamination.

[1] For a discussion of the physical significance of S^*/S in terms of mixing times in the ocean see H. Craig's paper in this issue.

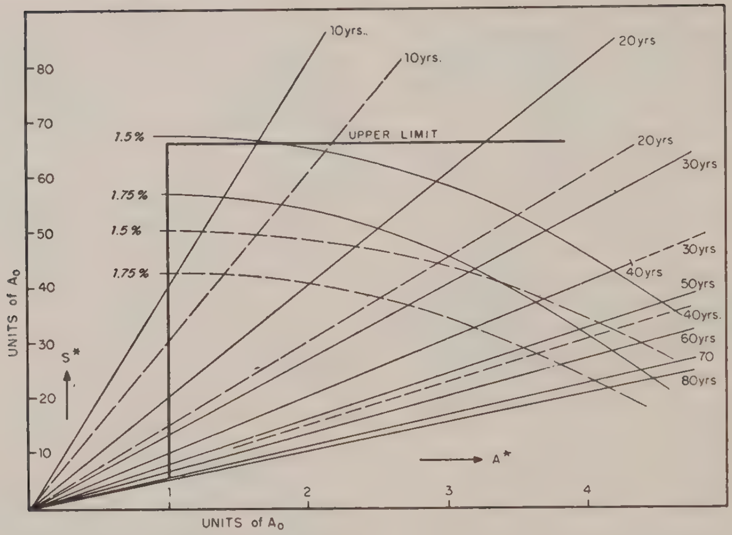

Fig. 1. Graphic solutions of Eq. (1 a) for values $1/k_1$ ranging from 10 to 80 years (straight lines), and of Eq. (5 a) for $r^* = 1.5$ % and 1.75 % (curved lines), for average apparent C^{14} age of sea water $1/k_2 = 400$ years (solid lines) and 300 years (broken lines). Points of intersection of straight lines and curves are possible solutions of the two equations for effective reservoirs A^* and S^*.

effect from industrial fuel combustion needs further experimental investigation.

We conclude that the exchange time τ (atm) $= 1/k_1$, defined as the time it takes on the average for a CO_2 molecule as a member of the atmospheric carbon reservoir to be absorbed by the sea, is of the order of magnitude of 10 years. This corresponds to a net exchange rate of the order of 10^{-7} mol CO_2 per second and square meter of the ocean surface, larger by a factor of 100 than that postulated by PLASS (1956) and smaller by a factor of 10,000 than that deduced by DINGLE (1954) as a lower limit from numerical values of the various rate controlling constants. These are, as HUTCHINSON (1954) has forcefully pointed out, too uncertain to allow any definite conclusions. On the other hand, our exchange data give a value for the "invasion coefficient" of carbon dioxide close to that determined experimentally by BOHR (1899) for a stirred liquid surface.

Secular variation of CO_2 in the atmosphere

In the preceding section of this paper, two simplifying assumptions were made when estimating the exchange rate of CO_2 between the atmosphere and the oceans: (1) that the rate constants k_1 and k_2 were not affected by a small increase of the exchangeable carbon reservoir such as that from industrial fuel combustion, and (2) that, except for that increase, no other changes in the sizes of the oceanic and atmospheric carbon reservoirs have taken place. If these assumptions were rigorously correct, the increase in atmospheric CO_2 due to an addition of C^{14} free CO_2 would be nearly equal to r, as given by Eq. (5) and in table 4, and equal to the decrease in the specific C^{14} activity r^*, multiplied by a factor A^*/A.

Because of the peculiar buffer mechanism of sea water, however, the increase in the partial CO_2 pressure is about 10 times higher than the increase in the total CO_2 concentration of sea water when CO_2 is added and the alkalinity remains constant (BUCH, 1933, see also HARVEY, 1955), so that under equilibrium conditions at a given alkalinity

$$\frac{r}{A_0} = \frac{\gamma s}{S_0} \text{ or } \frac{A_0}{S_0} = \frac{k_1}{k_2} = \frac{r}{\gamma s},$$

γ being a numerical factor of the order of 10

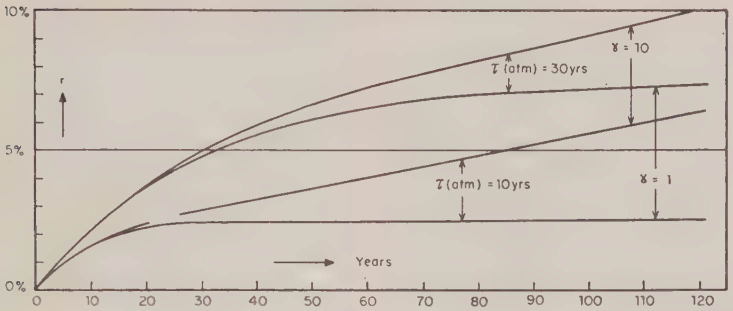

Fig. 2. Expected secular increase in the CO_2 concentration of air (r) according to Eq. (7), for average lifetimes of CO_2 in the atmosphere $\tau(\text{atm}) = 10$ years and 30 years, with and without correction for the increase in the partial CO_2 pressure with total CO_2 concentration of sea water (curves for $\gamma = 10$ and $\gamma = 1$ respectively), for a constant rate of addition of industrial CO_2 of $i = 2.5 \cdot 10^{-3} \times A_0$.

for r and s small compared to A_0 and S_0 respectively.

As a reasonable approximation we may write instead of Eq. (3):

$$s = it\frac{k_1}{k_1 + \gamma k_2} - i\frac{k_1}{(k_1 + \gamma k_2)^2}\left(1 - e^{-(k_1 + \gamma k_2)t}\right) \quad (6)$$

or

$$r = it\frac{\gamma k_2}{k_1 + \gamma k_2} + i\frac{k_1}{(k_1 + \gamma k_2)^2}\left(1 - e^{-(k_1 + \gamma k_2)t}\right) \quad (7)$$

Figure 2 shows r as a function of time calculated from Eq. (7) for two values of k_1 corresponding to an exchange time of 10 and 30 years respectively, assuming constant addition of industrial CO_2 equal to 0.25 % of the CO_2 in the atmosphere per year. At present the integrated amount of industrial CO_2 corresponds to about 40 to 50 years of addition at this constant rate. The increase in CO_2 in the atmosphere plus biosphere and soil due to industrial fuel combustion should therefore at present amount to 3 to 6 %, depending on the assumptions made with respect to the size of the "effective" atmospheric carbon reservoir that exchanges with the ocean.

Eq. (7) and figure 2 show that addition of industrial CO_2 at a constant rate should eventually lead to a situation in which the secular increase in CO_2 in the atmosphere plus biosphere and soil equals $\frac{i\gamma k_2/k_1}{1 + \gamma k_2/k_1}$ per year. With $S_0/A_0 = k_1/k_2 \approx 60$ and $i = 0.25$ an increase of 3.6 % per century is obtained. We have neglected the present rate of increase in alkalinity, which is small compared to the rate of CO_2 production from fossil fuels. However, over a sufficiently long period of time the alkalinity of the ocean must be expected to rise more rapidly as a consequence of the higher total CO_2 concentration in the atmosphere and ocean which will tend to increase the rate of rock weathering and to decrease the rate of deposition of $CaCO_3$. The secular increase in r should therefore be less than that calculated from Eq. (7) with $\gamma = 10$ and somewhere between the curves shown in figure 2 for $\gamma = 10$ and $\gamma = 1$.

It seems therefore quite improbable that an increase in the atmospheric CO_2 concentration of as much as 10 % could have been caused by industrial fuel combustion during the past century, as Callendar's statistical analyses indicate. It is possible, however, that such an increase could have taken place as the result of a combination with various other causes. The most obvious ones are the following:

1) Increase of the average ocean temperature of 1° C increases P_{CO_2} by about 7 %. However, such increase would also raise the sea level by about 60 cm, due to thermal expansion of the ocean water. Actually, according to MUNK and REVELLE (1952), although the sea level has risen about 10 cm during the last century, this rise can be accounted for almost quantitatively by addition of melt water from retreating glaciers and ice caps. The increase in the average ocean temperature is probably not more than 0.05° C, which corresponds to an increase in P_{CO_2} of 0.35 %. In the case of slow oceanic mixing, the increase could be somewhat larger, if only

the top layers of the sea were affected by a rise in temperature.

2) Decrease in the carbon content of soils: Hutchinson (1954) considers this the most probable additional cause of the Callendar effect. The increase in arable lands of about 4×10^{16} cm^2 since the middle of the 19th century has resulted in a corresponding decrease of forest land of about 10 %. Assuming that 70 % of all the soil carbon is in forests (probably a considerable over-estimate), and that cultivation reduced this by 50 %, the total decrease in soil carbon would correspond to 9×10^{16} gms of CO_2 which is 4 % of that in the atmosphere. At least four-fifths of this amount should have been transferred to the ocean.

3) Change in the amount of organic matter in the oceans. About 7 % of the marine carbon reservoir consists of organic material. The amount of organic matter must depend on the balance between the rates of reduction of CO_2 by photosynthesis and of production of CO_2 by oxidation. As pointed out previously, a change in the CO_2 content of sea water by a certain factor without a corresponding change in alkalinity changes P_{CO_2} by about 10 times this factor. Therefore a 1 % change in the concentration of organic material in the sea will change the partial CO_2 pressure and hence the atmospheric CO_2 by roughly 1 %. During the past 50 years, the increase in marine carbon from absorption of industrial CO_2 of about 0.2 % might have increased the rate of photosynthesis without a corresponding change in the rate of oxidation per unit mass of organic matter, and thus decreased P_{CO_2}. An increase in the temperature of surface water might have increased the rate of oxidation per unit mass of organic matter, and hence increased P_{CO_2}. We suspect that fluctuations in the amount of organic marine carbon might be an important cause for changes in the atmospheric CO_2 concentration.

Erikson and Welander (1956) have discussed a mathematical model of the carbon cycle between the atmosphere, the land biosphere and dead organic matter, and the ocean, in which it is assumed that the rate of input of carbon to the biosphere is directly proportional, not only to the total size of the biosphere but also to the amount of CO_2 in the atmosphere. Their estimate of the land biosphere is 7 times larger than that given in Table 3. They conclude that most of that part of the CO_2 added by fossil fuel consumption, which has not been absorbed by the ocean, has probably gone into the biosphere. Erikson and Welander's basic assumption that the amount of atmospheric carbon dioxide limits the growth of the terrestrial biosphere seems highly unlikely, in view of the fact that the principal photosynthetic production on land is in forests, where a deficiency of plant nutrients might be expected. In any case as Hutchinson (1954) has shown, the amount of carbon in the biosphere and soil humus has probably decreased, rather than increased, during the past century, because of the clearing of forests.

In contemplating the probably large increase in CO_2 production by fossil fuel combustion in coming decades we conclude that a total increase of 20 to 40 % in atmospheric CO_2 can be anticipated. This should certainly be adequate to allow a determination of the effects, if any, of changes in atmospheric carbon dioxide on weather and climate throughout the earth.

Present data on the total amount of CO_2 in the atmosphere, on the rates and mechanisms of CO_2 exchange between the sea and the air and between the air and the soils, and on possible fluctuations in marine organic carbon, are insufficient to give an accurate base line for measurement of future changes in atmospheric CO_2. An opportunity exists during the International Geophysical Year to obtain much of the necessary information.

Acknowledgements

A paper on the same subject by James R. Arnold and Ernest C. Anderson appears in this issue of this journal; we are grateful to Drs. Arnold and Anderson for the opportunity of discussing the problem before publication. We are happy to note that these authors have simultaneously and independently derived essentially the same conclusions as presented in this paper. We hope that the somewhat different approach will make both contributions equally valuable to the reader. We also wish to thank Dr. Carl Eckart for valuable discussions and Dr. Harmon Craig for much constructive criticism. Dr. Craig's own careful analysis of the subject appears in a separate paper in this issue.

REFERENCES

Arrhenius, Svante, 1903: *Lehrbuch der kosmischen Physik* **2**. Leipzig: Hirzel.

Bohr, C., 1899: Die Löslichkeit von Gasen in Flüssigkeiten. *Ann. d. Phys.* **68**, p. 500.

Buch, K., 1933: Der Borsäuregehalt des Meerwassers und seine Bedeutung bei der Berechnung des Kohlensäuresystems. *Rapp. Cons. Explor. Mer.* **85**, p. 71.

Callendar, G. S., 1938: The artificial production of carbon dioxide and its influence on temperature. *Quarterly Journ. Royal Meteorol. Soc.* **64**, p. 223.

Callendar, G. S., 1940: Variations in the amount of carbon dioxide in different air currents. *Quarterly Journ. Royal Meteorol. Soc.* **66**, p. 395.

Callendar, G. S., 1949: Can carbon dioxide influence climate? *Weather* **4**, p. 310.

Chamberlin, T. C., 1899: An attempt to frame a working hypothesis of the cause of glacial periods on an atmospheric basis. *J. of Geology* **7**, pp. 575, 667, 751.

Conway, E. J., 1942: Mean geochemical data in relation to oceanic evolution. *Proc. Roy. Irish Acad., B.* **48**, p. 119.

Craig, H., 1953: The geochemistry of the stable carbon isotopes. *Geochim. et Cosmochim. Acta* **3**, p. 53.

Craig, H., 1954: Carbon 13 in plants and the relationship between carbon 13 and carbon 14 variations in nature. *Journ. Geol.* **62**, p. 115.

Dingle, H. N., 1954: The carbon dioxide exchange between the North Atlantic Ocean and the atmosphere. *Tellus* **6**, p. 342.

Erikson, E., and Welander, P., 1956: On a mathematical model of the carbon cycle in nature. *Tellus* **8**, p. 155.

Fergusson, G. J., and Rafter, T. A.: *New Zealand C-14 Age Measurements III.* In press.

Fonselius, S., Koroleff, F., and Wärme, K., 1956: Carbon dioxide variations in the atmosphere. *Tellus* **8**, p. 176.

Harvey, H. W., 1955: *The Chemistry and Fertility of Sea Water.* Cambridge: University Press.

Hayes, F. N., Anderson, E. C., and Arnold, J. R., 1955: Liquid scintillation counting of natural radiocarbon. *Proc. of the International Conference on Peaceful Uses of Atomic Energy, Geneva*, **14**, p. 188.

Hutchinson, G. E., 1954: In *The Earth as a Planet*, G. Kuiper, ed. Chicago: University Press. Chapter 8.

Munk, W., and Revelle, R., 1952: Sea level and the rotation of the earth. *Am. Journ. Sci.* **250**, p. 829.

Nier, A. O., and Gulbransen, E. A., 1939: Variations in the relative abundance of the carbon isotopes. *Journ. Am. Chem. Soc.* **61**, p. 697.

Plass, G. N., 1956: Carbon dioxide theory of climatic change. *Tellus* **8**, p. 140.

Rafter, T. A., 1955: C^{14} variations in nature and the effect on radiocarbon dating. *New Zealand Journ. Sci. Tech. B.* **37**, p. 20.

Rubey, W. W., 1951: Geologic history of sea water. *Bull. Geol. Soc. Amer.* **62**, p. 1111.

Slocum, Giles, 1955: Has the amount of carbon dioxide in the atmosphere changed significantly since the beginning of the twentieth century? *Monthly Weather Rev.* Oct., p. 225.

Suess, H. E., 1953: Natural Radiocarbon and the rate of exchange of carbon dioxide between the atmosphere and the sea. *Nuclear Processes in Geologic Settings*, National Academy of Sciences — National Research Council Publication, pp. 52—56.

Suess, H. E., 1954: Natural radiocarbon measurements by acetylene counting. *Science* **120**, p. 5.

Suess, H. E., 1955: Radiocarbon concentration in modern wood. *Science* **122**, p. 415.

Sverdrup, H. U., Johnson, M. W., and Fleming, R. H., 1942: *The Oceans.* New York: Prentice-Hall, Inc.

United Nations, 1955: World requirements of energy, 1975—2000. *International Conference on Peaceful Uses of Atomic Energy, Geneva*, **1**, p. 3.

Urey, H. C., 1952: *The Planets.* New Haven: Yale Univ. Press.

PRINTED IN SWEDEN ESSELTE, STHLM 57

Reprinted from
THE EFFECTS OF ATOMIC RADIATION ON OCEANOGRAPHY AND FISHERIES
PUBLICATION No. 551, NATIONAL ACADEMY OF SCIENCES—NATIONAL RESEARCH COUNCIL, 1957

GENERAL CONSIDERATIONS CONCERNING THE OCEAN AS A RECEPTACLE FOR ARTIFICIALLY RADIOACTIVE MATERIALS[1]

ROGER REVELLE and MILNER B. SCHAEFER, *Scripps Institution of Oceanography*
and
Inter-American Tropical Tuna Commission, La Jolla, California

I. INTRODUCTION

IN THIS report, we have attempted to summarize both the present knowledge and the areas of ignorance concerning the oceans that must be taken into account in considering the biological effects of radiation.

The oceans of the world furnish essential sources of food and other raw materials, vital routes of transportation, recreation, and a convenient place in which to dispose of waste materials from our industrial civilization. These different ways in which men use the sea, however, are not always compatible. The use of the sea for waste disposal, in particular, can jeopardize the other resources, and hence should be done cautiously, with due regard to the possible effects. Waste products from nuclear reactions require special care: they constitute hazards in extremely low concentrations and their deleterious properties cannot be eliminated by any chemical transformations; they can be dispersed or isolated, but they cannot be destroyed. Once they are created, we must live with them until they become inactive by natural decay, which for some isotopes requires a very long time.

Waste products from nuclear reactions arise in two ways: (1) from the slow controlled reactions involved in laboratory experimentation, in the production of materials for nuclear weapons, the production of reactor fuels, and the "burning" of fuels in power reactors; (2) from the rapid, uncontrolled reactions involved in testing of weapons or in warfare. Up to the present time, the largest quantities of fission products introduced into the aquatic environment have been from weapons tests; most of the products from controlled reactions have been isolated on the land, and only relatively small quantities have been introduced into the sea or fresh water. In the future, however, industrial nuclear wastes will present difficult disposal problems and the sea is a possible disposal site, particularly for small, densely populated nations with long sea coasts. We have, therefore, given particular attention to the long-range problems that may arise from the large-scale disposal of both high-level and low-level industrial wastes, as well as to the effects of weapons tests.

Among the variety of questions generated by the introduction of radioactive materials into the sea, there are few to which we can give precise answers. We can, however, provide conservative answers to many of them, which can serve as a basis of action pending the results of detailed experimental studies. The large areas of uncertainty respecting the physical, chemical, and biological processes in the sea lead to restrictions on what can now be regarded as safe practices. These will probably prove too severe when we have obtained greater knowledge. It is urgent that the research required to formulate more precise answers should be vigorously pursued. Fortunately, the use of radioactive isotopes is one excellent means of acquiring the needed information, and the quantities of these isotopes required for pertinent experiments are well within limits of safety. Moderate quantities of the very waste products we are concerned with can, therefore, provide one means of attacking the unsolved scientific problems.

II. THE NATURE OF THE OCEAN AND ITS CONTAINED ORGANISMS

The ocean basins cover 361×10^6 square kilometers and have an average depth of 3,800 meters, giving a total volume of 1.37×10^9 cubic kilometers. They are characteristically bordered by a continental shelf, which slopes gently out to a depth of about 200 meters. Inside it is a steeper slope extending down to the

---

[1] Contribution from the Scripps Institution of Oceanography, New Series, No. 901.

Reproduced by Permission

deep sea floor with depths of 4,000 meters or more. The average width of the continental shelf is about 30 miles, varying from almost nothing off mountainous coasts, such as the West Coast of South America, to several hundred miles in the China Sea. The shelf is not everywhere smooth, but is often intersected by submarine valleys and canyons. In the deep ocean basins there are high mountains and long, deep trenches, features larger than any on land. Some of the deeper parts are isolated by submarine ridges which restrict the exchange of water between adjacent areas.

The waters of the oceans are stratified. Within a relatively thin layer at the surface, varying in thickness in different places but averaging about 75 meters, vertical mixing caused by winds is fairly rapid and complete. In consequence, the temperature, salinity and density are nearly uniform from top to bottom. Relatively fast wind-driven currents exist in this upper mixed layer; these are the "surface" currents of the oceans depicted on many charts. Here also the horizontal mixing is relatively rapid. The mixed layer is the region of the sea in which most of man's activity takes place.

Below the mixed layer is a zone within which the temperature decreases and the density increases rapidly with depth. This thermocline, or pycnocline, separates the surface mixed layer from the layers of intermediate and deep water, the latter extending to the bottom, within which there are gentle gradients of decreasing temperature and increasing salinity and density with depth. Vertical movement in the intermediate and deep layers is much slower than in the mixed layer, and horizontal currents are more sluggish. The strong density gradient across the pycnocline tends to inhibit physical transport across it, because work is required to move water vertically in either direction, and thus the pycnocline acts as a partial barrier between the mixed layer and the lower layers. There is, however, some interchange of both living and non-living elements; indeed the continued existence of some marine resources depends on such interchange.

MARINE RESOURCES

Living resources

The most important extractive industry based on the resources of the sea is the harvesting of its living resources.

On land the cycle of life is relatively simple; we may describe it in four figurative stages. First is the grass, which by a subtle and complex chemistry captures the energy of sunlight and builds organic matter. Sheep and cows live on the grass; tigers and men eat them. The cycle is closed by bacteria, which decompose the dead bodies and the excreta of all living creatures, making their constituent substances again available as building materials for the plants. In the sea, the cycle is longer. Instead of grass there are the tiny floating plants called phytoplankton; in place of cows, the zooplankton animals that eat the plants are small crustaceans, no bigger than the head of a pin. Many kinds of tigers eat the cows, but they are mostly also zooplankton, only a fraction of an inch in length. Other intermediate flesh-eaters exist between them and the fishes of our ocean harvest. Because every link in this long food chain is inefficient, we reap from the sea only a small fraction of its organic production.

Other characteristics of the ocean also tend to limit the harvest as compared to that from the land. One is its giant size; more than 70 per cent of all the sunlight that penetrates the atmosphere falls on the sea; moreover, this sunlight can act throughout the top 20 to 100 meters, thus the living space for plants and animals is far greater than on land. This great areal extent and volume, combined with the fluidity of the oceans, results in a low concentration of organisms per unit volume and therefore inefficiency in harvesting.

On land, the standing crop of plants and animals is of the same order of magnitude as the amount of organic production per year, while in the ocean the crop is very small, compared to the production, because of rapid turnover. The average rate of organic production per unit area is probably about the same on land and in the sea, but the efficiency of harvesting depends more on the size of the crop than on the total amount of organic matter produced.

The plants of the sea, on which all other living things depend, grow only in the waters near the surface where bright sunlight penetrates. These waters differ widely in fertility. Like the land, the ocean has its green pastures where life flourishes in abundance, and its deserts where a few poor plants and animals barely survive.

The fertility of the land depends on four things: water, temperature, intensity of sunlight, and available plant nutrients—substances that usually occur in very small amounts but are essential for plant growth. In the sea, water is, of course, always abundant; the plants are well adapted to the narrow range of temperature; the intensity of sunlight determines the length of the growing season and the depth of growth, but usually not the differences in fertility. These depend only on the plant nutrients in the waters near the surface. As in any well-worked soil on land, the nutrients in the waters must be replenished each year. They are continually depleted by the slow sinking of plant and animal remains from the brightly lighted near-surface layers into the dark waters of the depths.

Men plow the soil to restore its fertility; the fertility of the sea is restored when nutrient-rich deeper waters are brought up near the surface. The "plowing" of the sea is accomplished in three ways. In some regions winds drive the surface waters away from the coast or away from an internal boundary, and nutrient-rich waters well up from mid-depths. In other areas, the surface waters are cooled near to freezing in the winter, become heavy and sink, and mix with the deep waters. Elsewhere, violent mixing occurs along the boundaries between ocean currents, and deeper waters are thereby brought into the brightly lighted zone.

The influx of nutrients to the upper layer, and the corresponding loss from this layer by sinking of plant and animal remains, do not directly involve the deep waters. Upwelling and vertical mixing take place only in the upper few hundred meters. The exchange between these mid-depths and the abyssal deep is a very much slower process, of the scale of hundreds of years.

Most of the commercially important marine organisms are harvested in coastal waters or in offshore waters not very far from land. Several factors are involved: (1) Profitable fisheries can be conducted more easily near ports and harbors; (2) the coastal waters are of high fertility, because of greater upwelling and turbulent mixing and the ease of replenishment of plant nutrients from the shallow sea floor, and perhaps also because of the supply of nutrients and organic detritus from land; (3) the standing crop of plants and animals attached to or living on the bottom in coastal areas is large, relative to the total organic production.

None of the animals of the great depths are the objects of a commercial fishery. Even the truly pelagic, high seas fisheries, such as the great offshore fisheries for tuna, herring, redfish and whales, harvest animals that live primarily in the surface layer. Some of these animals, however, do much of their feeding in the deeper layers. The sperm whales, for example, feed on deep-sea cephalopods at great depths. Moreover, much of the food for commercially harvested organisms consists of small animals, including crustaceans, squids, and fishes, that perform vertical diurnal migrations from several hundred meters depth to the surface.

The sea fisheries produce about 25 million metric tons per year of fishes and marine invertebrates, in addition to about 4 million tons of whales. The great bulk of the harvest is taken, at present, from the waters of the northern hemisphere, despite the fact that the southern oceans constitute 57 per cent of the world's sea area. The following table indicates the production in 1954 by latitude zones:

TABLE 1 Harvest of Fishes and Marine Invertebrates in 1954, by Latitude Zones (From FAO, 1957)

Zone	Millions of metric tons	%
Arctic region	1.2	5
Northern hemisphere-temperate zone	17.5	72
Tropical zone	4.1	17
Southern hemisphere-temperate zone	1.4	6
Antarctic regions	0*	0*

* About 4 million tons of whales were taken in the Antarctic, but few fish or marine invertebrates.

The disproportionately large yield in the northern hemisphere is related to three factors: (1) Human populations are heavily concentrated there; (2) the major fishing nations are the industrialized maritime nations, which are mostly located in the north; (3) except for some of the fisheries for tuna, salmon, herring, and whales, the important fisheries are located in the relatively shallow areas along the continents, and the extent of these areas is much greater in the northern than in the southern hemisphere.

The sessile algae of shallow coasts are also the object of important industries in Japan, the United States, the United Kingdom, Norway, and some other countries. Some of these plants are used directly for human consumption, while others are employed indirectly in pharmaceutical and food products.

Petroleum and natural gas

It is estimated that about 30 million cubic meters of possible oil-bearing sediments underlie the 11.8 million square miles of the submerged continental shelves. These sediments contain some 400 billion barrels of recoverable crude oil.

Exploitation of these deposits of petroleum and the associated natural gas has commenced in the waters of the Gulf of Mexico; intensive geophysical prospecting has been conducted offshore from California and in the Persian Gulf. It may be expected that this source of fossil fuels will be extensively utilized in the near future. The resource is confined to the subsoil of the marginal seas, since only there do we find oil-bearing sediments.

Minerals

Extraction of sea salt for sodium chloride is an ancient industry, and is now highly developed also for production of sodium sulfate, potassium chloride, and magnesium chloride. Bromine is extracted directly from sea water for the manufacture of ethylene dibromide. Magnesium metal has been produced commercially from seawater by chemical and electrolytical procedures for nearly two decades.

All of these industries use sea water taken from near the surface at the shore but the quantity of water utilized is insignificant. For example, a single cubic kilometer of sea water contains over a million tons of magnesium, about five times the peak world annual production of this metal.

The floor of the deep sea is known to contain low-grade deposits of cobalt, nickel and copper (0.1 to 0.7 per cent by weight of the metals) associated with deposits of iron and manganese. The problems of mining these materials, in the face of the great depths and pressure, have not been solved, and they certainly will not soon be economically useable.

Ocean transportation

Long-distance transportation of large cargos by sea is the indispensable basis of international commerce. The economy of the United States and of other industrial nations is in large part dependent on the sea-borne commerce that flows through the seaports.

Contamination of the sea by nuclear wastes will certainly not present a hazard to shipping, since acceptable levels of such materials in the surface layer of the sea will be limited by other considerations (such as the effects on the fisheries) to much lower levels than would constitute a hazard to ships' personnel. On the other hand, it is almost certain that nuclear power plants will be extensively used in merchant vessels; they are already in use in naval craft.

Serious hazards may arise in confined waters from collisions in which the reactor is damaged and the fuel elements with their contained fission products are lost in the water. Suppose for example that a 50,000 kilowatt reactor (probably fairly typical for a large fast freighter) has been in service without refueling for one year on a ship that has spent half its time under way. Approximately 10 kilograms of fissionable material will have been used up and the total amount of fission products will be approximately 10^7 curies. If, owing to a collision, the reactor is lost in a harbor, say 8 miles long by 3 miles wide by 50 feet deep, and the fission products become uniformly distributed, the water in the harbor would contain 10^{-2} curies per cubic meter giving an almost constant radiation dose of about 0.5 r per day on the surface. Dock pilings, ship bottoms and other structures covered with fouling organisms would accumulate a much higher level of radioactivity, and local concentration in the water might be extremely high.

Recreation

For coastal populations in the temperate, subtropical, and tropical regions, the sea and its contents provide healthful sports and satisfaction of men's curiosity and their desire for beauty. Boating, swimming, sport fishing, and other recreations are engaged in by millions of people, and are the basis of tourist and service industries of very considerable monetary value.

Waste disposal

Disposal of domestic sewage and industrial wastes is often conveniently accomplished near coastal population centers by running them into the sea. The large volume and rapid mixing of the ocean waters dilute the wastes, and the bacteria in the sea break down the organic constituents. Unless care is exercised, however, this discharge into inshore sea areas may be deleterious to other resources. Dumping of excess volumes of sewage and industrial wastes, without proper regard to the local characteristics of the sea bottom, currents, and other factors, has already resulted in ruining some harbors and beaches for recreation, damage to the living resources of adjacent areas, and even serious problems of corrosion to ships.

The use of the sea for the disposal of atomic wastes has, fortunately, been so far approached with great caution and with due regard to the possible hazards. The problems, because of the dangerous character of small amounts of atomic wastes, are of a different order of magnitude than those of the disposal of other kinds of wastes.

III. POTENTIAL HAZARDS FROM RADIOACTIVE MATERIALS

Direct hazards

A direct hazard to human beings from radiation may exist if the levels of radiation in the environment are sufficiently high.

The natural radioactivity of the sea is very much lower than that of the land. According to Folsom and Harley (Chapter 2 of this report), a man in a boat or ship receives only about half a millirad per year from the radio isotopes in the sea, compared with about 23 millirads per year from sedimentary rock or 90 millirads per year from granite. Thus, it would be necessary to increase the radioactivity of the sea many fold to equal the radiation that man normally receives from the land on which he lives. Due to the rather rapid mixing in the upper layers of the sea, and to its very large volume, even large quantities of activity introduced at the surface in the open sea become sufficiently dispersed to constitute no direct hazard after a relatively short time, as has been shown by the dispersion of the activity resulting from weapons tests in the Pacific. If the direct hazard were the only consideration, sea disposal of radioactive wastes would give rise to difficulties only in small areas near the disposal sites.

Some radioactive wastes have been disposed of in the sea by placing them in containers designed to sink to the sea bottom. In this way, the wastes are isolated and not dispersed by the ocean currents. Direct hazards could arise if the containers in some manner were to come into contact with humans, such as through accidental recovery during fishing or salvage operations or if, through improper design, the containers were to float to the surface and come ashore.

Indirect hazards

The most serious potential hazards to human beings from the introduction of radioactive products into the marine environment are those that may arise through the uptake of radio isotopes by organisms used for human food. There are several reasons why these indirect hazards are more critical than the direct hazards: (1) The radiation received from a given quantity of an isotope ingested as food is much greater than the dose from the same quantity in the external environment; (2) many elements, including some of those having radioactive isotopes resulting from nuclear reactions, are concentrated by factors up to several thousand by the organisms in the sea; (3) the vertical and horizontal migrations of organisms can result in transport of radioactive elements and thereby cause distributions different from those that would exist under the influence of physical factors alone; for example, certain elements may be carried from the depths of the sea into the upper mixed layer in greater amounts than could be transported by the physical circulation.

It is quite certain that the indirect hazard to man through danger of contamination of food from the sea will require limiting the permissible concentration of radioactive elements in the oceans to levels below those at which there is any direct hazard. Any part of the sea in which the contamination does not cause dangerous concentrations of radioactive elements in man's food organisms will be safe for man to live over or in.

A reduction of the harvestable living resources of the sea could conceivably occur through the effects of atomic radiations on the organisms that are the objects of fisheries, or on their food. This might result from mortality induced by somatic effects, or from genetic changes. There is no conclusive evidence that any of the living marine resources have yet suffered from either of these, and they are not likely to be undesirably influenced at radiation levels safe from other standpoints. The knowledge of radiation effects on marine organisms is, however, inadequate for firm conclusions.

Pollution in general

The introduction of atomic wastes into the aquatic environment is but one aspect of the general problem of pollution.

Man's record with respect to pollution of lakes, streams, and parts of the sea by sewage and industrial wastes has not been good. In many places, the waters have been ruined for recreation and useful living resources have been destroyed or made unfit for human consumption. This unhappy record results from two factors: (1) the insidious nature of pollution of the aquatic environment, and (2) the fact that the waters and most of their resources are not private property, but are the common property of a large community (in the case of the high seas, the whole world); what is everyone's business often becomes no one's business.

The ruin of an aquatic resource by pollution seldom has been rapid. Quantities of waste products, at first very small, increase year by year until finally the concentrations become so large as to have obvious deleterious effects. For example, in the depletion of oxygen by organic wastes, sharp critical levels of tolerance of low oxygen content exist for some of the living resources, so that there is little adverse effect until a critical concentration of pollutant is reached, whereupon catastrophic mortality occurs. In other cases, the effects are more or less proportional to the concentrations. The destruction of a resource may then proceed gradually and it may not even be clear whether the pollutant has, indeed, been the cause rather than some other environmental change. For these reasons, it is necessary that the introduction of waste materials of any kind into the aquatic environment be carefully monitored, so that the effects may be detected before they become serious. Unfortunately, such monitoring is seldom the concern of those who produce the pollutants.

The record of the control and monitoring of the disposal of atomic pollutants has, so far, been excellent. We are, however, at the threshold of a tremendous growth of the atomic energy industry, and it behooves mankind to make sure that as much caution is exercised in the future as in the past.

Ordinary pollutants in sewage and industrial wastes are rapidly neutralized by the chemical and biological processes in the sea, and when effects of pollution are detected they can be rather quickly reversed by the cessation of introduction of the waste. A number of the radio isotopes, on the other hand, are very long-lived. Having reached harmful concentrations in the sea, they will diminish only by very slow decay, so that the effect of any serious pollution is not reversible. For this reason, the *prevention* of atomic pollution is of paramount importance.

URGENCY OF THE PROBLEM

Estimates of the rate of economic development of nuclear power vary widely. This source of power is already competitive with conventional sources in some places, and research on reactor development with consequent reductions in cost is proceeding rapidly. Thus, we can expect that very large quantities of nuclear power will be generated in the quite near future, even though the relative urgency of nuclear power requirements differs greatly in different countries. In countries with high costs from conventional (fossil) fuels there is encouragement to proceed immediately with the commercial construction of reactors of proved design. In such countries as the United States, where conventional power costs are low, major efforts are being devoted to experimental construction of new types of reactors that hold promise of economical operation in the future.

One megawatt-year of heat produced by a nuclear reactor results in 365 grams of fission products. The Committee on Disposal and Dispersal of Radioactive Wastes, also a part of the National Academy of Sciences' study of the biological effects of atomic radiation (1956), estimates that by 1965 the United States will be generating about 11,000 megawatts of reactor heat, some 20 per cent of which will be for naval vessels. This will result in the production of about 4 tons per year of fission products. According to recent statements of government officials, reported in *Nucleonics* (1957), the United Kingdom has a 1965 target of 6,000 megawatts of electricity from Calder Hall-type reactors; "Euratom" has a goal of 15,000 megawatts by 1967, and Japan will produce 1,000 megawatts by 1965 and 10,000 megawatts by 1975. If the reactors are of 25 per cent efficiency in conversion of heat to electricity (the Calder Hall reactor has a net thermal efficiency of 21.5 per cent, *Nucleonics* 1956), for each

1,000 megawatts of electrical power there will be produced 1.46 tons per year of fission products. Thus, the fission products from the foregoing programs will amount to: United Kingdom 8.8 tons, "Euratom" 21.9 tons, Japan 1.5 to 14.6 tons.

If we further assume that all other areas of the world will in the next ten years develop nuclear power equal to the sum of that generated in the United States, Japan, the United Kingdom, and "Euratom," there will be a total of some 80 tons per year of fission products. This represents, after 100 days' cooling, according to the values given by Renn (see Chapter 1, Tables 2 and 3), 3.9×10^4 megacuries of beta radiation and 2.5×10^4 megacuries of gamma radiation, or over ⅒ of the total natural radioactivity of all the oceans (Revelle, Folsom, Goldberg and Isaacs 1955). The annual production of the isotope of greatest long-range hazard, strontium 90, will be 200 megacuries. Craig (Chapter 3) has shown that a thousand tons of fission products per year would result from a 2.7-fold increase in the present world energy consumption of about five million megawatts, if 10 per cent of this energy were derived from the heat of nuclear fission at 50 per cent efficiency. World energy consumption is now doubling once every thirty years and a 2.7-fold increase would be expected by about the year 2000. An annual production of a thousand tons of fission products corresponds to an equilibrium quantity of 7.7×10^5 megacuries of radiation or about 1.6 times the total natural radioactivity of the oceans. The equilibrium amount of strontium 90, plus its daughter yttrium 90, would be 2.2×10^5 megacuries. Carritt and Harley (Chapter 6) have made calculations based on an annual production of 4,000 tons of fission products, corresponding to two million megawatts per year of nuclear heat production from fission. If no new sources of power, such as thermonuclear reactions, become available, this production would be expected in the very early part of the twenty-first century because of the limited world fossil fuel reserves.

Our knowledge of just what share of these fission products can be safely introduced into the oceans is woefully incomplete because we simply do not know enough about the physical, chemical, and biological processes. If the sea is to be seriously considered as a dumping ground for any large fraction of the fission products that will be produced even within the next ten years, it is urgently necessary to learn enough about these processes to provide a basis for engineering estimates.

As shown in the several chapters of this report, the necessary information can be obtained only by extensive fundamental research. In the next decade we should attempt to learn far more about the ocean and its contents than has been learned since modern oceanography began 80 years ago.

Some of the required investigations of physical, chemical, and biological processes involve the employment of naturally occurring or experimentally introduced radioactive tracers. Pollution of the seas by the dumping of atomic wastes, even at levels that are "safe" from the standpoint of human health hazards, will make such experiments progressively more difficult because the presence of introduced pollutants will add an unknown background variability. The sooner the work can be commenced and the cleaner our oceanic laboratory, the more precise will be the experimental results. At the very least, it is urgent that the details of any interim introductions of radio isotopes be carefully documented, so that researchers can take account of them in their investigations.

INTERNATIONAL IMPLICATIONS

The oceans and their resources cannot be separated into isolated compartments; what happens in one area of the sea ultimately affects all of it. Moreover, the greater part of the oceans and their contained resources are the common property of all nations. Even the relatively narrow territorial seas are amenable only to juridical and not physical control; no nation can effectively modify the natural interchange of the biological and physical contents of its territorial sea with those of the high seas or of the territorial seas of other nations. The continuity of the oceans, and their status as international common property require that the oceanic disposal of radioactive wastes be treated as a world problem.

It is, first of all, urgent that the nations of the earth formulate agreements for the safe oceanic disposal of atomic wastes, based on existing scientific knowledge. Second, because of the vastness, complexity, and immediacy of the underlying scientific problems, it is important that pertinent oceanographic research be intensified on a world-wide basis. Third, from the standpoint both of research and of proper control of this new kind of pollution, careful records should be maintained of the kinds, quantities, and physical and chemical states of all radio isotopes introduced into the seas, together with detailed data on locations, depths and modes of introduction. This can probably best be done by national agencies reporting to an international records center.

Although we are urgently concerned with preventing possible deleterious effects of atomic wastes, atomic radiations can also be of benefit. Large-scale experiments employing radioactive isotopes might contribute importantly to our knowledge of the flux of materials through the food chains from the phytoplankton to the harvestable fishes, invertebrates, and whales (Schaefer, Chapter 13 of this report). Such knowledge will not only make possible assessment of the ocean's potential for providing food to mankind, but is a basic prerequisite for the effective conservation of marine populations, to permit maximum harvests to be taken year after year. Other experiments using radioactive tracers could lead to improved knowledge of the processes of circulation and mixing in the sea (Folsom and Vine, Chapter 12; Craig, Chapter 11). In both types of experiments, inter-

TABLE 2 ELEMENTS IN SOLUTION IN SEA WATER (EXCEPT DISSOLVED GASES)[1, 2]

Element	mg/kg Cl = 19.00‰	Total in oceans (tons)	Natural activities		
			Nuclide	Total (tons)	Curies
Chlorine	18,980	2.66×10^{16}			
Sodium	10,561	1.48×10^{16}			
Magnesium	1,272	1.78×10^{15}			
Sulfur	884	1.23×10^{15}			
Calcium	400	5.6×10^{14}			
Potassium	380	5.3×10^{14}	K^{40}	6.3×10^{10}	4.6×10^{11}
Bromine	65	9.1×10^{13}			
Carbon	28	3.9×10^{13}	C^{14}	56	2.7×10^{8}
Strontium	13	1.8×10^{13}			
Boron	4.6	6.4×10^{12}			
Silicon	0.02 –4.0	$0.028–5.6 \times 10^{12}$			
Fluorine	1.4	2×10^{12}			
Nitrogen (comp.)	0.01 –0.7	$0.14–9.8 \times 10^{11}$			
Aluminum	0.5	7×10^{11}			
Rubidium	0.2	2.8×10^{11}	Rb^{87}	1.18×10^{11}	8.4×10^{9}
Lithium	0.1	1.4×10^{11}			
Phosphorus	0.001–0.1	$0.014–1.4 \times 10^{11}$			
Barium	0.05	7×10^{10}			
Iodine	0.05	7×10^{10}			
Arsenic	0.01 –0.02	$1.4–2.8 \times 10^{10}$			
Iron	0.002–0.02	$0.28–2.8 \times 10^{10}$			
Manganese	0.001–0.01	$0.14–1.4 \times 10^{10}$			
Copper	0.001–0.01	$0.14–1.4 \times 10^{10}$			
Zinc	0.005	7×10^{9}			
Lead	0.004	5.6×10^{9}			
Selenium	0.004	5.6×10^{9}			
Cesium	0.002	2.8×10^{9}			
Uranium	0.0015	2.1×10^{9}	U^{238}	2.8×10^{9}	3.8×10^{9}
Molybdenum	0.0005	7×10^{8}	U^{235}	2.1×10^{7}	1.1×10^{8}
Thorium	< 0.0005	$< 7 \times 10^{8}$	Th^{232}	1.4×10^{7}	8×10^{6}
Cerium	0.0004	5.6×10^{8}			
Silver	0.0003	4.2×10^{8}			
Vanadium	0.0003	4.2×10^{8}			
Lanthanum	0.0003	4.2×10^{8}			
Yttrium	0.0003	4.2×10^{8}			
Nickel	0.0001	1.4×10^{7}			
Scandium	0.00004	5.6×10^{7}			
Mercury	0.00003	4.2×10^{7}			
Gold	0.000006	8.4×10^{6}			
Radium	$0.2–3 \times 10^{-10}$	28 –420	Ra^{226}	4.2×10^{2}	1.1×10^{9}

[1] Sverdrup, H. U., M. W. Johnson, and R. H. Fleming, OCEANS (1942).

[2] Revelle, R., T. R. Folsom, E. D. Goldberg, and J. D. Isaacs (1955).

national scientific cooperation will often be essential for optimum results.

IV. Chemical Processes and Radioactive Materials

Elements in sea water

Sea water is a solution of a large number of dissolved chemicals containing small amounts of suspended matter of organic and inorganic origin. The ratios of the more abundant elements are very nearly constant, despite variations in absolute concentrations in different parts of the sea. Lower than average absolute amounts are encountered in coastal areas and near river mouths, while higher amounts are encountered in areas of high evaporation, such as the Red Sea. Vertical variations are usually small; in general, in the open ocean in mid-latitudes, the quantity of dissolved materials, measured by the *salinity,* first decreases slightly with depth, then increases slowly in the deep water.

Table 2 (from Carritt and Harley, Chapter 6) shows the concentrations of some of the elements in solution in sea water at a chlorinity of 19.00‰, which is near average for the sea, and the total amounts in the ocean as a whole. Also shown are the total amounts and total radioactivity of the principal naturally occurring radio isotopes. In addition to the listed elements, there are variable amounts of dissolved gases, including nitrogen, oxygen, and the noble gases. A range of values is given for some elements present in small quantities, such as nitrogen, phosphorus, silicon, iron, and copper. These are substances necessary for living organisms, and the inorganic phases may be reduced to nearly zero in surface waters where they have been almost completely removed by organic uptake.

Behavior of introduced materials

A number of things can happen to materials introduced into the sea either in solution or as particles. The particles may go into solution. The dissolved substances may be precipitated as particles of colloidal or larger size either by coprecipitation with other elements, by sorption on organic or inorganic particles already present in the sea, or by interaction with other sea water constituents. Both dissolved materials and particles may be ingested by organisms and enter into the biochemical cycles.

Particles in the sea are continually removed by settling out on the bottom. The rates of settling depend on the size and density of the particles, as modified by various physical and biological factors.

Normal removal of elements from sea water

The results of geochemical studies provide very approximate estimates of the fractions of some elements supplied to the ocean that are eventually removed from solution. In Table 3 are listed a number of elements, including some of the elements having long-lived fission-product isotopes, with their concentrations in the supply to the ocean and in the ocean itself. Assuming steady-state equilibrium, the ratio of the concentration in the ocean to the concentration in the supply, the *transfer percentage,* indicates what share of the supply stays in solution. Large values of the transfer percentage indicate that a relatively large fraction remains dissolved; small values indicate that relatively much is removed.

TABLE 3 Geochemical Balance of Some Elements in Sea Water (From Goldschmidt, Quoted in Rankama and Sahama, 1950, Table 16.19)

Element	Total supplied (ppm)	Amount present in ocean (ppm)	Transfer percentage
Na	16,980	10,560	62
K	15,540	380	2.4
Rb	186	0.2	0.1
Ca	21,780	400	1.8
Sr	180	13	7.2
Ba	150	0.05	0.03
Fe	30,000	0.02	0.00007
Y	16.9	0.0003	0.002
La	11	0.0003	0.003
Ce	27.7	0.0004	0.001

These data give no information on the removal processes or on the time rate of removal. The latter can be obtained from estimates of rates of natural sedimentation together with chemical analysis of sediments or from study of rates of sedimentation of radio isotopes following weapons tests or waste disposal operations (Carritt and Harley, Chapter 6).

Goldberg and Arrhenius (in press), from a study of natural sediments, have estimated residence times in the ocean for several elements. They conclude that one half the amount of strontium present at a given time is deposited in the sediments in about ten million years. For other elements the residence times relative to strontium are roughly proportional to the transfer percentages. Thus they estimate that the residence time for iron is of the order of a hundred years.

Introduction of radioactive materials

Radioactive materials in large quantities can be introduced into the sea from reactor wastes, from weapons tests, or in warfare.

In Table 4 is a listing of the important fission products, their half-lives, and the quantities resulting from 10^{11} megawatt hours of nuclear power production (Carritt and Harley, Chapter 6). The column "specific activity" shows the ratio of the quantity of radioactivity of a particular isotope to the total amount of isotopes of that element in the sea for this amount of energy. The specific activity will, of course, be lower for smaller amounts of fission. It is also obvious that a uniform specific activity in all parts of the sea would be obtained only if the fission products were evenly distributed. Since, under any practical method of introduction, this will not occur, there are bound to be gradients of specific activity decreasing from the sites of introduction, and depending on the mixing characteristics of the ocean.

Nuclear explosions have been the principal source of fission products introduced into the sea to date. The total quantity of fission power from such explosions so far may be estimated at 40 to 60 megatons of TNT equivalent, from the data summarized by Lapp (1956). This corresponds, with 20 kilotons equal to 1 kilogram of fission products (Libby, 1956a), to two to three metric tons of fission products.

The amount of fission products reaching the sea from nuclear explosions depends on a number of factors such as the location of the burst, the distance above (or below) the surface, and the size of the weapon or device. For the smaller devices with a TNT equivalent of several kilotons, most of the fallout is immediate and local, although an appreciable fraction remains in the troposphere for a few weeks (Libby, 1956a, b). Subsurface explosions will result in local deposition of a larger fraction of the fission products; a deep underwater burst will deposit practically all of the activity locally, with nearly $\frac{1}{3}$ being in the surface layer and about $\frac{2}{3}$ below (Revelle, 1957). In the case of

TABLE 4 Fission Product Activity After 100 Days Cooling From 10^{11} Megawatt Hours of Nuclear Power Production [1]

Isotope	Half-life	Tons (metric)	Curies at 100 days	Specific activity curies per ton [2]
Kr^{85}	94 y	7.3	3.3×10^{9}	—
Sr^{89}	55 d	86	2.3×10^{12}	0.128
Sr^{90}	25 y	463	7.5×10^{10}	0.0042
Y^{90}	62 h	—	7.48×10^{10}	178
Y^{91}	57 d	111	2.8×10^{12}	6,660
Zr^{95}	65 d	152	3.2×10^{12}	—
Nb^{95}	35 d	161	6.3×10^{12}	—
Ru^{103}	45 d	46	1.3×10^{12}	—
Rh^{103}	57 m	—	1.3×10^{12}	—
Ru^{106}	290 d	35	1.5×10^{11}	—
Rh^{106}	30 sec	—	5.15×10^{10}	—
I^{131}	8.0 d	—	5.2×10^{9}	0.0743
Cs^{137}	33 y	705	5.63×10^{10}	20.1
Ba^{137}	2.6 m	—	5.1×10^{10}	0.728
Ba^{140}	12.5 d	2	1.5×10^{11}	2.14
La^{140}	1.7 d	—	2.5×10^{11}	595
Ce^{141}	28 d	45	1.5×10^{12}	268
Pr^{143}	13.8 d	2	1.4×10^{11}	—
Ce^{144}	275 d	490	1.6×10^{12}	386
Pr^{144}	17 m	—	2.4×10^{12}	—
Pm^{147}	94 y	7.3	3.3×10^{9}	—
Sm^{151}	73 y	0.7	2.0×10^{7}	—

[1] Adapted from data of Culler (1954) and Revelle et al. (1955).
[2] Based on tonnage shown in Table 2.

large, megaton devices, half or more of the total fission products are injected into the stratosphere from which there is a slow leakage into the troposphere (of the order of 10 per cent per year) and subsequent fallout fairly evenly over the entire northern hemisphere, with lesser amounts in the southern hemisphere (Libby, 1956a, b). Of this long-term fallout, up to 71 per cent falls on the oceans, since this is the proportion of the earth's surface covered by them. (The proportion of land to sea is higher in the northern hemisphere than in the southern, and since most of the long-term fallout occurs in the northern hemisphere, the amount entering the ocean will be less than 71 per cent.) On the other hand, some of the fallout on the land will eventually reach the sea through land drainage or river runoff.

Except in the case of deep underwater bursts, all of the fission products reaching the sea from weapons tests are deposited in the upper layer of the ocean. Removal into the deeper water is relatively slow. Despite the rapid mixing within the upper layer by vertical and horizontal wind stirring, the products from a large weapon remain in measurable concentrations over many months. A survey made 13 months after the 1954 weapons tests in the Pacific showed low-level activity over a vast area (Harley, 1956).

Radio isotopes in fallout on the land remain largely in the upper few inches of the soil. Fallout on the sea, on the contrary, is rapidly diffused through the upper mixed layer, some 75 meters deep on the average. Consequently, for conditions of equal fallout, the concentrations of radio isotopes in the part of the sea from which they are taken up by man's food organisms are less than in the soil. Thus, even though the calcium concentration of sea water is lower than in most soils, the ratio of strontium 90 to calcium in the marine environment is now much less than in agricultural lands of the mid-western United States. In 1955 (Libby 1956b) these soils contained about .025 microcuries of strontium 90 per kilogram of calcium available to growing plants. Revelle (1957) has calculated that for an equal amount of widely distributed fallout (from approximately 25 megatons TNT equivalent of fission) about .00015 microcuries of strontium per kilogram of calcium would be present in the upper mixed layer of the sea, half of one percent of the amount in soils.

In addition to fission products, neutron irradiation of elements in the environment immediately after the detonation produces other radioactive isotopes. With ordinary land or marine materials, the amounts of this neutron-induced radioactivity are small (Libby, 1956a). However, soon after the 1954 tests in the Pacific, quantities of zinc 65 were discovered in marine fishes, and subsequently cobalt 60 was recovered from clams in the Marshall Islands. These isotopes probably originated from neutron irradiation of metals, other than the fissionable materials, in the test device.

Comparison of table 2 and table 4 demonstrates that the mass of radioactive isotopes introduced into the sea from weapons tests, or which might be introduced from disposal of waste products, will be very small compared with the amounts of their normal isotopes already present. The introduction of the radioactive material does not, therefore, appreciably modify the chemical and physical properties of normal seawater, so that the chemistry of the introduced radioactive substances is the same as for the corresponding non-radioactive isotopes in the sea.

Introduced radioactive isotopes will partition into a soluble and an insoluble fraction. The physical states of a given element under equilibrium conditions depend upon whether or not the solubility product of the least soluble compound has been exceeded. Since the ionic activities of the elements in the complex chemical mixture that is sea water are not accurately known, it is difficult to attack this problem from theory. Greendale and Ballou (1954) have determined the distribution among soluble, colloidal, and particulate states of important fission product elements by simulating the conditions of an underwater detonation; their results are given in Table 5. Elements of Groups I, II, V, VI and VII usually occur as ionic forms, while other elements, including the rare earths, occur as solid phases. Some of these results have been confirmed by field observations following weapons tests (see Chapter 6 of this report by Carritt and Harley, and Chapter 7 by Krumholz, Goldberg and Boroughs). Those elements in Table 5 that have sufficiently long half-lives to contribute a significant share of the total activity after one year of decay are marked with an asterisk. Cesium 137 and strontium 89 and 90 remain in solution, while ruthenium 106, cerium 144, zirconium 95, yttrium 90 and 91, and niobium 95 are largely in the solid phase.

The solid fractions, whether they be chemical precipitates or solids produced by accumulation in the bodies of organisms, will tend to settle out. As they settle, they may encounter environmental conditions which will prevent or hinder deposition. There will be, however, some net transport toward the deeper water and the bottom from the settling process. Because of biological uptake, the removal of the particles from the upper layers of the sea may be quite slow. For example, cerium 144, a rare earth which has a half-life of 275 days, and which is present in the sea primarily in particulate form, and its daughter Pr 144 were found to account for 80 to 90 per cent of the activity in plankton samples from the upper layer taken in the Pacific by the TROLL survey 13 months after weapons tests (Harley, 1956).

TABLE 5 PHYSICAL STATES OF ELEMENTS IN SEA WATER[1] (FROM GREENDALE AND BALLOU, 1954)

	Percentage in given physical state		
Element	Ionic	Colloidal	Particulate
Cesium *	70	7	23
Iodine	90	8	2
Strontium *	87	3	10
Antimony	73	15	12
Tellurium	45	43	12
Molybdenum	30	10	60
Ruthenium *	0	5	95
Cerium *	2	4	94
Zirconium *	1	3	96
Yttrium *	0	4	96
Niobium *	0	0	100

[1] Elements introduced by simulated underwater detonation of atomic bomb, Greendale and Ballou, 1954.

* Indicates element has important fission product isotope.

A very rough idea of the reduction in activity that would eventually be obtained by removal from the ocean can be gained from the transfer percentages of Table 3. The fraction of an introduced fission product remaining in the sea will, at equilibrium, be equal to or greater than the transfer percentages for the corresponding element. (The transfer percentage reflects, in part, retention on land as well as sedimentation from the sea.) An important factor is the time required for equilibrium to be reached; if it is very long in relation to the half-life of the element in question, reduction of activity may be negligible. The long-lived and dangerous isotope, strontium 90, has a relatively high transfer percentage and a long equilibrium or "residence" time; the same would be expected for cesium 137, which is an alkali and should behave somewhat like potassium or rubidium.

Disposal of atomic wastes by deep sea burial in various sorts of packages has been proposed. Dispersion of the activity would then be by slow diffusion from concreted wastes, or would be delayed until rupture of an impermeable container occurred. Because the deep ocean sediments have appreciable exchange capacities, much of the wastes would be retained in this highly absorptive environment. The upper layers of the sediments would, presumably, tend to become saturated, and the further removal of radioactive elements by exchange or absorption would be controlled by the rate of diffusion into the deeper sediments.

There are wide gaps in our knowledge of many of the processes mentioned above. These, and suggestions for research needed to fill them, are discussed by Carritt and Harley (Chapter 6). Much of the required information can be obtained by the use of radioactive tracers, introduced in weapons tests and experimental waste disposal operations, as well as in purposive experiments.

V. PHYSICAL PROCESSES AND RADIOACTIVE MATERIALS

Physical structure of the sea

The physical properties of sea water of importance to the present study are functions of temperature, salinity, and pressure. The temperature ranges from about 30° C to about $-2°$ C, which is the initial freezing point. The highest temperatures occur at the surface or in the mixed near-surface layer; below this the temperature decreases to about 5° C at 1,000 meters and to 1° to 2° at greater depths. In the deepest parts of the ocean there is a slight increase of temperature due to adiabatic heating. Hydrostatic pressure increases about one atmosphere for each 10 meters of depth. In the open ocean in mid-latitudes the salinity generally decreases slightly with depth in the upper few hundred meters, then increases slowly. In high latitudes the salinity normally increases with depth throughout the water column.

The density of sea water increases with decreasing temperature and with increasing salinity and pressure. Except in quite dilute sea water, the temperature of maximum density is lower than the freezing point. The range of density in the open sea is between about 1.02 and 1.06. It may, of course, be lower in inshore waters in the vicinity of river mouths. At constant pressure the major changes in density in the sea are associated with temperature, so that to a first approximation the change of density (computed for constant pressure) with depth is inversely proportional to the change of temperature.

Many processes in the sea depend on the density distribution. The ocean basins are largely filled with water of relatively high density formed in high latitudes; overlying this dense water in middle and low latitudes, and separated from it by the pycnocline, is the subsurface mixed layer, varying from a few meters to several hundred meters in thickness but averaging about 75 meters, of water of high temperature and low density. The relative rate of change of density with depth may be taken as a measurement of the vertical *stability* of the water (Sverdrup, Johnson and Fleming, 1942, p. 417). Stability in the region of the pycnocline is much higher than above or below it, so that exchange of water across it tends to be small.

All parts of the ocean and its bordering seas are in communication with each other, and are in continuous motion. The rates of movement, however, differ greatly in different areas. Thus, although there is eventual complete interchange of water between all oceans and seas, some parts are partially isolated from others, the exchange between these parts being much slower than within them.

Near-surface currents and mixing within the upper layer

Currents in the upper, mixed layer of the sea are primarily generated by winds, and, consequently, the major horizontal surface currents of the ocean correspond to the field of wind stress (Munk, 1950). The average locations and velocities of the important surface currents are well known from numerous observations of merchant ships and research vessels, and appear on many charts.

The velocities and volume transports of the major near-surface currents are large. For example, the mean speed of the Florida Current is about 193 cm/sec. and of the Kuroshio about 89 cm/sec. The volume of water flowing through the Florida Straits in 15 years is equal to the volume of the upper 500 meters of the whole North Atlantic, and the transport of water by the Kuroshio between the Northern Ryukus and Kyushu in 50 years is equal to the upper 500 meters of the whole North Pacific.

Because of the large surface currents, introduced materials tend to be carried away from the sites of introduction to other parts of the upper mixed layer of the sea. Thus, no area of surface water in the ocean is isolated for long periods from the remaining areas.

The currents are not steady streams, but have a complicated fine structure, with many eddies, jets, and filaments. In consequence of this turbulence, on both large and small scales, dissolved materials in seawater are rapidly dispersed horizontally. The rate of dispersion is about a million times the rate of molecular diffusion, and depends on wind speed, current shear, vertical and horizontal density gradients, direction of dispersion, and the dimensions of the area considered. Because of this large number of variables and the lack of knowledge of turbulent processes, it is not possible to predict accurately the horizontal dispersion in particular areas. If even moderately precise values are required, experiments must be conducted in the area of interest. Some of the results of such studies are reported by Wooster and Ketchum (Chapter 4).

The rate of vertical diffusion in the upper, mixed layer, although much less than that for horizontal dispersion, is nevertheless about a thousand times greater than molecular diffusion. The extent of vertical stirring in the upper layer depends on the magnitude and uniformity of the wind stress and on the vertical density gradient. Convective processes, and, in coastal areas, strong tidal currents, also contribute to vertical mixing. The mixing rate in the upper layer has been measured by changes in the vertical distribution of radio isotopes following weapons tests. Revelle, Folsom, Goldberg, and Isaacs (1955) report that in one such test the lower boundary of the radioactive water moved downward at about 10^{-1} cm/sec. until it reached the thermocline, where it abruptly stopped,

Circulation and mixing within the intermediate and deep layer

Within the pycnocline and for some distance below it, it is believed that most of the motion takes place along surfaces of constant potential density, so that transport and diffusion in the lateral direction are very much greater than in the vertical. This belief has been confirmed by experiments with radioactive tracers, reported by Revelle, Folsom, Goldberg, and Isaacs (1955), in which it was shown that the radioactive water spread out over an area of about 100 square kilometers while maintaining a thickness of the order of a few meters.

Much of our knowledge of deep and intermediate currents has been inferred from the distributions of properties. These indicate that the average velocities of the deep currents are only a few cm/sec. or less. However, Wüst (1957) has recently made calculations on data from the Atlantic which indicate velocities of meridional currents of 3 to 17 cm/sec. in the deep sea, along the western margin of the western trough, in depths between 3,000 and 5,000 meters. The calculated currents on the eastern side of the deep South Atlantic, especially in the region of the Angola Basin were, on the contrary, very weak. Dietrich (1957) has likewise computed mean current velocities of about 10 cm/sec. for the deep Antarctic Circumpolar Current, and for the Subarctic Bottom Current in the northern North Atlantic, the latter increasing to as much as 40 cm/sec. when flowing across the Greenland-Scotland ridge. He states, however, that in the largest part of the ocean the bottom currents are below 2 cm/sec.

Direct measurements of deep currents are technically difficult. The few successful measurements summarized by Bowden (1954) show mean velocities from less than a cm/sec. to 13 cm/sec. Recently Swallow (1955 and unpublished data) has measured subsurface currents by tracking a neutrally buoyant float at a fixed depth. His measurements in the North Atlantic give mean resultant velocities of 1.7 to 9.1 cm/sec. Tidal currents of about 10 cm/sec. have been obtained by Swallow and others in deep water. It appears that the mean current in many parts of the deep sea may be less than the periodic variable currents.

The turbulence of these variable tidal currents, especially near the bottom, contributes to vertical and horizontal mixing in deep water. Mixing should also occur along the boundaries of the rapid deep resultant currents indicated by Wüst and Dietrich, where there must be considerable shear.

Dietrich (1957) also suggests that horizontal spreading of near-bottom water may occur in regions of turbidity currents, which occur especially on the continental slopes.

Exchange between the open sea and coastal areas

In coastal areas and estuaries where precipitation and land runoff exceed evaporation, there is a net seaward drift of dilute surface water and an inshore drift of sub-surface water from the open sea. This is superimposed on the flow of wind-driven currents through the coastal areas.

Some idea of the average time involved in interchange of coastal waters can be obtained from the volume in and transport through various areas along the American Atlantic seacoast. Calculations give a mean age of $2\frac{1}{2}$ years for the waters over the Continental Shelf from Cape Hatteras to Cape Cod, about 3 months for the Bay of Fundy, and 3 to 4 months for Delaware Bay (Wooster and Ketchum, Chapter 4).

Exchange between the deep and intermediate layers and the mixed sub-surface layer

Evidence of local cross pycnocline interchange was obtained from measurements of the vertical distribution of radioactivity following the 1954 Pacific weapons tests (Japanese Fishery Agency, 1955 and Harley, 1956); it is not, however, clear whether the observed phenomena were entirely the result of physical exchange of the water and its contents or were in part due to settling of particles and to biological transport.

The major exchange between the near-surface and deeper waters takes place in the following regions:

In areas where the pycnocline is maintained, by the distribution of mass related to the general circulation, at a sufficiently shallow depth to be eroded away by wind stirring. Such areas exist near the equator, along the north edge of the Equatorial Counter Current, and at the centers of strong cyclonic eddies.

In regions of upwelling, where vertical currents carry water toward the surface and stir the surface and intermediate layers. Water from as deep as about 500 meters may be brought to the surface by this process. Upwelling occurs along the western coasts of continents in intermediate and low latitudes, wherever the wind-driven circulation removes surface water from the coast. This water is replaced by deeper water moving upward. Such coastal upwelling has been found to be of the order of 1 to 3 meters per day. Upwelling also occurs in mid-ocean where there are surface current divergences, most notably along the equator in the eastern and central Pacific.

In regions of surface convergence, where sinking waters may extend to the oceanic depths, or may spread out at intermediate levels, according to their density. In tropical and temperate latitudes such sinking is confined to the upper few hundred meters, but at high latitudes the waters may reach great depths. Indeed, it is in the convergence regions of high latitudes that much of the intermediate and deep water of the oceans are formed.

In regions where increase of surface density by evaporation, freezing out of ice, or cooling, causes the surface waters to sink and be replaced by the formerly deeper water. Deep thermal convection occurs in high latitudes and extends in some areas to the bottom; for example, Antarctic bottom water is formed in the Weddell Sea by the cooling and sinking of the surface waters, and the Atlantic deep water is formed in a similar manner east of Greenland. Haline convection takes place in regions where evaporation exceeds precipitation or where freezing prevails over melting. The latter in high latitudes increases the intensity of the thermal convection. Haline convection in winter is responsible for the characteristics of the deep water of the Mediterranean Sea. This water flows out into the North Atlantic at depths of 1,000 to 1,500 meters, and can easily be identified even on the western side of the ocean.

The exchange between the surface layer of the ocean and the deeper layers may be either continuous or discontinuous. Some idea of the rate of exchange can be obtained from various estimates of the "age" or average residence time of the water in the deeper layers. These estimates, which differ widely depending on the data and assumptions used, have been summarized by Wooster and Ketchum (Chapter 4 of this report) and by Craig (Chapter 3).

Three estimates for the water in the intermediate layer of the Atlantic Ocean give residence times between 7 and 140 years. Estimates for the water below 2,000 meters vary from 50 to 1,000 years. An estimated upper limit based on the measured heat flow through the sea floor under the Pacific Ocean indicates that the Pacific deep water is replenished in less than 1,000 years. The deep water in the Pacific may be older than in the Atlantic because of the larger volume of the Pacific.

EXCHANGE FROM CONFINED BASINS

The few data available for estimating the age of water in confined basins have been considered by Wooster and Ketchum (Chapter 4). These indicate that the mean residence time of water in the Mediterranean Sea is about 75 years. In the Caribbean Sea the mean age cannot be less than 6 years and, in the deeper part, may be as much as 140 years. The deep waters of the Black Sea apparently remain isolated for very long periods. Transport considerations lead to an estimated age of at least 2,500 years, while, from consideration of phosphorus accumulation, the age has been estimated at 5,600 years.

VI. BIOLOGICAL PROCESSES AND RADIOACTIVE MATERIALS

Uptake and accumulation of elements in organisms

Organisms take up from their environment and their food and incorporate into their bodies those elements required for their maintenance, growth, and reproduction. The proportion of various elements required by the organisms are different than the proportions in the environment, and this results in concentrations of some elements in the biosphere.

The energy that drives the whole life cycle is the energy of sunlight. This energy is bound chemically in organic compounds by the photosynthesis of plants, and is passed along, through the food chain, in the food of all the organisms beyond the plants. The flux of energy, and hence the flux of carbon, through the various trophic levels measures the *productivity* of the organisms at each level. Since the efficiency at each stage of the chain is low (of the order of 10 per cent to 30 per cent) the flux decreases at each step. The standing crop, or biomass, of organisms at the different levels, or, in other words, the amount of carbon present in the organisms at each level, may be greater or less than the amount at the next lower level, depending on the rates of turnover of the populations involved.

In addition to the abundant elements carbon, oxygen and hydrogen, the bodies of organisms contain a number of elements in smaller amounts, such as nitrogen, phosphorus, calcium, strontium, copper, zinc, and iron, which are essential to the life processes. These may be obtained by organisms above the plants in the food chain either from their ingested food, or by direct uptake from the sea water. Since the requirements for different elements are different in different kinds of organisms, the fluxes of the various elements are variable from one to another, and at different trophic levels.

The concentration factors of some of the important elements in different kinds of organisms are tabulated in Table 6, taken from Krumholz, Goldberg and Boroughs (Chapter 7 of this report). Certain elements, for example, sodium, occur in some organisms at lower concentrations than in the water; they are selected against. On the contrary, those elements, such as phosphorus, that are essential to the organisms but occur in low concentration in the sea water, are concentrated by several orders of magnitude. In some parts of the sea, the phosphorus may be nearly completely removed from the water by the organisms. Such elements are often limiting constituents for further increase of the populations of a particular part of the sea, and any quantities added will be soaked up by the biosphere very rapidly.

Both dissolved and particulate materials can be taken up from the environment. Iron, for example, occurs in the sea almost entirely in particulate form and is used in that form by diatoms. Fishes can take up ionic calcium and strontium directly from the sea water. Observations in conjunction with weapons tests, reported in Chapter 7 of this report, have shown that particulate feeders among the zooplankton ingest particles of inorganic compounds and retain them.

TABLE 6 APPROXIMATE CONCENTRATION FACTORS OF DIFFERENT ELEMENTS IN MEMBERS OF THE MARINE BIOSPHERE. THE CONCENTRATION FACTORS ARE BASED ON A LIVE WEIGHT BASIS (FROM KRUMHOLZ, GOLDBERG AND BOROUGHS, CH. 7 OF THIS REPORT)

Element	Form in sea water	Concentration in sea water (micrograms/l)	Algae (non-calcareous)	Concentration factors			
				Invertebrates		Vertebrates	
				Soft	Skeletal	Soft	Skeletal
Na	Ionic	10^7	1	0.5	0	0.07	1
K	Ionic	380,000	25	10	0	5	20
Cs	Ionic	0.5	1	10		10	
Ca	Ionic	400,000	10	10	1,000	1	200
Sr	Ionic	7,000	20	10	1,000	1	50
Zn	Ionic	10	100	5,000	1,000	1,000	30,000
Cu	Ionic	3	100	5,000	5,000	1,000	1,000
Fe	Particulate	10	20,000	10,000	100,000	1,000	5,000
Ni *	Ionic	2	500	200	200	100	0
Mo	Ionic-Particulate	10	10	100		20	
V	?	2	1,000	100		20	
Ti	?	1	1,000	1,000		40	
Cr	?	0.05	300				
P	Ionic	70	10,000	10,000	10,000	40,000	2,000,000
S	Ionic	900,000	10	5	1	2	
I		50	10,000	100	50	10	

* Values from Laevastu and Thompson (1956).

The uptakes of various elements by organisms are not entirely independent of one another. Elements of similar chemical properties tend to be taken up together very roughly in the same proportions as they exist in the environment. This is true, for example, of calcium and strontium. Sometimes one element has an inhibiting effect on another. There can also be synergistic effects, such as the enhancement of phosphorus uptake of diatoms by increased concentration of nitrogen.

Certain elements are deposited, in large part, in particular organs. Perhaps the best known examples are the deposition of iodine in the thyroid glands of vertebrates, or the deposition of calcium and strontium in the bones of vertebrates and in the shells and other hard parts of invertebrates.

The length of time an organism retains the average atom of a given element varies greatly from one element to another. This is sometimes measured as the biological half-life, although the relative rate of loss is not a simple linear function of time as is the case with radioactive decay. Much is known about the retention times of different elements in man (see, for example, Handbook 52 of the National Bureau of Standards, 1953), but there are few data for most marine organisms. The rate of excretion of an element and the amount ultimately retained, will be quite different if the element is taken up quickly from a single dose or is taken up slowly over a long time.

The processes of uptake, accumulation, and loss of elements by marine and other aquatic organisms, are discussed in more detail by Boroughs, Chipman and Rice (Chapter 8 of this report), Krumholz, Goldberg, and Boroughs (Chapter 7), and by Krumholz and Foster (Chapter 9).

Effects of organisms on spatial distributions of elements in the sea

Those elements of which a large proportion is cycled through organisms are modified profoundly in their spatial distributions by the effects of the biosphere, so that they are quite differently distributed in the sea than elements in which the distribution is determined only by physical and inorganic chemical processes. We have already mentioned phosphorus as a notable example. Ketchum (Chapter 5 of this report) has written a detailed discussion of the general effects of the ecological system on the distribution of elements in the sea.

The marine biosphere acts as a reservoir for those elements that are removed selectively from sea water by organisms. This reservoir is not stationary in space, however, because many of the living organisms make both vertical and horizontal migrations of large extent, while their dead bodies and fecal materials continually fall toward the bottom under the influence of gravitation. The effects of the living reservoir in the distribution of elements vary not only from one part of the sea to another, but also seasonally in the same area.

Because organisms in the sea are more abundant in the upper layers than deeper down, those elements in scarce supply that are essential to life tend to be retained by the biosphere in the upper layers and to be returned to solution in the deeper layers. Stationary populations, such as attached benthic organisms, act as a fixed reservoir.

Where there are currents at different levels in opposite directions, the accumulation of elements by pelagic organisms, together with gravity effects on their dead bodies and fecal materials, can result in local concentrations of elements at intermediate depths greater than the concentrations in either the overlying or the deeper waters. This pattern, as noted by Ketchum, is common in estuaries, continental shelves, and in the vicinity of coastal upwelling.

Migration of organisms may result in a net transport of elements from areas of high concentration to areas of lower concentration. Thus, for example, the vertical migrations of the organisms of the deep scattering layer can result in a transport from the deeper layers into the upper mixed layer. Salmon which spawn and die in fresh waters after accumulating elements in the sea can transport significant quantities of some elements from the sea to fresh waters.

Finally, the remains of organisms, falling out as particulate matter, are an important component of the sedimentation process in the deep sea, and are thus important in the geochemical cycle, as noted by Carritt and Harley (Chapter 6) and others.

Although we have some understanding of the various processes involved, data for making useful quantitative assessments are almost entirely lacking.

Effects of introduction of radioactive elements

Since the isotopes of most chemical elements are similar in chemical behavior, it can be assumed that organisms do not appreciably distinguish between the radioactive and non-radioactive isotopes, and that, to a good degree of approximation, the path of a radioactive element through the biological system is the same as that of its non-radioactive isotopes.

The accumulation of radio isotopes in organisms will, therefore, depend on the same factors as the accumulation of normal isotopes (their concentration in the water where the organisms are located, the concentrations of other elements by which uptake is influenced, the size of the population of organisms concerned, the concentration factors of the organisms for each element, and the rates of excretion, and *in addition* will depend on the decay rates of the radioactive isotopes).

The most important radio isotopes from the standpoint of accumulation in organisms are, therefore, those which are concentrated in large degree by organisms, are retained by them for relatively long periods of time, and have slow decay rates. An additional consideration from the standpoint of human hazards is the uptake and biological half-life of the elements in humans who may consume the marine organisms as food.

The most important fission product from all these considerations is strontium 90 and its daughter yttrium 90. This isotope has a large fission yield and a long physical half-life, is concentrated by organisms, and can be tolerated in human food only in very low amounts.

Ce 144 is another isotope with a large fission yield, which is concentrated by organisms (Harley, 1956), and has a moderately slow decay rate. Due to its small uptake and low retention by humans, it can, however, be tolerated in human food in much greater concentrations than Sr 90.

Zn 65 and Co 60, although not fission products, are sometimes produced in relatively large quantities in weapons tests. They are concentrated by very large factors in fish and mollusks used for human food, but fortunately they possess a relatively high tolerance level in humans.

Because of its biological role both in marine organisms and in humans, strontium 90 dominates consideration of depositing mixed fission products in the sea. For other radioactive wastes, and for mixed fission products from which Sr 90 has been removed, other elements will be the critical determinants, but in most cases, prior removal of Sr 90 will permit the safe disposal in the sea of larger quantities than would otherwise be possible.

The safe quantity of fission products depends on the concentrations that reach man's food organisms. The quantity will be greater if sites of introduction are chosen to give either long periods of isolation of the wastes or high dispersion (and thus low concentration) of the fractions that come into the environment (both physical and biological) of human food organisms.

Somatic and genetic effects on marine organisms

It is sometimes suggested that sufficient quantities of radioactive elements may be accumulated by marine organisms to endanger their populations, either by direct somatic effects or through genetic changes. Some aspects of this problem are discussed by Donaldson and Foster in Chapter 10 of this report.

So far as somatic effects are concerned, experimental data indicate that primitive forms are more resistant to ionizing radiation than the more complex vertebrates. It has not been possible to demonstrate any large-scale radiation damage to marine populations in the vicinity of large weapons tests. Levels of radiation safe from the standpoint of human hazards are also probably safe for the populations of marine organisms that are used as human food.

By analogy with results from genetic studies on laboratory animals, it may be inferred that significant genetic population effects will occur in marine organisms at much lower levels of radiation than will produce somatic effects. These genetic effects might be related to the increase in amount of total body radiation above the natural background. As shown by Folsom and Harley (Chapter 2), the normal radiation background of organisms in the deep sea is very low, so that appreciable quantities of radioactive wastes would significantly increase the radiation received by them. Craig (Chapter 3) has shown that the deposition of 1,000 tons per year of fission products in the deep sea would, at secular equilibrium, almost triple the average radiation level in the deep water. This could, conceivably, result in genetic effects in the marine populations in these waters, which might seriously upset the ecological system of the oceans. At the present state of knowledge, however, this is pure speculation. The matter does require, nevertheless, serious investigation.

VII. PREDICTED EFFECTS OF INTRODUCED RADIOACTIVE MATERIALS

Prediction of the effects of the introduction of radioactive materials into the different domains of the oceans must take into account the various physical, chemical, and biological processes discussed above. While our knowledge of these processes is very imperfect, we can make rough evaluations of the effects of disposal of fission products in different parts of the sea. Because of the limitation of knowledge, these evaluations must, of necessity, be conservative. Under some circumstances this necessity could involve considerable cost to society. Those sites and methods of disposal, both on the land and in the sea, that provide the least hazard may also involve the greatest disposal costs, so that, to the extent we must include a safety factor because of ignorance, there can be economic loss.

In disposing of radioactive materials in the sea, we aim at two things: (1) isolation of the materials, so that their entry into the part of the sea and its contents used by man is limited, (2) dispersal of the materials that do enter the domain important to man, to keep the concentrations of radioactive elements at tolerable levels. Depending on the quantity of materials to be dealt with, we may need to consider either or both of these possibilities.

Introduction in the upper mixed layer

Radioactive materials introduced into the upper mixed layer will, because of the rapid transport and large horizontal and vertical mixing within this layer, be carried away from the site of introduction and rapidly dispersed. Dispersion may be more rapid in coastal areas than in the open sea, but in some situations there may be a net transport inshore, particularly in or near estuaries, if the materials are introduced below the surface.

Direct evidence of near-surface transport and dispersion of fission products in the open sea has been obtained by the surveys of the "Shunkotsu Maru" (Miyake, Sugiura and Kameda, 1955) and the "Taney" (Harley, 1956), respectively four and thirteen months after the Pacific weapons tests of March 1954. The indicated transport of these products was in good agreement with current velocities measured by conventional means. These data from the open sea and earlier measurements on the partially confined waters of Bikini Lagoon (Munk, Ewing and Revelle, 1949) demonstrate the rapid dispersal of fission products in the surface layer.

Dispersion in an inshore situation (the Irish Sea) was measured with fluorescein by Seligman (1955) as a preparatory study for the discharge of low-level wastes from a power reactor installation. Subsequent experience with liberation of the radioactive wastes (Anon., 1956) confirmed that they were rapidly dispersed.

Radioactive materials introduced into coastal waters enter directly into that part of the ocean most utilized by man, from which he removes the greater share of his harvest of marine food organisms. The sessile algae, bottom living invertebrates, and fishes of these waters heavily concentrate certain of the elements, such as strontium, cesium, zinc, and cobalt that has radioactive isotopes most hazardous to man. While dispersion due to physical transport and dispersion in these waters is high, they are usually shallow, so that the volume is limited and there can also be considerable accumulation in shallow bottom sediments from which the isotopes can be again taken up by man's food organisms.

In some coastal areas the combination of physical and biological processes can result in local concentrations of radioactivity in the waters themselves (Ketchum, Chapter 5).

Because of the above considerations, the quantity of radioactive materials that can be introduced safely into coastal waters near shore is very limited, of the order of a few hundred curies per day. The particular physical, chemical, and biological factors vary so widely from one coastal area to another, that careful study is required to determine the safe amount in any particular locality, and continuous monitoring should be conducted to guard against effects of unforeseen variability in environmental factors.

The rather low level of discharge of radioactive products that can be tolerated in coastal waters imposes the necessity of providing adequate safeguards against discharge of high-level atomic wastes from accidents to power reactors, either at locations on the shore or shipborne reactors.

The quantity of radioactive material that can be safely deposited in the mixed layer in the open sea depends on such local characteristics as the direction and rate of transport, the rate of horizontal dispersion, the rate of uptake by organisms, and the contiguity of fishing areas. However, in general, the quantities will be much greater than those permissible for coastal waters. An idea of the order of magnitude of mixed fission products that can be safely introduced in a fairly typical situation is given by the results of weapons tests in the Pacific where a quantity of mixed fission products of the order of half a ton was introduced into the mixed layer in a short time period. That this was near the limit of safety is evidenced by the capture in adjacent areas of specimens of tunas and other fishes with sufficient radioactivity to be doubtful for human consumption (Kawabata, 1956, and Hiyama and Ichikawa, 1956).

Deep water introduction

The only place in the ocean in which we can be confident at this time that radioactive wastes of the order of some tons a year can be safely deposited is in the depths of the sea. Knowledge is, however, insufficient to determine whether radioactive materials of the order of the expected production from power reactors in the next few decades could be disposed of in this way.

Radioactive materials introduced into the deeper layers will be partially isolated from the upper layer for time periods related to the residence time of the water in the deeper layer. During this time there will be a decrease of radioactivity due to decay, and dilution due to dispersion. Since, as we have noted above, the residence times are variable in different depths and different locations, a much greater time of isolation will be obtained in some places than others.

The longest average time of isolation will be obtained in deep nearly enclosed basins such as the Black Sea. It has been suggested by Wüst (1957) that there may also be a long isolation period in the abyssal trenches of the central equatorial regions, such as the Romansch Deep or the Tonga Trench, but no data on currents in these deeps are now available.

Craig (Chapter 3 of this report), assuming an estimated average residence time in the deep sea of 300 years, the introduction into the deep sea of 1,000 tons per year of fission products after 100 days cooling, and complete uniform mixing within the deep water, has calculated the activity in the deep and surface layers at secular equilibrium. This calculation indicates that the total fission product activity in the mxed layer would be about equal to that at present from natural sources (primarily K^{40}). The concentration of Sr 90 would, however, be about 6.5×10^{-5} microcuries per liter, or 0.16 microcuries per kilogram of calcium in solution in sea water.

Studies of the uptake of strontium by marine fishes indicate a discrimination against strontium with respect to calcium approximately by a factor between 3 and 10. Thus for human populations such as the Japanese (Hiyama, 1956), in which much of the dietary calcium is obtained from marine fishes (including the bones and skin of some species), the amount of strontium 90 ingested per unit weight of calcium would be of the order of .04 microcuries per kilogram of calcium. A human population that obtained all its calcium from marine fishes after equilibrium was established with about 1,000 tons of fission products per year (1.1×10^5 megacuries of strontium 90) in the deep sea would have a burden, primarily in the bones, of approximately .005 microcuries of strontium 90 per kilogram of calcium. This is 5 per cent of the maximum permissible concentration for the population at large, estimated by the National Bureau of Standards (1955).

Weapons tests resulted in an average amount of .025 microcuries of strontium 90 per kilogram of calcium available to growing plants in the United States in 1955. By 1970, the amount will be .08 microcuries per kilogram of calcium even in the absence of further weapons tests (Kulp, Eckelmann, and Schulert, 1957). Because of discrimination against strontium with respect to calcium in food grains and grasses, and the additional discrimination in cows' milk and in human beings, it is expected that by 1970 an average of about .002 microcuries of strontium 90 per kilogram of calcium will exist in the United States population, 2 per cent of the maximum permissible concentration.

From the above considerations it is uncertain whether reactor-fuel wastes of the order of 1,000 tons a year could be deposited safely in the deep sea. Craig's calculation is most useful in orienting our thinking, but is, of course, very much oversimplified. No account is taken of the removal of activity from the sea by sedimentation. On the other hand, it does not take into account any biological transfer of material across the pycnocline, nor can we assume that effective concentration of Sr 90 per unit weight of calcium for some commercially important organisms will not be greater than the values we have taken.

Moreover, such a calculation assumes even distribution of the radioactive materials throughout the deep layer. This could only occur if they were evenly distributed when introduced, or if there were uniform and complete mixing in all parts of the deep layer.

A priori we should expect that neither the physical circulation and mixing in the deep sea nor the transfer between the deep layer and the mixed layer would be uniform. There is some evidence, however, from carbon 14 measurements made by the Lamont Geological Observatory that in fact fairly complete mixing occurs within the deep sea during the average residence time of a water particle.

Another calculation, based on very conservative assumptions concerning the mixing processes, was made in the report of a meeting of scientists from the U.S. and U.K. (Anon., 1956). It was assumed that fission products deposited on the ocean floor in mid-latitudes would drift and disperse for at least 10 years before surfacing, at which time the contaminated area would be a disc about 2 km. thick and 70 km. in diameter, which would be subsequently dispersed throughout the surface layer. Repeated deposits of 1 megacurie of Sr 90 (0.4 tons of mixed fission products) made at the rate of ten per year would result in an average concentration of Sr 90 of not over 10^{-5} microcuries per liter in the mixed layer, or .025 microcuries per kilogram of calcium.

Although we cannot say at this time with any precision what quantities of reactor-waste products can be safely deposited in the deep sea, it appears certainly safe to employ quantities up to a few tons a year in careful experimental studies. It is not impossible that 1,000 tons a year can be safely disposed of in deep, isolated basins where the residence time is much greater than the 300-year average estimated for the deep sea generally. For quantities of the order of 100 tons a year or more, effects on the animal populations of the deep sea, and resulting effects on the whole ecology of the sea could become important; as to this no information is at present available.

VIII. What We Need to Know

Our knowledge of most of the processes in the oceans is altogether too fragmentary to permit precise predictions of the results of the introduction of a given quantity of radioactive materials at any particular place. In order to obtain the necessary knowledge, an adequate, long-range program of research on the physics, chemistry, and geology of the sea, and on the biology and ecology of its contained organisms is required. Such research must be directed toward the understanding of general principles, not simply to the *ad hoc* solution of a particular local problem for immediate application. The latter sort of study is, of course, desirable in order to provide engineering solutions to particular waste-disposal problems as they arise. Such engineering solutions must necessarily be of limited application and, moreover, they must always be conservative, at least until sufficient broad understanding is obtained.

MAJOR UNSOLVED PROBLEMS

Some of the major basic problems that should be included in the research program can be briefly outlined:

1. Dispersion in the upper mixed layer

Fairly extensive information is available on the mean velocities and transport of the major surface currents. The transient currents and eddies that result in dispersion in both the horizontal and vertical directions are, on the contrary, not understood. Some empirical parameters approximately describing the relationships of diffusivity to time and to size of area have been developed, but understanding of the detailed physical principles is lacking. In consequence, it is not possible to predict on the basis of more elementary properties the dispersion of materials introduced into the upper layer at a given point. Direct measurements must be made, and these are costly and not necessarily reliable. Basic research on the turbulent motion of water in the upper layer is needed.

2. Circulation in the intermediate and deep layers

For the region of the sea below the surface layer, we not only do not understand the nature of the turbulent motion, we do not even have a description of the mean currents. The charting of the deep currents, and investigations toward elucidating the physical principles involved should be vigorously pursued.

3. Exchange between the surface layer and deeper layers

It is important to determine the average rate of exchange of water between the surface and the deep layers, as a basis of estimating average "hold up" times of dissolved materials deposited in the deep layer. It is probably even more important to measure the heterogeneity in the exchange system, that is to measure the rates of exchange in different areas and depths. We know that vertical exchange is much more rapid in some parts of the oceans than others, but describing it in quantitative terms can be done only in a very sketchy manner. Quantitative data on this subject are required as one basis of arriving at estimates of the amount of atomic wastes that can be deposited safely in specified parts of the deep sea.

4. Sedimentation processes

Sedimentation processes constitute an important mechanism for removing atomic wastes from the waters of the oceans. In order to evaluate their role, however, we need to measure the average times that different elements remain in the sea before being deposited in the sediments, the rates of sedimentation in different parts of the deep sea, and the ability of the sediments to capture and retain various fission products.

5. Effects of the biosphere on the distribution and circulation of elements

As we have noted, marine organisms have profound effects in modifying the distribution and circulation of elements in the sea. It is vitally necessary that the biological processes be studied in sufficient detail to enable their effects to be quantitatively evaluated. Such investigations need to include: The flux of various elements through the different trophic levels, and the variations in different ecological realms such as inshore coastal waters, offshore surface waters and the deep sea; the effects of vertical and horizontal migrations of organisms on redistribution of elements; the effects of the uptake, modification of the physical state, and elimination of elements by members of the marine biosphere on their subsequent distribution in the sea.

6. Uptake and retention of elements by organisms used as food for man

Related to the foregoing, but of separate importance, is the study of the quantities of radioactive elements deposited in different situations in the sea that can be expected to be taken up by organisms harvested for food, the length of time such elements are retained in the food organisms, and, consequently, the levels of concentration. Some parts of some organisms are not eaten by man, but are discarded or used for other purposes. The sites of accumulation of different radioactive elements in the organisms must therefore be determined.

7. Effects of atomic radiation on populations of marine organisms

In order to determine what quantities of atomic wastes can be safely deposited in the sea without upsetting the ecology of the sea through destruction of important populations of organisms, research is needed on the somatic and genetic effects of atomic radiation on marine populations. This is especially important for organisms of the deep sea which may come in contact with very high concentrations of radioactive elements, if deep sea disposal of large quantities proves feasible in other respects.

RESEARCH METHODS

Much of this required research can be accomplished by the intensive application of classical techniques of physics, chemistry, geology, and biology. In addition, however, the availability of radioactive isotopes provides us with a powerful new tool, which is especially valuable for studying *processes.* The use of radioactive elements as tracers permits the paths of various elements, both in the physical environment and within the biosphere, to be determined, and the fluxes of the elements through various parts of the system to be measured.

Radioactive tracers are useful both in laboratory experiments and in field studies of various kinds. The use of tracers in the laboratory and in small scale field experiments is already familiar. Information from the tracers introduced into the sea by weapons tests has provided valuable information. What has not yet been done, and what we believe will be a fruitful approach, is the employment of fairly large quantities of radio isotopes to study the various processes in the open ocean in a planned fashion. In Chapters of this report by Folsom and Vine and by Schaefer, suggestions are made for some experiments that should be useful and are currently feasible.

Naturally occurring radioactive isotopes can also provide a fruitful means of attack. Craig, in Chapter 11, discusses some of these avenues of research in detail.

FACILITIES REQUIRED

The Committee has not attempted to draw up detailed estimates of men, ships, and facilities which will be required for an adequate attack on this problem. These requirements will, however, be large. The problems outlined above are among the most difficult in the marine sciences. Adequate solutions will demand the collection of much more knowledge about the sea and its contents than the total obtained in the past hundred years.

Because of the urgency of these problems, and because of the large costs involved, it is essential that research be coordinated on both the national and international levels. Coordination among scientists engaged in these studies should be easier in the future than it has been in the past.

OTHER BENEFITS OF THE RESEARCH TO MANKIND

The potential requirement for disposal of atomic wastes in the sea is sufficient reason for pursuit of these investigations. However, mankind will derive additional, and perhaps even greater, benefits in other ways. For example, the flux of materials through the various trophic levels of the biosphere is the fundamental process underlying the harvest of the sea fisheries. This process must be studied to provide part of the basis for atomic waste disposal, but its elucidation will also provide much of the scientific base for the optimum exploitation and conservation of the seas' living resources by man.

IX. CONCLUSIONS AND RECOMMENDATIONS

We repeat here the conclusions and recommendations that were agreed upon by the members of the Committee at the time they prepared the Summary Report published by the Academy in 1956:

1. Tests of atomic weapons can be carried out over or in the sea in selected localities without serious loss to fisheries if the planning and execution of the tests are based on adequate knowledge of the biological regime. The same thing is true of experimental introduction of fission products into the sea for scientific and engineering purposes.

2. Within the foreseeable future the problem of disposal of atomic wastes from nuclear fission power plants will greatly overshadow the present problems posed by the dispersal of radioactive materials from weapons tests. It may be convenient and perhaps necessary to dispose of some of these industrial wastes in the oceans. Sufficient knowledge is not now available to predict the effects of such disposal on man's use of other resources of the sea.

3. We are confident that the necessary knowledge can be obtained through an adequate and long-range program of research on the physics, chemistry, and geology of the sea and on the biology of marine organisms. Such a program would involve both field and laboratory experiments with radioactive material as well as the use of other techniques for oceanographic research. Although some research is already under way, the level of effort is too low. Far more important, much of the present research is too short-range in character, directed towards *ad hoc* solutions of immediate engineering problems, and as a result produces limited knowledge rather than the broad understanding upon which lasting solutions can be based.

4. We recommend that in future weapons tests there should be a serious effort to obtain the maximum of purely scientific information about the ocean, the atmosphere, and marine organisms. This requires, in our opinion, the following steps: (1) In the planning stage committees of disinterested scientists should be consulted and their recommendations followed; (2) funds should be made available for scientific studies unrelated to the character of the weapons themselves; (3) the recommended scientific program should be supported and carried out independently of the military program rather than on a "not to interfere" basis.

5. Ignorance and emotionalism characterize much of the discussion of the effects of large amounts of radioactivity on the oceans and the fisheries. Our present knowledge should be sufficient to dispel much of the overconfidence on the one hand and the fear on the other that have characterized discussion both within the Government and among the general public. In our opinion, benefits would result from a considerable relaxation of secrecy in a serious attempt to spread knowledge and understanding throughout the population.

6. Sea disposal of radioactive waste materials, if carried out in a limited, experimental, controlled fashion, can provide some of the information required to evaluate the possibilities of, and limitations on, this method of disposal. Very careful regulation and evaluation of such operations will, however, be required. We, therefore, recommend that a national agency,

with adequate authority, financial support, and technical staff, regulate and maintain records of such disposal, and that continuing scientific and engineering studies be made of the resulting effects in the sea.

7. We recommend that a National Academy of Sciences—National Research Council committee on atomic radiation in relation to oceanography and fisheries be established on a continuing basis to collect and evaluate information and to plan and coordinate scientific research.*

8. Studies of the ocean and the atmosphere are more costly in time than in money, and time is already late to begin certain important studies. The problems involved cannot be attacked quickly or even, in many cases, directly. The pollution problems of the past and present, though serious, are not irremediable. The atomic waste problem, if allowed to get out of hand, might result in a profound, irrecoverable loss. We, therefore, plead with all urgency for immediate intensification and redirection of scientific effort on a world-wide basis towards building the structure of understanding that will be necessary in the future. This structure cannot be completed in a few years; decades of effort will be necessary and mankind will be fortunate if the required knowledge is available at the time when the practical engineering problems have to be faced.

9. The world-girdling oceans cannot be separated into isolated parts. What happens at any one point in the sea ultimately affects the waters everywhere. Moreover, the oceans are international. No man and no nation can claim the exclusive ownership of the resources of the sea. The problem of the disposal of radioactive wastes, with its potential hazard to human use of marine resources, is thus an international one. In certain countries with small land areas and large populations, marine disposal of fission products may be essential to the economic development of atomic energy. We, therefore, recommend: (1) that cognizant international agencies formulate as soon as possible conventions for the safe disposal of atomic wastes at sea, based on existing scientific knowledge; (2) that the nations be urged to collaborate in studies of the oceans and their contained organisms, with the objective of developing comparatively safe means of oceanic disposal of the very large quantities of radioactive wastes that may be expected in the future.**

10. Because of the increasing radioactive contamination of the sea and the atmosphere, many of the necessary experiments will not be possible after another ten or twenty years. The recommended international scientific effort should be developed on an urgent basis.

11. The broader problems concerned with full utilization of the food and other resources of the sea for the benefit of mankind also require intensive international collaboration in the scientific use of radioactive material.

REFERENCES

Anon. 1956. Report of a meeting of United Kingdom and United States scientists on biological effects of radiation in oceanography and fisheries. Nat. Acad. Sci.—Nat. Research Council, Oct. 31, 1956, 8 pp. (mimeographed).

Bowden, K. F. 1954. The direct measurement of subsurface currents in the oceans. *Deep Sea Research,* Vol. 2, pp. 33-47.

Culler, F. L. 1954. Notes on fission product wastes from proposed power reactors. ORNL Central File No. 55-4-25.

Dietrich, G. 1957. Selection of suitable ocean disposal areas for radioactive waste. (A preliminary report with 6 charts.) M.S., 10 pp.

Food and Agriculture Organization of UNESCO. 1957. Yearbook of fishery statistics. FAO, Rome, Vol. 5 (1954-55).

Goldberg, E. and Arrhenius, G. O. S. 1957. Chemistry of Pacific pelagic sediments. In press.

Greendale, A. E., and N. E. Ballou. 1954. Physical state of fission product elements following their vaporization in distilled water and sea water. USNRDL Document 436, pp. 1-28.

Harley, John E. (Editor). 1956. Operation Troll. U.S., A.E.C., N.Y. Operations office 1956. 37 pp.

---

* The President of the Academy, Dr. Detlev W. Bronk, has requested that the present committee undertake to develop and carry forward this continuing program.

** As a first step in this direction an informal discussion was held by members of this committee with scientists from the United Kingdom at North Falmouth, Massachusetts, on September 27 and 28, 1956. A brief summary of the meeting was published by the National Academy of Sciences (Anon., 1956).

HIYAMA, Y. 1956. Maximum permissible concentration of Sr 90 in food and its environment. Records of Oceanographic Work in Japan, Vol. 3, No. 1, March 1957, pp. 70-77.

HIYAMA, Y., and R. ICHIKAWA. 1956. Movement of fishing grounds where contaminated tuna were caught. Japan Society for the Promotion of Science; Research in the Effects and Influences of the Nuclear Bomb Test Explosions, pp. 1079.

JAPANESE FISHERY AGENCY. 1955. Report on the investigations of the effects of radiation in the Bikini region. Res. Dept., Jap. Fish. Agency, Tokyo, 191 pp.

KAWABATA, T. 1956. Movement of fishing grounds where contaminated tuna were caught. Japan Society for the Promotion of Science; Research in the Effects and Influences of the Nuclear Bomb Test Explosions, pp. 1085.

KRAUSKOPF, K. B. 1956. Factors controlling the concentration of thirteen rare metals in sea water. *Geochim. et Cosmochim.* Acta 9, pp. 1-32.

KULP, J. L., ECKELMANN, W. R., and A. R. SCHULERT. 1957. Strontium 90 in man. *Science,* Vol. 125, No. 3241, pp. 219-225.

LAEVASTU, T., and T. G. THOMPSON. 1956. The determination and occurrence of nickel in sea water, marine organisms, and sediments. *Jour. du Cons.,* Vol. 21, pp. 125-143.

LAPP, RALPH E. 1956. Strontium limits in peace and war. *Bull. Atomic Scientists,* Vol. 12, No. 8, pp. 287-289, 320.

LIBBY, W. F. 1956a. Radioactive fallout and radioactive strontium. *Science,* Vol. 123, pp. 657-660.

1956b. Radioactive strontium fallout. *Proc. Nat. Acad. Sci.,* Vol. 42, No. 6, pp. 365-390.

MIYAKE, J., SUGIURA, Y., and K. KAMEDA. 1955. On the distribution of radioactivity in the sea around Bikini Atoll in June 1954. *Pap. Meteorol. Geophys.,* Tokyo, Vol. 5, No. 3-4, pp. 253-262.

MUNK, W. H. 1950. On the wind-driven ocean circulation. *Jour. Meteorol.,* Vol. 7, No. 2, pp. 79-93.

MUNK, W. H., EWING, G. C., and R. R. REVELLE. 1949. Diffusion in Bikini lagoon. *Trans. Am. Geophys. Union,* Vol. 30, No. 1, pp. 59-66.

NATIONAL BUREAU OF STANDARDS. 1953. Maximum permissible amounts of radio isotopes in the human body and maximum permissible concentrations in air and water. U.S. Dept. of Commerce, Nat. Bureau Standards. Handbook 52, 45 pp.

1954. Radioactive waste disposal in the ocean. Nat. Bureau of Standards. Handbook 58, 31 pp.

NUCLEONICS. 1956. Calder Hall, over-all description. *Nucleonics,* Vol. 14, No. 12, pp. S10-S11.

1957. Roundup of key developments in atomic energy. *Nucleonics,* Vol. 15, No. 6, pp. 17-28.

RANKAMA, K., and T. C. SAHAMA. 1950. Geochemistry. Univ. of Chicago Press, 1950.

REVELLE, R. R. 1957. Statement by Professor Roger Revelle before the joint Committee on atomic energy, 28 May 1957. The Nature of Radioactive Fallout and its Effects on Man; *Hearings before the Special Subcommittee on Radiation of the Joint Committee on Atomic Energy.* Congress of the United States, 1957.

REVELLE, R. R., FOLSOM, T. R., GOLDBERG, E. D., and J. D. ISAACS. 1955. Nuclear Science and Oceanography. Int. Conf. on the Peaceful Uses of Atomic Energy. A/Conf. 8/P/277, 22 pp. (mimeographed).

SELIGMAN, N. 1955. The discharge of radioactive waste products into the Irish Sea. Part I: First experiment for the study of movement and dilution of released dye in the sea. Proc. Int. Conf. on Peaceful Uses of Atomic Energy, United Kingdom paper number 418, 25 pp.

SVERDRUP, H. U., JOHNSON, M. W., and R. H. FLEMING. 1942. The Oceans. Prentice Hall, New York, 1942, 1060 pp.

SWALLOW, J. C. 1955. A neutral-buoyancy float for measuring deep currents. *Deep Sea Research,* Vol. 3, pp. 74-81.

VINOGRADOV, A. P. 1953. The elementary composition of marine organisms. Sears Foundation for Marine Research, Memoir No. 2, 647 pp.

WÜST, G. 1957. Report on the current velocities, volume transports and mixing effects in the Atlantic deep sea as physical processes important to the transport and dispersal of radioactive wastes. M. S. (mimeographed), 19 pp.

Reprinted from
THE EFFECTS OF ATOMIC RADIATION ON OCEANOGRAPHY AND FISHERIES
PUBLICATION NO. 551, NATIONAL ACADEMY OF SCIENCES—NATIONAL RESEARCH COUNCIL, 1957

CHAPTER 7

ECOLOGICAL FACTORS INVOLVED IN THE UPTAKE, ACCUMULATION, AND LOSS OF RADIONUCLIDES BY AQUATIC ORGANISMS[1]

LOUIS A. KRUMHOLZ, *Department of Biology, University of Louisville,* Louisville, Kentucky

EDWARD D. GOLDBERG, *Scripps Institution of Oceanography, University of California,* La Jolla, California

HOWARD BOROUGHS, *Hawaii Marine Laboratory, University of Hawaii,* Honolulu, T. H.

Introduction

THIS paper is concerned with the uptake, accumulation, and loss by living organisms, of radioactive materials that may be added to or induced in an aquatic environment. These aquatic organisms may live in either fresh, salt, or brackish water and include vascular plants, algae, protozoans, plankton, all the other invertebrate forms such as aquatic insects, bottom-living crustaceans and molluscs, and representatives of each of the five classes of vertebrate animals.

The accumulation and loss of any radioisotope will depend not only upon its own physical half-life but also upon the biological factors that contribute to its incorporation in, retention by, and disappearance from the organism involved. In general, all isotopes of any one chemical element are similar in chemical behavior, and thus it can be assumed, when tracing the paths of most chemical elements through biological systems, that a radioactive atom will behave in the same way as a non-radioactive atom of the same species. However, relatively little is known about the actual mechanisms of uptake, accumulation, and loss by marine and fresh-water organisms of the elements whose isotopes constitute fission products and other radiomaterials.

For the purposes of this discussion, the following terms will be defined:

Uptake is the amount of material that enters the organism in question and the speed at which the material enters is the rate of uptake.

Loss is the amount of material that leaves the organism, and the speed at which it leaves is the rate of loss.

Accumulation is the amount of material that is present in the organism at a given time, and the rate of accumulation is the amount accumulated per unit time. In practice, the accumulation is the difference between the uptake and the loss.

Metabolic processes include all the chemical changes concerned in the building up and destruction of living protoplasm. During these changes, energy is provided for the vital processes and for the assimilation of new materials.

Specific activity is the ratio between the amount of radioactive isotope present and the total amount of all other isotopes of that same element, both radioactive and stable. Most commonly, it is given as the microcuries of radioisotope per gram of total element.

Although the higher animal forms are dependent upon the primary concentrators, the plants, for their source of energy, these animals may or may not be dependent upon the lower forms for many elements. Some elements may enter the bodies of the higher forms directly from the water, while others must be supplied from the lower trophic levels through the food web. These food webs are not the same for all organisms and may even be different for the same organism at various seasons of the year. In some instances certain elements, although present in the environment, are not in the proper physical and/or chemical state to be utilized by the organisms and thus are not available for metabolism.

Radionuclides may become associated with an organism either through adsorption to surface areas, through engulfment, or through metabolic

---

[1] Contribution No. 9 (New Series) from the Department of Biology, University of Louisville. Contribution from the Scripps Institution of Oceanography, New Series, No. 901a. Contribution from the Hawaii Marine Laboratory, No. 94.

Reproduced by Permission

processes; in some instances assimilation may take place following the engulfment of living or inert particulate matter. A radionuclide may also be incorporated into an organism by simple exchange of the radioactive isotope for the stable isotope of the same species. It is therefore important to know the physical and chemical state necessary for metabolism, the mode of entry, and the ability of all organisms at each of the different trophic levels to concentrate the various radionuclides.

Physical and Chemical Factors Concerned with the Uptake of Radionuclides by Living Organisms

a. *Acute versus chronic exposure*

Chronic exposure of an aquatic organism, even to low concentrations of radiomaterials, usually has a markedly different effect on the organism than an acute exposure; the principal difference lies in the amount of radiomaterial accumulated in the tissues. Because many aquatic organisms have the ability to concentrate radiomaterials from their environments by factors up to several hundred thousand, much radiomatèrial may be accumulated during a chronic exposure for a relatively long period of time. A state of equilibrium is ultimately reached at which there is a constant uptake and a constant loss with a resultant constant maximum level of accumulation. Conversely, in an acute exposure, such as a single feeding or a single injection of radiomaterials, only a certain relatively small fraction of the radiomaterial is accumulated in the body and the remainder is lost. In such an instance, the maximum level to which an organism is capable of accumulating the radiomaterial in question is seldom reached and certainly not maintained.

Krumholz and Rust (1954) reported an accumulation of one microcurie of strontium 90 per gram of bone in the entire skeleton of a muskrat (*Ondatra zibethica*) which had been utilizing foods of its own choice in the area contiguous to the Oak Ridge National Laboratory. Certainly this instance can be presumed to represent a chronic exposure inasmuch as the animal was at least two years old and had probably lived in the area during her entire lifetime. Aquatic organisms in the Columbia River below the Hanford Works and those in White Oak Creek, Tennessee, below the Oak Ridge National Laboratory, have all suffered chronic exposures to radiomaterials and have accumulated considerable amounts of those materials in their tissues. Hiatt, Boroughs, Townsley, and Kau (1955) found that the daily feeding of strontium 89 to the fish *Tilapia* for short periods of time (four days) did not increase the level of strontium retention after an apparent steady-state condition had been reached. However, there are no published reports of the results of long-term, controlled experiments of chronic exposures of aquatic organisms to radiomaterials.

The literature contains many reports concerned with acute exposures of aquatic organisms to radiomaterials. Martin and Goldberg (unpublished data), who gave single feedings of strontium 90 to Pacific mackerel (*Pneumatophorus japonicus diego*), found that less than five per cent of the amount fed was retained in the body after 48 hours. Much of the five per cent that was incorporated in the skeleton remained there for the duration of the experiment (235 days). Boroughs et al. (1956) reported that between only one and two per cent of the strontium 89 fed to ten yellowfin tuna (*Neothunnus macropterus*) remained in the body after 24 hours. The small amount retained in the body was largely incorporated into the skeletal structures. However, other fish (*Tilapia*) which had been fed similarly prepared strontium 89 capsules retained about 20 per cent of the ingested material after 24 hours. After four days, the amount retained finally levelled off at values that ranged from 1.5 to 19.5 per cent of the amount ingested; the average amount retained was about 7.5 per cent. Here, again, the retained materials were incorporated mainly in the skeletal structures and integument.

b. *Chemical and physical states of the elements in the environment.*

The chemical composition of the marine environment cannot be rigorously defined. The concentrations of elements depend upon the type and location of the water mass. Although more than 90 per cent of marine waters occur at depths greater than 1000 meters, the majority of chemical analyses have been made for shallower waters. Because of the biological activity of the oceans and the movements and origins of water masses, the abundance of certain elements appears to vary by factors greater than two orders of magnitude. However, as a

(40)

first approximation, the chemical constituents may be considered to be much the same in all places. Fairly good approximations of the concentrations of elements in sea water are listed in Table 1 as the numbers of atoms per million atoms of chlorine. The reported values of concentrations of elements on which Table 1 is based frequently fail to distinguish between the solid and dissolved phases.

Whereas the oceans may be considered very roughly as a homogeneous mass, most bodies of fresh water must be examined on an individual basis because of the tremendous range in their physical and chemical characteristics. Many of the elements that occur normally in the oceans are in concentrations too small to be detected by present methods or are present in only trace amounts in fresh water. The pH of fresh waters ranges from perhaps as low as 2.2 to a high of about 10.5 although the pH of most lakes and streams falls somewhere between 6.5 and 8.5. The total dissolved solids in fresh waters ranges

TABLE 1 CHEMICAL ABUNDANCES IN THE MARINE HYDROSPHERE

	mg/l	atoms/10^6 atoms Cl
H	108,000	202,000,000
He	0.000005	.002
Li	0.2	50
Be		
B	4.8	830
C	28	4,300
N	0.5	70
O	857,000	100,000,000
F	1.3	130
Ne	0.0003	0.03
Na	10,500	850,000
Mg	1,300	100,000
Al	0.01	0.7
Si	3	200
P	0.07	4
S	900	52,000
Cl	19,000	1,000,000
A	0.6	28.5
K	380	18,000
Ca	400	19,000
Sc	0.00004	0.002
Ti	0.001	0.04
V	0.002	0.08
Cr	0.00005	0.002
Mn	0.002	0.07
Fe	0.01	0.3
Co	0.0005	0.02
Ni	0.0005	0.02
Cu	0.003	0.09
Zn	0.01	0.3
Ga	0.0005	0.01
Ge	< 0.0001	< 0.003
As	0.003	0.07
Se	0.004	0.1
Br	65	1,500
Kr	0.0003	0.007
Rb	0.12	2.2
Sr	8	160
Y	0.0003	0.006
Zr		
Nb		
Mo	0.01	0.2
Tc		
Ru		
Rh		
Pd		
Ag	0.0003	0.005
Cd	0.000055	0.0009
In	< 0.02	< 0.3
Sn	0.003	0.05
Sb	< 0.0005	< 0.008
Te		
I	0.05	0.7
Xe	0.0001	0.001
Cs	0.0005	0.005
Ba	0.0062	0.008
La	0.0003	0.004
Ce	0.0004	0.005
Pr		
Nd		
Pm		
Sm		
Eu		
Gd		
Tb		
Dy		
Ho		
Er		
Tm		
Yb		
Lu		
Hg		
Ta		
W	0.0001	0.001
Re		
Os		
Ir		
Pt		
Au	0.000004	0.00004
Hg	0.00003	0.0003
Tl	< 0.00001	< 0.00009
Pb	0.003	0.03
Bi	0.0002	0.002
Po		
At		
Rn	9.0×10^{-15}	8.0×10^{-14}
Fr		
Ra	3.0×10^{-11}	2.0×10^{-10}
Ac		
Th	0.0007	0.006
Pa	0.003	0.03
U		

from very low concentration (less than 5 ppm) in the "battery-water" lakes to very high concentrations (more than 400 ppm) in the "alkali" lakes. The fertility of fresh waters ranges from the almost sterile bog lakes to the highly productive lakes in the midwestern prairies.

The physical states and ionic speciation of elements in sea water cannot be as well defined as their absolute concentrations. However, using the known physicochemical constants, and assuming a pH of 8 and a salinity of 35 parts per thousand for sea water, Krauskopf (1956) postulated that the principal valence states of the ions of a number of metals in sea water are as listed in Table 2. From these data it may be concluded that most monovalent or divalent ions, except the noble metals, will occur as cations whereas most metals with valences higher than two, and the noble metals, will occur as anions.

TABLE 2 CALCULATED VALENCE STATES FOR METALLIC IONS IN SEA WATER
(From Krauskopf, 1956)

Element	Ion
Zinc	Zn^{++}, $ZnCl^{+}$
Copper	Cu^{++}, $CuCl^{+}$
Bismuth	BiO^{+}
Cadmium	$CdCl^{+}$, $CdCl_2$
Nickel	Ni^{++}, $NiCl^{+}$
Cobalt	Co^{++}
Mercury	$HgCl_4^{-}$
Silver	$AgCl_2^{-}$
Gold	$AuCl_4^{-}$ (Calculated by Goldberg)
Chromium	CrO_4^{-}
Vanadium	$H_2VO_4^{-}$, $H_3V_2O_7^{-}$
Magnesium	Mg^{++}
Calcium	Ca^{++}
Strontium	Sr^{++}
Barium	Ba^{++}

The physical states of a given element under equilibrium conditions depend upon whether or not the solubility product of the least soluble species has been exceeded. Greendale and Ballou (1954) have determined the distribution of elements among the soluble, colloidal, and particulate states by simulating the conditions of an underwater detonation of an atomic bomb. Their data are presented in Table 3.

It is not known whether the elements that occur in colloidal or particulate phases are homogeneous entities or are sorbed in other solid phases. Nevertheless, it appears that elements of Groups, I, II, V, VI, and VII usually occur as ionic forms in sea water, whereas other elements, excluding the rare gases, occur predominantly as solid phases. These generalizations have been confirmed in field tests after underwater detonations where more than 50 per cent of the resultant radioactivity was associated with solid phases retained by a molecular filter of pore size 0.5 micron (Goldberg, unpublished data).

Although the data supplied by Greendale and Ballou (1954) are of value for the physical states of elements following the detonation of an atomic bomb, they are at best only suggestive of the steady-state conditions which might result from the continuous spilling of fission product wastes into the sea on a long-term basis.

TABLE 3 PHYSICAL STATES OF ELEMENTS IN SEA WATER

(From Greendale and Ballou, 1954)

	Percentage in given physical state		
Element	Ionic	Colloidal	Particulate
Cesium	70	7	23
Iodine	90	8	2
Strontium	87	3	10
Antimony	73	15	12
Tellurium	45	43	12
Molybdenum	30	10	60
Ruthenium	0	5	95
Cerium	2	4	94
Zirconium	1	3	96
Yttrium	0	4	96
Niobium	0	0	100

Metabolic processes concerned with the uptake, accumulation, and loss of radionuclides

There are many factors concerned with metabolic processes which are to be considered among the biological aspects of the accumulation of radiomaterials. It has been demonstrated that the metabolism of all forms of life is remarkably similar at the cellular level even though the morphological differences among aquatic organisms range from the bacteria through the vertebrate forms, and from the algae through the vascular plants. Nevertheless, differences do exist. These differences are governed by the complex anatomies, life histories, and physiological processes, and the relationships of the organisms with each other and with their environment. All of these differences must be considered in the light of the physical and chemical states of the elements involved.

In different organisms, ionized or particulate fission-product wastes and other radiomaterials may be either adsorbed, engulfed, or accumulated by metabolic processes. For example, Rothstein and his associates (1951) demonstrated that uranium as the uranyl ion was adsorbed by yeast cells. Hamilton and co-workers (see Hevesy, G., 1948, p. 441) showed that particulate radiomaterials such as various uncomplexed rare earths at physiological pH's were adsorbed by the gut lining of rats. In these experiments practically no accumulation of these particular radiomaterials by the animal was observed. On the other hand, Goldberg (1952) demonstrated with radioactive iron that a marine diatom assimilated particles of hydrated iron oxide, but that these organisms were unable to take up ionic iron in a complexed form.

The first biological experiments in which radioactive atoms were used were performed by Hevesy in 1923. In those classical experiments it was demonstrated that plants could take up lead from solution and translocate it throughout the vascular system.

The accumulation of radioelements is also dependent upon many chemical characteristics of the water in question. Among the parameters affecting accumulation are the salinity, percentage composition of the dissolved solids, pH, the oxygen-carbon dioxide ratio, and the presence of complexing agents.

a. *Chemical composition of marine organisms*

A modern systematic study of the inorganic constituents of marine organisms is yet to be made. The best summary of existing knowledge may be found in Vinogradov (1953).

However, certain generalizations can be drawn from the recent literature on the concentration of metals by marine organisms. Goldberg (in Treatise of Marine Ecology, volume II, edited by J. Hedgpeth, in press) has pointed out that the marine biosphere tends to concentrate such heavy metals as copper, nickel, zinc, etc., over the marine hydrosphere by factors of 100 to 100,000 on a weight-for-weight basis (Table 4). These metals are strongly bound in the organisms and cannot be easily removed by elution. Further, the elements most strongly concentrated in the biosphere are those that form the most stable complexes with organic chelating agents. As an example, copper is concentrated over sea water in the soft parts of most marine organisms by factors of 10^2 to 10^4 whereas calcium shows concentration factors of less than 1 to 50. Copper forms very strong complexes with many organic compounds whereas calcium does not. Although the exact role of most metals in the physiology of organisms is not known, nevertheless, one might *a priori* expect that some heavy metals introduced into the ocean from nuclear reactions would concentrate in the biosphere.

b. *Concentration in the environment*

The concentration of a given radiomaterial by an organism is sometimes proportional to the concentration of that material in the environment. This generalization applies both to aquatic and to terrestrial organisms. The uptake of cesium 137 by the oyster (*Crassostrea virginica*) has been shown to be dependent upon the external concentration of cesium in the sea water (Chipman, et al., 1954). Prosser, et al. (1945), noted that with the addition of strontium to the environment there was an increase in the uptake of that element by goldfish (*Carassius auratus*). Also, it has been demonstrated that as the carrier concentration in the nutrient environment is increased, the concentration factor for a particular fission product in terrestrial plants tends to increase (Rediske, et al., 1955).

c. *Effect of the presence of one element on the uptake of another element*

The uptake of one radioelement by an organism may be altered by the relative abundance of another element in the environment. In instances in which more than one element is involved, one of three phenomena may be observed:

First, elements of similar chemical properties may substitute for one another. For example, it has been shown by Prosser, et al. (1945), that when the amount of calcium in the water was low, there was an increase in the uptake of strontium 89 by goldfish. Conversely, as the amount of calcium was increased, the uptake of strontium decreased. Rice (1956) observed that cells of *Carteria* grown in artificial sea water took up strontium in proportion to the strontium/calcium ratio in the medium. Bevelander and Benzer (1948) have shown that a modification of the constituents of sea water resulted in a change in the constituents of the shells deposited by mollusks.

Second, some elements may have an inhibitory effect on others. A classical example of this phenomenon is that in which calcium inhibits the stimulatory action of potassium on heart muscle.

Third, there may be a synergistic effect of one element on another. Ketchum (1939) has shown that the uptake of phosphorus by marine diatoms was enhanced with increased concentrations of nitrogen.

d. *Specificity of organisms and tissues for given elements*

The specific activity of a radionuclide in any organism is dependent upon the ability of the organism or any of its parts to concentrate that nuclide. If the stable counterpart of the radionuclide does not normally enter into the physiological processes of an organism, neither will the radioactive material.

It is well known that certain tissues have a predilection for concentrating specific elements. For instance, iodine is concentrated in the thyroid tissue of animals and hence radio-iodine will also be concentrated there. Strontium, like calcium, is a bone seeker and the radioisotopes of both of those elements will be concentrated in the bony skeletons of animals. Similarly, both strontium and calcium are concentrated in certain parts of vascular plants and so are the radioisotopes. Phosphorus is one of the principal constituents of bone and radiophosphorus is also concentrated in that tissue. The compound adenosine triphosphate is commonly present in the flight muscles of some birds and it has been shown that radiophosphorus is incorporated into the flight muscles of migratory waterfowl (Krumholz, 1954).

Although many different kinds of aquatic organisms have the ability to concentrate phosphorus in their tissues, there are few that show such a specificity for that element as the various plankters. The uptake of phosphorus 32 by plankton algae in a lake has been demonstrated by Coffin and his associates (1949) and others, and Whittaker (1953) showed that phytoplankters from the Columbia River concentrated radiophosphorus by factors as great as 300,000. Krumholz (1954, 1956) found that attached fresh-water algae (*Spirogyra*) concentrated radiophosphorus by a factor of 850,000, and that many fresh-water zooplankters concentrated that radionuclide by factors of more than 100,000. Approximate concentration factors for marine organisms are given in Table 4.

TABLE 4 Approximate Concentration Factors of Different Elements in Members of the Marine Biosphere. The Concentration Factors are Based on a Live Weight Basis.

				Concentration Factors			
				Invertebrates		Vertebrates	
Element	Form in Seawater	Concentration in seawater (micrograms/1.)	Algae (Non-calcareous)	Soft	Skeletal	Soft	Skeletal
Na	Ionic	10^7	1	0.5	0	0.07	1
K	Ionic	380,000	25	10	0	5	20
Cs	Ionic	0.5	1	10	—	10	—
Ca	Ionic	400,000	10	10	1,000	1	200
Sr	Ionic	7,000	20	10	1,000	1	200
Zn	Ionic	10	100	5,000	1,000	1,000	30,000
Cu	Ionic	3	100	5,000	5,000	1,000	1,000
Fe	Particulate	10	20,000	10,000	100,000	1,000	5,000
Ni[1]	Ionic	2	500	200	200	100	—
Mo	Ionic-Particulate	10	10	100	—	20	—
V	?	1	1,000	100	—	20	—
Ti	?	1	1,000	1,000	—	40	—
Cr	?	0.05	300	—	—	—	—
P	Ionic	70	10,000	10,000	10,000	40,000	2,000,000
S	Ionic	900,000	10	5	1	2	—
I	Ionic	50	10,000	100	50	10	—

[1] Values from Laëvastu and Thompson (1956).

e. *Osmotic and ionic regulation*

Osmotic and ionic regulation are known to occur in a variety of ways. The usual pathways of excretion are through the urine, feces, skin, respiration, and particle ejection, and the method of excretion depends upon the particular organism and element involved. Ionic regulation may also occur by way of the chloride secreting cells in the gills of those fishes that migrate from salt to brackish water (Keys, 1931). Unfortunately, no experiments on such ionic regulation have been performed with radionuclides.

f. *Reproductive processes*

The reproductive processes of plants and animals range from simple fission among the unicellular organisms to the very complex relationships among the gametogenic forms. During reproduction there is a transfer of materials from the parent to the offspring.

In simple fission, the parent cell splits in two and each offspring receives approximately half of the parent material and thus only half of any radiomaterial that may have been present. Under conditions of chronic exposure, the offspring of organisms that reproduce by fission will incorporate usable radiomaterials into their bodies and a state of equilibrium eventually will be reached.

Among the egg-laying forms, most of the material received by the offspring is derived from the contents of the egg. In this form of reproduction, once the egg is laid there will be no further loss of radiomaterials from the mother or gain to the offspring. This applies even when the environment is contaminated and there is chronic exposure of the parents, because the protective coverings of the egg prevent the entrance of radiomaterials.

Among the forms that bear their young alive, however, there is usually some continuous transport of materials between the mother and the embryo. In such an instance it is probable that the embryo will accumulate radiomaterials with a resultant loss to the mother. If chronic exposure of a mother carrying an embryo continues during pregnancy, a state of equilibrium may eventually be reached between the mother and the environment and between the mother and the embryo.

During embryological development of all kinds there is a "biological dilution" of radiomaterials through cell division and growth. This statement applies primarily if there has been an acute exposure to radiomaterials or if the exposure has stopped with the commencement of the embryological development.

g. *Molting*

In instances where the embryos pass through a series of metamorphic stages, there is a loss of radiomaterials from stage to stage as, for example, the loss from instar to instar in insects through molting. Furthermore, it has been demonstrated by Chipman and coworkers (personal communication) that there is an increased accumulation of elemental constituents in crustaceans prior to molting, and a loss of such materials when the carapace is lost.

h. *Age and growth*

It has been established (Olson and Foster, 1952) that younger, more rapidly growing fishes accumulate relatively greater amounts of radiomaterials than do older, more slowly growing individuals. This phenomenon is probably a reflection of the more rapid metabolism that accompanies the growth of the younger fishes. It is not known whether the accumulation of radiomaterials by other aquatic vertebrates and invertebrates is a function of age and growth.

i. *Effect of temperature on cold-blooded and warm-blooded animals*

In general, the body temperatures of warm-blooded animals are more or less constant whereas the body temperatures of cold-blooded animals largely depend upon the temperature of the environment. Similarly, the rate of metabolism in warm-blooded animals is generally independent of temperature changes in the environment while that in the cold-blooded animals is largely dependent upon external temperatures. Changes in temperature affect the rates of chemical reactions and hence chemical processes that involve the accumulation of elements in the body tissues are temperature dependent.

Generally speaking, all cold-blooded aquatic organisms exhibit seasonal changes in the uptake and accumulation of radiomaterials from the environment. Davis, et al. (1953), and Krumholz (1954, 1956) have shown that there is a direct correlation between an increase in temperature and an increase in the accumulation of radiomaterials in fishes of the Columbia River, Washington, and of White Oak Lake, Tennessee, respectively. This increase in accumulation is apparently a reflection of the increase in the speed of the metabolic processes with rising water temperatures. However, Krumholz (1956) suggested that the fishes in White Oak Lake entered a period of dormancy following August 1 and lost about two-thirds of their accumulated radioactivity during the subsequent two months even though the water temperatures were much the same as they were during the earlier part of the summer.

In studies of the uptake of strontium 89 by oysters and other shellfish at the Radiation Laboratory of the Fish and Wildlife Service (Chipman, unpublished data) it was found that the rate of uptake was slowed down and the retention time was extended when the animals were kept in sea water at low winter temperatures. Conversely, the rate of uptake was speeded up and the retention time was shortened when the animals were kept at summer temperatures. In other experiments at the same laboratory, it was found that larvae of the winter flounder (*Pseudopleuronectes americanus*) took up strontium 89 much more rapidly at higher water temperatures than at lower.

So far as is known, there is no demonstrable seasonal pattern of accumulation of radiomaterials among the warm-blooded aquatic vertebrates. It is generally believed that inasmuch as the body temperatures of those animals remain more or less constant throughout the year there will be no marked seasonal changes in the uptake of radiomaterials based on changes in rates of metabolism.

j. *Effect of light*

Light affects the uptake and accumulation of radioelements by plants. For example, it has been clearly shown by Scott (1954) that the uptake of radiocesium by the algae *Fucus* and *Rhodymenia* was greatly enhanced in the presence of light.

k. *Radiation effects*

Many aquatic organisms have the ability to concentrate radiomaterials in amounts deleterious to their well-being. These deleterious effects range from those in which only the individual is concerned to those in which the population as a whole may be affected. Elsewhere in this series of reports there is a paper on the effects of radiation on aquatic organisms.

Aspects of the accumulation of radionuclides through the ecosystem

For purposes of this paper, the aquatic biosphere can be divided into three trophic levels based on energy sources:

1. Primary producers, such as the photosynthetic plants.
2. Primary consumers, the herbivores, such as water fleas (cladocerans).
3. Secondary consumers, the carnivores, such as the largemouth bass or the tunas.

The community biomass (the total weight of all organisms in the community) is unequally divided between the three trophic levels. Usually there is a progressive decrease in both the biomass and the number of organisms from the first trophic level through the third, and a progressive increase in the size of the organisms. However, most community populations are constantly changing and are affected by seasonal, diurnal, and other cycles of abundance. These changes frequently have a profound effect on the environment and any changes in the environment in turn affect the stability of the community.

Generally speaking, the smaller organisms have a higher reproductive potential, a shorter life span, and a shorter time between generations; the length of the life span and the time between generations usually give a fair indication of the length of the embryological period. Furthermore, the smaller animals usually serve as food for the larger ones.

The discussion will consider the following aspects of the accumulation of radiomaterials in the three trophic levels: (1) the distribution of elements among the three levels, (2) the concentration factors in different organisms within the same level, and (3) the transport of radiomaterials from one trophic level to another.

Problems of the distribution of radionuclides among the trophic levels and the degree of concentration of radionuclides by different organisms can be approached most readily through separate consideration of the effects from an acute exposure and those from a chronic exposure.

A steady-state condition will be approximated when the amounts of radiomaterials introduced into the environment is equal to the amount that disappears through physical decay. Any organisms living in such an environment will suffer chronic exposure to the radioactivity, the level depending, of course, on their ability to concentrate the radiomaterials introduced and on the steady-state concentration of these materials in the surrounding medium. An approximation of the concentration factors for some organisms is given in Table 4.

Davis and co-workers (1952) showed that there was a progressive decrease in the amount of radioactivity found in the aquatic organisms of the Columbia River downstream from the Hanford Works. There, the principal radionuclide was phosphorus 32, which has a physical half-life of about 14 days. It is apparent that when following the steady-state transport of radiomaterials through the ecosystem the following parameters must be considered: (1) the physical half-life of the radionuclide, (2) the distance of the organism from the source of radioactive contamination, and (3) the dilution of the radiomaterials between the point of introduction and the area in which the organism lives.

The results from acute exposure cannot be as definitely approximated as for chronic exposure. In such instances, the time element is very important, and the following must be known: (1) the rate of dilution of the radioactive water mass with non-radioactive water; (2) the rate of transfer of radiomaterials from one trophic level to another with the concurrent dilutions and losses or gains in concentration by the organisms; and (3) the life span of the organisms involved.

In general, the radiomaterials taken up by organisms of the first trophic level will be primarily in the ionized state although a certain amount of particulate radiomaterials will be adsorbed to the body surfaces. When uptake occurs, the rate of uptake will probably be more rapid than the rate of uptake in the other trophic levels.

Particulate radiomaterials tend to be concentrated in the second trophic level. Findings from the Wigwam and Castle tests (Goldberg, unpublished data) showed that the principal organisms which concentrated particulate radiomaterials were the mucous, ciliary, and pseudopodial feeders among the zooplankters. These organisms contained much more radioactivity per unit weight than either the algae or the setal or rapacious feeders.

In addition to the differences in concentration of radiomaterials from one trophic level to another, there are marked differences among species in the same level. For instance, it has been shown by Chipman, et al. (1953), that some phytoplankters will concentrate radiostrontium by a factor of about 20 times whereas others will concentrate the radioelement by factors as much as 1500 times. Comparable data have been recorded by Krumholz (1954) for the accumulation of radiophosphorus by the phytoplankters of White Oak Lake.

Differences also exist between individuals of the same species. Very large differences in the amounts of radiomaterials accumulated by individual fishes in White Oak Lake were described by Krumholz (1956). For instance, he reported that the amounts of radiostrontium in the bones of three bluegills (*Lepomis macrochirus*) differed by more than five-fold. These three fish were taken from the same place in the lake on the same day, August 27, 1952. Comparable differences were found in the amounts of accumulated radiomaterials in most other tissues.

The transfer of radiomaterials from one trophic level to another is not only dependent upon the concentration of the radiomaterial in the organism but also is governed by the rate of growth of the organism and the rate of increase in the size of the population. These factors of transfer are of particular importance in the event of an acute exposure because the dilution brought about through cell division and growth may well minimize any radiation effect. In any event, there is always a loss in the total amount of radiomaterials in the transfer from one trophic level to another (though not necessarily a decrease in the concentration in individual organisms). Such a loss may be relatively small or it may be very great depending upon the organism and the particular food web involved.

Not all radiomaterials that enter the first trophic level are passed on to higher levels. At each trophic level there are certain species that, for one reason or another, are not widely used as food by the organisms of higher levels. Also, some of the plants of the first trophic level may die before they are eaten and thus will be returned to the environment as organic matter. In this case the primary producers may be of little or no importance as a source of radiomaterials to the organisms of the second and third trophic levels.

If relatively large quantities of radiomaterials are accumulated in certain hard parts of an organism, such as the shell of an oyster or the bones of a fish, they will, in all probability, remain in those parts during the greater part of the life of the animal concerned, and will not be available to other animals in the biosphere until the animal dies.

Chipman and co-workers (1953) showed that oysters fed on *Chlorella* assimilated only very little of the radiophosphorus from these algae. On the other hand, oysters fed upon other phytoplankters that contained no more radiophosphorus than the *Chlorella* accumulated relatively large amounts of radiophosphorus and incorporated that element into their tissues as organic phosphorus compounds. It appears that the particular food web used by any organism is of primary importance in the transfer of radiomaterials from one trophic level to another.

Problems for further research

One of the fundamental questions to be answered concerns the mechanism of incorporation of the heavier elements, such as the fission products, in aquatic organisms. To date, no metal heavier than molybdenum has been shown to be necessary for metabolic processes. Specifically, we need to know:

1. How are the radioactive elements passed through membranes and where and why do they concentrate in the organisms?
2. What are their biological half-lives of the different radioactive elements in different organisms?
3. What are the average and extreme concentration levels of these elements in various organisms and in the biosphere?

The revolution in biological thought brought about by the use of labelled atoms is manifest in all branches of biological research today. Radioisotopes have permitted the study of rate processes that could not have been investigated in any other way. Such processes include the pumping rates of water and other biological fluids, and the transfer of molecules or portions of molecules from tissue to tissue, or, on the ecological level, from organism to organism.

REFERENCES

Bevelander, G., and P. Benzer. 1948. Calcification in marine molluscs. *Biol. Bull.* **94**:176–83.

Boroughs, H., S. J. Townsley and R. W. Hiatt. 1956. The metabolism of radionuclides by marine organisms. I. The uptake, accumulation and loss of strontium 89 by fishes. *Biol. Bull.* III:336–351.

Chipman, W. A., T. R. Rice, and T. J. Price. 1953. Accumulation of radioactivity by marine invertebrate animals. U. S. Fish and Wildlife Service Radioisotope Laboratory, Progress Report, April 1953, (Typewritten).

1954. Accumulation of fission products by marine plankton, fish, and shellfish. U. S. Fish and Wildlife Radioisotope Laboratory, Progress Report, July-December 1954, (Typewritten).

Coffin, C. C., F. R. Hayes, L. H. Jodrey, and S. G. Whiteway. 1949. Exchange of materials in a lake as studied by the addition of radioactive phosphorus. *Canad. Jour. Research* **27**:207–222.

Davis, J. J., R. W. Coopey, D. G. Watson, C. C. Palmiter, and C. L. Cooper. 1952. The radioactivity and ecology of aquatic organisms of the Columbia River. *In* Biology Research — Annual Report, 1951, USAEC Document HW-25021, pp. 19–29.

Goldberg, E. D. 1952. Iron assimilation by marine diatoms. *Biol. Bull.* 102, 243–8.

Greendale, A. E., and N. E. Ballou. 1954. Physical state of fission product elements following their vaporization in distilled water and seawater. USNRDL Document 436, pp. 1–28.

Hevesy, G. 1923. Absorption and translocation of lead by plants. *Biochem. Jour.* **17**:439–45.

1948. Radioactive indicators. Interscience Publishers, New York, xvi+555 pages.

Hiatt, R. W., H. Boroughs, S. J. Townsley, and Geraldine Kau. 1955. Radioisotope uptake in marine organisms with special reference to the passage of such isotopes as are liberated from atomic weapons through food chains leading to organisms utilized as food by man. Hawaii Marine Laboratory, Annual Report, AEC project number AT(04–3) 56, pp. 1–29, (Mimeographed).

Ketchum, B. H. 1939. The adsorption of phosphate and nitrate by illuminated cultures of *Nitzchia closterium, Am. J. Botany* **26**:399–402.

Keys, A. B. 1931. Chloride and water secretion and absorption by gills of the eel. *Zeitsch. Vergl. Physiol.* **15**:364.

(48)

Krauskopf, K. B. 1956. Factors controlling the concentrations of thirteen rare metals in sea water. *Geochim. et Cosmochim. Acta* **9**:1–32.

Krumholz, L. A. 1954. A summary of findings of the ecological survey of White Oak Creek, Roane County, Tennessee, 1950–1953. USAEC Document ORO-132, pp. 1–54, (Mimeographed).

1956. Observations on the fish population of a lake contaminated by radioactive wastes. *Bull. Amer. Mus. Nat. Hist.* **110**(4):277–368.

Krumholz, L. A., and J. H. Rust. 1954. Osteogenic sarcoma in a muskrat from an area of high environmental radiostrontium. *A.M.A. Arch. Path.* **57**:270–278.

Laevastu, T., and T. G. Thompson. 1956. The determination and occurrence of nickel in sea water, marine organisms and sediments. *J. du Cons.* **21**:125–143.

Olson, P. A., Jr., and R. F. Foster. 1952. Effect of pile effluent water on fish. *In* Biology Research — Annual Report, 1951. USAEC Document HW-25021, p. 41.

Prosser, C. L., W. Pervinsek, Jane Arnold, G. Svihla, and P. C. Tompkins. 1945. Accumulation and distribution of radioactive strontium, barium-lanthanum, fission mixture and sodium in goldfish. USAEC Document MDDC-496, October 13, 1954.

Rediske, J. H., J. F. Cline, and A. A. Selders. 1955. The absorption of fission products by plants. *In* Biology Research — Annual Report, 1954. USAEC Document HW-35917, pp. 40–46.

Rice, T. R. 1956. The accumulation and exchange of strontium by marine and planktonic algae. *Limnology and Oceanography* **1**(2):123–138.

Rothstein, A., and R. Meier. 1951. The relationship of cell surface to metabolism VI, the chemical nature of the uranium complexing groups of the cell surface. *J. Cell. Comp. Physiol.* **38**:245–70.

Scott, R. 1954. A study of cesium accumulation by marine algae. Proc. Second Radioisotope Conference, pp. 373.

Vinogradov, A. P. 1953. The elementary composition of marine organisms. Sears Foundation for Marine Research, Memoir No. 2.

Whittaker, R. H. 1953. Removal of radiophosphorus contaminant from the water in an aquarium community. *In* Biology Research-Annual Report, 1952. USAEC Document HW-28636, pp. 14–19.

Reprinted from
THE EFFECTS OF ATOMIC RADIATION ON OCEANOGRAPHY AND FISHERIES
PUBLICATION NO. 551, NATIONAL ACADEMY OF SCIENCES—NATIONAL RESEARCH COUNCIL, 1957

CHAPTER 11

ISOTOPIC TRACER TECHNIQUES FOR MEASUREMENT OF PHYSICAL PROCESSES IN THE SEA AND THE ATMOSPHERE[1]

HARMON CRAIG, *Scripps Institution of Oceanography, University of California,*
La Jolla, California

I. *Introduction*

THROUGHOUT this report reference has been made to the need for a fundamental understanding, on a long-term basis, of mixing phenomena in the ocean and the atmosphere. In a general sense the ocean and the atmosphere may be regarded as a two-phase system, in which the phases are separated by the fundamental discontinuity of the ocean-atmosphere interface. Each phase is further divided into two parts by a second order discontinuity; the atmosphere, divided by the tropopause at about 12 km, into the troposphere and the stratosphere, etc., and the oceans, divided by the thermocline at some 100 meters, into an upper and lower layer.

The basic problems in determining the effects of both radioactive waste disposal and the dispersal of debris from nuclear explosions may be formulated in terms of a single objective. Given the ocean-atmosphere system under normal steady state conditions, and given some substance introduced at any point in one of the four designated zones, we wish to be able to predict quantitatively the concentration of the substance as a function of latitude, longitude, altitude or depth, and time. These problems thus involve studies of (1) the intra-phase mixing, above, below, and across the second-order discontinuities within each phase, and (2) the inter-phase mixing across the ocean-atmosphere interface, with the aim of predicting the effects of perturbations on the system.

The dominant mixing processes in the various spheres are processes of mass movement or turbulent mixing. In such processes, for elements undergoing no change of phase, there is little or no separation of components, and thus, in general, isotopic tracer techniques may involve a wide range of materials of quite different chemistry. It is this phenomenon of mass movement dominance, and the relative unimportance of diffusive transfer except in special cases, that makes the tracer technique so powerful; a tagged isotope for each element is not required, and one can choose for each particular study the elements most useful for tracing the movement of a mass of heterogeneous material.

As mentioned at several points in this report, both artificial and natural isotopic tracers may be used for the study of transfer phenomena in the sea and the atmosphere. Artificial tracers are of value in such studies because they allow the investigator to introduce perturbations in the system at convenient times and places; they are especially valuable for the study of short term fluctuations in local systems. However, for the general understanding of mass transfer phenomena, artificial tracers are of value mainly as experimental checks on deductions based on other data, with the exceptions of a few special cases to be described below. The reason for this is that mass transfer phenomena are by nature subject to long term periodic fluctuations such as convection, with periods often longer than the time range available for observation. A second reason for this is the high cost of radioisotopes and the large amounts of activity required to tag adequately the large masses of water necessary for ocean studies.

Revelle, Folsom, Goldberg and Isaacs (1955) have discussed in their Geneva report the problems involved in adapting radioisotope tracer techniques to transfer studies in the ocean, and the requirements for usable isotopes. If one introduces some 10 curies of a gamma emitter in solution at some point below the thermocline, it is found that within a reasonable duration of observation time the activity will be concentrated in a layer of the order of 1 meter thick

---

[1] Contribution from the Scripps Institution of Oceanography, New Series, No. 902.

Reproduced by Permission

spread over a horizontal area of radius r. They find that with the best of present instruments, the horizontal spread in which the concentration of the introduced radioactivity can be determined corresponds to r=1 km. With the possibility of improved instrumentation, and the use of specially selected nuclides, it may be possible to raise the area of detection and determination of activity concentration to about 100 km², an area which is still negligible with respect to oceanic expanses.

The radioisotopes suitable for such measurements must of course have a half-life compatible with the mixing rates to be studied and yet short enough so as not to constitute a permanent hazard, namely of the order of a week to a month. Moreover, they must be available in multi-curie amounts at reasonable cost, should form soluble ionic species in sea-water, have a high specific activity, and, for instrumental reasons, should be gamma emitters with energy between .2 and 1.3 Mev. Revelle, et al., were able to list three such isotopes, which, together with half-life, cost, and other data, are listed in the following table:

Isotope	Half-life	Cost per curie	Specific activity available	Gamma energy Mev
Rb^{86} . . .	19.5 day	$1000	9 mc/gram	1.1
I^{131} . . .	8.0 day	750	Carrier-free	0.36, 0.72
Ba^{140} . . .	12.8 day	500	Carrier-free	0.16, 0.54

Comparison of the cost of these isotopes with the maximum area of detection cited above shows that the study of large-scale transfer phenomena in the oceans, using deliberately introduced artificial radioactivity in the form of specific isotopes, is so costly as to be infeasible with the estimated best instrumentation which will be available in the near future. It is evident that such isotopes are at best adapted only to short-term, small scale studies of local phenomena. The use of mixed fission products on a large scale, discussed elsewhere in this report, is somewhat more feasible but is beset with many difficult problems of transportation and handling.

From these considerations it seems evident that the critical data in studies of atmospheric and oceanic mixing and interaction will come from the use of the naturally occurring isotopic tracers, which reflect in their material balance adjustments the differential rates of transfer from source, through reservoir, to sink, and loss by decay. It is from these transfer rates, adjusted to the steady state geochemical and geophysical cycles of the various elements, that we can hope to gain an understanding of the long period variations in natural transfer phenomena. The importance of gaining a clear understanding of the long period transfer rates, when problems such as storage of potentially hazardous radioactive wastes and cumulative effects of nuclear detonations are considered, cannot be overemphasized.

In the following sections we discuss the present status of our knowledge of the distribution and properties of the various naturally occurring isotopes which are useful for studies of atmospheric and oceanic transfer phenomena. In addition, mention is made of the nuclides produced in nuclear detonations and supplied by reactors which have properties such that they are also useful in such studies and which have been studied to some extent.

II. *Distribution of naturally occurring isotopes of elements adapted for transfer studies*

In this section we discuss the production and occurrence of radioactive and stable isotopes showing measurable isotopic variations, and the distribution factors which determine their relative concentrations in natural materials.

Carbon 14

Carbon 14 is formed in the atmosphere by the reaction of neutrons with nitrogen, i. e.

$$N^{14}+n=C^{14}+p+620\text{ kev};$$

the neutrons being the result of the interaction of primary cosmic rays with the atmosphere (Libby, 1955). The carbon 14 is naturally radioactive, decaying by β-emission back to nitrogen 14 with a half-life of 5570 years. Thus the half-life is so short that radiocarbon depends, for its existence, on the continual production in the stratosphere, with which it is presumably in steady state. The assumption of a steady state condition for at least the last 15,000 years is justified by the observation that radiocarbon dates on historic samples agree with the calendar dates. The steady state production rate, which is equal to the steady state disintegration rate, can be calculated from measurements on the neutron flux in the lower stratosphere and compared with the observed specific activity of carbon. Anderson (1953) who has made the most recent and detailed considerations of the production rate, finds a rate of 2.6 carbon 14 atoms per cm^2 and per sec.

The carbon 14 atoms are oxidized to CO_2 and thus enter the normal geochemical and biological cycles of carbon via the atmosphere. The distribution through the atmosphere and the terrestrial plants is rapid, and the steady state radiocarbon concentration in these reservoirs is taken as the basis for the so-called "modern" specific activity of carbon, namely about 15 disintegrations per minute per gram of carbon.

On the other hand, the transfer of carbon from the atmosphere to the sea is slow enough, compared to the half-life, to produce a significant difference between the predicted and observed activity of carbon in the surface layers of the oceans. Carbon, as one of the lighter elements, is subjected to natural fractionation of its isotopes in the various reactions it undergoes in its biogeochemical cycle (cf. section on stable isotope variations, below). The steady state isotopic separation of the stable isotopes C^{12} and C^{13} produces a C^{13} concentration in surface ocean water bicarbonate and shell carbonate which is about 2.5 per cent higher than the C^{13} concentration in terrestrial plants. It is thus known that the C^{14} concentration in ocean bicarbonate and carbonate should be about 5 per cent higher than the concentration in land plants, namely about 15.75 disintegrations per minute per gram of carbon (Craig, 1954). In actual fact, however, measurements show that the specific activity of bicarbonate and carbonate from the ocean is about the same as the specific activity of land plants. Thus the atmospheric C^{14} activity has been increased 5 per cent by slow exchange of CO_2 between atmosphere and sea, resulting in an "apparent age," relative to wood standards, of 400 years for the bicarbonate and carbonate shells in the surface layers of the ocean (Craig, 1954, 1957 (a)). Some 10 measurements have now been made on marine plants, animals, and sea-water from the Atlantic (Suess, 1954) and from the New Zealand area (Rafter, 1955) which indicate that the radiocarbon "age" of surface marine carbonate is about 400 years; it is thus clear that radiocarbon age determinations made on deep ocean waters must all be referred to this baseline, rather than to the modern specific activity displayed by the terrestrial plants and the atmosphere.

The evaluation of the exchange time of CO_2 between atmosphere and sea from data on the natural distribution of C^{14}, is discussed in Section IV of this paper.

The most recent and accurate measurement of the absolute radiocarbon concentration is that of Suess (1955), based on comparisons with an absolute standard obtained from the National Bureau of Standards. Suess finds a concentration of 1.238×10^{-12} atoms of C^{14} per atom of carbon for average 19th century wood, corrected for decay to the present date and corrected for isotopic fractionation. Based on this value and a half-life of 5568 years, we give below the amounts of C^{14} in metric tons, and the activities in megacuries present in the major reservoirs on the earth (Craig, 1957 (a), calculated from his Table 1). The figures for the atmosphere and terrestrial living matter are normalized for isotopic fractionation, while the organic and inorganic carbon in the ocean was assumed to have an average age of 600 years relative to corrected 19th century wood, or 200 years relative to surface ocean bicarbonate (see Section IV, this paper).

Reservoir	Total C^{14} metric tons	Total activity megacuries
Atmospheric CO_2	0.96	4.4
Terrestrial living matter + humus	2.2	11.0
Ocean: Total organic matter	3.8	17.6
Ocean: Total inorganic carbon	49.8	228.6
Totals	56.8	261.6

The total activity of radiocarbon present on the earth thus corresponds to some 260 megacuries, practically all of which is in the ocean. Using Anderson's figure for the production rate, cited above, and the decay constant of 3.945×10^{-12} sec^{-1}, the calculated total inventory of radiocarbon on the earth is 78.4 tons, which differs from the figure of 56.8 metric tons, obtained in Table II, by about 28 per cent. However, the production rate, as estimated from cosmic ray data and the counting of atmospheric neutrons, is uncertain to at least 20 per cent because of the uncertainty in the reactor flux from which the neutron counters are calibrated. More recent estimates of the production rate are lower than the figure cited above and all that can be said about the agreement between the calculated and predicted radiocarbon inventories is that they agree within present limits of error.

Tritium

Tritium (H^3) is made in the upper atmosphere, primarily in the "stars" or nuclear explosions produced by the collisions of primary cosmic ray particles with the atmospheric molecules; it is naturally radioactive, decaying by β^- emission to helium 3 with a half-life of about 12.5 years (Kaufman and Libby, 1954). The T atoms "burn" very quickly to HTO and enter the precipitation — evaporation cycle of water. A very small amount of tritium is produced in rocks by the nuclear reaction of lithium with neutrons produced by spontaneous fission of uranium and from (α,n) reactions (Morrison and Pine, 1955); the production of tritium by this process is insignificant relative to the atmospheric production.

Detailed studies of the distribution of tritium in natural waters have been made by Libby and his co-workers at Chicago. The natural concentration of tritium (before thermonuclear tests) in continental waters averages about 5×10^{-18} atoms of tritium per atom of hydrogen. (Following Libby's usage, such a concentration will hereafter be referred to as 5 tritium units, abbreviated as T.U.) The concentration in oceanic rains is about 1 T.U., while in the surface waters of the ocean itself the concentration appears to be as low as 0.2 T.U. The sea is, of course, the ultimate resting place of the tritium formed in the atmosphere, and the low concentration in the oceanic rains relative to continental rains is principally due to tritium removal by direct molecular exchange with the sea surface (see below).

Kaufman and Libby (1954) calculated the tritium production rate in the atmosphere by equating it with the rate at which tritium disappears from the atmosphere into the ocean, taken as the sum of the tritium entering the ocean by run-off from continental rains and the tritium entering directly via oceanic rains. For this calculation only the average run-off and ocean precipitation figures, and measured average tritium content of such waters, are needed. They obtained a net production rate, averaged over the earth's surface, of .12 T atoms per cm² per second. Von Buttlar and Libby (1955) measured many more rain samples, and also analyzed 5 samples of ocean water, from which they could estimate the tritium content of the water vapor which evaporates from the sea surface. Using this latter figure they calculated the production rate over the oceans, assuming that tritium is lost from the atmosphere only by oceanic rain, and gained by production and oceanic evaporation, and obtained a figure of 0.11 to 0.12 T atoms per cm² per sec. A similar calculation was made for the production rate over land, assuming tritium is lost from the continental atmosphere only by continental rains running off into the ocean, and gained by production, and by transport of ocean vapor onto the continents. Using the tritium data for average Mississippi Valley rains, they obtained a figure of 0.16. Their estimated world average production rate is 0.14 with a probable uncertainty of less than 20 per cent. This value agrees precisely with the expected world production rate calculated by Currie, Libby, and Wolfgang (1956) from their experimental measurements on tritium production in nitrogen and oxygen by bombarding protons of 450-Mev and 2-Bev energies. Previous experiments and calculations by Fireman and Rowland (1955) gave an expected production rate of 0.2 T atoms/cm² sec, also in good agreement with the rate apparently observed.

However, the tritium production rate must be a good deal higher than the figures given above. Von Buttlar and Libby calculated that, with such a production rate, and with the observed surface sea concentration of about 0.24 T.U., then the mixed layer of the sea is about 100 meters deep if one assumes that all the tritium of the sea is in the mixed layer. Though this depth is consistent with observational data on the sea, such a calculation assumes that the mixed layer is sealed off from the deep sea so that no tritium mixes below the thermocline, and the question then arises as to just how much mixing across the thermocline does, in fact, occur.

As discussed by Wooster and Ketchum in a separate paper in this report, various observations on ocean currents and on the heat flux through the ocean floor, indicate that the deep ocean water turns over, or mixes with surface water, in times of the order of a few hundred years. Assuming a generalized two-layer model of the sea, consisting of a shallow mixed layer about 75 meters deep on the average, and a homogeneous deep sea below the thermocline marking the interface between the layers, Craig (In press (a)) derived equations relating the production rate of a radioactive isotope to the concentrations of the isotope in the two layers of the sea and the mixing time through the thermocline. (These functions are discussed briefly in a separate paper by the writer in this report, in which calculations on the disposal of fission products in the sea and their ultimate steady state concentrations are discussed.) The applications of such calculations to the distribution of radiocarbon in the atmosphere and sea were demonstrated; these results are discussed in Section IV of this paper.

Application of such calculations to the distribution of natural tritium (Craig, 1957 (b) and manuscript in preparation) shows that for reasonable internal mixing rates of the sea, most of the world inventory of tritium must actually be in the deep sea below the thermocline. Thus for a deep water replacement time, or residence time of a water molecule in the deep sea before mixing into the surface layer, of 0 to 1000 years, and with a surface concentration of 0.24 T.U., the tritium flux into the sea must be between 7.6 and 0.3 atoms cm^2/sec. For the most reasonable deep sea residence time of the order of a few hundred years, the flux must be somewhere between 0.4 and 0.8. It is found that about $\frac{3}{4}$ of the total tritium in the sea is below the thermocline, with a deep-sea tritium concentration of about 0.014 tritium units.

The tritium production rate over the North American continent was recalculated (Craig, op. cit.) by taking into account the removal of tritium from the continent by the outgoing water vapor which does not condense over the land. This calculation gives a world average production rate of from 0.6–0.8 after correction for the latitudinal geomagnetic effect on the incoming cosmic rays. A tritium production rate of this order of magnitude indicates an average deep-sea residence time of water of about 250 years, for a simple two-layer ocean. Calculations based on a second-order ocean model in which the deep sea reservoir is exposed to the atmosphere at high latitudes would give a longer residence time relative to the mixed layer of the sea because of direct entry of tritium from the atmosphere to the deep sea. (See the discussion of radiocarbon residence times in Section IV of this paper.)

However, if the bulk of the tritium is not produced by cosmic radiation, but by solar accretion (see below), the world average production may be as high as 1.7 atoms cm^2/sec because the geomagnetic correction applies only to tritium produced by cosmic rays in the troposphere.

The calculated production rate over the oceans of about 0.14 is obtained by considering only the transfer of tritium into the sea by rainfall. Since rainfall appears to account for only about one-tenth of the tritium which actually enters the sea, it appears that the transfer of tritium from atmosphere to sea by direct molecular exchange across the sea surface is about 9 times as effective as the scrubbing action of precipitation.

A production rate of 1.4 atoms of tritium/cm^2sec means that the world inventory of tritium, before thermonuclear tests, was about 20 kg of tritium, or 200 megacuries, essentially all of which is in the ocean. However, from the experimental data obtained by the workers cited above on the production of tritium by the action of protons on nitrogen and oxygen, it appears very doubtful that the cosmic ray production rate can be much higher than about 0.2. In fact it is probably necessary to assume that tritium is produced on the surface of the sun and is directly accreted into the earth's atmosphere, rather than being a secondary result of the action of the cosmic ray protons on the atmosphere, as postulated by Feld and Craig (Craig, 1957(b)).

From a study of the fall-out rate of strontium 90 pushed into the stratosphere by large atomic detonations, Libby (1956a, b) calculates the stratospheric residence time of strontium to be about 10 years (cf. Section IV of this paper). Since at least half of the tritium production should take place in the stratosphere even if all the production is due to the action of protons on the earth's atmosphere, slow mixing through the tropopause will pile up tritium in the stratosphere in the same way that slow exchange across the sea surface builds up the radiocarbon concentration in the atmosphere. One-sixth of the atmosphere is above the tropopause on the average, but the water vapor concentration is so low that only about 0.3 per cent of the total water vapor in the atmosphere is in the stratosphere; thus the tritium concentration of the stratospheric water vapor will be much higher than that of the tropospheric vapor, which averages about 1 T.U. From the strontium data we assume that the mixing time of water vapor through the tropopause is at least 10 years.

Assuming a tritium production rate of 1.4, half of which is in the stratosphere, the tritium concentration of stratospheric water vapor is then calculated to be at least 300,000 tritium units. This is an astounding concentration factor relative to tropospheric water vapor. Recently the present writer and F. Begemann analyzed a series of samples of atmospheric molecular hydrogen for deuterium and tritium content respectively. Mass spectrometric measurements showed that all samples contained about 2–10 per cent less D than ocean water, falling just in the range of meteoric waters, and containing far too much deuterium to represent thermodynamic equilibrium with water vapor. These data confirmed a few previous measurements (cf. Harteck, 1954) which showed that the molecular hydrogen in the atmosphere must form by direct photodissociation of water vapor in the region around 70 km altitude, rather than by bacterial decomposition of organic matter which has been shown to produce hydrogen in isotopic equilibrium with water. We may thus assume that the tritium content of stratospheric molecular hydrogen is about the same as that of the stratospheric water vapor.

Assuming that the hydrogen is statistically distributed in the atmosphere, so that $\frac{1}{6}$ is above, and $\frac{5}{6}$ below, the tropopause, and taking again the mixing time through the tropopause as 10 years, we then calculate the tritium content of the molecular hydrogen in the troposphere. This figure is found to be 100,000 tritium units, probably as a minimum figure because of slow vertical mixing from the base of the stratosphere to the 70 km level where the hydrogen is made, and because of the indication that more than half the tritium is found initially in the stratosphere. The tritium contents measured by Begemann on a dozen samples of tropospheric hydrogen range from 50,000 to 100,000 tritium units, averaging about 80,000 T.U., in excellent agreement with the calculated value when the various uncertainities are considered.

It thus appears that the high tritium content of tropospheric hydrogen can be satisfactorily explained by purely geophysical reasoning based on the stratosphere-troposphere exchange time as estimated from Libby's Sr^{90} data, and the known concentration of water vapor in the stratosphere. This explanation seems more likely than the intricate series of photochemical mechanisms proposed by Harteck (1954) which at best may account for a tritium concentration of about 1000 T.U. in the molecular hydrogen.

Beryllium 7

Beryllium 7 is formed in cosmic ray stars, the peak production occurring at about 15 km. It decays by electron capture to lithium 7 with a half-life of about 53 days. The discovery, and the elucidation of the geochemical history, of this cosmic ray produced nuclide is due to Arnold and Al-Salih (1955).

Once formed in the atmosphere, the beryllium burns to the nonvolatile BeO or possibly $Be(OH)_2$, either of which diffuses until encountering a dust particle and adhering thereon. It is thus a tracer for the atmospheric dust, on which it is washed out of the atmosphere by rain, ultimately going into the ocean. Arnold and Al-Salih detected radioberyllium in 22 rain and snow samples from Chicago and Indiana, the average absolute assay being 6×10^6 atoms/liter. The estimated world-wide average production rate is 0.04 atoms per cm² per second, based on estimated rates of transfer and mixing in the stratosphere and troposphere. Most of the mixing rates involved are of the order of magnitude of the half-life, which makes calculation of the production rate difficult but greatly enhances the utility of the isotope for studying atmospheric processes, especially when used in conjunction with tritium.

A detailed discussion of the beryllium 7 production rate and atmospheric residence time has recently been given by Benioff (1956). He calculates the production rate to be 5.0 atoms/cm²min in the stratosphere and 1.3 atoms/cm²-min in the troposphere, and he finds that a stratospheric residence time of the order of years is required to match these production rates. Thus his stratospheric residence time agrees with that found by Libby for fission products.

Beryllium 10, a β^- emitter with a half-life of 2.5×10^6 years, is also formed in the cosmic ray stars. J. R. Arnold has recently identified this isotope in deep sea sediment samples (manuscript in press); it should be of great

(56)

importance, because of the long half-life, for the dating of such sediments.

Deuterium and Oxygen 18

Deuterium and oxygen 18 are stable isotopes of hydrogen and oxygen respectively, and it is now well known that the isotopes of these elements, as well as of other light elements such as carbon, nitrogen, and sulphur, are fractionated, or separated, by chemical and physical processes in natural systems. Since the fractionation factors for stable isotopes are measurable and/or calculable for many separation processes, and since the magnitude of these factors is mainly a function of temperature and process, the stable isotopes are extremely well adapted for the study of natural transfer rates in the geochemical cycles of their elements.

The concentrations of these isotopes show rather wide variations in different natural materials, these variations generally ranging from a few tenths of a per cent to a few per cent. In this report we shall mainly be concerned with the distribution of these isotopes in marine and fresh waters and in the atmosphere. Craig and Boato (1955) have recently reviewed the present status of natural isotopic studies, and reference is made to that paper for a more extended discussion.

VAPOR PRESSURES AND RELATIVE ABUNDANCES OF THE ISOTOPIC WATER MOLECULES

Species	Relative abundance (ocean water)	Mass	p (mm Hg)	
			30° C	100° C
H_2O	1	18	31.5	760
HDO	1/3230	19	29.4	741
H_2O^{18}	1/500	20	31.3	756

The above table shows the three most prominent members of the family of isotopic water molecules, their masses, relative abundances in average ocean water, and their vapor pressures at two temperatures. Other members of the family are much less abundant and can be neglected. One sees from the table that the vapor pressures are not a direct function of the molecular weight; the vapor pressure difference between HDO and H_2O is 10 times larger than the vapor pressure difference between H_20^{18} and H_2O, at 30°C. The isotopic separation in an evaporation or condensation process is directly proportional to these vapor pressure differences, so that in water vapor in equilibrium with water at 30°, the percentage depletion in deuterium, relative to the water, is ten times larger than the percentage depletion in oxygen 18.

The natural isotopic variations are customarily given in terms of per mil enrichment or depletion relative to a standard, similar to the way the density parameter is given in an oceanographic temperature-salinity diagram. The data are presented in terms of a function δ, defined as follows:

$$\delta(\%) = [(\text{Rsample}/\text{Rstd}) - 1] \times 1000$$

where R is the isotopic ratio $0^{18}/0^{16}$ or D/H. In the case of deuterium, however, the quantity in the brackets is multiplied by 100 and the δ values are given in per cent, because of the ten times higher isotopic separations encountered. Rstd here refers to the isotopic ratio in average ocean water.

Since H_2O^{16} is the most volatile isotopic species, the water vapor over the oceans is depleted in the heavy isotopes relative to the surface ocean water. As this vapor moves over the continents, the first rain to fall out is enriched in the heavy isotopes relative to the vapor, again because of the higher volatility of the lightest species. Removal of the heavy isotopes, in the form of rain, then causes the vapor to become continually depleted in deuterium and oxygen 18. In general enough rain falls out of an air mass over the oceans so that by the time the mass reaches the continents the rain is already "lighter" in isotopic content than ocean water, and as the air mass moves inland and poleward the rain which falls out becomes more and more depleted in deuterium and oxygen 18.

In a recent study by Craig (ms. in preparation) several hundred fresh water samples from all over the world were analyzed for deuterium and oxygen 18 concentration. The deuterium concentration varies by about 30% relative to mean ocean water, δD ranging from +3 to −27%, while the oxygen 18 concentration varies by only 4%, δO^{18} ranging from +6‰ to −34‰. The delta values for the two isotopes show a linear correlation such that $\delta D = 9\delta O^{18}$, corresponding to the vapor pressure difference ratio at about 25°C. The reason for the high value of the average temperature at which liquid and vapor equilibrate in the atmosphere is as yet unknown; the uncertainty in the vapor pressure data is such that the value could hardly be less than about 20°. The delta values for fresh waters show a general correlation with latitude or distance from the ocean; there is a general decrease in the heavy isotope concentration as the latitude varies from equatorial to polar, reflecting the continuous loss of vapor from the poleward moving air masses.

Isotopic variations such as mentioned above can be measured quite simply and precisely with the mass spectrometer, and it is evident, from the ranges of variation cited, that such studies on meteoric waters can provide a wealth of information concerning meteorological transfer and mixing phenomena in the atmosphere. The average water vapor of the earth has roughly the composition $\delta D = -10\%$, $\delta O^{18} = -11‰$, but large variations, related to the amount of liquid water which has condensed out of the vapor, occur, and thus such studies are directly adapted to problems of water vapor transport over both the oceans and continents.

The situation in the oceans themselves is somewhat more complicated. The oxygen isotopic composition of ocean waters has been studied by Epstein and Mayeda (1953), and the deuterium variations in the same samples by Friedman (1953); these writers also analyzed nine fresh water samples and first elucidated the D-O^{18} relationship in natural waters. The surface layers of the oceans are in general enriched in the heavy isotopes relative to mean ocean water because of the net storage of H_2O^{16} in the stagnant and circulating fresh water and vapor; the extent of this enrichment reflects the hold up at the boundary of the mixed surface layer, namely the thermocline. On the other hand, the deeper layers of the ocean are depleted in deuterium and oxygen 18, relative to mean ocean water, because of the influx of glacial melt water in polar latitudes, the glacial waters having δ values at the lightest ends of the ranges cited in the preceding paragraphs. Thus the oceans are isotopically upside down with the heavy isotopes concentrated at the surface, and the isotopic composition parameters in general correlate with salinity.

Epstein and Mayeda (op. cit.) showed that the salinity-oxygen 18 variations in marine waters were consistent with a model in which the oceanic precipitation is progressively depleted in the heavy isotopes as a function of the extent of precipitation from the local atmospheric reservoir. Salinity, of course, is uniquely related to the direct amount of fresh water removed by evaporation or added by meltwater dilution, but the relationship in the case of isotopic composition is more complex. This is because the isotopic composition of fresh water precipitating over the oceans, or added by runoff or melting of ice, is variable, depending on the history of the air mass from which it was precipitated. The correlation between isotopic composition and salinity is therefore more or less local, reflecting the particular relations obtaining on the average in the area. As a result, the isotopic composition parameters, rather than being simply transforms of salinity, and thus not inherently very useful for the study of transfer problems, become important parameters for such studies because of the reflection of areal conditions in a manner different from, but related to, the salinity parameter. Examples of this effect are discussed in Part IV, where applications to transfer studies are treated.

The isotopic composition of atmospheric oxygen is an interesting case of adjustment of a reservoir composition to steady state nonequilibrium biogeochemical transfer processes. Oxygen would exist in the atmosphere in the absence of living plants because of photodissociation of water vapor in the atmosphere, with subsequent escape of hydrogen from the earth. However, oxygen is cycled through the biosphere so rapidly that its isotopic composition, rather than reflecting its mode of formation, may be adjusted to a steady state balance between photosynthetic formation and respiratory uptake. The oxygen produced in photosynthesis is in isotopic equilibrium with the water taken up by the plants and is very close in isotopic composition to this water; however the atmospheric oxygen is some 23‰ enriched in oxygen 18 relative to average ocean water. Lane and Dole (1956) have measured the preferential uptake of oxygen 16 by various animals and land plants and concluded that the net fractionation is such as to account quantitatively for the atmospheric oxygen composition. Respiration in the oceans shows a much smaller selective oxygen 16 uptake (Rakestraw et al., 1951; Dole et al., 1954) and the isotopic composition of oxygen dissolved in ocean water is variable and dependent on the amount of oxygen which has been taken up from the local reservoir. There is some doubt as to whether the data of Lane and Dole can actually yield a material balance without invoking some special mechanisms relating the productivities of the oceans and the land, and a good deal of further study on this question is needed. The intent here is to point out that the isotopic transfer rates involved in this problem of the isotopic composition of atmospheric oxygen, and the variations in the isotopic composition and amounts of oxygen dissolved in ocean waters, may well be important parameters for the study of transfer phenomena in the oceans and the atmosphere and the interaction between them.

Carbon 13

About one per cent of natural carbon consists of the stable isotope C^{13}; the ratio C^{13}/C^{12}, and thus effectively the C^{13} concentration, in natural material shows a range of variation of about 6 per cent. The details of the natural variation have been described (Craig, 1953, 1954), and reference is made to these papers for extended discussion. The delta values for carbon are referred to a standard which has the composition of average limestone; on this scale the characteristic compositions of natural materials are shown below:

Material	δC^{13} (‰)
Limestones and shell	0
Ocean bicarbonate	— 1.5
Atmospheric CO_2	— 7
Marine biosphere	—13
Terrestrial biosphere	—25
Coal	—25
Petroleum	—28
Shales	—28

The difference between the compositions of atmospheric carbon dioxide and ocean bicarbonate probably reflects the isotopic equilibrium constant for the exchange of carbon isotopes between these compounds; the other variations shown in the table are due to kinetic factors which cause a selection of the isotopes in the various processes involved in the biogeochemical cycle of carbon. The carbon 14 variations caused by such processes should be almost exactly twice the C^{13} values shown above, and, as noted previously, the knowledge of the C^{13} variations has been of great value in understanding the transfer rates and mixing phenomena involved in the distribution of radiocarbon.

A particularly fertile field for study is the marine biosphere and the phenomena involved in the isotopic partition of carbon between carbonate and organic matter. One critical parameter in the kinetic processes involved is the rate of uptake of CO_2 by photosynthesis versus the relative rates of CO_2 replenishment by mixing and by reassociation of bicarbonate ions, and such studies may well lead to an improved knowledge of the carbon flux through local ecological systems and the interaction of the local system with the general marine reservoir. Keeling (manuscript in preparation) has studied the isotopic variations in carbon dioxide over the land, and has found that the isotopic parameters are critical indicators of the atmospheric transfer phenomena through local biotopes, as a result of the large difference in isotopic composition between normal atmospheric carbon dioxide and carbon dioxide produced in respiration during the night.

III. *Contribution of radioisotopes to the geosphere by nuclear fission and detonations*

The steady state isotopic distributions discussed in the preceding section have, in the case of radioactive elements, been altered to some extent by contribution to the geosphere of radioisotopes produced in nuclear fission in both reactors and nuclear detonations. Such contributions, rather than being detrimental to the study of natural transfer phenomena, have, on the whole, provided extra parameters of great value for such studies. It is of course obvious that addition of such elements under carefully controlled conditions in selected locations and at planned times would have contributed a great deal more to our knowledge of geophysical phenomena than the actual dispersal of the material has resulted in; nevertheless it is possible, even though working in almost total ignorance of the amounts of material added, to deduce a great deal of valuable information about mixing rates and even to make detailed studies of certain specific problems.

The fission of uranium in reactors and nuclear weapons results in a great variety of elements distributed mass-wise into a spectrum known as the fission yield curve; the proportions of the various masses produced are a unique function of the atomic mass and vary little with neutron energy or substitution of plutonium for uranium 235. For our purposes, the elements of most interest produced by fission are krypton 85, strontium 90, and cesium 137, ranging in half-life from 10 to 33 years; tritium, which is not a fission product, is also of great importance. Measurable additions to the geosphere of tritium, strontium 90, and krypton 85 have been noted and are discussed in Part IV in connection with general applications to transfer study phenomena. In this section we estimate the total amounts of these nuclides which have been produced; these estimates are also of some interest in connection with the magnitude of the disposal problem, both present and future.

One result of the advent of nuclear fission is that all the krypton in the atmosphere has become contaminated with radiokrypton. De Vries (1956) has measured the specific activity of atmospheric krypton, taken in March of 1955, as 25,000 counts per minute per mole. The activity is due to contamination with krypton 85, which decays by β^- emission with a half-life of ten years. From DeVries' measurement, we readily calculate that 56.4 moles, or 4700 grams, of Kr^{85} are now present in the atmosphere, and in ignorance of the rate of production, we make only a small error by assuming this figure as the total amount of radiokrypton produced and not correcting for decay. From the fission yield of 0.24 per cent for this isotope, it appears that some 23,500 moles, or 5500 kg, of U^{235} and plutonium have undergone fission since the advent of anthropogenetic fission, resulting in an atmospheric krypton activity of 2 megacuries. It is assumed, as seems reasonable, that all fission produced krypton finds its way into the atmosphere.

From the fission yield data, we calculate the total amounts of radiostrontium and cesium which have been produced; the data for the three elements are shown below. Only the strontium and cesium produced by detonation of nuclear weapons will escape into the atmosphere and be deposited over the surface of the earth and sea. Because the krypton figure is uncorrected for decay, and because some krypton must have gone directly into the stratosphere and is not included in the measured activity, the values all represent lower limits and should be slightly larger.

Radioisotope	Half-life	Fission yield (%)	Total activity produced by all fission (megacuries)
Krypton 85	10 years	0.24	2
Strontium 90	28 years	5.0	15
Cesium 137	33 years	6.3	16

Libby (1956a, b) has given detailed discussions of the fall-out patterns of strontium 90 and cesium 137, based on the Project Sunshine measurements on world-wide samples. Geophysically, the most significant finding is that, as mentioned previously, the residence time in the stratosphere of material pushed through the tropopause is about 10 years. The most recent measurements on the distribution of fission products from nuclear explosions (Libby: Address before American Association for the Advancement of Science, Washington, D.C., October 12, 1956) indicate that the amount of strontium 90 scattered over the surface of the earth is now equivalent to an average activity concentration of about 16 millicuries per square mile. In addition, the amount now held in the stratosphere is equivalent to another 12 millicuries per square mile. The total amount so far distributed is thus about 5.6 megacuries of Sr^{90}, of which about 2.4 are still in the stratosphere, and, assuming purely statistical distribution, some 2.3 megacuries have fallen directly into the sea, while about 0.9 megacuries have fallen on the land surface. Because of the similar half-life and fission yield, the figures for cesium 137 will be almost identical to those for strontium 90. Comparing these figures with the ones given in the above table, we see that roughly 5.6/17.4 or $\frac{1}{3}$ of all the solid fission products so far produced, by all fission, have been distributed over the atmosphere, the land, and the sea, by atomic weapons testing.

The most important of these elements for studying mixing rates in the sea should be cesium 137, which being soluble, should be an excellent tracer for the mixing rate of surface ocean water down through the thermocline. Krypton 85 should ultimately prove important for atmospheric mixing studies, especially for comparison of mixing rates of gaseous and solid elements across the tropopause.

Thermonuclear weapons may also be expected to produce some carbon 14 because of the neutrons released into the atmosphere in the explosion. A contemporary sample of grass, collected in the summer of 1955 in S.W. Kansas by the writer, was analyzed for C^{14} content by M. Rubin at the U.S. Geological Survey laboratory. This grass was found to be about 2.5 per cent higher in C^{14} content than the 19th century wood, corrected for age, used as the U.S.G.S. radiocarbon standard (Suess, 1955). The samples and standard were analyzed for C^{13} content by the writer and the results corrected for isotopic fractionation, and the sample was counted twice. Thus the measurement is quite precise, and probably indicates that the atmospheric radiocarbon content has risen about 2 per cent above normal at the present time, due to thermonuclear neutron production. For future geochemical studies with natural radiocarbon it will be important to monitor continuously the activity of contemporaneous plants and atmospheric carbon dioxide, though the effect will be insignificant for radiocarbon dating studies for some time yet.

The situation with tritium is different. The earliest rain ever analyzed for tritium content fell in Chicago in May of 1951; since October 1952 Libby and his co-workers at Chicago have produced an essentially continuous record of the tritium content of Chicago rain, and have analyzed a great many other samples from many parts of the world. Their data show that there was no significant production of tritium in the November 1952 Ivy test (Kaufman and Libby, 1954). However, the March 1954 Castle thermonuclear tests produced an increase in tritium concentration of Chicago rain from an average value of 9 to a maximum value of 450 atoms $T/10^{18}$ atoms H; i.e., a factor of 50 (von Buttlar and Libby, 1955). Even more striking was the discovery that the tritium content of southern hemisphere waters showed no significant increase in tritium concentration, and snow samples collected from the Antarctic as late as February of 1955 showed that during this interval no significant amounts of artifically produced tritium had crossed the equator (Begemann, 1956).

Begemann's recent data show that the tritium rained out of the northern hemispheric atmosphere with a mean-life of about 40 days for the decrease in tritium concentration; as late as the end of 1955 the tritium concentration of Chicago rain was still about three times normal. In Section II above it was concluded that the world inventory of tritium was about 20 kg, with about 5 kg in the mixed layer of the sea, and about 15 kg in the deep sea. The Chicago data show that the tritium content of the surface ocean waters has increased by at least a factor of four, indicating that the order of magnitude of 20 kilograms of man-made tritium has so far rained out into the ocean. Thus the amount of tritium produced by man is now about equal to the natural steady-state inventory.

IV. *Applications of tracer techniques to the study of physical processes in the sea and atmosphere*

In this section we describe a few of the more obvious applications of the tracer techniques and isotopes described in the previous sections to specific problems of transfer phenomena in the oceans and atmosphere. The topics are subdivided in terms of the isotopes discussed, in order to facilitate reference to points in preceding sections and parts of this section.

Carbon 14

Carbon 14 is perhaps the most useful of the isotopic tools available for geophysical and geochemical studies, especially when used in conjunction with oxygen 18 data; the 5700 year half-life and the universal distribution of carbon in organic and inorganic reservoirs make it ideal for such purposes. The most obvious application of immediate interest is the dating of the bicarbonate of the deep-sea waters, in order to determine the mixing rate of the oceans. Unfortunately, only one definitive set of measurements of this type has been made, namely the U. S. Geological Survey laboratory measurements of waters east of the Lesser Antilles at approximately 57° W. and 16° N., made by M. Rubin (personal communication). These data are shown below:

Depth (meters)	Carbon 14 age (years)
Surface	652
640	634
1640	628
1750	841

The absolute values are probably not better than ±150 years, but the relative values are more precise. The age of the surface bicarbonate is somewhat older than the 400-year average age mentioned in Part II as the result of slow transfer of atmospheric carbon into the sea, perhaps as a result of local conditions; however, the important figure is the age difference between surface and deeper waters and it is unfortunate that still deeper waters were not sampled. The importance of a great many vertical profiles of this sort from both oceans, and their fundamental import for knowledge of the mixing rates in the ocean, is obvious.

Because of the requirements of steady state balancing, the amounts of water transferred, per unit time, downward and upward through the thermocline in the sea must be equal, but because the mixed layer contains only about 2 per cent of the sea, this balance requires that a water molecule remain, on the average, some 50 times longer below the thermocline than above. As a consequence of this relationship, an uncertainty of 10 years in the residence time of material in the mixed layer results in an uncertainty of 500 years in the residence time of the material below the thermocline, considering the world average rate of general cross-thermocline mixing of the substance. As we shall see below, the half-life of radiocarbon happens to be so long, that considerations of the extensive data on C^{14} distribution in the atmosphere, biosphere, and mixed layer of the sea, do not yield important information on the internal mixing rate of the ocean itself. In fact, the distribution of tritium above the thermocline of the sea furnishes a much more precise estimate of the general turnover time of water in the deep sea.

Thus the application of radiocarbon analysis to mixing problems within the sea itself can be made only by actually getting below the mixed layer and studying the deep-sea distribution of C^{14} directly; such studies, coupled with chemical analyses and physical data serving as parameters for the identification of continuous water masses, will probably prove to be the most fruitful method for the delineation of large scale mixing phenomena in the sea.

On the other hand, the distribution of radiocarbon in the atmosphere and mixed layer of the sea is strongly dependent on the rate of exchange of carbon dioxide between the atmosphere and sea, and from a study of the relationship between the exchange rates and the radioactive decay rate, it is possible to derive rather precise values for the flux of carbon into the sea and downward through the thermocline. For such calculations it is necessary to assume a model of the atmosphere-sea system based on simplifying assumptions as to the nature of the sea below the thermocline. Calculations of this type, outlining the factors affecting the natural distribution of radiocarbon, have recently been made by Suess (1953), Arnold and Anderson (1957), Craig (1957 (a)), and Revelle and Suess (1957). The conclusions of these papers, though reached by various means, are quite similar, and we shall briefly summarize the general results.

There are two empirically observed effects, of different origin, by which factors affecting the natural distribution of radiocarbon may be evaluated. The first of these is the observation that the carbon in the surface layers of the sea (bicarbonate, shell, and organic matter) has an apparent age of about 400 years relative to the terrestrial wood used as standards for radiocarbon dating. The second is the observation that contemporaneous wood has a radiocarbon activity some 2 per cent lower than the activity of 19th century wood, corrected for age to the present date. This decrease in activity, reflecting the contribution of C^{14} free CO_2 to the atmosphere by the combustion of fossil fuel, was first found by Suess (1953) and we shall refer to it as the Suess effect.

The "apparent age" of carbon in the mixed layer of the sea has been measured on Atlantic ocean samples (and one Pacific sample) by Suess (1954), and on Pacific ocean samples around New Zealand by Rafter (1955). The average age determined by Suess is 430 years, while that of the Pacific samples was reported by Rafter as only 290 years. However, the Suess measurements are relative to the 19th century wood standard, corrected for decay to the present, while the Rafter measurements were made relative to a contemporaneous standard which has suffered a decrease in activity due to the Suess effect. Measurement of the effect in the New Zealand standard shows that 110 years must be added to the ages reported by Rafter (1955) in order to correct for this effect and make the ages comparable to those reported by Suess (Rafter, manuscript in press).

Thus the average ages reported for the two oceans are in almost exact agreement, and we may consider the 400 year apparent age well established as a world-wide phenomenon.

The 400 year apparent age of mixed-layer carbon is simply a less meaningful way of stating that the radiocarbon activity of mixed-layer carbon is 5 per cent lower than the activity in modern wood, uncontaminated by the Suess effect. Actually it is observed that the activities in wood and in surface ocean carbon are measured to be the same, but the measurements must be corrected for natural isotopic fractionation in the physical and chemical processes involved in the carbon cycle (see section on carbon 13 variations). Marine shells concentrate carbon 13 by 2.5 per cent relative to terrestrial wood, and must therefore concentrate carbon 14 by 5 per cent; since this concentration factor is not observed, we see that the activity of carbon in the mixed layer is, in fact, 5 per cent lower than expected. The relationships between carbon 13 and carbon 14 variations expected on theoretical grounds, and on the basis of laboratory measurements, were discussed in detail by Craig (1954) who showed that the 5 per cent discrepancy must be the result of slow transfer of carbon from the atmosphere to the sea, and cannot be explained by any other cause. Rafter (1955) verified the conclusion that the carbon 14 difference between atmospheric CO_2 and wood must be twice the carbon 13 difference, by direct measurement.

The exchange rate of carbon dioxide between atmosphere and sea may be deduced from considerations of the steady state relationships between the exchange rate and the radioactive decay rate; this type of evaluation is independent of considerations based on the magnitude of the Suess effect and the kinetics of the transient state. The general equations governing the transfer of a radioactive isotope between its various exchange reservoirs have been given by Craig (1957(a)) in terms of the relationship between the uniform activity which would be observed if all of the sea and the atmosphere were mixed together at a rate infinitely faster than the radioactive decay rate, and the percentage deviations from this uniform activity which are actually observed in the different reservoirs. Mixing rates are expressed in terms of the residence time of a molecule in a particular reservoir, which corresponds to the operational definition of flushing time or replacement time, used by oceanographers, and, for the first order processes with which we are concerned, to the reciprocal of the exchange rate constant.

The constant radioactive decay rate of carbon 14 furnishes a built-in clock which monitors the transfer rate of carbon between its various reservoirs. For example, if a barrier is interposed between the atmosphere and sea, so that the transfer rate of carbon between these reservoirs is slowed down, the radiocarbon atoms formed in the atmosphere have less probability of getting into the sea and thus of leaving the atmosphere by physical removal. However, the steady state requires that the total number of C^{14} atoms leaving the atmosphere by all mechanisms be equal to the production of radiocarbon atoms by the cosmic rays, and thus the number undergoing radioactive decay in the atmosphere must increase. The number of radioactive atoms decaying per unit time is a constant fraction of the total number present (the exponential decay law), and therefore the piling up of radiocarbon in the atmosphere because of such an exchange barrier results in an increase in the number decaying in just the way required to maintain the steady state secular equilibrium with the production rate. The percentage increase in the C^{14} activity of the atmosphere is a function of the ratio between the exchange rate and the decay rate, or, what is the same thing, between the atmospheric residence time and the radioactive mean life.

Considering then, the percentage change in the radiocarbon activity of atmospheric CO_2 and terrestrial wood, relative to the activity which would characterize these materials in the hypothetical state of infinitely rapid mixing between atmosphere and sea, it is found that for each year of residence time of a CO_2 molecule in the atmosphere as a result of slow exchange, the atmospheric activity will increase by 0.74 per cent. The activity in the sea would, of course, decrease as a result of the slower transfer of radiocarbon into the ocean, but since there is some 60 times as much carbon in the sea as in the atmosphere, the percentage decrease of activity in the sea will be only 1/60 of the atmospheric increase, namely about 0.01 per cent, which is not observable.

We can make a more detailed model of the carbon exchange system by breaking the sea up into a two-layer ocean, taking the upper layer to be about 75 meters deep corresponding to the average mixed layer as actually observed in the sea. (The 75 meter estimate was made by Dr. Warren Wooster, who kindly studied the question of the average depth of the mixed layer over the year in the various areas of the oceans.) The lower layer, extending to a depth of 4000 meters on the average, is termed for convenience the "deep sea," though it is of course obvious that such a uniform layer has little resemblance to the actual structure of the sea below the thermocline. Nevertheless, it is found that the consequences of such an assumption about the nature of the deep sea are not serious insofar as affecting the validity of the calculations on the atmospheric residence time, and the treatment of the relationships existing between the atmosphere, mixed layer, and main body of the sea, is of course improved immensely by assuming such a model. If we then add a barrier between the mixed layer and the deep sea, representing slow mixing across the thermocline, the radiocarbon is further piled up in both the atmosphere and the mixed layer, in the same manner as previously described. Calculation shows that the activities in the atmosphere and mixed layer are both increased by about 1.2 per cent, relative to the case of a rapidly mixed, uniform sea, for each 100 years of residence time in the deep sea, or, what is almost the same thing, for each 100 years of "age" of the deep water. The activity in the deep sea is reduced by 0.05 per cent for each 100 years of deep-sea residence time.

For deep-sea residence times up to several thousand years, the interpolation of a mixing barrier at the thermocline in the sea causes very close to the same activity increase in both the atmosphere and the mixed layer, and thus the activity difference observed between the atmosphere and mixed layer is sensitive only to the atmosphere-sea exchange rate for internal mixing times of the sea of the order of a few thousand years or less. The physical evidence discussed by Wooster and Ketchum in a separate paper in this report, and the tritium calculations cited previously in this paper, clearly show that the average mixing time of the sea is at least within this range.

Thus the figure cited above of a 0.74 per cent increase in atmospheric activity for each year of atmospheric residence time, indicates that the residence time of a CO$_2$ molecule in the atmosphere, before entering the sea, is about 7 years, corresponding to the 5 per cent activity difference between carbon in the atmosphere and in the mixed layer of the sea.

An independent calculation of the atmospheric residence time can be made by considering only the steady-state material balance in the atmosphere as a function of the production rate of radiocarbon, taken as $(2\pm.5)$ C^{14} atoms/cm^2 sec, and the rate at which carbon enters the sea. This calculation gives an atmospheric residence time of about 6 years. Considering the errors to be assigned the numerical values in both these calculations, it appears that the best value of the atmospheric residence time of carbon dioxide may be taken as 7 ± 3 years, corresponding to a rate constant $k_{a-m}=0.14$, where k is the fraction of the carbon in the atmosphere transferred to the mixed layer per year (Craig, 1957 (a)).

The average annual exchange flux of carbon dioxide, into and out of the sea each year, is thus found to be about 2×10^{-8} moles per square centimeter of sea surface. This rate is lower by a factor of 10,000 than the rate recently obtained by Dingle (1954) from consideration of the various rate constants involved, and the discrepancy thus serves to emphasize the power of natural isotopic studies to yield quantitative data, as compared with more traditional methods.

An entirely independent calculation of the atmospheric residence time, not based on steady-state considerations, may be made from the magnitude of the so-called Suess effect described previously. It is known that since the beginning of the industrial revolution, man has added an amount of carbon dioxide to the atmosphere by fuel combustion equivalent to about 12 per cent of the amount originally present. The degree of dilution of radiocarbon activity in contemporaneous wood by incorporation of C^{14}-free CO$_2$, measured relative to the activity of 19th century wood, is then a measure of the rate at which the dead CO$_2$ has been removed from the atmosphere into the sea. The first measurements of this effect, made by Suess (1953), indicated a dilution of about 3 per cent, and from these data Suess deduced an atmospheric CO$_2$ residence time of 20–50 years.

More recent and extensive measurements by Suess (1955) have shown that the figure of

3 per cent is higher than the average world-wide figure, and represents an increased local contamination in trees growing near sites of industrial activity. The latest measurements indicate a world-wide effect of about 1.7 per cent. Revelle and Suess (1957) have discussed the relationships between the exchange rate, the Suess effect, the effect of an increase in the atmospheric CO_2 content on the atmospheric and oceanic reservoirs, and the buffering effect of the sea water alkalinity on carbon transients. They conclude that, all things considered, the residence time of CO_2 in the atmosphere, relative to exchange with the sea, is of the order of 10 years. Though the uncertainty in their estimate is a good deal larger than in the case of the steady-state considerations discussed above, the close agreement of the figures obtained by these different considerations is gratifying, and indicates that the factors governing the natural distribution of radiocarbon are now fairly well understood.

The size of the terrestrial biosphere and the annual rate of photosynthesis on land have been estimated by Schroeder and Noddack, and from their figures it appears that the terrestrial plants consume about 3 per cent of the atmospheric CO_2 per year, corresponding to an atmospheric residence time before entrance into the biosphere of 33 years. With a residence time of 7 years, prior to exchange into the sea, the total residence time of a CO_2 molecule in the atmosphere is 6 years, after which it goes either into the sea (9 chances out of 11) or into the terrestrial biosphere (2 chances out of 11). Thus the carbon dioxide flux into the sea is about 4.5 times larger than the flux into the biosphere, and about 82 per cent of the CO_2 leaving the atmosphere goes into the sea, while only about 18 per cent goes into the terrestrial plants. This ratio represents a considerable departure from previous estimates, and indicates that the spatial distribution of plants and soils is probably not the dominant factor in determining the steady-state CO_2 concentration in the atmosphere. In fact it appears more likely that the spatial pattern of absorption and release of CO_2 by the sea, and the seasonal variations in this pattern, are the dominant factors.

The various considerations outlined above are all consistent with any deep-sea residence time of carbon up to a few thousand years, and do not yield any closer estimate for this figure. Recent unpublished data by Broecker and co-workers at the Lamont Geological Observatory indicate that the bicarbonate of deep ocean waters probably averages about 8 per cent lower in C^{14} content than the surface mixed layer, corresponding to a radiocarbon "age" of the order of 670 years. However, considerations by Craig (in press), based on a second order oceanic model in which the deep sea reservoir is exposed to the atmosphere in high latitudes, show that about half of the radiocarbon in the deep sea is derived directly from the atmosphere. The other half enters the deep sea from the surface mixed layer of the ocean by the mixing and interchange of water.

Because of this dual source of radiocarbon, the residence time calculated for carbon in the deep sea is only about half of the actual residence time of a water molecule in the deep sea relative to the mixed layer; thus the deep-sea residence time of water relative to the mixed layer is probably of the order of 1000 years as a world-wide average. However the actual interpretation of such residence times in the sea is quite complicated, and reference is made to the paper cited above for a detailed discussion of carbon and water residence times.

Deuterium and Oxygen 18

As discussed previously, the stable isotopes are of great value in the study of ocean water mixing as additional parameters related to salinity. One particular case in which information can be gained from such studies is the problem of meltwater dilution of the oceans in the polar regions. A salinity decrease can be caused by addition of fresh water from river runoff, or from the melting of sea ice, and from salinity data alone these sources cannot be differentiated. However, the isotopic composition of the two sources is quite different; the sea ice should have a composition quite similar to that of the ocean water, while, as shown above, the runoff of rivers in polar areas is greatly depleted in deuterium and oxygen 18 relative to ocean water. Thus from consideration of salinity and isotopic data taken together, a quantitative evaluation of the mixing conditions can be made. Friedman of the U. S. Geological Survey is currently studying such problems with deuterium analyses of Atlantic waters. The isotopic data should also be useful in material balance studies over various sections of the oceans, because of the latitudinal decrease in deuterium and oxygen 18 concentration of oceanic water vapor, and the known temperature dependence of the isotopic selection in evaporation.

Craig, Boato, and White (1956) have shown how deuterium and oxygen 18 measurements can be usesd to determine the proportions of juvenile or magnetic water to reheated ground water in thermal springs, and volcanic steam. These isotopes, together with tritium, have important applications to practically all hydrologic problems, and the exploitation of such techniques has barely begun.

Tritium and Strontium 90

As described in Part II, the tritium measurements made by Libby and his co-workers furnish an independent value for the mixing rate in the sea; more detailed studies will surely provide important information on the oceanic mixing phenomena. The production of tritium in thermonuclear explosions provides an isotopic tracer for determination of atmospheric mixing times across the face of the earth and storage times in the atmosphere.

The measurement of the world-wide distribution of strontium 90 produced by nuclear detonations has been done by W. F. Libby and E. A. Martell at the University of Chicago. The results of their work have recently been described by Libby (1956 a, b). The radionuclides produced by low-yield kiloton weapons, and part of the activity produced by the higher-yield megaton weapons, are distributed within the troposphere in a belt corresponding to the latitude of the test site. This material has a tropospheric life which is a function of particle size; some of the activity may circle the earth two or three times within the hemisphere in which it was produced before being washed out of the atmosphere. However, the mean life of this tropospheric material is only a few weeks.

More interesting is the fact that Libby and Martell find that half or more of the radiostrontium produced by the megaton weapons is distributed over both hemispheres and falls out much more slowly, the mean storage time in the atmosphere being of the order of ten years. They conclude that this material is carried up into the stratosphere, above the tropopause, where it is mixed horizontally in a time comparable to the storage time at this level.

The contrast between the distribution of megaton weapon produced radiostrontium and tritium is extremely significant. As noted in Part III, Begemann and Libby find that the artificially produced tritium is confined to a single hemisphere and is rapidly washed out of the atmosphere; this material thus follows the pattern of the activities which remain in the troposphere. The tritium and fission product data thus show that over a period of months there is virtually no cross-hemispheric mixing in the troposphere, but that over a period of years the stratosphere is well-mixed horizontally. The failure to detect tritium carried up into the stratosphere with the megaton weapon produced radiostrontium may be due to the instantaneous combustion of tritium to HTO by the catalytic action of the oxides of nitrogen produced in the blast (Harteck, personal communication). As water, the tritium may be frozen out at the lower cold trap, in the tropopause, where the temperature is about −70°C, and thus prevented from entering the stratosphere.

On the other hand, Martell points out (personal communication), that the thermal energy of the fireball is still quite large by the time a fireball produced by a megaton weapon has risen to the height of the tropopause. In order for HTO to condense and thus be trapped below the tropopause, it is necessary to assume that the lighter constituents of the fireball have diffused into the cooler outer layers. Martell suggests that if such is the case, then the actual explanation may be that the portion of the cloud containing the HTO may not have sufficient thermal energy to penetrate the tropopause, and as a result, this portion of the cloud merely expands horizontally below the tropopause.

V. *Conclusions*

From the discussion in the preceding parts of this report, it is apparent that the advent of manmade nuclear reactions introduced a series of geophysical and geochemical experiments on a vast scale. It is fortunate that the introduction of such experiments came at a time when geochemists were well underway towards the understanding of natural transfer phenomena by means of studies based on naturally occurring isotopes in their steady state biogeochemical cycles. It should be clear that the need for this knowledge is such that every effort should be made to prevent irreversible procedures which might eliminate the opportunity to study such mixing at the natural level where evaluation of the long term variables is possible. On the other hand, it is also evident that the introduction of artificially produced radioisotopes into the geosphere has been productive of a great deal of new knowledge that might otherwise not have been obtained.

The importance of continuous monitoring of the levels of such substances as tritium cannot be overemphasized. As an example of this, it may be pointed out that one reason that carbon 14 is such a powerful tool for the evaluation of ocean-atmosphere interaction that we have relatively precise records on just how much dead carbon has been produced by the combustion of fossil fuels; were this information not available the use of radiocarbon in such studies would be exceedingly difficult, if not impossible.

From the carbon 14 inventory discussed in Part II, and assuming an average depth of about 150 meters for the oceanic thermocline, it appears that about 4 per cent of the carbon 14 in the sea lies above the thermocline; this corresponds to an activity of about 10 megacuries. It is thus evident that introduction of artificially produced radiocarbon in 10,000 curie amounts above the thermocline would begin to produce a critical level which would interfere with the natural radiocarbon studies of such fundamental importance. Introduction of 100–1000 curie amounts above the thermocline would produce activity sites which could be traced for years, but such experiments could not be done more than once every decade or so if the natural level is to be preserved. It would thus seem highly desirable that some international body be constituted to record and monitor the material put into the sea and the atmosphere as wastes and for tracer experiments. It is a truism to point out that a contaminated laboratory is rather easily replaced, but that the laboratory of the earth scientists is not easily renovated.

CONCLUSIONS

ANDERSON, E. C. 1953. The production and distribution of natural radiocarbon. *Ann. Rev. Nuclear Science* **2**:63–78.

ARNOLD, J. R., and H. A. AL-SALIH. 1955. Beryllium-7 produced by cosmic rays. *Science* **121**:451–453.

ARNOLD, J. R., and E. C. ANDERSON. 1957. The distribution of carbon-14 in nature. *Tellus* **9**:28–32.

BEGEMANN, F. 1956. Distribution of artificially produced tritium in nature. Nuclear Processes in Geologic Settings: Proceedings of the Second Conference. *National Academy of Sciences — National Research Council Publication* **400**:pp. 166–171.

BENIOFF, P. A. 1956. Cosmic-ray production rate and mean removal time of Beryllium-7 from the atmosphere. *Phys. Rev.* **104**: 1122–1130.

CRAIG, H. 1953. The geochemistry of the stable carbon isotopes. *Geochim. et Cosmochim. Acta* **3**:53–92.

1954. Carbon 13 in plants and the relationships between carbon 13 and carbon 14 variations in nature. *J. of Geology* **62**: 115–149.

1957 (a). The natural distribution of radiocarbon and the exchange time of carbon dioxide between atmosphere and sea. *Tellus* **9**:1–17.

1957 (b). Distribution, production rate, and possible solar origin of natural tritium. *Phys. Rev.* **105**:1125–1127.

In press. The natural distribution of radiocarbon: II. Mixing rates in the sea and residence times of carbon and water. *Tellus.*

CRAIG, H., and G. BOATO. 1955. Isotopes. *Ann. Rev. Phys. Chem.* **6**:403–432.

CRAIG, H., G. BOATO, and D. E. WHITE. 1956. The isotopic geochemistry of thermal waters. Nuclear Processes in Geologic Settings: Proceedings of the Second Conference. *National Academy of Sciences — National Research Council Publication* **400**:pp. 29–38.

CURRIE, L. A., W. F. LIBBY, and R. L. WOLFGANG. 1956. Tritium production by high-energy protons. *Phys. Rev.* **101**:1557–1563,

DE VRIES, H. 1956. Purification of CO_2 for use in a proportional counter for ^{14}C age measurements. *Appl. Sci. Res.* (B) **5**: 387–400.

DINGLE, A. N. 1954. The carbon dioxide exchange between the North Atlantic ocean and the atmosphere. *Tellus* **6**:342–350.

DOLE, M., G. A. LANE, D. P. RUDD, and D. A. ZAUKELIES. 1954. Isotopic composition of atmospheric oxygen and nitrogen. *Geochim. et Cosmochim. Acta* **6**:65–78.

Epstein, S., and T. K. Mayeda. 1953. Variation of O^{18} content of waters from natural sources. *Geochim. et Cosmochim. Acta* **4**:213–224.

Fireman, E. L., and F. S. Rowland. 1955. Tritium and neutron production by 2.2-Bev protons on nitrogen and oxygen. *Phys. Rev.* **97**:780–782.

Friedman, I. 1953. Deuterium content of natural water and other substances. *Geochim. et Cosmochim. Acta* **4**:89–103.

Harteck, P. 1954. The relative abundance of HT and HTO in the atmosphere. *J. Chem. Phys.* **22**:1746–1751.

Kaufman, S., and W. F. Libby. 1954. The natural distribution of tritium. *Phys. Rev.* **93**:1337–1344.

Lane, G. A., and M. Dole. 1956. Fractionation of oxygen isotopes during respiration. *Science* **123**:574–576.

Libby, W. F. 1955. Radiocarbon dating. Univ. of Chicago Press, Chicago: 2nd edition, 175 pp.

1956(a) Radioactive fallout and radioactive strontium. *Science* **123**:656–660.

1956(b) Radioactive strontium fallout. *Proc. Nat. Acad. Sci.* **42**:365–390.

Morrison, P., and J. Pine. 1955. Radiogenic origin of the helium isotopes in rock. *Ann. New York Acad. Science* **62**:69–92.

Rafter, T. A. 1955. ^{14}C variations in nature and the effect on radiocarbon dating. *New Zealand J. Sci. Tech.* (B) **37**:20–38.

Rakestraw, N., D. Rudd and M. Dole. 1951. Isotopic composition of oxygen in air dissolved in Pacific ocean water as a function of depth. *J. Amer. Chem. Soc.* **73**: 2976.

Revelle, R., T. R. Folsom, E. D. Goldberg, and J. D. Isaacs. 1955. Nuclear science and oceanography. Intern. Conf. on Peaceful Uses of Atomic Energy, Geneva, also Contr. Scripps Inst. Ocean. *N. S.* **794**: 22 pp.

Revelle, R., and H. E. Suess. 1957. Carbon dioxide exchange between atmosphere and ocean and the question of an increase in atmospheric CO_2 during the past decades. *Tellus* **9**:18–27.

Suess, H. E. 1953. Natural radiocarbon and the rate of exchange of carbon dioxide between the atmosphere and the sea. Nuclear Processes in Geologic Settings. *National Academy of Sciences — National Research Council Publication,* pp. 52–56.

Suess, H. E. 1954. Natural radiocarbon measurements by acetylene counting. *Science* **120**:5–7.

1955. Radiocarbon concentration in modern wood. *Science* **122**:415–417.

Von Buttlar, H., and W. F. Libby. 1955. Natural distribution of cosmic-ray produced tritium. 2. *J. Inorganic and Nuclear Chem.* **1**:75–91.

Reprinted from

THE EFFECTS OF ATOMIC RADIATION ON
OCEANOGRAPHY AND FISHERIES

PUBLICATION NO. 551
NATIONAL ACADEMY OF SCIENCES—
NATIONAL RESEARCH COUNCIL
1957

DISPOSAL OF RADIOACTIVE WASTES IN THE OCEAN: THE FISSION PRODUCT SPECTRUM IN THE SEA AS A FUNCTION OF TIME AND MIXING CHARACTERISTICS

CHAPTER 3

DISPOSAL OF RADIOACTIVE WASTES IN THE OCEAN: THE FISSION PRODUCT SPECTRUM IN THE SEA AS A FUNCTION OF TIME AND MIXING CHARACTERISTICS[1]

HARMON CRAIG, *Scripps Institution of Oceanography, University of California,*
La Jolla, California

I. *Introduction:* Estimated output of nuclear heat and fission products at "steady state" nuclear power production

IN TWO other papers in this report, Wooster and Ketchum discuss mixing rates in the oceans on the basis of oceanographic data, and the present writer reviews the natural isotopic studies which bear on the problem. In this paper we attempt to construct a detailed quantitative picture of the fission product spectrum in the ocean, in steady state with a given fission rate. Such an attempt may well be termed premature, in view of our sketchy knowledge of the internal mixing rate in the sea. Nevertheless, we know a good deal more today than was known five years ago, enough at least to make some simple model calculations which may well yield correct results to an order of magnitude. Moreover, the construction of a model and the calculation of its characteristics are often highly informative, and, at the very least, provide a basis for the orientation of future studies.

The following figures, available in various sources, are pertinent to the estimation of future consumption rates of nuclear power.

Present U. S. electrical energy:
6×10^8 mwh/yr.

Present world electrical energy:
10^9 mwh/yr.

Present world energy consumption (all sources) is about 4.5×10^{10} mwh/yr, doubling every 30 years.

For the present calculations, we shall assume a stationary world fission rate of U^{235} equal to 1000 metric tons/yr, supplying all the fission products to be disposed of in the sea. We shall then attempt to construct as reasonable a picture as possible of the fission product activity in the sea, when this activity reaches steady state with the rate of fission, i.e., when the decay rate of each fission product in the sea is equal to the rate at which it is being dumped into the sea, so that its concentration remains constant. We shall also make some calculations for a linear build up to such a fission rate in 50 years.

Since 1 gram of U^{235} is equivalent to 24 mwh, our assumed fission rate of 1000 tons of U^{235} per year is equivalent to 2.4×10^{10} mwh/yr of nuclear heat. At 50 per cent efficiency, this is equivalent to a world nuclear power consumption of 1.2×10^{10} mwh/yr. If this latter figure represents 10 per cent of the total world energy utilization, we are then assuming a world consumption of 1.2×10^{11} mwh/yr, which seems not unreasonable as an estimate for the year 2000 A. D.

Thus a fission rate of 1000 tons of U^{235}/yr represents a 2.7 fold increase in the present world energy consumption, 10 per cent being derived from nuclear heat with 50 per cent efficiency, which should be reached in about the year 2000 based on the present trend in energy consumption (see above). Our calculations will all be linear with the fission rate, so that data for other fission rates are easily derived from the present calculations.

The build up of fission products in a reaactor is given by:

$$\frac{dN}{dt} = fR - \lambda N$$

where f = fission yield (per cent of fissions yielding an individual fission product, the sum equalling 200 per cent), R is the rate of fission (atoms U^{235}/yr) here assumed constant and equivalent to 1000 tons of U^{235}/yr, and N = the

---

[1] Contribution from the Scripps Institution of Oceanography, New Series, No. 902a.

(70)

Reproduced by Permission

number of atoms of an individual fission product present in the reactor at any time.[2]

Integration with appropriate limits gives the number of atoms of a given fission product in the reactor as a function of time:

$$N = \frac{fR}{\lambda}(1 - e^{-\lambda t}) \qquad (1)$$

where the build up factor $(1 - e^{-\lambda t})$ varies from 0 to 1 as t varies from 0 to infinity, and gives the fraction of the equilibrium amount attained at any time. At secular equilibrium in the reactor, $dN/dt = 0$, and $\lambda N = fR$; we then have:

$$N_{eqlb} = \frac{fR}{\lambda} \qquad (2)$$

from which one sees that at any time in the reactor, $N = N_{eqlb}(1 - e^{-\lambda t})$.

The assumed fission rate of 1000 tons U^{235}/yr is equivalent to 2.2×10^6 megacuries of fission (1 curie $= 3.7 \times 10^{10}$ disintegrations/sec), and since the sum of the fission yields is 200 per cent, at equilibrium the total activity of all fission products present in the world, in megacuries, could be roughly estimated by multiplying 4.4×10^6 by the average number of radioactive members per fission chain. The amount of an individual fission product would be fR/λ, using the appropriate decay constant, and its activity would simply be fR, using the appropriate fission yield.

The lengths of the fission chains are difficult to estimate because of the extremely short half-lives of the first members. However, Dr. E. C. Anderson (personal communication) has studied the experimental data on the activity of fission product mixtures directly after fission, and concludes that for times beyond one day after cessation of fission, on the average only $\frac{1}{6}$ of the chains are still active (i.e. from this time on there are left only about 0.3 radioactive members per pair of fission chains initiated). Thus he points out that assuming a fission rate of 1000 tons U^{235}/yr as used above, and taking one day as an assumed minimum delay between accumulation and disposal, the steady activity in the sea for continuous stripping and disposal after one day would be roughly 7×10^5 megacuries. This is about the same total activity as that found below for an average irradiation time of one year with a 100-day cooling period before disposal, namely 7.7×10^5 megacuries (see calculations in Section IV and Table 1). The rough agreement of these numbers merely emphasizes the great predominance of the few long-lived isotopes of high fission yield in the fission product activity after very short times.

II. *Rate of introduction of fission products into the sea*

A more realistic picture is obtained by considering the irradiation time, or reactor holding time for uranium slugs, which is limited by structural weakening from irradiation, poisoning by fission products, etc., and the cooling period necessary for safe handling and for the growing in of plutonium in breeder piles. We assume the fission products of the world are distributed between (1) reactors, (2) cooling pits, and (3) the oceans (or any gross disposal site for that matter). The distribution among these reservoirs and the fission product spectrum in each depends on the irradiation and cooling times.

We shall assume an irradiation time of t_r years, equivalent to any of the following physical interpretations:

1. The reactors of the world are operated, on the average, t_r years, then stripped down and rebuilt.
2. The reactor slugs are continuously pushed through the reactors, each spending, on the average, t_r years in the reactor.
3. Continuous stripping into a holding tank which is opened every t_r years for removal of fission products.

---

[2] The above equation actually applies only to the first member of a fission chain; for the build up of the second member (y) of a chain with initial member (x), the correct expression is:

$$\frac{dN_y}{dt} = [f_x(1 - e^{-\lambda_x t}) + f_y]\,R - \lambda_y N_y$$

where f_x and f_y are the individual direct fission yields, and so forth for the succeeding members of each mass number chain. However the decay constants are very large for the first members of a chain, and thus one can neglect the exponential terms and assume a fission yield which is the total yield of the isotope under consideration plus all preceding members of the chain, for all irradiation times with which we shall be concerned. The experimental fission yield figures generally refer to the total chain yield, but because of the very low production of the later members of a chain by direct fission, there is no error involved in applying them to the first significantly long-lived chain member.

From these sources, the fission products are assumed to enter the cooling pits, from which they are dumped into the sea.

At the end of the irradiation time t_r, the amount of a fission product is given by (1) as:

$$N_{t_r}=\frac{fR}{\lambda}(1-e^{-\lambda t_r}) \qquad (3)$$

Assuming for the moment no cooling time, the fission products are stripped out every t_r years and dumped into the sea. Thus the introduction rate into the sea of a given fission product is equal to its activity A_s in the sea at steady state, and is given by N_{t_r}/t_r or:

$$A_{s(t_0=0)}=\frac{fR}{\lambda t_r}(1-e^{-\lambda t_r}) \qquad (4)$$

where t_o denotes the cooling time, here assumed to be 0.

The activity of the fission products in the world reactors at any time, A_r, may be evaluated in the following way. The fission products are stripped out every t_r years, and N_r, the amount in the reactors, varies from 0 to N_{t_r} in cycles, as t varies from 0 to t_r. For many reactors operating independently (the sum of the fission rates being R) with random distribution on the t_r cycle, we take the average of N_r consistent with R by integrating equation (1) from 0 to t_r and dividing by t_r; i.e., the steady state value of N_r is:

$$\bar{N}_r=\frac{1}{t_r}\int_0^{t_r}\frac{fR}{\lambda}(1-e^{-\lambda t})\,dt$$

Performing the integration, and setting $A_r=\lambda N_r$, we have for the steady state activity of a fission product in the reactors of the world:

$$A_r=\frac{fR}{\lambda t_r}[\lambda t_r-(1-e^{-\lambda t_r})] \qquad (5)$$

and from equations (4) and (5) we see that $N_s+N_r=fR/\lambda=N_{eqlb}$, the total amount of the fission product in the world, as of course it must.

Still neglecting cooling time, the fraction of the world total of a fission product which is in the sea is given by $N_s/N_{eqlb}=A_s/A_{eqlb}=F_s$, and:

$$F_{s(t_0=0)}=\frac{(1-e^{-\lambda t_r})}{\lambda t_r} \qquad (6)$$

Neglecting cooling time, the effect of irradiation time may be demonstrated by considering the long and short-lived radioisotopes of strontium, calculating the fraction of the world totals, for the assumed fission rate, which is in the sea, as a function of t_r, as given below.

	F_s (%)	
t_r (years)	Sr^{90} (28y)	Sr^{89} (54d)
0.1	99.9	79.8
0.5	99.4	38.6
1	98.8	21.2
2	97.5	10.7
10	88.5	2.1

Equation (6) shows the following characteristics:

For long half-lives (λt_r small): $F_s=1-\frac{\lambda t_r}{2}$ . . .(approaching 1).

For short half-lives ($\lambda t_r>5$): $F_s=\frac{1}{\lambda t_r}$

For $t_r=1$ year, and for any isotope with a half-life of less than 60 days:

$F_s=0.4t_{1/2}$ (where $t_{1/2}$ is here in days, $t_o=0$).

Thus, as shown above, increasing the irradiation time from 0.1 to 1 year cuts the fraction in the sea of a 60 day isotope by ¼, neglecting cooling time effects, but does not affect the long-lived isotopes.

We next interpose the cooling time between the reactor stripping and the disposal in the sea. The amount of an isotope left after the cooling period is:

$$N_o=N_{t_r}e^{-\lambda t_o}$$

and from (4), the steady state activity of a given fission product in the sea, equal to its introduction rate, now becomes:

$$A_s=\frac{fR}{\lambda t_r}(1-e^{-\lambda t_r})(e^{-\lambda t_o}) \qquad (7)$$

and F_s is reduced to:

$$F_s=\frac{(1-e^{-\lambda t_r})(e^{-\lambda t_o})}{\lambda t_r} \qquad (8)$$

III. *Fission product concentration in the sea as a function of linearly increasing fission rate*

We can get some idea of the transient characteristics of the fission product spectrum in the sea by examining the build-up of fission products with an increasing rate of fission. We shall take R, the world rate of fission, as 0 at the present time ($t=0$) and increasing linearly from the present time until it reaches the 1000 ton rate in 50 years. We shall further assume *continuous stripping* of fission products into the sea, and examine the transient characteristics of long-lived and a short-lived fission product.

The rate of increase of a fission product in the sea is given by:

$$\frac{dN}{dt}=f\left(\frac{R}{t}\right)t-\lambda N$$

where (R/t) is a constant by virtue of the assumed linear increase from $R=0$. N is now the amount of a fission product in the sea at any time t. We thus have:

$$dN+[\lambda N-(fR/t)t]dt=0$$

Multiplication by $e^{\lambda t}$ makes the equation exact, and the solution is:

$$N_t=ce^{-\lambda t}+\left(\frac{fR}{t}\right)\frac{(\lambda t-1)}{\lambda^2}$$

Evaluating the constant from $N=0$ at $t=0$, we have the general solution:

$$N_t=\frac{fR}{\lambda^2 t}[\lambda t-(1-e^{-\lambda t})] \qquad (9)$$

where N_t is the amount in the sea at the time t. Multiplication by λ to give the activity is seen to give an equation of the same form as (5) for the steady state amount in reactors, except that in (9) both R and t are variables, with R/t being constant.

We take $R=0$ at the present time, increasing linearly to 1000 tons U^{235}/year in 50 years. As noted previously, this rate is equivalent to 2.2×10^6 megacuries of fission, and thus $R/t=4.4\times10^4$ megacuries/year. Thus the activity of a fission product in the sea at any time t is given by:

$$A_t=4.4\times10^4\frac{f}{\lambda}[\lambda t-(1-e^{-\lambda t})] \qquad (10)$$

where A_t is in megacuries, $\lambda=\text{yrs}^{-1}$, t is in years, and f is the fission yield. We tabulate below the increasing activity in the sea for a long-lived and a short-lived isotope with continuous stripping into the sea.

Activity (megacuries) in the sea

	Sr^{90}	I^{131}
	$t_{1/2}=28y$	$t_{1/2}=8d$
t (years)	$f=0.05$	$f=0.028$
1	26.4	1200
10	2640	12,300
50	4.8×10^4	6.2×10^4
100	1.4×10^5	1.2×10^5
200	3.5×10^5	2.4×10^5
1000	2.1×10^6	1.2×10^6

At 50 years, when the fission rate of 1000 tons/year is reached, the Sr^{90} activity is half the amount which would be in steady state with this fission rate with an irradiation time of 1 year (see below and Table 1). If R continues to increase at the same rate, the steady state Sr^{90} activity for constant R is reached in about 100 years, and thereafter the activity increases linearly at a rate given by: $A_t=2200(t-40)$, the mean life of Sr^{90} being 40 years. The factor $(1-e^{-\lambda t})$ grows in to 95 per cent at 3 mean lives or 4 half-lives.

With a constant fission rate of 1000 tons U^{235}/year, irradiation time one year, and no cooling time, the I^{131} steady state activity in the sea would be 2000 megacuries (calculated as in Table 1, but with no cooling time). With the linear increase of fission rate and continuous stripping as shown above, this level is surpassed in two years. These data illustrate rather strikingly how rapidly the short half-life isotopes build up to secular equilibrium with an increasing fission rate. Sr^{90} does not equal the I^{131} activity until after 100 years of dumping into the sea, under the above conditions. For all species which have grown into secular equilibrium with the increasing fission rate, the activity ratios in the sea are simply given by the fission yield ratios.

IV. *Steady state fission product spectrum in a homogeneous, rapidly mixed sea*

The first three columns of Table 1 list all the fission products of any significance, together with their half-lives and fission yields. Columns 4 and 5 show the total amounts of each isotope in the sea, in metric tons and megacuries of activity respectively, in secular equilibrium with a fission rate of 1000 tons U^{235}

per year (2.2×10^6 megacuries of fission), assuming an irradiation time (t_r) of one year, and a cooling time (t_c) of 100 days (0.274 years). With such conditions, the expression for the activity of each fission product in the sea, as given by equation (7), becomes:

$$A_s = \frac{}{\lambda}(1 - e^{-\lambda})(e^{-0.274\lambda}) \times 2.2 \times 10^6 \text{ megacuries} \qquad (11)$$

where λ is in years^{-1}.

For half-lives greater than 1 year there is essentially no reduction in the oceanic activity by the cooling time. For all isotopes with half-lives greater than 5 years, more than 90 per cent of the isotope will be in the sea at steady state.

Of the 30 isotopes shown, 22 are independent and 8 are short-lived daughters which come quickly into secular equilibrium with their parents, decaying thereafter with the activity of the parent. Cs^{137} has a branching decay with 8 per cent going directly to the ground state of Ba^{137}; thus the secular activity of Ba^{137m} is only 92 per cent of the parent activity. The activities listed are beta activities only, for all isotopes except Ba^{137m}, Te^{129m}, and Cd^{115m}, which decay from their excited states by gamma emission. The Sm and Eu activities depend on the actual rate of burn-up in the reactors, and may vary considerably with different reactor conditions.

In the calculations, the first long-lived member of each fission chain was taken, and the fission yield for the entire chain was used for this isotope. The direct fission yield for the 11-day Nd which lies above the 2.5-year Pm in the 147 fission chain is not known, and thus this isotope has been neglected; the Nd comes quickly into secular equilibrium in the reactor, so that the total chain fission yield can be used for the Pm calculation.

The fission products are listed in order of decreasing total activity in the sea, with radioactive daughters paired with their parents. The total amount of all fission products in the sea is found to be about 3200 metric tons, corresponding to almost one million megacuries of activity. This represents almost twice the present activity in the sea, which is mainly due to the radioactivity of potassium 40. The figures for K^{40} and Rb^{87} are shown for comparison, the activity of the other radioactive elements in the sea being negligible relative to these isotopes.

We shall now discuss the effects of the mixing barrier at the thermocline in the sea on the distribution of the fission products between the deep sea and the upper mixed layer of the sea.

V. *Distribution of fission products between the deep sea and the mixed layer*

We shall assume a simple model, convenient for calculation, in which we divide the ocean into two geophysical reservoirs: a mixed layer above the thermocline, and the bulk of the ocean, termed the "deep sea," below the thermocline. The exchange of fission products between these two reservoirs is assumed to be a first order process, the rate of removal of a fission product from a reservoir being simply proportional to the amount of the isotope in the reservoir. The thermocline is assumed to represent the boundary across which the hold-up in mixing takes place.

Thus, for example, the rate of transfer of water from the mixed layer to the deep sea is assumed to be $k_m N_m$, where N_m is the mass of water in the mixed layer and k_m is the exchange rate constant for transfer of material from the mixed layer to the deep sea. In general, we write k_i as the fraction of material in reservoir i removed per year.

The residence time of a molecule in a reservoir, τ, is defined as the average number of years a molecule spends in the reservoir before being removed by the physical mixing process. The meaning of τ may be shown by the following derivation which gives a rigorous definition.

Assume a reservoir with a steady-state fixed content of N molecules of a substance, and a continuous flux into and out of the reservoir of ϕ molecules/year. At a particular time, $t = 0$, we have N_0 particular molecules in the reservoir, and at some later time t, we have N' of these original N_0 molecules still present. Then we define the average life of a molecule in the reservoir in the usual way, as

$$\tau = \frac{\Sigma_i t_i n_i}{\Sigma_i n_i} \approx -\frac{1}{N_0} \int_{t=0,\ N'=N_0}^{t=\infty,\ N'=0} t\, dN'$$

where n_i is the number of molecules of the original N_0 which remain in the reservoir for each time t_i, and dN' is the number of molecules removed in the interval t and $t+dt$, i.e., the number of molecules with a reservoir lifetime equal to t.

The number of molecules of the original particular set of N_0 which are removed in any interval dt is simply given by the concentration of such molecules in the reservoir, multiplied by the total flux from the reservoir, i.e.:

$$dN' = -\frac{N'}{N}\phi dt$$

which yields on integration $N = N_0 \, exp \, (-\phi t/N)$.

Substituting for dN' and then for N' in the integral expression for τ, and integrating between $t=0$ and infinity, we obtain:

$$\tau = \frac{N}{\phi}$$

and from the expression for N' one sees that τ, the average life, is also the time required for the original number of N_0 particular molecules to be reduced to $1/e$ times the initial number. τ is thus formally equivalent to a radioactive mean life.

In our particular model we are assuming the rate of removal to be dependent only on the total amount of substance, N, in the reservoir, so that the outgoing flux is given by $\phi = kN$. In such cases we see that $\tau = 1/k$, just as the radioactive mean life is equal to $1/\lambda$. The total removal rate of a radioactive isotope from a reservoir is of course the sum of the physical removal rate and the radioactive decay; τ as defined above refers only to the residence time relative to physical removal.

The symbols used in the following discussion are listed below, where i refers to the subscripts m and d for the mixed layer and deep sea.

N_i, V_i: mass and volume, respectively, of water in reservoir i.

N_i^* = amount of any fission product in reservoir i.

A_i = activity of any fission product in reservoir i $(=\lambda N_i^*)$, in megacuries.

a_i = activity of any fission product per unit volume of sea water in reservoir i.

k_i = exchange rate constant, = fraction of material in reservoir i removed per year.

τ_i = residence time in reservoir i relative to physical removal, $=1/k_i$.

m = average depth of mixed layer of the sea (taken as 100 meters).

D = average depth of the ocean (taken as 3800 meters).

We assume that the fission products are introduced into the deep sea after the 100 day cooling period, the disposal rate or flux of a given fission product isotope, termed ϕ, being equal to the steady-state total activity in the sea A_s as given by equation (11). ϕ is thus in "megacuries of flux," = atoms/sec divided by 3.7×10^{10}. We wish to ask what steady-state activity per unit volume of water will be in the mixed layer, as a function of the rate of cross-thermocline exchange of sea water and fission products.

The water balance between the reservoirs is given by:

$$k_m N_m = k_d N_d$$

or, neglecting density differences which are not important for these calculations,

$$\frac{N_d}{N_m} = \frac{\tau_d}{\tau_m} \approx \frac{D-m}{m} \qquad (12)$$

The fission products are introduced into the deep sea with a rate of introduction for any give isotope ϕ. The radioactive balance in the two reservoirs is then given by:

Deep sea: $\phi + k_m N_m^* = k_d N_d^* + \lambda N_d^*$ (13)

Mixed layer: $k_d N_d^* = k_m N_m^* + \lambda N_m^*$ (14)

Total: $\phi = \lambda(N_m^* + N_d^*) = A_s = A_m + A_d$ (15)

From (12) and (14)

$$\frac{N_d^*}{N_m^*} = \frac{\tau_d}{\tau_m} + \lambda\tau_d$$

or:

$$\frac{A_d}{A_m} = \frac{D-m}{m} + \lambda\tau_d$$

Thus for a stable element $(\lambda = 0)$ the partitioning is simply statistical. From (15):

$$A_m = \frac{\phi}{D/m + \lambda\tau_d} \qquad (16)$$

which gives the total activity of any fission product in the mixed layer as a function of decay constant, relative sizes of the mixed layer and deep sea, and exchange rate between the reservoirs as given by τ_d.

Various estimates of the value to be assigned to τ_d may be obtained from the separate papers by Wooster and Ketchum, and by Craig, in this report, and are discussed in relation to this particular model in the paper by Craig. From these discussions, we choose for the present calculations a value $\tau_d = 300$ years as perhaps the best guess. As discussed by the writer in a separate chapter of this report, radio carbon data indicate a residence time for water of about 1000 years, as a world-wide average. Mixing in the Atlantic is probably a good deal faster than in the Pacific, and 300 years is probably a safe lower limit estimate for the Atlantic, considering the material to be deposited on the bottom. Thus the mixed-layer activities we calculate should be upper limits, which would be approached more closely in the Atlantic than in the Pacific.

The average world-wide depth of the mixed layer, m, is taken as 100 meters, and the average depth of the sea is taken as 3800 meters. The volume of the sea is 1.4×10^{21} liters; thus the volume of the mixed layer is taken as 1/38 of this or 3.7×10^{19} liters. Putting these numerical values into (16), and noting that $\phi = A_s$, we have for the activity of any fission product per unit volume of sea water in the mixed layer:

$$a_m = \frac{10^{-8} A_s}{300\lambda + 38} \text{ dps/liter} \qquad (17)$$

in disintegrations per second per liter, where A_s is in megacuries, as tabulated in column 5 of Table 1, and λ is in years^{-1}. From this equation the values tabulated in column 8 of Table 1 were calculated, and were converted to microcuries per liter for column 9.

From the relation $a_d/a_m = (A_d V_m / A_m V_d) = (A_d/A_m)(m/D\text{-}m)$ we obtain:

$$\frac{a_d}{a_m} = \lambda \tau_m + 1$$

where τ_m, the residence time of a water molecule in the mixed layer, is given by (12) as 1/37 of $\tau_d = 8.1$ years. We thus write:

$$\frac{a_d}{a_m} = 8.1\lambda + 1 = \alpha \qquad (18)$$

from which, given the values of a_m computed above, the values of a_d tabulated in column 7 of Table 1 were computed. We call α the "oceanographic partition factor." It is a function of the mixing rate of the sea and the decay constant of the individual isotope, and is a measure of the effectiveness of the cross-thermocline exchange rate in buffering the mixed layer from the fission products introduced into the deep sea. Values of α are tabulated in column 6 of the table, and range from about 1 for the longest lived isotopes to about 250 for an isotope with a half-life of 8 days. For stable isotopes λ is 0, α is 1, and (18) reduces to simple statistical partitioning.

From (17) we see that as λ, the decay constant of an isotope, increases, the activity in the mixed layer decreases; i.e., if more of the isotope can be removed from the deep sea by decay, less needs to be transferred to the mixed layer to preserve the steady state. If the half-life were so long that the radioactivity did not affect the distribution between the mixed layer and the deep sea, we would have simply a statistical partitioning of the isotope between these reservoirs, such that the activity per unit volume in each reservoir would be the same. From the above equations we can derive the ratio of the activity in the mixed layer for an isotope to the activity per unit volume which would be observed if the partitioning were statistical:

$$\frac{a_m}{a_m(stat)} = \frac{\tau_d + \tau_m}{\alpha \tau_d + \tau_m} \approx \frac{1}{\alpha} \qquad (19)$$

and we see that α^{-1} is approximately the fraction of the statistical activity per unit volume attained by a fission product in the mixed layer. Equation (19) can be written exactly as:

$$\frac{a_m}{a_m(stat)} = \frac{t_{1/2}}{t_{1/2} + 5.5} \qquad (20)$$

where $t_{1/2}$ is the half-life of the isotope in years. The ratio $a_m/a_m(stat)$ is plotted in Figure 1 as a function of the half-life, and one reads, for example, that an isotope with a 5 year half-life attains about 48 per cent of the activity per unit volume in the mixed layer which it would have if its half-life were so long, relative to the mixing rate in the sea, that its radioactivity had no effect on its distribution.

The values of a_m, a_d, and α are tabulated in Table 1, in which the isotopes are arranged in order of their activity in the deep sea. For comparison, the activities of potassium 40 and rubidium 87, which provide essentially all the radioactivity in the sea, are also listed. In the deep sea, the predicted fission product activity is 19.3 disintegrations per second per liter, as compared with the natural activity of 12.2 dps/liter; thus the fission products in steady state with the 1000 ton fission rate would almost triple the deep-sea activity.

TABLE 1 FISSION PRODUCT SPECTRUM IN THE OCEAN AT STEADY STATE DISPOSAL INTO DEEP SEA. CALCULATED FOR FISSION RATE OF 1000 TONS U^{235}/YR (2.4×10^{10} MWH/YR OF NUCLEAR HEAT), IRRADIATION TIME OF 1 YR AND COOLING TIME OF 100 DAYS. AVERAGE LIFE OF A WATER MOLECULE IN THE DEEP SEA TAKEN AS 300 YEARS; AVERAGE DEPTH OF THE MIXED LAYER TAKEN AS 100 METERS.

			Total amount in ocean			Activity (dps/liter)		
Isotope	Half-life	Fission yield %	Metric tons	Activity megacuries	$\alpha = a_d/a_m$	a_d Deep sea	a_m Mixed layer	a_m Microcuries per liter
${}_{55}\text{Cs}^{137}$	33 y	6.3	1750	1.4×10^{5}	1.17	3.64	3.12	8.4×10^{-5}
${}_{56}\text{Ba}^{137m}$	2.6 m	—	—	1.3×10^{5}	—	3.35	2.87	7.7×10^{-5}
${}_{38}\text{Sr}^{90}$	28 y	5.0	780	1.1×10^{5}	1.20	2.90	2.42	6.5×10^{-5}
${}_{39}\text{Y}^{90}$	64 h	—	0.20	1.1×10^{5}	—	2.90	2.42	6.5×10^{-5}
${}_{58}\text{Ce}^{144}$	280 d	5.3	19	6.0×10^{4}	8.32	1.62	0.19	5.2×10^{-6}
${}_{59}\text{Pr}^{144}$	17.5 m	—	—	6.0×10^{4}	—	1.62	0.19	5.2×10^{-6}
${}_{61}\text{Pm}^{147}$	2.5 y	2.6	48	4.6×10^{4}	3.24	1.23	0.38	1.0×10^{-5}
${}_{62}\text{Sm}^{151}$	100 y	0.7	630	1.5×10^{4}	1.06	0.40	0.38	1.0×10^{-5}
${}_{40}\text{Zr}^{95}$	65 d	6.4	0.58	1.2×10^{4}	32.5	0.33	1.0×10^{-2}	2.7×10^{-7}
${}_{41}\text{Nb}^{95}$	36 d	—	0.32	1.2×10^{4}	—	0.33	1.0×10^{-2}	2.7×10^{-7}
${}_{39}\text{Y}^{91}$	60 d	5.9	0.39	9.4×10^{3}	35.1	0.25	7.2×10^{-3}	1.9×10^{-7}
${}_{44}\text{Ru}^{106}$	1 y	0.5	2.0	6.6×10^{3}	6.61	0.18	2.7×10^{-2}	7.2×10^{-7}
${}_{45}\text{Rh}^{106}$	35 s	—	—	6.6×10^{3}	—	0.18	2.7×10^{-2}	7.2×10^{-7}
${}_{38}\text{Sr}^{89}$	54 d	4.6	0.22	6.0×10^{3}	38.9	0.16	4.1×10^{-3}	1.1×10^{-7}
${}_{44}\text{Ru}^{103}$	40 d	3.7	7.2×10^{-2}	2.3×10^{3}	52.0	6.1×10^{-2}	1.2×10^{-3}	3.2×10^{-8}
${}_{45}\text{Rh}^{103}$	55 m	—	—	2.3×10^{3}	—	6.1×10^{-2}	1.2×10^{-3}	3.2×10^{-8}
${}_{58}\text{Ce}^{141}$	32 d	5.7	6.3×10^{-2}	1.8×10^{3}	65.0	4.9×10^{-2}	7.6×10^{-4}	2.0×10^{-8}
${}_{63}\text{Eu}^{155}$	2 y	0.03	0.44	5.1×10^{2}	3.8	1.4×10^{-2}	3.6×10^{-3}	9.7×10^{-8}
${}_{52}\text{Te}^{129m}$	33 d	0.3	3.4×10^{-3}	1.0×10^{2}	63.4	2.8×10^{-3}	4.4×10^{-5}	1.2×10^{-9}
${}_{52}\text{Te}^{129}$	70 m	—	—	1.0×10^{2}	—	2.8×10^{-3}	4.4×10^{-5}	1.2×10^{-9}
${}_{59}\text{Pr}^{143}$	13.7 d	5.4	—	40	151	1.1×10^{-3}	7.2×10^{-6}	2.0×10^{-10}
${}_{56}\text{Ba}^{140}$	12.8 d	6.1	—	30	161	8.0×10^{-4}	5.0×10^{-6}	1.3×10^{-10}
${}_{57}\text{La}^{140}$	1.7 d	—	—	30	—	8.0×10^{-4}	5.0×10^{-6}	1.3×10^{-10}
${}_{50}\text{Sn}^{123}$	130 d	1.2×10^{-3}	—	6.8	16.8	1.8×10^{-4}	1.1×10^{-5}	3.0×10^{-10}
${}_{48}\text{Cd}^{115m}$	44 d	8×10^{-4}	—	0.64	47.4	1.7×10^{-5}	3.6×10^{-7}	9.8×10^{-10}
${}_{53}\text{I}^{131}$	8 d	2.8	—	0.35	256	9.5×10^{-6}	3.7×10^{-8}	1.0×10^{-12}
${}_{63}\text{Eu}^{156}$	15.4 d	0.01	—	0.15	134	4.0×10^{-6}	3.0×10^{-8}	8.0×10^{-13}
${}_{55}\text{Cs}^{136}$	13.7 d	0.01	—	7.5×10^{-2}	151	2.0×10^{-6}	1.3×10^{-8}	3.6×10^{-13}
${}_{50}\text{Sn}^{125}$	10 d	0.02	—	1.7×10^{-2}	206	4.7×10^{-7}	2.3×10^{-9}	6.2×10^{-14}
${}_{47}\text{Ag}^{111}$	7.6 d	0.018	—	1.4×10^{-3}	268	3.9×10^{-8}	1.4×10^{-10}	3.9×10^{-15}
Totals:			3230	7.7×10^{5}		19.3	12.1	3.2×10^{-4}
Natural potassium and rubidium in the sea:								
K^{40}			6.3×10^{10}	4.6×10^{5}	1	12	12	3.2×10^{-4}
Rb^{87}			1.2×10^{11}	8.4×10^{3}	1	0.22	0.22	5.9×10^{-6}

All activity values are Beta activities only, except where isomeric transitions are indicated.

Conversion: 1 disintegration per second = 2.7×10^{-5} microcuries.
1 curie = 3.7×10^{10} disintegrations per second.

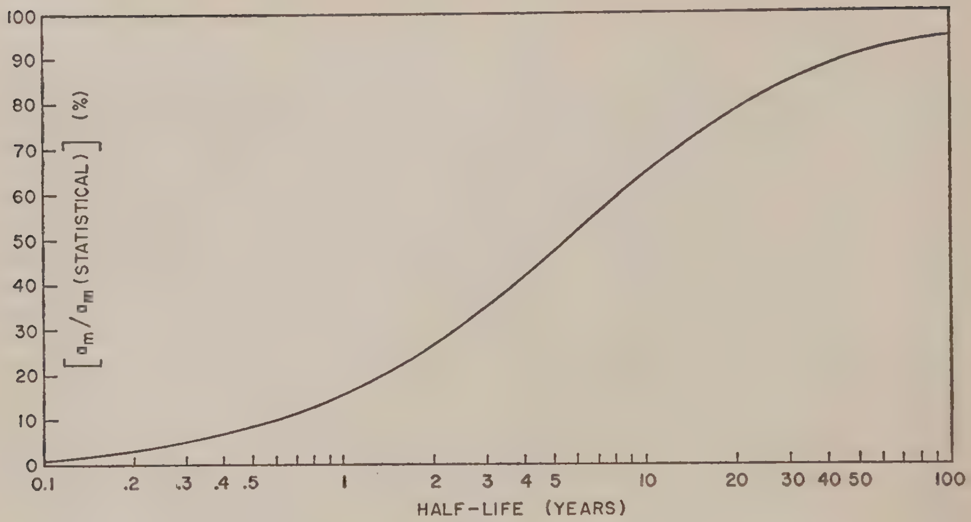

FIGURE 1

However, the effect of the internal mixing rate of the sea in the model adopted, is to cut the activity in the mixed layer down to 12.1 dps/liter which is, by coincidence, just equal to the natural activity and which would thus just double the activity in the mixed layer.

It should be noted that the figures given in the table for the predicted activities in the mixed layer refer only to cross-thermocline mixing by physical processes, exclusive of biological transfer through the thermocline. However, the figures listed provide a basis for speculation on the hazardous effects of the mixed layer activity, in that comparison may be made with biological concentration factors, discussed elsewhere in this report, to predict the activity levels in marine organisms. In this way, rough predictions may be made of the hazard to man, not only by direct exposure to the waters of the mixed layer of the sea, but by the activity concentrated in marine organisms used for food.

Reprinted from
THE EFFECTS OF ATOMIC RADIATION ON OCEANOGRAPHY AND FISHERIES
PUBLICATION No. 551, NATIONAL ACADEMY OF SCIENCES—NATIONAL RESEARCH COUNCIL, 1957

CHAPTER 4

TRANSPORT AND DISPERSAL OF RADIOACTIVE ELEMENTS IN THE SEA[1]

WARREN S. WOOSTER, *Scripps Institution of Oceanography,* La Jolla, California

and

BOSTWICK H. KETCHUM, *Woods Hole Oceanographic Institution,* Woods Hole, Massachusetts

THE FATE of radioactive elements in the sea differs from that of non-radioactive elements since they are subject to radioactive decay. Otherwise, concentrations of radioactive elements are changed by the same physical and biological processes as are those of other isotopes in the same physical state. Thus the fate of radioactive material introduced into the sea depends on:

1. What is introduced — the nuclide, its radioactive properties (half-life, nuclear reaction, kind and energy of radiation), its physical state in sea water (whether particulate, colloidal or ionic) and its chemical properties (including its role in biological processes).
2. Where it is introduced — position and depth with respect to the density and velocity structure of the sea.

This paper describes the physical processes whereby radioactive elements in true solution are diluted by mixing and are carried from one part of the ocean to another. Although all parts of the open ocean appear to be in continuous motion and in communication with each other, the rates of this motion and exchange cover such a wide range that it is convenient to consider separately the questions of near-surface vertical and horizontal exchange, intermediate and deep circulation, and the exchange between the deep sea, coastal areas and enclosed basins.

Near-surface circulation

In middle and low latitudes the surface layer of the ocean, from 10 to 200 meters thick, is separated from the colder deep waters by a layer of rapid density change and great stability, the pycnocline or thermocline. This intermediate layer varies in depth and stability from time to time and from place to place. At times there are two such layers, the seasonal thermocline and a deeper main thermocline. The surface layer is often called the "stirred" or "mixed" layer[2] because of its relative uniformity in temperature and in concentrations of dissolved substances.

It is believed that radioactive material introduced into this surface layer will be rapidly distributed vertically throughout the layer. The general uniformity of concentrations within this layer suggests that forces are present which tend to bring it about. Because density increases only slightly with depth through the layer, little energy is required for vertical stirring.

Some evidence of the rapidity of vertical mixing in the upper layer is given by Folsom (Revelle, Folsom, Goldberg and Isaacs, 1955), who observed that when fission products were introduced at the surface in an area where the surface layer was about 100 meters thick, the lower boundary of the radioactive water reached the bottom of this layer in about 28 hours. Within this period of time radioactivity had become uniformly distributed vertically throughout the layer.

Rapid vertical mixing in the upper layer is brought about primarily by the following two processes:

1. Convection: When the density of surface water is sufficiently increased, owing to either

---

[1] Contribution from the Scripps Institution of Oceanography, New Series, no. 903. Contribution no. 870 from the Woods Hole Oceanographic Institution. This paper, in part, represents results of research carried out by the University of California under contract with the Office of Naval Research. Reproduction in whole or in part is permitted for any purpose of the United States Government.

[2] A distinction is made here between stirring and mixing. In stirring, one causes relative motion of different parts of the liquid, and the average value of the gradient is increased. Mixing then takes place, the gradients disappearing and the liquid becoming homogeneous (Eckart, 1948).

a decrease in temperature or an increase in salinity, the surface water sinks and mixes with deeper water. Convection is maintained by (a) surface cooling due to long wave radiation and heat conduction to the atmosphere, (b) the loss of latent heat and water vapor in evaporation, or (c) the increase of surface salinity from freezing of surface water.

2. Wind stirring: Vertical turbulence in the upper layer results from wind action on the sea surface. The extent of wind stirring depends both on the magnitude and uniformity of wind stress and on the vertical density gradient. Stirring is effective only to a depth where there is sufficient energy to overcome the effect of stability. Both the homogeneity and the depth of the upper layer are affected by wind. Single gales have been observed to deepen the surface layer on the average by about 20–30 feet, (Francis and Stommel, 1953).

Rapid vertical mixing may be brought about by other processes. Thus in shallow coastal areas stirring by strong tidal currents is important. Stirring may also be accomplished by the vertical component of currents, particularly in regions of upwelling and sinking.

It should be noted that even above a well-developed pycnocline there is not complete homogeneity within the so called "mixed" layer. Concentrations of those elements affected by biological activity (such as oxygen and phosphorus) may show significant variation within the euphotic zone. Even so-called "conservative" concentrations (temperature and salinity) may not be uniform within the surface layer. Such heterogeneity may be attributed to incomplete vertical mixing or to vertical shear in the surface layer.

When radioactive materials are introduced into the near-surface layer, they are transported away from the area of introduction by surface currents. These currents extend, in general, through the entire depth of the upper layer and seem to be driven, directly or indirectly, by the wind.

The average locations and velocities of the important surface currents of the world ocean have been studied for many years and are well known (see, for example, Deutsche Seewarte, 1942; U. S. Navy Hydrographic Office, 1947 a and b, 1950; Sverdrup, Johnson, and Fleming, 1942, ch. 15). This knowledge comes primarily from averages of countless ship-drift observations, and from computations based on the observed subsurface distribution of density.

These calculations give mean speeds as high as 193 cm/sec (90 miles per day) in the Florida Current (Montgomery, 1938a) and 89 cm/sec (41 miles per day) in the Kuroshio (Koenuma, 1939). The volume of water flowing through the Florida Straits in 15 years is about equal to that of the upper 500 meters of the whole North Atlantic. Similarly, between the northern Ryukyus and Kyushu, the Kuroshio transports a volume equivalent to that of the upper 500 meters of the North Pacific in about 50 years. It seems likely that there is no area of surface water in the ocean that can be considered as isolated from the remaining surface waters.

Recent intensive studies of the Gulf Stream and other surface currents, using such modern instruments as the bathythermograph, electronic navigational aids, and geomagnetic electro-kinetograph (GEK), have revealed complicated fine structures, with filamentous jets and countercurrents not apparent in the average picture (Fuglister, 1951). Characteristic maximum surface velocities measured by GEK and Loran dead reckoning in the Gulf Stream were found to fluctuate between 150 and 300 cm/sec or 70 to 140 miles per day (von Arx, Bumpus and Richardson, 1955). Thus, in estimating the time at which radioactive materials will be found at various distances from the area of introduction, one must be cautious in the use of average surface current speeds.

Direct evidence of the transport of radioactive materials by surface currents in the western Pacific is given by "Shunkotsu-Maru" survey (Miyake, Sugiura and Kameda, 1955) and the "Taney" survey (U. S. Atomic Energy Commission, 1956) four months and thirteen months respectively after nuclear weapons tests in the Marshall Islands in March, 1954. The earlier survey found significant levels of radioactivity at a distance of 2000 kilometers from Bikini, suggesting a westward drift of more than 9 miles per day (about 20 cm/sec). The later survey found significant levels of radioactivity at least 7000 kilometers downstream from Bikini; this gives about the same minimum westward drift.

In addition to being drifted away from the area of introduction, radio-active materials are dispersed by diffusion. Diffusion in the ocean is caused by turbulence or eddies, and the coefficient of eddy diffusivity is usually more than a million times the corresponding molecular coefficient. The rate of eddy diffusion depends on wind speed, current shear, density gradient, gradient of the diffusing concentration, direction of diffusion, and the dimensions of the phenomenon. The calculated rates depend upon the magnitudes of eddy diffusivity coefficients used, and they have been estimated by a number of methods (Sverdrup et al., 1942, p. 484–485; Munk, Ewing and Revelle, 1949).

Because of both the large number of variables concerned and the present unsatisfactory state of our quantitative knowledge of turbulence in the ocean, it is difficult to predict the diffusion of radioactive materials under any given circumstances. The most satisfactory approach at present is to conduct diffusion studies and experiments at the place and under the conditions of contemplated release. The results are only applicable to the particular areas.

During the 1946 preliminary survey in Bikini Lagoon, the state of turbulence was determined by a variety of measurements, and the subsequent observed distribution of radioactivity was in close agreement with the predicted values (Munk, Ewing and Revelle, 1949). A mean value for the radius of the contaminated area was 3 km., which approximately doubled between the first and second days after the burst. The initial distribution of radioactivity as deposited by the atomic bomb was patchy, and the turbulent eddies, which spread the contamination over a larger area, did not appreciably reduce this patchiness during the first three days.

Another pertinent study was made by Ketchum and Ford (1952) who examined the rate of dispersion of acid-iron wastes in the wake of a barge at sea. Computed mixing coefficients showed a tendency to increase with increasing time, and thus with the dimensions of the mixing field, and the radius of the contaminated area was observed to double in time periods ranging from 0.5 minutes to 35 minutes. It should be noted that the scale of this phenomenon was about 10^{-2} that of Munk, Ewing and Revelle (1949); they show that the ratio of lateral eddy diffusivity coefficient to the radius of the area considered is relatively constant over a range of radius between 10^3 and 10^8 cm.

A large scale tracer experiment was carried out in the Irish Sea prior to the discharge of radioactive effluent (Seligman, 1955). During each experiment, 10 tons of 6.7 percent fluorescein solution were introduced near the surface during a 20-minute period, and the sensitivity of subsequent detection was believed to be of the order of 1 part in 10^9. Maximum concentrations detected directly after release were 10^{-4} of the original concentration; 12 hours after release, they were down to 5×10^{-7} of the original concentration. The trial area was probably part of an eddy and was subject to tidal mixing, so the results may not be generally applicable.

Exchange between near-surface and intermediate waters

Since the surface layer is separated from deeper waters by a layer of rapid density increase, and hence of great stability, vertical transfer of materials across this layer by eddy diffusion must be much less rapid than is vertical diffusion in the upper layer. Thus radioactivity introduced at the surface by fallout may remain in the upper layer for a long time and be diluted by only a small part of the total volume of the sea. Conversely, radioactive materials introduced below the pycnocline should only slowly contaminate the upper layer where they are most likely to endanger human activities. However, organisms and particles of sufficient density may readily cross the pycnocline, due both to gravity and to vertical migrations.

There are few observations which show directly the existence of cross-pycnocline exchange on a local scale. In the western Pacific, both the "Shunkotsu-Maru" survey (Japanese Fishery Agency, 1955) and the "Taney" survey (U. S. Atomic Energy Commission, 1956) reported patches with significant concentrations of radioactivity below the thermocline four months and thirteen months, respectively, after mixed fission products were introduced at the surface in the Marshall Island area. It is not known, however, whether this exchange was effected by mixing processes, or by particulate or ecological processes.

Exchange of properties between the near-surface and deeper waters is most likely to take place under the following conditions:

1. In regions where the pycnocline is sufficiently shallow to be eroded at the top by wind stirring. In coastal waters the pycnocline is usually shoaler than in midocean, and shallow pycnoclines may also be found in high latitudes, at the equator, along the north edge of the Equatorial Countercurrent, and at the center of strong cyclonic eddies. This process is not effective to great depths, but could serve to bring radioactive materials into the surface waters from the pycnocline layer.

2. In regions of upwelling, where the pycnocline is relatively weak and where vertical currents not only carry water toward the surface but also stir surface and deeper waters. It is unlikely that water from depths of more than 500 meters is ever brought to the surface by this process. Upwelling is common along western coasts of continents in the trade wind belt, such as the coasts of Peru and Northern Africa. In a simple sense, the persistent trade winds blowing parallel to or offshore develop an offshore component of transport in the surface waters, and deeper waters upwell to maintain the volume continuity. Upwelling may also occur along other coasts when the winds are suitable. The process has been extensively studied along the coast of California where it is not continuous because of the variability of the winds (Sverdrup et al., 1942, p. 725). The speed of coastal upwelling has been variously estimated as 0.6 m/day (McEwen, 1934), 2.25 m/day (Saito, 1951) and 2.7 m/day (Hidaka, 1954). However, since these estimates are theoretical mean values, they may differ significantly from actual instantaneous upwelling rates.

Midocean upwelling, associated with divergence of the surface currents, occurs in a band along the equator in the eastern and central Pacific Ocean (Cromwell, 1953). Observations indicate that the effects of this upwelling extend to 50 meters in the eastern Pacific and to 100–150 meters in the central Pacific (Wooster and Jennings, 1955). Similar but less pronounced upwelling has been observed in the equatorial Atlantic (Bohnecke, 1936).

3. In regions of surface convergence, where sinking waters may fill the depths of the ocean, or may spread at intermediate depths according to their density. In tropical and temperate latitudes such sinking is confined to the surface layer. In such regions mixing in the upper layer may be facilitated but exchange across the pycnocline probably is not, since the sinking water tends to increase the density gradient in the pycnocline.

In high latitudes, on the other hand, sinking waters may reach great depths, and it is in such regions that most of the intermediate and deeper water masses of the ocean are formed. The most extensive and pronounced of these convergences is the Antarctic Convergence which occurs at 50 to 60°S in a band around the entire Antarctic Continent. The cold, low-salinity water which sinks there forms an identifiable water mass, the Antarctic Intermediate Water, which spreads at depths between 800 and 1200 meters in all southern oceans. This water can be identified everywhere in the South Atlantic and extends across the equator as far as 22°N in the North Atlantic (Deacon, 1933; Iselin, 1936).

In the Irminger Sea, between Iceland and Greenland, and in the Labrador Sea, warm high salinity water of the Gulf Stream is partly mixed with cold low-salinity water flowing out of the Arctic Ocean. The resulting mixture may spread in small quantities as Arctic Intermediate Water, or when sufficiently dense may form the deep and bottom water of the North Atlantic (the possibility that the formation of this deep water is not a continuous process is discussed later). Intermediate waters of the North Pacific are probably formed in winter at the convergence between the Kuroshio Extension and the Oyashio (Sverdrup et al, ch. 15). There is apparently no deep or bottom water formed by this process in the Pacific.

4. In regions where the density of surface waters is so increased by evaporation, cooling or freezing, that they sink to intermediate or greater depths. Active formation of Antarctic Bottom Water takes place in the Weddell Sea due to the freezing of high salinity surface waters. In the Mediterranean and Red Seas, bottom water is formed by winter cooling of waters whose salinity has been greatly increased by evaporation. Mediterranean water flows out into the North Atlantic at depths of 1000 to 1500 meters and can readily be identified near Bermuda, 2500 miles from its source.

In summary, exchange between near-surface and deeper waters takes place most commonly (1) in high latitudes, (2) along the equator, and (3) in coastal regions, particularly along the western coasts of continents. Conversely, such exchange is least likely in temperate and tropical latitudes in the vast central regions of the northern and southern oceans.

Exchange between the open sea and coastal areas

In coastal areas or enclosed basins where precipitation exceeds evaporation, there is a seaward surface drift of diluted water and a landward subsurface drift of water derived from the open sea. If radioactive materials were released in such a coastal area, the material which remained in the surface layer would be carried seaward, but the part of the material which mixed or settled to the deeper water would move toward shore and the estuaries of rivers. Conversely, if radioisotopes were liberated in the open sea, some would eventually be carried inshore as a result of the coastal and estuarine circulation.

It is clear that the ultimate distribution in coastal areas of radioactive materials added to the sea would depend on the location of the release, the vertical distribution of radioactivity and density in the area of release, the length of time required for the transport to the coastal area or estuary, and the location of the source sea water which provides for the counter drift. The number of variables involved makes it difficult to discuss the effects in general terms, but it is worthwhile to note that the circulation in coastal areas is rapid, and water bathing the North Atlantic beaches is not uncommonly 90 per cent sea water even off large rivers such as the Hudson and Delaware.

An idea of the lengths of time involved in the coastal circulation can be obtained from the mean age of waters in various parts of the Atlantic seacoast. Such mean ages are computed from the volume of water contained in the region and the estimated transport of water through the region. The waters of the continental shelf from Cape Hatteras to Cape Cod have a mean age of about 2½ years, those of the Bay of Fundy about 3 months, and those of Delaware Bay from the ocean to the height of tide about 3–4 months (Ketchum and Keen, 1953, 1955). The source sea water for all of these circulations is the "slope water" which is formed between the Gulf Stream and the edge of the continental shelf.

A few data are available for confined basins and seas from which estimates of the mean age of the water can be derived. In most cases, however, the sources of water entering into the circulation are uncertain, and it should be emphasized that in all cases some of the waters within the basin will be older or younger than the mean age.

The source waters of the Florida Current are funnelled through the Caribbean Sea. The mass transport is 26 million cubic meters a second (Sverdrup et al., 1942, p. 638), so that this current carries annually a volume of water equivalent to one-sixth of the total volume of the Caribbean. However, there is evidence that the renewal of the deep water of the Caribbean proceeds at a much slower rate than the six year mean age that this ratio implies. Worthington (1955) has calculated, on the basis of loss of oxygen from this deep water during the last 30 years, that the age of the deep water in the various parts of the Caribbean may range from 93–142 years. The mean age of the waters above 2000 meters would be reduced to about 5 years if the deepest ⅕ of the volume of the basin is isolated from the present circulation.

The same current passes through the Yucatan channel into the Gulf of Mexico, before emerging as the Florida Current. No estimate of the mean age of the waters of the Gulf of Mexico is possible, however, since the current data in the Gulf indicate an anticyclonic eddy in the western portion, and suggest that the waters of the Gulf of Mexico are drawn into the Florida Current to only a slight extent (Dietrich, 1939, Sverdrup et al., 1942, p. 642).

The Black Sea probably contains the most isolated and the oldest deep water to be found anywhere in the oceans. Precipitation and runoff exceed evaporation, and the surface waters are dilute (salinities less than 18 per cent) and isolated from the deep water by an intense density gradient. The deep waters are anaerobic; hydrogen sulfide reaches large concentrations below about 200 meters. The sill at the Bosporus is only 90 meters below the surface so that this deeper water is isolated from the more rapid surface circulation. The inflow of sea water is so small that it would take about 2500 years to replace the deep water in the basin (Sverdrup et al., 1942, p. 651). The mean replacement time for the surface layers to a depth of 200 meters is equivalent to about 200 years. Gololobov (1949) has computed the mean age of the deep water on the basis of the annual contribution of phosphorus in the river inflow and the quantity accumulated in the depths. This computation indicates an accumulation time of 5600 years.

The Arctic Basin receives its major inflow north of Scotland and a much smaller inflow through the Bering Strait. Additional sources are from the river runoff and excess of precipitation over evaporation. The outflow is primarily through the Denmark Strait (Sverdrup et al., 1942, p. 655). These flows would provide a volume equal to that of the Arctic Ocean in about 160 years. The Arctic is also stratified because of the addition of fresh water from rivers and melting ice, and it is not known how isolated some of the waters in the deeper basins may be. However, recent analyses have shown that the deeper water in the Arctic Ocean is far from anaerobic, so that it seems unlikely that this water can be considered as isolated from the circulation.

The Mediterranean is a basin in which evaporation exceeds precipitation and runoff. Through the Strait of Gibralter there is an inflow of oceanic surface water and a subsurface outflow of high salinity Mediterranean water. The exchange is sufficiently rapid to replace the entire Mediterranean in about 75 years (Sverdrup et al., 1942, p. 647). The Mediterranean is divided into eastern and western basins by a 500-meter sill between Sicily and Tunisia, and it is not know to what extent the deep waters of these basins are involved in the over-all exchange.

Deep circulation

Most of our present knowledge of the intermediate and deep circulation (see Sverdrup et al., 1942, ch. 15) has been obtained indirectly from the observed distribution of properties. The general uniformity of temperature and dissolved substances in deep water suggests that deep currents are very slow, perhaps at most a few centimeters per second. But deep currents cannot be computed by the geostrophic method because only relative velocities can be thus obtained. Furthermore, small errors in the measurement of salinity or temperature produce uncertainties in velocity of the same magnitude as the currents being computed. The direction of movement in the deep and bottom water has been deduced from the observed distribution of properties such as salinity and potential temperature, but little can be learned about current speeds from such observations.

Existing direct measurements of subsurface currents have been summarized by Bowden (1954). Such measurements have been made since the time of the CHALLENGER Expedition (1873–76), but because of practical difficulties (such as the problem in the open sea of referring observations to a fixed frame of reference) they have taught us little about the deep oceanic circulation. The few successful measurements at depths greater than 1000 meters reported by Bowden showed mean speeds ranging from "negligible" to about 13 cm/sec. At nearly all stations and depths at which current measurements have been made, semidiurnal tidal currents of the order of 10 cm/sec. have been recorded.

Recently measurements of subsurface currents have been made in the North Atlantic by tracking for three days a neutral-buoyant float stabilized at a given depth (Swallow, 1955 and unpublished). These measurements show small resultant speeds (1.7 to 9.1 cm/sec or 0.8 to 4.2 miles/day at depths from 600 to 1900 meters), tidal components of about 10 cm/sec, and in two successive three-day measurements at 1900 meters, a change in direction of 124°. Thus it seems likely that motion below the pycnocline is characterized by more variation, periodic or otherwise, than previously supposed and indeed that the mean drift may represent only a small part of the total motion.

Little is known about the nature and extent of lateral and vertical mixing in the deep sea. It is generally believed, however, that flow and mixing take place along surfaces of constant potential density (isentropic surfaces) and that below the upper layer vertical mixing is very slow except near coastlines and areas where upwelling may occur (Montgomery, 1938). An observation supporting this belief was reported by Revelle, et al. (1955). Introduction of mixed fission products below the pycnocline led to the formation of a lamina of high radioactivity about one meter thick and 100 or more square kilometers in area. The radioactive water apparently spread out along an isentropic surface and resisted destruction by vertical mixing for at least three days.

Age of intermediate and deep waters

It is generally accepted that intermediate and deep waters in most parts of the oceans acquired their characteristics while at or near the surface. Thus the low temperature and relatively high oxygen content of deep water can only be explained by assuming an exchange between deep and surface waters. The problem of the disposal of radioactive wastes in the deep sea has stimulated the oceanographer's natural curiosity as to the rate of this exchange.

The North Atlantic receives surface waters from the South Atlantic and loses deep water to the South Atlantic. Assuming a surface flow from the South to the North Atlantic of 6 million cubic meters per second (Sverdrup et al., 1942, p. 685), and considering only the upper kilometer of the North Atlantic to be affected, the mean replacement time is about 140 years. The gyral in the North Atlantic, which includes the Gulf Stream, carries about ten times the volume of water exchanged between the South and North Atlantic, so that the mean circulation time is only about one-tenth the replacement time.

This surface exchange between the North and South Atlantic is balanced by a deep current from North to South. The mean displacement time for the deep water of the North Atlantic (2000–4000 meters) is calculated as about 250 years. This time is in reasonable agreement with more recent estimates of the age of the deep water discussed below.

Between these surface and deep layers are the intermediate waters which appear to circulate even more rapidly. Deacon (1933) calculated rapid rates of northward flow of the Antarctic intermediate water in the South Atlantic, based upon alternate maxima and minima in the concentrations of oxygen in the oxygen minimum layer. These were interpreted as representing annual cycles when the waters were formed at the surface. He estimated a transit time of about 4½ years between the Antarctic convergence and the equator. Seiwell (1934) has similarly computed rapid flows and a mean transport time of 7–8 years for the drift of the oxygen minimum layer of the North Atlantic Ocean. Deacon's and Seiwell's interpretations have been questioned (see Riley, 1951, p. 77) on various grounds. However, their rates of flow agree with direct current measurements at comparable depths (see earlier) which also indicate rapid rates of circulation.

The deep outflow from the Mediterranean sinks from sill depth to 1000–1500 meters in the North Atlantic Ocean. This water, although much diluted by Atlantic water, is characterized by relatively high salinity and temperature, and spreads out in a sheet which may be identified in most of the temperate North Atlantic, and some spreads into the South Atlantic. It can be readily identified near Bermuda, 2500 miles from its source. Iselin (1936) computed that sufficient excess salt would be produced by the Mediterranean outflow to produce the observed anomaly in 12–15 years. He pointed out that the actual replacement would be more rapid because he neglected admixture of Atlantic water in the immediate vicinity of the Straits of Gibraltar. Defant (1955) has evaluated the mixing processes involved in dissipating the Mediterranean water within the Atlantic Ocean, and has concluded that the total accumulation in the Atlantic Ocean represents the contribution resulting from six years of flow through the Straits of Gibraltar. The rapid dissipation of this large water mass at mid depths suggests a more rapid circulation than had been generally accepted for intermediate waters.

During recent years other lines of investigation have led to the belief that the overturn of water in the ocean basin takes place in less than a thousand years and probably in 200 years or less. Evidence supporting this belief follows. (Carbon-14 and carbon dioxide exchange estimations are discussed in greater detail by Craig elsewhere in this report.)

1. *Heat flow measurements:* Measurements reported by Revelle and Maxwell (1952) have shown a heat flow through the floor of the Pacific Ocean of 1.2×10^{-6} calories per square centimeter per second, or 38 calories per square centimeter per year. If not dissipated by circulation and mixing, this heat flow would lead to warming of the deep and bottom water during its passage from the Antarctic to the equator. From considerations of meridional circulation, observed temperature gradients and mixing in the deep sea, Revelle and Maxwell estimate that the deep water is replenished in less than 1000 years.

2. *Secular change of oxygen:* Worthington (1954) has shown that the North Atlantic Deep Water has suffered a loss of dissolved

oxygen of about 0.3 ml/L over the last twenty years. Assuming a steady rate of attrition he computes that the date at which this water was saturated, presumably while at the surface, was about 1810. A further study (Worthington, 1955) suggests that the Caribbean Deep Water was formed at the same time. Thus it seems possible that formation of the North Atlantic Deep Water, which composes about half of the contents of the Atlantic, is not continuous but sporadic.

3. *Carbon-14 dating:* In recent years the techniques of carbon-14 age determination have been applied to deep sea water samples. The most reliable measurements (Rubin, unpublished), of samples from east of the Lesser Antilles, show the carbon at 1750 meters to be about 200 years older than the surface carbon.

Present estimates of the age of deep waters are based primarily on measurements in the North Atlantic and on geochemical calculations for the entire world ocean. That the deep circulation of the Pacific is significantly slower than that of the Atlantic is suggested by the apparent absence of regions of deep and bottom water formation in the Pacific and the relatively high nutrient salt content and low dissolved oxygen content of deep Pacific waters. In order to determine whether the deep waters of the Pacific would provide a longer period of isolation for radioactive wastes than elsewhere, deep Pacific oceanographic data must be carefully scrutinized.

REFERENCES

BOHNECKE, G. 1936. Atlas: Temperatur, Salzgehalt und Dichte an der Oberflache des Atlantischen Ozeans. Deutsche Atlantische Exped. *Meteor*, 1925–27, Wiss. Erg. **5**: vii+76 pp.

BOWDEN, K. F. 1954. The direct measurement of subsurface currents in the oceans. *Deep-Sea Res.* 2:33–47.

CROMWELL, T. 1953. Circulation in a meridional plane in the central equatorial Pacific. *J. Marine Res.* **12**:196–213.

DEACON, G. E. R. 1933. A general account of the hydrology of the South Atlantic Ocean. *Discovery Rep.* **7**:171–238.

DEFANT, A. 1955. Die Ausbreitung des Mittelmeerwassers im Nordatlantischen Ozean. Pap. Mar. Biol. and Oceanogr., *Deep-Sea Res.*, suppl. to **3**:465–470.

DEUTSCHEN SEEWARTE. 1942. Weltkarte zur Ubersicht der Meeresstromungen. Deutschen Seewarte No. 2802.

DIETRICH, G. 1939. Das Amerikansiche Mittelmeer. Gesellsch. Erdkunde zu Berlin, Zeitschr., 108–130.

ECKART, C. 1948. An analysis of the stirring and mixing processes in incompressible fluids. *J. Marine Res.* **7**:265–275.

FRANCIS, J. R. D., and H. STOMMEL. 1953. How much does a gale mix the surface layers of the ocean. *Quart. J. Roy. Meteorol. Soc.* **79**:534–536.

FUGLISTER, F. C. 1951. Multiple currents in the Gulf Stream System. *Tellus* **3**(4): 230–233.

GOLOLOBOV, Y. K. 1949. Contribution to the problem of determining the age of the present stage of the Black Sea (in Russian). *Dokl. Akad. Nauk SSSR* **66**:451–454.

HIDAKA, K. 1954. A contribution to the theory of upwelling and coastal currents. *Trans. Am. Geophys. Union* **35**(3):431–444.

ISELIN, C. O'D. 1936. A study of the circulation of the western North Atlantic. *Pap. Phys. Oceanogr. Meteorol.* **4**(4):1–101.

JAPANESE FISHERY AGENCY. 1955. Report on the investigations of the effects of radiation in the Bikini region. Res. Dept., Japanese Fishery Agency, Tokyo, 191 p.

KETCHUM, B. H., and W. L. FORD. 1952. Rate of dispersion in the wake of a barge at sea. *Trans. Am. Geophys. Union* **33** (5):680–684.

KETCHUM, B. H., and D. J. KEEN. 1953. The exchanges of fresh and salt waters in the Bay of Fundy and in Passamaquoddy Bay. *J. Fish. Res. Bd. Can.* **10**:97–124.

1955. The accumulation of river water over the continental shelf between Cape Cod and Chesapeake Bay. Pap. Mar. Biol. and Oceanogr., *Deep-Sea Res.*, suppl. to vol. **3**: 346–357.

KOENUMA, K. 1939. On the hydrography of south-western part of the North Pacific and the Kuroshio. *Kobe Imper. Marine Observ., Memoirs* **7**:41–114.

McEWEN, G. F. 1934. Rate of upwelling in the region of San Diego computed from serial temperatures. *Fifth Pac. Sci. Congr.,* Toronto **3**:1763.

MIYAKE, Y., Y. SUGIURA, and K. KAMEDA. 1955. On the distribution of radioactivity in the sea around Bikini Atoll in June, 1954. *Pap. Meteorol. Geophys.,* Tokyo **5**(3, 4):253–362.

MONTGOMERY, R. B. 1938a. Fluctuations in monthly sea level on eastern U. S. coast as related to dynamics of western North Atlantic Ocean. *J. Marine Res.* **1**:165–185.

1938b. Circulation in upper layers of southern North Atlantic deduced with use of isentropic analysis. *Pap. Phys. Oceanogr. Meteorol.* **6**(2):1–55.

MUNK, W. H., G. C. EWING, and R. R. REVELLE. 1949. Diffusion in Bikini Lagoon. *Trans. Am. Geophys. Union* **30**(1):59–66.

REVELLE, R., and A. E. MAXWELL. 1952. Heat flow through the floor on the eastern North Pacific Ocean. *Nature* **170**:199.

REVELLE, R., T. R. FOLSOM, E. D. GOLDBERG, and J. D. ISAACS. 1955. Nuclear science and oceanography. United Nations International Conference on the Peaceful Uses of Atomic Energy, Geneva, Paper no. 277: 22 pp.

RILEY, G. A. 1951. Oxygen, phosphate and nitrate in the Atlantic Ocean. *Bull. Bingham Oceanogr. Coll.* **13**, Art. 1:1–126.

SAITO, Y. 1951. On the velocity of the vertical flow in the ocean. *J. Inst. Polytech., Osaka City Univ.* **2**(1) Ser. B.:1–4.

SEIWELL, H. R. 1934. The distribution of oxygen in the western basin of the North Atlantic. *Pap. Phys. Oceanogr. Meteorol.* **3**(1):1–86.

SELIGMAN, H. 1955. The discharge of radioactive waste products into the Irish Sea. Part 1. First experiments for the study of movement and dilution of released dye in the sea. Proceedings of the International Conference on the Peaceful Uses of Atomic Energy, Geneva. Paper **9**:701–711.

SVERDRUP, H. U., M. W. JOHNSON, and R. H. FLEMING. 1942. The oceans, their physics, chemistry and general biology. Prentice-Hall, N. Y., x+1087 pp.

SWALLOW, J. C. 1955. A neutral-buoyancy float for measuring deep currents. *Deep-Sea Res.* **3**:74–81.

U. S. ATOMIC ENERGY COMMISSION. 1956. Operation Troll. U. S. Atomic Energy Commission, New York Operations Office, NYO 4656, Ed. by J. H. Harley, 37 pp.

U. S. NAVY HYDROGRAPHIC OFFICE. 1947a. Atlas of surface currents, north Atlantic Ocean. H. O. Pub. 571, First Ed., reprinted 1947.

1947b. Atlas of surface currents, northeastern Pacific Ocean. H. O. Pub. 570, First Ed.

1950. Atlas of surface currents, northwestern Pacific Ocean. H. O. Pub. 569, First Ed., reprinted 1950.

VON ARX, W. S., D. F. BUMPUS, and W. S. RICHARDSON. 1955. On the fine structure of the Gulf Stream front. *Deep-Sea Res.* **3**:46–65.

WOOSTER, W. S., and F. JENNINGS. 1955. Exploratory oceanographic observations in the eastern tropical Pacific, January to March, 1953. *Calif. Fish and Game* **41**: 79–90.

WORTHINGTON, L. V. 1954. A preliminary note on the time scale in North Atlantic circulation. *Deep-Sea Res.* **1**:244–251.

1955. A new theory of Caribbean bottom-water formation. *Deep-Sea Res.* **3**:82–87.

Reprinted from
THE EFFECTS OF ATOMIC RADIATION ON OCEANOGRAPHY AND FISHERIES
PUBLICATION No. 551, NATIONAL ACADEMY OF SCIENCES—NATIONAL RESEARCH COUNCIL, 1957

CHAPTER 13

LARGE-SCALE BIOLOGICAL EXPERIMENTS USING RADIOACTIVE TRACERS [1]

MILNER B. SCHAEFER, *Inter-American Tropical Tuna Commission, Scripps Institution of Oceanography,* La Jolla, California

ONE OF the major difficulties in evaluating the probable results of the introduction of radioactive materials into the sea is the lack of adequate knowledge respecting the effects of the organisms in the sea on the distribution and transport of such materials. Some information, which has been reviewed in earlier sections of this report, has been obtained on the uptake and excretion of elements by different kinds of marine organisms. This information is, however, not sufficiently extensive. The even more important problems of the quantitative interrelationships and movements of the populations of organisms at the several trophic levels are among the least understood biological phenomena of the oceans. These, together with physical factors, will determine the fluxes of the radioactive materials.

Measurements of the fluxes of materials through physical-biological systems, or ecosystems in the sea are of vast and fundamental importance not only for evaluating the probable distribution of radio-active products introduced into the sea, but also as a basis of evaluating the sea as a source of food and other biological products for the use of mankind. With the approaching full utilization of the land, increasing attention is being directed to the sea as a source of such products, but the basic biological knowledge for realistic evaluation of the potential harvest of the sea is quite inadequate.

The availability of rather large quantities of radioactive materials, as by-products of the development and utilization of nuclear energy, makes possible the study, *in situ,* of the biological and ecological processes in the sea by the use of tracer techniques. A start has been made, in connection with the introduction of radioisotopes into the marine and fresh waters by weapons tests and by the disposal of low-level wastes, but the opportunities for obtaining useful information by these means have not been fully exploited. Also it should be possible by introducing radioisotopes in a planned, controlled, and purposive fashion to obtain even better information than is possible through observation of introductions ancillary to operations having a different primary purpose.

Observation in connection with weapons tests

Observations in connection with weapons tests have the advantages that (1) very large quantities of radioisotopes are introduced into the sea, sometimes over a rather large area, so that radioactivity is sufficiently high to be detected in the sea waters and organisms over a considerable time after the event, and (2) the difficulty of being certain that the organisms have actually remained in the water containing the isotopes is minimized. On the other hand, the determination of exact amounts of isotopes introduced, of their spatial distribution, and of their physical state presents some difficulty.

Biological studies, in connection with the various weapons tests in the Western Pacific ocean, have been primarily directed toward determining the concentration of gross activity in different organisms, the localization of such activity in different parts of the organism, and the rates of decline of activity with time. There has also been limited determination of the isotopes concerned. The most extensive data are from the lagoons of the atolls at and near the test sites. In the open sea, outside the lagoons, usually only limited collections of organisms have been made, incidental to other operations.

Following the test series of 1954, however, two rather extensive surveys were made of the distribution of activity in the sea, and in organisms at different trophic levels, over a large sea area at intervals of approximately 4 months and 13 months after the test.

---

[1] Contribution from the Scripps Institution of Oceanography, New Series, No. 903a.

These observations have been directed primarily to possible human hazards through contamination of edible marine products. Only minor attention has been given to ecological processes, probably because of lack of facilities for the extensive, systematic collecting required.

Soon after the underwater test in the Eastern Pacific in the spring of 1955, some collections were made that indicate which organisms in the food chain are the primary concentrators of certain radioisotopes, and that give some indication of the time scale in passage to the next step of the food chain. Unfortunately, it was not possible to follow the passage of isotopes farther through the system.

Following a weapons test a series of observations and collections taken in a carefully planned pattern in space and time could provide information on the time scale involved in the passage of material through the system of prey and predators, and on the efficiency of this transfer from one stage to another, two of the little understood basic problems in marine ecology. Data from experiments with radioactive tracers, together with more limited field data, indicate that the transfer efficiencies are different for different elements.

In those situations, following weapons tests, where there is a fairly extensive body of water containing radioisotopes at some particular level, say at the surface, it should be possible by means of collections at various depths over a period of time to obtain worthwhile information on the vertical migrations of organisms, and also to determine how the feeding and excretion patterns of such organisms transport radioisotopes from one level to another.

These and similar studies would require the assignment of a vessel, with necessary equipment and a team of scientists, to the exclusive pursuit of such studies. Since results will depend on systematic, serial observations, the vessel must be available to take them when and where required, which precludes the commitment of the vessel to other activities. Although a sizable cost is involved, it is believed that the results to be obtained are of sufficient value to more than justify it.

It should also be pointed out that effective planning of such studies requires considerable knowledge of the types of organisms to be encountered in the test area, the sizes of their populations, and some knowledge of their migration patterns, as well as data on the currents and other physical parameters to be considered. A pre-survey of the test areas by standard methods of biological investigation is, therefore, an important element in the adequate planning and execution of post-test investigations by means of the radioisotopes produced by the test.

Observations in connection with waste disposal

The disposal of wastes from the fission industry by introduction into the marine environment offers another means of studying the uptake of elements by aquatic organisms, their fluxes in the ecosystem, and their effects on the organisms concerned. Advantages over weapons tests are: (1) the wastes are usually introduced in such a manner that their amount, distribution and physical state can be readily determined, (2) disposal is usually continuous, even though not of constant magnitude, thus permitting systematic study over considerable periods of time.

Disposal in the United States has consisted of relatively low-level wastes introduced into fresh waters by the Hanford works on the Columbia River, the Oak Ridge National Laboratory, and the Plant on the Savannah River. At the first named locality, field observations, supplemented by laboratory experiments, are being made on the uptake of radioisotopes by organisms, their fluxes through the food chain, and their distribution in the river as the result of the combined effects of physical and biological processes. The phosphorous cycle has been investigated in particular detail. At the Oak Ridge Laboratory, observations were made over a period of years on the uptake of fission products by various organisms, the sites of deposition of radioisotopes in the organisms and the effects on some of their populations. Continuous disposal into marine waters is not practiced at present in this country. Reports by H. Seligman, H. J. Dunster, D. R. R. Fair and A. J. McLean at the 1955 Geneva Conference on Peaceful Uses of Atomic Energy describe introduction of low-level wastes into the Irish Sea, and briefly review studies of the uptake of various isotopes by different kinds of organisms.

With the exception of limited work at Hanford and Oak Ridge, it appears in all these cases that primary attention has been concentrated on monitoring aspects, that is measurement of the quantity and distribution of radioisotopes to insure against hazards to human or other animal populations. The work of Richard Foster and others on the radiophosphorus cycle in the Columbia River, and the work of Louis A. Krumholz on seasonal variations in quantities of fission products in different groups of organisms, indicate however, that locations where wastes are being continuously introduced into aquatic environments offer a good opportunity to study the ecological processes of the aquatic populations through the tracers provided by the introduced isotopes. It may be expected with the development of the fission industry in the next few years, that there will be disposal of some low-level wastes into marine waters, which will provide opportunities to investigate the ecology of estuaries and inshore ocean waters by these means.

These introductions also constitute large-scale experiments on both the direct and genetic effects of long-term exposure of marine organisms to atomic radiations. It is important that these effects be carefully investigated, because it is possible that the larger organisms in the sea, which are subjected to much lower rates of natural radiation than terrestrial forms (due to the shielding effects of water on cosmic rays, as well as to the low gamma-ray activity per unit volume of sea water compared with the rock and soil of the land), may show proportionally a greater genetic effect from a given amount of radiation.

Planned experiments

Much useful information may be obtained by well conceived biological observations in connection with weapons tests and routine disposal of industrial atomic wastes. Much more precise information could be obtained, however, by planned experiments introducing measured quantities of known isotopes into the marine environment in a controlled manner. Furthermore, it is evident that the fluxes of different elements through the ecosystem vary according to their abundance in the sea and their physiological roles in the organisms. Some of the most important elements biologically are not fission products, nor are they present in wastes in appreciable quantity. The outstanding example is carbon. The energy which supports most of the life in the sea, as on the land, is fixed as chemical energy of complex carbon compounds synthesized by plants. To study the flux of energy through the different trophic levels of the ecosystem it is necessary, therefore, to measure directly or indirectly the flux of carbon. One of the most promising possibilities, discussed further below, is the use of radiocarbon in tracer experiments on a scale larger than the present laboratory-type experiments.

The need for large scale experiments under natural conditions arises because we require knowledge concerning the quantitative interrelationships of the various populations of organisms, and it is not possible to reproduce natural marine communities, especially the pelagic elements, in the laboratory. It is probably not possible yet to study some aspects of open-sea communities by radioactive tracers, either, but it may be possible to improve on present techniques by larger scale *in situ* experiments than have been attempted.

Large scale experiments, employing either mixed fission products or single isotopes isolated from mixed fission products, appear feasible (at least in selected locations in the open sea) to determine what organisms take up which elements and the quantitative aspects of how these elements are passed through the food chain. It may also be feasible to introduce sufficient quantities of radioisotopes in particular situations to make possible a study of the transport of such elements by migrations of organisms. In general, however, in the open sea, it will be necessary to confine attention to those elements which are naturally present in seawater in very small concentrations, so that the organisms may be expected to take up a relatively large fraction of the isotope in question. In the case of elements such as carbon, only a small fraction of which is taken up by the organisms, experiments in unconfined volumes of open sea would appear to require larger quantities of the radioisotope than are feasible on a cost basis, and experiments therefore will have to be limited, in the near future at least, to small enclosed arms of the sea or artificially bounded volumes of water in the open sea.

In order to conduct experiments in the open sea it is necessary to (1) introduce the radioisotopes into an area sufficiently large so that it can be located and followed, to insure the or- (91)

ganisms under study being in it over a known period of time, and (2) have a sufficiently high radioactivity that it may be followed from shipboard. If we use only fission products which organisms concentrate; then, since longer counting periods are feasible for samples of the organisms than are feasible for the equipment used to locate and follow the water mass, the radioactivity required to determine the position of the contaminated water mass is expected to be the limiting factor in the experiment.

Revelle, Folsom, Goldberg and Isaacs (1955) have indicated that, in the slow-mixing levels of the sea below the thermocline, vertical mixing is almost negligible, so it may be expected that while the area in which the isotopes can be detected spreads over a radius of 4.1 km., vertically it will be limited to about .1 meter. In these circumstances, it has been calculated that 10 curies of gamma emitter may be detected until it has spread laterally to a radius of 4 km., or a mean concentration of about 2×10^{-7} curies per cubic meter. They do not specify the time involved, but it may be presumed to be of the order of one week to one month. For biological experiments, it would be necessary to make observations over a longer period of time, also we cannot commence significant biological observations until the contaminated area is sufficiently large to ensure knowledge of which animals are or have been in the active water. For these reasons the time involved should perhaps be increased by a factor of 10. If the diffusion of the contaminated water, both vertically and horizontally follows the "random walk" law, the volume containing the activity will increase linearly with time, and, in consequence, about 100 curies of gamma activity will be required.

Experiments in the upper mixed layer will require much larger quantities of fission products. Mixing to the top of the thermocline is very rapid; according to the authors above cited the lower boundary of radioactive water moves down at about 10^{-1} cm/second. If we select an area, such as that off Central America where there is a fairly shallow sharp thermocline at a mean depth of about 20 meters, mixing down to the top of the thermocline would be complete in less than ten hours. Thereafter downward mixing should be negligible. Recent experiments suggest that the radius over which the water spreads laterally is increased as about the 0.8 power of time. In Bikini lagoon it has been found that the radius of the radioactive area increased to 4 kilometers in 3 days. If we ran an experiment for 90 days, which is probably the time necessary to follow the flux of radioelements through two or more trophic levels, we would, then, expect the radius to approximate

$$r = 4(30)^{.8} = 60 \text{ kilometers.}$$

The volume would then be (with a 20 meter thermocline)

$$\pi \times 36 \times 10^8 \times 20 \text{ cubic meters}$$
$$\text{or about } 225 \times 10^9 \text{ cubic meters}$$

To be still detectible at this dilution, using the above estimate of 2×10^{-7} curies/cubic meter, an initial quantity of some 4×10^4 curies would be required. The logistics of handling large quantities of fission products will be difficult, but not perhaps impossible.

Because of the smaller volume of water to be dealt with, it may be most desirable, at least initially, to conduct such experiments in a small enclosed arm of the sea. Such an environment is different in many respects from the open ocean, but much useful information about fluxes of radioelements through the several trophic levels could be obtained. It would not be difficult to select a small bay, with a narrow, shallow entrance, which could be cut off temporarily from the sea for this purpose. A body of, say, one square kilometer with an average depth of ten meters might be used, giving a volume of 10^7 cubic meters. Since the problem of locating the water mass is eliminated, and fairly large volumes of water can be filtered for organisms, rather small quantities of fission products, which would not be hazardous, could be employed. One curie would be ample, and the contamination of the water itself would be within safe levels for human hazards.

It was noted earlier that one of the important fundamental ecological problems is to measure the flux of carbon through different trophic levels. Since the fraction of the carbon taken up by plants is a very small part of the total in the sea water, experiments with radio-carbon in the open sea are not feasible. Experiments using samples in bottles have been conducted *in situ* in recent years, but these have two deficiencies: (1) the surface and other effects of the container modify the environment so that the resulting computations for photosynthesis probably are not those that would have occurred naturally in the sea and (2) only the uptake of carbon at the phytoplankton level is measured. It seems feasible to improve on the experiments in bottles by conducting experiments in small lagoons, or by employing larger partly-enclosed volumes in the open sea.

From experience with such experiments in bottles, it can be shown that there is sufficient uptake of carbon by the phytoplankton, if grown in a concentration of 0.3 micro-curie per liter for one day, to measure it if a one liter sample is filtered and the radioactivity of the filtered plants determined in a counter of 20 per cent efficiency. By increasing either the counting time or the volume of water filtered, the initial concentration of C^{14} can be decreased correspondingly.

For an experiment in a lagoon, we might use a body of water of, say, 500 meters long by 200 meters wide with an average depth of 10 meters, giving a volume of 1×10^6 cubic meters or 1×10^9 liters. By filtering 100 liters of water for phytoplankton, C^{14} at a concentration in the water of 3×10^{-9} curies per liter would suffice, or 3 curies for the experiment. Since there is probably between a 50 per cent and 90 per cent loss at each step up the food chain, correspondingly larger volumes would have to be strained for the higher forms, but this is a simple problem by the use of standard nets, etc.

To get improved measurements of the uptake of carbon by phytoplankton in the open sea, and the passage of carbon to the smaller grazing organisms, it is suggested that a moderately large rubber tank open at the surface be employed to isolate a piece of the top of the sea, yet have a sufficiently small surface-to-volume ratio that the processes will more nearly approach normal conditions than is obtained in bottle experiments. We might employ such an apparatus of 20 meters diameter by 10 meters deep, having a volume of $\pi\, 10^3$ cubic meters, or $\pi \times 10^6$ liters. By filtering 10 liter samples for phytoplankton, with 20 per cent efficient counting equipment, we would need to provide about 3×10^{-8} curies per liter, or a total of about 1/10 curie of C^{14}.

Some cost and logistic considerations

For the two experiments with C^{14}, discussed immediately above, the problems of handling the amounts of activity involved present no particular difficulty. Since C^{14} is a pure beta emitter, the shielding problem for even the experiment requiring 3 curies is a simple matter. The cost of the isotope, however is fairly high; at present about $30,000 per curie. This might be reduced somewhat if the present demand were to increase. The cost, notwithstanding, however, the information to be gained is well worth the outlay.

In the case of an experiment using gamma emitters in the slow-mixing layer below the thermocline, where about 100 curies would be required, it is suggested that mixed fission products from wastes from processing of reactor fuel elements be used. A large quantity of such wastes will be available, probably at no charge. If one used HNO_3 salted waste product from a natural uranium-plutonium reactor, after 100 days "cooling," the reactor waste will contain about 200 curies/gallon. Approximately half a gallon will be needed, requiring about 10″ of lead shielding for transportation and handling. A cubical container will require 10.05 cubic feet of lead, weighing 7,175 pounds. This is feasible to handle by freight and on shipboard.

For the kilocurie quantities required for an experiment in the upper mixed layer of the sea, the handling problem reaches a different order of magnitude. It becomes quite infeasible to handle waste liquids in the volume required. It may be possible, because of the much higher activity per unit volume to employ slugs of U^{235} from a reactor, which, after 30 per cent burning and 100 days "cooling" have about 2×10^5 curies per kilo of fairly long term gamma activity. Even then some 2/10 kilos of "used" U^{235} would be required. The problems of transporting and handling this are somewhat difficult as are methods of dissolving and liberating the material at sea, but probably feasible. Further detailed consideration needs to be given to this problem. It may, of course, be that the use of an explosive reaction — a small nuclear detonation for oceanographic and biological experimental purposes — is the only logistically feasible method.

REFERENCES

Revelle, R., T. R. Folsom, E. D. Goldberg, and J. D. Isaacs. 1955. Nuclear Science and Oceanography. United Nations International Conf. on Peaceful Uses of Atomic Energy, Geneva, Paper no. 277:22 pp.

Reprinted from

THE EFFECTS OF ATOMIC RADIATION ON
OCEANOGRAPHY AND FISHERIES

PUBLICATION NO. 551
NATIONAL ACADEMY OF SCIENCES—
NATIONAL RESEARCH COUNCIL
1957

COMPARISON OF SOME NATURAL RADIATIONS RECEIVED BY SELECTED ORGANISMS

Chapter 2

COMPARISON OF SOME NATURAL RADIATIONS RECEIVED BY SELECTED ORGANISMS[1]

Theodore R. Folsom, *Scripps Institution of Oceanography, La Jolla, California*

and

John H. Harley, *Health and Safety Laboratory, U. S. Atomic Energy Commission*

In attempting to consider in numerical terms possible consequences to populations from mutations caused by very low levels of artificial radioactivity, it is instructive to collect for quick comparison some estimates of the natural doses to which certain organisms have been exposed for geological periods. These data emphasize that doses from natural sources vary widely and depend not only upon the habitat but also upon the physical size of the organism; this natural radiation background varies particularly widely amongst aquatic organisms.

A very useful summary of natural and artificial radiation to which human beings are now exposed has been published by Libby (1955); it has already been quoted and some of his comparisons will be repeated here. Nevertheless, additional radiological factors must be included whenever the natural exposures of marine organisms are to be evaluated.

Only sources contributing substantially to the average dose to the organisms as a whole will be listed here. The major contributors are (a) cosmic rays, (b) radioactivity in local surroundings, and (c) radioactivity spread through the tissue inside the organism itself.

Cosmic rays

Cosmic ray intensity decreases far more rapidly from sea level downward than it increases with increasing elevation above the earth. Figure 1 and Table 1 show the trend of the ionizing component of these rays with elevation above sea level, and with depth in water. The absolute dose which is used in Table 3 and Figure 2 is the average of the two values Libby (1955) uses for the geomagnetic equator and for 55° geomagnetic north latitude. (See Figure 1 and Table 1.)

External activity

Most organisms live close to either (a) igneous or metamorphic rock, (b) sedimentary rock, or (c) water. Sea water has a characteristic natural radioactivity — much lower than that of terrestrial rocks but quite appreciable when

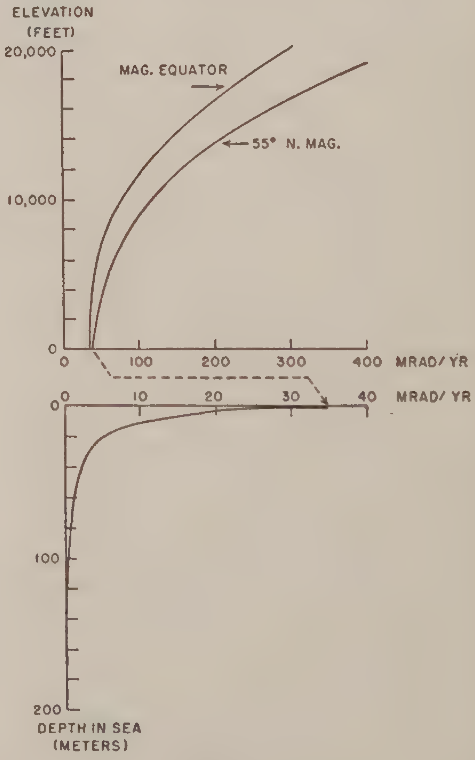

Figure 1

---

[1] Contribution from the Scripps Institution of Oceanography, New Series, No. 904.

TABLE 1 Trend of Cosmic Rays with Distance Above and Below Sea Level

Variation with elevation above sea level, values of intensity of ionizing component (in mrads/year) taken from Libby (1955).

Elevation in feet	Mrad/year Equator	 Latitude 55° N (mag)
0	33	37
5,000	40	60
10,000	80	120
15,000	160	240
20,000	300	450

Variation with depth in water, values computed from average attenuation compiled by George (1952) using Libby's average absolute intensity for mean sea level.

Depth in meters	Mrad/year	Percent of surface value
0	35	100
10	10.1	28.8
20	4.86	13.9
50	1.40	4.0
100	0.47	1.35
200	0.15	0.42
300	0.074	0.21
500	0.030	0.087
1,000	0.009	0.025
4,000	0.007	0.002

compared to that of most natural fresh waters. The major activity in sea water comes from radiopotassium (Revelle, Folsom, Goldberg and Isaacs 1955), and only this constituent will be considered here. Of the metamorphic and igneous rocks, granite has the highest activity; for our comparisons the same average radioactivities used by Libby (1955) are used here for granite and sedimentary rocks.

Internal sources of activity

The bodies of large animals contain a much higher concentration of potassium than is found in sea water. A value of 0.2 per cent is used herein for human tissue (Burch and Spiers, 1954) and 0.3 per cent is used for the potassium concentration of large fish (Vinogradov, 1953). Since radio-potassium contributes the major portion, aside from cosmic rays, of the radiation contributing to the average dose to the total body of any marine organisms, the character and distribution of this important natural activity has been compiled in Table 2.

Geometrical factors influencing dose

A man standing above a granite plane surface receives from the granite roughly one half the radiation which might strike him if he were completely surrounded by granite; likewise a man in a row boat receives from the sea only one half the dose which the sea gives to any submerged organism.

Potassium yields both beta and gamma activity; roughly three fourths of the total energy comes from the beta rays. Nevertheless, because of its short range, the beta particle from the potassium in the surrounding sea contributes

TABLE 2 Potassium Radiation Data

Distribution and Intensities

Material	Potassium content		Beta rays d/m/g	 mrad/yr	Gamma rays d/m/g	 mrad/yr	
Sea water (35‰ salinity)	0.038%	(1)	0.66	2.7	0.068	0.9	
Man	0.2%	(2)	3.5	15	0.36	2.3	(4)
Fish (large)	0.3%	(3)	5.8	24	0.3	3.7	(4)

Physical Nature of Potassium Activity
Beta activity = 29 d/s/gram of total potassium
Beta ray energy (average) = 0.5 mev
Gamma activity = 3 d/s/gram of total potassium
Gamma ray energy ≐ 1.5 mev

Sample Calculations for Potassium Activity

$$\frac{\text{Beta d/m/g} \times 1440 \times 365 \text{ m/yr} \times 0.5 \text{ mev/d} \times 1.6 \times 10^{-6} \text{ erg/mev } 1000}{100 \text{ erg/rad}} = \text{mrad/yr beta which reduces}$$

to, Beta d/m/g × 4.2 = mrad/yr beta; and correspondingly, Gamma d/m/g/ × 12.6 = mrad/yr gamma.

(1) Sverdrup, Johnson and Fleming (1942).
(2) Sherman (1941).
(3) Vinogradov (1953).
(4) Assume half of the gamma rays from internal activity are absorbed inside the body.

very little to the total dose of a large animal. On the other hand the beta rays from the surroundings can appreciably affect very small organisms and can in fact become the predominant contributor to dose whenever the organism has dimensions much smaller than the range of the beta particles in water and tissue.

The effect of beta rays starting from internal sources also depends upon the size of the organism. If the organism is very small the beta bombardment from the outside sources may contribute much more than does internal activity even though the source of activity is more concentrated in the tissue than it is in the surrounding water. It would appear from the character of beta penetration (Friedlander and Kennedy,

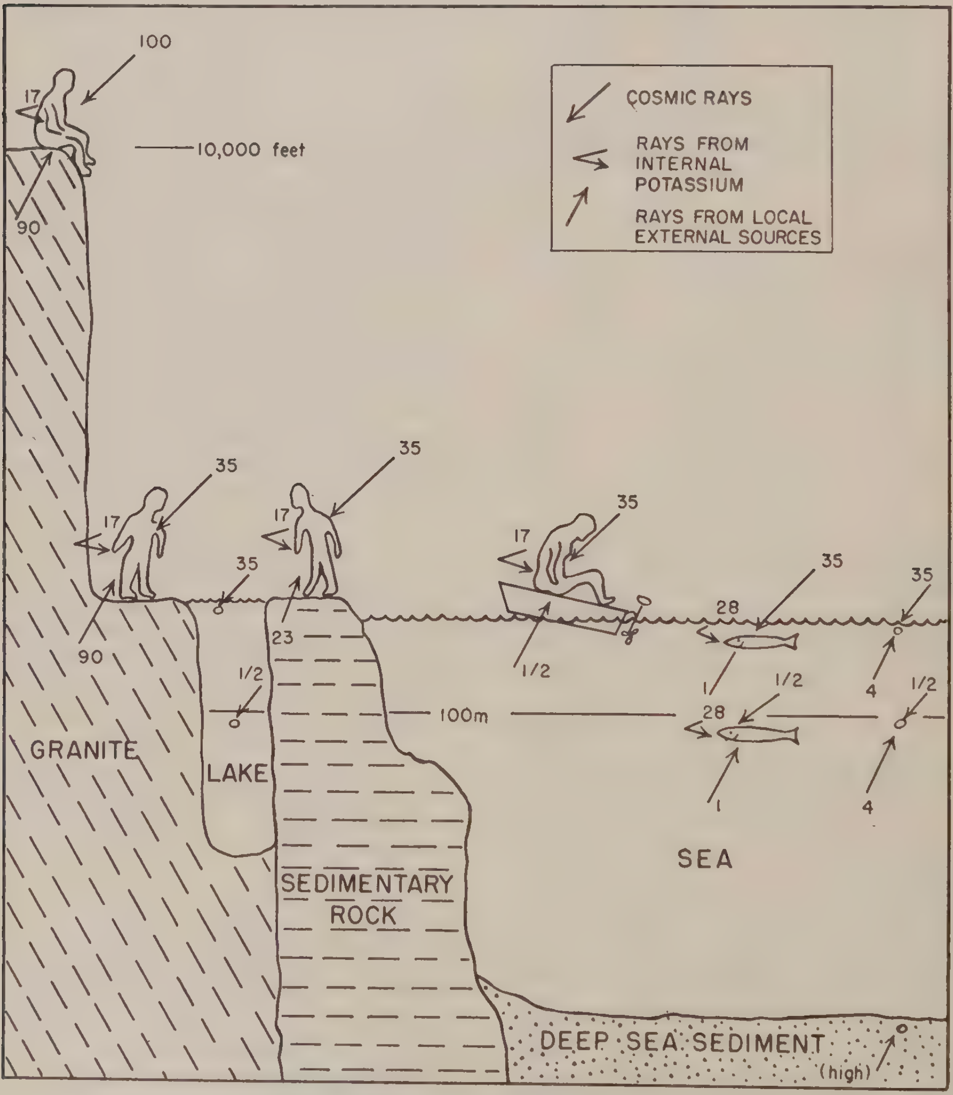
100
17
90
10,000 feet
COSMIC RAYS
RAYS FROM INTERNAL POTASSIUM
RAYS FROM LOCAL EXTERNAL SOURCES
35
17
90
35
35
17
23
1/2
GRANITE
LAKE
SEDIMENTARY ROCK
100m
35
17
1/2
35
28
1
1/2
28
1
35
4
1/2
4
SEA
DEEP SEA SEDIMENT
(high)

TOTAL NATURAL DOSES (mrad/year)

Man over granite		Man over sedimentary rock	Man over sea	Large fish in sea		Micro-organism in sea	
10.000	m.s.l.			at surf.	100 m.	at surf.	100m.
207	142	75	52	64	30	39	5

FIGURE 2

1949) that any potassium beta particle which originates inside a small organism will deposit most of its energy outside the organism; apparently less than 10 per cent of the total ionization can take place inside a sphere having a mean radius of 0.1 mm, and perhaps from the activity concentrated inside a phytoplankter having a mean radius of 0.01 mm only 1 per cent of the energy would be felt by the organism itself. Thus we see that the constitution of the surrounding medium dominates the life of the marine microorganism in a radiological sense as well as in those other manners more familiar to biologists.

Units used

For quantitative statements concerning such feeble radiations as these it is logical to use a very small unit and preferably one which is defined in terms of energy absorbed; the millirad per year (mrad/yr) is such a unit and is used here. The rad unit is only slightly larger than the more familiar roentgen unit, since 1.0 rad by definition causes 100 ergs to be absorbed per gram of matter, and this is approximately the energy deposited by 1.1 roentgen of gamma rays. For converting beta activity to equivalent rad dosage the average beta energy of potassium has been taken as being 0.5 mev.

Comparison of natural doses in several domains

Figure 2 attempts to bring into a single picture the magnitudes of the main components making up the radiation in each of several domains of interest. The approximate total dose to the organism is listed below the figure so that numerical comparisons can be made. In the sea and in deep lakes the dose to small organisms must be evaluated separately from that experienced by large organisms. Circumstances in each domain are given in more detail in Table 3. (See Figure 2 and Table 3.)

Discussion

Small organisms must be considered separately from large ones. Only a small fraction of the energy coming from activity inside a very small organism can be absorbed by the organism, whereas a large organism cannot escape so well from its own radioactivity.

Near the sea surface a large fish receives about half its total natural exposure from the rays originating in the radio-potassium in its own tissues. On the other hand near the sea surface cosmic rays appear to outweigh all other radiations received by a microorganism.

At depths of the order of 100 meters the attenuated cosmic rays no longer contribute significantly to marine organisms either large or small. However, the beta and gamma rays from potassium in sea water can give small organisms doses amounting to about ten per cent of the total dose they receive at the sea surface; the small marine organism cannot escape this exposure to radioactivity in the surrounding water.

It is the deep fresh water which makes possible the most extreme variation in natural exposure. In the deeper waters living things can hide from external bombardment; fresh water generally contains such small amounts of radioactivity that this source can be neglected even in comparison with the feeble effect of cosmic rays remaining at depths of several hundred meters or more.

In pure fresh water the total dose from strongly ionizing rays depends largely upon the size of the organism and upon its living habits. If the organism is small in the sense already discussed, if it lives in deeper waters, if it stays away from the bottom sediments, if it avoids the neighborhood of large masses of living tissue or of detritus, and if it avoids as far as possible accumulating excessive amounts of those elements which can be radio-active — then it can remain remarkably free from the ionizing bombardment received by all other living things.

It would be interesting to find out how the phytoplankton that seek the deeper portion of the euphotic zone of clear lakes respond to their extremely low external dose. If morphological or other differences are discovered between surface specimens and deep-water specimens, then one of the origins of these differences might possibly be the extremely different amounts of strongly ionizing rays in the two biospheres.

Geneticists should not overlook another aspect of the minute cell in feeble radiation; an individual cell has an extremely small probability of being struck at all during one generation. In a deep lake the radiation intensity can be so low that only one phytoplankter in about five hundred would experience an ionizing ray before it divided; at least this is the probability of a cosmic ray hitting an area 0.1 mm square at 100 meters depth. Furthermore, should an individual plankter accidentally concentrate an excessive amount of radioactive material in its tissue there is little probability that this individual would ever pass along any effect of it; there would be very little chance of a disintegration occuring before division. Purely physical reasoning therefore indicates that mutations leading to a capability for accumulating relatively large amounts of activity might be carried to offspring for ten or more generations before any nuclear energy would be released in any cell whatever.

Because of the "patchiness" of the radiation, the use of a unit like the millirad per year for feeble doses of strongly ionizing radiation unfortunately cannot convey the complete picture of the interesting bombardments which must be experienced by the very small organism.

TABLE 3 RADIATIONS IN ELEVEN RADIOLOGICAL DOMAINS

Man over granite	Total mrads/year
1. At 10,000′ elevation	
Cosmic rays 100 + granite 90 + internal 17	= 207
2. At sea surface	
Cosmic rays 35 + granite 90 + internal 17	= 142
Man over sedimentary rock	
3. At sea level	
Cosmic rays 35 + rock 23 + internal 17	= 75
Man over sea	
4. Cosmic rays 35 + sea 0.5 [1] + internal 17	= 52
Large fish in sea	
5. Near surface	
Cosmic rays 35 + sea 0.9 [1] + internal 28	= 64
6. 100 meters deep	
Cosmic rays $\frac{1}{2}$ + sea 0.9 [1] + internal 28	= 30
Micro-organism (mean radius 0.01 mm or less) in water	
7. Near sea surface	
Cosmic rays 35 + sea 3.6 [1] + internal [3]	= 39
8. 100 meters deep in sea or more	
Cosmic rays 0.5 + sea 3.6 [1] + internal [3]	= < 5
9. Buried in deep sea sediments	
Cosmic rays 0.000 + clay 40–620 + internal [4]	= 40–620
10. Near fresh water surface	
Cosmic rays 35 + water activity [2] + internal [2]	= 35
11. 100 meters deep in a fresh lake	
Cosmic rays < 0.5 + water activity [2] + internal [2]	= < 0.5

[1] For every radiopotassium disintegration there are 10 betas having average energy 0.5 mev and also one gamma ray having 1.5 mev. The man receives half the gammas from activity in the sea; the large fish, substantially all the gammas; while the micro-organism receives gammas and betas together.

[2] In fresh water natural activity is extremely low and little of this energy stays in the cell. For example (Robeck et al., 1954) in the Columbia River the beta background of the water is at or below 1×10^{-8} microcurie per ml (2×10^{-4} d/m/g) while the activity of aquatic organisms is at or below 1×10^{-6} microcuries per gram (2×10^{-2} d/m/g). For comparison, the beta activity in normal sea water is 0.66 d/m/g.

[3] The marine microplankton probably carries more internal activity than does the lake plankton, nevertheless effect can be neglected unless activity is concentrated more than 100 fold.

[4] All deep-water organisms have not escaped radiations. Micro-organisms buried in true deep-sea sediments have exceptionally high exposure to radium (Love, 1951); they receive 40-620 mrads/year depending upon the type of sediment.

CONCLUSIONS

1. Some humans actually live under exposure levels surprisingly near the magnitude, 10 roentgen during 40 years, which has been suggested as a genetic tolerance level, i.e., see Figure 2 and Table 2 (domain 1, high elevation over granite).

2. A man may experience 207 mrad/year on high mountains, or 142 on a sandy shore; he may reduce this further by half, say, by staying aboard a ship.

3. A large fish experiences a 50 per cent reduction in dose when going to a depth of 100

meters; it carries along its own source of internal radiation, however.

4. A marine microorganism, having a mean radius of 0.01 mm, receives only about 10 per cent of the surface dose at a depth of 100 meters in the sea; most of the dose comes from sea water activity unless exceptionally high internal activities are accumulated.

5. In a deep fresh water lake those microorganisms living in deep water (but not right at the bottom) receive from their surroundings what is probably the lowest natural ionizing dose within the biospheres of the earth. It would appear that geneticists should consider seeking evidence of abnormal mutation rates amongst microorganisms which live in deep waters of clear lakes, particularly amongst those which have low affinity for radioactive elements.

REFERENCES

Burch, P. R. J., and F. W. Spiers. 1954. Radioactivity of the human being. *Science* **120**:719–720.

Friedlander, G., and J. W. Kennedy. 1949. Introduction to radiochemistry. J. Wiley and Sons, New York: xiii+412.

George, E. P. 1952. Progress in cosmic rays. J. C. Wilson, ed. '52 Interscience, North-Holland Publ. Co.: xviii+557.

Libby, W. F. 1955. Dosages from natural radioactivity and cosmic rays. *Science* **112** (3158): 57–58.

Love, S. K. 1951. Natural radioactivity of water. *Ind. Eng. Chem.* **43**:1541.

Revelle, R. R., T. R. Folsom, E. D. Goldberg, and J. D. Isaacs. 1955. Nuclear science and oceanography. International conference on the peaceful uses of atomic energy, Geneva. Paper no. **277**:22.

Robeck, G. G., C. Henderson, and R. C. Palange. 1954. Water quality studies on the Columbia River. U. S. Dept. of Health, Education, and Welfare. Robert A. Taft Sanitary Engineering Center; Cincinnati, Ohio: viii+294.

Sherman, H. C. 1941. Chemistry of food and nutrition. 6th Ed., McMillan, New York: x+611.

Sverdrup, H. U., M. W. Johnson, and R. H. Fleming. 1942. The oceans, their physics, chemistry and general biology. Prentice-Hall, Inc.: x+1087.

Vinogradov, A. P. 1953. The elementary chemical composition of marine organisms. Trans. Julia Efron and Jane K. Setlow, Sears Foundation for marine research, Yale Univ., New Haven: xiv+647.

Reprinted from
THE EFFECTS OF ATOMIC RADIATION ON OCEANOGRAPHY AND FISHERIES
PUBLICATION NO. 551, NATIONAL ACADEMY OF SCIENCES—NATIONAL RESEARCH COUNCIL, 1957

CHAPTER 12

ON THE TAGGING OF WATER MASSES FOR THE STUDY OF PHYSICAL PROCESSES IN THE OCEANS[1]

THEODORE R. FOLSOM, *Scripps Institution of Oceanography,* La Jolla, California

and

ALLYN C. VINE, *Woods Hole Oceanographic Institution,* Woods Hole, Massachusetts

FINDING, identifying, and plotting the courses of characteristic masses of water in the oceans are major activities of the physical oceanographer. Assistance from the new techniques that have come with the use of radioactive materials has been welcomed by him; some of these techniques have already been put into service for tracing the water. It is not generally realized how much experience has been gained, beginning with the 1946 tests in Bikini Lagoon, in tracing water masses contaminated with radioactive materials from weapons' tests. And many thoughts are now turning toward the radioactive tagging of ocean water by other means in regions where knowledge of underlying physical processes are meager, especially in the very deep waters. Proposals for the disposal in the sea of atomic energy wastes cannot be properly evaluated until estimates can be improved concerning the motion of this deep water.

Many of the advantages (familiar in the laboratory) of using radioactive identifying tags can be realized at sea, even though rendered difficult by the very large physical dimensions of the oceans. What appeals most to the oceanographer is his new ability, under certain circumstances, to make very rapid identifications of water lying on the surface or deep below his ship; thus allowing large volumes to be surveyed in three dimensions and in more detail than ever before possible.

Three layers in the ocean are distinguished clearly by structure and behavior: the mixed layer near the surface; the intermediate layer lying just below wherein the temperature changes rapidly with depth (this thermal stratification bringing about great stability); and finally, the large, nearly uniform bottom water mass extending to the sea floor with so little variation in density that very stable stratification is not possible. Each water mass reacts differently when disturbed, and therefore, mixing occurs differently in response to currents and mass intrusions. Experiments conducted in any one of these domains must take into consideration the special features that exist, and must call upon equipment most suited to these sections. Equipment specialized for radiological survey work in any of these oceanographic domains is still primitive. However, it can be said that equipment for detecting and measuring radiation is not a bit less highly developed than are the equipment and techniques needed for navigating a ship, and for maneuvering detectors at sea, especially at great depth. So much information now can be reported by radiological means in a short time that a ship now has more reason than heretofore for precise navigation. In some cases, the depth and position of the detector relative to the ship must be known instantly, and almost always must be controlled far better than has been accepted by traditional hydrography. It is difficult to record data in full detail in many cases, and in others it is difficult to evaluate features rapidly enough to alter maneuvers to best advantage; an oceanographer can now expect to be aware of a strongly active layer in less than one second after his electronic probe makes contact, and he even may make use of a fast moving airplane to outline radioactive areas on the surface.

---

[1] Contribution from the Scripps Institution of Oceanography, New Series, No. 905.

Contribution No. 929 from Woods Hole Oceanographic Institution. Part of Table 2 was computed with the collaboration of John Harley of AEC, New York City Operations Office, who gave much other counsel for which the authors are grateful.

Instrument Sensitivity and Natural Backgrounds

Many promising measuring schemes have been proposed. However, it is profitable to compare the equipment and techniques which have been used already at sea. At the top of Table 2 is presented the background radiations coming from cosmic rays and from the natural potassium in the sea, and the activity level now believed tolerable for drinking water also is given for comparison.

At the bottom of Table 2 are listed, in the brief numerical form in which they are commonly stated, the sensitivities of three measuring techniques which actually have been used for radiological exploration at sea. Many aspects of the measurement problem are oversimplified by a comparison of this sort, but the table does indicate that present shipboard beta analysis is capable of measuring beta tracer activity below the background beta activity due to the potassium in the sea water, whereas gamma detectors so far have been limited at levels above the gamma backgrounds of the sea. On surveys covering large distances, such as on Operation TROLL (U. S. Atomic Energy Commission 1956), and on the SHUNKOTU MARU Expedition (Mujoke, Sugiura, and Kameda 1954), there is ample time for water analyses, and advantage can be made of beta techniques. Nevertheless, there are many circumstances where direct measurements by gamma devices are necessary for rapidly locating small contaminated water masses, and it is likely that gamma techniques will be perfected so as to allow use at levels far below their present capability.

There are occasions at sea in which a gamma detector must indicate the presence of tracer activity within a few seconds after making contact. The limitations imposed by this sort of time restriction in the presence of statistical fluctuations in the signals are discussed in Appendix A, and are summarized in Table 3.

Other important details concerning the radioactive background in the sea have not been thoroughly explored. It may be too late to estimate the background level that existed a decade ago for some isotopes, and this should not be forgotten in planning future surveys. Of particular interest are background conditions near the sea floor where radium and thorium activity are known to accumulate in sediments; but little is known in detail about the lateral distribution of bottom activity.

More complete utilization of weapons' tests for the marine sciences

It appears likely that large weapons will continue to be tested in oceanic areas and that radioactive materials will be strewn from time to time over the surface of the sea. Valuable oceanographic data already has come from such sources; for example, direct measurements have been made of the rate of mixing downward from the surface to the thermocline, and also, direct information has been obtained regarding mass motion and lateral mixing. One special feature of benefit in studying weapons tests is the unique initial boundary condition provided by the arrival of fallout activity almost simultaneously over an area having dimensions very large compared with the depth of water involved; downward mixing appears as a relatively simple phenomena following this initial condition, and can be studied under almost ideal circumstances.

Two expeditions mentioned above have proven that further information concerning lateral mixing and flow can be gained for many months after a weapons' test, and obviously this fact should be exploited fully by marine scientists of all nations. Ancillary benefits might come from more or less fixed monitoring stations; if, for example, following the 1954 test, repeated sampling had been done off Guam it would have furnished data of value for interpolating observations made in the two follow-up cruises mentioned.

Bottom exploration following weapons' tests has not been given deserved attention, and insufficient attention has been paid to getting even purely oceanographic information from these sources into the form needed by those people who are charged with making decisions regarding the ominous waste disposal problem.

Hazards involved in the deliberate tagging of ocean waters

Safety of the research staff is always a consideration; at sea because of special circumstances the handling of extremely large amounts of activity is not too difficult or hazardous. Protection can be secured very cheaply by towing the larger sources of radioactivity aft of the ship, preferably slightly submerged on a suitable barge or special vessel. Bringing large quantities of activity to the waterfront promises to be more expensive, but practical experience in this should be valuable for later planning of large-scale disposals.

The more controversial question of how much radioactivity can safely be introduced into the sea is not without reasonable solutions; but the recommendations depend upon the circumstances, especially, upon the particular part of the oceans to be studied. At the outset, barren areas of ocean rather than those productive of things leading to human food must be selected since the former can yield equally good information regarding purely physical phenomena.

Deliberate tagging of surface waters (*Operation PORK CHOP*)

Surface waters mix in a turbulent manner due to forces not yet fully understood. Better knowledge of this layer is badly needed justifying the consideration of water tracing experiments involving introduction of fairly large amounts of activity. Greatest care must be exercised here because these waters are those most close to humans, in several senses.

Rate of mixing to the bottom of the mixed layer, and rate and character of lateral motion as functions of the usual parameters of the sea are of most immediate interest, and observations lasting even a few days or few weeks would be of great value at the outset, especially if repeated frequently. A simple surface water experiment now will be proposed in briefest possible outline.

Figure 1 presents schematically some of the procedure which might be used and some of the phenomena to be expected. Guided by suitable navigational aids, here represented by deep-anchored buoys No. 1 and No. 2, the ship A proceeds on a straight course while dropping two quantities of radioactive materials (a and a′) mixed with enough surface water to leave near the surface a small contaminated patch having nearly neutral buoyance. These are essentially point-source initial conditions in this scale of dimensions; although, they are not as convenient as the plane-source initial conditions

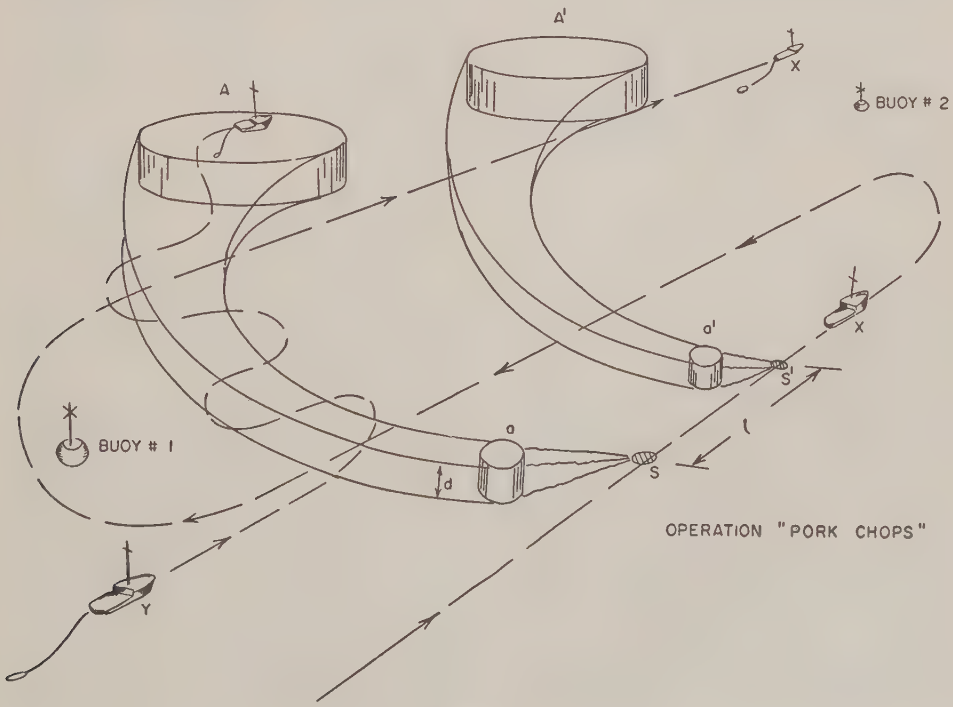

FIGURE 1

(105)

provided by fallout, they have some mathematical simplicity. It would appear economical and informative to drop two sources almost simultaneously, some distance apart — say one to ten kilometers; this would permit large-scale advection also to be studied at little extra ship cost.

From the sources s and s′ will grow a larger more dilute patch of water finally ceasing to penetrate rapidly downward at depth d. The rate and lateral spread prior to this time as functions of wind velocity are of special interest. After further downward penetration is retarded, the areas a and a′ move and expand to the larger areas A and A′ conserving most of the original radioactive material, and the product of activity and area should be almost constant after correction is made for the known rates of decay of radioactive constituents.

Dual ship operations

Experience has shown that operations on the scale of this sort can scarcely hope to be successful unless more than one ship is used; even with the best facilities one ship may lose contact with the invisible patch and waste valuable time locating it. One ship, X, must stay in or near the tagged mass while the other one, Y, may survey the area in detail, inspecting sections across the mass, studying the bottom for reference features, and chasing missing buoys if necessary.

Ultimate disposal of hazard in surface waters

Reduction of activity to a level below that of the natural activity of sea water is one criterion which has been used for planning disposals (Glueckoff 1955), and this is fairly reassuring provided the specifically dangerous and the long-lived activities are eliminated, for example, after radiostrontium and radiocesium are removed from raw fission wastes. Present evidence permits the conclusion that in the open ocean, when winds are above the critical white-cap level and under circumstances where mixing ceases at a depth of about 30 to 50 meters, as much as 1,000 curies would mix to a safe dilution in less than 40 days. An example of the dispersal rate in the open sea will now be given.

Brief outcome of an experimental tagging of surface waters in the open sea

Surface water made active by introducing fission products concentrated within a few square kilometers was intercepted by a ship 36 days after inoculation and traversed for 10 days. After corrections were made for the drift of the water during the survey, and for radioactive decay, a synoptic picture could be drawn roughly locating the contours of activity. This estimate of radioactive distribution was referred to the time of 40 days after the start of dispersal.

The contamination had mixed significantly only to about 30 to 60 meters, although the thermocline lay nearer to 100 meters depth. The following tabular description of this synoptic sketch can be made.

TABLE 1 Approximate Distribution of Radioactivity Found in the Surface Waters of the Open Seas 40 Days After Being Introduced Suddenly as a "Point Source." (A Synoptic Picture Computed from Measurements Made on Several Different Days.)

Areas inside contours of equal concentration in square kilometers.	Areas inside the contours as percentages of the area of the maximum contour.	Concentration of radioactivity (as per cent of the maximum concentration measured).
40,000 (km^2)	100%	10%
24,000	65	20
14,000	38	30
8,000	22	40
800	2	60
490	1	80
35	0.1	100

At the end of 40 days, the center of gravity of this distribution was about 120 miles from the point of inoculation and the pattern was about four times longer than broad. The wind was 3 and 4 of Beaufort's scale for the first 20 days, but was much calmer for the last 20 days.

If the average mixing depths are taken as 50 meters, then, 1,000 curies distributed over 40,000 square kilometers would result in an average concentration of $1.5 \times 10^{-10}/\mu c/ml$. This would certainly be safe sea water in most senses; and even in the smaller areas where much less than the average dispersal took place the water should also be safe. In fact, the experiment indicated that it is likely that after 40 days, following the introduction of 1,000 curies of activity into the surface waters of the open sea, only about 0.1 per cent of the total area should retain contamination above the tolerance concentration permitted for potable water, and even in this small region the residual artificial activity would amount to less than the normal natural activity of sea water.

It is evident from Table 2 and Table 3 that shipboard beta measurements would suffice to detect the more radioactive spots if there were initially 1,000 curies of slowly decaying beta activity; it is apparent, however, that direct measurements by gamma detectors might be sufficient for several days or even weeks. Surface experiments are by far the easiest to conduct and implement — they are limited largely by considerations of hazard to humans. Two more difficult experiments will now be described.

Investigations in the thermocline layer by use of radioactivity

The thermocline lying between perhaps 100 meters depth on an average, and 800 meters or more, can be thought of as being a lid which restrains deeper water from reaching the surface. Experiments in this stable region must take into consideration the fact that any liquid introduced here will seek the level of its own density and will then spread out in a very thin layer. An experiment in this layer has been

TABLE 2 Approximate Sensitivities of Three Detecting and Measuring Techniques Presently Available for Use At Sea Compared With the Activity of Sea Water and With That of Fresh Water.

A *Common background radiation levels:*	d/m/l	curies/l	microcuries/ml	rad/hr[2]	mrad/yr[8]
Activity in normal sea water due to potassium:[1]					
Gamma rays	70	3×10^{-11}	3×10^{-8}	1×10^{-7}	0.9
Beta rays	660	3.0×10^{-10}	3.0×10^{-7}	—	—
Maximum permissible[4] *concentration of unknown mixed beta activities in drinking water:*					
Beta rays	220	11×10^{-10}	1×10^{-7}	—	—
Cosmic ray background at sea surface:[5]					
At equator	61	—	—	—	33
At 55°N (mag)		—	—	—	37
B *Sea water activities at which present measurements are significant.*					
Shipboard water analysis[6] *for mixed beta emitters, 60 minutes count after removal of potassium:*					
	50 ± 15	2×10^{-11}	2×10^{-8}	—	—
Uderwater gamma detector,[7] *1956 scintillation rate-meter of AEC-NYOO:*					
(0.6 MEV gammas assumed)	220 (approx)	—	—	1.4×10^{-7}	1.2
Underwater gamma detector,[8] *1955 geiger instruments of SIO. (counting pulses):* (See also table 3 for other cases)					
Case A: Used in deep water where net background is 15 CPM, assume photons of 0.6 Mev; assume short measurements required, $t = 5$ sec.	6600	3×10^{-9}	3×10^{-6}	3.8×10^{-6}	30
Case B: Towed on surface, assume constant background 60 CPM, assume photons of 0.6 Mev; assume long measurements permitted, $t = 5$ min.	520	2×10^{-10}	2×10^{-7}	0.3×10^{-6}	3

---

[1] Assuming normal sea water has 3.8×10^{-4} gk/g sea water, that beta activity is 29 d/s/gk and that gamma activity is 3 d/s/gk.

[2] The rad unit is somewhat larger than the more familiar roentgen unit; 1 rad = 1.1 roentgen approximately for gamma rays. Values in this column were computed upon the assumption that the activity was uniformly distributed in the water and that the detector was a meter or more from any boundary.

[3] Referring to beta ray activity in rad units in roentgen units is a dangerous practice—much further specification depending upon the individual experiment is required.

[4] Handbook 52 of the National Bureau of Standards. The values given refer to the case where the nature of the activity is unknown; certain radioisotopes can be tolerated at much higher levels.

[5] See Table 1 in the accompanying paper "Comparisons of Some Natural Radiations Received by Selected Organisms" by T. R. Folsom, and John H. Harley for variation of cosmic rays with depth and altitude.

[6] Cosmic rays are counted by most geiger counters at the average rate of approximately one count/min/sq cm of counter area.

[7] This information was supplied by J. H. Harley from personal communication with H. D. LeVine of the New York City Operations Office of the Atomic Energy Commission who designed this equipment.

[8] This detector was not intended previously for use at low intensities, but rather for measuring a wide range of intensities of gamma rays. Additional geiger tubes might easily be added to increase the sensitivity by at least five fold. Still more sensitive gamma devices are now used in oil well logging.

TABLE 3 COMPARISON OF MINIMUM DETECTABLE CONCENTRATIONS USING SEVERAL MEASURING TIMES AND ASSUMING SEVERAL BACKGROUNDS

(a) Minimum detectable anomolous activity if potassium of the sea produced the only background, i.e., $B = 1.2 \times 10^{-3}$ gammas/sec/ml.

Counting time in secs. t	Minimum detectable concentration γ/sec/ml	= γ/min/l	Net signal counts/min $C_aVe = 30C_a$	Total net counts $30C_at$	Rads/hour	
					Photons .6 mev	Photons 1.5 mev
	C_a					
3	.19	11,000	5.7	17	6.5×10^{-6}	16×10^{-6}
5	.11	6,600	3.3	17	3.8	9.5
60	.010	600	0.3	18	.3	.8
180	.0039	230	.12	22	.13	.33
300	.0026	160	.078	23	.09	.22
600	.0016	99	.048	30	.06	.14
Very large	$0.025/\sqrt{t}$					

(b) Minimum concentration detectable if backround were 15 CPM, i.e., an actual background signal experienced in deep water.

Counting time in secs. t	Minimum detectable concentration γ/sec/ml	= γ/min/l	Net signal counts/min	Total net counts	Photons .6 mev	Photons 1.5 mev
	C_b					
3	.19	11,000	5.7	17	6.5×10^{-6}	16×10^{-6}
5	.11	6,600	3.3	17	3.8	9.5
60	.010	590	.29	17	.33	.84
180	.0058	350	.17	32	.20	.50
300	.0049	290	.15	45	.17	.42
600	.0032	190	.096	58	.11	.28
Very large	$0.067/\sqrt{t}$					

(c) Minimum detectable concentration if total background were 60 CPM, i.e., an actual background signal experienced at the sea surface.

Counting time in secs. t	Minimum detectable concentration γ/sec/ml	= γ/min/l	Net signal counts/min	Total net counts	Photons .6 mev	Photons 1.5 mev
	C_c					
3	.205	12,000	6.1	18	7.1×10^{-6}	18×10^{-6}
5	.133	8,000	4.0	20	4.6	12
60	.0222	1,330	.67	40	1.9	7.5
180	.0116	700	.35	63	.4	1.0
300	.0087	520	.26	78	.3	.74
600	.0059	354	.17	102	.2	.51
Very large	$0.13/\sqrt{t}$					

described in some detail by Revelle, Folsom, Goldberg, and Isaacs (1955), and discussed in several of the accompanying papers. It will be discussed here only in the matter of difficulty of survey. Although mixing is known to be very slow in the thermocline, it is not certain how direct is the path from this *fringe* biosphere to human food supply, so that the hazard of a long remaining concentration of activity is not easily evaluated. Revelle et al., prefer to suggest the experimental use of the conservative amounts of 10 to 100 curies, and they then show that such small sources of radioactivity might be practical none the less.

Actual field experience has shown that layers as thin as one or two meters thick are extremely difficult to sample for water analyses even after being located by gamma ray detectors. Folsom (1956) has emphasized that future deep surveys with radioactive tags must rely heavily upon discovery of radioactive water by means of gamma detectors, and has urged that specialized forms of these be brought to perfection.

In this particular layer, geometric factors are not adverse for maneuvering a detector into the water mass to be studied; a probe is dropped rapidly and more or less vertically so as to intersect and pierce a rather broad horizontal lamina, sharply confirming the activity. Some difficulty would be encountered in holding the probe in the thin layer long enough to permit accurate measurements after the activity falls to such a low level that statistical fluctuation becomes the predominant source of error; however, the major difficulty even at these depths is holding the ship in the general area of active pools of small size. Any area of less than a square mile below the surface is a tiny detail in the open sea, and oceanographers never before have realized how hard it is to navigate and maneuver to study areas so small. Multiship operation, the use of the best position-locating gear, and careful crew training and teamwork are necessary for subsurface radiological surveys even at these moderate depths.

Outline of tagging experiment in the thermocline layer

Figure 2 illustrates certain features which must be considered in this region. The ship, A, may lower a gamma sonde through an activated pool and detect its presence by the receiving of a signal like that shown on the right side of the figure; the hydrographer may obtain a water sample by triggering electrically a water sampler at the moment the detector indicates that the sampler is within the active layer. The data in Table 3 make it clear that rapid response is important during this sort of measurement; a statistically significant signal must be accumulated in the short period during which the probe is passing through the active layer.

Attention is called to the need for navigational and maneuvering aids here by including schematically the parachute-drogue C. It is difficult to maneuver a weighted detector horizontally in order to study the lateral distribution in detail. The use is suggested of towed gamma detectors depressed to the desired level by hydrofoils controllable from the surface, more or less as illustrated schematically at the left of Figure 2. By means of a swivel-clamp, SC, a pennant several meters long containing a row of Geiger tubes or other gamma detectors, might be suspended above the depressor so as to present a vertical, linear array, thus giving a high probability of intersecting wide lateral distributions of activity. This sort of gear should not be too awkward nor fragile for deck handling at sea. Signals might be recorded partially, or entirely inside the depressor, or reported to the ship electronically or sonically.

Ship A or a sister ship with similar gear might stay in the pool during the whole experiment, however, if the pool were lost after its depth was established, then Ship B would likely be the first to find it again with its towed detector.

Difficulties in sounding and exploring very deep waters

Bottom exploration so far has been confined largely to sonic plotting and sounding by solid cable; very deep wire casts are very time consuming and difficult; the ship generally is moved laterally by surface currents before the

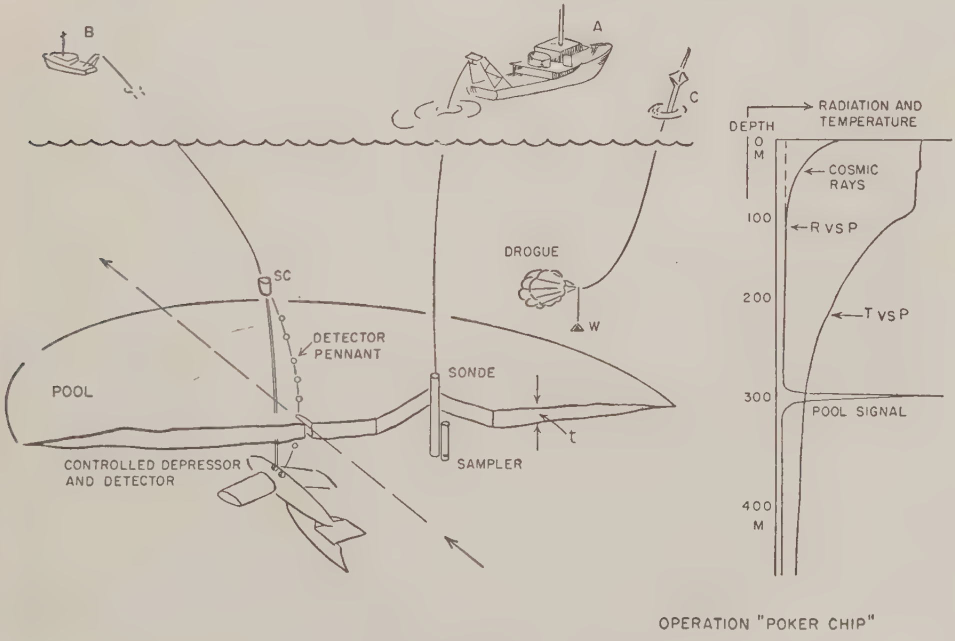

FIGURE 2

wire touches bottom. Oceanographers seldom hope to place their sondes and coring tools upon any pre-selected topographic detail of small area. However, it is quite likely that a technique can be perfected for dragging a detecting instrument along the bottom in many areas of the oceans' floor, and with a dragged detector a large region might be traversed rapidly, and tagged water masses near the sea floor might be located and surveyed. A proposal for tagging bottom waters now will be outlined.

Difficulties in tagging bottom waters

Fortunately, little hazard to human populations would result from putting into the deep bottom waters in certain latitudes almost any amount of activity which might be readily available in the near future, or which would be easy to handle safely ashore and on ordinary surface vessels. After all, these amounts would be only the feeble forerunners of what may have to follow.

The problem is that of displaying even a relatively large radioactive source economically in face of the immensity of the abyssal reaches. One can think of many things which must not be done; heavy, radioactive liquid cannot be merely poured overboard, for example. Matching density at intermediate layers or attempting to insert a strata at a selected depth also would appear experimentally difficult in view of the limited knowledge presently available; an unequilibrated liquid mass might wander about like a sinking dinnerplate — and soon become lost. In the absence of the restraining forces found in more stable waters, the pouring of streams of dense solution downward from a height above the bottom, or alternately the releasing of lighter material upward from the bottom would surely cause mass motion which might not cease until the streams had moved long distances and perhaps had curled into configurations quite unsuited as initial boundary conditions for water tracing experiments. Furthermore, activity spread initially in more or less vertical lines would make very poor targets for detectors trailing on the end of wires three miles long, and would be wasteful in terms of radioactive material and of expedition time.

One might, of course, carefully select a perfect basin, and might gently introduce into it a dense radioactive solution. This certainly should be considered since only a small amount of activity might suffice for tagging the waters in a small basin and valuable information regarding motion and dispersion in basins might result, but results would not lead to a realistic picture of the large scale flow over bottom which may have to disperse the wastes dumped in the future. The results of an experiment set up in this way would be inadequate, and, in fact, might be misleading in a dangerous direction.

Production and use of horizontal line-sources near the bottom

"Operation HARE and HOUND"

It is evident that distribution of activity in a horizontal line near the bottom would be most easy to intercept by a detector dragged along the bottom, and it appears also to be something which would be relatively easy to produce, and economical. It should be possible to hold tagged water near the bottom by mixing it with a very dense solution; and there are two ways immediately evident for effectively spreading streaks of dense solution for long distances over the bottom terrain.

Figure 3 illustrates the two methods proposed for tagging bottom water, and the method proposed for locating the tagged masses later. The Ship B' is shown dragging a "Hare" D, across the bottom leaving behind a streak of contaminated water. Alternately, Ship B is shown just after it has dropped to the sea floor a specialized water blending device which might well be called a "quern" [1], C, which generates for a few minutes or hours, a stream of dense, radioactive solution on the slope of a carefully selected large topographical ridge b — d; this stream flows away very much like one of the submarine currents which are now called "turbidity currents" by geologists. Violence of this sort of free current might theoretically be controlled through wide limits by adjusting the densities of the solution. The essential features of a water-tagging quern are shown in the upper right of Figure 3. Radioactive material, AS, is combined in predetermined proportions with a heavy salt solution by metering pump, P, and the two are then fed to a fan-type mixer, and are there blended with a large volume of

---

[1] Old English name for a mill for grinding all sorts of things. (Ruggoff, 1949.)

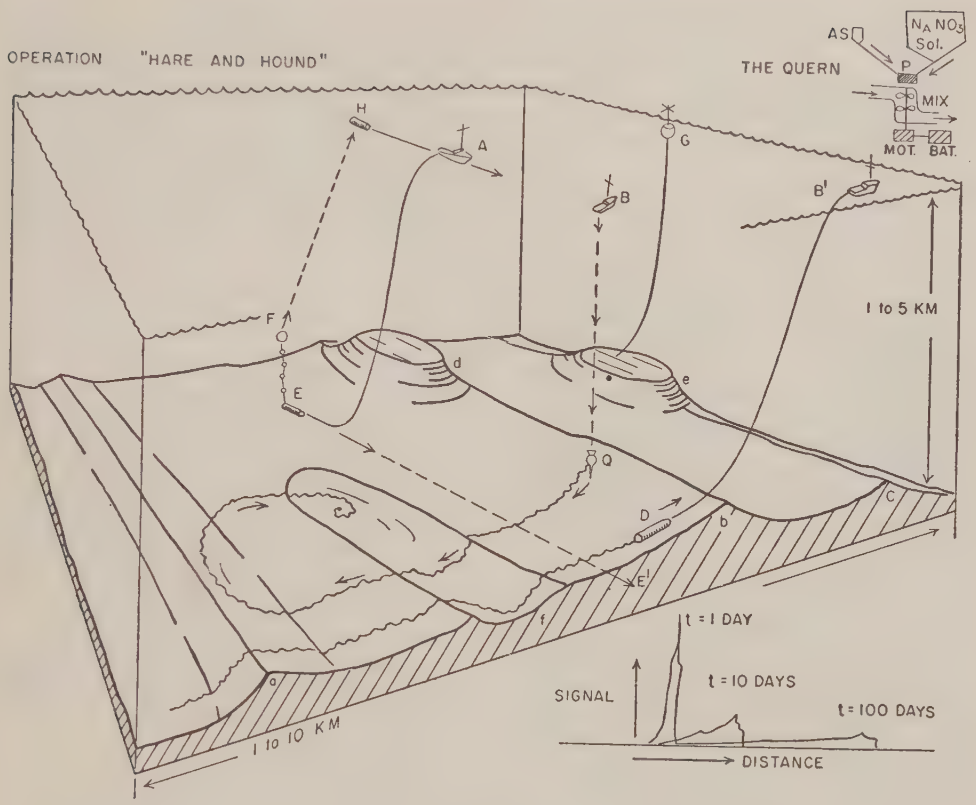

FIGURE 3

local water. There are several reasons for preferring a design leading to inexpensive construction and single use; the cost of decontamination of apparatus of this type would outweigh any benefit from repeated use. Suggestion is made of the use of a salt such as sodium nitrate which has both high solubility, and an endothermic heat of solution which would serve to overcome the adiabatic heat set free during lowering. It would appear that one or more tons of a nitrate salt, mixed into bottom water by use of a few kilowatt hours of energy, stored in oil-sealed accumulators, could produce a compact body of very heavy water which would rush like a freight train across the terrain dropping a streak of traceable radioactive eddies as it traveled.

A fixed, water-mixing quern, of the sort described, might produce a tagged water mass behaving in a manner appearing realistic to both the disposal planner and the submarine geologist; however, its use is not likely to lead directly to the extremely simple results needed for the very first experiments. The employment of a dragged hare might be preferable at the outset — and its metering machinery might be somewhat less elaborate than that of the quern just described.

One might contemplate using 1,000 or more curies for making streaks several kilometers long so that location would not be difficult with a simple gamma device dragged by a ship. In Figure 3, Ship A is shown dragging such a detector which might be called a "hound" for obvious reasons. For very great depths, no electrical wire is presently available with the durability equal to that of an ordinary dredging cable. It would, therefore, be wise to first consider the use of a compact multichannel chart recorder inside the dragged pressure shell E so as to make permanent records of signals picked up by a set of gamma detectors suspended by an oil-filled float F. Numerous accessories might profitably ornament this sort of gear, but the one which might prove most rewarding would be a sound producer capable of reporting the moment of contact with the tagged water mass; even a crude sonic signal sent from a transducer on the float, F to the ship, A, via the towed hydrophone, H, would suffice. Details of the gamma signals need only be recorded so that they might be inspected later on the recorder chart, however, it would be important for the navigator to recognize instantly when contact was made so that he could maneuver the ship economically.

The operations proposed above are not unlike those used successfully by cable ships when retrieving submarine wires. Careful preliminary surveys of the whole area, the selection of identifying landmarks, and the laying of the marking buoys also appear essential for success in work of this type.

The final results might have the general character of the hypothetical signals shown graphically at lower right in Figure 3. Change in amplitude and displacement, and skewness of the signal records should lead to estimates of both velocity and rate of mixing. If each survey included ten or more intersectings, and if each contact brought separate gamma signals from several detectors distributed along the hound's vertical "tail," then the data of the sort needed would accumulate quickly.

Rough estimate of effectiveness of 1,000 curies for tagging bottom waters

It appears possible to distribute radioactivity uniformly along the course of a device dragged over the sea bottom, and it would appear possible also to deposit the material so gently that it would come to rest within a few meters of the precise course. If, for a rough evaluation, we assume that local diffusion sooner or later produced a uniform distribution within a radius of 10 meters, and that the total activity, M, was 1,000 curies, then the length of the water mass which might be tagged can be stated

$$l = \frac{M}{C\pi r^2}. \qquad (1)$$

where C is the average concentration of activity within the tagged mass.

If now we assume that only 10 seconds can be allotted for traversing 20 meters (that is the ship's speed is about 4 knots), then the equation (9) of Appendix A indicates that a single detector like the 1955 SIO Geiger instrument could detect, in the presence of a realistic deep-water background of 15 cps, a limiting gamma source concentration of 0.061 disintegrations/sec/ml, or $C = 0.061/3.7 \times 10^{-10}$ curies/ml, and the length of traverse which could be tagged with 1,000 curies would be, under these assumptions,

$$l = \frac{1000}{1.65 \times 10^{-12} \pi (1000)^2} = 1900 \text{ Km} \qquad (2)$$

It would appear feasible to locate and allocate by ordinary navigational means a geographical line in the deep sea floor of less than two kilometer's length, so that the hypothetical example just given suggests that 1,000 curies could equally well be used to produce a very concentrated streak of activity having a length of two or three kilometers which might still be detected with ease after it had diffused, mixed, or decayed to less than one percent of its initial concentration. Thus it can be concluded that 1,000 curies, or even less activity, put into bottom water would be quite adequate for tracing movements on a scale large enough to contribute information useful in disposal planning.

SUMMARY AND CONCLUSIONS

1. Consideration has been given some of the problems involved in tagging water masses in the open ocean.
2. The problems are different in the three major strata; the surface layers, the thermocline, and the deep water layer.
3. It appears that under certain circumstances water tagged with even moderate quantities of activity can be followed for at least several weeks; surface waters contaminated by large activities such as result from fallout can certainly be followed for a year or more.
4. Much field experience in radiological oceanography has been gained already. A fairly clear direction for development of instruments has been indicated.
5. The need is seen for attention to the perfection of navigational aids, for use of specialized vessels and gear, and for the use of several vessels simultaneously in oceanic surveys of this sort.

APPENDIX A

In practice, many factors tend to limit the effectiveness of an under sea gamma detector, but the random fluctuation of a feeble radiation may alone prevent its recognition in the presence of a background of similar magnitude. The lowest detectable concentration, limited only by statistical considerations, may be expressed in terms of the strength of the background, the time permitted for measurement, and the measuring efficiency of the instrument.

Let the sea water be contaminated with a concentration of radioactivity N curies/ml, and let this activity cause m counts/sec to be indicated by the instrument, and let the average background be b counts/sec. The relative accuracy, n, of a single measurement made during t seconds will depend upon signal strength and background strength; if the fluctuations are purely random, the error, 95 per cent of the time will be equal to, or less than,

$$n=\frac{2\sigma}{mt}=\frac{2\sqrt{\sigma_M^2\div\sigma_B^2}}{mt}=\frac{2\sqrt{mt\div bt}}{mt} \qquad \text{A.1}$$

and solving for the net signal gives,

$$mt=\frac{2+2\sqrt{1\div n^2bt}}{n^2}. \qquad \text{A.2}$$

Now, the counting efficiency of the instrument logically should be derived from the ratio of counts recorded to the photons striking the instrument. This ratio would be impossible to evaluate, but it is approximated when the instrument is small, and easily penetrated by,

$$e=\frac{mt}{3.7\times10^{10}Nvt} \qquad \text{A.3}$$

that is by the ratio of the net counts recorded to the photons emitted in a volume of liquid, v, equal to that displaced by the detector. Solving this equation for concentration,

$$N=\frac{mt}{3.7\times10^{10}vet} \qquad \text{A.4}$$

curies/ml, and substituting here the value for net count, mt, obtained in equation (2) when the background rate is b, and accuracy is, n, the limiting concentration can be expressed,

$$N=\frac{2+2\sqrt{1+n^2bt}}{3.7\times10^{10}n^2vet} \qquad \text{A.5}$$

curies/ml, wherein b expresses the background rate actually indicated when the instrument is surrounded by clean sea water. If no other background exists except that coming from a surrounding solution having specific activity B, and if the instrument counts this activity with the same efficiency, e, than the limiting detectable concentration becomes, in curies/ml,

$$N=\frac{2+2\sqrt{1+Bn^2vet}}{3.7\times10^{10}n^2vet}. \qquad \text{A.6}$$

Numerical examples applying to an actual undersea instrument

The sensitive portion of the 1955 model of the Scripps Institution of Oceanography's Geiger instrument has a volume of about 1,000 ml. The ratio e, applying to hard gamma rays, was measured directly by submerging the instrument in a tank containing potassium solution of known concentration, and was found to be approximately 0.03.

If by "detection" is meant the measurement of the concentration with an error of not more than 50 per cent, then, n=0.5.

Formulas (5) and (6) may now be applied to three characteristic background circumstances:

Case 1: Here no other background is evident except that caused by a solution having specific activity $B=1.2\times10^{-3}$ gammas/sec/ml such as comes from the natural potassium in normal sea water. From (6), the limiting detectable concentration,

$$C_1=\frac{2+2\sqrt{1+0.009t}}{7.5t} \qquad \text{A.7}$$

gammas/sec/ml, and when t becomes very large this approaches,

$$C_1=\frac{0.035}{\sqrt{t}} \qquad \text{A.8}$$

Case 2: In deep water cosmic rays may be neglected, and the S. I. O. probe is likely to indicate a total background of about 15 CPM, or b=0.25 counts/sec, therefore, the concentration just delectable is,

$$C_2=\frac{2+2\sqrt{1+0.063t}}{\sqrt{t}} \qquad \text{A.9}$$

gammas/sec/ml, which approaches as t increases to a large value,

$$C_2=\frac{0.067}{\sqrt{t}} \qquad \text{A.10}$$

Case 3: In shallow water where cosmic rays are unattenuated, the background on the S. I. O. probe amounts to about 60 CPM, or b=1.0

counts/sec, therefore the minimum detectable concentration becomes,

$$C_3 = \frac{2 + 2\sqrt{1 + 0.25t}}{7.5t} \qquad \text{A.11}$$

gammas/sec/ml which approaches for very large values of t,

$$C_3 = \frac{0.13}{\sqrt{t}}. \qquad \text{A.12}$$

Tabulations

Table 3 compares the effect of increasing the period of measurement with the effect of diminishing the background. It is evident that a substantial change in background has relatively small practical effect on any measurement made so rapidly that only a very poor sample is taken out of the fluctuating signal; however, when sufficient time can be alloted for good sampling, the background level becomes the limiting factor. It should not be overlooked that in practical field work, instrument imperfections may contribute to the overall error more or less proportionally with time of measurement, and that measurement time must be spent economically on almost all oceanographic expeditions. It is apparent therefore that efforts should be made towards increasing the counting rate, ve, while reducing the relative value of the background count by all possible means. Technique for cleanliness and for discrimination of background by electronic means have not yet been fully developed for this purpose.

REFERENCES

Folsom, Theodore R. 1956. Problems peculiar to direct radiological measurements at sea. Paper presented at Nat. Acad. of Science Meeting, 29 Feb.-1 Mar. 1956. Washington, D. C. Proceedings (in press).

Glueckoff. 1955. Long term aspects of fission product disposal. United Nations Conference on the Peaceful Uses of Atomic Energy, Geneva. Paper No. 398: 11 pp.

Miyake, Y., Y. Sugiura, and K. Kameda. 1954. On the distribution of radioactivity in the sea around Bikini Atoll in June 1954. Paper in meteor and geophys., Meteorol. Research Institute, Tokyo, 5:253–262.

Revelle, R. R., T. R. Folsom, E. D. Goldberg, and J. D. Isaacs. 1955. Nuclear science and oceanography. United Nations International Conference on the Peaceful Uses of Atomic Energy, Geneva. Paper No. 277:22 pp.

Ruggoff, Milton D. (Editor) Why the sea is salt (an abstract from a translation from the Norse by Sir George Weble) pp 672–676 in Harvest of World Folk Tales. XViii+734 pages, Viking Press.

U. S. Atomic Energy Commission and Office of Naval Research. 1956. Operation TROLL. Health and Safety Laboratory, U.S.A.E.C., New York Operations Office, NYO-4656, Ed. by J. H. Harley: 37 pp.

U. S. Department of Commerce. 1953. Maximum permissible amounts of radioisotopes in the human body, and maximum permissible concentrations in air and water. National Bureau of Standard Handbook 52:445 pp.

Reprinted from Journal of Applied Physics, Vol. 28, No. 2, 205–211, February, 1957
Copyright 1957 by the American Institute of Physics
Printed in U. S. A.

Reproduced by Permission

Air Bubbles in Water*

Leonard Liebermann
University of California, Marine Physical Laboratory of the Scripps Institution of Oceanography, La Jolla, California
(Received September 4, 1956)

The solubility of air bubbles is observed in a variety of experiments. Freely rising bubbles exhibit a solution rate more than twice that of bubbles which are stationary: i.e., trapped on the walls of the container. The theory of solution of stationary bubbles is given but the theory of a free bubble is difficult and has not been solved. Stationary bubble observations lead to a determination of the coefficient of diffusivity: 2.9×10^{-5} cm^2/sec at 27°C; the temperature dependence is considerable, obeying Einstein's equation relating diffusion and viscosity. The effect of surface contamination on diffusion is analyzed; bubble solution in the presence of contaminants is not greatly altered. Experiments are described showing that air bubbles of dimension less than 1μ lodged on hydrophobic particles are not soluble and can exist indefinitely. It is shown that hydrophobic particle residues frequently remain after bubble solution, even in relatively pure water. These residues function as bubble nuclei for boiling or for cavitation.

I. INTRODUCTION

Gas bubbles in the interior of liquids are unstable. If a liquid is undersaturated with gas, bubbles diminish in size as the gas diffuses into the liquid; similarly, bubbles in oversaturated liquids increase in size. The length of time during which bubbles can persist in an undersaturated liquid is of considerable interest. For example, the presence of relatively few bubbles in a liquid can produce profound changes in its acoustical properties; serious errors in ultrasonic measurements have been attributed to the presence of bubbles. In fact, thermal, viscous, and elastic properties of a liquid all may be considerably affected by the presence of bubbles.

Although gas bubbles in liquids are a familiar sight, they are nearly always observed in a trapped state, i.e., on the sides or bottom of a container. Free bubbles are less commonly observed because they rapidly ascend and disappear unless extremely small, and not easily visible. The theory of the diffusivity of a stationary bubble is known, but the theory of diffusion of an ascending bubble is of extreme difficulty and thus far has not been attempted.

The experiments which follow show that the rate of diffusion of a stationary (or trapped bubble) is considerably different from free bubbles. These experiments also yield the determination of the coefficient of diffusivity of air into water. This coefficient is surprisingly independent of contamination of the interfacial boundary between the air and water.

II. OBSERVATIONAL TECHNIQUES

A. Free Bubble Solubility

The observational technique for studying the solution of a free bubble is simple and direct: A 1-m vertical glass tube, with lower end open, is filled with water and stoppered at the upper end. The inside diameter of the tube is small (1 cm), so that water remains in the tube although the lower end is open. Small bubbles, created by vigorously shaking a water-filled bottle, are introduced into the column by momentarily placing the bubble filled water in contact with the open end.

Bubbles introduced in this manner slowly ascend the column and their velocity is observed with the aid of a stop watch and scale. Whenever the water in the column is undersaturated with air the velocity is observed to diminish as the bubble ascends the column. This diminution of velocity is a consequence of the decrease in size of the bubble as its air goes into solution; a definite relationship exists between bubble velocity and bubble size as is discussed in detail below. Hence, both bubble velocity and bubble radius are observed as a function of time for freely rising bubbles. A sample

---

* This work received support from the Bureau of Ships, Navy Department; Contribution from the Scripps Institution of Oceanography, New Series, No. 906.

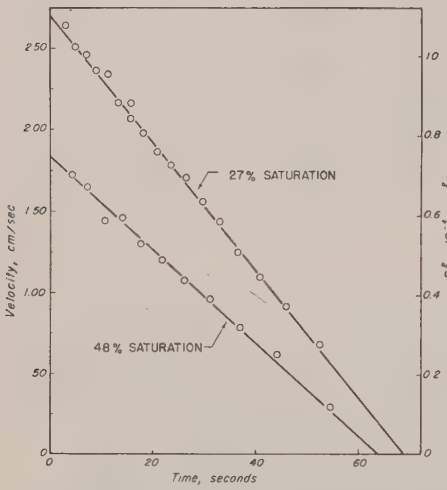

FIG. 1. Observations of the velocity of rise (and solubility) of two individual free bubbles. The bubble radius R given on the right of the figure, is derived from the velocity observations by Stokes' equation. The degree of saturation of the water is the ratio of actual air concentration to saturation concentration, c_∞/c_s.

set of observations illustrating the method is shown in Fig. 1. Note that the velocity decreases linearly with increasing time. As is shown in the following section, the terminal velocity is proportional to the square of the radius; hence the square of the radius also decreases linearly with time.

B. Ascent Velocity and Bubble Radius

A familiar relationship between terminal velocity and spherical diameter is that of Stokes[1]:

$$v = (2/9)gR^2(\rho-\rho')/\eta, \tag{1}$$

where $(\rho-\rho')$ is the difference in densities of the sphere and surrounding liquid; η is the viscosity, g the acceleration of gravity, and R is the bubble radius. As stated above, the velocity is proportional to the square of the radius.

Stokes' formula applies to a sphere with a rigid or extremely viscous boundary. The assumption that the air-liquid interface of a bubble is rigid may appear doubtful. Rybczynski[2] elaborated Stokes' calculation for a viscous boundary and obtained a modified formula:

$$v = [(2/9)gR^2(\rho-\rho')/\eta](3\eta'+3\eta)/(3\eta'+2\eta), \tag{2}$$

where η' and η are the viscosities of air and water, respectively. Inasmuch as η'/η is of the order of 10^{-2}, the expression outside the brackets is approximately 1.5. Hence the fluidity of the boundary might be expected to increase the Stokes velocity by the factor, 1.5.

An important objection to the preceding formula was raised by Boussinesq.[3] It has been known since the time of Descartes and Rumford that the viscosity of a liquid measured at its surface can be considerably greater than the usual shear viscosity. Rayleigh showed that this apparent surface viscosity does not occur with purely shearing motion, but with surface dilatation (or compression). Undoubtedly it results from surface contamination, invariably present on liquid surfaces. According to Boussinesq the correct terminal velocity should lie between that of the rigid boundary of Stokes and the fluid boundary of Rybczynski, or greater than the Stokes velocity by 1 to 1.5.

A direct answer to this question was obtained by measuring the diameter of a bubble by means of a measuring microscope at the instant of striking a horizontal glass plate. The terminal velocity of the same bubble at the instant of striking was observed as described in Part *A*. These data demonstrate that the terminal velocity of a bubble less than 0.2 mm (the size used here) is correctly given by Stokes, i.e., it behaves as if dynamically rigid. This result is confirmed by the experiments of Bond and Newton[4] using highly viscous liquids, as well as by the older work of Allen.[5] Hence the Stokes formula, Eq. (1), was used throughout in computing these results.

C. Stationary Bubble Observations

Observations on the rate of solution of a stationary bubble were made with a measuring microscope. A droplet of water was suspended on the underside of a carefully cleaned microscope slide. The air bubble, introduced by means of a micropipette, remained stationary against the underside of the glass. The diameter of the bubble was measured at regular time intervals. All observations were made in a thermostatically controlled chamber whose temperature could be varied.

Preparation of the partially saturated water used in all observations, was as follows: Distilled water was permitted to remain in contact with air at reduced pressure for more than 24 hours, in order to establish oxygen-nitrogen equilibrium; equilibrium is important inasmuch as the diffusion rates of these two gases are different. The oxygen content in solution was then analyzed by a standard chemical titration method and the result used to obtain the degree of air saturation. The degree of saturation could also be obtained approximately from the value of the reduced atmospheric pressure at which equilibrium was established; the oxygen determination provided a more precise check.

---

[1] G. G. Stokes, Math. and Phys. Papers 2, 10 (1880).

[2] W. Rybczynski, Bull. Acad. Sci. Cracovie, 40 (1911).

[3] J. Boussinesq, Ann. chim. phys. 29, 349 (1913).

[4] W. N. Bond and D. A. Newton, Phil. Mag. No. 7, 5, 794 (1928).

[5] H. S. Allen, Phil. Mag. No. 5, 50, 323 (1900).

III. INTERPRETATION OF OBSERVATIONS

It was found from the preceding observations that the rate of solution of stationary bubbles is quite different from that for free bubbles. Consequently, this represents two types of diffusion processes which are best treated separately in the following discussion.

A. Solubility of Stationary Bubbles

The theory of diffusion is closely analogous to the theory of heat conduction. A similar problem, the cooling of a perfectly conducting sphere in an infinite medium is found in texts.[6] In terms of the temperature, θ,

$$(d\theta/dr)_R=(\theta_s-\theta_\infty)[1/R+1/(\pi\kappa t)^{\frac{1}{2}}], \tag{3}$$

where θ_s is the temperature of the sphere and θ_∞ is the temperature of the medium far from the sphere; κ is the coefficient of thermal diffusion. In the present problem the concentration of gas in the solution is exactly analogous to the temperature and can be interchanged in the above equation; for example θ_s is replaced by c_s the gas concentration at saturation. From the definition of the coefficient of diffusion it follows that

$$dm/dt=4\pi R^2\kappa(dc/dr)_R.$$

Inasmuch as $dm/dt=4\pi R^2\rho dR/dt$, Eq. (3) can be written as

$$dR/dt=(\kappa/\rho)(c_s-c_\infty)[1/R+1/(\pi\kappa t)]. \tag{4}$$

In the present observations, diffusion is sufficiently slow that the last term on the right containing the time can be neglected. The solution is then

$$R^2=R_0^2-(2\kappa/\rho)(c_s-c_\infty)t, \tag{5}$$

where R_0 is the radius at $t=0$.

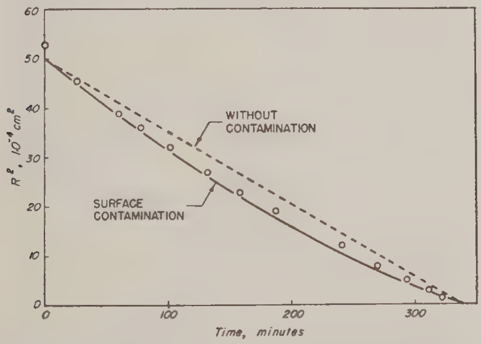

FIG. 2. Observations of a stationary (trapped) air bubble dissolving in water at 14.5°C, 60% saturation. The bubble radius is R. The dotted line (without contamination) is given by Eq. (5); the solid curve represents Eq. (6), assuming the presence of an unavoidable contaminant on the bubble surface.

According to Eq. (5) the square of the bubble radius should diminish linearly with time. It is seen from Fig. 2 which gives the dependence of R^2 on t, that this behavior is very nearly, but not exactly, observed.

The slight departure from linearity appears to result from the inescapable contamination at the surface of the bubble; this effect was discussed briefly in connection with surface viscosity. Suppose the thin film of contamination of thickness ΔR possesses another diffusion coefficient, κ_1. It is entirely possible that the quantity $\kappa_1\Delta R/\kappa$ is not negligible compared to R. In this case it may readily be shown that bubble solubility is given by

$$R^2=R_0^2-(2\kappa/\rho)(c_s-c_\infty)t+(2\kappa_1\Delta R/\kappa)(R_0-R). \tag{6}$$

Equation (6) is plotted in Fig. 2 with κ and κ_1 chosen to give the best fit with the data. The quantity $\kappa_1\Delta R/\kappa$ in this case is 0.06 cm, or nearly the same as R_0. It is clearly impossible to assign a value to the constant κ_1, for the thickness as well as the nature of the contaminant may vary from one trial to the next.† The slight curvature observed in all decay curves of stationary bubbles, in spite of elaborate cleanliness procedures, is evidence that surface contamination is practically unavoidable.

B. Coefficient of Diffusion of Air into Water

The preceding discussion suggests the use of Eq. (6) for the determination of the coefficient of diffusion. Before applying this equation it is important to consider those properties of real bubbles which were ignored in its derivation. For example, the surface tension of a bubble was neglected. Epstein and Plesset[7] have given the theory of solution of a stationary bubble in which this effect is included. Surface tension increases the gas pressure in the bubble and thus increases c_s. This effect becomes important only when $c_\infty \simeq c_s$ (near to saturation). The present observations were deliberately made at lower air concentrations where the surface tension correction can be neglected.

The boundary of the observed stationary bubble was not entirely free but was in contact with a plane surface. The glass surface was chemically clean so that the bubble remained essentially spherical with an extremely small contact area. It can be shown that the effect on diffusion of a plane surface tangent to a sphere is to reduce the diffusivity by $\ln 2=(0.69)$.‡ Hence a correction must be made for this effect in the determination of the diffusion coefficient.

Finally the theory neglects the influence on diffusion of the motion of the boundary as the bubble slowly collapses. This effect might slightly increase the rate of diffusion, but it is believed to be negligible.

---

[6] H. S. Carslaw and J. C. Jaeger, *Conduction of Heat in Solids* (Oxford University Press, London, 1947), p. 217.

† It is quite likely that ΔR, the film thickness, is not constant but gradually increases as the film becomes compressed with diminishing bubble diameter.

[7] P. S. Epstein and M. S. Plesset, J. Chem. Phys. 18, 1505 (1950).

‡ This is readily proven using the methods of electrostatics. For example, the capacitance of a conducting sphere is reduced by ln2 when placed close to an infinite plane ungrounded conductor.

Table I gives the coefficient of diffusivity for air into water, derived from observations on stationary bubbles using Eq. (6). The correction for the presence of the plane surface adjacent to the bubble has been included.

The most widely accepted determination of diffusivity is that of Mache.[8] As in the present work, Mache observed the solubility of a stationary air bubble. Brandstaetter[9] attempted to repeat Mache's result but obtained diffusivity values nearly 50% higher. His explanation for this wide discrepancy was that Mache's low diffusion rates resulted from surface contamination. Previously Mache had criticized an earlier determination (i.e., Huffner) as being too high; Mache attributed the "error" to the presence of advection currents.

This disagreement apparently resulted from a failure to realize that diffusion is temperature dependent. Mache's experiments were made at 9°C; Brandstaetter's were primarily at 20°C; Huffner's results were very likely at room temperature. The theory of diffusion predicts an increase in the diffusion constant with temperature. For example, it is reasonable to utilize Einstein's[10] relation for the diffusion of small spheres in a viscous fluid; this theory has been verified in many instances for a solute diffusing into a liquid solvent:

$$\kappa = K\theta/3\pi D\eta, \tag{7}$$

where D is the molecular diameter of air, and K is the Boltzmann constant; η is the viscosity of water.

By means of this equation the measurement of diffusivity gives a determination of the average molecular diameter of air; the value obtained is 1.8 A. Figure 3 shows the temperature variation of diffusion predicted by Eq. (7) using the above molecular diameter; the present observations together with those of Mache and Brandstaetter are included. The present observations are somewhat higher than the previous work, resulting from the different treatments of contamination. The earlier workers ignored the curvature in the rate of diffusion and simply computed the mean slope; this is equivalent to using Eq. (5) rather than Eq. (6) in computing κ. It appears that both of the earlier values would be in close agreement with this work if Eq. (6) had been used for computing the diffusion.

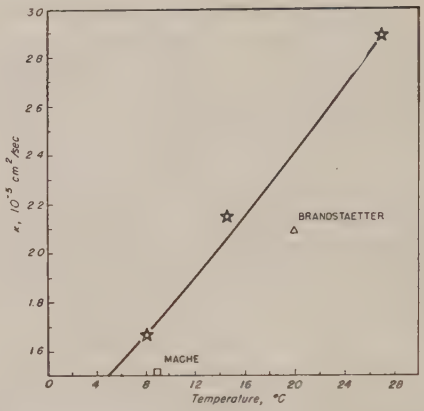

Fig. 3. Observations of the temperature dependence of the coefficient of diffusivity. Present observations are symbolized by stars. The solid curve is the Einstein diffusivity, $\kappa = K\theta/3\pi\eta D$ with the air molecular diameter D taken to be 1.8 A. The previous determinations of Mache and Brandstaetter would be in close agreement with the present work if the effect of contamination were included in calculating κ.

Table I. Determinations of the coefficient of diffusion, κ, at various temperatures. Another coefficient, κ', is defined for freely rising bubbles.

Air saturation	Temperature (°C)	Initial radius	Final radius	κ	κ'
		(10^{-3} cm)		(cm^2/sec)	
		Stationary bubble diffusion			
50%	8	75	3	1.7×10^{-5}	
35%	8	39	5	1.6×10^{-5}	
46%	14.5	64	8	2.1×10^{-5}	
46%	14.5	61	5	2.2×10^{-5}	
70%	27	60	4	2.9×10^{-5}	
60%	27	70	2	3.0×10^{-5}	
		Free bubble diffusion			
70%	25	10	4		6.3×10^{-5}
44%	25	9	4		6.2×10^{-5}
27%	25	10	3		6.3×10^{-5}
10%	25	9	4		6.2×10^{-5}

C. Free Bubbles

As noted in the foregoing, the solution times of free bubbles bears the same linear relationship with R^2 as observed with stationary bubbles. Consequently, the stationary bubble equations given above can be used to define another characteristic constant: the coefficient of diffusivity for free bubbles. The column headed κ' in Table I was derived in this manner treating free bubbles as if they were stationary. It is seen that the effect on the diffusivity of the ascending motion as slow as $\frac{1}{2}$ cm/sec is by no means negligible; it increases the diffusivity by approximately the factor 2.

It is surprising that the observed rate of diffusion of a free bubble is apparently independent of velocity. Clearly some velocity range must exist in which the diffusivity varies from its free to stationary values. Unfortunately, applicable theory is practically nonexistent, for the problem is one of extreme difficulty. The special case of the very slowly moving sphere has been treated by Breiman.[11] However the Péclet number

---

[8] M. Mache, Wien. Akad. IIA 138, 529 (1929).

[9] F. Brandstaetter, Österr. Akad. Wiss. IIa 161, 107 (1952).

[10] A. Einstein, Ann. Physik. 17, 549 (1905).

[11] L. Breiman, California Institute of Technology Repo t No. 27-2, Office of Naval Research (1952).

($\mathrm{Pe}=2vR/\kappa$) is assumed to be less than unity in this approximation and in the present observations the Péclet number was of the order of 100. Boussinesq[12] calculated the heat transfer assuming the temperature gradient in the direction of flow to be negligible compared to the gradient normal to it; in other words, the heat conductivity was low and the velocity, high. He obtained the result, $\kappa'=0.35(\mathrm{Pe})^{\frac{1}{2}}\kappa$. Johnstone, Pigford, and Chapin[13] derived a similar heat transfer expression by making the assumption that the fluid flow remains parallel to the sphere's surface with velocity equal to the undisturbed flow; this is the tendency at high Reynold's numbers. They obtained $\kappa'=0.5(\mathrm{Pe})^{\frac{1}{2}}\kappa$. Kramers[14] has measured the heat transfer of spheres in flowing media. He obtained the empirical expression for water, $\kappa'=\kappa[2+0.5(\mathrm{Re})^{\frac{1}{2}}]$ where Re is the Reynold's number, $2Rv/\eta$. However, in Kramers' experiments the flow was not entirely free, but was confined to a 3-cm diam pipe with a 1-cm diam sphere on the axis. Although corrections were made, it is questionable whether these observations pertain to free flow.

The preceding formulas although differing in detail all agree in predicting that the diffusivity in flowing media should be a function of velocity (and diameter). Present observations, on the contrary, yield a constant coefficient of diffusivity independent of velocity. The foregoing formulas are supposedly applicable for Reynold's numbers of the present work. Apparently important factors were neglected in the above approximations which cancel the variation with velocity, but not the effect of velocity.

It is interesting to note that in spite of this fundamental disagreement, the foregoing formulas predict a diffusivity of the order of that observed. For example, the Péclet number in the middle velocity range of Fig. 1 is 100. In this region both theoretical formulae give, $\kappa'\sim 5\kappa$, or greater by the factor 2 from observation. The empirical formula of Kramers for Reynold's number 1, gives $\kappa'\sim 2.5\kappa$ in the neighborhood of the observed value.

The effect of hydrostatic pressure was considered in the free bubble solubility. During observation a bubble may have changed its water depth from 60 cm to nearly 0; the pressure variation resulting is 6%. However, the combination of the pressure variation resulting from surface tension ($\sim$5%) and the variation of depth tend to keep the pressure increase nearly constant during an observation. The slight increase in diffusivity resulting is not significant.

IV. PERSISTENT BUBBLES

It is a common belief that bubbles can persist for long periods in water. The preceding observations illustrate that this notion is incorrect for pure undersaturated water. For example, a beaker of water at 50% saturation will be completely free of bubbles (except for those stuck on the walls) in less than ½ minute.§ Although the solution times of large bubbles may be lengthy, these ascend rapidly and are lost at the liquid surface unless trapped on a rigid boundary. This behavior is characteristic of pure water; the slight inhibition of diffusivity resulting from the unavoidable contamination described earlier, suggests the possibility that the relatively large amount of impurities in natural waters might significantly alter bubble stability.

The experiments described in the next part represent an attempt to observe diffusion effects when the contamination is deliberately large.

A. Influence of Contaminants on Diffusivity

The diffusivity of bubbles was measured under two types of contamination and the following conclusions established: In sea water, the solution rate of bubbles was found to be not significantly lower than in pure water; the sea water was unfiltered, containing the usual particulate organic material. In a second series of experiments, bubbles were created by shaking a bottle of water in which a surface contaminant had been introduced. Contaminants tried, one at a time were: oleic acid; palmitic acid; neutral detergent, soap, mineral oil, and vegetable oil. The rate of solution was measured with the contaminated bubble dissolving in pure water. It was concluded that none of the above surface contaminants significantly diminished (by as much as a factor, 2) the rate of diffusion of the bubble. Although every reasonable attempt was made, *no laboratory condition could be found in which the rate of bubble diffusion was significantly altered.*

B. Persistence of Bubbles on Hydrophobic Surfaces

As discussed previously, surface tension increases the internal pressure of free bubbles. On a hydrophobic surface the effect of surface tension can reverse; surface tension may act oppositely to the aqueous

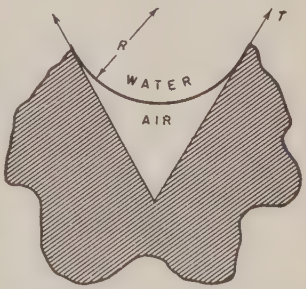

FIG. 4. A condition whereby an air bubble can remain stable indefinitely, without solution, on a hydrophobic particle possessing a concave surface. If the external pressure,

$$P\leqq 2T/R$$

then bubble stability results.

---

[12] J. Boussinesq, Liouville Journal 1, 285 (1905).

[13] Johnstone, Pigford, and Chapin, Trans. Am. Soc. Chem. Engrs. 37, 95 (1941).

[14] H. Kramers, Physica XII, 12, 61 (1946).

§ See Fig. 1. Even at 100% saturation all free bubbles would be absent in less than two minutes because of the effect of surface tension.

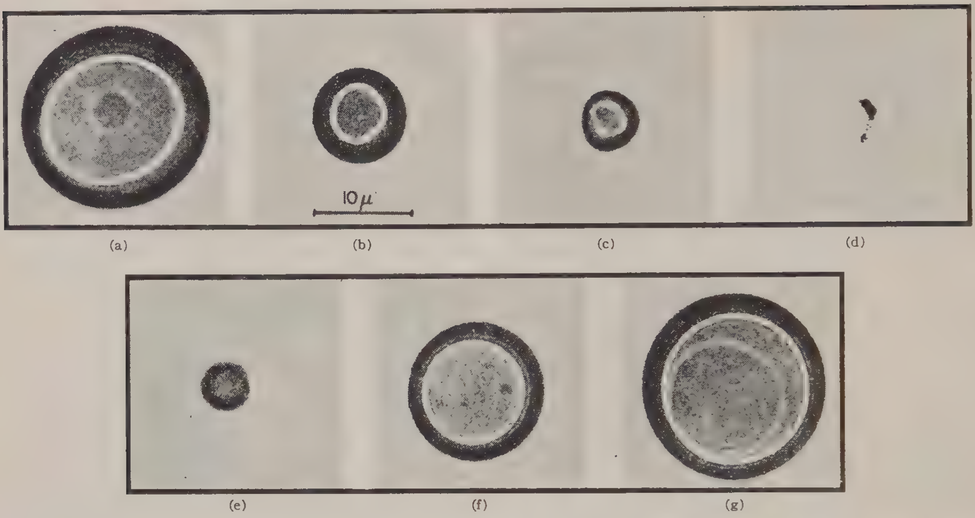

(a) (b) (c) (d)

(e) (f) (g)

FIG. 5. (a)–(c) Sequential photomicrographs of the solution of a single bubble; the length of the line is 10μ; the time lapse between photographs is in the neighborhood of 20 sec. (d). The insoluble stable residue remaining on the underside of the glass slide at the site where the bubble dissolved, termed the nucleus. (e)–(g). The growth of a bubble from the same nucleus when the external pressure was reduced to $\frac{1}{4}$ atmos.

pressure, reducing the total pressure. As an illustration, Fig. 4 shows schematically a bubble trapped on a particle whose surfaces are hydrophobic. It is seen that the curvature of the aqueous surface results in surface tension opposing the hydrostatic pressure in the liquid. Whenever these opposing pressures are equal, i.e., when $2T/R \sim 10^6$ dynes/cm^2 (T is the surface tension constant), solution ceases and the bubble can persist indefinitely. Hence bubbles of dimension less than 1 μ, lodged upon hydrophobic surfaces in water ($T=70$), would be expected to remain stable.

In order to test this hypothesis the following experiment was performed: A droplet of undersaturated water was suspended on the underside of a microscope slide; to the water had been added a small amount of very fine oily chalk dust serving as a hydrophobic contaminant. A small air bubble was introduced into the droplet by means of a micropipette. The bubble was observed microscopically using a 1.9-mm oil immersion objective. The bubble was seen to diminish and then vanish from sight; but remaining on the underside of the glass at the site of the bubble collapse was a microscopic deposit of chalk debris. Figures 5(a), 5(b), and 5(c) are a series of photomicrographs taken at various time intervals showing the bubble going into solution; *d*, shows the insoluble nucleus remaining after the solution.

The next stage in the experiment demonstrates the likely existence of a persistent submicroscopic bubble: the water droplet containing the insoluble nucleus shown in Fig. 5(d), was then subjected to a reduced pressure of approximately $\frac{1}{4}$ atmos. Almost immediately a visible bubble appeared. The bubble rapidly grew in size as shown in Figs. 5(e), 5(f), and 5(g). Clearly the increase in size resulted from the water droplet becoming oversaturated at the reduced pressure.

Although it is readily apparent that a bubble, once formed in an oversaturated solution will grow, its initial formation requires explanation. The tensile strength of water is known to be in excess of 200 atmos[15]; the relatively small pressure reduction used in this experiment is far insufficient to cause a rupture in pure water. A more reasonable explanation of bubble formation is to postulate the presence of a permanent submicroscopic bubble, stable against solution because of the presence of a hydrophobic surface. It is not surprising that this stable bubble "nucleus" is invisible; with the microscope optics used 1 μ would be at the limit of visibility. In addition, gas bubbles are relatively poor objects for microscopy.

Once formed, a bubble "nucleus" is exceedingly stable. There appears to be no time limit beyond which it is not possible to regenerate a bubble from a hydrophobic collapse site. In these experiments as much as 48 hours were permitted to elapse between bubble collapse and regeneration.

C. Cavitation Nuclei

Similar hydrophobic sites may well be the explanation for ordinary cavitation (or boiling). It is a familiar fact that cavitation (and boiling) often occurs when the pressure is small but positive, although the tensile strength of a liquid would require a large negative pressure for cavitation.

---

[15] L. Briggs, J. Appl. Phys. 21, 721 (1950).

It is unnecessary to add a contaminant, such as chalk dust, in order to observe bubble regeneration. The above experiments were repeated using multiply distilled water on a chemically clean glass support instead of the chalk-dust contaminated water. In spite of precautions to preclude the introduction of contaminants *a permanent insoluble deposit remained after bubble collapse in every trial.* Some (not all) of these collapse sites were demonstrated to be capable of regenerating bubbles exactly in the manner described previously.

Hence, it seems reasonable that submicroscopic bubbles can persist indefinitely in supposedly pure liquids. The surface of a collapsing gas bubble provides a mechanism for concentration of the invariable debris existing in all but the purest liquids.‖ These debris sites may then provide the proper environment for the stable existence of the nuclei of cavitation.

V. CONCLUSIONS

Lifetimes of air bubbles in water are paradoxical: the larger the bubble, the longer the persistence time; but sufficiently small bubbles, below 1 μ in diameter, are often able to persist indefinitely, stable against solution. The rate of solution of bubbles larger than 1 μ has been shown to be relatively rapid; within minutes all bubbles in a container of water (except for those stuck on the walls) will have vanished, either by solution or by rising to the surface. Thus, the effect of bubbles of this size on physical experiments in water can be expected to be negligible (unless bubble generation occurs). The same conclusion undoubtedly holds in the ocean; it was shown that organic stabilizers do not significantly inhibit bubble solution. It is not easy however, to eliminate air bubbles of sizes less than 1 μ from water. Very likely it is the presence of these small stable bubbles which are responsible for the phenomenon of boiling and cavitation in water and in other liquids.

‖ Cavitation experiments with extremely pure liquids have demonstrated that negative pressures approaching the tensile strength must be provided for the onset of cavitation in these liquids.

JOURNAL OF SEDIMENTARY PETROLOGY, VOL. 27, NO. 1, PP. 41–55
FIGS. 1–8, MARCH, 1957

A FABRIC AND PETROLOGIC STUDY OF THE PLEASANTVIEW SANDSTONE[1]

GENE A. RUSNAK
Scripps Institution of Oceanography, University of California,
La Jolla, California

ABSTRACT

The Pleasantview sandstone is a typical Pennsylvanian cyclothem sandstone in western Illinois exhibiting both channel and non-channel phases. In order to describe the sandstone and to interpret the sediment transport direction and the environmental conditions existing at the time of deposition, an investigation was made of the texture, composition, depositional structure, cross-bedding, and dimensional fabric. Results of this study indicate that the sandstone is a subgraywacke which was deposited in a north and northwest direction. It is concluded that the process which cut the Pleasantview channel was to a large degree independent of the processes which later filled the channel with sediment. No conclusive evidence could be found for the exact nature of the processes operating at the time of channel cutting and filling. However, it is suggested that the environmental conditions of the Pleasantview most closely resemble those conditions existing at present in the Dutch Wadden Sea.

INTRODUCTION

The Pleasantview sandstone occurs in the lower part of the Carbondale between the Colchester (No. 2) and the Springfield (No. 5) coals and represents the basal member of the Summum Cyclothem. This sandstone is typically bluish-gray, fine-grained, micaceous, carbonaceous, and massive to thin-bedded. In the non-channel phase the sandstone is in apparent conformity with the subjacent Purington shale, but in the channel phase the sandstone rests unconformably on the underlying channeled sediments. The thickness of the sandstone ranges from 6–10 feet in the non-channel areas to 100 feet in the deep channels. The stratigraphic section, which includes the Pleasantview, has been previously described in papers by Ekblaw (1930) and Wanless (1931) and is generalized in figure 1.

Although the origin of the cyclothem channels has been ascribed to several possible causes (Wanless, 1950, 1952, 1955; Weller, 1956; Stout, 1931), there has been little work done to determine the direction of current flow within these channels. Ekblaw (1930, 1931) investigated the field relations of the Pleasantview channel system and succeeded in delineating the channel boundaries. From the dendritic pattern obtained, Ekblaw concluded that the currents producing the channels flowed from north to south. The direction of transport of the sandstone fill was not determined at that time, however. The present writer, therefore, attempted to answer the question of transport direction by making a field and petrologic study of the Pleasantview sandstone and channel of Fulton County, Illinois (fig. 2). A secondary objective of this study was the description of the sediment and an attempt at understanding some of the conditions of sedimentation.

GROSS LITHOLOGY

The Pleasantview channel in Fulton County has a width of about 1¼ miles and a length of about 22 miles. The depth of this channel and the thickness of the sandstone fill increases from 50 feet at the northern border of Fulton County to 100 feet 22 miles further south where the channel opens out at its mouth. Because the Pleasantview sandstone in the non-channel areas differs from that of the channel areas it is here described separately as "non-channel phase" and "channel phase."

Non-channel phase.—In the non-channel areas the sandstone is fine-grained, bluish-gray, thin-bedded, and contains very little carbonaceous material. This sandstone is in apparent conformity with the underlying Purington shale and exhibits a gradational contact with shale-to-sandstone transition zones ranging in thickness from 6 to 18

---

[1] Contribution from The Scripps Institution of Oceanography, New Series 907.

Reproduced by Permission

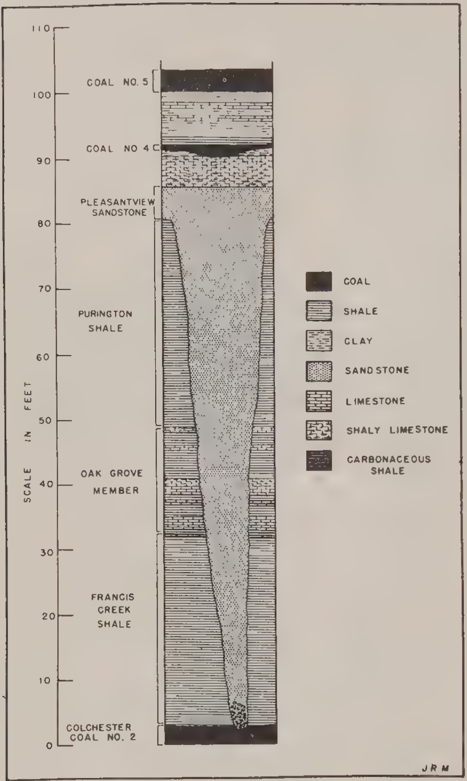

FIG. 1.—Generalized stratigraphic section containing the Pleasantview sandstone (after Ekblaw, 1930 and Wanless, 1931).

inches. Above this contact the sandstone is uniform and evenly bedded. The top of the sandstone is marked by calcareous beds which grade upward into an overlying sandy shale. The total thickness of the non-channel phase ranges from 6 to 10 feet.

Unlike the channel sandstone, the non-channel phase shows some prominent ripple marks. The ripple marks observed by the writer were wave (oscillation) ripple marks rather than current ripple marks. An exceptionally good exposure of these was noted in the NW¼ NE¼ sec. 32, T. 6 N., R. 3 E. of the Havana Quadrangle. The strike of the ripples at this location measured N. 35° E. and thus would indicate a wave oscillation of northwest-southeast. Ekblaw (1930), however, reported current ripples from this same area which indicated a northwest (N. 30° W.) flowing current.

Channel phase.—The Pleasantview sandstone in the channels is also fine-grained, but is very micaceous, and very carbonaceous. The color ranges from bluish-gray to yellowish-gray and locally to black where there is a great abundance of fossil plant material. Although local variations of lithology exist, a generalized description of the channel phase can be made.

The lowermost 15 inches of the sandstone commonly exhibit isolated conglomeratic layers of clay ironstone, limestone, and shale pebbles (long dimensions lying parallel to the bedding planes) which appear to be derived from the underlying sediments. Above this conglomeratic zone is a sandstone, 3 to 5 feet thick, containing many fossil wood fragments carbonized to form coaly streaks. These two basal units are not everywhere present and are often represented only by thin-bedded carbonaceous shales.

The sediments of the next higher zone consist of very thick massive and lenticular sandstones alternating with sandy carbonaceous shales. The bedding planes of this unit are marked by abundant, large mica flakes and plant remains. Although poorly displayed because of inadequate exposures, the massive sandstone commonly contains highly variable cross-bedding. Where cross-bedding was observed, the dip inclinations and dip directions were measured and summarized as in table 1. Normals to these cross-bedding planes are graphically shown in figure 3 and the average dip direction for each sample site is shown in figure 2.

The uppermost 20 feet of the channel sandstone is very shaly and contains much carbonaceous material, thin coaly streaks, and lenses of massive calcareous and stone concretions. This unit grades upward into the shaley and calcareous zone marking the top of the Pleasantview.

Whereas the contacts of the sandstone and the underlying shale appear gradational in the areas far removed from the channels, the contacts at the channel borders are sharp and distinct. Here, the undersurface of the sandstone disclosed markings, resembling minute ripple marks, similar to those described as "groove casts" by Shrock

(1948, p. 163–165) and attributed to subaqueous scour by Rich (1950). These markings are discontinuous and patchy and have an average crest-to-crest width of 6 mm and an average crest height of 2 mm. Groove casts appear to be associated with gentle wall slopes. With steep wall slopes, however, a lobate form of cast is more common (fig. 4). Rich (1950) calls such lobate forms "flow rolls" and describes them also as scour marks. Along the eastern border of the channel, the orientation of both groove and lobe casts is down the channel walls and to the southwest. Hence, if scour formed these marks, the scour was directed down towards the channel from northeast to southwest along the eastern border. This would agree, in general, with the erosion gradient as evidenced by the southward increase in channel depth.

The channel fill has distinctive depositional structures. Along the sides of the channel the sandstone bedding is characteristically parallel to the slope of the channel walls. Thus, the sandstone dips into the channels and is in angular contact with the essentially horizontal underlying channel-cut sediments. In the central portions of the channel, the sandstone beds assume a horizontal attitude. Hence, there is a strong suggestion that this channel was filled from outside the channel rather than by aggradation within channel flowing streams. The channel-flanking sandstone beds are not peculiar to

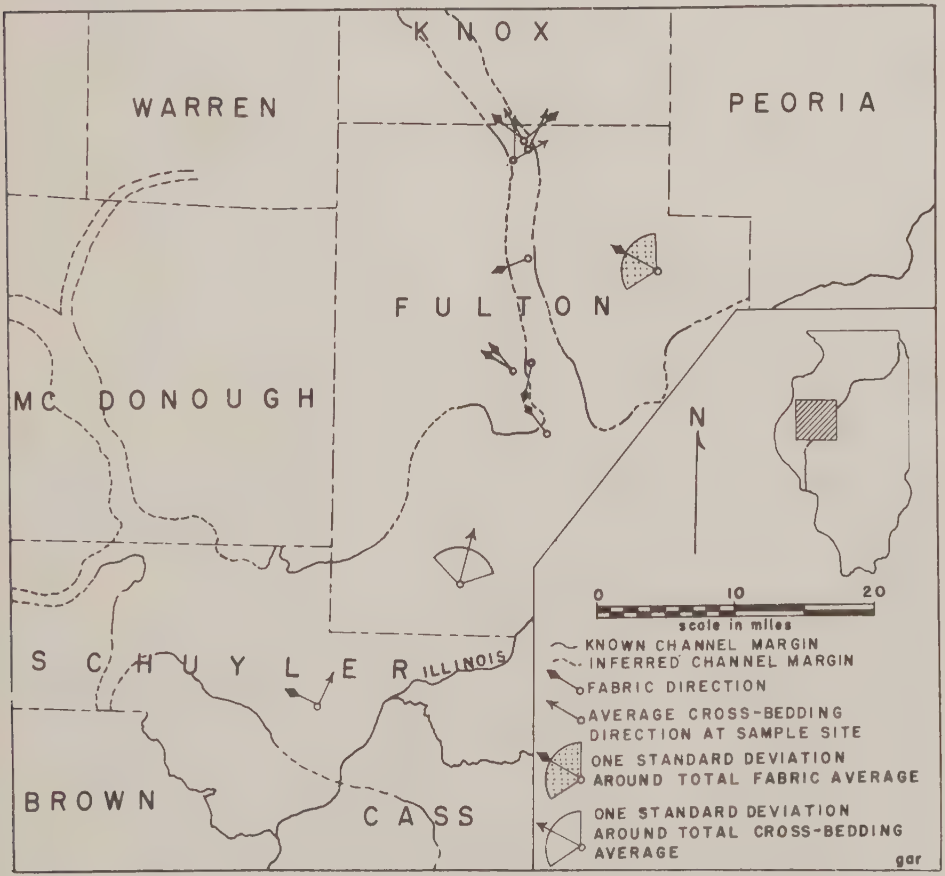
KNOX
WARREN
PEORIA
FULTON
MC DONOUGH
SCHUYLER
ILLINOIS
BROWN
CASS
N
0
10
20
scale in miles
KNOWN CHANNEL MARGIN
INFERRED CHANNEL MARGIN
FABRIC DIRECTION
AVERAGE CROSS-BEDDING DIRECTION AT SAMPLE SITE
ONE STANDARD DEVIATION AROUND TOTAL FABRIC AVERAGE
ONE STANDARD DEVIATION AROUND TOTAL CROSS-BEDDING AVERAGE
gar

Fig. 2.—Distribution of samples of fabric and cross-bedding directions (Channels after Ekblaw, 1930).

TABLE 1.—*Observed cross-bedding dip direction and inclination*

Location	Direction	Inclination
SE ¼ NW ¼ sec. 31, T. 2 N., R. 1 E. Schuyler County	1	12
	45	10
	69	22
	70	15
	78	8
	96	28
	110	6
	280	12
	285	13
	335	19
	352	26
	355	5
	357	25
NE ¼ SW ¼ sec. 17, T. 8 N., R. 3 E. Fulton County	5	25
	325	22
	340	15
	340	28
SW ¼ NE ¼ sec. 19, T. 8 N., R. 3 E. Fulton County	15	22
	130	17
	331	4
SW ¼ NE ¼ sec. 20, T. 8 N., R. 3 E. Fulton County	40	22

this single channel but have been reported from other Pleasantview channels by Ekblaw (1930, 1931). More recently, van Straaten (1951, 1952) has described similar relations from the sediments in the tidal-cut channels of the Dutch Wadden Sea and makes a distinction between vertical sedimentation (resulting in horizontal beds) and lateral sedimentation (resulting in inclined beds). Although the Dutch Wadden Sea area has this and other similarities to the Pleasantview, differences do exist. Further discussion of the differences and parallels between these two areas is made in the concluding section of this paper.

Near the western margin of the channel in the SW ¼, NE¼, SW ¼ sec. 19, T. 8 N., R. 3 E., Canton Quadrangle, three contorted and disconnected sandstone lenses are imbedded in what is apparently reworked Purington shale (fig. 5). These lenses lie one foot below the gradational contact of the channel sand and the shale. The internal structure of these lenses resembles nappe structure (fig. 6), with overturning and crumpling, and the streamline shape of the lens outlines suggests the lenses were lodged into the enclosing shale *en masse* and in a semifluid state as a sand slide or flow. The horizontal bedding of the surrounding shale does not appear to be disturbed in any way that would suggest mass slumping. Therefore, it might be concluded that, here at least, the shale must have been a very fluid mud at the time the lenses were incorporated. The direction of lens implacement appears to be to the south and may indicate that when the unstable sands started to flow they followed the local gradient of the channel. Other indications of unstable sediments are also present.

Within the shaly members of the channel fill in the NW ¼ SE ¼ sec. 19, T. 8 N , R. 3 E., Canton Quadrangle, two small "slump" folds were observed. One of these folds was noted near the base of the channel and the other was observed near the top of the channel. Neither of these slump folds exceeds 6 feet from limb-to-limb and 3 feet from base to crest (fig. 7). The asymmetry of the folds indicates that the fold at the base of the channel slumped toward the west and the fold near the top of the channel slumped toward the south. Although this deformation might have occurred at a much later time (possibly during Pleistocene glaciation), the horizontal beds above and below the folds show no apparent disturbance and hence strongly indicate that the folds are contemporaneous with the deposit.

Good exposures of the Pleasantview are rather limited because of overburden and strip mining activity. However, a complete cross-section of this Pleasantview channel, showing all the previously mentioned salient features, can be seen in a series of outcrops along Coal Creek in the Canton Quadrangle near the northern border of Fulton County.

METHODS

Because the study was made primarily to determine the direction of sediment transport, the sampling was made for the most part from the channel sandstone deposits. Samples were collected both vertically and laterally along the channel in an effort to evaluate possible textural and compositional variations. Moreover, several areas were sampled which were not bounded by the channel in order to assess variations outside the channel proper. In all, a total of 37 hand specimens was collected for study. Macroscopic examination of these hand specimens

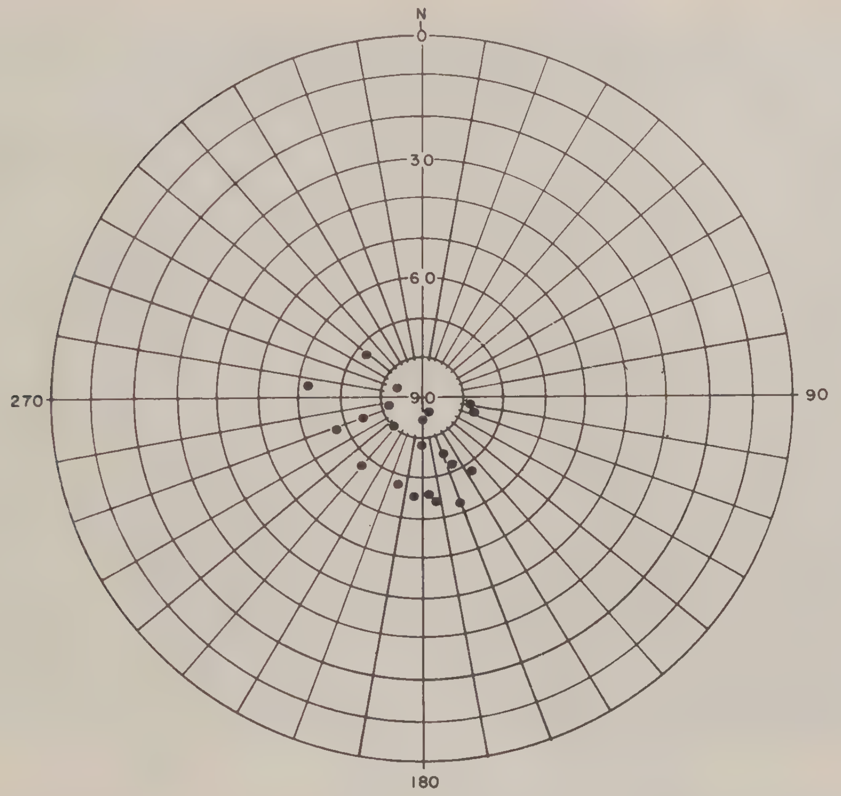

FIG. 3.—Directions of normals to the cross-bedding. Predominant direction to the north. Plotted on the lower hemisphere.

did not reveal any apparent variation in sandstone texture. Hence, to save time in the analyses, only a small number of representative samples was selected for complete textural and compositional study.

At the time of collection, all hand specimens were marked with their orientation in the field. These oriented samples enabled the writer to obtain oriented thin sections cut normal and parallel to the bedding planes. Thin sections cut normal to the bedding were used specifically for microscope and integrating stage analysis of the mineralogical composition (Krumbein and Pettijohn, 1938). The thin sections cut parallel to the bedding were used only for "dimensional fabric" study and a full discussion of this method of analysis is given later in this paper.

The samples selected for size analysis were disaggregated by crushing and then dispersed in a solution of N/100 sodium oxalate. After dispersion, the size fractions greater than 1/16 mm were sieved and the finer material was run through pipette analysis. A small fraction of the clay-sized material was set aside and later run through X-ray analysis by the writer for identification of the minerals constituents.

Heavy minerals were identified from the $\frac{1}{8}$-to-1/16 mm-size fractions and counted until the total mineral count included at least 250 non-opaque grains per sample. Apatite was excluded from this analysis because it is believed that the rigorous method of clarification by boiling in dilute HCl tended to destroy this mineral much more rapidly than any others. Barite, although present, is not considered valid for correlation purposes (because it may be authigenic)

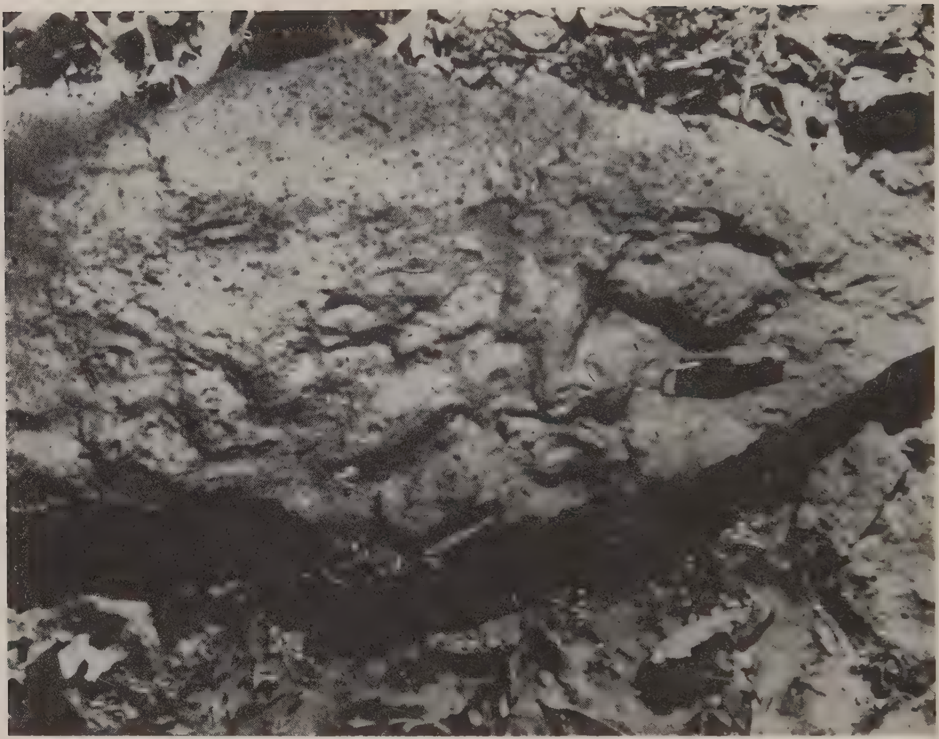

FIG. 4.—Flow rolls occurring at the base of the Pleasantview sandstone on the steep slopes of the channel wall.

and was also excluded. In the final results, all mineral species were expressed as percent of the total heavy-mineral count.

COMPOSITION AND TEXTURE

The results of the analyses of composition and texture, shown in table 2 and figure 8, clearly indicate that the Pleasantview sandstone is a subgraywacke. The dominant detrital components are quartz, rock fragments, and the fine-grained matrix of silt and clay. Feldspar and mica are present in minor amounts only. Texturally the Pleasantview sandstone is uniform and well sorted, with about 70 percent of the material in the very-fine sand size. The uniformity of the size frequency distributions of the several samples analyzed is demonstrated by the range between cumulative curves of figure 8.

In thin sections the detrital quartz grains commonly exhibit euhedral overgrowths of secondary or authigenic quartz. Where the original grain boundaries could be distinguished from these overgrowths by dusty inclusions, the detrital quartz roundness could be estimated by the visual roundness chart of Krumbein (1941). Average roundness was 0.3 with a range from 0.1 to 0.5. Feldspar showed a slightly higher roundness with an average of 0.5.

Very minor constituents of the sandstone are glauconite and the heavy minerals. Glauconite, in amounts less than one percent, was noted in nearly all thin sections. However, because the mineral is only found in these very small quantities, no particular significance is attached to its presence, although it might indicate marine conditions if it is not reworked material.

The heavy minerals of the Pleasantview consist mostly of opaques and the very stable non-opaques. The opaques are represented by leucoxene 31%, black opaques (ilmenite-magnetite) 3% and pyrite 5%. The non-opaque minerals include 41% zircon, 7% rutile, 6% garnet, 4% tourmaline, 2% chlorite, and less than 1% sphene.

The sandstone matrix material consists of clay and silt sized mineral grains, carbonate, and secondary silica cement. The clay sized minerals were identified by X-ray and consist of illite, kaolinite, quartz, chlorite, and sericite in order of decreasing abundance. The carbonates of the matrix consist of siderite and calcite. Siderite is apparently the dominant carbonate in the lower and middle members of the sandstone and calcite is the dominant carbonate in the upper members. It is of interest to note that when calcite makes up a high percentage of the constituents, as in sample A-16 of Table 2, the sandstone has the appearance of a "washed" graywacke; i.e., a graywacke which appears to have the fine-grained matrix winnowed out. However, the extensive replacement of detrital constituents by the calcite cement might indicate that the "washing" was accomplished, wholly or in part, by the replacement of the finer materials.

The order of cementation in the Pleasantview is evidenced by the calcite-filled pore spaces where calcite has partially replaced some of the detritals and is itself replaced by euhedral rhombes of siderite. Both calcite and siderite are subsequently replaced by euhedral overgrowths of secondary quartz on the detrital quartz grains. Hence, it is apparent that the initial binding agent was silt and clay and was followed, in turn, by calcite, siderite, and silica cements.

DIMENSIONAL FABRIC

The use of dimensional fabric analysis in sedimentary petrology is relatively new and until recently has been primarily concerned with pebble orientation. Dapples and Rominger (1945), however, made an experimental study of the orientation of inequidimensional sand-size particles and have

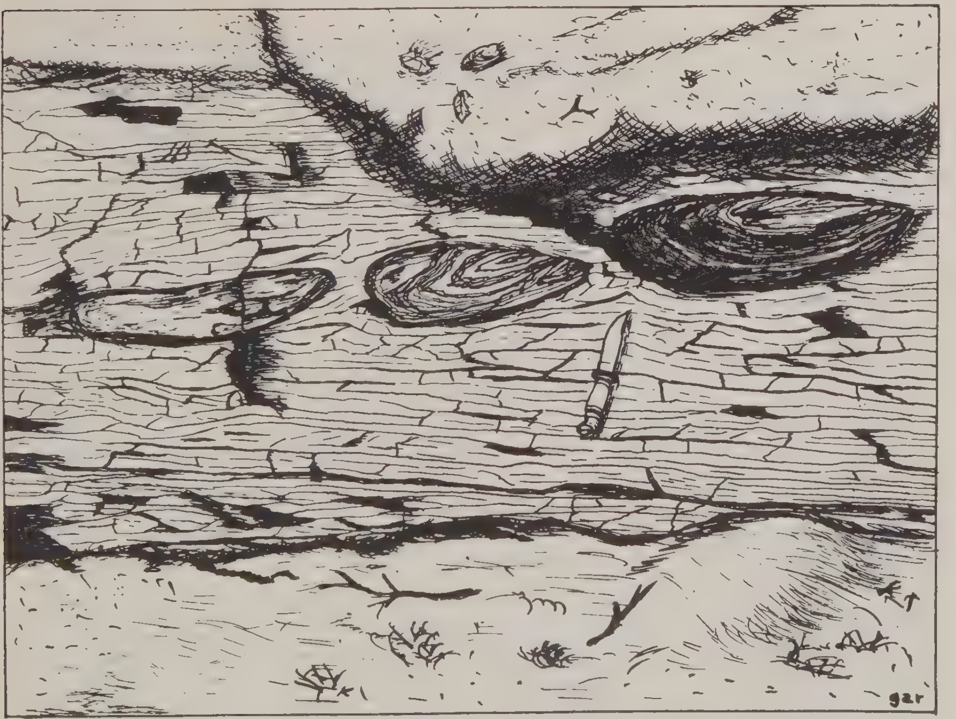

FIG. 5.—Highly contorted sandstone lenses emplaced in reworked Purington shale. The base of the Pleasantview sandstone is visible in the upper left hand corner. Drawn to scale from a photograph. The outcrop is sloping towards the reader.

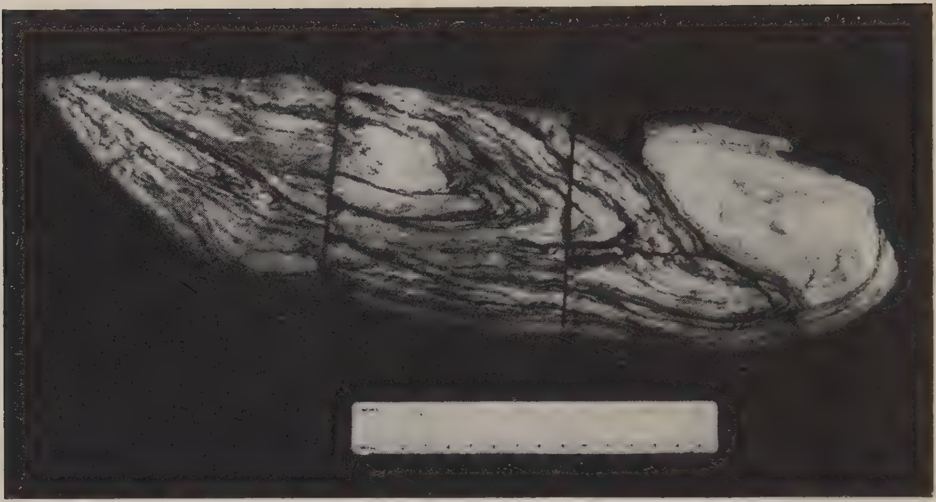

FIG. 6.—Cross-section of a sandstone lense cut to show the internal structure. The angle of the sandstone lense approximates the angle of emplacement in the field. The blunt end points to the south. A six inch rule is used for scale.

shown that the long axes tend to align themselves parallel to the direction of flow of the transporting medium. These authors made several statistical studies of water, wind, and gravitational-influenced orientation and demonstrated that preferred orientation is best developed in water transport. Moreover, Dapples and Rominger found that those sand grains having a "tear-drop" shape tended to orient themselves with the blunt end upstream and into the current. Hence, the results of their experimental study indicated that the mean value of the long-axis orientation distribution gave a preferred azimuth orientation parallel to the current and the pointed ends of the "tear-drop" shapes gave the direction of flow along this resultant azimuth.

More recently, Schwarzacher (1951) also investigated the existence of sand-grain orientation under experimental conditions and concluded that the long axes aligned themselves parallel to the current just as Dapples and Rominger had previously described. The significant finding of Schwarzacher's experiments, however, was that the sand grains displayed imbrication in the same way that pebbles do in a stream bed. As a supplement to the experimental study, an example of both long-axis preferred orientation and imbrication was demonstrated by Schwarzacher in his analysis of a sandstone sample.

These earlier studies of sand-grain orientation thus demonstrated the possible applicability of sand-grain fabrics for determining transport directions in sandstones. With this purpose in mind, the present writer applied the above methods of analysis to determine the transport direction in the Pleasantview sandstone.

Methods of grain orientation analysis.—Thin sections cut parallel to the bedding planes were used for the analysis of dimensional orientation. These thin sections were placed in a microprojector and the sand-grain images were projected onto a sheet of cross-section paper.[2] The long axes of the least projection rectangles and the pointed ends of the tear-drop shapes were then determined from the grain images.[3] Tear-drop shaped grains were drawn as arrows indicating the direction of the pointed ends and

[2] Polaroids inserted into the microprojector helped to distinguish grain boundaries and greatly expedited the analysis.

[3] A full treatment of this method of drawing long axes and pointed ends has been previously described by Dapples and Rominger (1945). The long axis of the least projection rectangle has been defined by them as the axis which lies parallel to the two parallel lines which can be drawn tangent to a grain with a minimum of separation.

acicular or lath-shaped grains, which did not have a tear-drop shape, were drawn simply as direction lines. By plotting all the quartz grains projected (with the obvious exception of equidimensional grains), bias in the analysis was kept at a minimum; i.e., no particular grain shapes were given undue weight. After 300 or more grains were plotted in this manner, the directions of the long axes were measured and counted on a tally sheet arranged in 20° group intervals from 0° to 360°. A statistical test based on Chi-square and vector summation was then applied to each distribution to obtain the direction of preferred orientation (Tukey, 1954; see also the appendix at the end of this paper).

The statistical test of orientation was performed on a 180° distribution by placing all diametrically opposed long axes in the same group interval from 0° to 180°. The test was then carried out and a preferred-direction line of orientation determined, if one existed. In some cases the sample distribution proved to be insufficiently different from a uniform distribution (i.e., a distribution with an equal number of observations in each group interval) and had to be discarded. During the test, the acceptance level of orientation was arbitrarily chosen at the 90th percentile of significance (i.e., there is a chance of being wrong 10 percent of the time).

After a preferred-direction line of orientation (or azimuth) was determined for a sample, the number of grains pointing in the two opposite directions of this line was counted for the entire sample. If 60 percent or more of the grains pointed in one direction of the preferred line, this direction was chosen as the direction of transport (Dapples and Rominger, 1945). In one case, it was found that the number of grains pointing in either direction was about equal and therefore transport direction was not defined by this criterion. To overcome this difficulty the

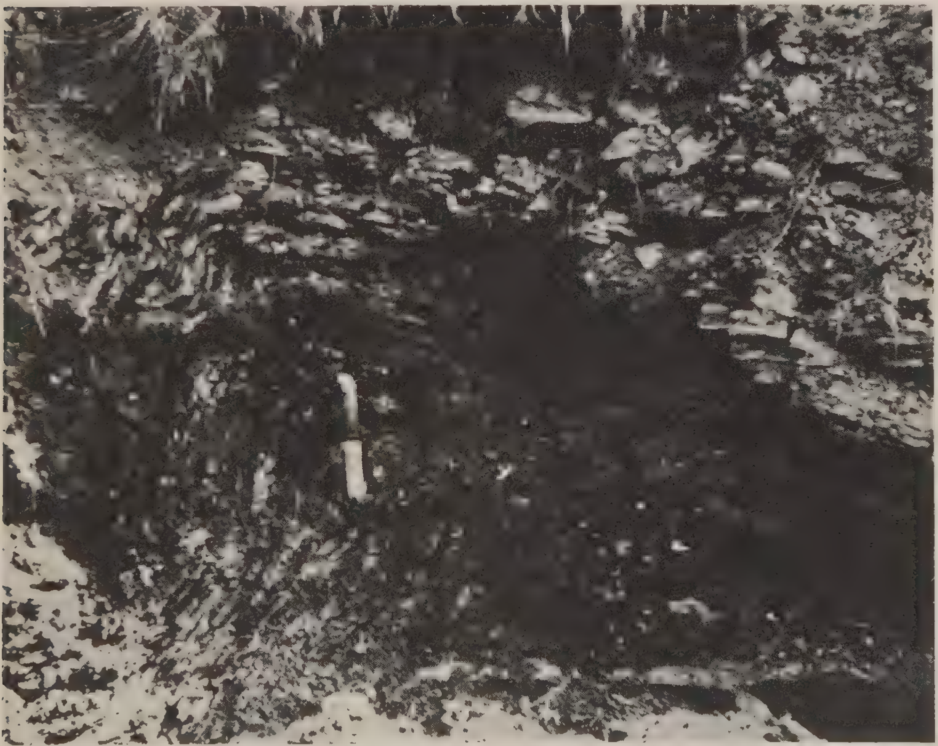

FIG. 7.—Small scale slump anticline in the shaly member of the Pleasantview. Knife is used for scale.

Table 2.—*Mineralogical composition of the Pleasantview sandstone*

	Components	Specimen Number[1]									
		A17	A16	A18	A14	A15	A25	A12	A22	A51	A10
Detrital	Quartz										
	strain-free	25.3	21.0	33.4	18.3	25.5	33.2	24.3	28.1	28.5	20.0
	strained	15.7	9.0	16.7	11.7	21.0	13.8	19.2	17.2	10.5	18.0
	Rock Fragments										
	quartzite	7.0	4.7	5.3	4.3	9.5	8.2	4.8	7.6	4.0	6.0
	chert	3.0	2.8	4.3	3.5	4.5	4.3	2.3	1.0	3.2	3.0
	argillite	0.7	1.3	3.6	3.2	5.3	6.0	1.9	7.1	3.3	1.0
	phyllite	0.6	0.3	3.0	1.3	6.2	6.0	2.6	2.9	1.0	1.9
	Feldspar										
	Na-feldspar	1.0	1.6	2.3	1.5	2.0	2.3	1.3	4.7	2.2	2.1
	K-feldspar	1.2	1.0	2.3	1.5	1.5	1.7	1.0	1.9	2.0	1.9
	Mica	1.8	1.9	4.7	4.7	2.0	5.0	5.2	6.2	3.5	5.3
Secondary or Interstitial	Carbonates										
	siderite	4.0	6.2	3.7	22.0	3.5	2.3	3.6	8.0	11.3	7.0
	calcite	13.0	42.2	0.0	0.0	0.0	1.0	4.5	0.0	1.0	2.1
	Quartz	5.3	0.7	3.0	2.2	2.1	2.4	3.6	1.0	2.7	1.0
	Clay-Silt	21.4	7.3	17.7	25.8	16.9	13.8	25.7	14.3	26.8	30.9

[1] *Sample Location:* A17, middle non-channel; A16, upper non-channel; A18, basal channel; A14, A15, A25, lower channel; A12, A22, A51, middle channel; A10, upper channel.

writer cut a thin section perpendicular to the bedding plane and parallel to the preferred direction line. A plot of grains from this section was then made to determine whether imbrication, such as that found by Schwarzacher, existed. The results of this plot demonstrated that the sand grains were imbricated. The direction of imbrication was then chosen as the direction of transport for the sample. It thus appears that imbrication direction may be a more reliable method of determining transport direction along an azimuth than are pointed ends.[4]

Results of transport direction analyses.—Eleven samples, taken from channel and non-channel areas, were analyzed for dimensional orientation direction. Of these, 9 proved to be statistically significant with a definite preferred orientation. The resultant directions of the significantly oriented samples have been indicated by the arrows in figure 2. The preferred directions, from one sample to another, appear to be as variable as the cross-bedding directions.

The vector mean direction (Krumbein, 1939) of the 6 samples analyzed from within the channel is 320°; and, for the 2 samples from the non-channel area is 310°. The one sample analysis from Schuyler County has a preferred orientation of 318°. Thus, it would appear that the transport direction of the sediment was to the northwest.

Cross-bedding, on the other hand, shows a vector mean direction (from 8 measures) of 0° for the channel in Fulton County and a direction of 24° (from 13 measures) for Schuyler County. These results would indicate a transport direction to the north; a difference in direction of about 60° from that obtained by grain orientation study. Although it is hazardous to speculate on such a small number of direction measures, one might consider the possibility that two factors influenced the transportation of the sediment. That is, the grain fabric of the uncross-bedded members might represent weak currents such as coastal currents and cross-bedding might represent stronger currents such as tidal currents.

Speculations might also be made for

---

[4] Experimental work carried out by the writer after this study was completed substantiated the criteria of imbricate and long-axis direction as the direction of transport. The data on the reliability of these measures will soon be ready for publication.

fluvial transport conditions, but it would be difficult to explain the observations since the direction of transport exhibited by both fabric and cross-bedding is diametrically opposed to the apparent erosion gradient of the channel (as previously discussed). For example, grouping of both fabric and cross-bedding directions (a total of 30 direction elements) results in a vector mean direction of 357° with a standard deviation of ±67°. That is, the sediment transport direction indicates the sediment was deposited towards the north whereas the channel gradient indicates that the channel was cut to the south. It seems, therefore, that the process of channel filling was to a large degree independent of the process or processes which cut the channel.

COMPARISON WITH THE DUTCH WADDEN SEA

The Dutch Wadden Sea is an area of broad tidal flats incised by channels of tidal current origin (van Veen, 1950, van Straaten, 1949). The tidal channels are bordered by areas of relatively continuous sedimentation of tidal sands, plant material, and marine organisms (van Straaten, 1952) and the channels themselves are presently being filled with sands swept in from the tidal flats and the North Sea. The result of this sedimentation is described by van Straaten (1951) as vertical sedimentation (resulting in horizontal beds on the tidal flats) and lateral sedimentation (resulting in inclined beds flanking the channel walls). Although the deposits in the channels are mainly sand, thick deposits of mud are also present (van Straaten, 1952). Some of the characteristic features of the channel deposits are the occurrences of slump structures, cross-bedding, and local basal conglomerates (derived from the eroded walls, mainly shells, van Straaten, 1950b, 1951). The cross-bedding (van Straaten, 1950a) may be directed up channel in areas subjected mainly to flood tides and may be directed down channel in those areas dominated by ebb tides (both kinds can also be present in one channel).

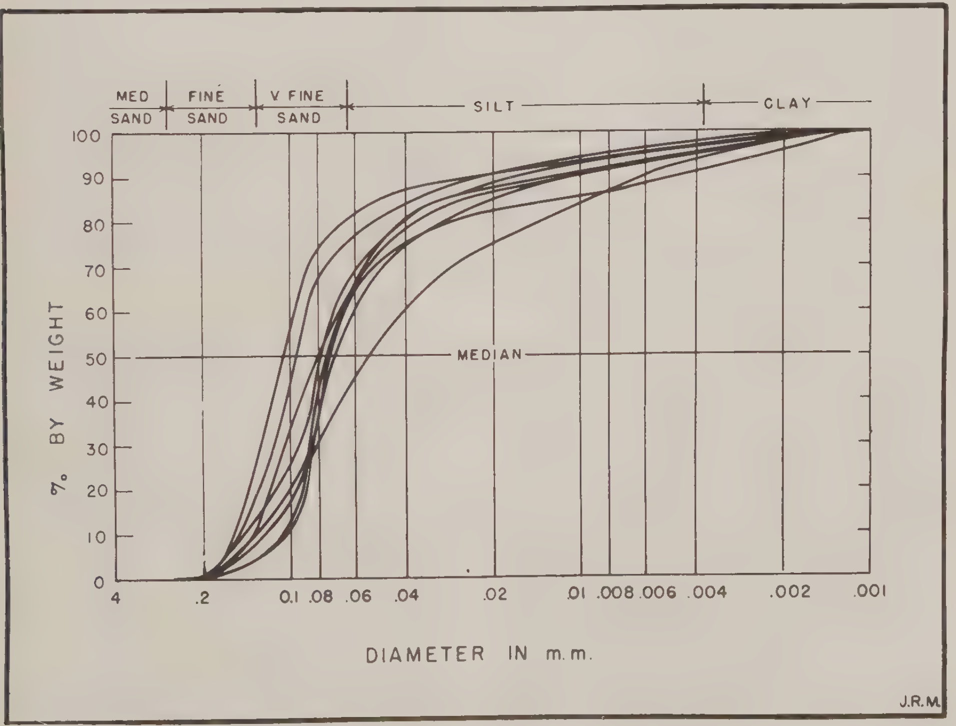

FIG. 8.—Cumulative size frequency distributions of 8 selected Pleasantview sandstone samples.

With the exception of marine organisms all of the examples above, or modifications thereof, are present in the sediments of the Pleasantview. Hence, the environment of the present Wadden Sea is believed to be very near the possible, if not probable, kind of environment which existed during Pleasantview sedimentation.

SUMMARY AND CONCLUSIONS

The study of the Pleasantview sandstone, and the channel which it fills in Fulton County, Illinois, was undertaken in order to describe (1) some of the properties of the sandstone, (2) its depositional transport direction, and (3) the environmental conditions under which it was deposited. It is felt by the writer that the first two objectives of this study have been fulfilled, but the answer to the third is still somewhat tenuous.

The results of the analyses of texture and composition place the Pleasantview sandstone in the subgraywacke classification of Pettijohn (1949). The quartz, rock fragments, and heavy-mineral varieties indicate that the source area of this sediment was made up of a series of rock types ranging from igneous to high and low metamorphics and to pre-existing sediments. Quartz varieties show that igneous and metamorphic rocks (the ultimate source) contributed almost equally to the sediment. However, the fact that only chert, the very stable heavy minerals, and a small amount of feldspar is present indicates that the detritus is of high maturity (Pettijohn, 1949); i.e., the detritus has gone through several cycles of sedimentation. It seems reasonable, therefore, to conclude that the Pleasantview sandstone was largely derived from pre-existing sediments. This conclusion is in agreement with the recent studies made by Siever and Potter (1956) of Pennsylvanian sediments in the Eastern Interior Basin.

The field relations suggest that the Pleasantview can be conveniently described as two-phased; the non-channel phase, and the channel phase. The non-channel phase is thin-bedded, ripple marked, and in apparent conformity with the underlying shales, while the channel phase is massive to thin-bedded, cross-bedded, shaly, and is unconformable with the underlying beds in the channel. Along the channel borders, the sandstone dips into the channel, but in the central portion of the channel the sandstone is essentially horizontal. These relationships, along with the evidences of slump structures and scour markings, are considered by the writer as indications that the Pleasantview sandstone was deposited when both the channel and non-channel areas were submerged. The non-channel areas represent conditions of relatively continuous sedimentation and the channels represent areas of contemporaneous erosion and later filling.

Directional properties which could be measured in the Pleasantview include the following: (1) channel gradient, (2) scour marks, (3) slump and slide structures, (4) ripple marks, (5) cross-bedding, and (6) preferred orientation of sand grains. The results of these measures can best be summarized by a short table as in table 3.

The first three directional properties of table 3 are related to the erosional gradient and reflect the local gradient direction. The last three directional properties reflect the sediment transport direction. From the table, it seems that the directed process which cut the channel was independent of the processes which later filled the channel with sediment because the resultant directions are diametrically opposed. In the writer's opinion the observations can best be explained by considering the channel first to have been cut by tidal current action and later to have been filled with sediments through the action of both coastal (longshore) and tidal currents. Examples from the Dutch Wadden Sea demonstrate that this suggestion is not unreasonable.

ACKNOWLEDGEMENTS

The writer wishes to express his appreciation to Dr. F. J. Pettijohn for his many thoughtful and stimulating comments and advice. Thanks are extended to Dr. H. R. Wanless for his generous and invaluable aid in pointing out many critical sample sites and for his critical discussions of the problem with the writer. Acknowledgements are also due Drs. J. M. Weller, H. A. Lowenstam, Leland Horberg, P. E. Potter, R. Siever, R. L. Miller, F. P. Shepard, and Mr. P. W. Vitanage and Mr. J. R. Curray for the helpful comments, criticisms, and suggestions. Mr. J. R. Moriarty's help in preparing several of the illustrations is also appreciated. Thanks are also extended to

TABLE 3.—*Results of directional-properties measures*

Measure	Resultant Direction	Kind and Number of Measurements
Channel Gradient	South	Increasing depth of channel and thickness of channel fill
Scour marks	Down the channel wall and south	2 outcrops (qualitative orientation of casts)
Slump and slide structures	South (?)	3 structures (direction of asymmetry)
Ripple marks	Northwest-Southeast and Northwest	1 outcrop and 1 reported measure from Ekblaw (1930) (strike and asymmetry)
Cross-bedding	North	21 (foreset dip directions)
Sand grain orientation	Northwest	9 (preferred long-axis directions)

Dr. John W. Tukey for permission to publish a summary of the statistical test of significance of orientation which he designed. The writer takes sole responsibility for any mistakes or omissions in the paper and in the opinions set forth. The major part of this paper represents work carried out by the writer in the spring of 1952 while at the University of Chicago.

APPENDIX

The Tukey (1954) Chi-square test of significance for orientation data from a 180° distribution is based on the departures of the observed data from a distribution which is completely uniform; i.e., from a distribution having an equal number of observations in each class interval.[5] If the distribution were completely uniform, the expected number of observations in each class interval would be the total number of observations divided by the number of class intervals. This expected number in each class interval has been called the "contemplated" by Tukey. The measure of deviations from an expected uniform distribution is given by the following:

$$x=\frac{\text{observed}-\text{contemplated}}{\sqrt{\text{contemplated}}}$$

where x is the frequency deviation measure in each class interval. Vector summation over all class intervals results in the following:

$$C=\frac{\sum x\cos 2\theta}{\sqrt{\sum\cos^2 2\theta}}\quad\text{and}\quad S=\frac{\sum x\sin 2\theta}{\sqrt{\sum\sin^2 2\theta}}$$

where θ is the mid-point of each class interval and the resultant squared is given by $C^2+S^2=\chi^2$. This value of Chi-square, χ^2, is then compared with the tables given in standard statistics books for two degrees of freedom. If there is significant departure from uniformity at a chosen level of significance, the preferred direction of orientation is derived from the relation

$$\tan 2\theta=\frac{S}{C}\,.$$

Where θ plus the mid-point value of the first class interval is then the preferred orientation direction.

Example—Using the data from one of the orientation analyses (grouped in 20° intervals from 0° to 180°); where N, the total number of observations is 590 or contemplated is $590/9=65.6$; and, in tabular form we have the following:

Class Interval in Degrees	θ	Observed	Observed-Contemplated	x	$\cos 2\theta$	$\sin 2\theta$
0–20	0	60	−5.6	−0.69	1.00	.00
20–40	20	60	−5.6	−0.69	.75	.64
40–60	40	90	24.4	3.01	.17	.98
60–80	60	74	8.4	1.04	−.50	.87
80–100	80	71	5.4	0.67	−.94	.34
100–120	100	60	−5.6	−0.69	−.94	−.34
120–140	120	64	−1.6	−0.20	−.50	−.87
140–160	140	60	−5.6	−0.69	.17	−.98
160–180	160	51	−14.6	−1.80	.76	−.64

---

[5] As has been pointed out to the writer by Dr. H. J. Pincus (personal communication), "uniform" and "random" are not synonymous.

From this table we can obtain the values of C and S by following the previously outlined procedure.

$$C=-1.22 \qquad S=2.78$$

Squaring these values and adding we have the resultant squared which is, in our case equal to the Chi-square value of 9.21. Referring to the Chi-square tables in Dixon and Massey (1951, p. 308) for 2 degrees of freedom at the 90th percentile of significance we find that our value is well above the tabled value 4.61. Therefore, we conclude that there is sufficient evidence our population did not arise from a uniform distribution; i.e., the distribution is not isotropic.

To determine the preferred direction of orientation we have simply to determine

$$\tan 2\theta=\frac{S}{C}=-2.28$$

and distinguish between the two roots by the requirement that the signs of S and C be those of $\sin 2\theta$ and $\cos 2\theta$ respectively, from which we obtain the preferred angle

$$\theta=\frac{180^\circ-67^\circ}{2}=57^\circ.$$

However, since θ is the mid-point of our class interval, we have 10° for the mid-point of our first observed interval. Hence, we have to add this to our preferred angle with the result that the preferred direction of orientation for our distribution is 67°. Because we did not make a distinction between diametrically opposed directions, the preferred direction could also be 247°. As it turns out, the sand grains are imbricated to the northeast in this sample and therefore we choose 247° as the vector direction; i.e., the direction of sand transport.

REFERENCES

Dapples, E. C., and Rominger, J. F., 1945, Orientation analysis of fine-grained clastic sediments: Jour. Geology, v. 53, p. 246–261.

Dixon, W. J., and Massey, F. J., 1951, Introduction to statistical analysis. McGraw-Hill Book Co., New York, 370 p.

Ekblaw, S. E., 1930, The stratigraphic relations of the Pleasantview Sandstone in western Illinois: Unpublished Master's Thesis, University of Illinois.

———, 1931, Channel deposits of the Pleasantview Sandstone in western Illinois: Illinois Acad. Sci. Trans. 23, p. 391–399.

Krumbein, W. C., 1939, Preferred orientation of pebbles in sedimentary deposits: Jour. Geology, v. 47, p. 673–706.

———, 1941, Measurement and geological significance of shape and roundness of sedimentary particles: Jour. Sedimentary Petrology, v. 11, p. 64–72.

Krumbein, W. C., and Pettijohn, F. J., 1938, Manual of sedimentary petrography, Appleton-Century, New York, 549 p.

Pettijohn, F. J., 1949, Sedimentary rocks. Harper and Brothers, New York, 526 p.

Rich, J. L., 1950, Flow marking, grooving, and intra-stratal crumpling as criteria for recognition of slope deposits, with illustrations from Silurian rocks of Wales: Am. Assoc. Petoleum Geologists Bull., v. 34, p. 717–641.

Schwarzacher, W., 1951, Grain orientation in sands and sandstones: Jour. Sedimentary Petrology, v. 21, p. 162–172.

Shrock, R. R., 1948, Sequence in layered rocks. McGraw-Hill Book Co., New York, 507 p.

Siever, R., and Potter, E., 1956, Sources of basal Pennsylvanian sediments in the Eastern Interior Basin: part 2, sedimentary petrology: Jour. Geology, v. 64, p. 317–335.

Stout, E., 1931, Pennsylvanian cycles in Ohio: Illinois Geol. Survey Bull., v. 60, p. 195–216.

Straaten, L. M. J. U, van, 1949, Quelques particularités du relief sous-marin de la Mer des Wadden (Hollande): Comptes Rendus du Congrès de Sedimentation et Quaternaire in France, p. 139–145.

———, 1950a, Giant ripples in tidal channels: Tidjschr. Kon. Nederl. Aardr. Gen., v. 67, p. 76–81.

———, 1950b, Environment of formation and facies of the Wadden Sea sediments. Tijdschr. Kon. Nederl. Aardr. Gen., v. 67, p. 94–108.

———, 1951, Texture and genesis of Dutch Wadden Sea sediments: Proc. 3rd Int. Congress Sedimentology Netherlands, 5–12, July, 1951, p. 225–244.

———, 1952, Biogene textures and the formation of shell beds in the Dutch Wadden Sea: Konikl Nederl. Akademie van Wetenschappen, Amsterdam, Series B, v. 55, p. 500–516.

Tukey, J. W., 1954, Chi-square test of orientation, comment no. 1A, Earth Sciences Panel Review Group, CSPS—ASA, unpublished communication.

Veen, J. van, 1950, Eb-en vloedshaar-systemen in de Nederlandse getijwateren (with an English summary): Tijdschr. Kon. Nederl. Aardr. Gen., v. 67, p. 43–65.

WANLESS, H. R., 1931, Pennsylvanian cycles in western Illinois: Illinois Geol. Survey Bull., v. 60, p. 179–193.

———, 1950, Late Paleozoic cycles of sedimentation in the United States: International Geological Congress "Report of the Eighteenth Session, Great Britain 1948," part IV, p. 17–28.

———, 1952, Studies of field relations of coal beds: Nova Scotia Research Foundation, Second Conference on the Origin and Constitution of Coal, p. 148–175.

———, 1955, Pennsylvanian rocks of Eastern Interior Basin. Am. Assoc. Petroleum Geologists Bull.. v. 39, p. 1753–1820.

WELLER, J. M., 1956, Diastrophic control of late Paleozoic cyclothems: Am. Assoc. Petroleum Geologists Bull., v. 40, p. 17–50.

Reprinted from Deep-Sea Research, 1957, Vol. 4, pp. 211 to 217.
Reproduced by Permission

Composition of the swim-bladder gas in bathypelagic fishes

JOHN KANWISHER and ALFRED EBELING

(*Received* 7 *February* 1957)

Abstract—Measurements were made of swim-bladder size and gas composition on pelagic fish in the eastern Pacific. The physiological problem of vertical migration with a swim-bladder is discussed. It is concluded that some gas-containing fish migrate vertically but that net-collecting data is too fragmentary to determine if such fish are primarily responsible for scattering layers.

THE gas in the swim-bladder of a fish is at the hydrostatic pressure of its depth. This may be 100 atmospheres or more. In contrast, the dissolved gases in the water itself have been introduced at the surface, and total only one atmosphere of tension. Since the increased pressure of the gases in the swim-bladder indicate active secretion, their composition is of great interest. SCHOLANDER and co-workers (1951, 1953) found that in a series of marine coastal bottom fishes, the oxygen percentage increased with depth. Although the percentage of nitrogen decreased, its partial pressure was larger at greater depths, reaching as much as 15 atmospheres. Similar data are presented here for bathypelagic fishes. The problem of vertical migration with a swim-bladder is also considered since these fishes are thought to be a component of the scattering layer.

Material was collected at various depths with the 10 ft ISAACS-KIDD mid-water trawl towed at 2-3 knots (ISAACS and KIDD, 1953) over much of the eastern tropical Pacific, during the Eastropic Expedition of the University of California Scripps Institution of Oceanography. Surface fishes and vertically migrating species were taken under a light at night with a dip net.

Collections with nets are incomplete, possibly because many of the faster-swimming animals escape. The squid and lantern fishes seen in large numbers on the surface at night were almost never captured during the daytime tows below the surface. There may be many faster fishes at all depths that are not represented in such collections. BEEBE's direct bathysphere observations (1935) led him to conclude that there was a much more abundant fish fauna than he had surmised from years of trawling with the best oceanographic collecting equipment available. This imposes a severe limitation on statements concerning the kinds of animals in the various scattering layers.

The ISAACS-KIDD trawl is also limited in that it cannot be opened and closed at depth. There is always the possibility that specimens have entered the net while it was being lowered or raised. Whenever possible control tows were made, in which the net was brought back up immediately without towing it at depth. By comparing the two tows one is more certain which fishes were caught at which depth. Some species appeared regularly only in the deeper net tows. The hatchet fishes, *Argyropelecus lychnus* and *Sternoptyx obscura*, were commonly caught in nocturnal tows at depths greater than 200 metres, but were rare in collections from lesser depths. Other fishes (adult ceratioids, alepocephalids, certain stomiatoids, melamphaids, etc.) were characteristic of the fishes collected in the still deeper tows.

As soon as the trawl was brought on board, the cod end was removed and the contents emptied into trays. The fishes were immediately separated and placed in a bucket of sea water. Those with swim-bladders which had come from any depth were distended with gas and floated to the surface. Several of the non-floating ones (ceratioids, alepocephalids, bathylagids, some myctophids, etc.) were checked for gas both by needle puncture and in a pressure chamber, with negative results.

The techniques were the same as those of Scholander and van Dam (1953). The fish that floated were held underwater and the gas withdrawn through a hypodermic needle into a syringe lubricated with an acid citrate solution. With the needle capped, such a sample could be stored for several hours without appreciable change in composition. Thus, samples could be taken immediately from all of the desired material and analysed when convenient.

The analyses were performed in a syringe analyser (Scholander *et al.*, 1955) for carbon dioxide, oxygen, and nitrogen to an accuracy of 0·5 per cent of the total volume. Carbon dioxide was always less than 2 per cent, and was not considered significant since it increases on standing and is probably at a very low level in the live fishes. Samples of about 30 mm^3 were transferred from the storage syringe to the analyser. Duplicate analyses were done on all but the smallest fishes which did not contain enough gas.

The volume of gas in some of the fishes was determined before sampling in the apparatus shown in Fig. 1. The fish is placed in the chamber, taking care that no bubbles adhere to it. With the chamber brimming with water, the cap is inserted and clamped down. Thus the only gas in the chamber should be that in the swim-bladder of the fish. Pressure is now applied with the syringe until the manometer indicates that the pressure has doubled. Harden Jones (1951) has shown that fish probably do not resist such a volume change with their musculature. Applying Boyle's law, the excursion of the syringe to produce this pressure change will be $\frac{1}{2}$ the volume of the swim-bladder. A small blank is subtracted for the gas in the manometer. It is essential that such a system be as rigid as possible and that bubbles be scrupulously avoided. Fortunately it is easy to check the system by filling the chamber with water only. The blank value is obtained in this way. Such a check was usually repeated after each measurement.

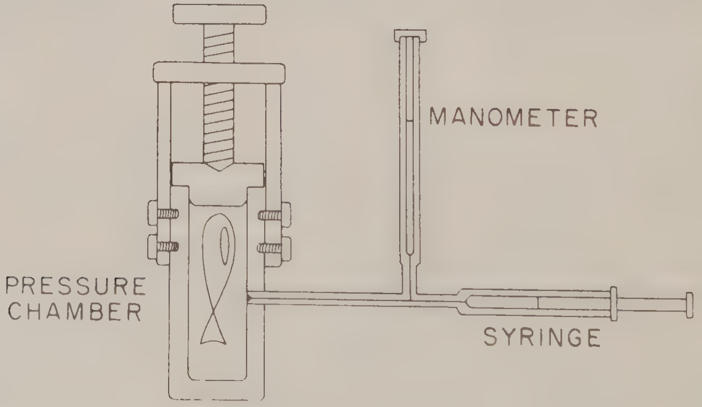

Fig. 1.

RESULTS

Swim-bladders of surface pelagic species contained 27 to 33 per cent oxygen, only slightly above that of air. This is the same as inshore marine fish taken at the surface. The fishes dip-netted at night, which are believed to have migrated up from depth, had 74 to 91 per cent oxygen. These agree well with the species taken at depth by trawling which also had 53 to 93 per cent oxygen in their swim-bladders.

Below is a list of species divided into these arbitrary categories. A range of oxygen values indicates that more than one individual of the species was measured. The amount of gas is indicated by the per cent of the total volume of the inflated fish made up by the swim-bladder gases at 1 atmosphere at the surface. The compressed gas at depth would be in a much smaller volume.

Table 1.

	Per cent O_2	*Per cent volume of gas*
I. *Surface pelagic species*		
Exocoetidae		
Exocoetus monocirrhus	33	3·5
Cypselurus xenopterus	23–25	
Hirundichthys sp.	33	3·1
Hemiramphidae		
Hemiramphus sp.	29	
II. *Bathypelagic fishes taken at the surface*		
Myctophidae		
Myctophum evermanni	74–91	3·2–5·0
Myctophum spinosum	77–91	4·0–5·5
Myctophum affine	90	
III. *Bathypelagic fishes taken at depth* (*all below* 100 *metres*)		
Sternoptychidae		
Argyropelecus lychnus	72–92	32–65
Argyropelecus affinis	67–93	42–55
Sternoptyx obscura	71–88	
Vinciguerria lucetia	78–90	32–52
Ichthyococcus sp.	77–83	
Melamphaidae		
Melamphaes macrocephalus	73–87	37–65
Melamphaes nigrofulvus	67–77	56
Melamphaes opisthopterus ?	71	
Melamphaes nycterinus	54–93	48–54
Melamphaes cristiceps ?	61–81	
Myctophidea		
Lampanyctus omostigma	89	53
Lampadena bathyphila	85	

Several factors tend to produce errors in the compositions and amounts of gas in the deep fishes. When a fish enters the net it is forced back into the cod end where it probably does not live very long. Since some of the tows lasted several hours, a fish may have been dead nearly this long before being sampled. In such a fish, diffusion will have begun to bring the bladder gases into equilibrium with the rest of the fish and the outside sea water. This will lower the oxygen and raise the nitrogen percentage. Experiments at the surface showed that the oxygen percentage could decrease as much as 10 to 20 per cent in a few hours. Several members of the genus *Melamphaes* were particularly sensitive to this.

The swim-bladders in some of these relatively fragile mid-water fish may have ruptured into the body cavity. Diffusion would then work more quickly to vary the gas composition. Gas would also likely be lost in such a fish. Thus the oxygen content and the amount of gas shown above for the deep fishes can only be considered minimal values. There is little point in computing the size of the swim-bladder at depth from these figures. All that can be said is that the deep fishes had much more gas than those taken on the surface. This is to be expected since a greater absolute amount of gas is necessary to maintain a constant swim-bladder volume at depth due to the pressure.

Oxygen increases with the depth of the fish and at about 200 metres can constitute more than 90 per cent of the gas mixture in the bladder. All deep fish tended toward 80 to 90 per cent. The lower values are probably due to the errors mentioned above.

DISCUSSION

The scattering of sound by horizontally layered marine organisms has been observed over most of the oceans of the world. The identity of the animals that make up these scattering layers had been discussed in several articles (RAITT, 1948; MOORE, 1950). MARSHALL (1951) has shown that fish with functional swim-bladders are widely distributed and may be a principal cause. This is an attractive hypothesis since a gas-filled bladder is a much more efficient scatterer of sound that invertebrates or fishes without enclosed gases.

Since the tissue of fishes is denser than sea water, a gas-filled swim-bladder is necessary if a fish is to adjust itself to neutral buoyancy. An amount of gas equal to about 4 per cent of the body volume of the fish is needed. If these fish migrate vertically, the gas will expand or contract with the changes in hydrostatic pressure. To keep the swim-bladder at the same relative volume, gas must be either secreted or absorbed. PARR (1937) recognized that this places limitations on the amount and speed with which such fishes can change their depth. The secretion of a gas under pressure represents work that must be done by the fish. It is interesting to compute the rate and amount of work represented by some observed migrations in the scattering layer.

A fish must keep its swim-bladder a constant size if its buoyancy is not to change during migration. On this assumption, the work performed in migrating between pressures p_1 and p_2 will vary as :

$$W = 2{\cdot}3\, v\, p_2 \log \frac{p_2}{p_1}$$

where v is the volume of the swim-bladder.

Fig. 2 shows the accumulated work necessary to migrate from the surface to various depths if the swim-bladder is kept constant at 4 per cent of the volume of the fish. The figures are for a 10 g fish with a 0·4 ml swim-bladder. Another atmosphere of gas must be supplied for every 10 metres increase in depth. Since this has to be secreted at continually higher pressure, the rate of doing work increases with depth. This is shown by the increasing slope of the curve with depth. This is only true if the fish keeps in step with the pressure and maintains neutral buoyancy at all depths. MARSHALL (1951, 1954) has discussed the amount of work necessary to migrate vertically. He apparently believes the amount of gas is not increased by secretion in going down, so that the fish gets heavier at great depths.

One can compute the amount of work represented by gas secretion and relate this to what fishes are capable of metabolically. Since many assumptions are necessary the accuracy of such a calculation is open to question. From data of SCHOLANDER *et al.* (1953), a 10 g fish would use about 0·4 ml oxygen per hour. This is equal to 2 g calories under conditions of aerobic oxidation of food stuffs. Anatomically it seems likely that not more than one third of a fish's circulation would go to the swim-bladder. Let us assume that the secretion process is 25 per cent efficient, and that one third of a fish's metabolic work is available for the task. This would allow the fish to secrete an amount of gas equivalent to about 0·15 g calories of work per hour. A scale is included in Fig. 2 representing the number of hours necessary at this rate to attain neutral buoyancy at a given depth. Thus 33 hr would be needed to go to a depth of 400 metres. Such a figure is unrealistic since the scattering layer migration must be made daily. If fishes with swim-bladders make up part of such a layer, their specific gravity probably differs appreciably from sea water at either the top or bottom of their migration. This cannot be too severe a handicap since many species have no swim-bladder. They are successful in spite of having to swim all the time to keep from sinking.

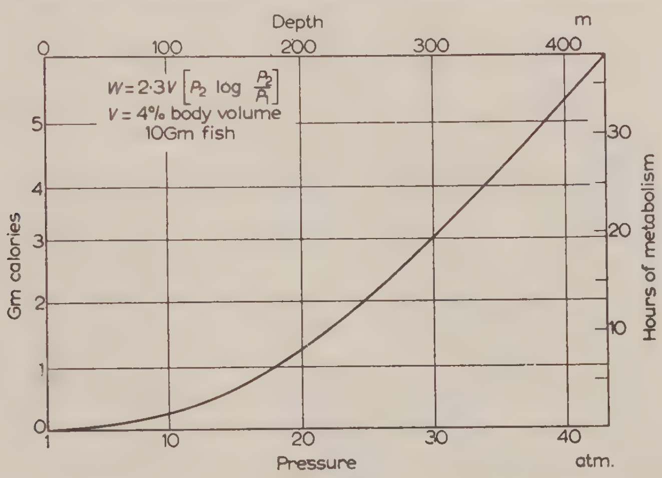

Fig. 2.

LANTERN FISHES

The various lantern fishes taken with a dip net at the surface at night all had swim-bladders with high percentages of oxygen. SCHOLANDER and co-workers (1951, 1953) only found such a gas composition in fishes taken at a considerable depth. Considering this, the high oxygen values in the present fishes strongly infer that the gas was secreted at depth before they migrated to the surface. The amount of gas was 3 to 5·5 percent of total body volume. This is just the quantity necessary to make the fish neutrally buoyant at the surface. None of these species were caught at depth during daytime tows. This is not surprising since they showed great speed on the surface when chased by squid. If they are part of the most persistent scattering layer, they spend the daytime between 300 and 400 metres. From the metabolic considerations in Fig. 2, it seems unlikely that they could also secrete enough gas to be weightless at depth. Yet one wonders how the fish would determine the proper amount of gas to secrete at depth to give it the correct-sized swim-bladder, 4 per cent of body volume, at the surface. Whether daily secretion occurs during vertical migration one cannot say without the necessary daytime data. However, the lantern fish do seem to be migrating vertically with a swim-bladder containing gas. Since they are so common they may well be an important sound scatterer.

OXYGEN MINIMUM

The eastern tropical Pacific form which these collections were made has a highly developed oxygen minimum. The dissolved oxygen in the sea water is generally below 0·25 ml per litre from the thermocline at about 100 metres down to 600 or 800 metres. Below this it gradually increases. WINKLER oxygen determinations of less than 0·1 ml per litre are common. In spite of these low values very rich collections were made in this water. In addition, scattering layers were always seen at these depths during both the day and night. One component of the layer appeared to migrate wholly within this region. MARSHALL (1954) has noted that a variety of animals seem to thrive in the oxygen-poor waters of the ocean. It is not clear whether they are the cause or effect of the oxygen minimum.

The hatchet fishes in particular were taken in large numbers in the oxygen minimum, as many as several hundred being caught in one haul. All of them were bloated with large amounts of gas, which was mostly oxygen. HARDEN JONES and MARSHALL (1953) state that the proportion of oxygen in the swim-bladder decreases when fish are kept in low-oxygen water. This is apparently not so for these species.

At depth the partial pressure of oxygen in the swim-bladders of these fishes may amount to 25 or 50 atmospheres, while the oxygen tension in the surrounding sea water is only 1/250 of an atmosphere. The fish maintains its swim-bladder oxygen against a diffusion gradient of 10,000 to 1. MARSHALL (1954) noted that the swim-bladders of deep living fishes have much more developed *retia mirabilia* and gas gland than those of shallow fishes. SCHOLANDER (1954) has shown that the *rete* can function as a counter current diffusion system capable of maintaining a large tension gradient across the bladder wall. Some such special system must be present for blood to flow in and out of the bladder without the gases being lost. It is not known whether the gas is initially secreted at these depths and at these low oxygen concentrations in the sea water.

PARTIAL MIGRATIONS

Since the hatchet fish seemed abundant enough to account for sound scattering, an attempt was made to see if they made a diurnal migration. A series of tows before and after the evening ascent indicated that they were associated with a layer which in the daytime was at 380 to 450 metres. At night it rose to 300 to 350 metres. Since this does not represent a large percentage change in pressure, the fish could probably let the swim-bladder change in volume without having to secrete or absorb during such a migration.

At the same time diffuse scattering at grater depths during the daytime moved up at night and concentrated at about 400 metres. *Melamphaes* with swim-bladders and other black fish characteristic of greater depths were caught here at night.

There are not enough daytime hauls to be certain such species are at greater depths. However, collection records of past Scripps Institute of Oceanography expeditions indicate that these species are caught at shallower depths at night than during the day.

Many mid-water fish with swim-bladders seem to perform partial vertical migrations that do not carry them all the way to the surface. These movements may be limited by the amount of distension the swim-bladder can withstand. For a given fractional change in pressure, a deep fish has much more vertical range than a shallow one. HARDEN JONES (1952) has shown that some fresh water fishes can stand a 20 per cent change in pressure without compensating. This may also be the case for these marine fishes.

CONCLUSIONS

(1) Measurements were made of the composition and amount of swim-bladder gases in some pelagic fishes of the eastern Pacific. In deep fishes the oxygen content approached 80 to 90 per cent of the gas. In strictly surface fish the gas contained slightly more oxygen than air. Some fishes taken at the surface at night had high oxygen. The gas was thought to have been secreted at depth since it was from species that are known to migrate vertically.

(2) Net tows indicated that some gas-containing fishes are associated with scattering layers which rise but do not come all the way to the surface at night.

(3) Energy considerations make it unlikely that neutral buoyancy can be maintained by gas secretion during very extensive diurnal vertical migrations.

Acknowledgements—We are indebted to Mr. MARK CLAFF for his expert craftsmanship in constructing the chamber used to determine gas volumes. The work would also have been impossible without the net tows made by the members of the crew of the R/V *Horizon*.

Contribution No. 888 *from the Woods Hole Oceanographic Institution and from Scripps Institution of Oceanography, new series, No.* 908

REFERENCES

BEEBE W. (1935) *Half mile down* John Lane, London.

HARDEN JONES F. R. (1951) The swim bladder and the vertical movements of teleostean fishes, I. Physical factors. *J. Exp. Biol.* **28**, 553-566.

HARDEN JONES F. R. (1952) The swim bladder and the vertical movements of teleostean fishes, II. The restriction to rapid and slow movements. *J. Exp. Biol.* **29**, 94-109.

HARDEN JONES F. R. and MARSHALL N. B. (1953) The structure and functions of the teleostean swim bladder. *Biol. Rev.* **28** (1), 16-83.

ISAAC J. D. and KIDD L. W. (1953) Isaacs-Kidd midwater trawl. *Scripps Institution of Oceanography*, Ref. 53-3 (unpublished manuscript).

MARSHALL N. B. (1951) Bathypelagic fishes as sound scatterers in the ocean. *J. Mar. Res.* **10** (1), 1-17.

MARSHALL N. B. (1954) *Aspects of deep sea biology* Philosophical library, New York.

MOORE H. B. (1950) The relation between the scattering layer and the Euphausiacea. *Biol. Bull.* **99** (2), 181-212.

PARR A. E. (1937) Concluding report on fishes. *Bull. Bingham Oceanog. Coll.* 3 (7), 1-79.

RAITT R. W. (1948) Sound scatterers in the sea. *J. Mar. Res.* 7, 393-000.

SCHOLANDER P. F. CLAFF C. L. TENG C. T. and WALTERS V. (1951) Nitrogen tension in the swim bladder of marine fishes in relation to depth. *Biol. Bull.* **101** (2), 178-193.

SCHOLANDER P. F. and VAN DAM L. (1953) Composition of the swim bladder gas in deep sea fishes. *Biol. Bull.* **104** (1), 75-86.

SCHOLANDER P. F. (1954) Secretion of gas against high pressures in the swim bladder of deep sea fishes. *Biol. Bull.* **107** (2), 260-277.

Reproduced by Permission

Särtryck ur Tellus nr 2, 1957

(147)

An Observation of an Oceanic Front

By JOHN A. KNAUSS, Scripps Institution of Oceanography, University of California[1],
La Jolla, California

(Manuscript received September 9, 1956)

Abstract

A detailed temperature section across an oceanic front in the Eastern Equatorial Pacific is described. The frontal zone was moving at about one knot from the colder water toward the warmer water. The temperature difference across the front was 5° F. In the temperature section it is possible to see the cold water overrunning the warm water and creating an unstable zone approximately 100 yards wide.

On the Scripps Institution Eastropic Expedition we were able to observe an oceanic front in somewhat more detail than had been described previously (CROMWELL and REID, 1956). The measurements were made 12 October 1955 in the vicinity of 3° N and 120° W. The nearest land, Clipperton Island, was 1,000 miles to the north-northeast.

Observations

Movement and orientation of the front: The Scripps research vessel, HORIZON, was traveling south, completing a long north-south series of stations along 120° W, when the front was first registered by the recording surface thermograph at 0415 PST, 12 October. The surface temperature suddenly dropped 4.8° F. The ship's position at this first crossing was 2° 46′ N, 120° 39′ W. The front's orientation was not observed by anyone aboard the ship. The HORIZON continued to steam south to her last station and returned to the front late the same afternoon. At evening star sights at 1820 the ship's position at the front was 3° 08′ N, 120° 36′ W. The front was observed to be oriented on a line running about 225°—45°. If we assume the front was moving on a line normal to itself, the average velocity for this fourteen-hour period was about one knot.

The Scripps research vessel SPENCER F. BAIRD, which was working a similar north-south series of stations 300 miles to the east, did not observe the front on her north-south traverse.

Appearance of the front: The frontal zone was easy to observe with the eye. The cold water (which was to the south) was darker, the waves were shorter crested, and the sea state value was lower than on the warm side. The wind was from 170° T and was blowing between 18—20 knots during the time of observations.

High biological activity was associated with the front; however, there was no floating debris. The cold water was relatively sterile; most of the life appeared to be concentrated in the relatively narrow frontal zone. A dip-net collection made while drifting across the front yielded squid, colonial tunicates (*Pyro-*

---

[1] Contribution from the Scripps Institution of Oceanography, New Series No. 909. This paper represents the results of research carried out by the University of California under contract with the Office of Naval Research. Reproduction in whole or in part is permitted for any purpose of the United States Government.

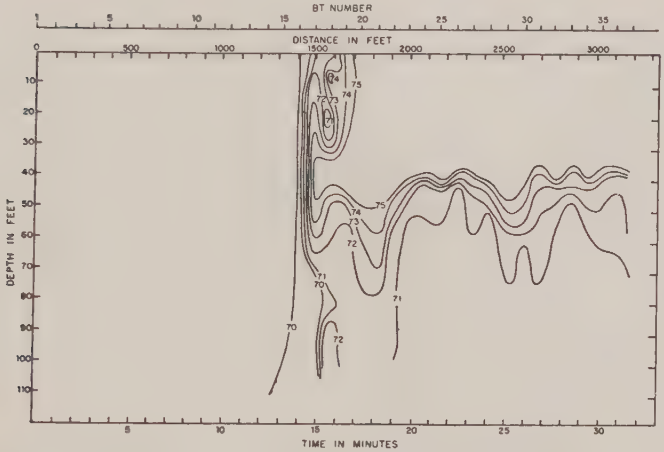

Fig. 1. Temperature (°F) profile based on BT's which were made while ship drifted across front. BT's are plotted against time.

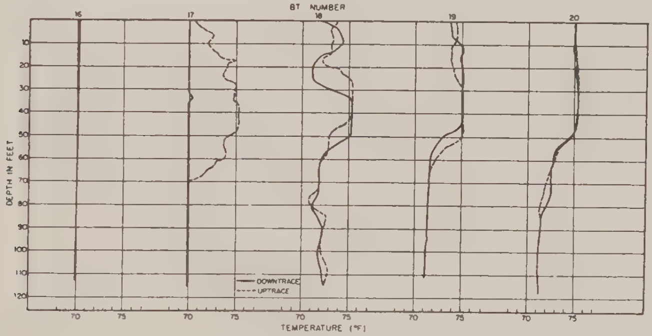

Fig. 2. Copies of individual BT's taken across frontal edge. "Down trace" is assumed to be that which indicated colder surface temperature.

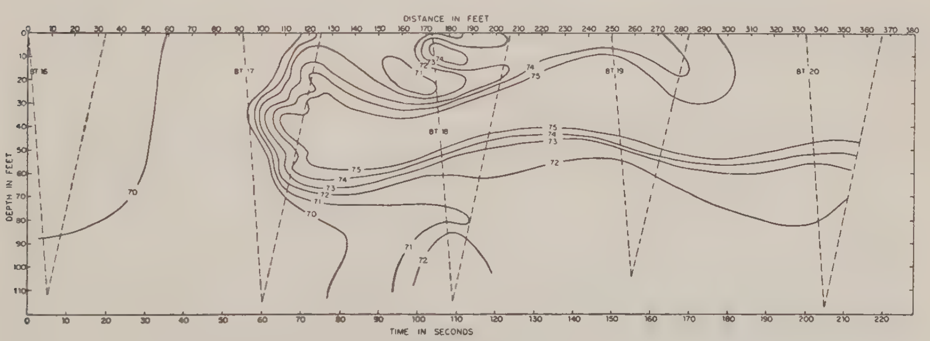

Fig. 3. Frontal edge of Fig. 1 plotted with no vertical exaggeration. The assumed position of BT's shown by dashed lines.

soma atlantica), flying fish (*Cypselurus xenopterus*, and *Exocoetus* sp.), sauries (*Cololabis adocetus*), and lantern fish (*Hygophum reinhardi*, and *Myctophum affine*).

Temperature measurements: Because of the strong wind at almost right angles to the front, it was possible to drift the R/V HORIZON through the frontal zone. As the ship drifted, shallow bathythermographs (BT's) were taken as rapidly as possible (about one every 50 seconds). The drift of the ship relative to the front was estimated at one knot.

Fig. 1 is a temperature profile based on the BT's taken from the drifting ship. The positions of the BT's are plotted as a function of time; the distance scale is based on the assumed one-knot rate of drift. In Fig. 2 are plotted the five BT's (16—20) taken as the ship drifted across the edge of the front. Note that 16 was completely in the cold water as were 1—15; 17 was lowered in cold water and raised in warm water; 18 shows a confused unstable trace, as does 19 to a somewhat lesser extent. By the time 20 was taken, some two minutes later, and approximately 80 yards from the frontal edge, the BT trace showed a stable configuration, similar in most respects to the remaining 17 BT's in the series.

In Fig. 3 these five BT's have been plotted without vertical exaggeration. For this plot both the up and down trace were used; the assumed position of the BT is indicated by the dashed lines. It was assumed that the BT took five seconds to reach depth and 15 seconds to return to the surface, and it was further assumed the "down trace" was that trace which registered the lower surface temperature, an assumption substantiated by the surface recording thermograph which registered a steadily increasing temperature as the ship drifted across the front.

Table 1

BT	Temp. (°F)	Salinity	Density
1	70.2	34.54	1.0241
3	70.2	34.52	1.0241
9	70.2	34.51	1.0241
16	70.5	34.49	1.0240
19	74.7	34.46*	1.0233
23	75.4	34.46	1.0232
37	75.4	34.46	1.0232

* salinity sample taken during BT's "uptrace"

Surface temperature and salinity measurements and calculated surface density values from samples collected as the HORIZON drifted across front. Positions of samples with respect to frontal zone are indicated by BT number and can be located in Fig. 1.

Salinity: Surface salinity was measured in conjunction with seven of the BT's as the ship drifted across the front. Their values, along with the surface temperatures and calculated density values are listed in Table I.

Velocity measurements: The surface velocities measured by the BAIRD and the HORIZON in this area are shown in Fig. 4 along with the surface temperatures recorded in the area. Measurements were made by the geomagnetic electrokinetograph (GEK), using "neutrally buoyant" cables.

The highest velocities were those recorded by the BAIRD in the vicinity of the equator

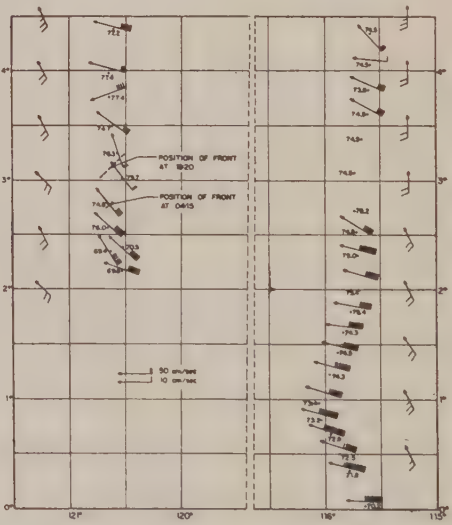

Fig. 4. Surface currents, surface temperatures and average winds as recorded by HORIZON and BAIRD on their north-south traverses. Temperature and current data are plotted at position of observation. Then the average wind data are plotted alongside in the Beaufort scale. The front was first observed at 0415, 12 October, while the HORIZON was traveling south. On returning from southernmost station, the front was observed at 1820 the same day. The two current and temperature observations shown between the 0415 and 1820 positions of the front were made while the HORIZON was traveling south. Hence these observations were made north of the front.

where the current was flowing 3—5 knots west to west-northwest (1 knot = 51 cm/sec). These high velocities recorded by the GEK are in general agreement with as yet unpublished measurements made at the equator at the same time by free-floating parachute drogues. In the vicinity of the front the water had a strong north component and was moving almost at right angles to the front.

A series of four GEK measurements was made a few hundred yards on either side of the front. The two measurements in the cold water to the south were 94 cm/sec-335° and 105 cm/sec-324°, respectively. The two measurements north of the front were less consistant: 84 cm/sec-307° and 62 cm/sec-268°.

Discussion

It is believed that the temperature measurements shown in Fig. 1—3 are the most detailed yet made in an oceanic front (or in any open-ocean convergence zone). Although the details in Fig. 3 are subject to personal interpretation, the picture of cold water overrunning the less dense warm water and then plunging downward is inescapable. On this particular crossing the unstable area was no more than 100 yards wide.

The concept of the frontal wall being continuously destroyed by cold water overrunning the warm water and then mixing with the warm water is not inconsistent with the observations of: (1) the front moving as a "cold front" at a speed of about one knot and (2) the cold water to the south moving at right angles to the front at speeds in excess of two knots. The cold water is probably part of the South Equatorial Current.

It should be pointed out that this is an observation of a single front. Fronts have been reported in this area which move as warm fronts (Cromwell, personal communication). It is unlikely in these cases that mixing at the frontal wall of the type suggested here could occur.

Acknowledgement

The observations of biological activity were contributed by A. E. Ebeling.

REFERENCE

Cromwell, T., and J. L. Reid, Jr., 1956: A Study of Oceanic Fronts. *Tellus*, 8, pp. 94—101.

PRINTED IN SWEDEN
ESSELTE, STHLM 57

Reprinted from PACIFIC SCIENCE April, 1957

Records of Bioluminescence in the Ocean[1]

BRIAN P. BODEN and ELIZABETH M. KAMPA[2]

DURING THE MONTH of June, 1955, while measurements were being made of the depth of penetration of moonlight into the sea off the Kona Coast (S. W. coast) of the island of Oahu in the Hawaiian group, some information was obtained on bioluminescence in deep water in this region and on the effect of moonlight on the vertical distribution of luminescent organisms. Observations of bioluminescence were also made off San Diego, California, during the month of January, 1956.

An underwater photometer (Kampa, 1955; Snodgrass *et al.*, 1957 in press) designed for work in the deep sonic-scattering layers was used for these measurements. This was equipped with a depth-indicator (Boden *et al.*, 1955) so that a precise knowledge of the depth of the instrument was available at all times. The instrument utilizes a 931-A photomultiplier tube oriented with the sensitive surface facing up. In front of this is a collimating tube at the base of which is a filter-holder for interference filters. The collimator ensures that the 5° useful angle of the filters is not exceeded. At the distal end of this tube is a diffusing plastic disc, which is a true Lambert-type collector—that is, under a uniform sky the intensity (I_θ) collected from the direction Θ would be

$$I_\theta = I_0 \cos \Theta.$$

Thus the instrument measures irradiance. The collimating tube and filter-holder are free-flooding. The dark-current level of the instrument changes less than 0.2 millivolts on the 0–10 millivolt recorder range through the temperature range 10–30°C. It fluctuates about 0.03 millivolts at any particular temperature. The instrument registers down to 1×10^{-6} μ watts/cm^2.

Observations of bioluminescence in surface waters were made off San Diego (Lat. 32° 38′ N., Long. 117° 35′ W.) on the morning of January 18, 1956.

The photometer was lowered with its sensitive surface pointed downward. The sky was cloudless and moonless, and the first cast was made immediately before the beginning of official twilight. Luminescence was clearly visible at the surface at this time, and porpoises were seen to leave bright trails of light in their wakes.

Flashes, or bursts of light, were observed by the instrument, and recorded on a Leeds and Northrup Speedomax recorder, from the surface to a depth of 60 meters. From a depth of about 25 meters downward the flashes were superimposed on the dark-current level of

---

[1] Contribution from the Scripps Institution of Oceanography, New Series, No. 910, and from the Marine Laboratory, University of Hawaii, No. 90. This paper represents the results of research carried out by the University of California in part under contract with the Office of Naval Research. Reproduction in whole or in part is permitted for any purpose of the United States Government.

[2] Scripps Institution of Oceanography, University of California, La Jolla, California. Manuscript received February 27, 1956.

Reproduced by Permission

the instrument, and at times apparently single flashes reached a level of 2×10^{-3} μ watts/cm^2.

A later cast, with the photometer still pointed downward, revealed that at sunrise (0652 hrs.) the flashes were first recorded at a depth of about 110 meters.[3] All facts known to us indicate that these flashes are generated *in situ* and we interpret them as due to luminescent organisms, possibly both nekton and plankton.

Records of bioluminescence at depth were first made in Hawaii at midnight on the night of June 9, 1955. The moon, three days past the full, had just appeared over the mountains. Its angle of elevation at 2400 hours was 19°. The instrument was lowered without color filters, and total irradiance, as seen by the instrument, was recorded. The sky was partly cloudy, but the moon remained clear throughout the observations.

Figure 1 is a tracing of the actual recording made on the Leeds and Northrup Speedomax recorder. Total irradiance (H) at any depth was obtained from

$$n = k\,H = \int_0^\infty E\,S\,d\,\lambda,$$

where n = recorder reading, E = energy of the source through the wave-length interval $d\,\lambda$, S = relative spectral sensitivity of the photomultiplier tube through the wave-length interval, $d\,\lambda$ (300–700 mμ). The value of k was obtained by calibration of the entire instrument against a Bureau of Standards source. The inset shows the relative spectral sensitivity of the 931-A tube used.

The dark-current level of the photometer was reached at 200 meters. From about 50 meters downward numerous brilliant flashes of light were recorded.

At some depths, for example 120–130 meters and 150–170 meters, the background light level appears to have remained constant or to have increased rather than to have decreased with depth.

Many types of luminescent marine animals, e.g., euphausiids, generate a steady glow of light for limited periods in contrast with the discrete flashes produced by others (Harvey, 1940). Possibly the sustained light level (Fig. 1) on which the flashes are superimposed at depths of 120–130 meters and 150–170 meters was due to a background glow produced by concentrations of such types, or by numerous flashes at varying distances.

An alternative explanation of the flashes can be found by visualizing a distribution of steadily-glowing organisms similar to that of stars in the sky, and a flashlike increase in the level of light due simply to the instrument's approach to and retreat from a glow during its descent. The rate of descent of the instrument was about 32 meters/minute. For this to be the true explanation, the glows would have had to be about 1 meter of depth apart, for the frequency of the flashes was about 36/minute.

Many luminescent organisms flash brightly when irritated mechanically or chemically. It is impossible at present to determine whether the observed flashes were due to spontaneous luminescence or whether the luminescence was intensified by agitation of the animals by the instrument.

Four more casts were made, using narrowband interference filters, during the forty-five minutes after midnight. The angle of elevation of the moon varied between 21° and 31° during this period. The interference filters employed were G. A. B. filters, manufactured in Liechtenstein, with half-peak band widths of about 10 mμ. Block filters are incorporated to reduce stray light and eliminate secondary transmission peaks. Peak transmissions, measured by a Beckman Model DU spectrophotom-

---

[3] The possibility that these are artifacts due to instrument failure is to be considered. It is improbable that distortion due to pressure affected the circuitry, for the phenomenon was not observed when the instrument had been lowered to greater depths during daylight. It is improbable, too, that the effect could have been caused by water leakage, for moisture in the system has been shown to raise the dark current to such a high level that the recorder is immediately sent off scale. Furthermore the fact that color filters placed in the light-path reduced the amplitude of recorded flashes discounts the possibility that loose electrical connections were responsible. Another photometer, similar to the one employed here, has since shown that the flashes are not recorded when the sensitive element is covered but are when it is exposed immediately afterward at the same depth. Thus we believe that the instrument was sensing real light flashes.

Flashes of this nature could not have been caused by tilt of the instrument since it was pointed downward.

(154)

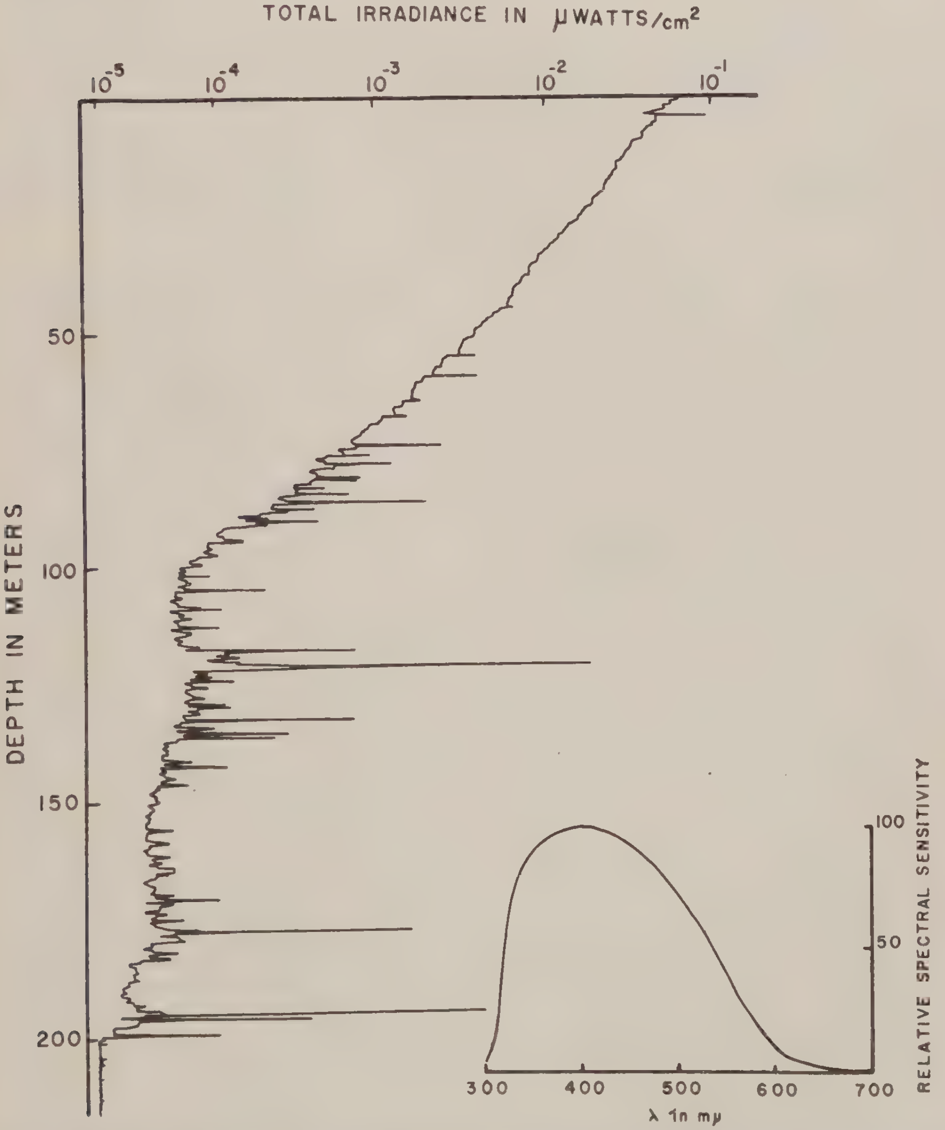

FIG. 1. Tracing of total irradiance recorded on Leeds and Northrup Speedomax recorder by bathyphotometer without color filters. Spectral sensitivity of the 931-A photomultiplier tube is shown in inset. This is from manufacturer's specifications and is an average curve. The record was made at 2400 hours, June 9, southwest of Oahu.

eter, are at 418, 491, 552, and 630 mμ (see inserts in Fig. 2).

Irradiance (H) was obtained from

$$n = k\,H = \int E\,T_f\,S\,d\,\lambda,$$

where n = recorder reading, E = energy of the source through the wave-length interval $d\,\lambda$, T_f = measured transmission of the individual interference filter through the wave-length interval $d\,\lambda$, and S = the relative sensitivity of the photomultiplier tube through the wave-length interval $d\,\lambda$. The value of k was obtained as indicated above.

Tracings of the recordings are shown in Figure 2. Orange light (λ max, 630 mμ) is seen to cut out at 11 meters, and no flashes are apparent. With the 418 mμ filter, the dark-current level of the instrument was reached at a depth of 280 meters.

The 418 mμ cast reveals an actual increase in irradiance with depth between 100 and 220 meters. Sudden flashes again occurred between 100 and 280 meters, but these, as recorded, were of lower amplitude than those in the unfiltered cast, presumably because of the narrowness and reduced intensity of the transmitted band.

These observations indicate that the light generated at depth is blue-violet (see Harvey, 1940, for spectral distribution of bioluminescence). It can be seen too (Fig. 2) that the flashes produced in the surface layers are greener.

The greater depth attained with a 418 mμ filter in the instrument (cf. Figs. 1 and 2) and the deeper flashes may be explained on the assumption that some of the light-generating constituents of the population had by then sought greater depths as the moon cleared the mountains and approached its zenith. The possibility that these constituents comprise a photoregulated community similar to the Californian deep-scattering layer may be inferred from this assumed downward migration with increasing illumination.

This inference is substantiated by observations made off San Diego (Lat. 32° 38′ N., Long. 117° 35′ W.) on January 17, 1956. At this time EDO fathograms and light measurements were made simultaneously during the periods of the twilight migration of the sonic-scattering layer. Figure 3A (1640–1650 hours) shows that flashes were first recorded as the photometer reached the depth of the scattering layer. Thirty minutes later (1720–1728 hours) the top of the scattering layer had reached a depth of 120 meters. Figure 3B shows that the first flashes recorded by the photometer were now at this same depth. On the day of these observations sunset was at 1706 hours.

We have recorded flashes, during our scattering-layer studies, in the Pacific, Atlantic and Mediterranean. They appear to increase both in frequency and amplitude during the twilight migration of the layer and at night. On this account it is extremely difficult to obtain an accurate picture of the spectral distribution of moonlight in the sea, or even of sunlight at scattering-layer depths.

Since the completion of this paper we have heard from Professor George L. Clarke of Harvard University (Clarke and Backus, in preparation) that he too has recorded flashes of luminescence off the Florida coast.

This phase of work on the sonic-scattering layers received additional support from the National Science Foundation and the Pauley Fund of the University of California. The inquiry was pursued from the Marine Laboratory of the University of Hawaii. The Californian data were obtained from the "USS EPCE(R) 855." Acknowledgment is made of the generous loan of the Research Vessel "Makua" by Mr. Vernon Brock, Director of the Territorial Fish and Game Commission, Hawaii. The U. S. Air Force and Marine Corps were unstinting in their loan of equipment and facilities. Data were analyzed and most of this paper was written at The Laboratory, Plymouth, England. The hospitality of the director, Mr. F. S. Russell, F. R. S., is most gratefully acknowledged. Professors

(156)

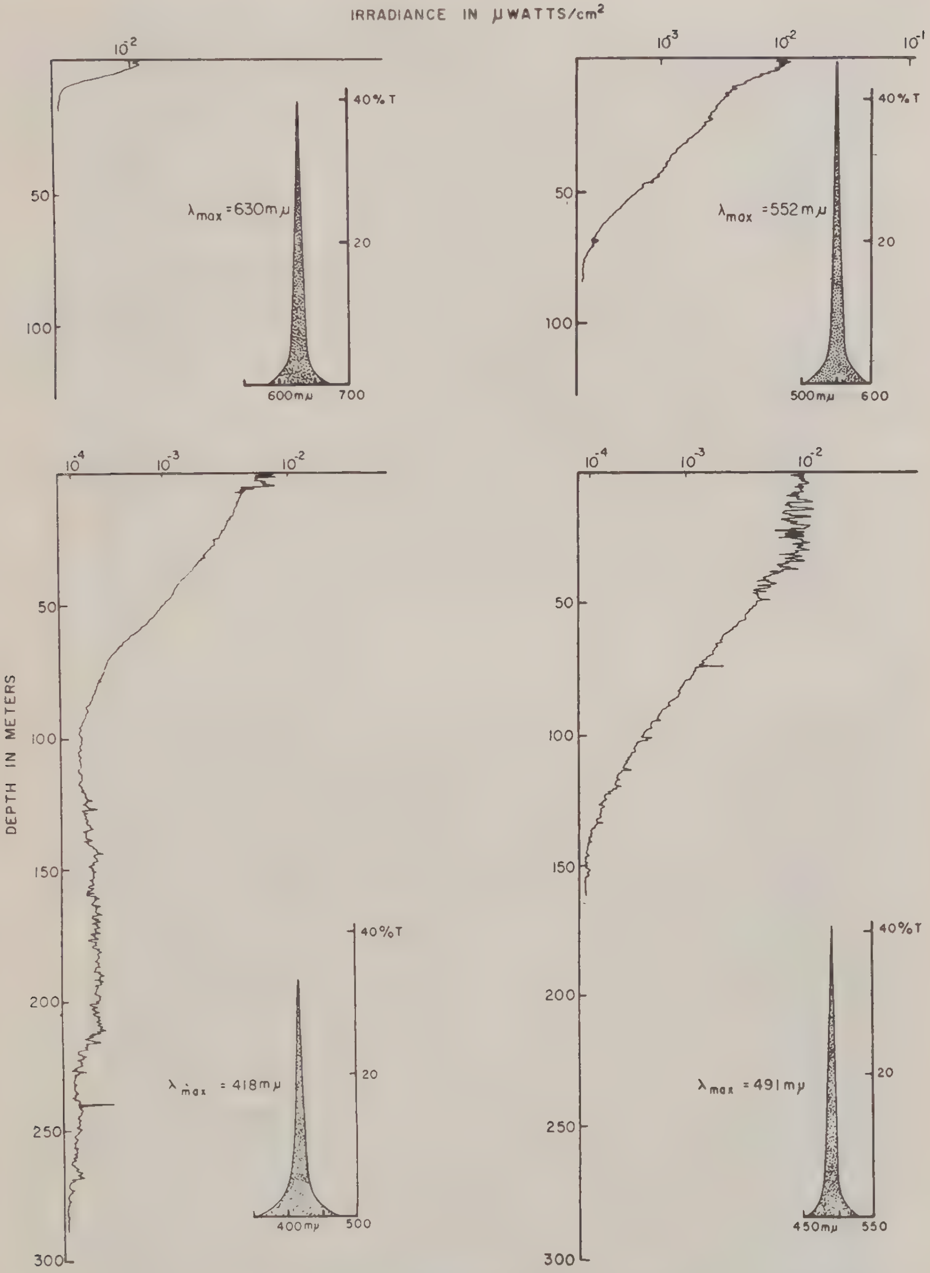

FIG. 2. Tracings of irradiance record at four different wave lengths as determined by bathyphotometer using interference filters. Insets show measured transmission curves of filters used. The records were made at the following times: 630 mµ—0020 hrs.; 552 mµ—0030 hrs.; 491 mµ—0044 hrs.; 418 mµ—0058 hrs.; all on June 10, southwest of Oahu.

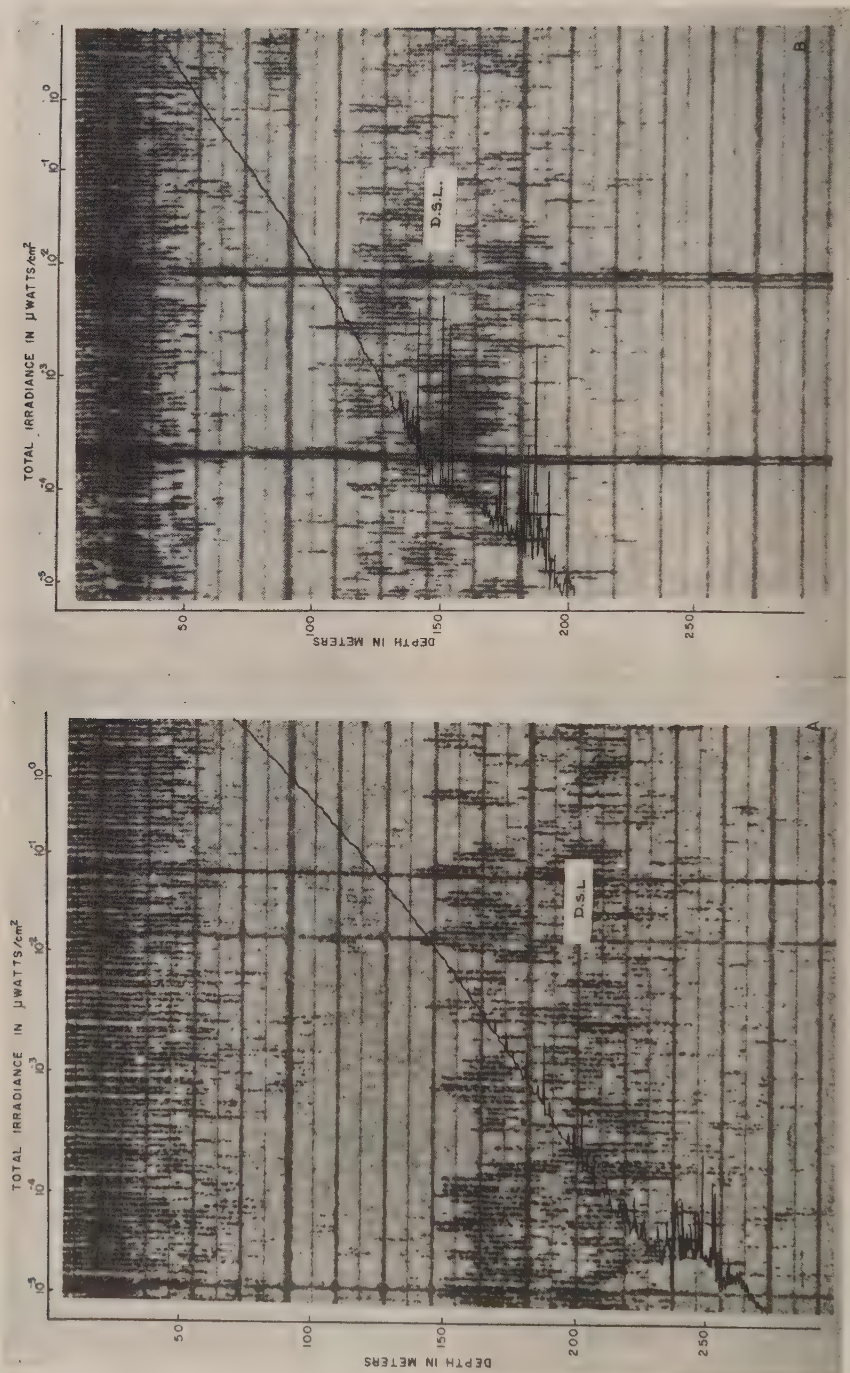

FIG. 3. Tracing of total irradiance recorded 17 January 1956, in the San Diego Trough, Latitude: 32° 38′ North; Longitude: 117° 35′ West. The superimposed fathograms were recorded at the same time. A: 1640–1650 hrs., B: 1720–1728 hrs. The light curve does not reach the surface because the upper limit of the photometer's range is about 2μ watts/cm².

(158)

Carl Eckart and Carl L. Hubbs of the Scripps Institution and Mr. John Tyler of the Visibility Laboratory of the Scripps Institution subjected the manuscript to vigorous and stimulating criticism.

REFERENCES

Boden, Brian P., Elizabeth M. Kampa, James M. Snodgrass, and Robert F. Devereux. 1955. A Depth Telerecording Unit for Marine Biology. *Jour. Mar. Res.* 14(2): 205.

Clarke, G. L., and R. H. Backus. Light penetration in relation to vertical migration and records of luminescence of deep sea animals. *Deep Sea Research.* [In preparation.]

Harvey, E. N. 1940. *Living Light.* Princeton University Press.

Kampa, Elizabeth M. 1955. A Discrepancy between Calculation and Measurement of Submarine Illumination. *Natl. Acad. Sci., Proc.* 41(11): 938.

Snodgrass, J. M., R. F. Devereux, and J. H. Cawley. 1957. A Telerecording Bathyphotometer. [In press.]

Reprinted from the JOURNAL OF CELLULAR AND COMPARATIVE PHYSIOLOGY
Vol. 49, No. 1, February 1957

Reproduced by Permission

CHARACTERISTICS OF THE DIURNAL RHYTHM OF LUMINESCENCE IN GONYAULAX POLYEDRA[1,2,3]

BEATRICE M. SWEENEY AND J. WOODLAND HASTINGS
Division of Marine Botany, The Scripps Institution of Oceanography La Jolla,
California, and Department of Biological Sciences,
Northwestern University, Evanston, Illinois

SIX FIGURES

INTRODUCTION

The production of light by living organisms is to a great extent associated with the marine environment (see Harvey, '52). *Gonyaulax* is a marine dinoflagellate which is both photosynthetic and luminescent, being one of the many organisms which contribute to the frequently observed "phosphorescence" of the ocean. Its luminescence occurs upon stimulation, as a bright flash having a duration of about 0.1 sec. When large numbers of these organisms are stimulated in the ocean, as by the passage of a school of fish or by wave action, the disturbed water glows as a result of their flashing. Fishermen locate sardine schools by such luminescence.

Dinoflagellates in general have been reported to lose their ability to luminesce in daylight (see Harvey, '52). Such a phenomenon is also known in other luminous forms, particularly the ctenophores. In the latter, the ability to luminesce

---

[1] This research has been supported in part by grants from The National Science Foundation and the Graduate School of Northwestern University and in part by a grant from Rockefeller Institute to Scripps Institution of Oceanography.

[2] We are grateful to Mr. William K. Purves for his assistance in carrying out these experiments.

[3] Contribution from the Scripps Institution of Oceanography, University of California, New Series No. 911.

is rapidly inhibited in light, but recovers after a sojourn of 20 to 30 minutes in darkness. In the case of dinoflagellates, however, reports by several observers (Zacharias, '05; Moore, '08; Kofoid and Swezy, '21; Harvey, '52) suggest that luminescence is under the control of a type of diurnal rhythmic mechanism. This conclusion is based mainly on visual observations that dinoflagellates kept in total darkness fail to luminesce during the day, but regain their ability to do so during the nighttime. The studies described in this paper confirm this general conclusion with quantitative measurements, and give additional information concerning other effects of light.

MATERIALS AND METHODS

A unialgal culture of *G. polyedra* was isolated by one of the authors (B. M. S.) from a net sample collected off the pier at Scripps Institution of Oceanography, on September 22, 1952. Since that time, the cultures have been maintained in Fernbach flasks placed in a window (north exposure, 400–800 foot candles) at room temperature (23°–26°C.). The culture medium was composed of 75% filtered sea water, 2% soil extract (Pringsheim, '46), 2×10^{-3} M KNO_3, 2×10^{-4} M K_2HPO_4, 6×10^{-6} M $FeCl_3$, and 2.7×10^{-5} M ethylendiaminetetraacetic acid (EDTA) at pH 8.0–8.2. All distilled water used in these experiments was distilled a second time in a Pyrex glass still.

For experimental purposes, some cultures were grown and maintained in a temperature-controlled cabinet (25°C.) under constant illumination at an intensity of about 700 foot candles. Illumination was provided by "cool white" fluorescent lamps. Cultures grown in the window were used for experiments in which it was desired that organisms be exposed to normal day-night changes in light intensity. Cultures were inoculated at a cell density of about 800 cells per milliliter, and were used for experiments 10–15 days later at a population density of 6000–13000 cells per milliliter.

The luminescence of *Gonyaulax* may be induced by mechanical stimulation. After a few seconds of agitation, the luminescent response is markedly decreased. Agitation during the pipetting of population samples is unavoidable. Although recovery was not studied in any detail, it was determined that a rest period of two hours in the light is sufficiently long to permit recovery from agitation coincidental to the preparation of samples. For experimental studies, 2 ml aliquots from cultures were pipetted into groups of test tubes and given a recovery period of at least six hours in the light. Luminescence was assayed by stimulating the cells in test tubes with a fine jet of purified air from a compressed air tank. Since it was impossible to determine luminescence accurately from the intensity recordings, the output from the phototube was accumulated in a capacitor, giving a measure of the total light emission (see fig. 1). This method was used for all assays.

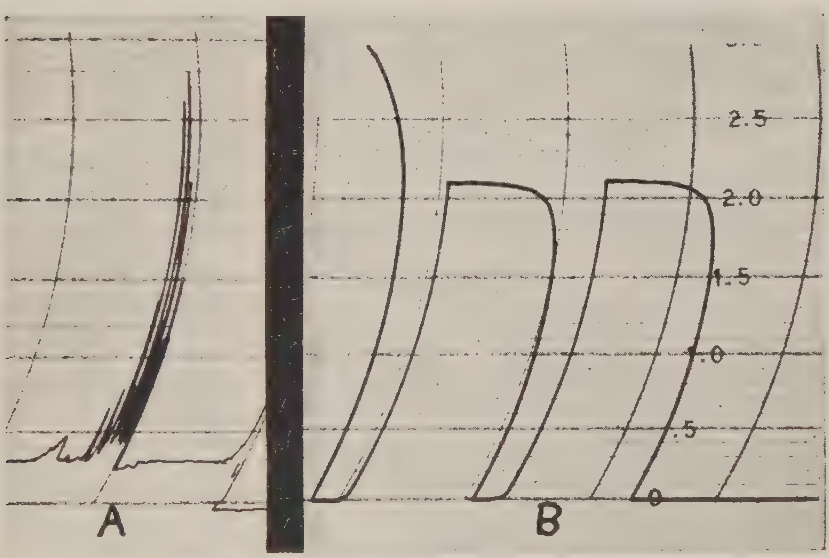

Fig. 1 Recordings of *Gonyaulax* luminescence. A. Intensity measurement. B. Measurement by integration. Time scale, one minute between vertical divisions. Intensity measurement does not give an accurate record of flashing since the flashes have a duration of 0.1 sec. and the time constant of the meter was 0.5 sec. Direction of time axis is from right to left.

Since essentially all luminescence was exhausted within one minute, the values for luminescence of cells are expressed in terms of total (integrated) light emitted during one minute of stimulation, expressed as arbitrary total light units. With the exception of this integration circuit, the light-measuring apparatus was essentially the same as described previously (Hastings, McElroy and Coulombre, '53), utilizing a 931A photomultiplier tube and an Esterline-Angus graphic meter for recording. Provision for precision voltage regulation makes the sensitivity of the instrument independent of time of day.

After each determination, the experimental tube was discarded. Determinations made from a number of aliquots from a given culture under similar conditions generally agreed within 10%, but very occasionally greater variations were encountered. These cases may have been due to any of a variety of factors, and we were not successful in eliminating them. Individual experimental determinations which varied widely from others, although included in the figures, are therefore not considered to be highly significant.

Time of day is expressed throughout in Pacific Daylight Time, and the hours are numbered consecutively from 0100 (1 A.M.) to 2400 (midnight).

EXPERIMENTAL RESULTS

Haxo and Sweeney ('55) have shown that cells grown in bright continuous illumination have a dim luminescence which shows no detectable rhythmic variation. Using cells grown under these conditions, they found that changes in luminescence could be initiated by placing the cells in total darkness. Cells kept in darkness over a period of 40 hours were observed to increase in brightness during the first 6–8 hours followed by a decline. A second increase in luminescence followed this with a maximum between 20 and 24 hours after the first peak.

We have repeated these experiments with cells which had been cultured in constant light for 8 weeks and extended the period of darkness up to 100 hours. The results of such an experiment are shown in figure 2. The fluctuations suggest that *Gonyaulax* cells possess a type of "biological clock," or an inherent mechanism of rhythmicity which is inhibited in continuous illumination but which may be initiated at any time by subjecting them to darkness. The period between peaks has been found to be about 23 hours in these experiments. The magnitude of each succeeding peak is progressively lower, suggesting the exhaustion of the energy stores. Since energy in this organism is derived from light through photosynthesis, this is an expected consequence of continuous darkness. The fall in peak height with time is

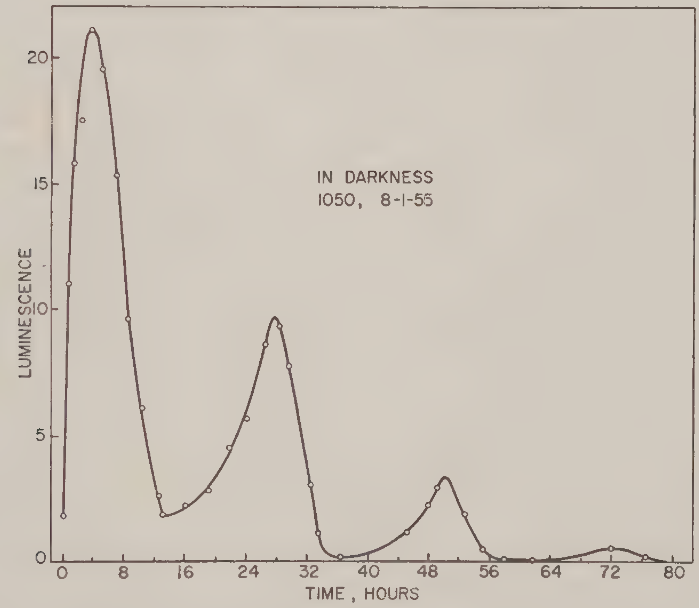

Fig. 2 Spontaneous rhythmic changes in luminescence of cells grown in constant light and placed in total darkness. Luminescence in constant light, 1.8 light units. Time in hours after placing in darkness. Each point represents the average of 2–4 determinations.

slightly greater than logarithmic over the long continued dark period, while cell counts decrease only slightly, and there is no detectible decrease in the per cent of cells which are motile. Consequently, the progressive reduction in the magnitude of successive peaks in luminescence probably reflects a progressive starvation of all the cells of the population, rather than a reduction in the per cent viable cells.

It was of interest to re-examine whether or not cells retained any detectible rhythmicity while in constant illumination. This was done in two ways. We first made additional measurements to determine whether or not there were any significant fluctuations in the dim luminescence of cells kept in constant light. No variations which indicated a rhythm were observed. Secondly, an experiment was planned to test whether or not the initiation of the rhythm in cells grown in constant light was independent of time of day. Aliquots of cells which had been grown in continuous light were removed to total darkness at three hour intervals over a 24 hour period. The first part of the rhythmic luminescent cycle of each group was determined. The results of this experiment are summarized in figure 3, and show that in light-grown cultures, the rhythm may be initiated with equal rapidity at any time of day. A systematic variation in the maximum luminescence attained was observed, the greatest luminescence being developed between 1300 and 1500. An experiment carried out over a longer time period is necessary to determine whether or not this variation represents a vestigial rhythmic pattern, displaced in time. However, it is apparent that the time intervals of the newly-developed rhythmic pattern are not affected.

It may also be noticed in the experiments shown in figures 2 and 3 that there is a considerable difference in the ratio of luminescent intensity in constant light to the maximum intensity in darkness. Wide variations in this ratio were encountered from culture to culture. Since aliquots from any one culture at any given time behaved uniformly, this variation appears to be caused by differences in the pretreatment of cultures. It was not possible to standardize pretreatment with precision with the equipment available and a growth medium which is not completely defined.

The changes in the luminescence of *Gonyaulax* exposed to natural day-night variations in light intensity was next studied, and the results are shown in figure 4. For this purpose, samples were pipetted from window-grown cultures and placed in the window. They were then assayed for luminescence at the times indicated. Figure 6 shows a more detailed measurement of a nighttime excursion.

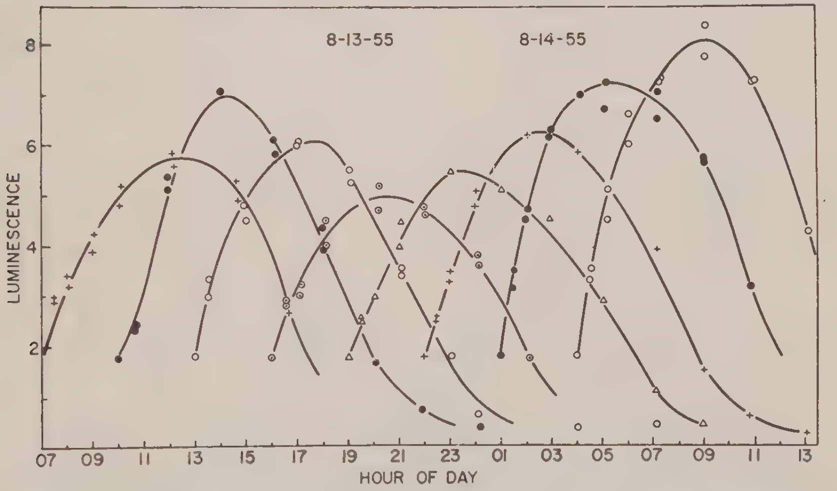

Fig. 3 Plot of the first cycle of luminescence (as in fig. 2, first 12 hours) in a series of experiments in which cells grown in constant light were placed in darkness at 3 hour intervals over a 24 hour period. Time (PDT) from 0700 hours (7 A.M.) of first day through 1300 hours (1 P.M.) of second day. The first determination of each curve was made at the time the aliquots of this group were darkened. Each point represents a single determination.

It can be noted (see fig. 6) that the luminescence begins to increase only at the onset of darkness, but begins to decrease before any light of morning has appeared. This suggests that the same mechanism is functional in the early morning decline of luminescence as in the decline observed in continuous darkness (fig. 2). To test this assumption, a number of aliquots from the window were removed during darkness (at midnight) and placed in total darkness. Their luminescence was assayed and found to decrease from the nighttime peak in the same manner as those left in the window (see fig. 4). Moreover, although the cells were kept in darkness all the while, their luminescence increased the following night. They differed from those left in the window in that the increase in luminescence the second night was not as great as that of those which were left in the window, and it occurred somewhat earlier. This latter point is more clearly demonstrated in a similar experiment shown in figure 5.

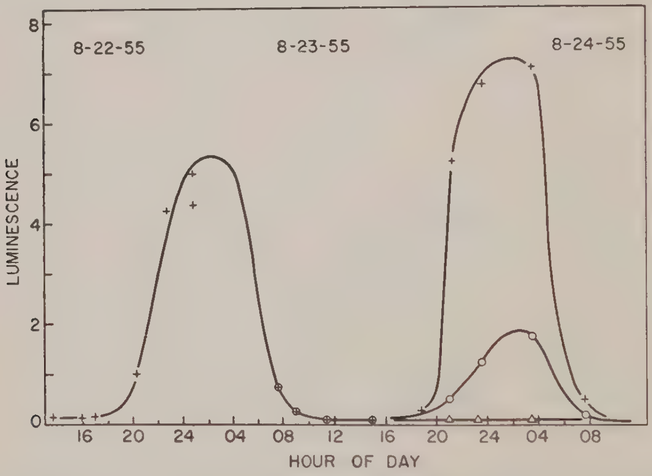

Fig. 4 Variation in luminescence over the course of two days of cultures grown and kept in window (indicated by crosses). Some cultures were removed from the window at midnight on the first day and put in total darkness (circles). Other cultures were removed from the window at noon and placed in constant light (triangles). Hour of the day plotted as in figure 3. Each point represents 1–2 determinations.

With the exception of the two effects noted above, the rhythm of the luminescence of *Gonyaulax* in the window continues unaltered when the cells are placed in total darkness at any time of the day or night. This is apparent from figure 5, where aliquots from the window were placed in continuous darkness at three different times during daylight. As can be seen, there was no increase in the luminescence in any of the experimental tubes until early evening, about one hour before the controls from the window began to increase in intensity. It may be possible that this earlier rise is related to the 23-hour period observed in cultures placed in continuous darkness (fig. 2). Moreover, the magnitude of the evening peak is related to the duration of the exposure to daylight, suggesting that "day length" (i.e. time × intensity) is effectively the important factor with regard to the magnitude of the night-time peak. It seems probable that restoration of energy stores through photosynthesis is responsible for this light effect although direct evidence to support this assumption is not yet available.

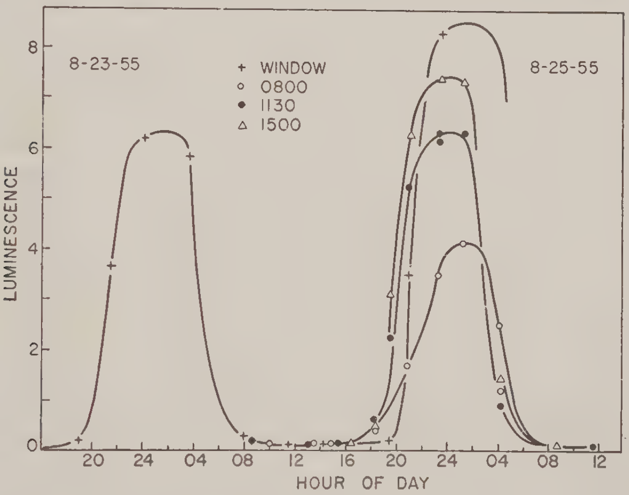

Fig. 5 Variation in luminescence over two days as in figure 4 (crosses). During the day three groups were removed from the window at the times indicated and placed in total darkness. The luminescence of each group was assayed at the times indicated, showing the effect of light during the day upon the amount of luminescence at night. Hour of the day plotted as in figure 3. Each point represents a single determination.

Another series of experiments was concerned with the effect of removing cells from the day-night regime in the window to the illuminated incubator. When cells were removed from the window to continuous light at any time during daylight, no subsequent increase in luminescence was observed (fig. 4). But on the other hand, if the cells were removed from the window and placed in constant light during the nighttime period (i.e., at any time after an increase in luminescence had already occurred) luminescence was decreased in all cases (fig. 6), as previously described by Haxo and Sweeney ('55) for cells exhibiting maximum luminescence. However, in no case is the luminescence decreased to the low day-time level, even when measurements were extended to 1100 the following morning. Thus, although light will inhibit any increase in luminescence when illumination is begun during daylight, once this increased luminescence has begun to develop in darkness, then inhibition by light is only partial. Thus light during the

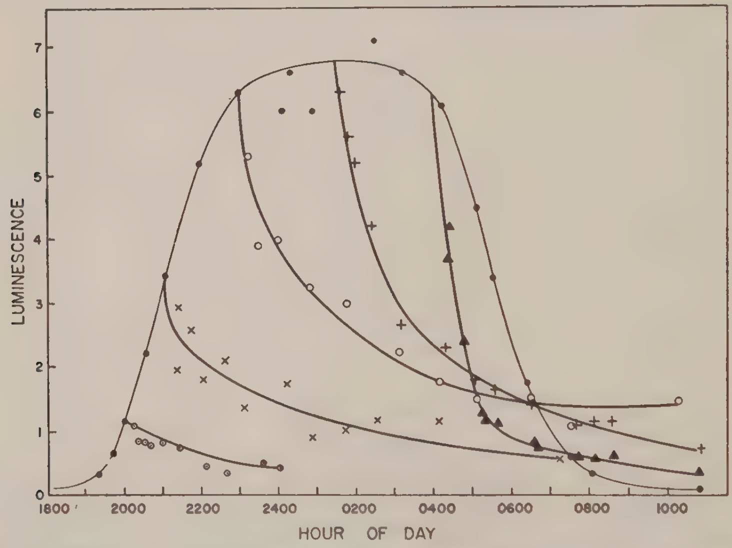

Fig. 6 Effect of light during the night upon the luminescence of cultures growing in the window. At 2000, 2107, 2300, 0130 and 0400 cultures were removed from the window and placed in constant light in the incubator, and the luminescence of these along with the control in the window was determined at the times shown. Time of day plotted as in figure 3. Each point represents a single determination.

night prevents the maximum excursion of the luminescent cycle, both up-swing and down-swing.

DISCUSSION

From the experiments described, it is clear that the luminnescence in *Gonyaulax* cannot be maintained at maximum brightness under any of the experimental conditions used. A maximum is always followed by a fall in luminescence. This alteration of bright and dim periods is observed in continuous darkness as well as during the normal succession of day and night, and so may be considered an endogenous diurnal rhythm, similar in nature to rhythms which have been described for a variety of activities in numerous organisms (see Bünning, '52; Kleitman, '49; Grossenbacher, '39; Welsh, '38). Since *Gonyaulax* is a unicellular form, the origin of the rhythmicity is evidently intracellular.

Under normal conditions of daily changes in light intensity luminescence is maximum during darkness and minimum during daylight. It has been possible recently (Hastings and Sweeney, '57) to demonstrate luminescence in cell-free extracts and to separate substrate and enzyme (luciferin and luciferase) from one another. It was found that extracts prepared from cells during nighttime were from 5 to 15 times more active than those prepared during daylight. At least part of the diurnal fluctuation in light intenstity may therefore be attributed to actual changes in the concentrations of luciferin and luciferase. It has been shown by Buck ('37) that spontaneous firefly flashing involves a diurnal rhythm. In the case of the firefly, however, the rhythm is evidently linked to the control of flashing and not to the production of photogenic substance. We have made some observations which suggest that *Gonyaulax* cells also may be inherently more susceptible to stimulation during the nighttime period than during the day. Cells from the window placed in a test tube in total darkness but not stimulated show a marked increase in the frequency as well as magnitude of what appears to be spontaneous flashing during the nighttime period. This may account for the fact that the difference in the luminescence of intact cells between day and night is greater than the corresponding difference in the activity of extracts by day and night. It is thus possible that both factors are involved in the changes in luminescence, and that both are linked to a rhythmic mechanism.

The shifting of the rhythm has not been studied in any detail. The results obtained thus far suggest that it may be shifted at will with the proper manipulation of light and dark periods. Certainly after long exposure to continuous light it may be initiated at will. This condition is similar to that found by Buck ('37) for spontaneous firefly flashing.

It was not possible to determine how long the rhythm itself might persist, since the cells apparently die within about 100 hours in continuous darkness. The fact that cells in constant light retain the mechanism over a long period of time suggest, but does not prove, that the mechanism is a persistent one. This point might be settled if a substance supplied in the medium could be utilized by the organism as an energy source. A number of compounds have been tried in this connection, but none have substituted for light insofar as growth is concerned (W. H. Thomas, '55). It is also possible, as indicated in preliminary experiments of Haxo and Sweeney ('55) that the blue-violet portion of the spectrum is most effective in inhibiting luminescence. In this case red light might be used to keep the cells alive while not disturbing the rhythms of luminescence.

Light may evidently affect the cells in a number of different ways. First it provides an energy source for the organism through photosynthesis. Luciferin and luciferase would be expected to be synthesized and destroyed daily via reactions which require energy. A decreased exposure to light with consequent reduction in photosynthesis would therefore result in a lower concentration of the photogenic compounds. Secondly, light will apparently inactivate or inhibit the luminescent system or its components. At the light intensities used, the inactivation is never complete. This may be a consequence of a balance between a photoinactivation and biosynthesis. Alternatively, the decrease in luminescence may be the result of the photoproduction of an inhibitor which, in the concentrations produced, is not 100% effective. Finally, as an independent effect, light appears to inhibit rhythmic changes in the intensity of luminescence.

A clarification of these various effects of light, and to what extent they are independent of one another, will be greatly aided by a determination of their respective action spectra. Studies of this nature are being carried out at the present time.

SUMMARY

The luminescence of cultures of the marine dinoflagellate, *Gonyaulax polyedra*, receiving light from the window, is dim during the day and about sixty times brighter at night. These variations may be described as a type of inherent diurnal rhythmicity, since a number of experiments demonstrate that the periodicity is maintained in the absence of normal day-night variations in light intensity. If the cultures are transferred from the window to total darkness at any time, the rhythmic changes in luminescence continue to occur, approximately in phase with cells left in the window. Continuous exposure to light will inhibit the rhythm, but it may be initiated in such light-treated cultures at any time by placing them in total darkness. The rhythm will then persist for about four days. The amount of luminescence which develops at night is directly related to the amount of light received during the day. This is probably related to the energy stores derived from photosynthesis. Light will also directly inhibit luminescence at any time during the night. The changes in luminescence are at least partially due to synthesis and destruction of luciferin and luciferase. It is also possible that the cells are more susceptible to stimulation during the night phase.

LITERATURE CITED

BUCK, JOHN B. 1937 Studies on the firefly. I. The effect of light and other agents on flashing in *Photinus pyralis*, with special reference to periodicity and diurnal rhythm. Physiol. Zool., *10:* 45–58.

BÜNNING, E. 1952 Morphogenesis in plants. In: Survey of biological progress. (G. S. Avery, Jr., ed.) Vol. 2, pp. 105–140. Academic Press, New York, N. Y.

GROSSENBACHER, K. A. 1939 Autonomic cycles of rate of exudation of plants. Am. J. Bot., *26:* 107–109.

HARVEY, E. N. 1952 Bioluminescence. Academic Press, New York, N. Y.

HASTINGS, J. W., W. D. MCELROY AND J. COULOMBRE 1953 The effect of oxygen upon the immobilization reaction in firefly luminescence. J. Cell. and Comp. Physiol., *42:* 137–150.

HASTINGS, J. W., AND B. M. SWEENEY 1957 The luminescent reaction in extracts of the marine dinoflagellate, *Gonyaulax polyedra.* J. Cell. and Comp. Physiol., *49:* (in press).

HAXO, F. T., AND B. M. SWEENEY 1955 Bioluminescence in *Gonyaulax polyedra.* In: The luminescence of biological systems. (F. H. Johnson, ed) pp. 415–420. A.A.A.S. Press, Washington, D. C.

KLEITMAN, N. 1949 Biological rhythms and cycles. Physiol. Rev., *29:* 1–30.

KOFOID, C. A., AND O. SWEZY 1921 The free-living unarmoured dinoflagellata. Mem. Univ. Calif., *5:* 1–562.

MOORE, BENJAMIN 1909 Observations on certain organisms of (a) variations in reaction to light and (b) a diurnal periodicity of phosphorescence. Biochem. J., *4:* 1–29.

PRINGSHEIM, E. G. 1946 Pure cultures of algae pp. 41–42. Cambridge Univ. Press. 119 pages.

THOMAS, W. H. 1955 Heterotrophic nutrition and respiration of *Gonyaulax polyedra.* Abstract No. 14 J. Protozool. 2 — supplement.

WELSH, J. H. 1938 Diurnal rhythms. Quart. Rev. Biol., *13:* 123–139.

ZACHARIAS, O 1905 Beobachtungen über das Leuchtvermögen von *Ceratium tripos* (Müll). Biol. Zbl., *25:* 20–30.

Reprinted from the JOURNAL OF CELLULAR AND COMPARATIVE PHYSIOLOGY
Vol. 49, No. 2, April 1957

Reproduced by Permission

THE LUMINESCENT REACTION IN EXTRACTS OF THE MARINE DINOFLAGELLATE, GONYAULAX POLYEDRA[1]

J. WOODLAND HASTINGS AND BEATRICE M. SWEENEY
Department of Biological Sciences, Northwestern University, Evanston, Illinois, and Department of Marine Botany, Scripps Institution of Oceanography, La Jolla, California

NINE FIGURES

INTRODUCTION

Bioluminescence, or the production of light by living organisms, occurs in a great variety of unrelated and diverse animals and plants (Harvey, '52). The nature of the luminescent display may vary, but the reaction in all cases is evidently an enzymatic chemiluminescence, usually an oxidation. The bioluminescent reaction has been carefully studied in only three groups of organisms, namely *Cypridina,* fireflies and bacteria. The light emitting reaction of each differs markedly in requirements (Tsuji, Chase and Harvey, '55; McElroy and Hastings, '55; Strehler, '55; Hastings and McElroy, '55). The present paper, which describes characteristics of the reaction in *Gonyaulax,* indicates that this reaction differs from the three previously described.

Gonyaulax polyedra is a marine armored dinoflagellate which is both photosynthetic and luminescent. The so-called phosphorescence or, more properly, luminescence of the ocean at night is generally believed to be due principally to the luminescence of dinoflagellates (Harvey, '52). *Gonyaulax* has recently been isolated and grown in pure culture by one of the authors (B.M.S.), making possible a study of its physiology and biochemistry. The characteristic luminescence of *Gonyaulax* occurs upon stimulation as a brilliant flash, having a duration of about 0.1 sec. (fig. 9). Maximum luminescent responses occur in darkness and are about 40 to 60 times as bright as the responses in daylight. A preliminary account of the luminescence of living *Gonyaulax* has been given by Haxo and Sweeney ('55) and more detailed studies along these lines are published elsewhere (Sweeney and Hastings, '57).

---

[1] This research has been supported in part by grants from The National Science Foundation and the Graduate School of Northwestern University. Contribution from the Scripps Institution of Oceanography, University of California, New Series No. 912.

MATERIALS AND METHODS

Cells were grown in Fernbach flasks, each containing 1500 ml of medium, placed on shelves in windows (north exposure) at room temperature (23°–26°C.). The culture medium was composed of 75% filtered sea water, 2% soil extract (Pringsheim, '46), 2×10^{-3} M KNO_3, 2×10^{-4} M K_2HPO_4, 6×10^{-6} M $FeCl_3$, and 2.7×10^{-5} M ethylenediaminetetraacetic acid (EDTA) at pH 8.0–8.2. All distilled water used in these experiments was distilled a second time in a glass still.

Cells were inoculated at a cell density of about 800 cells per milliliter and harvested 6 days later at a density of about 6000 cells per milliliter. In preliminary studies it was found that extracts from cells harvested at midnight were about 10 times more active than those from cells harvested at noon, so the procedure was carried out thereafter at midnight. The cells were harvested with a Buchner funnel on Wratten no. 4 filter paper, washed several times with distilled water to remove residual salts and plunged into cold acetone at —25°C., removing a considerable amount of the pigment. The acetone was removed by filtration and the resultant powder dried *in vacuo* over calcium chloride and paraffin. A yield of about 45 mg of dry powder per liter of culture was generally obtained. Light intensity was measured with highly sensitive apparatus, utilizing a photomultiplier tube as described previously (Hastings, McElroy and Coulombre, '53), and recorded on an Esterline-Angus graphic meter.

EXPERIMENTAL RESULTS

Crude extracts

When initial preparations of the dry powder were mixed with distilled water a very faint, slowly decaying luminescence was observed. However, when distilled water was replaced with sea water, the intensity was increased several fold, suggesting a salt requirement in the reaction. In subsequent preparations care was taken to remove residual salt by washing the cells with distilled water, as described above. Such salt free powders then gave essentially no light when mixed with distilled water, but when optimum salt was added, a dim, but readily visible, luminescence occurred. The salt-free powder therefore was routinely extracted with distilled water (20 mg/ml) in the cold with a Potter homogenizer and centrifuged for 10 min. at 20,000 RPM in a Spinco preparative centrifuge (head no. 40) for 10 minutes at 0°C. The clear yellow-green supernatant contained the activity.

It was found that NaCl would completely replace sea water in stimulating luminescence. As shown in figure 1, unusually high concentrations of salt, about 1.2 M, are required for maximum activity. It was found that KCl, $(NH_4)_2SO_4$, and sodium and potassium phosphates (pH 6.6) were equally effective at the same concentration in replacing NaCl for the stimulation of luminescence. Versene (EDTA) was not inhibitory in a final concentration of 10^{-3} M when added secondarily. The salt requirement was also found in partially purified preparations of the enzyme (see below). The role of salt in this reaction is not clear and has not been studied in any detail. Salt in lower concentrations is known to affect light production in other luminescent reactions however (Anderson, '37; McElroy, Hastings, Sonnenfeld and Coulombre, '54).

The reaction is markedly dependent upon pH, as shown in figure 2, with an optimum at about pH 6.6. Similar results have been obtained using sodium phosphate and potassium phosphate buffers, including the sharp drop in activity above

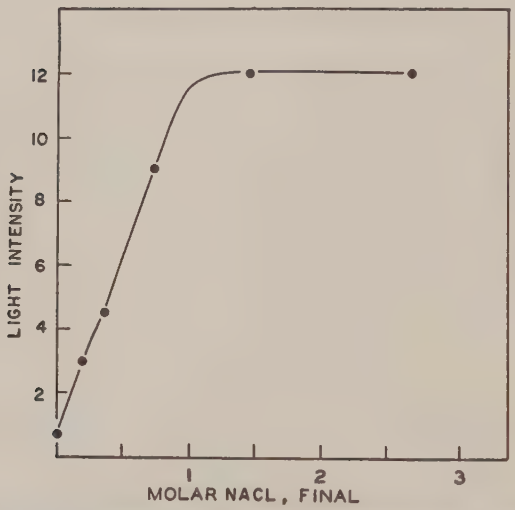

Fig. 1 Relationship between NaCl concentration and light intensity. Reaction mixture contained 1.0 ml crude extract, 0.4 ml 0.05 M tris-maleate buffer pH 6.4, water and NaCl to a total volume of 2.5 ml.

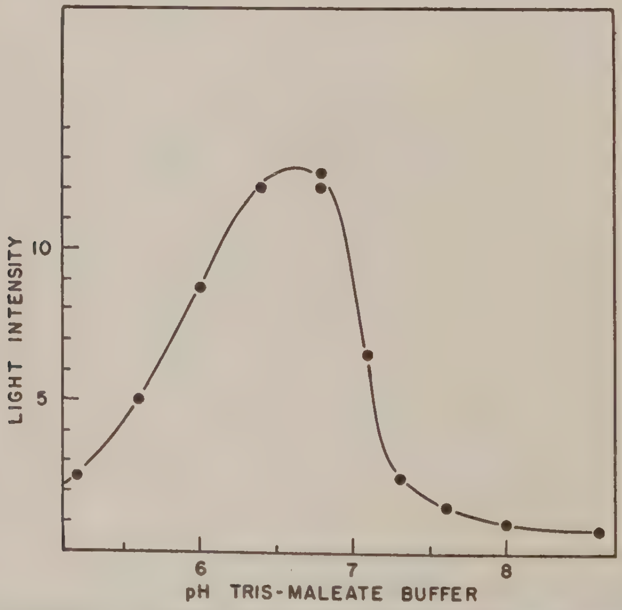

Fig. 2 Relationship between pH and light intensity. Reaction mixture contained 1.0 ml crude extract, 0.4 ml 0.05 M tris-maleate buffer, 0.6 ml 6.1 M NaCl, and 0.5 ml H_2O.

pH 7. There was little difference betwen different buffers in the maximum luminescence obtained, and tris-maleic acid buffer (trihydroxyamino-methane and maleic acid adjusted to pH with NaOH) was used routinely in all experiments.

The light emitted by the living cells is blue to blue-green. Utilizing concentrated extracts, it has been possible to determine the emission spectrum of the *in vitro* reaction. As shown in figure 3, the emission peak is at about 478 mμ. Since ammonium sulfate in place of NaCl had been found to result in a much slower decay of luminescence, it was used in these experiments. The reaction mixture was placed at the entrance slit of a Bausch and Lomb grating monochromator, and the photomultiplier tube at the exit slit. Both slits were set at 5 mm and the light intensity was recorded at various wave length settings. The values obtained were corrected both for

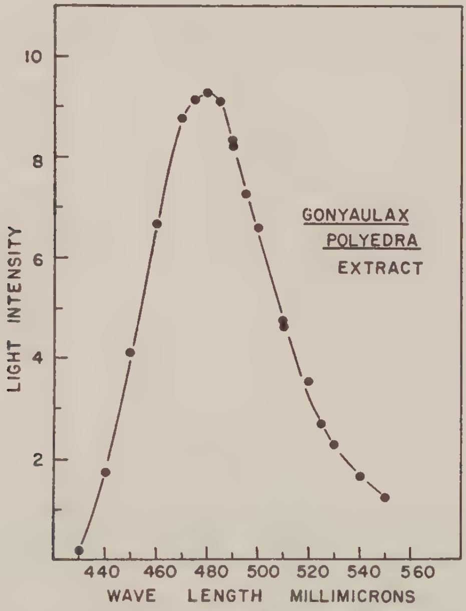

Fig. 3 Emission spectrum of *Gonyaulax* extracts. Reaction mixture contained 1.6 ml crude extract, 0.2 ml 0.1 M tris-maleate buffer pH 6.6, and 0.2 ml 6 M $(NH_4)_2SO_4$. Time during determinations, 6 min.

the decay of the reaction and for the color sensitivity of the phototube.[2] A second determination gave identical results.

The effect of temperature upon the reaction was determined both with the crude extract and with the purified enzyme (see below). In both cases the optimum was found to be at about 24°C., and a curve for the purified enzyme is shown in figure 4. The reaction mixture without enzyme was adjusted to the desired temperature and placed in front of the phototube. Enzyme was rapidly added to initiate the reaction and the initial light intensity recorded as the reaction rate. An Arrhennius plot of the data indicates an activation energy of about 9000 calories, and a similar plot for the rate of enzyme inactivation by heat gives an activation energy of about 60,000 calories.

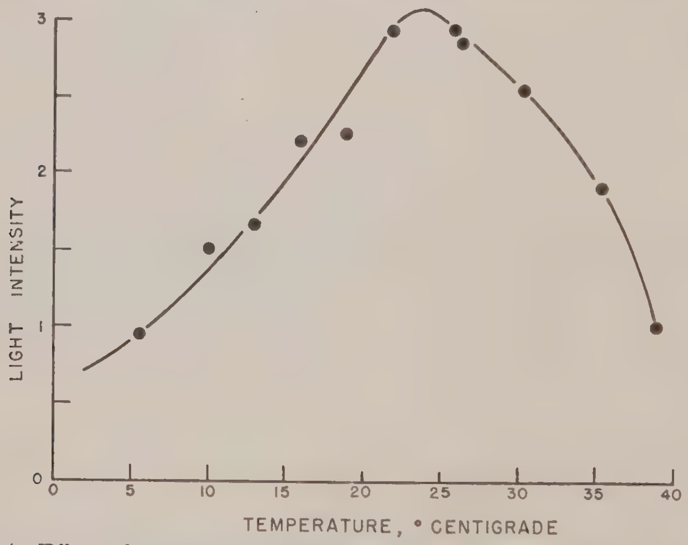

Fig. 4 Effect of temperature upon luminescence. Reaction mixture contained 0.2 ml purified enzyme, 1.0 ml boiled crude extract, 1.2 ml 6.1 M NaCl, 0.4 ml 0.1 M tris-maleate buffer pH 6.6, and 1.2 ml H_2O.

Enzymatic activity was completely destroyed at 100°C. for one minute, but the loss of activity of purified enzyme was less than 5% after two hours at 22°C. However, the crude extract is quite unstable and loses activity relatively rapidly, as shown in figure 5. In this experiment the crude extract was kept in an ice bath at about 4°C. and at the times indicated was assayed for activity. Varying the temperature of the extract from 4° to 30°C. during this period had only a relatively small effect upon the rate of decay. This suggests that the decrease is not due to enzyme destruction since denaturation is generally characterized by a large temperature coefficient. Additional evidence for this is presented in a later section. The possibility that a slow auto-oxidation of substrate was taking place was tested by bubbling aliquots with pure oxygen and pure nitrogen. In each of three trials oxygen not only failed to accelerate the decay of the extract but actually resulted in a slight increase in activity. It is considered possible that the decay is due to the production of potent in-

---

[2] We are grateful to Mr. John Tyler for determining the color sensitivity of our phototube.

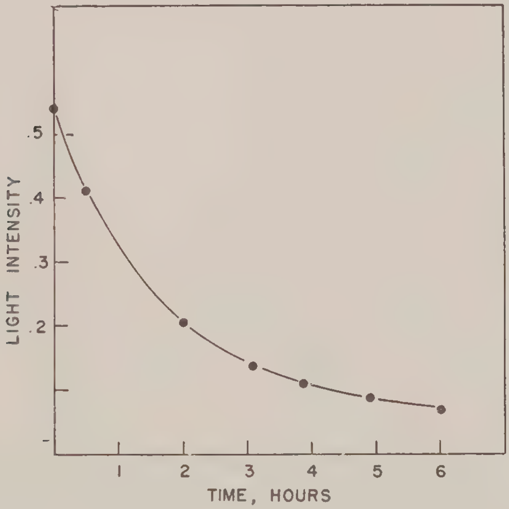

Fig. 5 Spontaneous decay in activity of crude extract kept at 4°C. Aliquots were taken at time intervals indicated and assayed for luminescence. Reaction mixture contained 0.5 ml crude extract, 0.4 ml 0.05 M tris-maleate buffer pH 6.6, 0.6 ml 6.1 M NaCl, and 0.5 ml H_2O.

hibitors since old extracts which have decayed are highly inhibitory to fresh extracts.

The effect of concentration of crude extract is shown in figure 6. The shape of the curve indicates that a second factor, presumably substrate, is limiting in the reaction at low concentrations.

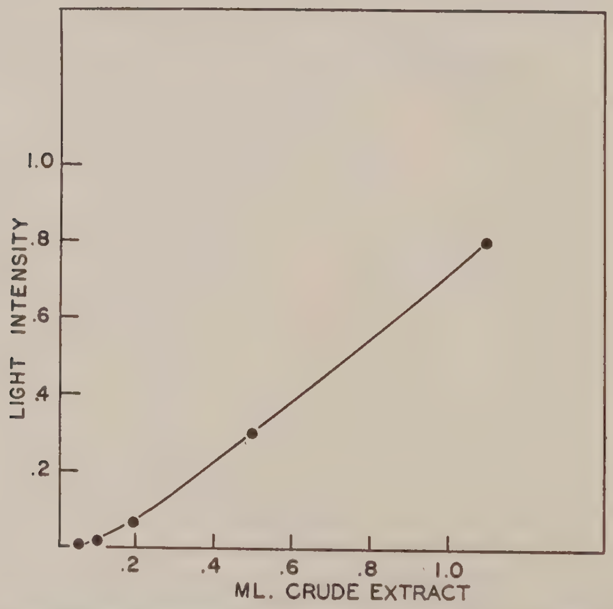

Fig. 6 Relationship between the concentration of crude extract and light intensity. Reaction mixture consisted of 0.5 ml 6.1 M NaCl, 0.4 ml 0.05 M tris-maleate buffer pH 6.6, and water and enzyme to a volume of 2.0 ml.

The intensity of luminescence of the crude extract is dependent upon oxygen concentration. When hydrogen is bubbled through a luminescing reaction mixture, the intensity decreases to a low level. When air is subsequently readmitted, the intensity is increased. No excess flash of luminescence, such as has been reported in the case of extracts of *Cypridina,* (Chance, Harvey, Johnson and Millikan, '40), the firefly (Hastings, McElroy and Coulombre, '53) and the luminous bacteria (Hastings, '55), was observed. It may be concluded however that the *Gonyaulax* reaction is an oxidative one similar, in this respect, to other bioluminescent reactions.

Purified enzyme

Preliminary purification procedures have resulted in the separation of the enzyme from the heat stable substrate or substrates. Ammonium sulfate was added to the crude extract to 35% saturation, and allowed to stand for 15 minutes at 5°C., and centrifuged at 25,000 RPM (Spinco, Head no. 40) for 12 minutes. A green precipitate resulted, which was inactive, insoluble in water, methanol soluble, and showed absorption suggesting a mixture of chlorophyll and carotenoid pigments. Ammonium sulfate was added to the supernatant to 75% saturation and the resulting precipitate was clear and readily soluble in water. By itself this fraction was completely inactive, but when added together with a boiled crude extract, excellent activity resulted. Figure 7 shows the effect of purified

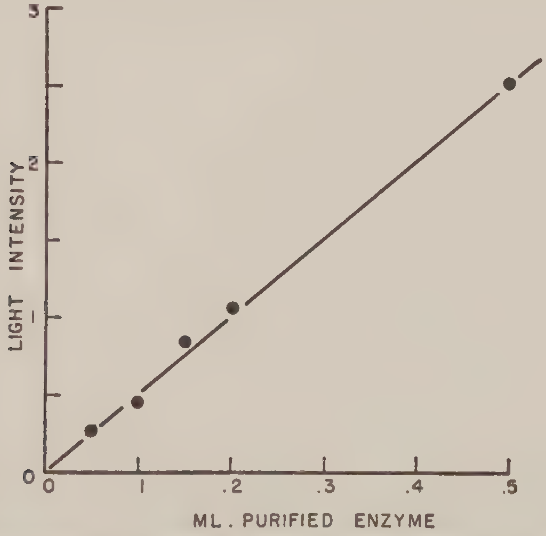

Fig. 7 Relationship of purified enzyme concentration to light intensity. Reaction mixture contained 0.6 ml 6.1 M NaCl, 0.5 ml heated crude, 0.2 ml 0.1 M tris-maleate buffer pH 6.6, and water and enzyme to a volume of 2.0 ml.

enzyme concentration upon initial light intensity with boiled crude extract (non-saturating concentration) added, indicating that no other factor was carried along in the enzyme fraction. The reaction with the purified enzyme appears to have the same characteristics as the crude extract insofar as the salt requirement, pH optimum and temperature coefficient are concerned.

Figure 8 shows the effect of different added amounts of a boiled crude extract upon the initial light intensity. The boiled crude extract appears to be relatively stable, but different preparations have given different values for maximum light intensity at saturation. This again suggests that inhibitors in crude extracts may influence the reaction, and that in such experiments they may have been present in greater or lesser concentrations.

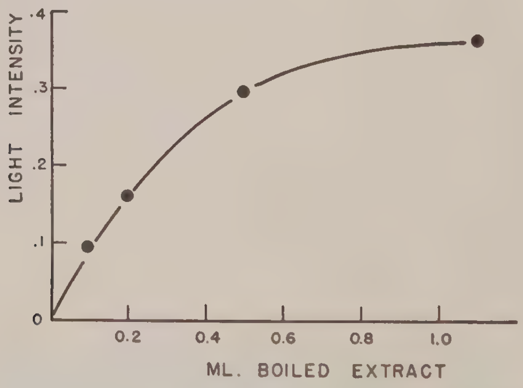

Fig. 8 Effect of the concentration of boiled crude extract upon luminescence of purified enzyme. Reaction mixture was composed of 0.6 ml 6.1 M NaCl, 0.2 ml 0.1 M tris-maleate buffer pH 6.6, 0.1 ml purified enzyme, and boiled crude extract and water to a volume of 2.0 ml.

Since it was thought that the decrease in activity of the crude extract (fig. 5) was not due to enzyme destruction, it was of interest to check this by determining the activity of an ammonium sulfate fraction from freshly prepared crude extract together with the activity of a similar fraction prepared from crude extract in which the activity had decayed

The activities before fractionation were in the ratio of 7.0 to 1.3 for fresh extracts and decayed extracts respectively, while the purified fractions had relative activities of 3.5 and 2.0 respectively, indicating that a major portion of the enzyme is recoverable after the decay of the crude extract.

The nature of the factor in the heat stable fraction has not been determined. In preliminary dialysis experiments it has not been possible to demonstrate any activity in the dialysate. A variety of cofactors, intermediates and other compounds have been tested with regard to their effect upon the reaction, and for their ability to replace this factor. None have been found to be active. Those tested include adenosine triphosphate, oxidized and reduced diphosphopyridine nucleotide, triphosphopyridine nucleotide, dodecyl aldehyde, oxidized and reduced flavins (riboflavin, riboflavin-5-phosphate, and flavin mononucleotide), thiamine pyrophosphate, coenzyme A, vitamin B_{12}, choline, acetylcholine, lipoic acid, liver and yeast concentrates, glucose, and glucose-6-phosphate. Crude homogenates of various organs of the rat and of the Pacific mussel were also tested and found to be either inactive or inhibitory. Irradiation with ultraviolet light, which has been shown to be effective in increasing enzyme activity in extracts of luminous bacteria, was found to have no similar effect upon the *Gonyaulax* enzyme. Cross tests between *Cypridina* luciferin and luciferase and similar *Gonyaulax* preparations did not give luminescence.

As mentioned previously, luminescence of the living organism is from 40 to 60 times greater at night than by day. Similarly, crude extracts prepared at night were found to be more active than those prepared in the daylight, but only by a factor of from 5 to 15 times. By ammonium sulfate fractionation it has been found that at least part of this difference in activity can be ascribed to enzyme concentration, and part to the activity of the heat stable fraction. In one experiment the crude extract from the night harvest was 8 times as active as the one from the daytime harvest. The purified enzymes from these fractions differed in activity roughly by a factor of 4 and the activities of the boiled crude extracts differed by a factor of about two, the fraction from the night harvest being more active in each case. Presumably therefore, both enzyme and substrate vary in concentration during the course of the day.

The decrease in luminescence with time in the reaction mixture is approximately logarithmic, suggesting that the reaction is first order in nature. In crude extracts the decay during the first two or three minutes is more rapid than during the later logarithmic period. In the purified extracts this phenomenon is much less marked. When $(NH_4)_2SO_4$ is used in place of NaCl in the reaction, the velocity constant is decreased by a factor of approximately 3/5.

It is of interest to mention that the classical luciferin-luciferase test does not give a positive reaction with *Gonyaulax* extracts. The test involves restoring luminescence to a reaction mixture which is dark following luminescence by adding an extract which was boiled before the decay of luminescence (see Harvey, '52). This is interpreted as a demonstration of the oxidation or utilization of a heat stable substrate, usually called luciferin, by the enzyme luciferase. The dark mixture contains only luciferase (the luciferin having been utilized in the luminescent reaction), and the boiled extract unoxidized luciferin. In the case of *Gonyaulax*, when boiled crude extract is added to a reaction mixture which is dim following luminescence a very slight (up to 10%) stimulation sometimes occurs, and at other times none at all. From the experiments with the purified enzyme it is clear that both an enzyme and a heat stable factor are involved in the reaction in a classical type luciferin-luciferase mechanism. It is not clear why the usual luciferin-luciferase test is negative, but the possibility that a product of the luminescent reaction itself is highly inhibitory is an attractive one. Extracts which have decayed spontaneously or those which have decayed with luminescence are inhibitory to the luminescent reaction, and the inhibition may be such that little or no response is obtained in the luciferin-luciferase test. It is also of interest that the living cell, which emits a flash upon stimulation, is rapidly (within 10–20 sec.) and almost completely fatigued with continuous stimulation. It is possible that this decrease in luminescence is due not to the exhaustion of the substrate but to the intracellular accumulation of the inhibitory products of the reaction.

DISCUSSION

A rhythmic expression of a variety of activities has been observed in a large number of organisms (Welsh, '38; Kleitman, '49). The present studies however, have provided evidence for the nature of the biochemical changes which may be correlated with the physiological rhythmicity of the organism. Although the variations in enzyme and substrate concentrations found in *Gonyaulax* occurred in phase with the diurnal changes in light intensity, there is good evidence from studies with living cells (Sweeney and Hastings, '57) that similar changes occur when the organisms are kept in the dark. Cells kept in continuous darkness show persistent fluctuations in light intensity. In preliminary studies it has been found that these fluctuations are correlated with similar changes in the activities of the extracts. The rhythmicity is therefore evidently at least partially the result of changes in concentration of the luminescent system. Further studies should provide information relevant to the general problem of the mechanisms controlling enzyme synthesis and destruction.

Certain properties of *Gonyaulax* extracts suggest that the reaction is a relatively simple oxidation such as occurs in *Cypridina,* where the reaction is often written as

$$\begin{aligned} LH_2 + \tfrac{1}{2}O_2 &\xrightarrow{\text{luciferase}} L^* + H_2O \\ L^* &\xrightarrow{\hphantom{\text{luciferase}}} L + \text{light} \end{aligned} \tag{1}$$

where LH_2 is the reduced substrate, luciferin, present as such in the extracts. When luciferin is oxidized in the presence of the enzyme (luciferase) an excited molecule results (L^*) which subsequently falls to the ground state with the emission of a quantum of light. All three bioluminescent reactions which have been studied are known to involve such a terminal oxidative reaction, which is characteristically very rapid (Hastings, McElroy and Coulombre, '53; Chance, Harvey, Johnson and Millikan, '40; Strehler and Cormier, '54; Hastings, '55). In both the firefly and bacterial extracts however, there are dark reactions preliminary to the oxidative step which are relatively slow, resulting in high overall

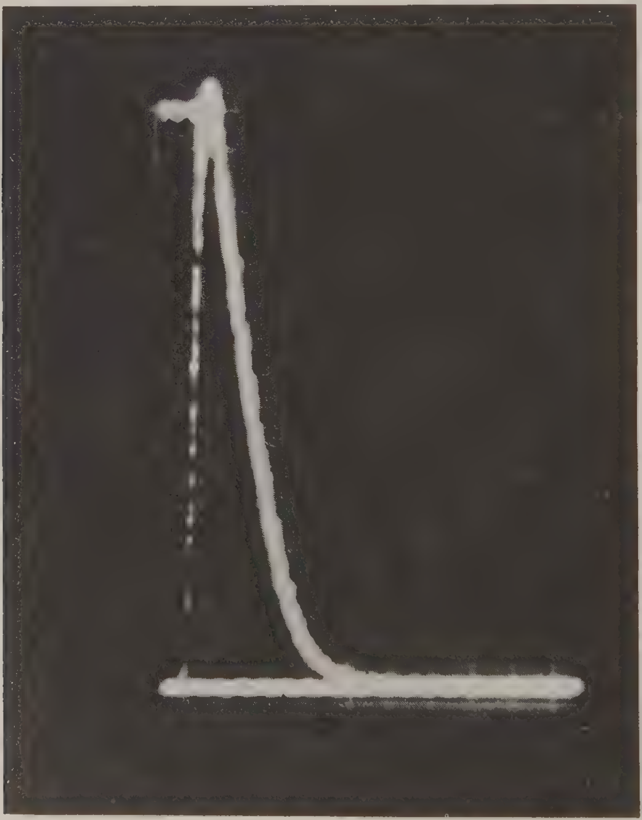

Fig. 9 Luminescent flash of *Gonyaulax* in response to mechanical stimulation, as photographed from the oscilloscope screen. Ordinate light intensity, abscissa time. Sweep time, 0.25 sec. One small division equals 0.025 sec. A test tube containing 5 ml of culture (about 1000 cells/ml.) was placed in front of the phototube and tapped very lightly. The flash is presumably the response of a single cell or of several cells flashing simultaneously.

activation energies (Strehler, '55; McElroy and Strehler, '49). Since the activation energy of *Gonyaulax* luminescence is lower (somewhat higher than *Cypridina),* it suggests that only a terminal rapid oxidation is involved in the luminescence of the extracts. If, as is possible, additional reactions preceding the oxidation are involved, they must be very rapid. The logarithmic decay is also in agreement with such a mechanism.

The blue color of the light is very similar to that of *Cypridina.* Since no light was obtained when *Cypridina* luciferin was added to crude or purified *Gonyaulax* enzyme, it must be concluded that the luciferins are different, even though it is possible that the mechanisms may be similar. It also seems certain that neither bacterial nor firefly components are involved in the reaction. It seems that not only has luminescence evolved independently in a great variety of unrelated organisms, but also, as Harvey ('53) has pointed out, that a considerable number of different luminescent systems have arisen independently.

The very rapid flash of *Gonyaulax* (fig. 9) is an excellent example of a precisely controlled biological reaction, and it is most logical to consider it as a type of cellular excitation. The mechanism by which an enzymatic reaction may be so regulated constitutes a major problem in modern physiology and biochemistry. As pointed out by Harvey ('52), the unicellular luminescent forms may be of great value in the study of these fundamental cellular processes.

SUMMARY

The extraction, partial purification and properties of the luminescent system in the marine dinoflagellate *Gonyaulax polyedra* are described. Crude cell-free water extracts of acetone powders emit light in the presence of salts, such as NaCl. The reaction also requires oxygen, and shows an optimum activity at pH 6.6 and 24°C. The light is blue-green with the emission peak at 478 mμ. The enzyme, purified by ammonium sulfate fractionation, requires for luminescence a

factor present in boiled crude extracts. It is suggested that this factor may be designated as *Gonyaulax* luciferin. The reaction appears to involve an oxidation of the luciferin. The intensity of luminescence of living cells shows a type of diurnal rhythmicity. The amount of both luciferin and luciferase which can be extracted from cells is correlated with these rhythmic intensity fluctuations. This phenomenon, as well as the mechanism of the reaction, is discussed.

LITERATURE CITED

ANDERSON, R. S. 1937 Chemical studies on bioluminescence. IV. Salt effects on the total light emitted by a chemiluminescent reaction. J. Amer. Chem. Soc., *59:* 2115–2117.

CHANCE, B., E. N. HARVEY, F. H. JOHNSON AND G. MILLIKAN 1940 The kinetics of bioluminescent flashes. A study in consecutive reactions. J. Cell. and Comp. Physiol., *15:* 195–215.

HARVEY, E. N. 1952 Bioluminescence. Academic Press, New York, N. Y.

——— 1953 Bioluminescence: Evolution and comparative biochemistry. Federation Proc., *12:* 597–600.

HASTINGS, J. W. 1955 The effect of oxygen upon the luminescence of bacterial extracts. Anat. Rec., *122:* 458.

HASTINGS, J. W., W. D. MCELROY AND J. COULOMBRE 1953 The effect of oxygen upon the immobilization reaction in firefly luminescence. J. Cell. and Comp. Physiol., *42:* 137–150.

HASTINGS, J. W., AND W. D. MCELROY 1955 Purification and properties of bacterial luciferase, in The Luminescence of Biological Systems (F.H. Johnson, ed.) pp. 257–264. A.A.A.S. Press, Washington, D.C.

HAXO, F. T., AND B. M. SWEENEY 1955 Bioluminescence in *Gonyaulax polyedra*, in The Luminescence of Biological Systems (F. H. Johnson, ed.) pp. 415–420. A.A.A.S. Press, Washington, D.C.

KLEITMAN, N. 1949 Biological rhythms and cycles. Physiol. Rev., *29:* 1–30.

MCELROY, W. D., J. W. HASTINGS, V. SONNENFELD AND J. COULOMBRE 1954 Partial purification and properties of bacterial luciferin and luciferase. J. Bacteriol., *67:* 402–408.

MCELROY, W. D., AND J. W. HASTINGS 1955 Biochemistry of firefly luminescence, in The Luminescence of Biological Systems (F. H. Johnson, ed.) pp. 160–198. A.A.A.S. Press, Washington, D.C.

MCELROY, W. D., AND B. L. STREHLER 1949 Factors influencing the response of the bioluminescent reaction to adenosine triphosphate. Arch. Biochem., *22:* 420–433.

PRINGSHEIM, E. G. 1946 Pure Cultures of the Algae. pp. 41–42. Cambridge Univ. Press., 119 pages.

STREHLER, B. L. 1955 Factors and biochemistry of bacterial luminescence. in The Luminescence of Biological Systems (F. H. Johnson, ed.) pp. 209–255. A.A.A.S. Press, Washington, D. C.

STREHLER, B. L., AND M. J. CORMIER 1954 Kinetic aspects of the bacterial luciferin-luciferase reaction *in vitro*. Arch. Biochem. and Biophys., *53:* 138–156.

SWEENEY, B. M., AND J. W. HASTINGS 1957 Characteristics of the diurnal rhythm of luminescence in *Gonyaulax polyedra*. J. Cell. and Comp. Physiol., *49:* 115–128.

TSUJI, F. I., A. M. CHASE AND E. N. HARVEY 1955 Recent studies on the chemistry of *Cypridina* luciferin, in The Luminescence of Biological Systems (F. H. Johnson, ed.) pp. 127–159. A.A.A.S. Press, Washington, D.C.

WELSH, J. H. 1938 Diurnal rhythms. Quart. Rev. Biol., *13:* 123–139.

Reproduced by Permission

Reprinted from Journal of Bacteriology
Vol. 73, No. 4, pp. 563-568, April, 1957
Printed in U.S.A.

BAROPHILIC BACTERIA IN SOME DEEP SEA SEDIMENTS[1]

CLAUDE E. ZOBELL AND RICHARD Y. MORITA[2]
Scripps Institution of Oceanography, University of California, La Jolla, California

Received for publication October 29, 1956

Barophile is a term coined by ZoBell and Johnson (1949) to describe bacteria which grow preferentially or exclusively at moderately high hydrostatic pressures (Johnson *et al.*, 1954). Most terrestrial bacteria appear to be affected adversely by pressures of 200 to 600 atm. Similar results were obtained by Oppenheimer and ZoBell (1952) working with marine bacteria, virtually all of which were inhibited by pressures ranging from 200 to 600 atm, although a few deep sea cultures reproduced at 1,000 atm.

Little is known regarding the occurrence, characteristics, and physiological activities of bacteria on the deep sea floor, where pressures approaching 1,100 atm prevail, although fragmentary observations indicate that shallower marine muds on the continental slopes support bacterial populations comparable to those occurring in soil (ZoBell, 1946; Limberg-Ruban, 1952). Even organic-poor pelagic sediments, including red clay and globigerina ooze collected at stations several hundred miles from the nearest land and from water depths ranging from 1,707 to 5,942 meters during the Mid-Pacific Expedition to the Marshall Islands, were shown by Morita and ZoBell (1955) to contain from 10 to 10^4 viable bacteria per gram. The Danish *Galathea* 'Round-the-World Expedition (Spärck, 1952) afforded an opportunity to demonstrate bacteria in a large number of sediment samples taken from depths of 7,000 to more than 10,000 meters. The pressures at these depths are about 700 to more than 1,000 atm, the pressure depth gradient in the sea being approximately 0.1 atm per meter. One atmosphere is equivalent to 1.0332 kg per cm^2, 1.0133 bars, or 14.696 psi.

MATERIALS AND METHODS

The R.D.N. *Galathea,* a 1,630-ton corvette converted for studying the deep sea floor, was equipped with radar, loran, sonic depth recorders, and other modern navigational aids. Locating oceanic deeps and staying on station for prolonged periods while taking bottom samples required the best of navigation, for which a high tribute is due Captain Sven Greve and his staff of 90 Danish seamen. The ship was equipped with a tapered dredging cable having dimensions as shown in table 1. The tapering was designed to provide a cable that could support its own weight in the water with a load of 26,000 kg from the greatest depths in the sea (Wüst, 1950; Carruthers and Lawford, 1952).

Radially central subsections of bottom sediment were taken aseptically from cores or grab hauls of mud for bacteriological examination immediately after being hauled on deck. Hauling samples from a depth of 10,000 m required from 8 to 18 hr, during which the pressure changed from 1,000 atm at the bottom to about 1 atm at the surface, and the temperature changed from about 3 C at the bottom to 30 C at the surface in tropical waters. The effect of these changes in climate on the deep sea bacteria is yet to be determined. Many survived, but we have no way of knowing how many perished. Obviously our observations are on the survivors, which slowly die off at 30 C or when held in the refrigerator at normal atmospheric pressures. Most marine bacteria are thermosensitive, many being killed in 10 min at a temperature of 30 C or less (ZoBell and Conn, 1940). In order to minimize mortality, samples were processed as soon as possible. Part of the material was used at once to inoculate nutrient media for incubation at different temperatures and pressures. The remainder of the sediment sample was stored in the refrigerator (3 to 5 C) in pressure cylinders at *in situ* pressures (700 to 1,000 atm).

The nutrient medium employed for demon-

---

[1] Contribution from the Scripps Institution of Oceanography, New Series No. 913. This work was supported in part by grants from the Rockefeller Foundation and from the Office of Naval Research, U. S. Navy Department.

[2] Present address: Biology Department, University of Houston, Houston, Texas.

TABLE 1

Dimensions of dredging cable

Section No.	Diameter	Length
	(mm)	*m*
1	9.3	3,600
2	11.6	1,750
3	13.2	770
4	14.7	1,330
5	17.1	1,730
6	19.6	1,080
7	20.2	980
8	21.8	1,060
Total		12,300

strating the most probable number (MPN) of bacteria by the minimum dilution method consisted of peptone (Difco), 5.0 g; soluble starch, 2.0 g; KNO_3, 1.0 g; yeast extract (Difco), 1.0 g; and $FePO_4$, 0.1 g. per L of aged sea water (salinity 25 per mille). Following autoclave sterilization the pH was 7.7. It was dispensed in 9.0-ml quantities in 15-ml screw cap bottles for preparing proper dilutions of inoculated sediment sample (diluted seriatim by powers of 10) and for incubating at 1 atm. Portions of the inoculated medium were transferred aseptically to small glass vials (10 by 50 mm) for incubation at high pressures. The vials were closed with tapered No. 000 Neoprene stoppers, which functioned as pistons when the tubes were subjected to pressure in steel cylinders (ZoBell and Oppenheimer, 1950) filled with hydraulic fluid. Air was introduced in part of the vials for estimating MPN of aerobes; free oxygen was excluded from other vials employed for estimating MPN of anaerobes. Sulfate reducing bacteria were detected and cultivated in medium M-10E: K_2HPO_4, 0.2 g; $MgSO_4 \cdot 7\ H_2O$, 0.2 g; Ca lactate, 3.5 g; ascorbic acid, 1.0 g; $FeSO_4\ (NH_4)_2SO_4 \cdot 6\ H_2O$, 0.1 g; peptone (Difco), 1.0 g; yeast extract (Difco), 1.0 g; agar (Difco), 3.0 g; and aged sea water (salinity 25 per mille), 1000 ml.

The inoculated media were incubated for a minimum of 2 weeks at the stated temperatures and pressures. Turbidity and direct microscopic examination (in questionable cases) were employed as criteria of growth or reproduction of bacteria. Portions of media in which bacteria grew were treated with iodine reagent to determine starch hydrolysis. Other portions were examined for the appearance of nitrite or for the disappearance of nitrate as criteria of nitrate reduction. An increase in the ammonium content of the medium was indicative of the activity of ammonifiers. The production of black ferrous sulfide in the anaerobic series indicated the activity of sulfate reducers.

(194)

RESULTS AND DISCUSSION

Data summarized in table 2 are representative of results which, for the first time, prove the presence of living bacteria at depths exceeding 10,000 meters. Prior to the *Galathea* Expedition, 5,942 meters was the greatest depth at which bacteria had been found. In numerous sediment samples taken at depths of about 10,000 meters were found from 10^4 to 10^5 viable bacteria per gram wet weight. In overlying water, except that closely associated with bottom deposits, the bacterial population was generally sparse, ranging from less than 1 to no more than 10^3 viable bacteria per ml. This should dispel any doubt that the bacteria detected in the bottom sediment samples could possibly be contaminants from overlying water through which the deep sea sampling devices passed. Moreover, unlike most bacteria collected from shallow depths, most of those in the deep sea sediment samples grew preferentially or exclusively at high pressures and at refrigeration temperatures. Less than 10 per cent of the aerobic bacteria from the bottom of the Philippine Trench grew at either 30 C or at 1 atm.

Direct phase contrast microscopic examinations of sediment samples showed appreciably larger bacterial populations than the MPN indicated by growth in nutrient media, probably owing to the death of some bacteria in transit to the surface and to the inadequacy of the media to provide for the cultural requirements of all deep sea bacteria. Since there is evidence for the activity of bacteria on the deep sea floor, we were not surprised to find large bacterial populations. Nor did it seem surprising that bacteria grew at the high hydrostatic pressure and low temperatures characteristic of oceanic deeps. It seems singularly significant, though, that most of the bacteria from the Philippine Trench behaved as obligate barophiles. A good many tests made on those which grew at 1,000 atm demonstrated their inability to grow in similar media incubated at 1 atm. Similarly, among the many cultures tested, none which grew at 1 atm did so when incubated at 1,000 atm.

TABLE 2

MPN of different physiological types of bacteria detected per gram of wet sediment from the Philippine Trench in selective media incubated at different hydrostatic pressures at 3 to 5 C

	Galathea Station							
	No. 418		No. 419		No. 420		No. 424	
Latitude	10°13 N		10°19 N		10°24′ N		10°28′ N	
Longitude	126°43′ E		126°39′ E		126°40′E		126°39′ E	
Water depth	10,190 m		10,210 m		10,160 m		10,120 m	
	Incub. pressure (atm)							
	1	1,000	1	1,000	1	1,000	1	1,000
Total aerobes	10^3	10^6	10^3	10^5	10^4	10^5	10^4	10^6
Total anaerobes	10^3	10^5	10^4	10^5	10^3	10^5	10^4	10^5
Starch hydrolyzers	10^2	10^3	10	10^2	10	10^2	10^2	10^3
Nitrate reducers	10^2	10^5	10^2	10^4	10^3	10^5	10^2	10^5
Ammonifiers	10^3	10^5	10^3	10^4	10^3	10^5	10^3	10^5
Sulfate reducers	0	10^2	0	10	0	10^2	0	0

The significance of these latter cultures from the deep sea floor which grow at 1 atm but not at 1,000 atm nor at 30 C is unknown. Whether they would grow at other pressures or temperatures in media providing different combinations of nutrients or cultural conditions has not been examined exhaustively. These apparently alien bacteria may represent species which have settled from the surface to the sea floor where they remain dormant or, more probable, they are passive mutants. Incidentally, only a small percentage of them form endospores. There are numerous analogous anomalies on the apparent temperature requirements of bacteria. Bartholomew and Rittenberg (1949), for example, report finding up to 800 thermophilic bacteria per gram in long cores of deep sea mud (3,000 to 4,000 feet) having a temperature of about 3 C. These bacteria grew in nutrient medium at 60 C, but not at 20 C nor at 37 C. In frozen Arctic soils McBee and McBee (1956) similarly found many thermophilic bacteria which grew in nutrient medium at 55 C.

Nearly as many bacteria from the Kermadec-Tonga Trench (table 3) grew in nutrient media at 1 atm as at high *in situ* pressures. Actually, more anaerobes were detected in nutrient medium inoculated with sediment from a depth of 6,790 m (Station No. 650) when incubated at 1 atm than at 700 atm. Likewise, more aerobes were detected in medium incubated at 1 atm than at 1,000 atm in a sediment sample from a depth of 10,080 m (Station No. 686). Bacteria which are unable to grow at the high pressures where they are found may be alien to the deep sea floor or they may be passive mutants. Finding numerous aerobes buried at depths where ostensibly there is no free oxygen suggests their dormancy. From 10^4 to 10^6 aerobes per gram were found in mud cores 25 to 30 cm long, and from 10^3 to 10^4 aerobes per gram were found in 85- to 90-cm strata at the bottom of the Kermadec-Tonga Trench (ZoBell and Morita, 1957).

In most cases only a small percentage of the bacteria isolated from aerobic enrichment cultures grew when transferred to a similar medium from which oxygen was excluded. Conversely, a majority of the "anaerobes" grew readily when transferred to oxygenated medium, thereby indicating that they are either facultative aerobes or pseudo-anaerobes which can activate nitrate as an hydrogen acceptor. Many of the deep sea bacteria reduced nitrate at high hydrostatic pressures. This is noteworthy because not only is nitrate reduction by most surface dwelling bacteria, which we have investigated, inhibited when compressed to 400 to 600 atm, but their nitratase dehydrogenase system is irreversibly inactivated in a few hours at 1,000 atm (ZoBell and Budge, unpublished manuscript, 1957). This suggests that the enzyme systems of certain deep sea bacteria may differ from such systems of surface-dwelling prototypes.

Besides a few clostridia, sulfate reducers were the only strict anaerobes from deep sea sediments which developed at high hydrostatic pressures. From 10 to 100 bacteria per gram of sediment

TABLE 3

MPN of bacteria detected per gram of wet sediment from the Kermadec-Tonga Trench in selective media incubated at different hydrostatic pressures at 3 to 5 C

	Galathea Station							
	No. 649		No. 650		No. 658		No. 686	
Latitude Longitude Water depth	35°15′ S 178°40′ W 8,500 m		32°20′ S 176°54′ W 6,790 m		35° 51′ S 178°31′ W 7,900 m		28°30′ S 176°53′ W 9,800 m	
	Incub. pressure (atm)							
	1	850	1	700	1	800	1	1,000
Total aerobes	10^5	10^6	10^6	10^6	10^4	10^6	10^6	10^5
Total anaerobes	10^4	10^5	10^6	10^5	10^5	10^5		
Starch hydrolyzers	0	0	10	10				
Sulfate reducers	0	0	0	0				

TABLE 4

MPN of bacteria detected per gram of wet sediment from deeps in Indian Ocean in selective media incubated at different hydrostatic pressures

	Pressure	*Galathea* Station	
		No. 463 (Soenda Deep): 10°16′ S x 109°51′ E; water depth 7,020 m	No. 492 (Weber Deep): 5°31′ S x 131°01′ E; water depth 7,250 m
	atm		
Total aerobes	1	690,000	810,000
	700	1,050,000	2,300,000
	1,000	4,800	17,000
Starch hydrolyzers	1	100	10
	700	1,000	1,000
	1,000	0	0
Nitrate reducers at	1	10,000	1,000
	700	10,000	10,000
	1,000	10	10
Sulfate reducers at	1	0	0
	700	100	10
	1,000	0	0

from the Philippine Trench (table 2) reduced sulfate at 1,000 atm. A like number of bacteria from the Soenda Deep (7,020 m) and the Weber Deep (7,250 m) in the Indian Ocean reduced sulfate in medium incubated at 700 atm (table 4). There was no activity of sulfate reducers in these deep sea sediments incubated at 1 atm, although sulfate reducers which grow at 1 atm have been recovered from depths down to nearly 5,000 m (ZoBell and Rittenberg, 1948; Morita and ZoBell, 1955).

Growth of the obligate barophilic sulfate reducers from the Philippine Trench which grew at 1,000 atm but not at 1 atm was retarded at 1,200 atm. These cultures were killed during 2 weeks' compression at 1,500 atm at 3 C. They survived for several weeks in nutrient medium and in raw mud stored at 1 atm in the refrigerator. Although these cultures grew preferentially or exclusively when compressed to a pressure approximating that of their native habitat, like most barophilic bacteria that we have studied, their best growth is generally much slower than the normal growth of surface-dwelling bacteria at atmospheric pressure. Similarly, psychrophiles from the deep sea, high latitudes, or from frozen foods whose optima for growth are under 20 C reproduce much more slowly at these lower temperatures than mesophiles multiply at their higher optima, 20 to 45 C.

Incubation for from 2 weeks to 2 years in the refrigerator (3 to 5 C), or compression to from 700 to 1,000 atm may be required for psychrophilic or barophilic bacteria, respectively, to reproduce sufficiently to be detected by increased turbidity in nutrient media. Routinely an attempt is made in this laboratory to hold barophilic and psychrophilic cultures for at least 2 months before discarding as negative, and some cultures have developed only after being incubated for 2 years. Part of this prolonged period of incubation required for evidence of activity is attributable to a long lag phase or to slow acclimatization, but it is often attributable to a long generation time at low temperatures and high pressures.

Sulfate reducers from the Weber Deep have been maintained compressed to 700 atm at 3 to 5 C for more than 5 years and are still under observation at the Scripps Institution. Upon decompressing and opening the pressure vessels for examination of some of the original sediment sample, the emanation of hydrogen sulfide indicated the activity of sulfate reducers during storage. Shortly after collection, several small quantities of the mud were used to inoculate appropriate medium in piston stoppered vials for enrichment in the refrigerator at 700 atm. After incubation for 60 days there was no evidence of sulfate reduction, but after 10 months sulfide was found in most vials inoculated with 0.1 or 0.01 g of mud from the Weber Deep. The uninoculated controls were negative. Likewise there was no evidence of sulfate reduction after incubation for 26 months at 1 atm in similar medium inoculated with some of the original mud sample or with enrichment cultures which developed at 700 atm.

The obligate barophilic sulfate reducing bacteria from the Weber Deep have been transplanted five successive times and kept growing when compressed to 700 atm at 3 to 5 C. Morphologically they appear as small ovoid cells about 0.3 μ in width and 0.5 to 0.8 μ in length, thus differing in both size and shape from sulfate reducers commonly classified as species of the genus *Desulfovibrio*. Though highly pleomorphic (Butlin *et al.*, 1949; Pochon and Chalvignac, 1952), known *Desulfovibrio* species are ordinarily comma shaped organisms 0.5 to 1.0 μ wide and 3 to 5 μ long. The barophilic sulfate reducer from the Weber Deep is gram negative and has neither flagella nor endospores. It is believed to be a new species, but further studies must precede its naming. Pressure tolerance is probably not a sufficiently distinctive characteristic to delineate species, particularly since deep sea bacteria may be remnants of surface dwelling forms which have become acclimatized to high pressures while sinking to the sea floor. Pressure is known to affect the morphology of bacteria (ZoBell and Oppenheimer, 1950) and it may have mutagenetic effects.

Barophilic bacteria in abundance were also found on the integument and in the gut of many deep sea animals. The observations on such bacteria, though, have little quantitative significance because of the crushed or contaminated condition of the animals. All of the deep sea animals were dead upon reaching the ship's deck, presumably killed by the rigorous change in climate during transit from the deep sea floor to the surface, coupled with mechanical attrition with marine material in nets, dredges, and trawls. Many of the animals are normally mud eaters or detritus feeders, and may obtain an appreciable part of their nutrition from the ingestion and digestion of bacteria. The "standing crop" of bacteria in the topmost 1-cm layer of deep sea mud was estimated (ZoBell, 1954) to contain between 0.001 and 0.005 g of organic carbon per m². If these bacteria reproduce at rates comparable to rates observed in the laboratory under normal conditions of temperature, pressure, and nutrients, the annual "crop" or yield may amount to 0.5 g of organic (bacterial) carbon per m² in the topmost 1 cm of mud.

Spärck (1952) estimated that the total animal life on the deep sea floor amounts to 1 g per m². Among the many animals shown by the *Galathea* Expedition to live at depths of 10,000 m or more were Actinia, Amphipoda, Holothuriodea, Lamellibranchiata, Sipunculoidea, and Tanaidacea. Additionally from depths of 7,000 to 9,000 m were recovered Asteroidea, Branchyura, Cirripedia, Crinoidea, Echinoidea, Echiouroidea, Gastropoda, Hydroidea, Pisces, Polychaeta and Spongia.

ACKNOWLEDGMENTS

The authors are grateful to Dr. Anton Fr. Bruun (1955), scientific leader of the *Galathea* Expedition, as well as to other scientists, officers, and crew members whose cooperation and contributions made these collections and observations possible. Special thanks are due Commander Tage Feddersen, the ship's physician, who helped with many aspects of the bacteriological work.

SUMMARY

Bacterial populations ranging from 10^3 to 10^6 per g of wet mud were demonstrated in several samples taken from depths of 7,000 to 10,000 m or more. Some of the deep sea bacteria appear to be obligate barophiles which grow when com-

pressed to 700 to 1,000 atm. Deep sea bacteria which grow at 1 atm but not at the high pressures of the environment where found may be dormant aliens from shallower depths, or they may be passive mutants, or all of their cultural requirements may not have been satisfied by the laboratory conditions.

Even under optimum conditions for reproduction barophilic bacteria, like psychrophilic forms, grow very slowly. Cultures of obligate barophilic sulfate reducing bacteria have been transplanted several times and maintained in the laboratory for more than 5 years.

Many barophilic bacteria were found associated with deep sea fauna. On the deep sea floor bacteria may contribute substantially to the nutrition of animals

REFERENCES

Bartholomew, J. W. and Rittenberg, S. C. 1949 Thermophilic bacteria from deep ocean bottom cores. J. Bacteriol., **57**, 658.

Bruun, A. F. 1955 Life and life conditions of the deepest deep sea. Proc. 8th Pac. Sci. Congr., **1**, 399–409.

Butlin, K. R., Adams, M. E., and Thomas, M. 1949 The morphology of sulfate-reducing bacteria. J. Gen. Microbiol., **3**, 3–4.

Carruthers, J. N. and Lawford, A. L. 1952 The deepest oceanic soundings. Nature, **169**, 601–603.

Johnson, F. H., Eyring, H., and Polissar, M. J. 1954 *The kinetic basis of molecular biology*, pp. 286–368. John Wiley & Sons, Inc., New York.

Limberg-Ruban, E. L. 1952 Number of bacteria in the water and floor of the northwestern part of the Pacific Ocean. Akad. Nauk. SSSR Zool. Inst., **3**, 138–141.

McBee, R. H. and McBee, V. H. 1956 The incidence of thermophilic bacteria in Arctic soils and waters. J. Bacteriol., **71**, 182–185.

Morita, R. Y. and ZoBell, C. E. 1955 Occurrence of bacteria in pelagic sediments collected during the Mid-Pacific Expedition. Deep-Sea Research, **3**, 66–73.

Oppenheimer, C. H. and ZoBell, C. E. 1952 The growth and viability of sixty-three species of marine bacteria as influenced by hydrostatic pressure. J. Marine Research, **11**, 10–18.

Pochon, J. and Chalvignac, M. A. 1952 Sur l'instabilité des charactères d'une souche de Sporovibrio. Ann. inst. Pasteur, **82**, 399.

Spärck, R. 1952 Revealing the secrets of the deep. The Galathea Expedition of 1950–52. Danish Foreign Office J., **6**, 1–7.

Wüst, G. 1950 Die grössten Tiefen des Weltmeeres in kritischer Betrachtung. Die Erde, **3**, 203–214.

ZoBell, C. E. 1946 *Marine microbiology*, 240 pp. Chronica Botanica Co., Waltham, Mass.

ZoBell, C. E. 1954 The occurrence of bacteria in the deep sea and their significance for animal life. Pub. Intern. Union Biol. Sci., Series B, No. **16**, 20–29.

ZoBell, C. E. and Budge, K. M. 1957 Pressure inhibition of nitrate reduction. Manuscript.

ZoBell, C. E. and Conn, J. E. 1940 Studies on the thermal sensitivity of marine bacteria. J. Bacteriol., **30**, 223–238.

ZoBell, C. E. and Johnson, F. H. 1949 The influence of hydrostatic pressure on the growth and viability of terrestrial and marine bacteria. J. Bacteriol., **57**, 179–189.

ZoBell, C. E. and Morita, R. Y. 1957 Deep sea bacteria. In *Galathea Reports*, 43 pp. Copenhagen.

ZoBell, C. E. and Oppenheimer, C. H. 1950 Some effects of hydrostatic pressure on the multiplication and morphology of marine bacteria. J. Bacteriol., **60**, 771–781.

ZoBell, C. E. and Rittenberg, S. C. 1948 Sulfate-reducing bacteria in marine sediments. J. Marine Research, **7**, 602–617.

THE ORIENTATION OF SAND GRAINS UNDER CONDITIONS OF "UNIDIRECTIONAL" FLUID FLOW. 1. THEORY AND EXPERIMENT

GENE A. RUSNAK

Reprinted for private circulation from
THE JOURNAL OF GEOLOGY
Vol. 65, No. 4, July 1957
PRINTED IN U.S.A.
Reproduced by Permission

THE ORIENTATION OF SAND GRAINS UNDER CONDITIONS OF "UNIDIRECTIONAL" FLUID FLOW

1. THEORY AND EXPERIMENT[1]

GENE A. RUSNAK
La Jolla, California

ABSTRACT

Recent interest in dimensional orientation of sand-sized particles has indicated that detailed studies of the orienting process are necessary in order to understand better and apply this tool for directional investigations in ancient sedimentary rocks. Based on the laws of fluid mechanics, the theoretical considerations of the present and earlier investigators indicate that the most stable position which an ellipsoidal particle acquires in depositional transport is one in which the long axis lies parallel to the direction of fluid motion, with a slight dip into the current.

In the present study, experiments were performed with varied sediment parameters and varied fluid-flow conditions. Although large perturbations exist in the process of sedimentation, these experimental measurements reveal that the theory is valid in a statistical sense. The statistically preferred direction of orientation of sand-grain long axes parallels the fluid-flow direction; in addition, there is a statistically preferred imbricate direction dipping into the current. This orientation is dependent both upon the sediment parameters of size and shape and upon the fluid-flow conditions.

ORIENTATION

INTRODUCTION

The use of dimensional orientation as an indicator of sedimentary transport direction has received a great deal of interest because it appears to be a workable geological tool. Orientation, however, is also recognized as one of the fundamental properties of a sediment (Pettijohn, 1942, p. 43–61).[2]

In the past, most of the studies of particle orientation have been restricted to pebble-size material because of the ease with which such studies could be undertaken. Some examples of the application of pebble orientation studies are: to till deposits (Richter, 1932, p. 62–66, and 1936, p. 197–206; Holmes, 1941, p. 1299–1354; Virkkla, 1951, p. 5–66; Hoppe, 1952, p. 1–72; the last two give an excellent introduction to the European literature), to glacial outwash (Wadell, 1936, p. 74–92), to talus deposits (Swineford, 1942, p. 1–41), and to river and marine gravels (Cailleux, 1938, p. 171–196, and 1945, p. 375–404; Krumbein, 1940, p. 636–676, and 1942*a*, p. 1355–1402).[3]

Only recently has dimensional orientation of sand-size particles received attention (notable exceptions are the pioneering works of Sander, 1930, p. 279–281; the later works of Wayland, 1939, p. 99–109; and Ingerson, 1940, p. 557–574). Most of the early investigators of sand-grain orientation have restricted their studies to single laboratory experiments or to isolated examples of orientation within sedimentary rocks, for example, Dapple and Rominger (1945, p. 246–261), Rowland (1946, p. 547–564), Gryaznova (1947, p. 647–650), Griffiths (1949, p.

---

[1] This study was made at the University of Chicago and represents a joint contribution from the University of Chicago and the Scripps Institution of Oceanography, University of California, La Jolla, California. Contributions of the Scripps Institution of Oceanography, New Ser., No. 914. Manuscript received December 20, 1956.

[2] Pettijohn describes the fundamental properties as being size, shape, roundness, surface texture, lithology, and orientation. All other properties are considered to be dependent upon these more fundamental properties.

[3] Two articles on pebble orientation have been published since this paper went to press; one on fluviatile gravels by Kalterherberg (1956) and another on till fabrics by Harrison (1957). The writer thanks Dr. W. Zimmerle, of the California Research Corporation, and Dr. R. Brinkmann, of the University of Bonn, Germany, for bringing the article by Kalterherberg to his attention.

138–163), Griffiths and Rosenfeld (1950, p. 202–236; 1953, p. 192–214), and Schwaracher (1951, p. 162–172).[4] More recently, extensive quantitative study of dimensional orientation in modern beach sands has been made by Nanz (1955) and Curray (1956*a*, p. 117–131; 1956*b*, p. 2440–2456). However, the only extended geological applications of sand-grain orientation as a transport criterion are those of Kopstein (1954) and Rusnak (1957 p. 41–55). Incidental application of sand-grain orientation for determining bedding planes is also noted in the studies of sediment flow by Vitanage (1954, p. 493–500) and Van Straaten (1949, p. 9–18).

"Dimensional orientation" is defined as the spatial relation of some geometric property of a particle to an arbitrary co-ordinate system. The geometric property which uniquely determines the complete orientation of a non-spherical particle is a combination of an axis and a plane (Krumbein, 1939, p. 673–706). Most commonly, the longest axis and the maximum projection plane have been used to express the orientation of a particle. With fine-grained material, however, the handling and measuring of individual particles is much more difficult than the handling of pebbles, and workers in the field have restricted their studies to the orientation of some property of particle elongation. The difficulties in measuring an axis and a plane are especially obvious when one tries to apply these techniques to indurated sediments.

"Dimensional fabric" is defined as the spatial arrangement of an aggregate of individual particles making up a unit of sediment and, in this sense, is restricted entirely to a textural property of the sediment. When it can be shown by statistical methods that there is a significant departure from a uniform distribution (i.e., a distribution in which an equal number of grains occurs in all possible positions), the fabric of the sediment is said to have a "preferred orientation." The "preferred direction of orientation" can be thought of as the center of gravity of such a distribution and has been found to correspond, in some way, to the direction of depositional transport.

Orientation can be studied from the viewpoint of kinematics without reference to the forces that cause motion or from the viewpoint of kinetics with reference to the dynamics of the actual forces causing motion and resultant orientation. The earlier studies of dimensional orientation have been restricted entirely to the former view. Unless we have a better understanding of the dynamics of the orienting process, however, we can hope for little more than a superficial understanding of orientation—with consequent inadequacies in application.

The conditions of the orienting process are dependent upon the complex interrelationships of size, shape, roundness, and density of the sedimentary particles to those of the nature, magnitude, and direction of the transporting medium. In order to understand better these relationships, an evaluation of orientation with regard to fluid mechanics has been the prime purpose of the present study (pt. 1). The application of this method of analysis to a geological situation having rigid directional control will be presented in part 2.

FLOW CHARACTERISTICS

Distinction of flow types in the study of fluid mechanics is made by considering all possible types of motion based on the properties of length, time, mass, and force. In general, fluid flow is classified as "steady" (streamline or laminar) or "unsteady" (turbulent), depending upon whether or not at a given point the fluid has a velocity constant with respect to time, magnitude, and direction. When the motion is steady and a viscous fluid moves over a hydrodynamically smooth solid boundary, the flow resembles the slipping of thin plates over one another and is described as "laminar." The term may also be applied to unsteady, non-uniform flow as long as the individual streamlines conform in general to the shape of the solid boundary, but this restricted usage is not applied in the following discussion.

---

[4] Two papers by Vollbrecht (1953*a*, *b*), dealing with sand-grain orientation, were brought to the attention of the writer by Joseph R. Curray after this paper had gone to press.

When the fluid exhibits random velocity fluctuations, it is considered "turbulent." However, if the solid boundary is hydrodynamically smooth, there will be a thin fluid layer adjacent to the boundary which still exhibits laminar motion.

Fluid mechanics engineers have found that the character of flow for any fluid could be adequately described by a dimensionless quantity of the form $uL\rho/\mu$, where u is the velocity, L is a unit of length, ρ is the density of the fluid, and μ is the dynamic viscosity. If we substitute for μ/ρ the equivalent ν, the kinematic viscosity, the quantity describing the character of the flow can be written as

$$R = \frac{uL}{\nu}, \tag{1}$$

where R is the Reynolds number characterizing the type of flow. For cases of free surface flow (e.g., open channels) the unit of length, L, takes the form of the hydraulic radius, P.[5] For small values of R, the flow is laminar, and for higher values it is turbulent.

In natural watercourses, turbulence is predominant, and laminar flow can exist only near a smooth bottom. In the turbulent zone the velocity of flow at a given point is described as the average velocity, $\bar{u}$. The velocity of flow at any instant of time (the instantaneous velocity) is, however, the vector sum of the average velocity, $\bar{u}$, and the random velocity component, u', related to turbulence (Sverdrup *et al.*, 1942, p. 471):

$$u_i = \bar{u} + u' . \tag{2}$$

The Von Kármán–Prandtl equation for the velocity distribution near a rough bottom (*ibid.*, p. 479) is

$$\bar{u} = \frac{u_*}{k_0} \ln \frac{z + z_0}{z_0}, \tag{3}$$

where u_* is called the friction velocity and is equal to $\sqrt{\tau/\rho}$, where τ is a function of the fluid shear exerted on the bottom,[6] k_0 is Von Kármán's constant, z is the height at which $\bar{u}$ is measured, and z_0 is the roughness length.

Near a smooth bottom, however, the velocity distribution in the turbulent zone, from the Von Kármán equation (*ibid.*, p. 479), is

$$\bar{u} = 5.5 u_* + \frac{u_*}{k_0} \ln \frac{u_* z}{\nu}, \tag{4}$$

where the symbols have the same meaning as previously and ν is the kinematic viscosity. While in the laminar boundary layer, the velocity distribution takes the form

$$u = u_*^2 \frac{z}{\nu}. \tag{5}$$

The relative roughness of the bottom is dependent upon the height at which the roughness elements project above the bottom and upon the thickness of the laminar layer. In the experiments[7] of Nikuradse (1933) and Fage (1933) it became clear that the criteria for distinguishing between rough and smooth bottoms could be written in the dimensionless form of a Reynolds number so that:

When $\dfrac{u_* d}{\nu} > 3.5$, the bottom is rough,

When $\dfrac{u_* d}{\nu} < 3.5$, the bottom is smooth;

here d is the height of the roughness elements. In this case, d is the diameter of the particles making up the bottom surface.

Using the foregoing relationships, one can determine the forces acting on any point in the flow, and the character of the flow can be defined.

FLUID FORCES

In a treatment of particle orientation under conditions of fluid flow, it becomes immediately apparent that one has to deal with the same forces that are involved in the process of particle transport by surface creep, saltation, and suspension. In general, the fluid forces acting on a particle can be considered as (1) the tangential drag of viscous shear and/or (2) the dynamic or inertial forces associated with pressure differences, caused by variations in magnitude and direction, of the fluid elements.

---

[5] Where the channel can be considered infinitely wide, however, P takes the value of depth, D.

[6] If one assumes the turbulence to be isotropic, this relation is the mean of the absolute value of the fluctuations.

[7] Cited by White (1940, p. 324–325).

A particle immersed in a moving fluid exerts a stress on the fluid, so that there is resistance to motion. This resistance is expressed as the "drag" of the fluid on the solid and is a function of the above forces. In laminar flow or at very low Reynolds numbers, the resistance of a particle to flow is entirely due to distortion of the surrounding flow pattern and is referred to as "deformation drag." At higher Reynolds numbers, the distortion of the surrounding flow pattern is limited to the boundary layer, and shear along the boundary leads to "surface-drag" resistance. Finally, with still higher Reynolds numbers, if the shape of the particle is such that separation[8] occurs, there is an area of low pressure in the wake that results in a force which opposes motion with a resistance expressed as "form drag."

Rouse (1938, p. 209–210) gives three fundamental geometric shapes which are involved in form drag: (1) a very thin plate, which, when held parallel to the flow, presents an ideal form to a streamline flow pattern but, when held at right angles to the flow, represents complete angularity of profile; (2) a sphere, which has appreciable curvature but with a curvature gradual enough to cause the point of separation to be controlled, in part, by the conditions within the boundary layer; and (3) a streamline shape, with a very slight curvature, so that the point of separation occurs close to the rear of the particle and thereby reduces to a minimum the size of the wake.

Considering the foregoing, it becomes apparent that shape alone does not completely describe the resistance of a particle but that orientation is involved as well. Further, when the particle surface is not smooth, turbulence in the boundary layer occurs at lower Reynolds numbers. This, in turn, decreases the size of the turbulent wake and thereby results in decreased resistance. Thus the resistance of a particle will depend upon the Reynolds number and on the shape, surface roughness, and orientation of the particle.

The conventional form of expressing the drag force exerted on a particle is

$$F_d = C_D A \rho \frac{v^2}{2}, \qquad (6)$$

where C_D is the coefficient of drag, A is the projected area of the particle in the direction of motion, ρ is the density of the fluid, and v is the velocity of the particle with respect to the fluid. A large number of experimental studies have established the values to be applied to C_D for various shapes and orientations at specific values of R. However, to the writer's knowledge, the actual effects of particle surface roughness have not been definitely established.

A special case of the resistance encountered by a particle is that of a sphere. Stokes (Lamb, 1945, p. 597) showed that the resistance, p', of a sphere moving through a viscous fluid would be

$$p' = 3\pi\mu\, vd\ , \qquad (7)$$

where the symbols have the same meaning as before. Equating this resistance to the combined forces of gravity and buoyancy acting on the particle leads to Stokes's law for the viscous settling velocity, s_v, of a particle:

$$s_v = \frac{1}{18}\frac{g}{\mu}\rho' d^2\,, \qquad (8)$$

where ρ' is the density difference between the particle and the fluid and g is the acceleration due to gravity. This equation has been found to hold only in the region of viscous settling, and experimental evidence has shown that this region exists only when $R < 1$. In terms of quartz grains settling in water (at 20° C.), the largest diameter for which Stokes's law holds is about 0.08 mm.

---

[8] Separation occurs when the fluid-flow lines no longer follow the solid boundaries.

Above this diameter, turbulence is set up by the grain, and the viscous effects become secondary to the inertial (or dynamic) effects.

The Stokes equation becomes important in any theory of suspension transport because, if the upward velocity of turbulent eddies exceeds the settling velocity of a given-sized particle, the particle will remain in suspension. Inman (1949, p. 51–70) has recently improved and summarized the theory of suspension transport and suspended sediment concentration gradient.[9]

Study of sediment transport along the bottom of a watercourse by surface creep reveals that the resistance of the sediment to movement is a function of the tractive forces exerted by fluid shear. For a spherical particle, the shear which just balances the resistance to motion is expressed in the form

$$\tau_t = \alpha p \rho' g d \tan \gamma \ , \qquad (9)$$

where α is a coefficient determined by experiment, p is a packing coefficient equal to d^2 times the number of grains exposed per unit area, and γ is taken as the angle of repose of the grains. This expression holds only for $u_* d/\nu$ greater than 3.5, at which point α has a constant value of 0.25 (White, 1940, p. 322–338). Substitution of τ_t by the friction velocity, u_*, leads to an expression for the threshold velocity of particle movement (Bagnold, 1942, p. 99). Because minor fluctuations of velocity may momentarily exceed the threshold velocity and result in particle movement, the instantaneous velocity (eq. [2]) must be considered. Thus, whenever the threshold velocity is exceeded, the particle is put into motion and is transported by rolling or sliding along the bottom.

Very high instantaneous velocities may momentarily lift a particle from the bottom and cause it to travel by a series of leaps. When this phenomenon occurs, the particle is said to be transported by "saltation." The exact nature of the forces acting in this process is not clearly understood. Jeffreys (1929, p. 272–276) has partly explained this process by considering the pressure differences acting on a particle in the vicinity of a steep velocity gradient. More recently, the lift force has been measured by Einstein and El-Samni (1949, p. 520–524).

Saltation in air becomes very important to particle transport, since the impact of the bounding grains is sufficient to dislodge other grains and initiate movement. In water, however, the impact momentum is insufficient to impart motion to the bottom-lying grains. Saltation is therefore relatively unimportant in water-transported sediments (Bagnold, 1942, p. 102) except at high velocities.

ORIENTATION THEORY

Under conditions of fluid flow, the orientation which a particle will obtain can be determined by considering, in terms of stability, the forces acting on it. The position of a particle will be stable when all forces acting on it are in equilibrium. Any displacement of equilibrium will result in a force couple which will tend to restore equilibrium. The magnitude of this restoring force couple can be expressed in terms of its moment of force.

For purposes of simplicity, let us consider the motion of a perfect prolate ellipse, suspended in a uniform stream under conditions of steady inviscid flow. If we neglect the forces due to gravity, the moment acting on the particle can be expressed only in terms of the dynamic forces of the density and the velocity of the fluid. Under these assumptions, it is found (Milne-Thomson, 1949, p. 165) that the moment, M, is

$$M = -\pi \rho (a^2 - b^2) u^2 \sin \beta \cos \beta \ , \quad (10)$$

where a and b are the major and minor axes of the ellipse and β is the angle between the major axis and the direction of motion. The negative sign indicates that the ellipse is acted upon by a couple which tends to set it broadside into the direction of motion. Examination of the equation shows that there are two positions in which the moment goes to zero: (1) when $\beta = \pi$ and (2) when $\beta = \pi/2$. The maximum moment occurs when

---

[9] See also Rouse (1950, p. 790–803).

$\beta = \pi/4$, and the product $\sin \beta \cos \beta$ is equal to $\frac{1}{2}$.

When the ellipse is either broadside or end-on into the stream, the resultant of the sum of the forces coincides with the line of motion passing through the center of the ellipse, and there can be no force couple. In the end-on position, however, the ellipse is unstable, and any fluctuations of the flow will cause the disturbing force couple to come into effect and result in setting the ellipse broadside. Therefore, the only stable position is broadside into the direction of flow.

Although we have considered only the dynamic forces of the fluid, the analysis of Jeffery (1922, p. 161–179) on the motion of an ellipse and a disk in a viscous fluid results in a similar conclusion. Experiments carried out by Taylor (1923, p. 58–61) on disks and ellipsoids in *moving fluids* with a fixed velocity gradient have demonstrated that Jeffery's analytical conclusions are correct. However, Taylor found that the preferred orientation did not become fully established until the particles had been subjected to the forces of laminar flow for a prolonged period of time. More recently the experiments of Krumbein (1942, p. 622–633), Davies (1947, p. 25–39), Kunkel (1948, p. 1056–1058), and McNown and Malaika (1950, p. 74–82) have shown that particles falling through a *quiet fluid* do not acquire a preferred orientation when the inertial forces are negligible, but, when the inertial forces become effective, all symmetrical particles oriented themselves with their maximum cross-sectional area perpendicular to the direction of motion.

Under gravitational conditions of suspension transport, the point about which a particle rotates in obtaining equilibrium is identical with the center of mass. Consequently, for varied geometric shapes, a particle will have a stable orientation when the resultant of the sum of the forces lies on the line of motion passing through the center of mass. A streamline shape, for example, will be stable when the forces are symmetrically disposed (resulting in zero torque) about the line which passes through the center of mass and the apex. In addition, since the apex of the streamline shape represents the point farthest from the center of mass, the only stable position will be obtained when the apex points in the direction of relative fluid motion. This has been demonstrated in experiments by Kunkel (1948, p. 1056–1058).

The same conditions of stability should hold true whether the fluid motion is laminar or turbulent. In laminar motion a given geometric shape will maintain one orientation with respect to the fluid throughout its transport, as long as the flow remains the same. In turbulent flow, however, if one assumes the turbulence to be isotropic, then the orientation of a group of individual particles in suspension should also be isotropic. In any given instant of time the instantaneous velocity, u_i, within a small volume of the fluid may influence the particles in such a way that the orientation within that volume would no longer be isotropic. Therefore, the orientation of a group of particles can be isotropic only when considered over a long period of time in a large volume of fluid, where the entire spectrum of eddies has been operative.

Should the suspended particles settle to the bottom, they would not maintain spherical isotropicity. In the absence of fluid forces on the bottom, gravitational forces would still be operative, and the particles would be in a stable position only when their long dimension lies in the plane parallel to the bottom. Hence isotropicity could exist only within this plane.

When fluid forces are acting on the bottom, they will tend to induce motion and influence particle orientation. Here, however, the pivot point of a particle will no longer be the center of mass but the point of contact of the particle with the bottom surface. Thus an ellipsoid in contact with a smooth bottom will pivot around its small diameter and behave approximately as it would in suspension; i.e., it will roll with the major axis perpendicular to the line of motion. This has been noted both experimentally (Hunzicher, 1930, p. 1–72) and in a natural deposit (Lane and Carlson, 1954, p. 453–462) of pebbles resting on a sand bed.

With increasing size of the bottom-roughness elements, the ellipsoid will act more erratically as each roughness element presents a new fulcrum point for the rolling grain. So long as the roughness elements are isolated, the ellipsoid will continue to move by sliding or rolling around the obstacle. When the roughness elements are uniformly distributed, as in the case of particles in a bottom sediment, the spaces between the particles act as "pockets" into which the ellipsoid can fall. Hence the ellipsoid will roll only when the fluid forces are capable of overcoming the resistance offered by these obstacles.

Since the fluid forces acting on a particle are proportional to the projected area, an ellipsoid will more easily overcome the obstacles in its path when set broadside into the stream. Where minor fluctuations of velocity are not sufficient to overcome the supporting action of the underlying grains so that the ellipsoid can pivot broadside, an end-on position into the stream would be more stable. Thus, for a broadside threshold velocity, an ellipsoid will not move when set end-on into the stream.

Further reasoning along these lines leads one to conclude that, aside from a horizontal (or planar) stability, a vertical stability under fluid forces needs also to be considered. For example, an end-on position into the stream with a positive angle of attack (i.e., where "positive" denotes an upward inclination into the direction of fluid motion and "negative" denotes a downward inclination into the direction of fluid motion) will lead to a lift force resulting from a high pressure under the particle and a low pressure above and behind it. This lift force will make the particle more susceptible to movement and will tend to flip the particle either over or broadside. When the ellipsoid has a negative angle of attack, the reverse is true. The fluid forces will then help to keep the grain from moving: the fluid forces will supplement the gravitational forces holding the particle both on the bottom and against the obstacle. The latter can be true only when the point of contact with the obstacle lies on a line above the center of gravity; for, when the point of contact lies below the center of gravity, the particle will be unstable and will topple or roll. For a uniform size distribution of particles, an estimate of the maximum negative angle of attack would be somewhat less than the angle of repose. For sands, the angle of repose is about 30°.

With turbulent flow over a rough bottom, the velocity gradient is relatively small. Thus a more uniform velocity can be expected from bottom to top of the particle. This should result in a slightly higher negative angle of attack than would occur in the case of turbulent flow over a smooth bottom, where a steeper velocity gradient exists in the laminar boundary layer. With a steep velocity gradient, the force at the top of a bottom-lying grain is greater than the force at the bottom of the grain and results in a high torque.

The sum of these effects taken over a given area of the deposit leads to the phenomenon referred to as "imbrication." This has most commonly been defined as the overlapping, shingling effect of elongate pebbles (or sand grains) resting on one another in a manner analogous to shingles on a roof. The pebbles would be dipping in an upstream direction (Becker, 1893, p. 53–54; summarized by Pettijohn, 1930, p. 568–573).

In the present study the writer restricts the meaning of the word "imbrication" to the statistically preferred angle of dip (of elongate particles) in a plane perpendicular to the bedding and parallel to the flow direction. That is, particles may lie at any vertical angle from 0° to 180° with respect to the bedding plane; but stability requires that the mean angle of dip be in an upstream direction. Figure 1 shows schematically the azimuth relations of elongation direction in the vertical and horizontal planes.

Schwarzacher (1951, p. 162–172), for example, has noted in his orientation analyses that imbrication existed in several experimentally deposited sands. Three of his water-deposited samples show imbrication as well as orientation. However, the degree of both orientation and imbrication of the wind-deposited sediments examined by Schwarzacher is less pronounced than that of water-laid sands. The two-dimensional analysis by Dapples and Rominger (1945, p. 246–261) of a wind-deposited sand also shows a less pronounced orientation than that exhibited by water-laid sands. Although the phenomenon was noted by these writers, no attempt at explanation was made. The writer believes that the explanation is connected with the effects of saltation. For, although saltation is a highly effective agent in the movement of particles under conditions of wind transport, it also has the effect of disturbing the surface grains. Therefore, it might be reasonable to expect that all wind-deposited sands will show a lower degree of orientation than water-laid deposits. This, then, may be an effective means of distinguishing subaqueous from aeolian deposits.

In summary, then, we might conclude that the most stable positions which particles will acquire on the bottom will be with lengths parallel to the direction of fluid motion and with a slight negative angle of attack. This would be true only when the roughness elements of the bottom surface are of the same order of magnitude as the size of the depositing particles. When the roughness elements are very small compared to the depositing particles, we should expect

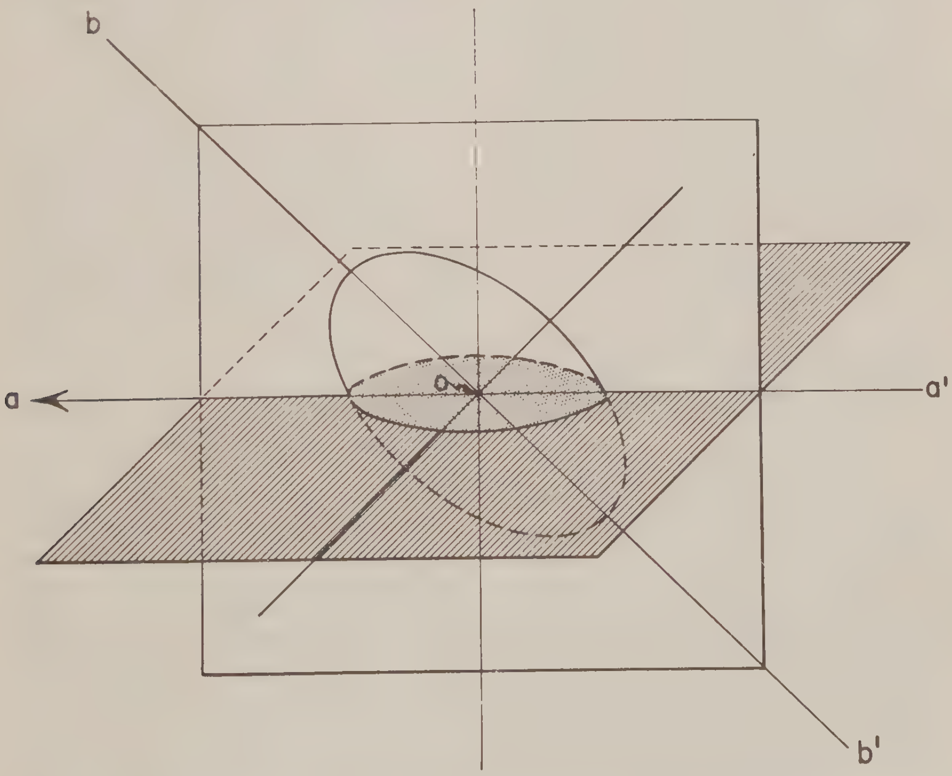

Fig. 1.—Schematic diagram showing the preferred azimuth direction, *a′–a*, in the horizontal plane and the preferred azimuth direction, *b′–b*, in the vertical plane. The direction of flow is from *a′* to *a*, and the angle of imbrication is the angle *a′ob′*.

a transverse orientation to the direction of fluid motion. In the latter case a negative angle of attack might also be expected of the intermediate diameters of blade-shaped particles.

Extension of these ideal considerations cannot be made to sedimentary deposits without keeping in mind the perturbations that exist in the process of sedimentation. Here the orientation is influenced by (1) the elongation of the particles, (2) the velocity of fluid flow, (3) the distribution of eddies in turbulent flow, (4) the roughness of the bottom, (5) the individual eddies shed by the adjacent particles, (6) the packing of the adjacent particles, and (7) the rate of sediment supply. Although these factors do not exhaust the possibilities, it is believed that they are the primary factors contributing to orientation. The difficulty in trying to determine the magnitude of these effects analytically makes it advisable to evaluate them by experiment. The end result of the factors controlling the orientation should be a mean orientation, with a degree of dispersion around this mean that is dependent upon the effectiveness of the above perturbations.

EXPERIMENT

INTRODUCTION

The desirability of using the experimental approach as a device for the better understanding of natural processes has been summarized by Rubey (1938, p. 122) as follows:

> If the objective is an analysis or the better understanding of some particular process rather than a synthesis of the combined effects of many different processes, the data from the laboratory may be more useful than data from natural streams, because under controlled conditions some at least of the many extraneous and confusing factors of nature are thereby eliminated or held constant. The behavior in natural streams, of course, remains the final criterion by which conclusions founded on the relatively simple conditions of the laboratory must ultimately be tested.

Those criteria which may be derived from a series of experiments performed in a flume, where conditions of flow as well as the parameters of the sediment are subject to control, lie clearly in the foregoing category. Experimentally, the effects of elongation (sphericity) of particles, the velocity of fluid flow, the relative roughness of the bottom, and the rate of sediment supply may be controlled in a flume.

If one endeavors to extend the results derived by experiment to those conditions existing among naturally occurring sedimentary deposits, cognizance must be taken of the fact that natural velocities of flow must have been sufficient to transport material to the site of deposition but not of so great a magnitude that wholesale erosion could take place. It would then follow that experimental validity may be gained through the use of those velocities just capable of moving particles of a given grain size, assuming that minor velocity fluctuations around the critical velocity will cause some sediment to be brought in, but little eroded.

DESCRIPTION OF SAMPLE MATERIAL

In order to vary the sediment parameters in these experiments, use was made of several characteristic particulate materials. The choice of material was conditioned by the need for obtaining a wide range of sphericity values and sizes. To fulfil this need, the following materials were employed:

Sand A—a gneissic sand obtained by reducing a deeply weathered till stone
Sand B—an artificially colored sand used commercially for "roofing-shingle"
Sand C—a beach sand
Sand D—a commercial grade of St. Peter sand

The writer's original intention was to use samples in the grade sizes for very fine sand (0.062–0.125 mm.), medium sand (0.250–0.500 mm.), and very coarse sand (1.00–2.00 mm.). However, during the process of sieving, it was determined that this range of sizes was represented only by sands A and C. The range in sizes of sand B was so limited that the entire supply of material was used. Sand D did not have sufficient material in the 1.00–2.00-mm. size grade, and so the size grade 0.500–1.00 mm. was used instead.

These sands were further analyzed for the size distribution within each grade. A series of sieves based on $\sqrt[4]{2}$ grade scale was used for this purpose. Figures 2 through 5 graphically express the size-frequency distribution and size range of the sands utilized for experiment.

The roundness and sphericity of each sand grade used for experiment were determined by standard methods of visual comparison. Each grade was split into fractions for microscopic analysis, using a Jones sample splitter and an Otto "microsplit." These fractions were then examined under a binocular microscope. A series of parallel traverses was run, to insure randomness, and all grains in each field of view were compared with standard charts until 100 grains were evaluated. The Krumbein Roundness Chart (1941, p. 64–72) and the Rittenhouse Sphericity Chart (1943, p. 79–81) were used for this purpose. The mean and the standard deviation of each sand grade was then computed from the shape and roundness frequency distributions. Table 1 shows the results of these roundness determinations, and table 2 shows the results of the sphericity determinations. As may be seen in these tables, the mean roundness varies from 0.14 to 0.62, and the mean sphericity varies from 0.68 to 0.84.

DESCRIPTION OF FLUME

The flume used for all the experiments was 29.5 feet long, 0.95 foot wide, and had a slope of 0.00467. Water for the experiments was supplied through a stilling basin from a constant-head tank, and discharge from the flume was measured by means of a 90° *v*-notch weir. The mean velocity and the depth of flow were controlled by means of an adjustable tail gate at the end of the flume. Throughout all experiments, the water depth was kept essentially constant at 0.5 foot.

METHODS

The experimental procedure consisted of (1) establishing an essentially uniform flow in the flume at a mean velocity just capable of moving the particle-size sediment to be deposited and (2) depositing a uniform layer of given sediment on the bottom, out of suspension, by adding small increments of sediment to the flow. To insure a uniform layer of sediment on the bottom, the writer added small amounts of sediment to the flow at each of a series of traverses along the length of the flume. In this manner, a fairly even distribution of sediment was obtained on the bottom. However, at these flow velocities, ripples were formed at the head of the flume and progressed downstream with time. Therefore, to avoid ripples, the water flow was stopped before the ripples progressed to the area of sampling.

Published curves of velocity versus size, established by Inman (1949, p. 51–70) and Menard (1950, p. 148–160), were used to determine the mean velocities for these experiments. Inman's curves are based on friction velocity, u_*, which is a preferred measure of expressing velocity conditions. However, friction velocity is not directly measurable, and for the purpose of these experiments it was necessary to convert friction velocity to mean velocity by the Von Kármán equations for turbulent flow over smooth and rough boundaries (Rouse, 1938, p. 245):

$$\bar{V} = 1.45u_* + 5.75u_* \log\left(u_* \frac{P}{\nu}\right) \quad \text{(smooth)} \qquad (11)$$

and

$$\bar{V} = 4.43u_* + 5.75u_* \log\left(\frac{P}{d}\right) \quad \text{(rough)}\,. \qquad (12)$$

The relations of mean velocity versus size are shown graphically in figure 6, where the experimental velocities used for each size have also been entered. It should be stated emphatically that the mean velocities versus size shown are comparable only when identical conditions are maintained between experiments. For this reason, the universally accepted friction velocities, which are ap-

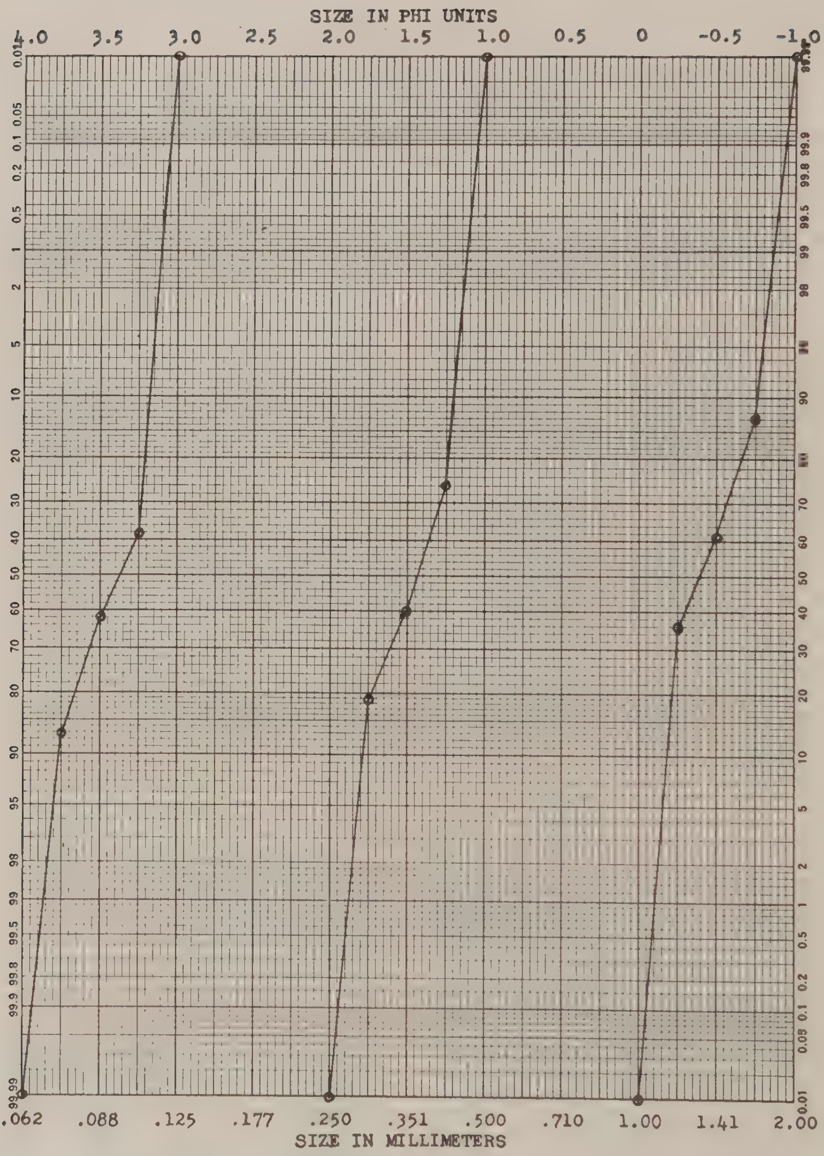

FIG. 2.—Cumulative curves of Sand A size distribution plotted on probability paper in weight per cent. Ordinate is weight per cent, and abscissa is size.

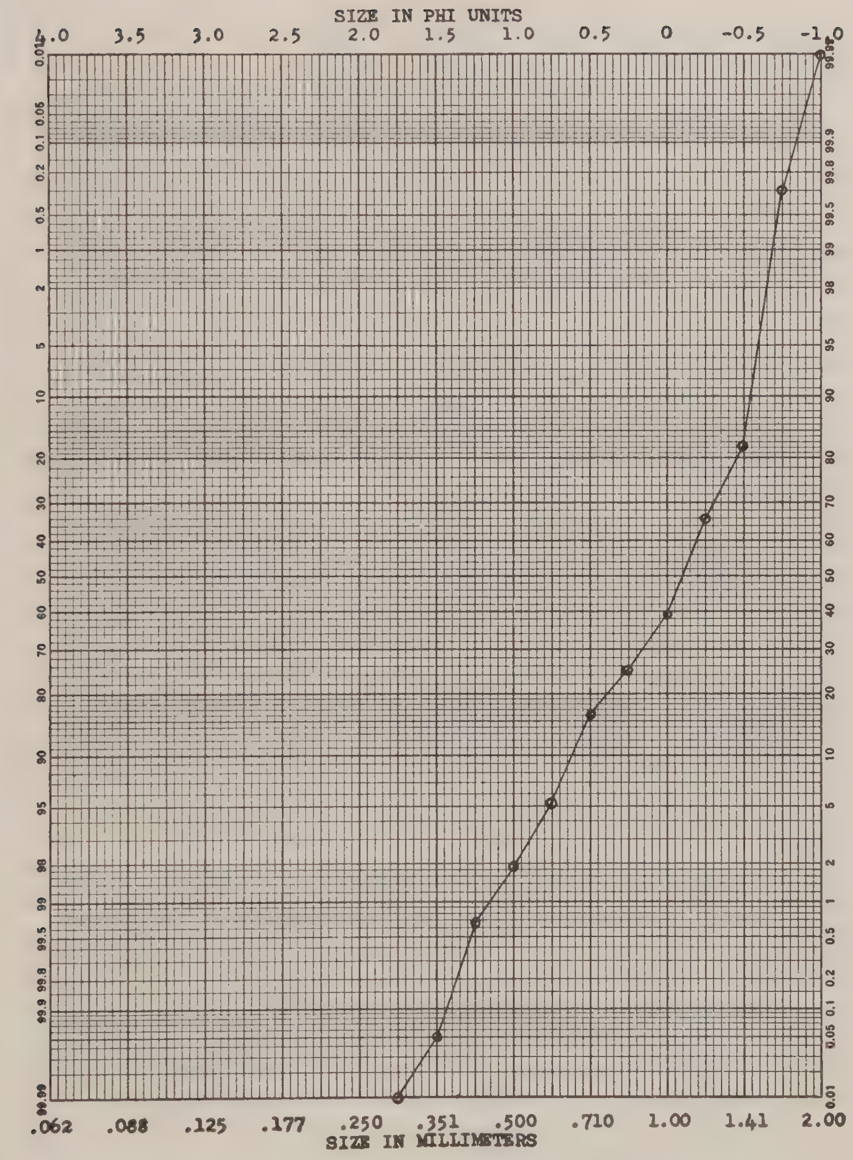

Fig. 3.—Cumulative curve of Sand B size distribution plotted on probability paper in weight per cent. Ordinate is weight per cent, and abscissa is size.

(211)

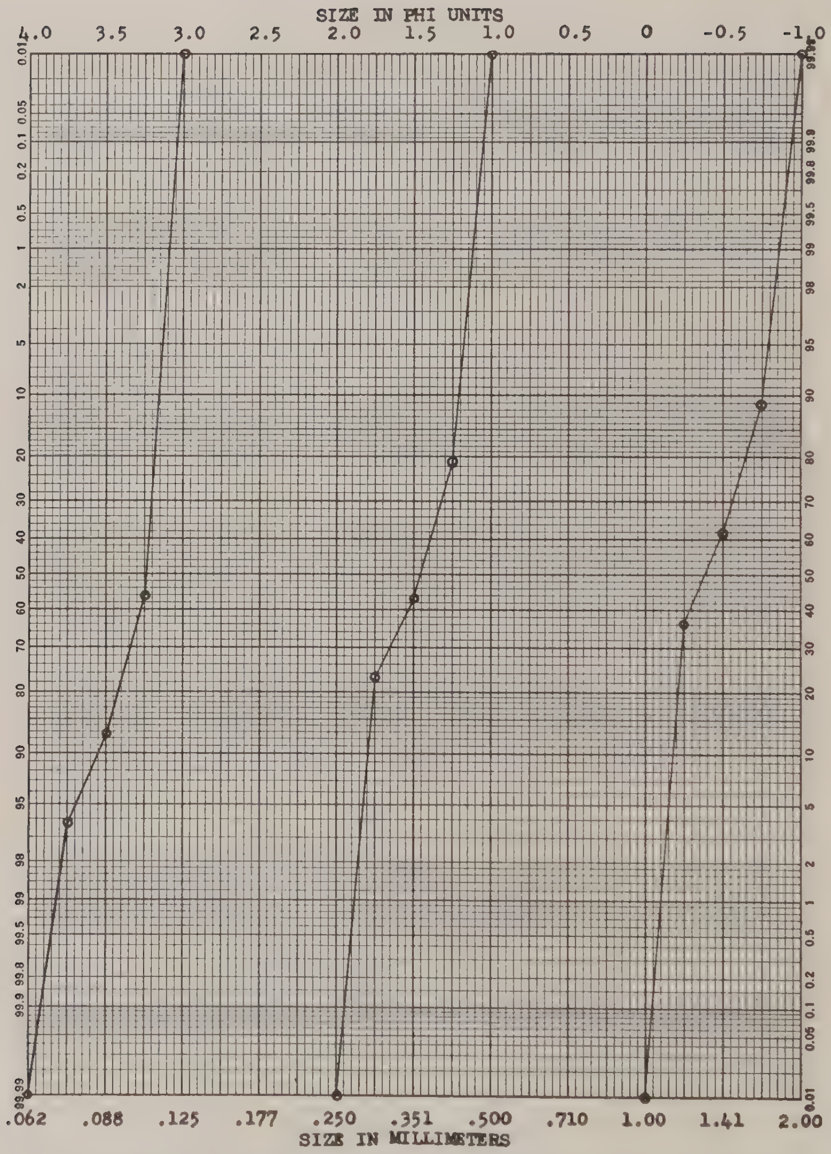

FIG. 4.—Cumulative curves of Sand C size distribution plotted on probability paper in weight per cent. Ordinate is weight per cent, and abcissa is size.

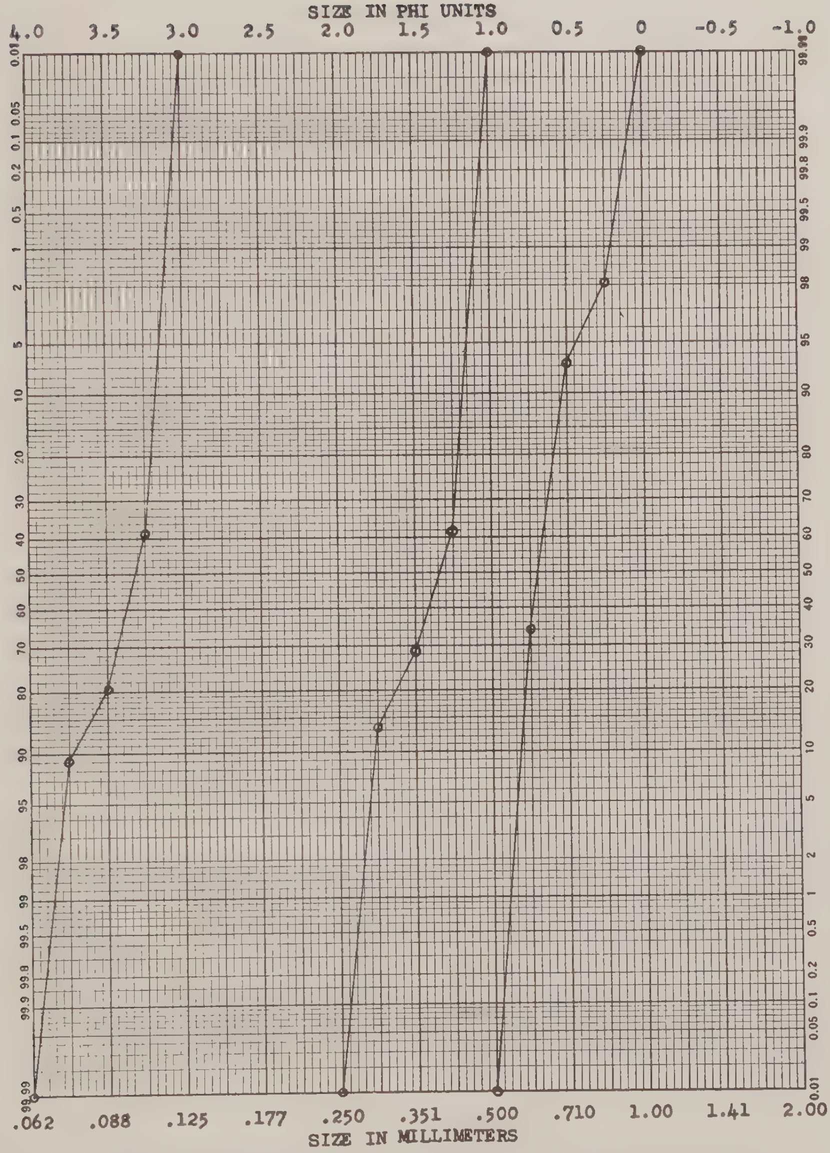

FIG. 5.—Cumulative curves on Sand D size distribution plotted on probability paper in weight per cent. Ordinate is weight per cent, and abscissa is size.

(213)

TABLE 1

ROUNDNESS, *Ro*, FREQUENCY DISTRIBUTION

	SAND*									
	A			B	C			D		
Size†	a	b	d	e	a	b	d	a	b	c
Ro:										
0.9	....	....	....	....	....	....	....	....	....	4
.8	....	....	....	....	....	2	3	1	6	13
.7	....	....	....	....	1	11	6	9	13	22
.6	....	....	....	....	1	26	17	15	31	33
.5	....	1	....	3	16	30	27	40	33	18
.4	7	4	....	18	21	15	17	20	11	9
.3	12	6	10	45	21	10	15	12	6	1
.2	23	22	24	31	27	6	14	2	....	....
0.1	58	67	66	3	13	....	3	1	....	....
Av. *Ro*	0.17	0.15	0.14	0.29	0.31	0.50	0.45	0.48	0.55	0.62
s_{Ro}‡	0.09	0.09	0.07	0.08	0.14	0.14	0.17	0.13	0.12	0.13

* The sands are of the following varieties: A, weathered gneiss; B, artificial sand; C, beach sand; D, St. Peter sand.

† The sizes are as follows: a, 0.062–0.125 mm.; b, 0.250–0.500 mm.; c, 0.500–1.00 mm.; d, 1.00–2.00 mm.; e, 0.297–2.00 mm.

‡ This is one standard deviation around the mean value of roundness.

TABLE 2

SPHERICITY, ψ, FREQUENCY DISTRIBUTION

	SAND*									
	A			B	C			D		
Size†	a	b	d	e	a	b	d	a	b	c
ψ:										
0.97	....	....	....	....	....	....	....	1	2	1
.95	....	....	....	....	....	....	....	....	....	4
.93	....	....	....	....	....	3	....	....	1	5
.91	....	....	....	....	....	1	....	....	3	7
.89	1	....	1	....	2	8	5	3	8	13
.87	1	1	1	1	6	10	9	7	13	15
.85	4	7	8	3	9	8	13	12	11	11
.83	7	7	6	11	9	9	11	10	10	12
.81	8	8	5	7	12	10	5	12	11	12
.79	8	6	7	6	8	12	10	13	13	9
.77	10	6	13	17	12	10	7	7	5	4
.75	6	3	4	11	8	5	8	11	4	2
.73	1	1	2	6	4	5	4	3	5	1
.71	6	8	4	3	6	5	5	4	3	2
.69	9	7	5	2	4	5	5	1	3	1
.67	6	6	3	5	5	4	5	6	4	1
.65	6	8	7	8	4	1	8	4	3	....
.63	6	8	8	7	4	2	1	4	1	....
.61	2	3	3	1	2	2	....	2	....	....
.59	5	5	2	1	1	....	1	....	....	....
.57	6	4	6	4	2	....	2	....	....	....
.55	3	4	6	1	....	....	1	....	....	....
.53	1	4	1	4	1	....	....	....	....	....
.51	....	1	4	1	1	....	....	....	....	....
.49	2	2	3	1	....	....	....	....	....	....
.47	1	1	1	....	....	....	....	....	....	....
0.45	1	....	....	....	....	....	....	....	....	....
Av. ψ	0.71	0.68	0.70	0.72	0.76	0.80	0.77	0.78	0.81	0.84
s_ψ‡	0.10	0.10	0.11	0.09	0.09	0.08	0.08	0.08	0.08	0.06

* The sands are of the following varieties: A, weathered gneiss; B, artificial sand; C, beach sand; D, St. Peter sand.

† The sizes are as follows: a, 0.062–0.125 mm.; b, 0.250–0.500 mm.; c, 0.500–1.00 mm.; d, 1.00–2.00 mm.; e, 0.297–2.00 mm.

‡ This is one standard deviation around the mean value of sphericity.

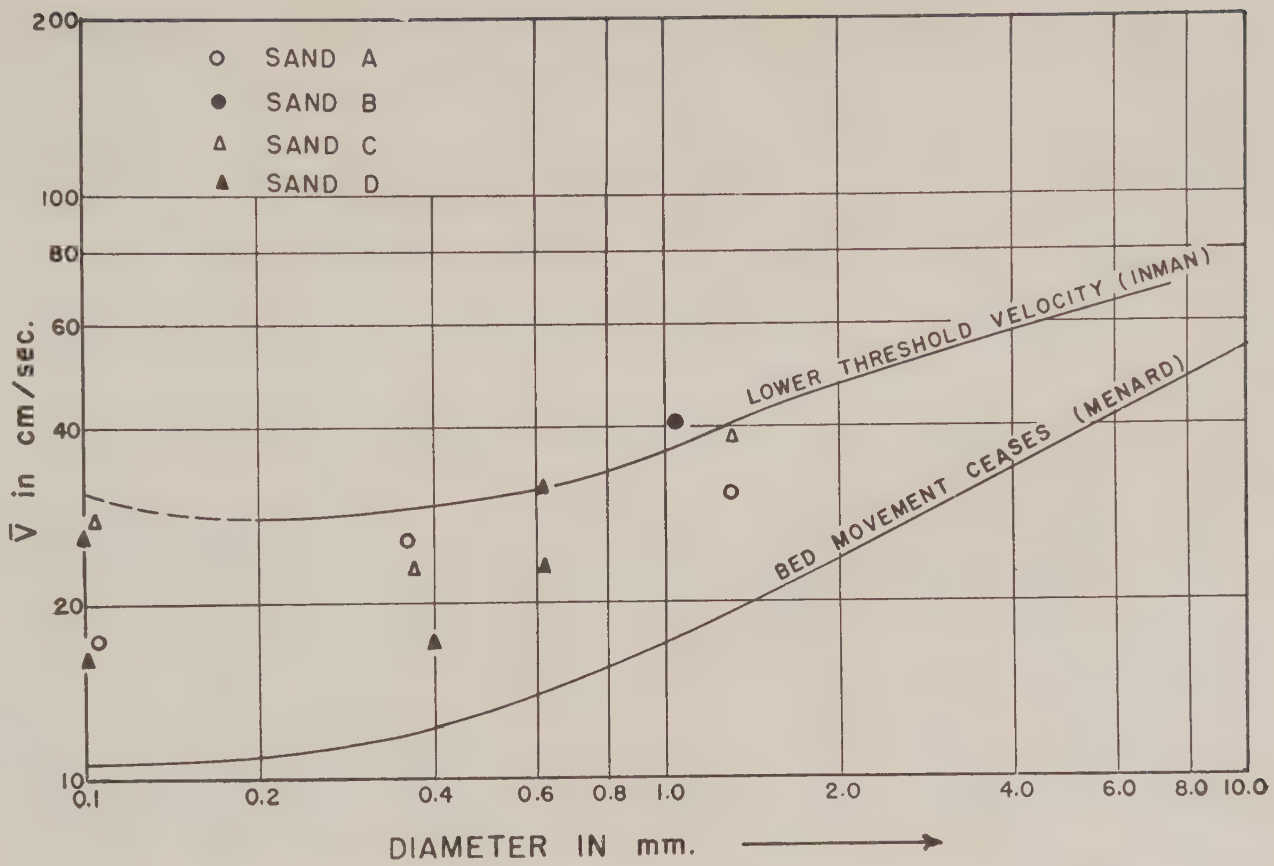

FIG. 6.—Relations of size versus mean velocity and velocities used in the experiments. The mean velocities shown as the threshold velocities were calculated from eqs. (11) and (12), using the friction velocity values given by Inman (1949, p. 56). These mean velocities represent the mean of all velocities taken over the entire cross section of the 0.5-foot depth of flow established in the flume. Mean velocity in the flume was determined from discharge rate as measured by means of the 90° *v*-notch weir.

(215)

plicable to any experiment, have been entered in table 3 along with the mean velocities.

Subsequent to the deposition on the bottom of the flume of a quantity of sand, the water was drained and the sediment dried. In order to insure an undistributed surface, a fine screen was fixed to the end of the flume so that it could be drained gradually. A 300-mesh screen was used, since this gave sufficient resistance to flow that draining was both gradual and uniform.

The surface of the dried sediment was then sprayed with Krylon plastic and allowed to harden. This hardened material was then marked with an arrow indicating the direction of flow and removed from the flume to be examined for orientation. Since the surface was essentially parallel to the flume bottom, it acted as a convenient reference plane comparable to the bedding plane in nature.

Each sample thus obtained was mounted on a glass slide and placed under a binocular microscope equipped with a rotating stage. To establish reference lines, the microscope was fitted with cross-hairs and a micrometer ocular, with which individual grains could be measured. Series of traverses were then taken across the surface of the mount in both east-west and north-south directions, and the orientation of *each grain* was determined as it passed the intersection of the cross-hairs. All these data were then grouped into 20° class intervals.

Since the area of least cross section has hydrodynamic significance (see p. 387), the method of measuring orientation was dependent upon this property. In addition, the stability of a grain is related to the long dimension of the particle, so that a measure combining both these properties was needed. For this purpose, the procedure followed by Dapples and Rominger (1945, p. 251) of using "least projection elongation" was found to be entirely adequate. The least projection elongation has been described by Dapples and Rominger in the following manner: "Elongation direction is considered as that of the two parallel lines with the minimum amount of separation which can be drawn tangent to the grain projection."

In addition to the measure of elongation, a visual estimate of end position (i.e., apex direction) was used, because it was anticipated that the end position would correspond to the apex orientation of a streamline body under fluid forces. That is, theoretically, the apex of a streamline shape should point in the direction of relative fluid motion. Although the few samples tested by Dapples and Rominger (1945, p. 246–261) indicated that the end position was a possible criterion by which flow direction could be determined, the small sample left much to be desired. Thus the apex, or end position, of each grain in the present analysis was also determined. When the end position could not be distinguished, azimuthal directions only were noted. In every sample, at least five hundred grains were measured in the bedding plane in this manner. These measurements resulted in a two-dimensional test of orientation within the bedding plane.

Sections of each sample, cut perpendicular to the bedding and parallel to the flow direction, were used for studies of imbrication. The method outlined in the foregoing section was also used in this analysis. Here, however, the bedding plane, along with the direction of flow, was used as the line of reference for the analyses. Thus a combination of a horizontal plane and a vertical plane gave an apparent three-dimensional picture of the orientation pattern. A total of twelve samples, with varied parameters, was studied for orientation in this manner.

For purposes of three-dimensional analysis by means of a universal stage, samples of Sand C_b (subscript refers to size) and Sand B_e were used. Each grain of the sample field was examined by means of a standard four-axis universal stage in combination with a binocular microscope and was oriented either parallel or perpendicular to the axis of the microscope. Here the elongation was used in the same sense as the optic-axis orientation in optical petrofabrics, where these axes are plotted as poles in the lower hemisphere of a spherical projection. Each value was plotted with a Schmidt equal-area net. These values were then statistically contoured as a petrofabric diagram.[10]

Although no attempt was made to measure end position in the universal-stage analysis, each grain in the sample of Sand B_e was classified into one of the four shape classes defined by Zingg (1935, p. 39–140) as disks, equants, rods, and blades. The shape classification was undertaken in an effort to determine the effects of these four shapes on the orientation pattern. Classification of shapes was simplified by preparing a special chart on which visual estimates could be made with images of the limiting forms. Figure 7 is an illustration of the chart designed for this purpose. The chart is subdivided into the four shape groups on the basis of the axial ratios: $b/a = \frac{2}{3}$ and $c/b = \frac{2}{3}$, where a is the long axis, b is the intermediate axis, and c is the short axis.

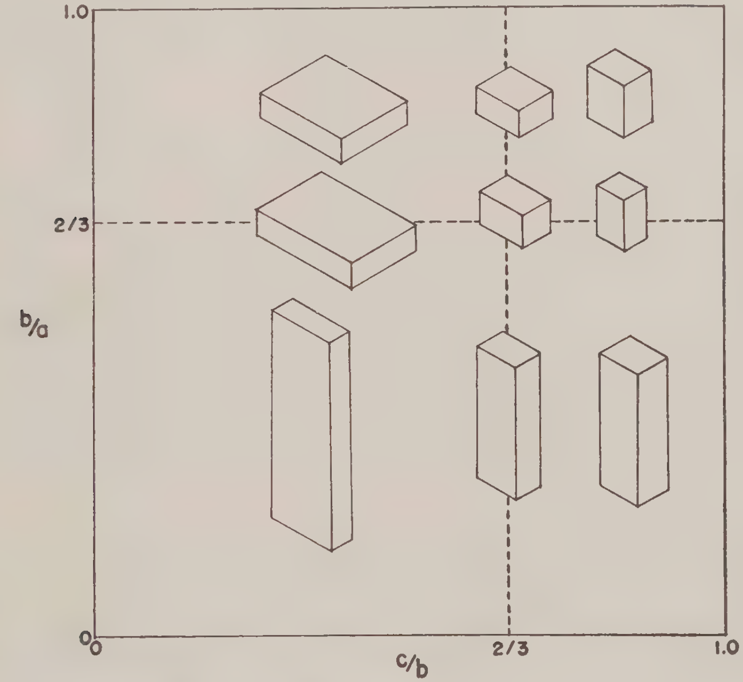

FIG. 7.—Modified Zingg chart used for visual estimates of the four shape classes: equants (*upper right*), rods (*lower right*), blades (*lower left*), and disks (*upper left*). Limiting forms have been drawn by using the values at the boundaries of the shape classes.

EXPERIMENTAL RESULTS

As a result of the flume experiments, twelve samples with varying sediment and fluid-flow parameters were obtained for orientation study. The distribution of least-projection elongation in each of these samples was tested for preferred orientation direction and degree of dispersion. Statistically significant orientation was determined with a test combining the method of vector summation and chi-square. This test was specifically designed by Tukey (1954, p. 1–5) for determining the significance of orientation. In short, the test consists of determining the difference between the number of observations in each class interval or sector and the number that would occur if that same sample were completely isotropic.[11] Results of these tests showed every sample to have a significant orientation,[12] with a preferred direction of orientation (resultant vector) that varied little from the direction of fluid flow. That is, the preferred elongation direction in the horizontal plane approximately paralleled the flow direction.[13] In addition, the statistically preferred direction within the vertical plane showed a very decided imbrication in the upstream direction. The analysis of pointed-end direction reveals that, although in most examples a greater percentage of the grains point in the direction of flow, this percentage is so small that it can lead to unreliable estimates of direction. The complete results of the orientation study have been summarized in table 3.

---

[10] For a complete description of petrofabric methodology, beyond the scope of this paper, the reader is referred to a standard text, such as Ingerson and Knopf (1938).

TABLE 3

SUMMARY OF ORIENTATION STUDY EXPERIMENTS

Sand	Median Diam.*	ψ	Ro	$\bar{V}$†	u_*‡	Preferred Direction§	Dispersion (σ)	Imbrication	End Position‖	Histogram No.
A_a....	0.106	0.71	0.17	17.40	0.88	97.5°	47.48	16°	− 3.2	1
A_b....	0.365	.68	.15	25.65	1.45	81.5°	44.28	14°	+12.0	2
A_d....	1.300	.70	.14	30.73	2.11	66.5°	47.02	20.5°	+ 2.0	3
B_e....	1.060	.72	.29	40.26	2.68	83.5°	47.00	13.5°	+ 3.6	4
C_a....	0.106	.76	.31	27.94	1.43	91°	48.00	3.5°	+ 0.8	5
C_b....	0.370	.80	.50	23.00	1.93	89.5°	47.80	18.5°	+11.2	6
C_d....	1.300	.77	.45	39.12	2.69	99°	48.80	13°	+10.4	7
D_a....	0.100	.78	.48	16.26	0.82	66°	48.90	7.5°	+10.4	8
	0.100	.78	.48	25.91	1.32	80°	45.20	5.6°	+ 4.4	9
D_b....	0.395	.81	.55	17.14	0.98	74°	49.03	14°	+ 1.2	10
D_c....	0.610	.84	.62	22.86	1.39	58°	46.86	16.5°	+ 0.6	11
	0.610	0.84	0.62	32.00	1.95	85.8°	47.92	25.7°	+10.3	12

* In millimeters.

† Mean velocity in centimeters per second.

‡ Friction velocity in centimeters per second.

§ In every case the flow direction was fixed at 90° as the reference.

‖ These values are in per cent; + is in direction of flow, − is opposite of flow. Values determined by subtracting the percentage opposite to flow direction from the percentage in the direction of flow.

To test the variability within a sample, the writer examined two fields from the sample surface of Sand C_d. The results of this examination gave a preferred orientation of 101° and 98°, with standard deviations of 48.7° and 48.8°, respectively. From this it was concluded that there were no differences in the two fields, and they were plotted together as histogram *7* in figure 8. The preferred orientation of this histogram is 99°, with a standard deviation of 48.8°. These values have been entered in table 3.

Another test was made for the variability between the surface of sample Sand D_c and the underside of the same sample. The vertical distance between these two surfaces was several grain diameters, and the horizontal distance between the two fields examined was 2 inches. The results of this test gave preferred directions of orientation of 51° and 58°, with standard deviations of 47.8° and 46.9°, respectively. There appeared to be no differences between the two surfaces, and hence the data were combined for histogram *11* in figure 8. The preferred direction of orientation of this combination is 58°, with a standard deviation of 47.84°. It is this result which has been entered in table 3.

---

[11] For a completely worked example of this test, the reader is referred to the appendix at the end of the paper by Rusnak (1957); see also the paper by Harrison (1957).

[12] The test recently presented by Curray (1956*a*, p. 117–131) was used as a check on the significance of this orientation and resulted in identical conclusions.

[13] The preferred orientation in those samples which were deposited under low velocities, however, show rather marked departures from the flow direction.

Referring to table 3 and figure 6, it can be seen that the greatest departure of preferred orientation from the flow direction (at the fixed value of 90°) occurs in those samples which had been deposited at low mean velocities, that is, at velocities well below the threshold velocity. From this it is concluded that the critical velocities of particle movement were not reached in the experiment; hence the orientation direction was only partly controlled by the fluid-flow forces. Two of these sands (D_a and D_c) were redeposited at slightly higher mean velocities and reanalyzed for preferred orientation direction. Both sands D_a and D_c showed less departure from the flow direction at the higher velocities. Figure 8 illustrates the results of the azimuth distributions in the form of histograms for all samples studied.

The only noticeable effect of changing the sediment size appears to be a decrease in the preferred angle of imbrication with decreas-

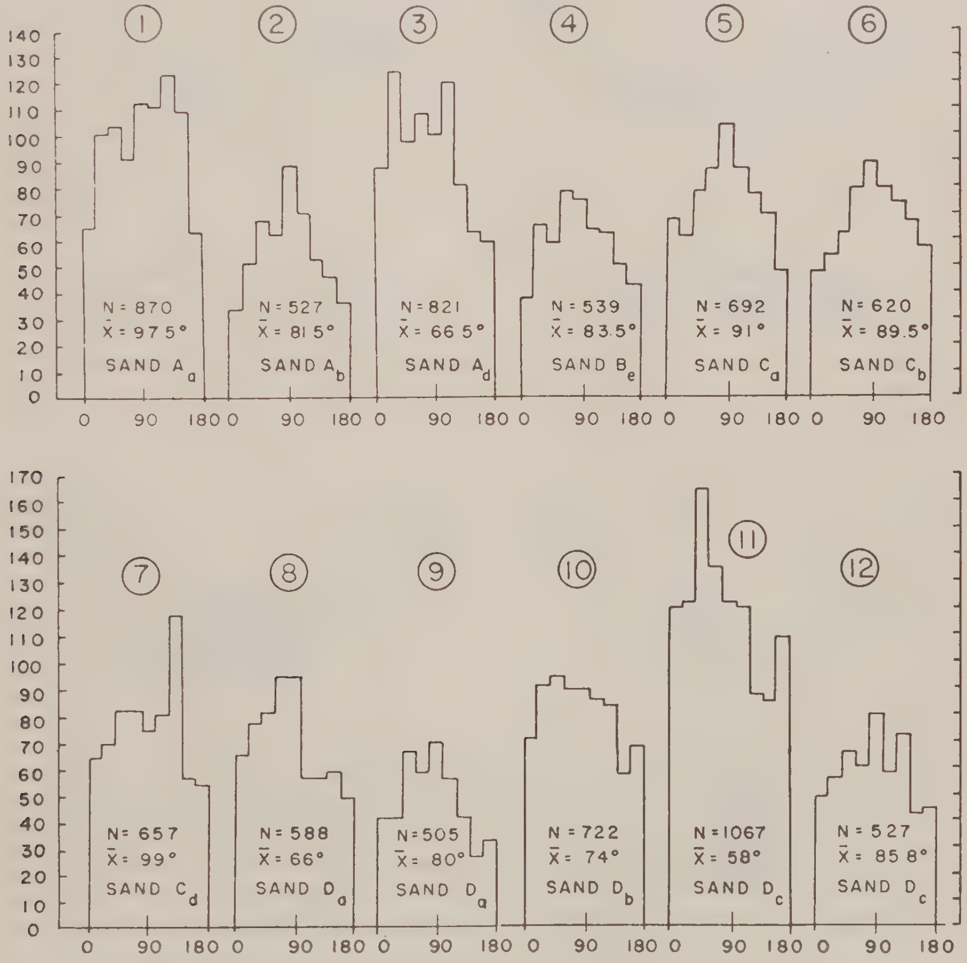

FIG. 8.—Histograms of the long-dimension azimuth distributions of orientation results from experiments. The ordinate is in terms of the number of grains, and the class intervals along the abscissa are in steps of 20° from 0° to 180°.

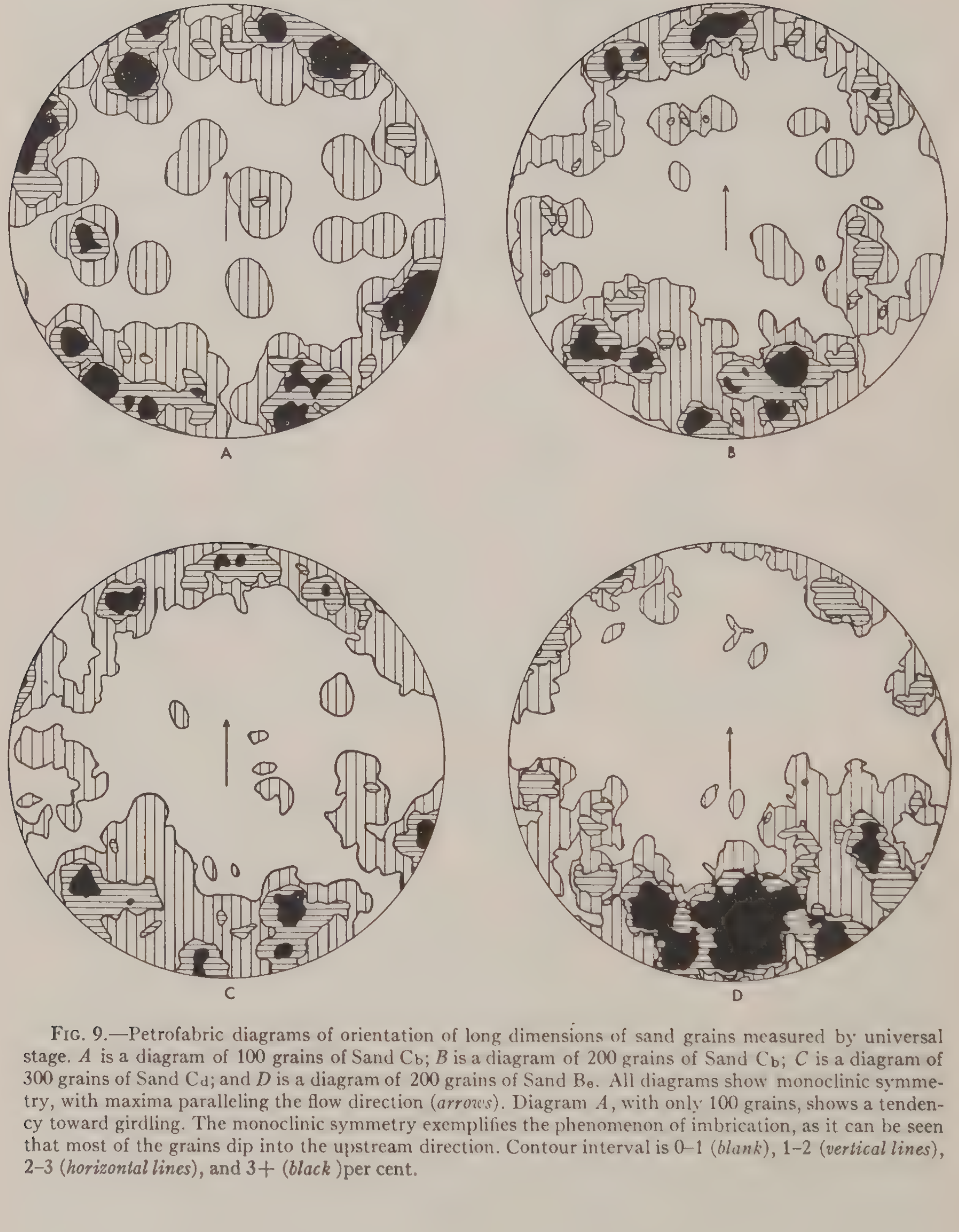

FIG. 9.—Petrofabric diagrams of orientation of long dimensions of sand grains measured by universal stage. *A* is a diagram of 100 grains of Sand C_b; *B* is a diagram of 200 grains of Sand C_b; *C* is a diagram of 300 grains of Sand C_d; and *D* is a diagram of 200 grains of Sand B_e. All diagrams show monoclinic symmetry, with maxima paralleling the flow direction (*arrows*). Diagram *A*, with only 100 grains, shows a tendency toward girdling. The monoclinic symmetry exemplifies the phenomenon of imbrication, as it can be seen that most of the grains dip into the upstream direction. Contour interval is 0–1 (*blank*), 1–2 (*vertical lines*), 2–3 (*horizontal lines*), and 3+ (*black*)per cent.

TABLE 4

COMPARISON OF METHODS IN PREFERRED ORIENTATION ANALYSIS

PETROFABRIC DATA (Long Axes Projected onto a Plane)			TWO-DIMENSIONAL DATA (Long Axes in Plane of Sample Surface)		
Sample	Orientation Direction	No. of Grains	Sample	Orientation Direction	No. of Grains
Sand C_b........	88°	200	Sand C_b........	89.5°	628
	88.5°	300			
Sand B_e........	81°	200	Sand B_e........	83.5°	539

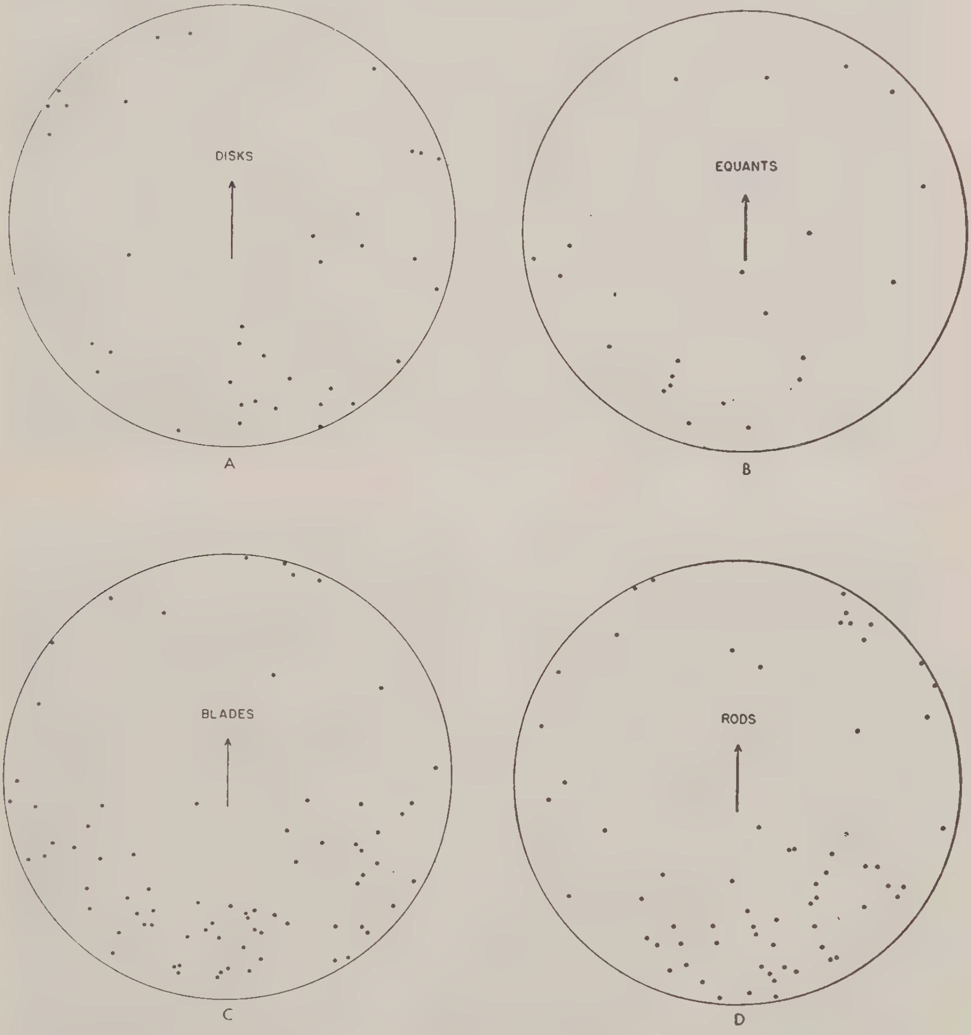

FIG. 10.—Point plot of the four shape classes of Zingg, showing the effect of each shape on the petrofabric diagram of Sand B_e.

The number of points plotted in each shape class represents that portion of the 200 grains used in determining the petrofabric diagram. Disks = 36 grains, equants = 23 grains, blades = 73 grains, and rods = 66 grains.

ing grain size. This change takes place when the bottom becomes effectively smooth. According to the published data of Inman (1949, p. 56), the bottom becomes smooth for flow of threshold velocity when the particles making up the bottom become smaller than about 0.18 mm. It may be seen that three of the samples below this size show a very marked decrease in the angle of imbrication, while only one does not. This effect of lower angle of imbrication is explained by the consideration of the steep velocity gradient discussed in the theory (see p. 390).

As was anticipated from theory, an increase in sphericity (i.e., a decrease in elongation) results in an increase in the degree of dispersion around the preferred direction of orientation. Here the standard deviation, computed around the preferred direction, was used as the measure of dispersion. Although there is a general increase in the standard deviation with increasing mean sphericity, the correlation is low, and these data can be accepted as only suggestive. The low correlation is most probably due to the fact that, within any one sand, there is a wide spread of sphericities represented and the mean sphericity is inadequate for correlation.[14]

The results of the universal-stage analyses show that the inferences drawn from the two-dimensional studies about the nature of

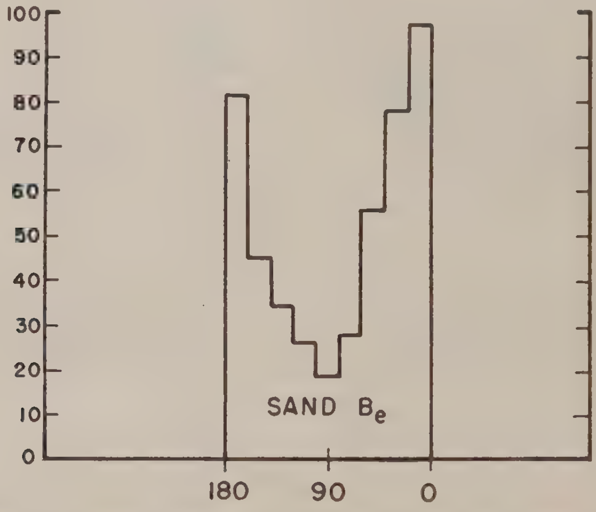

FIG. 11.—Histogram of azimuth distribution in the vertical plane of the long axis, showing the dominant number of grains to be dipping into the current from 0° to 90°. The preferred angle of dip is an imbrication of 13.5°.

---

[14] It is evident from fig. 10, however, that the more elongate grains within one sample show the greatest parallelism to transport direction.

PLATE 1

Two photographs of the same area of Sand B_e taken in the flume after deposition was stopped and the flume drained. The arrows indicate the direction of flow. The difference in the photographs is due to the phenomenon of imbrication. In both photographs the lighting was the same and the camera angle was the same. In *A*, the reader is looking downstream and at the maximum projection planes of the grains. In *B*, the reader is looking upstream and end-on at the grains.

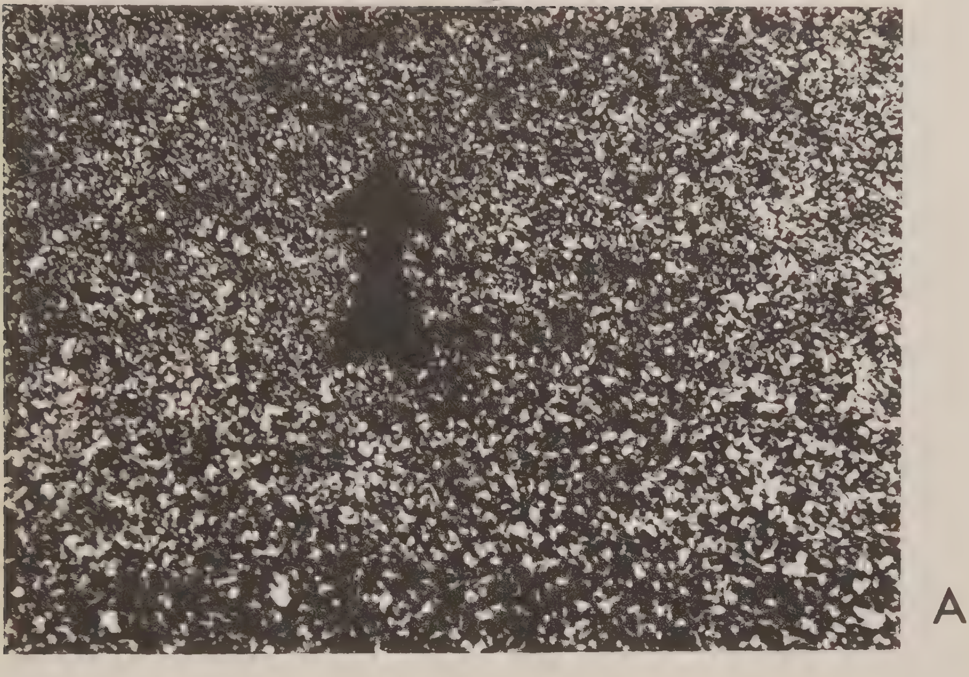

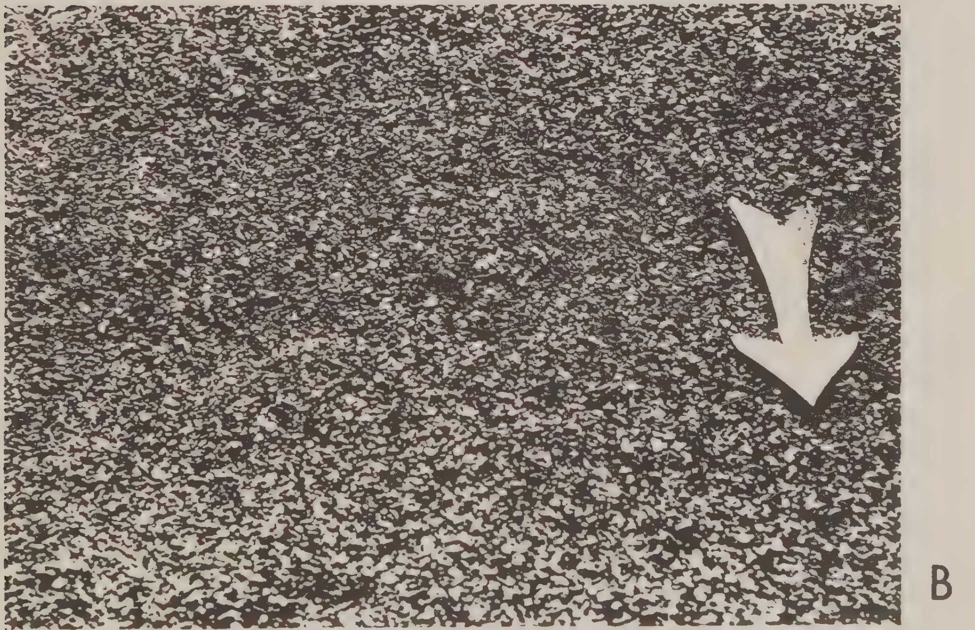

Sand surfaces

three-space orientation are correct. Figure 9 illustrates the three-space orientation results in the form of petrofabric diagrams. By projecting the long axes from the petrofabric diagrams onto a plane, these data were subjected to the same statistical tests of preferred orientation direction used in the two-dimensional studies. The comparative results of this analysis are shown in table 4. The sample of Sand C_b with only 100 grains did not have statistically significant orientation and has not been entered in this table.

The effect of various shapes on the orientation pattern of the petrofabric diagrams is illustrated in figure 10 and is the result of the shape-study orientation of Sand B_e. Here the rod-shaped grains show the greatest concentration around the current direction. The imbrication exhibited by these petrofabric diagrams is vividly demonstrated in the photographs of the sand surface shown in plate 1 and in the histogram of figure 11.

Summarizing the experimental results, we might conclude that the experimental data agree surprisingly well with the theory. That is, although large perturbations exist which tend to disturb orientation, a statistically significant orientation is detectable:

1. The long axes of sand grains tend to align themselves parallel to the fluid-flow direction.
2. The more elongate (rod-shaped) sand grains tend to be more nearly parallel to the fluid-flow direction than less elongate grains.
3. The sand grains are imbricated (shingled) with the direction of dip upstream.
4. The angle of imbrication is larger for turbulent flow over a rough bottom (large-grain size) than it is for turbulent flow over a smooth bottom (small-grain size).
5. The fluid-flow direction of the depositing medium can be determined from an orientation analysis of the dimensional fabric of a sand deposit.

REFERENCES CITED

BAGNOLD, R. A., 1942, The physics of blown sands and desert dunes: 265 p., London, Methuen & Co.

BECKER, G. F., 1893, Finite homogeneous strain, flow, and rupture of rock: Geol. Soc. America Bull., v. 4, p. 13–90.

CAILLEUX, A., 1938, La disposition individuelle des galets dans les formation détritiques: Rev. géog. phys. et géol. dynam., v. 11, p. 171–196.

——— 1945, Distinction des galets marins et fluviatiles: Soc. géol. France Bull., v. 15, ser. 5, p. 375–404.

CURRAY, J. R., 1956*a*, The analysis of two-dimensional orientation data: Jour. Geology, v. 64, p. 117–131.

——— 1956*b*, Dimensional grain orientation studies of Recent coastal sands: Bull. Am. Assoc. Petroleum Geologists, v. 40, p. 2440–2456.

DAPPLES, E. C., and ROMINGER, J. F., 1945, Orientation analysis of fine-grained clastic sediments: Jour. Geology, v. 53, p. 246–261.

DAVIES, C. N., 1947, The sedimentation of small suspended particles: Supp. to Institution of Chemical Engineers Trans., v. 25, p. 25–39.

EINSTEIN, H. A., and EL-SAMNI, EL-SAYED A., 1949, Hydrodynamic forces on a rough wall: Rev. Modern Physics, v. 21, p. 520–524.

GRIFFITHS, J. C., 1949, Directional permeability and dimensional orientation in Bradford sand: Pa. State Coll. Min. Indus. Expt. Sta. Bull., v. 54, p. 138–163.

——— and ROSENFELD, M. A., 1950, Progress in measurement of grain orientation in Bradford sand: Pa. State Coll. Min. Indus. Expt. Sta. Bull., v. 56, p. 202–236.

——— ——— 1953, A further test of dimensional orientation of quartz grains in Bradford sand: Am. Jour. Sci., v. 251, p. 192–214.

GRYAZNOVA, T. E., 1947, K metodike izucheniya orientirovki chastits v peschanykh otlozheniyakh: Akad. Nauk. S.S.S.R., Doklady, v. 58, no. 4, p. 647–650.

HARRISON, P. W., 1957, New technique for three-dimensional fabric analysis of till and englacial debris containing particles from 3 to 40 mm. in size: Jour. Geology, v. 65, p. 98–105.

HOLMES, C. D., 1941, Till fabric: Geol. Soc. America Bull., v. 52, p. 1299–1354.

HOPPE, G., 1952, Hummocky moraine regions: Geog. Annaler, no. 1–2, p. 1–72.

HUNZICHER, A., 1930, A laboratory study of antidune traction and the transportation and deposition of ellipsoidal and disk-shaped pebbles: Unpublished S.M. Dissert., Univ. of Wisconsin.

INGERSON, E., 1940, Fabric criteria for distinguishing pseudo-ripple marks from ripple marks: Geol. Soc. America Bull., v. 51, p. 557–574.

——— and KNOPF, E. B., 1938, Structural petrology: Geol. Soc. America Mem. VI.

INMAN, D. L., 1949, Sorting of sediments in the light

(225)

of fluid mechanics: Jour. Sed. Petrology, v. 19, p. 51–70.

Jeffery, G. B., 1922, The motion of ellipsoidal particles immersed in a viscous fluid: Royal Soc. London Proc., v. 102A, p. 161–179.

Jeffreys, H. B., 1929, On the transport of sediments by streams: Cambridge Philos. Soc. Proc., v. 25, p. 272–276.

Kalterherberg, J., 1956, Ueber Anlagerungsgefüge in grobklastischen Sedimenten: Neues Jahrb. Geologie u. Paleontologie Abhandl., v. 104, no. 1, p. 30–57.

Kopstein, F. P. H. W., 1954, Graded bedding of the Harlech Dome: Ph.D. thesis, Univ. of Groningen, Pub. 81, p. 97.

Krumbein, W. C., 1939, Preferred orientation of pebbles in sedimentary deposits: Jour. Geology, v. 47, p. 673–706.

——— 1940, Flood gravel of San Gabriel Canyon, California: Geol. Soc. America Bull., v. 51, p. 639–676.

——— 1941, Measurement and geological significance of shape and roundness of sedimentary particles: Jour. Sed. Petrology, v. 11, p. 64–72.

——— 1942*a*, Flood deposits of Arroyo Seco, Los Angeles County, California: Geol. Soc. America Bull., v. 53, p. 1355–1402.

——— 1942*b*, Settling-velocity and flume-behavior of non-spherical particles: Am. Geophys. Union Trans., p. 621–633.

Kunkel, W. B., 1948, Magnitude and character of errors produced by shape factors in Stokes' law estimates of particle radius: Jour. Applied Physics, v. 19, p. 1056–1058.

Lamb, Sir H., 1945, Hydrodynamics: 738 p., New York, Dover Pubs.

Lane, E. W., and Carlson, E. J., 1954, Some observations on the effect of particle shape on the movement of coarse sediments: Am. Geophys. Union Trans., v. 35, p. 453–462.

McNown, J. S., and Malaika, J., 1950, Effects of particle shape on settling velocity at low Reynolds numbers: Am. Geophys. Union Trans., v. 31, p. 74–82.

Menard, H. W., 1950, Sediment movement in relation to current velocity: Jour. Sed. Petrology, v. 20, p. 148–160.

Milne-Thomson, L. M., 1949, Theoreticol hydrodynamics: 600 p., London, Macmillan & Co., Ltd.

Nanz, R. H., 1955, Grain orientation in beach sands: a possible means for predicting reservoir trend (abs.): Program Soc. Econ. Paleontologists and Mineralogists 29th Ann. Mtg., New York.

Pettijohn, F. J., 1942, Quantitative and analytical sedimentation: Natl. Research Council, Comm. on Sedimentation, Rept. 1940–1941, Exhibit G, p. 43–71.

Richter, K., 1932, Die Bewegungsrichtung des Inlandeises rekonstruiert aus den Kritzen und Längsachsen der Geschiebe: Zeitschr. f. Geschiebeforschung, v. 8, p. 62–66.

——— 1936, Ergebnisse und Aussichten der Gefügesforschung im pommerschen Diluvium: Geol. Rundschau, v. 27, p. 197–206.

Rittenhouse, G., 1943, A visual method of estimating two-dimensional sphericity: Jour. Sed. Petrology, v. 13, p. 79–81.

Rouse, H., 1938, Fluid mechanics for hydraulic engineers: 422 p., New York, McGraw-Hill Book Co.

——— 1950, Engineering hydraulics: 1,039 p., New York, John Wiley & Sons, Inc.

Rowland, R. A., 1946, Grain shape fabrics of clastic quartz: Geol. Soc. America Bull., v. 57, p. 547–563.

Rubey, W. W., 1938, The force required to move particles on a stream bed: U.S. Geol. Survey Prof. Paper 189-E, p. 121–141.

Rusnak, G. A., 1957, A fabric and petrologic study of the Pleasantview sandstone: Jour. Sed. Petrology, v. 27, p. 41–55.

Sander, B., 1930, Gefügekunde der Gesteine: 352 p., Vienna, Springer.

Schwarzacher, W., 1951, Grain orientation in sands and sandstones: Jour. Sed. Petrology, v. 21, p. 162–172.

Straaten, L. M. J. U. van, 1949, Occurrence in Finland of structures due to subaqueous sliding of sediments: Comptes Rendus Soc. géol. de Finlande, v. 22, p. 9–18.

Sverdrup, H. U., Johnson, M. W., and Fleming, R. H., 1942, The oceans, their physics, chemistry, and general biology: 1,087 p., New York, Prentice-Hall.

Swineford, A., 1942, Fabric of a gravel talus: Unpublished S.M. Dissert., Univ. of Chicago.

Taylor, G. I., 1923, The motion of ellipsoidal particles in a viscous fluid: Royal Soc. London. Proc., v. 103A, p. 58–61.

Tukey, J. W., 1954, Chi-square test of orientation: 5 p., Comment no. 1A, Earth Sci. Panel Rev. Group, CSPS-ASA, unpublished communication.

Vitanage, P. W., 1954, Sandstone dikes in the South Platte area, Colorado: Jour. Geology, v. 62, p. 493–500.

Virkkala, K., 1951, Glacial geology of the Suomussalmi area, East Finland: Full. Comm. Géol. Finland, no. 155, p. 5–66.

Vollbrecht, K., 1953*a*, Zur Quarzachsenregelung sandiger Sedimente: Acta Hydrophysica, v. 1, no. 2, p. 61–88.

——— 1953*b*, Zur Unterscheidung von Sinkstoff- und Geschiebebarren: Geologie, v. 2, no. 4, p. 268–276 (Berlin).

Wadell, H., 1936, Volume, shape, and shape position of rock fragments in openwork gravel: Geog. Annaler, no. 1, p. 74–92.

Wayland, R. G., 1939, Optical orientation in elongate clastic quartz: Am. Jour. Sci., v. 237, p. 99–109.

White, C. M., 1940, The equilibrium of sand grains on the bed of a stream: Royal Soc. London Proc., v. 174A, p. 322–338.

Zingg, T., 1935, Beitrag zur Schotteranalyse: Schweiz. mineralog. u. petrol. Mitt., v. 15, p. 39–140.

APPENDIX

Symbols and Dimensions

All units are in terms of the c.g.s. system; M is mass in grams, L is length in centimeters, and T is time in seconds.

Symbol	Quantity	Dimensions
a	Major axis of the ellipse in equation (10)	L
A	Projected area of a particle in the direction of motion	L^2
b	Minor axis of the ellipse in equation (10)	L
C_D	Coefficient of drag	Dimensionless
d	Particle diameters in centimeters for equations and millimeters for graphs	L
F_d	Frictional drag force on a particle	MLT^{-2}
g	Acceleration due to gravity	LT^{-2}
k_0	Von Kármán's flow constant, equals approximately 0.4	Dimensionless
ln	Natural logarithm	
log	Logarithm to the base 10	
M	Moment of force in equation (10)	ML^2T^{-2}
p'	Resistance of a sphere in equation (7)	ML^2T^{-2}
p	Packing coefficient in equation (9)	Dimensionless
P	Hydraulic radius of equations (1), (11), (12)	L
R	Reynolds number	Dimensionless
Ro	Roundness	Dimensionless
s_v	Settling velocity	LT^{-1}
u	Velocity in laminar flow	LT^{-1}
$\bar{u}$	Mean downstream velocity	LT^{-1}
u'	Random velocity component related to turbulence	LT^{-1}
u_*	Friction velocity	LT^{-1}
u_i	Instantaneous velocity	LT^{-1}
v	The velocity of a particle with respect to the fluid	LT^{-1}
$\bar{V}$	Mean velocity in equations (11) and (12)	LT^{-1}
z	Vertical axis; positive upward	L
z_0	Roughness length, related to the height of the roughness elements above the bottom	L
α	Experimental coefficient of equation (9)	Dimensionless
β	Angle between the major axis and the flow direction of equation (10)	Dimensionless
γ	Angle of repose	Dimensionless
μ	Dynamic viscosity	$ML^{-1}T^{-1}$
ν	Kinematic viscosity	L^2T^{-1}
ρ	Density of the fluid	ML^{-2}
ρ'	Density difference between the particle and the fluid	ML^{-2}
τ_t	Tractive force per unit area exerted on the bottom by fluid shear	$ML^{-1}T^{-2}$
τ	Intensity of fluid shear	$ML^{-1}T^{-2}$
$\bar{X}$	Angle of preferred orientation (degrees)	Dimensionless
ψ	Sphericity	Dimensionless

Vol. 38, No. 3 Transactions, American Geophysical Union June 1957

The Effects of Cable Design on the Accuracy of the GEK*

JOHN A. KNAUSS AND JOSEPH L. REID

Abstract—Simultaneous observations with a GEK and a drifting drogue were made in order to test the validity of the GEK for surface current measurements. The average current velocity was obtained by plotting the drogue trajectory by celestial fixes and other navigational means. Tests were conducted using various types of GEK cables. A cable having a density greater than that of sea water creates an error termed 'cable droop'; a lower cable density creates an error termed 'windage.' Good agreement between the average GEK velocity and the average drogue velocity is obtained when allowance is made for windage and droop.

The basic assumptions in GEK measurements—The method of towed electrodes, the Geomagnetic Electrokinetograph or GEK, as a technique for measuring ocean currents was first described by *von Arx* [1950]. Since then it has been widely used for surface current measurements in the open ocean, by *von Arx* [1952], *Bowden* [1953], *Murray* [1952], and others.

The theory of the GEK and the underlying assumptions involved in the interpretation of its results are best described by *Longuet-Higgins*, *Stern*, and *Stommel* [1954, referred to hereafter as *LSS*]. It is there shown that the potential E measured by the GEK is given by

$$\mathbf{E} = (\nabla\varphi - \mathbf{V}' \times \mathbf{H})\cdot\mathbf{S} \qquad (1)$$

where $\mathbf{V}'$ represents the velocity of the electrodes, $\mathbf{H}$ the Earth's magnetic field, and $\mathbf{S}$ the vector distance between electrodes. $\nabla\varphi$ is the potential gradient in the ocean and is given by

$$\nabla\varphi = \mathbf{V} \times \mathbf{H} - \rho\,\mathbf{i} \qquad (2)$$

where $\mathbf{V}$ is the velocity of the water, ρ the electrical resistivity of the water, and $\mathbf{i}$ the electrical current density.

The velocity of the electrodes $\mathbf{V}'$ consists of three components: the course and speed of the ship, her leeway (if any), and the set and drift of the current itself. Hence,

$$\mathbf{V}' = \mathbf{V}'' + \mathbf{V}''' + \mathbf{V} \qquad (3)$$

where the seconds and thirds refer to course and speed and leeway respectively. $\mathbf{V}'' + \mathbf{V}'''$ is the velocity of the ship relative to the water, which we will call $\mathbf{V}^*$. If there is any current shear, so that the current moving the electrodes is different from the current moving the ship, there must be one more velocity component in (3) to represent this difference. However, for most of the arguments that follow, the current difference component can be lumped with the windage component.

In making GEK measurements the electrodes are towed in two directions, x and y, (usually at right angles) and the two potential components are added vectorially: $\mathbf{E} = \mathbf{E}_x + \mathbf{E}_y$. If (1) is expanded (making the single assumption that $V'_z = 0$ where the z direction is normal to the surface of the water) then the potential measured when the ship is on the x leg is

$$E_x = \frac{\partial\varphi}{\partial x}S_x + \frac{\partial\varphi}{\partial y}S_y + \frac{\partial\varphi}{\partial z}S_z - V_yH_zS_x + (V_x + V^*_x)H_zS_y - (V_x + V^*_x)H_yS_z + V_yH_xS_z \qquad (4)$$

(Although V'_z may not be zero at any instant, it most certainly has to be almost zero when averaged over a two to four-minute interval, the usual time for a GEK fix.) By the 'x leg' we mean that x is the direction of $\mathbf{V}^*$, not of $\mathbf{V}''$. A similar expression holds when the electrodes are towed on the y leg. In interpreting the potential measured by the GEK in terms of ocean currents the assumption is usually made that all terms but one in (4) are small and that to a good approximation

$$V_y \cong -E_x/H_zS_x \qquad (5)$$

To go from (4) to (5) requires two assumptions

(a) $|\nabla\varphi| \ll |\mathbf{V} \times \mathbf{H}|$

(b) $S_y = S_z = 0$, that is, $\mathbf{V}^* \times \mathbf{S} = 0$.

The conditions which must be satisfied in the open ocean for the first assumption to be valid are discussed in detail by *LSS* [1954]. It is assumed in what follows, unless otherwise specified, that the first assumption is valid. The second assumption is related to the manner in which the electrode

---

* Contribution from the Scripps Institution of Oceanography, New Series No. 915.

Reproduced by Permission

cable tows behind the ship and is the subject of this paper.

Cable droop—Until a few years ago nearly all GEK's in this country were equipped with Navy-type 'demolition cable' which has a diameter of approximately 0.35 inches and a specific gravity of about 1.8. This cable tows directly in the path the ship makes relative to the water (that is, $S_y = 0$ in (4)) but being denser than water it tows the far electrode at a greater depth than the near electrode (that is, $S_z \neq 0$). When this type of cable is used (4) becomes

$$E_x \cong -V_y H_z S_x - V^*_x H_y S_z - V_x H_y S_z \qquad (6)$$

In practice the third term can usually be neglected. First, the current component V_x is usually much smaller than the ship velocity, V^*_x. Secondly, V_x is often cancelled because of the way in which GEK measurements are made. Since the electrodes tend to drift with respect to one another the usual practice is for the ship on at least one course to tow the electrode in first the x direction and then the $-x$ direction. The mean of the two observed potentials is used as the zero reference so that $\bar{E}_x$, the value used in determining V_y in (5), is simply

$$\bar{E}_x = E_x - \tfrac{1}{2}(E_x + E_{-x}) \qquad (7)$$

In this manner any fixed potential between electrodes (as long as it remains constant over the period of measurement) is cancelled out. Thus the third term in (6) is cancelled. Both S_x and V^*_x change sign as the ship changes direction, but V_x does not. Hence, when a cable with a density greater than that of sea water is used, the current component is related to the measured potential such that

$$V_y = \frac{-\bar{E}_x}{H_z S_x} - V^*_x \frac{H_y}{H_z} \tan \psi \qquad (8)$$

where $\tan \psi = S_z/S_y$, where ψ is the angle the cable makes with the horizontal plane. By towing the electrodes at right angles and adding the components vectorially as in (3), it can be demonstrated that (8) becomes

$$\mathbf{V} = \mathbf{s}\frac{\bar{E}}{H_z S} + \mathbf{t}V^* \frac{H_h}{H_z} \tan \psi \qquad (9)$$

where H_h is the horizontal component of the Earth's magnetic field, $\mathbf{t}$ is a unit vector pointing toward magnetic north, and $\mathbf{s}$ a unit vector pointing 90° to the left (to the right in the southern magnetic hemisphere) of the vector $\mathbf{V}$. (In practice, of course, towing the electrodes at right angles is almost impossible. However, the difference between 'ship's heading' and the actual path of the ship is usually not more than a few degrees and results in a relatively small error [see *LSS*, 1954].) It is assumed here that the magnitude of V^*, the speed of the ship through the water, is the same on both legs. This assumption may not be true when the sea is heavy or the wind strong.

If one neglects the S_z terms and calculates the current on the basis of (5), one arrives at (9) without the second term. Since this is the assumption that is usually made in GEK measurements, one can write (9) as

$$\mathbf{V} = \mathbf{V}_c + \mathbf{V}_f \qquad (10)$$

where $\mathbf{V}$ is the 'actual current' assuming (6) is true, $\mathbf{V}_c$ is the current calculated in the usual manner from (5), and $\mathbf{V}_f$, which always points toward magnetic north, is the false signal caused by the fact that $S_z \neq 0$, and must be added to the calculated current in the usual way in order to arrive at the actual ocean current.

In order to know the magnitude of this false current it is necessary to know the value of $\tan \psi$. On four cruises in the past four years (Scripps Institution Cruises SHELLBACK, CAPRICORN, and EASTROPIC; and Pacific Oceanic Fishery Investigations Cruise 16 of the *Hugh M. Smith*) ships equipped with GEK's have made measurements at the magnetic equator (where H_z is zero) and in this way we have been able to measure the value of $\tan \psi$ for different ship speeds. The results are shown in Figure 1. The mean value of the direction of these 34 measurements was one degree east

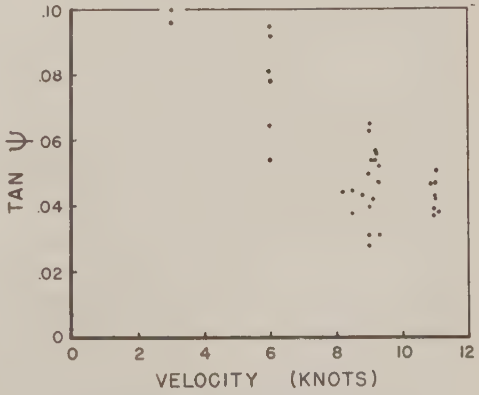

FIG. 1 – The angle a demolition cable makes with the surface when towed through the water at different speeds

Table 1 – *Representative values of the 'false current' caused by cable droop*

Area	H_z	H_h	V_f	Dir.
	oersted	oersted	cm/sec	°
Equatorial Countercurrent (Eastern Pacific)	0.18	0.33	40 ± 9	010
Kuroshio	0.32	0.31	21 ± 5	355
Florida Current	0.44	0.25	12 ± 3	360
California Current	0.43	0.25	13 ± 3	015
Gulf Stream	0.52	0.16	6 ± 1	345

from magnetic north with a standard deviation of three degrees. The mean standard deviation of $\tan \psi$ for ship speeds of 8.5 to 9.5 knots is $\tan \psi = (4.66 \pm 1.05) \times 10^{-2}$. In Table 1 are listed the values of $\mathbf{V}_f$ for a few representative areas assuming a ship's speed of nine knots.

In the area of the Gulf Stream and the Florida Current the assumption of $\nabla\varphi \cong 0$ is not in general valid, because the currents are still strong at depths which are not "small compared to the depth to the bottom" [*von Arx*, 1952; *Murray*, 1952]. The assumption of $S_z = 0$ results in a trivial error in the Gulf Stream (where the ratio of H_h/H_z is small and the currents are of the order of 50 to 250 cm/sec), and the error is still very small in the Florida Current where the currents are even stronger. It has been the experience of the authors in studying the California Current and the Equatorial Current system that the assumption $\nabla\varphi \cong 0$ is apparently valid. The droop correction on the other hand is large, amounting in both cases to a correction which is of the same order as the currents measured.

Neutrally buoyant cables—Over the past few years there have been several attempts to use cables which did not droop. This has been done by either floating the demolition cables or using neutrally buoyant cables. On the 1955 EASTROPIC Expedition to the Eastern Equatorial Pacific, neoprene cables (with a density about that of sea water) were used successfully. They were towed at the magnetic equator and showed no indication of droop. However, although $S_z = 0$ with this type of cable, it is not necessarily true that $\mathbf{V}^* \times \mathbf{S} = 0$. A cable which floats upon the water partly exposed to the air may be subject to transverse forces caused by the drag of the wind on the cable. In this case $S_y \neq 0$. Under these circumstances (4) becomes

$$E_x = -V_y S_x H_z + (V_x + V^*_x)\, H_z S_y \quad (11)$$

The sign of S_y does not change when the electrodes are towed in the opposite direction, and the equivalent equation to (8) in the case of wind-blown electrodes is

$$V_y = \frac{-\overline{E}}{H_z S_x} + V^*_x \tan\theta \qquad (12)$$

where $\tan\theta = S_y/S_x$ and θ is the angle in the horizontal plane that the electrode cable makes with the path of the ship relative to the water. This angle is a function of the athwartship component of wind velocity. The equivalent of (10) is

$$\mathbf{V} = \mathbf{V}_c - \mathbf{V}_w \qquad (13)$$

where the direction of $\mathbf{V}_w$ is approximately down wind. (If $\tan\theta$ is a simple linear function of the athwartship wind speed, then the direction of $\mathbf{V}_w$ is exactly down wind.)

For comparison we have, on two occasions, simultaneously towed both neutrally bouyant and demolition cables, the ship running in squares for a number of hours. The mean values of GEK measurements made simultaneously with neutrally buoyant cables $\overline{\mathbf{V}}_{nb}$ and demolition cables $\overline{\mathbf{V}}_d$, are shown in Figure 2. Values of $\overline{\mathbf{V}}_d$ have been corrected for droop. The vector differences given in Table 2 are defined by

$$\overline{\Delta\mathbf{V}} = \overline{\mathbf{V}}_d - \overline{\mathbf{V}}_{nb}, \qquad (\overline{\Delta\mathbf{V}^2})^{\frac{1}{2}} = \overline{[|\,(\mathbf{V}_d - \mathbf{V}_{nb})\,|^2]}^{\frac{1}{2}}$$

Directions are in conventional notation: currents are 'toward', wind is 'from.' On other occasions the two types of cable were towed together, but with only one recorder aboard ship it was necessary to record first one and then the other. In Figure 2 the difference in velocity of successive GEK's as measured by the two cables is plotted against wind direction. The magnitude of the individual vectors is the difference between successive measurements with first a neutrally buoyant cable and then a demolition cable; demolition cable values have been corrected for droop. The time between the two measurements is of the order of 20 min. The directions of the vectors in Figure 2 have been plotted against the observed wind direction, and the wind during the period of observation varied between 5 and 18 knots from 270° through 045°.

As can be seen from these tests the neutrally buoyant cable shows a consistent 'down-wind component' as predicted from (12). However, the interpretation of these data is somewhat ambiguous. The electrodes on the demolition cable tow at a depth of between 8 and 15 m. The electrodes of the neutrally buoyant cable are in the top meter. One might expect a wind-driven current superimposed upon the 'geostrophic current' to give a

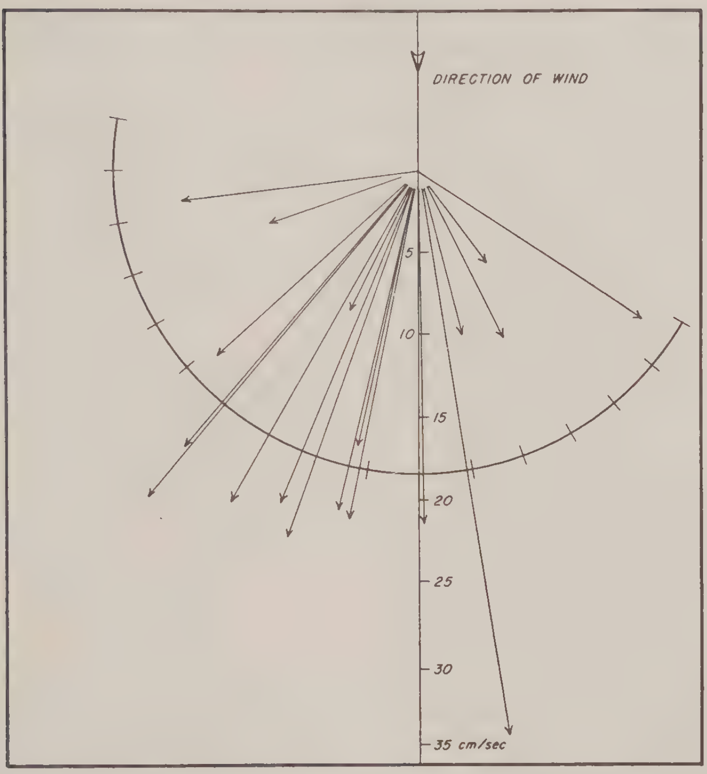

FIG. 2 – The difference in velocity as measured by a demolition cable and a neutrally buoyant cable

TABLE 2 – *Comparison with mean wind speed of the mean values of GEK measurements made simultaneously with neutrally buoyant cables* ($\mathbf{V}_{nb}$) *and demolition cables* ($\mathbf{V}_d$)

Date	Length of obs.	Number of observations	$\overline{\mathbf{V}}_d$	Dir.	$\overline{\mathbf{V}}_{nb}$	Dir.	$\overline{\Delta\mathbf{V}}$	Dir.	Wind		$\overline{(\Delta\mathbf{V}^2)}^{1/2}$
									speed	dir.	
	hr		cm/sec	°	cm/sec	°	cm/sec	°	cm/sec	°	cm/sec
July 26–27, 1955	22.5	43	8.9	339	2.6	283	7.4	171	9	285	16
Nov. 29–30, 1955	39.3	63	13.4	186	16.6	159	7.6	103	14	300	11

shear not unlike that observed, even though the interpretation of these GEK measurements as a measure of near-surface shear is rather complex [see *LSS*, 1954].

We have not yet been able to satisfy ourselves whether the observed difference is due to current shear, wind-blown electrodes, or both. There are two reasons for thinking the difference is not real, but caused by windage on the electrodes. One is discussed in the next section on tests of GEK validity. The other is essentially a negative argument. For the tests summarized in Table 2, the two cables were towed for a total of 106 observations. In addition there are the 30 successive measurements in Figure 2. In all of the 136 measurements the difference between the two cables was a vector which was always in the down-wind semicircle. The rms vector for the 106 cases where the measurements were made simultaneously is 13 cm/sec. (A simple calculation of the ratio of form to surface drag for a cable 10 to 50 pct exposed to air indicates that angles of this order (θ = 1 to 3°) might be expected.) More direct measurements of current shear [*Stommel*, 1954] indicate that although one might expect a down-wind component on the average, it would be unlikely that there always would be a down-wind component.

TABLE 3 – *Comparison of the mean GEK velocity with the mean drogue velocity*

Region	Date	Length of observations	Depth of drogue	Drift of drogue	$\bar{\mathbf{V}}_g$	Dir.	$\bar{\mathbf{V}}_t$	Dir.	$\bar{\mathbf{V}}_g - \bar{\mathbf{V}}_t$	Dir.	Maxi-um error in $\bar{\mathbf{V}}_t$ area positioning
		hr.	m	mi	cm/sec	°	cm/sec	°	cm/sec	°	cm/sec
Equatorial Countercurrent	Oct. 30, 1955	11.5	5	8.2	38.0	081[a]	37	076	3	330	6.7
California Current (near Channel Islands)	Jan 21–24, 1952	65.3	20	7.3	4.3	060	5.7	070	1.6	277	0.8
	Jan. 24–27, 1952	69.0	10	25.8	15.1	187	19.3	179	4.8	335	0.8
	July 26–27, 1955	22.5	5	6.6	8.9	339	15.1	342	6.3	167	4.6
					2.6	383[a]			14.6	171	4.6
	Nov. 29–Dec 1, 1955	39.3	5	9.8	13.4	186	129	179	1.6	255	3.3
					16.6	159[a]			6.2	110	3.3

[a] Neutrally buoyant cable, no droop correction applied.

Tests of GEK validity—One way of testing the validity of the assumptions and the applied corrections is to make continuous GEK measurements around a free-floating surface drogue. The average velocity of the water can be ascertained by plotting the trajectory of the drogue by celestial fixes or other navigational means, and the average drogue velocity can be compared with the average GEK velocities during this period. This experiment has been performed once in the Equatorial Countercurrent with a neoprene 'neutrally buoyant' cable, twice in the California Current with demolition cable, and twice in the California Current with both demolition cable and neutrally buoyant cable. The results are shown in Table 3 in which $\bar{\mathbf{V}}_g$ is the mean corrected GEK velocity and $\bar{\mathbf{V}}_t$ the mean drogue velocity. In all cases the calculations were carried out under the assumption $\nabla\varphi = 0$. The false current due to cable droop was calculated from the data in Figure 1.

The agreement between mean GEK velocity and mean drogue velocity is good in most cases. The agreement between drogue and neutrally buoyant cable in the Countercurrent is excellent, and it is well within the possible error due to uncertainty of drogue positioning. This test was conducted in a calm sea. The two tests in which both demolition and neutrally buoyant cable were used show the drogue velocity in better agreement with the demolition cable than with the neutrally buoyant, which is another reason for thinking the down-wind component discussed in the last section is due to windage rather than current shear.

Summary and conclusions—The calculation of surface currents by (5) implies two important assumptions

$$\text{(a) } |\nabla\varphi| \ll |\mathbf{V}\times\mathbf{H}|$$

$$\text{(b) } \mathbf{V}_* \times \mathbf{S} = 0$$

The conditions which must be satisfied for (a) to be true are discussed in detail in *LSS* [1954]. The second assumption concerns the GEK cable and how it tows behind the ship. The use of a cable heavier than sea water results in the far electrode's towing deeper than the near electrode and introduces an error, which in the calculation of the current vector shows up as a 'false current' whose direction is toward magnetic north and whose magnitude increases as one approaches the magnetic equator. Measurements have been made of the cable droop for different ship speeds, the results of which are shown in Figure 1. Examples of the magnitude of the false vector are given in Table 1.

Tests with a neutrally buoyant cable towed in conjunction with a demolition (heavier than sea water) cable show that the difference in the two currents always results in a vector whose direction is 'down wind.' This current difference may be the result of shear, but it is more likely the result of the neutrally buoyant cable's making more leeway than the ship. This windage vector is of the order of 10 to 15 cm/sec and is independent of the magnetic latitude.

GEK measurements have been made around a drifting drogue and the mean value of the GEK observation compared with the mean velocity of the drogue as indicated by the drogue trajectory. When proper corrections are applied for cable droop, the two are in good agreement.

Acknowledgments—This paper represents in part the results of work carried out by the University of California under contract with the Office of Naval Research.

This paper also represents one of the results of research conducted under the Marine Life Research Program, the Scripps Institution's component of the California Cooperative Oceanic Fisheries Investigations, a project sponsored by the Marine Research Committee.

REFERENCES

BOWDEN, K. F., Measurements of wind currents in the sea by the method of towed electrodes, *Nature*, **71**, 735–737, 1953.

LONGUET-HIGGINS, M. S., M. E. STERN, AND H. STOMMEL, The electrical field induced by ocean currents and waves, with applications to the methods of towed electrodes, *Pap. Phys. Oceanogr.*, **13** (1), 37 pp., 1954.

MURRAY, K. M., Short period fluctuations of the Florida Current from geomagnetic electrokinetograph observations, *Bul. Mar. Sci., Gulf Carib.*, **2**, 360–375, 1952.

STOMMEL, H., Serial observations of drift currents in the central North Atlantic Ocean, *Tellus*, **6**, 203–214, 1954.

VON ARX, W. S., An electromagnetic method for measuring the velocities of ocean currents from a ship under way, *Pap. Phys. Oceanogr.*, **11** (3), 62 pp., 1950.

VON ARX, W. S., Notes on the surface velocity profile and horizontal shear across the width of the Gulf Stream, *Tellus*, **4**, 211–214, 1952.

Scripps Institution of Oceanography, La Jolla, California.

(Communicated manuscript received December 3, 1956; open for formal discussion until November 1, 1957.)

(235)

Reproduced by Permission

[Reprinted from The Journal of General Physiology, May 20, 1957,
Vol. 40, No. 5, pp. 715–733]
Printed in U.S.A.

SENSITIVITY TO LIGHT IN THE SEA ANEMONE METRIDIUM SENILE (L.)

II. Studies of Reaction Time Variability and the Effects of Changes in Light Intensity and Temperature*

By WHEELER J. NORTH

(*From the Laboratory of the Division of Marine Biochemistry, Scripps Institution of Oceanography, University of California, La Jolla*)

(Received for publication, November 23, 1956)

In the first paper of this series it was shown by North and Pantin (1) that the sea anemone *Metridium senile* is not uniformly sensitive to radiation throughout the visible spectrum; maximum sensitivity generally occurred in the blue-green at about 500 mμ, although considerable variability was found from animal to animal. Light and dark adaptation phenomena were also demonstrated.

The entire body surface of *Metridium* is apparently photosensitive, and the animal usually responds to light by local contraction of the parietal musculature; unilateral stimulation, therefore, results in bending, Bohn (2), Parker (3), Batham and Pantin (4). North and Pantin were unable to find either macroscopic or microscopic units suggestive of photoreceptors in the animals, hence the actual site of light perception is still unknown. Both Batham and Pantin and North and Pantin used high light intensities for times up to several minutes. Responses were often movements of a centimeter or more and there was a delay of 20 to 40 seconds between commencement of illumination and the onset of bending. Neither the magnitude of bending, however, nor the time delay were free from variability.

The present investigation deals with much dimmer stimuli and a response of slightly different character. The magnitude of this response is rarely a bending traverse of more than a millimeter; here only bending is involved whereas the high intensity stimuli occasionally cause complete closure, suggesting a more general effect, perhaps even an avoidance reaction. The low intensity response is also involved at high intensities, but may escape notice since it is completed in less than a second with a movement of perhaps a millimeter or less. The action spectra of the two responses are similar, however, and each under the proper conditions displays a reaction time (delay between initiation of stimulus and response). Because of its greater uniformity, the present study will utilize only the low intensity response.

---

* Contribution from Scripps Institution of Oceanography, University of California, New Series, No. 918.

Materials and Methods

The illuminator used to supply test stimuli was a model 370 Spencer microscope lamp supplied with a General Electric, vertical ribbon filament, 110 watt projection bulb, type 18AT10/1–6v. The lamp was fitted into a holder containing an additional lens, a 5 cm. plexiglas cell filled with 0.1 M acidic copper sulfate solution, and a slotted holder for 8¼ cm. square filters. The illuminator produced a 1½ × 8 cm. rectangular image of the filament, which was sharply defined at distances from 22 to 35 cm. in front of the forward lens of the system. The input voltage was stabilized by two Sola constant voltage transformers, types CV and CVH, rated at 500 watts each and connected in series. Both transformers were rated to give 1 per cent or better regulation through ±20 per cent fluctuations in line voltage; through the series connection, the regulation was refined to 0.01 per cent. Daily and momentary line voltage fluctuations at the laboratory rarely exceed ±10 per cent.

The regulated voltage was transformed to 6 volts through a triad No. F22-A transformer connected to a variac which controlled the voltage to the illuminator. The latter voltage was kept constant at 6.00 volts by means of a Weston AC voltmeter.

Within the illuminator infrared radiation was removed by a Corning aklo No. 3966 heat filter, 2.5 mm. thick, and by copper sulfate kept in the aforementioned plexiglas cell of 5 cm. pathlength. An Ilford No. 603 spectrum filter, 8¼ × 8¼ cm., made of gelatin, was used to provide blue-green light. This filter had a maximum transmission of 12 per cent at 493 mμ (near the maximum of the anemone's action spectrum) and a transmission of 1 per cent at 473 and 520 mμ; transmissions substantially lower than 460 mμ or beyond 550 mμ were 0.001 per cent or less. Intensities were regulated with Ilford neutral density gelatin filters. All filters were calibrated in a Beckman DU spectrophotometer.

The illuminator was calibrated with the aklo, copper sulfate, and 603 filters in place, by means of an Eppley No. 2470 vacuum thermopile, placed 25 cm. in front of the forward lens of the system, and positioned in the center of the image. The thermopile was calibrated by means of a National Bureau of Standards secondary radiation standard No. C-613, and the output was measured with a Leeds and Northrup type 2284B reflecting galvanometer. Corrections for losses due to absorption, reflection, and scattering by glass surfaces and sea water in the aquarium and aquarium housing totalled 10 per cent and were determined with a General Electric type DW-68 exposure meter.

Throughout the experiments to be described, the animal was illuminated from above by a 2 watt GE 46 radio bulb, 40 cm. distant, shining through an Ilford No. 608 red filter. Voltage across this bulb was regulated as described above. This arrangement cast a general illumination of about 10^{11} quanta/cm.^{2} of light with wave length values greater than 620 mμ upon the surface of the anemone. Light of this dimness and spectral character was assumed to impose no adaptation to the blue-green stimulus. Variation of the intensity of the red light by about threefold did not change the sensitivity of animals to the blue-green stimulus.

The containing aquarium had a capacity of about 10 liters and was kept in a heat-insulated housing in a dark room. The housing was sufficiently large to permit moisture, condensed on the exterior of the aquarium, to be wiped away before each determination. Sea water in the aquarium was circulated continuously by a Jabsco stainless steel pump, through a stainless steel cooling coil and a charcoal column 45 cm. high. Plexiglas tubing was used for interconnecting the components of the circulating system, and water was cycled completely through the aquarium at a continuing rate of about once every 5 minutes. Temperature was controlled by a Fenwall No. 17851 thermoswitch which maintained constancy of ±¼°C. The entire system was drained and flushed with 40 liters of fresh sea water once or twice weekly. At this time the walls of the aquarium were thoroughly cleaned.

An upright grid of inert black bakelite bars 2 mm. square in cross-section, and arranged to provide 8 mm. square holes, was positioned in the aquarium between the anemone and the eye of the observer. During stimulation the head of the observer was fixed by a rest, the direction of view being perpendicular to the stimulating light beam. Any motion by the animal was readily apparent through the bars of the grid. The anemone was kept on a rotatable, tiltable dais which enabled the observer cautiously to line up the leading edge of the animal with one of the vertical bars of the grid; movements of ½ mm. or less were thus readily detectable. Before each stimulation the anemone was closely observed for at least 30 seconds to ensure that no movement might be in process. If movement was detected, observations were continued until none occurred during a 30 second period. During an experiment the stimulus was extinguished a few seconds after response and at least 5 minutes of darkness intervened between successive stimuli. Measurements of height and diameter were made at intervals during the course of an experiment to ensure that an animal maintained approximately the same shape and volume. Any radical changes in these quantities might alter the total number of photoreceptive units within the illuminated area. Short times (120 seconds or less) were measured with a stop-watch.

Moderate sized specimens of *Metridium* (about 3 cm. diameter and 10 cm. high while expanded) were collected intertidally along the California coast between Pt. Conception and Pt. Reyes. They were allowed to adhere to plexiglas discs and when not under observation were maintained in running sea water cooled to 13°C. Healthy specimens have been thus maintained at La Jolla for 18 months, being fed occasionally on living *Artemia salina*, a small pelagic brine shrimp which *Metridium* readily captures on contact. All data presented were obtained using the white color phase of this anemone, although most of the other color phases described by Fox and Pantin (5) are available. Any variations in sensitivity due to different concentrations of insensitive body pigments were thus minimized.

RESULTS

Variability of the Reaction Time.—The reaction time in *Metridium* (the period elapsing from the instant of illumination until a response is observed) is a feature of great importance, since at any given intensity it is a measure of the number of quanta delivered to the animal. Illumination is apparently necessary for the entire duration of the reaction time; in 70 trials no response was observed if the light was extinguished before the onset of bending.[1] The magnitude of the response (the distance moved during bending) does not appear to correlate with the length of the reaction time.

Unfortunately even under the most uniform environmental conditions obtainable, all animals studied displayed considerable variations in reaction time from one stimulus to the next. Fig. 1 *a* shows a typical record obtained on an anemone from 38 observations during a 7 hour period. Since a light source of constant intensity was used to stimulate, the number of quanta necessary to cause a response varied fivefold in this graph. A sevenfold variation was, in fact, common.

Irregular and large as the fluctuation was, the reaction times of any given anemone always appeared to oscillate around a given average value which did not change over periods of at least a week. It was found, in fact, that when large numbers of observations were studied, statistical similarities among data from different anemones became apparent, and a scheme could be constructed to predict the expected error when only small numbers of observations were available.

If, say, 100 observations were made on an animal, and the reaction times were grouped into classes (for example, out of the 100 observations, 7 might be in the 1.6 to 2.5 second class; 11 in the 2.6 to 3.5 second class; 18 in the 3.6 to 4.5 second class, etc.), a characteristic skewed distribution was always obtained with a degree of kurtosis (peakedness) somewhat greater than ordinarily found in a normal or Gaussian distribution. The anemone data could be adequately fitted by curves calculated from the Poisson distribution

$$F_t = \frac{(Kt)^m e^{-Kt}}{m!}, \qquad (1)$$

in which F_t is the frequency of any class of reaction time t, and K and m are constants characteristic of each distribution. The reasons for choosing the Poisson distribution will become apparent below but it should be pointed out that the experimental data could probably be adequately fitted by other distributions as well, such as the Gram-Charlier with a correction factor for kurtosis.

Fig. 1 *b* shows the results of 4 large groups of observations made upon 4 different animals under uniform conditions of environment and stimulus. The data were calculated as cumulative frequency, plotted upon probability paper, and the Poisson distribution of closest fit was drawn. The most obvious difference among the curves is their vertical separation, evidenced by the different values of K needed to fit the curves to the data. This difference suggests that the average reaction time for each animal is different, or the average number of quanta necessary to cause a response varies from animal to animal. North and Pantin (1) have shown that there are factors, such as body pigmentation, that can cause permanent variations in base line sensitivity to blue-green light among individuals of *Metridium*. Undoubtedly there are unknown causes as well, and the existence of such differences is hardly surprising, although well worth future study. The main point to be made here is that the vertical spread of the curves does not necessarily indicate fundamental differences in the patterns of variability found in the animals studied.

---

[1] *Metridium* is different in this respect from certain other animals such as *Ciona* and *Mya* (Hecht (6, 7)), *Lampetra* (Steven (8)), or *Cerianthus* (Moore (9)) possessing dermal photosensitivity. The reaction times in the latter group are divisible into a "sensitization period" during which the stimulating light must continue if a response is to be obtained, and a "latent period" during which the animal may remain in darkness and still respond. Both sensitization periods and latent periods might run into several seconds' duration. Any latent period in *Metridium* is probably less than a second, as the animal responds in less than a second to intense flashes of about 1/100 second duration.

(240)

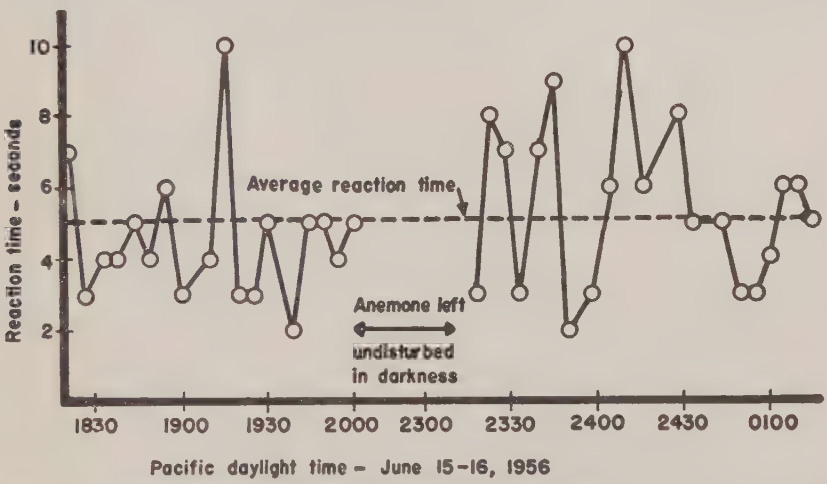

FIG. 1 *a*. Fluctuations in the length of reaction time observed over a 7 hour period; $T = 12°C$. The points were arbitrarily connected by straight lines. Since any latent period is a negligible fraction of the reaction time, the length of the latter can be used as a measure of the radiant energy necessary to elicit a response. Energy of the stimulus was 8.6×10^8 quanta/cm.^{2} sec. of blue-green light.

Variation of K in Equation 1 involves a slight change of slope in the curves of Fig. 1 *b*, but the top curve is of such different slope that it requires an increase in the value of m to best fit the data. In order to determine whether this might indicate a fundamental difference between this animal and the others, a simple statistical device was constructed to run analyses.

The device consisted of a number of marbles of the same size and weight, placed in an opaque urn. Several colors of marbles were available, and a given color was assigned to each reaction time class. F_t values for $m = 5$ $K = 1.00$ (see Equation 1) were then calculated, and the number of marbles corresponding to each F_t were placed in the urn. Marbles were withdrawn by touch one at a time, the class noted, the marble replaced, and the urn shaken thoroughly before the next withdrawal.

Ten distributions of 100 withdrawals each were thus obtained, and the two distributions with the most extreme slopes are plotted in Fig. 1 *c*. These extremes are closely fitted by curves for which $m = 4$ and $m = 8$, hence it is concluded from the available data that the differences of slope in the curves of Fig. 1 *b* probably have no fundamental significance. A total of eight distributions of 60 or more observations each on eight different anemones have not shown significant deviations from each other when analyzed in the above manner.

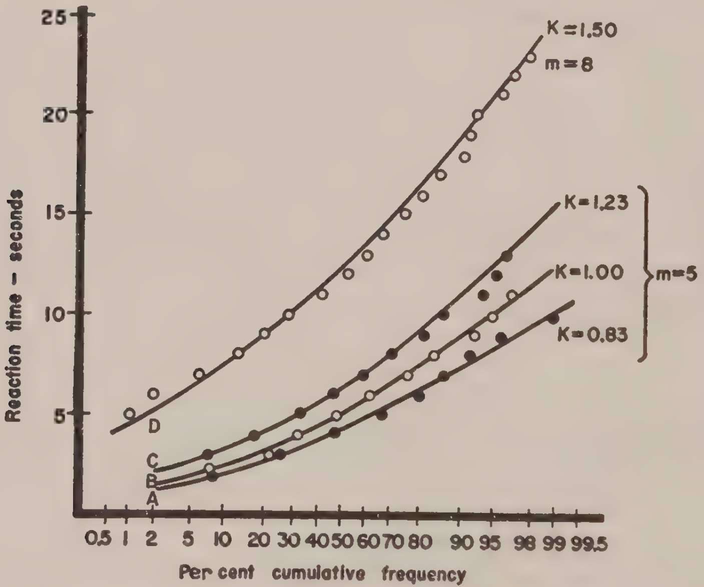

FIG. 1 *b*. Cumulative frequency curves for reaction time distributions gathered from four different anemones at 11.3–12.5°C. The points are experimental data and the lines are calculated values for the Poisson distribution discussed in the text. The record shown in Fig. 1 *a* forms a part of the data used for the points of distribution *A* in this figure. *A* and *D* represent 100 observations, *B* 98 observations, and *C* 81 observations. Energy of the stimulus was as in Fig. 1 *a*.

It would seem, then, that the patterns of variability in different anemones appear essentially alike when sufficiently large numbers of observations are analyzed. This suggests that the cause of the variability may be a mechanism common to all anemones of this species.

One further question needs to be answered; is there a correlation between the values of consecutive reaction times when series of observations are made, or do the values distribute themselves at random? A rapid and easy way of determining autocorrelation is to count the number of oscillations in a given series of observations. If the values occur at random, the number of maxima and the number of minima found should each be about 1/3 of the total number of observations. Large deviations from the 1/3 value indicate that autocorrelation exists.

To take an example, the record shown in Fig. 1 *a* consists of 38 observations and contains 11 maxima and 11 minima (a point at the start or the end of a series being arbitrarily judged a maximum or a minimum if it deviates from the average by more than 1 second). The series of observations is therefore almost certainly composed of values distributed at random. This conclusion is supported by data obtained from the distributions of Fig. 1 *b*, collected in Table I. In addition, the range of variation is shown in the 10 distributions obtained from the random marble withdrawals which illustrate the variation that can be expected. Our conclusion is that there may be a factor or mechanism in the photosensory processes of *Metridium* which causes as much as a sevenfold random variation in reaction time.

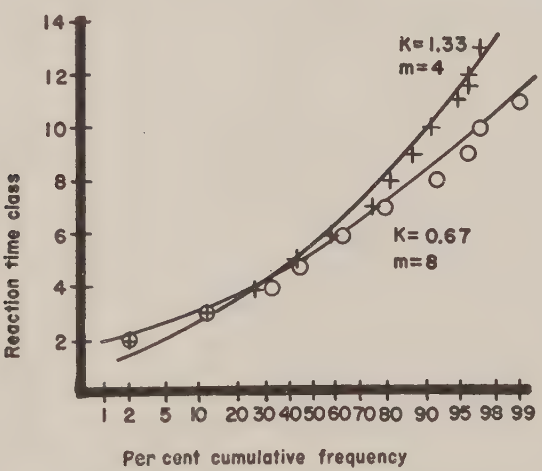

FIG. 1 *c*. Extremes of variation in slope found in 10 distributions obtained from a statistical analyzer described in the text.

Expected Error for Small Numbers of Observations.—Determination of the large distributions shown in Fig. 1 *b* requires not only considerable time but also a degree of good fortune, since animals may not maintain constant position, shape, or activity for the necessary long periods. Many easier yet significant experiments could be performed, however, based upon smaller numbers of observations, if the experimenter had a fairly accurate estimate of the errors that might be expected in the procedure he employs. In experiments to be discussed below, for example, it was found necessary to determine the means, the per cent deviation from the mean, and the degree of randomness of small groups of reaction time determinations. A description of the method of determining the expected error in these quantities follows.

It was decided to adopt ten observations as a convenient total for a given series. This number can usually be made in an hour or less, and, as will be seen presently, does not give rise to large expected errors.

Since it has been shown that large numbers of observations of reaction times occur randomly in a distribution resembling the Poisson, it is possible to calculate theoretically the expected error of, say, the mean of a group of 10 observations. It is much less laborious, however, to perform a thousand marble withdrawals in the statistical analyzer, divide them into groups of ten, determine the means of each group, and plot a frequency curve. The validity of this curve can then be checked against results obtained from anemones. Fig. 2 shows the results of such determination of the means, per cent deviations from the mean, and degree of randomness, employing the series of 1000 marble withdrawals used in the previous section. Likewise included in the figures are values obtained from the four anemone distributions shown in Figure 1 *b*. The correspondence is fairly close, and the curves of Fig. 2 will be used in the following section as a basis for estimating the expected error or the expected range of variation when groups of about ten observations each are studied.

TABLE I

Statistical Data on Four Large Distributions of Reaction Time from Four Different Specimens of Metridium senile and from Ten Distributions Obtained from a Statistical Analyzer Described in the Text

Experiment (Fig. 1 *b*)	No. of observations × 1/3	No. of maxima	No. of minima
C	27	27	28
A	33.3	32	31
B	32.7	31	32
D	33.3	29	29
Range of variation in 10 marble distributions....	33.3	34–28	33–28

Relationship between Reaction Time and Light Intensity.—

Over the range of intensities studied, it has been found that the photosensitive response of *Metridium* obeys, on the average, the Bunsen-Roscoe law of reciprocity

$$I \times t = K, \tag{2}$$

(244)

in which I is the intensity of the stimulating light, t is the length of illumination time necessary to elicit response (for the case of *Metridium*, the reaction

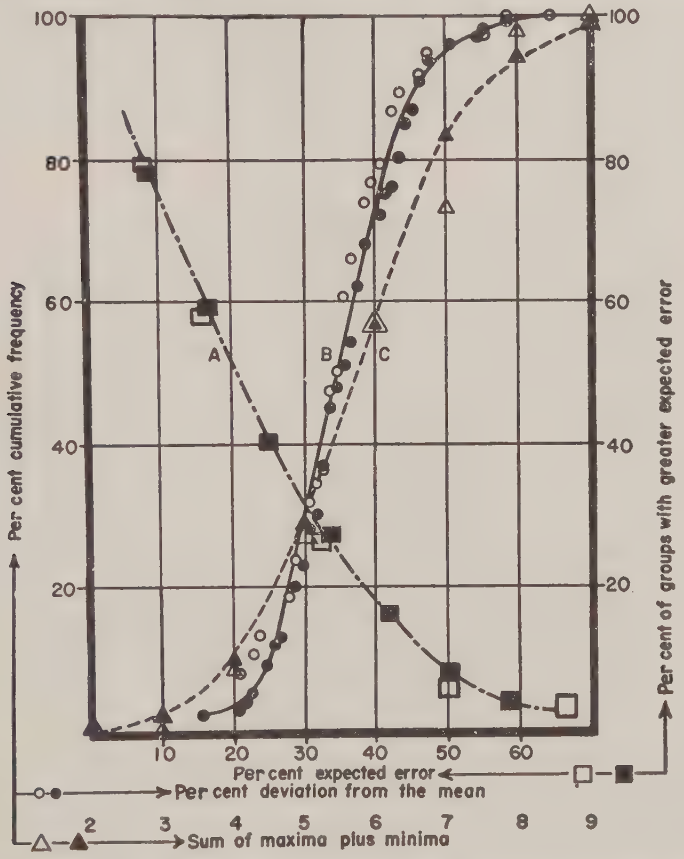

FIG. 2. A. Graph used to determine the expected error in the mean when using groups of ten observations; B. Cumulative frequency curve showing the range of variation to be expected for the per cent deviation from the mean for groups of ten observations. C. Cumulative frequency curve showing the range of variation to be expected for the sum of the maxima and minima found in groups of ten observations. The sum is used as a measure of the randomness within a distribution. Full symbols represent values obtained from marble data, open symbols are values obtained from experimental anemone data.

time), and K is a constant which for *Metridium* appears to be in the neighborhood of 5×10^9 blue-green quanta/cm.^{2}, but varies among individuals by a factor of perhaps three.

Fig. 3 *a* shows the results of 62 observations over a 55 hour period, made on a white animal at different intensities. Each point represents the mean of ten or eleven consecutive observations. Assuming that the animal obeyed the Bunsen-Roscoe reciprocity relationship, the 62 observations were recalculated as if they had been determined at a constant intensity and the mean of the entire group taken. On the basis of this mean, still assuming reciprocity, the theoretical mean at the different intensities of Fig. 3 *a* was then determined, as well as the limits within which it could be expected that nine out of ten points, such as are shown in the figure, would lie. The limits are indicated by the dotted lines, and it is seen from the points that a satisfactory hyperbolic relationship was obtained between the reaction time and the intensity of the stimulating light. 306 observations on eight different anemones, covering the range shown in Fig. 3 *a*, have produced no evidence to suggest that the reciprocity relationship is incorrect.

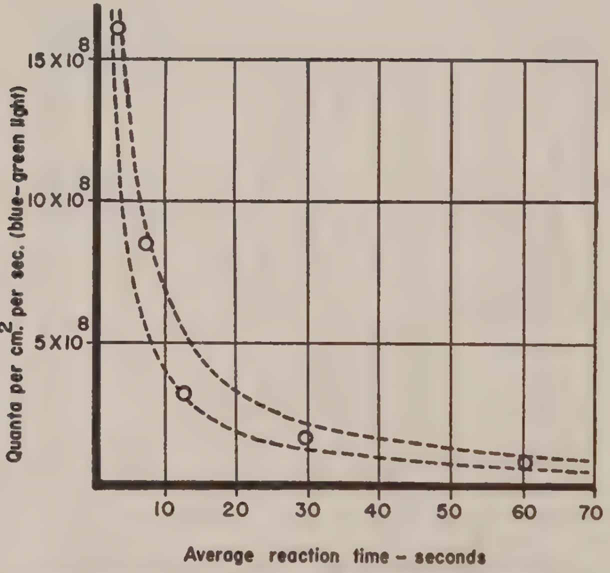

FIG. 3 *a*. Diagram showing the relationship between the length of the reaction time and the intensity of the stimulating light. The points represent the average of 10 to 11 observations on one animal and the dotted lines indicate the limits within which 9 out of 10 of such points might be expected to fall, assuming that *Metridium* obeys the Bunsen-Roscoe law; $T = 12.0°C$.

We are now in a position to eliminate an uncertainty of Fig. 1 *a*. It will be recalled that in constructing this figure the points were arbitrarily connected by straight lines. Suppose, however, that the fluctuations in reaction time occur much more rapidly and instead of connecting the points with straight lines, two or three or more oscillations between each observation should be indicated. If such were the case, it would be expected that records made at dim intensities in which reaction times may average a minute or so, would show not only a decrease in the per cent deviation from the mean, but also in randomness, since minor peaks would be levelled as uniform readings.

Fig. 3 *b* shows the effect of change of average reaction time on the per cent deviation and on the randomness. Many of the readings were taken at higher temperatures in the hope that this would increase the number of fluctuations per unit time and enhance the effect we are seeking, but the next section will show that there is apparently no temperature effect.

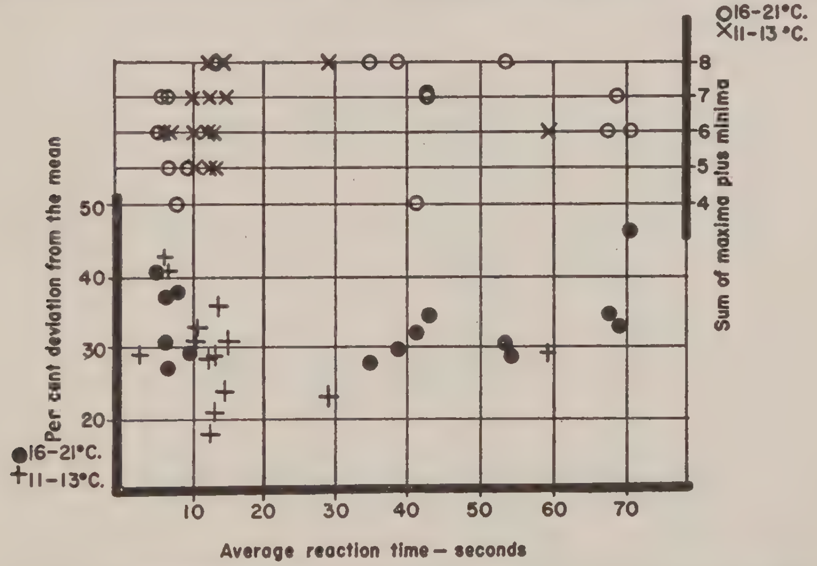

FIG. 3 *b*. Data calculated from 300 observations of reaction time on eight different anemones, showing the distribution of per cent deviation from the mean and of the degree of randomness as a function of the average length of the reaction time. One point (at $\bar{t}$ = 55.1 sec.) was obtained from 7 observations; the rest from 10 to 11 observations.

There is no marked change in either the randomness or the per cent deviation at longer average reaction times. There is perhaps an unexpectedly large number of values of 8 for the maxima plus minima sum, but in three of the four instances at the longer times they are caused by minor fluctuations such as 52, 54, 51 seconds, which at ten times the intensity would have been recorded as 5, 5, 5, seconds (readings are taken to the nearest second).

The values of per cent deviation at the longer reaction times are slightly low, lying mostly in the second quartile of the frequency curve of Fig. 2. The significance of this will be left for a future investigation, but it is felt that the slight change does not constitute evidence for a short period fluctuation.[2] We conclude that if irregular fluctuations in the state of the animal are responsible for the observed variability in reaction time, they are probably fairly accurately portrayed by observations made every 5 minutes.

Anemones often require about a minute to respond to light stimuli of 10^8 quanta/cm.^{2} sec. This is roughly the illumination cast by an ordinary street light upon a normal surface about a mile away. About half an hour of dark adaptation is required before an investigator can accurately judge responses by the animals.

TABLE II

Average Reaction Times Found for Two Anemones over a Range of about 12°C

Anemone 1			Anemone 2		
Temp.	No. of observations	Average reaction time	Temp.	No. of observations	Average reaction time
°C.		sec.	°C.		sec.
4.9	10	6.0	5.7	10	7.3
8.4	10	6.3	7.7	10	8.6
10.0	10	6.4	10.0	9	8.4
12.2	10	5.5	12.9	10	8.2
14.1	10	6.0	14.5	10	8.6
17.1	10	6.8	17.5	10	7.3
Limits within which 9 out of 10 average reaction times would be expected to fall......................		5.0–7.4			6.5–9.7

Effects of Temperature upon the Reaction Time.—Table II shows the average reaction times found for two anemones over a range of about 12°C. There seems to be no significant trend or change over this range, which approximately covers the environmental temperatures for the regions where *Metridium* is found along the Pacific coast. A total of 300 observations were made on eight different anemones over the temperature range 4.3—21.0°C., and no significant changes in average reaction time with temperature were found.

As noted above, if a latent period exists in the response of *Metridium* to light it is very short, probably less than a second in duration. A latent period might include thermally affected processes such as nerve conduction time, muscular contraction time, etc., which could conceivably require less than a second to execute. Although muscular contraction is often a slow process

---

[2] For an oscillation of average wave length 2 minutes or less the per cent deviations should lie between 0 and 18; for an oscillation of average wave length 2 to 4 minutes the per cent deviation should be distributed around 18 as an average.

(Batham and Pantin (10)), *Metridium* can execute a considerable contraction of the longitudinal musculature in a fraction of a second, and conduction in the nerve net of *Metridium* has been shown by Parker (11) to proceed at a rate of about 13 cm./sec. at 21°C. Pantin (12) found similar rates in *Calliactis* for the general nerve net. Photochemical reactions, on the other hand, are well known to be independent of temperature. Since average reaction time does not vary with temperature, it seems safe to assume that most of the reaction time involves photochemical processes.

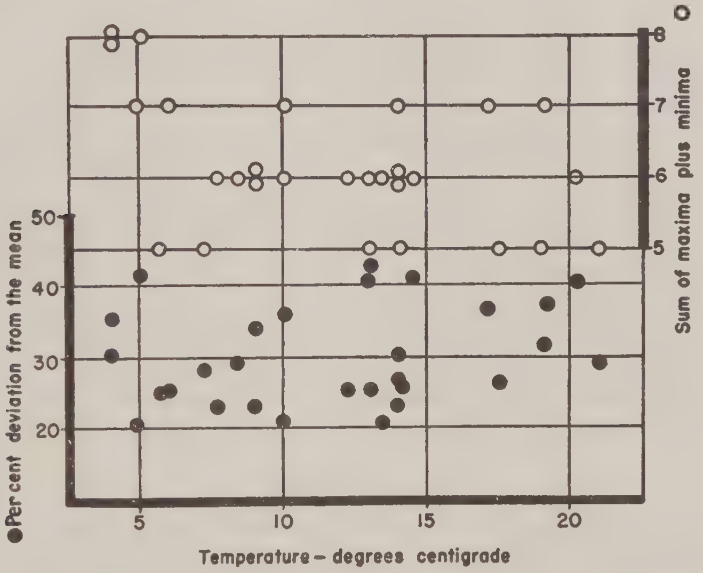

FIG. 4. Data calculated from 290 observations of reaction time on eight different anemones, showing the distribution of per cent deviation from the mean and of degree of randomness at different temperatures. Each point represents 9 to 11 observations. Energy of the stimulus in all cases was 8.6 × 10^8 quanta/cm.^{2} sec. of blue-green light.

Lack of a temperature effect upon the length of the reaction time would thus have a plausible explanation. If, however, the variability should arise from changes in physiological state within the animal, one might expect the rate of such changes to display a temperature effect. By way of illustration, suppose that the variability is caused by variance in the tone of the musculature. The body column of a normal *Metridium* is in a state of constant activity, bending about (Batham and Pantin (13)); so a short reaction time might represent an instance when the animal was stimulated just as it was about to execute a forward (*i.e.* "lightward") bend, while a long reaction time might represent an instance when the stimulus arrived just prior to a backward (or "darkward") bend. The rate of such complex activity should, however, be affected by temperature, and it is indeed found that animals at low temperature are much freer of perceptible random movement and therefore much easier to study. Hall and Pantin (14) found a Q_{10} of 2 for the rate of contraction and relaxation in *Metridium*. The rate of spontaneous bending should, therefore, be considerably retarded at low temperatures. If our hypothesis about muscular tone is correct, the effect on a record such as depicted in Fig. 1 *a* would be to lengthen the time scale. Thus, at 2°C. the abscissa of Fig. 1 *a* might be expected to cover a period of 14 hours or more instead of 7 hours, without any other change in the diagram. This suggests that the average number of oscillations per unit of time would be expected to decrease, which could be detected in our measure of degree of randomness. If the temperature effect were considerable, then, for a small number of observations, the per cent deviation from the mean might also decrease. These predictions are not, however, borne out by the experimental evidence, presented in Fig. 4. Over the range of temperatures shown, at least a three- to fourfold change in the rate of ordinary physiological reactions might be expected. Such a change would decrease the sum of maxima and minima to around 2 or 3, for ten observations taken 5 to 7 minutes apart. It can be concluded that the response of *Metridium* to photic stimulation exhibited no temperature effect in experiments so far devised to test for such an effect.

DISCUSSION

Ecological Aspects of the Photosensitive Response.—The experiments with different intensities have shown that *Metridium* is able to integrate absorbed photic energy over periods of a minute or more, and to utilize the effect to produce a directional response. Several eyeless animals have been shown to possess this ability. Probably the most intensive studies were done on *Ciona* and *Mya* by Hecht (6, 15).

The mechanism of integration of light might conceivably be of advantage to an anemone in a dark environment,[3] causing orientation of the body and tentacles towards steady but weak sources of bioluminescence, thus perhaps increasing the chances of catching microplanktonic luminescent animals for food. Flashes of bioluminescence, presumably from single cells, are often observed in the experimental aquarium, and appear to the human eye many times brighter than illuminations eliciting anemone responses in say, 5 seconds. The ability to integrate radiant energy over the entire body surface might have great potential survival value to other animals as well in the unlighted depths of the oceans where translucency or transparency among organisms is common. Clearly the phenomenon needs to be studied further, not only with regard to its occurrence, already demonstrated in several phyla, but also with regard to actual uses of it in nature.

---

[3] *Metridium* is dredged from depths of 300 to 400 meters in Puget Sound (D. L. Ray, personal communication).

(250)

Cause of Reaction Time Variability.—Pirenne (16) notes that many investigators have observed variability of response to light in their experimental material when the region of the threshold is approached. In the case of the human eye the source of the variability arises from the uncertainty of quantum capture at dim threshold intensities. For *Limulus*, however, Hartline *et al.* (17) were unable to distinguish between quantal uncertainty and the possibility of variation in nerve thresholds known to occur.

With *Metridium*, for lack of further data, we are at the present time faced with something of the same dilemma, although the current experimental evidence favors the hypothesis of quantal uncertainty. As mentioned above, any variable physiological state such as the tone of a muscle or the threshold of a nerve, depending upon a vast array of physiological and biochemical reactions within the organism, can be expected to display a temperature effect of some sort. In order to explain the observed variability by assuming a fluctuating change in the condition of the animal, we should probably look for a single simple temperature-independent chemical process or, at most, two balancing processes, one with a positive and the other with a negative temperature coefficient. Such processes would need to cause sevenfold changes in photosensitivity of the animal over short periods of time; they have yet to be discovered.

If one assumes that *Metridium* has such a low concentration of photosensitive pigment that only a few quanta may be captured in the brief exposure time at the intensities used, explanation of variability in the reaction times follows. This hypothesis of uncertainty of quantum capture has so far proven entirely adequate as an explanation of the data. Since any latent period is a negligible part of the anemone's reaction time, the latter could be expected to be entirely temperature-independent under this hypothesis. Reaction time distributions would need to conform to the Poisson distribution. And indeed they do, although this is a necessary but not a sufficient requirement. If we assume quantal uncertainty, cumulative curves derived from experimental data have all shown values of m (as defined in Equation 1 above) less than 10, suggesting that the animals responded to less than ten absorbed quanta.

At first thought it seems difficult to conceive that when more than one billion quanta are administered to an anemone, the animal would effectively absorb less than 10 of these. Indeed this is probably not so; measurements upon the body wall of white *Metridium* by North and Pantin (1) have shown transmissions of roughly 50 per cent at 500 mμ. Of the remaining 50 per cent a large fraction is undoubtedly reflected, scattered, or otherwise dispersed, but nonetheless considerably more than 10 quanta are probably absorbed by the

(251)

tissues. It must be remembered, however, that there is apparently a specific pathway by which absorption of quanta must occur and still elicit a response by the animal; action spectra for *Metridium*, with maxima lying between 500 and 600 mμ, have been found by North and Pantin (1), suggesting that quanta must be absorbed by a certain pigment or perhaps a few pigments. The concentration of such a photosensitive pigment, therefore, is the critical factor that must be considered.

Unfortunately hardly a beginning has been made towards isolating possible photosensitive pigments from *Metridium*. Indeed if we assume that the hypothesis of quantal uncertainty is correct, even a rough calculation quickly indicates the futility of attempting to isolate such a pigment in any reasonable quantity, much less determine the concentration accurately[4]. We note

[4] Let us assume, as a rough conservative estimate from the data presented above, that on the average 1 quantum in 10^9 is absorbed by the photosensitive pigment in the illuminated area of the animal. Assume, further, a quantum efficiency of unity and let the concentration of pigment be c, its molar extinction coefficient at the wave length of maximum absorption be E, and assume that the thickness of the body wall of the anemone is 10^{-1} cm. Then

$$c = \frac{ln(I_o/I)}{E \times l} = \frac{ln\left(\frac{10^9}{10^9 - 1}\right)}{E \times 10^{-1}} = \frac{10^{-8}}{E}\text{, expressed as moles/liter}$$

In order to obtain a fairly good absorption spectrum in a Beckman DU spectrophotometer, with a 1 cm. path-length cell, the concentration of pigment should be such as to render the maximum per cent absorption not much less than 10 per cent. Such a concentration of pigment would be

$$c = \frac{ln(100/90)}{E \times 1} = \frac{10^{-1}}{E},$$

again expressed as moles/liter. A concentration factor of 10^7 is therefore indicated.

An average sized *Metridium* contains perhaps 10 cc. of tissue, therefore, one million such animals would be expected, according to our calculation, to yield 1 cc. of dilute extract for spectrophotometric analysis, assuming no losses during the extraction procedure. To conduct such an experiment in California would require several man-years of effort just to collect the necessary anemones; the chemical extraction might well be complicated by similar but non-photosensitive pigments which would almost certainly be present in the 100 tons or so of material. To attempt the collection and analysis hardly seems practical.

The hypothesis of quantal uncertainty can be shown to lead to sensible results if we assume a value of E in the equation above, of 10^5, a value common among carotenoids at the wave length of maximum absorption. It can then be calculated that our average sized *Metridium*, fully expanded, would have 10^6–10^7 photosensitive pigment molecules per cm.^{2} of body surface. The animal would need perhaps 10^{14} of such molecules per cm.^{2} before it would appear faintly colored.

in passing that *Metridium* may represent a biological extreme in photosensitive machinery. On the one hand we have receptors such as the human eye, where evolution has conveniently concentrated the photosensitivity pigment. Threshold studies here must deal with the uncertainty of the exact number of quanta contained in any stimulating flash. In similar studies with *Metridium*, on the other hand, the number of quanta per stimulus is readily determinable with sufficient accuracy, but the uncertainty element may still be present, since the pigment concentration may be so dilute as to render any adequate determination of it all but impossible.

In retrospect, the critical data that support the hypothesis of quantal uncertainty are the variabilities in reaction time and especially the demonstration of a complete lack of a temperature effect. At the same time the length of the reaction time is intimately related to illumination since it can easily be varied by changing the intensity of the stimulus. While these considerations constitute strong arguments for the hypothesis, they are perhaps not the conclusive proof that is needed for complete acceptance. In dealing with the properties of such a dynamic fluid as protoplasm, of which we possess only a fragmentary knowledge, it would seem wise to view with reservation conclusions dependent upon indirect evidence.

SUMMARY

1. The reaction time of the photosensitive response of *Metridium* was found to be composed almost entirely of a sensitization period. If a latent period exists, it is too short to be detected by the methods used and is probably less than a second in duration. The length of the reaction time, therefore, was used as a measure of the radiant energy necessary at any intensity to elicit a response.

2. The length of the reaction time was found to vary randomly by a factor of seven under constant environmental and stimulating conditions. Determination of large numbers of reaction times on several anemones, grouped according to length, gave closely similar distributions resembling Poisson distributions. It was suggested that the variability may be caused by the same factor or mechanism in each individual. An experimental scheme was presented for determining the expected error and variation in statistical quantities when groups of ten observations are used.

3. The means of groups of reaction times determined at different intensities formed a hyperbolic relationship when plotted against intensity, suggesting that the animal obeys the Bunsen-Roscoe law of reciprocity. No marked changes were noted of per cent deviation from the mean or of randomness at different intensities. Stimulation of *Metridium* requires roughly 5×10^9 incident quanta/cm.^{2} of blue-green light.

4. No temperature effect could be found on either the means, the per cent

deviation from the mean, or the degree of randomness of series of about ten observations, studied over a 17°C. range. It was concluded that the variability in reaction time was not due to changes in any complex physiological state such as muscular tone.

5. A possible use of the photosensitive response is suggested and the potentialities of "integrative" photosensitivity are discussed.

6. Possible mechanisms to explain the variability in reaction time are discussed. In the light of evidence presented, the most likely hypothesis appears to be the uncertainty of quantum capture caused by low concentrations of photosensitive pigment. Assuming the validity of this hypothesis, evidence suggests that the anemones responded to less than 10 quanta of absorbed light. Caution, however, is recommended in accepting the hypothesis because of the indirect nature of the supporting evidence.

Grateful acknowledgment for helpful criticism and advice is made to Drs. Brian Boden, Frederick Crescitelli, Carl Eckart, Denis L. Fox, Francis T. Haxo, Elizabeth Kampa, Leonard Liebermann, C. F. A. Pantin, and W. A. H. Rushton, and for aid in collecting specimens to Messrs. Raymond J. Ghelardi and Conrad Limbaugh.

It is a pleasure to acknowledge the support given by the George Allen Bisbee Donation and The Rockefeller Foundation Donation for Research in Marine Biology.

REFERENCES

1. North, W. J., and Patin, C. F. A., Sensitivity to light in the sea-anemone *Metridium senile* (L.). I. Adaptation and action spectra, data in preparation.
2. Bohn, G. M., Sur les courbures dues a la lumière, *Compt. rend. Soc. biol.*, 1906, **58,** tome 2, 420.
3. Parker, G. H., The effector systems of actinians, *J. Exp. Zool.*, 1916, **21,** 461.
4. Batham, E. J., and Pantin, C. F. A., Slow contraction and its relation to spontaneous activity in the sea-anemone *Metridium senile* (L.), *J. Exp. Biol.*, 1954, **31,** 84.
5. Fox, D. L., and Pantin, C. F. A., The colours of the plumose anemone *Metridium senile* (L.), *Phil. Tr. Roy. Soc. London, Series B*, 1941, **230,** 415.
6. Hecht, S., The photic sensitivity of *Ciona intestinalis*, *J. Gen. Physiol.*, 1918–19, **1,** 147.
7. Hecht, S., Sensory equilibrium and dark adaptation in *Mya arenaria*, *J. Gen. Physiol.*, 1918–19, **1,** 545.
8. Steven, D. M., Some properties of the photoreceptors of the brook lamprey, *J. Exp. Biol.*, 1950, **27,** 350.
9. Moore, M. M., Tropistic reactions of *Cerianthus membranaceus*, *J. Gen. Physiol.*, 1923–24, **6,** 385.
10. Batham, E. J., and Patin, C. F. A., Muscular and hydrostatic action in the sea-anemone *Metridium senile* (L.), *J. Exp. Biol.*, 1950, **27,** 264.
11. Parker, G. H., The rate of transmission in the nerve net of the coelenterates, *J. Gen. Physiol.*, 1918, **1,** 231.

(254)

12. Pantin, C. F. A., The nerve net of the actinozoa. II. Plan of the nerve net, *J. Exp. Biol.*, 1935, **12,** 139.
13. Batham, E. J., and Pantin, C. F. A., Inherent activity in the sea-anemone *Metridium senile* (L.), *J. Exp. Biol.*, 1950, **27,** 290.
14. Hall, D. M., and Pantin, C. F. A., The nerve net of the actinozoa. V. Temperature and facilitation in *Metridium senile, J. Exp. Biol.*, 1937, **14,** 71.
15. Hecht, S., The photochemical nature of the photosensory process, *J. Gen. Physiol.*, 1919–20, **2,** 229.
16. Pirenne, M. H., Physiological mechanisms of vision and the quantum nature of light, *Biol. Rev., Cambridge Phil. Soc.*, 1956, **31,** 194.
17. Hartline, H. K., Milne, L. J., and Wagman, I. H., Fluctuation of response of single visual sense cells, *Fed. Proc.*, 1947, **6,** 124.

Reprinted by permission of the publishers from
"The Physiology of Fishes", Brown, Margaret Elizabeth, Ed.
New York, Academic Press, 1957. pp.367-385.

Chapter VII

THE PIGMENTS OF FISHES

D. L. Fox*

		Page
I.	Introduction	367
II.	Flavines	368
III.	Pterins	369
IV.	Melanins	370
V.	Carotenoids	371
	References	383

I. INTRODUCTION

"Our minds seem naturally inclined to devote special attention to all coloured substances" (M. Tswett). Transcending its universal esthetic appeal, pigmentation holds special attraction and significance for the biochemist and the physiologist. The colors of organic compounds are manifestations of fractional light absorption by molecular resonance, the frequency of which is retarded by chemical unsaturation. The degree of unsaturation, in turn, is a deciding factor not only of the wavelength of light selectively absorbed, but of relative chemical or biochemical reactivity; it may, for example, confer upon a compound a role as an oxidant or as a reducing agent (Fox, 1953).

Excelling the other vertebrate classes in the richness and variety of their integumentary pigmentation, the fishes thus perhaps display a sign of relatively greater diversity in their metabolism and disposition of colored molecules. Yet the compounds responsible for biochromy in fishes belong to but a few classes, namely, carotenoids, indoles (melanins), flavines, tetrapyrroles, and the pterin and purine group.

Of these classes, the yellow, orange, or red carotenoids and the brown, grey, or black melanins are by far the predominant members. The pale yellow, fluorescent flavines and the pterins are not ordinarily conspicuous, since they occur internally for the most part, or at great dilutions in some scales. The red endogenous cyclic heme tetrapyrroles, found in the blood of all vertebrates (and in the body fluids of many invertebrates), contribute in but a minor way to the external coloration of fishes; moreover, their physiological function is sufficiently well known as to demand no space for special discussion in this chapter. Their open-chained derivatives, the bilichromes, are not of very common manfestation in fishes, but impart striking green or blue-green colors to the flesh, skin, mucus, and skeleton of a few groups of fishes (Fox, 1953; Fox and Millott, 1954).

---

* (Contribution from the Scripps Institution of Oceanography, University of California; New Series No. 919.)

Finally, the purines, notably guanine, hardly belong to the true pigments, since they manifest no colors of molecular resonance. These cyclic, nitrogenous protein catabolites are mentioned here, however, because they are responsible for countless manifestations of mat whiteness (e.g., in ventral scales), of silvery iridescence or of specular blue or green colors in the skins of fishes. The interference colors of iridescence and manifestations of Tyndall blue are greatly fortified by underlying dark pigment, serving as a light screen for penetrating rays. Green aspects often arise from the combined effects of reflected blue Tyndall rays and a yellow pigment (Fox, 1953).

II. FLAVINES

Riboflavine (benzisoalloxazine-6, 7-dimethyl-9-D-riboflavine) is crystallizable from alcohol as stellate yellow-orange needles which decompose between 274 and 293° C. The compound shows reversible optical activity in alkaline systems and, in neutral aqueous media, exhibits maximal light absorption at 445 mμ, with three ultraviolet peaks, at 372, 269, and 225 mμ, respectively.

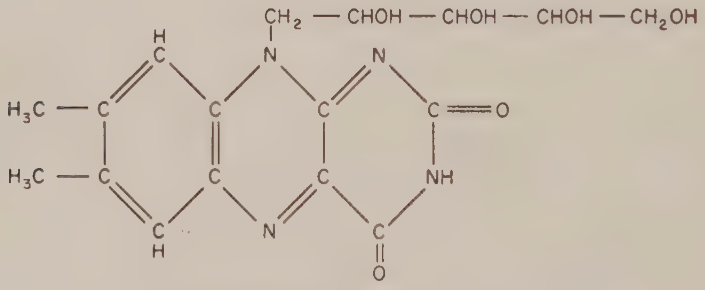

RIBOFLAVINE

It is strongly fluorescent in pyridine, and mildly so in aqueous systems, emitting therein maximally in the green at 562–565 mμ. This property shows little variation between pH 3 and 9, and is nearly constant between pH 5.5 and 8.0. Conjugated as flavoproteins, the natural state *in vivo*, these compounds are not fluorescent, and possess molecular weights of from 60,000 to 77,000.

Concentrations of flavines, amounting to but a few micrograms per gram, show progressive decreases in the eggs of several elasmobranch species after fertilization, and in the developing embryonic shark, *Car-*

charhinus commersonii (Fontaine and Gourevitch, 1936).

But developing free-swimming stages of the eel, *Anguilla anguilla,* show increasing concentrations of flavines, reaching a peak in the adult male, wherein the dorsal and flank skin (but not the white ventral) carries the richest supplies, closely associated with maximal concentrations of carotenoids and melanins, and with minimal or no guanine-containing leucophores (Fontaine, 1937). The correlation of rich flavine deposits with localization of epidermal melanophores holds not only for the eel but also for the scales of the carp and in the conger, *Conger conger,* the blennies, *Blennius gattorugine* and *Muraena helena,* and the lamprey, *Petromyzon marinus* (Fontaine and Busnel, 1938).

Riboflavine has been found to catalyze, *in vitro,* the photochemical oxidation of some pterins, aromatic amino acids, and purines, while aliphatic amino acids are hardly affected (Isaka and Kato, 1952). Cupric, ferric, and to lesser degrees, cobaltous, manganous, nickelous, and zinc ions inhibit this oxidative power of photoactivated riboflavine, while magnesium and calcium ions are ineffective. The inhibitory divalent cations lead to decreases in fluorescence intensity, presumably through chelation between the metal and the photoriboflavine (Isaka and Ishida, 1953).

III. PTERINS

Pterins, involving 30–40% organically combined nitrogen, are somewhat amphoteric, showing limited solubility in mild acids or alkalis, less in neutral aqueous media, and insolubility in common organic solvents. Some of them give a positive murexide reaction, like the purines. The pterins tend to decompose rather than to melt, hence must be diagnosed by their relative nitrogen content, their absorption spectra, fluorescent properties, and behavior toward adsorptive substances (Fox, 1953, and cited references).

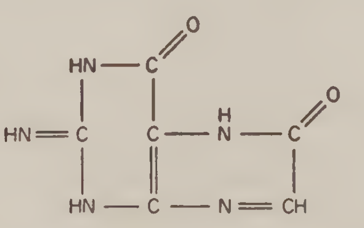

Xanthopterin

Like the flavines, pterins occur in very minute concentrations, in various tissues of fishes and other animals, but possess certain important physiological attributes. Simmons and Norris (1941) and Norris and Simmons (1945) determined that xanthopterin, a yellow member of the series, injected in doses of but 30–50 μg., restored juvenile salmon (several *Oncorhynchus* species) from nutritional anemia.

A blue-fluorescing pterin, fluorescyanin (ichthyopterin, $C_7H_8O_3N_4$), encountered by Fontaine and Busnel (1939) in fishes' scales, is discussed extensively by Polonovski, Busnel, and Pesson (1946). Like riboflavine, fluorescyanin occurs as a chromoprotein and, when free, is reduced by dithionate to a non-fluorescing leuco form, but less rapidly so than riboflavine. Its more ready reoxidation by atmospheric oxygen has led to the hypothesis that it may serve as a hydrogen transporter. The more richly pigmented dorsal scales of carp or goldfish yield more fluorescyanin than do the pale ventral scales, and consume about ⅓ more oxygen per hour. Physiological experiments have indicated a similarity between fluorescyanin (and certain other pterins) and B_1 and B_2 vitamins (Polonovski *et al.*, 1946).

Some Japanese workers have studied the possible photochemical role of some pterins. Yagi (1954) reports the inhibition of the photodecomposition of riboflavine by pterins (in frog skin) but not through any primary role as light-absorbing screens. Kushibiki, Hama, and Gota (1954) describe some violet-fluorescing pterins, cyprinopurple A_1 and A_2 (very similar to fluorescyanin) and cyprinopurple B (a photochemical derivative of A_2) from the scales of carp, *Cyprinus carpio* and *Carassius auratus*. The three pterins, separated by paper chromatography, are all reversibly reducible by dithionate, and exhibit characteristic changes in fluorescence with varying pH and on ultraviolet irradiation.

The consumption of oxygen by dopa is accelerated by xanthopterin, the more so if in the presence of cupric ions, while leucopterin is ineffective, whether alone or with copper. This was found by Isaka and Shuzo (1953), who also confirmed the role of zinc ions in catalyzing the oxidation of dopa-chrome (red) to the colorless phase, regarded as the second step in melanogenesis. Addition of xanthopterin to the system weakens the effect of the zinc, perhaps by chelative binding, or perhaps, according to Isaka (1952), by inhibiting the oxidative reaction, i.e. by competing with dopa for the available oxygen, giving rise to phenylalanine quinone, leucopterin, and water.

IV. MELANINS

The dark, endogenous melanins, which are oxidized, polymerized end-products from the metabolism of tyrosine and allied phenolic compounds, are well known for their black pigmentation of eyes, peritoneal lining, and exposed areas of skin. Mobile melanin granules within the dendritic chromatophores of fishes' scales are responsible for the striking reversible chromatic changes (Sumner, 1940; Parker, 1948; and see Chap. VIII). Melanin aggregates in deeper layers of skin, beneath pigment-free, turbid overlayers of tissue, give rise to the familiar Tyndall blue colors.

Many ceratioid fishes display intensely black pigmentation over the entire body surface, e.g. the black sea devil *Melanocetus johnsoni*, a deep-sea angler fish, has a naked, slimy skin of shiny, jet-black color, save for the small eyes and the conical luminescent tip of the esca or whip-like lure extending from the snout.

At least one species of crestfish (*Lophotus*) stores copious melanin pigment in a specialized glandular sac, whence it is expelled forcibly through a post-anal aperture by muscular contractions against the bifurcated air-bladder lying against either side of the gland. The viscid, adhesive ink has a musty or seminal odor, and, on extraction with ether–acetone solution, yields a little yellow sterol-containing lipid material (cf. octopus ink; Fox and Crane, 1942). The melanin, believed to be conjugated with protein, can be dissociated therefrom by alkaline hydrolysis, and is thereafter readily reprecipitable by mild acidification. Also, like other melanins, the black or sepia-colored centrifugate in this instance was insoluble in ether, alcohol, or acetone, but dissolved in pyridine and in ethylene chlorhydrin. It was readily bleached by hydrogen peroxide (Fox and Hubbs, unpublished).

Pronounced melanogenesis has long been recognized in association with pathological conditions and with moribundity in fishes. Gordon (1948) has reviewed the genetically linked development of melanotic tumors from aggregations of aberrant macromelanophores in several species of fishes (see Chap. X). And Blackburn (1950) discusses the rapid integumentary blackening of the Tasmanian whitebait *Lovettia seali* in the post-spawning, moribund condition. The melanophores increase conspicuously in numbers with successive stages of sexual maturity, especially in the males, and spawned individuals exhibit large dark areas or, notably when dying, complete blackening of the skin. These observations emphasize the association between degradation of tyrosine into melanin, and accelerated protein metabolism, whether concerned with the rapid proliferation of cells, either gonadal or neoplastic, or with cellular decomposition.

V. CAROTENOIDS

Because the carotenoids show considerable contrast with the other biochromes of fishes, in respect to their extensive variety within the chemical class, their relatively high local concentrations, and their visible and metabolic conspicuousness, they have been assigned most of the limited space allotted to this chapter. They are lipoid-soluble, chemically unsaturated, nitrogen-free compounds of high molecular weight (ca. 536), involving only carbon and hydrogen (carotenes; $C_{40}H_{56}$), or these elements plus oxygen (xanthophylls or esters thereof). The molecular configuration responsible for color manifestation is a so-called conjugated double-bond system, wherein the unsaturated linkages occur between alternative pairs of carbon atoms in a long, multiply branched chain. Most, but not all of the known carotenoids have an ionone-like trimethyl substituted cyclohexenyl ring at each end of an 18-carbon chain.

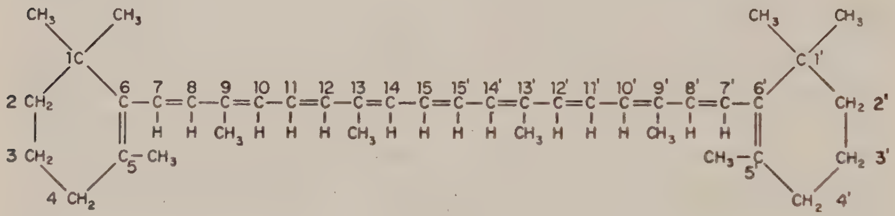

β-carotene

At certain C atoms, one H is replaced by oxygen-containing polar groups, e.g. by —OH at C—3 or C—3′ in cryptoxanthin, at each of these loci in zeaxanthin and in astaxanthin, which has also enolizable (thus acidogenic) keto O at both C—4 and C—4′, while its artifact, astacene, is 3,3′,4,4′-tetraketo-β-carotene. α-Carotene and its hydroxy derivatives contain the double bond between C—4′ and C—5′, thus involving less symmetry. Absence of the bond between C—1 and C—6 characterizes γ-carotene, encountered in the plant dodder and in some fungi, while a completely open chain (by absence of the opposite link between C—1′ and C—6′ as well) represents lycopene, the red pigment of tomatoes and watermelons. There is a very large family of oxygen-containing carotenoids, the formulae for which are depicted in several standard treatments of the subject (e.g. Karrer, Jucker, and Braude, 1950).

Carotenoids occur in fishes, as in most animals, chiefly dissolved in fatty droplets present in eggs, gonads, liver, and skin, to which latter they often confer strikingly conspicuous yellow, orange, or red colors. The xanthophylls, or oxygen-containing carotenoids, often as esters, predominate greatly over the carotenes or hydrocarbon members, both in incidence and in relative concentrations. Indeed, many species of fishes apparently store solely xanthophylls, rejecting or destroying dietary carotenes completely.

Methods for the recovery and resolution of carotenoids into their various fractions are described in other publications (e.g., Fox 1953 and cited references). Diagnostic characteristics of this general class of biochromes may be summarized as follows:

(1) Color in solution red, orange, or yellow, depending on molecular polarity, concentration, and solvent.

(2) Soluble in various organic fat solvents; insoluble in water.

(3) Blue or green colors on treatment of a chloroformic solution with concentrated sulfuric acid or with a solution of antimony trichloride in chloroform.

(4) Distribution between petroleum ether and 90 to 96% methanol (the so-called partition or phase test):
  (a) Carotenes persistently epiphasic (remaining in petroleum ether).
  (b) Free xanthophylls hypophasic (migrating to the aqueous methanol layer).
  (c) Esters of xanthophylls or of acidogenic carotenoids epiphasic.
  (d) Following saponification and dilution, carotenoid acid soaps collect as colored layer at interface.

(5) Chromatographic adsorption:
  (a) Xanthophylls selectively adsorbed from petroleum ether upon powdered calcium carbonate.
  (b) Carotenes, unadsorbed by calcium carbonate, adsorbed upon powdered magnesia, alumina, or calcium hydroxide.

(6) Absorption spectra:
  (a) Solutions of carotenes and of most xanthophylls manifest two absorption bands, in the blue-green, blue or blue-violet, sometimes with a faint third shadow in the violet region of the spectrum.
  (b) Solutions of carotenoid acids, and of certain unusual neutral xanthophylls, show a single broad absorption band in the blue region.

The body of evidence accumulated to date indicates that fishes belong to a class of metabolic selectors of conventional xanthophylls, rejecting all or most of the dietary carotenes. A comparative biochemical survey has yielded little, to date, of an evolutionary trend. Table I presents a review of the occurrence of carotenoids in numerous species of fishes (see Goodwin, 1952; Fox, 1953), listed in successive order of ascending families.

Carotenes (largely β-carotene) seem to occur but rarely in fishes, in very small concentrations, and then usually in glandular structures such as liver and ovaries or eggs. Traces have been reported in the flesh of certain salmons and in the skin of only two or three of the species listed, namely the burbot, *Lota lota,* the river perch, *Perca fluviatilis,* and possibly the goldfish, *Carassius auratus.* Zeaxanthin-like carotenoids are likewise scarce in fishes, having been reported in the eggs of the trout, *Salmo irideus,* in the skin of *Perca fluviatilis,* and questionably also in that of the two species of topminnow, *Xiphophorus,* the goldfish, *Carassius auratus,* and the gourami, *Macropodus.* Astaxanthin-like carotenoids were detected in about a third of the fourscore genera listed. Of these, some 18 instances referred to skin, flesh, or eyes, and 9 to liver, ovaries, or eggs. There are no conspicuous differences between the incidence of astaxanthin among the soft-rayed or intermediate classes of teleosts on the one hand, and the spiny-rayed group on the other.

The predominant integumentary carotenoids of fishes belong chiefly to the taraxanthin and lutein classes. No outstanding differences in the distribution of these two xanthophylls are yet apparent, and there is need for a more extensive survey. Neglecting the two cyclostome species and the pair of elasmobranchs at the lower end of the evolutionary scale, each of whose skin yielded lutein, the skin of soft-rayed and intermediate teleost species seem to be about equally distributed as to incidence of lutein and of taraxanthin, while a slight preponderance of taraxanthin is apparent in the spiny-rayed group. Of 40 species in the first group, 10 (25%) contain only lutein, while 9 contain taraxanthin alone, and another 9 (22% each) yield both types. In the skins of 40 spiny-rayed species, there are 13 (32%) carrying taraxanthin alone, only 7 (17%) lutein alone, and 12 (30%) yielding both lutein and taraxanthin (or violaxanthin). It should be pointed out that the terms "lutein," "taraxanthin," "violaxanthin," and the like, as used here, are not sharply definitive, but commonly refer to xanthophyllic carotenoids which are undifferentiable from those respective compounds in spectral and other properties, save perhaps by mixed chromatography.

The food and feeding habits are insufficiently different to lead to any correlations with type of carotenoid stored, since the great majority of fishes are carnivorous, and a fair number omnivorous. There appear to be somewhat more "lutein selectors" and fewer "taraxanthin selectors" among the freshwater species, most of which belong to the lower or to the intermediate evolutionary group.

Fishes seem, despite the wide occurrence and conspicuousness of their red, orange, and yellow pigmentation, to store but few unusual carotenoids, adhering chiefly to xanthophylls of the taraxanthin, lutein, and astaxanthin types, probably in that order of frequency. The brightly colored opah, *Lampris regius*, is exceptional, storing in its lips, tongue, and fins a striking red esterified xanthophyll, neutral after hydrolysis, but showing a single broad symmetrical absorption band with a maximum at 472 mμ in petroleum ether, and at 502–504 mμ in carbon disulfide, thus close to the respective maxima of astacene. The opah's heavy diet of nautiloid cephalopods suggests that its pigment may have an ultimate crustacean origin, but there remains the question as to how astaxanthin may be converted by the fish, or by the molluscan intermediary, into a nonacidogenic carotenoid (Goodwin and Fox, 1955).

Less surprising than the rejection of carotenes by most fishes is the finding, in one species at least (*Fundulus parvipinnis*) of an apparent ability to convert dietary β-carotene into the familiar taraxanthin class of pigment. Moreover, another taraxanthin-selecting species, the bright orange marine goldfish *Hypsypops rubicunda*, ultimately stores small amounts of carotene in its skin after having been long maintained upon a xanthophyll-free, carotene-rich diet (see below).

Relatively little quantitative work has been done on carotenoid metabolism in fishes, but brief summaries of such experiments should be presented here. Both immature sexes of the Pacific killifish, *Fundulus parvipinnis*, yield approximately 1 mg. of taraxanthin-like xanthophyll per 100 g. of fresh tissues. Sexually mature males store as much as 36% more of the pigment in their skins than do the females, which mobilize relatively large amounts of the unesterified xanthophyll into the eggs. Despite pronounced associated chromatophoric color changes in the direction of matching and concealment, immature *Fundulus* yielded little or no variations in xanthophyll content after protracted residence (1–2 months) in black, white, red, or yellow containers. Nor did 6 weeks in total darkness elicit any measurable change in this regard.

Not only did growing *Fundulus* suffer no losses in total quantities of integumentary xanthophylls after 14 weeks on a carotenoid-deficient diet, but gains occurred in both concentration and total quantities of taraxanthin when a diet rich in that pigment was maintained over the same interval. Moreover, in a third lot of specimens fed no xanthophylls but only β-carotene, significant increases in the quantities of taraxanthin stored led to the conclusion that the fish were able to effect conversion of a carotene into a xanthophyll (Sumner and Fox, 1933, 1935a).

The brilliant omnivorous marine goldfish or Garibaldi, *Hypsypops rubicunda*, bears rich supplies of taraxanthin-like esters in its skin, yielding from about 24 to 98 mg. per 100 g. of skin according to age. The stores of integumentary xanthophyll remain unchanged for long periods, decreasing but slowly after months on carotenoid-free diets. Individuals captive for 2 to 3 years lost from 81 to 88% of their skin carotenoids. Gradual losses in xanthophyllic pigment were found even after rich supplies of β- and α-carotene had been included in the food

TABLE I

DISTRIBUTION OF CAROTENOIDS THROUGH THE ASCENDING GROUPS OF FISHES

Class, Order, Family	Genera, Species (food habit: C = carnivores D = detritus feeders O = omnivores H = herbivores P = plankton eaters)	Tissues	Carotenoid Types				
			Tara-xanthin	Lutein	Zea-xanthin	Asta-xanthin	Caro-tene
CYCLOSTOMES							
Petromyzontidae (lampreys)	*Lampetra fluviatilis*						
	larva (D)	Whole larvae		+			
	adult (C; parasitic)	Adult skin		+			
	Lampetra planeri						
	larva (D)	Whole larvae		+			
	adult (does not feed)	Adult skin		+			
ELASMOBRANCHS							
Rajidae (skates)	*Raja batis* (C)	Skin		+			
	Raja clavata (C)	Skin		+			
TELEOSTS							
A. Soft-rayed fishes							
Clupeidae (herrings, sardines)	*Clupea harengus* (P)	Skin	+	+			
Anguillidae (eels)	*Anguilla anguilla* (C)	Skin		+			
Coregonidae (whitefishes)	*Coregonus albula* (P)	Flesh				+	
		Ovaries, eggs				+	
		Skin				+	
Salmonidae (salmons. trouts)	*Salmo gairdneri* (C)	Flesh, skin				+	
	Salmo irideus (C)	Flesh				+	

		Eggs		+	+	+	+
		Skin		+		+	
	Salmo salar (C)	Flesh				+	(+)
		Eggs	+				
		Liver		+			
		Skin, fins		+		+	
	Salmo trutta (C)	Flesh (red)		+		+	(+)
		Eggs	+	+			+
		Liver		+			+
		Skin, fins	+	+		+	
		Eyes	(xanthophyll traces)				
	Salvelinus spp. (C)	Skin				+	
	Oncorhynchus nerka (C)	Flesh				+	
		Skin				+	
Esocidae (pikes)	*Esox lucius* (C)	Skin	+				
Cyprinidae (minnows)	*Barbus nigrofasciatus* (C)	Skin				+	
	Carassius auratus (O)	Skin	+	+	+?	+	(+)
	Leuciscus						
	(= *Rutilus*) *rutilus* (O)	Liver		+		+	
Erythrinidae (characins)	*Copeina guttata* (C)	Skin	+				
Cyprinodontidae (killifish)	*Fundulus parvipinnis* (O)	Skin, viscera	+				
	Oryzias latipes (C)	Skin		+			
Poeciliidae (topminnows)	*Platypoecilus* (= *Xiphophorus*)						
	maculatus (O)	Skin		+	+?		
	Xiphophorus helleri (O)	Skin		+	+?		
B. Intermediate Groups							
Anacanthines							
Gadidae (cods)	*Eleginus navaga* (C)	Eggs, ovaries	(three unidentified xanthophylls)				
	Gadus (= *Melanogrammus*)						
	aeglefinus (C)	Skin	+				
	Gadus callarias						
	(= *Gadus morrhua*, see below)						

TABLE I (Continued)
DISTRIBUTION OF CAROTENOIDS THROUGH THE ASCENDING GROUPS OF FISHES

Class, Order, Family	Genera, Species	Tissues	Carotenoid Types				
			Tara-xanthin	Lutein	Zea-xanthin	Asta-xanthin	Caro-tene
	Gadus (= *Odontogadus*) *merlangus* (C)	Skin	+				
	Gadus (= *Trisopterus*) *minutus* (C)	Skin	+	+			
	Gadus morrhua (C)	Skin	+	+			
		Eggs		+		+	+
	Gadus (= *Pollachius*) *pollachius* (C)	Skin	+				
	Gadus (= *Pollachius*) *virens* (C)	Skin	+	+			
	Gaidropsarus (= *Enchelyopus*) *cimbrius* (C)	Skin		+			
	Gaidropsarus mustelus (= *Ciliata mustela*) (C)	Skin		+			
	Lota lota (C)	Skin	+				+
		Eggs		+			+
	Raniceps raninus (C)	Skin		+			
Allotriognaths							
Lampridae (opahs)	*Lampris regius* (C)	Skin				+ (nonacidogenic ester)	
Regalecidae (oarfish)	*Regalecus glesne* (C)	Liver				+	
Flatfishes							
Scophthalmidae (= Bothidae)	*Bothus maximus* (= *Psetta maxima*) (C) (= *Scophthalmus maximus*)	Skin	+				

	Bothus (= *Scophthalmus*) *rhombus* (C)	Skin	+	+			
	Scophthalmus (= *Phrynorhombus*) *norvegicus* (C)	Skin				+	
Pleuronectidae	*Hippoglossus hippoglossus* (C)	Eggs, ovaries		+		+	+
	Pleuronectes (= *Platichthys*) *flesus* (C)	Skin		+			
	Pleuronectes (= *Microstomus*) *kitt* (C)	Skin	+	+			
	Pleuronectes (= *Limanda*) *limanda* (C)	Skin	+	+			
Soleidae	*Solea vulgaris* (= *Solea solea*) (O) (D)	Eggs, ovaries					+
C. Spiny-rayed Fishes							
Berycoids							
Berycidae	*Beryx decadactylus* (C)	Skin				+	
Bass-like fishes							
Serranidae (sea basses)	*Centropristes striatus* (C)	Eyes	+				
Percidae (perches)	*Perca fluviatilis* (C)	Skin	+		+	+	+
Carangidae (jacks, yellowtails)	*Caranx trachurus* (C)	Skin		+			
Scombridae (mackerels)	*Scomber scombrus* (C)	Skin	+	+			
Sparidae (porgies)	*Stenotomus chrysops* (= *versicolor*) (C)	Eyes	+				
Embiotocidae (viviparous perches)	*Cymatogaster aggregata* (C)	Skin, gut	+				
Pomacentridae (damselfishes)	*Hypsypops rubicunda* (C, H)	Skin	+				
Labridae (wrasses)	*Centrolabrus exoletus* (C)	Skin	+	+		+	
	Crenilabrus melops (C)	Skin	+ or	+			

TABLE I (Continued)
DISTRIBUTION OF CAROTENOIDS THROUGH THE ASCENDING GROUPS OF FISHES

Class, Order, Family	Genera, Species	Tissues	Carotenoid Types				
			Tara-xanthin	Lutein	Zea-xanthin	Asta-xanthin	Caro-tene
	Ctenolabrus suillus (C)	Skin	+ or	+			
	Labrus bergylta (C)	Skin		+			
	Labrus ossifagus (C)	Skin		+			
Girellidae (opaleyes)	*Girella nigricans* (O)	Skin	+				
Scorpaenoids							
Scorpaenidae (scorpionfishes)	*Scorpaena scrofa* (C)	Skin				+?	
	Sebastes marinus (C)	Skin				+	
Cottidae (sculpins)	*Cottus bubalis* (C)	Skin	+	+			
Triglidae (gurnards)	*Trigla gurnardus* (C)	Skin	+				
	Prionotus carolinus (C)	Eyes				+	
Cyclopteridae (lumpfishes)	*Cyclopterus lumpus* (C)	Skin				+	
		Liver				+	
Gobies							
Gobiidae (gobies)	*Aphia minuta* (C)	Skin	+				
	Gillichthys mirabilis (C)	Skin	+				
	Gobius niger (C)	Skin		+			
Labyrinthfishes							
Anabantidae (gouramis)	*Betta splendens* (C)	Skin		+	(also violaxanthin?)		
	Colisa fasciata (C)	Skin		+	(also violaxanthin?)		
	Colisa lalia (C)	Skin		+	(also violaxanthin?)		
	Macropodus opercularis (C)	Skin		+	+?		
Trachiniforms							
Trachinidae (weevers)	*Trachinus draco* (C)	Skin	+				

Callionymidae (dragonets)	*Callionymus lyra* (C)	Skin	+				
Blennioids							
Pholidae (gunnels)	*Pholis gunnellus* (C)	Skin	+	+			
Zoarcidae (eel-pouts)	*Zoarces viviparus* (C)	Skin	+	+			
Ammodytidae (sand-lances)	*Ammodytes* (= *Hyperoplus*) *lanceolatus* (C)	Skin	+				
	Ammodytes tobianus (C)	Skin	+				
		Ovaries, eggs	+				+
Syngnathiforms							
Gasterosteidae (sticklebacks)	*Gasterosteus aculeatus* (C)	Skin	+				
Syngnathidae (pipefishes, sea horses)	*Nerophis* (= *Entelurus*) *aequoreus* (P)	Skin		+			
	Nerophis ophidion (P)	Skin	+				
	Siphostoma typhle (P)		+	+			
	Syngnathus acus (P)		+	+			
Pediculates							
Lophiidae (anglers)	*Lophius piscatorius* (C)	Liver	+	+		+	+?
Plectognaths							
Molidae (molas)	*Orthagoriscus* (= *Mola*) *mola* (C)	Liver				+	+?

although it was ultimately determined that traces of carotene had been assimilated and stored as such after a long period on the specialized diet (Kritzler *et al.,* 1950).

The remarkably euryhaline long-jawed goby, *Gillichthys mirabilis,* likewise possesses integumentary taraxanthin, in concentrations about half those of *Fundulus.* Like *Fundulus, Gillichthys* demonstrated no recognizable quantitative changes in xanthophyll following protracted residence on the various colored backgrounds to which they adapted their body color. Again, like *Fundulus,* this goby may be capable of converting dietary carotene into integumentary xanthophyll (Sumner and Fox, 1933). Mr. Arthur Lockley, working in the writer's laboratory, has verified this, and has found a loss of skin xanthophyll in gobies which had been required to adapt themselves osmotically to concentrations of sea salts above normal. Decreases in skin xanthophyll were associated with increased respiratory activities, suggesting that work may have been performed by the skin in order to maintain an osmotic equilibrium.

Immature greenfish or opal-eye, *Girella nigricans,* unlike *Fundulus* and *Gillichthys,* lose their integumentary taraxanthin in captivity, despite the inclusion of such carotenoids in their diet. Moreover, the rate of loss is more rapid when the fishes are kept on white backgrounds than when on yellow or red, and least rapid on black (Sumner and Fox, 1935b).

The yellow-banded viviparous surf perch, *Cymatogaster aggregata,* feeding upon shrimp (e.g. *Hippolyte californiensis*), rejects therefrom the carotenes, as well as an astaxanthin-like, acidogenic carotenoid which is, nevertheless, first hydrolyzed from its esterified condition in the gut. A taraxanthin-like xanthophyll ester from the shrimp was also hydrolyzed, then absorbed in part and stored, in re-esterified form, in the skin. Any quantities which may exceed the consumer's apparent threshold of assimilation (ca. 0.27 mg. per 100 g. of wet, eviscerated fish) remain uncombined and are stored in the rectal segment of the gut, temporarily conferring upon it a yellow, rich orange, or reddish color. When the critical xanthophyll is withheld from the diet, the rectal segment readily loses its color, while the appearance of the skin and the quantity of xanthophyll extractable therefrom remain unchanged even after some weeks(Young and Fox, 1936).

We owe to Steven (1948, 1949) a better understanding of the kinds, disposition, and metabolism of carotenoids in the brown trout, *Salmo trutta.* Carotene is present in liver and ovaries, lutein and astaxanthin in skin, muscles, and ovaries, lutein alone in eyes, and predominantly in the liver. The integumentary xanthophylls are esterified, as in many if not most other fishes; the optical lutein is also esterified, while the xanthophylls of muscles and ovaries are uncombined, and those of the liver partly esterified, partly free. Direct comparative microspectrophotometric inspection led Steven (1948) to conclude that the yellow xanthophores carry only lutein esters (1 to 3×10^{-5} γ per cell), and the red erythrophores some 2 to 3.5×10^{-5} γ of astaxanthin per cell. Trout deprived of dietary carotenoids lost most of their red and yellow pigmentation, which could be restored by feeding a natural supply of the appropriate source of pigment. Grangaud *et al.* (1952) conducted similar feeding experiments on other salmon species with like results. *Salmo trutta* is, like most fishes, apparently unable to convert one type of carotenoid into another.

Mature female trout seem to lose free lutein and astaxanthin from their muscles to the developing ova, while the esterified skin xanthophylls remain undepleted. The free yolk xanthophylls are absorbed by the embryo, re-esterified, and ultimately deposited chiefly in skin and fins. β-Carotene, detectable in freshly deposited eggs, was not recognized in any of the developmental embryonic stages. Microsurgical removal of 90% of the yolk carotenoids resulted in the larvae appearing normal in all respects save for slight reduction in size and bearing none save a few pale chromatophores (Steven, 1949).

The metabolism of astaxanthin in the fertilized egg of *Salmo salar* has been followed by Glover, Morton, and Rosen (1952) who found it to be the sole carotenoid present; not even any A vitamins or 7-dehydrocholesterol were detectable during the first 3 months of development. Most of the astaxanthin is assimilated by the developing embryo, and there stored in esterified form.

One may hardly survey the extensive occurrence of carotenoids in the skin and ovaries of fishes, and indeed in comparable tissues of countless invertebrates as well, without reflecting on the possibility of a biochemical role played therein by these biochromes, comparable to functions fulfilled by the related A vitamins in other animals.

ACKNOWLEDGMENTS

I acknowledge with gratitude the invaluable help of my colleagues Dr. Grace L. Orton and Professor Carl L. Hubbs in arranging the evolutionary table of fishes and in verifying current nomenclature.

REFERENCES

Blackburn, M. (1950). *Australian J. Marine and Freshwater Research* **1,** 155. The Tasmanian Whitebait, *Lovettia seali* (Johnston) and the Whitebait Fishery.

Fontaine, M. (1937). *Compt. rend.* **204,** 1367. Sur la teneur en flavine de divers organes de l'Anguilla.

Fontaine, M., and Busnel, R. G. (1938). *Bull. inst. oceanog.* **35,** (742), 1. Recherches sur la flavine contenue dans la peau de quelques Poissons.

Fontaine, M., and Busnel, R. G. (1939). *Bull. inst. oceanog.* **36,** (782), 1. Nouvelles recherches sur la repartition des flavines et de quelque autres pigments fluorescents dans la peau et les yeux des Téléostéens.

Fontaine, M., and Gourevitch, A. (1936). *Compt. rend. soc. biol.* **123,** 443. Sur les variations de la teneur en flavine, pendent la développement des oeufs et embryons des Sélaciens.

Fox, D. L. (1953). "Animal Biochromes," 379 pp. Cambridge, London.

Fox, D. L., and Crane, S. C. (1942). *Biol. Bull.* **82,** 284. The pigments of the two-spotted octopus and the opalescent squid.

Fox, D. L., and Millott, N. (1954). *Experientia* **10,** 185. A biliverdin-like pigment in the skull and vertebrae of the ocean skipjack, *Katsuwonus pelamis* (Linnaeus).

Glover, M., Morton, R. A., and Rosen, D. G. (1952). *Biochem. J.* **50,** 425. Astaxanthin, cholesterol and lipins in developing salmon eggs.

Goodwin, T. W. (1954). "Carotenoids: Their Comparative Biochemistry," 356 pp. Chem. Publ. Co., New York.

Goodwin, T. W., and Fox, D. L. (1955). *Nature* **175,** 1086. Some unusual carotenoids from two nudibranch slugs and a lamprid fish.

Gordon, M. (1948). *N. Y. Acad. Sci. Spec. Publ. IV,* 216. Effects of five primary genes on the site of melanomas in fishes and the influence of two color genes on their pigmentation.

Grangaud, R., Dieuzeide, R., Massonet, R., and Douard, T. (1952). *Compt. rend.* **253,** 213. Saumonization de *Salmo irideus* Gibb. par administration d'astaxanthine.

Isaka, S. (1952). *Nature* **169,** 74. Inhibitory effect of xanthopterin upon formation of melanin *in vitro.*

Isaka, S., and Ishida, S. (1953). *J. Coll. Arts and Sci. Chiba Univ.* **1,** 90. Photochemistry of riboflavin. II. Effect of divalent metallic ions upon the oxidative power of photoactivated riboflavin.

Isaka, S., and Kato, J. (1952). *J. Coll. Arts and Sci. Chiba Univ.* **1,** 43. Photodynamic activities of riboflavin.

Isaka, S., and Shuzo, S. (1953). *Nature* **171,** 303. Effects of some chelate compounds upon the formation *in vitro* of melanin.

Karrer, P., Jucker, E., and Braude, E. A. (1950). 384 pp. "Carotenoids." Elsevier, New York.

Kritzler, H., Fox, D. L., Hubbs, C. L., and Crane, S. C. (1950). *Copeia* p. 125. Carotenoid pigmentation of the pomacentrid fish, *Hypsypops rubicunda.*

Kushibiki, K., Hama, T., and Gota, T. (1954). *Compt. rend. soc. biol.* **148,** 759. Quelques ptérines de la peau ou les écailles de la Carpe et leur transformation photochimique.

Norris, E. R., and Simmons, R. W. (1945). *J. Biol. Chem.* **158,** 449. The hematopoietic activity of xanthopterin in young salmon.

Parker, G. H. (1948). 377 pp. "Animal Colour Changes and their Neurohumours." Cambridge, London.

Polonovski, M., Busnel, R. G., and Pesson, M. (1946). *Helv. Chim. Acta* **29,** 1328. Propriétés biochimiques des ptérines.

Simmons, R. W., and Norris, E. R. (1941). *J. Biol. Chem.* **140,** 679. Xanthopterin, the fish anemia factor.

Steven, D. M. (1948). *J. Exptl. Biol.* **25,** 369. Studies on animal carotenoids. I. Carotenoids of the brown trout (*Salmo trutta* Linn.).

Steven, D. M. (1949). *J. Exptl. Biol.* **26,** 295. Studies on animal carotenoids. II.

Carotenoids in the reproductive cycle of the brown trout.

Sumner, F. B. (1940). *Biol. Revs. Cambridge Phil. Soc.* **15,** 351. Quantitative changes in pigmentation resulting from visual stimuli in fishes and Amphibia.

Sumner, F. B., and Fox, D. L. (1933). *J. Exptl. Zool.* **66,** 263. A study of variations in the amount of yellow pigment (xanthophyll) in certain fishes and of the possible effects upon this of colored backgrounds.

Sumner, F. B., and Fox, D. L. (1935a). *Proc. Natl. Acad. Sci. U. S.* **21,** 330. Studies of carotenoid pigments in fishes. III. The effects of ingested carotenoids upon the xanthophyll content of *Fundulus parvipinnis.*

Sumner, F. B., and Fox, D. L. (1935b). *J. Exptl. Zool.* **71,** 101. Studies of the carotenoid pigments of fishes. II. Investigations of the effects of colored backgrounds and of ingested carotenoids on the xanthophyll content of *Girella nigricans.*

Yagi, K. (1954). *Compt. rend. soc. biol.* **148,** 752. Action inhibitrice des ptérines sur la decomposition photochimique dans la peau de *Rana nigromaculatus.*

Young, R. T., and Fox, D. L. (1936). *Biol. Bull.* **71,** 217. The structure and function of the gut in surf perches (*Embiotocidae*) with reference to their carotenoid metabolism.

Reprinted from JOURNAL OF THE OPTICAL SOCIETY OF AMERICA, Vol. 47, No. 6, 499–506, June, 1957
Printed in U. S. A.
Reproduced by Permission

Image Transmission by the Troposphere I*

SEIBERT Q. DUNTLEY, ALMERIAN R. BOILEAU, AND RUDOLPH W. PREISENDORFER
Scripps Institution of Oceanography,† University of California, La Jolla, California

(Received November 15, 1956)

Quantitative treatment of the apparent luminance of distant objects and the reduction of apparent contrast along inclined paths of sight through real atmospheres has been accomplished by means of optical data taken from an aircraft in flight. Sample data from a single flight are used to illustrate some of the principles involved. Correlation has been found between the humidity profile of the atmosphere and its optical properties.

INTRODUCTION

DISTANT objects are usually viewed, photographed, or televised by means of some path of sight through the atmosphere. Conventional principles of geometrical and physical optics suffice to describe the nature of the final image except for effects due to the atmosphere. In most circumstances, however, the configuration of the image and its information content is affected, often seriously, by its transmission from the object to the receiver. The atmosphere can be regarded as a transmission link in the object-to-image chain and the concomitant effect of the pertinent optical atmospheric properties can be regarded as governing its *image transmission*.

This paper is intended as the first of a series describing the results of an extensive on-going research program which has already been in progress for several years. Results from numerous theoretical and experimental investigations of image transmission phenomena are ready to be reported and further research of many kinds is in progress. Experimental results from a single flight comprise the factual content of this first paper and the equations are limited to certain general relations needed for the practical utilization of the data; this is in keeping with the scope of the oral version of the paper as presented at the Cambridge meeting of the International Commission on Optics.

The specially instrumented B-29 aircraft used to collect the data reported in this paper has, on other flights, secured data up to 30 000 ft under several different atmospheric and lighting conditions; and subsequent papers in the series will present data from these and other flights. The optical properties of the troposphere are of special interest because most viewing takes place through it. Roughly three-fourths of the atmosphere lies within the troposphere and because this lower air often contains haze, clouds, dust, and rain it seriously affects image transmission more frequently than do the higher strata. Exploration of image transmission phenomena in the stratosphere must await an opportunity to instrument a vehicle having greater altitude capability.

SOME GENERAL PRINCIPLES‡

Introduction

In the absence of appreciable atmospheric boil[1] the apparent radiance of any distant object is the sum of two independent components: (1) residual image-forming light from the object that has traversed the atmospheric path without having been scattered or absorbed; (2) radiance created by the scattering of ambient light throughout the path of sight, including sunlight, skylight, earth-shine, etc. Only the first component contains information about the object, for the second is the result of scattering processes throughout the path of sight and is, therefore, independent of the nature of the object. In this paper the image transmission of any path of sight will be specified in terms of the transmittance of the entire path and the path radiance. No theoretical model for the atmosphere is needed; consequently, nearly all restrictive assumptions are avoided and the equations can be used to describe any path of sight through all real isotropic atmospheres with any lighting condition. To be useful in practice, these equations must be supplied with data and these are becoming available as a result of the flight research program now in progress.

Notation

The notation used in this paper has been adopted with great care and on the basis of experience accumulated over many years. It is designed to fulfill many

---

* Presented at the Fourth Congress of the International Commission of Optics, held in Cambridge-Boston, Massachusetts, March 28–April 3, 1956. Published with financial assistance from UNESCO and the International Union of Pure and Applied Physics.

† Contribution from the Scripps Institution of Oceanography, University of California, New Series No. 921. This work has been supported by the Geophysical Research Directorate of the Air Force Cambridge Research Center and the Bureau of Ships of the U. S. Navy under contracts NObs–43356, NObs–50274, NObs–72039, and NObs–72092.

‡ The principles presented in this paper and in subsequent papers of this series were formulated in unpublished lecture notes used within the Visibility Laboratory of the Scripps Institution of Oceanography which include, generalize, and extend earlier work by the authors and others (R. W. Preisendorfer, "Lectures on photometry, hydrological optics, atmospheric optics," Fall, 1953, Vol. I).

[1] Duntley, Culver, Culver, and Preisendorfer, J. Opt. Soc. Am. 42, 877A (1952); publication of this paper is planned.

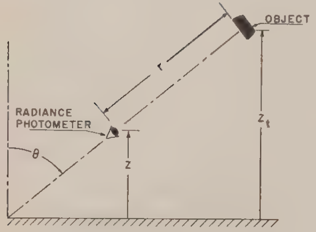

FIG. 1. Illustrating the geometry of the path of sight.

requirements: It is suited to the terrestrially-based system of altitudes and directions in which flight data must be taken and it is fully compatible with the more powerful vector notation required for the generalized theoretical treatments of image transmission and radiative transfer phenomena to follow. It is compatible also with the notation commonly used in several mathematically allied fields of physics, as for example, neutron diffusion theory. It is extendable to hydrological optics, a natural counterpart of meteorological optics, in which the authors of this paper are deeply interested.

The basic symbol employed for the spectral radiance is N, and the symbol for luminance is B. The altitude of the photometer is denoted by z, the height above mean sea level. The direction of any path of sight is specified by a zenith-angle θ and an azimuth angle ϕ, the photometer being directed upward when $0\leq\theta<\pi/2$, as in Fig. 1; z, θ, and ϕ are always written as parenthetic attachments to the parent symbol. When the post subscript r is appended to any symbol, it denotes that the quantity pertains to a path of length r. The subscript 0 always refers to the hypothetical concept of a photometer located at zero distance from the object, as, for example, in denoting the *inherent* radiance of a surface. Pre-subscripts identify the object, thus the pre-subscript b refers to background, and t to object or visual target. Thus, the (monochromatic) *inherent spectral radiance* of an object t at altitude z_t as viewed in the direction (θ,ϕ) is ${}_tN_0(z_t,\theta,\phi)$ and the corresponding apparent radiance observed in the direction (θ,ϕ) at any other altitude z is ${}_tN_r(z,\theta,\phi)$ where $z_t=z+r\cos\theta$. A post-superscript *, or post-subscript $_*$ is employed as a mnemonic symbol signifying that the radiometric quantity has been generated by the scattering of ambient light reaching the path from *all directions*. Thus $N_r^*(z,\theta,\phi)$ is the spectral path radiance observed at altitude z in the indicated direction, and (N_*z,θ,ϕ) is used to denote *path function*, a quantity defined later in this paper.

The (monochromatic) *apparent spectral radiance* of any distant object t is

$$ {}_tN_r(z,\theta,\phi)=T_r(z,\theta,\phi)\ {}_tN_0(z_t,\theta,\phi)+N_r^*(z,\theta,\phi), \quad (1)$$

where the first term on the right is the residual image-forming light from the object and the second term is the path radiance due to scattering processes throughout the path. $T_r(z,\theta,\phi)$ is the spectral transmittance of the path for image-forming rays; it includes the factor $[n(z)/n(z_t)]^2$ required by geometrical optics whenever the index of refraction of the medium at the observer $[n(z)]$ differs from the index of refraction of the medium at the target $[n(z_t)]$. In the case of paths of sight through the troposphere the departure of $[n(z)/n(z_t)]^2$ from unity is negligible. The transmittance of the path is a property of the atmosphere throughout the path and is independent of the distribution of the ambient lighting; in the case of any path of sight through the troposphere it is the same for upward or downward transmissions, thus $T_r(z,\theta,\phi)=T_r(z_t,\pi-\theta,\pi+\phi)$ where $z_t=z+r\cos\theta$. Because forward scattering generally exceeds backward scattering, reversibility is not true of the path radiance $N_r^*(z,\theta,\phi)$ except for a few symmetrical lighting conditions, such as (1) horizontal paths of sight under a uniform overcast, and (2) a horizontal path at right angles to the plane of the sun provided both the radiance distributions of the sky above and the earth below the path are symmetrical with respect to the plane.

The image transmitting properties of the atmosphere can be separated from the optical properties of the object by the introduction of the *contrast* concept:

The *inherent spectral contrast* $C_0(z_t,\theta,\phi)$ of an object is, by definition,

$$C_0(z_t,\theta,\phi)=[{}_tN_0(z_t,\theta,\phi)-{}_bN_0(z_t,\theta,\phi)]/{}_bN_0(z_t,\theta,\phi). \quad (2)$$

The corresponding definition for *apparent spectral contrast* is

$$C_r(z,\theta,\phi)=[{}_tN_r(z,\theta,\phi)-{}_bN_r(z,\theta,\phi)]/{}_bN_r(z,\theta,\phi). \quad (3)$$

The apparent and inherent background radiances are related by the expression

$${}_bN_r(z,\theta,\phi)=T_r(z,\theta,\phi)\ {}_bN_0(z_t,\theta,\phi)+N_r^*(z,\theta,\phi). \quad (4)$$

Theorems

Subtracting Eq. (4) from Eq. (1) yields the relation

$$[{}_tN_r(z,\theta,\phi)-{}_bN_r(z,\theta,\phi)] =T_r(z,\theta,\phi)[{}_tN_0(z_t,\theta,\phi)-{}_bN_0(z_t,\theta,\phi)]. \quad (5)$$

Thus, radiance differences are transmitted along inclined paths with the same attenuation as that experienced by each image-forming ray.

If Eq. (5) is divided by the apparent radiance of the background ${}_bN_r(z,\theta,\phi)$ and combined with Eq. (3), the result can be written:

$$C_r(z,\theta,\phi)=T_r(z,\theta,\phi) \times[{}_tN_0(z_t,\theta,\phi)/{}_bN_r(z,\theta,\phi)-{}_bN_0(z_t,\theta,\phi)/{}_bN_r(z,\theta,\phi)]. \quad (6)$$

When the inherent radiance of the background is very dark, as in the case of an object at high altitude, the second term in the brackets on the right side of Eq. (6) may be negligible.

Combining Eqs. (2) and (6) yields the expression

$$C_r(z,\theta,\phi)/C_0(z_t,\theta,\phi) = T_r(z,\theta,\phi)\;{}_bN_0(z_t,\theta,\phi)/{}_bN_r(z,\theta,\phi). \quad (7)$$

The right-hand member of Eq. (7) is an expression for the *contrast transmittance* of the path of sight; it is independent of the optical properties of the object. Equation (7) is the law of contrast reduction by the atmosphere expressed in its most general form.[2]

An interesting variant of Eq. (7) formed by combination with Eq. (4) is the following expression in which *contrast transmittance* is characterized in terms of path radiance and inherent background radiance:

$$C_r(z,\theta,\phi)/C_0(z_t,\theta,\phi) = 1 - [N_r^*(z,\theta,\phi)/{}_bN_r(z,\theta,\phi)]. \quad (8)$$

The apparent indeterminateness of Eqs. (7) and (8) when applied to the case of objects outside the atmosphere can be avoided by the use of the limiting form of Eq. (6), as follows:

$$C_r(z,\theta,\phi) = T_r(z,\theta,\phi)\;{}_tN_0(z_t,\theta,\phi)/{}_bN_r(z,\theta,\phi). \quad (9)$$

It should be emphasized that Eqs. (1) through (9) are completely general; they apply rigorously to any path of sight regardless of the extent to which the scattering and absorbing properties of the atmosphere or the distributions of lighting exhibit nonuniformities from point to point. No theoretical model of the atmosphere is involved and no restrictive assumptions have been made. The equations can be used in treating all real atmospheres and all real lighting conditions. This is in sharp distinction to treatments of the subject which are based upon theoretical models of the atmosphere which invariably involve major assumptions such as horizontal uniformity, exponential lapse rate of air density, vertical uniformity of particle size distribution, negligible earth curvature, etc.

Equation of Transfer

Image-forming light is lost by scattering and absorption in each elementary segment of the path of sight and contrast-reducing path radiance is generated by the scattering of the ambient light which reaches the segment from all directions. The quantitative description of this scattered component of path-segment radiance involves a quantity called the *path function* and denoted by the symbol $N_*(z,\theta,\phi)$, where the mnemonic subscript symbol $_*$ is used both to suggest light reaching the path segment from all directions and to denote that the quantity is a point function. The parenthetical symbols (z,θ,ϕ) indicate that the path function depends upon the direction of image transmission and upon the location of the segment in the path of sight. The path function depends upon the directional distribution of the lighting on the segment due to its surroundings; it can be operationally defined in terms of the (limiting) ratio of the path radiance associated with a short path to the path length by the relation $N_*(z,\theta,\phi) = \lim(\Delta r \rightarrow 0) \times N_{\Delta r}^*(z,\theta,\phi)/\Delta r$. In experimental practice, the path length Δr should be sufficiently short that no change in the ratio can be detected if Δr is made shorter. Apparatus for path function measurement has been built and will be described elsewhere.

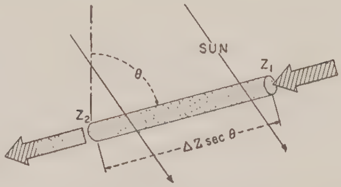

FIG. 2. Illustrating the derivation of the equation of transfer. Δz is defined as $z_1 - z_2$, so that $\Delta r = \Delta z \sec\theta$ is always non-negative. The difference $\Delta N(z,\theta,\phi)$ between output and input is $N(z_2,\theta,\phi) - N(z_1,\theta,\phi)$.

The loss in image-forming light due to attenuation by scattering and absorption within any path segment is proportional to the amount of image-forming light present; the coefficient of proportionality will be written in the reciprocal form $1/L(z)$, and $L(z)$ will be referred to as the *attenuation length*. $L(z)$ is a function of position within the path of sight; it does not depend upon the image transmission direction unless the aerosol is anisotropic, as sometimes occurs in the case of falling snow; it is independent of the manner in which the path segment is lighted by the sun or sky; it is a physical property of the atmosphere alone. Attenuation includes loss of image-forming radiance by absorption and by scattering. Absorption refers to any thermodynamically irreversible transformation of monochromatic radiant energy including, primarily, conversion of light into heat but also fluorescence phenomena, photochemical processes, etc. Attenuation by scattering results from any change of direction sufficient to cause the radiation to fall outside the summative radius of the detector mosaic.

In any path segment of length $\Delta r = \Delta z \sec\theta$, as illustrated by Fig. 2, the difference $\Delta N(z,\theta,\phi)$ between output and input radiance is attributable to a gain term $N_*(z,\theta,\phi)\Delta r$ and a loss term $N(z,\theta,\phi)\Delta r/L(z)$, so that $\Delta N(z,\theta,\phi) = N_*(z,\theta,\phi)\Delta r - N(z,\theta,\phi)\Delta r/L(z)$. This relation may be rewritten

$$\Delta N(z,\theta,\phi)/\Delta z \sec\theta = N_*(z,\theta,\phi) - N(z,\theta,\phi)/L(z). \quad (10)$$

In conformity with usage in other fields of physics Eq. (10) will be referred to as the incremental form of the *equation of transfer*. It is implicit in this equation that Δz must be taken sufficiently small so that over this interval $L(z)$ and $N_*(z,\theta,\phi)$ may be regarded as constants within the precision of experimental data.

---

[2] Equation (7) is a generalization of Eq. (15) on p. 183 of S. Q. Duntley, J. Opt. Soc. Am. 38, 179 (1948).

Equation (10) is a steady-state equation of continuity,[3] based upon the conservation of energy principle; it refers only to nonemitting atmospheres, since an additional term would be needed to represent emission of radiation in the path, as by fluorescence, recombination phenomena, particle excitation, etc. Self-radiosity within the visible spectrum appears to be of negligible importance in the troposphere. Equations (1) and (4) may be regarded as integral forms of the equation of transfer.

The equation of transfer and the concepts of attenuation length and path function share the same generality as the concepts associated with Eqs. (1) through (9): No theoretical model atmosphere has been employed; each of the equations in this paper is applicable to all real isotropic atmospheres, all lighting conditions, and all paths of sight. The use of the equation of transfer in numerical summation procedures involving experimental data will be illustrated in a later section of this paper. Only when Eq. (10) is simulated by a differential equation and an analytic integration performed does the introduction of a theoretical model for the atmosphere become necessary; this will not be done in the present paper.

Equilibrium Radiance

Many image transmission phenomena are most clearly understandable in terms of the concept of *equilibrium radiance*. This concept is a natural consequence of the equation of transfer, which indicates that some unique *equilibrium radiance* $N_q(z,\theta,\phi)$ must exist at each point such that the loss of radiance within the path segment is balanced by the gain, i.e., $\Delta N_q(z,\theta,\phi)=0$. Thus

$$0=N_*(z,\theta,\phi)-N_q(z,\theta,\phi)/L(z), \quad \text{so that} \quad N_q(z,\theta,\phi)=N_*(z,\theta,\phi)L(z) \tag{11}$$

and the equation of transfer (10) may be rewritten as follows:

$$\Delta N(z,\theta,\phi)/\Delta z\sec\theta=[N_q(z,\theta,\phi)-N(z,\theta,\phi)]/L(z). \tag{12}$$

Equation (11) shows that each segment of every path of sight has associated with it an equilibrium radiance, and Eq. (12) states that the average space rate of change in image-forming radiance caused by the path segment is in such a direction as to cause the output radiance to be closer to the equilibrium radiance than is the input radiance. This segment-by-segment convergence of the apparent radiance of the object to the dynamic equilibrium radiance is illustrated by the data in Fig. 6 of this paper.

When the path of sight is horizontal and optically uniform both in terms of the composition of the aerosol and its lighting, the equilibrium radiance is identical with the apparent radiance of the horizon. The apparent radiance of distant objects inherently more radiant than the equilibrium value decreases toward the equilibrium radiance as an asymptote; conversely the apparent radiance of any dark distant object approaches the same asymptote.

Equilibrium Contrast

Many of the foregoing equations can be rewritten in terms of *equilibrium contrast*, $C_q(z,\theta,\phi)$, which is defined by the relation

$$C_q(z,\theta,\phi)=[{}_tN_r(z,\theta,\phi)-N_q(z,\theta,\phi)]/N_q(z,\theta,\phi). \tag{13}$$

Notation of the type defined by Eq. (13) enables the equation of transfer (10) to be written

$$\Delta C_q(z,\theta,\phi)/\Delta z\sec\theta=-C_q(z,\theta,\phi)/L(z) \tag{14}$$

or

$$\Delta C_q(z,\theta,\phi)/C_q(z,\theta,\phi)=-\Delta z\sec\theta/L(z), \tag{15}$$

provided that the equilibrium radiance $N_q(z,\theta,\phi)$ is constant on the segment of path under discussion. In this case the fractional change in equilibrium contrast depends only upon the ratio of the length of the path segment to the attenuation length. The negative signs throughout Eqs. (14) and (15) signify that equilibrium contrast decreases in absolute magnitude in the segment.

EXPERIMENTAL METHODS

Introduction

The apparent radiance of any distant object can be computed by means of Eq. (1) if the transmittance of the path of sight and the path radiance are calculated from experimental data. This can be done from profiles of attenuation length and path function for the path of sight by means of the relations

$$T_r(z,\theta,\phi)=[n(z)/n(z_t)]^2\prod_{i=1}^{m}\exp\{-\Delta r/L(z_i)\}$$

$$=[n(z)/n(z_t)]^2\exp\{-\Delta r\sum_{i=1}^{m}1/L(z_i)\} \tag{16}$$

and

$$N_r^*(z,\theta,\phi)=\Delta r\sum_{i=1}^{m}T_{r_i}(z,\theta,\phi)N_*(z_i,\theta,\phi), \tag{17}$$

where the vertical height $|z_t-z|$ of the path is divided into m equal segments of length Δz, and $\Delta r=\Delta z\sec\theta$. $L(z_i)$ and $N_*(z_i,\theta,\phi)$ are the mean values of L and N_* in the ith segment. $r_i=(i-1)\Delta r$, $i=1,\cdots,m$.

---

[3] The equation of transfer has been generalized to the transient case, and rigorously derived for an arbitrary optical medium, using the concepts of measure theory. R. W. Preisendorfer, "A mathematical foundation for radiative transfer theory," Doctoral dissertation, U.C.L.A., May 1956. An exposition of this theory has been submitted for publication in the Journal of the Optical Society of America.

Attenuation Profile

An experimental technique for measuring the vertical profile of attenuation length in horizontally uniform atmospheres has been devised around an air-borne version of an instrument based upon principles described earlier.[4,5] Figure 3 shows this attenuation meter mounted on the B-29 aircraft used by the Visibility Laboratory in its flight research program. The optical system is shown diagrammatically in Fig. 4. The forward telephotometer is directed toward the horizon and measures the equilibrium radiance of the horizontal path of sight in the direction of flight of the aircraft. The rear telephotometer measures the radiance of a path of unit length; this is numerically equal to the path function. The attenuation length is the ratio of the equilibrium radiance to the path function, as shown by Eq. (11). Recording potentiometers within the aircraft record the outputs of both telephotometers as well as their ratio.

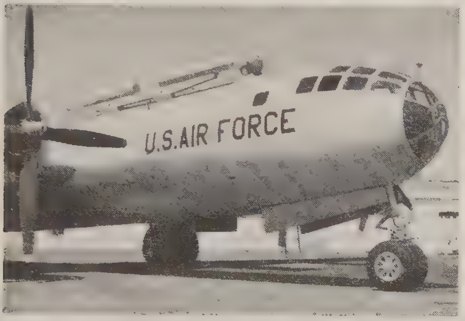

Fig. 3. Specially instrumented B-29 aircraft used to collect the data presented in this paper. The long cylindrical apparatus on top of the fuselage is the *attenuation meter*, shown schematically in Fig. 4. The smaller cylindrical device which appears slightly forward of the attenuation meter is the sky-scanning telephotometer. It consists of an end-on type multiplier phototube mounted at the focal point of a parabolic front-surfaced mirror 12 in. diam. Scanning is accomplished automatically by means of a turret and trunion mounting; scanning time for the entire hemisphere is 90 sec. Field of view, adjustable by means of interchangeable field stops, was circular, 5° in angular diameter in the case of the data shown in Fig. 6. Sensitivity is sufficient to map even the darkest high-altitude night skies. Spectral response is controlled by absorption filters. A similar (downward-viewing) telephotometer is mounted beneath the aircraft but is not shown by this photograph.

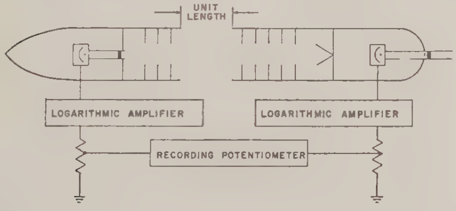

Fig. 4. Schematic diagram of the air-borne attenuation meter. The forward photoelectric telephotometer measures the equilibrium radiance; the rear telephotometer measures the radiance of a path of unit length. The latter radiance is numerically equal to the horizontal path function in the direction of flight. Multiplier phototubes and Sweet-type logarithmic circuits enable direct recording of the ratio of these radiances, i.e., of the attenuation length [see Eq. (11)]. Wind-tunnel tests of the aerodynamic design showed ambient pressure throughout the unit path. Light trap design, stray-light treatment, and photoelectric sensitivity are sufficient to enable measurement of attenuation lengths up to 200 nautical miles when the phototube spectral sensitivity is rendered photopic by means of absorption filters.

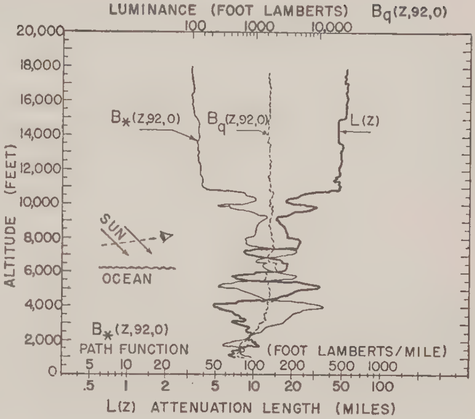

Fig. 5. Measured profiles of path function and attenuation length over the Atlantic Ocean off the coast of Florida, March 10, 1956. Flight 77. Sun position: zenith angle = 48°, azimuth = 140° clockwise from true north. Path function: zenith angle $\phi=92°$; azimuth $\theta=0°$ from the plane of the sun. Sky condition: cloudless, blue. Approximately 36 hr after the passage of a major front. Very light ground haze with top at 4000 ft. The profile of equilibrium luminance was computed by means of Eq. (11).

Despite the use of multiplier phototubes, the low level of radiance produced by scattering processes in clear high altitude air precluded the use of narrow-band interference or absorption filters in the airborne attenuation meter. Because it was not possible to measure the spectral radiances called for by the equations given in this paper, each phototube was carefully corrected by means of specially constructed absorption filters to measure luminous quantities. For reasons of rigor the equations in this paper are written with the symbol N, denoting spectral radiance, but it will be understood that these same equations have been used with N replaced by B, denoting luminance, in the treatment of the illustrative data shown in Figs. 5 through 8.

During the flight for which data is given in this paper, the aircraft maintained a constant (southerly) heading and a fixed attitude which held the attenuation meter pointed at the desired portion of the horizon sky while making a controlled, rapid descent from 18 000 ft to 1000 ft at a rate of approximately 1500 ft per min. The resulting profiles of path function, equilibrium luminance, and attenuation length are shown in Fig. 5.

---

[4] S. Q. Duntley, U. S. Patent No. 2,661,650.

[5] S. Q. Duntley, J. Opt. Soc. Am. 39, 630A (1949).

It will be noted that the equilibrium luminance (horizon luminance) was nearly independent of altitude. Repeated descents have demonstrated that the major details of these curves are repeatable.

The transmittance of any inclined path of sight having terminal altitudes between 1000 and 18 000 ft can be calculated from the attenuation profile in Fig. 5 by means of equations corresponding to Eq. (16).

Path Function Profiles

The aircraft is not equipped for the direct measurement of path functions for vertical and inclined paths of sight. It is capable, however, of measuring the radiance of the sky in any direction, above or below, during flight. A photoelectric telephotometer is located in a trunion mounting on top of the fuselage near the forward end of the attenuation meter, as shown in Fig. 3. This instrument performs an automatic scan of the entire sky above the aircraft in approximately 90 sec. Another telephotometer in a fixed vertical mount provides a continuous record of the radiance of the zenith during the controlled rapid descent described in the preceding section. A corresponding pair of telephotometers is mounted on the bottom of the fuselage. Figure 6 shows zenith luminance data secured by the fixed telephotometer during the same descent to which Fig. 5 applies. Similar profiles of sky luminance for any upward path of sight inclined at angles θ, ϕ can be constructed from the record of the sky-scanning telephotometer, which is designed to be operated continuously during the descent.

The profile of the path function for any path of sight can be calculated from the sky radiance profile and the attenuation profile by means of Eq. (10) after rearrangement as follows:

$$N_*(z,\theta,\phi)=\Delta N(z,\theta,\phi)/\Delta z\sec\theta+N(z,\theta,\phi)/L(z). \quad (18)$$

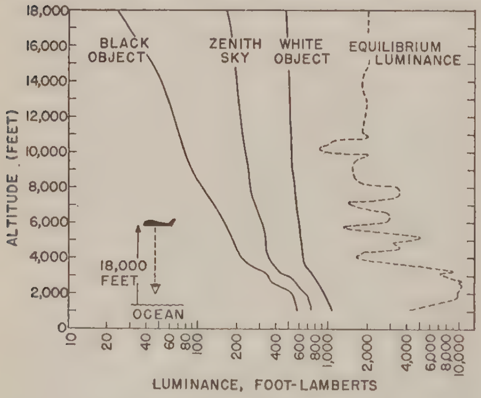

Fig. 6. Measured profile of the luminance of the zenith sky. Flight 77. Calculated profiles of the apparent luminance of black and white objects at 18 000 ft. Calculated profile of vertical equilibrium luminance.

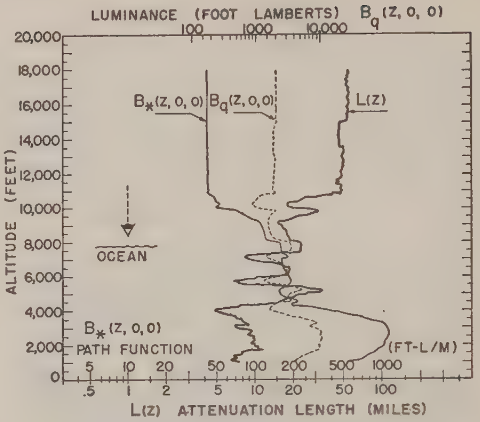

Fig. 7. Calculated profiles of vertical path function and vertical equilibrium luminance. Flight 77. The profile of attenuation length is identical with that in Fig. 5.

Figure 7 shows the result of such a calculation for the vertical path of sight which corresponds with the zenith luminance profile given in Fig. 6.

Equilibrium Radiance Profiles

An expression for the equilibrium radiance for each element of any path of sight can be found by combining Eqs. (11) and (18) as follows:

$$N_q(z,\theta,\phi)=L(z)(\Delta N(z,\theta,\phi)/\Delta z\sec\theta)+N(z,\theta,\phi). \quad (19)$$

Figure 6 shows the result of the use of Eq. (19) for a calculation of the equilibrium luminance profile for the upward vertical path of sight; the same profile appears in Fig. 7.

In every case the radiance of the sky $N(z,\theta,\phi)$ as observed from any altitude z is the path radiance generated by the portion of the path above the observer. That is, $N(z,\theta,\phi)=N_\infty{}^*(z,\theta,\phi)$, where $0\leq\theta<\pi/2$. Because $N(z,\theta,\phi)=0$ outside the atmosphere (except for light from the stars) and $N(z,\theta,\phi)>0$ within, it follows from Eq. (19) that the equilibrium radiance exceeds the apparent radiance of the clear sky and, therefore, the measured radiance of a clear sky increases as the photometer descends.

When clouds are present or when the image transmission direction is upward, the apparent radiance reaching any particular path segment may exceed the equilibrium radiance for that segment, so that a decrease of apparent radiance is possible. In such cases it often happens that the apparent radiance of highly radiant objects decreases while that of objects of small inherent radiance increases. Illustrative data for upward-transmitting paths of sight are planned for presentation in a subsequent paper.

Profiles of Apparent Object Luminance

Profiles of the apparent luminance of any specific object can be calculated for any path of sight provided that the inherent luminance of the object in the direction of interest is known. Two such profiles appear in Fig. 6; they refer to hypothetical "black" and "white" objects, respectively, located at a fixed altitude of 18 000 ft and viewed from directly below on the occasion to which the data in this paper applies. The profiles were calculated by means of Eq. (1). Alternatively, they could have been generated step-wise by successive applications of either Eq. (10) or Eq. (12). The complexity which characterizes the attenuation, path function, and equilibrium luminance profiles is scarcely noticeable in these vertical profiles of apparent object luminance. In the case of paths of sight inclined at large zenith angles, however, the object luminance profiles exhibit the complexities due to atmospheric structure much more prominently.

Profiles of Apparent Contrast

Figure 8 shows profiles of apparent object contrast generated by means of Eq. (3) from the apparent luminance profiles in Fig. 6. The same profiles could have been generated by use of the Eq. (7).

METEOROLOGICAL CORRELATIONS

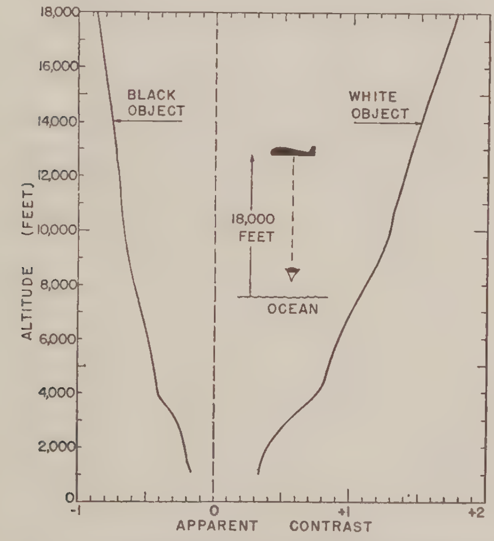

FIG. 8. Calculated profiles of the apparent contrast of black and white objects at 18 000 ft. Flight 77.

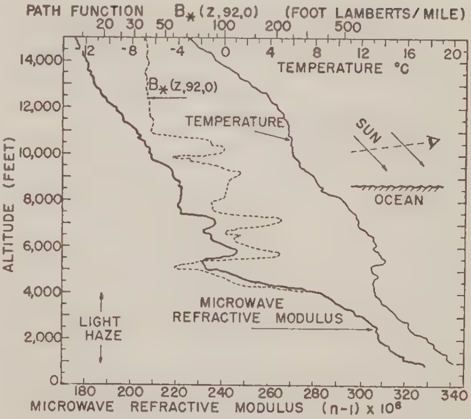

FIG. 9. Profiles of microwave refractive modulus, path function, and free air temperature. Flight 77. Correlations between the profiles of microwave refractive modulus and path function can be noted.

The complex profiles of attenuation length and path function can only be the result of sharply defined layers of scattering particles. Repeated descents have demonstrated that the major features of the profiles are reproducible in space and time; the layers must, therefore, be horizontal strata of great extent which characterize the air mass. Such strata must also be observable in terms of nonoptical meteorological phenomena. Initial attempts to discover correlations with the temperature and humidity profiles produced routinely by the meteorological services from radiosonde observations met with failure. This was attributed to the long time constant associated with the humidity sensing elements carried by the balloons. It was believed necessary to measure the humidity profile during the controlled rapid descent of the B-29 with equipment having a fractional second time constant in order to record faithfully the presence of strata only a few feet in thickness. This was accomplished by means of an airborne microwave refractometer[6] of the type described by Crain and Deam.[7] The microwave refractive index recorded by this instrument is governed primarily by the water vapor concentration in the atmosphere; it is related to pressure, temperature, and the partial pressure of water vapor by an equation derived by Debye and discussed by numerous authors in connection with microwave propagation.[8] An expression for the partial pressure of water vapor obtained from the usual microwave approximation of Debye's equation is:

$$\epsilon=\frac{(\text{microwave refractive modulus})(\text{Kelvin temp.})^2}{(77.6)(4810)}-\frac{(\text{total pressure})(\text{Kelvin temp.})}{4810}.$$

---

[6] The authors are indebted to Mr. Thomas J. Obst, Director of Range Development, Patrick Air Force Base, for suggesting the use of the microwave refractometer and for arranging for the availability of this equipment for the flight experiment described in this paper.

[7] C. M. Crain and A. P. Deam, Rev. Sci. Instr. 23, 149 (1953).

[8] E. K. Smith, Jr., and S. Weintraub, J. Research Natl. Bur. Standards 50, 39 (1953).

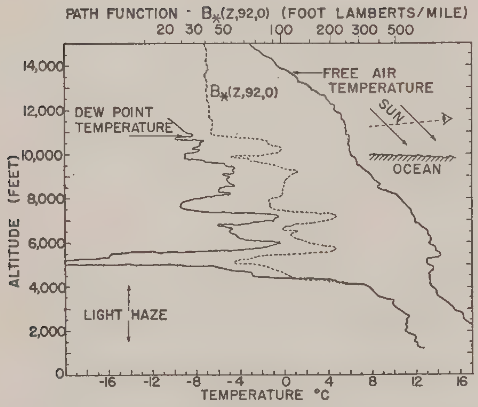

FIG. 10. Profile of dew point temperature calculated by means of Debye's equation from the profile of microwave refractive modulus in Fig. 9. Profiles of path function and free air temperature are identical with those in Fig. 9. Correlations between profiles of dew point temperature and path function are obvious.

In this equation ϵ is in millibars, the Kelvin temperature is of the stratum, the total pressure is in millibars, and the *microwave refractive modulus* of the stratum for microwaves is defined by the expression $(n-1)\ 10^6$, where n is the refractive index of the stratum.

An Air Force C-131 equipped with a microwave refractometer flew in formation with the B-29 throughout the descent during which the optical data reported in this paper was secured. The resulting profile of microwave refractive modulus is shown in Fig. 9. The profile of horizontal path function from Fig. 5 also appears in Fig. 9 for purposes of comparison.

Debye's equation was used to calculate a humidity profile from the microwave data. This profile, expressed in terms of dew-point temperature, is given in Fig. 10. The close correlation between humidity and path function is obvious.

The following speculations on the reasons for the observed correlation are offered: In terms of visible light water vapor exhibits virtually no absorption and it contributed only molecular scattering, the magnitude of which is too small to be responsible for the observed effects. The atmosphere invariably contains, however, suspended material such as sea-salt ions, silica, ammonia, or oxides of nitrogen and sulfur which can form condensation nuclei for water droplets. A tenuous haze of these tiny droplets will form in any stratum having a water vapor content above some critical minimum. These droplets will grow until the vapor pressure just outside the curved surface of the drop equals the partial pressure of water vapor in the surrounding air.[9] Liquid droplets ranging from 4×10^{-7} to more than 10^{-4} cm are known to be present in the atmosphere.[10] In the case of spherical water droplets small in diameter compared with a wavelength of light that component of the scattering coefficient which is due to droplets increases as the sixth power of their diameter,[11] assuming the number of droplets per unit of volume to remain fixed. In view of this, the observed correlation between the path function and the humidity within tenuous haze layers appears to be understandable.

ACKNOWLEDGMENTS

The number of individuals involved in an experimental program of the complexity, scope, and duration of the flight research partially described by this paper is too great to be listed properly here. Special mention should be made, however, of the technical contributions of Brig. Gen. Victor A. Byrnes, USAF, through whose efforts the program was initiated; Lt. Col. George E. Long, USAF; Major Joseph X. Brennan, USAF; and research pilot Capt. Robert L. Baron, USAF. Important contributions to the detailed design of the apparatus were made by John M. Hood, Roswell W. Austin, W. Joseph Woodside, Thomas H. Glenn, Romuald Anthony, Merril D. Hobt, and David J. A. Hooton.

---

[9] W. E. K. Middleton, *Vision through the Atmosphere* (Toronto Press, Toronto, 1952), Chap. 3.

[10] C. Junge, *Nuclei of Atmospheric Condensation*, Compendium of Meteorology (American Society for Metals, Cleveland, 1951).

[11] Lord Rayleigh, Proc. Roy. Soc. (London) **A90**, 219 (1914).

Reprinted from SYSTEMATIC ZOOLOGY, Volume 6, Number 2, June 1957
Reproduced by Permission

The Bearing of Larval Evolution on Some Problems in Frog Classification

GRACE L. ORTON

THE extreme specialization of the frogs (Order Salientia) and their poor early fossil record hamper our efforts to discern the principal evolutionary lines in this relatively small but seemingly inscrutable taxonomic group. From the nature and limitations of the data that have accumulated, interpretations of frog phylogeny are unavoidably conjectural, and understanding perhaps depends as heavily on one's ability to use concepts of systematics and evolution theory in general as it does on the direct evidence from the frogs. Classifications based on various combinations of external characters, on certain features of the skeleton and musculature, etc., have helped to clarify many problems, but none of the classifications proposed in the literature thus far are adequate by the exacting standards of modern systematics. It is increasingly apparent that major progress in frog systematics will require both more extensive and more closely integrated studies than have been customary in the past. The basic comparative anatomy and developmental morphology of the frogs need very thorough investigation, on a much broader scale than has yet been attempted. Developmental characters, in particular, are still commonly underrated and neglected as materials for the study of frog systematics, though they offer very rewarding clues to evolutionary trends and taxonomic understanding.

The present paper discusses some general aspects of larval evolution in the frogs, and some problems in the use of larval characters to help designate the more primitive families and to interpret their relationships, together with brief comments on some analogous problems in the fishes which may contribute indirectly toward a better understanding of larval evolution in the frogs. The presentation is deliberately speculative, in the hope that the disagreement thus invited may help to stimulate some of the needed studies.

It should be pointed out that I apply the term "tadpole" only to the larva of the frogs, in contrast to the less restricted and sometimes misleading use of the term by some authors to designate various unrelated chordate larvae which are very different from the frog larva in their morphology and their evolutionary background.

Geological History

The rich variety of adaptive specializations and structural peculiarities which tadpoles display can easily divert our attention from the long time gap in the early geological history of the frogs from which we have very little useful information but during which extensive evolution must have occurred in the larval as well as the adult characters of these animals. As noted earlier (Orton, 1953), the major characters that differentiate the Salientia from all other known amphibians, fossil and living, are features that have fundamental effects on the structural plan in both larval and adult stages, notably the drastically altered proportions and peculiar adjustments to internal space limits associated with the excessively shortened vertebral column. It seems highly probable that a block of characters with such far-reaching effects as these must have been established through coordinated evolutionary changes that modified the whole ontogeny as a unit. It is unlikely that such a sharply different structural plan could be produced by discordant changes that brought one developmental stage to the salientian level without simultaneously remodelling the other stage. The genetic changes that installed the frogs as a distinctive group were certainly attained long ago, but the early part of that history is still very inadequately known. All of the known Recent frogs and all of the well-preserved fossil frogs have essentially the same peculiar structural plan, and presumably they represent a sampling of the evolutionary lines that have branched off since the frog stock first became genetically isolated. *Protobatrachus,* of the Upper Triassic, has generally been considered a very primitive frog or a near-predecessor of the typical frogs, but recently Griffiths (1956) has interpreted the single known specimen as a partly metamorphosed tadpole, an illuminating idea which can account for virtually all of the peculiarities of the specimen and which—if correct—implies that the tadpole-frog structural plan was probably already well established by Upper Triassic times.

Cope (1889) essentially predicted the modern view of the evolutionary significance of the tadpole when he suggested: "The larval life of the Salientia has probably undergone important modifications during the course of geologic time . . . these peculiarities of larval life . . . have been gradually assumed by the larvae of the Salientia in the course of their existence, as though they were adult animals, and probably in obedience to the same kind of laws." This suggestion, which differed from the interpretation of specialized larval stages which prevailed in his time, was an obscure detail buried in his vast amount of published work, hence it is scarcely surprising that it was not followed up and that tadpole evolution received little further serious attention until G. K. Noble began his life-history studies in the 1920's.

Noble made many important contributions to frog systematics, both from his own studies and from skilled appraisal of the work of others. His most original interpretive work began when he noted that revisions based on adult characters regrouped some frogs that not only had important adult characters in common but also shared an unusual type of life history or a distinctive larval character. He followed up this clue to life-history evolution by investigating the status of frogs that shared similar life-history specializations but were supposedly unrelated, and analyzing supposed related groups which included forms with discordant life-history patterns. From this co-ordinated survey of life-history and taxonomic problems (in salamanders as well as in frogs) he concluded that the nature of the life history, including the larval characters, is an important indicator of evolutionary relationships among the amphibians.

Evolution of Developmental Characters

There is well substantiated experimental evidence from both vertebrates and invertebrates that certain developmental characters have a genetic basis. One can extrapolate from the limited known genetic evidence, and from the much more extensive observational studies on many kinds of larvae, and infer that the developmental process in general is under genetic control and hence is subject to genetic evolutionary changes. If larval and other growth characteristics had no such basis, the developmental resemblances and differences between species would be entirely random, and it would not be possible to recognize and define higher group catgeories on the basis of developmental characters. Keys to the larvae of genera (e.g., Orton, 1952) or of other group categories could not be written. That species groups can be recognized and defined in early developmental stages and that they coincide well with categories defined on adult characters implies that these developmental features do have a genetic basis and also that they have had sufficient genetic stability through time to be retained as a common heritage by a group of diverging descendent species. Although there is much evidence to support this working hypothesis, the adoption of developmental studies as a regular working tool in the systematics of the lower vertebrates is still very slow, as one can note from almost any recent taxonomic paper on fishes or amphibians. Conspicuous advances in the use of larval and other developmental characters in systematics have been made chiefly by students of such groups as parasitic worms and certain insects in which the larval stages are economically or medically important. These cases amply show that early stages provide good taxonomic material, and that much can be accomplished in their study when there is sufficient incentive. The general lag in interest probably traces back to the persistent older practice of "granting" taxonomic value only to the characters of the mature adult (preferably the male in breeding plumage, or equivalent), and disregarding all else. It should be obvious, however, that the nature of evolutionary change in any morphological character can be determined more accurately when the whole ontogeny of that characteristic is well understood.

Since the origin of the frogs marked a fundamental departure in both larval and adult structure from all other known amphibian stocks, it should be glaringly obvious that the evolution of this group offers far more challenging problems when it is studied from the broader viewpoint of developmental systematics, utilizing evidence from the whole ontogeny. The key to successful integration of larval characters into the frog classification lies in deciphering the main patterns of tadpole evolution and determining which patterns are of basic importance and which are secondary in the broad phylogenetic sense. With some understanding of these trends, one can then apply larval data most effectively to help solve particular problems, and in addition can more easily view the origin and history of the tadpole as a part of the broader problem of vertebrate larval evolution as a whole.

Variations and specializations in tadpoles follow very orderly and definable patterns of evolution, with both conservative basic characters that help to delimit major taxonomic groups, and an elaborate network of secondary adaptive trends that cut across taxonomic lines (Orton, 1953, and unpublished data). Larval adaptive radiation and convergent adaptation have produced an abundance of modifications for pond life, stream life, arboreal life, terrestrial life (direct development), for surface feeding, and for predatory habits, and other specializations of less obvious ecological significance. These adaptive modifications are not always sharply defined morphologically, for there are many intermediates, and they have evolved repeatedly in unrelated groups throughout the order. Although such plastic adaptive trends as these are of secondary importance to the main lines of frog phylogeny, they must be worked out and understood in order to clarify the more conservative basic larval history. The combination of independent secondary trends superimposed on (and often obscuring) stable phylogenetic lines is a familiar pattern of animal evolution. It is not surprising that tadpoles follow such standard evolutionary procedures; indeed, it would be most surprising if they did not do so.

Primitive Tadpoles and Primitive Frogs

Much of the disagreement at the family level of frog classification stems from the general difficulty of discerning criteria of primitiveness and advancement within any group that is very highly specialized and presumably long isolated from all known related stocks, and yet has an uninformative fossil record. All of the known frogs are so specialized in their entire structure that characters which ordinarily help us to judge primitiveness or advancement in the amphibians as a whole are obscured, and it is difficult to find anything of clearly primitive nature in any of the frogs. Hence, in this group there is a particular need to explore all possible clues throughout the entire life cycle, because valid evidence of relationship is not confined to any single developmental stage.

The suborder and family arrangement of the frogs proposed by Noble (1931) represented a major advancement in knowledge of this difficult group, and it has been widely adopted. Parker, Davis, and others have since made important improvements in certain sections of the classification, but Noble's conclusions still dominate most discussions of frog systematics. Studies on morphology and evolutionary trends in the tadpole stage (Orton, 1953 and unpublished data) have suggested a taxonomic grouping and phylogenetic organization that differ sharply from Noble's interpretation. Consideration of larval and adult characters together suggests a classification of the frogs into four basic groups of families, each group possessing a distinctive type of tadpole (see Orton, 1953, fig. 6). These four groups do not coincide with Noble's five suborders, but the latter have gradually lost validity with the increasing number of known exceptions to the characters on which they were based. On present knowledge, I consider a formal category of suborder in the Salientia to be both unnecessary and undesirable. In such small taxonomic groups as this, it is generally best to avoid excessive use of the supplementary named categories, in order to permit greater flexibility as knowledge advances and to avoid pedantic clutter.

The four definable larval types in the extant frogs are so stable, regardless of specific secondary specializations, that their real long-term phylogenetic significance appears virtually certain. It seems probable that the four groups of families which they help to characterize represent four major branches of salientian evolution that have been separate for a very long time. They probably do not represent all of the significant lines that have branched off during the long history of the Salientia, but simply lines that have survived. Larval characters thus suggest the way to an apparently more natural grouping of the frogs and to a better understanding of their main phylogenetic trends. In the suggested arrangement into four groups of families, I consider the Ascaphidae, Discoglossidae, and Pipidae to be comparatively primitive, as did Noble, but differ greatly from him in the interpretation of these families and in moving the Rhinophrynidae and Microhylidae to the primitive end of the scale.

The first of the four proposed groups contains the Pipidae and Rhinophrynidae. The known larval and adult characters together suggest that these are probably the most primitive Recent frogs. It would be difficult to find two series of frogs that contrast more sharply in general appearance in the adult stage than do these two families. The Pipidae are the most specialized aquatic frogs known, and *Rhinophrynus* is probably the most specialized of all known burrowing frogs. The Pipidae have long been placed at or near the primitive end of the scale, but the status of *Rhinophrynus* was long in doubt. Early authors treated it variously as a bufonid or leptodactylid, or as a monotypic family of uncertain relationships. Noble placed it in a monotypic subfamily of his very inclusive Bufonidae. The Zoological Record for 1953 still included it in the Bufonidae. Walker (1938), however, showed definitely that *Rhinophrynus* is not related to the bufonids or to the leptodactylids and that its primitive characters together with its many peculiar specializations isolate it well and fully justify its separation as a monotypic family. The tadpole of *Rhinophrynus* agrees very strikingly with those of the Pipidae, which are widely and completely separated from all other known tadpoles by the structure of the mouthparts, by the paired instead of single spiracle, and by other characters. Developmental characters of the African genus *Xenopus* and of the South American genus *Pipa* (including *Protopipa* and *Hemipipa*) are well known, but tadpoles of the other African genera, *Hymeno-*

chirus and *Pseudhymenochirus*, have apparently not yet been reported. The adult of at least one of these incompletely known forms, *Hymenochirus boettgeri*, has wide labial folds along the jaws, perhaps derived from conspicuous labial folds of the still unknown tadpole. From current knowledge of larval and adult characters it is postulated that the Rhinophrynidae are most closely related to the Pipidae; that these two families are endforms of a very ancient adaptive radiation which represents the oldest known surviving level of frog evolution; that their phylogenetic line split off at a very primitive level before the more advanced tadpole characters had evolved; and that they retain some larval characters probably very close to the ancestral basic type in the earliest true frogs. Although it may seem startling to bracket together such extreme adaptive opposites as the adult pipids and rhinophrynids, it should be noted that their suggested ancient origin would give their phylogenetic line a very long history (probably going far back into the Jurassic) with ample time to undergo an elaborate adaptive radiation with an extreme range of types, and ample time for extinction to eliminate most of them, leaving a wide gap between the known survivors.

The second basic group contains the Microhylidae. This relatively large and predominantly tropical family presents many interesting problems. The microhylids are extremely specialized, chiefly for burrowing, and their relationships both among themselves and to other frogs are difficult to interpret. Noble considered the microhylids to be a very advanced family derived from the Ranidae, and accordingly he placed them at the upper end of his classification. Parker (1934), however, found that the evidence does not indicate ranid ancestry for the microhylids, and he suggested that they are probably a much older stock than the ranids. This view is well supported by the larval characters. The single midventral spiracle of the microhylid tadpole, the distinctive pattern of mouthparts and other characters, together with the nature of the evolutionary trends (compared with characteristics and trends of tadpoles as a whole) strongly suggest a relatively primitive phylogenetic position for the microhylids. Differences from the type of tadpole that characterizes the higher families (Bufonidae, Ranidae, etc.) are of such nature that derivation of the microhylid tadpole from any stock in that group, ranid or otherwise, seems highly unlikely. The microhylid larval jaw structure most nearly resembles the pipid type, but is more complicated and shows a different pattern of evolutionary trends. The large number of forms and wide distribution of the Microhylidae give us a good opportunity to determine the stability of its peculiar type of tadpole under various ecological conditions. Microhylid tadpoles display an interesting range of specializations, in part associated with differences in feeding habits, unusual ecological adaptations, and direct development. So far as known, however, these differences are all variations of the single basic structural plan, and this stable larval type occurs throughout the Microhylidae and is restricted to this family. On present knowledge it seems probable that the microhylids originated at a comparatively primitive level in salientian history and have long been completely separate from other frogs, and that they are a terminal group which has not given rise to any of the known higher and more modern stocks.

The status of the genus *Phrynomerus* is uncertain. Parker (1934) excluded it from the Microhylidae, giving it monotypic family rank largely because it possesses intercalary cartilages. The tadpole attributed to *Phrynomerus* in the literature is a typical microhylid, and more recent authors have tended to return this genus to the Microhylidae. More extensive information on both its development and its adult anatomy would be very desirable.

The third apparently natural group of frogs comprises the Ascaphidae and Discoglossidae. On the basis of vertebral structure and other adult characters, Noble regarded the Ascaphidae (his Liopelmidae) as the most primitive known frogs, and designated the suborder Amphicoela for this single family. This opinion and rank designation have been widely adopted in the general zoological literature. In known larval characters, however, *Ascaphus* is essentially a discoglossid. The tadpole of *Ascaphus* is highly modified for life in swift streams, but its basic characters are those of the discoglossids and its specializations modify typical discoglossid features. These characters include a single median spiracle as in the microhylids and complex mouthparts similar in many respects to those of the higher group of families. The important recent work by the Stephensons on the direct development and adult anatomy of *Leiopelma* provides long-needed material for comparative study and should help to clarify the relationships of this genus. The development of the Philippine discoglossid, *Barbourula,* is apparently still unknown. The early fossil histories of both the discoglossid-ascaphid and the microhylid lines are apparently unknown, but these two groups probably branched off separately and are not directly related to each other. In larval characters, certainly, they have evolved along quite different lines. Their puzzling combinations of larval characters provide one of the reasons for thinking that not all of the major branches of frog evolution, particularly at the more primitive levels, have survived to Recent times.

The five families of frogs that are considered here to be the most primitive of the extant forms thus fall into three well-defined groups, and each group is characterized by a distinctive larval type. All other frogs, so far as their classification is currently understood, comprise one large group that is characterized throughout by one basic larval type, the well-known "standard polliwog" with horny mouthparts and sinistral spiracle. In this largest major section of the classification the abundant life-history material shows that the basic internal and external characters remain stable under the very wide range of known adaptive specializations which more or less drastically modify the general appearance of the tadpole. The only known forms in which basic characters are obscured are some of those with direct development (notably, *Eleutherodactylus* spp.), in which suppression of larval characters has gone to an extreme and some of the diagnostic structures simply fail to develop at all. The higher families offer many interesting problems in larval evolution and many points of disagreement and uncertainty in classification, but time limitations prevent their discussion here.

The temptation to generalize widely from thin lines of evidence is a well-known hazard in evolutionary research, and is a special problem in studies on the frogs because of the traditional reluctance of vertebrate taxonomists to rely on unfamiliar developmental data. Since the suggested re-grouping of frog families departs sharply from the widely-used Noble classification, the interpretation of larval characters and their validity in systematics may be questioned. A more conservative taxonomist may favor the idea that some or all of the presumed basic larval characters might have resulted from secondary convergent adaptations rather than from stable phylogenetic events. However, the extensive comparative study of tadpoles on which this work is based has shown clearly that the characters in question have remained stable under the impact of taxonomic diversification, extreme adaptive modification, and geographic dispersal which tadpoles (and, of course, the Salientia as a group) have obviously undergone. The apparent integrity of the four larval types and their apparent reliability as indicators of basic evolutionary lines are inferred from their restriction to, and constancy within, the particular taxonomic group which each larval type characterizes. Regardless of how specialized the known tadpoles have become in their ecological adjustments (including their feeding adaptations), they do not escape from the basic structure of their group. On present knowledge the reality of these larval group characters seems beyond question, but of course the use to which they are put in tracing phylogenetic details may reflect differences of interpretation now, and it is well recognized that future discoveries may necessitate changes.

The suggestion that the very specialized pipids and rhinophrynids probably represent a more ancient stock than does *Ascaphus* poses an interesting problem in the interpretation of taxonomic characters. Primitiveness implies both relatively ancient origin and possession of relatively ancient characters, but in an incomplete record (either geologically or morphologically) these two attributes do not always appear to coincide precisely in any known species. A Recent species that is extremely primitive in the sense of coming from a very ancient stock may be so specialized in its adult characters that it has lost most of the obvious primitive features of its group. In contrast, a different Recent form that derives from a somewhat less ancient stock may have kept a more generalized adult structural plan with fewer losses of ostensibly primitive characters through secondary specializations, and may thereby wear the most obvious "primitive look" among its contemporaries. Relationships may be obscure or seem contradictory if judgement is based on too narrow a segment of the obtainable evidence, hence the importance of coordinated study of the whole animal through its whole ontogeny should be obvious. Present knowledge suggests that the Pipidae and Rhinophrynidae derive from a very ancient salientian stock and retain some very stable archaic larval characters in common, although adaptive evolution has taken these families into conspicuously opposite extremes of adult specialization. The available evidence further suggests that the relatively more advanced status of the discoglossid-ascaphid group is obscured largely because their more generalized adult format retains more features that fit our idea of what a primitive frog ought to look like.

Supplementary Evidence from the Fishes

Tadpole studies are no exception to the general rule that any research can benefit from consideration within a wider framework. There is much to be learned by treating tadpole evolution as a part of the broader problem of developmental evolution in the lower vertebrates as a whole. For example, comparative study of phylogenetic trends in jaw modifications in fishes (both skeletal and soft parts) can be very instructive in the analysis of comparable problems in tadpole history, for there are some remarkable similarities in morphological adjustments in the jaw region between tadpoles and certain fishes. Study of the external mouthparts of many kinds of tadpoles and the labial structures of salamander larvae and of certain kinds of fishes reveals convincing evidence that the lips of tadpoles are morphologically derivable from the simple labial folds that are common throughout these groups. The larvae of flyingfishes (Exocoetidae) have complex lip and barbel structures that yield important taxonomic clues comparable to the sort of information obtainable from tadpole mouthparts. Many adult fishes, especially among the Ostariophysi, have complex labial specializations which bear a striking superficial resemblance to certain kinds of lip modifications of tadpoles, as noted by Annandale and Hora (1922). Internal anatomy also reveals some notable structural analogies between tadpoles and certain fishes. In certain of the fish skulls described by Gregory (1933), most conspicuously in the catfish *Plecostomus commersoni,* the jaw pattern more or less closely suggests the condition in a typical ranid-type tadpole, particularly in the forward inclination of the quadrate, the contours of the shortened and displaced jaws, and the small mouth. It is noteworthy that modifications may follow similar designs in both vertebrate classes, and that such modifications may evolve either as temporary larval characters (in tadpoles, larval flyingfishes, etc.) or as permanent adult characters (in certain fishes). The occurrence of analogous jaw patterns in tadpoles and certain fishes strongly suggests that a thorough comparative study of developmental stages, with emphasis on basic principles, would materially advance our understanding of the morphogenetic background of evolution in both groups. The richer evolutionary diversity of the fishes may supply more easily analyzed evidence than can be obtained from the frogs on such problems as the extent of convergence in adaptive structural modifications of the mouthparts at different phylogenetic levels, and the extent to which secondary changes in specializations may be confused with primitive simplicity. For example, present knowledge of Recent tadpole anatomy is inadequate to demonstrate unequivocally whether the possession of certain similar lip and jaw characters by tadpoles of both the discoglossid-ascaphid and the ranid types stems from a remote common ancestral stock that had attained this general level of buccal complexity, or whether these similar jaw patterns originated independently in the two groups from less complex ancestral mouthparts. Since the likelihood of solving this problem directly from fossil discoveries of such delicate tadpole structures is remote, the best approximation will be achieved indirectly from extensive comparative study of the trends in modification of the labial folds and jaw patterns that are evident throughout the extant amphibians and fishes.

Summary

To summarize: evolutionary processes can modify any characteristic that is genetically regulated, whether this be manifested in structure, function, or development, and since these attributes are unified in the life of the animal their evolution is best treated as a unified problem. The origin of the tadpole and its subsequent history form an integral part of the evolutionary history of the frogs. Coordinated study of the larval and adult characters suggests a way toward a more natural grouping of the families of frogs and a better understanding of their main lines of evolution. The likelihood that further improvements in frog classification will depend significantly on comparative study of the evolution of jaw mechanisms and labial specializations in fishes is but one example of the unexpected and interwoven trails one must be prepared to follow in systematics.

LITERATURE CITED

ANNANDALE, N., and HORA, S. L. 1922. Parallel evolution in the fish and tadpoles of mountain torrents. *Rec. Indian Museum, 24*:505–509.

COPE, E. D. 1889. The Batrachia of North America. *Bull. U. S. Nat. Mus., 34*:7–525.

GREGORY, W. K. 1933. Fish skulls: a study of the evolution of natural mechanisms. *Trans. Amer. Philos. Soc., N. S., 23*: vii + 75–481 pp.

GRIFFITHS, I. 1956. Status of *Protobatrachus massinoti. Nature, 177*:342–343.

NOBLE, G. K. 1931. The biology of the Amphibia. McGraw-Hill Co., xiii + 577 pp.

ORTON, GRACE L. 1952. Key to the genera of tadpoles in the United States and Canada. *Amer. Midl. Nat., 47*:382–395.

——— 1953. The systematics of vertebrate larvae. *Syst. Zool., 2*:63–75.

PARKER, H. W. 1934. A monograph of the frogs of the family Microhylidae. British Mus. (Nat. Hist.), viii + 208 pp.

STEPHENSON, N. G. 1951. On the development of the chondrocranium and visceral arches of *Leiopelma archeyi. Trans. Zool. Soc. London, 27*:203–253.

——— 1955. On the development of the frog, *Leiopelma hochstetteri* Fitzinger. *Proc. Zool. Soc. London, 124*:785–795.

WALKER, C. F. 1938. The structure and systematic relationships of the genus *Rhinophrynus. Occ. Papers Univ. Michigan Mus. Zool.*, No. 372, pp. 1–11.

GRACE L. ORTON, Scripps Institution of Oceanography, University of California, La Jolla, California. The work reported here is derived in part from the author's doctoral studies, conducted at the University of Michigan under the direction of Dr. Norman Hartweg. Contribution from the Scripps Institution of Oceanography, New Series No.922.

Reprinted from BULLETIN OF THE SEISMOLOGICAL SOCIETY OF AMERICA
VOLUME 47 • NUMBER 3 • JULY, 1957

NORTHWARD CONTINUATION OF THE SAN ANDREAS FAULT

By FRANCIS P. SHEPARD

A RECENT article by Tocher[1] gives some interesting information concerning the earthquake epicenters off the northern Pacific coast of the United States. The article is chiefly concerned with the northward continuation of the San Andreas Fault. As Tocher points out, there are two significant trends among the epicenters. The group with the largest number of epicenters of major earthquakes between 1922 and 1955 follows the Gorda Escarpment as closely as could be expected, in view of the inaccuracy of epicenter locations (fig. 1). The other, which contains the epicenter with the highest energy but a distinctly smaller concentration, is referred to by Tocher as the probable northward continuation of the San Andreas Fault.

The writer[2] has presented evidence which suggested that the San Andreas Fault might make a westward bend along the Gorda Escarpment somewhat like the trend changes to the south. The evidence for this projection of the fault, briefly recapitulated, includes (1) the displacements at Shelter Cove during the great 1906 earthquake, presumably along the San Andreas;[3] (2) the northwestward tracing of the fault zone along the coast with the cutting off of the head of Delgada Submarine Canyon;[4] (3) the existence of unique types of gash cracks or small rift valleys in the continental shelf northwest of the beheaded canyon and pointing toward the scarp (fig. 2); and (4) the 40-mile displacement of the 1,000-fathom curve off Punta Gorda, which could be due to the right lateral slip characteristic of the San Andreas Fault. When this evidence was presented, seismologists working in the California area pointed out that epicenters (then far less certainly located) showed a much more probable northward continuation along a line which is essentially that shown in the recent article by Tocher.[5] They maintained that the Gorda Escarpment could not be the continuation of the San Andreas Fault since it was not an area of earthquake epicenters. Now, however, that Tocher's more detailed and improved study has shown that the Gorda Escarpment actually has more large earthquakes than the other trend, it would seem only reasonable for the California seismologists to reconsider this opinion. Yet Tocher still persists in the old idea, using as a new argument the large bend away from the general trend of the San Andreas Fault to the south made by the Gorda Escarpment.

A study of various geological maps of California will show that along the San Andreas Fault there are several significant changes in trend. Near the Tehachapi

---

Manuscript received for publication January 16, 1957.

[1] Don Tocher, "Earthquakes off the North Pacific Coast of the United States," *Bull. Seism. Soc. Am.*, 46: 165–173 (1956).

[2] F. P. Shepard, "Structures in Prolongation of the San Andreas Fault Zones," *Bull. Geol. Soc. Am.* (abstract), 53: 1821–1822 (1942); F. P. Shepard and K. O. Emery, "Submarine Topography off the California Coast: Canyons and Tectonic Interpretation," Geol. Soc. Am., *Special Paper* 31 (1941).

[3] F. E. Matthes, quoted in A. C. Lawson *et al.*, *The California Earthquake of April 18, 1906. Report of the State Earthquake Investigation Commission*, Carnegie Institution of Washington, pp. 54–58 (1908).

[4] Shepard and Emery, *op. cit.*, fig. 15.

[5] *Op. cit.*, fig. 1.

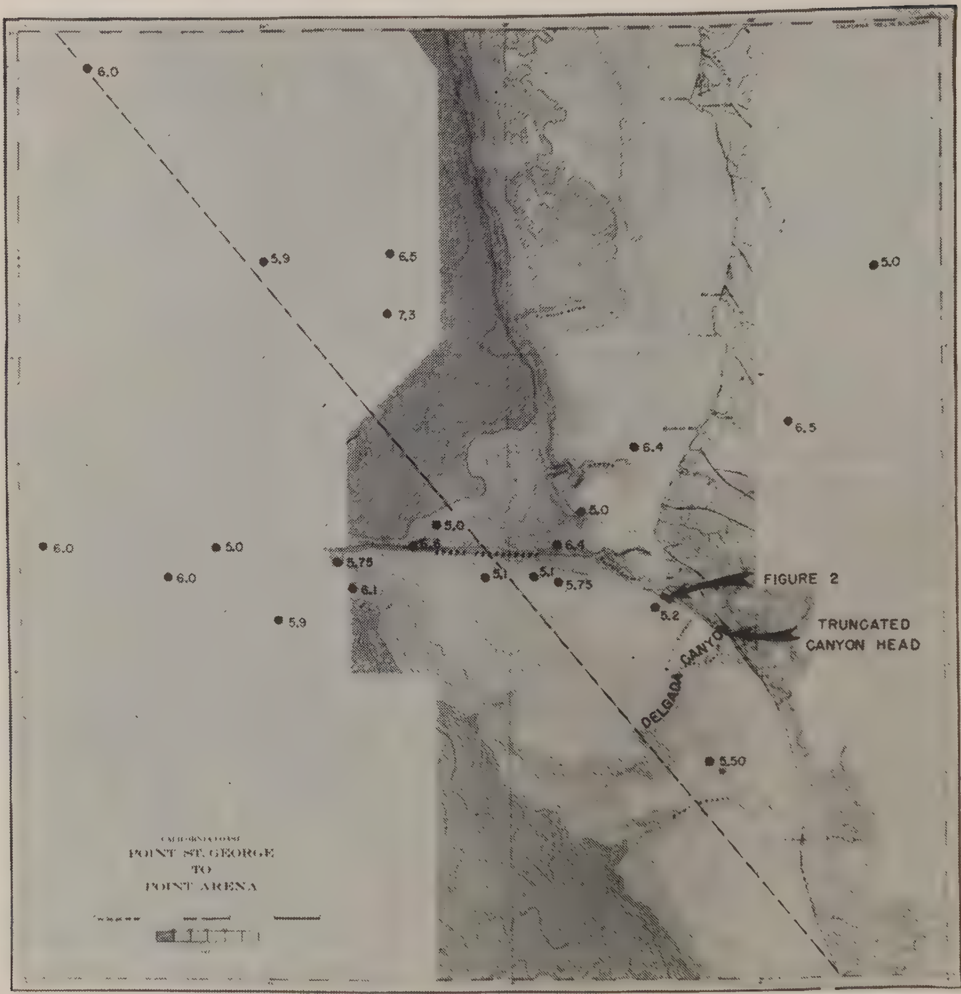

Fig. 1. Relating submarine topography (Shepard and Emery, 1942, as cited in fn. 2) to epicenters of large earthquakes between 1922 and 1955 (Tocher, 1956, as cited in fn. 1). Note that the great-circle extension of the San Andreas fault defended by Tocher shows no indication of a strike-slip displacement of submarine contours either at the Gorda Escarpment or where the line crosses the submarine canyons, whereas the trend favored by the writer is in accord with large horizontal displacement both of the continental slope and Delgada Canyon (for more detail of the latter see Shepard and Emery, 1942, fig. 15, *c*).

Mountains, according to Hill and Dibblee,[6] there is a trend of east and west at Frazier Mountain and of N 80° W at Mount Pinos. Both of these approximate the same trend as that of the Gorda Escarpment. Just northwest of Mount Pinos the general trend of the fault is mapped as N 40° W, so that changes of trend of up to 50° appear to exist here, not much less than the 70° change in trend which is suggested by the Gorda Escarpment. In both trends the change is gradual.

---

[6] M. L. Hill and T. W. Dibblee, Jr., "San Andreas, Garlock, and Big Pine Faults, California: A Study of the Character, History, and Tectonic Significance of Their Displacements," *Bull. Geol. Soc. Am.*, 64: 443–458 (1953).

(294)

It is perhaps significant that there are several changes in trend of the San Andreas Fault to the east of the area where Menard[7] found the Murray fracture zone extending out from the continental slope off the Santa Barbara area. Farther north, Menard's Mendocino fracture zone is clearly a westward continuation of the Gorda Escarpment. It is, therefore, not by any means surprising that the San Andreas Fault should show an even larger deflection where it encounters this great submarine structural trend. Beyond the relatively short Gorda Escarpment the trend may again continue to the northwest.

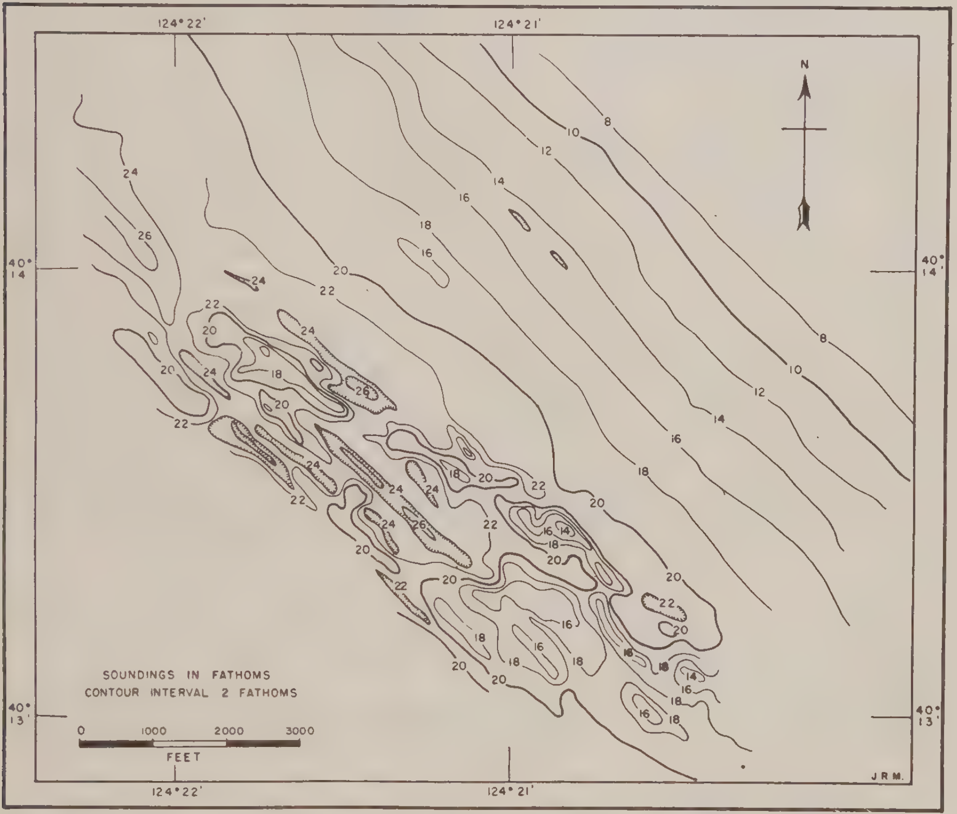

Fig. 2. Detailed contours of part of the shelf near Punta Gorda (see fig. 1) showing small "rift valleys" and short ridges along the suggested trend of the San Andreas fault. Detailed soundings terminate at the outer part of the contouring. Contoured from U. S. C. and G. S. unpublished Hydrographic Sheet no. 6164.

A relationship of more importance than trend is the topographic expression of a large strike-slip fault where it crosses a steep submarine slope. This has been neglected by Tocher. The hypothesis of a continuation of the San Andreas Fault along the Gorda Escarpment fits the supposed character of the fault, namely, that it has had a large right lateral shift. The large scale of this movement along the San

---

[7] H. W. Menard, "Deformation of the Northeastern Pacific Basin and the West Coast of North America," *Bull. Geol Soc. Am.*, 66:1149–1198 (1955).

Andreas fault system was doubted for a long time by many California geologists, but the carefully documented evidence by Noble,[8] Wallace,[9] Hill and Dibblee,[10] and Crowell[11] seems to show that actually there is very substantial evidence in favor of many miles of horizontal displacement along the San Andreas and associated faults. It would be surprising if the northward extension of this fault system into the ocean basin did not have a displacement of the contours of the continental slope out of their general north–south trend. The 1,000-fathom curve at Punta Gorda is offset about 40 miles (fig. 1). This amount is not out of line with the amount of displacement indicated along the San Andreas and adjacent faults in southern California. The line drawn by Tocher to show his concept of the northern continuation of the San Andreas Fault, on the other hand, crosses the Gorda Escarpment in a well-sounded area but shows no offset at all. Furthermore, the submarine canyons south of the Gorda Escarpment cross Tocher's hypothetical fault either without displacement, or, in the case of Delgada Canyon, with a bend in the wrong direction, whereas the fault inferred by the writer is supported by the unique shoreward termination of Delgada Canyon.

The foregoing discussion does not solve the problem but may indicate the importance of further examination of the various aspects. Quite clearly Tocher has considered the matter entirely from the point of view of seismology and general trends, and seems to have given no consideration to the significance of the extraordinary displacement of the contours which occurs at Punta Gorda. The northwesterly line of epicenters shown by Tocher may be related to the San Andreas Fault, but it clearly has no indication of being a zone of major strike slip. Perhaps a split in the fault occurs at the inner end of the Gorda Escarpment, and the energy may be divided.

---

[8] L. F. Noble, "Geology of the Valyermo Quadrangle and Vicinity, California," *U. S. Geol. Survey*, 1954.

[9] R. E. Wallace, "Structure of a Portion of the San Andreas Rift in Southern California," *Bull. Geol. Soc. Am.*, 60: 781–806 (1949).

[10] *Op. cit.*

[11] J. C. Crowell, "Probable Large Lateral Displacement on San Gabriel Fault, Southern California," *Bull. Amer. Assoc. Petrol. Geol.*, 36:2026–2035 (1952).

University of California,
Scripps Institution of Oceanography,
La Jolla, Calif.

(Contribution from the Scripps Institution of Oceanography, N. S., no. 923.)
Reproduced by Permission

Vol. 38, No. 3 Transactions, American Geophysical Union June 1957
Reproduced by Permission

Photography of Submerged Vertical Structures*

Raymond F. McAllister

Abstract—A device is illustrated and described with which photographs of the vertical walls of the La Jolla Submarine Canyon were obtained to a depth of 625 ft. Brief description of a number of the photographs is given, and photographs are reproduced. It is concluded that such an apparatus can provide pictures of sheer underwater scarps, reef faces, and, with suitable modifications, of dams, breakwaters, and bridge supports.

Introduction—During an investigation, undertaken by H. B. Stewart, to determine the geology of the La Jolla Submarine Canyon (Fig. 1) it became desirable to obtain photographs of the walls below diving depth [*Shepard*, 1949] to learn, if possible, something of the nature of the bedrock, sediment veneer, and organic incrustation. Since in many places the walls of this canyon are vertical and even overhanging, some method differing from those in the literature was needed to obtain pictures. After experimentation, the apparatus described below was developed by the author. Good photographs were obtained at a depth of over 600 ft.

The apparatus—Figure 2 shows the apparatus and method of suspension. Considerable modification can be made in size and material without impairing the usefulness of the device. The trip nose operates the camera upon contact with hard bottom by compressing a normally extended spring in the nose and allowing the cable within to become slack. The release mechanism of the camera case operates when unloaded; thus, a slack cable trips the camera and fires the flash bulbs which are electrically synchronized with the shutter. An NDRC underwater camera case, employing the German-made Robot camera, was used [*Ewing* and *Worzel*, 1942]. The canvas sail serves to keep the camera headed in the direction of the boat's travel and hence into the canyon wall. Suspension of the device forward of its center of resistance in a manner similar to a windvane helps maintain the required orientation.

The flash bulbs used were unprotected, types SM, SF, and #5. They were pretested for implosion by submerging them to a depth of more than 1000 ft before use, and gave adequate light for a camera-to-subject distance of more than 16 ft. Various inclinometers were used to indicate the vertical in the finished photographs, but results were rather unsatisfactory. Observations by divers with self-contained underwater breathing apparatus during early tests in 80 ft of water revealed that the device was very nearly horizontal at the moment of contact.

An attempt was made to obtain stereo photographs of the canyon walls by mounting two camera cases side by side and tripping them simultaneously. The picture separation was too great, however, to permit stereo viewing of the photographs.

For horizontal photography, most underwater camera cases may be used in a modification of the frame herein described, although one holding a camera with a larger negative size would be desireable.

Operation—A small boat with good speed control ahead and astern, equipped with a power winch, is most satisfactory. A DUKW was used with great success.

Ranges, determined by two objects of fixed and known location kept in direct line with each other, were selected. Using a comparatively accurate bathymetric chart of the canyon, areas of interest crossed by certain ranges were selected for survey. Using predetermined sextant angles and the ranges, it was possible to lower the apparatus to the required depth in the middle of the submarine canyon, with the trip nose directed toward a precise location on the canyon wall. The DUKW moved forward slowly during lowering, thus maintaining the orientation. Contact with the canyon wall was determined by the sudden tension in the wire rope, at which time the clutch on the winch was 'slipped' and the DUKW thrown into reverse. After the apparatus was free of potential snags it was retrieved, recocked, and new bulbs were inserted readying it for another lowering. With the DUKW on the range, a sextant angle was recorded at the moment of contact with the canyon wall. Proof of the accuracy of this

---

* Contribution from the Scripps Institution of Oceanography, New Series, No. 924. Contribution from the Department of Oceanography of the Agricultural and Mechanical College of Texas, Oceanography and Meteorology Series, No. 81.

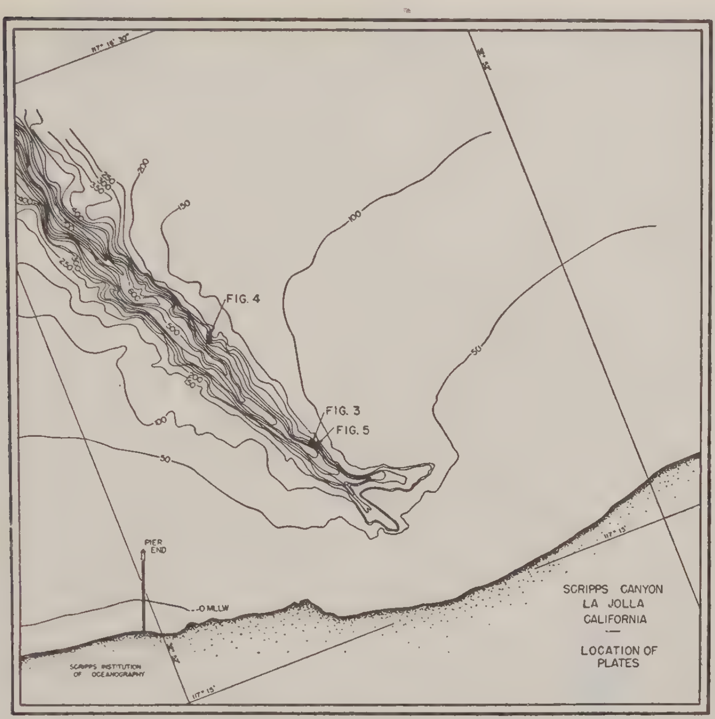
117° 18' 30"
32° 52'
200
150
100
50
FIG. 4
FIG. 3
FIG. 5
PIER END
0 MLLW
117° 15'
SCRIPPS INSTITUTION OF OCEANOGRAPHY
SCRIPPS CANYON
LA JOLLA
CALIFORNIA
LOCATION OF PLATES

FIG. 1 – Index to location of photographs

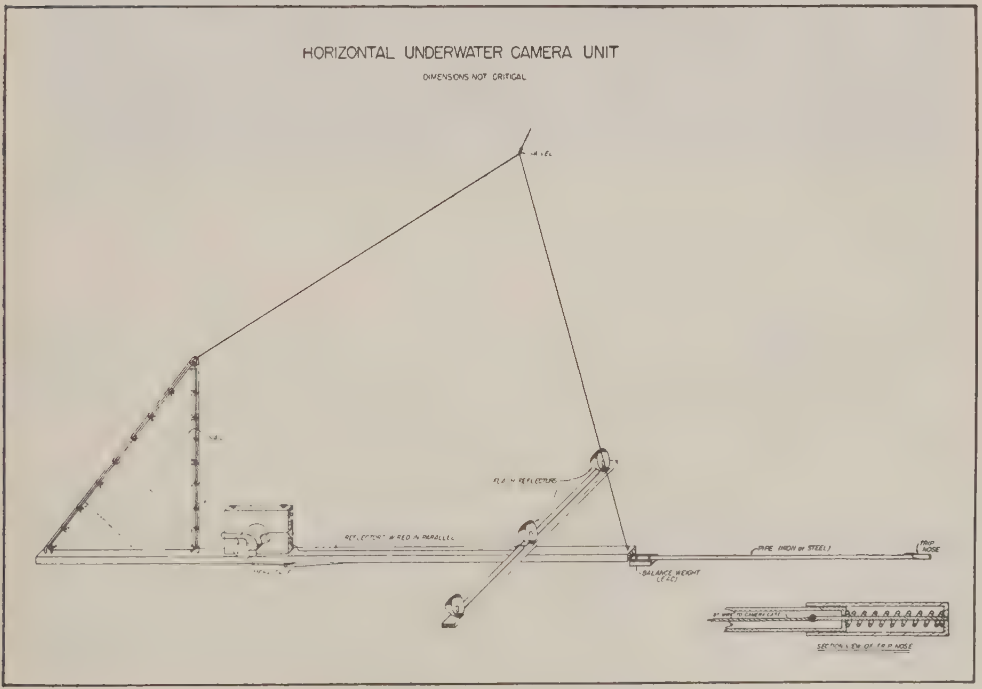
HORIZONTAL UNDERWATER CAMERA UNIT
DIMENSIONS NOT CRITICAL
FLASH REFLECTORS
REFLECTORS WIRED IN PARALLEL
PIPE (IRON or STEEL)
TRIP NOSE
BALANCE WEIGHT (LEAD)
TO CAMERA CASE
SECTION VIEW OF TRIP NOSE

FIG. 2 – The horizontal underwater camera unit

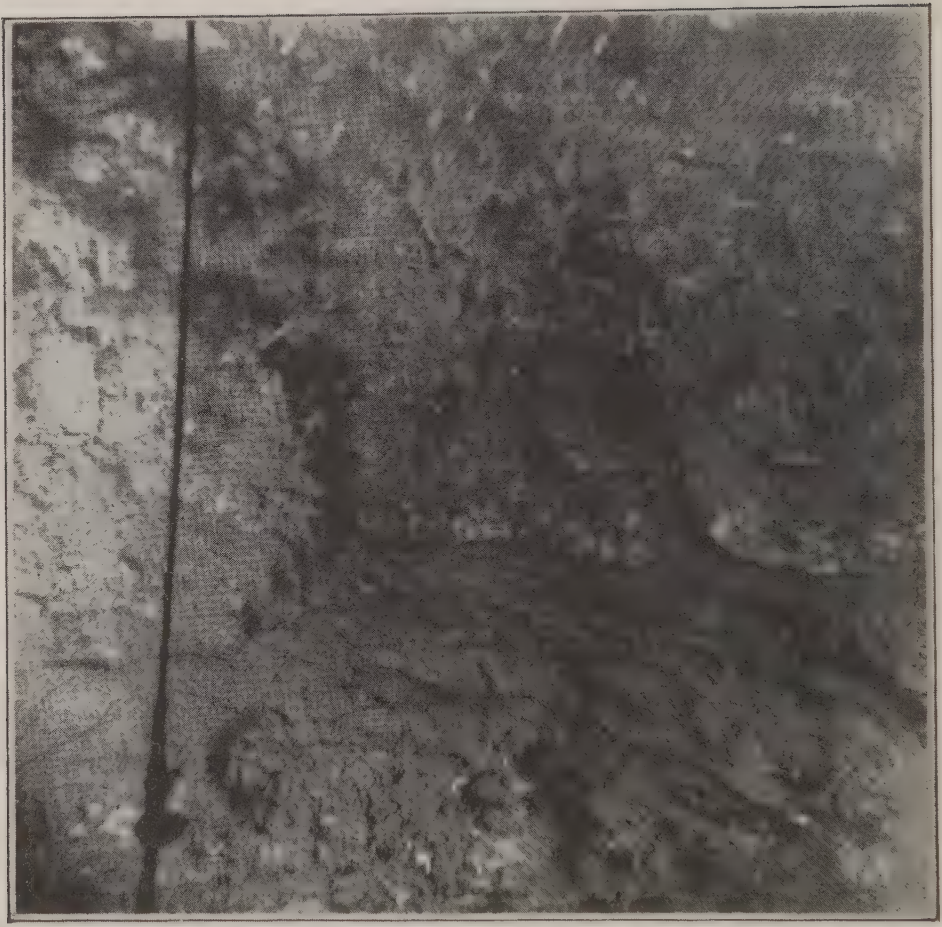

FIG. 3 – Narrow ledge with nearly sheer rock face behind it; this area rephotographed one year later, showed no change in organisms or sediment cover; 300 ft deep, NW wall, Scripps Canyon; area about 3.5 ft square; vertical black line is suspending wire rope; photo data: f 5.6, $\frac{1}{100}$ sec, one SF flash bulb, Plus X film, camera to subject about 7.5 ft.

method of positioning is shown by two photographs taken one year apart which include the same area of the canyon wall while registering only a few minutes of angle difference at contact and very nearly the same depth by the amount of cable out (see below).

Adjustment of focus must be made to take into account the difference between the refractive indices of water and air (which also much reduces the field of view). For accurate focus, the camera should be set for 75 pct. of the underwater distance from lens to subject. A wide-angle lens effectively increases the field of view of the camera.

Results of the survey—From 88 lowerings made in 1952, 57 printable negatives were obtained from depths of 95 to 625 ft. These photographs, taken with a camera-subject distance of 7½ ft, covered an area approximately 3½ ft square. When sloping walls were photographed the area was much increased.

Most of the photographs show rock in various attitudes. Bedding planes, rock faces encrusted with organisms, and ledges laden with sediment were photographed. A number of pictures interpreted as showing conglomerate were taken. Dredging from various places in this canyon had previously revealed conglomerate [*Shepard* and *Emery*, 1941].

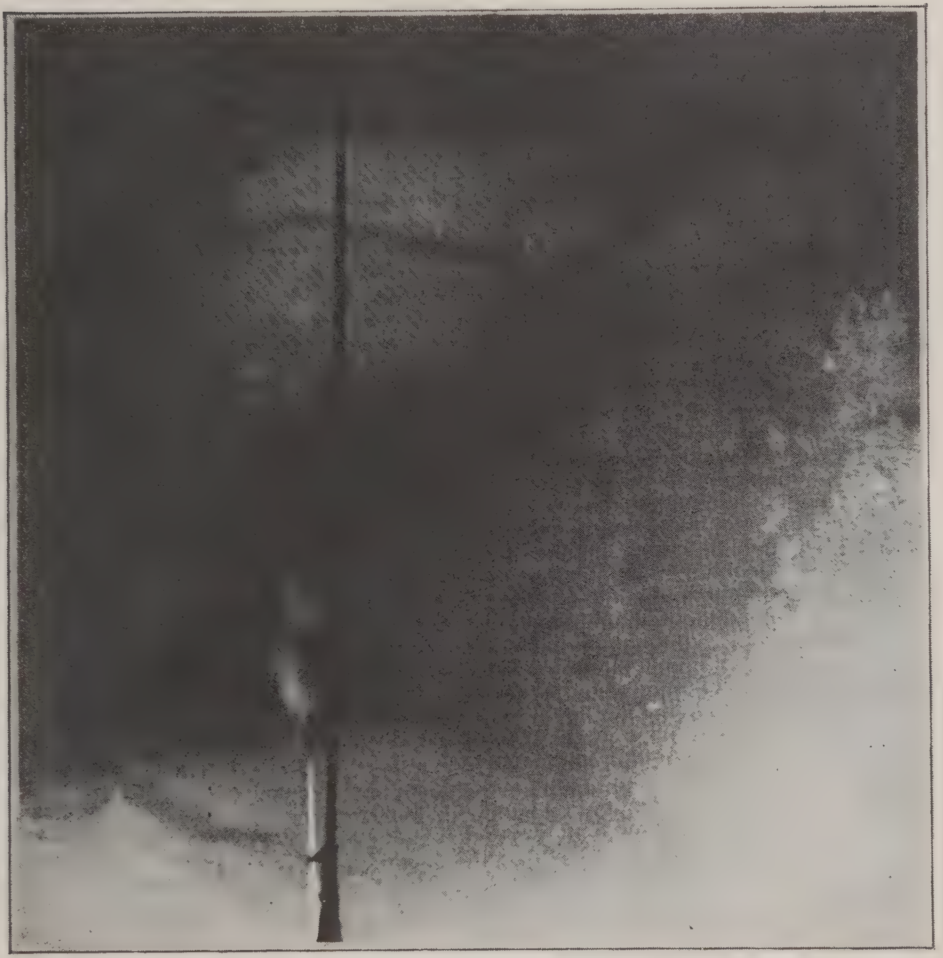

FIG. 4 – Jutting ledge at 300 ft on NW wall, Scripps Canyon; area of photograph unknown; photo data: f 10, $\frac{1}{100}$ sec, two #5 flash bulbs, Plus X film, camera to subject distance unknown

Extensive attempts were made to photograph terraces which might correlate with a Pleistocene lowering of sea level of 250 to 350 ft. No such terrace was found, although the wall between these depths was repeatedly photographed. Coverage, however, was not thorough enough to be certain that there are no terraces. The ledges shown in several photographs are much like the one in Figure 3, and seem hardly significant in this respect, being about 12 in wide. They probably represent nothing more than resistant beds of rock.

Heavy organic (animal) incrustation occurs at all depths photographed. No important changes in organisms seems to occur with increasing depth except the disappearance of the sea anemones. Fan and tube worms, starfish, and sponges and tunicates occur with greater frequency below 200 ft. In some photographs the fan worms almost cover the sheer rock faces with their extended arms (upper portion, Fig. 3).

Operations in 1952–53 with a longer frame resulted in 11 printable negatives from 25 lowerings. They included a much larger area of the canyon wall. A rock ledge photographed in August 1952 (Fig. 3) was rephotographed in August 1953 and found to have suffered no noticeable change in sediment veneer or organic growth. The 1953 picture has insufficient density to permit reproduction.

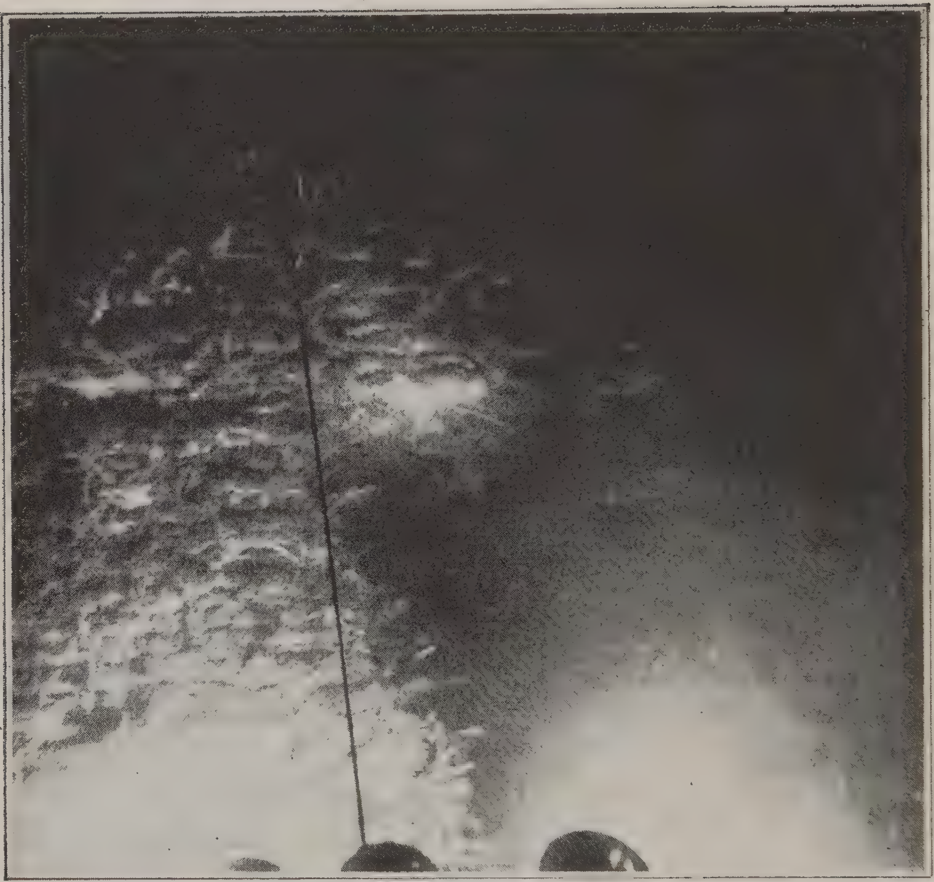

FIG. 5 – Angular re-entrant at 300 ft on NW wall, Scripps Canyon; area of photograph approximately 7.5 ft square; note thin bedded rock; photo data: f 5.6, $\frac{1}{100}$ sec, two #5 flash bulbs, Plus X film, camera to subject about 11.5 ft

Figure 4 very clearly shows a thin bedded rock ledge protruding from the canyon wall. This is one of several pictures illustrating ledges and angular irregularities along the course of the canyon. Figure 5 shows an angular re-entrant at a depth of 300 ft.

Conclusions—The equipment and methods herein presented should enable one to take photographs to a depth of more than 600 ft, and thus to delineate the features of near vertical walls of submarine canyons, and of fault scarps and reef faces, hitherto known only from dredging and sounding information. A more sturdy camera case should extend the depth range considerably. Manmade structures, such as bridge supports, dams, and piers, may be photographed using a modification of the equipment. Since the boat from which it is suspended is normally considerably ahead of the apparatus, it may not be used when the object to be examined extends above the surface. By suspending the unit from a boom and orienting it with cables extending laterally to the surface, one need only draw the far end slowly forward with another line, to obtain pictures of shallow structures.

The choice of frame size must depend upon the requirements of the survey, with long frames permitting examination of larger areas in each picture, and it is not unlikely that a close-up camera built along similar lines could be used to reveal microstructure of sediments, and details of the organisms.

Acknowledgments—This project was supported by the Office of Naval Research under contract *N6-ori-111* (Task b). The DUKW was loaned to the project by the Beach Erosion Board, through D. L. Inman. Ted Anstead, the DUKW driver, saved the apparatus several times when it seemed irretrievably snagged deep in the submarine canyon. H. B. Stewart and M. A. Beal assisted with operations during 1952 and 1953 respectively. F. P. Shepard made the study possible by his support and encouragement, and this assistance s gratefully acknowledged.

REFERENCES

EWING, M. AND WORZEL, J. L., Photography of submerged wrecks: *NDRC Report C4-sr 31-135*, June 24, 1942.

SHEPARD, F. P., Terrestrial topography of submarine canyons revealed by diving; *Bul. Geol. Soc. Amer.* **60**, 1597–1612, 1949.

SHEPARD, F. P., AND EMERY, K. O., Submarine topography off the California coast, canyons and tectonic interpretations; *Geol. Soc. Amer. Spec. Paper 31*, 1941.

Scripps Institution of Oceanography, La Jolla, California

(Communicated manuscript received July 16, 1956, and, as revised, January 15, 1957; open for formal discussion until November 1, 1957.)

LABORATORY STUDIES ON THE RATE OF GROWTH OF THE FORAMINIFER, "*STREBLUS BECCARII* (LINNÉ) VAR. *TEPIDA* (CUSHMAN)"

BY

JOHN S. BRADSHAW

Reprinted from
Journal of Paleontology
Vol. 31, No. 6, November, 1957
Reproduced by Permission

Contributions from the Scripps Institution of Oceanography, New Series, No. 925

(305)

JOURNAL OF PALEONTOLOGY, VOL. 31, NO. 6, P. 1138–1147, 5 TEXT-FIG., NOVEMBER 1957

LABORATORY STUDIES ON THE RATE OF GROWTH OF THE FORAMINIFER, "*STREBLUS BECCARII* (LINNÉ) VAR. *TEPIDA* (CUSHMAN)"

JOHN S. BRADSHAW
Scripps Institution of Oceanography, University of California, La Jolla

ABSTRACT—Many generations of "*Streblus beccarii* (Linné) var. *tepida* (Cushman)" have been cultured successfully in the laboratory over a period of two years. During this time, experiments have been carried out on the effects of temperature and salinity upon the rate of growth and reproductive activity.

Temperatures below 10°C. and above 30–35°C. result in a cessation of growth, temperatures lower than 10°C. allow life, but temperatures above the upper extreme cause death in a short time. Between these limits growth is observed, the rate increasing with the temperature. Reproduction takes place at temperatures between approximately 20°C. to 30°C.

Temperature also affects the duration of each generation; at 20°C. it may take four times as long to reach reproductive maturity as at temperatures of 25° to 30°C. Under the latter conditions reproduction occurs on the average of once per month.

Salinities between 20 and 40 °/₀₀ allow normal growth and reproduction. Above and below these limits growth and reproductive activity decline until growth finally ceases at salinities higher than 67 °/₀₀ or below 7 °/₀₀. Reproduction occurs only at salinities between 13 °/₀₀ and 40 °/₀₀. The time required to reach reproductive maturity also increases as the extreme tolerance limits are approached so that it requires twice as long for each generation at 13 °/₀₀ as it does within the normal range.

INTRODUCTION

Few experimental data have been published emphasizing the effect of environmental factors upon the Foraminifera. External factors such as temperature and salinity presumably exert a selective effect by direct action on fundamental metabolic processes and undoubtedly play an important role in determining which species will be excluded and which will be found in any given area.

Each species appears to have its own range of environmental conditions within which it will flourish, the limits being determined by its physiological makeup. If a species is continuously exposed to conditions outside these limits it will sooner or later fail in competition with other better-adapted forms and must eventually die out. According to Andrewartha & Birch (1954, p. 26) even slight changes in environmental conditions are shown to affect longevity, fecundity, and rate of development, and these in turn will determine the rate of increase or decrease of the population. Knowledge of these limits and of the reactions of Foraminifera to the extreme conditions of their environment is, therefore, of great importance.

A paper describing the results of some preliminary laboratory experiments on two species of Foraminifera has been published (Bradshaw, 1955). Many of the methods and techniques used for the present study are similar to those used in the earlier work.

The study has been supervised by Fred B. Phleger. The laboratory work was supported in part by a contract of the University of California with the Office of Naval Research, and in part by American Petroleum Institute Project 51. Species illustrations were prepared by Robert R. Lankford. Appreciation is expressed to Dr. Zach M. Arnold of the University of California at Berkeley and Miss Frances L. Parker of Scripps Institution for helpful suggestions received during preparation of this manuscript. This is a contribution from the Scripps Institution of Oceanography, New Series, No. 925. Contribution No. 26, Marine Foraminifera Laboratory.

MATERIALS AND METHODS

The living specimens of "*Streblus beccarii* (Linné) var. *tepida* (Cushman)" (Text-fig. 1) used in the experiments came from several samples of sediment collected by R. R. Lankford from a depth of six feet in Lower

(306)

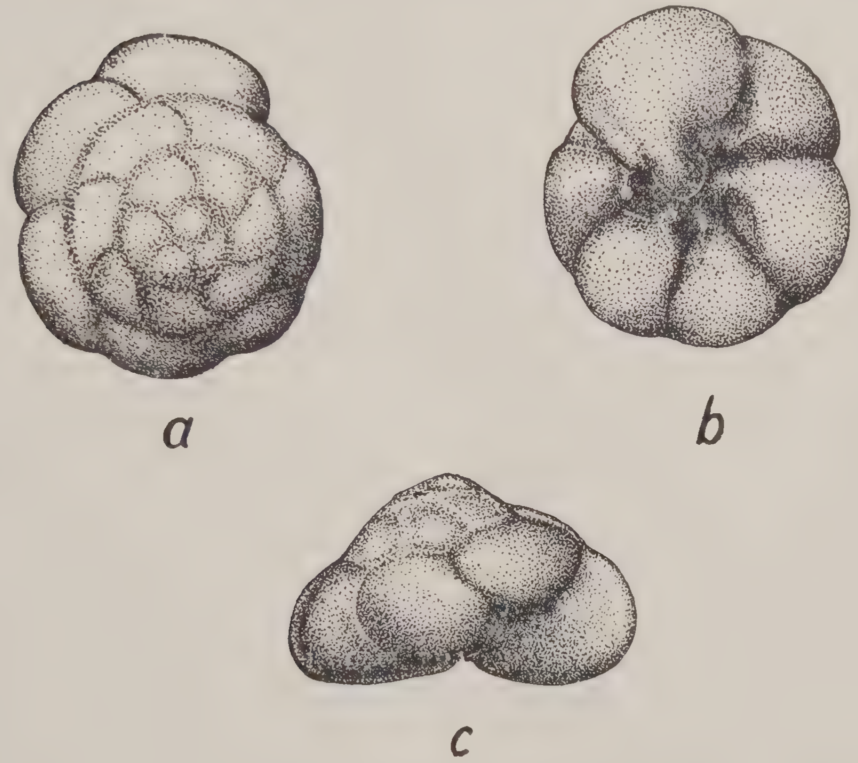

TEXT-FIG. *1*—"*Streblus beccarii* var. *tepida* (Cushman)," 5×170. a, Dorsal view; b, ventral view; and c, side view.

San Antonio Bay, Texas. The taxonomic status of this variety is in doubt but the name used should sufficiently identify the form. A description has been given by Parker, et al., (1953, p. 13, pl. 4, fig. 25–28).

The following discussion is based largely on test morphology. Laboratory generations appear to follow one another at approximately equal intervals, the exact time depending upon environmental conditions. No good evidence has been seen of a dimorphic alternation of generations and most of the forms, with very few exceptions, have a prolocular diameter of approximately 57μ. According to observations made by Lister (1895, p. 436) on a related form, this size should be indicative of the megalospheric generation. Very rarely, young individuals were observed with a proloculus of approximately 33μ but these never developed beyond the two-chambered stage and eventually died. Nuclear staining with aceto-carmine has, thus far, shown only one nucleus.

The direction of coiling appears to be so distributed that approximately half of the adult specimens coil to the right and the other half turn to the left. The offspring of either a right or left coiled parent have approximately a 50-50 ratio of coiling direction. Changes in temperature or salinity appear to have little effect upon this character. The number of young produced varies from about 17 to 44 individuals, usually averaging from 28 to 32.

The young foraminifer emerges from the parental test at the two-chambered stage (maximum diameter approximately 78μ). At first the young adhere closely to the empty adult but after several hours gradually move away. When food is plentiful and environmental conditions are optimal the addition of chambers is so rapid that three chambers are present by the second day and four chambers by the fourth day. The rate of addition becomes slower as the individual grows larger. Under optimum conditions reproduction occurs at any time after a total of 13 or more chambers has been attained. Reproduction typically terminates the life of the parent, although occasionally some protoplasm showing pseudopodial activity may remain behind in the test for several days before decomposing.

A series of experiments was designed to assess the importance of two environmental factors, temperature and salinity. If hereditary differences can be disregarded it may be assumed that the rate of growth of an individual is directly related to the fitness of its environment. Since it could not be shown that all the individuals had a uniform heredity, an attempt was made to minimize the possible effect of any hereditary differences by selecting the groups of six to ten young Foraminifera in a random manner from the same mass culture.

Watch glasses, containing the young forms were placed in covered petri dishes and kept under the following temperatures at a constant salinity of 33.5‰. Duplicate cultures were kept at temperatures of 15°, 20° and 30°C.

	Temperature °C.					
	10°	15°	20°	24–27°	30°	35°
Mean number of chambers at start of experiment	10.3	7.3	8.3	8.7	8.5	8.7
Range of chamber number	8–17	6–9	7–11	8–11	8–9	6–11
Number of specimens	7	17	16	7	15	9

Similar groups (at 24–27°C.) were kept at the following salinities.

	Salinity ‰									
	2	7	13	20	27	30	33.5	40	50	67
Mean number of chambers at start of experiment	9.1	8.8	9.0	8.9	9.2	8.5	8.7	7.8	8.4	9.7
Range of chamber number	7–11	7–11	8–10	7–12	7–10	6–10	8–11	6–10	6–11	8–11
Number of specimens	10	10	8	9	8	10	7	10	10	7

Rate of growth could be determined either by number of chambers added or linear addition to the maximum test diameter. In the present study chamber number was used. For some purposes, however, linear measurement may be more applicable since this would enable an approximate calculation of protoplasmic volume increase. Text-figure 2 compares the maximum diameter of the test with that of chamber number so that the number of chambers given in the subsequent figures can be converted to linear measurement if desired.

On Monday and Thursday mornings during the course of the experiment the maximum diameter of each individual, at a magnification of 75×, was measured with an ocular reticle and the total number of chambers was counted. Each specimen was then carefully pipetted into a freshly prepared sterile sea water medium and again placed under the prescribed environmental conditions. An "artificial detritus" composed of freshly heat-killed *Chlamydomonas* was used for feeding. Preliminary experiments showed that the addition of approximately 200,000 cells to each culture at equal intervals twice a week was sufficient to allow ten Foraminifera to grow normally.

The curves (Text-fig. 3,4, and 5) showing the rate of growth under various environmental conditions cover the period from the beginning of the experiment to the onset of reproduction. The length of life from birth can be approximated by extrapolation of

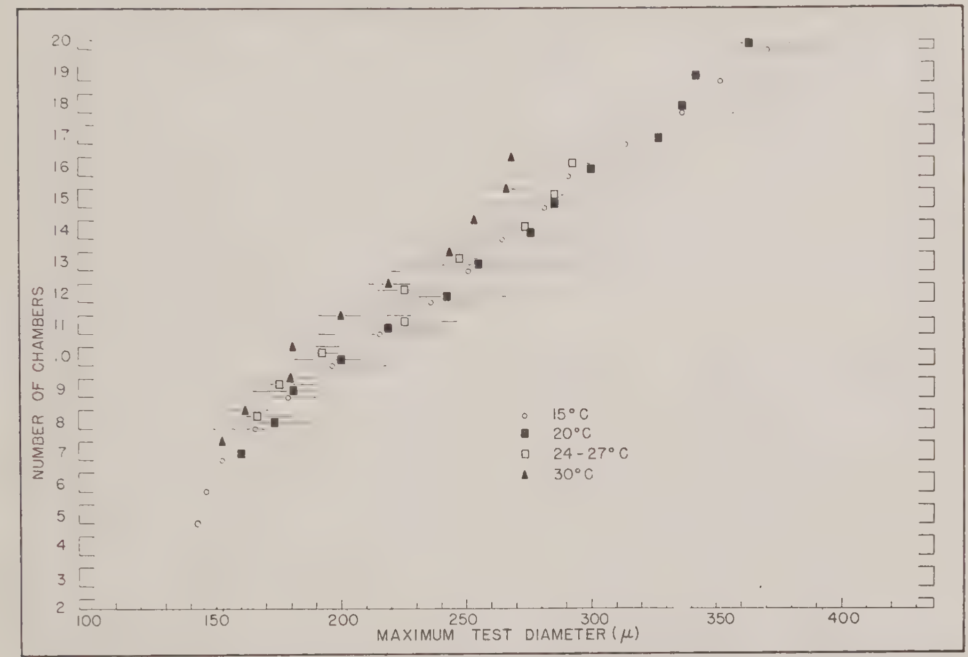

TEXT-FIG. 2—Relation between chamber number and maximum test diameter. Symbols indicate the mean maximum test diameter and the observed range of the specimens cultured at different temperatures.

these observed growth curves. The length of time from birth to reproductive maturity will vary somewhat among the different individuals of a culture. For the purposes of graphic representation the first occurrence of reproduction in each culture marks the end of that particular experiment. In the text discussion, however, the average length of life of all the specimens in each culture has been used when comparing the results of environmental influences.

EXPERIMENTAL RESULTS

Temperature Experiments

Text-figure 3 shows the mean rate of addition of chambers in cultures containing from six to ten specimens when kept at the indicated temperatures and at a salinity of 33.5°/₀₀. At 10°C. no growth was observed. At 15°C. there was some growth amounting to approximately one new chamber every six days. Temperatures of 20°C. permitted one new chamber every four days. At temperatures of 24–27°C. and 30°C., however, the test growth rate was doubled so that one new chamber was added every two days. When cultures were kept at 35°C. no growth was observed and the specimens died within twenty-four hours.

Although no observable growth occurred in cultures kept at 10°C., metabolism did not cease entirely and the individuals appeared to live indefinitely long periods without reproducing. The culture was transferred to room temperatures of 24–27°C. after 27 days of no growth, and the specimens grew rapidly and reproduced 25 days later.

The 15°C. culture grew very slowly for 134 days with no evidence of reproduction; however, at the end of this period, reproduction occurred within eight days when the culture was transferred to temperatures of 24–27°C.

At 20°C. there was one peculiar instance of possible reproductive activity after 72 days. At this time many spherical prolocula or small *Allogronia*-like forms were found embedded in the umbilicus of a mature adult. Normal calcareous tests never developed and the individuals degenerated after several weeks of no growth. This phenomenon has been observed on several occasions and may represent an abortive attempt at reproduction. Seventy-six days after the start of the experiment one specimen had a normal brood but the remaining specimens did not reproduce until 22 days later.

At 24–27°C. the average time from the beginning of the experiment to reproductive maturity was 19 days whereas at 30°C. the main period was only 15 days. At 35°C. the specimens lived less than one day.

The relationship between chamber number and mean maximum test dimension at different temperatures, shown in Text-figure 2 reveals that Foraminifera grown at warm temperatures (30°C.) tend to add chambers having a smaller size than do specimens kept at cooler temperatures. Warm temperatures also seem to encourage the development of misshapen individuals which have chambers of variable size.

There may be a significant difference in the total number of chambers and the maximum test diameter for the parent test at the time of reproduction for specimens cultured at different temperatures, as shown by the following table:

	Temperature °C			
	15°C.*	20°C.	24–27°C.	30°C.
Mean number of chambers at reproduction	20	19	15	15
Range of chamber number at reproduction	18–21	17–21	13–17	13–17
Mean size at reproduction (μ)	355	357	293	266
Number of specimens examined	14	9	5	12

* No reproduction at indicated temperature.

Salinity Experiments

Text-figures 4 and 5 show the mean rate of growth of cultures containing from six to ten specimens when kept at the indicated salinities and at temperatures varying between 24 to 27°C. At salinities of 20–40°/oo, one new chamber was added approximately every two days. At salinities of 13°/oo and 50°/oo chambers were added at the rate of one every three days. The culture kept at a salinity of 67°/oo showed no growth for a 35-day period, but was still viable as shown by the resumption of its normal rate of growth when transferred to a salinity of 33.5°/oo.

Within the salinity range of 20°/oo to 40°/oo, the average length of time for reproduction to occur was 23 days. Specimens kept at 13°/oo required an average of 48 days to reproduce. Below 13°/oo cultures failed to grow, although this may have been partly an effect of low pH as well as salinity.

The tests of specimens grown at 2°/oo and 7°/oo dissolved within a few days after introduction to the experimental media. The pH values were 7.2 and 7.4 respectively, which are too low to allow the existence of carbonate tests. This low pH was a result of the use of distilled water instead of river water in the dilution of the sea water for the experimental media. Natural river water usually contains large amounts of carbonate and other anions which act as buffers to resist the lowering of pH caused by respiration and atmospheric CO_2. Distilled water, on the other hand, contains none of these buffers and consequently when it is used to dilute sea water to very low salinity the remaining ions are insufficient to buffer effectively. The experimental results shown for the low salinity cultures, therefore, must not be considered indicative of those to be expected in natural environments where river water is mixed with sea water.

Subsequent experiments using Mississippi River water for dilution have shown slight growth in a salinity of 7°/oo but none in 2°/oo although the Foraminifera remain alive and have intact tests.

Salinities of 50°/oo and higher not only retard growth but also appear to inhibit the reproductive process, since no reproduction occurred during the time the cultures were kept under the experimental conditions.

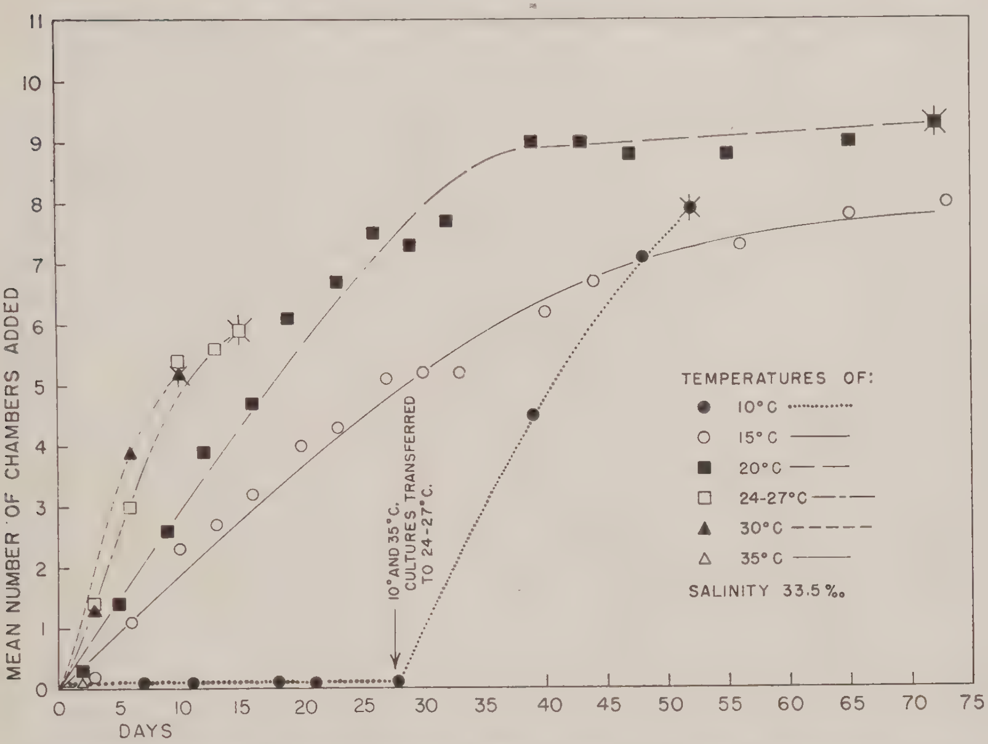

TEXT-FIG. 3—Growth of "*Streblus beccarii* var. *tepida* (Cushman)" at different temperatures. * Indicates first occurrence of reproduction in culture.

When transferred to salinities of 33.5°/oo, however, the specimens eventually reproduced.

Specimens cultured at different salinities may show a significant difference in the total number of chambers and in the mean maximum test diameter at the time of reproduction. The relationship is shown by the following table:

DISCUSSION

Experimental results have shown that in the life cycle of "*Streblus beccarii* var. *tepida*," growth and eventually reproduction will take place as long as environmental factors are favorable. Furthermore, as the environmental factors, e.g. temperature and salinity depart from the optimal values, the rate of growth and the frequency of repro-

	Salinity °/oo						
	13	20	27	30	33.5	40	50*
Mean number of chambers at reproduction	19.7	18.2	17.1	16.5	15.0	18.5	18.5
Range of chamber numbers	17–21	17–19	15–19	15–17	13–17	16–21	15–21
Mean maximum diameter (μ)	296	298	293	285	293	300	300
Number of specimens	8	9	6	6	5	6	7

* No reproduction at indicated salinity.

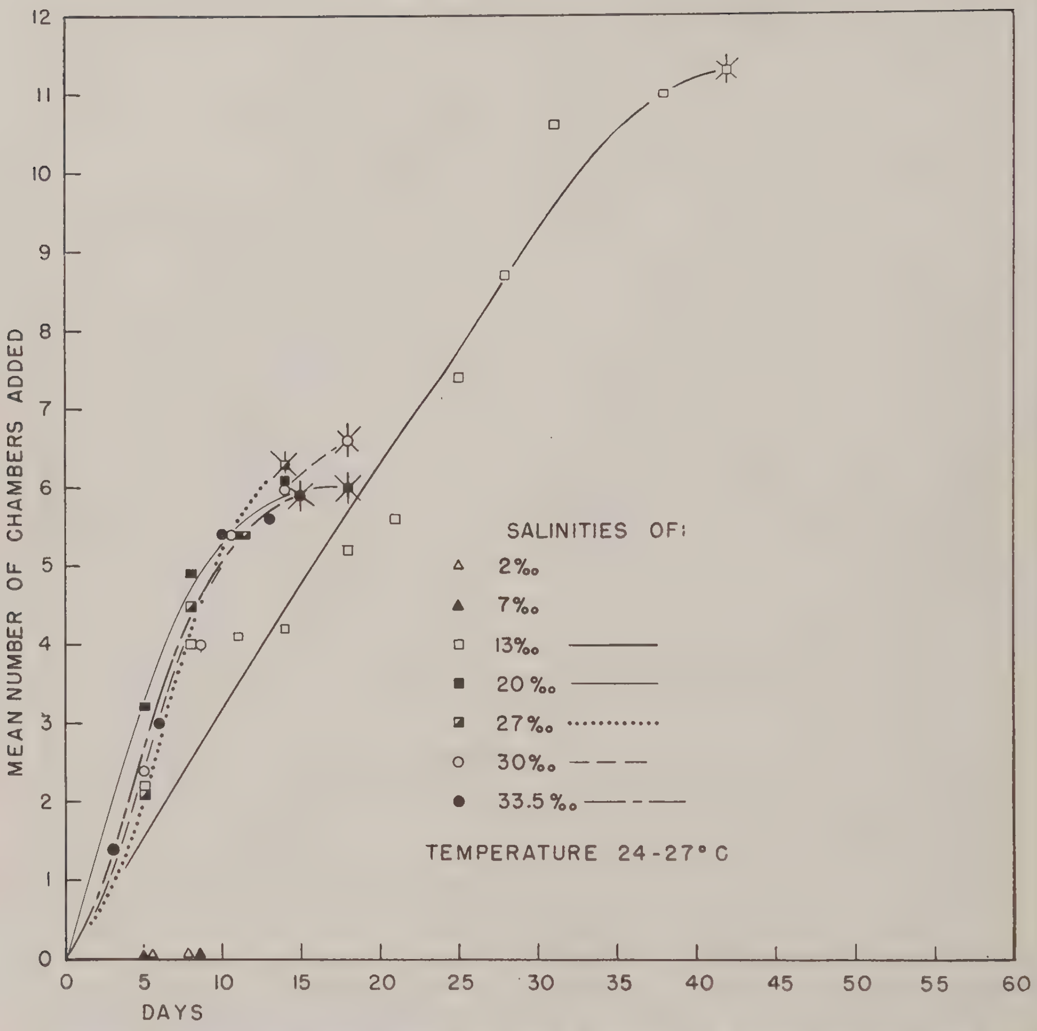

TEXT-FIG. 4—Growth of "*Streblus beccarii* var. *tepida* (Cushman)" at salinities less than that of normal sea-water. * Indicates first occurrence of reproduction in culture.

duction decline. At any given temperature or salinity within the tolerance of the species the growth as measured by rate of chamber increase is not uniform but occurs more rapidly in young individuals and slows down as reproductive maturity is reached. The reason for the decline of growth and subsequent reproduction at the end of life is not known. Mazia (1956) shows that it may not be merely the attainment of a critical size but also the completion of important nuclear processes that "triggers" reproduction in *Amoeba proteus*. This may be true also in the Foraminifera but further studies are necessary.

The present experiments tend to substantiate Mazia's findings. In the experimental cultures of Foraminifera, reproduction has not occurred until a total of at least 13 chambers has been reached. As was true

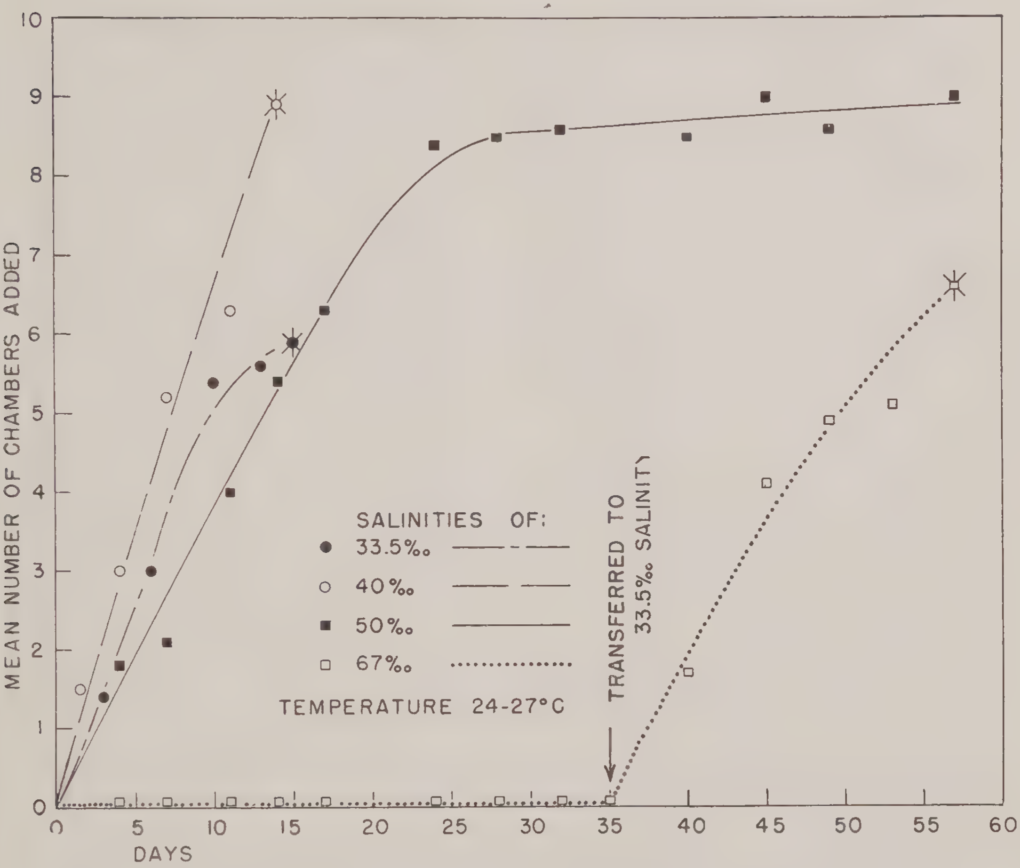

TEXT-FIG. 5—Growth of "*Strebulus beccarii* var. *tepida* (Cushman)" at salinities greater than that of normal sea-water. * Indicates first occurrence of reproduction in culture.

of *Amoeba*, however, the mere attainment of this size will not in itself guarantee successful reproduction since presumably a period of nuclear reorganization also must precede the production of young forms.

For reproduction to occur the environmental factors must be within certain limits. In the cultures grown under optimum conditions, for example, temperatures of 24–30°C. and 33.5°/₀₀ salinity (Text-figure 3) reproduction occurred soon after the "critical size" was reached.

The cultures kept at 15° and 20°C. and also those at 50°/₀₀ salinity. Text-figures 3 and 5, however, illustrate the situation when conditions are such that reproductive activity cannot easily be carried out. Here, even though the "critical size" has been reached, the reproductive process appears to be inhibited by the prevailing conditions. If the cultures are returned to optimal conditions, however, reproduction usually follows within a few days.

When reproduction is delayed by unfavorable temperatures and salinities, and other factors, food, etc., remain favorable, growth may continue, as long as the conditions are not excessively detrimental. The specimens may thus finally reproduce at a larger size and with a greater number of chambers than would be true under more favorable circumstances.

If the conclusions derived from the laboratory experiments are valid and may be applied to natural populations of Foraminifera the larger specimens of the same species would be expected in the unfavorable environments and the smaller specimens under the most favorable conditions. Nicol (1944) shows such a relationship between size, temperature and latitude in his study of West Coast species of *Elphidium*. He noted that "increase in size of specimens is related to decrease in temperature and increase in degrees north latitude." He further states that temperature may be the controlling factor although he does not say in what manner the temperature may control the size. Hesse, Allee & Schmidt (1951) state that "the larger size of northern and cold water marine forms is a frequent phenomenon, both as applying to the individuals of a wide ranging species and to the northern or cold water species that replace tropical forms within a given genus. Delayed sexual maturity, which favors growth in size, appears to be directly dependent on retardation of growth at lower temperatures. . . ."

The results from laboratory culture experiments are interesting for they may give us a clue to the behavior of Foraminifera in nature. So long as temperature and other factors remain within a "favorable range" in the laboratory, "*S. beccarii* var. *tepida*" will reproduce continuously with the result that under optimum conditions of 30°C. one generation will follow another at approximately 28-day intervals. Temperatures this high occurring under natural conditions during the summer may allow several generations of this form with the resulting addition of many empty tests to the sediments. Assuming that about 28 young are produced per parent and that all the offspring grow to maturity and reproduce, at the end of three such generations, a total of 22,765 empty tests would have been contributed to the sediments from one ancestral test. This extreme rate of test deposition is not realized in nature because of predation and other factors; nevertheless, there may be a more significant addition of tests to the sediments in the warmer months than during the remainder of the year.

With the advent of more adverse temperatures (20 to 24°C.) in the fall, the growth rate declines and a longer interval is required between successive generations. Reproduction does not occur below approximately 20°C. With temperatures of 10° and lower, such as may occur in the San Antonio Bay area in winter, there should be a complete cessation of growth, although these Foraminifera may remain alive and resume growth when favorable temperatures again occur. In winter the minimal addition of empty tests to the sediments is expected. Myers (1942) has shown similar seasonal changes in growth rate for natural populations (Plymouth, England) of *Elpidium crispum* (Linné). Growth was rapid in spring and summer, declined in the fall and did not occur during the winter.

In "*S. beccarii* var. *tepida*" normal growth and reproduction occur between salinity values of $20^{\circ}/_{\circ\circ}$–$40^{\circ}/_{\circ\circ}$. Beyond these limits growth and reproductive activity decline until finally growth ceases at salinities higher than approximately $67^{\circ}/_{\circ\circ}$ or below $7^{\circ}/_{\circ\circ}$; other life activities may continue, however, at salinities as low as $2^{\circ}/_{\circ\circ}$ (and perhaps even lower).

A knowledge of the reactions of laboratory cultures of Foraminifera to different salinities makes it possible to explain certain anomalous occurrences under natural conditions. Lankford (personal communication) reported that living specimens of "*S. beccarii* var. *tepida*" were found in water of $1^{\circ}/_{\circ\circ}$ salinity off the mouth of the Mississippi River. The salinity near the mouths of estuaries may vary widely because of variations in the amount of river discharge, reaching minimal values in winter and spring with maximal values in summer and fall. A station located hear the mouth of the Mississippi River, for example, having a bottom salinity of less than $1^{\circ}/_{\circ\circ}$ in February was found to have a salinity of almost $32^{\circ}/_{\circ\circ}$ in November. A form such as "*Streblus beccarii* var. *tepida*," with a high degree of salinity tolerance could be expected to survive these conditions of extremely low salinity and to flourish when conditions are once again within the reproductive range.

It must not be assumed that the results from the preceding experiments will be applicable to all species of Foraminifera. The limited work that has been done so far on the tolerance of Foraminifera shows that many and perhaps most species have narrower limits than these reported for survival and reproductive activity. It may be possible, however, that in variable environments similar to San Antonio Bay, the results described for "*S. beccarii* var. *tepida*" may serve as a general pattern for other species found in similar habitats.

BIBLIOGRAPHY

ANDREWARTHA, H. G., & BIRCH, L. C., 1954, The distribution and abundance of animals: Chicago, University of Chicago Press, 782 p.

BRADSHAW, J. S., 1955, Preliminary laboratory experiments on ecology of foraminiferal populations: Micropaleontology, vol. 1, p. 351–358.

HESSE, R., ALLEE, W. C., & SCHMIDT, K. P., 1951, Ecological Animal Geography: John Wiley and Sons, New York, 715 p.

LISTER, J. J., 1895, Contributions to the life-history of the Foraminifera: Philos. Trans. Roy. Soc., London, Ser. B., vol. 186, p. 401–453.

MAZIA, D., 1956, The life history of the cell: Amer. Scientist, vol. 44, p. 1–32.

MYERS, E. H., 1942, A quantitative study of the productivity of the Foraminifera in the sea: Proc. Amer. Philos. Soc., vol. 85, p. 325–342.

NICOL, D., 1944, New West American species of the foraminiferal genus Elphidium: Jour. Paleont., vol. 18, p. 172–185.

PARKER, F. L., PHLEGER, F. B., & PEIRSON, J. F. 1953, Ecology of Foraminifera from San Antonio Bay and Environs, Southwest Texas: Contr. Cushman Found. Foram. Res., Spec. Publ. No. 2.

Reprinted from JOURNAL OF BACTERIOLOGY
Vol. 74, No. 2, pp. 251-255, August, 1957
Printed in U.S.A.

EFFECT OF HYDROSTATIC PRESSURE ON SUCCINIC, FORMIC, AND MALIC DEHYDROGENASES IN *ESCHERICHIA COLI*[1]

RICHARD Y. MORITA[2]

Department of Biology, University of Houston, Houston, Texas

Received for publication February 25, 1957

ZoBell and Morita (1957) demonstrated the existence of barophilic bacteria in various deeps and trenches of the Pacific and Indian Oceans where hydrostatic pressures up to 1,100 atm exist. However, the relationship between hydrostatic pressure and the activity of life in the deep sea is still unknown.

Johnson *et al.* (1954), for convenience of discussion, divided hydrostatic pressure into moderate or high pressures (*ca.* 1 to 1,000 atm) and very high pressures (*ca.* 1,000 atm and above). The effect of very high pressures has been known to inactivate certain enzymes (Macheboeuf *et al.*, 1933; Vignais *et al.*, 1951; Matthews *et al.*, 1940; Curl and Jansen, 1950*a*, 1950*b*). Using moderate pressures, Borrowman (1950) reported that hydrostatic pressures up to 700 atm at 30 C had no effect on the rate of formic dehydrogenase activity of *Escherichia coli*. In the latter work a pressure cylinder with optical windows was employed as well as cells of *E. coli* which were heated to 65 C for 5 min in order to inactivate as many interfering enzymes as possible. Since the cells were subjected to heat the "biological whole" was not represented.

Morita and ZoBell (1956) studied the effect of hydrostatic pressure on the succinic dehydrogenase system in cells of *E. coli*, which had been previously subjected to pressure. These measurements were carried out by the Thunberg technique after the pressure was released to 1 atm. This paper deals with the effect of pressure on the rate of formic, succinic, and malic dehydrogenase by cells of *E. coli* during the time of compression.

MATERIAL AND METHODS

Preparation of cells. Cells of *E. coli* were grown in a Fernbach flask containing 200 ml of nutrient medium: glucose, 2 g; KH_2PO_4, 2 g; K_2HPO_4, 5 g; peptone (Difco), 5 g; distilled water, 1,000 ml. The pH of the medium after autoclaving was 7.0. This medium was inoculated with 20 ml of a similar medium in which *E. coli* had developed for 24 hr. The inoculated medium was incubated at 30 C for 16 hr. Cells were grown for each experiment.

The cells were harvested in a Servall type XL centrifuge and washed twice with equal volumes of M/100 phosphate buffer (pH 7.0) and resuspended in M/15 phosphate buffer (pH 7.0). The suspended cells were aerated with filtered air for 2 hr at room temperature (27 C). After aeration the cells were recentrifuged and the final suspension adjusted to a turbidity of 250 on the Klett-Summerson apparatus using a red filter (640 to 700 mμ). The zero setting was made with distilled water in a Klett tube. The final suspension was stored overnight in the refrigerator (5 C) and used the next morning.

Optical high pressure cylinder. Stainless steel pressure cylinders fitted with white sapphire windows were constructed (figure 1). A neutral piston prevented the mixing of the hydraulic fluid and the reaction mixture. This neutral piston was fitted with a 8/32 in. self-seal screw which had one side cut away to allow for the escape of gas and excess liquid in the optical high pressure cylinder. After filling the cylinder with the reaction mixture, the excess gas or liquid was replaced by the neutral piston and the self-seal screw was secured. The valve was attached and the optical high pressure cylinder attached to the pressure apparatus and pressurized to the desired hydrostatic pressure. The pressure apparatus was described by ZoBell and Oppenheimer (1950).

These optical high pressure cylinders were constructed to fit in a modified 10 cm cell compartment of a Beckman DU spectrophotometer. The

---

[1] Contribution from the Scripps Institution of Oceanography, New Series, No. 927. This paper represents results of research carried out by the University of California under a grant from the Rockefeller Foundation.

[2] Visiting investigator, Scripps Institution of Oceanography, University of California, La Jolla, California.

(317)

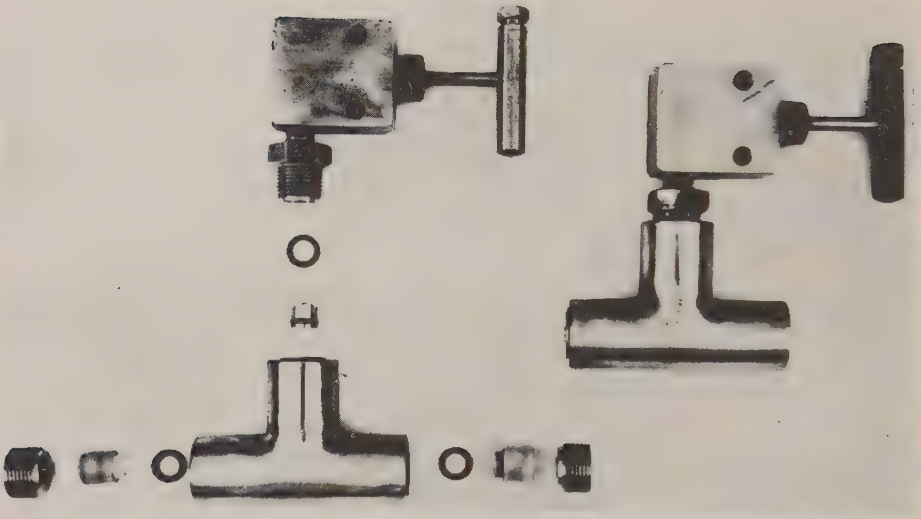

Figure 1. Optical high pressure cylinder

total liquid volume of the optical high pressure cylinder was 7.5 ml.

Deoxygenating unit. A deoxygenating unit (figure 2) was constructed from a connecting tube (with a suction tube, standard taper 24/40) and a pair of ground joints (full length, standard taper 24/40, ends sealed). An 18 gauge syringe needle was inserted near the contact between the rubber tubing and the connecting tube so that the point of the syringe needle was at the base of the suction tube of the connecting tube. This syringe needle was plugged when the unit was evacuated.

Vacuum pump assembly. The lower arm of a three-way T-shaped stopcock was attached by a rubber tubing to a Cenco-Megavac vacuum pump while the upper arm was attached by rubber tubing to a nitrogen reservoir. Rubber tubing from the horizontal arm of the stopcock was attached to the deoxygenating unit. Vacuum or a slight nitrogen pressure could be applied by moving the stopcock to the appropriate position.

Methylene blue reduction measurements. Methylene blue was employed as the hydrogen acceptor. No change in methylene blue could be detected by use of the Beckman DU spectrophotometer after subjecting the methylene blue at 1,000 atm for 30 min.

The following constituents were added into the male ground joint of the deoxygenating unit (figure 2): 0.5 ml of 1:1,000 (0.000267 M) methylene blue, 2 ml of M/50 substrate, 11.5 ml of M/15 phosphate buffer (pH 7.0). One ml of cell suspension was added to the female ground joint. This dexoygenating unit was assembled and attached to the horizontal arm of the stopcock (see vacuum pump assembly) by rubber tubing and the stopcock turned so that vacuum could be applied. After evacuation, the deoxygenating unit was flushed with gaseous nitrogen (all nitrogen used was first passed through a mixture of pyrogallic acid and NaOH solution) and re-evacuated. After the second evacuation the cells were mixed with the methylene blue-substrate-buffer mixture and nitrogen allowed to pass back into the deoxygenating unit. This unit was under slight nitrogen pressure to prevent the entrance of atmospheric oxygen. The syringe needle plug was removed and a syringe attached to the syringe needle. The re-

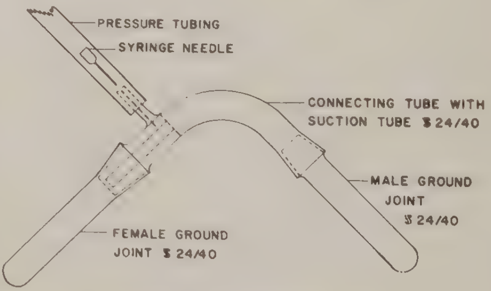
PRESSURE TUBING
SYRINGE NEEDLE
CONNECTING TUBE WITH SUCTION TUBE $ 24/40
MALE GROUND JOINT $ 24/40
FEMALE GROUND JOINT $ 24/40

Figure 2. Deoxygenating unit

TABLE 1

Micrograms of methylene blue reduced in the presence of malate by resting cells of Escherichia coli (0.5 ml, Klett turbidimetric reading of 250 employing a red filter) at various hydrostatic pressures

Reaction Time	1 Atm		200 Atm		600 Atm		1,000 Atm	
	Endogenous control, 26.7 C	With added malate, 26.8 C	Endogenous control, 27.5 C	With added malate, 27.5 C	Endogenous control, 27.5 C	With added malate, 27.2 C	Endogenous control, 27.2 C	With added malate, 27.6 C
min	*µg*	*µg*	*µg*	*µg*	*µg*	*µg*	*µg*	*µg*
0	0.0	0.0	0.0	0.0	0.0	0.0	0.0	0.0
3	0.4	2.7	0.3	2.5	0.2	1.5	1.5	2.2
6	0.7	8.7	0.9	6.7	0.4	6.3	3.1	4.2
9	1.8	12.6	2.5	12.0	1.2	12.1	3.8	5.6
12	1.9	16.0	2.7	16.5	2.2	15.8	5.6	7.5
15	2.2	20.5	2.9	20.1	5.0	20.5	6.7	8.6

action mixture was removed with the syringe and placed in the optical high pressure cylinder. The syringe and the optical high pressure cylinder were flushed with nitrogen before use. The optical high pressure cylinder was always kept under a nitrogen phase until the neutral piston was secured. The high pressure valve was attached to the optical high pressure cylinder and the entire unit connected to the hydrostatic pressure apparatus (ZoBell and Oppenheimer, 1950).

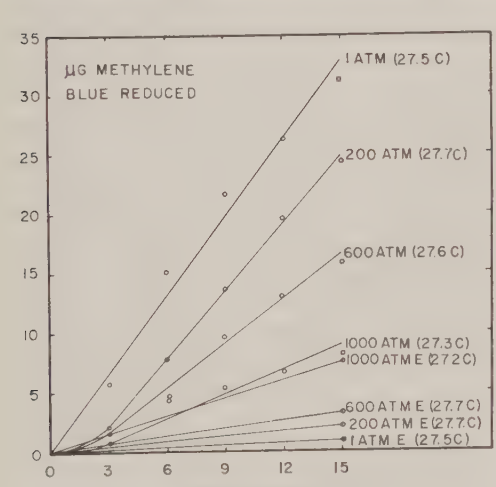

Figure 3. Micrograms of methylene blue reduced in the presence of succinate by resting cells by *Escherichia coli* (0.5 ml, Klett turbidimetric reading of 250 employing red filter) at various hydrostatic pressures.

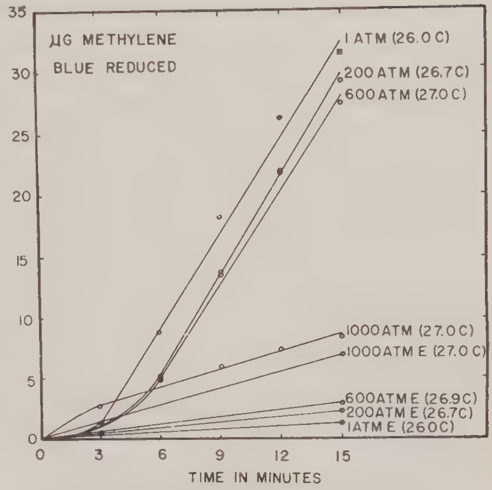

Figure 4. Micrograms of methylene blue reduced in the presence of formate by resting cells of *Escherichia coli* (0.5 ml, Klett turbidimetric reading of 250 employing a red filter) at various hydrostatic pressures.

All measurements of methylene blue reduction on the Beckman DU spectrophotometer were started exactly 5 min after the cells were mixed with the methylene blue-substrate-buffer mixture. The first reading (5 min after mixing) was considered time "zero" in table 1 and figures 3 and 4. The amount of methylene blue reduced at 3 min intervals was followed. By substracting the optical density reading at various time intervals from the initial optical density reading, the amount of methylene blue reduced could be determined.

The cell check (optical density of 0) for the Beckman DU spectrophotometer was made by employing the second optical high pressure cylinder filled with 7.5 ml of a solution: 1 ml cell suspension and 14 ml of phosphate buffer (pH 7.0).

RESULTS

Resting cells of *E. coli* show loss of succinic dehydrogenase activity during the period of applied hydrostatic pressure (figure 3). The amount of methylene blue reduced in 15 min, as well as the rate, decreased with increased hydrostatic pressure. At 1,000 atm the amount of methylene blue reduced in 15 min is just slightly more than

TABLE 2

Slope of the line of the methylene blue reduction for figures 3 and 4 and table 1. Corrected for endogenous methylene blue reduction

Atm	Malate*	Succinate†	Formate‡
1	1.27	1.93	2.67
200	1.26	1.70	2.60
600	1.20	1.00	2.43
1,000	0.17	0.04	0.01

* Slope calculated from data in table 1 for the 3 to 15 min period.

† Slope calculated from data in figure 3 for the 3 to 15 min period.

‡ Slope calculated from data in figure 4 for the 6 to 15 min period.

the 1,000 atm endogenous methylene blue reduction, which indicates very little succinic dehydrogenase activity. After correcting for the endogenous methylene blue reduction, the cells at 200 atm reduced about 0.75 times the amount of methylene blue in 15 min than cells at 1 atm. Cells at 600 atm reduced about 0.4 times the amount of methylene blue reduced by cells at 1 atm.

Room temperature was employed throughout these experiments. The observed temperatures of the optical high pressure optical cylinder were found to be between 27.2 C and 27.7 C for the data recorded in figure 3. This represents a temperature difference of 0.5 C. This temperature difference was not considered significant.

In determining the action of hydrostatic pressure on resting cells of *E. coli* when formate was employed as the substrate, it was noted that the amount of methylene blue reduced in 15 min decreased with increased pressure (figure 4). After correcting for the endogenous methylene blue reduction the cells at 200, 600, and 1,000 atm reduced about 0.83, 0.75, and 0.06 times the amount of methylene blue respectively as cells at 1 atm.

When malate was used as the substrate the amount of malate oxidized, as indicated by the methylene blue reduction, at 1, 200, and 600 atm is approximately equal (table 1). Again a large drop in the amount of methylene blue reduction is observed at 1,000 atm. The endogenous methylene blue reduction also increases with increasing pressure as noted in figures 3 and 4.

When the slopes of the line of the reaction rates at 1, 200, 600, and 1,000 atm on the oxidation of succinate, formate, and malate (as indicated by methylene blue reduction) were compared (table 2), it was noted that pressure applied does not affect each substrate in the same way. The differences in the slopes of the line at 1, 200, and 600 atm were small when malate was used as the substrate, increasing with formate and succinate respectively. In each case the slope of the line dropped drastically at 1,000 atm when compared to the increments of drop between other pressures.

The endogenous methylene blue reduction increased regularly with increasing pressure; at 1,000 atm a rate of 5 to 8 times the 1 atm value was observed.

DISCUSSION

The experimental data presented demonstrates the inactivation of formic, succinic, and malic dehydrogenase associated with the whole cells of *E. coli* during the period of compression. It is not known whether the effects of moderate hydrostatic pressure are direct or indirect. This problem still remains for further investigation.

The application of hydrostatic pressure does not appear to inhibit the action of the three dehydrogenases to the same degree (table 2). The slopes of the line for formic and malic dehydrogenase action at 1, 200, and 600 atm did not differ appreciably. On the other hand, the slope of the line for succinic dehydrogenase action decreased considerably between 1 and 200 atm, between 200 and 600 atm, and between 600 and 1,000 atm.

Borrowman (1950) observed that pressures up to 700 atm did not change the formic dehydrogenase activity of cells of *E. coli* which had been heated previously to 60 C for 5 min. Since heat was applied, the "biological whole" was not represented. Whether or not formic dehydrogenase associated with the "biological whole" is affected by hydrostatic pressure differently than crude or pure enzymes is not known. However, using cells of *E. coli* at 1,000 atm a great drop in the methylene blue reduction is observed. Borrowman's (1950) maximum pressure was 700 atm. Thus, a pressure of 1,000 atm nearly inactivated formic dehydrogenase as well as succinic and malic dehydrogenase (table 1 and figures 3 and 4). Since the "biological whole" was used in these experiments, it is not known how other protoplasmic factors (other enzymes, cell permeability, etc.) affect the action of the enzymes tested.

Endogenous methylene blue reduction increased with increased hydrostatic pressure. Since methylene blue did not appear to break down under a pressure of 1,000 atm, the donation of hydrogen to methylene blue probably comes about by the dehydrogenation of some unknown component(s) of the cell. It is too early to speculate what this component(s) might be.

The harmful effects of oxygen at high pressures are due to the oxidation of the —SH group (glutathione, coenzyme A, cysteine, —SH enzymes) (Barron, 1955). In these experiments precautions were taken to exclude atmospheric oxygen at all stages of the experiment.

ACKNOWLEDGMENTS

The author is indebted to Mr. James M. Snodgrass for aid in the development and construction of the optical high pressure cylinders, to Dr. Claude E. ZoBell for making space available in the laboratory at Scripps Institution, and to Dr. Galen E. Jones for his critical review of the manuscript.

SUMMARY

A method and apparatus for the measurement of dehydrogenase activity under various hydrostatic pressures has been described.

Employing resting cells of *Escherichia coli*, the rate of succinic, formic, and malic dehydrogenase activity decreased with increased hydrostatic pressure during a period of compression. Under the conditions of the experiment, the effect of hydrostatic pressure on the rate of succinic, formic, and malic dehydrogenase varied according to the applied pressure. The endogenous methylene blue reduction by the resting cells was found to increase with increased hydrostatic pressure.

REFERENCES

Barron, E. S. G. 1955 Oxidation of some oxidation-reduction systems by oxygen at high pressure. Arch. Biochem. and Biophys., **59,** 502–510.

Borrowman, S. R. 1950 Kinetics of the formic dehydrogenase system. Doctorate Dissertation, University of Utah.

Curl, A. L. and Jansen, E. F. 1950*a* Effect of high pressures on trypsin and chymotrypsin. J. Biol. Chem., **184,** 45–54.

Curl, A. L. and Jansen, E. F. 1950*b* Effect of high pressures on pepsin and chymotrypsinogen. J. Biol. Chem., **185,** 714–724.

Johnson, F. H., Eyring, J., and Polissar, M. J. 1954 *The kinetic basis of molecular biology.* John Wiley & Sons, Inc., New York.

Macheboeuf, M., Basset, J., and Levy, G. 1933 Influence des pressions très élévees sur les diastases. Ann. physiol. physicochim. biol., **9,** 713–722.

Matthews, F. E., Jr., Dow, R. B., and Anderson, A. K. 1940 The effects of high pressure on the activity of pepsin and rennin. J. Biol. Chem., **135,** 697–705.

Morita, R. Y. and ZoBell, C. E. 1956 Effect of hydrostatic pressure on the succinic dehydrogenase system in *Escherichia coli*. J. Bacteriol., **71,** 668–672.

Vignais, P., Barbu, E., Basset, J., and Macheboeuf, M. 1951 Modifications de l'état des acides ribonucléiques sous hautes pressions en presence ou en absence de nucléodepolymerase. Compt. rend., **232,** 2364–2366.

ZoBell, C. E. and Morita, R. Y. 1957 Deep sea bacteria. In *Galathea Reports*, 43 pp. Copenhagen.

ZoBell, C. E. and Oppenheimer, C. H. 1950 Some effects of hydrostatic pressure on the multiplication and morphology of marine bacteria. J. Bacteriol., **60,** 771–781.

Reproduced by permission of the
publishers, Williams and Wilkins Co.

Reprinted from THE JOURNAL OF PARASITOLOGY, August, 1957,
Vol. 43, No. 4, pages 470–473.
Reproduced by Permission

THE COPEPOD *CHONIOSPHAERA CANCRORUM* PARASITIZING A NEW HOST, THE GREEN CRAB *CARCINIDES MAENAS**

MARTIN W. JOHNSON
Scripps Institution of Oceanography of the University of California, La Jolla, California,
and The Marine Biological Laboratory, Woods Hole, Massachusetts

During recent years, the green crab, *Carcinides maenas* (L.) has greatly extended its range northward in the coastal waters of Maine where its enormous increase in numbers coupled with its habit of feeding upon young clams has been held responsible for an alarming reduction in the population of the soft-shell clam *Mya arenaria.* For this reason *Carcinides* has become the subject of detailed study by the Clam Investigations of the U. S. Fish and Wildlife Service in order to elucidate all aspects of its biology that may contribute to its control (Glude, 1955; Scattergood, 1952; Dow and Wallace, 1952).

As a part of this study, samples of green crab containing an unknown parasite inhabiting its egg masses were sent by Mr. Walter R. Welch, U. S. Fish and Wildlife Service, Boothbay Harbor, Maine, to Dr. Horace W. Stunkard at the Woods Hole Marine Biological Laboratory in July 1956. Here Dr. Stunkard kindly entrusted samples of the parasite to me for identification and study.

This parasite (Fig. 1) turned out to be a species of copepod which was described by C. J. Connolly in 1929 as a new genus and species, *Choniosphaera cancrorum* of the family Choniostomatidae. This family of crustacean parasites has received but a smattering of study on the American coasts. Aside from Connolly's paper the only other reports appear to be those of Blake (1929) in which 3 new species of the genus *Sphaeronella* are described, and of Paul Illg (in MacGinitie 1955) recording several specimens of *Choniostoma mirabile* Hansen from the shrimp *Eualus gaimardi* off Point Barrow, Alaska.

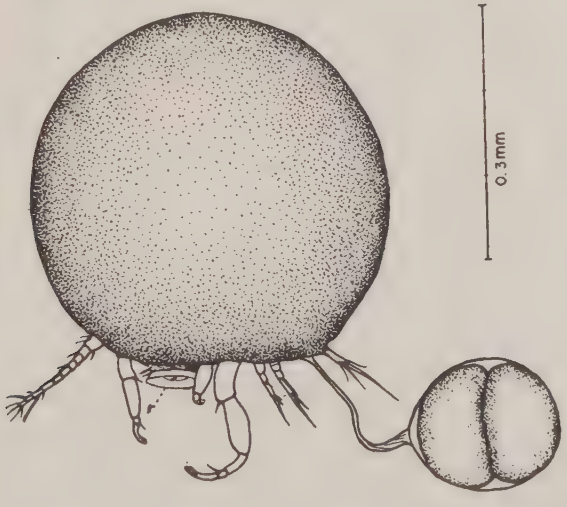

FIGURE 1. *Choniosphaera cancrorum.* Adult female with eggs. r, rostrum.

Received for publication February 28, 1957.

* Contribution from Scripps Institution of Oceanography New Series No. 928, and the Woods Hole Marine Biological Laboratory.

As the specific name indicates, Connolly found his species on the eggs of cancer crabs, *Cancer amoenus* Herbst, *Cancer irroratus* Say, and *Cancer borealis* Stimpson. He reports the species from St. Andrews, New Brunswick, and from Woods Hole, Massachusetts. Thus the specimens from Boothbay Harbor, Maine, fall well within the distributional range of the species.

Collections from the marsupium of the green crab

The finding of this same species of parasite on the eggs of the green crab, which belongs to a different family, is of some biological interest in view of Hansen's (1897) observation that several of the same species of Choniostomatidae may live on 2 or more host species of the same genus or of 2 closely related genera and "perhaps in exceptional cases they may be found on animals of different families."

The present specimens do not completely agree with the original descriptions given for *Choniosphaera cancrorum.* For example the caudal rami of the adult female, with 1 segment each (Fig. 2), are typical of copepods generally. Connolly states that the rami are 2-jointed. His figures and descriptions of the thoracic feet are incomplete but he infers that only the exopods are composed of 2 segments though his figures suggest also 2-segmented endopods. In the present material, the endopods possess 2 segments, a short first segment and a second longer segment (Figs. 3 and 4). Other minor differences occur in the spination of the thoracic legs.

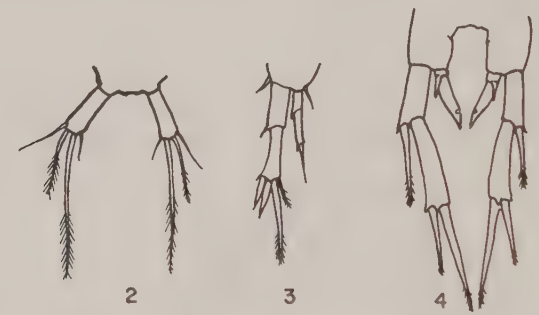

FIGURES 2, 3 and 4. *Choniosphaera cancrorum.* Adult female. (2.) caudal rami; (3.) first leg; (4.) second pair of legs.

In his "cyclops" stage he finds only 1 spine on the posterior lateral angles of the first urosome segment. In my specimens there are 2 spines as shown in Figure 5. It seems likely that all of these differences represent oversights or misinterpretations.

The adult females (Fig. 1) are spherical or subspherical in shape, range in size from 0.35 mm to 0.42 mm in length (evidently depending upon spawning condition) and rather closely resemble the eggs of the host crab in size and color. They were observed to be able to move freely about amongst the eggs and in this respect differ from the description which Wilson (1932, p. 493) gives for members of the Lernaeopodoida which includes the family Choniostomatidae. He says: "The female becomes a fixed parasite attached immovably to its host." In other respects *Choniosphaera cancrorum* appears to be less degenerate than other members of the suborder and also of the family Choniostomatidae (See Hansen 1897, 1923).

The adult female lays her eggs in small packets of 1 to 4 eggs each. These packets are attached to the genital area by a long slender cord. Many egg packets were also found scattered throughout the crab egg-mass where they are attached by shorter cords to the stalks of the crab eggs or to hairs of the swimmerets. A nauplius larva hatches from the egg.

In general appearance the nauplius is much like that of free-living copepods but differs greatly in details and, as already observed by Connolly, no well defined stages could be determined in its development (Figs. 6 and 7). The bases of the second antennae are not provided with masticatory hooks and the penultimate segment of the endopods bear 2 terminal setae (Connolly shows but 1) and a small lateral process or spur. A distinctive character of the larvae, but one difficult to observe in most specimens, is the presence of the funnel-like "rostrum" which is situated between the larval mandibular palps. This structure becomes a striking feature in the "cyclops" and adult stages when the mouth and mandibular blades can be observed within the membranous circle.

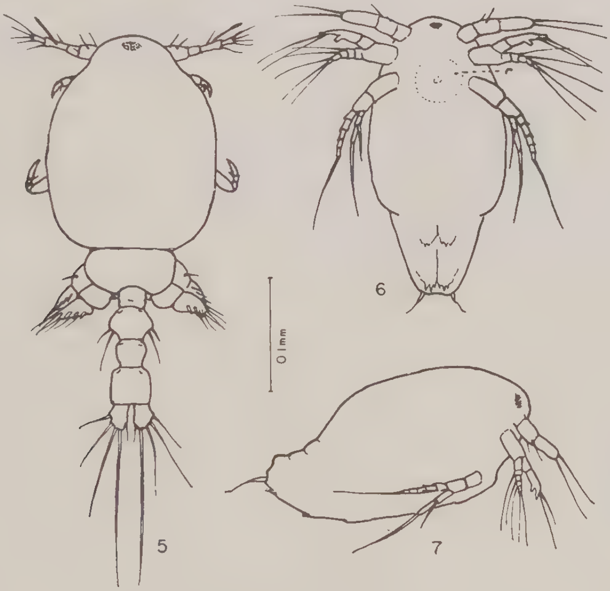

Figures 5, 6 and 7. *Choniosphaera cancrorum.* (5.) copepodid ("cyclops") stage; (6.) late nauplius stage, ventral; (7.) late nauplius stage, lateral. r, rostrum.

In addition to the adult female, numerous free-living nauplii and copepodid ("cyclops") stages were found in the marsupium of the crab. The male was not found.

The copepodid stage (Fig. 5) which metaporphoses from the nauplius is very active and probably represents the principal stage which spreads infection from host to host, though unattached eggs may also float into the water to hatch in the vicinity of uninfected crabs.

Glude (1955) introduces briefly the idea of green crab control through the agency of natural enemies. Such biological control might eventually stabilize the crab population in the new range to a level that will enable clam recruitment sufficient to support a moderate clam fishery. The effect of the present parasite as a natural control is not known and warrants further study in order to determine, if possible, whether or not the *Choniosphaera* attack on the green crab is indeed an adaptation coincident with the extension of *Carcinides* range. In the present study it has been possible to examine only a few crabs. Connolly's (1929) observations that the parasite occurs in the Woods Hole region on *Cancer amoenus* would lead one to believe that green crabs in that area might also be infected, but he makes no mention of having examined other crabs than *Cancer*.

BIBLIOGRAPHY

BLAKE, C. H. 1929 Crustacea. New crustacea from the Mount Desert Region. Biological Survey of the Mount Desert Region, Part 3: 3–34.

CONNOLLY, C. J. 1929 A new copepod parasite *Choniosphaera cancrorum*, gen. et sp. n., representing a new genus, and its larval development. Proc. Zool. Soc. London, Part 3: 415–427.

DOW, R. L. AND WALLACE, D. E. 1952 Observations on green crabs (*C. maenas*) in Maine. Maine Dept. Sea and Shore Fish., Fish Circular No. 8: 11–15.

GLUDE, J. B. 1955 The effects of temperature and predators on the abundance of the soft-shell clam, *Mya arenaria*, in New England. Trans. Amer. Fish. Soc. **84** (1954) : 13–26.

HANSEN, H. J. 1897 The Choniostomatidae. A family of Copepoda, parasites on Crustacea Malacostraca. Copenhagen. Andr. Fred. Høst and Son Pub., 205 pp.

——— 1923 Crustacea Copepoda. II. Copepoda parasita and hemiparasita. Danish Ingolf-Expedition, **3** (Part 7) : 1–92.

MACGINITIE, G. E. 1955 Distribution and ecology of the marine invertebrates of Point Barrow, Alaska. Smithsonian Misc. Coll. **128** (9), 201 pp.

SCATTERGOOD, L. W. 1952 The distribution of the green crab, *Carcinides maenas* (L.) in the Northwestern Atlantic. Maine Dept. Sea and Shore Fish., Fish. Circular No. 8: 2–10.

WILSON, C.B. 1932 The copepods of the Woods Hole Region, Massachusetts. United States National Museum. Bulletin 158, 635 pp.

Seismic-Refraction Studies of Eniwetok Atoll

By RUSSELL W. RAITT

Bikini and Nearby Atolls, Marshall Islands

GEOLOGICAL SURVEY PROFESSIONAL PAPER 260-S

A study of seismic-wave velocities
down to the Mohorovičić discontinuity

U.S. DEPARTMENT OF THE INTERIOR
March 3, 1849

UNITED STATES GOVERNMENT PRINTING OFFICE, WASHINGTON : 1957

UNITED STATES DEPARTMENT OF THE INTERIOR
FRED A. SEATON, *Secretary*

GEOLOGICAL SURVEY
Thomas B. Nolan, *Director*

For sale by the Superintendent of Documents, U. S. Government Printing Office
Washington 25, D. C. - Price 20 cents (paper cover)

(328)

CONTENTS

Page
Abstract 685
Introduction 685
Acknowledgments 685
Operating procedure 686
  Shore stations 687
  Reflection studies 687
  Lagoon survey 687
  Deep-sea survey 687
  Firing procedure 688
  Receiving equipment 688
Theory of interpretation of seismic-refraction observations 688
Travel-time plots 690
Accuracy of travel times 692
Velocities 694
Subsurface structure 695
  Reef structure 695
  First and second layers 695
  Third layer 696
  Fourth layer 696
  Fifth layer 697
  Sixth layer 697
Bibliography 698

ILLUSTRATIONS

Page
FIGURE 219. Location of shot lines and receiving stations 686
220. Model of subsurface structure assumed for interpretation of travel-time plots 689
221. Travel-time plots for section through stations A, B, C, D, E, K, and K′ 690
222. Travel-time plots for section northwest from station A 690
223. Travel-time plots for section through stations F, D, G, and L 691
224. Travel-time plots for section through station J 691
225. Travel-time plot of short profile across reef northwest of island of Elugelab 692
226. Travel-time plots for section through stations F, B, and A 692
227. Travel-time plots for section through stations E and G 693
228. Travel-time plots for section through stations M and I 693
229. Travel-time plots for shots received at station H 694
230. Oscillograms of ½-pound shots at short range and 80-pound shots at long range 694
231. Hypothetical subsurface section through Eniwetok Atoll from north to south 696
232. Hypothetical subsurface section through Eniwetok Atoll from west to east 697

BIKINI AND NEARBY ATOLLS, MARSHALL ISLANDS

SEISMIC-REFRACTION STUDIES OF ENIWETOK ATOLL

By Russell W. Raitt[1]

ABSTRACT

Observed seismic velocities at Eniwetok Atoll indicate the presence of 6 layers of rock, in which the average velocities are 2.44, 3.06, 4.15, 5.59, 6.90, and 8.09 kilometers per second, respectively. Previous drilling permits the identification of the first 2 layers as calcareous deposits and the third layer (4.15 kmps) as volcanic. The calculated depth of the third layer beneath the drilling sites was about 0.3 km greater than the depths at which volcanic rock was penetrated by the drill. This may be due to the fact that, in calculations, the vertical seismic velocities in the first 2 layers were assumed to be equal to the horizontal velocities measured in those layers, whereas the vertical velocities are probably less because of the presence of unconsolidated material between the cemented layers in the first 2 zones.

The fourth layer (5.59 kmps) is thought to be a hard crystalline rock, probably basalt. The fifth layer (6.90 kmps), identified with the crustal layer extensively present in the Pacific Ocean basin, is found at a depth of 9–10 km, and the sixth layer (8.09 kmps), characteristic of the layer just below the Mohorovičić discontinuity, is reached at a depth of 16–17 km.

INTRODUCTION

Seismic-refraction observations at Eniwetok Atoll in October and November 1952 had as their objective the delineation of the volcanic-rock layer immediately beneath the lagoon and the determination of the seismic-wave velocity as a function of depth down to the Mohorovičić discontinuity. Primary emphasis was placed on determining the seismic velocity in the layer of calcareous sediments forming the upper surface of the atoll and the configuration of the volcanic rock immediately beneath.

In planning the survey, the previous seismic-refraction studies at Bikini and Kwajalein (Dobrin, Perkins, and Snavely, 1949; Raitt, 1954) and the drilling at Eniwetok (Ladd, Ingerson, Townsend, and others, 1953) were very helpful. The Bikini studies indicated the form of the travel-time data to be expected. The drilling at Eniwetok reached a hard formation at a depth of 4,610 ft (1.41 km) beneath the island of Elugelab and 4,170 ft (1.27 km) beneath Parry Island. At Parry Island the hard formation was determined to be olivine basalt. This gave additional support to the identification of the 4-kmps (kilometers per second) layer at Bikini, found at an average depth of 4,300 ft (1.3 km), as volcanic rock and indicated that the structure at Eniwetok and Bikini is similar.

ACKNOWLEDGMENTS

This work was supported by the Office of Naval Research under Contract Nonr–233(05) and the Bureau of Ships under Contract NObsr–43356. Support from the Office of Naval Research was administered by J. W. Smith, who arranged for the delivery of the large quantities of explosives and other supplies needed in the investigation.

A seismic-refraction operation of the magnitude of the Eniwetok studies requires the cooperation of many people, whose help is gratefully acknowledged.

H. Kirk Stephenson of the Los Alamos Scientific Laboratory directed the project for that organization, and his active participation in the survey was an essential feature of its success. J. D. Isaacs was scientific leader, and Comdr. C. N. G. Hendrix was liaison officer for the Scripps Institution scientific group. Comdr. John Lofland, USN, and Comdr. Theodore Eunson, USN, arranged for the necessary shore installations, transportation, and ship facilities.

The officers and crews of U. S. S. *Lipan* (ATF *85*), R/V *Horizon*, and R/V *Spencer F. Baird* were of great help. Their commanding officers were Lt. R. M. Hughson, Noel L. Ferris, and Laurence E. Davis, respectively.

Members of the firing and recording groups were Joel H. Swartz, U. S. Geological Survey; Edwin M. Hamilton and Maxwell Silverman, U. S. Navy Electronics Laboratory; Chief Gunners Mate Daniel Howlett, USN; and Willard C. North, Daniel K. Gibson, Arthur D. Raff, Richard J. Smith, Alan C. Jones, Richard P. VonHerzen, and Winter D. Horton, Jr., Scripps Institution of Oceanography.

---

[1] Scripps Institution of Oceanography, University of California.

Note.—Contribution from Scripps Institution of Oceanography, New Series 929.

Reproduced by Permission

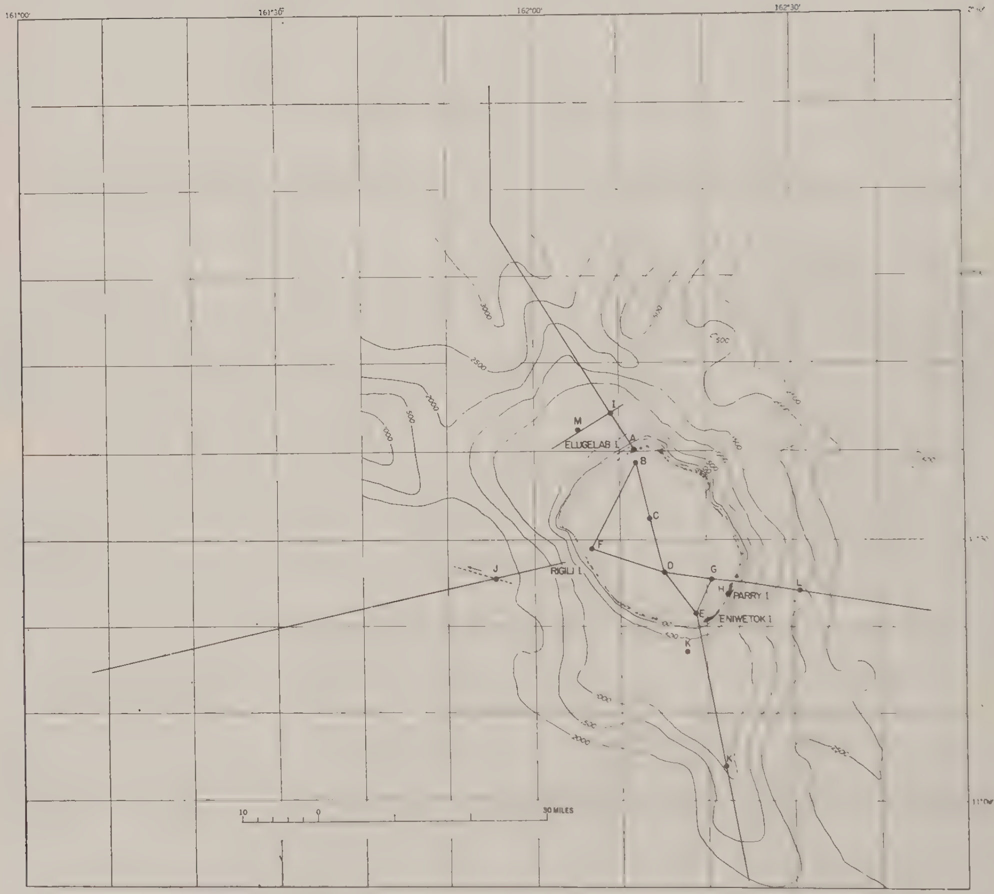

FIGURE 219.—Location of shot lines and receiving stations. Depth contours are in fathoms.

The author is indebted to Beauregard Perkins for suggestions made during his technical review of the paper.

OPERATING PROCEDURE

The plan of operation is shown in figure 219. The topography of the bottom surrounding the atoll was previously determined by K. O. Emery (Emery, Tracey, and Ladd, 1954). The letters represent receiving stations, and the heavy solid lines represent the lines along which shots were fired. The spacing of the stations and the directions of the lines in the lagoon were determined by the desired objective of optimum reversed control of the volcanic layer and by the necessity that the firing ship stay well clear of the coral shoals scattered throughout the lagoon. In extending the lines into deep water, advantage was taken of the two navigable passages on the southern and eastern sides.

Taken together, the lines of shots provide 2 sections across the atoll, 1 roughly north and south, and the other west and east. The north-south line, with eight stations, was laid out not only to obtain adequate data concerning the upper layers but also to extend the lines to maximum feasible range in the hope of achieving penetration to the Mohorovičić discontinuity beneath the atoll.

Three types of stations were occupied: shore stations, A and H, where portable equipment was set up in tents on Elugelab and on Parry Island; lagoon stations, B–G, at which the U. S. S. *Lipan* (ATF *85*), at anchor, served as receiving ship, using the same type of portable equipment used ashore; deep-sea stations, I–M, at which the Scripps Institution of Oceanography's R/V *Spencer F. Baird* served as receiving ship. The *Baird* was also used at lagoon station G for the line G–L. During this operation, and also while *Baird* was at K receiving shots fired on line D–E, the portable equipment from station A and the U. S. S. *Lipan* was used at station H.

SHORE STATIONS

In order to tie in the survey to the points at which drilling had determined the depth to volcanic rock (Ladd, Ingerson, Townsend, and others, 1953), receiving stations were occupied at the drill holes on the island of Elugelab and Parry Island. At Elugelab (station A) tests using conventional geophones at the surface were unsatisfactory owing to a high noise level. The signal-to-noise ratio of the refracted waves was much better for a hydrophone lowered into the drill hole. Consequently all shots used at station A were received on a hydrophone lowered to a depth of 250 ft in the test hole drilled on Elugelab. Shots received at this station were fired in the lagoon along the lines from F to B, and from B through C and D to E. Shot distance for these profiles was obtained with the help of a radio sonobuoy placed in the lagoon 800 yd from station A in about 10 fathoms depth. Shots outside the atoll were fired along a line bearing approximately 330° until well out from the base of the slope, thence bearing 0°. Shot distances for this line were obtained with the aid of a radio sonobuoy placed about 100 yd beyond the reef opposite station A.

A profile from station A to the edge of the outer reef was recorded to determine the differences, if any, between reef and lagoon structure, and to complete the short-range part of the profile extending northwestward to deep water. Shots were fired from a DUKW in water of about 4-foot depth normally covering most of the outer reef opposite Elugelab. The shot instant was transmitted by radio sonobuoy and the shot position was surveyed by taking sextant angles between known points near the Elugelab drill hole.

At Parry Island the noise level in the drill hole was higher than at Elugelab; hence the seismic waves were received on a hydrophone planted on the lagoon bottom (station H) about 500 yards from shore opposite the Parry Island drill hole. In this location, the noise level was much lower than in the drill hole. The depth was about 10 fathoms. At this station shots fired along lines D–E and G–L were recorded.

REFLECTION STUDIES

While setting up and testing the Elugelab shore station, about 2 days were spent attempting to obtain reflections from the volcanic rock, known from drilling (Ladd, Ingerson, Townsend, and others, 1953) to be at a depth of 4,610 feet at this point. Geophones and drill-hole hydrophones were used. Shots were fired at varying distances of as much as one-half mile from station A. Records of all shots showed irregular disturbances for several seconds following the first arrival, with no outstanding reflections identifiable with the volcanic rock or other subsurface interface.

Although these tests do not preclude the possibility that good reflections might be obtainable elsewhere, it was concluded that it would be inadvisable to plan a reflection survey when reflections were unobtainable at one of the principal control points.

LAGOON SURVEY

In the initial plans for the survey, the *Baird* was to serve as a receiving ship for all stations except the shore stations, and it was fitted out for this purpose. However, owing to a delay of about 2 weeks in the arrival of the *Baird*, the U. S. S. *Lipan* (ATF *85*) was used as a substitute. The receiving equipment, which consisted of the portable instruments from the Elugelab shore station, was more primitive than the multichannel installation on the *Baird*, but this was not a serious handicap to the lagoon survey as noise levels were generally low, and, except for the long profiles extending outside the lagoon to the south, the ranges were short.

At each receiving station, the receiving ship was carefully anchored with reference to gyrocompass bearings on the nearest island points. The receiving hydrophones were suspended at a depth of 75 ft and floated about 100 yd from the ship. Owing to the swinging of the ship at anchor, the hydrophone moved through a considerable arc, but the combined departure from the normal station positions shown in figure 219 due to this effect and to errors of position determination was probably no more than 200 yd. The firing ship similarly maintained position along the designated lines by gyrocompass bearings, and with the same probable departure. Distances between shot and hydrophone were obtained much more accurately than this by measurement of the travel time of the waterborne sounds; therefore the error in the ship's position would not affect the value of the depth calculation but would cause a maximum error of 200 yd in the location of the depth value.

DEEP-SEA SURVEY

Fortunately, the *Baird* arrived as the lagoon phase of the survey was completed. The deep-water survey could not have been carried out with the use of the *Lipan* as it had no deep-water echo sounder, which is essential for calculation of the water delay in deep-sea seismic-refraction work. The final deep-sea phase of the survey was completed with the *Baird*, and the portable station on the *Lipan* was moved to the Parry Island drill hole.

At deep-water stations I, M, J, K, K′, and L, anchoring was not practicable and the *Baird* either lay to or was underway slowly, attempting to maintain position. Throughout much of this phase the wind was high, frequently having a velocity of 17–21 knots, and the combined wind and current drift while lying to was between 2 and 3 knots. Attempts to maintain position by turning the screw slowly were only partially successful. Hence the positions shown are only rough estimates of the average position during the shot recordings. In most cases the *Baird* was probably within 1 nautical mile of the indicated position. An exception was the large drift during the shooting of the first part of profile J, indicated by a dashed line. During the shooting along the southwest end of this line, the *Baird* got underway and held position reasonably well. As stated above, these changes in position of the receiving ship affect only the location of the depth value. Seismic-refraction operations under these conditions, from the standpoint of noise level, firing conditions, and general operational difficulties, are marginal.

FIRING PROCEDURE

With the exception of a few experimental reflection shots and the short profile across the Elugelab reef (see Shore Stations), all shots were fired from the Scripps Institution of Oceanography's R/V *Horizon*, which proceeded along the courses indicated in figure 219 at speeds ranging from 6 to 11 knots. Shots were made up from tetrytol demolition blocks. The charges varied from one-half pound at distances less than 5 km from the receiving station to as much as 80 lb at the maximum range of 50–100 km. They were fired with slow-burning fuse ignited just before being dropped overside. The time of firing was recorded by picking up the direct blast on the *Horizon's* echo sounder and transmitting it by radio to the receiving ship, where it was recorded by the oscillograph used to record the seismic waves.

RECEIVING EQUIPMENT

The *Baird's* receiving equipment was very similar to that used in the Bikini survey (Raitt, 1954). Three hydrophones were suspended by their electrical cable from surface buoys to depths of 75 ft in the lagoon survey and 200 ft in the deep-sea survey. In the lagoon the very slow currents permitted the suspending cable to hang vertically and the hydrophone depth was very close to 75 ft. In the deep sea, however, the wind and current drift caused the suspension to assume a substantial angle with the vertical, and the average depth was therefore probably close to 120 ft. A multichannel oscillograph on the *Baird* recorded the outputs of the 3 hydrophones on 3 low-frequency (3–20 cycles per second) channels, on 3 intermediate-frequency channels (20–200 cps), and on 3 high-frequency channels (500–3,000 cps). All channels recorded at 2 levels of sensitivity of 20-decibel-level difference. Except at very short range the seismic waves through the earth were received only on the low-frequency channels. The higher frequencies were used to identify the waterborne waves, whose travel times were used to determine the shot distance.

Timing on the oscillograph was obtained by timing lines flashed every 1/100 second, with 1/10 seconds accented. The timing disk was driven by a fork-stabilized synchronous motor. The accuracy of the timing was controlled by frequent comparison with a break-circuit chronometer which was calibrated daily with time signals from radio station WWV.

A two-channel pen oscillograph was used at the portable station ashore and on the U. S. S. *Lipan*. One channel recorded the low-frequency seismic waves, the other performed the double function of recording the radio-transmitted firing signal and the high-frequency waterborne sound. Some records were made with 2 hydrophones, both recording the low-frequency waves but only 1 the high-frequency waves. The low noise levels and good signals obtained in the lagoon gave little additional advantage to the use of more than one hydrophone. However, in the deep-sea work the noise levels from rough sea conditions gave a real advantage to using three hydrophones, as was done on the *Baird*.

THEORY OF INTERPRETATION OF SEISMIC-REFRACTION OBSERVATIONS

Knowledge of the earth's interior is yielded both by travel times of sound waves and by the intensity and spectra of the waves. However, travel times are more tractable in analysis and more easily measured. In the present study, as in most seismic interpretations, the travel times form the sole basis for the interpretation of the subsurface structure.

The specific methods used in the interpretation were the same as those used by the author in the Bikini survey (see Raitt, 1954); the formulas and diagrams are repeated here for reference.

Figure 220 illustrates a subsurface section consisting of three layers in which the seismic velocities are c_0, c_1, and c_2. In seismic work at sea the upper layer is water. For the example illustrated, the velocities c_1

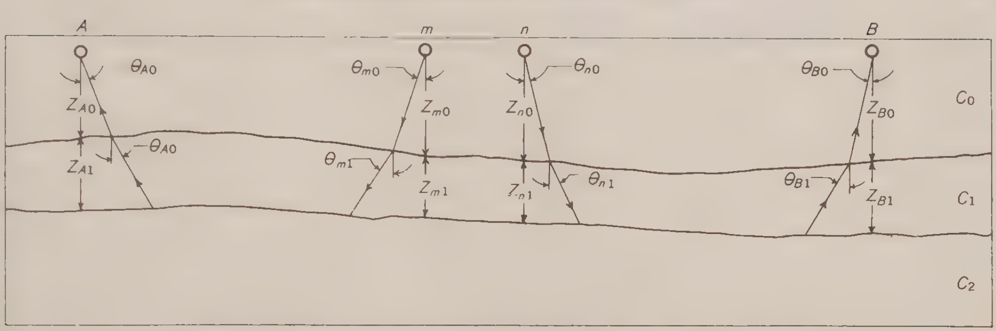

FIGURE 220.—Model of subsurface structure assumed for interpretation of travel-time plots.

and c_2 are 2 and 4 times as great, respectively, as c_0, the velocity in water. Points *A* and *B* represent receiving stations and *m* and *n* represent shot points. The sound rays shown are critically refracted through the third layer. The symbols for the various angles and the thicknesses of the layers, used in the calculations, are illustrated in the figure.

The travel time, T_{Am}, for a sound pulse to travel from *m* to *a* is

$$T_{Am}=\frac{X_{Am}}{c_2}+\frac{z_{A0}\cos\theta_{A0}}{c_0}+\frac{z_{m0}\cos\theta_{m0}}{c_0}+\frac{z_{A1}\cos\theta_{A1}}{c_1}+\frac{z_{m1}\cos\theta_{m1}}{c_1} \qquad (1)$$

and the travel time, T_{Bn}, for the pulse to travel from *n* to *B* is

$$T_{Bn}=\frac{X_{Bn}}{c_2}+\frac{z_{B0}\cos\theta_{B0}}{c_0}+\frac{z_{n0}\cos\theta_{n0}}{c_0}+\frac{z_{B1}\cos\theta_{B1}}{c_1}+\frac{z_{n1}\cos\theta_{n1}}{c_1}, \qquad (2)$$

where X_{Am} and X_{Bn} are the horizontal distances between shots and hydrophones.

In equation 1 the term $\left(T_{Am}-\frac{X_{Am}}{c_2}\right)$ is called the intercept time (Gardner, 1939). The four remaining terms of equation 1 are called delay times and are designated τ_{A0}, τ_{m0}, τ_{A1}, and τ_{m1}, respectively.

If the delay times for the water layer are subtracted from the total travel times, the corrected travel times are

$$T'_{Am}=\frac{X_{Am}}{c_2}+\tau_{A1}+\tau_{m1} \qquad (3a)$$

and

$$T'_{Bn}=\frac{X_{Bn}}{c_2}+\tau_{B1}+\tau_{n1}. \qquad (3b)$$

For gently sloping structures the seismic velocity in the third zone is, to a sufficient degree of approximation,

$$c_2=\frac{2}{\frac{dT'_{Am}}{dX_{Am}}+\frac{dT'_{Bn}}{dX_{Bn}}}. \qquad (4)$$

If the contact between the second and third layers is nearly horizontal and if shots *m* and *n* are fired at the same point *m*, τ_{m1} and τ_{n1} may be considered equal to a first approximation; and if a third shot is fired at point *A* and the resulting pulse is critically refracted through zone C_2 and recorded as a first arrival at point *B*, then the delay times at *A*, *m*, and *B* are determined by the three measured intercept times,

$$T'_{Am}-\frac{X_{Am}}{c_2}=\tau_{A1}+\tau_{m1}, \qquad (5a)$$

$$T'_{Bn}-\frac{X_{Bn}}{c_2}=\tau_{B1}+\tau_{m1}, \qquad (5b)$$

and

$$T'_{AB}-\frac{X_{AB}}{c_2}=\tau_{A1}+\tau_{B1}. \qquad (5c)$$

The values of τ_{A1}, τ_{m1}, and τ_{B1} may be derived by solving equations 5a–c simultaneously. The thicknesses of the second layer beneath points *A*, *m*, and *B* to a first approximation are

$$z_{A1}=\frac{c_1\tau_{A1}}{\sqrt{1-\left(\frac{c_1}{c_2}\right)^2}}, \qquad (6a)$$

$$z_{m1}=\frac{c_1\tau_{m1}}{\sqrt{1-\left(\frac{c_1}{c_2}\right)^2}}, \qquad (6b)$$

and

$$z_{B1}=\frac{c_1\tau_{B1}}{\sqrt{1-\left(\frac{c_1}{c_2}\right)^2}}. \qquad (6c)$$

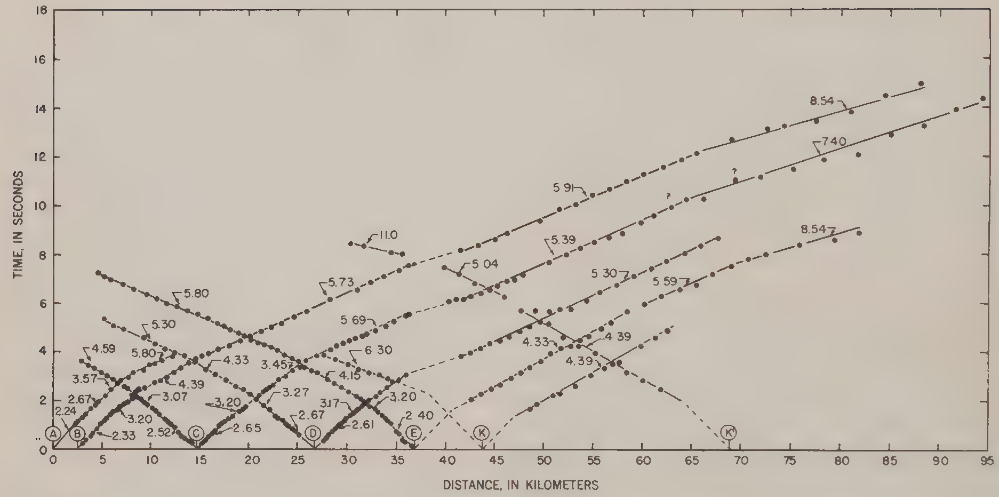

FIGURE 221.—Travel-time plots for section through stations A, B, C, D, E, K, and K'. Times are corrected for water delay; apparent velocities are in kilometers per second.

The process here outlined can, in principle, be repeated indefinitely for deeper horizons of successively higher speeds of transmission. The practical difficulties and cumulative errors become severe if the number of layers with small velocity contrasts is large.

TRAVEL-TIME PLOTS

The observed travel times of the bottom-refracted waves, corrected for water delay, are plotted in figures 221 to 229. In order to facilitate comparison of profiles, they are plotted together in related groups. For example, figure 221 contains all shots received at stations A, B, C, D, E, K, and K', fired along the lines that pass through each of these stations. For each time-distance graph the distance of each shot point from the corresponding receiving station is accurately plotted. Since the receiving station was fixed and the shot point varied for each profile, the zero point for each graph represents the true distance of the receiving station from the traverse reference station shown at zero distance (for

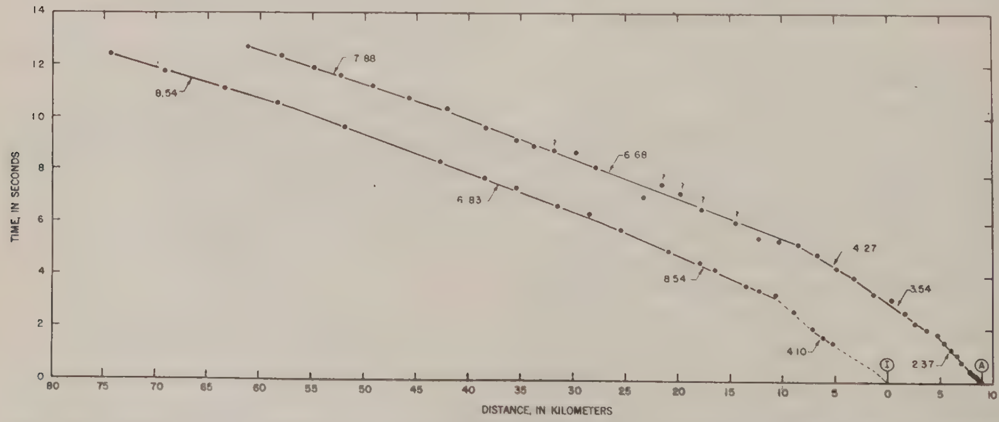

FIGURE 222.—Travel-time plots for section northwest from station A. Times are corrected for water delay; apparent velocities are in kilometers per second.

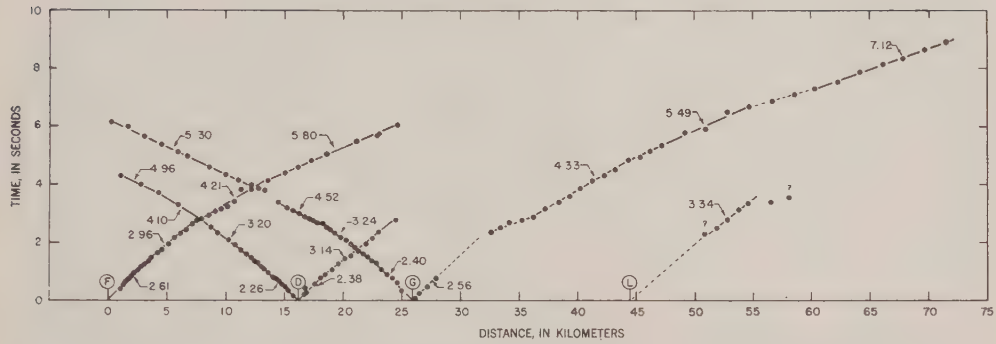

FIGURE 223.—Travel-time plots for section through stations F, D, G, and L. Times are corrected for water delay; apparent velocities are in kilometers per second.

example, from station A in figure 221). Because the receiving stations are generally not on a straight line, the distances from the shot points to stations other than the receiving station or between stations other than the reference station are only approximate in the graph.

It can be seen that most of the travel-time plots can be represented roughly by segments of straight lines. The lines drawn on the plots have been fitted by inspection, and the corresponding apparent velocity for each segment is indicated in kilometers per second (kmps). Just as in the Bikini survey, the data require at least six velocity groups or layers to represent the range of values. These are, roughly, 2.5, 3, 4, 5.5, 7, and 8 kmps.

One significant difference from the Bikini lagoon profiles is the greater prominence at Eniwetok of the 3-kmps layer, which was observed on so few profiles at Bikini that its existence throughout the lagoon was hypothetical. At Eniwetok, however, it is observed on every lagoon profile. This yields information about the structure of the calcareous deposits, but unfortunately it masks part of the important 4-kmps segment and increases the distance between the shot and the receiver at which this velocity is first observed. Hence, the segments representing the layer believed to be the upper part of the volcanic rock are short and the degree of reversed control is considerably less than expected. In order to obtain the maximum information about this layer, and to increase the accuracy of the determination of velocities from the short segments in the first 15 km of profile, the number of shots at short range was increased significantly above that used in the Bikini survey.

Gaps in the profiles, indicated by dashed lines, resulted from two causes: in sections E–K in figure 221

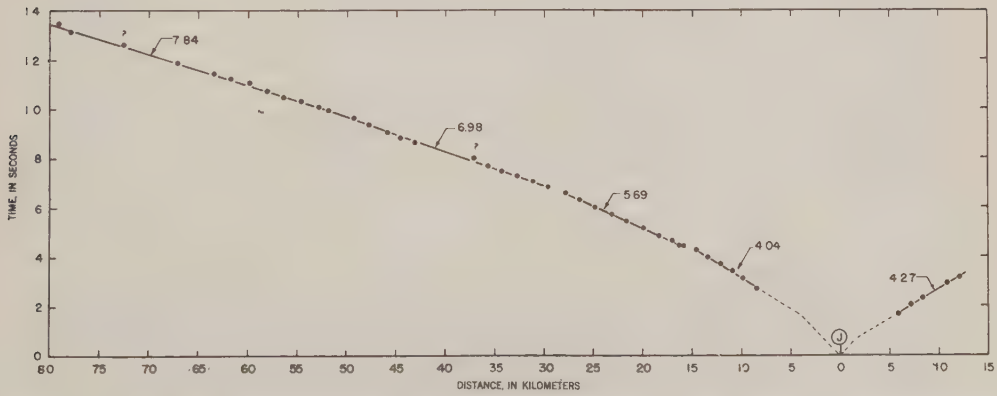

FIGURE 224.—Travel-time plots for section through station J. Times are corrected for water delay; apparent velocities are in kilometers per second.

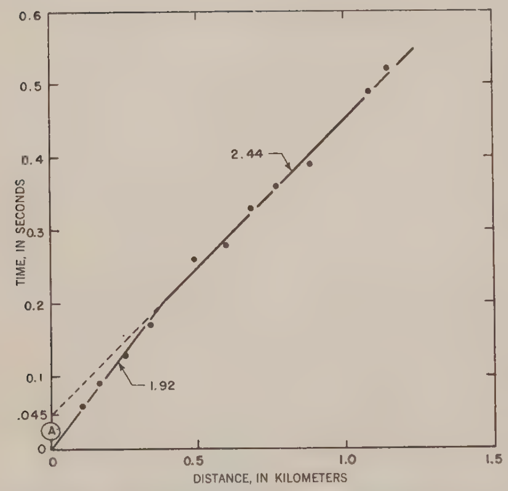

FIGURE 225.—Travel-time plot of short profile across reef northwest of Elugelab. The plotted distance is the direct distance $\sqrt{\Delta^2+0.076^2}$, where Δ is the horizontal distance and the hydrophone depth is 0.076 km.

and G–L in figure 223 the lines crossed areas where underwater shots were prohibited because of the risk of damage to or interference with undersea installations, and the short-range first arrivals at the deep-water stations were masked by bottom echoes and direct water waves. The gaps due to the first cause were not serious, but the loss of the short-range information in the deep-water stations made it impossible to determine the velocity in sediments outside the lagoon.

ACCURACY OF TRAVEL TIMES

At short ranges the first-arriving elastic pulse is sharply defined and its arrival time can be measured with little difficulty to 0.01 second (see fig. 230).

At greater ranges the pulse decreases in amplitude, and the initial pressure pulse is frequently masked by the background noise. This phenomenon is illustrated by figure 230*A*, which shows the initial part of the pulses produced by the first four ½-pound shots south of station B. In the uppermost record, at the shortest range, the beginning is sharp and unquestionable. In the lowest record the beginning is barely detectable and was estimated by comparison with the preceding

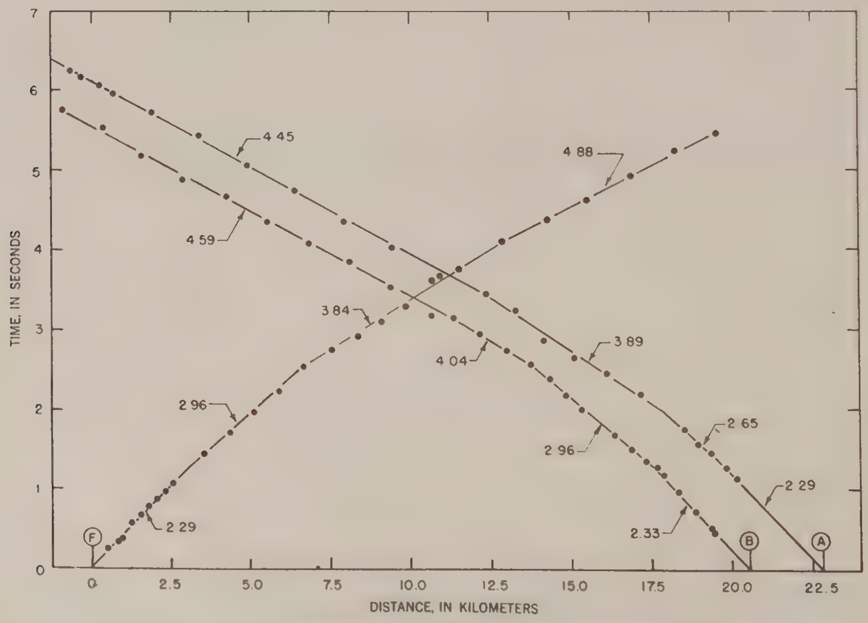

FIGURE 226.—Travel-time plots for section through stations F, B, and A. Times are corrected for water delay; apparent velocities are in kilometers per second.

records and with other comparable records to be 0.08 second ahead of the first negative swing.

This procedure of comparing records has been followed throughout the survey. The beginnings have been chosen by lining up groups of adjacent records on significant similar features and picking the beginnings with reference to the records which show the most conspicuous onsets. An example of this procedure for distant shots is shown by figure 230*B*, the record of three 80-pound shots at the end of the profile that extends south from station C for a distance of about 80 kilometers. Where similarity of form of the first wave is maintained for a considerable distance, this method of picking the beginning of the pulse yields an accurate slope of the travel-time curve, even though the arrival time may be questionable.

An ever-present potential source of error is the possibility that the true beginning wave group is too weak to observe and that the observed wave has taken a longer path but arrived with much greater intensity. This is particularly likely to occur in as complicated a structure as Eniwetok, where there are many possible paths for the waves to travel, and there is a good possibility that the initial ones frequently are much weaker than late arrivals. This possibility is greatest at greatest range, where even the strongest signals are weak. Hence, all of the sources of error tend to increase with range. The error in picking the beginning of the first observed wave is roughly $0.02\Delta^{1/2}$ second, where Δ is the range in kilometers. Failure to observe a weak first arrival can be reduced by multiple profiles like section A–K′ at Eniwetok, but there is no satisfactory way of estimating the expected error from this cause.

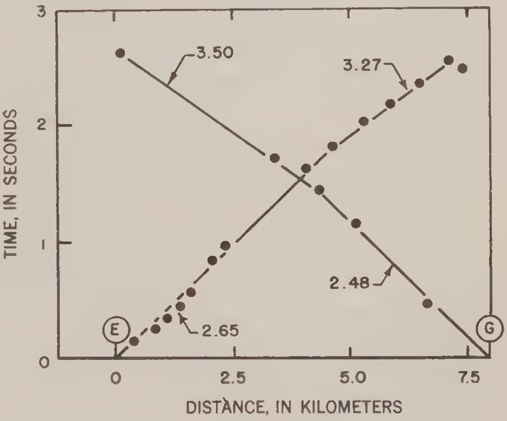

FIGURE 227.—Travel-time plots for section through stations E and G. Times are corrected for water delay; apparent velocities are in kilometers per second.

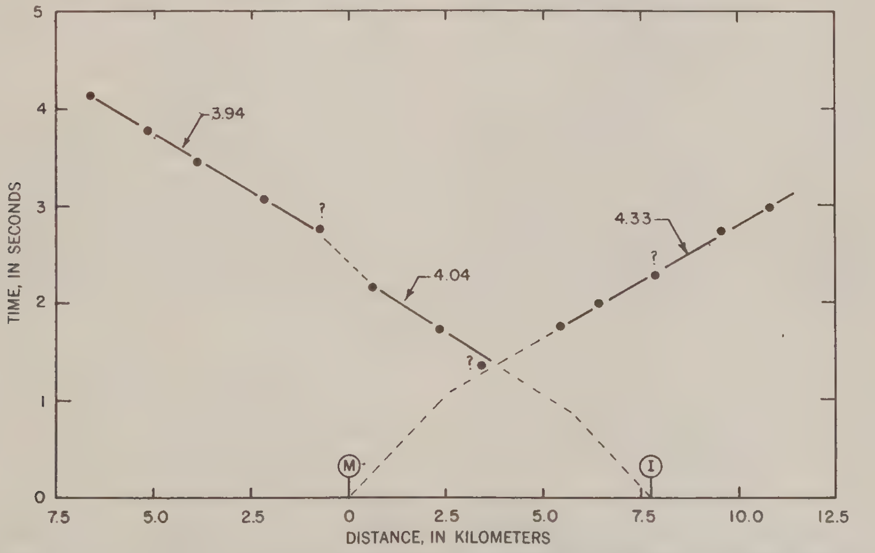

FIGURE 228.—Travel-time plots for section through stations M and I. Times are corrected for water delay; apparent velocities are in kilometers per second.

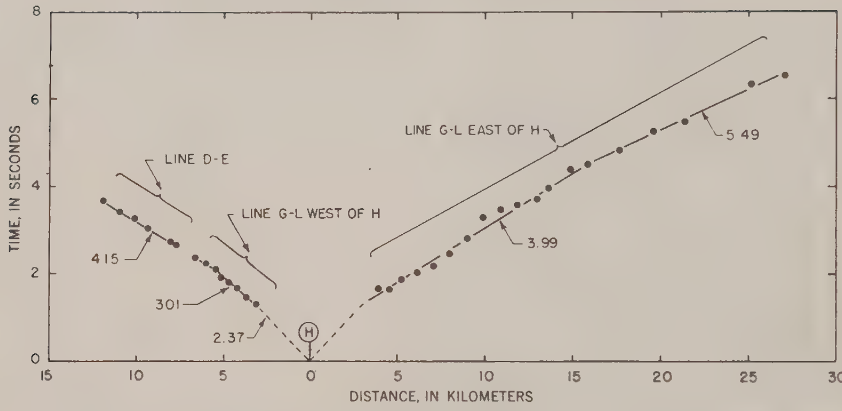

Figure 229.—Travel-time plots for shots received at station H. Times are corrected for water delay; apparent velocities are in kilometers per second.

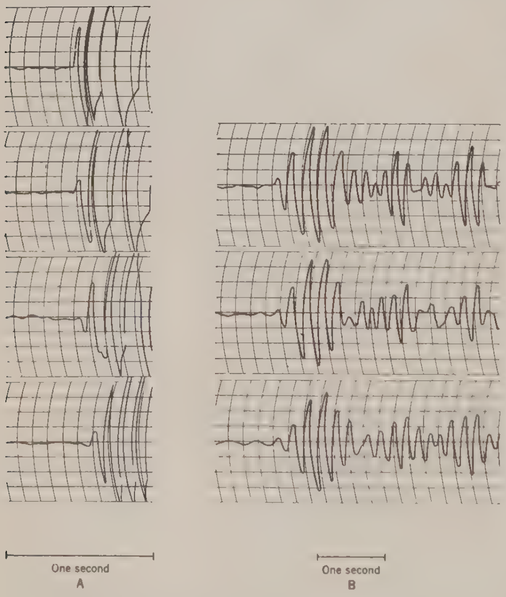

Figure 230.—Oscillograms of (*A*) the first four ½-pound shots south of point B and (*B*) three 80-pound shots at the outer end of the profile extending 80 km south of point C.

VELOCITIES

Even though many parts of the shooting lines were traversed by the firing ship as much as 5 and 6 times, it is apparent that the distance over any one layer in which true reversed control was established is very small. Consequently no attempt was made to determine true velocities for specific areas as was done at Bikini, where the reversed control of the third layer was better than at Eniwetok. Instead, velocities for each layer were averaged for the entire survey and a single velocity value, used for the entire area of the survey, was determined for each layer.

In making the averages it was assumed that the variations in apparent velocity were due primarily to irregularities in the thickness of the overburden rather than to changes in true velocity. Hence, following the procedure of equation 4, the harmonic mean of the apparent velocities is taken as the best measure of velocity in the formation. Not all of the data are equally suitable for this average. Some of the first arrivals are of poor quality, water delays may be of doubtful accuracy because of rough bottom topography, and drift of the receiving ship over a sloping bottom may give a spurious slope to the time-distance curve. The velocity segments that have been used in the averages are listed in the following table.

Station	Profile direction	Apparent velocity (kmps)	Station	Profile direction	Apparent velocity (kmps)
		First Layer			
A	NW	2.37	E	NW	2.40
	SW	2.29		NE	2.65
	S	2.24	G	SW	2.48
B	SW	2.33		W	2.40
	S	2.33		E	2.56
C	N	2.52	F	NE	2.29
	S	2.65		E	2.61
D	N	2.67			
	SE	2.61	Harmonic mean velocity		2.44
	W	2.56			
	E	2.38			

Station	Profile direction	Apparent velocity (kmps)	Station	Profile direction	Apparent velocity (kmps)
Second layer					
A	SW	2.65	E	SW	3.20
	S	2.67		NE	3.27
B	SW	2.96	G	W	3.24
	S	3.20	F	NE	2.96
C	N	3.07		SE	2.96
	S	3.20	H	NW	3.01
D	N	3.27			
	SE	3.17	Harmonic mean velocity		3.06
	W	3.20			
	E	3.14			
Third layer					
A	SW	3.89	F	SE	4.21
B	SW	4.04	I	NW	4.10
	S	4.39		W	3.94
C	N	4.59	M	E	4.33
	S	3.45	J	W	4.04
D	N	4.33	K	S	4.39
	W	4.10	K′	N	4.39
E	NW	4.15	H	W	4.15
	S	4.33			
G	W	4.52	Harmonic mean velocity		4.15
F	NE	5.84			
Fourth layer					
B	S	5.73	G	W	5.30
	S	5.91	F	SE	5.80
C	S	5.69	J	W	5.69
	S	5.39			
D	N	5.30	Harmonic mean velocity		5.59
	SE	5.30			
E	NW	5.80			
Fifth layer					
A	NW	6.68	J	W	6.98
G	E	7.12			
I	NW	6.83	Harmonic mean velocity		6.90
Sixth layer					
A	NW	7.88	J	W	7.84
I	NW	8.54	Harmonic mean velocity		8.09

SUBSURFACE STRUCTURE

Following the foregoing principles of theoretical interpretation, depths to the interfaces between the 6 principal layers have been estimated for the 2 north-south and east-west sections across the atoll and plotted in figures 231 and 232.

In these figures hachured interfaces indicate that the refracted waves from shots fired above that part of the interface have been received with a velocity corresponding to the layer immediately below. The dashed interfaces are extrapolations and interpolations from the areas of direct observations. The necessity of making these assumptions in order to calculate depths to deeper layers is one of the principal sources of error, for an error in estimating these dashed interfaces will be reflected in an error in the hachured interfaces beneath them. Because of the preponderance of dashed interfaces on the flanks of the atoll and in the deeper layers, the structure in these areas is necessarily schematic and the error can be large. For the shallow layers beneath the lagoon, the concentration of observations gives more complete control and more accurate detail.

REEF STRUCTURE

The detailed profile (fig. 225) across the reef northwest of Elugelab indicates the presence of a thin, low-velocity layer on the reef surface in which the seismic velocity is 1.92 kmps. The thickness of this layer is calculated to be 108 m, which puts the depth of its base about 50 or 60 m below the average depth of the lagoon. It is of interest to note that this depth is of a reasonable order of magnitude for a previous glacial lowering of sea level (Daly, 1910). It is nearly the same as the depth of the volcanic basement beneath Bermuda (Officer, Ewing, and Wuenschel, 1952), at 60 to 100 m, believed to have been eroded to sea level during the Pleistocene epoch. The lower seismic velocity in the material deposited since that time may be a result of relatively rapid deposition, or it may merely indicate that the relatively cavernous structure of the outer reef results in a lower seismic velocity than in the lagoon deposits. The properties of this low-velocity layer are similar to the layer indicated in the first survey of Bikini (Dobrin, 1950) at receiving stations on the periphery of the lagoon.

FIRST AND SECOND LAYERS

The first and second layers are considered together because drilling has shown that beneath the atoll they represent calcareous deposits formed by reef and lagoon organisms (Ladd, Ingerson, Townsend, and others, 1953). Velocities of 2.44 and 3.06 kmps, respectively, in these layers are characteristic of partly consolidated sediments.

The first layer is probably composed of material very similar to that now forming the lagoon floor. Although the short-range travel times show irregularities indicating inhomogeneity, there is no consistent tendency for the time-distance curve to have a positive intercept when projected to the time axis, which would be expected if there were a lower velocity layer above the first zone mapped. The observed irregularity in the arrival times of the pulses reduces the possibility of detecting a thin overlying layer, and it is possible that a layer of 2 kmps velocity and 50 m thickness, for example, would not be observed.

The thickness of the first layer decreases regularly from about 600 m at the edge of the atoll to about 200–300 m in the center. The discontinuity at its base is not definitely established, since the observations could also be explained by a moderately rapid increase of velocity with depth in the upper few hundred meters

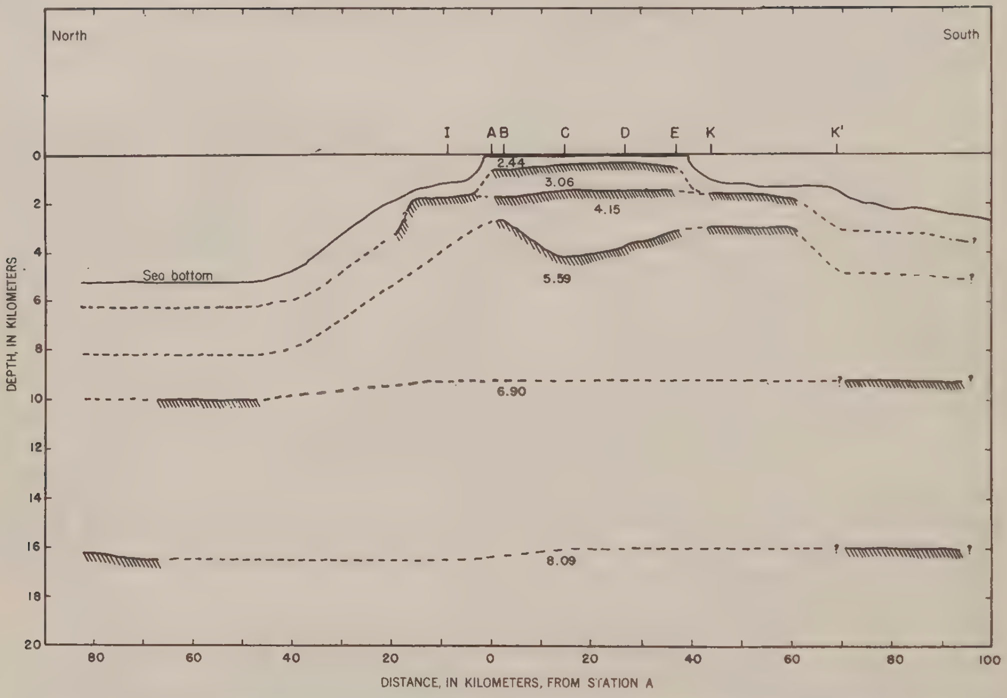

Figure 231.—Hypothetical subsurface section through Eniwetok Atoll from north to south. Velocities are in kilometers per second.

due to compaction caused by pressure of the overlying material.

The second layer is about 1 km thick. The irregular variation in thickness indicated by the time-distance graphs is probably no greater than the experimental error in reading arrival times and calculating the water delay. There is no systematic change of thickness toward the center of the lagoon. In calculating the structure outside the lagoon, the second layer was assumed to be absent since no direct evidence of its presence was obtainable.

THIRD LAYER

The third layer (4.15 kmps) is found at all points of the seismic survey to be deeper than the points at which it was penetrated by the drilling that identified it as volcanic rock (Ladd, Ingerson, Townsend, and others, 1953). It is difficult to explain why the seismic observations show this layer to be deeper than was determined by drilling. It is possible that the horizontal velocity in the first and second layers may be greater than the vertical velocity, owing to the presence of thin layers of consolidated material in which the velocity is higher. For example, if the second layer consists of 2 strata, an upper, thin stratum of hard rock in which the seismic velocity is 3.06 kmps and a lower, thick stratum in which the seismic velocity is about 2.44 kmps, the average vertical velocity would be such that the calculated depth to the third layer would be in agreement with the drilling results. Also, the upper part of the volcanic formation may be highly fractured or vesicular. Its average compressibility could be quite high, hence the velocity in it could be low even though the drilling was very hard through individual blocks. The velocity in such a formation might be little greater than the 3.06 kmps in the second layer and would be masked by it.

FOURTH LAYER

A seismic velocity of 5.59 kmps, the velocity in the fourth layer, is characteristic of a hard crystalline rock. It is in close agreement with one of the few values, 5.6 kmps, identified with basalt in the literature (Brock-

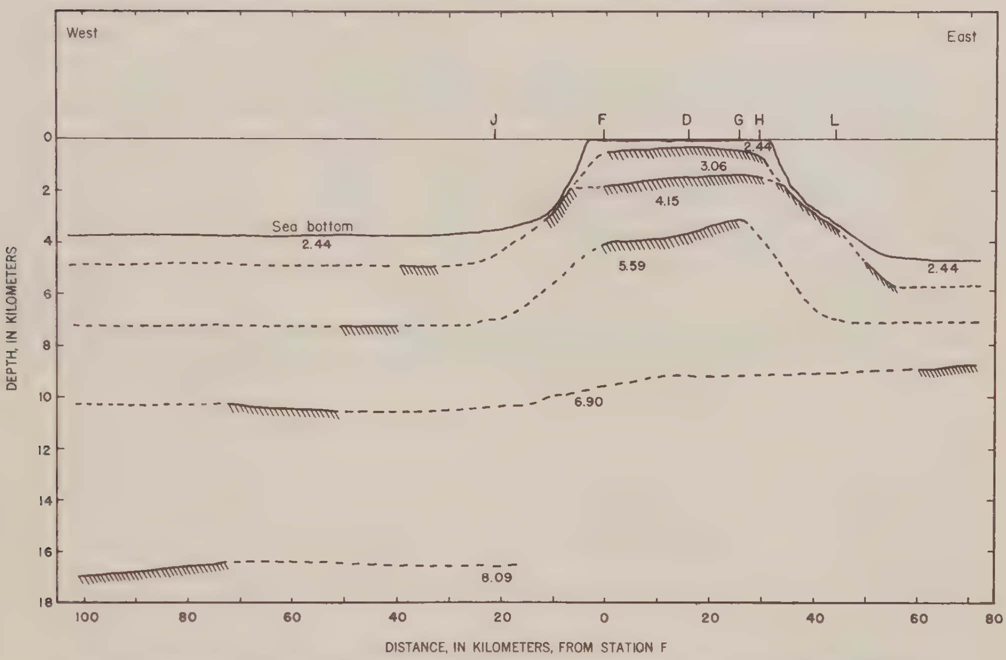

FIGURE 232.—Hypothetical subsurface section through Eniwetok Atoll from west to east. Velocities are in kilometers per second.

amp and Wölcken, 1929). The plotted interface between the third and fourth layers does not necessarily indicate a structural or lithologic discontinuity. It merely indicates the approximate depth at which a velocity of 5.59 kmps is reached. It is possible that the fourth layer is largely plutonic rock intruded from below, while the third layer is mostly extruded. On the other hand, it may all have been extruded. The higher velocity in the fourth layer could then be attributed to compaction or consolidation produced by the pressure of the rocks above.

FIFTH LAYER

The velocity of 6.90 kmps in the fifth layer identifies it with the crustal layer in the Pacific basin (Raitt, 1956) which has a velocity between 6.5 and 7.0 kmps. This is higher than field measurements of velocities in known rocks, and it may represent a rock type never observed at the earth's surface. Current petrologic doctrine indicates that it represents a dense basic rock, probably olivine basalt. Its depth below sea level, 9–10 km, is greater than the 7- to 9-km depth at Bikini (Raitt, 1954), and substantially greater than the 5- to 8-km depth considered to be characteristic of the Pacific basin.

Because it was observed at only a few places, its depth can only be roughly indicated, and practically nothing has been learned about the form of its surface. At the southern end of profile A–K′ (see fig. 221) the great irregularity of the points, owing to subsurface anomalies of unknown character, made it uncertain as to whether the pulses received had been refracted through the 6.90 kmps or the 8.09-kmps layer. The depths are therefore questionable, although consistent with those obtained on other profiles.

SIXTH LAYER

The velocity of 8.09 kmps in the sixth layer is characteristic of the velocity found at the base of the earth's crust below the Mohorovičić discontinuity. Its depth, 16–17 km, is greater than at Bikini (13 km). This is due primarily to the great depth of the fifth layer, whose thickness, about 6.5 km, is not much greater than that observed at Bikini or generally throughout the Pacific basin.

BIBLIOGRAPHY

Birch, Francis (editor), 1942, Handbook of physical constants: Geol. Soc. America Special Paper 36, 325 p.

Brockamp, B., and Wölcken, K., 1929, Bemerkungen zu den Beobachtungen bei Steinbruchsprengungen: Zeitschr. Geophysik, v. 5, p. 163–171.

Daly, R. A., 1910, Pleistocene glaciation and the coral reef problem: Am. Jour. Sci., 4th ser., v. 30, p. 297–308.

Dobrin, M. B., 1950, Submarine geology of Bikini lagoon as indicated by dispersion of water-borne explosion waves: Geol. Soc. America Bull., v. 61, p. 1091–1118.

Dobrin, M. B., Perkins, Beauregard, Jr., and Snavely, B. L., 1949, Subsurface constitution of Bikini Atoll as indicated by a seismic refraction survey: Geol. Soc. America Bull., v. 60, p. 807–828.

Emery, K. O., Tracey, J. I., Jr., and Ladd, H. S., 1954, Geology of Bikini and nearby atolls, Marshall Islands: U. S. Geol. Survey Prof. Paper 260–A, 265 p.

Gardner, L. W., 1939, An areal plan of mapping subsurface structure by refraction shooting: Geophysics, v. 4, p. 247–259.

Heiland, C. A., 1940, Geophysical exploration: New York, Prentice-Hall, Inc.

Ladd, H. S., Ingerson, Earl, Townsend, R. C., and others, 1953, Drilling on Eniwetok Atoll, Marshall Islands: Am. Assoc. Petroleum Geologists Bull., v. 37, p. 2257–2280.

Nettleton, L. L., 1940, Geophysical prospecting for oil: New York, McGraw-Hill Book Co., Inc.

Officer, C. B., Ewing, Maurice, and Wuenschel, P. C., 1952, Seismic refraction measurements in the Atlantic Ocean—Part 4, Bermuda, Bermuda Rise, and Nares Basin: Geol. Soc. America Bull., v. 63, p. 777–808.

Raitt, R. W., 1954, Seismic-refraction studies of Bikini and Kwajalein Atolls: U. S. Geol. Survey Prof. Paper 260–K, p. 506–527.

——— 1956, Seismic-refraction studies of the Pacific Ocean basin—Part 1, Crustal thickness of the central equatorial Pacific: Geol. Soc. America Bull., v. 67, p. 1623–1640.

U. S. GOVERNMENT PRINTING OFFICE: 1957

Chemical Erosion of Beach Rock and Exposed Reef Rock

By ROGER REVELLE *and* K. O. EMERY

BIKINI AND NEARBY ATOLLS, MARSHALL ISLANDS

GEOLOGICAL SURVEY PROFESSIONAL PAPER 260-T

A study of the solution of calcium
carbonate in the intertidal zone

U.S. DEPARTMENT OF THE INTERIOR
March 3, 1849

UNITED STATES GOVERNMENT PRINTING OFFICE, WASHINGTON : 1957

UNITED STATES DEPARTMENT OF THE INTERIOR

FRED A. SEATON, *Secretary*

GEOLOGICAL SURVEY

Thomas B. Nolan, *Director*

For sale by the Superintendent of Documents, U. S. Government Printing Office
Washington 25, D. C. - Price 65 (paper cover)

CONTENTS

	Page
Abstract	699
Introduction and acknowledgments	699
Measurements of diurnal variations in solution-basin and reef water	700
Results	703
Conclusions	705
References cited	706
Appendix—Method of calculation of the percentage saturation of calcium carbonate	709

ILLUSTRATIONS

[Plates follow page 710]

PLATE 225. Etching and solution basins in the intertidal belt, Bikini and nearby atolls.
226. Solution basins in the intertidal belt, Guam and Australia.
227. Undercut sea cliffs (nips), Tonga, Guam, and Australia.
228. "Mushroom" rocks, reef flats, and undercut sea cliffs (nips), Fiji.
229. Undercut sea cliffs (nips), reef flat, "mushroom" rocks, and sea cave, Australia, East Indies, Red Sea, and Tonga.

	Page
FIGURE 233. Changes in water characteristics of two solution basins at Bikini island	701
234. Changes in water characteristics of normal sea-water basin 4 at Guam	702

TABLES

	Page
TABLE 1. Summary of data for water from solution basins and reef flats	703
2. Computed amounts of calcium carbonate dissolved and precipitated in solution basins and on reef flats	704

(347)

BIKINI AND NEARBY ATOLLS, MARSHALL ISLANDS

CHEMICAL EROSION OF BEACH ROCK AND EXPOSED REEF ROCK

By Roger Revelle [1] and K. O. Emery [2]

ABSTRACT

Above the low-tide line the beach rock and reef rock of Bikini and nearby atolls have a highly irregular surface with numerous small depressions, many of which are separated only by knife-edge ridges. This and other geological evidence suggests that some process of solution is of great importance in removing limestone in the intertidal zone. Marked diurnal changes in the alkalinity-chlorinity ratio of the water in the depressions strongly indicate that intertidal solution of calcium carbonate does in fact occur, probably at a comparatively rapid rate. But computations based on the experimentally determined solubility product of calcium carbonate in sea water show an apparent supersaturation in the basin and reef water that ranges from 175 to 800 percent. Possible rationalizations of these opposing lines of evidence are that (1) solution may occur within the limestone of the basin floors or in the interstitial water of the algal mats which cover some of the floors; (2) solution may occur in the films of water left on the basin walls by the receding tide; or (3) much of the calcium may be complexed or hydrated, and the time involved in the formation and dissociation of complexes containing calcium is long relative to the time required to precipitate free calcium ions or to obtain them from solution of calcium carbonate. If this is true, solution can occur when the carbonate concentration or temperature, or both, are rapidly decreased even though the product of the concentrations of total calcium and carbonate remains above the equilibrium saturation value. Erosion of calcium carbonate in warm ocean water is very widespread but is confined to the intertidal zone, where marked diurnal changes in conditions occur. These facts, coupled with the slow attainment of calcium carbonate saturation equilibrium in the laboratory, support the hypotheses of slow complexing or slow hydration and dehydration.

In the intertidal basins, cooling at night and respiration by plants and animals cause a drop in temperature and pH and an increase in carbon dioxide content of the water, all of which favor solution. Precipitation of calcium carbonate during the daytime is facilitated by warming of the water and by the decrease in carbon dioxide and increase in pH corresponding to the excess of plant photosynthesis over respiration. In some of the basins the water shows a stable density stratification at night, with more extreme conditions for solution near the bottom.

INTRODUCTION AND ACKNOWLEDGMENTS

Above the low-tide line the beach rock and reef rock of Bikini and nearby atolls have highly irregular surfaces with numerous small basin-shaped depressions (pl. 225), many of which are separated only by knife-edge ridges. The walls of some basins are overhanging so that their maximum diameters are below their rims. Very irregular basins are obviously the result of lateral coalescence of two or more smaller ones. Where two basin floors are at different levels, their junction may form a steplike structure and cause complete drainage of the higher basin. The floors of the basins are fairly flat, but the floors and especially the walls exhibit small sharp irregularities suggestive of corrosion rather than abrasion. Similar irregularities are present on the surfaces of melting ice, dissolving saltpans, and some meteorites. The basins seldom contain cobbles that might have served as tools to abrade potholes; moreover, some are floored by a thin mat of fragile foraminiferal sand held together by filamentous algae.

Erosion of limestone in the intertidal zone has been reported from the warm and temperate belts in many parts of the world (see, for example, MacFadyen, 1930; Kuenen, 1933; Fairbridge, 1952; and Guilcher, 1953). Solution basins in the upper parts of reef flats (pl. 226), nips (deep notches or undercuts) and caves at the base of sea cliffs in all kinds of calcareous rock from Pleistocene reef material to dense Paleozoic limestone, and nips around negroheads atop reef flats are common and widespread (pl. 227–229). The very existence of the broad and dead reef flat just below low-tide level indicates the efficacy of erosion of limestone in the intertidal zone. This erosion is as effective in sheltered lagoons as on exposed shores.

In some respects the irregular microtopography of the intertidal zone is similar to that of the karrenfelds on the elevated limestones of Guam and other high islands of the western Pacific. These karrenfelds have extremely jagged surfaces formed by vertical and

---

[1] Scripps Institution of Oceanography, University of California.

[2] University of Southern California.

Note.—Contribution from the Scripps Institution of Oceanography, New Series, no. 930; Contribution from the Allan Hancock Foundation, no. 183.

Reproduced by Permission

lateral corrosion of the limestone. Parts of the surfaces are exposed only to the air, and here solution must be brought about by films of rain water rather than by ground water. Unlike the intertidal basins, many of the steep-walled hollows in the karrenfelds are not closed basins capable of retaining water.

The geologic evidence for solution in the intertidal zone of warm tropical waters is in conflict with the results of laboratory studies of the solubility of calcium carbonate in sea water. The problem has been well stated by Kuenen (1950, p. 436):

> Geological observations * * * appear to establish beyond doubt the solvent action of tropical surface waters on reef limestone * * *. Investigation of sea water from the surface in tropical seas has led chemists to the conclusion that it is always saturated or even supersaturated with lime. Hence they have concluded that solution of limestone is not possible. But it is exceedingly difficult to establish whether solution under natural conditions is really excluded.

He left the question essentially as it was in 1933 (p. 75) when he wrote that—

> * * * whether it is the greater range in temperature, the contact with the atmosphere, some influence of surface tension, the alternate wetting and drying, or some other unsuspected influence which was overlooked in the experimental work, I am unable to say.

Solution in the upper part of the intertidal zone has been attributed to rainwater or to fresh ground water by some workers (Wentworth, 1938; Hills, 1949), but this is not likely to be important where rainfall is slight and where ground water cannot reach basins and nips, as on negroheads. Other investigators have supposed that animals burrowing into or grazing upon the rocks and algae boring below the rock surface are chiefly responsible for intertidal erosion of limestone (Duerden, 1902, p. 326–332; Gardiner, 1931, p. 68; and Ginsburg, 1953, p. 61–68).

Emery (1946) demonstrated that in the relatively cool waters of La Jolla, Calif., basins in the sandstone along the shore form in part through solution by biochemically modified sea water. The calcium carbonate cement of the sandstone is dissolved during the nighttime, when the carbon dioxide content of the water in the pools is raised by animal and plant respiration. In the daytime carbon dioxide is removed by photosynthesis, and calcium carbonate is precipitated, probably as small loose crystals that wash out of the pool at the next high tide. Thus, by alternate solution of calcareous cement and flushing out of the precipitate, the calcium carbonate is removed. Growth of the pools is aided by sand-ingesting organisms, particularly snails of the genus *Littorina* (North, 1954, p. 190–194). At La Jolla the characteristics of intertidal rock surfaces indicate that some chemical and organic erosion also occurs outside of pools.

The basins at Bikini differ in several ways from those at La Jolla. Obvious points of difference are their presence in limestone instead of in sandstone, the absence of *Littorina*, the lesser abundance of other conspicuous animals and of algae, the greater rainfall, and especially the higher temperature.

A brief investigation of the chemical and physical processes taking place in the solution basins at Bikini was carried out in 1946 during Operation Crossroads. Measurements of temperature, oxygen content, and hydrogen-ion concentration of the water in basins and on the reef flat were made during the scientific resurvey in 1947 and the Mid-Pacific Expedition in 1950. In an attempt to resolve uncertainties resulting from these researches, supplementary studies of 13 basins at Guam were carried out by Emery in 1952. These included field determinations of alkalinity, temperature, oxygen content, and hydrogen-ion concentration of the basin and reef waters.

The field work at Bikini in 1947 was done by T. S. Austin and T. Goreau; the investigations in 1950 were under the direction of R. F. Dill and R. Y. Morita. Their careful work under difficult conditions is gratefully acknowledged. E. D. Goldberg, Wilson Orr, and N. W. Rakestraw made valuable suggestions concerning the interpretation of the results, particularly with regard to the problems of complexing or hydration of calcium. We are indebted to R. W. Fairbridge for helpful discussions, for assembling many of the photographs in plates 226 to 229, and for invaluable assistance in reviewing the literature. The studies at Guam were carried out during geologic mapping in the islands of the western Pacific accomplished as a part of a joint program of the Corps of Engineers, U. S. Army, and the U. S. Geological Survey.

MEASUREMENTS OF DIURNAL VARIATIONS IN SOLUTION-BASIN AND REEF WATER

Measurements of temperature, oxygen content, and hydrogen-ion concentration in basins and on the reef flat at Bikini were made at intervals of 2 to 4 hours over several days, and water samples were collected for later chlorinity determinations.

Dissolved oxygen was determined by the Winkler method. Hydrogen-ion concentration was measured with a pH meter, using a glass electrode. The meter was carried to each basin in turn, and the pH determined on a freshly collected water sample.

Five basins in the beach rock near the southeastern end of Bikini island were studied in 1950. Three of these were below mean-tide level and consequently were flooded much of the time. Basin 3 was near the high-tide line and was only occasionally flooded. Basin 4 was above high tide during the survey and was not reached by sea water. These two basins show a more extreme range of conditions than the others and serve more easily to elucidate the processes taking place on the reef. Measurements from the two basins are shown in figure 233; selected data are given in table 1, as are data from the reef flat. Results very similar to these were obtained during the investigations of 1946 and 1947.

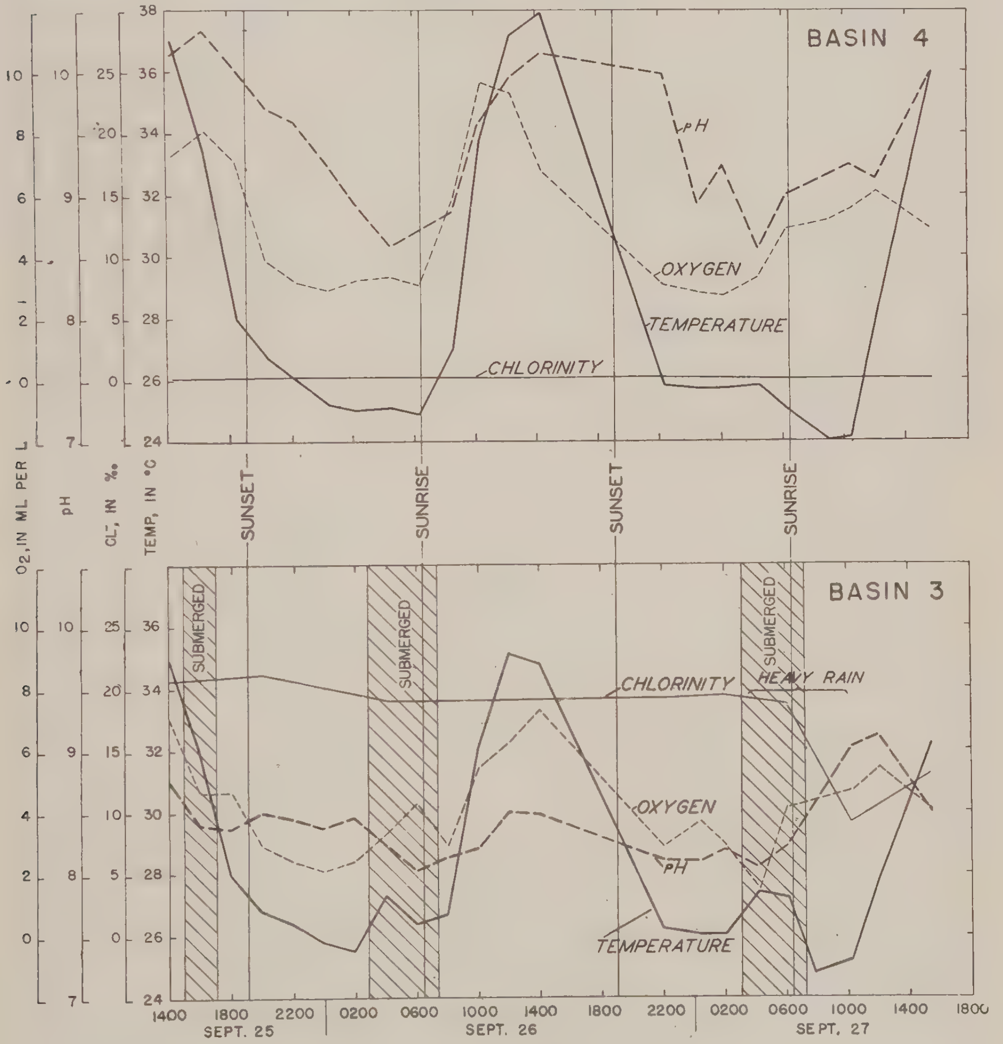

FIGURE 233.—Changes in water characteristics of two solution basins at Bikini Island in 1950. Basin 4 contains fresh rainwater; basin 3 contains normal sea water.

The basic difference between the two basins was in the chlorinity of the water. Basin 4 contained nearly fresh water having a chlorinity of less than 0.2 °/₀₀ (parts per thousand). Until the last morning, when a heavy rain diluted the water, the chlorinity in basin 3 was close to that of the sea water around the atoll, ranging between 18.4 and 21.0°/₀₀. In both basins the water temperature increased during the day and decreased during the night, with a total range of 13° C in the brackish basin and 9° C in the saltier one.

Oxygen content and pH showed marked diurnal cycles. Computations from the data given in figure 233 indicate that oxygen in basin 3 varied from about 30 percent of saturation at night to 180 percent of saturation in the afternoon. Roughly the same range of percentage saturation, 50 to 190 percent, occurred in basin 4. On the reef flat the diurnal variation was much smaller, from 85 to 140 percent. The oxygen increase in the daytime was due to the excess of photosynthetic-oxygen production by marine algae living on the basin floors and within the water, over oxygen consumption by animal and plant respiration. A corresponding decrease in carbon dioxide content must have occurred. At night, when photosynthesis ceased, oxygen was removed by respiration, and carbon dioxide was liberated. These inferred changes in carbon dioxide content are reflected in the observed cycle of pH, which was high during the day, when the carbon dioxide content was small, and low during the night, when the amount of carbon dioxide was relatively large.

Unfortunately, alkalinity was not determined in the field because it was believed that changes in the oxygen content would suffice to compute changes in carbon dioxide. Subsequent computations showed, however, that oxygen was being exchanged with the atmosphere so rapidly that the change in oxygen content was not a reliable measure of the change in carbon dioxide. Therefore, alkalinity of a few samples was measured nearly 2 years after the samples had been collected. Uncertainty in these results led to more complete field measurements of water in 13 basins and a reef flat at Guam in 1952 (Emery, in manuscript). In addition to measurements of temperature, oxygen content, and pH, water samples were filtered within a few hours after collection, and alkalinity was determined by the titration method of Wattenberg (1930). Representative data from the reef flat and from three basins of widely varying chlorinity (designated as brackish water, normal sea water, and hypersaline water) are given in table 1. A 24-hour series of observations of the normal sea-water basin (Guam 4) is illustrated in figure 234. The diurnal variations of alkalinity in the basins

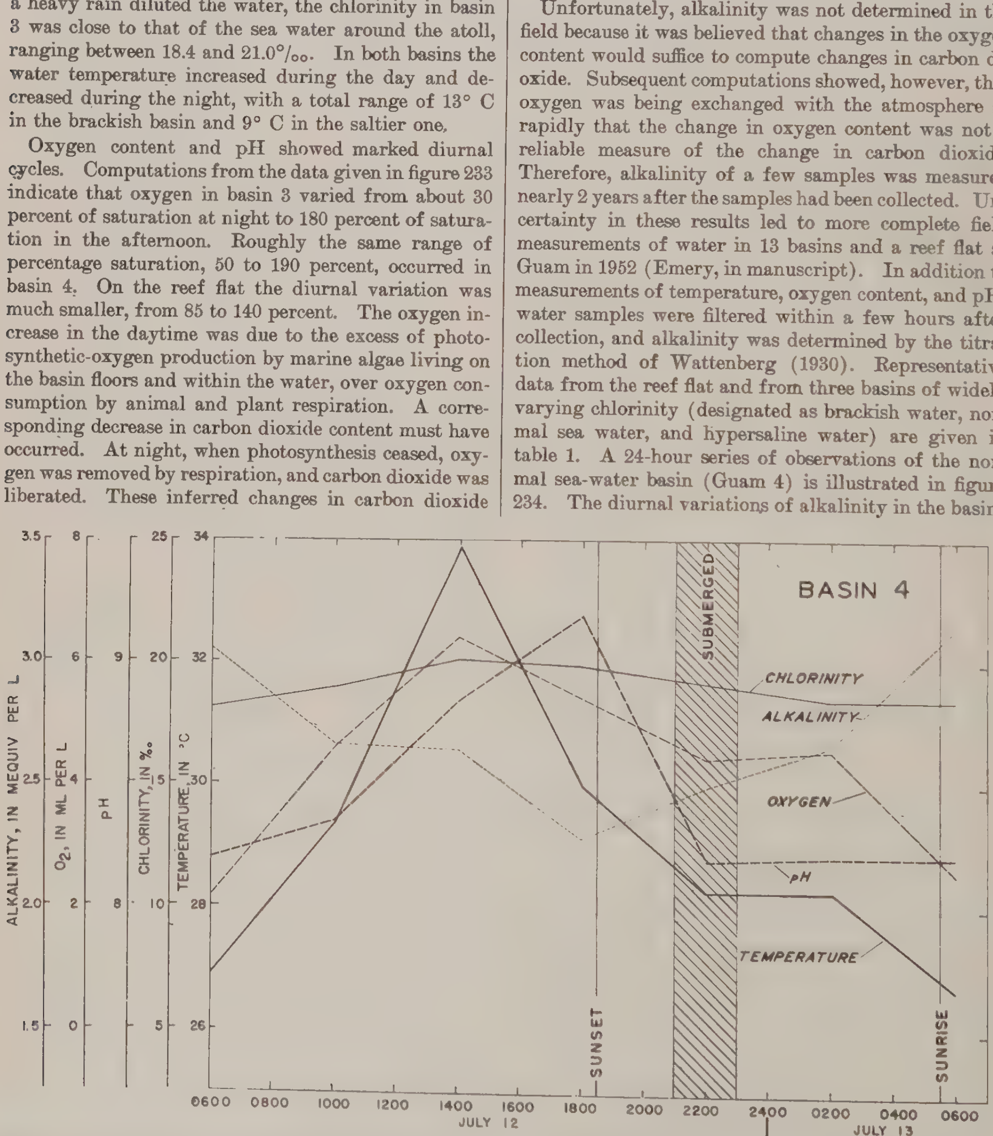

FIGURE 234.—Changes in water characteristics of normal sea-water basin 4 at Guam in 1952. Basin is 75 cm long, 50 cm wide, 10 cm deep.

were large and in any one basin were roughly inverse to the variation in pH.

RESULTS

In the eight solution basins at La Jolla investigated by Emery (1946), the carbonate concentration increased during the daytime as carbon dioxide and bicarbonate decreased; consequently, calcium carbonate was precipitated. This precipitation resulted in a proportionate decrease of the alkalinity. During the night the carbon dioxide content of the water increased; the alkalinity increased as calcium carbonate was dissolved. The water was apparently supersaturated with calcium carbonate in late afternoon but undersaturated at night. Computations based on Smith's (1941, p. 240) apparent solubility product for calcium carbonate (aragonite) show as much as 425 percent saturation in the daytime and only 45 percent saturation at night. A minor error in the previously published computations of percentage saturation, kindly pointed out to us by R. N. Ginsburg, is corrected in table 1.

Similar computations, using Smith's solubility product, indicate that at a temperature of 25° C, a chlorinity of 19°/₀₀, and an alkalinity of 2.34 mequiv per l (milliequivalents per liter), typical values for the tropics, solution can take place only if the pH is below 7.74. None of the pH values for tropical-basin and reef water given in table 1 are less than 8.00. The water is apparently supersaturated with calcium carbonate at all times. The greatest excesses occur in the afternoon and the least just before dawn, but the degree of saturation, using Smith's apparent solubility product for aragonite, is never less than 175 percent and rises to more than 800 percent (table 1). Thus, tropical sea water is apparently incapable of dissolving calcium carbonate at any time. This conclusion is opposed both by the geological evidence and by the observed changes in alkalinity.

TABLE 1.—*Summary of data for water from solution basins and reef flats*

[Symbols: B, bottom; T, top; X, 400 ft from shore; Y, 1,400 ft from shore]

Type of feature	Date	Local time	Sampled locality	Temp (°C)	Cl (°/₀₀)	pH	Oxygen		Total CO_2 (mg per l)	Alkalinity (mequiv per l)	Alkalinity: chlorinity	Calcium carbonate (percent saturation)[1]
							Ml per l	Percent saturation				
La Jolla												
	1944											
Normal sea-water basin	Apr. 28	0500	T	13.3	18.60	8.00			93.39	2.298	0.1234	125
	Apr. 28	1700	T	24.8	22.07	9.00			44.07	1.905	.0863	425
	May 6	0645	T	15.9	18.98	7.62			107.28	2.418	.1274	45
Bikini												
	1950											
Normal sea-water basin 3	Sept. 26	0615	T	26.4	18.95	8.00	4.30	89		[2] 2.302	0.1215	175
	Sept. 26	1415	T	34.8	19.10	8.50	7.30	178				
	Sept. 27	0200	T	26.0	19.34	8.20	2.95	61		[2] 2.474	.1279	265
Fresh-water basin 4	Sept. 25	1420	T	37.0	.10	10.10	7.33	146				
	Sept. 26	0430	T	25.1	.19	8.60	3.38	57				
	Sept. 26	1220	T	37.0	.11	9.95	9.35	187				
	Sept. 27	0430	T	25.8	.07	8.55	3.33	57				
	Sept. 27	1500	T	36.0	.02	9.95	4.91	96				
Reef flat	Sept. 25	1435		32.0	18.99	8.30	4.58	105				
	Sept. 26	0615		26.4	18.95	8.00	4.30	89		[2] 2.302	.1216	175
	Sept. 26	1200		31.1	19.00?	8.35	6.21	140				
	Sept. 27	0610		27.2	18.58	8.20	4.08	85		[2] 2.276	.1224	245
	Sept. 27	1545		30.0	18.71	8.25	4.80	106		[2] 2.421	.1294	325
Guam												
	1952											
Hypersaline-water basin	July 12	0600	T	26.7	22.75	8.41	2.29	50		3.73	0.164	625
	July 12	0600	B	27.3	22.89	8.27	H_2S	0		5.60?	.244	590
	July 12	1800	T	28.3	23.80	8.52	4.11	94		3.86	.162	785
	July 12	1800	B	29.9	23.61	8.50	3.15	74		3.82	.162	810
	July 13	0600	T	26.4	22.41	8.29	2.10	46		3.61	.161	495
	July 13	0600	B	27.2	22.89	8.20	H_2S	0		4.09	.179	515
Normal sea-water basin 4	July 12	0600	B	26.9	18.08	8.20	2.09	43		3.05	.169	330
	July 12	1400	B	33.9	20.10	8.84	6.41	143		2.64	.131	805
	July 24	1600	B	37.2	18.85	9.39	11.56	294		2.03	.108	770
	July 25	0400	B	27.8	18.85?	8.47	2.64	54		2.91	.154	490
Brackish-water basin	July 24	1600	B	27.8	.32	9.10	5.23	91		.80	2.50	180
	July 25	0400	B	26.4	.36	8.20	3.10	52		3.21	8.90	250
Reef flat [3]	July 5	1840	X	31.7	19.10	8.28	6.00	137		2.676	.140	395
	July 6	0610	X	22.8	18.90	8.24	3.44	67		2.676	.143	345
	July 5	1815	Y	30.0	19.12	8.17	5.27	117		2.750	.144	335
	July 6	0545	Y	28.8	19.50	8.24	3.36	73		2.793	.143	355

[1] Computed from Smith's (1941) apparent solubility product for aragonite.
[2] Analyses made nearly 2 years after collection of water samples.
[3] Reef flat 2,200 ft wide.

Reference to table 1 and figure 234 shows that in the brackish-water and normal sea-water (Guam 4) basins at Guam, and in the bottom of the hypersaline-water basin, the alkalinity increased at night and decreased in the daytime. These changes could have been caused by evaporation at night and dilution during the day, by solution of calcium carbonate at night and precipitation during the day, or possibly by other processes affecting the alkalinity. We are convinced that any other such processes were insignificant in the Guam and Bikini basins.

Under some circumstances the alkalinity may change because of solution or deposition of magnesium carbonate (Riviere, 1940, p. 41; Fairbridge, 1950, p. 385). This is probably not a significant factor at Bikini and Guam because magnesium carbonate is only a minor constituent of the rock. In localities where organic matter is rapidly decomposing, the alkalinity may be increased appreciably through production of salts of organic acids and, under extreme conditions, through reduction of sulfates to sulfides. In the clear and nearly colorless waters of the basins at Bikini and Guam, the concentration of organic material is undoubtedly too small to affect the alkalinity measurably. Hydrogen sulfide was noted in only one basin, and, as shown below, the amount was insufficient to account for more than a small fraction of the observed change in alkalinity.

Evaporation and dilution would have affected the chlorinity and the alkalinity in the same proportion. It is probable that the slight changes in alkalinity observed on the reef flats were due to these causes, because the alkalinity-chlorinity ratio was constant within the limits of experimental error. But table 1 shows that in the basins the alkalinity-chlorinity ratio was significantly lower in the daytime than at night, and therefore precipitation and solution, respectively, are indicated.

For the normal sea-water basin (Guam 4) the diurnal change of alkalinity on July 12 was 0.41 mequiv per l. This is not extreme either for this basin or for the other basins, even though it is very much larger than the changes observed in the reef water. The change in calcium computed from the change in alkalinity is illustrated in table 2. When this computed change in calcium concentration is corrected to a constant chlorinity, that of the reef water, it is found that 9 mg per l (milligrams per liter) of calcium was dissolved during the night and nearly 5 mg per l was precipitated during the day. If the calcium carbonate dissolved at night is derived entirely from solution of limestone, the rate of solution is such that about 33 years would be required to dissolve a layer of limestone 1 cm thick. This should be considered a minimum time because much of the calcium carbonate added to the water at night must have originated from solution of calcareous organic remains or re-solution of the calcium carbonate precipitated during the day. The net rate of removal of limestone depends in part on the tidal renewal of water at night and in part on the rate at which calcium carbonate, precipitated as small particles during the day, can be washed out of the basin by the tidal flow.

TABLE 2.—*Computed amounts of calcium carbonate dissolved and precipitated in a typical solution basin*

	Normal sea-water basin (Guam 4)		Reef-flat water (Guam)
	0600	1400	1815
Cl ‰	18.08	20.10	19.12
Ca balanced against weak bases, computed from measured alkalinity mg ions per l	1.53	1.32	1.38
Do. mg per l	61.1	53.0	55.1
Ca balanced against weak bases, computed from alkalinity-chlorinity ratio in reef water do	52.1	57.8	55.1
Ca dissolved do	9.0	0	
Ca precipitated do	0	4.8	
$CaCO_3$ dissolved do	22.5	0	
$CaCO_3$ precipitated do	0	12.0	
Volume of basin water cm^3	36,000	36,000	
Area of basin floor cm^2	3,900	3,900	
Thickness of $CaCO_3$ (assumed density 2.5) dissolved per 24 hr μ	.83		

In the bottom of the hypersaline-water basin at Guam, some of the nighttime increase in alkalinity evidently resulted from the reduction of sulfate to sulfide, a weak Brönsted base, during the latter part of the night after the free oxygen was depleted. Because of the relative inefficiency of anaerobic respiration, the rate of hydrogen sulfide production must have been lower than the rate of decrease of oxygen during the earlier part of the night. The total hydrogen sulfide produced was probably less than 1 ml per l (milliliters per liter). This corresponds to a change in alkalinity of only 0.05 mequiv per l whereas the observed changes in alkalinity were 0.3 and 1.8 mequiv per l. Thus, the larger part of the diurnal change in the alkalinity of the bottom water must have resulted from solution and precipitation of calcium carbonate.

The average alkalinity-chlorinity ratio of the reef-flat water at Guam is 10 percent higher than the value of 0.123 which is characteristic of surface water in the open sea. This difference probably means that the reef water contains a considerable admixture of island ground water which has dissolved calcium carbonate in its passage through the limestone. A mixture of 90 percent sea water with 10 percent brackish water having an alkalinity of 3 mequiv per l (similar to that in the brackish-water basin) would give the alkalinity-chlorinity ratio of about 0.142 found on the reef. Subsequent evaporation would raise the chlorinity to the prevailing value in the open sea around Guam. Water of the normal sea-water basin (Guam 4) is frequently exchanged with water from the reef, and consequently their average alkalinity-chlorinity ratios are nearly the same. In the hypersaline-water basin at Guam the higher average alkalinity-chlorinity ratio indicates that under the extreme conditions in this isolated basin more calcium carbonate remains dissolved throughout the day than in the basin with normal sea water. In the brackish-water basin the very high alkalinity-chlorinity ratio accords with the well-known fact that calcium carbonate is easily dissolved by fresh water.

Some of the calcium which the high alkalinities indicate as being present in solution actually may be in colloidal form. The water was filtered before the alkalinity titrations were made, but finely divided colloidal particles might have been able to pass through the filter paper. However, the existence of such a suspension could not explain the changes in alkalinity between day and night.

CONCLUSIONS

Geologic evidence suggests that some process of solution is of great importance in removing limestone in the intertidal zone. This process is faster than solution by rainwater, as indicated by the existence of intertidal nips in water sheltered from wave action (pl. 227–229). That it is much faster than solution below the intertidal zone is shown by the fairly level surface of the reef flat at a depth less than 30 cm below normal low tide.

The diurnal changes in alkalinity-chlorinity ratios given in table 1 strongly indicate that intertidal solution of calcium carbonate does in fact take place, probably at such a rapid rate that it is an important factor in reducing islands and raised reefs to the monotonously uniform level of the reef flat. The problem remains as to how solution can occur even though, in comparison with published solubility products, the water is apparently always supersaturated with calcium carbonate.

Smith's value for the apparent solubility product, K'_{CaCO_3}, is based on laboratory measurements of the ion product in samples of sea water, collected over the Great Bahama Bank, which had been equilibrated with calcareous bottom mud from the bank for periods of 11 to 38 days. The mud contained large numbers of minute aragonite needles. Other work (Hindman, 1943; Wattenberg and Timmerman *in* Sverdrup, Johnson, and Fleming, 1942, p. 206), in which equilibrium was approached by dissolving or precipitating calcite, yields values of the apparent solubility product for calcite about half as great as Smith's solubility product for aragonite. Revelle and Fleming (1934), in experiments in which aragonite was precipitated by passing air free of carbon dioxide through sea water for periods of several weeks, obtained an apparent solubility product for aragonite twice as large as Smith's value, but it is likely that the sea water was still supersaturated at the termination of their experiments. If solution and precipitation are determined by the apparent solubility product, the value of this product in the tropical basins must be at least twice that found by Revelle and Fleming, and 4 to 5 times Smith's value. Smith's apparent solubility product, when corrected for temperature and salinity, appears to be applicable to the La Jolla basins, and there is no evident reason why the solubility should be different in the tropics. Other explanations must be sought.

Clearly the diurnal cycles of oxygen, pH, and carbon dioxide reflect respiration by plants and animals, counterbalanced during the daytime by photosynthesis by plants. The greater range of the diurnal variations in the basin water, compared to the water of the reef flat or the open sea, is a result of the greater concentration of plant and animal tissue, relative to the amount of water, in the basins. Vertical gradients of chemical properties in the hypersaline-water basin indicate that more extreme conditions for carbonate solution or precipitation may exist at the bottom than within the main mass of water; this is in evident response to the bottom position of most organisms. In the hypersaline-water basin, bacterial respiration actually brings about anaerobic conditions near the bottom at night, with complete depletion of oxygen and production of hydrogen sulfide. Both sets of morning observations from this basin show a stable density gradient because the higher chlorinity near the bottom more than compensates for the slightly higher temperature. Evaporation during the daytime raises the density of the surface water so that overturning probably occurs in the late afternoon.

The presence of vertical gradients suggests that solution may occur under special local conditions. It may take place within the rock surface of the basin floors by organic acids liberated by boring algae, or by carbon dioxide produced in respiration beneath the algal mats that cover some of the floors. Measurements in 1953 by H. Rotschi while on the Capricorn Expedition of the Scripps Institution of Oceanography showed that the water beneath living algal masses on the reefs of Tahiti had a pH range of 6.0 to 8.7, much wider than in the overlying water. The diurnal changes of alkalinity given in table 1 demonstrate, however, that solution and precipitation wherever they occur are reflected in changes of chemical composition of the main mass of basin water.

Solution may take place on the walls of the basins above the pool of standing water, as indicated by the highly irregular surfaces and the fact that the basins coalesce by lateral enlargement. Although it has not yet been tested, the suggestion is made that solution of calcium carbonate on the walls occurs in the film of water remaining on the rock during ebb tide. The ratio of plant and animal bulk to water bulk must be very large in such films; consequently the films should exhibit extreme ranges of pH which may permit the solution of limestone. Examination of these films should be most fruitful for understanding the development of solution basins and nips in the intertidal zone.

But the universal solution of intertidal limestone suggests that something other than localized processes is involved. Two facts are characteristic of the problem: in warm ocean water, solution is confined to the intertidal zone, where rapid and profound changes in the water conditions occur; and in the laboratory, several weeks are required for apparent equilibrium to be attained when calcium carbonate is being dissolved or precipitated in sea water (Hindman, 1943). These two facts suggest that the problem is one of reaction rates. If the calcium is involved in two simultaneous reactions—solution or precipitation of calcium carbonate, and formation of complexes with chloride or sulfate or of hydrates—and if these reactions have markedly different reaction rates, the observations could be reconciled with the laboratory equilibrium values for the apparent solubility of calcium carbonate. This would require that much of the calcium is normally in the complex or the hydrated form and that the time constant for the complexing reaction or for hydration is much longer than the time required for solution or precipitation.

Let it be supposed that at a particular time the water is supersaturated; that is, calcium is slowly proceeding from the complex or the hydrated form to simple ionic form and is being precipitated as it is freed from the complex or the hydrated state. Let a marked change in conditions suddenly occur, for example a decrease in temperature and a decrease in pH, with a corresponding decrease in carbonate-ion concentration. Calcium carbonate will be dissolved, even though the overall concentrations of carbonate and of calcium in both complex or hydrated and simple ionic form are still sufficiently high that the apparent ion product is above the equilibrium saturation value. Eventually, if the new conditions continue, solution will cease and precipitation will again occur. But, if while solution is still proceeding, the temperature, pH, and carbonate-ion concentration are increased to the previously existing value, it is possible to restore the solution nearly to its original condition, provided the equilibrium constant for the complexing reaction or for hydration and the rates of complexing or hydration, solution, and precipitation vary sufficiently with temperature. A pseudoequilibrium may thus tend to persist, when there is a diurnal oscillation of pH and temperature, around a point where the average product of total calcium and carbonate considerably exceeds the laboratory equilibrium value.

Complexing of a sufficiently high proportion of calcium with organic substances could conceivably reduce the calcium activity to a level so low that the product of calcium and carbonate concentrations, multiplied by the activity coefficients, would be less than the solubility product, particularly at night. However, this would require a far higher content of organic matter in the water (of the order of 1 g per l) than has been observed. Fox, Isaacs, and Corcoran (1952, p. 42), found a 0.25 to 35 mg per l range of concentration of colloidal organic matter in inshore surface-water samples. It is concluded that either slow complexing with chloride or sulfate or slow hydration and dehydration are more probable explanations of the nightly solution of calcium carbonate by the apparently supersaturated basin water. An excellent review of the problem of complex-ion formation is given by Young and Jones (1952).

REFERENCES CITED

Duerden, J. E., 1902, Boring algae as agents in the disintegration of corals: Am. Mus. Nat. History Bull., v. 16, p. 326–332.

Emery, K. O., 1946, Marine solution basins: Jour. Geology, v. 54, p. 209–228.

Fairbridge, R. W., 1950, Recent and Pleistocene coral reefs of Australia: Jour. Geology, v. 58, p. 330–401.

—— 1952, Marine Erosion: Seventh Pacific Sci. Congr. Proc., New Zealand, 1949, v. 3, p. 347–359.

Fox, D. L., Isaacs, J. D., and Corcoran, E. F., 1952, Marine Leptopel: Jour. Marine Research, v. 11, no. 1, p. 29–46.

Gardiner, J. S., 1931, Photosynthesis and solution in formation of coral reefs: Proc. Linnean Soc. London for 1930–31, p. 65–71.

Ginsburg, R. N., 1953, Intertidal erosion on the Florida Keys: Marine Science of the Gulf and Caribbean Bull., v. 3, p. 59–69.

Guilcher, André, 1953, Essai sur la zonation et la distribution des formes littorales de dissolution du calcaire: Ann. de Geogr. (Paris), v. 62, p. 161–179.

Harvey, H. W., 1945, Recent advances in the chemistry and biology of sea water: London, Cambridge Press, 164 p.

Hills, E. S., 1949, Shore platforms: Geol. Mag., v. 86, p. 137–152.

Hindman, J. C., 1943, Properties of the system $CaCO_3—CO_2—H_2O$ in sea water and sodium-chloride solution: Scripps Institution of Oceanography, doctoral thesis.

Kuenen, Ph. H., 1933, The Snellius Expedition—Geology of coral reefs: Leyden, Brill, v. 5, p. 2, 126 p.

——— 1950, Marine geology: New York, John Wiley and Sons, Inc., 568 p.

MacFadyen, W. A., 1930, The undercutting of coral-reef limestone on the coasts of some islands in the Red Sea: Geog. Jour., v. 75, p. 27–34.

North, W. J., 1954, Size distribution, erosive activities, and gross metabolic efficiency of the marine intertidal snails, *Littorina planaxis* and *L. scutulata*: Biol. Bull., v. 106, p. 185–198.

Revelle, Roger, and Fleming, R. H., 1934, The solubility-product constant of calcium carbonate in sea water: Fifth Pacific Sci. Cong., Proc., Canada, 1933, v. 3, p. 2089–2092.

Riviere, André, 1940, L'eau de mer et les sediments calcaires: Comptes Rendus Sommaires, Soc. Géol. de France, no. 5, p. 40–42.

Smith, C. L., 1941, The solubility of calcium carbonate in tropical sea water: Jour. Marine Biol. Assoc., v. 25, p. 235–242.

Sverdrup, H. U., Johnson, M. W., and Fleming, R. H., 1942, The Oceans: New York, Prentice-Hall, Inc., p. 186–212.

Wattenberg Hermann, 1930, Über die Bestimmung der Alkalinität des Meerwassers: Annalen der Hydrographie und Maritimen Meteorologie, v. 58, p. 277–282.

Wentworth, C. K., 1938, Marine bench-forming processes—Part I, Waterlevel weathering: Jour. of Geomorph., v. 1, p. 5–32.

Young, T. F., and Jones, A. C., 1952, Solution of electrolytes: Ann. Rev. of Phys. Chemistry, v. 3.

APPENDIX—METHOD OF CALCULATION OF THE PERCENTAGE SATURATION OF CALCIUM CARBONATE

The apparent percentage saturation of calcium carbonate is given by the ratio of the product of the calcium and the carbonate concentrations to the apparent solubility product. Thus

$$\text{percentage saturation} = \frac{[\mathrm{Ca^{++}}] \times [\mathrm{CO_3^{--}}] \times 100}{K'_{\mathrm{CaCO_3}}}$$

For the usual range of temperature, chlorinity, and pH, the maximum changes of calcium, owing to solution or deposition produced by gains or losses of carbon dioxide, can amount to only about 0.5×10^{-3}g ions per l (gram ions per liter), or about 5 percent of the total calcium concentration. Under field conditions it is exceedingly difficult to measure the calcium directly with an accuracy of more than a few percent. Consequently the concentration of calcium was not determined experimentally but was estimated from the calcium-chlorinity ratio of sea water with the modification described below. In the open oceans the ratio of calcium to chlorinity is 0.02106 (Sverdrup, Johnson, and Fleming, 1942, p. 173), hence the concentration of calcium, expressed as gram ions per liter, is

$$[\mathrm{Ca^{++}}] = \frac{0.02106\ \mathrm{Cl} \times 1.025}{40}$$

if it is assumed that the concentration of calcium is governed by evaporation or dilution of sea water. This equation is accurate only when solution or precipitation of calcium carbonate has not occurred and when the sea water has not been diluted with fresh water in which the calcium-chlorinity ratio differs from that in the open sea.

Calcium totals about 400 mg per l (milligrams per liter) in ordinary sea water; of this amount, about 50 mg can be balanced against weak Brönsted bases, principally carbonate, bicarbonate, and borate. The concentration of weak bases, expressed in milliequivalents per liter (mequiv per l), is called the alkalinity. In water near the surface of the open sea the ratio between the alkalinity and the chloride concentration in grams per liter is 0.120; hence, the alkalinity-chlorinity ratio is about 0.123.

If it is assumed that measured changes in the alkalinity-chlorinity ratio correspond to changes in the calcium-chlorinity ratio, the concentration of the calcium is

$$[\mathrm{Ca^{++}}] = \frac{0.02106\ \mathrm{Cl} \times 1.025}{40} + \frac{([A] - 0.123\ \mathrm{Cl}) \times 10^{-3}}{2}$$

The carbonate concentration can be determined by measurement of chlorinity, temperature, hydrogen-ion concentration, and either alkalinity or total carbon dioxide. Measurement of total carbon dioxide content is impractical in the field, hence alkalinity was chosen for the study at Guam. The carbonate concentration in gram ions per liter was computed by means of the following equations adapted from Sverdrup, Johnson, and Fleming (1942, p. 198–200).

$$[\mathrm{CO_3^{--}}] = \frac{[A_{\mathrm{CO_2}}] \times K'_2 \times 10^{-3}}{[\mathrm{H^+}] + 2K'_2}$$

where

$$[A_{\mathrm{CO_2}}] = [A] - \left(\frac{K'_B \times [\Sigma \mathrm{H_3BO_3}]}{K'_B + [\mathrm{H^+}]} + [\mathrm{H^+}] - \frac{K_W}{[\mathrm{H^+}]} \right) \times 10^3$$

and

$$[\Sigma \mathrm{H_3BO_3}] = 0.0221\ \mathrm{Cl} \times 1.025 \times 10^{-3}.$$

Values of K'_2, K_W, and K'_B were taken from tables given by Harvey (1945).

For the basins within the normal range of chlorinity of sea water the apparent solubility constant of calcium carbonate was based upon Smith's (1941) value corrected, by Wattenberg's coefficients, for the observed chlorinity and temperature:

$$pK'_{\mathrm{CaCO_3}} = 5.933 + 0.019(20.0 - \mathrm{Cl}) + 0.012(30.0 - T).$$

For the brackish-water basin the apparently solubility was obtained by interpolation between Wattenberg's value of 18×10^{-8} at a chlorinity of 5 °/₀₀ and the solubility for distilled water, 0.5×10^{-8} (Sverdrup, Johnson, and Fleming, 1942, p. 205, 207). A "virtual chlorinity" corresponding to the supposed ionic strength of the solution was estimated from the measured chlorinity and alkalinity.

The symbols used above are as follows:

$[\mathrm{Ca^{++}}]$ = gram ions per liter of calcium
$[\mathrm{CO_3^{--}}]$ = gram ions per liter of carbonate
$[\mathrm{H^+}]$ = gram ions per liter of hydrogen $= 10^{-p\mathrm{H}}$
$[A]$ = total alkalinity $= ([\mathrm{HCO_3^-}] + 2[\mathrm{CO_3^{--}}] + [\mathrm{H_2BO_3^-}] + [\mathrm{OH^-}] - [\mathrm{H^+}]) \times 10^3$
$[A_{\mathrm{CO_2}}]$ = carbonate alkalinity $= ([\mathrm{HCO_3^-}] + 2[\mathrm{CO_3^{--}}]) \times 10^3$
K'_2 = apparent second-dissociation constant for carbonic acid $= 10^{-pK'_2}$
K_W = ion product for water $= 10^{-pK_W}$
K'_B = apparent first-dissociation constant for boric acid $= 10^{-pK'_B}$
$K'_{\mathrm{CaCO_3}}$ = apparent solubility product of calcium carbonate $= 10^{-pK'_{\mathrm{CaCO_3}}}$
Cl = grams of chlorine and chlorine equivalent of bromine and iodine per kilogram of sea water, in parts per thousand
T = temperature, in degrees centigrade.

PLATES 225–229

PLATE 225

A. Stereopair of karren (lapies) etched in beach rock on upper part of shore ramp, about 4–5 feet above low-tide level. Bikini island. (Photograph by J. I. Tracey, Jr.)

B. Solution basins, now partly filled with sand, on highest part of shore ramp, about 5–6 feet above low-tide level. Bikini island. (Photograph by K. O. Emery.)

C. Solution basins, showing coalescence; note relatively smooth floors, and jagged surfaces between basins. Latoback island, Rongerik Atoll. (Photograph by J. I. Tracey, Jr.)

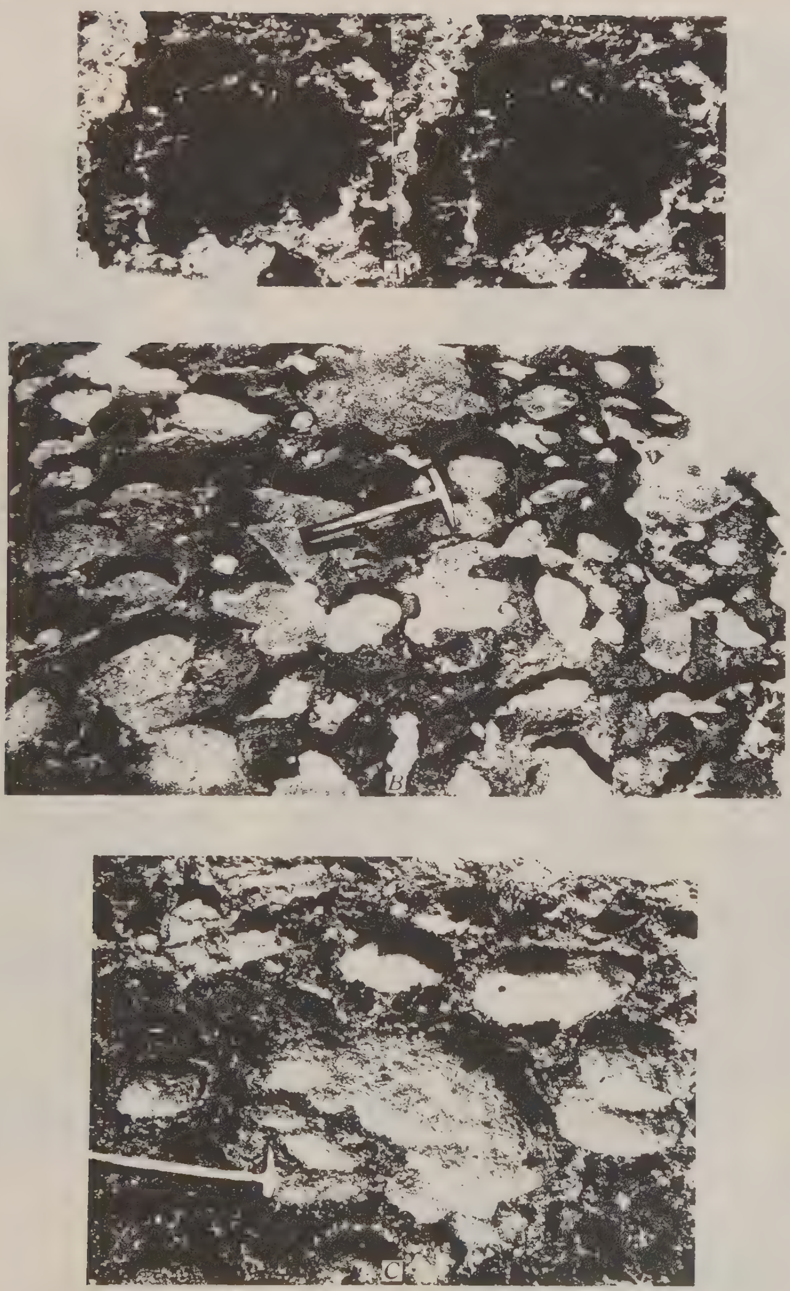

ETCHING AND SOLUTION BASINS IN THE INTERTIDAL BELT, BIKINI AND NEARBY ATOLLS

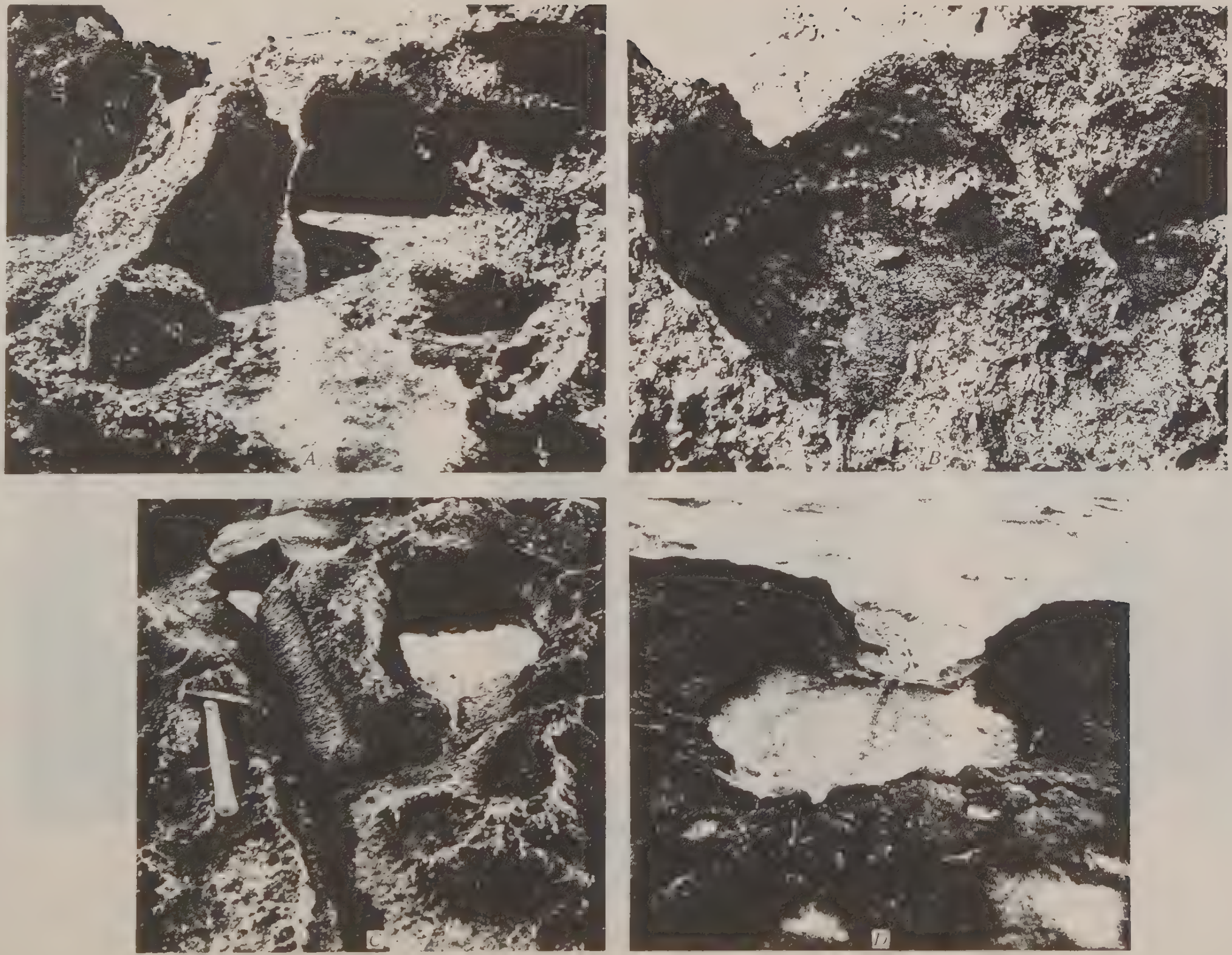

SOLUTION BASINS IN THE INTERTIDAL BELT, GUAM AND AUSTRALIA

PLATE 226

A. Solution basin 5, Toguan Bay, Guam. (Photograph by K. O. Emery.)

B. Solution basin 6, Gogna Cove, Guam. (Photograph by K. O. Emery.)

C. Marine solution basins, with rills and undercut runnels, etched in beach rock 5 feet above low-tide level. Western Australia, between Dongara and Geraldton. (Photograph by R. W. Fairbridge.)

D. Solution basin showing scalloped margins and undercuts and outlet channel following a joint plane. Western Australia, north of Murchison River. (Photograph by R. W. Fairbridge.)

PLATE 227

A. Undercut cliffs of an isolated island of emergent Pleistocene coral limestone in the protected bay of Vavau; undercuts reach from low-tide level to about 5 feet above it. Tonga Group, Vavau. (Photograph by J. B. MacFall.)

B. Undercut cliff of limestone in intertidal zone, 6 feet high. Guam, near Inarajan. (Photograph by K. O. Emery.)

C. Undercut cliff of Pleistocene coral limestone, 6 feet high; note protection from mechanical erosion by offshore reef; maximum depth of notch corresponds approximately to mean sea level. Western Australia, Port Denison, near Dongara. (Photograph by R. W. Fairbridge.)

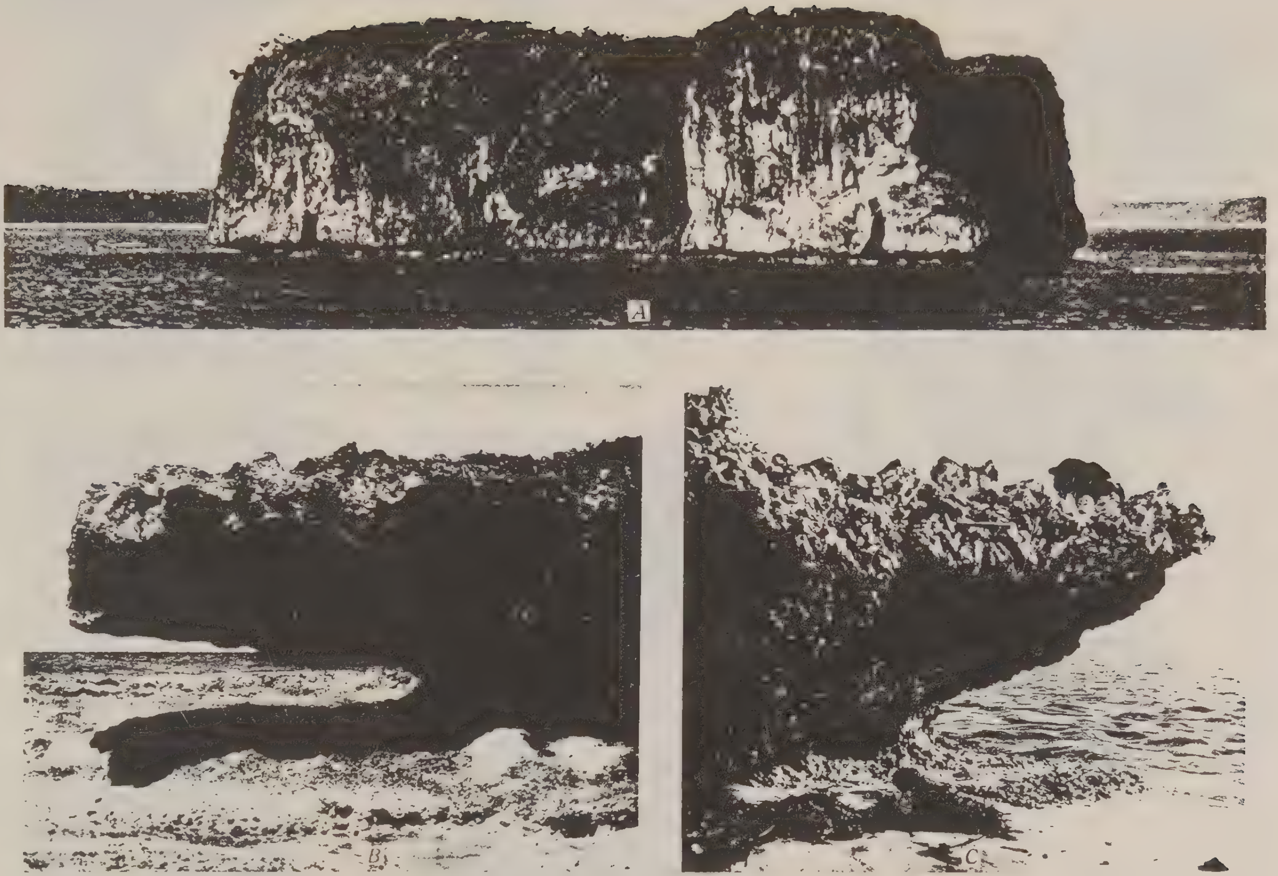

UNDERCUT SEA CLIFFS (NIPS), TONGA, GUAM, AND AUSTRALIA

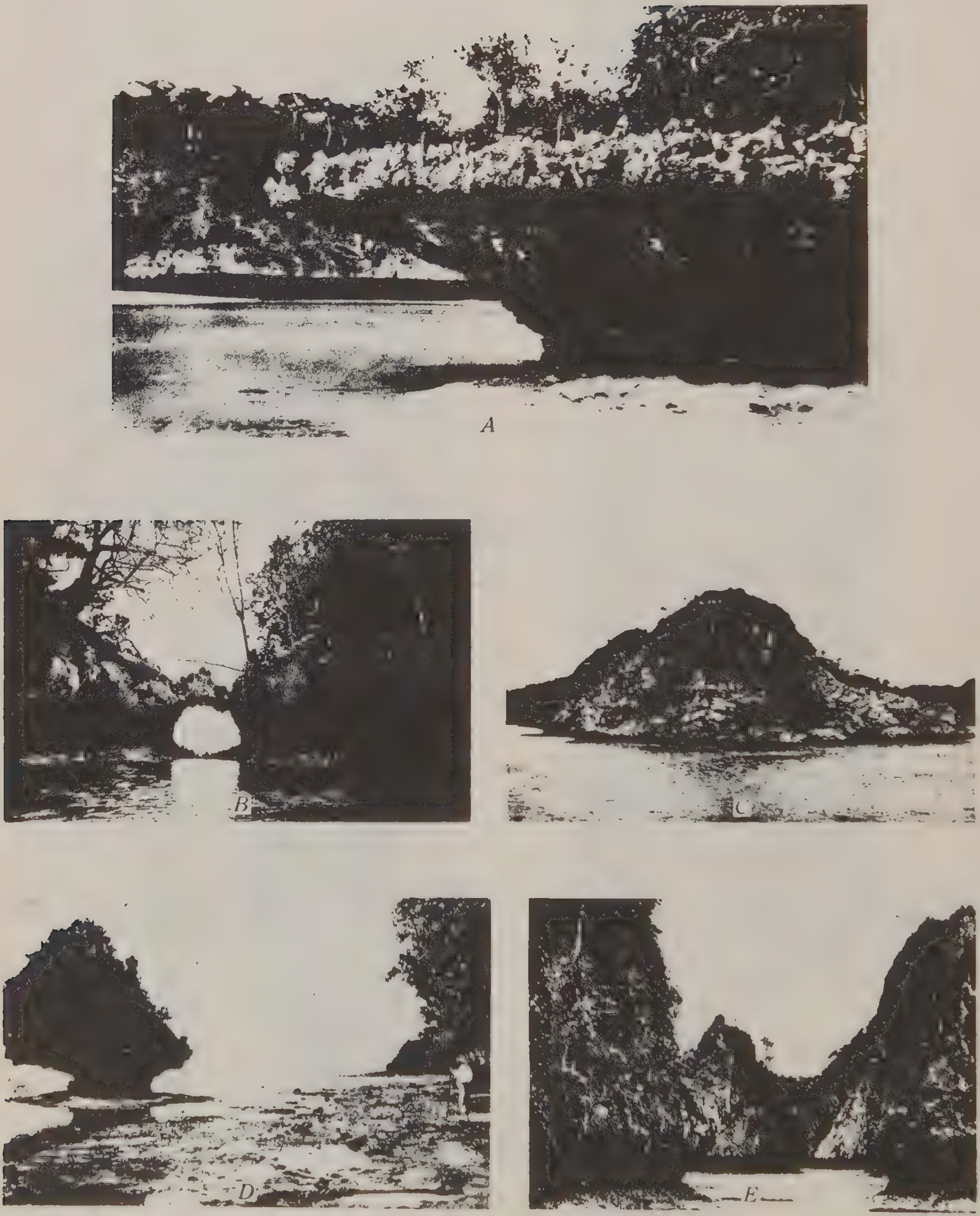

"MUSHROOM" ROCKS, REEF FLATS, AND UNDERCUT SEA CLIFFS (NIPS), FIJI

PLATE 228

A. Undercut cliff, showing remnants of horizontal reef platform approximately 10 feet above present reef flat. Passage between Ongea Levu and Yanuia. (Photograph by Edwin H. Bryan, Jr.)

B. Undercut islands nearly separated by progressive intertidal corrosion, leaving small natural bridge. Bay of Islands, Vanua Mbalavu. (Photograph by J. Edward Hoffmeister.)

C. Undercut cliff, with very deep notch that in places exceeds 20 feet in depth but is only 5–8 feet high; note extensive landslide due to collapse of undercut. North shore of Ongea Ndriki. (Photograph by Max Agassiz.)

D. Well developed "mushroom" rock (undercut stack) at low tide; top surface of undercut is 5–8 feet above reef flat. Mango. (Photograph by E. C. Andrews.)

E. Narrow protected bay with steep limestone cliffs undercut just as in exposed places. East shore of Ngillangillah. (Photograph by W. McM. Woodworth.)

PLATE 229

A. Undercut cliff, 10 feet high, in Pleistocene lagoon limestone; seen at low tide, tidal range being 3 feet; note horizontally eroded reef flat in protected lagoon. Western Australia, Middle Island, in Pelsart Lagoon, Houtman's Abrolhos islands. (Photograph by R. W. Fairbridge.)

B. Very deep notch, at least 20 feet deep and 5 feet high, in emergent Pleistocene coral limestone cliff. Shore is protected here by off-lying reefs and land. East Indies, west point of Waaf. (Photograph by Ph. H. Kuenen.)

C. Undercut cliffs and "mushroom" rocks, showing prominent overhang and horizontal top, which is the remnant of a former reef platform 10 feet above the present one. Red Sea, Farsan islands, east coast of Kamaran island. (Photograph by W. A. MacFadyen.)

D. Undercut cliffs leading into large sea cave (believed due to Pleistocene karst formation). Note that undercut extends into dark, protected waters of the cavern. Tonga islands, Vavau. (Photograph by Alan Jones.)

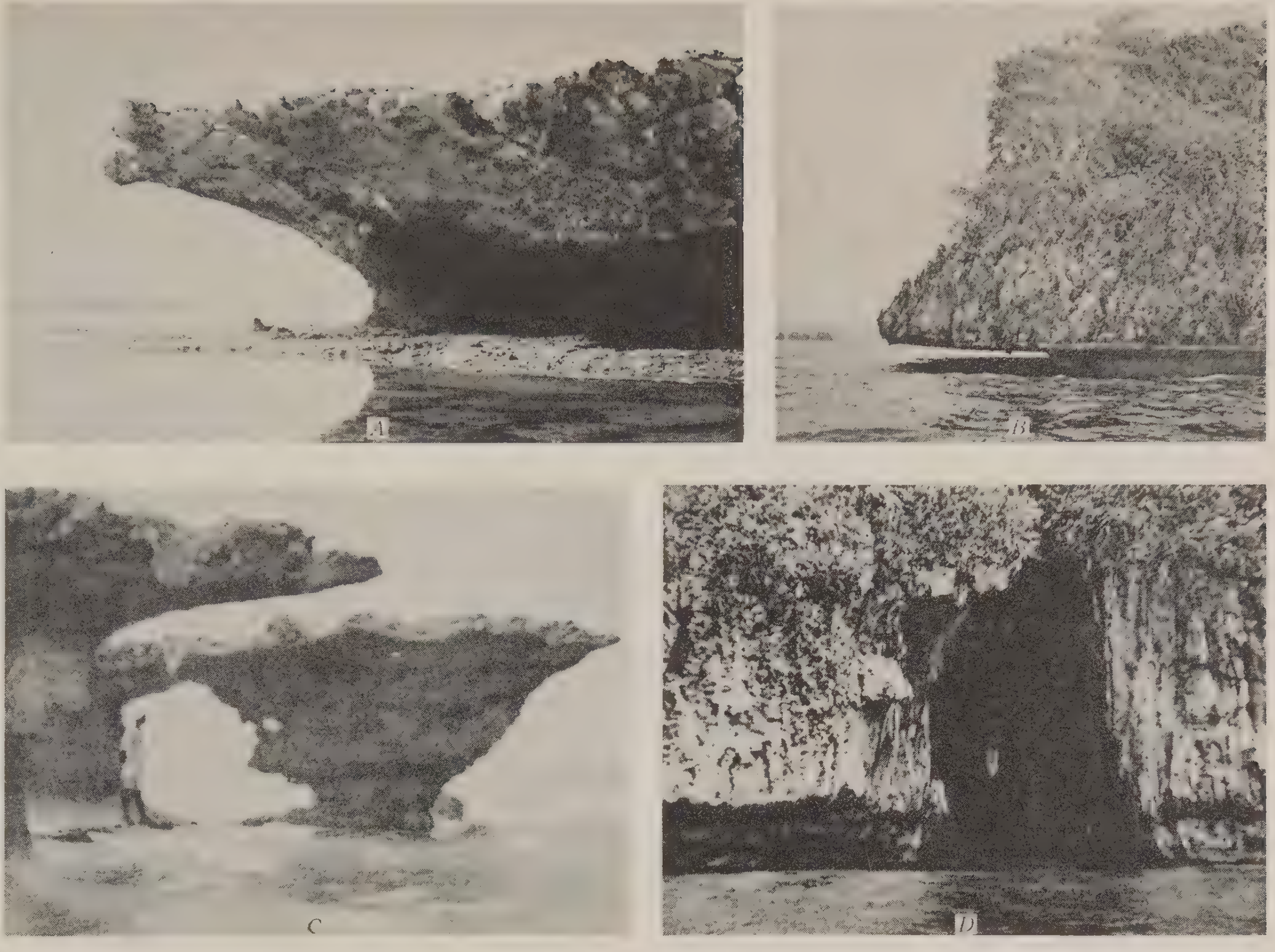

UNDERCUT SEA CLIFFS (NIPS), REEF FLAT, "MUSHROOM" ROCKS, AND SEA CAVE, AUSTRALIA, EAST INDIES, RED SEA, AND TONGA

BULLETIN OF MARINE SCIENCE
OF THE GULF AND CARIBBEAN

VOLUME 7 1957 NUMBER 2

THE MARINE BORER FAMILY LIMNORIIDAE (CRUSTACEA, ISOPODA).

PART I:

NORTHERN AND CENTRAL AMERICA: SYSTEMATICS, DISTRIBUTION, AND ECOLOGY[1,2]

ROBERT JAMES MENZIES
Lamont Geological Observatory,
Columbia University

ABSTRACT

The family Limnoriidae is reestablished with keys and diagnoses to all known species including *Limnoria* (*Limnoria*) *lignorum* (Rathke), *L.* (*L.*) *pfefferi* Stebbing, *L. (L.) japonica* Richardson, *L. (L.) septima* Barnard, *L. (L.) quadripunctata* Holthuis, and *L. (L.) tripunctata* Menzies. The following are described as new species: *L. (L.) platycauda,* Dutch West Indies, *L. (L.) saseboensis,* Sasebo, Japan, *L. (L.) simulata,* Virgin Islands, *L. (L.) multipunctata,* Kai Islands, *L. (L.) unicornis,* Ponape Island, *L. (L.) foveolata,* Kai Islands, *L. (L.) sublittorale,* N. S. Wales, Australia, *L. (L.) insulae,* Fiji Islands. Seaweed borers were assigned to the new subgenus *Phycolimnoria,* containing *segnis* (Chilton), *antarctica* (Pfeffer) and the new species *algarum,* California, *segnoides,* Misaki, Japan, *nonsegnis,* Port Arthur, Tasmania, *rugosissima,* Port Jackson, Australia, and *stephenseni,* Auckland Islands. The new genus *Paralimnoria* was instituted to receive the tropical *L. andrewsi* Calman. Variations in salinity, temperature, dissolved oxygen, and food supply are considered the major factors influencing the distribution of the species. Literature citations are reasonably comprehensive.

INTRODUCTION

The object of this paper is to present a systematic and zoogeographic account of the wood and sea-weed boring marine isopods of the northern and central Americas. It is optimistically hoped that

---

[1] Contribution from: The Pacific Marine Station, Dillon Beach, Marin County, California; the Zoology Department, University of Southern California and the Scripps Institution of Oceanography, New Series 931, and the Lamont Geological Observatory, No. 239, Biology Program No. 15.

[2] This work was supported by a grant-in-aid from the American Academy of Arts and Sciences, Boston, Massachusetts. The studies were further aided by a contract between the Office of Naval Research, Department of the Navy, and the University of California, SIO., NR 163-084, and finally a contract between the Biology Branch of the Office of Naval Research NONR 2664 and the Lamont Geological Observatory of Columbia University.

Reproduced by Permission

the introductory account of the morphology and the scientific keys are sufficiently elementary and lucid to permit a non-specialist to use them effectively.

The limnoria-like isopods which bore into wood are of such economic importance that they have been and are being studied by investigators of varied interest and training. It seems accordingly important that current systematic concepts and nomenclature be available and useful to the students of the subject.

The current concept suggests that only one species, *Limnoria lignorum* (Rathke) is widely present in the world. Other species which have been described have often been considered members of isolated endemic populations. This concept is apparently erroneous and thus highly misleading to students of the economic aspects, physiology, ecology, and geographic distribution of these animals. The evidence for the existence of other species, some of which seem to show even a wider distribution than *L. lignorum,* appears overwhelming to the writer and is here presented for a fairly wide geographic area.

In all, eight species are recorded from the area, including one apparently new genus, a new subgenus, and three new species. Five of the species had been known before, three from California alone.

Prior to the work of Richardson (1909, pp. 95-96, fig. 25) the characteristics used to distinguish the species were based mostly on the mouth parts, abdominal appendages, and the general body shape of the animals. While it is often true that features such as the shape of the maxillipedal epipod, and the number of articulations comprising the mandibular palp (both mouth parts) are useful in separating some species; these alone are insufficient to distinguish the many species now suspected to exist. In the course of this investigation it was found that the most useful diagnostic characteristics consisted of the gross and detailed shape and structure of ornamentations, tuberculations, and bristles on the dorsal surface of the last (most posterior) segment of the body, the *pleotelson.*

The following facts about the life habits of the animal are abundantly substantiated today. *Limnoria* and its close relatives (*Paralimnoria,* p. 147) eat the plant material, wood and seaweed, into which they bore. The habit of boring provides them with both nourishment and protection from enemies. The animals constitute a serious threat to wood, especially untreated wood, which is placed in sea water. They are exclusively marine and generally considered inhabitants of shallow water but have been collected from depths as great as 290 fathoms. The methods which have been thus far devised of preventing their damage to wood, consisting usually of paints and injected preservatives, are still imperfect, and the problem of extending the life of treated wood is almost as acute today in some harbors as it was 50 years ago. Attack on wood is instituted by crawling or swimming adults and not by larval forms. The larvae are incubated in a brood pouch and carried by the adult until capable of doing their own boring. The released young, however, in contrast to the adults, are poor swimmers. Structurally, the animals, except for extensive modifications of the mandibles, are generalized isopods belonging to the least morphologically modified isopodan suborder, the Flabellifera.

ACKNOWLEDGMENTS

The writer wishes first to thank the William F. Clapp Laboratories, Inc., of Duxbury, Massachusetts for their valuable assistance in supplying many of the specimens used in this study. The abbreviation "W.F.C.L." follows specimens which were received from that source. The encouragement of systematic studies by the late William F. Clapp was particularly stimulating to the writer. Surely his influence on marine borer studies will long be felt both here and abroad.

Numerous collecting trips were made to various harbors and bays in Southern California. On many of these excursions the companionship and collaboration with Dr. John Luther Mohr, Associate Professor of Zoology, University of Southern California, was both pleasant and intellectually rewarding.

Most of all the writer is indebted to the American Academy of Arts and Sciences for a grant-in-aid which permitted the procurement of essential literature and specimens from many parts of the world, as well as enabling the writer to participate in ecological studies of borers in San Francisco Harbor, Los Angeles Harbor, and other parts of California. In these studies, the use of laboratory and library facilities of the Pacific Marine Station, the Allan Hancock Foundation, and finally the Scripps Institution of Oceanography is especially appreciated as is also the assistance of the Office of Naval Research in supporting the terminal phase of this work.

Much of the descriptive material comes from a doctoral dissertation entitled "The phylogeny, systematics, distribution, and natural history

of *Limnoria*" which is deposited in the library of the University of Southern California, Los Angeles, California.

REVIEW OF THE LITERATURE

The literature dealing with *Limnoria* from North America may be conveniently divided into five major categories: taxonomy, distribution, ecology, anatomy, and physiology of the animals. It is the intent of this review to bring to the attention of the reader papers of outstanding importance to the general problem of each category rather than to discuss each paper.

Only one paper, that of Kofoid and Miller (1927) is of such scope as to cover all of the above subjects. It is based to a large extent on the findings of P.P.C. Hoek whose article "Betreffende de Levenswijze en de Werking van Limnoria lignorum" (1893) forms the starting point for much of our knowledge on the biology of the animal. A great deal of Hoek's work was both original and surprisingly accurate. The figures he gives of *Limnoria,* like those in the Kofoid and Miller paper (op. cit.), appear repeatedly in the works of later biologists concerned with the problem. Very recently Becker and Kampf, 1955. have reviewed the subject in a most comprehensive way.

Taxonomic Studies

Taxonomic studies on American *Limnoria* are most frequently found in treatises concerned with general isopodan systematics. The first to appear was that by Harger (1880), followed by Richardson (1905), and later by the Kofoid and Miller paper (op. cit.). The above papers mention only one species, *L. lignorum,* (Rathke), but in reality appear to treat several. Holthuis (1949) and Menzies (1951a) each added one species to the fauna, *L. quadripunctata* Holthuis and *L. tripunctata* Menzies. Without a doubt the most satisfactory taxonomic description of a species of *Limnoria* is that given by the venerable Norwegian scientist, George Ossian Sars (1897, pp. 76-77), and since he describes *L. lignorum,* a species which we consider, his study merits special note. The papers dealing with *Limnoria* on a world-wide scope are those by Chilton (1914a), Calman (1936), and Moll (1915). All of these suffer from the then prevalent concept that *L. lignorum* (Rathke) was the sole species having a world-wide distribution.

Distribution

With the exception of the papers by Richardson, Harger, and Kofoid and Miller, and some isolated reports by Holthuis (1949), Menzies (1951a), and Menzies and Mohr (1952), no other papers are known which deal with the distribution of the *Limnoria* in the Americas. As far as the general distribution of the genus is concerned the papers (op. cit.) by Calman, Moll, and Chilton should be consulted. Chilton, Moll, Kofoid and Miller, and especially Omer-Cooper and Rawson (1934) all present some ideas on the methods utilized by *Limnoria* in obtaining its wide distribution.

Ecology

The papers of Johnson (1935) and Johnson and Miller (1935), dealing with the seasonal migration of *Limnoria lignorum* at Friday Harbor are the first American works on that subject. Johnson's is the first paper in which the phenomenon is critically examined. Seasonal settlement by that species was later studied in even greater detail by Sømme (1940) in Norway who further points out that the subject had been investigated by Kramp in Europe as early as 1927. Kofoid and Miller did not find a seasonal settlement by *Limnoria* in San Francisco Bay, but their results might now be questioned due to the finding that two species are present there, neither of which is *lignorum* (see pp. 158-162). Both species could have overlapping migratory periods which would mask one another. It is interesting to note that Greenfield (1952) was unable to pick out distinct seasonal or ecological preferences by *Limnoria* at Miami where at least three species are now known to occur (pp. 135, 137, 141). The papers by Henderson (1924) and Kofoid and Miller (1927) are the only ones in which the habits of *Limnoria* are treated in any detail. Shiino (1950) is one of the first investigators to provide a detailed analysis of a natural population. He was dealing with *Limnoria tripunctata* Menzies and *Paralimnoria andrewsi* (Calman), both of which species occur in North America. The parasites of *Limnoria* are briefly mentioned by Kofoid and Miller (1927). Important observations on development as it relates to distribution and seasonal behavior are given by Coker (1923) and Johnson and Menzies (1956) in America and Sømme (1940) in Norway. Reish (1954) lists and discusses the polychaetous predators of *Limnoria*.

Physiology

The papers dealing with the physiology of *Limnoria* are rather scarce. Those dealing with the salinity tolerances of the animal by White (1929), Coker (1923), and Kofoid and Miller (1929), present some striking differences as far as results are concerned.

Some of the differences are evidently due to variations in experimental methods used by those writers; others are probably due to the fact that they were all working with different species. In general it can be said that a salinity of 15‰ is surely lethal to the animals within a few days and that death ensues quite rapidly in lower salinities. The subject is in need of re-examination with more standard techniques in light of the evidence that different species exist.

The question of cellulose utilization by *Limnoria* was first experimentally examined by C. M. Yonge (1927) who reported negative results. This conclusion has since been questioned by Ray and Julian (1952) using a chemical method to detect enzyme activity. The investigators came to the conclusion that the animal was able to use cellulose and all express the doubt that the cellulase could have been elaborated by bacteria. ZoBell (1946) suggested that the sources of nitrogen for the animal might come from bacteria present in the burrows and gut of the wood borer. Adsorbed organic matter, pelogloea, the importance of which is discussed by Fox, Isaacs, and Corcoran (1952), might also constitute a primary source of nitrogen for *Limnoria*.

Anatomy

Studies of the anatomy of *Limnoria* are particularly scarce and those available deal largely with its external features. In North America Henderson's (1924) paper is one of the first attempts to understand the workings of the animal from its anatomical structure. Her account is comparable with the first European treatise on the subject by Coldstream (1836). Only the papers by Hoek and Miller and Kofoid (op. cit.) show any attempt at an understanding of the internal structures and in several details their reports are inaccurate. Accounts of specialized structures of *Limnoria* as compared with other animals have appeared in European journals most comprehensive of which is an account of the accessory organs of the brain by Amar (1951, p. 224). Menzies (1954) has described the reproductive system and certain aspects of the reproductive biology of *Limnoria*.

ECONOMIC ASPECTS OF LIMNORIA ACTIVITY

No paper on marine wood-borers seems complete without an enumeration of the damages caused by the animals. There is, of course, no easy way to separate the damages caused by teredine borers from those caused by the isopods as far as cost alone is concerned. Generally the two types of organisms work together in their destruction of wood in the sea. In a few instances where the salinity of the water is reduced to the point of exclusion of *Limnoria*, such as certain rivers near Sydney, Australia; Lake Maracaibo, Venezuela, and Mira Flores Lake, Panama, only the teredines cause the damages reported. With the advent of extensive pressure creosoting of marine piling, it seems that the damages of teredines have become much lessened in importance, whereas those of *Limnoria* have been increased. This appears due to the unusual ability of *Limnoria tripunctata* (Menzies, 1952) and perhaps other species, to enter the creosoted shell of treated wood shortly after its immersion in sea water. Teredine larvae seem unable to accomplish this feat until leaching or injury to the pile exposes virtually untreated surfaces. The fact that teredines penetrate wood as larval forms, whereas *Limnoria* penetrates the wood as an adult, would seem to have much to do with this difference in ability between the two to attack creosoted wood. It is generally known from the results of studies made on fouling organisms, that larval forms are frequently about 100 fold more sensitive to toxins than are the adults. As far as borers are concerned, this relationship is further augmented by reports of adult teredo penetrating the creosoted parts of piling after once gaining entrance through untreated areas.

The annual cost of marine borer damage in the coastal waters around the United States is believed to exceed 50 million dollars according to the most recent estimates available (Greathouse, 1952). In San Francisco Bay alone during the years 1917 to 1921, it was estimated that marine borers caused 25 million dollars damage. Recently the "premature" failure of piling in the Guantanamo Bay at a U.S. Navy Installation cost many thousand dollars (Alexis, 1951). Were the records available, these examples could be multiplied many times. Because much of the damage caused by borers is slow and unspectacular, it is only the sudden and dramatic failures of marine structures that find their way into the published records, and receive public attention. In Los Angeles Harbor the inspection and replacement of defective piling is a constant job and because of this very few major accidents due directly to borer damage, such as is shown in Figure 1, are recorded but it is the estimate of Mr. Carrol M. Wakeman, Chief Testing Engineer at the Los Angeles Harbor Department Testing Laboratory, that borers, mainly *Limnoria*, cause about one million dollars' damage each year.

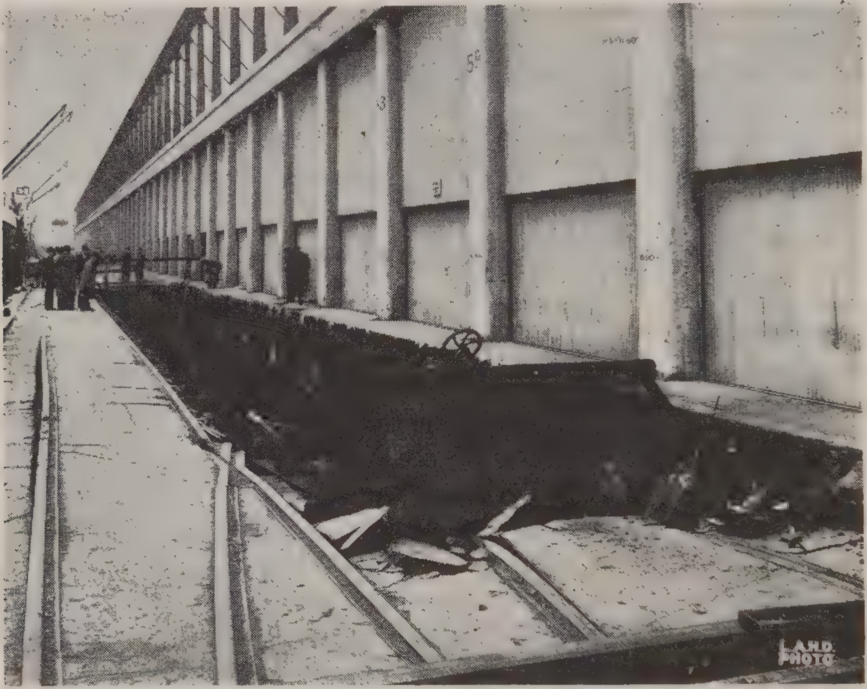

FIGURE 1. Collapse of creosoted wooden piles due to attack by *Limnoria tripunctata* at Berth 59, Los Angeles Harbor. Piles had been in service only 12-13 years. Photo courtesy of Los Angeles Harbor Department, via Mr. Carrol M. Wakeman, Testing Engineer.

COLLECTION, PRESERVATION AND EXAMINATION OF LIMNORIA FOR SYSTEMATIC STUDY

It is rather easy to detect the activities of the *Limnoria* which usually produce a multitude of minute holes at the surface of the wood. These holes are so numerous as to give the wood a lace-like appearance and a sponge-like structure. Attack on piling is often but not invariably most intense just above the mud line, giving the old piling the characteristic pencil-point appearance (Figure 2). The individual holes produced by *Limnoria* are seldom over one inch in length and generally penetrate less than one-half an inch into the wood. Usually the burrows are with the grain of the wood, the soft parts being more rapidly destroyed than the hard parts.

Not all samples of wood are equal in the number of animals they contain. Thus a sample taken from the soft and spongy outer part generally has much fewer animals than one taken deeper in the wood (Figure 3). Many of the animals will be situated very near the blind end of their burrows. A sample of wood ¾ inches deep and about one inch square should yield a good supply of specimens, if the wood has animals at all.

The above remarks apply to the activities of the wood-boring *Limnoria.* Those that burrow into sea-weeds are much more difficult to detect and even more difficult to collect (Figures 3 and 4). These animals burrow into the holdfasts of kelps belonging to the Laminariales. They are often burrowing into the living tissue of the plant and are accordingly parasitic on the kelp. Plants with compact holdfasts, such as *Egregia, Laminaria,* and *Postelsia* are best examined for *Limnoria* by slicing thin sections off the exposed (outer) part of the holdfast. If *Limnoria* is present, its burrow will be cut through and be detected. It is then a matter of following one burrow until the animals, which are usually found in pairs, are discovered. Plants

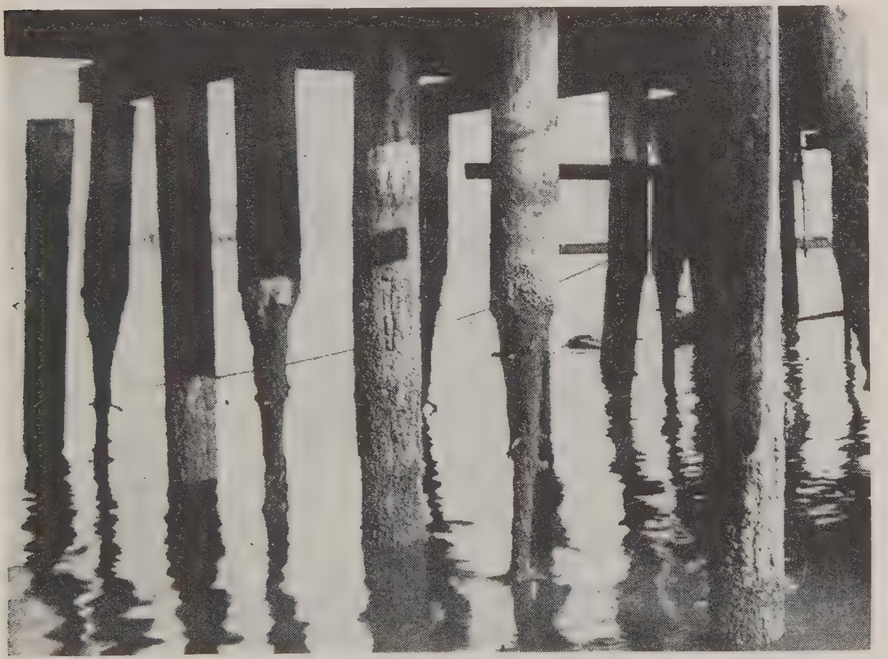

FIGURE 2. Untreated Douglas fir piling in San Francisco Bay showing the pencil-point erosion of the piling, characteristic of *Limnorial* attack within the intertidal zone. Photo reproduced from Hill and Kofoid, 1927, fig. 13, with permission of the University of California Press.

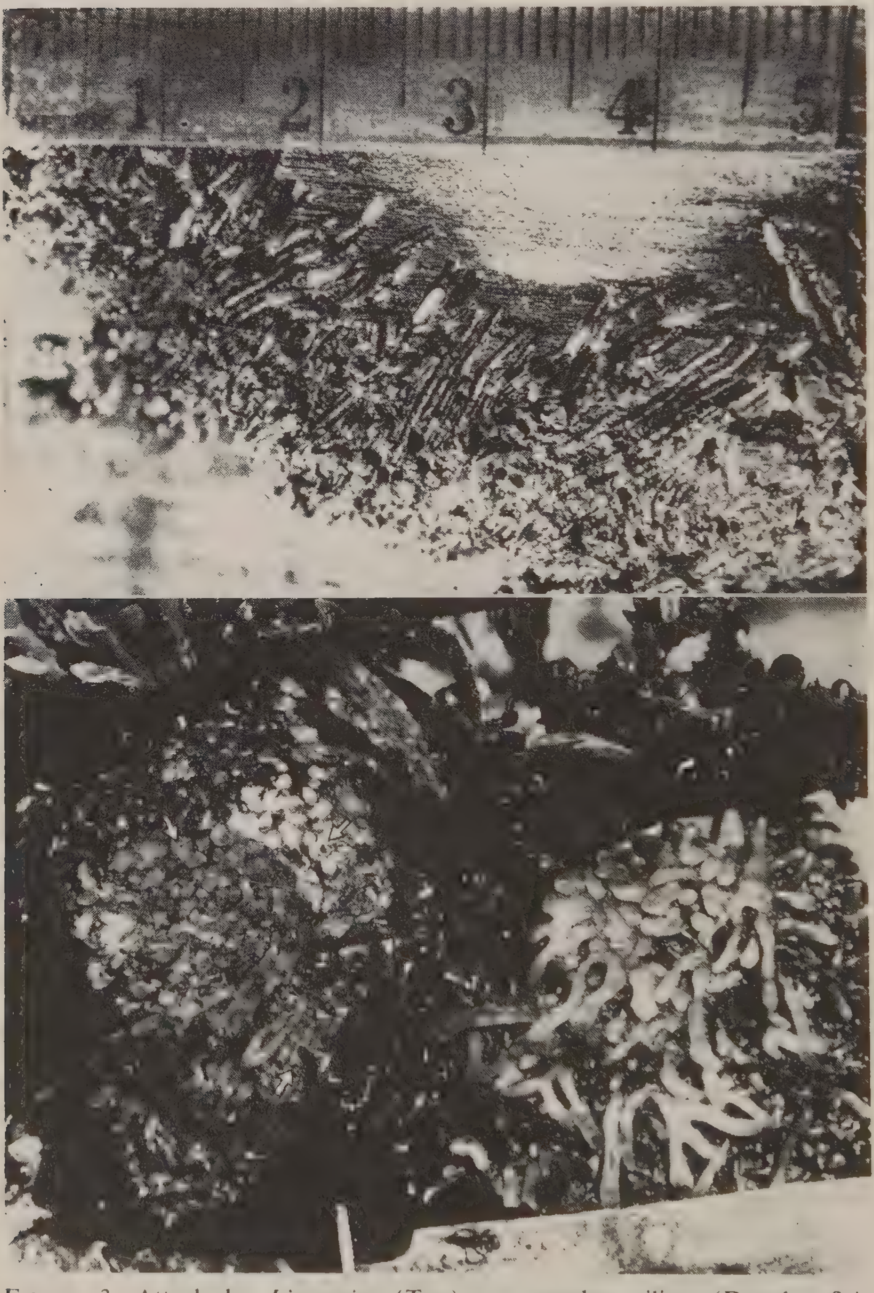

FIGURE 3. Attack by *Limnoria*. (Top), on wooden piling (Douglas fir). (Bottom), on the hold-fast of the alga *Egregia*.

(382)

with a diffuse holdfast, such as *Macrocystis,* have long narrow "roots" (=rhizoids). In this case, one rhizoid frequently has only one burrow. This is most easily detected in the old part of the rhizoid and are not in newly formed tissue as in the case of *Egregia.* The older parts of the burrows are often inhabited by polychaets and small crustaceans; frequently they are filled with sand. It would seem that the attack of a holdfast by *Limnoria* would weaken its holding capacity, making it more liable to be detached from its moorings than an unattached plant. Suggestive of this is the fact that the large kelps which are cast upon the beach after a storm are often rich sources of specimens of the kelp-burrowing *Limnoria.*

Specimens preserved in 75 percent ethyl alcohol show a maximum number of identifying structures. In contrast, specimens preserved in formalin, a solution which is or often becomes acid, generally have lost much of their carbonate to the preservative with a resultant obscuring of the delicate sculpturing which is so very useful in making specific determinations.

The ornamentation of the pleotelson is best observed with the aid of a powerful binocular stereoscope and a concentrated reflected light of strong intensity. Specimens, especially if they are taken from turbid water, may be covered with a dense layer of debris. This debris, consisting of silt, algal filaments, and wood particles must be removed from the pleotelson of the animal as it often obscures essential details in sculpturing.

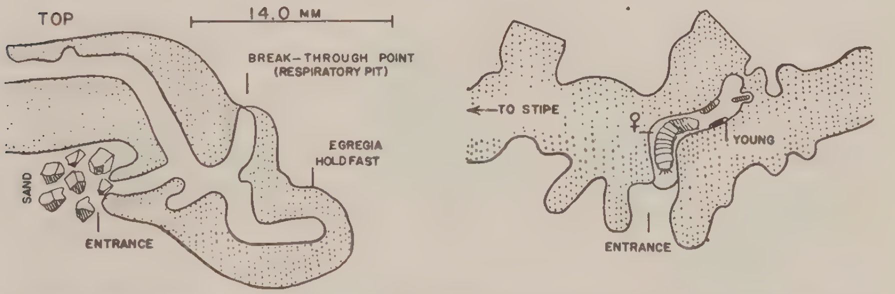

FIGURE 4. A sketch of the attack by *Limnoria* on the hold-fast of the seaweed *Egregia.*

For dissection of the mouth parts it is convenient to immerse the specimens in glycerin. The mouth parts can then be transferred to a microscope slide in the viscous drop of glycerin and readily examined.

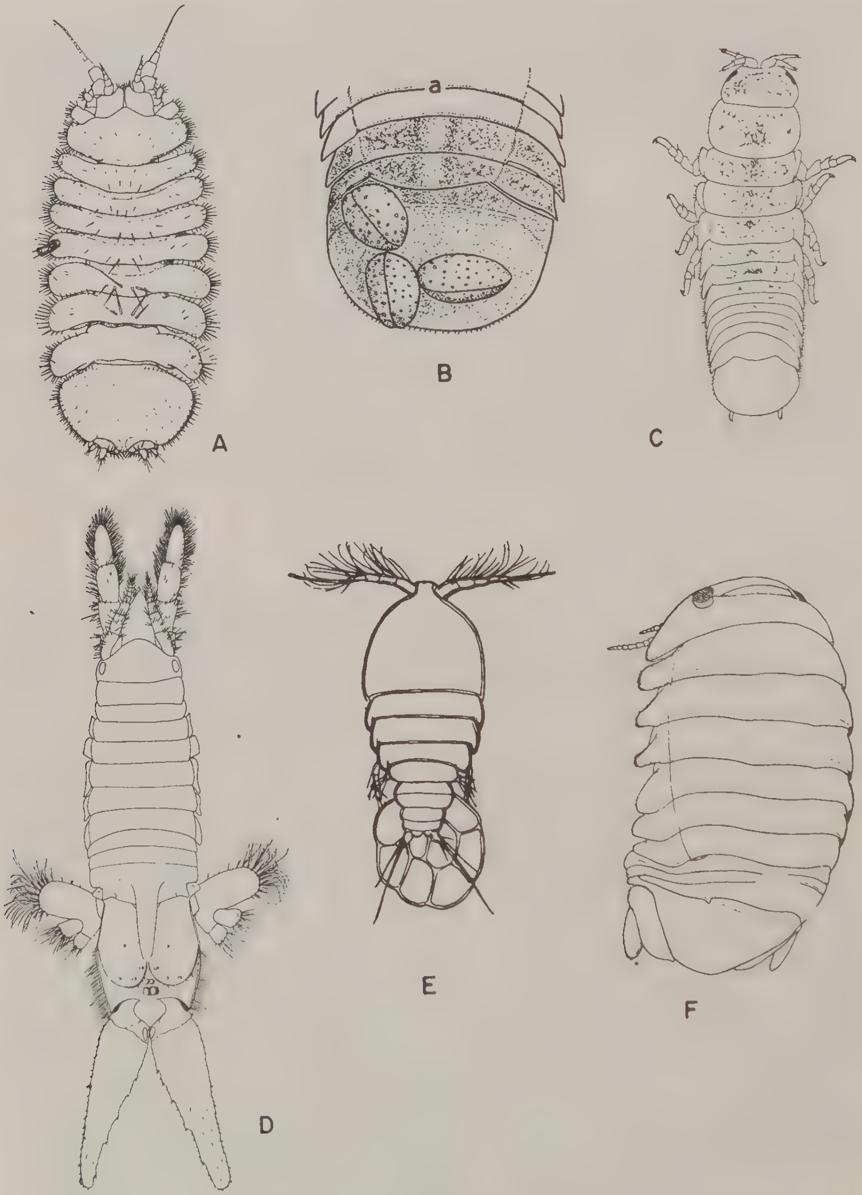

FIGURE 5. Crustaceans associated with *Limnoria* burrows. A, *Caecijaera* (after Menzies, 1951). B, *Aspidoconcha* (after DeVoss, 1953). C, *Limnoria* (after Shiino, 1950). D, *Chelura* (after Barnard, J. L., 1950). E, *Donsiella* (after Stephensen, 1935). F, *Gnorimosphaeroma* (after Menzies, 1954).

GENERAL MORPHOLOGY

Recognition of *Limnoria* cannot always be based on the removal of specimens from holes in wood. At times the burrows are occupied by secondary invaders, such as the amphipod *Chelura,* isopods like *Sphaeroma,* or such commensals with *Limnoria* as *Caecijaera.* These associated animals are shown in Figure 5. The amphipod *Chelura* is so abundant at times that it often has been considered more dangerous than *Limnoria* and once was mistaken for *Limnoria* in an important article concerned with the prevention of damages by borers (Clavenad, 1879, pp. 73-144). As far as is now known, it appears that *Chelura* is of minor importance, being secondarily but invariably associated with *Limnoria* in nature. Species of the genus *Sphaeroma* which do little damage in the northern hemisphere seem to have caused extensive damage to wood in Australia (Iredale, Johnson, and McNeill, 1932, pp. 21-22).

Like all isopods, the body of *Limnoria* is divisible into three major regions, the cephalon or head, the peraeon or body (also thorax), and the posterior area, the pleon or abdomen (Figure 6).

The cephalon is recognizable as the globular area bearing the eyes and the following paired appendages, going from front to rear, first antennae, second antennae, mandibles, first maxillae, second maxillae, and those covering the mouth area externally, the maxillipeds.

The peraeon consists of seven ring-like segments (somites) each of which bears a pair of *peraeopods* (or legs). In the maturing and adult female each of the first four pair of peraeopods has a leaf-like extension at its inner (medial) base called an *oostegite.* Collectively the interleaving oostegites of the egg-bearing female (gravid female) form the brood pouch (also called marsupial pouch). Each peraeopod has seven articles. The elongate article nearest the animal's body is called the *basis*; those following are called successively the *ischium, merus, carpus, propodus,* and *dactyl.*

The terminal body area or peraeon consists of five small ring-like somites each of which bears a pair of leaf-like plates, the gills or *pleopods,* and a large semicircular plate-like segment, the *pleotelson* which laterally bears the *uropods.*

The amphipod *Chelura* may be distinguished easily from *Limnoria* by the fact that it has only three pairs of pleopods. The isopod *Sphaeroma* has only three segments to its abdomen and not six as does *Limnoria.* The isopod *Caecijaera* besides being blind and much smaller than *Limnoria* has only two segments comprising its abdomen.

Other associated organisms are so greatly different from *Limnoria* that a misinterpretation of them as the gribble seems unlikely.

CHARACTERS OF SYSTEMATIC UTILITY

Diagnostic characteristics, those relatively constant for each species, are found on several areas of the body.

The first antenna has a prominent scale (actually a rudimentary branch) in the genus *Paralimnoria,* (p. 147), which is either reduced

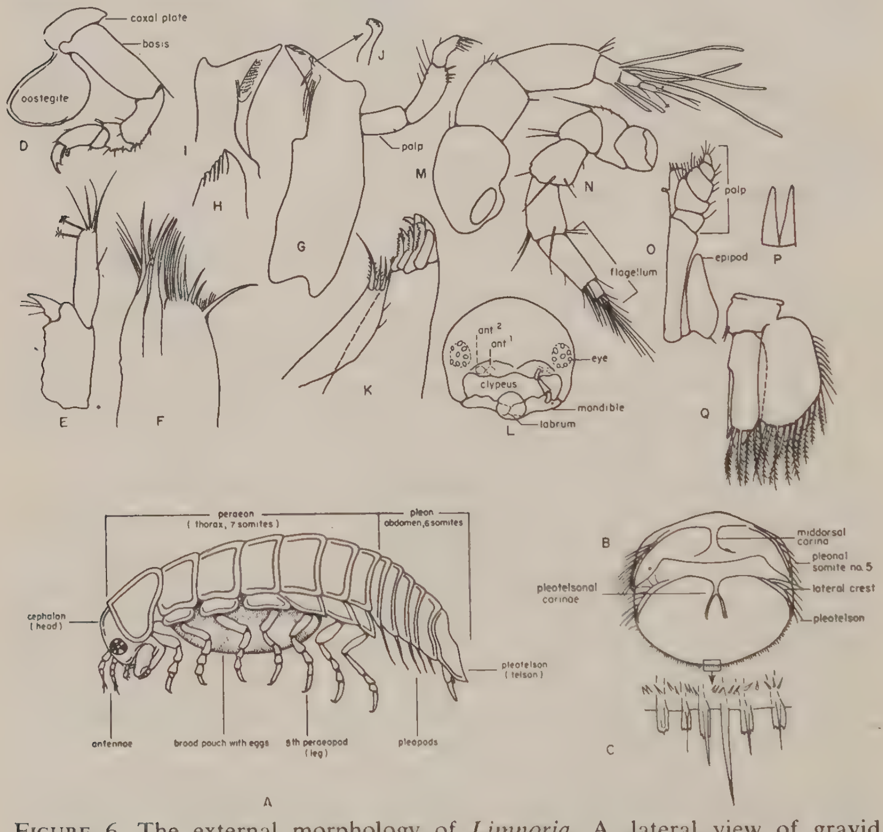
coxal plate
basis
oostegite
D
I
J
palp
M
N
palp
O
epipod
P
flagellum
H
G
E
F
K
ant 2
ant 1
eye
clypeus
mandible
labrum
L
Q
peraeon (thorax, 7 somites)
pleon abdomen, 6 somites
cephalon (head)
pleotelson (telson)
antennae
brood pouch with eggs
5th peraeopod (leg)
pleopods
A
B
middorsal carina
pleonal somite no. 5
lateral crest
pleotelsonal carinae
pleotelson
C

FIGURE 6. The external morphology of *Limnoria.* A, lateral view of gravid female (after G. O. Sars, 1897, and Menzies, 1954). B, Fifth pleonal somite and pleotelson. C, posterior border of pleotelson highly magnified. D, Leg of gravid female with attached oostegite. E, Uropod. F, First maxilla. G, right mandible of wood-borer. H, incisive part of right mandible of wood-borer, showing "file." I, Left mandible of wood-borer showing "rasp." J, Lacinioid seta of right mandible. K, Second maxilla. L, Frontal view of head. M, First antenna. N, Second antenna. O, Maxilliped. P, Penes (genital appophyses). Q, Second pleopod of male.

or absent in the genus *Limnoria* (sensu lato). The flagellum of the second antenna (Fig. 6) has four articles in some species (e.g. *L. (L.) pfefferi*) and five in others, (e.g. *L. (L.) lignorum*) or even six in *Paralimnoria*.

The mandible presents several important characteristics. The palp in all the species discussed herein has three articles (Fig. 6); whereas, in other species such as *L. (L.) segnis* Chilton (New Zealand) it has but two articles. The incisive process of each mandible bears a "rasp" and "file-like" series of grooves and teeth in the subgenus *Limnoria* (Fig. 6) and the genus *Paralimnoria*. These are lacking in the subgenus *Phycolimnoria*. The inner surface of the right mandible bears a lacinioid bristle or seta which is apparently distinctive for each species.

The epipod of the maxilliped (Fig. 6) has a shape and length peculiar to each species. In *L. (L.) lignorum* (Rathke) it does not quite reach to the articulation of the palp with the maxilliped; in other species it often extends farther.

The dorsal surface of the fifth somite of the pleon often has carinae (ridges) middorsally (*L. (L.) lignorum*) or elevated areas (*L. (L.) tripunctata*) or no ornamentation (*L. (L.) platycauda*) at all.

The dorsal surface of the pleotelson presents a multitude of useful characteristics. It can have rugosities (*L. (P.) algarum*) or be virtually smooth (*L. (L.) platycauda*). In some cases its margin has tuberculations (*L. (L.) tripunctata*) or no tuberculations, (*L. (L.) quadripunctata*). The setae or bristles fringing the posterior (distal) margin of the pleotelson are unique in their structure (microscopic) and arrangement. They consist only of simple closely set spike-like setae in *L.* (*P.*) *algarum* (p. 146), whereas they are delicate, often compound, and separated from one another in *L. (L.) tripunctata*. The lateral crests (Fig. 6) of the pleotelson have some characteristic tuberculations and setae.

In the species of the genus *Paralimnoria* the branches (*rami*) of the uropods are elongate and each taper to a point distally. On the other hand, the outer branch of the uropods (*exopod*) of *Limnoria* (sensu lato) is short and claw-like while the inner branch is elongated and not pointed, but blunt, at its apex.

SYSTEMATICS

As is so often the case with animals of economic importance, *Limnoria* has had a varied history regarding its classification and relationships. When first formally described, it was included within the genus *Cymothoa* (Rathke, 1799), a genus which today contains only fish parasites. In 1813 Leach described the genus *Limnoria*. This genus Leach placed in the family Cymothoidae of the tribe Asellides. According to Leach the tribe Asellides contained two additional families, the Anthuridae and Asellidae. The Cymothoidae then contained three genera, *Cymothoa, Limnoria* and *Sphaeroma*, each of which constitutes the type genus of a distinct family today. Subsequent to Leach (op. cit.), *Limnoria* has occupied a place in three other families. It was placed in the family Asellidae by White (1847, pp. 96-97) along with *Apseudes, Rhoea (=Tanais), Asellus, Jaera, Munna,* and *Oniscoda (=Janira)*. Today *Apseudes* and *Tanais* are not considered isopods while the other genera belong to the suborder Asellota. A few years later White (1850, p. 68; 1857, p. 226) erected the family "Limnoriadae" for *Limnoria, Asellus, Jaera, Munna,* and *Janira*. Bate and Westwood (1868, p. 313) continued White's classification of the Asellidae in a peculiar and unusual way by recognizing the differences noticed by White, but by instituting a new name for the Apseudidae, e.g. the Tanaidae, and by disregarding the name "Limnoriadae"; however, remarking that Leach had earlier considered *Limnoria* to form a "separate class amongst his Cymothoades."

Harger (1880, pp. 371-373) was the first to consider *Limnoria* the type of a unique family, the Limnoriidae. He was, however, uncertain of this placement because he writes, "I have preferred to constitute a new family for the genus, which has, however, evident relations with the Sphaeromidae, and perhaps should yet be united with that family." This Gerstaecker (1881) does, and without mention of his system as new he places *Limnoria* in the Limnorina group of the family Sphaeromidae. Hansen (1905, p. 98) is more emphatic about the relationship and considers *Limnoria* as belonging to the subfamily Limnoriinae of the family Sphaeromidae.

Subsequent investigators seem to have followed Harger or Hansen without questioning the merits of either system.

Harger (1880, pp. 371-373) effectively demonstrated that *Limnoria* was much more like *Sphaeroma* than any of the Asellota. Curiously, neither Hansen nor Harger compared *Limnoria* with *Cirolana*. It appears that both were misled into believing *Sphaeroma* and *Limnoria* were related because both roll into a ball when disturbed. Actually they accomplish this feat with entirely different methods. In *Limnoria* the head slides under the anterior margin of the first peraeon-

TABLE 1.

Comparison of Groups Related to *Limnoria*

Characteristic	Cirolanidae *Cirolana*	Cymothoidae *Cymothoa*	Sphaeomidae *Sphaeroma*	Limnoriidae *Limnoria*
1. Head with dorsal occipital groove	Present	Absent	Present	Present
2. Eye location	Dorsal	Dorsal	Dorsal	Lateral
3. Clypeus	Two pieces	Single piece	Single piece	Single piece
4. First Antenna anterior (dorsal) to second	Yes	Yes	Yes	No (antennae on a line with each other)
5. Antennal scale in Adult	None	None	None	Present
6. First Maxilla	Bilobed	One lobe	Bilobed	Bilobed
7. Molar process of mandible	Compressed but large	Reduced	Large	Absent
8. Lacinia mobilis on mandible	Present	Present	Present	Absent
9. Setal row on mandible	Present	Absent	Present	Present
10. Maxilliped with epipod	Present	Absent	Absent	Present
11. Maxillipedal palp with	Five articles	Less than five articles	Five articles	Five articles
12. Coxal plates separate from body	Always	Always	Seldom	Always
13. Number of digestive caeca	Six	Six	Six	Four
14. Sexes	Separate	Protandric	Separate	Separate
15. Testis	Trilobed	Trilobed	Trilobed	Unilobed
16. Separate somites comprising the pleon	Six	Six	Three	Six

al somite; whereas in *Sphaeroma* the head overrides the first peraeonal somite. Furthermore, *Sphaeroma* bends mostly between the peraeon and pleon; whereas *Limnoria* bends on either side of the fourth peraeonal somite while enrolling.

In Table 1 is shown a comparison of major characteristics which illustrate the differences and similarities between the families Cirolanidae (as exemplified by *Cirolana*), the Cymothoidae (e.g. *Cymothoa*), the Sphaeromidae (e.g. *Sphaeroma*) and the genus *Limnoria*. The table indicates that *Limnoria* shares more characteristics (eight of those considered) in common with the Cirolanidae than with any of the other families. It does, however, show marked differences from the other families and accordingly it is suggested that the familial status of *Limnoria*, the Limnoriidae, be retained but without the reservation suggested by Harger.

Order ISOPODA
Suborder *FLABELLIFERA*
Family LIMNORIIDAE Harger, 1880, emended

Synonymy:

Limnoriidae Harger 1880, pp. 371-373. — Dahl, 1916, p. 28. — Pfeffer, 1887, p. 60.—Richardson, 1904, p. 8; 1905, p. 268.— Sars, G. O., 1897, pp. 75-76.—Shiino, 1950, p. 334.—Stebbing, 1905, p. 713.—Vanhöffen, 1914, p. 508.—Zirwas, 1911, p. 86.

Limnoriadae White, 1850, p. 68 (and synonyms); 1857, p. 226.

Asellidae (part), White, 1847, p. 96, 1857, pp. 225-227. — Bate and Westwood, 1868, pp. 349-350.

Sphaeromidae (part), Gerstaecker, 1881-1883, p. 220, *Limnorina* group.

Limnoriinae Hansen, 1905, p. 98 (see also pp. 75, 83, 92-94, 100, 115); 1916, p. 177.—O. Cooper and Rawson, 1934, pp. 28-30.

Diagnosis. Cephalon ovoid in cross section. Eyes lateral. Clypeus consisting of a narrow, transversely elongated, undivided piece, lacking projections in its outer surface. Antennae separated along mid-line; not contiguous at the base. First and second pairs of antennae nearly in a transverse line, neither one markedly more anterior than the other. Obvious scale present on first antennae. Mandible lacking lacinia mobilis and molar process. Posterior part of cephalon slips under anterior margin of first peraeonal somite. Sexes separate. Penis (genital appophyses) consisting of a pair of elongate plates which articulate with the body. Only four digestive caeca (glands) present. Testes each with one lobe. Coxal plates present on peraeonal somites two to seven. Uropodal branches tubular (or claw-like), not expanded and flattened. Maxilliped with an epipod and a pentarticulate palp. Pleon consisting of five somites plus a large semicircular pleotelson.

Composition. Previously the family was considered to have only one genus, *Limnoria*. This genus, however, may be conveniently split into

(390)

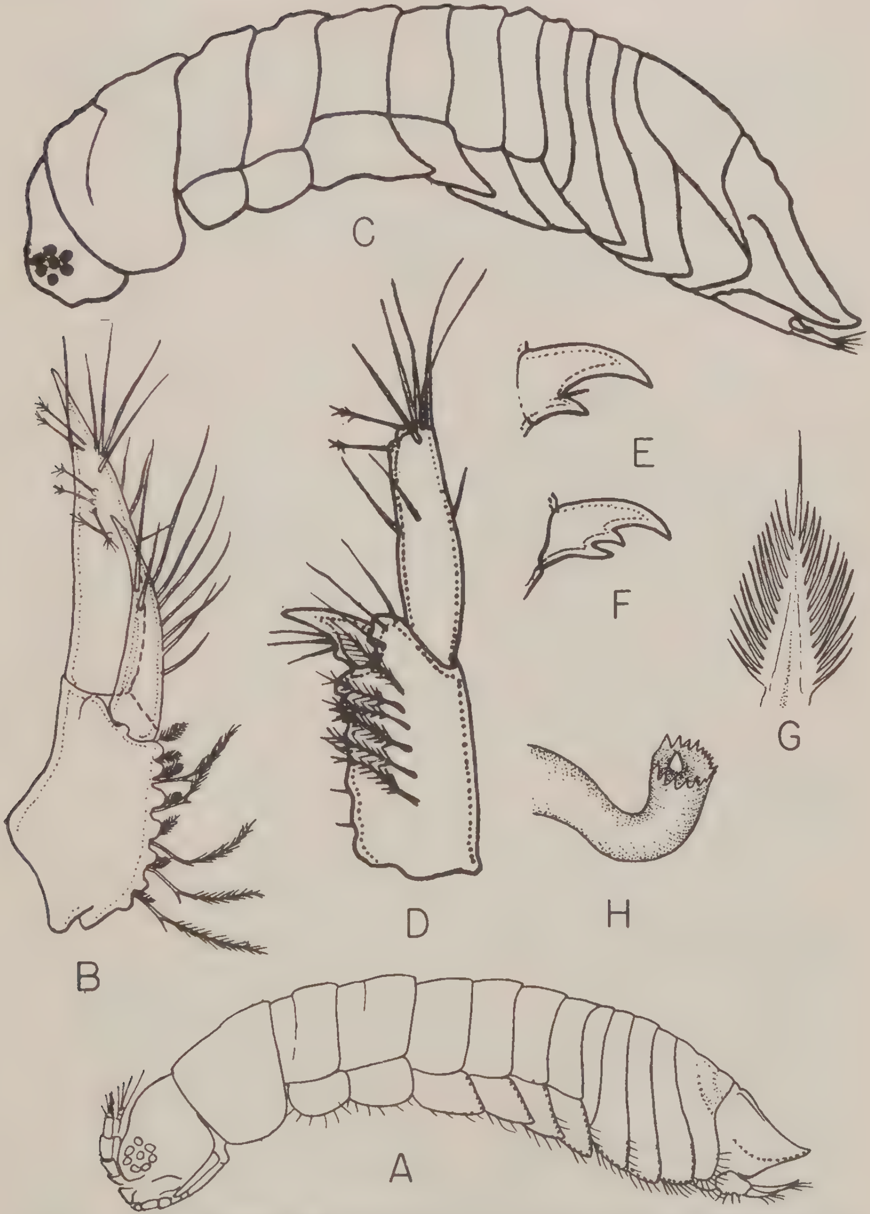

FIGURE 7. The distinguishing features of the genera of the Limnoriidae. A, *Paralimnoria,* lateral view. B, Uropod of *Paralimnoria.* C, *Limnoria,* lateral view. D, Uropod of *Limnoria.* E, Dactyl of first peraeopod of *Limnoria.* F, Dactyl of first peraeopod of *Paralimnoria.* G, Peculiar setae of peduncle of uropod of *Paralimnoria.* H, Lacinioid seta of mandible of *Paralimnoria.*

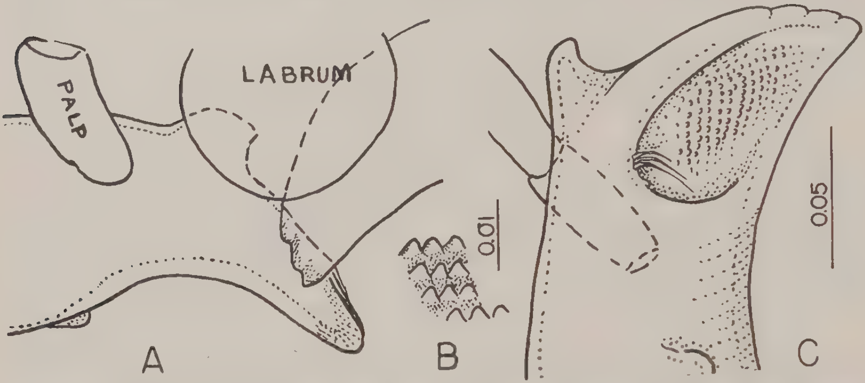

FIGURE 8. Mandibles of *Paralimnoria*. A, frontal view. B, "rasp" on inner surface of left mandible. C, inner surface of left mandible.

two genera, *Limnoria* Leach and a new genus *Paralimnoria*, which is herein described. The former genus may be further divided into two coordinate groups or subgenera; *Limnoria* (sensu stricto) containing only wood-boring species, and *Phycolimnoria* containing only algal-boring species. The distinguishing morphological characteristics between these divisions are shown in the following key and in Figures 7 and 8.

KEY TO THE GENERA AND SUBGENERA OF THE FAMILY LIMNORIIDAE

1. Branches of uropods dissimilar; exopod short, claw-like; endopod long and apically blunt. . . . . 2. Genus *LIMNORIA* (p. 121)

1. Branches of uropods similar; exopod and endopod elongate and each with an apical claw. . . . . Genus *PARALIMNORIA* (p. 147)

2. Incisor of right mandible with file-like ridges on upper surface; that of left with a rasp-like arrangement of strongly sclerotized scales. . . Subgenus *LIMNORIA* (p. 122)

2. Incisors of mandibles simple, lacking "rasp" or "file." . . . . . . Subgenus *PHYCOLIMNORIA* (p. 144)

CHARACTERIZATION OF GENERA, SUBGENERA, AND SPECIES

The systematics of isopods is currently so unstable, as compared with other orders of the Crustacea such as the Decapoda, that even modern descriptions have been necessarily long. Accordingly, it is believed that a general statement of the method used here is needed.

In the descriptions which follow of genera and species, none of the characteristics already mentioned in the diagnosis of the family will be repeated. Descriptions of species will similarly be treated without repetition of generic characteristics. The diagnoses are kept as parallel as possible to facilitate comparisons.

Genus *Limnoria* Leach, 1813 (1814)

Synonymy:

Limnoria Leach, 1813, p. 433. — Bate and Westwood, 1868, p. 351.—Coldstream, 1836, pp. 316-334.—Harger, 1880, p. 373.—Hansen, 1905, pp. 98-100.—Hoek, 1893, pp. 1-97.—Nierstrasz, Schuurmans, and Stekhoven, 1930, p. Xe 79.—Richardson, 1905, pp. 269-270.—Sars, G. O., 1897, pp. 76-77.

Lemnoria Humphreys, 1845, p. 22.

Lunovia Fox, 1878, pp. 189-194.

Diagnosis. Flagellum of first antennae with four articles. Flagellum of second antenna with three, four or five articles. Mandibular incisor with or without "rasp" and "file." Lacinioid seta of right mandible always flattened, never tubular, and with apex of variable structure. Exopod of uropod much shorter than endopod and provided with an apical claw; endopod elongate, apex blunt, lacking claw. Fifth pair of pleopods lack marginal setae.

The list of synonyms given above is by no means a complete list of references to the genus by name. It is, on the other hand, a complete list of papers which characterize the genus, alter its characteristics, or presented different spellings of the name.

The first reasonably comprehensive diagnosis of the genus was given by Sars (1897, pp. 76-77). This was slightly altered by Hansen (1905, p. 100). Since then the concept has not changed. The diagnosis given here, except for emphasis on the characteristics which separate *Limnoria* (sensu lato) and *Paralimnoria* (p. 147), is very close to that given by Sars (op. cit.), Hansen, (op. cit.) and Richardson (1905, pp. 269-270).

Remarks. Previous writers attached no importance to the variation in the number of articles comprising the flagellum of the antennae. Harger (1880), in fact, was not certain it was multiarticulate. This characteristic is important in separating the genus *Paralimnoria* from *Limnoria* (sensu lato) and is useful further in characterizing various species of *Limnoria*.

The genus *Limnoria* contains two subgenera, *Limnoria* (sensu stricto) and *Phycolimnoria*. Examples of these are found in all the major oceans of the world, except in truly Arctic or Antarctic areas where wood or large sea-weeds are lacking.

Subgenus *Limnoria*, comb. nov.

Diagnosis. Members of the genus *Limnoria* (sensu lato) which have a "rasp" and "file" arrangement of scales and ridges on the incisive process of the mandibles. The species are all wood-borers.

Type species. *Limnoria (Limnoria) lignorum* (Rathke)

Besides having a "rasp" and "file" on the mandibles, the species of this subgenus differ ecologically from the members of *Phycolimnoria* in being able to burrow into wood. They are able to burrow into agar and presumably could burrow into kelp; however, they have not been found in kelps in nature. Most known species are inhabitants of the intertidal zone, but the record of *L. (L.) japonica* Richardson, collected from 163 fathoms from off Japan indicates that deep water species might be more abundant than has been generally believed. Seven species, including three new species, are considered in this paper. All currently known and valid species except *L. (L.) septima* Barnard, 1936, pp. 174-175, (Indian Ocean), and *L. (L.) japonica* Richardson, 1909, pp. 95-96 (Misaki Light, Japan) are described herein (see part II, p. 164.)

KEY TO THE NORTHERN AND CENTRAL AMERICAN SPECIES OF THE SUBGENUS *Limnoria*.

1. Dorsal surface of distal border of pleotelson tuberculate (Fig. 16) . . . . 2.

1. Dorsal surface of distal border of pleotelson smooth, not tuberculate (Fig. 10) . . . . 4.

2. Flagellum of second antenna with four articles. Dorsal surface of pleotelson smooth with no elevated tubercles or ridges except at the tuberculate margin . . . . *L. (L.) platycauda* (p. 139)

2. Flagellum of second antenna with five articles. Dorsal surface of pleotelson with elevated tubercles or carinae . . . . 3.

3. Dorsal surface of proximal area of pleotelson, neither punctate nor rugose but with a single median tubercle followed distally by a pair of tubercles . . . . *L. (L.) tripunctata* (p. 137)

3. Dorsal surface of proximal area of pleotelson punctate and rugose, with at least a pair of tubercles, one on either side of midline, each followed by a carina . . . . *L. (L.) saseboensis* (p. 141)

4. Flagellum of second antenna with four articles. Pleotelson with two or no tubercles . . . . 5.

4. Flagellum of second antenna with five articles. Pleotelson dorsally with four tubercles . . . . . . *L. (L.) quadripunctata* (p. 127)

5. Epipod of maxilliped widest near distal end . *L. (L.) pfefferi* (p. 135)
5. Epipod of maxilliped widest near proximal end . . . . 6.
6. Dorsal surface of pleotelson with λ-shaped carina on midline . . . . *L. (L.) lignorum* (p. 123)
6. Dorsal surface of pleotelson medially with a pair of tubercles . . . . *L. (L.) simulata* (p. 144)

Limnoria (Limnoria) lignorum (Rathke)

Figure 9

Synonymy:

Cymothoa lignorum etc., Rathke, 1799, pp. 101-104, pl. III, figs. 14a-14d.

Limnoria terebrans Leach, 1813, p. 433.

Limnoria lignorum (Rathke), White, A., 1857, pp. 227-230. pl. XII, figs. 5.—Black and Elsey, 1948, pp. 1-29.—Calman, 1898, p. 261.—Fee, 1926, pp. 27-28.—Fraser, 1923, pp. 159-167.—Guberlet, 1936, p. 337, photograph, p. 336.—Hatch, 1947, pp. 211-212, fig. 81 (part).—Henderson, 1924, pp. 1-17.—Johnson, 1935, pp. 427-438, tab. 1-4.—Johnson and Miller, 1935, pp. 10-12, 17.—M'Gonigle, 1925, pp. 1-67.—Stafford, 1912, pp. 52, 60. —White, F. D., 1929, pp. 9-18.

Limnoria tenebrans Leach, Richardson, 1905, p. 269 (in part, a misspelling of *terebrans*).

Diagnosis. Scale of first antenna evident. Flagellum of second antenna with four articles. Epipod of maxilliped triangulate, about two and three-quarters times as long as wide, not quite reaching the articulation between palp and endopod. Mandibular palp with three articles. Fifth somite of pleon with a mid-dorsal longitudinal carina. Pleotelson with an anteriorly situated mid-dorsal longitudinal carina which bifurcates posteriorly and lacks tubercles. Posterior margin of telson lacks tubercles but has a dorsal fringe of spike-like bristles. Lateral crests of pleotelson slightly tuberculate. Lacinioid seta of right mandible with apex complex, trifid, and abruptly bent.

Type locality. Norway, probably Bergen (Rathke, 1799). Type specimens are not known to exist.

Measurements. The size of this species varies considerably. It is one of the largest of the wood-boring species, especially in the northern and colder regions of its range. A female of average size from Kodiak, Alaska was 3.5 mm in length and 0.8 mm in pleotelsonic width.

Remarks. The original description of *Cymothoa lignorum* by Rathke (1799, pp. 101-104, pl. III, figs. 14a-14d) presents one important nomenclatural problem. The description *per se* is polynomial and not binomial. The figure (part of the description in the broad sense) is given a binomial label. Subsequent writers have wisely considered, therefore, that Rathke satisfied the requirements of the Linnaean system of nomenclature. Linnaeus appears to have been unaware of *Limnoria*, but it is interesting to note, as Dahl (1916, p. 29) points

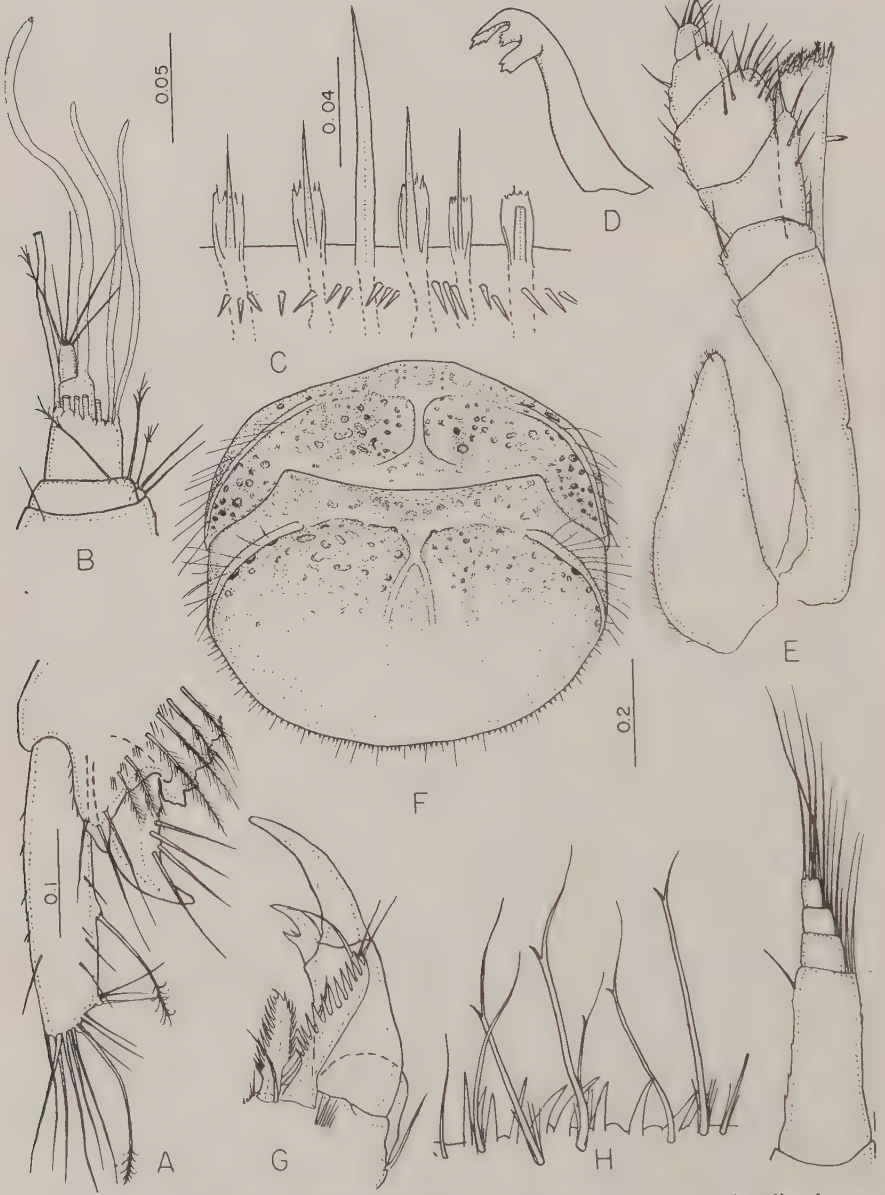

FIGURE 9. *Limnoria (L.) lignorum* (Rathke), topotypic male. A, distal parts of uropods. B, distal article of first antenna. C, apex of pleotelson. D, lacinioid seta of right mandible. E, maxilliped. F, pleotelson. G, distal parts of first peraeopod. H, lateral crest of pleotelson. I, flagellum of second antenna. Figures with similar magnification, A, E; B, G, H, I; C-, D-, F.

out, that Linnaeus' (Syst. Nat. ed. 10, 1758, p. 637) description of *Oniscus marinus* "semicylindricus, cauda ovato-oblonga integra," applies better to *Limnoria lignorum* (Rathke) than to the species known today by the name *Jaera marina* (Linne). Dahl (op. cit.) seems reasonably certain that Linnaeus had seen neither *L. lignorum* nor *J. marina* but, perhaps, a species of *Idothea.*

That the species *Cymothoa lignorum* Rathke belonged to the genus *Limnoria* Leach was recognized by White (1857, pp. 227-230, pl. XII, fig. 5) who considered Leach's species *L. terebrans* a synonym of Rathke's *lignorum*. Unfortunately, several writers subsequently cited the species as *"Limnoria lignorum* White" in an apparent attempt to credit White with the new combination. Actually such a citation means that White and not Rathke described the species which is, of course, not the case.

Through the courtesy of Dr. Isabella Gordon of the British Museum (Natural History), I was able to examine seven specimens (cotypes) of Leach's *Limnoria terebrans* collected from the Bell Rock lighthouse, Scotland, by Robert Stevensen in 1807. These specimens have been compared with over 200 specimens of *Limnoria (L.) lignorum* (Rathke) from Trφmso, Kristiansund, Flφdvigen, Rong, and Klosterelu Fjord in Norway and appear identical with Leach's specimens. White's (op. cit.) union of *terebrans* with *lignorum* accordingly is substantiated. This is a matter of considerable taxonomic importance in view of Holthuis' (1949, pp. 167-172) discovery of *Limnoria (L.) quadripunctata* in Holland where, however, *Limnoria (L.) lignorum* appears to be the common and indigenous species.

The figures and description given this species by Sars (1897, pp. 76-77, pl. 31) are outstanding and have been reproduced freely by subsequent investigators, including myself (Fig. 6A). Unfortunately Sars failed to notice the carinae on the dorsal surface of the pleotelson and the distinctive number of articles of the antennal flagellum, but beyond that he omitted few details. There is no real utility in enumerating errors in the descriptions and figures given by Leach and Rathke except to point out that both investigators figured the body of the animal as having more somites (segments) than it actually has. Detailed structures were even less accurately delineated.

Material examined. Including those mentioned above from Europe, the following specimens were examined from localities in North America:

Atlantic Coast

Newfoundland. *Argentia,* April 1, 1949, 6 specimens, W.F.C.L.

Nova Scotia. *Liverpool,* April 1, 1948, 8 specimens, December 1, 1949, 20 specimens, W.F.C.L.

Maine. *Casco Bay,* 1873, 9 specimens, U. S. Fish Commission, U.S.N.M. Cat. No. 2254. *Wicasset,* 1949, 7 specimens, W.F.C.L. *Fort Preble,* March 1949, 6 specimens, W.F.C.L. *Rockland,* 5 samples, 1948-1950, 47 specimens, W.F.C.L. *Portland,* 7 samples, 1949-1950, 76 specimens, W.F.C.L. *Southwest Harbor,* 5 samples, 1948-1950, 51 specimens, W.F.C.L.

New Hampshire. *Portsmouth,* 7 samples, 1948-1950, 59 specimens, W.F.C.L.

Massachusetts. *Boston,* 17 samples, 1948-1950, 174 specimens, W.F.C.L. *Quincy,* 2 samples, 1948, 1950, 12 specimens, W.F.C.L. *Salem,* 2 samples, 1948, 28 specimens, W.F.C.L. *Charleston,* 2 samples, 1948, 21 specimens, W.F.C.L. *Port Alleston,* January 1, 1950, 20 specimens, W.F.C.L. *Gloucester,* December 9, 1948, 5 specimens, W.F.C.L.

Rhode Island. *Newport,* April 8, 1949, 5 specimens, W.F.C.L.

Pacific Coast

Komandorski Islands, Bering Island, N. Grebnitski, no date, 75 specimens, U.S.N.M. Cat. No. 13081.

Alaska. *Adak,* 2 samples, 1948, 1950, 11 specimens, W.F.C.L.; 1950, 2 specimens, Charles H. Edmondson. *Dutch Harbor,* December 5, 1949, 9 specimens, W.F.C.L. *Kodiak,* February 16, 1949, 4 specimens, W.F.C.L.; 10 specimens, Charles H. Edmondson (date?). *Sitka,* March 9, 1949, 7 specimens, W.F.C.L.

British Columbia. *Victoria,* Departure Bay, Vancouver Isl., 1912, 1 specimen, Miss Pixell, British Museum (Natural History).

Washington. *Bellingham,* 2 samples, 1950, 12 specimens, W.F.C.L. *Hadlock,* March 18, 1949, 8 specimens, W.F.C.L. *Port Angeles,* 2 samples, 1949, 19 specimens, W.F.C.L. *Port Townsend,* 3 samples, 1948, 1950, 24 specimens, W.F.C.L. *Neah Bay,* 2 samples, 1949-1950, 22 specimens, W.F.C.L. *Friday Harbor,* 1949, 25 specimens, Dr. John L. Mohr. *Seattle,* December 6, 1948, 7 specimens, W.F.C.L.

Oregon. *Coos Bay,* Coos Co., August 1950, 23 specimens, Donald J. Reish.

California. *Samoa*, April 11, 1949, 2 specimens (with *L. (L.) quadripunctata*), W.F.C.L. *Point Arena*, 4 samples, 1948-1949, 40 specimens, W.F.C.L.

Geographical distribution. On the Pacific Coast the species extends from about 58°N (Kodiak Isl., Alaska) to 39°N (Point Arena, California). On the Atlantic Coast the distribution, as now known, appears restricted between 47°N (Argentia, Newfoundland) and 42°N (Rhode Island). Presumably it will be found farther north on the Atlantic side when more samples are available. It has been reported by Stephensen (1929) from Western Iceland (ca 63°N).

Factors associated with the distribution are discussed on p. 158.

Limnoria (Limnoria) quadripunctata Holthuis

Figures 10-14

Synonymy:

Limnoria quadripunctata Holthuis, 1949, pp. 167-172, fig. 2. — Menzies and Mohr, 1952, pp. 81-86.

Limnoria lignorum (Rathke). — Kofoid and Miller, 1927, p. 208, fig. 124 (not the remainder of the references and figures which might apply to other species).—MacGinitie, 1935, p. 703.—Schmitt, 1931, p. 217, fig. 41 (only this figure).

Diagnosis. Flagellum of second antenna with five articles. Epipod of maxilliped triangulate, not quite reaching the articulation between the palp and the endopod. Mandibular palp with three articles. Fifth somite of pleon dorsally with an x-shaped carina on mid-line. Pleotelson anteriorly with a pair of tubercles on mid-line followed by a similar pair of short distance from anterior pair. Each tubercle of posterior pair is followed by an indistinct longitudinal carina (especially evident in female specimens). Posterior margin of pleotelson dorsally lacks tubercles, spike-like bristles evident. Lateral crests of pleotelson lack tubercles. Lacinioid seta of right mandible expanded at apex which bears a fringe of serrations.

Type locality. North Sea coast of the Dutch province of Zuid-Holland between the villages of Katwijk and Noordwijk, not far from Leiden. October 24, 1948, S. Kroonenberg and L. B. Holthuis, more than 100 specimens (Holthuis, 1949, p. 172). The types are located in Rijksmuseum van Natuurlijke, Leiden.

Measurements. Length 3.0 mm; width 1 mm; (Holthuis, 1949, p. 167). Large female, length 3.4 mm, pleotelsonic width 1.0 mm.

Remarks. Holthuis' (1949) description is particularly good; however, a few points need elaboration and correction. The median carina of the fifth somite of the pleon is forked at both the anterior and posterior ends and not only at the anterior end. The eyes each have seven paired ocelli. The flagellum of the first antenna consists of five

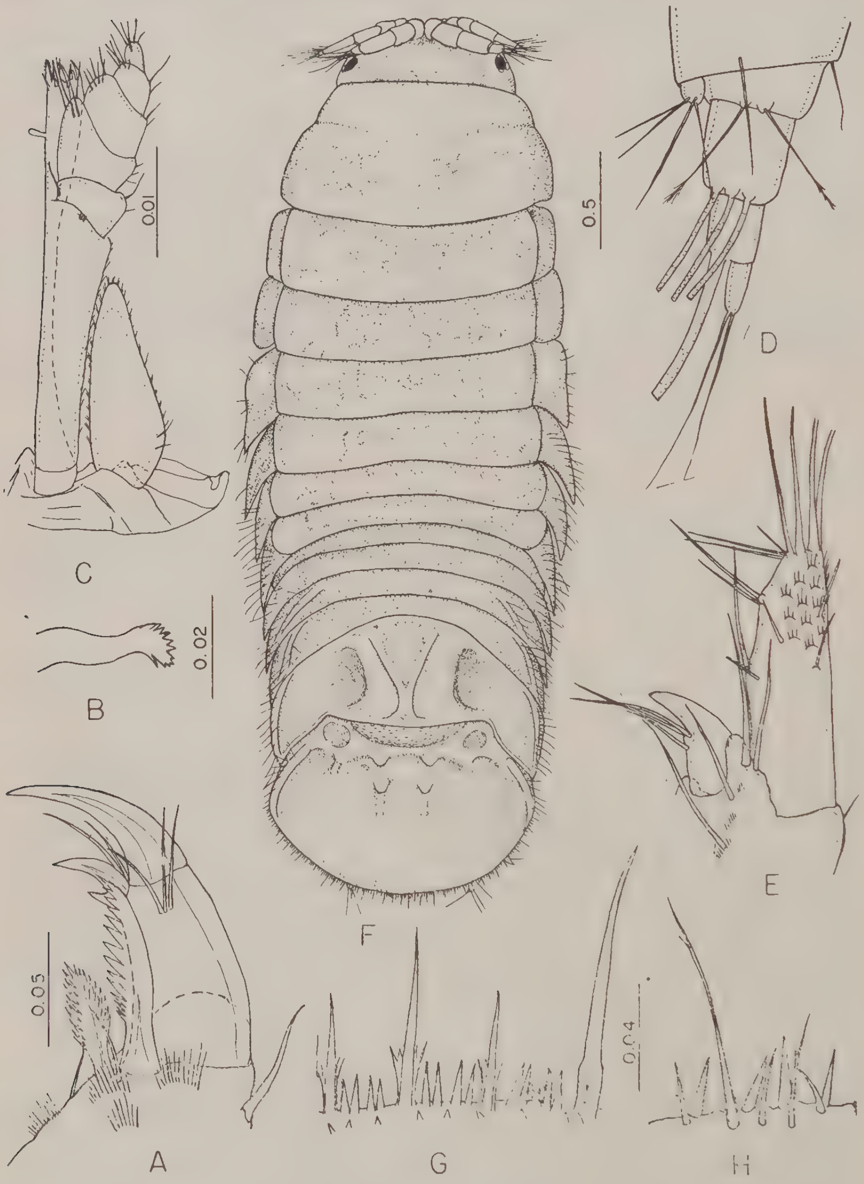

FIGURE 10. *Limnoria (L.) quadripunctata* Holthuis. A, distal part of first peraeopod. B, lacinioid seta of right mandible. C, maxilliped. D, distal articles of first antenna, note antennal scale. E, uropod. F, female, dorsal views, homoeotype. G, posterior edge of pleotelson. H, lateral crest of pleotelson. Figures with similar magnification, A, D, G, H; B; C; E; F.

(400

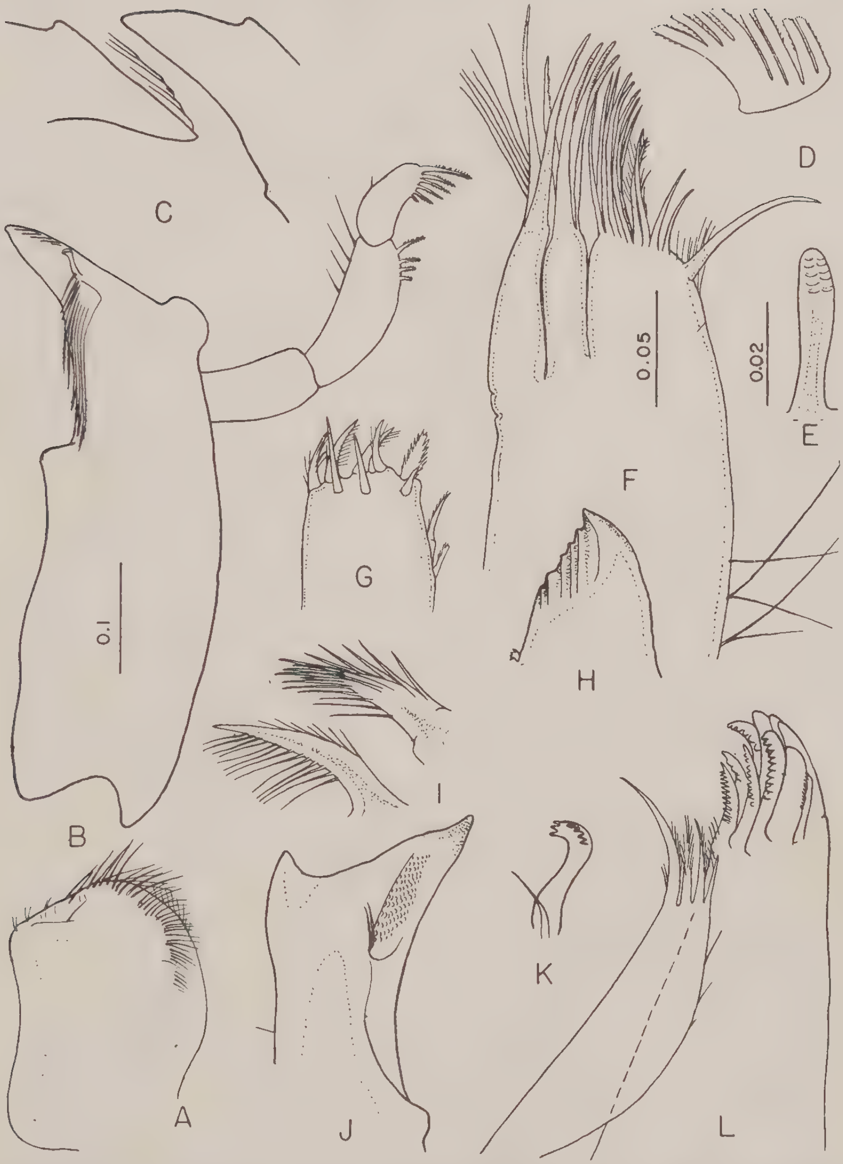

FIGURE 11. *Limnoria (L.) quadripunctata* Holthuis, mouth parts. A, labium, right. B, left mandible, inner surface. C, apices of left and right mandible *in situ,* showing functional relationship. D, setal row of left mandible. E, coupling hook. F, second maxilla. G, apex of endopod of maxilliped. H, upper (cutting surface) of incisive process of right mandible showing "file." I, peculiar setae at apex of endopod of maxilliped. J, inner surface, left mandible showing "rasp." K, lacinioid seta of right mandible. L, first maxilla. Figures with similar magnification, A, B, K, J; C, F, G, H, L; D, E, I, K.

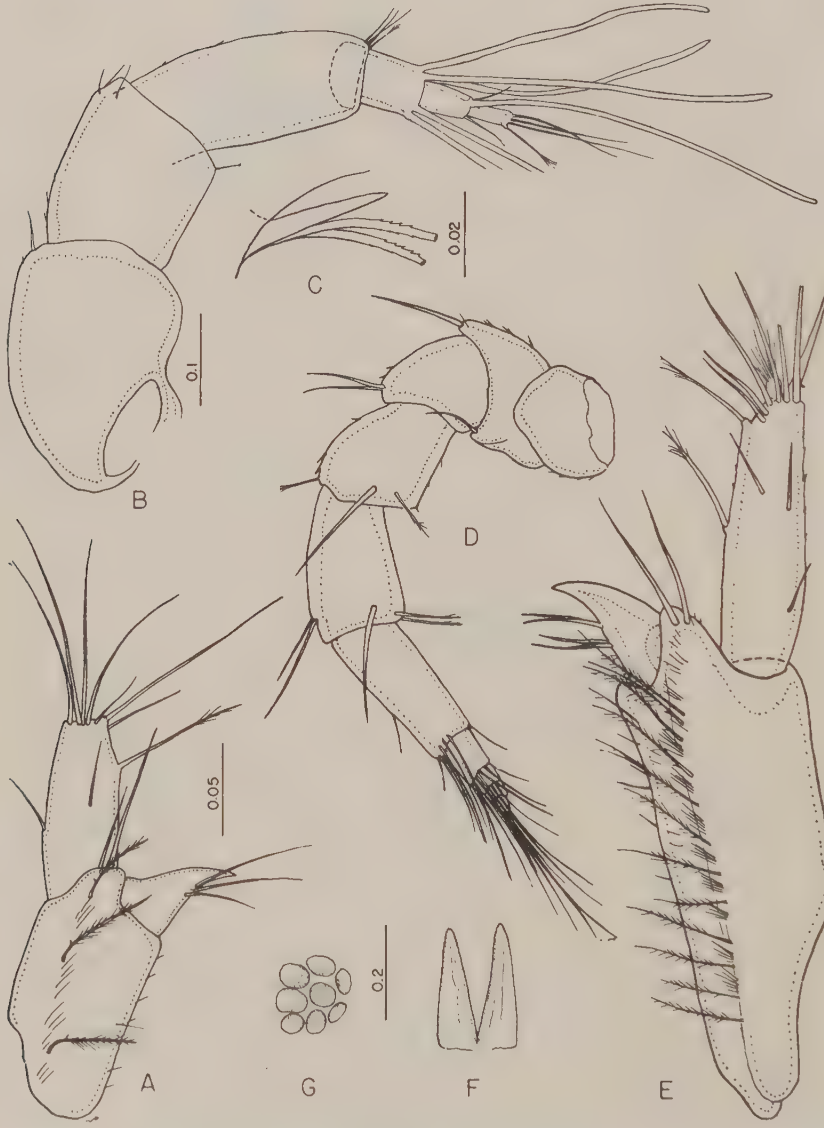

FIGURE 12. *Limnoria (L.) quadripunctata* Holthuis. A, uropod, juvenile, 1.0 mm length. B, first antenna. C, setal row of left mandible. D, second antenna. E, uropod. F, genital apophyses. G, eye, lateral view. Figures with similar magnification, A; B, D, E, F; C; G.

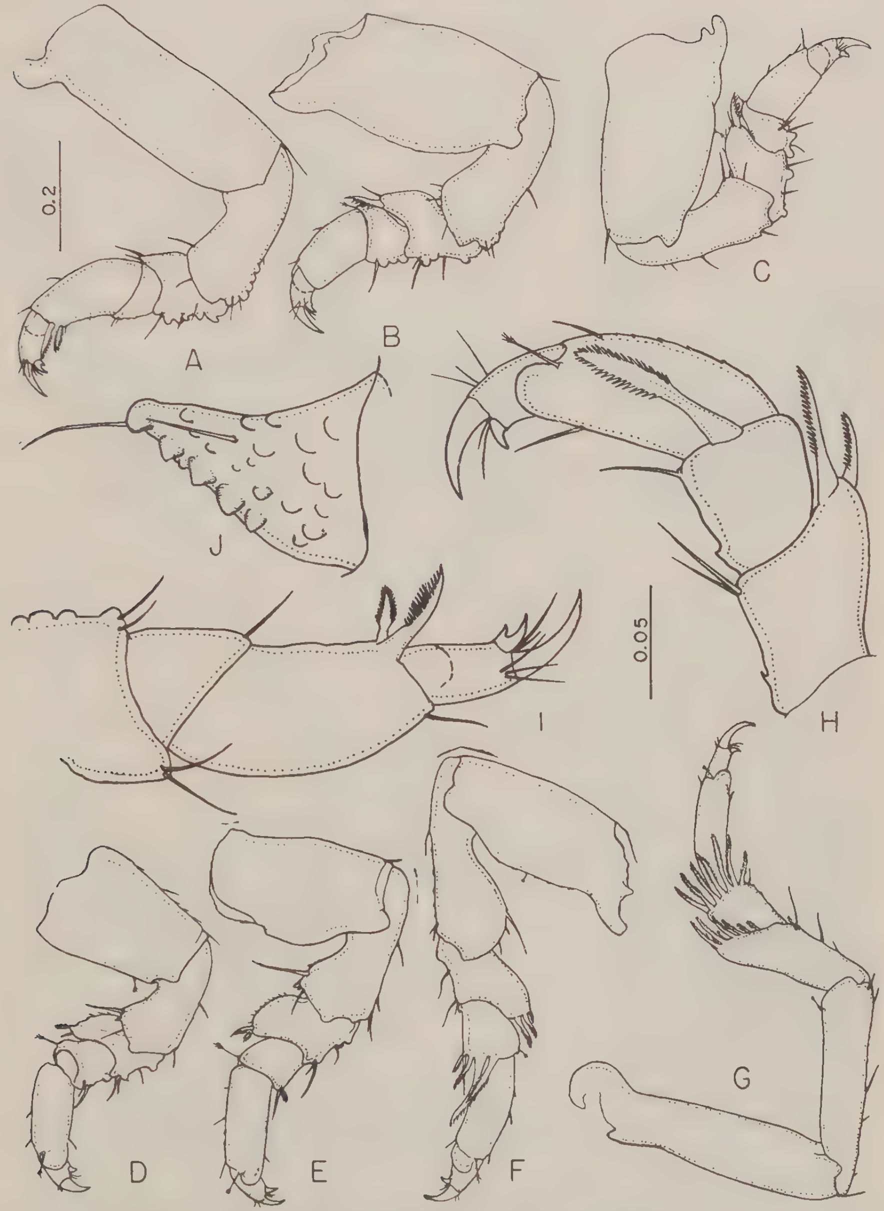

FIGURE 13. *Limnoria (L.) quadripunctata* Holthuis, peraeopods; A-G, in order, the first to seventh pair of adult. H, sixth of juvenile of 0.9 mm length. I, first of juvenile 0.9 mm in length. J, merus, outer surface, first peraeopod, adult. Figures with similar magnification, A-G; H-J.

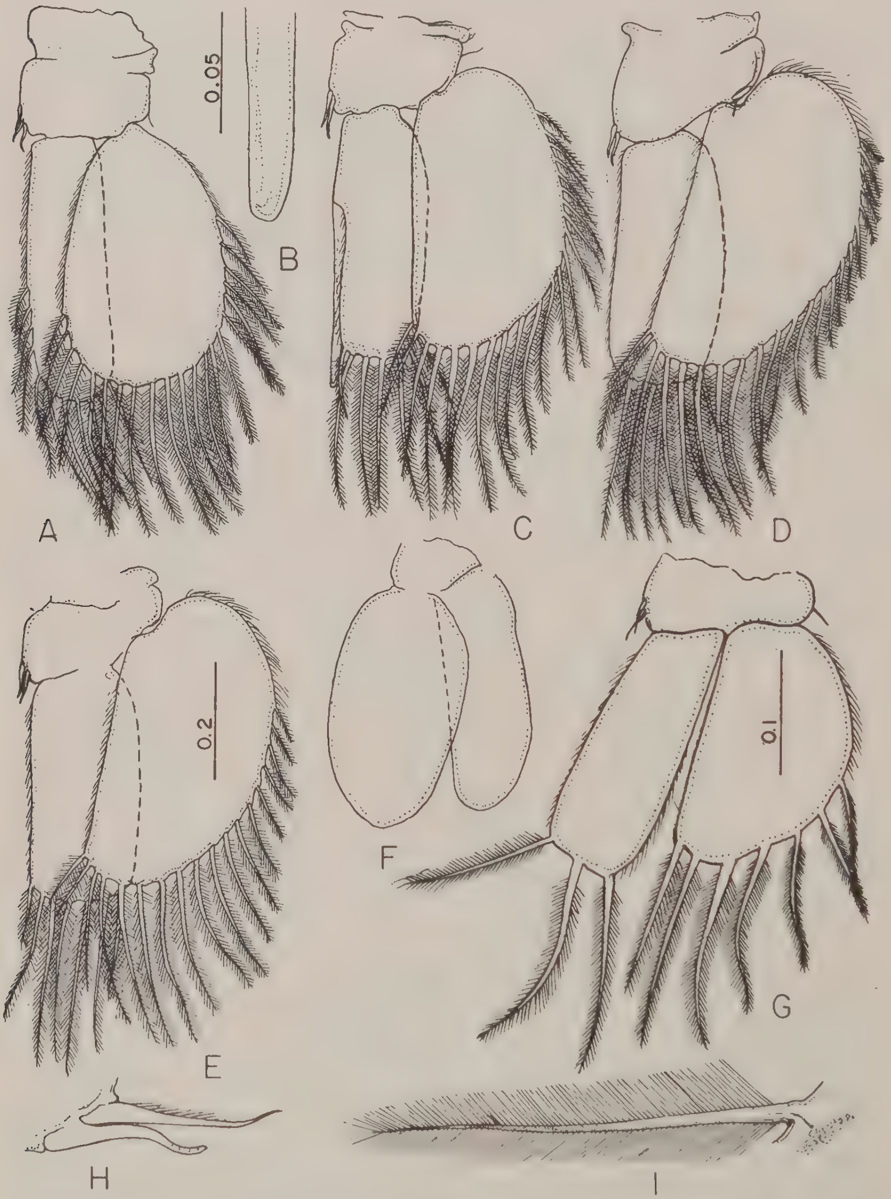

FIGURE 14. *Limnoria (L.) quadripunctata* Holthuis, pleopods. A-F, first to fifth of adult male. G, first, juvenile 0.9 mm length. H, accessory setae of sympod. I, plumose seta of pleopod. Figures with similar magnification, A, C, D, E, F; B, H, I; G.

articles and is thus unlike the quadriarticulate flagellum of *L. (L.) lignorum.* The maxillipedal epipod (Holthuis, 1949, p. 168, fig, 2e) is neither as short as figured nor is it shorter than that of *L. (L.) lignorum.* Each maxilliped has one coupling hook. The exopod of the uropod is not distinctly smaller than that of *L. (L.) lignorum,* but actually the two are very similar. The uropod is not similar to that of *L. (L.) septima* Barnard whose peduncle is markedly more elongate than that of *L. (L.) quadripunctata.*

Kofoid and Miller (1927, fig. 124) show, as Holthuis (op. cit.) pointed out. a clear series of photographs of *L. (L.) quadripunctata.*

Material examined. Including 15 specimens of Holthuis' type series, the following have been examined from the area under consideration:

Pacific Coast

California. *Samoa,* Humboldt Co., March 11, 1949, 10 specimens (with *L. (L.) lignorum*) W.F.C.L. *Bodega Harbor,* February and March, 1949, 61 specimens, R. J. Menzies and L. Miles. *Tomales Bay,* Nick's Cove, Vilich's Pier, Hamlet and Inverness, 1947-1949, 112 specimens, R. J. Menzies. *Duxbury,* April 12, 1949, 15 specimens, R. J. Menzies. *San Francisco Bay,* 1949-1950, several hundred specimens from Yerba Buena Isl., Belvidere, Parr-Richmond Pier, Aquatic Park, India Basin, Hunter's Point, Tiburon, N.W. Pac. R.R. ferry landing, Sausalito, Richmond at ferry landing, W.F.C.L., and Mr. R. J. Menzies and Mrs. Betty G. Menzies; Berkeley yacht harbor, September 8, 1950, 4 specimens, Dr. J. L. Mohr. *Monterey Bay,* 1949-1950, 59 specimens, W.F.C.L., July 22, 1947, 4 specimens, E. Polhemus and L. Kellen. *Elkhorn Slough,* July 1949, 5 specimens, R. J. Menzies. *Morro Bay,* 7 samples, 1949-1950, hundreds of specimens, R. J. Menzies and Dr. J. L. Mohr. *Santa Barbara,* 1949, 6 specimens, W.F.C.L. *Point Hueneme,* 1949, 14 specimens, W.F.C.L. *Los Angeles-Long Beach Harbors,* 1949-1950, hundreds of specimens, Southern California Marine Borer Council. *La Jolla,* August 24, 1949, 20 specimens, R. J. Menzies.

Geographical distribution. The species is noteworthy for its apparent absence from the Atlantic coast and from its restricted distribution between 41°N (Samoa, California) and 33°N (La Jolla, California). This corresponds roughly to areas having a mean annual sea water temperature (surface) near 15°C (10-20°C). In San Francisco Bay and south of Morro Bay the species appears restricted to the colder harbor entrances and does not penetrate into the warmer areas. It was the only species found at Tomales Bay.

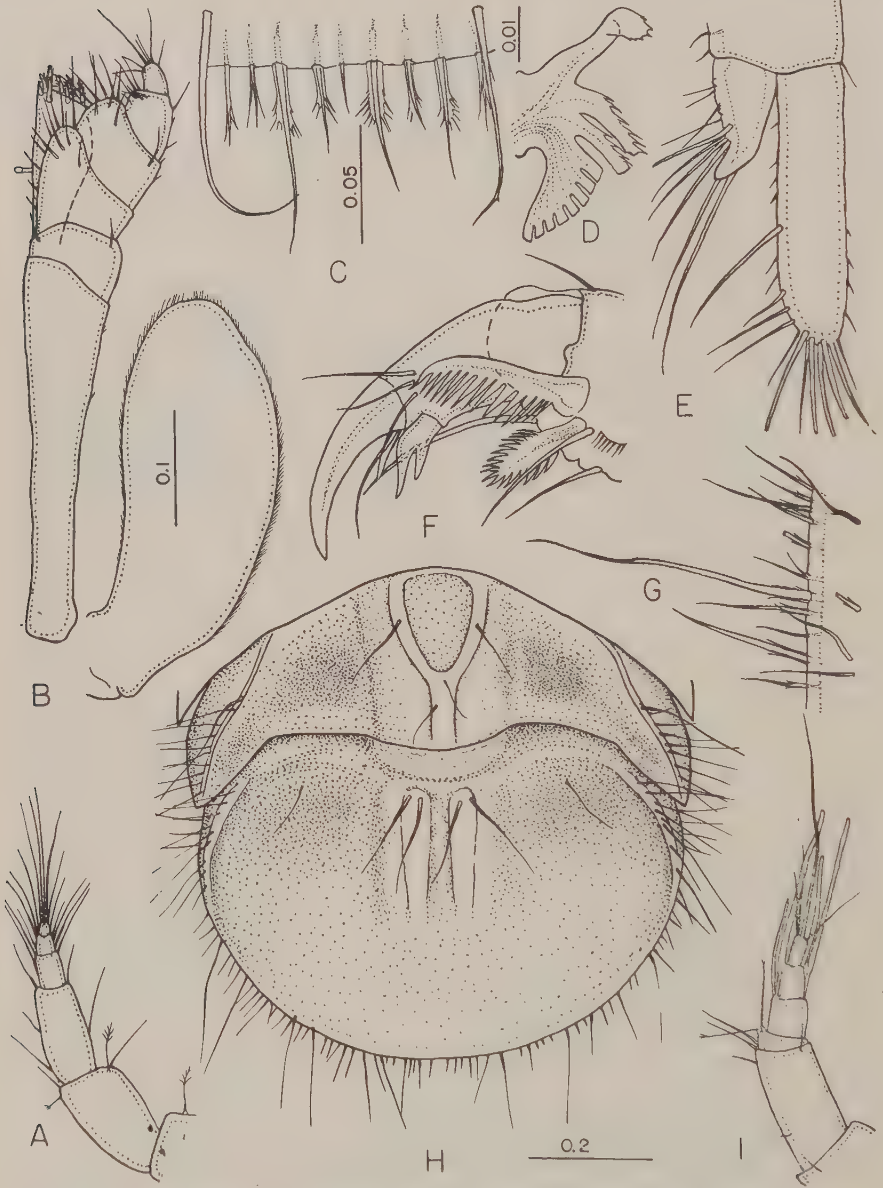

FIGURE 15. *Limnoria (L.) pfefferi* Stebbing, female cotype. A, second antenna. B, maxilliped. C, posterior edge of pleotelson. D, setal row and lacinioid seta of right mandible. E, uropod, distal parts. F, first peraeopod, distal parts. G, lateral crest of pleotelson. H, pleotelson, dorsal view. I, first antenna. Figures with similar magnification, A, B, E, F, I; C, G; H; D.

(406)

Limnoria (Limnoria) pfefferi Stebbing

Figure 15

Synonymy:

Limnoria pfefferi Stebbing, 1905, pp. 714-715. pl. LIIIa. —Chilton, 1914a, pp. 382, 387.—Kofoid and Miller, 1927, p. 309. —Holthuis, 1949, p. 170.—Moll, 1915, pp. 184-185, 188, fig. 7. *non Limnoria* (*pfefferi* Stebbing?), Stephensen, 1927, pp. 361-362 (=*Limnoria (Phycolimnoria)* sp).

Diagnosis. Flagellum of second antenna with four articles. Epipod of maxilliped just reaching the articulation of the first article of the palp with endopod; epipod clavate, widest near distal end, about two and one-half times as long as wide. Mandibular palp with three articles. Fifth somite of pleon dorsally with a median longitudinal yoke-shaped carina. Dorsal surface of posterior edge pleotelson lacks tubercles and spike-like bristles; lateral crests devoid of tubercles. Lacinioid seta of right mandible short, with five apical denticles.

Type locality. Minikoi Atoll, Indian Ocean, in rotten wood in lagoon (Stebbing, 1905, p. 715). The types are located in the British Museum (Natural History).

Measurements. Stebbing (1905, p. 715) records the species as being 3.5 mm in length and 1.25 mm in breadth. A large female cotype examined by me was 3.4 mm long and had a maximal pleotelsonic width of 0.75 mm.

Remarks. Stebbing (op. cit.) appears to have had two species at his disposal when describing *pfefferi*. The uropods figured by Stebbing belong to a species of *Paralimnoria* (p. 147) and not *Limnoria* (sensu lato). In other general features Stebbing's description applies to the cotypes (one male and one female) which are here figured and which kindly were sent to me for examination by Dr. Isabella Gordon of the British Museum (Natural History). Stebbing apparently failed to notice the conspicuous and characteristic carinae of the fifth somite of the pleon and pleotelson because he calls the area of the pleotelson on which the parallel ridges are present a "smoothly rounded median elevation."

The specimens from the Auckland Islands which Stephensen (1927, pp. 361-362) doubtfully assigned to as *pfefferi* have been examined and referred to the sea-weed borer, *L.* (*P.*) *sp.* (see part II).

Material examined. Besides the cotypes of this species, two males and one female were examined from the county causeway, Miami Beach, Florida. These were collected on September 1, 1950 by Mr. Leonard Greenfield of the University of Miami Marine Laboratory.

Geographical distribution. The species, besides having been first

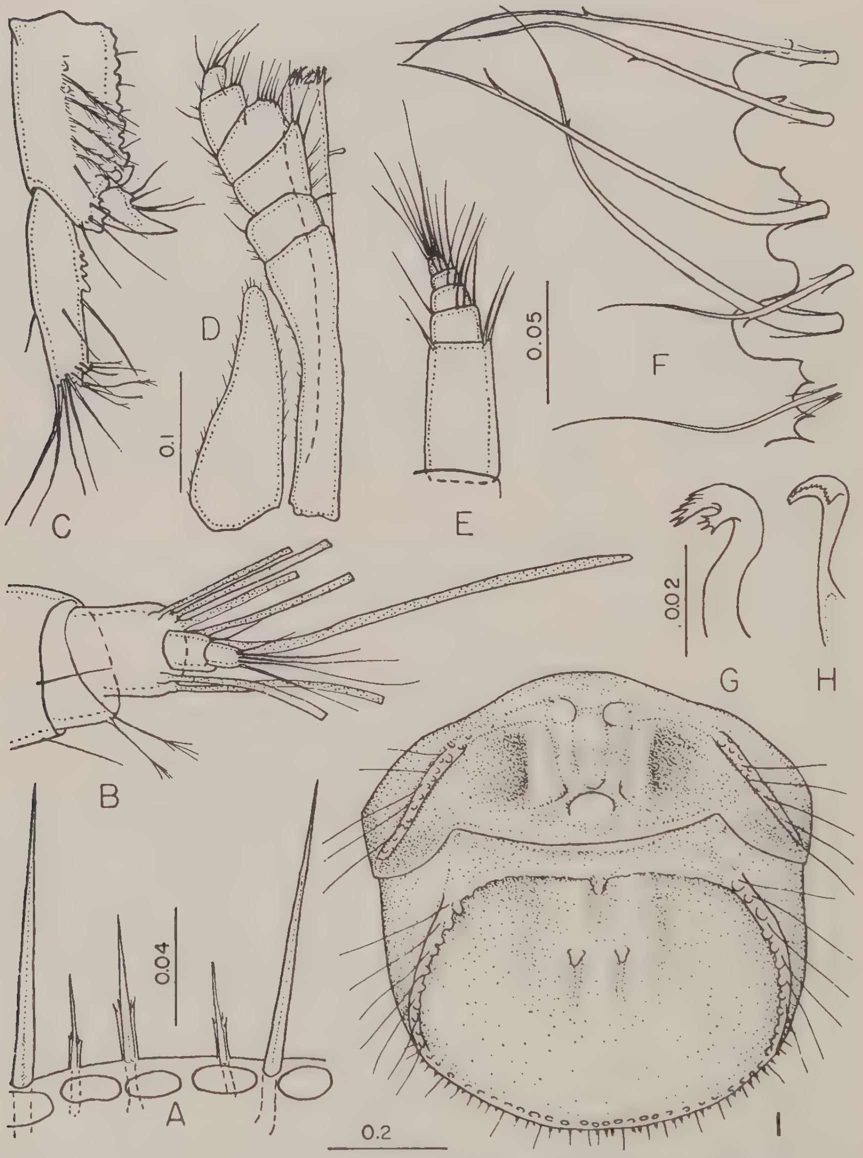

FIGURE 16. *Limnoria (L.) tripunctata* Menzies (from Menzies, 1951), paratype male. A, posterior edge of pleotelson. B, distal articles of first antenna. C, uropod. D, maxilliped. E, flagellum of second antenna. F, lateral crest of pleotelson. G-H, lacinioid seta of right mandible. I, pleotelson. Figures with similar magnification, A; B, E, F; C, D; G, H; I. (after Menzies, 1951)

collected from the Indian Ocean, is known in the Americas only from Miami, Florida.

5. *Limnoria (Limnoria) tripunctata* Menzies

Figure 16

Synonymy:

Limnoria tripunctata Menzies, 1951a, pp. 86-88, pl. 36.

Limnoria lignorum (Rathke). Allen and Carter, 1924, pp. 181-196. Anonymous, 1918, p. 58.—Coker, 1923, pp. 95-100.—Kofoid and Miller, 1927, pp. 308, 331 (in part).—Mohr and LeVeque, 1948, p. 26 (Newport reference).—Richardson, 1899, pp. 821-822 (H. Hemphill's specimens), 1900, p. 222 (South Carolina reference); 1905, pp. 268-279 (San Diego, California and Florida reference in part).—Shackell, 1923, pp. 221-230, figs. 1-4.—Shoemaker, 1949, pp. 1-13 (probable).

Limnoria terebrans, Leach, Gould, 1841, p. 338, (Massachusetts reference).

Diagnosis. Flagellum of second antenna with five articles. Epipod of maxilliped triangulate, two and one-half times as long as wide, just reaching the articulation of the palp with endopod. Mandibular palp with three articles. Dorsal surface of fifth somite of pleon medially with two anteriorly located elevated nodes and a single posteriorly elevated area; central part depressed. Pleotelson medially with one anteriorly located tubercle followed by a pair of tubercles, each of which is followed by a longitudinal carina. Dorsal surface of posterior margin of telson tuberculate, spike-like bristles lacking. Lateral crests conspicuously tuberculate. Lacinioid seta of right mandible abruptly curved distally bearing two prominent flattened, apically spinulate projections.

Type locality. San Diego County, Mission Bay, California. Collected by Mr. and Mrs. R. J. Menzies, December 23, 1948. Types are located in the United States National Museum, British Museum (Natural History) and the Rijksmuseum van Natuurlijke Historie, Leiden.

Measurements. Holotype male length 2.0 mm, width of telson (= pleotelson) at widest point 0.6 mm. Allotype length 2-4 mm, width of pleotelson 0.6 mm (Menzies, 1951, p. 86).

Remarks. In the original description the nodes and elevations on the fifth somite of the pleon were reversed from their actual location. This feature is evident from the figure (Menzies, op. cit., pl. 30, fig. i). It is correctly described in the above diagnosis.

This species has been collected frequently from the creosoted part of treated piling and has been often associated with cases of premature failure of creosoted piling in the United States (Menzies, 1951c, pp. M5-M6). This relationship might be due to the development of creosote tolerant strains of this species, to its being more tolerant originally, or perhaps more simply, to a more rapid leaching of the creosote in the warm water where this species is found.

Material examined. Including the type series (Menzies, 1951, pp. 86-88), specimens were examined from:

United States

Atlantic Coast.

Rhode Island, April 7, 1948, 2 specimens, W.F.C.L.

Massachusetts, *Boston,* August 9, 1948, 1 specimen, W.F.C.L.

New York, *New York Harbor,* Fisher's Island, October 1, 1948, 7 specimens, W.F.C.L. Sheepshead Bay, August 28, 1950, 50 specimens, H. N. Blume.

North Carolina, *Wilmington, South Port,* and *Kure Beach,* 1948, 1949, 1950, 151 specimens, W.F.C.L.

Bermuda, U. K., May 11, 1948, 15 specimens, W.F.C.L.

Florida, *Mayport, Fort Pierce,* 6 samples, 1949, 1950, 65 specimens, W.F.C.L.; *Miami Beach,* September 1, 1950, 25 specimens, Univ. Miami Marine Laboratory, Leonard Greenfield (with specimens of *L. (L.) pfefferi* and *L. (L.) saseboensis*).

Gulf of Mexico and Caribbean.

Florida, *Key West,* 1948, 1949, 8 specimens, W.F.C.L. *Panama City,* 1949, 1950, 8 specimens, W.F.C.L.

Texas, *Galveston, Corpus Christi,* 1948-1949, 22 specimens, W.F.-C.L. *Port Aransas,* 3 samples, 1948, 1949, more than 100 specimens, J. W. Hedgpeth (in creosoted wood).

Costa Rica. *Limon,* U.S.N.M. Cat. No. 39862, W. C. Mullins, over 100 specimens (identified by Harriet Richardson as *L. lignorum*).

Puerto Rico, *Mona Island,* January 15, 1950, 12 specimens, W.F.-C.L.

Cuba. *Guantanamo Bay,* 1949, U.S. Navy, over 100 specimens from creosoted wood.

Venezuela, *Amuay,* May, 1949, 37 specimens, W.F.C.L.

Pacific Coast.

California, *San Francisco Bay,* San Rafael, McNear's Beach, Sobrento, San Quentin, San Rafael Ferry slip, Belvidere (with *Chelura* and *L. (L.) quadripunctata*), San Mateo, Dumbarton Bridge, both approaches, South Double Basin, Parr-Richmond Pier, Berkeley Yacht Harbor, (with *L. (L.) quadripunctata*), Richmond, San Rafael Ferry Slip, Rodeo (in hole in telegraph pole), April-May 1950, over

100 specimens, R. J. Menzies; Berkeley Yacht Harbor, September 1950, 25 specimens, Dr. J. L. Mohr (with *L. (L.) quadripunctata*). *Port Hueneme,* January 6, 1950, 19 specimens, W.F.C.L. *Los Angeles-Long Beach Harbors,* 1949-1950, several hundred specimens from 14 different localities, Southern California Marine Borer Council. *Newport Bay,* upper part and at Highway 101, 1947, 50 specimens, Dr. J. L. Mohr, and February 14, 1950, 200 specimens. *Catalina Island,* July 15, 1950, 100 specimens, Allan Hancock Foundation (in creosoted timber). *La Jolla,* August 16, 1949, 25 specimens, R. J. Menzies (with *L. (L.) quadripunctata*).

Mexico. Pacific coast; *Ensenada,* September 7, 1949, 35 specimens, Allan Hancock Foundation. *San Quintin Bay,* April 7, 1950, 28 specimens, R. J. Menzies.

Gulf of California, *Santa Rosalia, La Paz harbor, San Marcos Island,* January 1-2, 1954, several hundred specimens, Drs. Gifford C. Ewing and R. J. Menzies.

Mexican mainland; *Mazatlan,* January 2, 1954, about 50 specimens, Drs. Gifford C. Ewing and R. J. Menzies.

Geographical Distribution. On the Atlantic coast from 44°N (Rhode Island, U.S.A.) to 12°N (Amuay, Venezuela) including the Gulf of Mexico; on the Pacific Coast from about 37°N (San Francisco area) to 23°N (Mazatlan, Mexico). The species appears to inhabit water ranging in mean temperature between 15°C and 30°C. It can be considered the most widely distributed species in Northern and Central America.

Limnoria (Limnoria) platycauda, new species

Figure 17

Diagnosis. Flagellum of second antenna with four articles. Epipod of maxilliped reaching nearly to the articulation between the first and second articles of palp; epipod semi-spatulate, narrowest at distal end, about three times as long as wide. Mandibular palp with three articles. Fifth somite of pleon dorsally with a median longitudinal ridge. Pleotelson dorsally lacking ridges or rugosities; posterior margin tuberculate, with few setae and no spike-like bristles. Lateral crests with conspicuous tubercles. Lacinioid seta of right mandible elongated, abruptly bent at distal end which bears a cup-shaped serrated apex.

Type locality. Mouth of Curacao Harbor, Dutch West Indies, J. W. Gonggrip, 1923. Specimens in greenheart timber, collector's note "planks 5 x 25 cm wholly severed at water line." Holotype, allotype, and 97 paratypes returned to the United States National Museum, Cat. No. 59975.

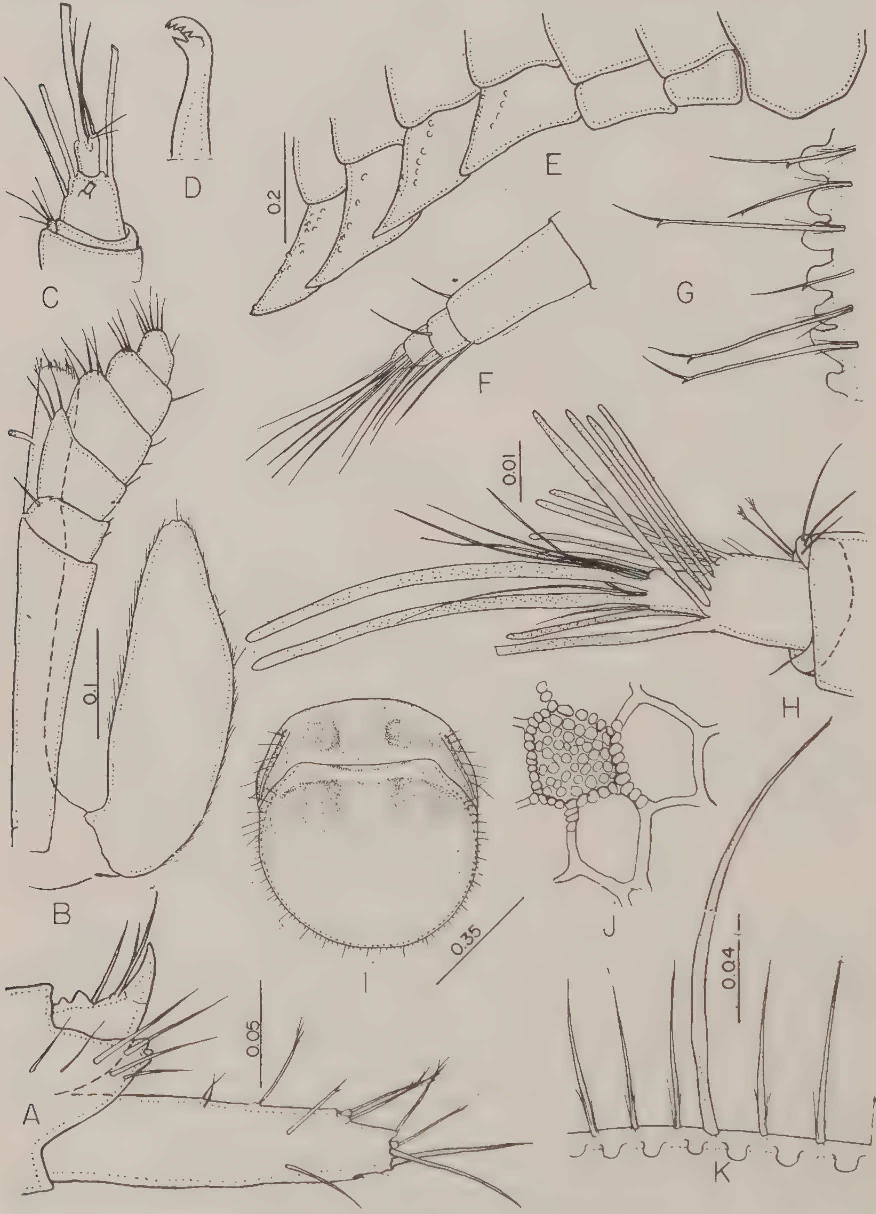

FIGURE 17. *Limnoria (L.) platycauda,* new species, paratype. A, uropod. B, maxilliped. C, distal articles of first antenna. D, lacinioid seta of right mandible, magnification not known. E, lateral margin of peraeon. F, flagellum of second antenna. G, lateral crest of pleotelson. H, distal articles of first antenna. I, pleotelson. J, dorsal surface of pleotelson. K, posterior margin of pleotelson. Figures with similar magnification, A, C, F, G; B; E; H; I; J, K.

Measurements. Holotype male length, 2.0 mm; pleotelsonic width 0.55 mm. Allotype length, 2.0 mm; pleotelsonic width 0.5 mm. Large paratype length, 2.5 mm; pleotelsonic width 0.7 mm.

Remarks. The dorsal surface of pleotelson has few setae or bristles, and thus the underlying structure of the integument is revealed. This consists of small hexagonal areas filled with minute globular bodies which appear more heavily calcified than the rest of the exo-skeleton. In this regard the species resembles *L.* (*L.*) *simulata* to a considerable degree. The species differs from all others noticeably in its lack of ridges, rugosities, or tuberculations on the dorsal surface of its pleotelson.

Material examined. In addition to the types, four specimens were examined from Mona Light, Puerto Rico, November 19, 1948, W.F.-C.L.

Geographical distribution. Caribbean, Puerto Rico to Curacao, Dutch West Indies.

Limnoria (Limnoria) saseboensis, new species

Figure 18

Diagnosis. Flagellum of second antenna with five articles. Epipod of maxilliped short, not reaching the articulation of palp with endopod by a distance about equal to 1/3 of its length; epipod strap-like, apically pointed being two and one-half times as long as wide, basal portion widest. Mandibular palp with three articles. Dorsal surface of fifth somite of pleon medially with a pair of subparallel longitudinal carinae which approach one another posteriorly. Pleotelson with two parallel carinae in dorsal surface; carinae tuberculate anteriorly and less so posteriorly; posterior edge tuberculate, margin with spike-like bristles; lateral crests tuberculate. Lacinioid seta of right mandible with two medially curved teeth at apex.

Type locality. The holotype and 11 paratypes were collected at Sasebo, Japan, August 22, 1949, W.F.C.L. With them were specimens of *L. (L.) tripunctata.* These have been sent to the United States National Museum.

Measurements. Holotype male, length 3.5 mm, width of pleotelson 0.95 mm.

Remarks. In having a pentarticulate second antennal flagellum and a tuberculate pleotelsonic margin this species resembles *L. (L.) tripunctata.* It differs markedly from the latter in having an unusually short maxillipedal endopod and parallel carinae on the dorsal surface of fifth somite of the pleon and pleotelson.

Material examined. In addition to the types, six specimens collected

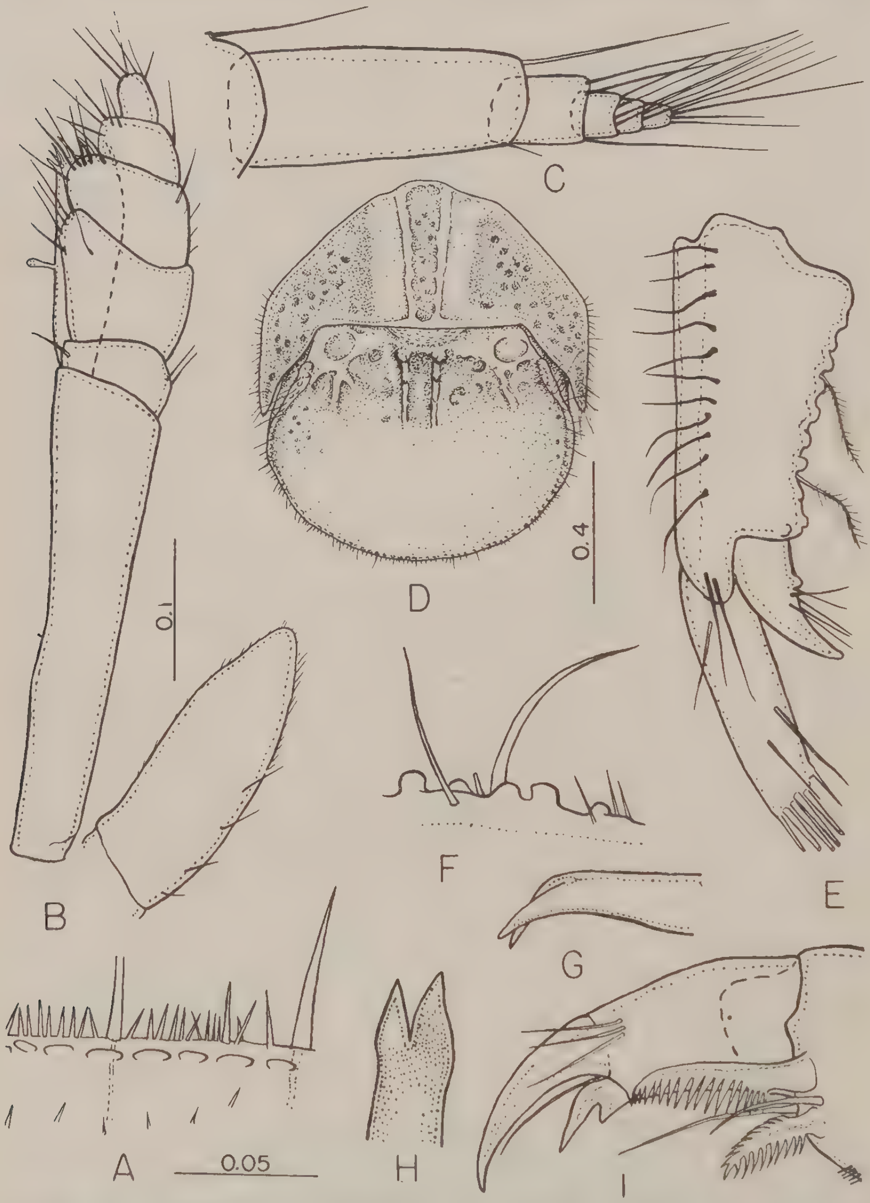

FIGURE 18. *Limnoria (L.) saseboensis,* new species, paratype. A, posterior margin of pleotelson. B, maxilliped. C, flagellum of second antenna. D, pleotelson. E, uropod. F, lateral crest of pleotelson. G, lacinioid seta of right mandible, lateral view. H, lacinioid seta of right mandible, medial view. I, distal articles of first peraeopod. Figures with similar magnification, A, F, I; B, C, E; D-, H, G (magnification not known).

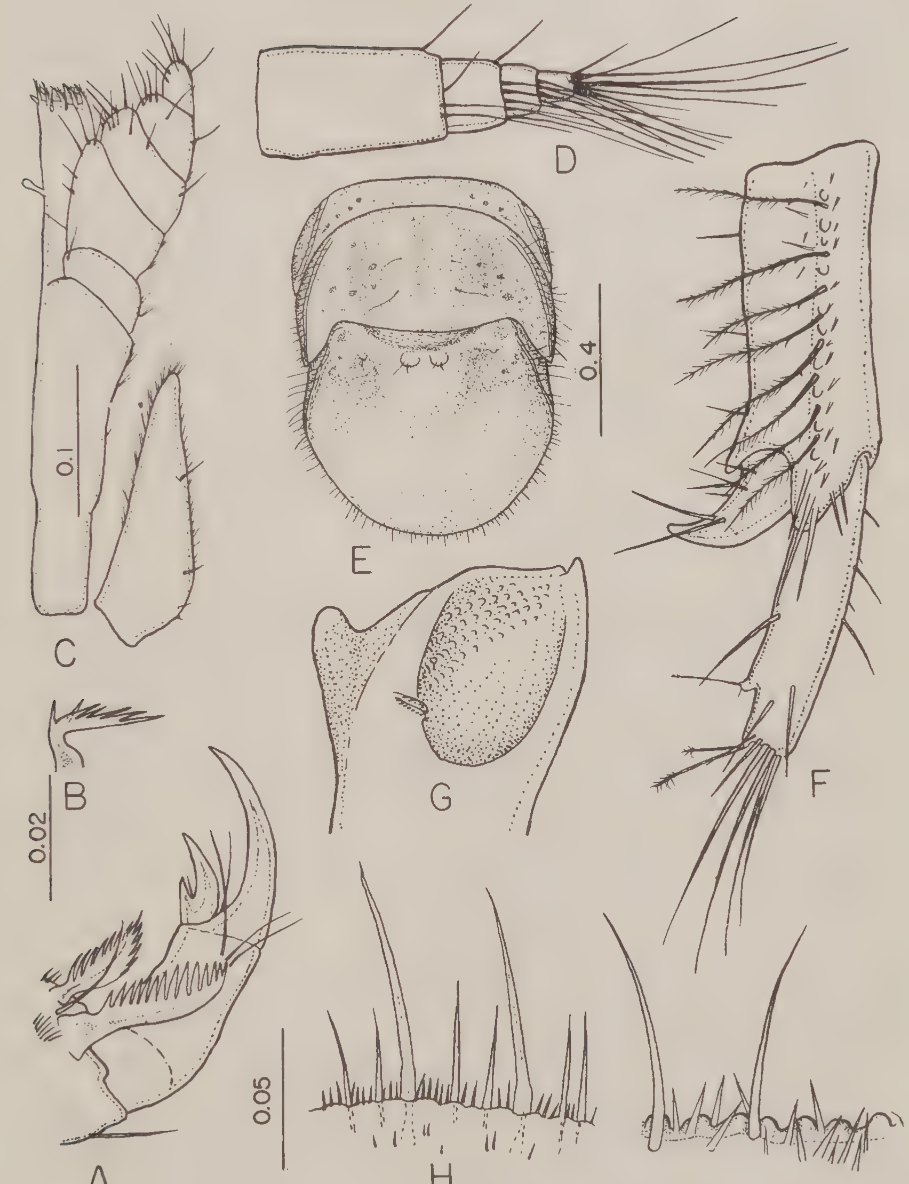

Figure 19. *Limnoria (L.) simulata,* new species, male paratype. A, distal articles of first peraeopod. B, lacinioid seta of right mandible. C, maxilliped. D, flagellum of second antenna. E, pleotelson. F, uropod. G, inner surface of left mandible, palp not shown. H, posterior margin of pleotelson. I, lateral crest of pleotelson. Figures with similar magnification, A, D, G, H, I; B; C-, E.

from the county causeway, Miami Beach, Florida, by Mr. Leonard Greenfield, September 1, 1950.

Geographical distribution. Known only from Miami, Florida, and Sasebo, Japan.

Limnoria (Limnoria) simulata, new species

Figure 19

Diagnosis. Flagellum of second antenna with four articles. Epipod of maxilliped triangulate, elongated, reaching to the articulation of first article of the palp with endopod; epipod three times as long as wide. Mandibular palp with three articles. Dorsal surface of fifth somite of pleon with a medial longitudinal sulcus. Dorsal surface of pleotelson with a pair of conspicuous tubercles on either side of the mid-line at anterior end lateral to each of which is a small tubercle; posterior margin irregular, lacking tubercles; lateral crests tuberculate. Lacinioid seta of right mandible provided with elongated spinules.

Type locality. Holotype male from Virgin Islands, West Indies, September 24, 1913 and one paratype male February 16, 1914. These have been returned to Dr. Torben Wolff, Universitetets Zoologiske Museum, Kopenhagen, Denmark.

Measurements. Holotype male length, 3.0 mm, width of pleotelson 0.55 mm.

Remarks. Although there were no data on the label indicating the habitat of this species, the mandibular structure would suggest that it is a wood-borer.

In over-all structure this species resembles *L. (L.) platycauda,* also a Caribbean species. It differs markedly from the latter in lacking a mid-longitudinal ridge on the dorsal surface of the fifth somite of the pleon and in having tubercles on the dorsal surface of the pleotelson which *L. (L.) platycauda* lacks.

Geographical distribution. The species is known only from the Virgin Islands.

Subgenus *Phycolimnoria,* new subgenus

Diagnosis. Members of the genus *Limnoria* (sensu lato) which lack a "rasp" and "file" arrangement of scales and ridges on the incisive process of the mandibles. All known species bore into sea weeds.

Type species. *Limnoria (Phycolimnoria) algarum* n. sp.

This subgenus includes the algal boring parasites, whose characteristic burrows were described on p. 109. Here only one species is treated, e.g. *L. (P.) algarum.* The other known species are *L. (P.) segnis* (Chilton, 1883, pp. 76-77) from Lyttelton Harbor, New Zealand which has a biarticulate mandibular palp and *L. (P.) antarctica* (Pfeffer, 1887, pp. 96-102) from the South Georgia Islands

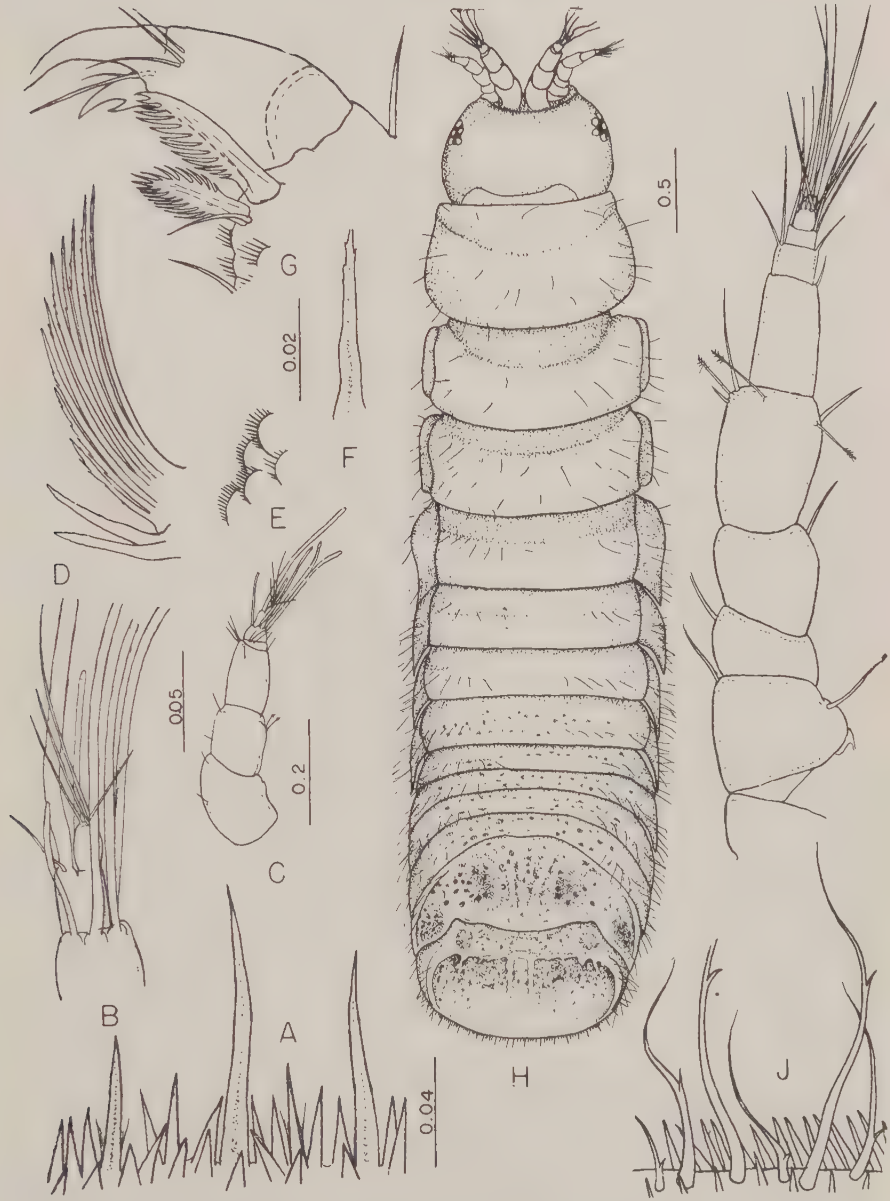

FIGURE 20. *Limnoria (P.) algarum*, new species, paratype. A, posterior margin of pleotelson. B, distal articles of first antenna. C, first antenna. D, setal row. E, scales of first antenna. F, lacinioid seta of setal row of right mandible. G, distal article of first peraeopod. H, *in toto,* dorsal view. I, second antenna. J, lateral crest of pleotelson. Figures with similar magnification, A; B, E, G, J; C; D, F; H; I.

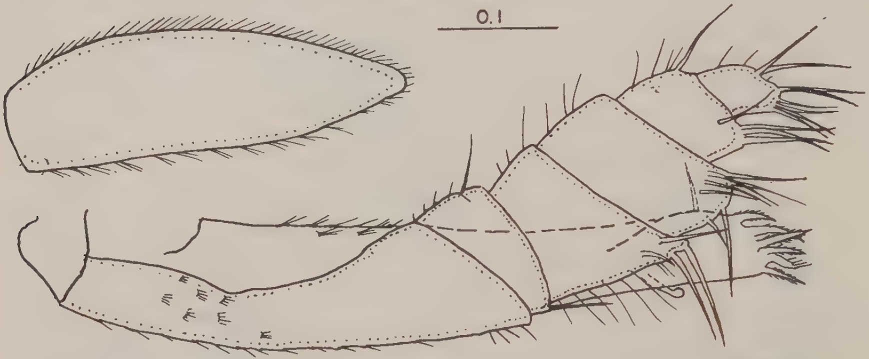

FIGURE 21. *Limnoria (P.) algarum*, new species, paratype, maxilliped.

in the Antarctic which like *L. (P.) algarum*, has a triarticulate mandibular palp. The two latter species may be distinguished from one another by the fact that the flagellum of the second antenna has four articles in *L. (P.) antarctica* and five in *L. (P.) algarum*.

The species thus far have been taken from nine genera of kelps (Laminariales), *Egregia, Macrocystis, Neriocystis, Laminaria, Sargassum, Lessonia, Lessoniopsis, Postelsia,* and *Eisenia*.

Limnoria (Phycolimnoria) algarum, new species

Figures 20-21

Diagnosis. Flagellum of second antenna with five articles. Epipod of maxilliped reaching the articulation of first article of palp with endopod; epipod strap-like, being three and one-half times as long as wide. Mandibular palp with three articles. Dorsal surface of fifth somite of pleon medially with a V-shaped carina. Dorsal surface of pleotelson medially with two weak parallel carinae. Pleon and pleotelson foveolate, posterior border fringed with many spike-like bristles and long setae; lateral crests and posterior margin lack tubercles. Lacinioid seta of right mandible simple, pointed, distally spinulate and not vastly different from other setae of the setal row.

Type locality. Dillon Beach, Marin County, California, April 25, 1949, 15 specimens from holdfasts of *Macrocystis* and *Egregia*, R. J. Menzies.

Measurements. Holotype male, length 3.00 mm, width of pleotelson 0.9 mm. Allotype (ovigerous), length 5.5 mm, width of pleotelson 1.0 mm.

Remarks. Besides differing from the two other known species in the number of articles comprising the flagellum of the second antenna and mandibular palp the ornamentation of the fifth somite of the pleon and pleotelson is further unique.

Material examined. Exclusive of the types, specimens were examined from the following localities all along the Pacific coast of North America.

Oregon. *Squaw Island*, Cape Arago, August 25-26, 1950, 55 specimens. Dr. J. L. Mohr; Gregory Point, August 27, 1950, 42 specimens, Dr. J. L. Mohr.

California. *Marin County*, Tomales Point and Duxbury Reef, July. August 1948, 15 specimens, Miss M. Barr. *Morro Bay*, San Luis Obispo Co., February 1-2, 1950, 13 specimens, R. J. Menzies and Dr. J. L. Mohr. *Point Fermin*, Los Angeles Co., February 14, 1949, 18 specimens, Dr. J. L. Mohr. *La Jolla*, San Diego Co., July 1953, about 50 specimens, R. J. Menzies.

Geographical Distribution. Oregon to Southern California, in holdfast of the algae *Egregia, Eisenia, Laminaria, Macrocystis*, and *Postelsia*.

Genus *Paralimnoria*, new genus

Diagnosis. Flagellum of first antenna with five articles. Flagellum of second antenna with five or six articles. Mandibular incisive processes with a "rasp" and "file" wood-boring apparatus. Lacinioid seta of right mandible tubular, with an apical circle of spines. Exopod and endopod of uropods subequal in length (exopod slightly shorter than endopod), each provided with a pointed spine-like (claw) apex, lateral margins of uropods with peculiar setae (Fig. 7) which do not occur in the genus *Limnoria* (sensu lato). Fifth pair of pleopods with marginal setae.

Type species. *Limnoria andrewsi* Calman, 1910, pp. 184-186, pl. V.

Distribution. In the Americas the genus appears to be restricted to Caribbean waters. The type species was described originally from the Indian Ocean.

Remarks. Only the type species is known to belong to this genus. This, however, presents some marked variations and may be divided into three *formae*. This term is used here to indicate a usually distinctive variation within one species or subspecies the cause of which is not known and which shows no evident correlation with ecologic, genetic, or geographic information.

When describing *L. andrewsi*, Calman (op. cit.) noted that the fifth pair of pleopods had marginal setae. He, therefore, modified Hansen's (1905, p. 98) diagnosis of the subfamily Limnoriinae (here considered a family). Calman did not observe the claw-like ends of each uropodal branch which are important characteristics separating the genus from *Limnoria* (sensu lato).

The conspicuous scale attached to the first antenna of *Paralimnoria* is also characteristic of the genus *Limnoria* and as Calman remarks of the genus *Bathynomus* (suborder Flabellifera) and cryptoniscian larvae (suborder Bopyroidea). It has since been found on *Mesantheura* (suborder Anthuridea, Miller and Menzies, 1952, p. 8) and the young of *Cirolana* (unpub. data) and it is possibly characteristic of isopods in general.

Paralimnoria andrewsi (Calman)

Figures 22-24

Synonymy:

Limnoria andrewsi Calman, 1910, pp. 184-186, pl. V, figs. 7-14. —Atwood and Johnson, 1924, pp. 24-25, pl. 1, figs. 3-5. Chilton, 1914a, pp. 382-387.—Holthuis, 1949, p. 170.—Kofoid and Miller, 1927, pp. 309, 331.—Miller, 1924, pp. 159-164.

Diagnosis. Flagellum of second antenna with five-six articles. Epipod of maxilliped slightly exceeding the articulation of first article of palp with endopod; epipod apically pointed, about two and two-thirds as long as wide. Mandibular palp with three articles. Ornamentation of dorsal surface of fifth somite of pleon and pleotelson variable. Lacinioid seta of right mandible tubular, bent near apex which is serrated around margins and has a central tooth.

Type locality. Christmas Island, Indian Ocean, 1908, collected by Dr. C. W. Andrews. Found in piles of pier at Flying Fish cove with the amphipod *Chelura insulae* Calman (Calman, 1910). Types located in the British Museum (of Natural History).

Formae

Three formae are recognizable, *Forma typica* (Calman's types), *Forma A* and *Forma B*. As a rule one sample contained specimens of only one forma; however, in some cases (not reported here) two formae occurred together. In some samples the characteristics of the formae seemed so mixed that a precise assignment was not possible.

Forma *typica*

Figures 22-24

Diagnosis. Fifth somite of pleon lacking central depressed triangulate area. Pleotelson dorsally with a pair of elevated tubercles near center, each followed posteriorly by a short, obscure carina. Lateral crest of pleotelson tuberculate, posterior margin sparsely tuberculate in most instances.

Specimens examined. Two female cotypes described by Calman (1910).

Forma *A*

Figure 24 A

Diagnosis. Fifth somite of pleon with a central depressed triangulate area. Pleotelson dorsally with a pair of elevated tubercles each followed posteriorly by a long carina which extends almost to the distal margin of pleotelson. Lateral crests and posterior margin of telson markedly tuberculate.

Specimens examined. Curacao, Dutch West Indies, 1923, 11 specimens, J. W. Gonggryp in greenheart timber with L. *(L.) platycauda* (p. 35), U.S.N.M. Cat. No. 59975.

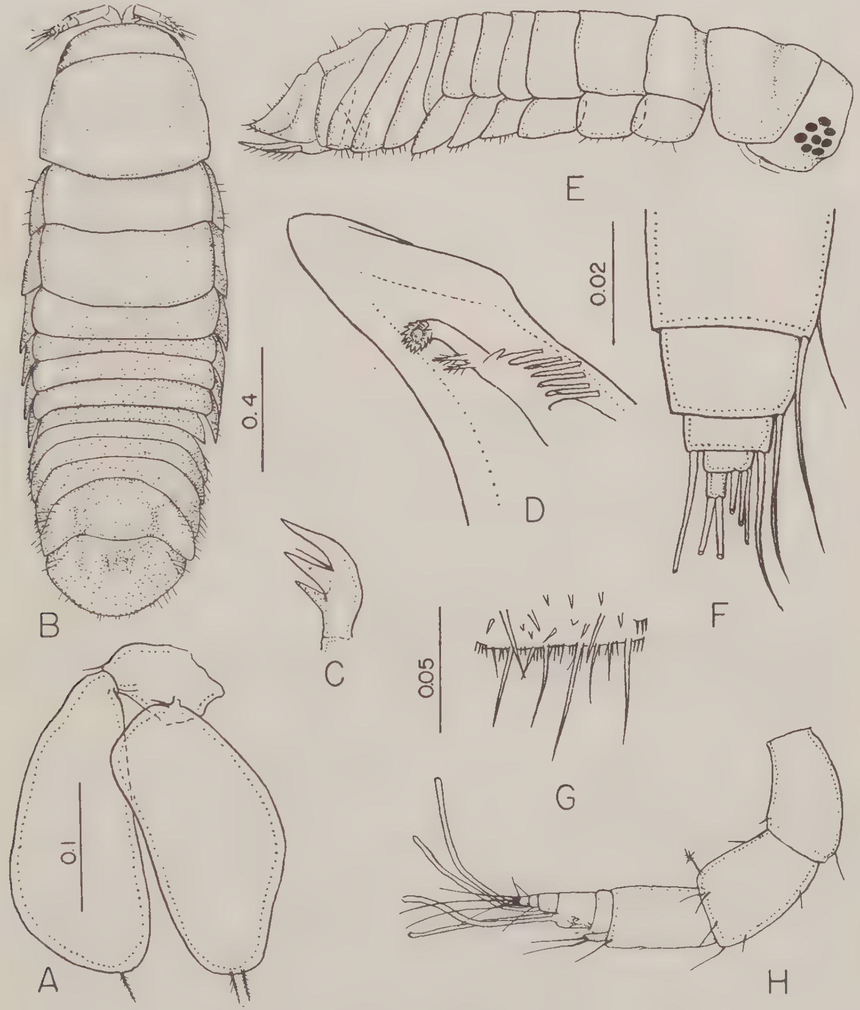

FIGURE 22. *Paralimnoria andrewsi* (Calman). A, fifth pleopod. B, *in toto*, dorsal view. C, accessory claw of first peraeopod. D, inner surface, right mandible. E, *in toto*, lateral view. F, apical articles of second antenna. G, apex of pleotelson. H, first antenna. Figures with similar magnification, A; B, E; C, D, F; G, H.

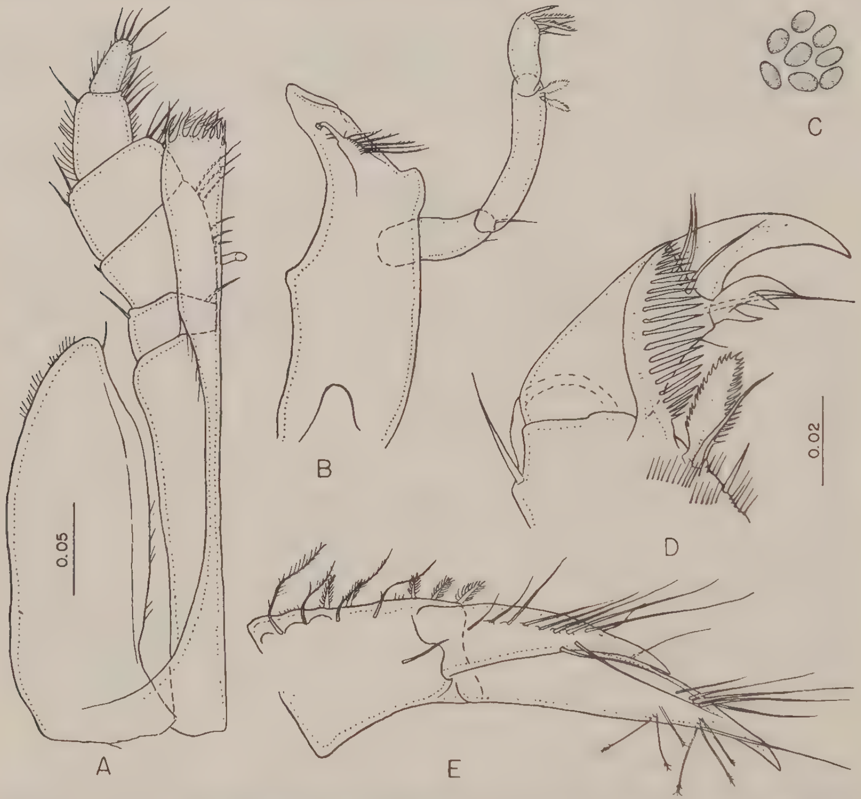

FIGURE 23. *Paralimnoria andrewsi* (Calman). A, maxilliped. B, right mandible. C, eye, lateral view. D, distal articles of first peraeopod. E, uropod. Figures with similar magnification, A, B, C, E; D.

Forma *B*

Diagnosis. Fifth somite of pleon with a central depressed area. Pleotelson as described for forma *typica*.

Specimens examined. Key West, Florida, April 4, 1949, 5 specimens, W.F.C.L.

Remarks. Calman (1910, fig. 7) did not indicate the evident coxal plates of this species and incorrectly figured the flagellum of the antennae. Beyond these corrections and those previously cited (p. 42) Calman's description is very accurate.

Distribution. In addition to the Caribbean localities mentioned, the species has been recorded from Samoa and the Hawaiian Islands (Miller, 1924) and Misaki and Tanabe Bay, Japan (Shiino, 1950).

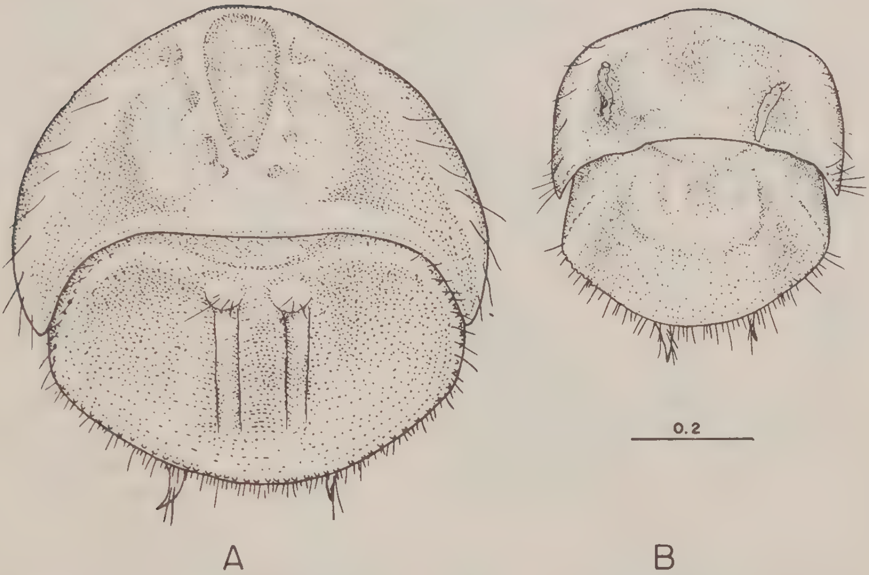

FIGURE 24. *Paralimnoria andrewsi* (Calman). A, pleotelson, forma B. B, pleotelson, forma typica; note protozoans on fifth somite of pleon. Magnification, both to same scale.

It accordingly appears to be a widely distributed (cosmopolite) tropical species.

DISTRIBUTION

The geographic distribution of individual species has already been given in detail as part of each description. Here distribution is treated in more general terms with emphasis on similarities and differences between species and with particular attention to the factors which appear to limit their distribution.

General

The collections of gribbles seem reasonably complete on the Pacific coast from Alaska to Mazatlan, Mexico and on the Atlantic coast from Maine to Miami, Florida. Outside of these areas the collections are spotty and the conclusions that may be drawn become more tentative (Figure 25).

The genus *Paralimnoria,* as far as North America is concerned, appears restricted to the Caribbean region, but might be expected to occur along the west coast of Central America in view of its wide distribution elsewhere.* The species *Limnoria (L.) platycauda, L. (L.)*

---

*unpublished data.

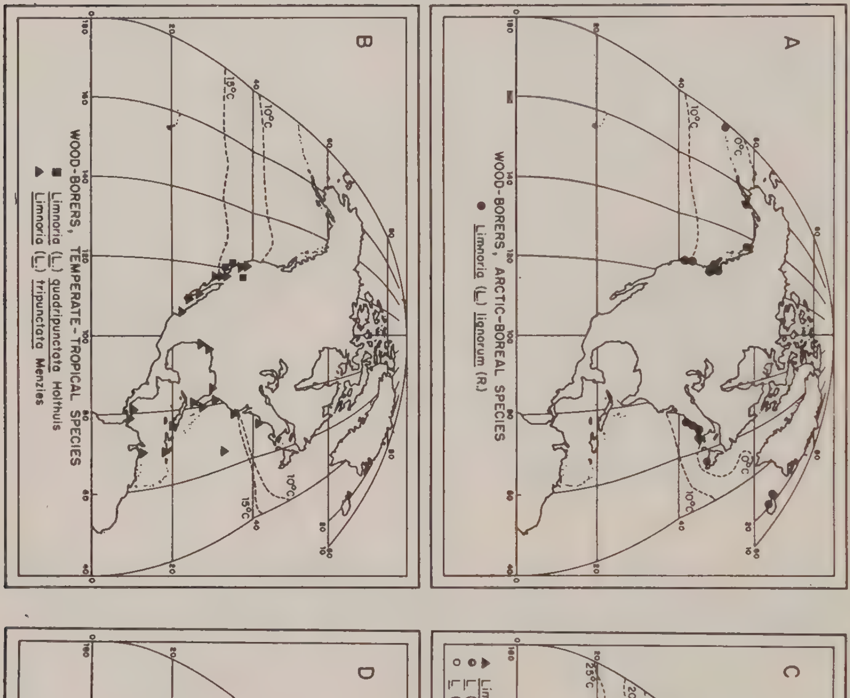
A
WOOD-BORERS, ARCTIC-BOREAL SPECIES
● Limnoria (L.) lignorum (R.)
B
WOOD-BORERS, TEMPERATE-TROPICAL SPECIES
■ Limnoria (L.) quadripunctata Holthuis
▲ Limnoria (L.) tripunctata Menzies
C
WOOD-BORERS, TROPICAL SPECIES
▲ Limnoria (L.) tripunctata Menzies
● L. (L.) platycauda n.sp
○ L. (L.) simulata n. sp.
● L. (L.) saseboensis n. sp.
● L. (L.) pfefferi Stebbing
+ Paralimnoria andrewsi (Calman)
D
SEAWEED-BORERS
● L. (Phycolimnoria) algarum n.sp
0°C
10°C
15°C
20°C
25°C

FIGURE 25. The distribution of the Limnoriidae in Northern and Central America. A, wood-borers, arctic-boreal. B, wood-borers, temperate-tropical species. C, wood-borers, tropical species. D, seaweed borers.

saseboensis, L. (L.) pfefferi, and *L. (L.) simulata* which also are known from other tropical regions, have a similar distribution. The apparent restriction of the species *L. (Phycolimnoria) algarum* to the Pacific Coast of North America may well be due only to a lack of any search for it on the Atlantic Coast. The genus at least may be suspected to occur wherever Laminariales grow. The following summarizes the general distribution of the American species.

Pacific Coast: four species.

1. *Limnoria (Limnoria) lignorum*
2. *Limnoria (Limnoria) quadripunctata*
3. *Limnoria (Limnoria) tripunctata*
4. *Limnoria (Phycolimnoria) algarum*

Atlantic Coast: four species (excluding Caribbean and Gulf of Mexico)

1. *Limnoria (L.) lignorum*
2. *Limnoria (L.) tripunctata*
3. *Limnoria (L.) pfefferi*
4. *Limnoria (L.) sasaeboenses*

Caribbean and Gulf of Mexico: four species

1. *Limnoria (L.) tripunctata*
2. *Limnoria (L.) platycauda*
3. *Limnoria (L.) simulata*
4. *Paralimnoria andrewsi*

Species common to both coasts: two species

1. *Limnoria (L.) lignorum,* a boreal circumpolar species
2. *Limnoria (L.) tripunctata,* a temperate-tropical cosmopolite

Factors Associated with the Distribution of Limnoria.

The environmental factors which are suspected or known to influence the distribution of *Limnoria* are food, depth with associated phenomena, dissolved oxygen, salinity, and temperature.

1. *Food.* The food supply of *Limnoria* is restricted either to seaweeds (subgenus *Phycolimnoria*) or wood (subgenus *Limnoria* and genus *Paralimnoria*). In the laboratory specimens of both subgenera have been kept for over a month on a diet of particulate cellulose in solid agar with no apparent adverse effects, indicating that their dietary requirements might be similar. In nature, however, the subgenus *Limnoria* has not been found in algae nor has *Phycolimnoria* been taken from wood. Members of both subgenera have been found to survive for as long as thirty days in the absence of food.

This ability to withstand starvation no doubt increases the opportunity for the animals to find food in nature. Limnorias have not been found where there was no available food, but on the other hand, areas with ample supplies of wood or kelp were found and although other environmental factors appeared to be ideal for their existence, no *Limnoria* were discovered. For example, drift wood and wooden floats examined along the entire peninsular side of the Gulf of California from Los Angeles Bay to Santa Rosalia Bay were found to be free from *Limnoria* but showed evidence of extensive teredine attack.

2. *Depth.* The extremely limited data available on the vertical distribution of *Limnoria* are such that little can be said about the influence of depth on their distribution. Wood is scarce at great depths and it seems remarkable that the animals are found at all in deep water. The collections on which this report is based were all taken from shallow water, e.g. surface to about 60 feet at a maximum. The species *Limnoria (L.) japonica* Richardson (1909) was reported from a depth of 163 fathoms off Suduz Misaki Light, Japan. Barnard (1936) reports *L. (L.) segnis* Barnard from 185-250 fathoms off the Andaman Islands in the Indian Ocean. Neither of these species has been collected from shallow water. Andrews (1875) recorded an attack by *Limnoria* on the guttapercha covering of a telegraph cable between Holyhead and Ireland. Chilton (1916) gave a similar report of cable damage by *Limnoria* from a depth of 60 fathoms off Sinclair Head in Cook Straight, New Zealand, and Calman (1936) records it from a submarine cable at a depth of 290 fathoms in the Mediterranean. Both Chilton and Calman identified the species with *L. (L.) lignorum* (Rathke) but these determinations are questionable in view of the multitude of species now believed to exist which were not known to those investigators.

3. *Dissolved oxygen.* The dissolved oxygen content of near-shore sea water, except in polluted areas, is rather high. It varies between 4 and 8 parts per million (ppm) in harbors in Southern California and is presumably higher in more northern localities. In Los Angeles-Long Beach Harbor *Limnoria* has been found in sea water whose dissolved oxygen ranged seasonally between 0.0 to 4.0 (mean 1.6) ppm. It was not found at a station where the oxygen concentration ranged seasonally between 0.0-1.4 (mean 0.12) ppm.[1] This suggests

---

[1] Data supplied through the courtesy of the Southern California Marine Borer Council, Box 786, Wilmington, California.

that an average dissolved oxygen content somewhat below 1.6 ppm might constitute a limiting factor in the survival of *Limnoria*. It was apparent from the data that populations could survive in areas having periodic oxygen depletion.

4. *Salinity*. In nature low salinity appears to be an important factor governing the distribution of *Limnoria*. This is particularly evident near shore in restricted localities where seasonal variations in salinity are common. Laboratory experiments by White (1929) and Henderson (1924, *L. (L.) lignorum*), Coker (1923, *L. (L.) tripunctata*), and Kofoid and Miller (1927, *L. (L.) quadripunctata*) all indicate that the animals cannot survive for more than a day in fresh water. Salinities between 10-18 ‰ had no unfavorable effect for as long as 8-12 days. Long-term experiments were not conducted by those investigators and accordingly the effect of lowered salinity on reproduction or the development of young is not known. The upper salinity limit tolerated by *Limnoria* has not been determined.

Areas having uniformly low salinities (below 10 ‰) and those having wide ranges of salinity (e.g. 0.00 ‰ to 35.00 ‰) might be considered as unfavorable for the development and establishment of *Limnoria*. Field data correlating salinity with the presence or absence of *Limnoria* are not abundant. The agreement with experimental results is far from perfect. As pointed out by Sϕmme (1940) part of this disagreement is because only surface salinities have been considered; whereas, *Limnoria* may be found at the bottom in water of a higher and more favorable salinity. This is especially well-illustrated in the data given by M'Gonigle (1925) where a surface salinity of 6.98 ‰ contrasted with that of 29.16 ‰ at a depth of only 14 feet at Sheet Harbor, Nova Scotia. The gribble, although scarce, was much more numerous at the bottom than at the surface. Black and Elsey (1948) found *Limnoria* at Shannon Bay, Queen Charlotte Island where the surface salinity was below 8 ‰ for short periods of time during November, January, and March. At Shannon Bay, attack was mild as compared with more saline localities and was markedly greater at the bottom than at the surface.

It is to be noted, however, that almost without exception the attack by *L. (L.) lignorum* was reported by the above investigators to be greatest at the bottom than at surface regardless of the magnitude of the seasonal salinity fluctuations. The wide tidal fluctuations may play an important role in such areas in keeping *Limnoria* attack near the bottom of piling, but there seems little doubt that salinities as low as 6.0 ‰ would have an adverse effect on *Limnoria* populations.

The gribble, *L. (L.) tripunctata* is not known to occur at the Carquinez Strait, California (vicinity of San Francisco Bay) or farther east in Suisun Bay. At Crockett the surface salinity (Kofoid and Miller, 1927) was below 12 ‰ for five months of the year and below 10 ‰ for four months of the year. Since other factors do not appear to be limiting such low salinity conditions are presumably unfavorable for *Limnoria* at that locality.

Watson *et al.* (1936) did not find *Limnoria* at Kangaroo Point, Port of Brisbane, Australia, where the salinity averaged 16 ‰ but was subject to reductions as low as 2 ‰ for several days during periods of heavy runoff. During dry seasons the salinity rose as high as 28 ‰.

On the other hand *Limnoria* (presumably *L. (L.) lignorum*) is reported by Sϕmme (1940) to occur on the Danish coast down to Kjels Nor where the yearly average salinity is only 14.3 ‰ with a minimum of 8.6 ‰ for one month and at Neustadt on the German Baltic coast at a salinity of only 9-10 ‰.

Clearly more field data over long periods of time are needed to establish more precisely the natural limits of salinity variations tolerated by *Limnoria.* The animal appears to be moderately euryhaline in its salinity tolerance as compared with other marine organisms.

5. *Temperature.* Variations in temperature appear to have a significant influence on the distribution of *Limnoria.* Temperature above or below an optimal range might adversely effect a species through: killing the adults; not killing the adults but causing a cessation of breeding activity, causing a serious slowing in the rate of egg production, rate of embryonic development, or in impairing the survival rate of gametes, embryos, or larvae, or any combination of these.

Mawatari (1949) found temperatures ranging between 2°C and 6°C to be lethal to adult *Limnoria* (probably *L. (L.) tripunctata*). A cooling of 5°C water to —9°C in the course of 2½ hours was found by Sϕmme (1940) to result in an 83% kill of *L. (L.) lignorum* in Norway. Temperatures of 2°C-6°C were not found to be lethal to adults of *L. (L.) lignorum*. The important feature here is that each of the two species shows a different limiting temperature for adults. Within the geographic range of *L. (L.) lignorum* temperatures as low as 2°C-6°C are often encountered seasonally. Such is not the case for *L. (L.) tripunctata.*

The breeding of *L. (L.) tripunctata* at Beaufort, North Carolina, is reported by Coker (1923) to cease when temperatures fall below 10°C. Coker also found lower egg numbers during periods of warm water (summer) and cold water (winter) than during periods having intermediate temperatures. Menzies (1954) reports that egg production of *L. (L.) tripunctata* in San Diego Harbor requires about twice as much time at temperatures near 15°C than when temperatures were near 20°C.

Sϕmme (1940) reports the embryonic development of *L. (L.) lignorum* to be retarded when temperatures fell below 6°C. At 6°C the entire incubation period was estimated to cover about three months rather than the two months needed at higher temperatures. She suggests that at temperatures near zero the brood might survive only in a more or less dormant state.

Both experimental and field data suggest that the reproductive capacities of these species are seriously impaired when the temperature is below a certain limit. For *L. (L.) lignorum* this limit seems near 0°C and for *L. (L.) tripunctata* it appears to be near 6°C. Data on the effect of high temperatures on the activities of the species are scarce. Sϕmme (op. cit.) reports an average temperature of 24.7°C (over a period of five days) to be unfavorable for the development of embryos of *Limnoria lignorum*.

The distribution of the species sheds some additional light on these problems. The species of *Limnoria* for which abundant collections are available show a northern (cold) and some show additionally a southern (warm) limit to their distribution in the northern hemisphere. Some species appear to have no upper temperature limit as far as temperatures normally encountered in the ocean are concerned. Because species do have geographic limits it is reasonable to suspect, if other ecologic conditions are within tolerable limits, that locations more to the north or south probably have conditions unfavorable for population by that species. Obviously temperature conditions at marginal areas are favorable enough to permit the existence of the species. It seems evident also that temperature conditions within the range of a species are at some points more favorable for its development than at other points (optimal temperature conditions). The precise determination of optimal temperature conditions naturally depends on the results of field studies, laboratory experiments, and detailed natural population analysis correlated with temperature measurements.

In the northern hemisphere four categories of marine animal distribution have been established by students of zoogeography; e.g. arctic, boreal, temperate, and tropical.

Arctic Species

No species of *Limnoria* or *Paralimnoria* is known to have a typical Arctic distribution. The species which has occasionally been found in the Arctic and which occupies the fringe of the Arctic is *Limnoria (L.) lignorum*. From Sφmme's data (op. cit.) which suggest that development does not progress at 0°C., it would seem probable that this species is limited by the 0°C isotherm which surrounds the Arctic Ocean. Wood and kelps are largely lacking from the Arctic Ocean and this scarcity of food is perhaps equally as important in keeping *Limnoria* out of the Arctic. Spring and summer melting of ice and the dilution of sea water might also be factors contributing to its absence at least from the surface water. At any rate, low temperature, lack of food, and wide seasonal salinity variations apparently add up to an environment unfavorable for the existence of *Limnoria* in the Arctic.

Boreal Species[2]

Only one species, *Limnoria (L.) lignorum* has a typical boreal distribution (Fig. 25). It is found on the Pacific coast as far north as Sitka, Alaska, and on the Atlantic coast as far north as the western part of Iceland (Stephensen, 1929, p. 16). Presumably at these extreme locations one approaches, seasonally at least, temperature minima tolerable for this species. The seasonal temperature curves for Sitka, Alaska and Eastport, Maine (which is somewhat similar in its temperature to Iceland) are shown in Figure 26. At Sitka the mean seasonal minimum is 4.2°C, the maximum 13.6°C, the mean 8.3°C. At Eastport these values in order are 1.1°C, 11.0°C, and 6.1°C. On the Pacific coast the species extend south as far as Point Arena, California. At Samoa, Humboldt Bay, California it was collected with specimens of *Limnoria (L.) quadripunctata*. Temperature curves are not available for Point Arena, and those for Crescent City, California have accordingly been used. There the minimum temperature is 10.0°C, the maximum 14.0°C, and the

---

[2] The temperature values given here represent means over a variable number of years depending upon the locality. They are derived from the publications TW-1 and TW-2, U.S. Coast and Geodetic Survey, Washington, D.C., which cover the "Surface water temperatures at Coast and Geodetic tide stations"; 1947 (TW-1, Atlantic and Gulf Coasts) and 1948 (TW-2, Pacific Ocean).

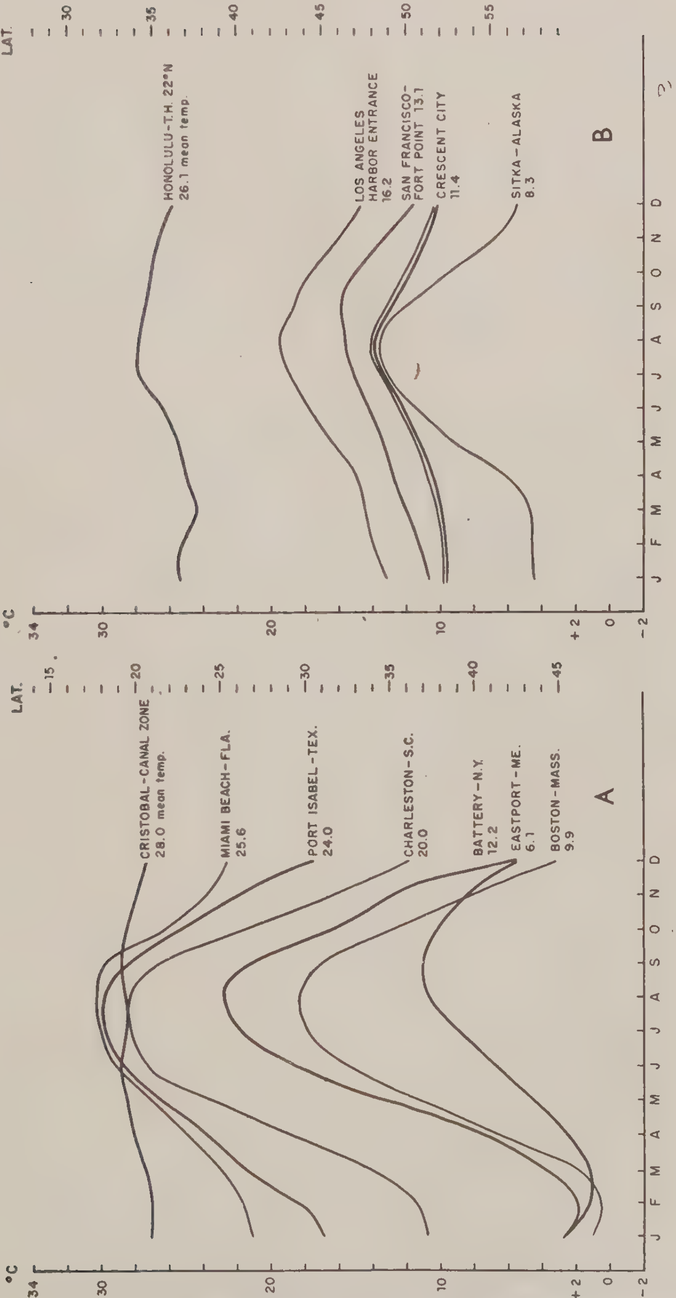

FIGURE 26. The monthly mean temperatures at various localities in America. A, Atlantic Ocean. B, Pacific Ocean.

(431)

mean 11.4°C. On the Atlantic coast *L. (L.) lignorum* is known as far south as Boston where the seasonal minimum is 0.4°C, the maximum 18.2°C, and the mean 9.9°C. It is interesting to note that temperatures lethal to adults are not encountered at either place but that low temperatures unfavorable for the development of the young do occur seasonally at all localities. The wide range of temperatures of localities between Boston and Eastport, allowing only a few consecutive months to have optimal temperatures would seem to offer less favorable conditions for *L. (L.) lignorum* than the narrower ranges encountered on the Pacific coast between Point Arena. California and Sitka, Alaska.

Temperate Species

Only one species, *Limnoria (L.) quadripunctata,* shows a temperate distribution. It is found between Humboldt Bay, California and La Jolla, California on the Pacific coast. However, its most southward extent in appreciable numbers is at the outer harbor of Los Angeles-Long Beach Harbors. It is not found on the Atlantic coast and this becomes a matter of considerable interest in view of the high number of collections available from the Atlantic coast. Temperatures from the outer harbor at Los Angeles are taken as representative of those at its southern limits. The minimum, mean and maximum seasonal temperatures at Crescent City are 10.0°C, 11.4°C, and 13.9°C. At Los Angeles harbor comparable values are 13.2°C, 16.2°C, and 19.4°C. If the mean temperatures of 11.4°C and 16.2°C at the extreme localities are assumed to represent limits containing within them an optimal range of temperatures for the development of this species then the absence of it from the Atlantic coast is easily accounted for. On the Atlantic coast from Eastport. Maine to Miami, Florida temperatures within that range are found only two successive months of the year and in total only three months out of the year (Table 2). In contrast within the range inhabited by the species the occurrence of assumed favorable temperatures is much more common; e.g. six months out of the year at Crescent City, seven months out of the year at Los Angeles and eleven months out of the year at San Francisco. At Sitka, Alaska four months of the year have temperatures within that range although the species is not known to occur here. If four successive months of the year having temperatures favorable for the species are insufficient for its establishment then two months of such temperatures, such as occur on the Atlantic coast would hardly seem adequate. Johnson, *et al.* (1947)

(432)

indicate that the duration of optimal temperatures appears to be important also in the control of the distribution of the snapping shrimps.

Temperate-Tropical Species

One species, *Limnoria (L.) tripunctata* extends from the temperate to the tropical areas on both coasts. On the Pacific coast its northward limit is San Francisco Bay. Its southward limit has not been defined but it has been collected at Mazatlan, Mexico and does occur in the tropical Pacific at Honolulu, Territory of Hawaii as well as at other islands in the central and south Pacific Ocean. Temperature records at Fort Point, San Francisco indicate a seasonal minimum of 10.6°C, a mean of 13.0°C, and a maximum of 15.8°C. The species has not been collected at Fort Point but has been collected at Berkeley Yacht harbor not far from there in company with *L. (L.) quadripunctata*. At Honolulu, a locality with temperatures approaching the upper limits tolerated by this species, the minimum is 24.3°C, the mean 26.1°C, and the maximum 27.8°C. On the Atlantic coast the species is found from New York harbor to the Caribbean and the Gulf of Mexico as far south as Panama. Again no upper temperature limit is evident. At the Battery in New York harbor the mean seasonal temperature shows a minimum of 1.8°C, a mean of 12.2°C, and a maximum of 22.8°C. At Cristobal in the Canal Zone of Panama the mean seasonal temperatures are at a minimum 26.8°C, at a mean of 28.0°C, and at a maximum of 28.8°C.

Tropical Species

In addition to *L. (L.) tripunctata* five species appear to fall in this category; *L. (L.) simulata, L. (L.) platycauda, L. (L.) pfefferi, L. (L.) saseboensis,* and *Paralimnoria andrewsi.* Two of the latter species of *Limnoria* have been collected at Miami but not elsewhere and the others occur in the Caribbean area but have not yet been reported from Miami or other parts of Florida. Obviously the data are too scarce to permit a delineation of the natural temperature requirements. It is doubtful, however, that they will be found much north of Miami on the Atlantic coast or north of Mazatlan on the Pacific coast where many collections have failed to reveal their presence. Presumably the temperature characteristics of these areas are too low and variable to allow their occurrence. If Miami is in fact the northernmost limit for these species, then the optimal conditions might be found in temperature ranges somewhere between those of Miami and the Caribbean areas. The seasonal temperature range at Miami has a minimum of 21.2°C, a mean of 25.6°C, and a maximum of 30.0°C. *Paralimnoria* also occurs in Honolulu where the seasonal averages are 24.3°C at minimum, 26.1°C at a mean and 27.8°C at a maximum.

SUMMARY

1) The systematics, geographical distribution and ecology of the wood and seaweed boring marine isopods of the family Limnoriidae occurring in North and Central America are described.

2) A brief review of the literature concerning taxonomic, distributional, ecologic, physiologic, and anatomical studies is given.

3) Directions are given for the collection, preservation, and examination of *Limnoria* for study.

The storage of specimens in 75% ethyl alcohol is recommended as the most satisfactory means of preservation.

4) The general morphology of *Limnoria* is described and characteristics having taxonomic utility are discussed.

5) A comparison of *Limnoria* with the related isopods *Sphaeroma, Cirolana,* and *Cymothoa* leads to the suggestion that *Limnoria* should be placed in a distinct family the *Limnoriidae* Harger (emend.).

6) The family Limnoriidae is characterized and a key is given to the genera it contains. The following genera and subgenera are recognized: genus *Limnoria* (sensu lato) (type *Cymothoa lignorum* Rathke), subgenus *Limnoria,* subgenus *Phycolimnoria n.* subg., (type *P. algarum* n. sp.), genus *Paralimnoria* n. gen. (type *Limnoria andrewsi* Calman).

7) A key is given to the various species occurring in the Americas. The following are described:

SPECIES	TYPE LOCALITY
Limnoria (Limnoria) lignorum (Rathke)	Norway
Limnoria (Limnoria) quadripunctata Holthuis	Holland
Limnoria (Limnoria) pfefferi Stebbing	Minikoi Atoll, Indian Ocean
Limnoria (Limnoria) tripunctata Menzies	San Diego, California
Limnoria (Limnoria) platycauda n. sp.	Curacao, Dutch West Indies
Limnoria (Limnoria) saseboensis n. sp.	Sasebo, Japan

(434)

Limnoria (Limnoria) simulata n. sp.	Virgin Islands, West Indies
Limnoria (Phycolimnoria) algarum n. sp.	Dillon Beach, California
Paralimnoria andrewsi (Calman), forma typica	Christmas Island, Indian Ocean
Paralimnoria andrewsi (Calman), forma A	Curacao, Dutch West Indies
Paralimnoria andrewsi (Calman), forma B	Key West, Florida

8) Four species have been found on the Pacific coast; *L. (L.) lignorum, L. (L.) quadripunctata, L. (L.) tripunctata, L. (P.) algarum.*

Four species have been found on the Atlantic coast, (excluding the Gulf and Caribbean); *L. (L.) lignorum, L. (L.) tripunctata, L. (L.) pfefferi, L. (L.) saseboensis.*

Four species are known from the Caribbean Sea and Gulf of Mexico; *L. (L.) tripunctata, L. (L.) platycauda, L. (L.) simulata,* and *P. andrewsi.*

Two species are common to both coasts; *L. (L.) lignorum* and *L. (L.) tripunctata* with the latter species occurring in the Gulf and Caribbean as well.

9) The following environmental factors are suspected or known to influence the distribution of *Limnoria:* Food supply, depth and associated phenomena, dissolved oxygen content, salinity, and temperature. Each factor is discussed and examples of the influence of each on distribution are given where possible.

An average dissolved oxygen concentration below 1.4 ppm (between 1.6 and 0.12) appears to limit the animals. Salinities below 10% similarly seem limiting. Temperature appears to be the major factor associated with the distribution of the various species. Low temperatures adversely affecting the reproductive capacity of the animals are considerably higher than those lethal to the adults. Temperature is believed to limit the distribution of the species primarily through its influence on the animal's reproductive abilities.

10) The absence of *L. (L.) quadripunctata* from the Atlantic coast is postulated as being due to its having a stenothermic reproductive range. Temperatures suspected to be entirely favorable for its development on the Pacific coast were found to occur only two successive months out of the year at locations on the Atlantic coast from Boston to Charleston, S.C. On the other hand, they occurred 6-11

successive months out of the year at localities within the range of the species on the Pacific coast.

11) No truly *Arctic* species was found. Of the wood-borers *L. (L.) lignorum* shows a typical *boreal* distribution on both sides of America. *L. (L.) quadripunctata* shows a *temperate* distribution. One species, *L. (L.) tripunctata,* shows a *temperate-tropical* distribution and is found on both coasts. The remaining species show a *tropical* distribution.

TABLE 2.

MONTHS DURING THE YEAR THAT TEMPERATURES BETWEEN 11.4°C AND 16.2°C PREVAIL AT VARIOUS LOCALITIES ALONG THE PACIFIC AND ATLANTIC COASTS. LOCALITIES HAVING THE SPECIES *L. (L.) quadripunctata* ARE MARKED WITH AN ASTERISK.

LOCATION	MONTH												Total No. Months
	J	F	M	A	M	J	J	A	S	O	N	D	
PACIFIC													
Sitka, Alaska	0	0	0	0	0	+	+	+	+	0	0	0	4
Crescent City*	0	0	0	0	+	+	+	+	+	+	0	0	6
San Francisco*	0	+	+	+	+	+	+	+	+	+	+	+	11
Los Angeles*	+	+	+	+	+	0	0	0	0	0	+	+	7
Honolulu, T. H.	0	0	0	0	0	0	0	0	0	0	0	0	0
ATLANTIC													
Eastport, Me.	0	0	0	0	0	0	0	0	+	0	0	0	1
Boston, Mass.	0	0	0	0	+	+	0	0	0	+	0	0	3
New York, N.Y.	0	0	0	0	+	0	0	0	0	+	+	0	3
Charleston, S.C.	0	+	+	0	0	0	0	0	0	0	0	+	3
Port Isabel, Tex.	0	0	0	0	0	0	0	0	0	0	0	0	0
Miami, Fla.	0	0	0	0	0	0	0	0	0	0	0	0	0

PART II:

ADDITIONS TO THE SYSTEMATICS

INTRODUCTION

The general features of classification, methods of collection, identification, anatomy, and nomenclature have been presented in Part I. Here it is my purpose to accomplish four things: first, to provide redescriptions of the known species in the four cases where such are needed, and second, to give descriptions to eight additional new species of *Limnoria,* four of which belong to the subgenus *Phycolimnoria* and five to the subgenus *Limnoria*, which have been subsequently discovered in the course of my studies on *Limnoria.* The third objective is to present a discussion of various taxonomic monstrosities which have arisen in the course of time since 1813 (1814) when Leach first gave the genus its present name. Finally a list has been compiled of the known and currently valid species with reference to their first description and subsequent revision.

DESCRIPTIONS OF WOOD-BORERS

REDESCRIPTIONS

Limnoria (L.) japonica Richardson

Figures 27-28

Synonymy:

Limnoria japonica Richardson, 1909, pp. 95-96, fig. 21. — Barnard, K. H., 1936, pp. 176-177.—Chilton, 1914a, pp. 382-387.—Kofoid and Miller, 1927, p. 309.—Holthuis, 1949, pp. 170-171.—Moll, 1915, p. 185, fig. 9.—Shiino, 1944, p. 2;—1950, p. 334.

Diagnosis. Flagellum of second antenna with four articles. Epipod of maxilliped not reaching the articulation of first article of palp with endopod; epipod semi-triangulate in shape, widest near the base and narrowing distally to a blunt point, length not exceeding three times the width. Mandibular palp with three articles. Fifth somite of pleon with two medially located tubercles, anterior tubercle separated from posterior one by a prominent sulcus. Pleotelson with a single prominent anterior medially located tubercle followed by a pair of large tubercles and their accompanying carinae. Posterior edge of pleotelson lacks tubercles and spike-like setae; lateral crests lack tubercles but have numerous spike-like setae. Lacinioid seta of right mandible with (usually) four distally spinulate branches near apex.

Measurements. Figured male paratype length 5.0 mm, pleotelsonal width 1.5 mm. Large ovigenous female paratype length 7.0 mm, telson width 1.7 mm. This species is evidently one of the largest of the genus, being excelled in size only by *L. (P.) stephenseni* n. sp. (p. 189).

Type locality. The types were taken from a depth of 163 fathoms at Lat. 37° 23′ N; Long. 137° 36′ E by the U. S. Fish Commission Steamer "Albatross" on the way from Nanoa, Hondo, Japan, to Isuruga, Hondo, Japan at Suduz Misaki Light (Richardson, 1909). The types are located in the U.S. National Museum, Cat. No. 39507.

Habitat. The types were taken from a water-logged fragment of bamboo.

Specimens examined. Over 30 cotypes were kindly sent to the writer by Dr. Fenner A. Chace, Jr., Curator, Marine Invertebrates, U. S. National Museum.

Geographical distribution. Known only from the type locality.

Remarks. Richardson's original description is erroneous in a number

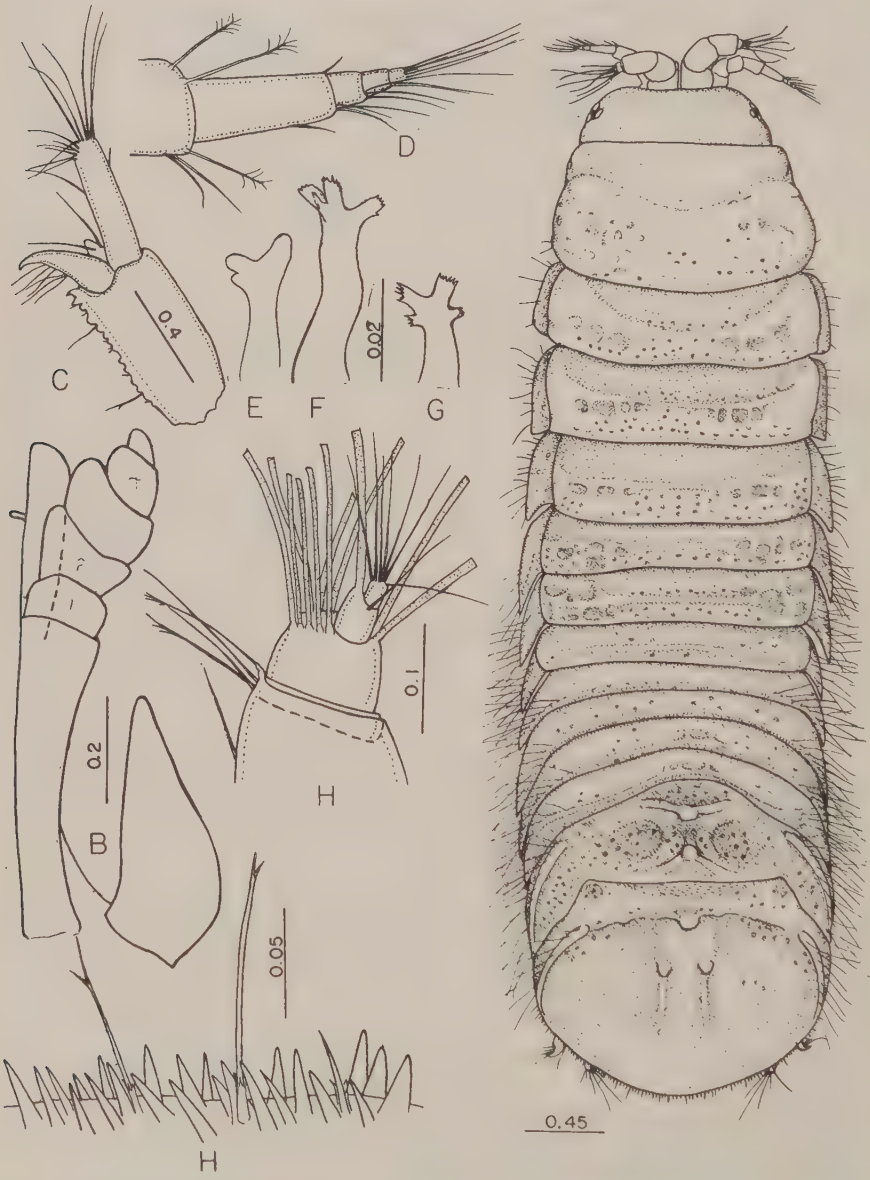

FIGURE 27. *Limnoria (L.) japonica* Richardson, cotype, male. A, lateral crest of pleotelson. B, maxilliped, setae omitted. C, uropod. D, flagellum of second antenna. E-G, lacinioid setae of right mandible. H, distal articles of first antenna. I, male. Figures with similar magnification, A; B, C; D, H; E, F, G; I.

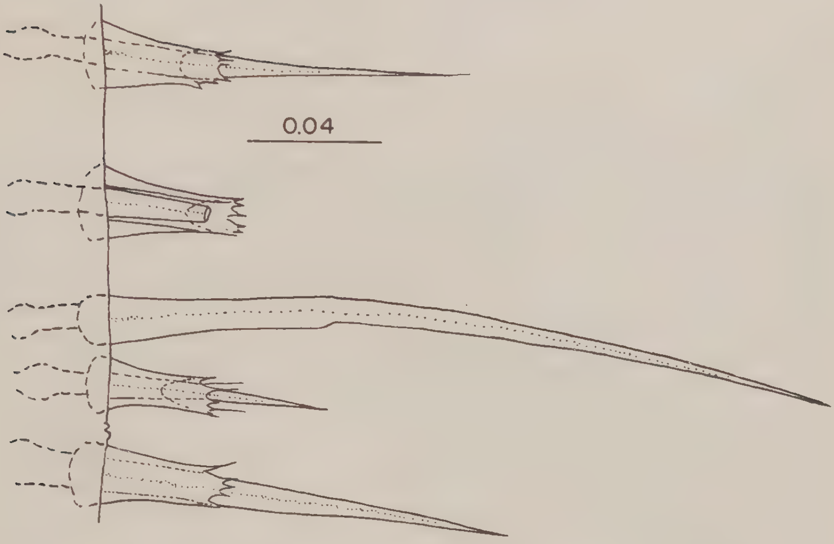

FIGURE 28. Pleotelsonic border of *L. (L.) japonica* Richardson.

of important respects. Most of these errors are corrected in the above diagnosis and therefore only a few additional notes need be given here. The first antenna consists of seven and not four articles. The flagellum of the second antenna has four and not five articles. Richardson did not mention the structure of the mandibles in her description and it is only by chance that Chilton (1914a, pp. 387-388) was correct when he assumed "that its mandible (palp) will be found to be three jointed and the epipods of the maxilliped to be short". Chilton in apparent disregard of this assumption however places *L. (L.) japonica* in his key with the species having "epipod of maxilliped longer than second joint". Holthuis (1949, p. 170) placed *L. (L.) japonica* in the group having the epipod of the maxilliped shorter than the second joint of the maxilliped, yet he, like the rest, had not seen specimens of *L. (L.) japonica*. Shiino (1944 and 1950) considered *L. (L.) japonica* a synonym of *L. (L.) tripunctata* (called *L. (L.) lignorum* by Shiino) and while the three tubercles on the pleotelson are similar to those of *L. (L.) tripunctata* the ornamentation of the fifth pleonal somite is different and the flagellum of the second antenna has four and not five articles and the pleotelsonal margin lacks the tuberculations characteristic of *L. (L.) tripunctata*.

Limnoria (?L.) septima Barnard

Figure 29

Synonymy:

Limnoria septima Barnard, 1936, pp. 174-177, text-figs. 11-12. — Holthuis, 1949, pp. 170-171.

Diagnosis. Flagellum of second antenna with five articles. Epipod of maxilliped not reaching the articulation of the first article of the palp with endopod; epipod semi-triangulate, narrowing distally to a point, and widest at base; length about three times the width. Mandibular palp with three articles. Structure of mandibular incisor not known. Fifth somite of pleon medially with a distal horseshoe-shaped carina and an opposing proximal horseshoe-shaped carina between which is an unornamented sulcus. Pleotelson with a medial elevated, bituberculate horseshoeshaped carina distal to which are two parallel carinae. Posterior margin of pleotelson with a dorsally directed fringe of spike-like setae, marginal setae numerous, tuberculations absent. Lateral crests devoid of tubercles. Structure of lacinioid seta of right mandible not known.

Measurements. Figured female cotype, length 6.4 mm, width of pleotelson 1.7 mm Barnard (1936) records the female cotypes as being 5.25 mm and 5.75 mm in length. Because he had only two adult female specimens the one examined by me should be one of them. There exists, therefore, a minimal difference of 0.65 mm. between the measurements. This may be due to a separation of the somites of the specimen and the resultant stretching of the body.

Type locality. The types were taken from a depth of between 185 and 250 fathoms in the Indian Ocean by the R.I.M.S. "Investigator" at two localities, North Sentinel, Andamans, 3 specimens, and Station 233, 13° 17′ 15″ N by 93° 10′ 25″ E, at 185 fathoms, Andamans. 1 juv. specimen (Barnard, 1936).

Habitat. No indication was given by Barnard as to the habitat of this species. In the absence of such information, three possibilities suggest themselves: (1) the specimens were taken from floating seaweed which was incidentally taken in the dredge haul; (2) they were taken from water-logged wood; (3) or they were taken free in the dredge haul in association with neither algae nor wood. The third possibility seems unlikely in view of the boring habits of the species of *Limnoria.* The others could be decided by a removal of the mandibles or an examination of the gut contents. Dissection of the cotype seemed inadvisable because the mandible were not movable without possible injury of the specimen. The food of this species and hence its subgeneric assignment will probably have to await the collection of more material.

Specimens examined. One female cotype was examined. This was

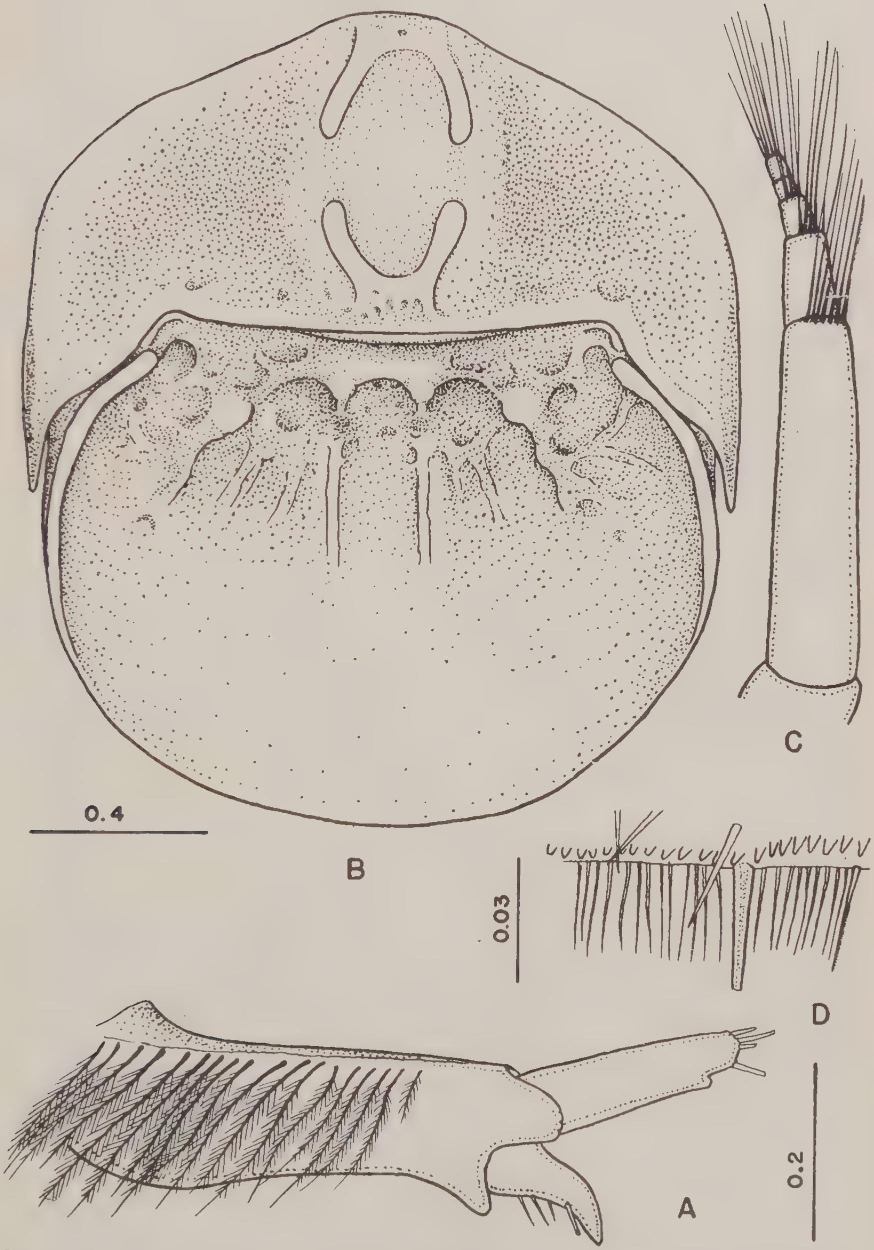

FIGURE 29. *Limnoria (?L.) septima* Barnard, female cotype. A, uropod. B, pleotelson. C, flagellum of second antenna. D, posterior edge of pleotelson. Figures with similar magnification, A, C; B; D.

(441)

very kindly sent as a loan to the writer by Dr. K. K. Tiwari, Carcinologist, Zool. Survey India, Calcutta, India.

Geographical distribution. Known only from the type locality.

Remarks. The description given this species by Dr. Barnard (1936) is in general very good; however, a few points need correction. The most anterior carina of the fifth somite of the pleon is horse-shoe shaped and not only a pair of parallel ridges as Barnard describes and figures. The second antenna is not "as in *lignorum*" because its flagellum consists of five and not four articles. Each maxilliped has one coupling hook which was not mentioned by Barnard. The maxillipedal epipod is not nearly as short as that figured by Barnard but extends at least three-fourths the length of the "end joint". Barnard (1936, p. 176) states that his specimens "bear most resemblance" to *L. (L.) japonica.* This is not the case because *L. (L.) japonica* belongs to the group of *Limnoria* characterized by having a second antennal flagellum with four and not five articles and an anterior medially located tubercle on the pleotelson.

Holthuis (1949, p. 171) thought that *L. (L.) quadripunctata* and *L. (L.) septima* were closely related because they resembled each other in the shape of the uropods. This is not the case because, as Barnard remarks, "the inner ramus is only one-half the length of the peduncle," whereas in *L. (L.) quadripunctata* Holthuis, the inner ramus (endopod) is, as Holthuis figures (Holthuis, 1949, fig. 2i), about equal to the length of the peduncle.

NEW SPECIES

Limnoria (L.) multipunctata, new species

Figures 30-31

Diagnosis. Flagellum of second antenna with four articles. Epipod of maxilliped reaching slightly beyond articulation of first article of palp with endopod; epipod spatulate in shape, blunt at distal end, being two and three-quarters times as long as wide. Mandibular palp with three articles. Fifth somite of pleon smooth medially. Pleotelson medially with an anteriorly located pair of tubercles followed by a larger more posteriorly located pair. This is followed by a multituberculate medially located carina. Posterior border of pleotelson with a conspicuous fringe of tubercles, spike-like setae lacking; lateral crests tuberculate. Lacinioid seta of right mandible reduced, simple, lacking spinules or serrations.

Measurements. Holotype male length, 1.9 mm; pleotelson width 0.4 mm. Allotype length, 2.0 mm; pleotelson width 0.4 mm.

Type locality. The type specimens were taken off the Kai Islands (5°-6° 5′ S by 131° 5′ to 133° 15′ E) in the South Pacific Ocean

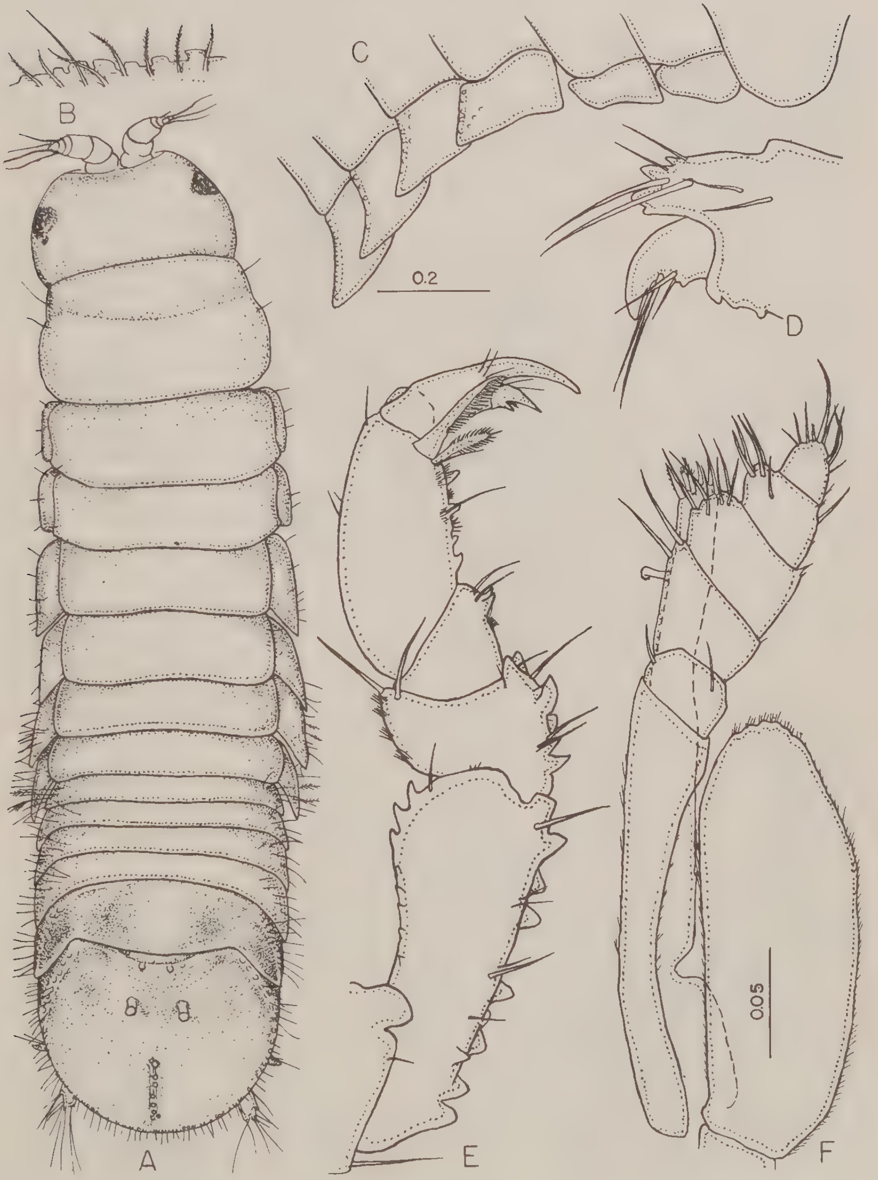

FIGURE 30. *Limnoria (L.) multipunctata,* new species, male paratype. A, male. B, lateral crest of pleotelson. C, lateral margin of peraeon. D, distal articles of uropod (endopod not figured). E, distal articles of first peraeopod. F, maxilliped. Figures with similar magnification, A, C; B, D, E, F.

(443)

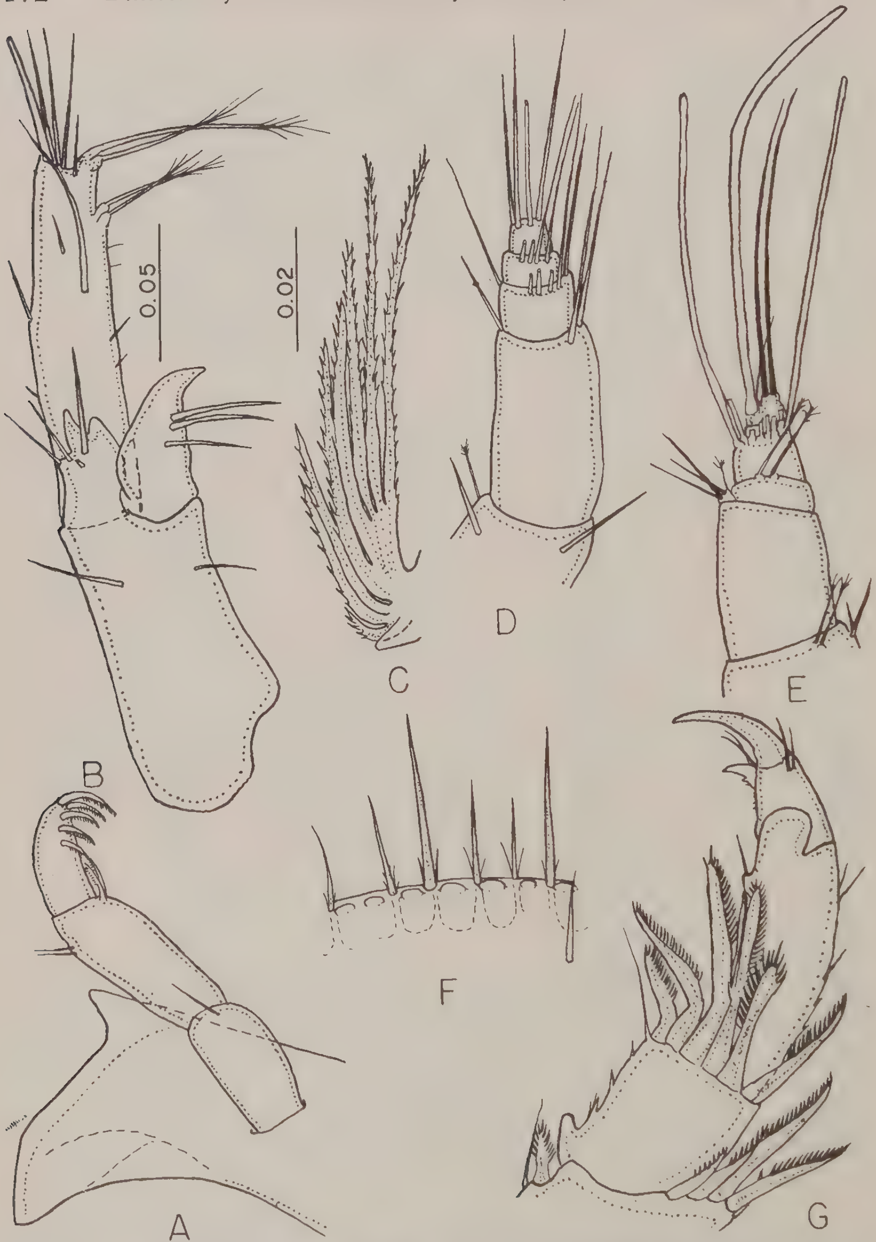

FIGURE 31. *Limnoria (L.) multipunctata,* new species, male paratype. A, mandible. B, uropod. C, setal row and lacinioid seta of right mandible. D, flagellum of second antenna. E, flagellum of first antenna. F, posterior edge of pleotelson. G, distal articles of seventh peraeopod. Figures with similar magnification, A, B, D, E, G; C; F.

(444)

from a depth of 13 meters on June 12, 1922, by the Danish Expedition to Kei-Oerne (Kai Isls.) in 1922. The specimens were lent to me by Dr. Torben Wolff, of the Universitetets Zoologiske Museum, København. The types consisting of a holotype, allotype and 55 paratypes have been returned to that institution. Five paratypes have been deposited in the collections of the United States National Museum, Washington, D. C.

Habitat. The specimens were removed from their burrows on a piece of *Teredo* infested wood.

Specimens examined. Other than the above mentioned types, specimens were examined which had been collected from the following localities in the Pacific Ocean. *Saipan Island,* U. S. Navy, July, 1948, 6 specimens, Charles H. Edmondson collection. *Canton Island,* Phoenix Isls., U. S. Navy, 1948-49 (?), 9 specimens, C. H. Edmondson collection. *Guam Island,* K. V. Bossler, July 30, 1946, 14 specimens, C. H. Edmondson collection. The specimens from Saipan were found in wood which was also attacked by *L. (L.) tripunctata* and *Paralimnoria andrewsi.*

Geographical distribution. South and Central Pacific Ocean at Guam, Saipan, Canton Isl., and the Kai Isls.

Remarks. The species appears similar to *L. (L.) platycauda* Menzies (p. 139), but differs markedly from the species in the tuberculations of the pleotelson and in the absence of a mid-longitudinal carina on the fifth somite of the pleon.

Limnoria (L.) unicornis, new species

Figure 32

Diagnosis. Flagellum of second antenna with four articles. Epipod of maxilliped short, not reaching the articulation of first article of palp with endopod; semi-triangulate in shape, three times as long as wide; apex acute. Mandibular palp with one article. Fifth somite of pleon with an anteriorly located, depressed, triangulate area on mid-line followed by a mid-longitudinal carina. Pleotelson with a large, elevated, median tubercle at proximal end. Posterior margin of pleotelson lacking tubercles; spike-like setae present. Lateral crests lack tubercles. Lacinioid seta of right mandible a simple, apically spinulate seta.

Measurement. Holotype male, length 2.9 mm, width of pleotelson 0.65 mm.

Type locality. Ponape, Caroline Isls., Pacific Ocean, 1948 (?), collected by U. S. Navy for C. H. Edmondson, holotype male, plus one pleon. These have been returned to Dr. Edmondson. In the vial with

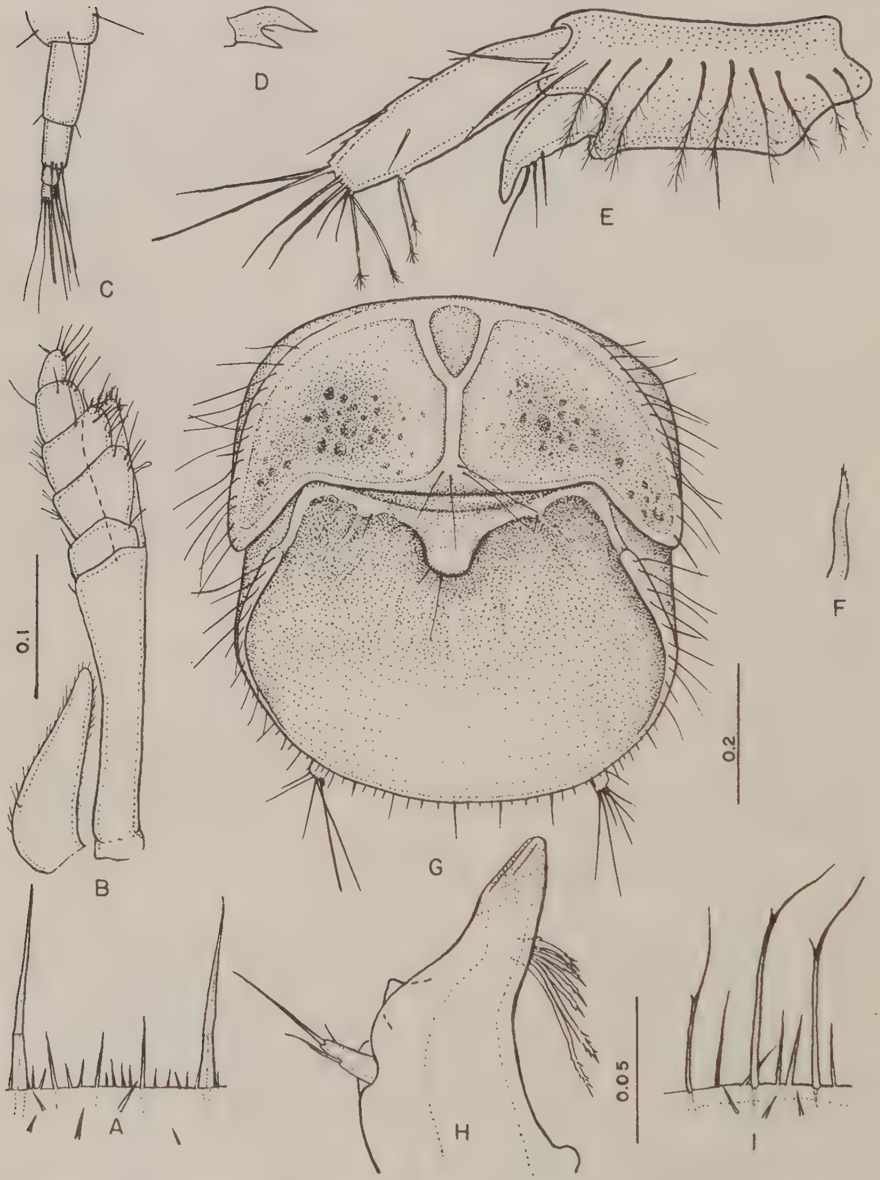

FIGURE 32. *Limnoria (L.) unicornis,* new species, male holotype. A, posterior edge of pleotelson. B, maxilliped. C, flagellum of second antenna. D, accessory claw of first peraeopod. E, uropod. F, lacinioid seta of right mandible. G, pleotelson. H, right mandible, outer surface. I, lateral crest of pleotelson. Figures with similar magnification, A, D, H, I; B, C, E; G; F (magnification not known).

this species were some specimens of *L.* (*L.*) *insulae* (p. 178).

Habitat. From wooden test sample.

Specimens examined. Types only.

Geographical distribution. Known only from Ponape Isl.

Remarks. This species is unique in having a mandibular palp consisting of only one article. In pleotelsonal ornamentation this species resembles the algal borers *L. (P.) segnis* (Chilton) and *L. (P.) segnoides* Menzies (p. 184) which species similarly exhibit a reduction in the number of articles of the mandibular palp.

Limnoria (L.) foveolata, new species

Figure 33

Diagnosis. Flagellum of second antenna with five articles. Epipod of maxilliped just reaching the articulation of palp with endopod. Epipod straplike but tapering gradually to a point at distal end, being three times as long as wide. Mandibular palp with three articles. Fifth somite of pleon foveolate, central portion raised and provided with deep pits and subparallel irregular ridges. Pleotelson medially with two tubercles at anterior end each followed by an irregular carina; lateral areas deeply foveolate. Posterior edge of pleotelson lacking tubercles and regularly arranged spike-like setae which are minute and delicate. Lateral crests of pleotelson devoid of tubercles. Lacinioid seta of right mandible with three medially recurved spines at apex.

Measurements. Holotype female, length 2.2 mm, width of pleotelson 0.5 mm.

Type locality. The holotype, and only specimen, was collected at Station 103 of the Danish Expedition to the Kei-Oerne (Kai Islands) in 1922 from a depth of 52 meters in the Sigsbee trawl. The specimen has been returned to Dr. Torben Wolff of the Universitetets Zoologiske Museum, København.

Habitat. Nothing was given on the label which might indicate from which material the specimen was taken. From the structure of the mandibles a wood-boring habit is clearly indicated.

Specimens examined. Type only.

Geographical distribution. Known only from the type locality.

Remarks. Superficially this species resembles *L. (L.) saseboensis* Menzies (p. 141) to a considerable degree. It can be distinguished from it by the lack of marginal tubercles on the pleotelson and by its much longer maxillipedal epipod.

Limnoria (L.) sublittorale, new species

Figure 34

Diagnosis. Flagellum of second antenna with five articles. Epipod of max-

(447)

illiped triangulate, elongated, reaching to the articulation of the first article of palp with endopod. Epipod three times as lòng as wide. Mandibular palp with three articles. Fifth somite of pleotelson with a pair of longitudinal carinae mid-dorsally. Pleotelson with a pair of parallel longitudinal carinae mid-dorsally; posterior margin with a fringe of upward-directed spike-like setae and a margin of simple setae of differing lengths. Lacinioid seta of right mandible with two recurved teeth at apex.

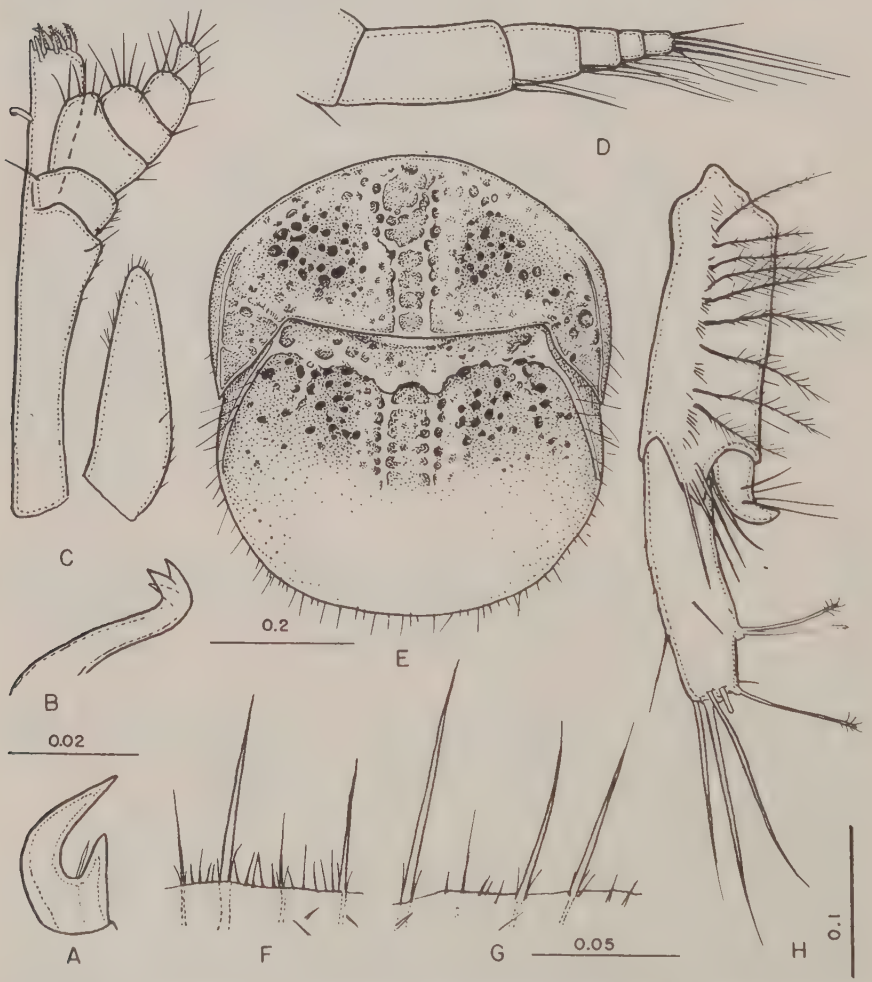

FIGURE 33. *Limnoria (L.) foveolata,* new species, holotype. A, accessory claw of first peraeopod. B, lacinioid seta of right mandible. C, maxilliped. D, flagellum of second antenna. E, pleotelson. F, uropod. G, posterior margin of pleotelson. H, lateral crest of pleotelson. Figures with similar magnification, B; D, H; E; F, G; A and C not known.

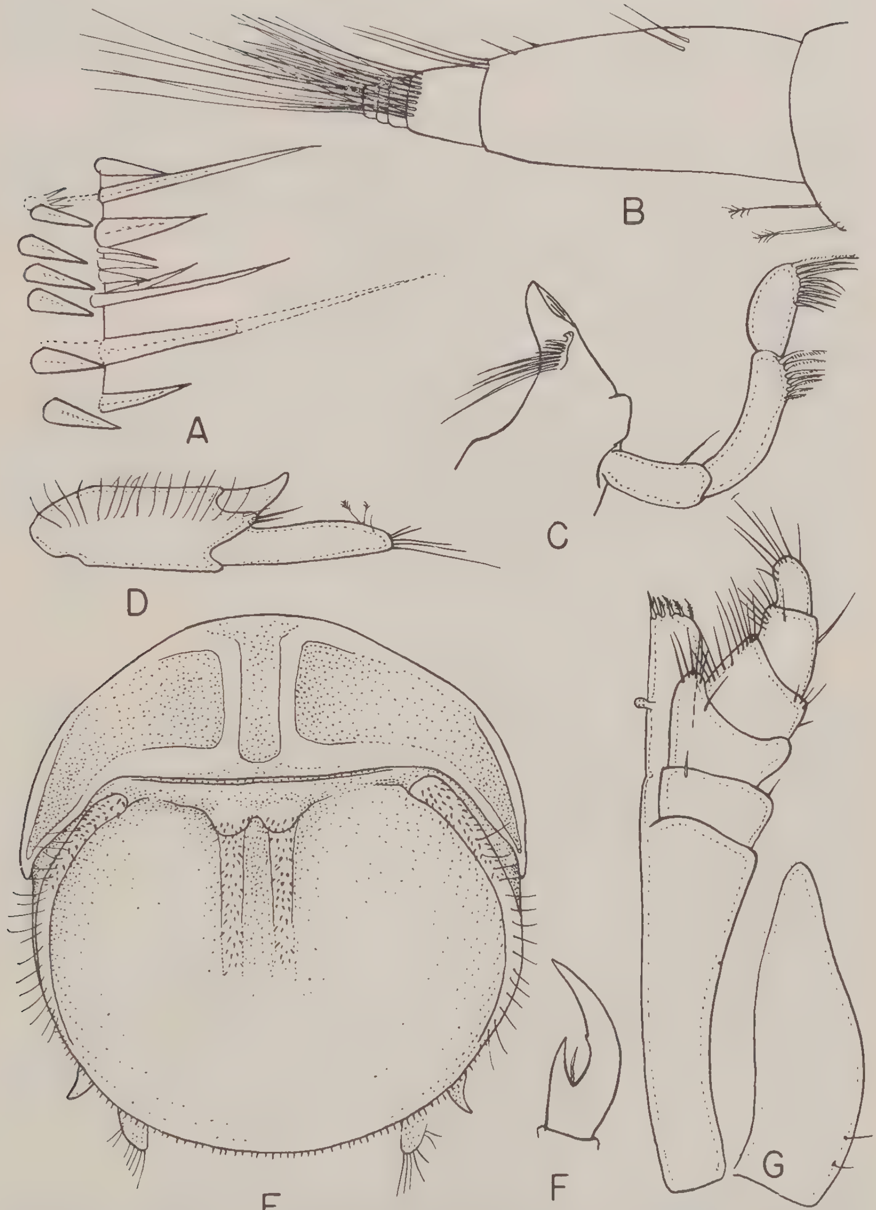

FIGURE 34. *Limnoria (L.) sublittorale,* new species, male paratype. A, posterior border of pleotelson. B, flagellum of second antenna. C, right mandible. D, uropod. E, pleotelson. F, accessory claw of dactyl of first peraeopod. Magnification, scales various, all taken from paratype 4 mm in length and 1.2 mm in width of pleotelson.

Measurements. Holotype male, length 5.0 mm, width of pleotelson 1.3 mm. Paratype male, length 4.0 mm, width of pleotelson 1.2 mm.

Type locality. From Oregon fir (Douglas fir) timber forming part of the frame of Otter board of Otter fish trawl retrieved from 60 fathoms off the coast of New South Wales, Australia. Collected by Frank McNeill, Australian Museum, Sydney, N.S.W., Australia. The specimens have been returned to Frank McNeill.

Specimens examined. Types only.

Geographical distribution. Known only from type locality.

Remarks. This species resembles *Limnoria (L.) quadripunctata* Holthuis and especially *L. (L.) saseboensis* Menzies (p. 141). It differs from *quadripunctata* in the structure of the carinae on the fifth somite of the pleon and from *saseboensis* in lacking tuberculations along the posterior margin of the pleotelson. It differs from *L. (L.) foveolata* in having a fringe of stout spike-like upward directed setae along the posterior margin of the pleotelson.

Limnoria (L.) insulae, new species

Figure 35

Diagnosis. Flagellum of second antenna with four articles. Epipod of maxilliped just reaching the articulation of first article of palp with endopod. Epipod spatulate, widest near middle, two and three-quarters times as long as wide. Mandibular palp with three articles. Fifth somite of pleon with a conspicuous hump on midline near distal border. In females the hump is markedly reduced to only a mid-longitudinal carina. Pleotelson lacking ornamentation but the lateral crests of the male particularly are much elevated and extend outward over the cup-shaped part of the pleotelson. Posterior margin of pleotelson tuberculate; spike-like setae lacking. Lacinioid seta of right mandible with two apical spines.

Measurements. Holotype male, length 3.8 mm, width of pleotelson 1.0 mm. Allotype length 3.0 mm, width of pleotelson 0.8 mm.

Type locality. Serua, Fiji Isl., December 15, 1952, low tide level, coconut tree trunk, 139 specimens collected by Dr. Martin W. Johnson. With this species were specimens of *L. (L.) tripunctata* Menzies and *L. (L.) saseboensis* Menzies.

Material examined. 137 paratypes from Fiji in addition to the holotype and allotype. *Guam Isl.*, one male, collected by K. V. Bossler, from C. H. Edmondson collection with specimens of *L. (L.) multipunctata* (p. 170). *Palmyra Isl.*, U.S. Navy, 2 specimens, collection of

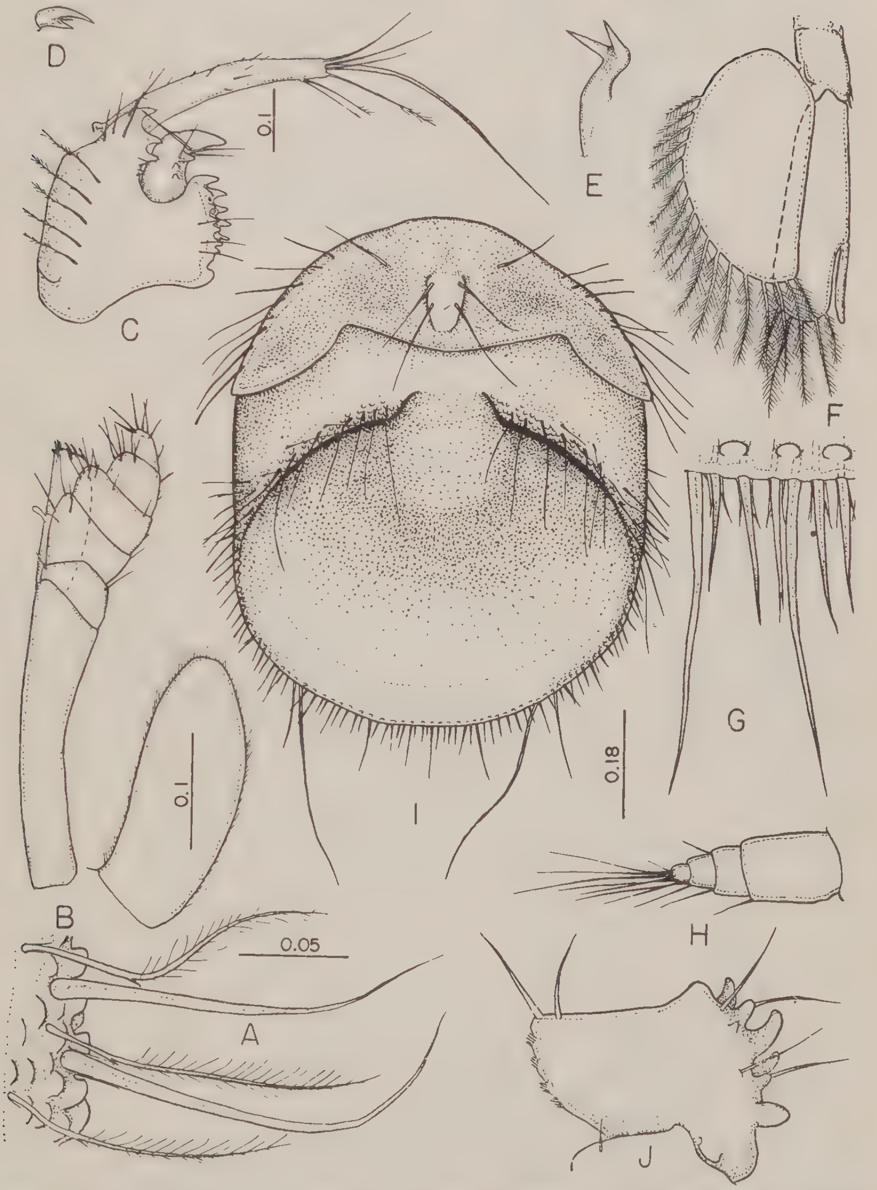

FIGURE 35. *Limnoria (L.) insulae*, new species, male. A, lateral crest of pleotelson. B, maxilliped. C, uropod. D, accessory claw of first peraeopod. E, lacinioid seta of right mandible. F, second pleopod. G, posterior edge of pleotelson. H, flagellum of second antenna. I, pleotelson. J, merus of first peraeopod. Figures with similar magnification, A, D, G, H, J; B; C, F, I; E.

C. H. Edmondson. *Ponape,* Caroline Isls., U.S. Navy, one male, collection of C. H. Edmondson.

Geographical distribution. South Pacific Ocean.

Remarks. The peduncle of the uropods of this species are markedly compressed and the tuberculations are spine-like. This characteristic and the cup-like nature of the pleotelson distinguishes this species from all others known to date.

DESCRIPTIONS OF ALGAL-BORERS

REDESCRIPTIONS

Limnoria (Phycolimnoria) antarctica (Pfeffer)

Figure 36

Synonymy:

> *Limnoria antarctica* Pfeffer, 1887, pp. 96-102, pl. 2, figs. 12-13, pl. 5, figs. 2-22; — 1890, p. 504. — Vanhöffen, 1914, pp. 509 510.

Diagnosis. Flagellum of second antenna with four articles. Epipod of maxilliped reaching slightly beyond the articulation of palp with endopod; epipod strap-like, slightly narrow at apex, slightly more than four times as long as wide. Fifth somite of pleon with a distinct transverse ovoid carina near distal margin and a pair of irregularly parallel carinae in the sulcus between them. Pleotelson medially with a large median swelling which is followed by a pair of parallel carinae; lateral to these are less distinct irregular carinae. Posterior margin of pleotelson with a dorsal fringe of large spike-like setae, margin with large distinctive setae. Entire pleotelson provided with distinct spike-like seta. Lateral crests devoid of tubercles. Lacinioid seta similar to other setae in setal row.

Measurements. Pfeffer (1887, p. 102) gives the length of one type as 4.5 mm, greatest width 1.6 mm. The longest specimen of the 58 type specimens examined by me was 5.0 mm in length.

Type locality. Süd-Georgian I., 1883, Ebbe unter Steinen, dieselbe Art ist in hohlen gangen in Tangwurzeln, No. K 19355, Hamburg Museum.

Habitat. This species was collected from algae under stones and from bore-holes in *Macrocystis* according to the label on the vials and from Pfeffer's (1887) description.

Specimens examined. A total of 58 type specimens were examined which were generously sent as a loan by Dr. A. Panning, Curator of Zoology, Hamburg Museum.

Geographical distribution. South Georgia Isl.—(Pfeffer, 1887), Kerguelen (Dreiinselhaven and Observatory Bay, Vanhöffen, 1914).

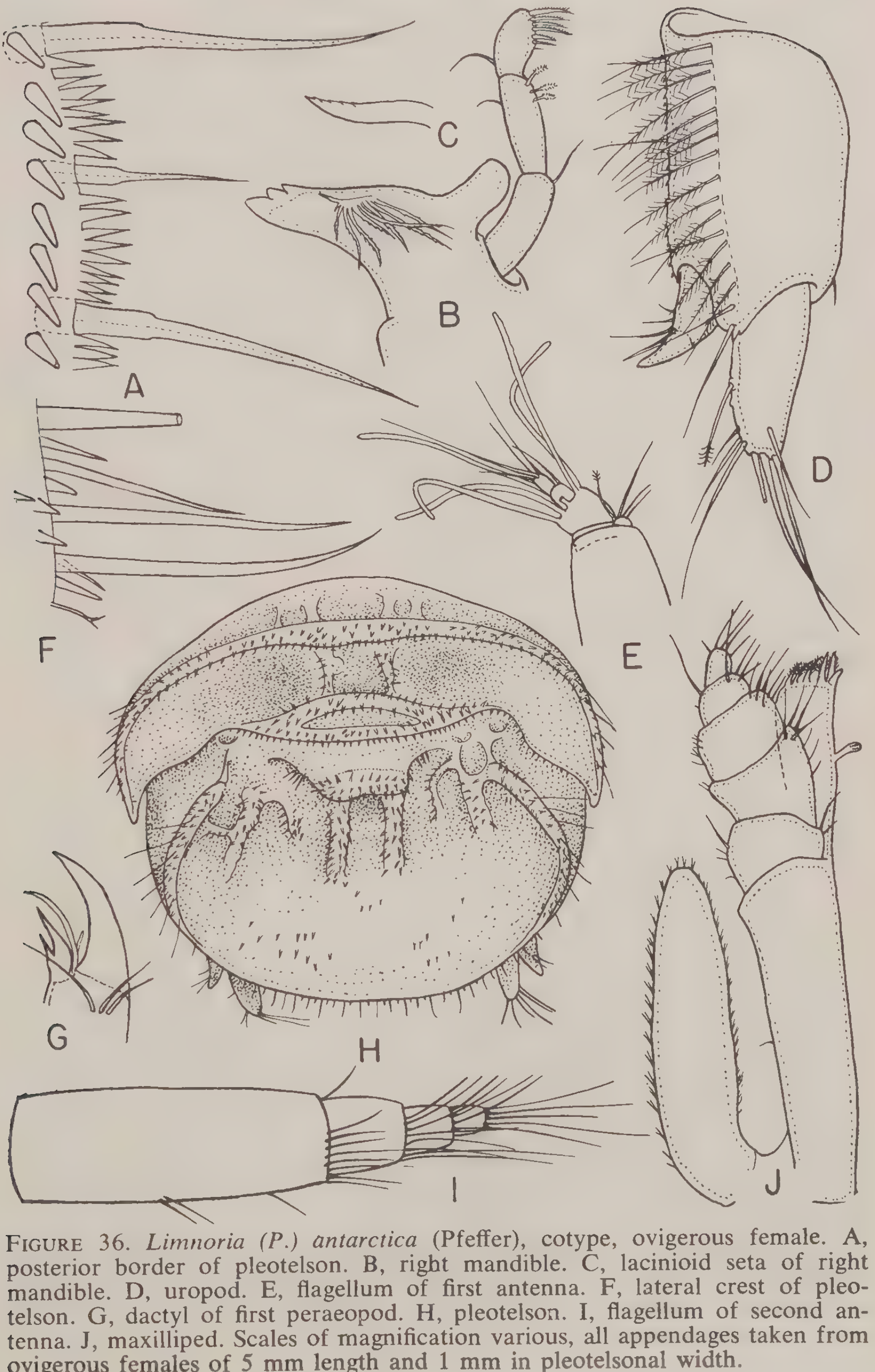

FIGURE 36. *Limnoria (P.) antarctica* (Pfeffer), cotype, ovigerous female. A, posterior border of pleotelson. B, right mandible. C, lacinioid seta of right mandible. D, uropod. E, flagellum of first antenna. F, lateral crest of pleotelson. G, dactyl of first peraeopod. H, pleotelson. I, flagellum of second antenna. J, maxilliped. Scales of magnification various, all appendages taken from ovigerous females of 5 mm length and 1 mm in pleotelsonal width.

Remarks. Pfeffer's elaborate description of this species is particularly good. The transverse carina on the fifth pleonal somite, a feature peculiar to this species, is shown by Pfeffer; however, the distinctive pleotelsonal carinae are only slightly indicated in the figures given by Pfeffer. The eyes have the usual seven facets and not only four. Pfeffer's figure of the uropod is incorrect because the exopod is claw-like and not a miniature of the endopod. Several of the illustrations given by Pfeffer are incorrect although they show the general form and proportions rather accurately.

It is doubtful that the specimens which Hale (1937) refers to this species actually belong to it. In the first place the mature specimens examined by Hale are twice the length of Pfeffer's specimens. Secondly, the uropodal exopod of *antarctica* is 2/3 the length of the endopod and not ½ the length of the endopod as it is in Hale's specimens. Hale's specimens have been referred to a new species, *L. (P.) stephenseni* which is described in this paper and which Stephensen had originally considered but with some doubt as equal to *Limnoria pfefferi* Stebbing. These specimens Hale considered as synonyms of *L. (P.) antarctica.*

It is now impossible, without examination of the specimens, to assign to a species the specimens which were reported by Richardson (1913) from the Deception and South Shetland Islands.

Limnoria (Phycolimnoria) segnis (Chilton)

Figure 37

Synonymy:

Limnoria segnis Chilton, 1883, pp. 76-77, pl. 2, fig. 1; 1914a, pp. 381-389, pl. XVII, figs. 1-5; — 1919, pp. 4-6, figs. 3, 5. — Kofoid and Miller, 1927, p. 309. — Holthuis, 1949, p. 170. — Moll, 1915, p. 184, fig. 6. — Stebbing, 1893, pp. 367-368; — 1905, p. 714.

Diagnosis. Flagellum of second antenna with three-four articles. Epipod of maxilliped reaching beyond the articulation of the first and second articles of the palp; epipod strap-like, elongated, being five times as long as wide. Mandibular palp with only two articles. Fifth somite of pleon with a median longitudinal carina which appears broken at the center, and anteriorly inconspicuously bifurcated. Pleotelson medio-anteriorly with a short transverse ridge having swollen tuberculiform areas at each end; each tuberculiform ridge followed distally by a short longitudinal ridge. Posterior edge of pleotelson lacks tubercles but bears a fringe of dorsally directed spike-like setae near the margin. Lacinioid seta of right mandible not markedly different from setae of setal row.

Measurements. Chilton (1883) remarks that the length of this species is one-sixth of an inch (about 4 mm). The largest cotype specimen

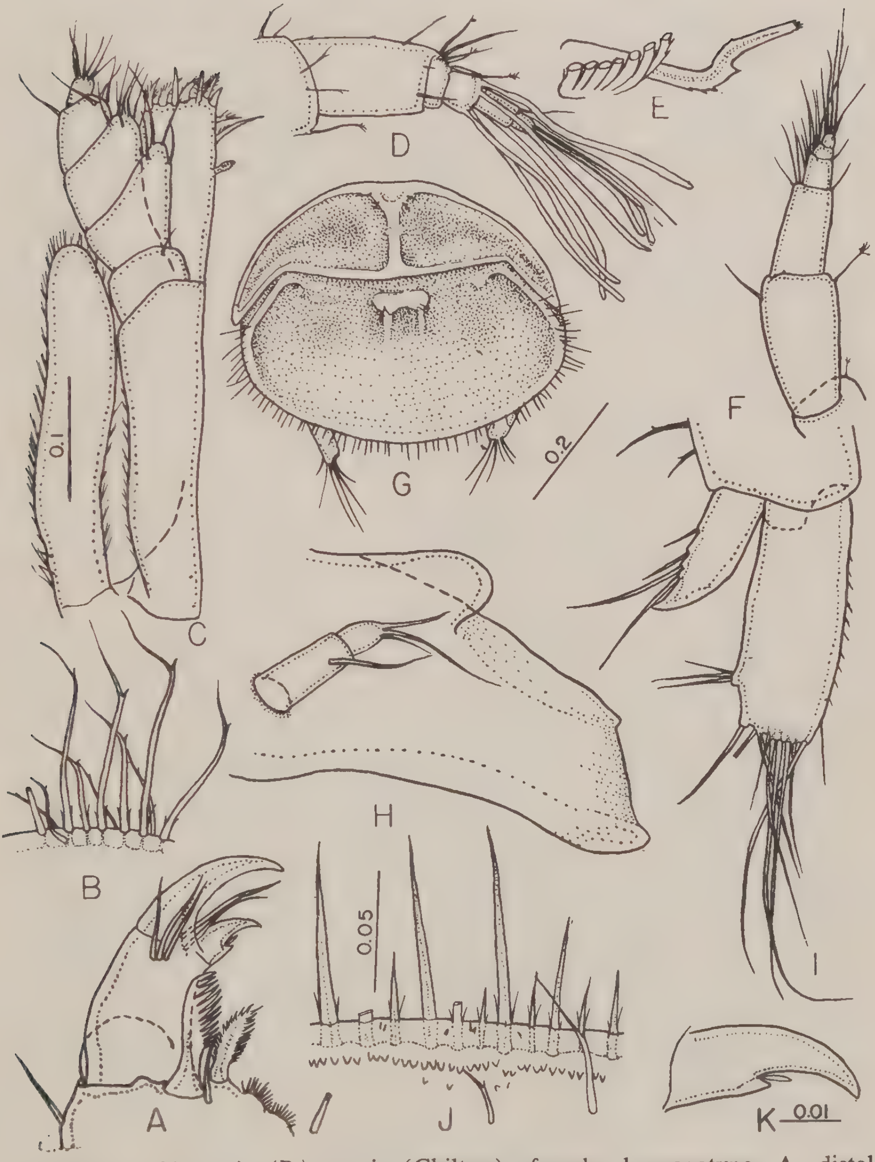

FIGURE 37. *Limnoria (P.) segnis* (Chilton), female, homoeotype. A, distal articles of first peraeopod. B, lateral crest of pleotelson. C, maxilliped. D, distal articles of first antenna. E, setal row and lacinioid seta of right mandible. F, apical articles, including flagellum, of second antenna. G, pleotelson. H, outer aspect of mandible. I, uropod. J, distal margin of pleotelson. K, accessory claw of first peraeopod. Figures with similar magnification, A, B, J, H; C, D, F, I; G; E, K.

examined by me was 4.0 mm in length and 1.0 mm in the width of the pleotelson.

Type locality. The species was originally taken "on seaweed" at Lyttelton Harbor, New Zealand (Chilton). Later Chilton (1914a, p. 382) notes that specimens were taken from holdfasts of *Macrocystis*. The types are located in Dr. Chilton's collection at Canterbury University College, Christchurch, New Zealand.

Specimens examined. Two lots of specimens were examined. Both were from Lyttelton Harbor and both were identified by Dr. Chilton. The first lot containing two ovigerous females and one male was sent to me by Dr. Isabella Gordon of the British Museum (Natural History). The second lot consisting of 14 cotype specimens was the loan of the Department of Biology, Canterbury University College, Christchurch. New Zealand, through the kindness of Dr. E. Percival, Professor of Biology.

Geographical distribution. The species thus far has been recorded only from Lyttelton and Akaroa Harbors, New Zealand (Chilton, 1914, p. 382).

Remarks. In the original description Chilton (1883) failed to record the sculpturing present on the dorsal surface of the fifth somite of the pleon and pleotelson. Later (1914, p. 383) he describes essentially what is shown in the figure reproduced here. His original figure of the maxilliped shows the palp consisting of only four articles. Later (1914a, pl. XVII, fig. 2) he indicates five articles; however in 1919 (fig. 5) he shows only four. In 1883 (fig. 1c) he shows a strap-like maxillipedal epipod; whereas in later papers he figures the epipod as club-shaped. The shape of the maxillipedal epipod is usually characteristic for each species; therefore, the possibility that Chilton confused two species should not be overlooked. The reduction of the mandibular palp from three to two articles is an interesting and useful specific characteristic. Chilton (op. cit.) was unable to find the scale of the first antenna, which is definitely present though concealed by an overgrowth of the preceding article of the antenna.

NEW SPECIES

Limnoria (Phycolimnoria) segnoides, new species

Figure 38

Diagnosis. Flagellum of second antenna lost. Epipod of maxilliped clavate, widest at mid-region, being about three times as long as wide and extending

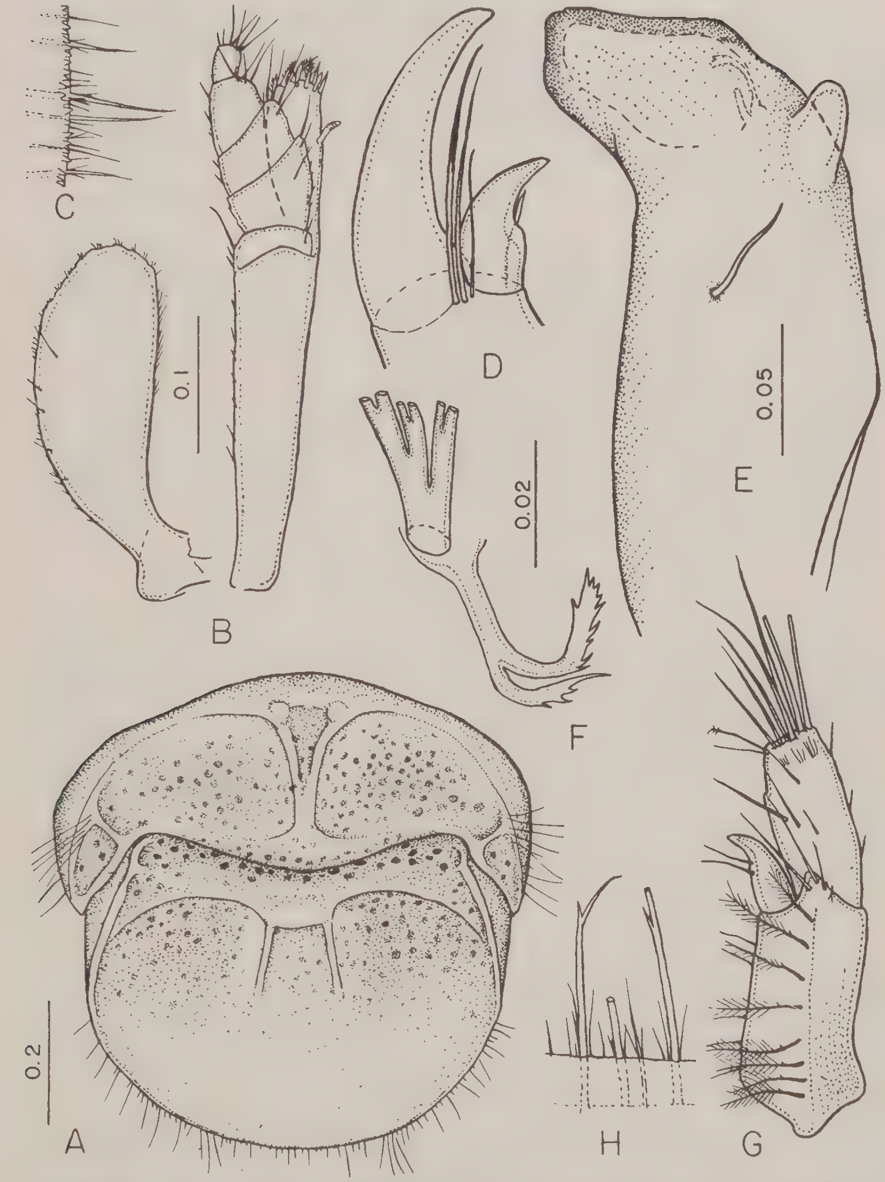

FIGURE 38. *Limnoria (P.) segnoides,* new species. A, pleotelson. B, maxilliped. C, posterior margin of pleotelson. D, distal parts of first peraeopod. E, outer surface of left mandible. F, lacinioid seta and setal row of right mandible. G, uropod. H, lateral crest of pleotelson. Figures with similar magnification, A; B, G; C, E, H; D, F.

to the articulation of palp with endopod. Mandibular palp lacking but is replaced by a stout long seta. Fifth somite of pleon with a median V-shaped carina. Pleotelson medially with an elevated anteriorly located region followed by two subparallel carinae. Posterior edge of pleotelson lacking tubercles but bearing a fringe of dorsally directed spike-like setae near margin. Lacinioid seta of right mandible composed of two simple marginally serrated setae which are similar to those in the setal row.

Measurements. Holotype female, length 2.7 mm, pleotelson width 0.6 mm.

Type locality. Misaki, Japan, collected by Dr. Th. Mortensen, May 26, 1914, low tide level, washed from the alga *Corallina.* The type and only one specimen is in the collections of the Universitetets Zoologiske Museum, København, Denmark.

Geographical distribution. Known only from the type locality.

Remarks. The structure of the mandibles and maxillipeds and the microscopic features of the pleotelson suggest that this species is closely related to *L. (P.) segnis.*

Limnoria (Phycolimnoria) nonsegnis, new species

Figure 39

Diagnosis. Flagellum of second antenna with three-four articles. Maxillipedal epipod strap-like, four times as long as wide, reaching the articulation of palp with endopod. Mandibular palp with three articles. Fifth somite of pleon with a mid-dorsal carina. Pleotelson with a mid-dorsal anteriorly located swelling followed by a pair of parallel carinae. Posterior edge of pleotelson with a fringe of dorsally directed spike-like setae but lacks tubercles. Lacinioid setae, two in number, are similar to the other setae of the setal row.

Measurements. Holotype male, length 3.0 mm, width of pleotelson 0.8 mm. Allotype, ovigerous, length 4.0 mm, width of pleotelson 1.0 mm.

Type locality. Port Arthur, Tasmania, holotype, allotype, and eleven female paratypes, from holdfast of *Macrocystis,* collected June 1951 by A. B. Cribb and sent to me by Frank McNeill, Curator of Invertebrates, at the Australian Museum, College Street, Sydney. The types have been returned to Frank McNeill.

Geographical distribution. Known only from the type locality.

Remarks. The ornamentation of the pleon and pleotelson resembles that of *L. (P.) segnis* considerably. It can be distinguished from *L. (P.) segnis* by its triarticulate mandibular palp and relatively short maxillipedal epipod.

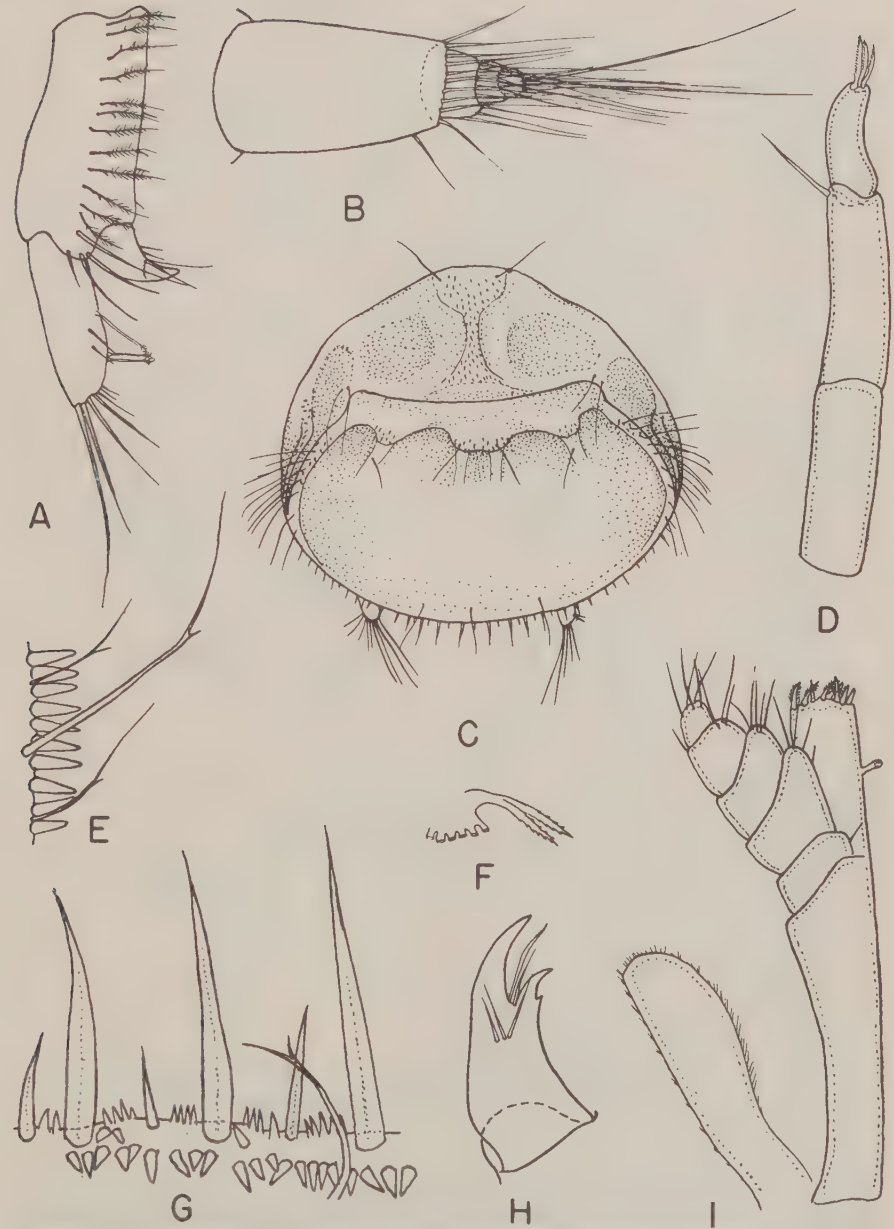

FIGURE 39. *Limnoria (P.) nonsegnis,* new species, female paratype. A, uropod. B, flagellum of second antenna. C, pleotelson. D, mandibular palp. E, lateral crest of pleotelson. F, setal row and lacinioid setae of right mandible. G, posterior margin of pleotelson. H, dactyl of first peraeopod. I, maxilliped. Figures with similar magnification, A, I; B, D, E, G, H; C; F (not known).

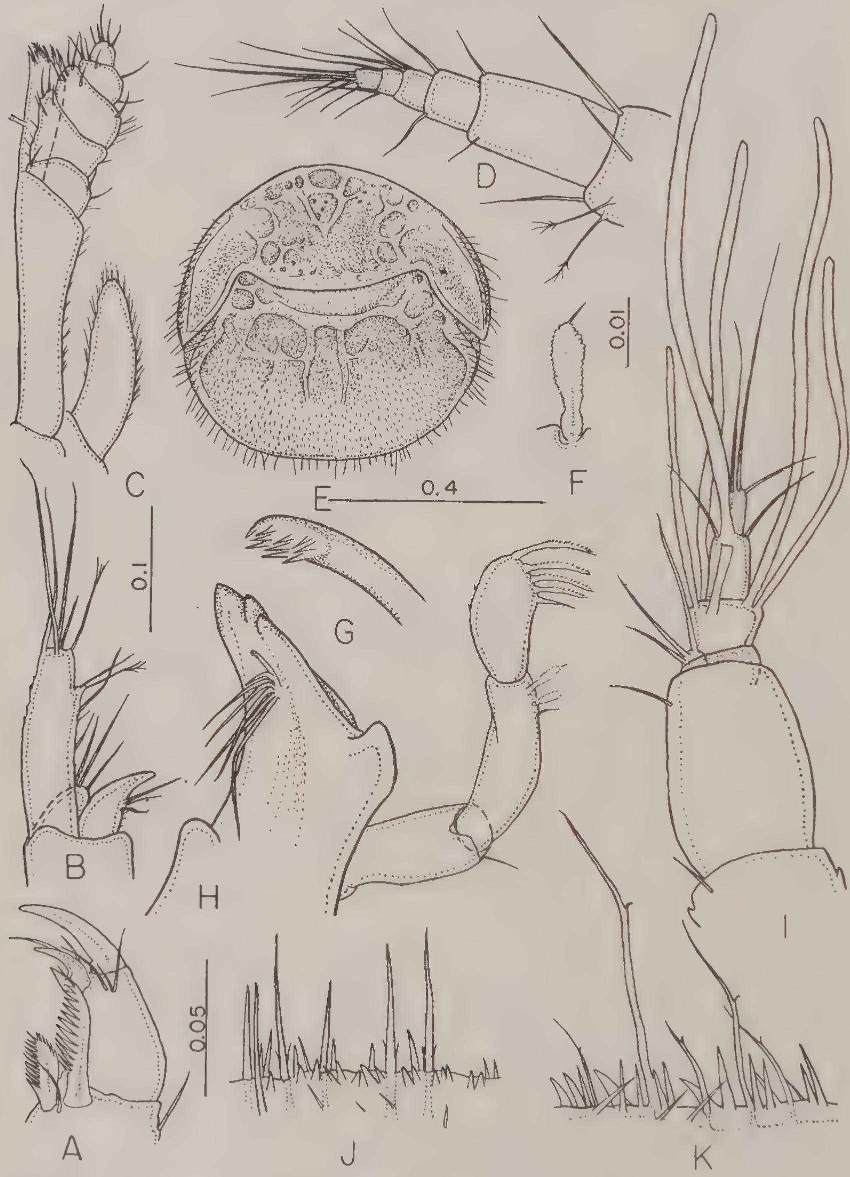

FIGURE 40. *Limnoria (P.) rugosissima,* new species, male paratype. A. distal article of first peraeopod. B, uropod. C, maxilliped. D, flagellum of second antenna. E, pleotelson. F, seta of penultimate article of mandibular palp. G, lacinioid seta of right mandible. H, right mandible inner surface. I, distal articles of first antenna. J, distal margin of pleotelson. K, lateral crest of pleotelson. Figures with similar magnification, A, D, H, I, J, K; B, C; E; F, G.

Limnoria (Phycolimnoria) rugosissima, new species
Figure 40

Diagnosis. Flagellum of first antenna with five articles. Epipod of maxilliped reaching only slightly beyond one-half the distance to the articulation of palp with endopod; epipod strap-like but with an acute distal end, being three and one-half times as long a wide. Mandibular palp with three articles. Fifth somite of pleon with large rugosities, pits, and ridges, irregular in pattern. Pleotelson with a pair of medial and lateral carinae; posterior margin with a fringe of dorsally directed spike-like setae near margin. Lacinioid seta of right mandible with an apical cluster of short, sharp denticles.

Measurements. Holotype, male, length 2.0 mm; width of pleotelson 0.5 mm. Allotype, length 2.0 mm, width of pleotelson 0.5 mm.

Type locality. The types, consisting of 14 specimens, were collected from Port Jackson, New South Wales, Australia. Twelve specimens were lent by Dr. E. Percival, Canterbury University College, Christchurch, New Zealand from the Chilton collection. Two paratypes also from the same collection were lent by Dr. Isabella Gordon, British Museum (Natural History). The specimens have been returned to Dr. Percival and Dr. Gordon.

Habitat. Although Chilton had identified the specimens as *Limnoria pfefferi* Stebbing, a wood-borer, the structure of the mandibles and the contents of the gut indicate this species is an algal borer.

Geographical distribution. Known only from the type locality.

Remarks. The rugose nature of the pleon and pleotelson, the pentarticulate second antennal flagellum, the triarticulate mandibular palp and the short maxillipedal epipod are features which distinguish this species from the other algal-boring species. Of the known species this one resembles *L. (P.) nonsegnis* most but is easily distinguished from it by the rugose pleotelson and short maxillipedal epipod.

Limnoria (Phycolimnoria) stephenseni, new species
Figures 41-42

Synonymy:

Limnoria antarctica Pfeffer. — Chilton, 1914a, pp. 382, 387 pl. XVII. — Hale, 1937, pp. 21-23, fig. 6. *Limnoria (pfefferi* Stebbing?), — Stephensen, 1927, pp. 361-362.

Diagnosis. Flagellum of second antenna with four articles. Epipod of maxilliped strap-like, about five times as long as wide and reaching beyond the articulation of palp with endopod. Mandibular palp with three articles. Fifth somite of pleon and pleotelson lacking ornamentation. Posterior margin of pleotelson with occasional large setae between which are small spike-like setae. Lacinioid seta of right mandible similar to the other setae in the setal row.

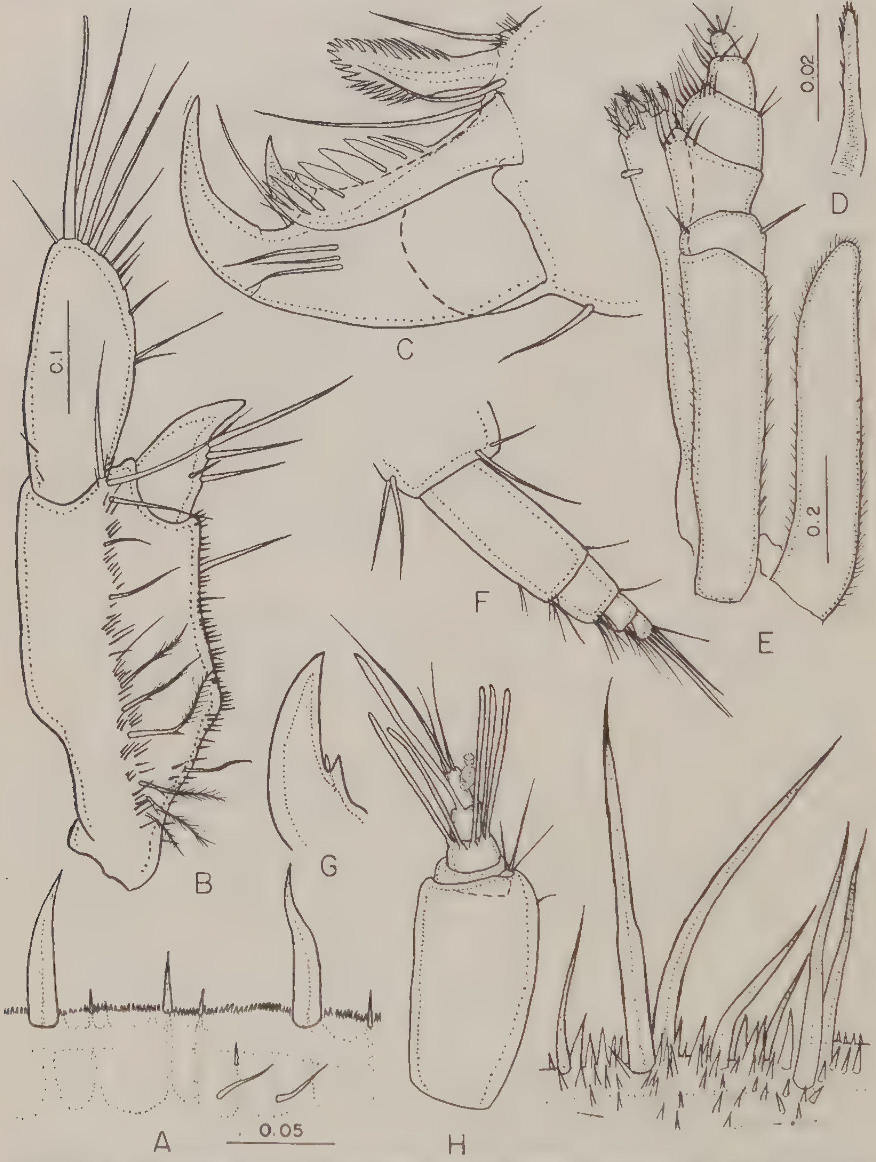

FIGURE 41. *Limnoria (P.) stephenseni*, new species, female. A, distal margin of pleotelson. B, uropod. C, distal parts of first peraeopod. D, lacinioid seta of right mandible. E, maxilliped. F, flagellum of second antenna. G, accessory claw, first peraeopod. H, distal articles of first antenna, note epizootic protozoan. I, lateral crest of pleotelson. Figures with similar magnification, A, C, H; B, F, G; D; E.

Measurements. One large female type was 8.0 mm in length and 2.6 mm in the width of the pleotelson.

Type locality. Auckland Islands, 33 type specimens, collected on Dr. Th. Mortensen's Pacific Expedition, 1914-1916. The specimens are in the collections of the Universitetets Zoologiske Museum, Copenhagen.

Geographical distribution. Auckland Isl., (Stephensen, 1927), *South Orkney* and *Macquarie Isls.* (Chilton, 1914a), *Macquarie Isls.* (Hale, 1937).

Remarks. Chilton (1914a) and Hale (1937) identified this species with *L. antarctica* Pfeffer but their figures show that this specimen had uropods more similar to those of *L. (P.) stephenseni*. Stephensen (1927) doubtfully referred the specimens to *L. (L.) pfefferi* Stebbing, a wood-borer, which however is large in size and similar to *L. (P.) stephenseni* in this respect. This species is the largest of all known species of *Limnoria* and is readily distinguished from the other algal-borers by the lack of ornamentation on its pleon and pleotelson. Hale's (1937) specimens were "found in burrows in roots of kelp—*Macrocystis*."

TAXONOMIC MONSTROSITIES, NOMINA NUDA, AND INVALID SPECIES

Limnoria, like many other genera of the animal kingdom, has its share of unrecognizable species, nomina nuda, and animals incorrectly

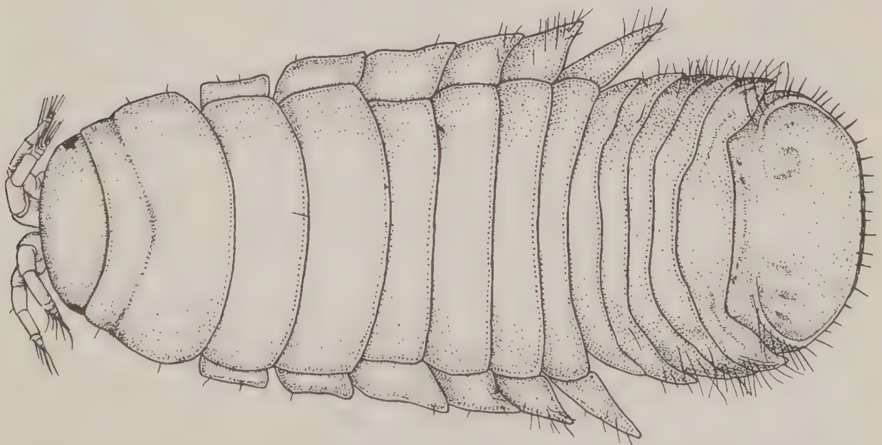

FIGURE 42. *Limnoria (P.) stephenseni,* new species, female slightly compressed, pleotelson foreshortened slightly, length of female 7.5 mm.

placed in the genus. Most writers have preferred to consider these as synonyms of *Limnoria lignorum* (Rathke). This treatment seems incorrect both biologically and taxonomically in every instance. Nomina nuda, names of animals lacking a description, are obviously not referable to any species until a description appears. It is equally inadvisable to consider names of animals which are not *Limnoria* as synonyms of *Limnoria*. For taxonomic and historical reasons it appears desirable that such troublesome forms be listed and discussed separately so that they may cause no further confusion with the valid forms of *Limnoria*.

1. *Limnoria Californica* Hewston, 1874, p. 24, *nomen nudum*.

In a report to the California Academy of Sciences, Dr. Hewston noted his find of a new species of *Limnoria* from San Francisco. This he provisionally called *Limnoria Californica*. No description ever appeared. Kofoid and Miller (1927, p. 309) considered this "species" to be undoubtedly *L. lignorum*." That this disposition of Hewston's name was incorrect is indicated by the fact that to date two species are known from San Francisco Bay (Menzies, Part I), neither of which is *L. lignorum*.

2. *Limnoria xylophaga* Hesse, 1868, pp. 101-120, pl. 9, figs. 1-37—Gerstaecker, 1882, p. 178.—Harger, 1880, p. 371.

This species is clearly an amphipod of the genus *Chelura*. Students of the Amphipoda have considered it a synonym of *Chelura terebrans* Philippi, 1839.

3. *Limnoria uncinata* Heller, 1886, pp. 734-735.—Carus, 1885, p. 451.—Gerstaecker, 1882, p. 178;—1883, p. 255.—Stalio, 1877, pp. 1367-1382.—Stossich, 1880, p. 228.

None of the writers subsequent to Heller added to his description or recognized his species. Most merely copied Heller's work or simply cited his paper. Harger (1880) considered this species a synonym of *Limnoria lignorum* (Rathke). Others have followed Harger's decision. Heller's species was collected "zu Verbosea auf der Insel Lesina" in the Adriatic. I have seen two species from the Adriatic *L. (L.) quadripunctata* Holthuis and *L. (L.) tripunctata* Menzies. Only one species, *L. terebrans* Leach, a synonym of *L. (L.) lignorum* was known to Heller. He distinguished between the two in the form of the uropods, being under the impression that the rami of those of *L. terebrans* were multiarticulate. His description of the uropods of *L. uncinata* corresponds generally with the structure

(464)

of those of all known species of *Limnoria*. Coldstream (1836, p. 321) described the uropodal rami of *L. terebrans* as multiarticulate and it is his error that lead Heller to believe that he had a new species. Indeed he probably did have one different from *L. lignorum* (=*L. terebrans*), but he in no way distinguished his species from *L. terebrans* (of Leach, not Coldstream). Had Heller been aware of Coldstream's error it is very doubtful that he would have described *L. uncinata*. There seems no real point in making either *L. (L.) quadripunctata* Holthuis or *L. (L.) tripunctata* Menzies, both of which are adequately described, synonyms of *uncinata* and reviving a name which has not been used since 1880.

4. *Limnoria gibbosa* Risso, Arcangeli, 1924, p. 7 (Carus, p. 451, ? Limnoria gibbosa Risso).

This species was assigned with doubt to *Limnoria* by Carus (1885, p. 451). Gourret (1891, p. 21-22) considered it a species of *Cymothoa*. Several of Risso's statements indicate that it does not belong to *Limnoria*. He states that the head is triangulate, which is not the case in *Limnoria* and, further, that "ses sept premiers segments sent ingaux," which is entirely unlike *Limnoria*.

A LIST OF THE KNOWN SPECIES OF LIMNORIIDAE

Present designation, original designation, most recent revision.

Wood-borers, *Limnoria (Limnoria)*

1. *lignorum* (Rathke), *Cymothoa lignorum* Rathke, 1799, this paper . . . . p. 123
2. *pfefferi* Stebbing, *Limnoria pfefferi* Stebbing, 1905, this paper . . . . p. 135
3. *japonica* Richardson, *Limnoria japonica* Richardson, 1909, this paper . . . . p. 165
4. *septima* Barnard, *Limnoria septima* Barnard, 1936, this paper . . . . p. 168
5. *quadripunctata* Holthuis, *Limnoria quadripunctata* Holthuis, 1949, this paper . . . . p. 127
6. *tripunctata* Menzies, *Limnoria tripunctata* Menzies, 1951, this paper . . . . p. 137
7. *platycauda* Menzies, *L. (L.) platycauda* Menzies, this paper . . . . p. 139
8. *saseboensis* Menzies, *L. (L.) saseboensis* Menzies, this paper . . . . p. 141

9. *simulata* Menzies, *L.* (*L.*) *simulata* Menzies, this paper . p. 144
10. *multipunctata* n. sp. . . . . p. 170
11. *unicornis* n. sp. . . . . p. 173
12. *foveolata* n. sp. . . . . p. 175
13. *sublittorale* n. sp. . . . . p. 175
14. *insulae* n. sp. . . . . p. 178

Seaweed-borers, *Limnoria (Phycolimnoria)*

15. *segnis* (Chilton), *Limnoria segnis* Chilton, 1883, this paper . . . . p. 182
16. *antarctica* (Pfeffer), *Limnoria antarctica* Pfeffer, 1887, this paper . . . . p. 180
17. *algarum* Menzies, *L.* (*P.*) *algarum* Menzies, this paper . . p. 146
18. *segnoides* n. sp. . . . . p. 184
19. *nonsegnis* n. sp. . . . . p. 186
20. *rugosissma* n. sp. . . . . p. 189
21. *stephenseni* n. sp. . . . . p. 189

Wood-borers, *Paralimnoria*

22. *andrewsi* (Calman), *Limnoria andrewsi* Calman, 1910, Menzies, this paper . . . . p. 148

LITERATURE CITED

ALEXIS, A. D.
1951. Field problems in the general maintenance of marine structures. *in* Proceedings Wrightsville Beach Marine Conference. Prevention of Deterioration Center National Research Council Publ. 203, pp. 4-7.

ALLEN, M. S. AND R. H. CARTER
1924. Toxicity of certain compounds on marine wood-boring organisms together with some physiological considerations. *in* Atwood and Johnson (1924), pp. 181-196.

AMAR, RAYMOND
1951. Formations endocrines cerebrales des Isopodes marins et comportement chromatique d'Idotea. Ann. Fac. Sci. Marseille, 2nd ser., 20 (3): 170-305.

ANDREWS, A.
1875. *Limnoria terebrans* attacking telegraph cable, exhibited. Q. J. Micr. Sci., *15*: 332.

ANONYMOUS
1918. Isopods from the Claremont-Laguna region. Pomona Coll. J. Entom. and Zool., *10* (3): 58.

ARCANGELI, A.
1924. Notizie sopra alcuni isopodi del mar Mediterraneo. Atti. Soc. Ital. Sci. Nat. Milano. *63*: 1-8.

ATWOOD, W. G. AND A. A. JOHNSON *et al.*
1924. Marine structures, their deterioration and preservation. 534 pp. Nat. Res. Council, Washington, D.C.

Barnard, K. H.

1936. Isopods collected by the R.I.M.S. "Investigator." Rec. Indian Mus., *38* (2): 147-191.

Bate, C. S. and J. O. Westwood

1868. A history of the British sessile-eyed Crustacea. *2*, 356 pp. London, J. Van Voorst.

Becker, G. and W. G. Kampf

1955. Die Holzbohrassel der Gattung *Limnoria (Isopoda)* und ihre Lebensweise, Entwicklung und Umweltabhängigkeit. Zeitschr. f. Angeu. Zoologie, *4*: 477-517.

Black, E. C. and G. R. Elsey

1948. Incidence of wood-borers in British Columbia waters. Fish. Res. Board Canada. Bull. *80*: 1-20.

Calman, W. T.

1898. On a collection of Crustacea from Puget Sound. Ann. N.Y. Acad. Sci., *11* (13): 259-292.

1910. On two new species of wood-boring Crustacea from Christmas Island. Ann. Mag. Nat. Hist., ser. 8, *5*: 181-186.

1936. Marine animals injurious to submerged structures. (revised by G. I. Crawford). British Mus. Nat. Hist., Econ. ser., *10*: 1-38.

Carus, J. V.

1885. Prodromus faunae Mediterraneae sive descriptio anunalium maris Mediterranei incolarum etc. Arthropoda, Assellidae, pp. 450-451. Stuttgart.

Chilton, C.

1883. Further additions to our knowledge of the New Zealand Crustacea. Trans. New Zealand Inst., *15*: 69-86.

1914a. The species of Limnoria, a genus of wood-boring Isopoda. Ann. Mag. Nat. Hist., ser. 8, *13*: 380-390.

1914b. Distribution of *Limnoria lignorum* (Rathke) and *Limnoria antarctica* Pfeffer. Ann. Mag. Nat. Hist., ser. 8, *76*: 448.

1916. The gribble (*Limnoria lignorum,* Rathke) attacking a submarine cable in New Zealand. Ann. Mag. Nat. Hist., ser. 8, *18*: 208.

1919. Destructive boring Crustacea in New Zealand. New Zealand J. Sci. & Techn., *11* (1): 3-15.

Clavenad, Mr.

1879. Restauration des fondations du batiment des subsistances de la marine, a Cherbourg, Mem. Soc. Nationale des Sc. Nat. et Mathématiques de Cherbourg. 3rd ser., *2* (22): 73-144.

Coker, R. E.

1923. The breeding habits of Limnoria at Beaufort, N.C., J. Elisha Mitchell Soc., *39*: 95-100.

Coldstream, J.

1836. On the structure and habits of the *Limnoria terebrans.* Edinburgh N. Philos. J., *16*: 316-334.

Dahl, F.

1916. Die Asseln oder Isopoden Deutschlands. 90 pp. Jena, G. Fischer.

de Vos, A. P. C.

1953. Three new commensal ostracods from *Limnoria lignorum.* Beaufortia (Zool. Mus. Amsterdam), *34* (4): 21-31.

FEE, A. R.
1926. The Isopoda of Departure Bay and vicinity with descriptions of new species, variations, and colour notes. Contr. Canad. Biol. Fish., n. ser., *3* (2): 15-45.
FOX, C. D.
1878. Discussion of the preservation of timber. Trans. American Soc. Civil Engineers. *6*: 189-194.
FOX, D. L., J. D. ISAACS AND E. F. CORCORAN
1952. Marine leptopel, its recovery, measurement and distribution. J. Marine Research, Sears Foundation, *11* (1): 29-46.
FRASER, C. M.
1923. Marine wood borers in British Columbia waters. Trans. R. Soc. Canada, ser. 3, *17* (5): 21-28.
GERSTAECKER, A.
1881-1883. Isopoda. *in* H. G. Bronn's Klassen und Ordnungen des Thier-Reichs. *5* (1), Arthropoda, Lief. 1-10, pp. 1-278. Leipzig.
GOURRET, P.
1891. Les Lemodipodes et les Isopodes du golfe de Marseille. Ann. Mus. Hist. Nat. Marseille. Zool. 4, Trav. sci. Memoire No. 1, pp. 1-44.
GOULD, A. A.
1841. Report on the Invertebrata of Massachusetts, comprising the Mollusca, Crustacea, Annelida, and Radiata. 373 pp., Cambridge, Folsom, Wells and Thurston.
GREATHOUSE, G. A.
1952. Foreword, *in* Proceedings Wrightsville Beach Marine Conference. Prevention of Deterioration Conter. Nat. Res. Council. Publ. 203.
GREENFIELD, LEONARD J.
1952. The distribution of marine borers in the Miami area in relation to ecological conditions. Bull. Mar. Sci. Gulf and Carib. *2* (2): 448-464.
GUBERLET, M. L.
1936. Animals of the seashore. 412 pp., Portland, Ore., Metropol. Press.
HALE, H. M.
1937. Isopoda and Tanaidacea. Australasian Antarctic Expedition 1911-14. Scientific Reports. ser. C., Zool. and Bot. *2* (2): 1-45.
HANSEN, H. J.
1905. Propogation, structure and classification of the family Sphaeromidae. Q. J. Micro. Sci., n. ser., *49* (1): 69-135.
1916. The Danish Igolf Expedition. Vol. III, part 5, Crustacea Malacostraca III, pp. 1-262.
HARGER, O.
1880. Report on the marine Isopoda of New England and adjacent waters. Rep. U.S. Comm. Fish and Fisheries, part 6: 297-462.
HATCH, M. H.
1947. The Chelifera and Isopoda of Washington and adjacent regions. Univ. Washington Publ. Biol., *10* (5): 155-274.
HELLER, C.
1886. Carcinologische Beiträge zur Fauna des adriatischen Meeres. Verhandlungen des Kaiserlich-Königlichen zoologisch-botanischen Gesellschaft in Wien, *16*: 723-760.
HENDERSON, J. T.
1924. The Gribble: A study of the distribution factors and life-history of *Limnoria lignorum* at St. Andrews, N. B., Contr. Canadian Biol., n. ser. *2*, part 1 no. 14: 309-325.

HESSE, M.
1868. Observations sur des crustacés rares ou nouveaux des cotes de France. Description d'un nouveau crustacé appartenant au genre Limnorie. Ann. Sc. Nat. 5th ser. Zool. et Paleontologie, *10*: 101-120.

HEWSTON, G.
1874. No title—Proc. California Acad. Sc., *5*: 24.

HOEK, P. P. C.
1893. Betreffende de Levenswijze en den Werking var *Limnoria lignorum. in* Rapport der Commissie uit de Koninklijke Akademie van Wetenschappen. Verhandelingen Koninklijke Akad. Wetenschappen te Amsterdam (Tweede sectie), *1* (6): 1-97.

HOLTHUIS, L. B.
1949. The Isopoda and Tanaidacea of the Netherlands, including the description of a new species of *Limnoria.* Zool. Mededelingen Rijksmuseum Van Natuurlijke Historie te Leiden. *30* (12): 163-190.

HUMPHREYS, H.
1845. Crustacea, in contributions towards a fauna and flora of the County of Cork, 30 pp. London.

IREDALE, T., R. A. JOHNSON AND F. A. MCNEILL
1932. Destruction of timber by marine organisms in the Port of Sydney. Sydney Harbour Trust, 148 pp.

JOHNSON, M. W.
1935. Seasonal migrations of the wood-borer *Limnoria lignorum* (Rathke) at Friday Harbor, Washington. Biol. Bull., *69* (3): 427-438.

JOHNSON, MARTIN W. AND ROBERT J. MENZIES
1956. The migratory habits of the marine gribble *Limnoria tripunctata* Menzies in San Diego Harbor. Biol. Bull., *110* (1): 54-68.

JOHNSON, M. W. AND R. C. MILLER
1935. The seasonal settlement of shipworms, barnacles, and other wharf-pile organisms at Friday Harbor, Washington. Univ. Washington Pub. Oceanogr., *2* (1): 1-18.

JOHNSON, MARTIN W., F. ALTON EVFREST AND ROBERT W. YOUNG
1947. The role of snapping shrimp (Crangon and Synalpheus) in the production of underwater noises in the sea. Biol. Bull., *93* (2): 122-138.

KOFOID, C. A. AND R. C. MILLER
1927. *in* Hill, C. L., and C. A. Kofoid *et al.*, Marine borers and their relation to marine construction on the Pacific coast being a final report of the San Francisco Bay Marine Piling Committee, 351 pp., San Francisco.

KRAMP, P. L.
1927. Undersøgleser over paeleorm og paelekrebs ved Hirtshals. Ingeniøren, no. 27, pp. 329-340.

LEACH, W. E.
1813. Crustaceology, *7*: 383-437, pl. 221, *in* Brewster's Edinburgh En-
(1814) cyclopaedia. London, Baldwin.

MACGINITIE, G. E.
1935. Ecological aspects of a California marine estuary. Am. Midland Naturalist. *16* (5): 629-765.

MAWATARI, SHIZUO
1949. Analytical study of various methods for the protection of wooden ships against marine borers. Miscellaneous Repts. Res. Inst. Nat. Res., Japan. *13*: 17-30 (in Japanese, with English resume).

M'Gonigle, R. H.
1925. Marine borers on the Atlantic coast of Canada. The Honorary Advis. Council Sci. and Indust. Res. Canada, Rept. 15: 1-67. Ottawa.
Menzies, Robert J.
1951a. A new species of *Limnoria* (Crustacea: Isopoda) from Southern California. Bull. So. California Acad. Sci., *50* (2): 86-88.
1951b. A new genus and new species of asellote isopod, *Caecijaera horvathi*, from Los Angeles-Long Beach harbor. American Mus. Novitates. No. 1542, pp. 1-7.
1951c. Limnoria and the premature failure of creosoted marine structures in North America. Rept. Mar. Borer Confer., U.S. Nav. Civil Eng. Res. and Evaluation Lab., Port Huenensa, California, pp. M-1—M-7 (offset private printing).
1954. The comparative biology of reproduction in the wood-boring isopod crustacean Limnoria. Bull. Mus. Comp. Zool., Harvard, *112* (5): 363-388.
1956. A study of the microscopic structure of isopod setae. Ann. Mag. Nat. Hist. Lond., Ser. 12, *9*: 698-699.
Menzies, R. J. and J. L. Mohr
1952. The occurrence of the wood-boring crustacean *Limnoria* and of Nebaliacea in Morro Bay, Calif., Wasmann J. Biol. *10* (1): 81-86.
Miller, M. A. and R. J. Menzies
1952. The isopod Crustacea of the Hawaiian Islands. III. Superfamily Flabellifera, Family Anthuridae. Occ. Pap. Bernice P. Bishop museum, *21* (1): 1-15.
Miller, R. C.
1924. Wood-boring Crustacea from Hawaii and Samoa. U.C. Pub. Zool., *26*: 159-164.
1926. Ecological relations of marine wood-boring organisms in San Francisco Bay. Ecology, *7* (3): 247-254.
Mohr, J. L. and J. A. LeVeque
1948. Folliculinids associated with *Limnoria* in California and Washington. J. Parasit. *34* (6): 26.
Moll, F.
1915. Holzzerstörende Krebse-Naturwiss. Zschr. Forst.-und Landwirt. *13*: 178-207.
1916. Bibliography of wood-boring crustaceans. American Wood-Preservers' Association. Twelfth annual meeting. Proceedings, pp. 409-413.
Nierstrasz, H. F. and J. H. Shuurmans Stekhoven, Jr.
1930. Isopoda genuina, *in* Grimpe and Wagler, Tierwelt der Nord-und Ostsee. Lief. 18, X. e2, pp. Xe5-Xe133.
Omer-Cooper, J. and J. Hedley Rawson
1934. Notes on the British Sphaeromatidae (Crustacea, Isopoda). Rep. Armstrong Coll., Dove Marine Laboratory. Ser. 3, no. 2, pp. 22-58.
Pfeffer, G.
1887. Die Krebse von Sud-Georgien nach der Ausbeute der Deutschen Station 1882-1883. I Teil, Naturhistorisches Mus. Hamburg. Jahrb. Wiss. Anst. Hamburg, 1886, pp. 43-105.
1890. Die niedere Thierwelt des Antarktischen Ufergebietes. No. 17, pp. 455-572, *in* Die Deutschen Expeditionen und ihre Ergebnisse, *2*. Dr. G. Neumayer. Die Internationale Polarforschung 1882-1883. Berlin, A. Asher Co.

PHILIPPI, A.
1839. Einige Zoologische Notizen. Arch. Naturgesch., *5*: 113-134.
RATHKE, J.
1799. Jagttagelser henhørende til Indvoldeormenes og Bloddyrenes Naturhistorie. Skrivter af Naturhistorie-Selskabet, *1* (11): 61-153, Copenhagen.
RAY, D. L. AND J. R. JULIAN
1952. Occurrence of cellulase in *Limnoria*. Nature, *169* (4288): 32-33.
REISH, DONALD J.
1954. Polychaetous annelids as associates and predators of the crustacean wood-borer, *Limnoria*. Wasmann J. Biol., *12* (2): 223-226.
RICHARDSON, H. E.
1899. Key to the isopods of the Pacific coast of North America, with descriptions of twenty-two new species. Proc. U.S. Nat. Mus., *21* (1175): 815-869.
1900. Synopsis of North American invertebrates VIII. The Isopoda, part I. American Naturalist, *34*: 207-230.
1901. Key to the isopods of the Atlantic coast of North America with the descriptions of new and little known species. Proc. U.S. Nat. Mus., *23* (1222), 493-571.
1904. Contributions to the natural history of the Isopoda. Proc. U. S. Nat. Mus., *27* (1350): 1-87.
1905. A monograph on the isopods of North America. Bull. U.S. Nat. Mus., no. 54, 727 pp.
1909. Isopods collected in the northwest Pacific by the U.S. Bureau of Fisheries steamer "Albatross" in 1906. Proc. U.S. Nat. Mus., *37* (1701): 75-129.
1913. Crustacés isopodes. 2nd Exped. Antarctique Française (1908-1910), pp. 1-24, Paris.
SARS, G. O.
1897. An account of the Crustacea of Norway. II., Isopoda, 127 pp., Bergen Museum, Christiania.
SCHMITT, W. L.
1931. Crustaceans, shelled invertebrates of the past and present. Smithsonian Sci. Ser., *10*, 247 pp., Washington, D.C.
SHACKELL, L. F.
1923. Toxicities of coal tar creosote, creosote distillates, and individual constituents for the marine wood borer *Limnoria lignorum*. Bull. U.S. Bu. Fish., *39* (952): 221-230.
SHIINO, S. M.
1944. Studies on marine wood-boring crustaceans. 1. On two species of *Limnoria* found in Japan. Miscel. Repts. Res. Inst. Nat. Resources. *6*: 1-19 (in Japanese).
1950. The marine wood-boring crustaceans of Japan. I. Limnoriidae. Wasmann J. Biol., *8* (3): 333-358.
SHOEMAKER, T. L.
1949. Recent developments in improving the marine borer resistance of lumber and plywood used in planking naval vessels. pp. 453-457 (Rept. Symposium on Wood) U.S. Nat. Res. Council and Office of Naval Research, 1949, 530 pp., Washington, D.C.
SØMME, O. M.
1940. A study of the life history of the gribble *Limnoria lignorum* (Rathke) in Norway. Nytt. Mag. f. Naturvidenskapene. *81*: 145-205.

STAFFORD, J.
1912. On the fauna of the Atlantic coast of Canada. Contrib. Canadian Biol., *5*: 45-67.

STALIO, L.
1877. Catalogo metodico e descrittivo dei crostacei dell' adriatico. Ordine III. Isopoda. Atti del Reale Instituto Veneto di Scienza, Lettere, ed Arti., ser. 5, *3*: 1345-1420.

STEBBING, T. R. R.
1893. A history of Crustacea. The International Scientific Series, 466 pp., New York, D. Appleton & Co.
1905. Marine crustaceans. XII. Isopoda, with the description of a new genus. S. Gardner, editor, *in* Fauna and Geography of the Maldive and Laccadive Archipelagoes, *2* (3): 699-721.

STEPHENSEN, K.
1927. Papers from Dr. Th. Mortensen's Pacific Expedition 1914-1916. XL. Crustacea from the Auckland and Campbell Islands. Vid. Medd. Dansk. Naturhist. Foren., *83* (40): 289-390.
1929. Marine Crustacea Isopoda and Tanaidacea. Zoology of the Faroes (Copenhagen), no. 24, pp. 1-23.

STOSSICH, M.
1880. Prospetto della fauna del mare Adriatico. Part 3. Crustacea. Boll. Soc. Adriatica Sc. Nat. Trieste. *6*: 178-271.

SUMNER, F., G. D. LOUDERBACK, W. L. SCHMITT AND E. C. JOHNSON
1914. A report on the physical conditions in San Francisco Bay. U.C. Pub. Zool., *14* (1): 1-198, pls. 1-13.

VANHÖFFEN, E.
1914. Die Isopoden der deutschen Südpolarexpedition 1901-1903. Deutsche Südpolar-Expedition 1901-1903. Zoologie, *7*: 449-598, Berlin G. Reimer.

WATSON, C. J. J., F. A. MCNIELL, R. A. JOHNSON AND T. IREDALE
1936. Destruction of timber by marine organisms in the Port of Brisbane. Queensland Forest Service. Bull. 12, pp. 1-107.

WHITE, A.
1847. List of specimens of Crustacea in the collection of the British Museum. 143 pp. London, British Museum (Natural History).
1850. List of the specimens of British animals in the collection of the British Museum, Part IV, Crustacea, 141 pp., London, British Museum (Natural History).
1857. A popular history of British Crustacea. 358 pp., London, L. Reeve.

WHITE, F. D.
1929. Studies on marine borers II. The effect of experimental variations in salinity and hydrogen ion concentration upon the wood borers of the Pacific coast of Canada. Contrib. Canadian Biol. and Fish., n. ser., *4* (2): 9-18.

YONGE, C. M.
1927. The absence of a cellulase in *Limnoria*. Nature, *119*: 855, London.

ZIRWAS, C.
1911. Die Isopoden der Nordsee. Wiss Meeresuntersuchungen Komm. Wiss. Untersuch. deutschen Meere in Kiel und d. Biol. Anst. auf Helgoland. Neue Folge, *12*: 75-115.

ZOBELL, C. E.
1946. Marine Microbiology. 240 pp., Waltham, Mass., Chronica Botanica.

[Reprinted from INSTITUTE OF MARINE SCIENCE, Vol. IV, No. 2, July, 1957]
Reproduced by Permission

Texas Bay Sediments[1]

FRANCIS P. SHEPARD AND GENE A. RUSNAK

Introduction

With the help of an American Petroleum Institute grant, a group of Scripps Institution scientists have been investigating the sediments of Texas bays during the past six years. In many respects these bays have proven ideal for a study of sedimentation. In the first place, with the climatic zonation found between the Louisiana border to the northeast and Laguna Madre to the southwest (Fig. 1), it has been possible to study the dif-

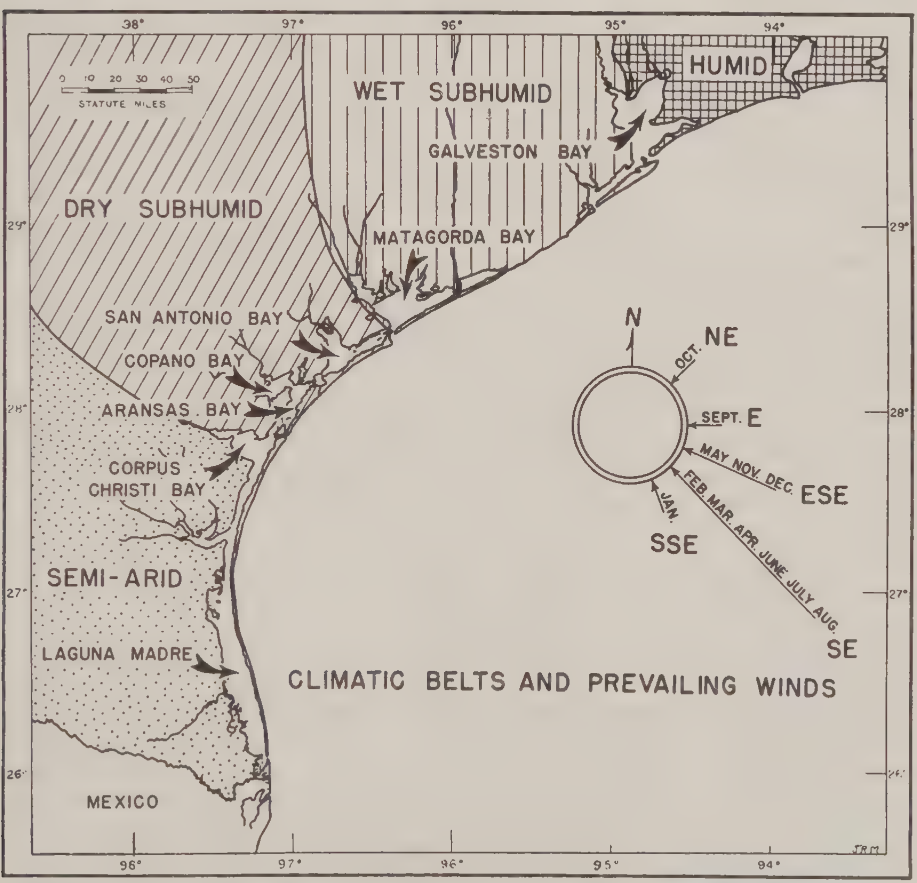
98°
97°
96°
95°
94°
0 10 20 30 40 50
STATUTE MILES
HUMID
WET SUBHUMID
GALVESTON BAY
DRY SUBHUMID
MATAGORDA BAY
SAN ANTONIO BAY
COPANO BAY
ARANSAS BAY
CORPUS CHRISTI BAY
SEMI-ARID
LAGUNA MADRE
MEXICO
29°
28°
27°
26°
N
OCT. NE
SEPT. E
MAY NOV. DEC. ESE
JAN. SSE
FEB. MAR. APR. JUNE JULY AUG. SE
CLIMATIC BELTS AND PREVAILING WINDS
JRM

FIG. 1. Index chart of Texas coast, showing climatic belts (after Thornthwaite, 1948) and prevailing wind directions (after Lohse, 1955).

---

[1] Contribution from the Scripps Institution of Oceanography, New Series No. 932. This investigation was supported by a grant from the American Petroleum Institute, Project 51.

ferences between sediments in bays of a humid area and those in areas of semiaridity. Streams provide large amounts of sediment to the bays in the humid areas, whereas windblown sands and washovers from the barrier islands provide the principal source for the semiarid bays. The differences in salinity in the bays, ranging from over 80‰ in Laguna Madre to approximately 1‰ at the mouths of some of the rivers entering the bays to the north, have a tremendous effect on the organisms and on the nature of sedimentation as it is related to these organisms. A second advantage of studying the Texas bays is that they are closed off from the open Gulf by almost continuous barrier islands so that sediments are more likely to be permanent than in open bays where sediments are often deposited and then removed by marine processes. Borings have shown that these bay sediments are present well below the bay bottoms. A third advantage of the Texas area to a student of sedimentation comes from the very complete surveys made by the U.S. Coast and Geodetic Survey around 1870 and again around 1934. These surveys provide a means of determining roughly the rate of sedimentation as related to other factors (Shepard, 1953).

It was thought at first that a very complete study should be made of the bays in the vicinity of Rockport, particularly San Antonio Bay into which the Guadalupe River enters. This has been done (see bibliography at end). It was realized, however, after some time had been spent on these concentrated studies, that a much better understanding of bay sedimentation in general and of the processes which contribute to it would come from making comparisons with other bays along the Texas coast. This became particularly evident when some rather large contrasts were found betweeen the sediments of the Laguna Madre, which is located in a semiarid climate and has virtually no entering streams, and the sediments of San Antonio Bay with its dry sub-humid climate, its entering streams, and its extensive oyster reefs. Furthermore, the importance of inlets on sedimentation soon became evident because tidal currents transport sediments into the bays from the barrier islands and from the shallow portions of the Gulf of Mexico.

In order to obtain some idea of the nature of Texas bay sedimentation, it is important to consider in some detail the characteristics which bays of these two contrasting types possess. Thus some description will be made of the bays of the Rockport-Aransas Pass area, especially San Antonio Bay, and of the Laguna Madre.

Rockport-Aransas Pass Area (San Antonio Bay)

Located almost in the center of the Texas coast, San Antonio Bay has many of the characteristics of the subhumid type of bay found along the coast from Corpus Christi to Galveston. The accompanying chart (Fig. 2) shows that, with the exception of oyster reefs, topographically this bay has only very minor bottom irregularities and is very shallow. In few places does it reach depths greater than six feet. To the north it is influenced by the Guadalupe River. At the present time this river flows into the isolated arm of the bay north of the delta, although in the not distant past it was entering directly into the upper San Antonio Bay through a series of channels cutting across the delta. The salinity, ranging under average conditions from about 4‰ at the northern end to about 25‰ at the southern end, shows fluctuations both seasonally and periodically because of the effect of drought on the one hand, and of floods on the other. A tongue of low salinity extends down the west side of the bay, whereas a tongue of relatively high salinity, ap-

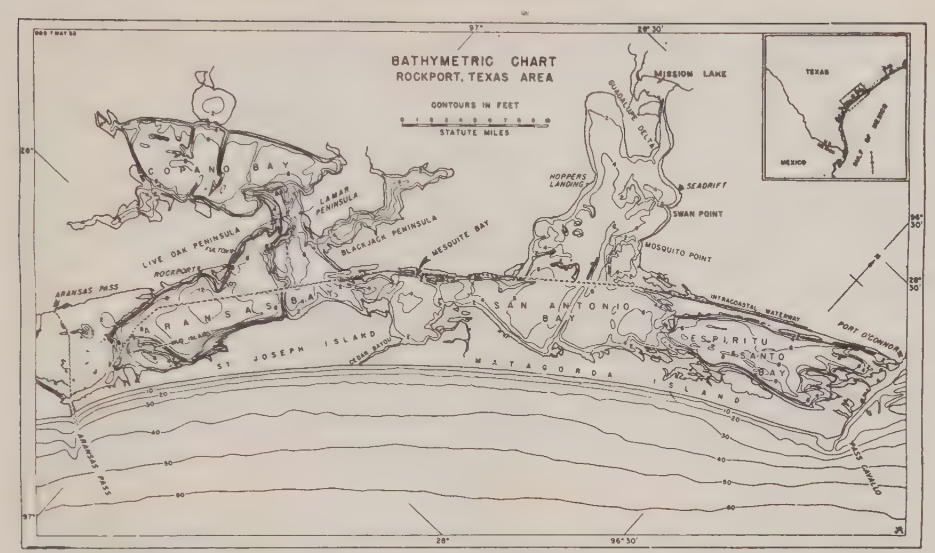
BATHYMETRIC CHART
ROCKPORT, TEXAS AREA
CONTOURS IN FEET
STATUTE MILES
COPANO BAY
LAMAR PENINSULA
LIVE OAK PENINSULA
FULTON
ROCKPORT
ARANSAS PASS
ARANSAS BAY
BLACKJACK PENINSULA
MESQUITE BAY
ST JOSEPH ISLAND
CEDAR BAYOU
HOPPERS LANDING
GUADALUPE DELTA
MISSION LAKE
SEADRIFT
SWAN POINT
MOSQUITO POINT
SAN ANTONIO BAY
INTRACOASTAL WATERWAY
PORT O'CONNOR
ESPIRITU SANTO BAY
MATAGORDA ISLAND
PASS CAVALLO
TEXAS
MEXICO
GULF OF MEXICO
97°
28°30'
96°30'
28°
10
20
30
40
50
60

FIG. 2. Bottom topography of Rockport bays and nearshore area (after Shepard and Moore, 1955). Bay contour interval 2 feet. Offshore contour interval, 10 feet.

parently coming in through Espiritu Santo Bay, extends up the east side of San Antonio Bay. Oyster reefs are most numerous in the central portion of the bay where they rise almost to or actually to the surface.

The barrier island, consisting largely of sand, contributes some sediment to the southern area as the result of wind action, although this does not appear to be very important, partly because much of the northern portion of Matagorda Island is marshy and has marsh vegetation which largely prevents the movement of the sand from the dunes farther south. A rather important source of sand comes into the adjoining Mesquite Bay through the small intermittent Cedar Bayou Inlet and elsewhere by washover storm waves. Also, during northers, rather strong currents come down Espiritu Santo Bay and carry sand into the southern portion of San Antonio Bay.

The result of these influences is seen on a map showing the general sediment types, as based on sand, silt, and clay contents[2] along with the oyster reefs (Fig. 3). Here we see that in the area around the delta the sediments are dominantly clayey with considerable silt, and a tongue of equally fine sediment extends down the center and west side of the bay as does the current of low salinity water mentioned previously. Very sandy sediments mixed with clay are found in Mesquite Bay to the southwest where the effect of the inlet and washovers seems to be very important. This is also true of southeast San Antonio Bay near Espiritu Santo Bay where, because of the locally shallow depths and currents due to occasional strong northeast winds, the sediments are relatively high in sand.

Examination under the binocular microscope of different sieve sizes of the sandy fraction of these sediments indicates other important characteristics of the sediment zones. Thus the sediments near the delta, and particularly those near the mouths of the present streams, have rather high content of wood debris. Furthermore, mica is more

---

[2] Dividing lines between sand and silt sizes are placed at 1/16 mm. and between silt and clay at 1/250 mm.

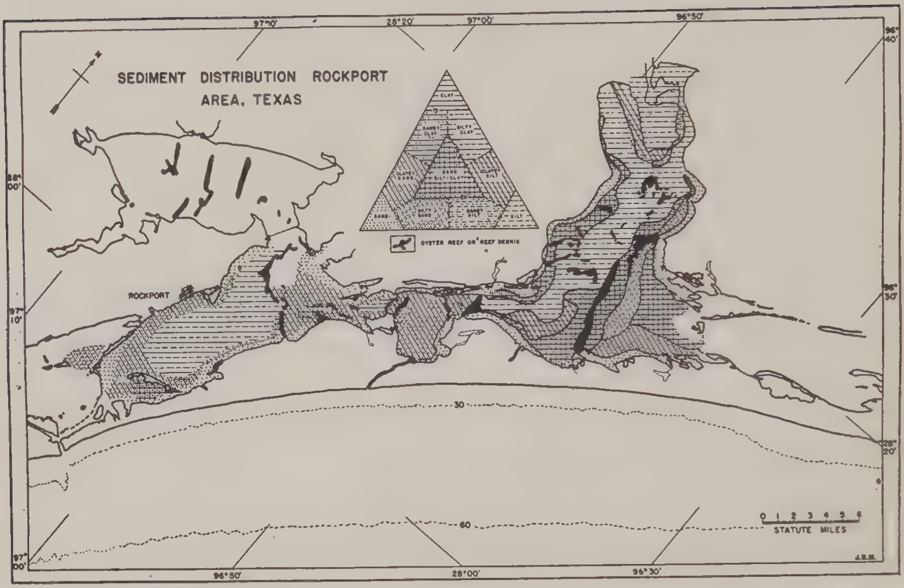
SEDIMENT DISTRIBUTION ROCKPORT AREA, TEXAS
CLAY
SANDY CLAY
SILTY CLAY
CLAYEY SAND
SAND SILT-CLAY
CLAYEY SILT
SAND
SILTY SAND
SANDY SILT
SILT
OYSTER REEF OR REEF DEBRIS
ROCKPORT
97°10'
28°20'
97°00'
96°50'
96°40'
28°00'
97°10'
96°30'
28°20'
97°00'
96°50'
28°00'
96°30'
30
60
0 1 2 3 4 5 6
STATUTE MILES

Fig. 3. Sediment distribution in Rockport area bays based on sand-silt-clay content (after Shepard and Moore, 1955).

abundant in these areas than elsewhere. There are also small ferruginous aggregates. Each of these constituents becomes negligible in the sediment farther down the bay, away from the influence of the river. In addition the cores of the sediments in the vicinity of the delta show occasional lamination, whereas farther down the bays the cores are rarely if ever laminated. The reason for this contrast in sediment structure is that the sediments around the river mouths are being deposited rapidly and they are not much disturbed by the burrowing activity of benthonic organisms, most of which cannot tolerate low salinities. On the other hand, at a position away from the delta where there is a much greater abundance of these bottom dwellers, the bottom becomes churned and stratification has little chance to be preserved. In the portions of the bays where sand is being introduced through inlets, there is a very crude type of stratification due to the alternate introduction of sandy sediments, on the one hand, and of clayey sediments, on the other. Because of the burrowing organisms, however, this alternation is not exhibited by good stratification.

Borings made into San Antonio Bay a few years ago (Shepard and Moore, 1955, pp. 1546–1576) showed that the characteristic sediments of the present day persist in many places to depths of as much as 50 or even 80 feet below the bottom. Some borings extended down through unstratified clayey material as much as 50 feet, and elsewhere oyster reefs were penetrated continuously for as much as 40 feet. Similarly, borings in the sandy barrier islands which border San Antonio and other bays along this part of the coast, show that the sand continues with very little change in character to depths of as much as 50 feet. The study of the sediments from these borings has indicated quite clearly that deposition has continued over a long period, probably as much as 9,000 years judging from carbon 14 dates, with conditions very similar to the present. This can mean simply that sandy barrier islands developed at an early stage during the rise in sea level that accompanied the melting of the great glaciers some 10,000 years ago (Flint, 1953). These islands caused an early development of the lagoons and estuaries so that bay sedimentation has probably occurred continuously over these long periods. If the barrier islands had not developed at this early stage and instead had been formed recently, the sediments under the bays would be far sandier than they are because open Gulf shelf deposits formed at shallow depths in this area contain a high percentage of sand. Also the free access of Gulf waters would undoubtedly have brought in an abundance of echinoids, which are so characteristic of the continental shelf deposits on the outside and are so rare in bays. Virtually no echinoid plates or spines have been found in these borings beneath San Antonio Bay. Glauconite also develops characteristically in the sediments of the open Gulf and it is virtually missing in the bays and in the borings made into the bays. Indications are that the present barrier islands have changed only slightly in position from time to time during their upgrowth.

Laguna Madre

The Laguna Madre is a linear coastal lagoon extending for approximately 120 miles south from Corpus Christi Bay almost to the Mexican border. This lagoon is mostly very shallow and a large portion, especially in the center of the bay, is rarely covered by water (see Figure 4). The Laguna Madre has very different conditions than those of San Antonio Bay. There are no streams of any consequence entering the bay at the present time, although in the past the southern end of the bay has been supplied from time to time with the waters of the Rio Grande. Also during the occasional heavy rains the Arroyo Colorado and the small streams coming into Baffin Bay estuary near the northern end provide large quantities of fresh water which radically reduces the salinity for short periods. Although the floods do not affect salinity very long they must discharge much clay into Laguna Madre. Ordinarily, however, the high evaporation in the bay maintains a high salinity commonly greater than that of the open Gulf except near the inlet at Port Isabel. The absence of large supplies of sediments introduced by streams is counteracted by a very considerable source of sediment from Padre Island. This island, because of the greater aridity of the climate here than to the north, is much less covered with vegetation and during wind storms great quantities of sand are brought into the Laguna. Furthermore, the occasional rises in sea level that accompany hurricanes, or to varying degrees nearby hurricanes, send large quantities of sands from the barrier island into the bay through a series of low passes developing washover fans. However, this source of sand would soon be exhausted were it not for continual replenishment from the Gulf by sediment transport of coastal sand by longshore currents (Bullard, 1942, pp. 1021–1044; Lohse, 1955, pp. 99–105).

As a result of these influences, the sediments in Laguna Madre are quite different from those of the more humid bays to the north. Figure 4 shows that sand forms a much larger constituent of the sediments. Although we have not sampled the central exposed area of the bay, sand is said to be prevalent in this area with dunes building over on the mud flats which are only occasionally flooded by the lagoon waters. The only area where clay (more than 75% clay sized material) is found is in the central part of the relatively deep Baffin Bay, which is somewhat deeper than San Antonio Bay. Elsewhere relatively deep areas with silty clays, sand-silt-clays, and clayey or silty sands occur in the northern Laguna, Baffin Bay and in the southern part of the Laguna (See Fig. 4). Much of the

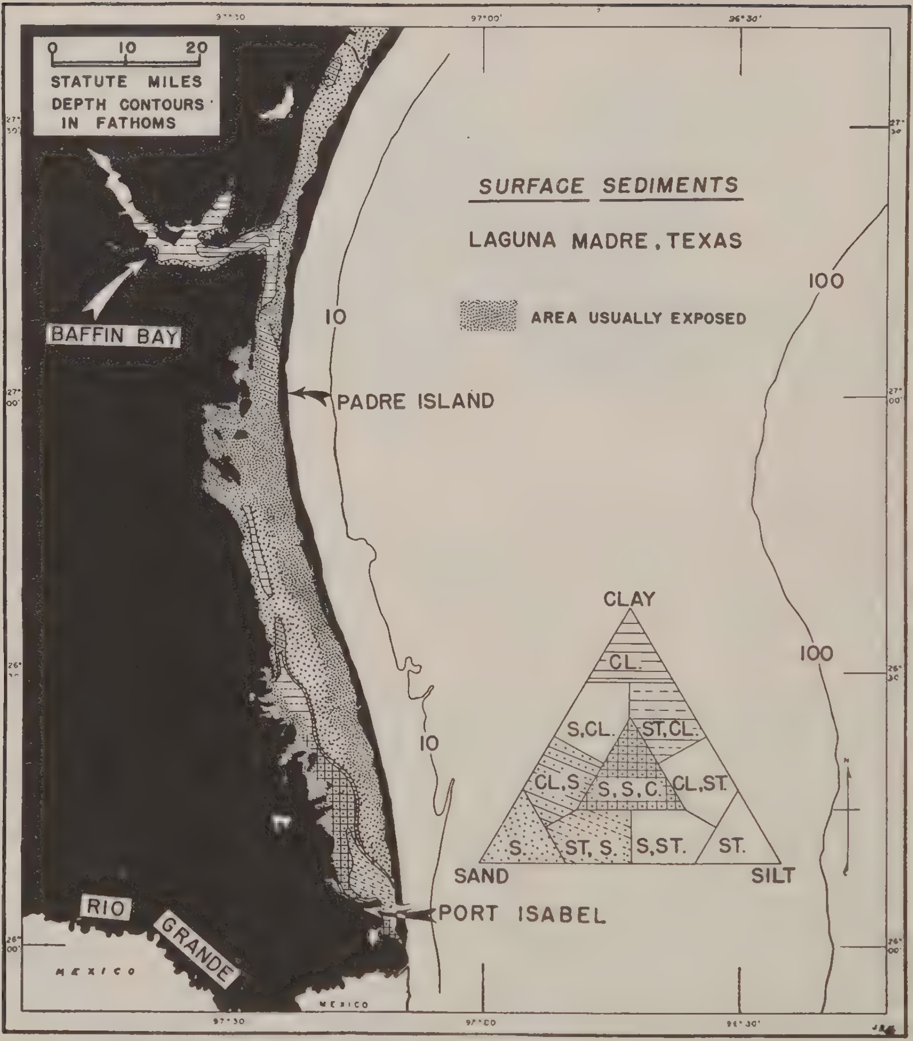
0 10 20
STATUTE MILES
DEPTH CONTOURS IN FATHOMS
SURFACE SEDIMENTS
LAGUNA MADRE, TEXAS
AREA USUALLY EXPOSED
BAFFIN BAY
PADRE ISLAND
10
100
CLAY
CL.
S,CL.
ST,CL.
CL,S
S,S,C.
CL,ST
S.
ST, S.
S,ST.
ST.
SAND
SILT
PORT ISABEL
RIO GRANDE
MEXICO
97°30'
97°00'
96°30'
27° 30'
27° 00'
26° 30'
26° 00'

FIG. 4. Sediment distribution in Laguna Madre based on sand-silt-clay content.

northern Laguna Madre consists of a shelly sand. Oyster reefs on the other hand are very scarce and hence do not contribute much to the sediment. However, extensive reef growths of serpulid worms have effectively closed off most of the mouth of Baffin Bay. These worms are not known to be active at present.

The study of the sand-sized material under the microscope has shown that in much of the Laguna Madre the sand includes numerous finely crystalline calcareous and gypsum aggregates, which are virtually missing in San Antonio Bay. They are found, however, in some of the shallow evaporating ponds and marshes along the northern fringe of the barrier islands in the subhumid area. In addition to these calcareous aggregates, the sand grains often have a coating of calcium carbonate which develops into ooliths. These ooliths seem to form especially along the shores of the landward side of the northern

Laguna. Both the ooliths and the calcareous aggregates are aragonitic and are an indication of the aridity of the climate and the resulting high evaporation which causes precipitation of calcium carbonate.

Foraminifera appear to be somewhat less abundant in the Laguna Madre sediments than in those of the bays to the north. Furthermore, the Foraminifera assemblage contains a larger percentage of the Miliolidae than is found in the humid bays. These Miliolidae also are important in the shallow water around the bay fringes of the barrier islands in the humid areas (Parker, *et al.*, 1953).

One large contrast between the bay deposits of this area of Laguna Madre and those to the north is the rather extensive development of stratification in the Laguna deposits. The greater part of the cores obtained to date show this stratification. Apparently the burrowing organisms which stir the bottom so extensively in the northern Texas bays are not nearly as active in the Laguna. This may be partly because of the hypersaline conditions found in the Laguna and the local development of black stinking muds which are inhospitable to the boring organisms. In the buried sediments of the Laguna rosettes of gypsum develop locally. These seem to develop in a zone several feet below the surface (Masson, 1955). The rosettes are found in some abundance on the spoil banks which have been built above the surface by the dredging operations of the intercoastal canal. In places where the water is either very shallow or where the surface is intermittently covered, an algal mat has formed on the surface of the sediments.

On the other hand, the Laguna Madre sediments do have some characteristics in common with those of the northern bays. Thus they lack echinoids and glauconite and the quartzose sand content varies directly with the distance from the barrier island, as is also the case in most of the northern bays.

Incidental Sediment Types in the Northern Bays

In addition to the types of sediment already discussed for the subhumid area, there are some rather special conditions which need to be considered. In an extensive portion of Aransas Bay the nature of the sediments indicates that they are accumulating very slowly. The map (Fig. 2) shows that this portion of Aransas Bay lies at a considerable distance from any stream mouth and it is far enough inside the bay to be away from much influence from Aransas Pass. Furthermore, the adjacent barrier island does not have many migrating dunes or excess supply of sand. Also, the relatively deep water, much of it over 12 feet, prevents the waves from introducing large quantities of sediments from the shallow margins. As a result of the slow sediment accumulation, the benthonic Foraminifera constitute an appreciable fraction, while quartzose sand percentage is diminished. This is particularly well shown in the ½–¼ mm. and ¼–⅛ mm. sievings from these bay sediments. These fractions commonly contain more than 80 per cent Foraminifera. This condition of slow deposition with high Foraminifera percentages is found also in a few samples from lower San Antonio Bay, but is better represented in some of the San Antonio Bay borings a short distance below the sediment surface. The increase in the Foraminifera content at depth has been used as evidence that the rate of deposition was slower in a period shortly preceding the present (Moore, 1955). A search for other localities with this high percentage of Foraminifera has not been very successful, although one zone was discovered in a sample presented to us by the Texas A. & M. Research Foundation from central Matagorda Bay, where again the water is relatively deep.

A few samples taken from the bays along the northeastern margin of Texas and into western Louisiana suggested that a special characteristic of the sediment may exist in these places. Much higher than normal wood fiber or plant fiber content was found in the sediments of some of these bays. Peaty material and tree remains form a significant portion of this sediment.

Summary and Conclusions

Texas bay deposits have such definite environmental characteristics that these bay facies should be easily recognized in the Tertiary sediments which are now largely buried by the Recent deposits along the Texas coast. In the older formations the finding of extensive thicknesses of unstratified clayey sediments, with occasional intercalation of calcareous deposits, consisting dominantly of oyster shells, should indicate that bay conditions in a relatively humid area have existed. The absence of echinoids and glauconite in the coarser fractions of the sediment would help to confirm the lagoonal or estuarine origin of such deposits. The macroorganisms, the Foraminifera, and the Ostracoda all have assemblages which are characteristic of bays, and they are quite distinct from those found in the open Gulf (see Parker *et al.*, 1953, Swain, 1955, and Parker, 1955). Where the sediments are intercalated with large quantities of sand, the nearness to inlets or to barrier islands is suggested. Where the sediments are predominantly clay and where they have an abundance of wood fragments the nearness to a stream mouth is indicated. Also an occasional finding of silt and clay laminations suggests conditions of deposition at a stream mouth.

Finding of roughly stratified sediments high in sand content and containing gypsum and carbonate aggregates would indicate deposition of the sediments under conditions of excessive evaporation. The abundance of the calcareous ooliths and of calcareous coatings around shells and sand grains would also indicate these semi-arid bay conditions.

REFERENCES

Beal, M. A., and F. P. Shepard. 1956. A use of roundness to determine depositional environments. Jour. Sed. Pet., 26: 49–60.

Bullard, F. M. 1942. Source of beach and river sands on Gulf Coast of Texas. Bull. Geol. Soc. Amer., 53: 1021–1044.

Flint, R. F. 1953. Probable Wisconsin substages and Late-Wisconsin events in northeastern United States and southeastern Canada. Bull. Geol. Soc. Amer., 64: 912.

Grim, R. E., and W. D. Johns. 1955. Clay mineral investigation of sediments in the northern Gulf of Mexico. 2nd Nat'l. Conf. on Clays and Clay Minerals, Nat'l Research Council, 81–103.

Inman, D. L., and T. K. Chamberlain. 1955. Particle-size distribution in nearshore sediments. Soc. of Econ. Paleon. Miner. Spec. Publ. No. 3, 106–127.

Ladd, H. S. 1951. Brackish-water and marine assemblages of the Texas coast, with special reference to mollusks. Pub. Inst. Mar. Sci. Univ. Texas, 2: 125–164.

Lohse, E. A. 1955. Dynamic geology of the Modern Coastal Region, Northwest Gulf of Mexico. Soc. Econ. Paleon. Miner., Spec. Pub., 3: 99–105.

Masson, P. H. 1955. An occurrence of gypsum in southwest Texas. J. Sediment. Petrol., 25: 72–77.

Moore, D. G. 1955. Rate of deposition shown by relative abundance of Foraminifera. Bull. Amer. Assoc. Petrol. Geol., 39: 1594–1600.

Norris, R. M. 1953. Buried oyster reefs in some Texas bays. J. Paleont., 27: 569–76.

Parker, Frances L., F. B. Phleger, and J. F. Pierson. 1953. Ecology of Foraminifera from San Antonio Bay and environs, southwest Texas. Cushman Foundation Spec. Pub., 2: 1–75.

Parker, R. H. 1955. Changes in the invertebrate fauna, apparently attributable to salinity changes, in the bays of central Texas. J. Paleont., 29: 193–211.

Puffer, E. L., and W. K. Emerson. 1953. The molluscan community of the oyster-reef biotope on the central Texas coast. J. Paleont., 27: 537–544.

Shepard, F. P. 1953. Sedimentation rates in Texas estuaries and lagoons. Bull. Amer. Assoc. Petrol. Geol., 37: 1919–1934.

————. 1955. Stratigraphic research that may pay off. Oil and Gas Journal, Feb. 21, 4 pp.

————. 1956. Late Pleistocene and recent history of the central Texas coast. J. Geol., 64: 56–69.

Shepard, F. P., and D. G. Moore. 1955. Central Texas coast sedimentation: characteristics of sedimentary environment, recent history, and diagenesis. Bull. Amer. Assoc. Petrol. Geol., 39: 1463–1593.

————. 1953. Sediment zones bordering the barrier islands of central Texas coast. Soc. Econ. Paleon. Miner. Spec. Publ. No. 3: 78–96.

Swain, F. M. 1955. Ostracoda of San Antonio Bay, Texas. J. Paleont., 29: 561–646.

Thornthwaite, C. W. 1948. An approach toward a rational classification of climate. Geogr. Rev., 38: 55–94.

Reprinted from JOURNAL OF THE OPTICAL SOCIETY OF AMERICA, Vol. 47, No. 8, 745–747, August, 1957
Printed in U. S. A.
Reproduced by Permission

Monochromatic Measurement of the Volume Scattering of Natural Waters

JOHN E. TYLER
Scripps Institution of Oceanography, University of California, La Jolla, California*

(Received April 12, 1957)

A laboratory method is proposed for measuring, as a function of wavelength, the scattering per unit volume of distilled and natural waters. The method employs special fixtures and techniques on the G.E. Spectrophotometer. It is best suited to hydrosols in which scattering and absorption are not excessive.

INTRODUCTION

IN many applications of Bouguer's law the absorption coefficient is so large compared to the scattering coefficient that the latter can be neglected in both the measurement and the calculation. A one-cm cell at the entrance port of the G.E. Spectrophotometer, for example, represents very little loss by fluid scattering and in most cases this loss can be largely compensated by the use of a reference cell of distilled water.

These techniques are not applicable, however, when one wishes to measure the constants of natural or distilled water. Writing Bouger's law to describe fully the beam transmittance of water we obtain

$$T=e^{-z(\mu'+s')},$$

where μ'† is the absorption coefficient for collimated light and s' is the scattering coefficient for collimated light. The sum $(\mu'+s')$ is commonly measured by oceanographers interested in the total attenuation of light by natural waters, and is called the total attenuation coefficient (β'). Various methods and instruments have been proposed for the independent measurement of s'.[1–6]

The method described here was devised for the measurement of natural waters and is best suited to media in which absorption and scattering are not excessive. It has the advantage of giving spectral data per unit volume throughout the visible region.

THEORY

The sphere of the G.E. Spectrophotometer is replaced by a somewhat modified sphere which is filled with the hydrosol to be measured. The exit ports are covered with reflectors having reflectances r_1 and r_2 and the instrument is allowed to come to balance.

In its passage through the sphere (see Fig. 1) the standard beam $(1+a)P_1$ will suffer losses at the various glass interfaces (represented by aP_1). A portion of the flux P_1 that enters the hydrosol will be scattered (sP_1 in the figure) and a portion mP_1 will arrive at the exit port. Of the latter, a fraction r_1 will be reflected. Thus the portions sP_1 and r_1mP_1 will be directed toward the phototube. In passing through the medium to the phototube these portions will suffer further loss due to absorption and the amounts actually reaching the phototube will be the fractions x and y, respectively, or

$$xsP_1+yr_1mP_1.$$

Similarly from the sample beam the amounts

$$xsP_2+yr_2mP_2$$

will finally reach the phototube.‡ Since this is for the balanced condition of the servo-mechanism,

$$xsP_1+yr_1mP_1=xsP_2+yr_2mP_2 \tag{1}$$

and the instrument reading

$$W=\frac{P_1}{P_2}=\frac{xs+yr_2m}{xs+yr_1m}. \tag{2}$$

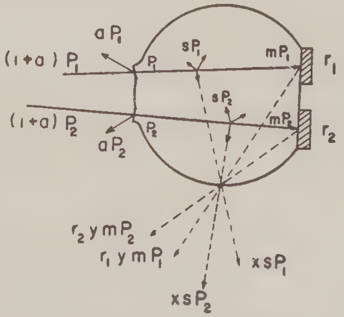

FIG. 1. Diagram of sphere for scattering measurements.

---

* Scripps Institution contribution No. 933. This work has been supported by the Bureau of Ships and by the Bureau of Aeronautics through contract NObs-72092.

† For a given sample the absorption coefficient for collimated light will differ from the absorption coefficient for diffuse light because of the difference in optical mean-free path. The measurement described here leads to the scattering coefficient for collimated light because of the geometry of the instrument used.

[1] B. S. Pritchard and W. G. Elliott, J. Opt. Soc. Am. 47, 113(A) (1957).

[2] R. G. Beuttell and A. W. Brewer, J. Sci. Instr. 26, 357–359 (1949).

[3] W. E. K. Middleton, *Vision Through the Atmosphere* (University of Toronto Press, Toronto, 1952), pp. 200–206.

[4] J. M. Waldram, Quart. J. Roy. Meteorol. Soc. 71, 319–336 (1945); Trans. Illum. Eng. Soc. (London) 10, 147–188 (1945).

[5] E. O. Hulburt, J. Opt. Soc. Am. 35, 698–705 (1945).

[6] J. E. Tyler, J. Opt. Soc. Am. 47, 346(A) (1957).

‡ It is, of course, important that the fractional losses at the interfaces, represented by (a), be the same for both beams if W is to be accepted without correction.

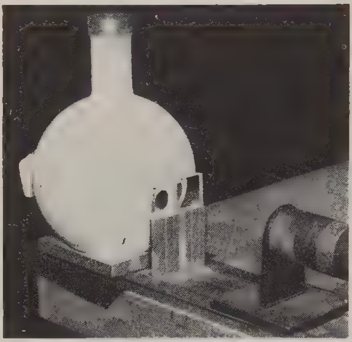

Fig. 2. Photograph of glass sphere in position on the Hardy spectrophotometer.

Referring back to Fig. 1, the portions sP_1, r_1mP_1, sP_2, and r_2mP_2 are all diffuse parcels of flux which are, on the average, optically equidistant from the phototube, or nearly so, and for which the attenuation coefficient is the same. Thus as the absorption coefficient becomes small the fractions x and y become equal. For hydrosols in which the absorption is small the instrument reading therefore becomes

$$W=(s+r_2m)/(s+r_1m). \tag{3}$$

By making $r_2=0$ and $r_1=1.0$ this reduces to

$$W=s/(s+m), \tag{4}$$

which in exponential form becomes

$$W=\frac{1-e^{-s'x_1}}{1-(e^{-s'x_1})(1-e^{-\mu'x_1})}, \tag{5}$$

where x_1 is the path length between entrance and exit ports.

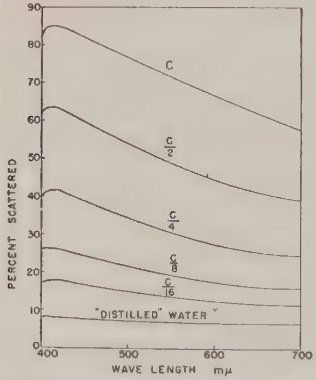

Fig. 3. Scattering data for a gum mastic preparation in various concentrations. Note that selective absorption, if present in the hydrosol, would result in an increase in the instrument reading.

EXPERIMENTAL

The outside surface of a five liter ring-neck flask was sand-blasted except for four clear spots left for entrance and exit ports. The exterior was then painted with white paint until it was opaque, again leaving appropriate ports. A plug was made for the neck which extended in, so as to finish off the inside sphere surface at this point. The finished sphere is shown in Fig. 2, mounted over the phototube of the Hardy spectrophotometer.§ Preliminary checks of the empty sphere showed that the two optical paths were very nearly alike.

The sphere was filled with a sample prepared by precipitating gum mastic from saturated alcohol solution. A series of curves was then run by progressively diluting as indicated‖ (see Fig. 3). It was not possible at this time to determine the absolute size or concentration of the scattering particles in this hydrosol. It was felt, however, that a method of progressive dilution would be most likely to preserve whatever particle size and state of aggregation existed in the original preparation. The curves exhibited in Fig. 3 represent samples having far greater scattering than is generally found in natural waters. Nevertheless, if absorption were absent, one would expect these data to conform to the equation,

$$\ln(1-S)=-s'cx_1, \tag{6}$$

or to Eq. (5) if absorption were present. Figure 4 shows that the data do indeed follow an exponential law indicating that absorption is not a dominant factor in these data. However, this is perhaps not a sufficiently sensitive test to show the degree of absorption in which we are interested when dealing with natural waters.

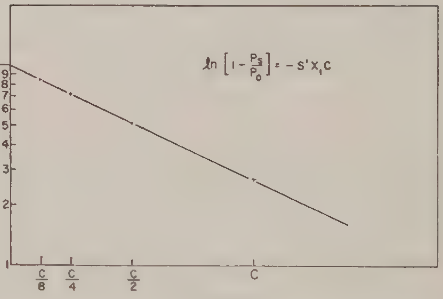

Fig. 4. Confórmity with Beer's law. These data are at 500 mμ. A linear relationship was also found at 410, 450, 550, 600, 650, and 700.

---

§ This refers to the original polarizing spectrophotometer built by A. C. Hardy and described by him in J. Opt. Soc. Am. **25**, 305–311 (1935). This instrument has been altered to some extent, and is still giving excellent service.

‖ In making these measurements it is essential to use an instrument equipped with a Stearns' plate [G. L. Buc and E. I. Stearns, J. Opt. Soc. Am. **35**, 521 (1945)] in order to get away from polarizing effects of the hydrosol.

Some idea of the effect of absorption on the reading at low levels of scattering and absorption can be gained from Fig. 5 which is a solution of Eq. (5) using values of s' and μ' likely to be found in the range for natural waters. Superimposed on these curves are the measured spectral values of absorption coefficient for distilled water given by Hulburt.[5] To be consistent these latter data should be referred to the calculated curve for $s'=0.931\times10^{-4}$/cm (not shown in Fig. 5) which is the measured value of the scattering coefficient obtained by Hulburt for distilled water. At these low levels of scattering and absorption the error in the instrument reading,

$$(W-S)/S,$$

depends only on the value of μ'. At higher levels the error depends upon s' as well. In either case an independent evaluation of μ' is needed.

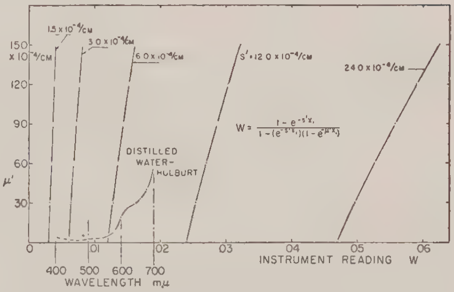

FIG. 5. Solution of Eq. (5) for same typical values of s' and μ'.

A direct experimental approach to the evaluation of μ' would be to measure the transmission of a known path length of the hydrosol using a cell mounted inside the standard G.E. Spectrophotometer sphere. In this way a fairly long path cell would be used without the associated danger of loss by scattering.

DISCUSSION

In the measurement of scattering of natural waters we are apparently not dealing with Rayleigh scattering but rather with large particle scattering in which air bubbles, organisms of various kinds, and detritus play an important part. Measurements made during field operations conducted by this laboratory indicate that we can expect "clear" water to have a scattering coefficient of the order of 0.004/cm and an absorption coefficient of about 0.002/cm. These data lie between the two lower curves of Fig. 3 and to the right of the curve marked $s'=24\times10^{-4}$/cm in Fig. 5. This method of measurement should be well suited to hydrosols in this region.

Because of the inherent precision of the Hardy spectrophotometer at low light levels and the fact that the sphere described here could easily be an integral part of a quartz distilling system designed to continuously purify a water sample, this method has been considered as a way of determining the spectral volume scattering for distilled water.

ACKNOWLEDGMENT

The author wishes to acknowledge with thanks the help of friends and associates who have assisted in carrying out this portion of our Hydrological Optics program.

Reprinted from THE REVIEW OF SCIENTIFIC INSTRUMENTS, Vol. 28, No. 7, 504–509, July, 1957
Printed in U. S. A.
Reproduced by Permission

Dielectric Recorder[*]

V. C. ANDERSON
University of California, Marine Physical Laboratory of the Scripps Institution of Oceanography, San Diego 52, California

(Received December 10, 1954; and in final form April 30, 1957)

A description is given of the dielectric recording technique wherein information is stored as a surface charge on a rotating dielectric coated drum. The specific application of the technique to a multiple channel recorder is shown. A general comparison between the properties of analog dielectric and magnetic drum recording is presented. The comparison shows dielectric recording to have important advantages for some applications.

INTRODUCTION

ONE of the perpetual problems of mankind is that of the storage of information. The steady pressure of this problem has given rise to a number of basic inventions which constitute an important part of our civilization today. These inventions range from the primitive invention of writing and paper up through inventions of printing and photography into the more recent inventions pertaining to analog recording of an electrical signal as typified by the phonograph and magnetic recorder. Each of these inventions represents the exploitation of some new physical phenomenon.

One of the more recent of the physical phenomena to appear in the field of information storage is the storage of an electrostatic charge on an insulating surface. The basic cause of its late arrival in the field may be traced to the fact that "perfect" insulators are not found in nature, and thus electrostatic storage is, of necessity, temporary in nature. It was not until the advent of more sophisticated information handling techniques as typified by modern analog and digital computers that the use of electrostatic storage has been seriously considered. The form of electrostatic storage most familiar to the reader is probably the Williams-type cathode-ray electrostatic storage as used in high-speed digital computers. The Williams-type storage tube uses an electron beam current and secondary emission to charge or discharge the dielectric storage surface. This type of storage is readily applicable to the problems of a digital computer; however, it cannot be applied to those problems where true analog recording is required. The technique to be described in this paper provides for true analog electrostatic recording using a bilateral recording head which can charge or discharge a dielectric surface with equal ease. Although the storage obtained with this technique is, of necessity, temporary, nevertheless it may find wide application where permanent recording is not required.

The secret of the dielectric recorder lies in the use of an ionization recording head to transfer charge to the dielectric recording surface. A review of the patent literature[1–5] reveals many ideas on the subject of electrostatic recording on a moving medium, none of which appear to be workable from a practical standpoint. In 1940, Grey[3] was granted a patent containing a broad claim of a method of imparting electric charges to the surface of an insulating medium, "such charges being of such a nature that they can be wiped off with a metallic contact." This is, of course, the obvious approach to the problem of establishing a charge on a dielectric surface, i.e., using a metallic contactor to apply and remove charges. As a matter of fact, this technique was the first one which was tried by the author in the development of the dielectric recorder. The early experiments showed that it was impossible to transfer charge in a linear fashion from a metallic contactor to a dielectric surface, and that the use of an ionization-type recording head in which a gaseous conductor makes intimate contact with the dielectric surface was required for successful operation.

In the course of development, a number of different ionization head designs were investigated. For a discussion of these investigations the reader is referred to an earlier report.[6] Only a general description of the technique and the characteristics of one of the most recent head designs will be given here, along with a description of a multichannel recorder used for electrically steering an acoustic array, which illustrates one of the several applications in which the dielectric recording technique has been used at the Marine Physical Laboratory.

PRINCIPLE OF OPERATION

The schematic representation of Fig. 1 illustrates the basic dielectric recording technique. The audio-

---

[*] This work is a result of research carried out under Contracts NObsr–43356 and 72512 with the Bureau of Ships, Department of the Navy. This is an SIO Contribution Number 934 (New Series).

[1] J. T. Tykociner, U. S. Patent Number 1,590,399, "Method and means for reproducing sound," (June 29, 1926).

[2] R. E. Tutherford, U. S. Patent Number 1,891,780, "Method and apparatus for recording and reproducing electrical impulses," (December 20, 1932).

[3] F. Grey, U. S. Patent Number 2,200,741, "Electrostatic recording and reproducing," (May 14, 1940).

[4] R. R. Riesz *et al.*, U. S. Patent Number 2,245,364, "Cathode ray device," (June 10, 1941).

[5] C. F. Pulvari, U. S. Patent Number 2,698,928, "Ferroelectric carrier, particularly tape recording and reproducing system," (January 4, 1955).

[6] V. C. Anderson, "A recording-reproducing system using a dielectric storage medium," University of California Marine Physical Laboratory of the Scripps Institution of Oceanography, SIO Reference 55–6 (January 4, 1955).

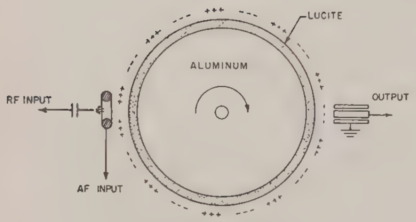

Fig. 1. Schematic representation of the dielectric recording process.

frequency signal is stored as a space varying surface charge on a rotating, dielectric-coated, conducting drum. The electric charge is transferred to the dielectric surface through a conducting path of ionized air which is produced by a stable rf corona discharge. As the surface of the drum passes through the discharge region, it is charged to the average potential of the region, which is the instantaneous value of the audio signal. Outside of the conducting region, a change in the surface charge distribution can only take place through volume or surface leakage in the dielectric medium, a relatively slow process. The varying surface charge induces a proportional change of potential on a conductor held near the surface of the rotating drum; a simple capacitative probe of this type is used as a reproducing head in the dielectric recorder.

A more detailed discussion of the three basic components of the dielectric recorder, i.e., the dielectric medium, the recording head, and the reproducing head will serve as a basis for the description of the operating characteristics, and general design considerations.

CHARACTERISTICS OF THE DIELECTRIC MEDIUM

The most important property of the dielectric material used to cover the recording drum is the decay time of a surface charge stored on it. This is determined by two factors: first, the volume resistivity, which gives rise to a characteristic decay time which is independent of both the geometry of the recorder and the surface charge distribution: second, the surface resistivity which gives rise to a decay time which is strongly dependent on both the drum geometry and the gradient of the surface charge.

The characteristic decay time of a surface charge due to the volume resistivity of a dielectric material is given by the product of the dielectric constant and volume resistivity of the material. A number of materials have decay times which are more than adequate for temporary storage applications. Commercially available plastics such as methyl methacrylate (Lucite), polystyrene, polyethylene, and Teflon have decay time constants ranging from 80 hr for Lucite to over 3000 hr for polyethylene.

In determining the effect of surface resistivity on the decay time of a sinusoidal surface charge, the geometry of the dielectric must be taken into consideration. It is readily shown[6] that the time constant due to surface resistivity for the geometry of the dielectric recorder is proportional to the square of the wavelength of the surface charge, for wavelengths long compared to the thickness of the dielectric, and directly proportional to the surface resistivity. Thus, surface leakage is most significant for the higher recorded frequencies. The surface resistivity depends not only on the dielectric material, but also strongly on the relative humidity of the atmosphere surrounding the dielectric as well as the roughness and cleanliness of the surface.

In addition to the storage properties of the dielectric materials, the stability of the material, both chemical and physical must be considered. The intense ionization and consequent strongly oxidizing atmosphere generated by the recording heads necessitates the use of a chemically inert material. The physical stability is also important since the drum must be machined to present and maintain a smooth, homogeneous surface for the recording.

Lucite has been a convenient material to use in the construction of dielectric recorders, and has been used exclusively in all applications of the dielectric recording technique mainly because of its ready machinability and the availability of large, thin wall extruded tubing from which homogeneous recording drums may easily be fabricated.

In practice, the 80-hr decay time constant for Lucite is only observed with a freshly cleaned surface. In normal operation in the laboratory, the time constant is somewhat less than this as a result of surface contamination from the atmosphere. Time constants for the Lucite drum recorders which have been constructed for operation in the laboratory have not fallen below one hour. Inasmuch as most of the applications require storage times ranging from a few milliseconds to less than one minute, the degradation of the signal resulting from the surface charge decay is negligible.

IONIZATION RECORDING HEAD

Basically the recording head is the component of the dielectric recorder which provides an electrical conducting path to the surface of the dielectric recording medium. A conductor placed on or near a dielectric

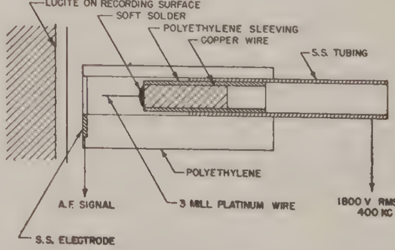

Fig. 2. Cross-section view of a dielectric recording head. The cylindrical body is $\frac{5}{8}$ in. in diameter and $\frac{9}{32}$ in. high.

surface always remains insulated from the surface by a thin layer of air. In order to transfer any electrical charge to the actual surface of the dielectric it is necessary first to break down the dielectric strength of this thin layer of insulating air. Thus, the use of a simple contactor as a recording head introduces a threshold potential which must be exceeded before any charge may be transferred. This threshold introduces intolerable nonlinearities in the recording properties. This difficulty may be circumvented if the air film is maintained in an ionized or conducting state at all times by some secondary source of energy. If this is done, then even minute amounts of charge may be transferred to the surface by a drift of the ions in the ionized gap. With a recording head of this type a very linear relationship exists between the charge transferred and the average potential difference between the recording head and the dielectric surface for potential differences of either polarity. Because of this bilateral linear relationship the recording head serves equally well in the dual roles of erasing a charge previously stored on the dielectric material while recording a new signal.

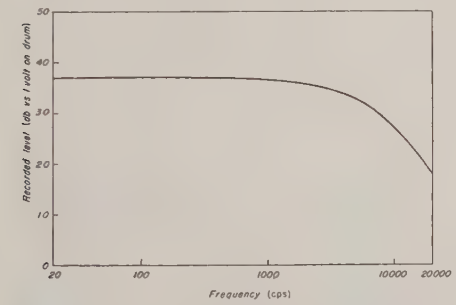

FIG. 3. Frequency response of a dielectric recording head. The surface speed of the drum is 2200 in./sec, the recording head is operated at 2200 v rms rf and driven with a 50 v rms af signal.

The erasing characteristics of the recording head are determined by the total conductivity of the ionized area exposed to the dielectric surface, while the sharpness of the boundary of this ionized area fixes the minimum wavelength of surface charge which may be recorded, thereby determining the upper frequency limit of the recorder. The dynamic range of the recorder is limited by the zero signal noise level of the surface charge which in turn will depend on the random fluctuations of the average potential of the ionized region at the surface of the recorder. It can be seen that, in general, a high ion intensity for high conductivity, a rapid decay of ionization for a sharp boundary, and a highly stable source of ionization for a low-noise level are to be desired in a recording head.

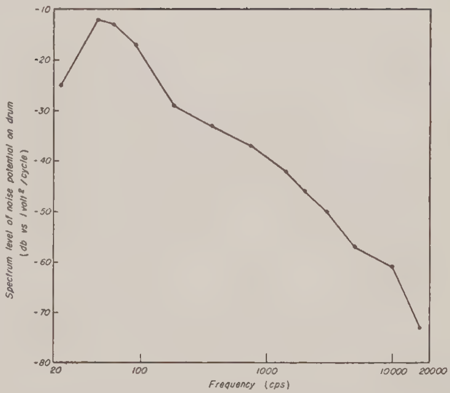

FIG. 4. Background noise spectrum obtained by octave band analysis. Drum surface speed is 2200 in./sec.

In line with the above requirement of a sharp boundary, it should be pointed out that, of all the common gases, air at atmospheric pressure has one of the highest ion recombination coefficients,[7] indicating a short ion lifetime and consequently a sharp boundary for the conducting region. For this reason, and because of the simplification of design, the recording heads used to date have been designed for operation in air at atmospheric pressure.

The construction of the dielectric recording head used in the multi-channel dielectric recorder is shown in Fig. 2. The body of the recording head is injection-molded from polyethylene. A polyethylene insulating sleeve provides dc isolation between the corona electrode and the rf supply, forming the coupling capacitor for the rf voltage. The audio electrode at the left of the cross-section view is made of stainless steel and maintains the average potential of the ionized region at or near the instantaneous potential of the audio signal applied to this electrode.

A large number of heads of this type may be driven from a single rf power supply thereby simplifying the circuitry for multichannel recording considerably. The compact design of these heads permits the use of three-eighths inch center-to-center track spacings

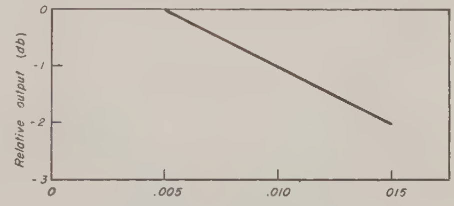

FIG. 5. Effect of recording head-to-drum gap on the amplitude of the recorded signal.

---

[7] L. B. Loeb, *Fundamental Processes of Electrical Discharge in Gases* (John Wiley and Sons, Inc., New York, 1949), p. 124.

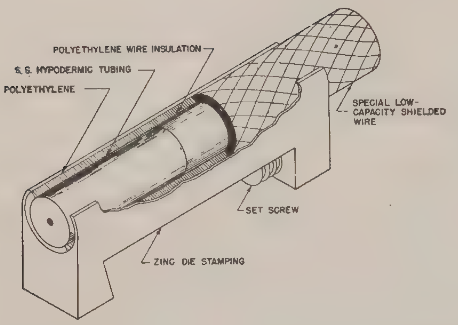
POLYETHYLENE WIRE INSULATION
S. S. HYPODERMIC TUBING
POLYETHYLENE
SPECIAL LOW-CAPACITY SHIELDED WIRE
SET SCREW
ZINC DIE STAMPING

Fig. 6. Cut-away sketch of the construction of a playback head. The over-all width of the head is 0.100 in., permitting close spacing around the drum.

on the recording drum. The impedance offered to the rf arises mainly from the 3-$\mu\mu$f stray capacity to ground. The impedance offered to the audio signal is also extremely high and again mainly reactive, appearing to be that of a capacity of less than 5 $\mu\mu$f exclusive of lead capacitance.

The frequency response of this recording head operating at a surface speed of 2200 in. per second is shown in Fig. 3. The curves are given in terms of charge potential on the dielectric surface. The major contribution to the high-frequency cutoff is the shunting effect of the rf coupling capacitor on the resistance of the ionized region. The corresponding background noise spectrum level for the recorder as determined by an octave band analysis is shown in Fig. 4. Here it can be seen that because of the slope of the noise spectrum, a wide dynamic range is maintained even if extensive high-frequency equalization is introduced to smooth out the frequency response up to the upper useable frequency limit of the recorder.

One of the most advantageous features of the dielectric recorder from the practical standpoint is illustrated in Fig. 5 where the recorded signal level is plotted as a function of the recording head to dielectric surface spacing. It can be seen that the amplitude recorded on the drum is very insensitive to changes in the head-to-drum spacing, thus permitting wide tolerances to be used in the construction of a recorder of this type.

The effect of the conductivity of the recording head in erasing a charge distribution on the drum is more noticeable than the effect of conductivity in recording. In practice it has not been possible to attain complete erasure with a single passage under the head. The maximum erasure which has been achieved is −20 db per head traversal, even at very slow surface speeds. The cause of this limitation has not been determined. At the 2200-in./sec surface speed used for Fig. 3 and Fig. 4, the erasure was less than this limit, approximately −15 db per head traversal.

Playback Head Characteristics

The basic requirements for the playback heads used on the multichannel dielectric recorder are that they be simple, compact, highly reproducible, and easily adjusted with regard to delay position or location around the drum. The final design of the playback head is shown in Fig. 6. The playback head bodies are zinc die stampings, and the electrodes and wire are crimped into the stamping after the electrode has been spot welded to the center conductor of the wire. After crimping, the electrodes are filed down to the correct dimension in a jig so that no additional head-to-drum adjustment need be provided.

For the particular head described here, a relatively long length of wire, approximately two feet, is required in order to permit the interconnection of the playback heads in the desired matrix. Inasmuch as the output level of the playback head is determined by the ratio of the head-to-drum capacitance to the shunting capacitances, a special, low-capacity, shielded wire was used for the playback head connections. This wire consists of an 0.008-in. diam stainless steel center conductor surrounded by a heavy polyethylene extruded insulation and covered with a single shielded braid. It has a capacity of 14 $\mu\mu$f per foot, a considerably lower capacity than commercially available wire of this over-all diameter.

The characteristics of the playback head as a function of head-to-gap spacing are shown in Fig. 7. Here again, it can be seen that the low sensitivity of the output with regard to the head-to-drum spacing permits the use of wide tolerances in recorder construction.

Another attractive feature of the dielectric recorder is the ease with which a number of pickup heads may be paralleled. The characteristic impedance of the playback head is strictly capacitive, hence, a simple capacitive mixing network is all that is required to combine a number of pickup head signals to a common output.

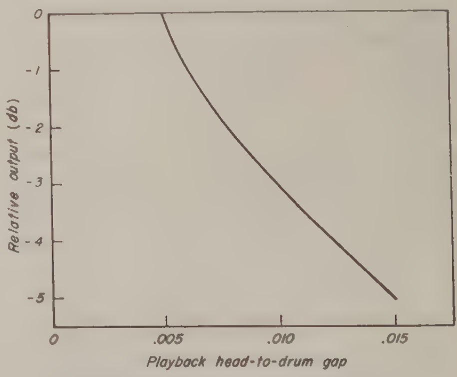

Fig. 7. Effect of playback head-to-drum gap on the amplitude of the reproduced signal.

The capacitive mixing networks used in the multichannel recorder described here were fabricated from double-copper-clad $\frac{1}{32}$-in. epoxy-glass board using printed circuit techniques. A number of these networks are shown in place in Fig. 8. Close-up views of the heads and a mixing pad are shown in Fig. 9.

MULTICHANNEL RECORDER

The construction of the multichannel recorder is shown in Fig. 8 to illustrate the manner in which the desirable properties of dielectric recording simplifies the design. The recording and playback heads for each channel are mounted on removable rings which in turn fit into an aligning support structure which positions the head-to-drum spacing, thereby eliminating the need for individual adjustments of the head-to-drum spacing on each head. The desired pickup head positions, corresponding to the time delays required, are preset by mounting the heads on the rings by the use of a calibrated jig. With the support structure shown, the head-to-drum spacing on the pickup and recording heads may be held uniform within ±0.002 in. Operating with a tolerance of this magnitude, the outputs of the heads are matched to within $\pm\frac{1}{2}$ db, a figure which was considered to be sufficiently reproducible for the purpose of steering an acoustic array.

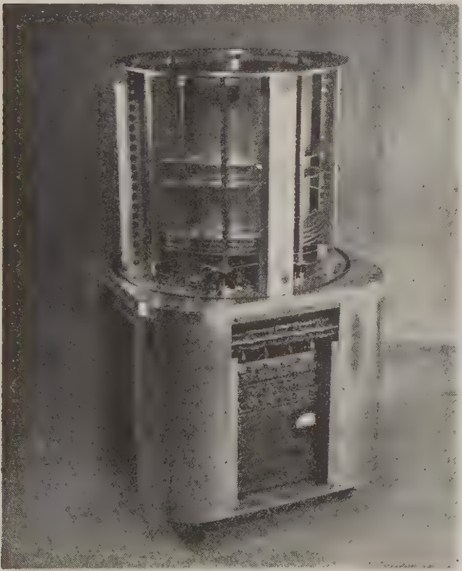

FIG. 8. View of a partially assembled multichannel dielectric recorder. The manner in which recording and playback heads are mounted around the 12-in. diam 12-in. high Lucite-coated drum is illustrated. A number of capacitative mixing pads are shown mounted in place on the recorder base plate. The 2500-v rf supply is shown at the bottom on the lower section, the 32 driving amplifiers are in the center, and the edge of the 48 playback amplifiers mounting plate with amplifiers in place may be seen just below the base plate.

A dovetail section of these rings serves as a mounting track for the playback heads. At one position on the ring this dovetail is machined flush with the ring base to provide for the mounting of the recording heads. The recording heads are lined up vertically with respect to each other so that simple direct connections to the rf power supply may be readily made. The rf inputs to the thirty-two recording heads are paralleled and brought through a metal-to-glass hermetic seal in the base plate to the rf power supply located beneath the base plate. The audio inputs of each individual head are also brought through a set of hermetic seals to the driver amplifiers in the bottom section of the recorder. The individual playback heads are brought to the capacitative mixing pads previously mentioned which are mounted directly on hermetic seals on the base plate. The output of each mixing pad is connected to one of the playback amplifiers which are mounted immediately beneath the base plate.

Complete hermetic sealing is provided for electrical connections through the base plate, so that an external case may be used over the entire drum assembly to control the atmosphere in which the recorder is operated. This is especially important when operating the recorder under adverse conditions, e.g., either humid air, or atmospheres contaminated with smoke and dust particles. Unfortunately the corona discharges in the recording heads serve as excellent dust precipitators and, in contaminated atmospheres, very quickly cause the growth of undesirable deposits in the recording head assemblies. High humidity greatly increases the corrosiveness of the nitrous oxide generated by the nitrogen fixing action of the corona discharge when operated in air. With the provision of hermetic sealing, dry air or even an inert gas may be used for the recording atmosphere, thereby overcoming these disadvantages.

COMPARISON OF DIELECTRIC AND MAGNETIC RECORDING

It is interesting to compare the properties of the dielectric recording technique with those of the more familiar magnetic drum recorder. The field in which the two techniques are competitive is in the field of temporary analog storage, e.g., dynamic time delay lines.

A comparison is made between the operating characteristics of the dielectric recorder and a typical spaced-head magnetic drum recorder[8] in Table I. It is apparent that one of the major advantages lies in the allowable tolerances in machining; a factor of 10 times larger tolerances may be used for the dielectric recorder for a given record-playback signal amplitude tolerance.

---

[8] Kenneth W. Goff, Proc. Inst. Radio Engrs. 41, 1578 (1953).

TABLE I. Comparison of operating characteristics of dielectric and magnetic drum recording.

	Dielectric drum	Magnetic drum
Surface speed	20 in./sec	100 in./sec
Head-to-drum spacing	5 mils	0.5 mil
Amplitude sensitivity of head spacing	0.5 db/mil	5–10 db/mil
Upper frequency response	400 cps	10 kcps
Low-frequency cutoff	<1 cps	100 cps
Min recorded wavelength	50 mils	10 mils
Dynamic range	60 db	50 db

Another major advantage is the broad band response of the recorder. Because no equalization is required in recording and playback, the low-frequency response of the recorder is determined only by the grid impedance of the input stage, and may be made almost arbitrarily low without encountering any basic long wavelength limitation as in magnetic recording.

The direct proportionality between the recording voltage and the playback voltage eliminates the phase distortion which normally accompanies the equalization process in magnetic recording.

The dielectric recorder offers an inherently high dynamic range; with existing recording heads, a dynamic range of 70 db has been measured using a recording voltage of 2800 v rms. Although this high a voltage is, in general, impractical, it serves to point out the contrast between the linear, nonsaturating medium of the dielectric recorder and the nonlinear magnetic medium with its troublesome saturation. The upper recording voltage limit is determined by breakdown along the surface of the dielectric, thus the limit is dependent mainly on surface cleanliness and the operating atmosphere rather than the properties of the medium.

OTHER APPLICATIONS OF DIELECTIC RECORDING

The dielectric recorder has been used for transient storage.[9] In this application the rf voltage is turned off one drum period after the arrival of a transient, and the transient may then be observed as a periodic signal and analyzed as desired.

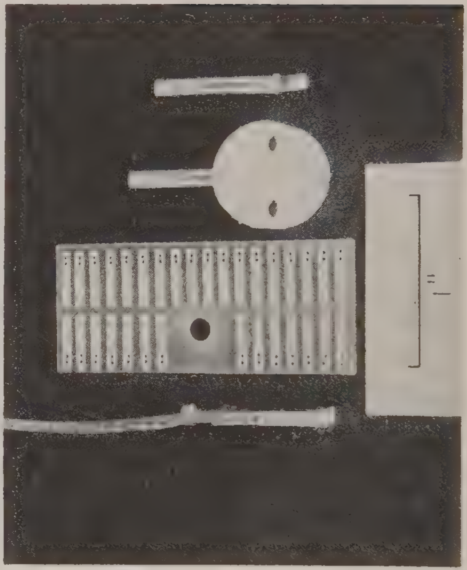

FIG. 9. Close-up view of a recording head, a playback head, and a capacitative mixing pad.

Another application of the dielectric recorder is as a multiple sweep integrator or comb filter.[10,11] Here the conductivity of the recording head is made intentionally small so that only a small fraction of the applied signal is transferred to the drum in a single revolution, and a correspondingly small fraction of the charge on the drum is removed in a single revolution. In this way that part of the applied signal which is periodic with the drum period builds up to the full potential on the drum while aperiodic portions tend to cancel out, producing an average charge distribution of zero.

The interest which has been shown in dielectric recording and the results obtained to date indicate the technique to be a fruitful field for future development and application.

---

[9] L. N. Liebermann, "Marine Physical Laboratory quarterly progress report," University of California Marine Physical Laboratory of the Scripps Institution of Oceanography, SIO Reference 54–32 (September 9, 1954), p. 5.

[10] B. L. Snavely, "Dielectric integrator and delay mechanism," Naval Ordnance Laboratory Report 4243, XD–1A, (October 25, 1956).

[11] V. C. Anderson, "The Deltic correlator," Harvard Technical Memorandum Number 37 (January 5, 1956).

CONTRIBUTIONS FROM THE CUSHMAN FOUNDATION
FOR FORAMINIFERAL RESEARCH
VOLUME VIII, PART 3, JULY, 1957

171. SEASONAL OCCURRENCES OF LIVING BENTHONIC FORAMINIFERA IN SOME TEXAS BAYS

By
FRED B PHLEGER and ROBERT R. LANKFORD
Scripps Institution of Oceanography, La Jolla, California

ABSTRACT

Seasonal collections were made from 32 stations in San Antonio, Mesquite, and Aransas bays during August and November, 1954, and January, March, May, and June, 1955. Studies of the seasonal living populations confirm the previously established faunal difference between the upper and lower bay areas. Living **Ammobaculites salsus**, a typical upper bay form, averages 27-59 specimens per station in the upper bay and 2-3 per station in the lower bay. The total living population in the upper bay is several times larger than that in the lower bay. This is attributed to the influence of the Guadalupe River bringing in food and/or trace materials conducive to high production. Populations in the lower bay are similar in size at all seasons. In the upper bay, on the other hand, the largest standing crops occurred in November and January. The reasons for this are obscure, but it is suggested that lower temperatures may cause reduced activity of bacteria in competition for food.

Plotting of distribution of sizes in **Streblus beccarii** at all stations shows a wide range of sizes at all seasons at all stations. This suggests that the population is composed of a wide range of age groups and that reproduction is occurring at frequent intervals. Plots of some species of **Quinqueloculina**, on the other hand, indicate seasonal reproduction and subsequent growth in average size of the specimens in some populations. Values for coefficient of variation generally are higher near the Guadalupe River than at other places in the lagoons.

INTRODUCTION

The area covered in this report includes San Antonio, Mesquite, and Aransas bays on the central coast of Texas, and extends from approximately 28° 20′ to 28° 47′ N. Lat. and 76° 30′ to 97° 03′ W. Long. The sedimentology of this area has been discussed in a comprehensive report by Shepard and Moore (1955), the basic patterns of dead foraminiferal populations have been described by Parker, Phleger, and Peirson (1953), and the living populations of Foraminifera at one season of collecting have been described by Phleger (1956). The purpose of the present report is to examine the distributions of living Foraminifera collected at two-month intervals for one year, and to attempt to discover the seasonal aspects of production, growth of the population and variability in population size distribution.

The field and laboratory work were supported by American Petroleum Institute Project 51. Final copies of the illustrations were drafted by Jean Peirson Hosmer.

DESCRIPTION OF AREA AND METHOD OF STUDY

Many of the features of this area have been described previously (Parker, Phleger, and Peirson, 1953; Phleger, 1956; Shepard and Moore, 1955). The bays are separated from the open ocean by a sand barrier island breached by only one perennial inlet at Aransas Pass in the southern corner of the area. The bays are very shallow with Mesquite Bay less than about 4 ft. in depth, San Antonio Bay averaging 5 to 6 ft., and Aransas Bay somewhat deeper. The Guadalupe River flows into the northeast corner of San Antonio Bay. The sediments are generally silty clays in the center of the bays grading into a narrow zone of sand at the margin: the area is traversed by numerous, elongate, shell reefs.

Thirty-two stations were occupied in Aransas, Mesquite, and San Antonio Bays during six seasons for one year; locations of the stations are shown on Figure 1. The periods of collections were August 26-29, 1954, November 9-11, 1954, January 5-7, 1955, March 7-9, 1955, May 2-4, 1955, and June 28-30, 1955. The stations are in all the principal foraminiferal assemblages previously established and give a reasonable coverage of the area. Surface-water samples for salinity and temperature observations were made at each station occupied during November, January, March, May, and June. Sediment samples were collected with a short coring tube previously described by Phleger (1951). The top 1 cm., comprising approximately 10 ml. of wet sediment, was taken from each core and preserved in neutralized formalin for study of Foraminifera. Neutralized formalin may break down into formic acid which will dissolve calcareous tests of Foraminifera in preserved material. A small amount of sodium carbonate was added to each sample to safeguard against solution and the pH of stored samples was determined frequently.

In the laboratory the sediment samples were washed over a screen having average openings of 0.062 mm. Specimens of Foraminifera alive at the time of collection were identified by the rose Bengal stain method

---

Contribution from the Scripps Institution of Oceanography, New Series, No. 935; Contribution from the Marine Foraminifera Laboratory, No. 25.

Reprinted from CONTRIBUTIONS FROM THE CUSHMAN FOUNDATION FOR FORAMINIFERAL RESEARCH
Volume VIII, Part 3, July, 1957
Printed by Dorr's Print Shop, Bridgewater, Massachusetts, U. S. A.

Reproduced by Permission

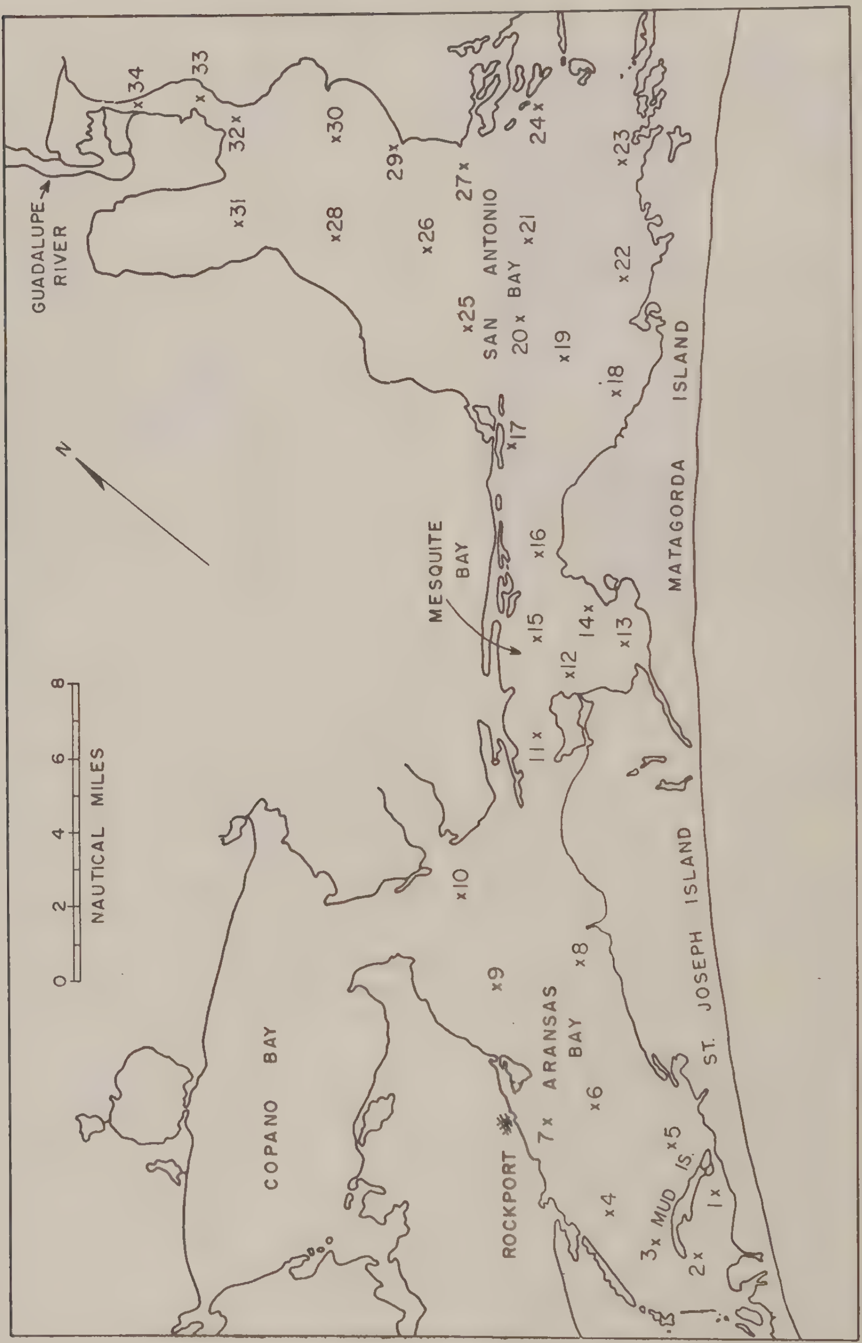
GUADALUPE RIVER
NAUTICAL MILES
0
2
4
6
8
N
COPANO BAY
ROCKPORT
ARANSAS BAY
MUD IS.
ST. JOSEPH ISLAND
MESQUITE BAY
MATAGORDA ISLAND
SAN ANTONIO BAY
1x
2x
3x
x4
x5
x6
7x
x8
x9
x10
11x
x12
x13
14x
x15
x16
x17
x18
x19
20x
x21
x22
x23
24x
x25
x26
27x
x28
29x
x30
x31
32x
x33
x34

FIGURE 1. Locations of stations.

(494)

described by Walton (1952). Living specimens were counted and in addition the maximum dimension of each living specimen was measured with a microscope micrometer disc. Sizes of specimens were listed according to divisions of the micrometer disc; each division is 0.025 mm. All measurements and detailed faunal data are on file at the Marine Foraminifera Laboratory, Scripps Institution of Oceanography. Illustrations of the species reported are in a previous paper (Parker, Phleger, and Peirson, 1953).

Temperature and salinity data have been summarized by Phleger (1956). Temperatures in Aransas Bay are reported by Hedgpeth (1951) to range from 13-31°C and the actual extremes over a long period of time probably are 5-10°C greater. Temperature data collected by the writers in 1954-55 are given in Table 1. Temperatures on November 9-11, 1954, ranged from 18-20°C. In January, 1955, measured temperatures were somewhat lower. They ranged from 14.7-21.6°C but were 15-18°C at most stations. In March temperatures averaged 16-18°C; these stations were occupied during a time of overcast and relatively cold weather when temperatures are expected to be somewhat lower than average. By May temperatures had risen to 25-26°C and in late June they were 29-30°C.

These surface temperatures are believed to give an approximate measure of the temperatures at all depths in the lagoons since the water is shallow and usually has daily wind mixing. There is obvious diurnal warming, as shown by average afternoon temperatures being 1-3°C higher than morning temperatures. These data may represent approximately normal yearly distribution but extreme maxima and minima apparently were not recorded.

Salinity data are discussed in terms of chlorinities in a previous paper (Phleger, 1956). Salinity data collected by the writers are listed in Table 2. In general, lowest salinities occur nearest the mouth of the Guadalupe River in Guadalupe Bay, and the salinities of both middle and lower San Antonio Bay are consistently lower than those of Aransas and Mesquite Bays. Salinities in Guadalupe Bay are quite variable depending upon runoff, and range from 2 o/oo to 24 o/oo. In upper San Antonio Bay the salinity usually is 33 o/oo or less, and in lower San Antonio Bay generally more than 33 o/oo. The highest salinities usually are found in Mesquite Bay; this was especially apparent in June, 1955, when the range was from 41.5-42.6 o/oo.

UPPER AND LOWER BAY FAUNAS

A faunal difference between upper and lower bays was demonstrated in previous papers (Parker, Phleger, and Peirson, 1953; Phleger, 1956). The present data confirm this and give further insight into the faunal differences in these two environments. In studying the faunal data it was apparent that the stations could be divided into two general groups, each of which seemed to be a faunal unit. The stations in Aransas, Mesquite, and lower San Antonio Bays which may be termed "lower bay" are 1-18, 21-24. "Upper bay" stations are 19, 20, 25-29, 31-34; station 30 is not included because its faunas are somewhat different from other stations; station 34 also is distinctive because of its very large populations and usually is not included.

Table 3 lists average total living populations in the upper and lower bay stations and average number of *Streblus beccarii* and *Ammobaculites salsus* at the various seasons of collection. An examination of these data shows that the average population per uniform size sample in the upper bay ranges from 188 to 352. The average number of specimens in the lower bay is much smaller, ranging from 53 to 106 per sample. The most striking difference between the different parts of the bay is the occurrence of *Ammobaculites salsus* which ranges from averages of 27-59/station in the upper bay to averages of 2-3 per sample in the lower bay. It is apparent that this species is better adapted to the upper than the lower bay. The average populations of *Streblus beccarii* in the upper bay were four to ten times larger than those in the lower bay at the times of sampling.

The living faunas in Aransas, Mesquite, and lower San Antonio Bays are also different from those in upper San Antonio Bay in containing several species which are more or less restricted to the lower bays or have generally higher frequencies in the lower bays than in the upper bay. These species are as follows:

Nonionella atlantica Cushman
Quinqueloculina funafutiensis (Chapman)
Q. lamarckiana d'Orbigny
Q. poeyana d'Orbigny
Rosalina floridana (Cushman)

Eponidella gardenislandensis Akers and *Miliammina fusca* (Brady) appear to be characteristic of upper San Antonio Bay, especially at the stations near the Guadalupe River.

There are some species typical of the open-ocean, nearshore environment which occur in the dead populations in lower San Antonio and Mesquite Bays, but have not been found living here. Living specimens of these species, however, occur in lower Aransas Bay. The following is a list of species which occur at station 23 in lowermost San Antonio Bay and which are not represented by living specimens:

Elphidium discoidale (d'Orbigny)
E. galvestonense Kornfeld

E. incertum mexicanum Kornfeld
Hanzawaia strattoni (Applin)
Massilina peruviana (d'Orbigny)
M. protea Parker
M. sp.
Quinqueloculina rhodiensis Parker
Q. wiesneri Parr

The following additional open-ocean species are not living in Mesquite Bay but are represented in the dead population:

Bigenerina irregularis Phleger and Parker
Reussella atlantica Cushman
Rolshausenia rolshauseni (Cushman and Bermudez)

The presence of *Palmerinella palmerae* Bermudez in the dead populations of the lower bays is not well understood. This species is not an open-ocean form and it has not been found living in the bays. It is suggested that this is a marsh form, apparently indigenous to the barrier island, and that it has been transported into the bays.

The locations where these open-ocean dead forms are found are on the inner side of a continuous barrier island and at a distance of several miles from permanent inlets. Most of the species have been found living in lower Aransas Bay, which is near an active inlet, and appear to indicate invasion of open-ocean water carrying the open-ocean species of Foraminifera. It is suggested that the presence of the dead open-ocean species in lower San Antonio and Mesquite Bays indicates either the former presence of inlets or occurrences of "wash-overs" over the barrier island during a storm such as a hurricane. Presence of wash-over channels on the barrier island in this area can be seen from the air. An inlet leading into Mesquite Bay is open occasionally. Open-ocean forms may have migrated into this area through the inlet and died out when the inlet became restricted or closed. It is also possible that some specimens were blown into the lower lagoon, but this seems less likely than in areas where more persistent winds of appreciable velocity blow from the ocean.

The distribution of the Miliolidae in the bays seems to be related to the type of substrate. They appear to prefer a sand or shell bottom, and numerous instances of living forms with their pseudopods attached to sand grains have been observed in the preserved samples.

Occurrences of living specimens of the various species are listed on Tables 5-10.

SEASONAL POPULATIONS AND VARIATION

There is no uniform relationship between size of living population and season of collection at the lower bay stations. Each of these stations seems to have its season of largest population more or less independently of nearby stations and no generalizations can be made about time of largest standing crop in this part of the area. In upper San Antonio Bay, on the other hand, the highest populations were collected during the winter season, November and/or January, at stations 26-29 and 31-34. This is also shown in the data for the average populations in the upper bay (Table 3) where the average populations for November and January are almost twice as large as those for the other seasons in the upper bay. In the lower bay there is a peak in the average population size in May but this does not occur at many stations.

Size-distribution histograms of the individuals of *Streblus beccarii* and *Ammobaculites salsus* were made at most stations, since these species have the highest consistent frequencies. Representative frequencies of sizes are shown in Figures 2-5. Size distributions for these two species show that there is a generally large range in size at all stations at all seasons, shown by the lateral spread of the histograms, and, moreover, that the spread in distribution is similar at all seasons at the same station. This suggests that the populations of these species are composed of mixed age groups. It appears, therefore, that reproduction in these populations is occurring at frequent intervals and during all seasons of the year. This conclusion is in agreement with results obtained by John S. Bradshaw (personal communication) on laboratory cultures of *Streblus beccarii.* He finds that under laboratory conditions this species will reproduce every four to eight weeks within the ranges of salinity and temperature to be expected in the environment represented by the Texas lagoons.

In contrast to this, some species of *Quinqueloculina* show evidence of seasonal reproduction. This is best shown by the size distribution of *Q. poeyana* at station 3 (Fig. 6) where there was a large population of relatively small specimens in August, 1954, but by March of the following year the total population had decreased and the average size of the individuals had increased. In the following June the average size of individuals was again relatively smaller. This suggests that summer is the season of reproduction for this species at station 3. The other *Quinqueloculina* species in Figure 6 also show some evidence of seasonal reproduction. Other species of living Foraminifera were not present in sufficient abundance to warrant plotting their size distributions.

It seems reasonable that the variability within an environment should be reflected in the genetic composition and morphology of individuals within a population. Species which are flexible in their adaptability are expected to inhabit more variable environments than those which are less adaptable. An index of variation of a population may therefore be an indication of the variability of the environment in which a population lived. The variation of size distribution within a population is expected to be somewhat different for different species and may differ because of the population growth stage, frequency of reproduction, and mortality rate.

An index of variation may be a useful tool in indicating the relative variability of the environment where a population lived and may be a clue to the actual environment. The Pearson coefficient of variation, $V = 100\ \sigma \div M$, has been calculated for living *Streblus beccarii* in all samples where the populations were large enough to be statistically significant. The coefficient of variation is an empirical measure based on the standard deviation, σ, and the mean, M, where the smaller coefficient numbers indicate less variation than the larger ones. Measurements of maximum diameter were used and the analysis is restricted to *S. beccarii* because the most reliable measurement data were obtained for this species.

Calculated coefficients of variation, V, are listed for *Streblus beccarii* on Table 4 along with the average values for V at all seasons at each station (V is given to the nearest whole number). The range for V is 17-43, and the range for the average of V is 20-34. In San Antonio Bay there are two geographic areas of average values. In the uppermost bay stations, 30-34, there are relatively high values of V, ranging from 30-34. These stations are nearest the Guadalupe River where there is most effect from the variable runoff of the river, the salinities are most variable, and it appears that there is most variation in the environment. South of station 30 the average values for V are lower, in the range of 20-26; most of the lower average coefficients of variation are confined to the lowermost bay at stations 17-19 and 22-24. There is some indication of higher values of V in the northern half of Aransas Bay, nearest the entrance to Copano Bay, than in the lower area, but the differences are not so marked as in San Antonio Bay.

In a previous paper on living Foraminifera from this area (Phleger, 1956) the ratio of living to total populations was calculated and estimations were made of relative sedimentation rates in these lagoons. Suggested relative rates of sedimentation on this basis were shown to be very low in the lower lagoons and significantly higher in the area in upper San Antonio Bay near the Guadalupe River. Live-total ratios have been estimated in the present samples and they appear to have the same orders of magnitude and to be distributed in the same pattern at all seasons as in the previous study of one season.

Duplicate samples were collected at two stations during March, 1955, in an attempt to discover whether collection methods were adequately sampling the living population. In four samples collected from station 15 the living population varied from 19-23 and the faunal composition was essentially the same. Five samples were collected at station 21 which had total populations varying from 10-19 with the larger population samples having more rare species but essentially the same basic faunal composition. These data probably indicate that a fairly good sample of the population is taken. It is suggested that the error of sampling probably is within the error of laboratory analysis of these populations.

DISCUSSION

There are significant differences between upper and lower bay faunas. There are fewer species at most stations in the upper than in the lower bay and the open-ocean species generally are restricted to the lower bay. The latter may be attributed to the immediate influence of open-ocean water invading through the inlets. The presence of higher living populations at all seasons in the upper bay than in the lower bay is more difficult to explain. It appears that the differences must be related to the influence of the Guadalupe River which is most pronounced in upper San Antonio Bay on the basis of salinity distribution. There is a marked increase in the size of the standing crop near the river with the largest population at all seasons at station 34 in Guadalupe Bay nearest the river mouth.

High populations near river mouths are established off some of the effluents of the Mississippi River near Main Pass and Pass a Loutre (Phleger, 1955). Living populations are higher in the direction of river mouths on the continental shelf off San Antonio Bay (Phleger, 1956).

The river-borne materials and/or factors which influence high standing crop, and probably high production, are believed to be numerous and are not known. Possible river influences are as follows:

1. An abundance of particulate food may be introduced by river water into a marine environment to which the populations are adapted.
2. Abundant nutrients may be introduced by river water into the marine environment and cause high production of plant materials which provide food for the Foraminifera.
3. It has been observed by Lankford that largest benthonic populations occur off the Mississippi River where there is a combination of high organic production and fast detrital sedimentation. It has been suggested that the sediment, which is very fine grained, may bring in attached detrital food on which the Foraminifera feed. It is interesting in this connection

that the highest populations are in San Antonio Bay in an area where the present sedimentation rate appears to be higher than elsewhere in the area.

4. It is well-known that the composition of dissolved salts in river water is quite different from that in ocean water. River water may also introduce trace materials, both organic and inorganic, which are conducive to growth of populations. Soils contain many such materials, and this fact is useful in laboratory foraminiferal cultures where soil extract is an essential ingredient for the living diatoms which are used as food in many such cultures.

No obvious explanation has been found for the higher populations in upper San Antonio Bay during November and January than at other seasons. Rainfall and meagre runoff data have been examined for this period and there do not seem to be any significant differences from other seasons. The salinities near the river mouth in November, 1954, ranged from approximately 25-34 o/oo and in January, 1955, were approximately 2.2-6.4 o/oo. At other stations in the upper bay salinities were essentially the same at both seasons and similar to salinities in the upper bay at other seasons. Water temperatures during this winter season, on the other hand, were significantly lower than at other seasons, being 18-20°C in November and 14.7-21.6°C in January. This infers that the low temperatures may have been conducive to growth of a large population. It has been suggested by D. L. Fox (personal communication) that the large populations at that winter season may be caused by lessened activity of bacteria in competing for the food supply.

REFERENCES

HEDGPETH, J. W., 1951, in Report of the committee on a treatise on marine ecology and paleoecology, no. 11, pp. 49-56.

PARKER, F. L., PHLEGER, F. B, and PEIRSON, J. F., 1953, Ecology of Foraminifera from San Antonio Bay and environs, southwest Texas: Cushman Found. Foram. Res., Spec. Publ. 2, pp. 1-75.

PHLEGER, F. B, 1951, Ecology of Foraminifera, northwest Gulf of Mexico. Part I, Foraminifera distribution: Geol. Soc. Amer., Mem. 46, pp. 1-88.

———, 1955, Ecology of Foraminifera in southeast Mississippi Delta area: Bull. Amer. Assoc. Petrol. Geol., vol. 39, pp. 712-752.

———, 1956, Significance of living foraminiferal populations along the central Texas coast: Contrib. Cushman Found. Foram. Res., vol. 7, pt. 4, pp. 106-152.

SHEPARD, F. P. and MOORE, D. G., 1955, Central Texas coast sedimentation: characteristics of sedimentary environment, recent history, and diagenesis: Bull. Amer. Assoc. Petrol. Geol., vol. 39, pp. 1463-1593.

WALTON, W. R., 1952, Techniques for recognition of living Foraminifera: Contrib. Cushman Found. Foram. Res., vol. III, pt. 2, pp. 56-60.

TABLE 1. Surface water temperatures in °C

Sta.	Nov.	Jan.	March	May	June
1	19.6		16.5	26.5	29.7
2	19.9	14.7	17.7	26.5	29.7
3	19.3	15.3	18.2	26.5	29.7
4	19.4	15.2	18.8	26.3	29.8
5	18.1	15.3	19.0	26.0	29.5
6	18.1	15.3	19.5		29.3
7	18.1	15.5		26.5	29.3
8	18.4	15.0	18.5	26.5	30.0
9	19.1	14.9	18.5	26.3	30.2
10	20.1	14.9	17.3	26.5	30.5
12	19.3	21.3	19.0	26.5	29.7
13	19.2	21.0	18.8	26.0	29.7
14	19.1	21.1	18.0	26.7	29.5
15	18.8	21.6	18.5	26.0	29.5
17	19.0	21.4	16.5	25.5	29.0
18	19.2	19.3	16.8	26.0	29.2
19	18.6	19.1	17.0	26.0	29.0
20	18.7	18.9	16.8	25.5	28.5
21	18.4	18.8	16.5	25.7	28.8
22	18.3	19.7	16.4	25.5	28.8
23	17.8	19.0	16.0	25.5	28.3
24	17.9	20.0	16.0	24.5	30.3
25	18.6	16.5		24.5	28.7
26	18.7	16.4		24.7	29.0
27	19.1	16.9		25.7	30.3
28	19.1	16.5		25.3	29.2
29	19.3	16.7		26.0	29.5
30	19.2	16.4		25.3	30.0
31	19.2	16.3		25.0	29.5
32	18.8	15.8		25.5	29.5
33	19.3	15.1		25.5	29.5
34	19.0	15.5		25.5	29.5

TABLE 2. Surface water salinities in o/oo

Sta.	Nov.	Jan.	March	May	June
1	36.51	36.59	34.42	35.41	40.82
2	36.35	36.30	33.78	35.67	39.60
3	36.35	36.12	34.04	35.60	39.52
4	36.68	36.09	33.33	35.47	39.30
5	36.63	36.00	33.52	35.82	39.46
6	36.56	35.89	33.15	36.25	39.33
7	34.47	35.91	33.46	35.16	39.18
8	36.18	36.16	33.73	35.88	41.17
9	35.22	35.37	33.84	36.75	41.34
10	35.48	35.42	34.22	35.94	41.07
12	36.77	37.04	33.08	36.18	42.51
13	36.51	36.82	32.29	34.34	42.55
14	36.53	36.75	31.67	36.17	42.60
15	35.10	36.68	31.73	36.43	41.57
17	33.58	35.52	29.31	33.30	41.76
18	34.66	35.15	33.95	34.11	36.99
19	33.83	34.72	33.87	33.69	36.67
20	34.21	34.57	32.09	33.04	34.23
21	34.69	34.24	31.72	34.75	36.85
22	33.64	35.24	33.18	34.52	36.96
23	33.69	35.41	33.13	35.32	36.01
24	33.19	35.41	33.14	35.34	36.31
25	32.32	33.07		33.16	31.26
26	33.11	30.66		33.05	28.05
27	33.52	34.51		32.84	30.82
28	30.48	29.33		30.90	29.22
29	33.48	35.37		34.08	31.24
30	34.22	32.54		30.59	28.60
31	28.96	27.61		32.09	26.71
32		6.35		24.90	4.92
33	24.85	3.00		14.83	2.56
34		2.19		15.75	2.30

TABLE 3. Comparison of populations of living Foraminifera in upper and lower bays

TOTAL POPULATION

Season	Av. no./sta. in lower bay	Av. no./sta. in upper bay
August, 1954	53	198
November, 1954	65	352
January, 1955	85	330
March, 1955	55	no samples
May, 1955	106	188
June, 1955	60	236

LIVING POPULATIONS OF *Streblus beccarii* (LINNÉ)

Season	Av. no./sta. in lower bay	Av. no./sta. in upper bay
August, 1954	15	92
November, 1954	22	266
January, 1955	32	158
March, 1955	10	no samples
May, 1955	24	91
June, 1955	18	106

LIVING POPULATIONS OF *Ammobaculites salsus* CUSHMAN AND BRONNIMANN

Season	Av. no./sta. in lower bay	Av. no./sta. in upper bay
August, 1954	3	48
November, 1954	3	40
January, 1955	3	53
March, 1955	3	no samples
May, 1955	3	27
June, 1955	2	59

TABLE 4. Coefficient of variation (Pearson) in *Streblus beccarii* (LINNÉ)

Sta.	Aug.	Nov.	Jan.	March	May	June	Average
1			25	28			26
4		26	17				22
5	20	24	23	24	23	22	23
6	40	25	24		27	24	28
7	24	33	21		20	17	23
8	32	22	18	26	22	32	25
9	28	34				27	30
17	15	24	29	32		25	25
18	26	25			22	20	23
19	19	18	17	25	20	20	20
20	26	20	21	13	25	18	20
22	21		22		24		22
25	24	21	23		23	34	25
26	23	29	35		21	24	26
27	19	18	32		18	22	22
28	24	23	18		31	23	24
29	28	22	19		24	26	24
30	35				29	27	30
31	23	24			30		28
32		32	34		36	26	32
33		31	32		43	29	34
34		34	31		31	35	33

STATION	1	2	3	4	5	6	7	8	9	10	12	13	14	15	17	18	19	20	21	22	23	24	25	26	27	28	29	30	31	32	33	34
TOTAL LIVING POPULATION AUGUST, 1954	25	12	158	70	119	65	42	52	100	45	38	24	9	8	68	100	340	24	11	38	50	24	266	428	73	131	79	117	104	317	216	186
Ammobaculites dilatatus	1				2	1	1		1			1				34	6				1			2		5	1	2				
salsus & vars	1				37	4	1	2	6	3					1	6	52	2	1	1			185	20	5	14	1	13	67	112	122	767
spp																													1			
Ammoscalaria pseudospiralis	3	1	1	5		2	9	9	2	5	3	6		1	7	9	37	1	1	9	3	8	2		20	1	21		3			
Bolivina lowmani								1																								
striatula					1		1				1	2			1	1		1		1			3				1					
Buliminella elegantissima																																
Elphidium delicatulum	1		2		5				3	1					2		2	1	2	1				9	2	3	1	3			5	21
discoidale																																
galvestonense			3																													
gunteri	4		4	4	4	2	2	10	3	7		1	2	1	1		9						5	9		2	4			1	6	14
incertum mexicanum																																
cf koeboeense														1									12									
matagordanum	1				3	2		2	4		1				38			3			1		49	9		2	2	5		2	1	
poeyanum					11	2	5	2	16	8	2		1	1	2		4	3	3		2			9	1	10	1	1	1	1		
spp															1																	
Entosolenia sp									2								1															
Eponidella gardenislandensis	1														1								3	10		1				70	21	234
Massilina peruviana																																
protea																																
sp				4																												
Miliammina fusca																																4
sp																1																
Nonionella atlantica																	2															
Quinqueloculina cultrata			1	1												2	2				1								1			4
funafutiensis		1	5	5			1		1		27	7	2	1							1											
lamarckiana	2	2		2																												
poeyana		6	103	11										1		8	18		1		2						1					
rhodiensis	2		1	4																												
seminulum			2	2							1	2																				
wiesneri			18	1				1																								
spp			6	4			1				1					3	4											1				
Reophax nana																																
Rosalina floridana	1						2																									
Streblus beccarii var A	2	2	7	9	35	40	15	26	59	9	2	3	3	2	1	12	157	13	3	23	31	5	99	359	39	85	28	82	24	95	37	81
beccarii var B	2		2	2	2	2	3	4	3	1			1		1	23	13			3	6		8	6	6	8	15	4	6	13	10	11
Triloculina sidebottomi	2		3	14								2			2	1	33										3	6	1	23	14	53
Other spp	2			2																	2											

TABLE 5. Distribution of living Foraminifera in surface sediment samples during August, 1954.

STATION	1	2	3	4	5	6	7	8	9	10	12	13	14	15	17	18	19	20	21	22	23	24	25	26	27	28	29	30	31	32	33	34
TOTAL LIVING POPULATION NOVEMBER, 1954	72	97	26	35	318	193	70	116	28	17	70	33	24	12	61	31	78	215	18	31	26	22	647	414	740	336	534	16	214	616	374	2608
Ammobaculites dilatatus	2	1			2	1										1		1			1				1	6		1	11	12		
salsus & vars	7				8	13	1	1	1	1	4	3	1		6	4	8	3	5	1	1	3	64	97	12	15	2		20	120	46	[illegible]
spp																										17	2	1	4	2	2	
Ammoscalaria pseudospiralis			1		2		1		2				1	1		2	1	3		5	2	10	7		103	21	79		17	1		
Bolivina lowmani		1				3						1											2		2							
striatula	2	3		1	4	6	2	1			3	1	2		4	1	1	2	2				12	2	10	5	6	1	4	2	2	
Buliminella elegantissima		1			1	1					1							1		1		1			1							
Elphidium delicatulum																							9	6	1	2	3		2	1	1	2
discoidale		4	1					1																								
galvestonense			1																													
gunteri	6	6	4		42	8		10	2	1	2	3	1	1	3	1	1	4		1	1	1	12	4	9	4	91	2	6	10	7	114
incertum mexicanum			1		7	3	1	1							1											1						
cf koeboeense												1						1					19		1		1					
matagordanum	1	1			4	1		1	2				1					48					140	8		1			7	4		
poeyanum	2			1	7	3	1	2	1	3		2	1		1	1	4	8	2				9	3	4		3	1		7	2	
spp	2				4												2						1									
Entosolenia sp.					1																				1			1		1		
Eponidella gardenislandensis		1			2			2															4	17		1				66	23	194
Massilina peruviana																																
protea											1										1											
sp																																
Miliammina fusca																					1											46
sp	1						1																		1							
Nonionella atlantica		5	1																													
Quinqueloculina cultrata	1	1									2			1	1		1						2	1	2	1			29	4	3	
funafutiensis	1	7	3	3							29	5	4	1		2				2	1						2					
lamarckiana	2	11		3			2				9	4	2							8	3				4							
poeyana	11	20	2	2					2						4					4	9	1		1	2	1				11	4	
rhodiensis	4	2					3																									
seminulum		8	1	2						1	12			4	1					1	4	1			6							
wiesneri	1	1																														
spp	3	3		1																								2	3		2	
Reophax nana	1				1			1							2																	
Rosalina floridana	2						5																									
Streblus beccarii var A	14	16	10	15	90	74	18	76	16	11	6	11	11	3	31	17	49	121	9	7	1	4	358	260	566	248	595	7	99	330	228	700
beccarii var. B	2	4	1	7	143	80	23	20	2			2			3	2	10	23				1	26	7	11	12	7		4		6	2
Triloculina sidebottomi	4	1					7				1			1	4					1	1		1		1	1	3		8	41	28	88
Other spp.	3						5										1						1		2					4		2

TABLE 6. Distribution of living Foraminifera in surface sediment samples during November, 1954.

STATION	1	2	3	4	5	6	7	8	9	10	12	13	14	15	17	18	19	20	21	22	23	24	25	26	27	28	29	30	31	32	33	34
TOTAL LIVING POPULATION JANUARY, 1955	110	166	78	83	391	104	125	44	19	3	85	79	53	20	265	19	160	134	9	30	7	18	239	1436	101	128	228	19	66	1050	491	2572
Ammobaculites dilatatus																										4	15		2	6		
salsus & vars	1				6	7			1			3			37		4	7	3				48	968	12	1	1	1	5	309	73	1660
spp																										2	1		1	6		
Ammoscalaria pseudospiralis	7	1	1	4					3		3	2	1	2	24	3	43	8		1	4	4	7		7	12	20		2			
Bolivina lowmani																																
striatula	1	4		1	2	2	4	1							4		2	3			1		4	12	2	5	9	1	1	9		
Buliminella elegantissima		3				1	1								1																	
Elphidium delicatulum															7								5	20		1			4		2	8
discoidale	1	1															1															
galvestonense																																
gunteri	6	2	16	2	161	1	5	4	2		1	1	1	5	64	1	4	5		1		1	6	52	8	26	87	4	25	51	15	52
incertum mexicanum																																
cf koeboeense			2												2		2						6		2	1						
matagordanum	1		1			2									41	1	7	9				1	35	12	2	9	2	1		126	58	48
poeyanum	3	13		24	51	12	23	1	1	1	3		3		2	5	12	27				3	1	36	11	8	2	3	11	72	14	
spp																																
Entosolenia sp					1										7								5	4		3	3			6	1	
Eponidella gardenislandensis					3	1									1		1	1					5	16	2					18	14	172
Massilina peruviana	3																															
protea																																
sp	4										1															1						
Miliammina fusca																														45	10	20
sp															1			1														
Nonionella atlantica																																
Quinqueloculina cultrata	2	8							1	1	3	1	1	1	5			2								1	5	2				
funafutiensis	6	7	5	8							29	45	20	4					1	2		1			2		2		1			
lamarckiana	8	8	5								7	9	7				3								1							
poeyana	5	18	35	6							1				2						2	1	1		1		7			12		
rhodiensis	11			1																												
seminulum	6	2	10								4	2		1	3		2	1														
wiesneri	1	1																														
spp	1			1	3						1	3	3		6					2					2	1			1	3	3	8
Reophax nana					1										2																	4
Rosalina floridana	1																															
Streblus beccarii var A	25	87	3	32	150	65	78	36	11	1	28	13	17	7	39	9	70	67	5	23		6	114	312	38	50	61	7	10	369	292	592
beccarii var B		10		4	13	12	14	1			4				2		9	3		1			2	4	8		10		1	9	7	
Triloculina sidebottomi	17	1						1							6										2	3	3		2	9	2	8
Other spp.						1									9							1			1							

TABLE 7. Distribution of living Foraminifera in surface sediment samples during January, 1955.

STATION	1	2	3	4	5	6	8	9	10	12	13	14	15	17	18	19	20	21	22	23	24
TOTAL LIVING POPULATION MARCH, 1955	116	78	72	25	39	28	50	22	5	48	54	143	19	331	45	183	41	10	17	16	14
Ammobaculites dilatatus				1								1									
salsus & vars	1				3	2			1		3			36	4	3	3				
spp																					
Ammoscalaria pseudospiralis	9	2		4				2	3			1	2	7	9	32	1	2			1
Bolivina lowmani																					
striatula	1	2			1					1	2	1		8		1		1			
Buliminella elegantissima		1								2	1			2							
Elphidium delicatulum	3													15	2	7	4				
discoidale																					
galvestonense			1																		
gunteri	4	4	10	1	3	14	7	1				1	4	61	3	4	2			1	
incertum mexicanum		8	3																		
cf. koeboeense														1							
matagordanum	4	2												6	1	2	6				
poeyanum	9	3		12	8	3	6	4		3	1	99	5	117	8	28	2				4
spp														7		1					
Entosolenia sp.								1						4							
Eponidella gardenislandensis					1		2							1		1	2				
Massilina peruviana		1																			
protea																					
sp.	1	1											1					1			
Miliammina fusca																					
sp.																					
Nonionella atlantica																					
Quinqueloculina cultrata	1												1	2							
funafutiensis	10	5	4	1						38	36	23	4		1	1			10	6	1
lamarckiana	3	2																			
poeyana	6	9	44	1										1					2	2	
rhodiensis	11		1																		
seminulum	2	5	6							2											
wiesneri		2																			
spp.	3	2												2						1	
Reophax nana	1																				
Rosalina floridana	8																				
Streblus beccarii var. A	22	3	2	3	21	7	22	14	1	1	10	10		32	13	86	21	4	5	5	7
beccarii var. B	7	4		2	2	2	13			1	1	7	2	2	4	16		2		1	
Triloculina sidebottomi	4	22	1											27		1					1
Other spp.	6																				

TABLE 8. Distribution of living Foraminifera in surface sediment samples during March, 1955.

STATION	1	2	3	4	5	6	7	8	9	10	12	13	14	15	17	18	19	20	21	22	23	24	25	26	27	28	29	30	31	32	33	34
TOTAL LIVING POPULATION MAY, 1955	109	149	12	47	292	107	157	156	9	132	33	82	139	38	45	57	139	149	9	73	432	25	370	165	151	113	372	158	92	248	84	653
Ammobaculites dilatatus	1									1								1					1		1	1						
salsus & vars			1		3	32	1	3			1	1			3	1	16	26					113	17	1	13		10	19	39	28	390
spp																							1									
Ammoscalaria pseudospiralis	21	4	1	8		1	10	5		9		3	13	1	2	12	16	15	1	18	2	2	4		20	2	66		3			
Bolivina lowmani							1											1										1				
striatula	3			1	1			1		2	1	5	2	2			1	4		5		1	2	1	2		10	2				
Buliminella elegantissima	8						1					1	1	1				2							1							
Elphidium delicatulum					5	1	2			1					4	2	2	1			6		21	15	1			10	2	1		19
discoidale																																
galvestonense																																
gunteri	4	1	1	2	71	1	8	16				2			17	1		1	1		3				4		24	3	1	3	2	2
incertum mexicanum		1																														
cf koeboeense													1								1		7									
matagordanum	2				2			5		6					4	2	1	6				1	31	2	2	6		7		66	1	5
poeyanum	2	4		10	0	1	21	6			2		2	4	1	5	3	11		1	9	4	4	3	13	15	28	3	5			1
spp					2																				1	3	1					
Entosolenia sp					1																			1			1					
Eponidella gardenislandensis					6			2										2					3	6						49	23	75
Massilina peruviana										1																						
protea	1																															
sp	1			1																1												
Miliammina fusca																																1
sp										1								1				2										
Nonionella atlantica							1																									
Quinqueloculina cultrata	1					1						1		2	1	1					2	1										
funafutiensis	14	65	2	7	1	2	4		1	3	20	51	79	13			1		1	6	4	3			7							
lamarckiana					1																											
poeyana	6	49	2	2							1	1	12	3		1				1	386		1		1		1					
rhodiensis	4	3		1																												
seminulum		6											3												3		1					
wiesneri																																
spp		5		2						2	2		1	2		1					5				1							
Reophax nana	1																															
Rosalina floridana	1		1				8			3																						
Strebius beccarii var A	14	7	3	7	115	37	45	90	7	2	5	13	12	9	11	18	90	67	5	32	2	8	166	116	56	60	111	111	60	88	28	158
beccarii var B	18	3	2	4	62	5	52	26				2	3	1	2	9	7	3	1	8	2	3	8	1	23	1	14		1	2	2	2
Triloculina sidebottomi	7	1		2	2		1	2				1				4	2	8		1	12		7	3	14	2	115	11	1			
Other spp.							4			1											4		1									

TABLE 9. Distribution of living Foraminifera in surface sediment samples during May, 1955.

STATION	1	2	3	4	5	6	7	8	9	10	12	13	14	15	17	18	19	20	21	22	23	24	25	26	27	28	29	30	31	32	33	34
TOTAL LIVING POPULATION JUNE, 1955	20	182	39	53	165	87	36	160	24	42	67	41	33	20	81	89	110	66	7	19	6	22	864	720	165	65	102	368	25	177	63	320
Ammobaculites dilatatus			1			1	1	1			1												2	1		2	1					
salsus & vars		2			16	11	1	1				1	2	3	1	3	8	3					431	53	6	4		19	9	62	21	202
spp																																
Ammoscalaria pseudospiralis		3	1	7				7	3	11	3	8	4	5	11	13	29	4	2	9	3	8		1	31		7	1				
Bolivina lowmani										1					1		1						2		1		1					
striatula	1	1		6	3		1			4	3	1				7		1		2			4	1	4		2	19	2			
Buliminella elegantissima		2		1		1							1	1	1					1			1									
Elphidium delicatulum					4	1	1	3			1				1	2		2					19	36			3	3		1		5
discoidale																																
galvestonense			1					1																								
gunteri		1		1	15	5	1	40						1	15	1		1	1			1	2	3	11	2	2	12	1	4	3	2
incertum mexicanum																																
cf koeboeense																							26		1		1					
matagordanum	1	1			4			1	2	2					7	1		11					133	5		13		58		40	2	1
poeyanum				1	2	1	4	7		1			3		2	7	6			1			2	10	4	2	3	10	3			
spp					3																			2				1				
Entosolenia sp.					1										1	1												4				
Eponidella gardenislandensis					1			1								1							14	15				1		8	17	42
Massilina peruviana																																
protea																																
sp.				3						2												2										
Miliammina fusca																											1					
sp																																
Nonionella atlantica		3																														
Quinqueloculina cultrata		10						1		1			2							1						1	1	2				
funafutiensis	2	3	2	3						4	20	15	2			4	3		1	2	1	1			4			3				
lamarckiana																																
poeyana	8	144	23	8				1			14		3	1		3				1						1		3				
rhodiensis	1																															
seminulum		9	1	1						4	1														1							
wiesneri																																
spp			1	1							3				1							1						1				
Reophax nana																																
Rosalina floridana	2			1																			1									
Streblus beccarii var A		2	4	14	80	39	24	60	17	9	14	10	14	7	18	31	59	42	2	2	1	8	202	567	79	30	43	127	9	50	19	66
beccarii var. B		1	2	4	36	28	2	35	2	2	6	4	1	2	20	13	4	2	1		1	1	22	25	23	9	29	38	1	12		1
Triloculina sidebottomi	3		3	1			1	1		1	1	1	1		2	2							3	1		1	8	61				
Other spp.	2			1								1																5			1	1

TABLE 10. Distribution of living Foraminifera in surface sediment samples during June, 1955.

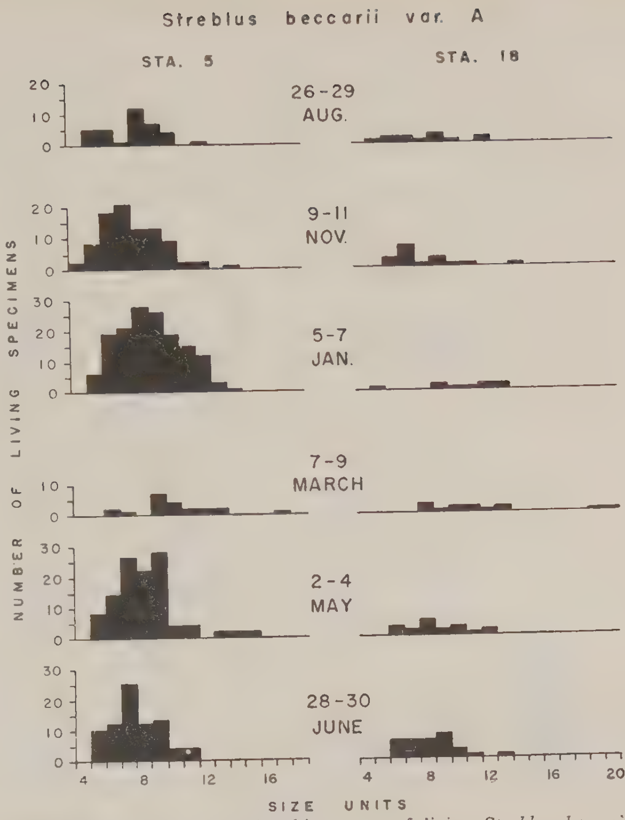

FIGURE 2. Size distribution histograms of living *Streblus beccarii* var. A at stations 5 and 18. Size divisions are 0.025 mm.

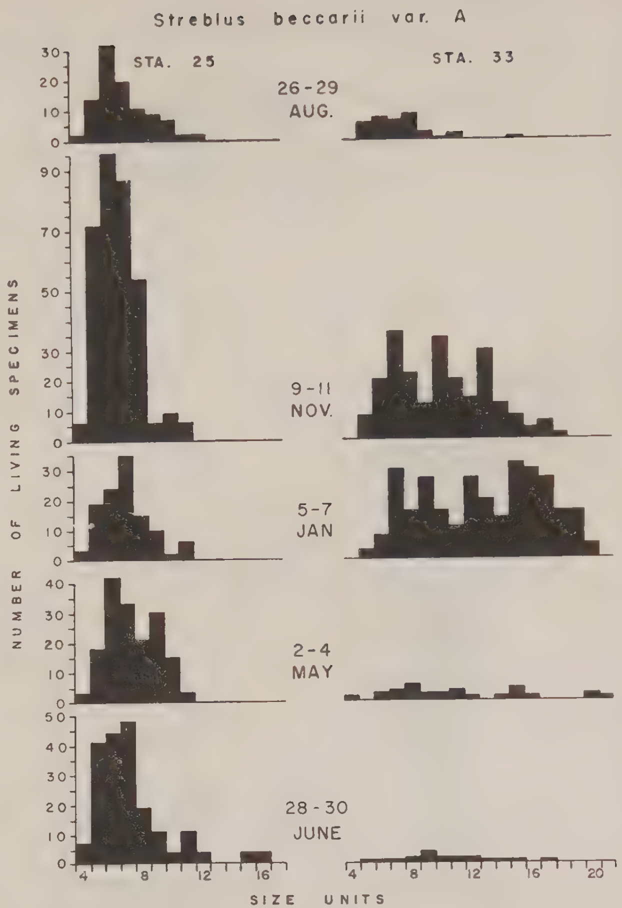

FIGURE 3. Size distribution histograms of living *Streblus beccarii* var. A at stations 25 and 33. Size divisions are 0.025 mm.

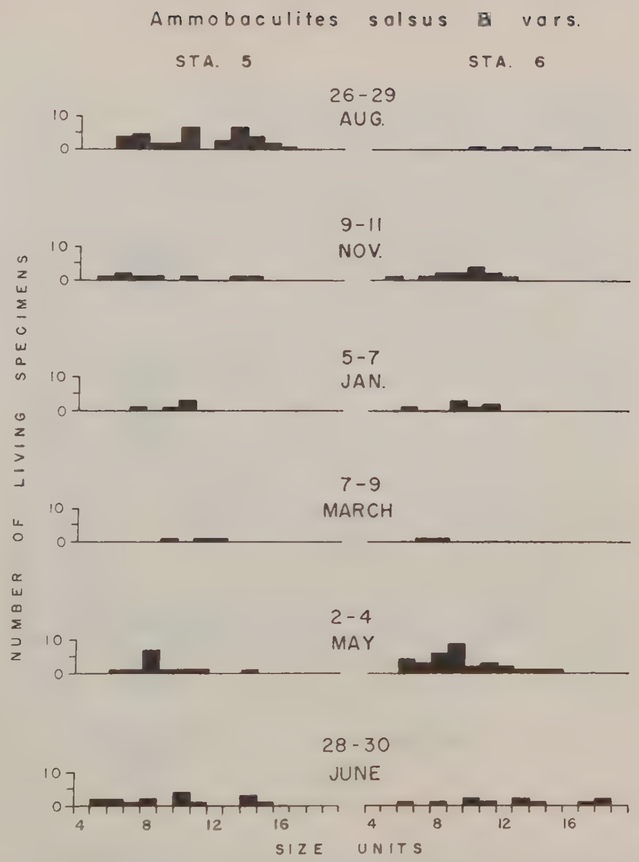

FIGURE 4. Size distribution histograms of living *Ammobaculites salsus* and vars. at stations 5 and 6. Size divisions are 0.025 mm.

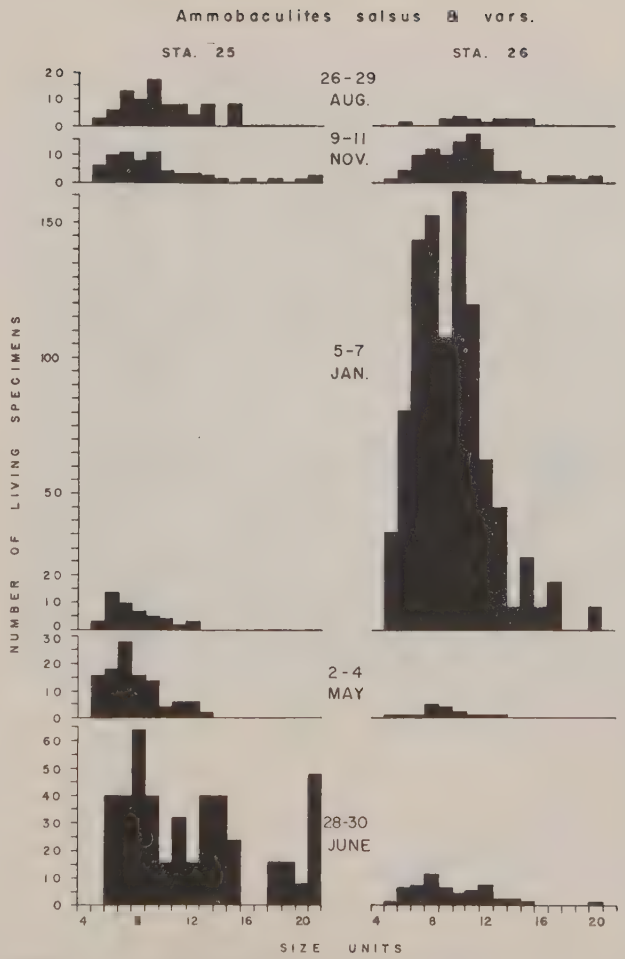

FIGURE 5. Size distribution histograms of living *Ammobaculites salsus* and vars. at stations 25 and 26. Size divisions are 0.025 mm.

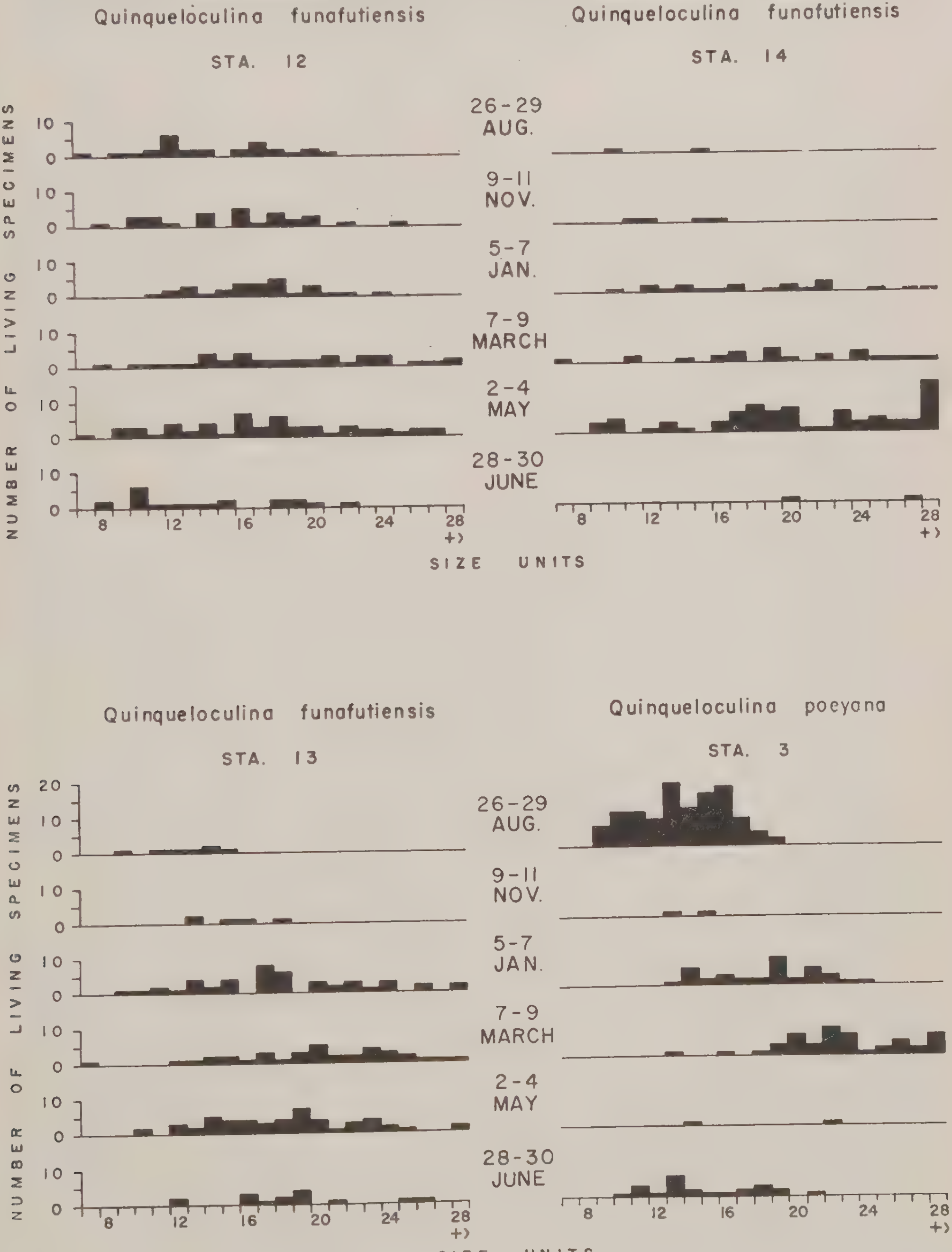

FIGURE 6. Size distribution histograms of living *Quinqueloculina funafutiensis* and *Quinqueloculina poeyana* at stations 3, 12, 13, and 14. Size divisions are 0.025 mm.

Reproduced by Permission
Reprinted from COPEIA, 1957, No. 3, pp. 173-185, August 26
Printed in U.S.A.

The Dentition of Eastern Pacific Mullets, with Special Reference to Adaptation and Taxonomy[1]

ALFRED W. EBELING

ALTHOUGH tooth characters are valuable in the taxonomy of mullets, descriptions of their dentition have generally been superficial and not quantitative. Furthermore, in these descriptions (with the notable exception of those of Schultz, 1946 and Thomson, 1954a-b), there has been little evaluation of tooth characters in respect to their value in classification, particularly as between species of *Mugil*. Uncertainties regarding the value of tooth characters in the distinction of species of eastern Pacific mullets were first brought to my attention by Dr. Boyd W. Walker at the University of California, Los Angeles.

The unusual feeding habits of mullets indicate a high degree of interspecific trophic specialization and, consequently, well-defined differences in their dentition. Schultz (1946) recognized, "... that the mouth parts of mugilid fishes have evolved and specialized, whereas the other anatomical structures have remained more or less constant for most of the genera." Schultz, Thomson (1954a-b), and Smith (1935), among others, have found unifid, bifid, and trifid teeth in the various genera of mullets. In addition to those on the jaws, some genera have teeth on the tongue (*Chaenomugil*), on the vomer and palatines (*Agonostomus*), or on the palate and tongue (*Joturus*, *Valamugil*). The oral teeth are restricted to the jaws in *Mugil* and *Xenomugil* (Schultz, 1946). Most mullets have toothed pads on the posterior roof of the pharynx.

This study is confined to the marine mullets (Mugilinae) of the eastern Pacific, currently referred to three genera (Schultz, 1946). Two of the genera, *Xenomugil* and *Chaenomugil*, are represented by the single well-defined species *X. thoburni* and *C. proboscideus*. The eastern Pacific species retained in *Mugil* are referable to the sharply distinct *curema* and *cephalus* species groups, generally distinguished by scale and fin-ray characters. In addition, I find that the inner teeth in the *curema* complex are simple; those in the *cephalus* assemblage bifid. Within each species group of *Mugil* there are recognized three species which stand in need of more thorough comparison and appraisal. The *curema* group includes *curema*, *setosus*, and *hospes*; the *cephalus* group, *cephalus*, "*peruanus*", and *rammelsbergi* (*M.* "*rammelsbergi*" from the Galápagos Islands may be a more extreme form than the mainland species, which was unavailable for study).

METHODS AND MATERIALS

An investigation was made of the morphology and histology of mullet teeth by means of dissections and microtome sections. The data obtained formed the basis for certain conclusions on the methods of tooth development and replacement in the aforementioned species. Since mullet teeth are generally minute, microscopic methods must be used to accurately determine their sizes, shapes, and arrangements.

In the observation of each specimen, dissecting needles were used to lift the gum away from the teeth so that their shape and arrangement could be observed. A thin jet of air would dry and shrivel the gum surrounding the teeth, rendering them more easily discernible. Using these methods, the gross arrangements and patterns of the teeth were revealed.

Young and half-grown specimens of *Mugil curema* were cleared in potassium hydroxide and stained in alizarin. Upper jaws of all the species except *M. setosus* were excised, skinned, cleared, and stained. Cross sections of these were obtained by carefully slicing through the jaw with a fine scalpel. Tooth attachments and replacement mechanisms were especially noted.

Individual teeth from both the upper and lower jaws were removed from all specimens studied. Balsam mounts of whole teeth, as well as small sections of gum with the embedded smaller teeth, were prepared. In these mounts there were representatives of the primary and secondary teeth of the upper jaw, as well as teeth from the mandible and pharyngeal pads.

---

[1] Contributions from the Scripps Institution of Oceanography, New Series, No. 937.

Upper-jaw and mandibular teeth from 46 specimens of *Mugil curema*, 24 of *Xenomugil thoburni*, 22 of *Mugil hospes*, 5 of *M. setosus* (Stanford University paratypes No. 309), 22 of *M. cephalus*, 12 of *M. rammelsbergi* (these were collected in the Galápagos Islands and

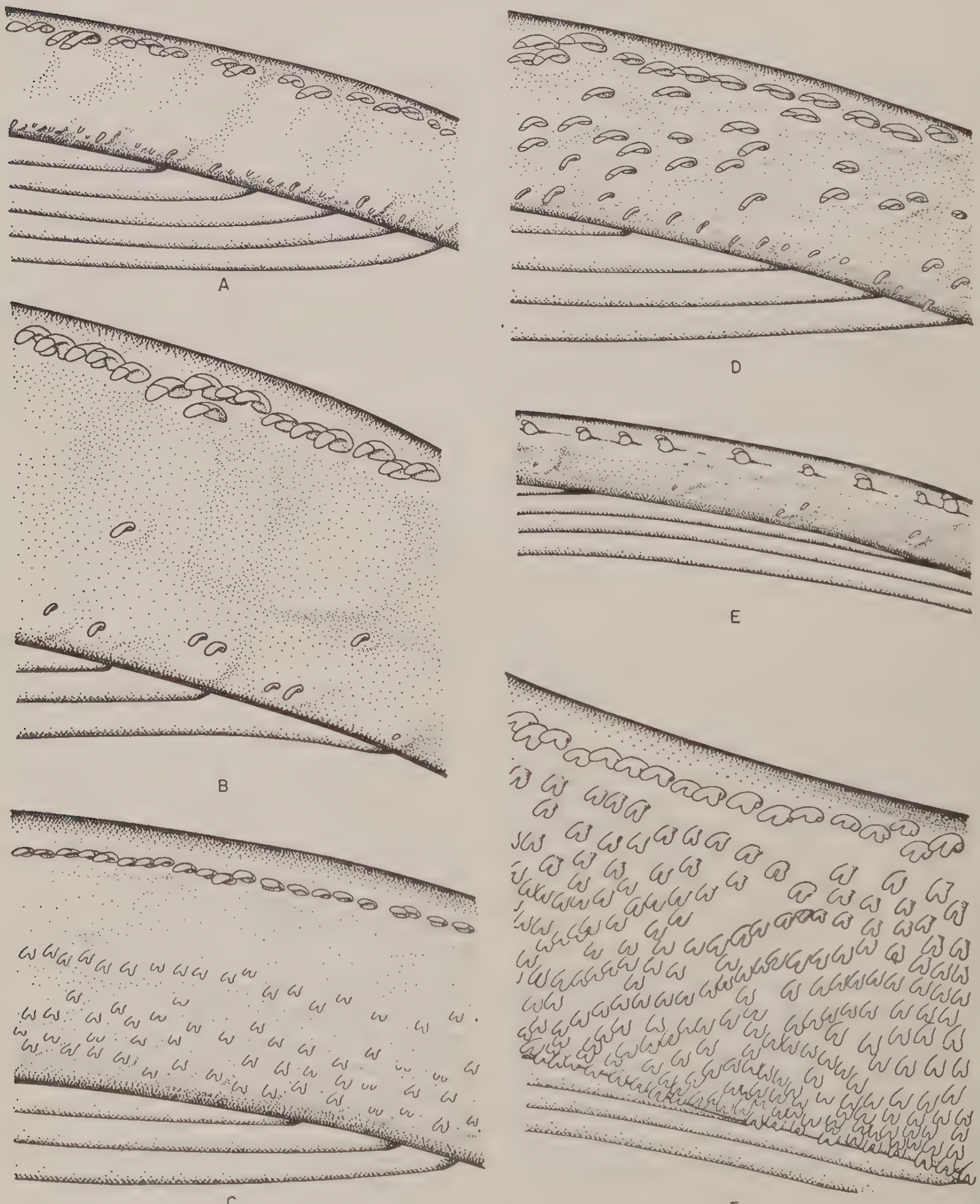

Fig. 1. Inner surfaces of the upper jaws showing typical parts of the mid-sections containing primary and secondary teeth. A, *Mugil curema*; B, *Xenomugil thoburni*; C, *Mugil cephalus*; D, *M. setosus*; E, *M. hospes*; F, *M. rammelsbergi*. ×17.

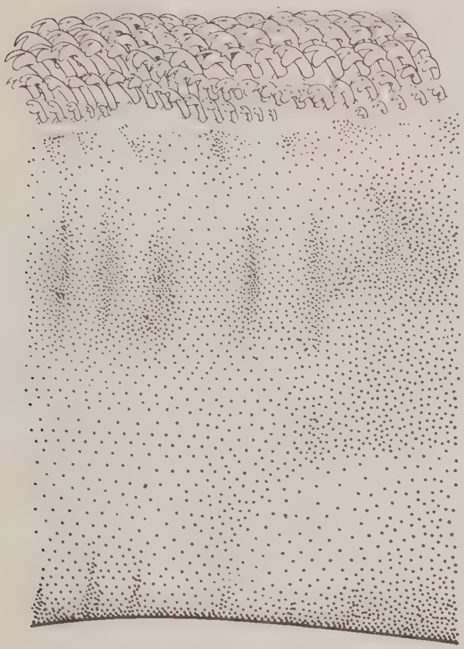

Fig. 2. Inner surface of the upper jaw of *Chaenomugil proboscideus*, showing a typical part of the mid-section containing primary teeth. ×17.

have not been compared with the mainland species), and 12 of *Chaenomugil proboscideus* were temporarily mounted on slides and their lengths measured with an ocular micrometer to the nearest hundredth of a millimeter. The length was considered to be the oblique distance from the enamel tip of the tooth to the farthest angle of the base. The teeth of *Chaenomugil proboscideus* are difficult to measure because the embedded ends of their long bony bases are often damaged during extraction. A faint partition was found near the base of the overt tooth, however, and the tooth length was taken as the oblique distance from an enamel tip to the anterior edge of this partition. Teeth measured from each specimen were taken from the group in the primary row nearest the symphysis of the upper jaw. The largest teeth in the jaw are usually in this group. The largest and most perfect tooth was extracted for measurement. Along with the measurements, information was obtained on the tooth arrangements, degree of completion of the rows of teeth, condition of the teeth and gums, and other pertinent features. Counts were made of the teeth in both the primary and the secondary row of the right half of the upper jaw and the mandible. The tooth lengths were plotted against the standard lengths of the fish from which they were extracted.

Cross and frontal sections were made from the jaws of 12 specimens representing 3 species (*Mugil curema*, *M. cephalus*, and *M. hospes*). The jaws were decalcified, embedded in celloidin, and sectioned. The sections were stained in acid Harris hematoxylin solution and counterstained in eosine. Photomicrographs and drawings were made of the clearer mounts.

Tooth Morphology

Mullet teeth range in size, shape, and structure from the minute, almost microscopic, teeth of *Mugil hospes* to the relatively complex, bifid, scoop-like teeth of *Chaenomugil proboscideus*. They also differ interspecifically in arrangement and attachment. Both the primary and secondary teeth are arranged uniserially or in bands and the primary teeth are attached to the jaw bone by either short or long fibers. Certain general conclusions on the arrangement, attachment, size, shape, and structure of mullet teeth are presented as a background for the observations on growth, development, and interspecific differences to follow.

Arrangement.—The primary or external row comprises relatively large teeth occupying the more prominent position in the jaw. The primary teeth in the upper jaw of the genera *Mugil* and *Xenomugil* that were studied are below the premaxillary bone (Figs. 1 and 3). In these genera this row is uniserial. In some specimens the teeth are in groups of 2 to 3, with the center tooth of the triad usually the longest. This center tooth may be the oldest in the group. The upper-jaw teeth of *Chaenomugil proboscideus* are in a compact band, in sharp contrast to the usual uniserial condition (Fig. 2).

The secondary row or band is composed of smaller teeth just behind the primary row, from which they are separated by a toothless area of gum. Minute teeth are developed here in all species except *Chaenomugil proboscideus*. Depending upon the species, these teeth are either widely scattered, alined in a single row, or arranged in a band (Figs. 1 and 3).

The mandible contains, in general, only primary teeth; however, the members of the

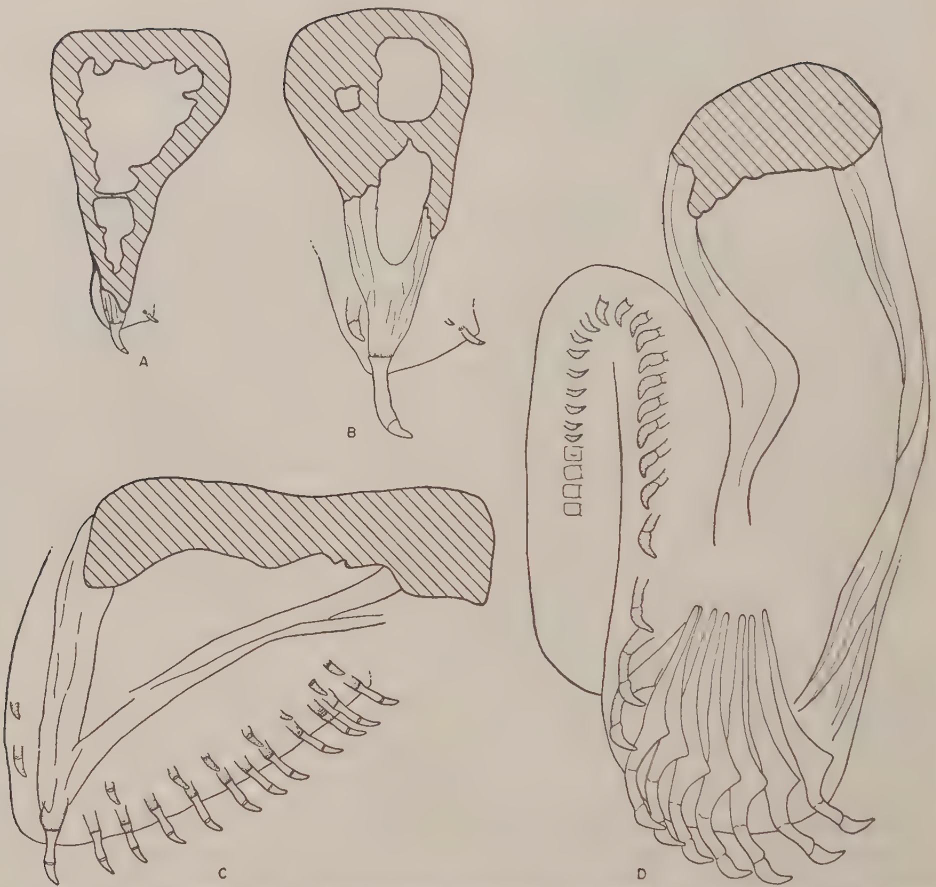

Fig. 3. Typical cross-sections from the mid-sections of the upper jaws of A, *Mugil hospes*; B, *M. curema* C, *M. rammelsbergi*; D, *Chaenomugil proboscideus*. The functional teeth and fibrous attachment strands are outlined, the replacement teeth and partially ossified bases of the primary teeth are stippled and the premaxillary bone is hatched. Parts of the epidermis and dermis are omitted. ×35.

Mugil cephalus group have both primary and secondary teeth. The mandibular teeth are uniserial in all species except *C. proboscideus*, in which they are in bands similar to those of the upper jaw, and in *Mugil cephalus* and *M. rammelsbergi*, which have a band of secondary teeth.

Attachment.—The primary teeth of the upper jaw are not anchylosed to the premaxillaries, but are attached by fibrous strands (Because of their flexible attachment with the jaw bones, mullet teeth appear loosely mounted and are easily movable in the gum). These strands are alined in two rows, one at the external margin and one at the internal margin of the jaw bone, in all species except *Mugil hospes*, which has teeth set rather near the premaxillary (Fig. 3 A and Pl. I C). The thicker external strands descend perpendicularly from the long axis of the jaw bone, but, in general, the internal fibers are more narrow in diameter and descend obliquely. A pair of such strands coalesces ventrally to form a fibrous base for each functional tooth (Fig. 3 B-C and Pl. I D). Figure 4 represents a section through two adjacent strands in both the internal and external rows. The proximal part of one strand (att. fib. pmx.) and the distal part of its neighbor (att. fib. pr.) are shown. The internal and external strands remain separate in *Chaenomugil proboscideus* and only the internal fibers appear to have any connection

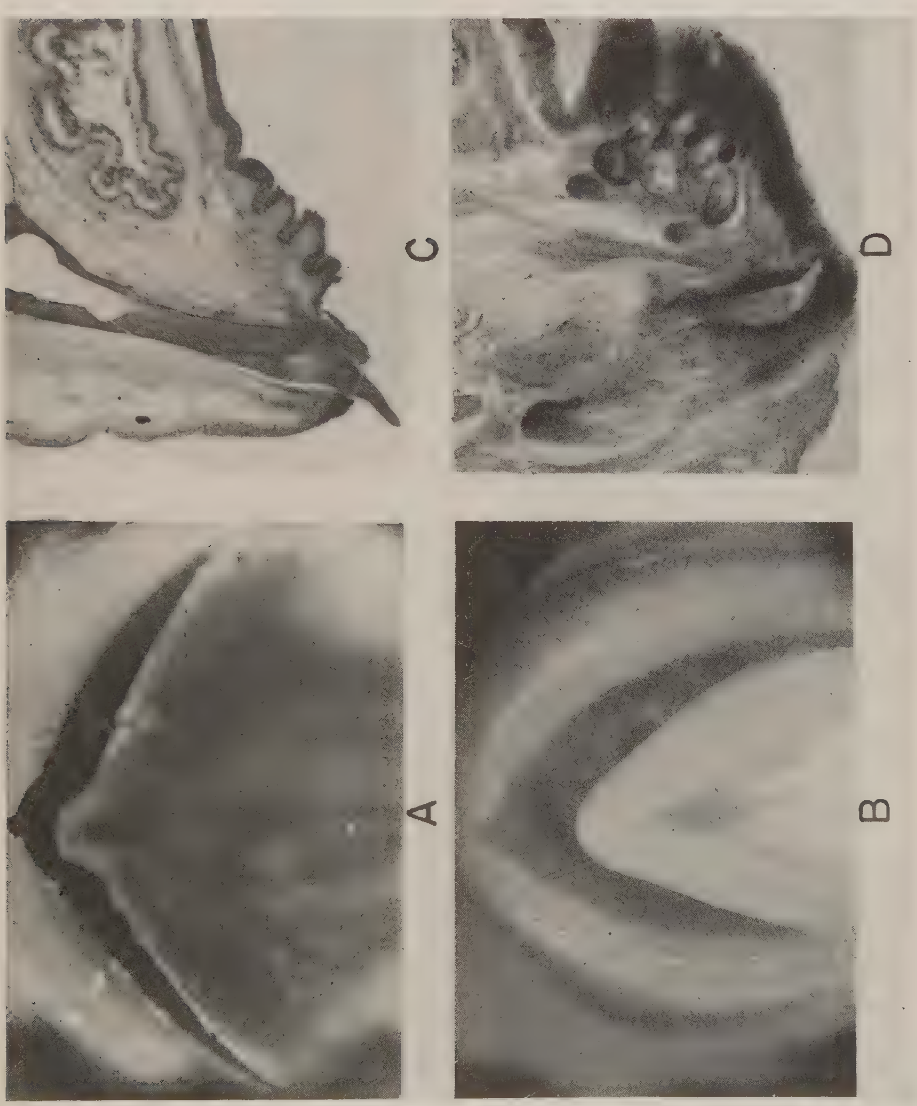

Plate I. Lips and teeth of A, *Mugil rammelsbergi*, and B, *Chaenomugil proboscideus*, ×6.7. Cross-sections from near the symphysis of the upper jaw of C, *Mugil haspes*, and D, *Mugil cephalus*; ×66.

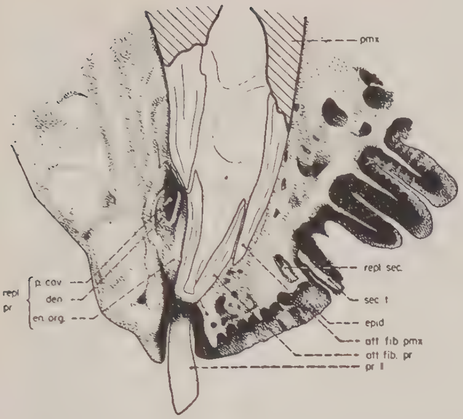

Fig. 4. Cross-section from near the symphysis of the upper jaw of *Mugil curema*. att. fib. pmx., proximal part of attachment fibers; att. fib. pr., distal part of attachment fibers; den., dentine; en. org., enamel organ; epid., epidermis; p. cav., pulp cavity; pmx., premaxillary bone; pr. t., primary tooth; repl. pr., replacement bud for primary tooth; repl. sec., replacement bud for secondary tooth; sec. t., secondary tooth. ×52.

with the functional teeth (Fig. 3 D). The functional teeth generally rest on short, partially ossified bases (Fig. 3 A–C). The teeth of *C. proboscideus*, however, have long thin bony bases which are deeply embedded in the gum area between the internal and external fibrous strands (Fig. 3 D).

The species that have wide lips (*C. proboscideus* and *Xenomugil thoburni*) also have very long attachment fibers in the jaws. The thin-lipped species (*Mugil hospes* and *M. curema*) have relatively short fibers. In *M. hospes* these fibrous strands are shorter than the teeth and do not bifurcate. *M. rammelsbergi* has a wider, flatter jaw bone than the other species; consequently, the internal fibrous strands extend diagonally from the posterior margin of the premaxillary bone to the functional tooth at the anterior margin of the jaw (Fig. 3).

The smaller secondary teeth in the upper jaw are loose in the gum. They are apparently not connected by fibers to the premaxillary bone (Figs. 3, 4 sec. t., Pl. I D).

In all the species the mandibular teeth are associated with the dentary bone in the same manner as the upper-jaw teeth are associated with the premaxillary. Usually, however, the annectant fibrous strands of the mandible are relatively longer than those of the upper jaw.

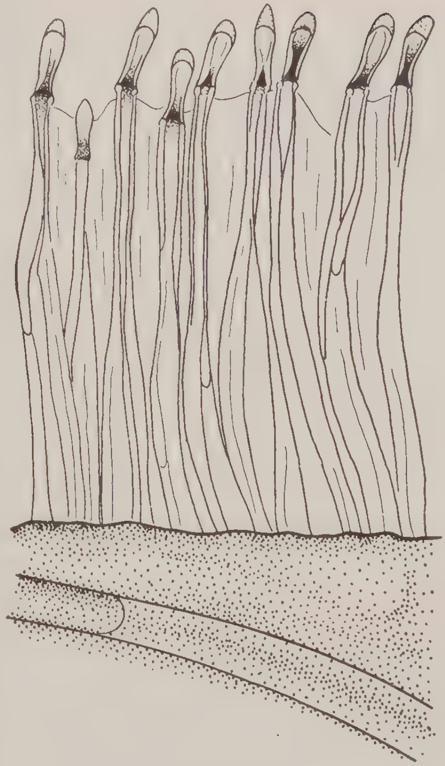

Fig. 5. Typical part of the lower jaw of *Mugil curema*, with the gum removed. ×29.

In *Mugil curema* they are several times as long (Fig. 5).

Size and Shape.—The teeth of the eastern Pacific Mugilinae vary in size among individuals of the same species or even within a particular series in a single jaw. For example, the primary teeth in both the upper and lower jaws are largest near the symphysis and decrease in size near the extreme distal ends. Also the newly erupted replacement teeth are always smaller than the functional teeth. The primary upper-jaw teeth are larger and stronger than either the primary mandibular teeth or the secondary teeth. The primary mandibular teeth are sometimes only slightly smaller than those of the upper jaw; however, they are less than one-half the size of the upper jaw teeth in *Mugil setosus* and some specimens of *M. curema*. The secondary teeth are generally minute; in *M. hospes* the secondary teeth sometimes require a compound microscope for detection, whereas the secondary bifid teeth of

TABLE I

TOOTH COUNTS AND SIZE RANGES IN THE RIGHT HALVES OF THE PRIMARY AND SECONDARY UPPER JAW AND MANDIBULAR TOOTH ROWS

The ranges of the tooth lengths are given as ten-thousandths of the standard length; the number of specimens is in parentheses. All counts and measurements are of the teeth in the right halves of the jaws, and, in each instance, the tooth measured is the largest and most perfect tooth near the symphysis of the jaw (see under methods).

Species	Standard length (mm.)	Teeth in primary upper jaw row		Teeth in secondary upper jaw row		Teeth in mandibular row	
		No.	Length	No.	Length	No.	Length
Mugil curema	29–57 (6)	21–30 (6)	59–68 (6)	0–1 (6)	—	21–42 (5)	23–35 (5)
	68–103 (7)	24–36 (6)	44–72 (7)	7–40 (4)	—	28–51 (4)	24–34 (3)
	108–172 (15)	28–48 (15)	32–53 (15)	11–60 (8)	13 (1)	41–73 (15)	19–29 (8)
	186–292 (18)[*]	40–63 (18)	18–30 (16)	4–68 (14)	6–8 (4)	74–115 (16)	9–18 (12)
Mugil setosus	118 (1)	—	61 (1)	—	—	—	—
	174–200 (4)	—	35–43 (4)	—	12–28 (4)	—	20 (1)
Mugil hospes	29–38 (5)	8–23 (5)	24–27 (5)	0 (5)	—	0 (5)	—
	97–119 (4)	26–37 (4)	13–16 (4)	0 (4)	—	65–84 (4)	9–10 (2)
	125–155 (8)	30–73 (8)	11–16 (8)	0 (8)	—	70–120 (8)	8–10 (8)
	162–186 (5)	30–75 (5)	8–10 (5)	2–30 (5)	4 (1)	115–130 (4)	8 (1)
Mugil cephalus	25–34 (6)	20–29 (6)	41–52 (6)	0–15 (6)	—	6–15 (6)	37–47 (5)
	49 (1)	58 (1)	36 (1)	—	—	45 (1)	—
	115 (1)	70 (1)	29 (1)	Many (1)	—	91 (1)	22 (1)
	148–183 (6)	70–95 (6)	19–21 (6)	Many (6)	9 (1)	100–104 (6)[†]	13–17 (6)
	190–250 (8)	57–101 (8)	14–18 (8)	Many (8)	8–9 (2)	97–149 (8)[‡]	10–14 (8)
Mugil rammelsbergi	29–34 (5)	23–26 (5)	43–46 (5)	30–45 (5)	—	9–17 (5)[§]	27–31 (5)
	46 (1)	32 (1)	38 (1)	73 (1)	—	20 (1)[§]	28 (1)
	131–140 (3)	55–75 (3)	17–21 (3)	Many (3)	—	51–63 (3)[‖]	13 (3)
	146–185 (3)	54–80 (3)	16–18 (3)	Many (3)	10–12 (2)	60–75 (3)[‖]	10–13 (3)
Xenomugil thoburni	37 (1)	25 (1)	70 (1)	0 (1)	—	5 (1)	—
	53–61 (2)	63–80 (2)	79–80 (2)	0 (2)	—	60–70 (2)	64–72 (2)
	69–94 (4)	63–82 (4)	66–74 (4)	0 (4)	—	62–87 (4)	51–58 (4)
	99–135 (10)	56–95 (10)	50–60 (10)	0–4 (10)	—	57–95 (10)	39–50 (10)
	148–169 (5)	73–91 (5)	40–52 (5)	8–25 (5)	17 (1)	70–89 (5)	36–47 (5)
	182–268 (2)	100 (2)	34–35 (2)	44–60 (2)	15 (1)	90–100 (2)	29–33 (2)
Chaenomugil proboscideus	41–45 (4)	3–4 rows (4)	38–44 (3)	—	—	2–3 rows (4)	31 (1)
	49–79 (5)	5 rows (5)	45–51 (5)	—	—	5–6 rows (5)	32–37 (2)
	92–122 (3)	5–6 rows (3)	43–49 (3)	—	—	7 rows (3)	30–31 (3)

[*] Small-toothed specimens from Cape San Lucas and Socorro Island.
[†] In the size range from 148 to 183 mm., the teeth in the secondary mandibular band increase from 0 to more than 100.
[‡] In the size range from 190–250 mm., the teeth in the secondary mandibular band are numerous.
[§] In the size range from 29 to 46 mm., the teeth in the secondary mandibular band increase from 1 to 8.
[‖] In the size range from 131 to 185 mm., the teeth in the secondary mandibular band are numerous.

the *M. cephalus* group are easily discernible at low magnification under a dissecting scope (Table I and Fig. 6).

The simplest type of tooth (e.g., that of *M. curema*) is shaped like the end of an upholsterer's needle, that is, slightly flattened and curved inward at the tip (Fig. 6E). The more specialized teeth of other species are bifid. Those of *Chaenomugil proboscideus* are shaped like miniature claw crowbars with the bifid tips and adjacent margins forming minute scoops, and are attached to long flexible bony bases (Fig. 6 G). The mandibular teeth are similar in form to the primary upper jaw teeth, while the secondary teeth (those of *M. cephalus* excepted) are generally minute counterparts of the primary teeth.

STRUCTURE.—The general plan of mullet tooth construction follows that of most teleosts. The bony dentine areas and pulp cavity, appearing black in some microscope preparations, can be easily seen (Figs. 4 den., p. cav., and

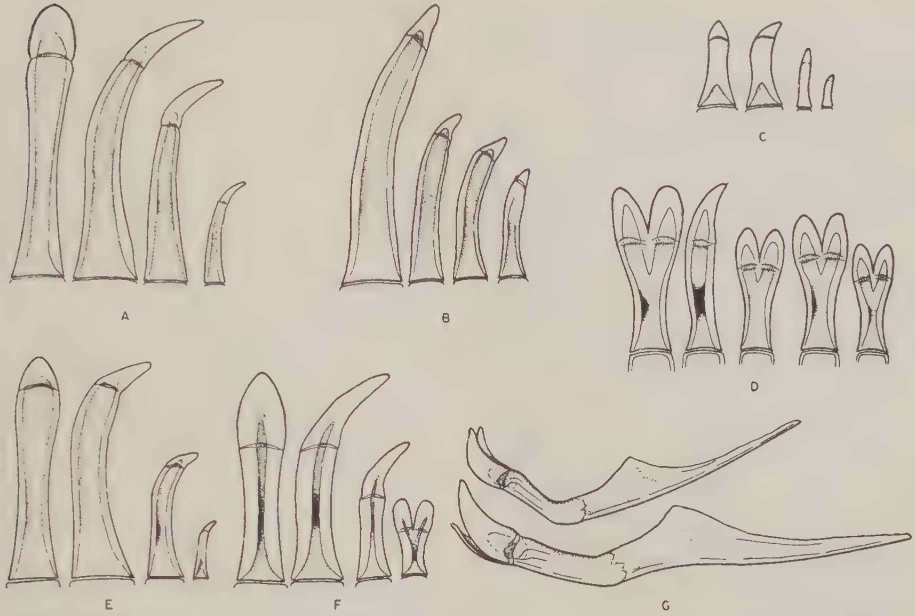

Fig. 6. Typical teeth of A, *Xenomugil thoburni*; B, *Mugil setosus*; C, *M. hospes*; D, *M. rammelsbergi*; E, *M. curema*; F, *M. cephalus*; G, *Chaenomugil proboscideus*. In A, C, E, and F both frontal and side aspects of a primary upper-jaw tooth are shown, followed, from left to right, by a mandibular and a secondary upper-jaw tooth. In B the side aspects of one primary and 3 secondary upper-jaw teeth are shown. In D, from left to right, the front and side aspects of a primary upper-jaw tooth, a primary mandibular tooth and the front aspects of a secondary upper-jaw tooth, and a secondary mandibular tooth are shown. In G side aspects of a mandibular tooth (upper) and upper-jaw tooth (lower) are shown. ×61.

6 E). The pulp cavity contains the "fibers of Korff", which, according to Levi (1939 a-c), contribute to the formation of dentine and enamel, i.e., these fibers may be the centers of calcium deposition.

Most teeth in both jaws have yellow tips at their apices. These tips are composed of what appears to be enamel, although the structure was not histologically determined. A distinct suture is visible between the tip and base of the tooth (Fig. 6). This is the weakest area of the tooth and is the first line of separation upon breakage. The tips are easily broken off by the slightest jarring from either dissecting needle or forceps. This may account for the absence of these tips on the teeth in some of the preserved specimens. The pulp cavity extends into the tip. The teeth of *Mugil hospes* apparently lack yellow tips; however, a suture is visible near the apex of the tooth (Fig. 6 C).

DEVELOPMENT

The growth and replacement of the teeth were investigated for whatever information might be revealed that could be related to their ultimate structural characteristics. The descriptions of tooth replacement apply only to the adult mullets. The development of teeth in small juveniles was generally not investigated, although observations were made of the teeth in a few small pelagic specimens. Contrary to the condition as observed in many fishes, the replacement of the primary teeth of mullets proceeds from the front of the jaw posteriorly so that the rows of replacement teeth are external to the functional teeth. These are continually being supplanted so that smaller teeth give way to larger ones as the fish matures.

REPLACEMENT.—Since the primary teeth are loosely attached in the gum, they are presumably often lost and then replaced. This may account for the size differences of the teeth and for frequent gaps in the rows. The replacement teeth are generally anterior to the external row of fibrous strands in the jaws; in *Mugil hospes*, however, the developing teeth appear to be almost in the same vertical plane as the functional teeth. Apparently a replacement tooth grows posteroventrad until it fills the space recently vacated by its functional predecessor. Another replacement tooth will then take its place (Figs. 3 and 4).

In *Mugil curema* the developing enamel (Fig. 4 en. org.), dentine (Fig. 4 den.), and pulp cavity (Fig. 4 p. cav.) of the replacement tooth are easily seen. The posteroventrad growth and movement of the tooth brings it alongside of the functional tooth of the primary row that it will replace. The replacement mechanism is similar in *M. cephalus*, *M. rammelsbergi*, and *Xenomugil thoburni* except that there are generally two rows of replacement teeth instead of one in these species (Fig. 3 C).

The replacement teeth of *Chaenomugil proboscideus* are remarkable in that they are arranged in many series, the cross-rows of which double back so that in cross-section they appear like sinuous chains of 30 or so teeth in different stages of development. The 7 or so terminal rows are functional teeth; the first few rows are pockets or alveoli in the gum in which the replacement buds will develop (Fig. 3 D). As a replacement tooth grows posteroventrad to become incorporated in the first functional row, it acquires the long bony base characteristic of a functional tooth (Figs. 3 D and 6 G). This base secures the tooth firmly in the gum. The terminal teeth of the chain are smaller than those in the middle functional rows. This is probably because they first grew into the functional position when the fish was smaller (Figs. 2 and 3 D). The point should be emphasized that the horizontal rows of teeth are not straight, but are wavy and that replacement may occur parallel to these rows instead of strictly posteroventrally (Fig. 2 and Pl. I B).

Replacement teeth in the secondary upper jaw rows are generally directly above the functional teeth (Fig. 3 A-C). Presumably, the teeth in the mandible are replaced in a similar manner to those in the upper jaw.

GROWTH.—The teeth of *Xenomugil thoburni* and *Chaenomugil proboscideus* (Fig. 7 A and C, respectively) appear to increase more rapidly in relative size with age than do those of the other species. *Mugil curema* exhibits a good deal of variation in the size of the primary teeth (Fig. 7 B). The largest specimens had relatively small teeth (Table I). This striking deviation from the tooth-body size relationships of the other species is graphically indicated by the group of points along the right hand margin of Figure 7 B that are encircled by the dotted line. These fish were all collected from Socorro Island and Cape San Lucas, Baja California. The disproportionately small teeth may be due either to racial variation or to the replacement of larger teeth by smaller ones in the large adults. A collection of young specimens (50 to 90 mm.) from near Balboa, Canal Zone had especially large teeth. These ranged from 0.59 to 0.74 per cent of the standard length.

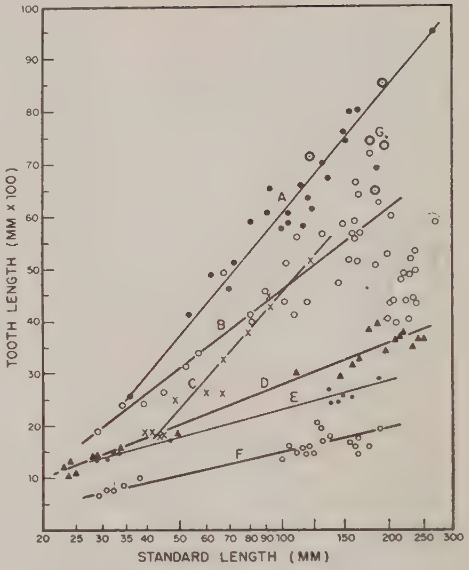

Fig. 7. Relation of tooth length to standard length in 6 species of mullets. A, *Xenomugil thoburni*; B, *Mugil curema*; C, *Chaenomugil proboscideus*; D, *Mugil cephalus*; E, *M. rammelsbergi*; F, *M. hospes*; G, *M. setosus*.

No juvenile examined of any species had a complete complement of teeth. The number of teeth increases with growth of the fish (Table I). Furthermore, the premaxillary teeth appear before the mandibular teeth. Several younger juveniles, which were still in the pelagic stage, were examined. Specimens of *Xenomugil thoburni*, 12 to 35 mm. in standard length, were dip-netted at night under a light about a mile from shore in the Galápagos Islands. Their mouths and lips are disproportionately small, with minute needle-like teeth in the jaws (in the larger specimens, some of the teeth are curved and have yellow tips like the adults). None have teeth on the mandible, while only those

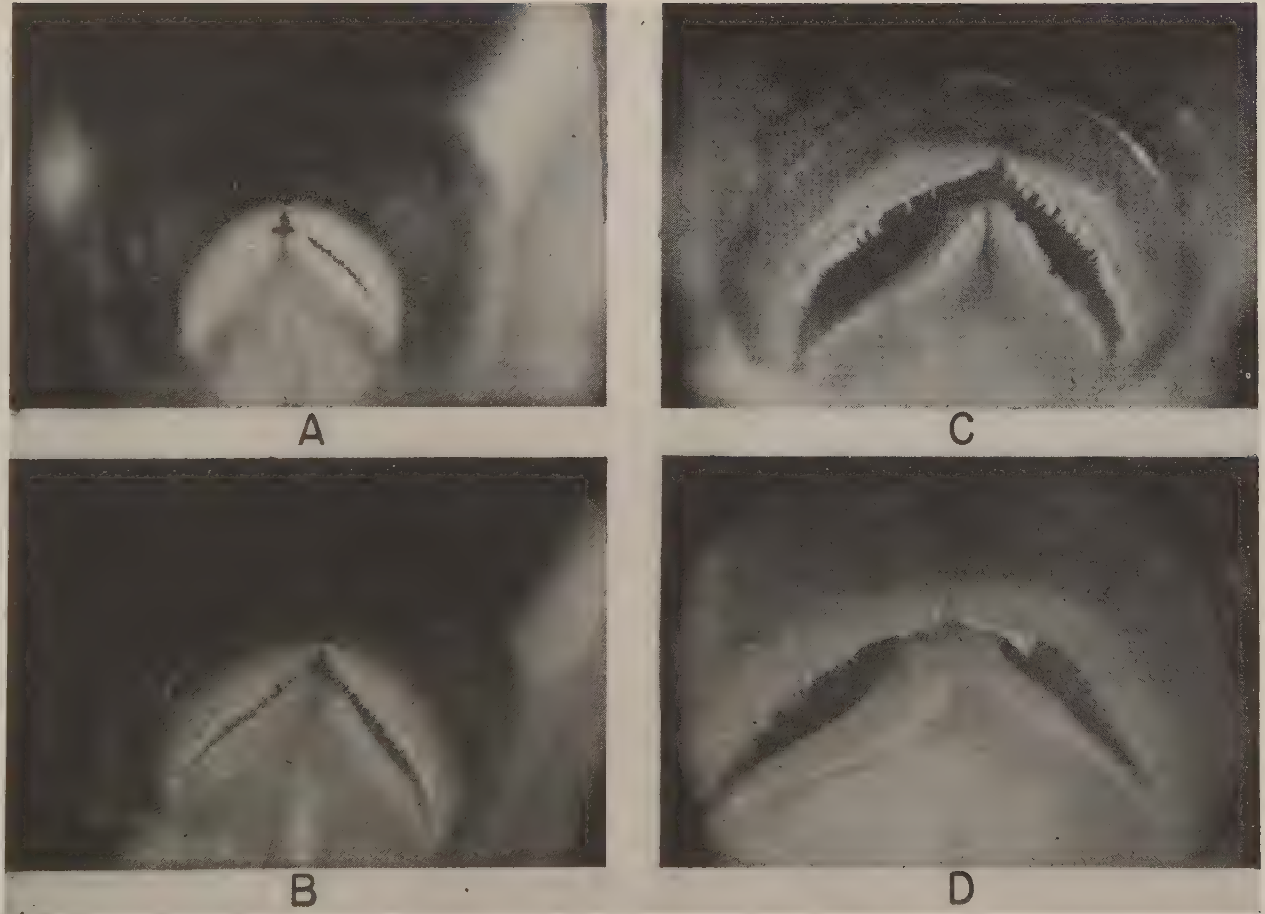

Plate II. Lips and teeth of *Xenomugil thoburni*, showing progressively greater turning under of the lower lip in the successive growth stages, represented by the standard lengths of A, 58 mm.; B, 78 mm.; C, 114 mm.; D, 157 mm. ×6.7.

TABLE II

Intraspecific Variation in the Condition of the Secondary Upper-Jaw Row in *Mugil curema*

Condition of secondary upper-jaw row	Number of specimens	
	Gulf of California	Socorro Island
No secondary row (or with fewer than 5 teeth)	1	1
Partial secondary row (incomplete on both sides)	1	2
Spotty (several wide gaps)	2	2
Almost complete, hidden by gum	4	4
Complete, easily visible	11	5
Complete, very densely packed	1	0
Totals	20	14

longer than 17 mm. have teeth in the upper jaw. Pelagic juveniles, tentatively identified as *Mugil hospes*, that were dip-netted off Costa Rica also have small mouths, toothless mandibles and minute teeth. Small pelagic juveniles of *Mugil rammelsbergi* and *Chaenomugil proboscideus* have characteristic bifid teeth in both jaws. The larger juvenile stages (longer than 25 to 35 mm.) of all species except *Chaenomugil proboscideus* have teeth forming only near the symphysis of the lower jaw. The teeth of these larger juveniles are disproportionately large (Table I).

In *M. curema* both the number and size of the secondary teeth vary between rather wide limits intraspecifically and even among the individuals within a single collection (Tables I and II).

In both *Chaenomugil proboscideus* and *Xenomugil thoburni* the lower lip becomes folded under, so that the teeth are directed either parallel with the horizontal axis of the body or obliquely downward (Pls. I B and II D). In the young of *Xenomugil* the lower lip is normal; the turning under is first apparent in individuals 60 to 100 mm. in standard length (Pl. II).

Interspecific Differences

The diagnostic tooth characters and geographical ranges for all the eastern Pacific Mugilinae except *M. peruanus*, which was not examined, are summarized by the following analytical key. These diagnoses may not generally apply to the smaller juveniles (see section under growth), some of which are pelagic and occur at some distance offshore. The genera and species groups can easily be diagnosed by tooth characters. The species of the *Mugil curema* group (*curema*, *setosus*, and *hospes*) have only simple teeth in the jaws, while those of the *M. cephalus* group (*cephalus* and *rammelsbergi*) have mostly bifid teeth (*M. cephalus* has a primary row of simple teeth in front of a secondary row of bifid teeth). Both *Xenomugil thoburni* and *Chaenomugil proboscideus* have the mandibular teeth directed downward in the adults. In both form and arrangement the peculiar bifid teeth of *Chaenomugil* are very different from any of the other species studied.

Analysis, Based on Dentition, of the Genera and Species of the Mugilinae of the Eastern Pacific

1a. Upper lip not wide and thick; lower lip normal in all growth stages (Pl. III). Area of gum behind primary teeth in upper jaw not especially wide or, if wide, crowded with bifid teeth (Fig. 1 A and C–F). Teeth in jaws, when bifid, never shaped like claw crowbars with long bases (Fig. 6 B–F). Secondary teeth in upper jaw bifid (Fig. 6 B–F), in definite rows or bands (Fig. 1 A and C–F), already developed in the larger juveniles, except in *M. hospes*, which has very minute secondary teeth only in the adults (Figs. 1 E and 6 C) (*Mugil*) 2

1b. Upper lip wide and thick; lower lip turned under (*Xenomugil*—adults, *Chaenomugil*—all stages) so that the mandibular teeth are directed downward (Pls. I B and II). Area of gum behind primary teeth especially wide, with or without relatively few scattered teeth (Figs. 1 B and 2). Teeth in jaws, when bifid, shaped like claw crowbars with long bases (Fig. 6 G). Secondary teeth in upper jaw either lacking (Fig. 2) or simple and developed, scatteringly, only in the larger half-grown and adult specimens (Fig. 1 B) 6

2a. Secondary teeth always simple (Fig. 6 B–C and E), and in uniserial rows or scattered behind the primary row (Fig. 1 A and D–E), never present in lower jaw (these teeth may be absent in juvenile and half-grown specimens). Primary teeth always simple (Fig. 6 B–C and E). (*Mugil curema* group) 3

2b. Secondary teeth always bifid (Fig. 6 D and F), in broad bands (narrow in juveniles) (Fig. 1 C and F), present in the upper jaws of all stages, and in the lower jaw of adults. Primary teeth simple or bifid (Fig. 6 D and F). (*Mugil cephalus* group) 5

3a. Primary teeth moderate to large, with yellow apical tips (Table I; Figs. 6 B, 6 E, 7 B, and 7 G); close-set or moderately spaced in adults (Fig. 1 A and D). Secondary teeth numerous, probably present in all stages except the smaller juveniles; typically more than 30 in adults, and moderate to large in size (Table 1).

Lips moderate (Pl. III A-B). Area of gum behind primary row of upper jaw moderate in width (Fig. 1 A and D) 4

3b. Primary teeth minute, only 0.2 to 0.5 as long as those of *M. setosus* and *M. curema* (Table I; Figs. 6 C and 7 F), without yellow tips (although a suture delimits the tip); widely spaced in adults (Fig. 1 E). Secondary teeth present only in the larger adults (longer than 160 mm.); in a single row comprising only 2 to 30 almost microscopic teeth (Table 1). Lips narrow (Pl. III C). Area of gum behind primary row of upper jaw narrow (Fig. 1 E). West coast of México to northern South America..... *Mugil hospes* Jordan and Culver

4a. Primary teeth in upper jaw moderate in size (Table 1; Figs. 6 E and 7 B), not very densely packed (in adults frequent spaces in row are 1 to 4 times as wide as a tooth). Generally, no teeth (occasionally one or two) scattered between secondary and primary rows (Fig. 1 A). Mandibular teeth usually 0.6 to 0.8 times as long as the primary upper-jaw teeth, in adults, but 0.4 to 0.5 times as long in juveniles (Table I and Fig. 6 E). Area of gum behind primary row of upper jaw narrower (Fig. 1 A). West coast of México (including the southern part of Baja California) to northern South America, Socorro Is........ *Mugil curema* Valenciennes

4b. Primary teeth in upper jaw large (Table 1; Figs. 6 B and 7 G), densely packed. Teeth of intermediate size scattered between a secondary row of small teeth and the primary row of large teeth (Fig. 1 D); these intervening teeth fewer in smaller adults (118–174 mm.). Mandibular teeth generally 0.4 to 0.55 times as long as primary upper-jaw teeth (Table I). Area of gum behind primary row of upper jaw moderately wide (Fig. 1 D). Clarion Island in the Revilla Gigedo Group *Mugil setosus* Gilbert

5a. Teeth in primary row of each jaw simple (Fig. 6 F), or at most a few bifid at ends of jaw in large adults; hiatus between this row and secondary band wide; area of gum behind primary rows not especially wide. Secondary teeth not densely packed (Fig. 1 C); those in upper jaw about 0.45 to 0.6 times as long as primary teeth (Table I and Fig. 6 F). Secondary band in upper jaw comprising about 3 to 4 rows in adults and one row in juveniles (shorter than 34 mm.). Secondary mandibular band present only in adults, comprising 1 to 3 rows. Southern California to northern South America (probably not insular)............... *Mugil cephalus* Linnaeus

5b. Teeth in primary rows of each jaw all bifid (Fig. 6 D); hiatus between this row and the secondary band narrow; area of gum behind primary row especially wide, to accommodate broad secondary bands. Secondary teeth densely packed (Fig. 1 F); those in upper jaw about 0.6 to 0.7 times as long as primary teeth (Table 1 and Fig. 6 D). Secondary band in upper jaw comprising about 12 to 13 rows in adults, and 1 to 3 rows in juveniles (shorter than 47 mm.). Secondary mandibular band developed in all stages and similar to upper-jaw band. Coast of Perú and nearby islands, Galápagos Islands........ *Mugil rammelsbergi* Tschudi (based on Galápagos specimens)

6a. Teeth in each jaw simple and without long bases (Fig. 6 A). Upper-jaw teeth of adults in 2 series, one uniserial row of larger teeth in front of scattered minute teeth (Fig. 1 B); only primary teeth in juvenile and some half-grown specimens. Lower lip turned under only in adults. Galápagos Islands, Perú, Panamá Bay *Xenomugil thoburni* (Jordan and Starks)

6b. Teeth in each jaw bifid, shaped like minute claw crowbars with long thin translucent bony bases, 2.5 to 3.5 times as long as the overt tooth (Fig. 6 G). Teeth in each jaw in broad bands comprising 6 to 7 rows in adults and 2 to 5 rows in juveniles (Fig. 2). No secondary teeth in any growth stage. Lower lip turned under in all stages. West coast of Middle America and offshore islands, Socorro Island *Chaenomugil proboscideus* (Günther)

PHARYNGEAL TEETH

The eastern Pacific Mugilinae have pharyngeal filtering devices consisting of gill rakers and toothed pads, which form the posterior roof of the pharynx. These resemble the pharyngeal mechanisms described by Al-Hussaini (1947), Pillay (1953), and Thomson (1954b), among others. The situation of the toothed pads is similar to that depicted in the Australian mullets by Thomson. The posterior gill rakers of the last pharyngeal arch form concavities on the floor of the pharynx in which fit the ventral convexities of the pads. Ingested material is filtered through the pharyngeal teeth, which span the narrow slit between the dorsal surface of the gill rakers and the ventral surface of the paired toothed pads.

In most of the species small hirsute papillae, which, in some instances, represent unerupted tooth buds, lie among the functional pharyngeal teeth. In all of the species except *Chaenomugil proboscideus* each tooth-base is covered by a hirsute, fleshy sheath. These sheaths, in conjunction with the smaller papillae, probably increase the efficiency of the filter. The largest teeth are at the anterior edges of the pads; the teeth are progressively smaller towards the posterior edges. Compared with the primary teeth of the upper jaw, these teeth are larger (*Mugil hospes*, *M. curema*), about equal in size (*C. proboscideus*), or smaller (*M. curema*, *Xenomugil thoburni*, *M. rammelsbergi*). Thev are in distinct rows in *C. proboscideus*.

The pharyngeal teeth are simple in all the species except *C. proboscideus*, in which they are bifid with slightly scooped tips. With one exception (*Mugil rammelsbergi*) these teeth resemble those in the jaws though they are

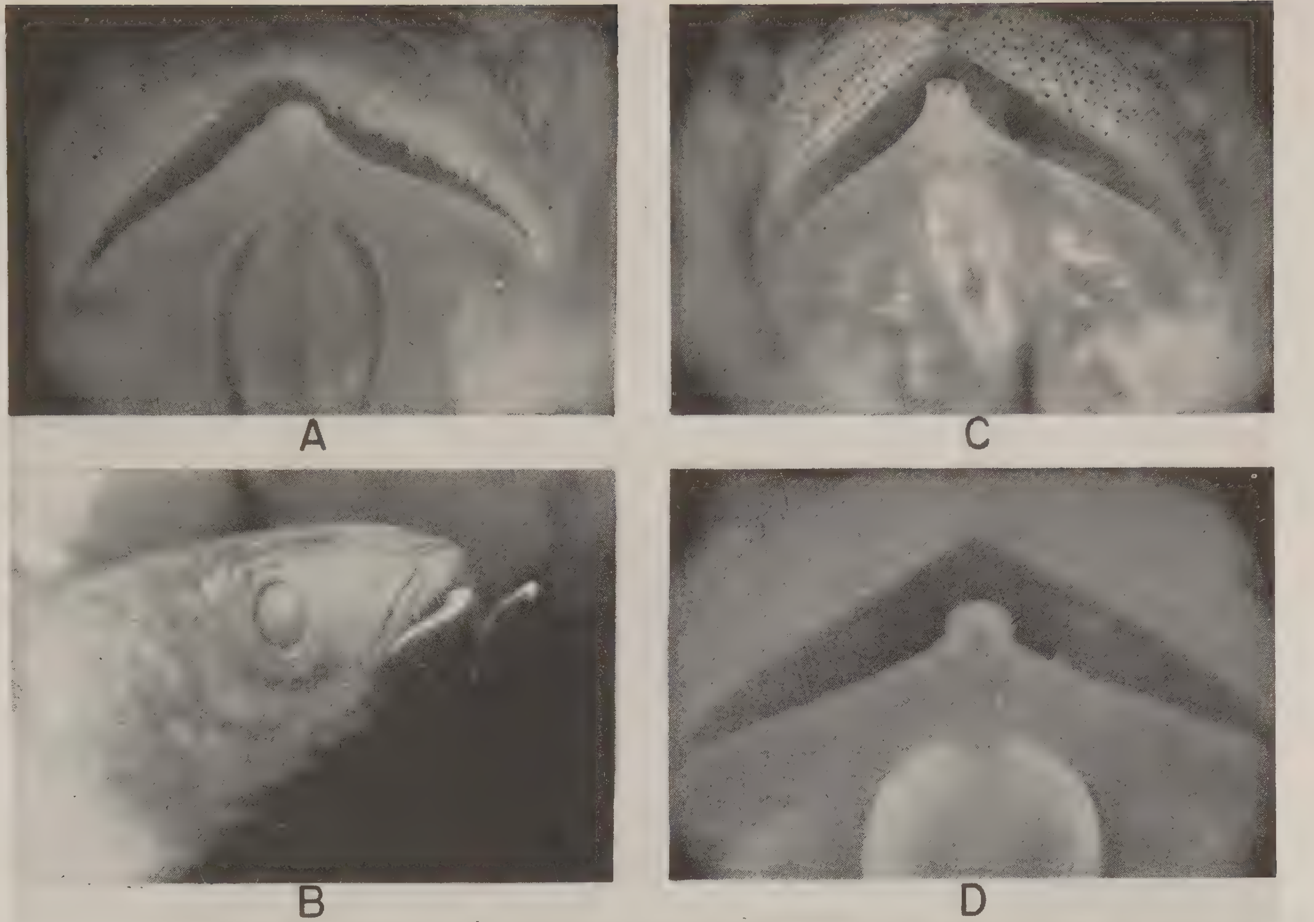

Plate III. Lips and teeth of A, *Mugil curema*; B, *M. setosus*; C, *M. hospes*; D, *M. cephalus*. ×6.7 (*M. setosus*, ×1.25).

more slender and curved. *M. rammelsbergi*, instead of having the pharyngeal teeth bifid like the oral teeth, have them simple, resembling those of *M. cephalus*. This possibly indicates a close relationship between these species.

The small pelagic juvenile mullets that were examined (*Xenomugil thoburni*, *Chaenomugil proboscideus*, and "*Mugil hospes*") have well-formed pharyngeal pads and teeth.

The Feeding Habits of Mullets

The adults of most mullet species are either vegetarians, which browse on minute epiphytes, or iliophagous, i.e. they stir up and gulp mouthfuls of bottom dirt and sand, expel the coarser granules, and digest the nutritive material off the mineral matter and non-nutritive detritus (an excellent survey of the pertinent literature on the food of mullets is given by Thomson, 1954b). The guts of the iliophagous mullets contain a high percentage of the finer mineral matter; the coarser material is probably removed by the pharyngeal filter (Al-Hussaini, 1947; Jacot, 1920; Pillay, 1953; Sarojini, 1951; Thomson, 1954b etc.). They feed by swimming head downward and protracting the premaxillaries to bring the mouth opening to a horizontal position, then shaking their heads over the bottom to facilitate ingestion of the surface mud layers (Hiatt, 1947). Observations by Conrad Limbaugh at Guaymas, Mexico demonstrate a tendency for the larger mullets, one foot or more in length, to feed by taking up and expelling mouthfuls of sand (this "spitting action" is described by Thomson, 1954b) and for the smaller 4 to 10 inch mullets to scrape algae off rocks.

That the juveniles feed on animal or plant plankton or on minute attached algae was born out by an examination of the gut contents of a collection of *Xenomugil* from the Galápagos Islands. The muscular crops of the young specimens (to 30 mm.) contained almost exclusively calanoid copepods of the planktonic genus *Acartia*, while all sizes of fish above 54 mm. had crops filled with filamentous algal bits, detritus, and littoral diatoms. The stomachs of specimens of lengths greater than 102 mm. contained bits of coral mixed with organic matter. In general the crops of *Mugil curema* held little else but diatoms and algal filaments.

Discussion

Schultz (1946) assumed, ". . . that the most primitive mullet had undergone the least amount of specialization. Such a mullet should retain largely unmodified teeth in bands on jaws, vomer, and palatines." He further stated that, "The lips would not be specialized with a thin edge or with modified teeth and papillae." On these probable assumptions, the dentitions of both the *Mugil curema* and *M. cephalus* species groups combine primitive and specialized characters. Though the three species that constitute the *curema* group have simple unmodified teeth on the jaws, these teeth are seldom in bands and the vomer and palatines are toothless. The *cephalus* group also lacks vomerine and palatine teeth, but the bifid secondary teeth are in more or less broad bands. The specimens of *M. rammelsbergi* from the Galápagos Islands, which have only bifid teeth, may represent the ultimate step in a trend toward bifidity of all the teeth in the jaws. Generally, in *M. cephalus*, only the secondary teeth are bifid; however, in older specimens, there may be a few bifid primary teeth at the ends of the jaws.

The peculiar bifid teeth and downward-folded lower lip of *Chaenomugil proboscideus* and the downward-folded lower lip of *Xenomugil thoburni* suggest that these species are the most specialized. Though *Chaenomugil* has highly specialized teeth on the jaws, it probably exhibits a primitive feature in the development of teeth on the tongue. Thus, this genus may also combine, as many organisms do, primitive and specialized characters. The teeth of these two species and *M. rammelsbergi* are well-developed and are relatively remote from the jaw bone; consequently, the fibrous attachment strands are long. These conditions may have resulted from three separate evolutionary trends, since the dental patterns in the species differ widely. These species are not as widely distributed as *M. cephalus* and *M. curema* along the mainland, but they are the most numerous insular species. Perhaps *C. proboscideus*, *X. thoburni*, and *M. rammelsbergi* were once endemic island forms, which have secondarily invaded the mainland. Other hypotheses of origin, however, are not excluded.

The relatively small size of the teeth in the adults of some species of mullets is indicative of a change-over from a juvenile predaceous or browsing eating habit to an adult iliophagous habit. The small mouths, toothless mandibles, and small teeth of some pelagic juveniles suggest a limited metamorphosis of the mouthparts to thicker lips and larger teeth concomitant to their movement into shallow, nearshore water. The minute secondary teeth may, in some cases, serve as gum supports.

Despite the fact that the teeth of mullets are small to minute, their shapes and arrangements were found to be useful taxonomic characters. Teeth are of particular value in the identification of the juvenile or querimana stages.

SUMMARY

This comparative study of the tooth morphology, development, and adaptation in the marine mullets (Mugilinae) of the eastern Pacific has disclosed valuable interspecific differences. The Mugilinae in the eastern Pacific comprise 3 genera, 2 species groups, and 7 or 8 species.

Mullet teeth are usually arranged so that smaller secondary teeth are behind a uniserial row of larger primary teeth, but one species lacks secondary teeth and has a broad band of primary teeth.

The primary teeth in the upper jaw are attached to the premaxillary by fibrous strands, very remotely in some species. The secondary, smaller teeth in the upper jaw are loose in the gum and have no connection with the premaxillary. The mandibular teeth are correspondingly remote from the dentary and are connected with this bone by fibrous strands, which are usually longer than the corresponding annectant strands of the upper jaw.

Mullet teeth are generally minute. The simplest type is shaped like the end of an upholsterer's needle, that is, slightly flattened and curved inward at the tip. The more specialized teeth are bifid, and in *Chaenomugil* are shaped like the end of a claw crowbar. In general the teeth have yellow apical tips.

Replacement teeth are usually anterior to the bases of the primary teeth. These developing teeth are in one or more rows and, presumably, rotate posteriorly to fill the gaps left by their missing functional predecessors. The replacements for the secondary teeth subtend their functional counterparts.

The teeth of some species appear to increase more rapidly in relative size with age than do those of others. The teeth of all the larger juveniles are disproportionately large. The few smaller pelagic juveniles examined had small mouths and very minute teeth; some had toothless mandibles. In two species, the lower lip turns under during development.

All the species have pharyngeal filtering devices consisting of gill rakers and toothed pads, which form the posterior roof of the pharynx.

It is generally agreed that mullets are mainly phytophagous, browsing on minute epiphytes. Although the adults of some species are iliophagous, the young are browsers or carnivores.

In dentition, both the *Mugil curema* and *M. cephalus* species groups combine primitive and specialized characters. The genera *Xenomugil* and *Chaenomugil* seem the most specialized. *Chaenomugil*, however, may have retained a primitive feature, teeth on the tongue. The dentition of mullets closely reflects their feeding habits.

ACKNOWLEDGEMENTS

I wish to acknowledge my gratitude to Dr. Boyd W. Walker, University of California, Los Angeles, for suggesting the problem on which the present investigation was based, and for aid and advice during the study; to Mr. Roy J. Pence, of the same campus, for advice and aid in photography; and to Dr. Walker and Dr. Carl L. Hubbs, University of California, Scripps Institution of Oceanography, La Jolla, for a critical review of the manuscript.

LITERATURE CITED

AL-HUSSAINI, A. H. 1947. The feeding habits and the morphology of the alimentary tract of some teleosts living in the neighborhood of the marine biological station, Ghardaqa, Red Sea. *Publ. Mar. Biol. Sta. Ghardaqa, Fouad I Univ., (5): 1–61, figs. 1–12.*

HIATT, ROBERT W. 1947. Food-chains and the food cycle in Hawaiian fish ponds. I. The food and feeding habits of mullets (*Mugil cephalus*), milk fish (*Chanos chanos*) and the ten-pounder (*Elops machnata*). *Trans. Amer. Fish. Soc., 1944, 74: 250–61.*

JACOT, ARTHUR PAUL. 1920. Age, growth and scale characters of mullets, *Mugil cephalus* and *Mugil curema. Trans. Amer. Microsc. Soc., 39: 199–299, figs. 1–7, pls. 20–26.*

LEVI, GIULIO. 1939a. Etudes sur le développement des dents chez les Téléostéens. I. Les dents de substitution d' *Ophidium, Trigla, Rhombus, Belone. Arch. Anat. Microsc. Paris, 35: 101–46.*

———. 1939b. Etudes sur le développement des dents chez les Téléostéens. II. Développement des dents pourvues de dentine trabéculaire (*Esox, Sphyraena*). *Ibid., 35: 201–21, figs. 1–7.*

(524)

———. 1939c. Etudes sur le développement des dents chez les Téléostéens. III. Développement des dents de substitution de *Merluccius*, *Chrysophrys*, *Cepola*, *Lophius* (suite et fin). *Ibid.*, *35: 415–55, figs. 1–12.*

Pillay, T. V. R. 1953. Studies on the food, feeding habits and alimentary tract of the grey mullet, *Mugil tade* Forskål. *Proc. Nat. Inst. Sci. India*, *19: 777–827, figs. 1–14, pls. 1–3.*

Sarojini, K. K. 1951. The fishery and biology of the Indian Grey Mullets—a review. *Jour. Zool. Soc. India*, *3: 159–79.*

Schultz, Leonard P. 1946. A revision of the genera of mullets, fishes of the family Mugilidae, with descriptions of three new genera. *Proc. U. S. Nat. Mus.*, *96: 377–95, figs. 28–32.*

Smith, J. L. B. 1935. The fishes of the family Mugilidae in South Africa. *Ann. South African Mus.*, *30: 587–644, figs. 1–17, pls. 15–22.*

Thomson, J. M. 1954a. The Mugilidae of Australia and adjacent seas. *Aust. Jour. Mar. Fresh. Res.*, *5: 70–130, figs. 1–16, pls. 1–2.*

———. 1954b. The organs of feeding and the food of some Australian mullet. *Aust. Jour. Mar. Fresh. Res.*, *5: 469–485, figs. 1–6, pls. 1–2.*

Scripps Institution of Oceanography, University of California, La Jolla, California.

(525)

(*Reprinted from Nature, Vol.* 180, *pp.* 85–86, *July* 13, 1957)

LOCALIZATION OF RADIOACTIVE AND STABLE HEAVY NUCLIDES IN OCEAN SEDIMENTS

By G. ARRHENIUS and M. N. BRAMLETTE
Scripps Institution of Oceanography, La Jolla, California
AND
E. PICCIOTTO
Laboratoire de Physique Nucléaire,
Université Libre de Bruxelles

A VARYING fraction of the sediment accumulating on the ocean floor consists of solids formed by precipitation from solution in the sea water, at the sediment surface, and in the sediment. Among these marine hydrogenous minerals are zeolites, manganite, goethite, barite and possibly some clay minerals, rutile and anatase. Also, a number of ionic species are transferred to the sediment by sorption in the molecular pores of the zeolites[1] and in the central layers of the manganites[2–4]. ('Manganite' is in this communication used as a chemical term, in accordance with Buser and coworkers[2]. The proper mineral name will be discussed elsewhere.) An extensive review of the distribution of rare metals in sedimentary rocks and an evaluation of the possible processes leading to this distribution have been published by Krauskopf[5]. There are few cases where the localization of trace elements in specific mineral constituents of fine-grained sedimentary rocks has been demonstrated directly.

The localization of trace metals in the minerals of ocean sediments is of special interest in the case of the naturally radioactive elements. The use of these elements for geochronological purposes depends largely on understanding the mechanism of transfer from the ocean to the sediment, and of redistribution following radioactive decay.

It is known that ionium (thorium-230) is at least partly separated from its predecessors in the ocean and carried to the ocean floor, where it generally gives rise to a high radium content. Several hypotheses have been advanced as to the mechanism of transfer of thorium from the ocean water to the sediment. Verification of any hypothesis by determining the localization of the thorium in particular constituents of the sediments has, however, been lacking, although Goldberg and Picciotto's finding[4] of a high thorium content in manganese nodules as well as Goldberg's theoretical considerations[3] point to the manganite as an important host mineral for this element.

Attempts to determine the ionium- and thorium-carrying minerals were started at Scripps Institution of Oceanography by E. D. Goldberg and us in 1954. Nuclear-emulsion techniques and β-counting demonstrated that most of the α- and β-activity from visible sources in the South Pacific sediments investigated was concentrated in authigenic crystals of phillipsite[2]. Further investigations were carried out in the Institute of Nuclear Physics of the University of Brussels, using sediments from the North Equatorial Pacific with a low content of phillipsite. The distribution of α-activity was studied by autoradiographs of sections of sediment cores, and by suspension of sediment in liquid nuclear emulsion. The results of the suspension studies can be summarized as follows:

(1) The biogenous opal (mainly in the form of diatom frustules and radiolarian skeletons) is entirely inactive.

(2) 10 per cent of the α-tracks originate from small crystals (of the order 1μ) with a high refractive index. The specific activity of this mineral, which is possibly barite, is very high.

(3) 15 per cent of the activity occurs in aggregates with an average size of 3–10μ, frequently with a barium content exceeding 10 per cent and with densities ranging from 2·1 to 2·3. These aggregates may be fæcal pellets of benthonic animals.

(4) 25 per cent of the activity is associated with amber-coloured, fibrous fragments of widely varying size, mostly 20–100μ. The specific activity is of the order of 10^{-7} curie per gm. These fragments were afterwards demonstrated to consist of fibrous apatite and organic matter, and to be skeletal debris of fish.

(5) The remaining 50 per cent of the α-tracks do not originate from any visible solid sources, and are supposed to indicate radioactive matter in true or colloidal solution in the pore water of the sediment, or displaced from the solids of the sediment upon suspension in the photographic emulsion.

Subsequent analysis of skeletal fish debris from pelagic sediments of late Pleistocene to Recent age revealed that this material has a remarkable composition. In addition to the very high content of radioactive elements, there were found several per cent of the rare-earth elements, 0·6–1·5 per cent zinc, 0·1–0·5 per cent copper, 0·05–0·15 per cent tin and 0·03–0·10 per cent lead.

By separation of the organic phase of the fish debris from the apatite phase, it was demonstrated that the rare-earth elements and most of the strontium and barium occur in the apatite structure, whereas the organic phase contains the zinc, tin, lead, titanium, copper and silver, and much of the magnesium, aluminium, chromium and nickel.

Some of the bone and scale debris could be identified as derived from various genera of bathypelagic fish (Hubbs, Dr. Carl L., personal communication). One fragment appeared to be a part of a squid beak.

Analysis of the ashed residue of macerated bathypelagic fish caught by tow-net did not reveal any high concentrations of heavy metals, except for copper (0·03–0·04 per cent), zinc (0·01 per cent) and lead (0·005–0·01 per cent). These amounts, however, are considerably smaller than those found in the fossil debris. The concentration of heavy metals in the fish debris, therefore, appears to have taken place after the death of the organism. Fish debris from the top stratum of the sediment, corresponding to a time period of about the past ten thousand years, had already reached the same high concentration of heavy metals which is found in debris from Tertiary strata. It is thus evident that the concentration takes place in an early phase of the accumulation of the sediment. The measurements of the uranium, ionium, radium and thorium content of the fish debris have not yet been completed. Several facts suggest, however, that the high radioactivity of the Recent and Pleistocene fish debris is mainly due to thorium isotopes and their daughter products. The limitation of the highly alpha-active spots to the upper strata in the cores excludes the possibility of dominant uranium support ; but, on the other hand, the active spots extend too far down to consist dominantly of unsupported radium. The high concentration of the rare-earth elements makes it highly probable that thorium, which has a geochemical behaviour similar to that of the raro-earth elements, is present in considerable amounts.

In a recent paper, Bowie and Atkin[6] have described skeletal material of Devonian fish with large amounts of associated uranium and especially thorium. In the case described, the uranium is mainly localized in the apatite structure, whereas the thorium is concentrated in the hydrocarbons which occur in the cavities of the bone structure. It is difficult at the present time to evaluate this finding in relation to the present observations on Cenozoic fish debris.

With long exposure on surfaces of especially low rate of accumulation, the biogenous apatite appears to dissolve at great ocean depth. The heavy-metal ions thus released seem to be resorbed in the secondary layer of the manganites, which are stable and offer a large active surface area. As a result, large amounts of thorium and rare-earth elements may be added to any already taken up in manganese nodules. In pelagic clays and oozes, where other components in addition to manganese micronodules contribute to a higher rate of accumulation, the fish debris is largely preserved, and the micronodules are lower in rare-earth elements.

Measurements of the crystallite size of marine apatites show a relation (that may be direct or indirect) of this parameter to the rare-earth content. The bathypelagic fish debris has a crystallite size of 300–400 A. along the Z-axis and has a rare-earth content as high as a few per cent. Whale bone fragments, exposed under similar conditions on the deep ocean bottom, but with a crystallite size of 600–1200 A., have a rare-earth content of the order of 0·1 per cent. Marine inorganic apatites, with crystallite sizes greater than 20,000 A., contain a total of rare earths of only 0·05 per cent or less.

It thus seems that ionium, produced from uranium-234 in solution in sea water, together with other thorium isotopes, the rare-earth elements and a number of other heavy metals, is carried to the sediment and sorbed to the surface of the microcrystalline apatite of skeletal debris. If a solid carrier is involved, this may not necessarily be the apatite itself but some other unidentified solid, such as organic matter, which is later dissolved. The details of these processes, as well as the redistribution of radium formed by the decay of ionium, are being further investigated, and a more extensive account of the results will be given on completion of the first phase of the work.

Support for this investigation was received from the Geological Society of America and the Office of Naval Research.

[1] Arrhenius, G., and Goldberg, E., *Tellus*, **7**, 226 (1955).

[2] Buser, W., and Grütter, A., *Schweiz. Min. u. Petr. Mitteil.*, **36**, 49 (1956).

[3] Goldberg, E., *J. Geol.*, **62**, 249 (1954).

[4] Goldberg, E., and Picciotto, E., *Science*, **121**, 613 (1955).

[5] Krauskopf, K., *Econ. Geol.*, **50**, 411 (1955); *Geochim. Cosmochim. Acta*, **9**, 1 (1956).

[6] Bowie, S., and Atkin, D., *Nature*, **177**, 487 (1956).

Contributions from the Scripps Institution of Oceanography, New Series, No. 938.

Printed in Great Britain by Fisher, Knight & Co., Ltd., St. Albans.

Reproduced by Permission

Reproduced by Permission

Reprinted from the Proceedings of the NATIONAL ACADEMY OF SCIENCES,
Vol. 43, No. 9, pp. 804–811. September, 1957.

*ON THE MECHANISM OF TEMPERATURE INDEPENDENCE IN A BIOLOGICAL CLOCK**

BY J. WOODLAND HASTINGS† AND BEATRICE M. SWEENEY

DEPARTMENT OF BIOLOGICAL SCIENCES, NORTHWESTERN UNIVERSITY, EVANSTON, ILLINOIS,
SCRIPPS INSTITUTION OF OCEANOGRAPHY, LA JOLLA, CALIFORNIA
AND
EARHART LABORATORY, CALIFORNIA INSTITUTE OF TECHNOLOGY, PASADENA, CALIFORNIA

Communicated by E. Newton Harvey, July 14, 1957

Introduction.—Diurnal rhythms which persist under constant conditions have been found in a variety of plants and animals (see Bünning;[1] Pittendrigh[2]). Most of the evidence points to the conclusion that diurnal rhythmicity is endogenous and results from oscillations of physiological processes of one sort or another. An unusual feature of many rhythms, however, is their temperature independence. In instances where study has been directed toward the temperature characteristics (Wahl;[3] Brown and Webb;[4] Pittendrigh;[5] Bruce and Pittendrigh;[6] Bühnemann[7]), it has been found that the period, or duration of a cycle, is unaffected or only slightly affected by temperature changes. The way in which this is achieved in organisms which are otherwise markedly temperature-sensitive is not known. It is possible that some uncontrolled environmental variable might be involved, i.e., that there is an exogenous factor which plays a role in determining the period in rhythmic organisms. Another possibility is that temperature compensation is incorporated as a part of the rhythmic mechanism. In either case, it may be noted that temperature independence constitutes support for the idea that a diurnal rhythm could be related to an accurate biological timing device, or clock. If, in fact, the rhythms are related to a chronometer mechanism, the significance of temperature independence is clear.

We have recently demonstrated (Hastings *et al.*[8]) that the dinoflagellate *Gonyaulax polyedra* possesses a diurnal rhythm of luminescence which persists under conditions of constant low light and constant temperature. Since *Gonyaulax* is a unicellular form which may be grown readily in large quantities and studied biochemically, it is an advantageous material for the study of rhythmicity. In addition, the quantitative measurement of light intensity provides an easy and accurate method for following rhythmic changes. The experiments reported here describe the effect of temperature upon the luminescent rhythm. The results suggest that temperature independence is achieved by means of a compensation mechanism.

Materials and Methods.—Gonyaulax polyedra is an armored marine dinoflagellate which is both photosynthetic and luminescent. This organism was isolated from a net sample collected off the pier at Scripps Institution of Oceanography and has been maintained in a unialgal culture in a medium composed of 75 per cent filtered sea water, 2 per cent soil extract, 2×10^{-3} M KNO_3, 2×10^{-4} M K_2HPO_4, 6×10^{-6} M $FeCl_3$, and 2.7×10^{-5} M ethylenediamine-tetraacetic acid (EDTA) at pH 8.0–8.2. Under optimal conditions of light and temperature, a growth rate of about one division per day has been measured. Bacteria-free cultures have been found to have a reduced viability and growth rate, apparently due to the lack of some unknown growth factor which may be supplied by the bacteria. In these experiments, therefore, bacteria-free cultures were not used.

Luminescence in *Gonyaulax* normally occurs only upon stimulation. The cell emits a flash of light having a duration of less than 0.1 second, a record of which has been published previously (Hastings and Sweeney[9]). In our experiments, luminescence was evoked by bubbling a fine stream of purified air through a 2-ml. aliquot of the cell suspension for 1 minute. With continued stimulation, the luminescent response declines sharply, so that after 1 minute, only a very small amount of light is emitted. Due to this fatigue characteristic, the luminescence of a suspension may be quantified by measuring the relatively brief bright burst of light emitted upon stimulation. The light emitted was measured with the photomultiplier apparatus previously described (Sweeney and Hastings[10]), which permits integration of light by accumulating the current output from the phototube on a capacitor. Our index of luminescence therefore is a fixed proportion of the total amount of light emitted by a cell suspension during a 1-minute period of stimulation. After each determination the cell suspension used for luminescence measurement was discarded.

The experiments illustrated in Figure 1 were carried out in the Earhart Laboratory of the California Institute of Technology, where eight different temperature-controlled rooms were available.[11] The temperatures of seven of these rooms and the extreme temperature variations recorded are noted in Figure 1. The eighth room was at 6° C. Unless otherwise stated, the only illumination in these rooms was provided by an overhead fluorescent fixture with two 40-watt "daylight" bulbs placed at a distance of 1 meter from the cultures, where the light intensity was about 100 foot-candles. Uniformity of illumination was achieved by means of a diffusing screen of white tracing paper placed under the fixtures.

Experimental Procedure.—*Gonyaulax* is an obligate photoautotroph. When cultures are grown with alternating light and dark periods of 12 hours each (= LD), their luminescence is much greater during the dark period than during the light period. If such cultures are then transferred either to total darkness or to continuous dim light (100–200 foot-candles), this rhythm of luminescence persists, retaining in both cases the period of approximately 24 hours. It has been shown (Sweeney and Hastings[10]) that in continuous darkness the amplitude of the rhythm is damped as a result of the depletion of its energy supply. In dim light, however, the luminescent rhythm persists with undiminished amplitude and has been observed for as long as fourteen consecutive days (Hastings *et al.*[8]).

The plan of the experiment was as follows: Two-milliliter aliquots from a culture of *Gonyaulax* which had been growing at 22° C. in LD conditions (light from 6:00 A.M. to 6:00 P.M. at an intensity of 800 foot-candles) were pipetted into each of 1,300 test tubes. The cell density at this time was 3,600 cells per milliliter. The tubes were placed in beakers and returned to the previous LD conditions at 22°. Two days later, just prior to 6:00 A.M., cultures were removed from the dark at 22° and placed in the dark in each of the eight rooms, at different temperatures. A few minutes later, at 6:00 A.M., the lights were turned on in all rooms. The cells therefore were exposed to the transition from dark to light almost simultaneously with the transition from 22° to a second temperature. Thereafter, at

(532)

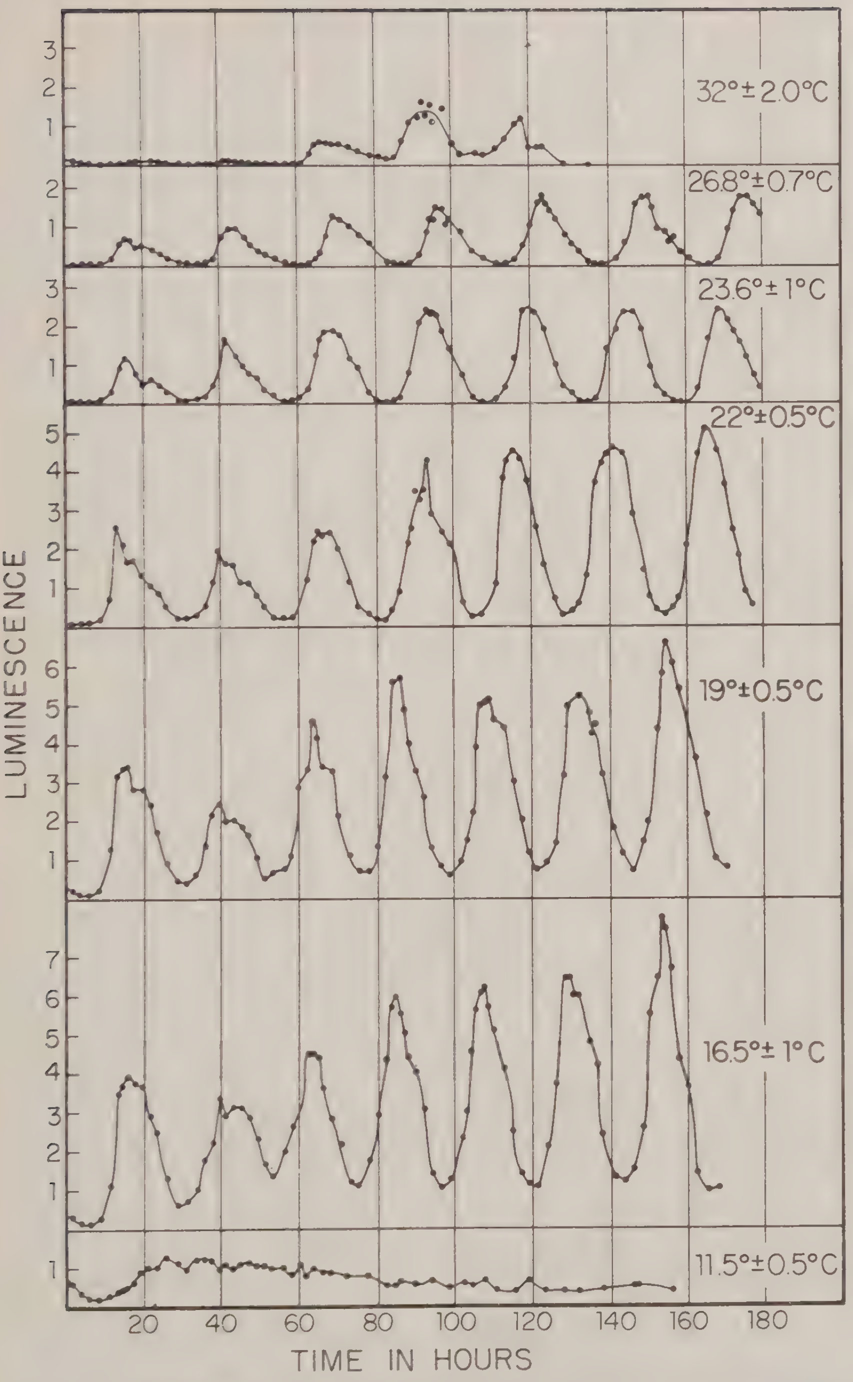

FIG. 1.—Characteristics of the persistent rhythm of luminescence at several different temperatures. The cells were kept at 22° C. in LD conditions prior to the beginning of the experiment shown on the graph. At that time the cells were transferred from the dark at 22° to the various temperatures, all in dim light, and left in these conditions throughout the experiment. The luminescence of the cells was determined approximately every 2 hours. At the dim light intensity used, there is little cell division, even at the optimal temperature for growth. The number of cells therefore remained essentially the same in all tubes at all temperatures.

approximately 2-hour intervals, two tubes were removed from each of the rooms, assayed for luminescence, and then discarded.

Results.—The results of this experiment are shown in Figure 1. At the five temperatures between 16.5° and 26.8° C. the experiments were continued for seven cycles. It is quite evident that the higher the temperature, the longer is the duration of a period. We have estimated the average time of a period at each temperature by taking the time at which the first and last peaks of luminescence occurred and dividing by the number of periods. The data from this computation are plotted in Figure 2.

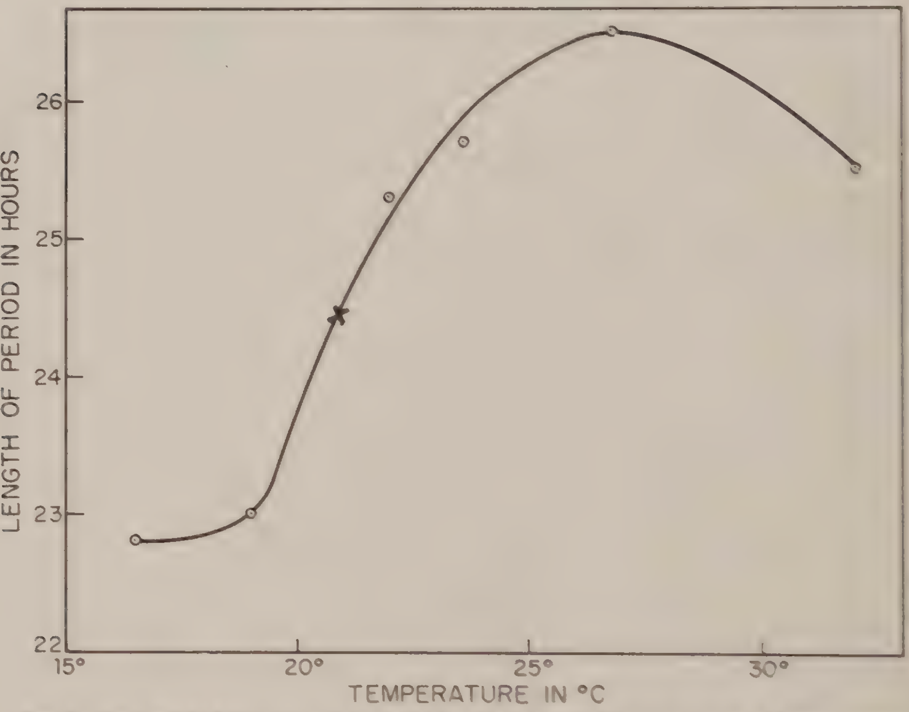

Fig. 2.—The effect of temperature upon the length of a period in the rhythm of luminescence. Data taken from the experiment shown in Fig. 1, except for the point indicated by the symbol X. This was obtained in an experiment (similar to those shown in Fig. 1) carried out in Evanston several months later at a temperature of 21.0° ± 0.1° C.

The temperature control in the room at 32° C. was poor, and the cells were killed on the sixth day of the experiment, when the temperature rose to 36°. The irregularity of the luminescence is probably due in part to the temperature fluctuations and in part to an adverse effect of the high temperature upon the cells. In spite of this, there is a clearly apparent rhythmicity with a period not far from 24 hours, the average duration being about 25.5 hours.

At a temperature of 11.5° C. the rhythmicity was lost, although the cells retained luminescence and viability. From previous experiments it is known that essentially no growth occurs at 11°. When the cultures at 11.5° were returned to a temperature of 22°, the rhythmicity was regained, but it was not determined whether or not the rhythmicity would persist for more than one cycle. It has been reported by Brown and Webb[4] that in the fiddler crab, *Uca*, a low-temperature treatment is equivalent to "stopping the clock" and that when the organism is brought back to a higher temperature, the rhythmicity resumes, with the phase displaced by a time period corresponding to the time of low-temperature treatment. This does not occur in *Gonyaulax*. The phase is determined by the time at which the cultures are returned to the higher temperature. Some cultures were removed from the 11.5° room and taken to the 22° room after 58 hours, and others after 67 hours at the lower temperature. In both cases, pronounced rhythms were initiated, having their first maximal luminescence 30 hours following the transfer. This suggests that a temperature shock may serve as a timing or setting device for rhythms.

Cell suspensions kept in constant dim light at 6° C. showed no measurable luminescence, even when warmed to 22° before assaying. Nevertheless, the cells remained viable, as evidenced by the fact that cultures transferred from 6° to continuous light at 22° regained the ability to luminesce after about 12 hours. The luminescence of such cultures showed no evidence of regaining a rhythmic character. It appears that cells which are kept at such a low temperature will not respond to the temperature shock as a stimulus to initiate rhythmicity.

The important finding in these experiments, namely, that the length of the period of the endogenous rhythm is greater at 26° than at 16° C., was confirmed by a later experiment carried out at La Jolla. This experiment was performed in essentially the same manner as described above, utilizing, however, only two temperature rooms (at 15.9° ± 0.2° and 26.6° ± 0.5°). In each case, only two periods were measured; at the higher temperature the durations of the periods were 27 and $26^1/_2$ hours, and at the lower temperature, 23 and 22 hours. This result confirms the previous finding. The cultures in these two rooms were then exchanged without any change in illumination. The persisting rhythm was somewhat irregular, but it was easily possible to measure the periods. In the cultures moved from 26° to 16°, three periods having durations of 20, 21, and 20 hours were observed. In those moved from 16° to 26°, two periods having durations of $24^1/_2$ and 24 hours were observed. The period may therefore be altered slightly by a temperature change alone.

From these experiments it is evident that, although the period does vary with temperature, the effect is not very great. The rates of various processes in chemical and biological systems usually differ by a factor of two or three at temperatures 10° C. apart. In our experiments the length of the period varies by only about 15 per cent at temperatures 10° apart. Since the temperature effect is relatively small, we may speak of this "clock" as being temperature-independent and comparable to the other cases of temperature-independent rhythms which have been reported.

However, the dependence on temperature which we do observe is worthy of consideration. First of all, it essentially eliminates the possibility that the period of the rhythm is regulated directly by some uncontrolled periodic variable in the environment. Second, in view of the fact that the observed Q_{10} is less than 1.0, it definitely suggests that a temperature-compensation mechanism is involved.[12]

(535)

If we were to assume that the duration of the period is governed by the rate of a single chemical reaction, then an increase in temperature should result in a period of shorter duration. The effect we observe in this case is precisely the opposite, i.e., the Q_{10} between 16.5° and 26.8° C. is 0.86. This result can be readily explained if we assume that temperature independence is achieved by means of compensation, and that this situation is an example of overcompensation.

There are several other compelling reasons to conclude that temperature independence, in biological clocks generally, results from a temperature-compensating mechanism. The pertinent considerations have been discussed in detail by Bruce and Pittendrigh[6] and by Pittendrigh.[2] For example, the effects upon endogenous rhythms in several organisms of repeated and nonrepeated temperature shocks, and the initiation of rhythms by single temperature shocks, favor the interpretation of a temperature-compensating mechanism.

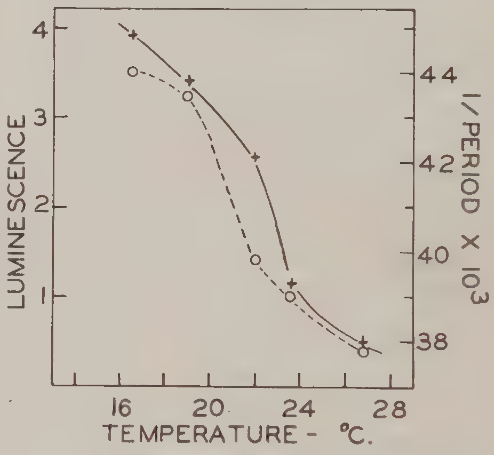

Fig. 3.—Plot showing the effect of temperature upon the amount of luminescence (measured 16 hours after the beginning of the experiment; data plotted with crosses, *solid line*), as compared with the temperature effect upon period (plotted as the inverse of period duration; data plotted with circles, *dotted line*). Data taken from the experiments shown in Fig. 1.

A temperature-compensation model can be expressed very simply in terms of two chemical reactions, A → B and C → D, both of which are temperature-dependent in the usual way. Let it be assumed that the rate of the first reaction controls the duration of the period, while D is an inhibitor of this reaction. If the two reactions have appropriate temperature coefficients, the rate of the first reaction, A → B, will remain essentially constant with temperature changes. If the temperature coefficient of the second reaction was too high in relation to the coefficient of the first reaction, an apparent Q_{10} for A → B of less than 1.0 would be expected. Also, the fact that the average period length in the experiment at 32° C. is less than at 26.8° and 23.6° may be understood in terms of the model reactions by assuming them to be enzymatic and to have different optimal temperatures. The observed result would be expected if the temperature optimum of C → D was somewhat lower than that of A → B.[13]

There is additional evidence for the suggestion that an inhibitor is acting in the luminescent system. In the experiments shown in Figure 1, it can be seen that the intensity of luminescence is less at higher temperatures. In Figure 3, the intensity of luminescence, measured 16 hours after the beginning of the experiment, is plotted against the temperature. On the same graph are plotted the data from Figure 2, using the inverse of time on the ordinate. The parallel between the two implies that both result from the action of the same postulated inhibitor system, even though the intensity of luminescence is changed by a greater degree than is

(536)

the periodicity with the temperature change. The unusual relationship between luminescence and temperature has been confirmed in many experiments, the details of which will be published elsewhere. We have found that light emission in the living cell increases with decreasing temperature to as low as 5° C.

In contrast to these findings, we have previously reported[9] that the luminescent reaction in cell-free extracts is temperature-dependent in the usual way. Luminescence increases with increasing temperature to an optimum at 25° C. and decreases thereafter as a result of enzyme denaturation. The growth rate of the cells is also temperature-dependent in a similar way, the optimum being at about 25°. It appears that the temperature relationships of both the periodicity and the intensity of luminescence in the living cell result from some particular and perhaps unique mechanism. It is at least certain that the entire metabolic pattern of the cell is not temperature-dependent in this unusual way.

Our experiments, as well as the previous studies of Bruce and Pittendrigh[6] with *Euglena gracilis*, demonstrate that a clock system may occur in unicellular forms. It is known, from studies which we have reported previously,[9] that luminescent rhythmicity in *Gonyaulax* is associated with diurnal fluctuations in the extractable components of the luminescent system—with respect to both enzyme and substrate. Pittendrigh[2] has pointed out that this is to be expected and that fluctuations of this sort, or indeed any overt and measurable manifestations of rhythmicity, may be merely "outputs," or reflections of the activity of some undefined but master cellular clock mechanism. In contrast to this view, we would suggest that rhythmicity may occur in particular and essentially discrete systems, such as the luminescent system, and that no special clock need be invoked to account for luminescent rhythmicity or, indeed, any other rhythmic process. In support of this idea, we point to the evidence that the temperature-compensation mechanism apparently acts in the luminescent system directly. If there were some other clock to which luminescence was tied, we would expect the clock itself rather than the luminescent system, to be temperature-compensated.

It seems that the general nature of persistent diurnal rhythms must eventually be understood in terms of oscillating chemical systems. On the assumption that discrete biochemical systems may undergo sustained autonomous oscillations, it appears worthwhile to investigate the biochemistry of such systems in detail.

---

* This research was supported in part by a grant to Northwestern University from the National Science Foundation. Contribution from the Scripps Institution of Oceanography, University of California, New Series, No. 939.

† Present address: Department of Chemistry, University of Illinois, Urbana, Illinois.

[1] E. Bünning, in *Handbuch der Pflanzenphysiologie*, ed. W. Ruhland (Berlin: J. Springer, 1956), **2**, 878–907.

[2] C. S. Pittendrigh, in *Perspectives in Marine Biology* (Berkeley: University of California Press, 1957).

[3] O. Wahl, *Z. vergleich. Physiol.*, **16**, 529–589, 1932.

[4] F. A. Brown, and H. M. Webb, *Physiol. Zoöl.*, **21**, 371–381, 1948.

[5] C. S. Pittendrigh, these Proceedings, **40**, 1018–1029, 1954.

[6] V. G. Bruce, and C. S. Pittendrigh, these Proceedings, **42**, 676–682, 1956.

[7] F. Bühnemann, *Naturforsch.* **10b**, 305–310, 1955.

[8] J. W. Hastings, M. Wiesner, J. Owens, and B. M. Sweeney, *Anat. Record*, **125**, 611, 1956.

[9] J. W. Hastings, and B. M. Sweeney, *J. Cellular Comp. Physiol.*, **49**, 209, 1957.

[10] B. M. Sweeney and J. W. Hastings, *J. Cellular Comp. Physiol.*, **49**, 115–128, 1957.

[11] We are grateful to Professor F. W. Went for his kindness and co-operation in making the space available to us.

[12] It is interesting to note that this is the second instance in which a Q_{10} of less than 1.0 has been reported for the length of the period in a rhythmic process. Bühnemann found that the rhythm of sporulation in *Oedogonium* had a period of longer length at higher temperatures.

[13] E. N. Harvey (personal communication) has recently suggested a model based on similar assumptions. We are not of the opinion that the intracellular reactions which are involved in rhythmicity and the temperature-compensation mechanism are as simple as those we have suggested. They are used merely for illustrative purposes. It does not seem worthwhile at the present time to suggest a more elaborate model, in the absence of more specific biochemical information. We would guess, however, that the chemistry of rhythmicity will be shown to involve a heterogeneous system rather than a homogeneous one.

(538)

FLUCTUATIONS IN POPULATIONS OF LITTORAL MARINE INVERTEBRATES

By

WESLEY R. COE
Scripps Institution of Oceanography
University of California
La Jolla, California

ABSTRACT

Fluctuations in populations of various species of marine invertebrates, several of them over many years, are recorded. Some of the data are quantitative, but most of them are merely estimates of relative abundance at the same season in successive years. Records of local fluctuations in populations of the Pismo clam extend over 25 years, those of dinoflagellates 20 years, and of *Donax* 58 years; records of the set of young oysters cover 70 years and those of the local production of oysters 100 years. These data offer no satisfactory evidence of persistent rhythmical periodicity in any of the species. Changes that have occurred in local populations of littoral invertebrates due to constantly changing environmental conditions and to the introduction of foreign species during the past half-century are recorded. Some of these changes have been catastrophic.

INTRODUCTION

The term annual fluctuation is used in this report to designate variations in the relative number of individuals of a particular species in the same locality in successive years. The estimated amount of fluctuation is based on samples which have been taken at the same season each year in order to avoid the complication of seasonal variations, which are often of considerable magnitude. The number of individuals usually have been largest shortly after periods of reproduction. Fluctuations have varied simultaneously in different parts of the range of a species, since they are largely dependent on local environmental conditions, including diseases.

The writer has recorded many observations of changes which have taken place in populations of various species of littoral invertebrates during the past half-century along the coasts of southern New England and southern California. Most of these changes have been minor fluctuations in numbers while others have been catastrophic, with the total elimination over considerable areas of all members of sus-

---

[1] Contributions from the Scripps Institution of Oceanography, of the University of California. New Series, No. 940.

Reprint from SEARS FOUND. JOURN. MAR. RES.
Reproduced by Permission

ceptible species or even of the entire littoral fauna. Catastrophic changes have obviously resulted from wide deviations in environmental conditions or from diseases, but no satisfactory explanations have been found for many of the observed fluctuations.

ANNUAL FLUCTUATIONS

Kemp (1938), Dexter (1944), Burkenroad (1946) and many others have published numerous examples of fluctuations among marine invertebrates, and others are known to every naturalist who is acquainted with the seashore.

At present many long-term records are available. Some of these are quantitative or semiquantitative in nature, while others are mere estimates of relative abundance which record whether many, few or none of a species were present. Some of these records were obtained in a survey of a particular locality at the same season in successive years. Some have reference to the entire local population of a species and others to only a single year-class. Also annual records of the production of some commercial species are available for a long series of years. It seems desirable to examine a few of these records in order to determine the magnitudes and intervals observed.

1. Pismo Clam.—In the population of the Pismo clam (*Tivela stultorum*) at La Jolla, California, changes which occurred in each year-class during five successive years (1945–1949) were determined by collections taken at monthly intervals, beginning at the time when the young clams first appeared on the beach. Of the average total of 297 individuals found on a restricted portion of the beach in September of these years, 214 were in the first year-class, 71 in the second, 8 in the third, and 4 in the fourth. The population on the beach in those five years indicated that there was an annual loss of 67 to 75% for each year-class and that less than 1% of the young individuals reached the age of four years (Coe, 1947; Coe and Fitch, 1950). A few individuals of more than 20 years of age have been found on the same beach.

Fig. 1 shows not only the number of individuals in each year-class at the end of September from 1945 through 1949 but estimates of the total population from 1938 to 1952 as well. It will be observed that the number of those one year of age increased rapidly in 1946 and decreased in 1949, that those aged two years increased in each successive year, and that the reduced populations of older clams remained nearly stationary. The estimated total population increased about six-fold during the five years preceding 1943. This was followed by a considerable decrease in numbers, with a resurgence in 1946. From 1949 through 1952 there was a rapidly declining population because of the failure of young clams to establish themselves on the beach at the end of the free-swimming larval periods. In 1953 the species had disappeared almost completely from the intertidal zone, not only locally but also in other formerly well populated areas. No significant deviation from average in temperature or salinity and no evidence of disease have been observed. Although some of the larger individuals were taken by poachers, it is concluded that deviations in the currents along the coast were mainly responsible for this pronounced decline. The larvae apparently have a pelagic life of two to three weeks or more, and during this period they may be carried far from their place of spawning by the ocean currents which on that part of the coast have an average velocity of four to five miles a day. Consequently the young clams in any locality may originate from populations living several, or even many, miles distant and the larvae are dependent upon favorable currents to bring them to the beach at the exact time when they are ready for transforming and settling in the sand. Presumably diseases similar to those recorded in this paper for *Donax* and oysters were responsible for many deaths; however, the causative agents were not determined. In some localities, every large clam observed showed macroscopic evidence of disease; some were moribund and others had died recently.

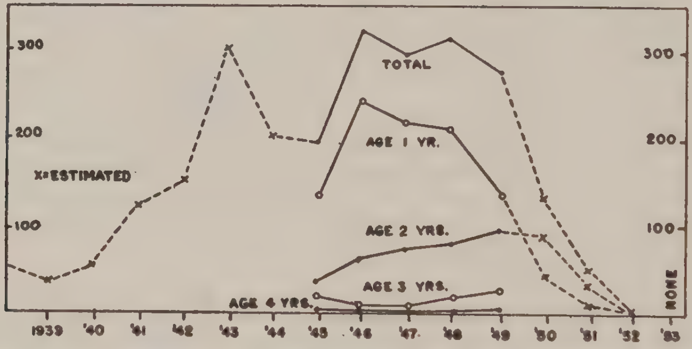

FIGURE 1. The constituent year-classes in the Pismo clam population on a restricted portion of the beach at La Jolla, California, during the last week in September of each year, 1938–1953. The numbers indicated for 1945 through 1949 are strictly quantitative and indicate an annual mortality rate of 67 to 75%. The total mortality from the first to fourth years was 97.5%. For the other years the population is estimated. No new set arrived in 1951 and the entire population disappeared in 1952.

The greater range in the fluctuations of the young as compared with older individuals is shown in the records of the Pismo clam populations at Pismo Beach, California, for the years 1923 through 1950. The samples were standard in that the same areas of the beach were covered in November of each year. The constituents of this population were described by Coe and Fitch (1950) but several of the data require further analysis. The first year-class is of particular interest. The numbers of young clams which settled in the measured areas and survived until the census was taken each year are shown in Fig. 2. The figures indicate variations ranging from 0 in 1934 and 1950, 1 in 1949, 6 in 1928, and 9 in 1938 to 743 in 1937, 758 in 1935, and 871 in 1931. The total of 4111 in the first year-class during the 19 years was 50% of the entire population not exceeding four years of age. Thus a high rate of mortality is indicated.

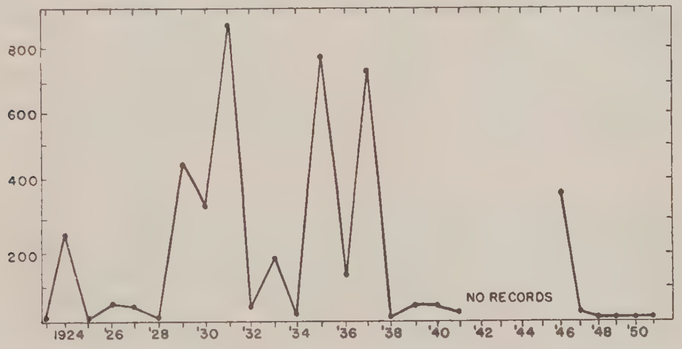

FIGURE 2. Fluctuations in the first year-class of Pismo clams at Pismo Beach, California, estimated from samples taken in November of each year by the California Bureau of Marine Fisheries. An increased population in alternate years as compared with each preceding year was of general occurrence.

It will be noted that during most of this period there was a biennial rhythm in the set or survival of young clams, the numbers in each alternate year being greater than those in the preceding year (Fig. 2). It seems possible that this may have been a chance occurrence due to variations in the water currents, but why there should have been five years in succession with no appreciable set on this beach remains unexplained (Fitch, 1952).

In order to avoid the possible influence of strictly local fluctuations, the collections were made in three well separated sections of the long beach (Fig. 3). The Pismo section was 1.4 miles from the Oceano section and 6.5 miles from the Le Grande section. The data compiled by Fitch (1952) show that, in spite of the distances separating the three sections, the fluctuations were generally parallel at each date of sampling (Fig. 3). This is presumably indicative of nearly uniform

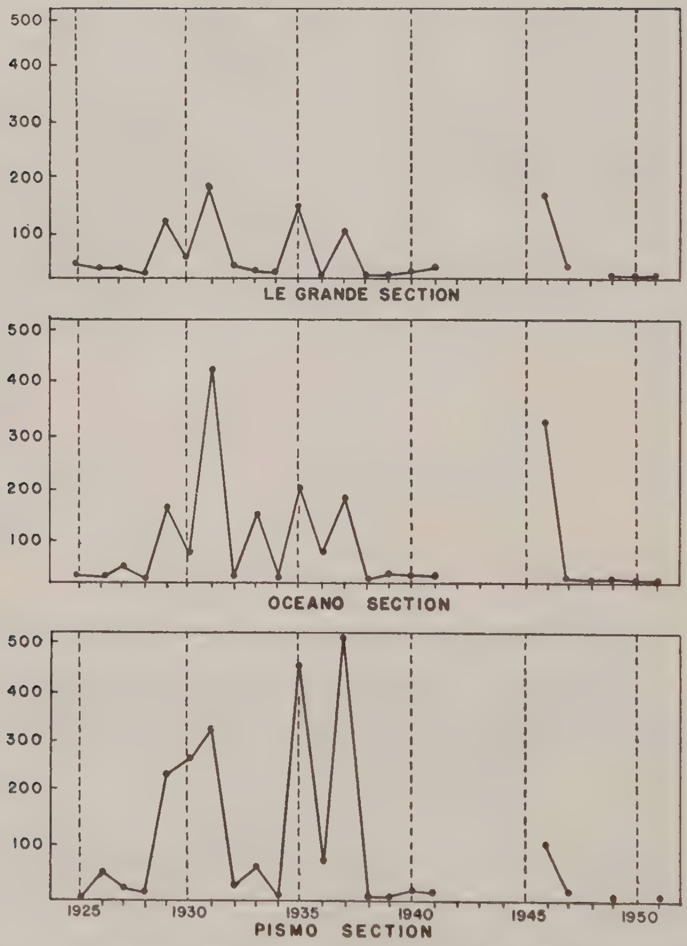

FIGURE 3. Fluctuations in the numbers of young Pismo clams found in the three sections of Pismo Beach, California, in November of the years 1925 to 1951, with the exception of 1942–1945. The same areas were covered each year. In all three sections, which were from 1.5 to 6.5 miles apart, each alternate (odd-numbered) year previous to 1940 generally showed an increased set as compared with the immediately preceding and following year, but in 1946 the trend was reversed. From 1946 to 1952 the set has been extremely small. Data from Fitch (1952).

environmental conditions along the entire extent of the beach in any given year although such conditions undoubtedly varied in different years.

The life span of individuals of this species may exceed ten years under favorable conditions, and each adult female may produce from 5 to 20 million eggs annually. During the years in which practically no young appeared there were many thousands of adults on the same beach, hence it is concluded that the immense numbers of potential young either failed to survive or were carried to other beaches, perhaps some miles distant. Presumably a large proportion of the young perished by being carried too far from shore; Johnson (1940) found larvae of the sand crab *Emerita* more than 90 miles from the nearest coast although the adults live only in the intertidal zone. Some were undoubtedly devoured, some probably died because of adverse temperature or lack of suitable nutrition, and possibly others succumbed to parasitic disease either before or after setting.

The older year-classes were less variable in numbers, the second year-class fluctuating from 2 in 1935 to 297 in 1947, the third year-class from 3 in 1946 to 245 in 1937, and the fourth year class from 4 in 1930 to 200 in 1946.

2. Oysters.—A quantitative study of variations in the number of young oysters (*Crassostrea virginica*) which set on 100 oyster shells in Long Island Sound has been made by Dr. Victor L. Loosanoff during 15 summers, 1937 through 1951, and by his permission the unpublished data are shown in Fig. 4. It will be noted that in two of these years the numbers were 40 times greater than those in the preceding year and were correspondingly larger than any set during the last five years. It appears that the number of survivors which reached the places for attachment fluctuated widely, but there is no evidence as to the number of larvae produced.

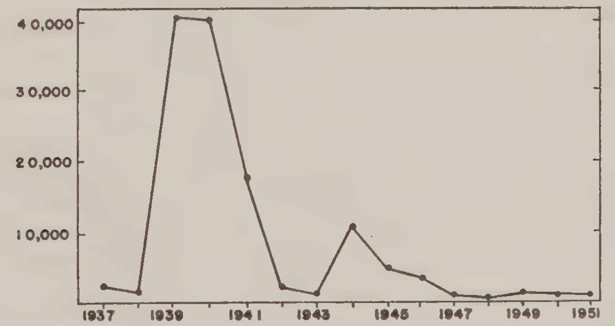

FIGURE 4. Yearly variation in the average set of young oysters on 100 oyster shells placed at various depths. Long Island Sound. Unpublished data supplied by Dr. V. L. Loosanoff.

The longest continuous record concerning fluctuations in populations of any American marine invertebrate may be found in the estimates of the relative abundance of the set of young oysters in the large oyster producing areas in Long Island Sound. It is obvious that a heavy set is generally, but not always, indicative of a large future population of adults. These records for the past 70 years have been compiled by Loosanoff and Engel (1940) and have been supplemented by personal communications from Dr. Loosanoff. Fig. 5 indicates that heavy sets were reported in 12 of the 18 years prior to 1900 whereas in only six years of the present century has the set been considered heavy. From 1906 to 1924 there were continual failures and light sets; medium sets occurred in 1926, 1934, 1937, 1941 and 1945, and heavy sets in 1904, 1925, 1928, 1930, 1939 and 1940.

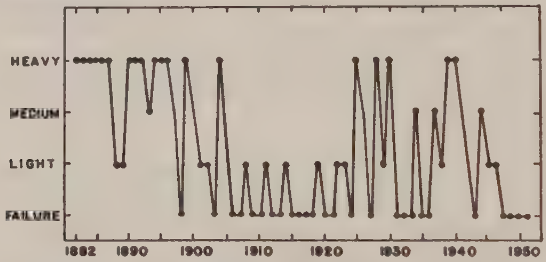

FIGURE 5. Fluctuations in the estimated set of young oysters in Long Island Sound during the past 70 years. Heavy sets were common in the years preceding 1900 and again in 1925 to 1929, but there were only light sets or failures from 1906 to 1924 and from 1945 to 1951. Data from Loosanoff and Engle (1940) and personal communications.

Note that in four of these years heavy sets occurred in the year immediately following one in which the set was a failure and that in only one year (1931) did a failure occur immediately following a heavy set. A sequence of six heavy sets was reported at the beginning of the record and a sequence of four failures followed 1914. In other years a maximum of three heavy sets or four failures followed in sequence. A cyclical periodicity in abundance is not evident. It is obvious that a light set accompanied by a low rate of mortality may be more productive than a heavy set with high mortality.

3. Starfish.—A quantitative study of the variations in the rate of attachment of young starfish (*Asterias forbesi*) on planted oyster shells for the years 1937 through 1951 was made by Dr. Loosanoff, who has kindly supplied the data indicated in Fig. 6. It will be seen that the numbers were much larger in 1938 and 1941 than in more recent years. It was mentioned in a preceding paragraph that the

associated set of young oysters was also much reduced in the five most recent years.

A cyclical periodicity has been reported by Burkenroad (1946) for the same species of starfish. From an examination of published reports of the oyster industry, of newspaper accounts and of testimony of oyster growers, he concluded that this starfish, which is the chief enemy of the adult oyster on the southern coast of New England, has been particularly destructive at intervals of about 14 years during the past 90 years. To Burkenroad the records seemed to indicate an interval of approximately 7 years between the periods of minimum and maximum abundance in each cycle. It seems doubtful, however, whether the data from the diverse sources mentioned, although of much interest, are sufficient to justify the conclusion that such definite periodic cycles prevail. He estimated that the population at peak periods might be 20 times that at trough periods.

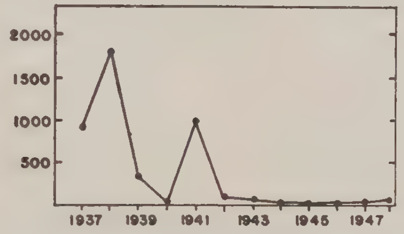

FIGURE 6. Fluctuations in the average seasonal set of young starfish on 100 oyster shells placed at various depths in Long Island Sound in the years 1937–1948. Unpublished data supplied by Dr. V. L. Loosanoff. The graph shows young populations in 1938 and 1941 which were many-fold larger than those in subsequent years.

The term "Resurgent Populations" is appropriately used for such populations as experience only minor fluctuations for a number of years and then increase rapidly to many times their former numbers with an increment of a hundred or even thousands. After one or several years of increase the population usually returns to approximately its former size. Such a resurgent population for the Pismo clam is shown in Fig. 1 and for the mussel *Septifer bifurcatus* in Fig. 8. Every naturalist familiar with seashore life must have noticed such resurgent populations, for they are common to all groups of invertebrates. A species formerly considered scarce suddenly becomes abundant and soon becomes scarce again.

4. *Donax.*—Conspicuous examples of this type of population are found in certain species of the little "bean clam," *Donax*. Of the two

species found in California, *D. californica* usually occurs only in small populations while *D. gouldii* remains relatively scarce locally for a number of years and then appears in countless millions. At such times the shells lie in contact or even in several layers in the intertidal zone over many miles of the sandy beaches.

After a life span of three years or less, the clams have sometimes disappeared so completely that not a single individual could be found in the intertidal zone on an extent of beach which was occupied by millions a few months earlier. Fig. 7 shows that these resurgent populations have been recorded at La Jolla in 1894–95, 1909–10, 1913–15, 1931–32, 1934, and 1937–38.

During the summer of 1949 there arrived a resurgent population which seems to have been of unprecedented magnitude. In the autumn of that year the beach had an average population of more than 20,000 young clams per square meter in a zone 2 to 5 meters wide which extended with some interruptions for more than five miles along the coast.

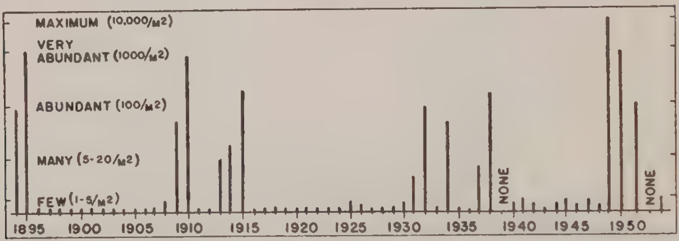

Figure 7. Resurgent populations of *Donax gouldii* in the intertidal zone at La Jolla, California. Estimated relative abundance: "few," less than 5 per square meter; "many," 5 to 20; "abundant," more than 100; "very abundant," more than 1000; "maximum," more than 10,000 per square meter. The populations in the years preceding 1926 and from 1928 to 1936 are estimated from the incomplete records by Dr. W. E. Ritter, Mr. Percy Barnhart, and others; those of 1926, 1927, 1937 and subsequent years are from personal observations by the writer. The entire populations died in 1939 and in 1952.

This dense population continued, but with considerable mortality, for almost two years. In July 1951 approximately half of the individuals died after spawning, but those remaining still formed a dense population in many areas. As soon as spawning began the following spring the mortality increased until about mid-July 1952, when only about 20 individuals per square meter, 0.1% of the early population, remained. The major portion of the mortalities occurred within a few days. The deceased included not only members of the resurgent population, which had then attained the ripe old age of nearly three years, but also most of the younger individuals which had reached the beach in the two intervening years and which had managed to survive in less crowded situations until the final catastrophe. Extended search along the beach, both in the intertidal zone and below, failed to reveal a dozen individuals, old or young, excepting one small area in which all members of the resurgent population died; the younger year-classes survived a few months longer. The miles of sandy beaches thickly strewn with empty shells bore vivid testimony as to what had occurred

Samples of the population had been examined microscopically once each month or oftener throughout the 3-year history of this phenomenon. Infestation with trematode parasites was common, but no evidence of truly pathogenic organisms appeared during the first two years. Thereafter the moribund individuals lay fully exposed on the surface of the sand for several days before death, apparently too feeble to bury themselves after having been washed out by the surf. The bodies were thin and watery, often with greenish exudations of blood and blood corpuscles, together with many minute unicellular parasites in the connective tissues, blood vessels, epithelium of gut and other tissues. On this evidence it is presumed that the minute parasites caused the epidemic.

In the year preceding this resurgence the population did not exceed one clam per square meter in the same area, although it is probable that some individuals were present below the tidal zone. It is not known whether this resurgent population originated from these few local individuals or were brought as larvae from a distance of many miles by ocean currents, as mentioned earlier. During the months preceding the appearance of this resurgent population at La Jolla there were populations of spawning adults at Coronado, about 12 miles south, at Sunset Beach, 65 miles north, and probably at other localities along the coast. With favorable current velocities of 2–5 miles per day, the larvae could have reached La Jolla from either of these localities during the larval period.

The occasional occurrence of these resurgent populations is presumably due to the chance combination of suitable conditions during the pelagic larval period and to favorable currents which bring the swarms of larvae to the beach at the exact time when they are ready for transforming and setting.

5. Mussels.—Not infrequently an introduced species multiplies with great rapidity for a few years and then declines or disappears. The bay-mussel (*Mytilus edulis diegensis*) offers an excellent example of the rise and fall of such a newly arrived population. In 1940 this subspecies attracted considerable attention in Newport Bay, California, because of its great abundance, and three years later, in August

1943, a small colony was found on the pier at the Scripps Institution of Oceanography, about 60 miles south of Newport Bay. Within a few months they multiplied so that by the following summer these mussels covered all available spaces in the intertidal zone on the pier as well as on adjacent rocks. Later they were found in Mission Bay, San Diego Bay and elsewhere along the coast, and soon they became a nuisance by clogging the intake pipes of salt-water systems. In many situations there were so many young that they could not possibly have grown to maturity because of lack of space. Thus vast colonies sprang up in situations unsuitable for long survival (Coe, 1946). Following the maximum during the second year after arrival, the numbers diminished slightly and then declined rapidly to a relatively sparse population in the seventh year (Fig. 8).

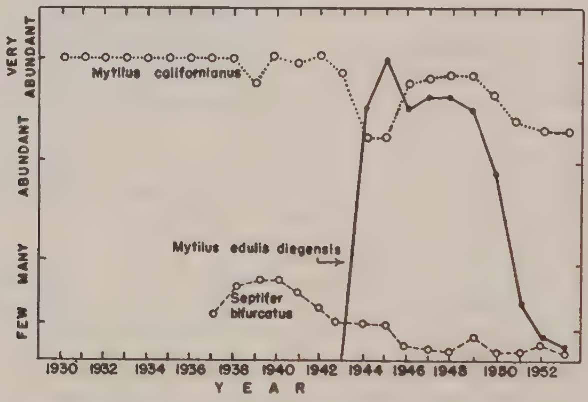

FIGURE 8. Comparison of populations of three species of mussels on the pier and rocks at La Jolla, California. The bay-mussel (*Mytilus edulis diegensis*) represents the temporary exuberance of a newly introduced stock. The sea-mussel (*Mytilus californianus*) has maintained an essentially maximum population with only minor fluctuations except in the years when the bay-mussel pre-empted the more favorable situations or when starfish were unusually numerous. The population of the ribbed mussel (*Septifer bifurcatus*) has been sparse except for a slight resurgence in 1938 to 1940.

In contrast with this briefly exuberant population, the native sea-mussel (*Mytilus californianus*) has long maintained maximum numbers, with only small fluctuations except for the years when many of the situations suitable for attachment of the young were pre-empted by the bay-mussel (Fig. 8).

A third species of mussel, *Septifer bifurcatus*, which occupies the same habitat, has maintained a sparse population except for a brief resurgence from 1938 through 1942 (Fig. 8).

6. Dinoflagellates.—Since the productivity of the sea is so largely dependent on phytoplankton for the nutrition of marine animals, it would naturally be expected that conditions favoring large phytoplankton populations would likewise be associated with large animal populations. An abundant crop of phytoplankton is normally accompanied by a large crop of grazing zooplankton which in turn serves directly or indirectly as food for larger animals, invertebrates as well as vertebrates. Thus the phytoplankton primarily, together with other marine plants and a comparatively small amount of detritus from the land, supplies the nutrition of all marine organisms. Hence if a rhythmical periodicity actually occurs in the production of phytoplankton over a series of years, associated changes in the animal populations should be predictable.

Statistical studies by Allen (1941) on the abundance of dinoflagellates on the coast of southern California, extending over a period of 20 years, have shown that the populations of dinoflagellates indicate an inverse correlation with the temperature of the water during the first quarter of the year. Low temperatures on that portion of the Pacific coast often indicate upwelling of deeper oceanic water which brings with it phosphates and other inorganic nutrients required for the growth of phytoplankton and animals. His data, however, do not show satisfactory evidence of cyclical periodicity.

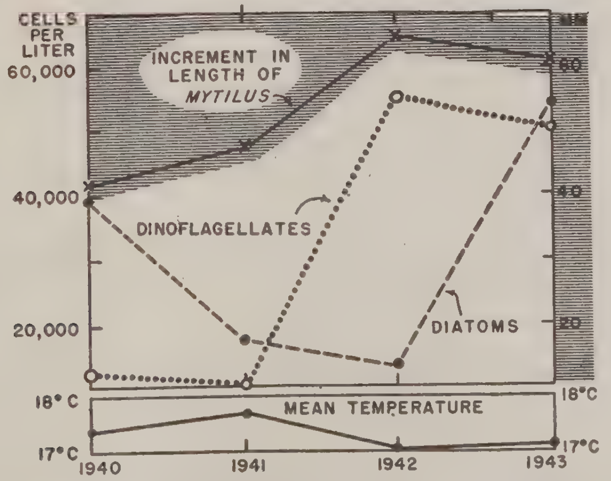

FIGURE 9. Fluctuations in the populations of diatoms and dinoflagellates as correlated with mean annual temperature of the water and increment in growth rate of mussels at the pier of the Scripps Institution of Oceanography, La Jolla, California. Low average temperature is associated with upwelling oceanic water, with large populations of dinoflagellates and relatively few diatoms, as well as with rapid growth of mussels.

In studies from 1940 through 1943, Coe and Fox (1944) found that the largest dinoflagellate populations occurred during 1942 when the lowest annual water temperature was recorded and that there was a more rapid growth of mussels in the same locality in 1942 than in the three years of higher temperatures. On the other hand, the populations of diatoms in 1942 were smaller than those of the other three years (Fig. 9).

CATASTROPHIC CHANGES

The littoral fauna, in contrast with fauna of the open ocean, is subject to great vicissitudes. During the half-century under observation there have been occasions when excessive cold in winter or heat in summer has destroyed all or nearly all individuals of susceptible species of the population over large areas.

Along the coast of southern New England during certain winters, particularly that of 1918, extensive populations of invertebrates were killed when the intertidal zone was exposed to temperatures far below the freezing point of sea water. Allee (1923) has shown that species having a more southerly range suffered greater losses than those which have a normal range extending farther northward. Blegvad (1929) described the high mortality among littoral invertebrates along the northern coasts of Europe during unusually cold winters. Heat combined with excessive salinity often produce similar catastrophes, as Gunter (1947) observed in the Gulf of Mexico.

MacGinitie (1939) has reported that the heavy rains and freshets of 1927, 1938, and 1941, and presumably of other years, lowered the salinity of the water in some of the bays along the coast of southern California to such an extent that only the more tolerant invertebrates in the intertidal zone were able to survive.

Severe storms and violent surf have in many winters washed out the intertidal substrate, thus destroying the associated invertebrates or crushing them as the surf pounded the rocks on or beneath which they had maintained flourishing colonies.

Epidemics of parasitic diseases have destroyed populations of sponges, oysters, clams, mussels and other invertebrates along many miles of seacoast within a single year. The epidemics in the bean clam, *Donax*, at La Jolla, California have been mentioned earlier. Diseases of an apparently similar nature, which have been destructive to oysters on the southern Atlantic and Gulf coasts of the United States in recent years, have long been known from other parts of the world (Mackin, 1951).

Sedentary invertebrates with a pelagic larval life are subjected to great vicissitudes because of their dependence upon favorable currents, as noted earlier. On both the Atlantic and Pacific coasts adverse currents have evidently caused the complete failure of young oysters and clams to establish themselves in many formerly populous localities.

Many marine invertebrates are more or less dependent upon vegetation for support or protection, and without it they perish. Mention may be made of the bay scallop (*Pecten irradians* = *P. gibbus*) which formerly lived in vast colonies in eelgrass (*Zostera marina*) in protected areas over a great extent of the Atlantic coast. Though not limited to such situations, the scallop populations suffered a rapid decline in numbers in 1931–1933 following destruction of the eelgrass by disease. A lucrative fishery disappeared in many localities. With the scallop went also many of the ophiurans, annelids, nemerteans, echiuroids, crustaceans, bivalves and other invertebrates that had found congenial homes in and beneath the vegetation. In some areas, however, the populations of scallops have more recently increased again in spite of the absence of eelgrass (Marshall, 1947).

The most spectacular catastrophes to both invertebrates and vertebrates along many miles of seacoast have been caused by a sudden heavy bloom of poisonous dinoflagellates, commonly referred to as "red water." These phenomena occur frequently in areas of upwelling. Brongersma-Sanders (1948) has shown that on some coasts they may be expected annually but that in most regions they occur at irregular intervals and cannot be predicted.

On the coast of southern California red tide has been observed either locally or over an extent of 100 to 200 miles or more in 1894, 1901, 1907, 1917, 1924, 1933, 1938, 1939, 1945 and 1952; thus the intervals have been 7, 6, 10, 7, 9, 5, 1, 6 and 7 years, with an average of nearly 6.5 years. Some of these occurrences have been highly destructive to both vertebrates and invertebrates while others have caused little injury. Although several species have been involved, the greatest destruction occurred when *Gonyaulax polyhedra* was the predominant organism. Not infrequently in years other than those noted above, the water has become more or less distinctly discolored locally in midsummer by populations of species of *Prorocentrum*, *Ceratium* and other dinoflagellates, but the populations did not reach the density characteristic of red water.

There are many records of the rapid elimination of flourishing populations due to pollution by oil and industrial wastes. Harbors and estuaries which formerly supported a vast assemblage of invertebrates have become barren wastes except for a few of the more resistant species. The effluent from sewers of certain communities, however, supplies additional nutrition for bivalve mollusks and other forms which feed on particles in suspension.

INTRODUCTION OF FOREIGN SPECIES

Some of the populations under observation have maintained themselves for many years with relatively little apparent change while others have fluctuated widely. Certain mussel beds, for example, with their associated invertebrates, have the same appearance today as they had 50 years ago whereas others have disappeared completely or have disappeared and repopulated repeatedly.

With few exceptions the species that constitute the marine invertebrate fauna of southern New England today are the same as those that were reported by Verrill (1873), although they have varied greatly in local abundance during the past 80 years. New species have been described each year, but most of these have been inconspicuous creatures that Verrill did not study or did not find. Changes in the local distribution of some of the species have been profound, due in large measure to the increased demand for seafood, the encroachment of industry, and the development of seashore properties, but none of the species appears to have been exterminated. Only three conspicuous species have become common since the publication of Verrill's report. The edible periwinkle (*Littorina litoria* L.) of European coasts was first noticed at Woods Hole in 1875 and soon became abundant along the coast as far south as Virginia. Another conspicuous, and sometimes abundant, species not reported by Verrill is the medusa *Gonionemus murbachi* Mayor; this was first found in the Eel Pond at Woods Hole in 1894. The sea-anemone *Aiptasiomorpha* (*Sagartia*) *luciae* (Verrill), discovered in 1887 on the southern coast of New England, became one of the most abundant constituents of the littoral fauna as far south as Florida and the Gulf of Mexico; it has fluctuated widely in abundance and local distribution in subsequent years.

Frequently the result of the introduction of a species of marine invertebrate, either accidentally or intentionally, into a foreign locality has been its speedy elimination. Even when environmental conditions seemed suitable for the existence of introduced individuals, conditions have seldom been favorable for reproduction and continuation of the species. Hence most of the attempts to introduce useful marine invertebrates have met with failure, but there have been some exceptions; a few of the useful species have been successful in establishing themselves in their new environments and have supplemented the human food supply.

The accidentally introduced Japanese little-neck clam (*Protothaca philippinarum*, also known as *Tapes semidecussata*) is an example. This highly palatable bivalve was first noticed on the coast of British Columbia in 1936. During the ensuing eight years it spread widely and in 1944 it had extended along the coast for a distance of more than 80 miles. It is stated by Neave (1944) that in some areas only two seasons of spawning were required to make it more abundant than any of the edible species of native clams. The species is now established at many localities along the Pacific coast and has become commercially important.

The intentional introduction of the soft-shell clam (*Mya arenaria*) of the Atlantic coast furnished the stock from which large crops of these succulent bivalves are now harvested commercially each year in many areas on the Pacific coast. Other introductions from the Atlantic to the Pacific include the horsemussel (*Volsella demissa*) and the quahog (*Venus mercenaria*). The snails *Ilyanassa obsoleta*, *Crepidula plana*, *C. glauca*, *C. fornicata*, *Busycon pyrum* and the gem clam (*Gemma gemma*) are among the immigrants who were transported from east to west coasts as stowaways among oysters.

Attempts to establish reproductive colonies of the Atlantic oyster (*Crassostrea virginica*) on the Pacific coast have not generally met with success; however, when the spat has been introduced it has grown to maturity in some localities, and it is said that normal reproduction occurs occasionally. Plantings of the lobster from the Atlantic coast have always failed.

Only a single species of marine invertebrate has been transported intentionally across the continent in the opposite direction, the reason being that edible invertebrates of the Atlantic coast are almost invariably more succulent than their relatives of the Pacific. Experimental plantings of the Japanese oyster have been made on the coast of New England in the hope that this species will thrive in situations that are unfavorable for the growth of the superior native species.

For many years on the Pacific American coast the Japanese oyster (*Crassostrea gigas*) has been successfully cultivated from young imported each year from Japan. This procedure has been necessary because of its failure to reproduce in the new localities. More recently, however, normal reproduction has occurred in certain areas at intervals of a few years, but most of the commercial crop is still grown from the imported young.

Unless great care is exercised there is always danger of introducing harmful species with beneficial species, and the former sometimes multiply more rapidly and prove to be even more injurious than they were in their native home. For example, in its native southern New England habitat the snail *Crepidula fornicata* is only occasionally injurious to the oyster beds, but on both shores of the English Channel it has become a great nuisance since it was accidentally introduced with American oysters. The snails quickly established themselves but the oysters did not. The boring snail or drill (*Urosalpinx cinerea*), which is so destructive to oysters and other bivalves, was brought to the Pacific coast and to the coasts of England in futile attempts to introduce oysters from the American Atlantic coast. The similarly destructive Japanese drill (*Tritonalia japonica*) has also become established on the American Pacific coast. The barnacle *Elminius modestus* from the southern hemisphere has now become a pest on British oyster beds, and species of *Teredo*, *Bankia* and *Limnoria*, which destroy wooden marine structures, have established themselves on all sea coasts except in the far north and far south.

PRODUCTION RECORDS

A summary of the commercial production in the various groups of marine organisms may be found in "Marine Products of Commerce" by Tressler, *et al.* (1951). However, these records of production do not afford reliable evidence as to the relative size of the population in any year or in any locality because they are influenced in large measure by economic factors such as demand, price and available manpower. Thus, from such records it may appear for a limited time that production is increasing when the population is actually being rapidly depleted. Records of oyster production in Maryland for more than a century, published by Beavan (1945), are typical of the production of most other invertebrates of economic importance. During the periods of maximum production between 1875 and 1892, 10 to 15 million bushels were harvested in that area annually. Then during the ensuing 13 years the rate of production declined rather rapidly, and more recently it has fluctuated irregularly between 2 and 3 million bushels a year, or one-fifth the previous maximum. In this case the production has been correlated with the size of the oyster population, since both have declined to about the same extent.

In most of the other oyster-producing areas on the Atlantic and Gulf coasts there has been a somewhat similar decrease in the past quarter century, but there have been some exceptions, such as that in Louisiana where the annual production has fluctuated widely but where there has been no downward trend during the 20 years preceding 1949 (Gunter, 1949).

Recently the commercial production of the various species of clams in most areas has declined even more rapidly than the production of oysters. On the contrary, lobster production in the New England and Middle Atlantic states has more than doubled in the 20 years between 1929 and 1949 (Scattergood and McKown, 1951).

POPULATION CYCLES

Many reports have been interpreted as indicating regular and predictable periodicities in the abundance of certain species of insects and mammals, and supposed cycles have been reported for commercial fish catches. However, the evidence is not conclusive, since there is always the possibility of chance coincidence. Irregularity in the periods of fluctuations is certainly the general rule. Cole (1951) and others have shown that purely random variations in environmental conditions would be consistent mathematically with practically all numerical maxima and minima observed in vertebrate populations and with variations in tree-ring width. The evidence presented by Burkenroad (1946) concerning a 14-year periodicity in the abundance of starfish has been noted previously.

From an examination of temperature variations in surface water off New Brunswick, Canada from 1921 to 1947, Hachey and McLellan (1948) concluded that cycles of 3.3, 9 and 15 years were involved, and they have indicated similar trends for other localities along the Atlantic coast. Four years of warmer water have alternated more or less regularly with similar periods of colder water, but the deviations have not been extensive and random fluctuation would seem to be a more plausible explanation.

Hutchinson (1950) concluded from a study of the guano deposits on the Peruvian coast that a well marked 7-year cycle in the inshore movement of warm water and in associated biological catastrophes had occurred regularly from 1864 to 1939; he found no evidence of such a cycle prior to 1864. He concluded therefore that this rhythm is nonpersistent, as are so many meteorological cycles. The deposits on one of the islands showed no trace of this periodicity.

If it should be proved that there are predictable long-term periodic cycles in meteorological conditions or in the physical and chemical phenomena of the environment, then it might be expected that populations of plants and animals would fluctuate accordingly (Allee, *et al.*, 1949; Dice, 1952), but thus far the available information on population abundance seems to indicate that nearly all of the fluctuations have occurred at irregular intervals and have resulted from irregular changes in one or more of the environmental conditions.

A full discussion of this subject may be found in "Symposium on cycles in animal populations" (Hewitt, 1954).

SUMMARY AND CONCLUSIONS

The foregoing examples of fluctuations in populations of marine invertebrates indicate that annual changes of considerable magnitude are of general occurrence. Some of these are evidently due to concurrent changes in environmental conditions (including chemical and physical alterations of the water), to enemies, to disease, and to changes in substrate and in ocean currents. Others are due to migration or introduction to new localities.

Records of local populations of dinoflagellates, starfish, oysters, clams and mussels over long periods show that maximum and minimum populations have sometimes followed each other immediately but that populations of medium size are more numerous than those with either extreme.

Maximum and minimum populations generally occur at irregular and unpredictable intervals with no satisfactory indication of long-term periodic or rhythmical cycles; it is concluded that the supposed periodicities are the result of random variations in the complex environmental conditions, including diseases.

The records show that the reproductive capacity of many marine invertebrates is such that relatively few individuals under favorable conditions can produce a maximum population in a single generation. Overpopulation has been frequent and has often been followed by a rapid decline in numbers, since the competition for space or food was too severe for survival.

Resurgent populations have sometimes resulted from the arrival of vast numbers of pelagic larvae transported from localities several miles distant by ocean currents. Except in bays and partially confined bodies of water, there is little chance that a large proportion of the larvae will settle in the immediate vicinity of their place of origin.

Introduction of a species to a new locality has sometimes resulted temporarily in a high rate of multiplication and territorial expansion, usually followed by a rapid decline in numbers. More frequently the introduced species has found the new locality unsuitable for reproduction and has been rapidly eliminated.

The populations of most commercially important species, with the exception of lobsters, have declined more rapidly during the past decade than at any earlier period of similar length.

Useful as well as harmful species, when introduced intentionally or accidentally, have sometimes become permanent members of the local fauna.

On the Pacific coast an inverse correlation was found between the mean annual temperature of the water and the growth rate of mussels, as well as the populations of dinoflagellates.

Catastrophic changes in the populations have been observed occasionally or at irregular intervals. These have resulted from excessive heat or cold, heavy rains and floods, heavy surf, adverse ocean currents, loss of associated vegetation, industrial wastes, excessive abundance of dinoflagellates, or epidemics of parasitic diseases, with the destruction of many or nearly all individuals of susceptible species over large areas.

LITERATURE CITED

ALLEE, W. C.
1923. The effect of temperature in limiting the geographical range of invertebrates in the Woods Hole littoral. Ecology, *4:* 351–354.
ALLEE, W. C., A. E. EMERSON, O. PARK, T. PARK AND K. P. SCHMIDT
1949. Principles of Animal Ecology. W. B. Saunders Co., Philadelphia. 837 pp.
ALLEN, W. E.
1941. Twenty years' statistical studies of plankton dinoflagellates of southern California. Amer. Midl. Nat., *26:* 603–635.
BEAVAN, G. F.
1945. Maryland's oyster problems. Maryland Dept. Res. and Educ., Educ. Serv., No. 8: 1–14.
BLEGVAD. H.
1929. Mortality among animals of the littoral region in ice winters. Rep. Danish biol. Sta., *35:* 49–62.
BRONGERSMA-SANDERS, MARGARETHA
1948. The importance of upwelling water to vertebrate paleontology and oil geology. Verh. Akad. Wet. Amst., Naturk., Sect. 2: 1–112.
BURKENROAD, M. D.
1946. Fluctuations in abundance of marine animals. Science, *103:* 684–686.
COE, W. R.
1946. A resurgent population of the California bay-mussel (Mytilus edulis diegensis). J. Morph., *78:* 85–104.
1947. Nutrition, growth and sexuality of the Pismo clam (Tivela stultorum). J. exp. Zool., *104:* 1–24.
1953. Resurgent populations of marine invertebrates and their dependence on ocean currents and tidal currents. Ecology, *34:* 225–229.
COE, W. R. AND J. E. FITCH.
1950. Population studies, local growth rates and reproduction of the Pismo clam (Tivela stultorum). J. mar. Res., *9:* 188–210.
COE, W. R. AND D. L. FOX
1944. Biology of the California sea-mussel (Mytilus californianus). Environmental conditions and rate of growth. Biol. Bull. Woods Hole, *87:* 59–72.
COLE, LAMONT C.
1951. Population cycles and random oscillations. J. Wildl. Mgmt., *15:* 233–252.
DEXTER, R. W.
1944. Annual fluctuation of abundance of some marine mollusks. Nautilus, *58:* 18–24.
DICE, L. R.
1952. Natural Communities. University of Michigan Press. 547 pp.

FITCH, J. E.
1952. The Pismo clam in 1951. Calif. Fish Game, *38:* 541–547.
GUNTER, GORDON
1947. Catastrophism in the sea and its paleontological significance, with special references to the Gulf of Mexico. Amer. J. Sci., *245:* 669–676.
1949. A summary of production statistics and facts related to development of the oyster industry in Louisiana, with a brief comparison with other Gulf states. Publ. Texas A. M. Res. Found., No. 2: 1–28.
HACKEY, H. B. AND J. B. MCLELLAN
1948. Trends and cycles in surface temperatures of the Canadian Atlantic. J. Fish. Res. Bd. Canada, *7:* 355–362.
HEWITT, O. H. (ed.)
1954. Symposium on cycles in animal populations. J. Wildl. Mgmt., *18:* 1–112.
HUTCHINSON, G. E.
1950. Survey of contemporary knowledge of biogeochemistry. 3. The biogeochemistry of vertebrate excretion. Bull. Amer. Mus. nat. Hist., *96:* 1–554.
JOHNSON, M. W.
1940. The correlation of water movements and dispersal of pelagic littoral animals, especially the sand crab, Emerita. J. Mar. Res., *2:* 236–245.
KEMP, STANLEY
1938. Oceanography and the fluctuations in the abundance of marine animals. Rep. Brit. Ass., 1938: 85–101.
LOOSANOFF, V. L. AND J. B. ENGEL
1940. Spawning and setting of oysters in Long Island Sound in 1937, and discussion of the method for predicting the intensity and time of oyster setting. Bull. U. S. Bur. Fish., *49:* 217–255.
MACGINITIE, G. E.
1939. Some effects of fresh water on the fauna of a marine harbor. Amer. Midl. Nat., *21:* 681–686.
MACKIN, J. G.
1951. Histopathology of infection of Crassostrea virginica (Gmelin) by Dermocystidium marinum Mackin, Owen, and Collier. Bull. mar. Sci. Gulf Carib., *1:* 72–87.
MARSHALL, N.
1947. An abundance of bay scallops in the absence of eelgrass. Ecology, *28:* 321–322.
NEAVE, FERRIS
1944. The spread of the Japanese little-neck clam in British Columbia waters. Prog. Rep. Fish. Res. Bd. Canada, Pacif. St., No. 61: 3.
SCATTERGOOD, L. W. AND D. A. MCKOWN
1951. United States lobster and spiny lobster production (1921–49) and imports (1923–49). U. S. Fish and Wildl. Serv., *13* (12): 1–11.
TRESSLER, D. K., J. MCW. LEMON, *et al.*
1951. Marine Products of Commerce. 2nd Ed. Reinhold Publ. Corp., New York. 782 pp.
VERRILL, A.-E.
1873. Report upon the invertebrate animals of Vineyard Sound and the adjacent waters, with an account of the physical characters of the region. Rep. U. S. Comm. Fish (1871–72): 295–778.

INTER-AMERICAN TROPICAL TUNA COMMISSION
COMISION INTERAMERICANA DEL ATUN TROPICAL

Bulletin – Boletín

Vol. II, No. 4

PRIMARY PRODUCTION, CHLOROPHYLL, AND ZOOPLANKTON VOLUMES IN THE TROPICAL EASTERN PACIFIC OCEAN

PRODUCCION PRIMARIA, CLOROFILA, Y VOLUMENES DEL ZOOPLANCTON EN LA ZONA TROPICAL DEL OCEANO PACIFICO ORIENTAL

by — por

ROBERT W. HOLMES, MILNER B. SCHAEFER, and—y BELL M. SHIMADA

La Jolla, California
1957

Reproduced by Permission

CONTENTS — INDICE

ENGLISH VERSION — VERSION EN INGLES

Page

Methods of measurement of chlorophyll, primary production, and standing crop of zooplankton 129
  Chlorophyll "a" 129
  Primary production 130
  Zooplankton standing crop 132
Results of *in situ* measurements in relation to oceanographic features 133
  Surface observations 133
  Sub-surface observations 134
Correlation of surface primary production and zooplankton volumes with surface chlorophyll 135
Carbon fourteen uptake of samples incubated on shipboard 137
Time variation in zooplankton volumes 138
Comparisons with observations in other oceanic regions 138

FIGURES — ILUSTRACIONES 140
TABLES — TABLAS 150

SPANISH VERSION — VERSION EN ESPAÑOL

Página

Métodos para la determinación de la clorofila, de la producción primaria y de la cantidad be zooplancton 158
  Clorofila "a" 158
  Producción primaria 158
  Cantidad de zooplancton 160
Resultados de las mediciones *in situ* en relación con las características oceanográficas 161
  Observaciones de la superficie 161
  Observaciones en aguas subsuperficiales 162
Correlación entre la producción primaria y los volúmenes del zooplancton con la clorofila de aguas superficiales 164
Asimilación de carbón catorce en muestras incubados a bordo 166
Variación en el tiempo en los volúmenes del zooplancton 167
Comparaciones con observaciones en otras regiones oceánicas 167

LITERATURE CITED — BIBLIOGRAFIA CITADA 169

PRIMARY PRODUCTION, CHLOROPHYLL, AND ZOOPLANKTON VOLUMES IN THE TROPICAL EASTERN PACIFIC OCEAN[1]

by

Robert W. Holmes[2], Milner B. Schaefer[2,3], and Bell M. Shimada[3]

Between 1 October and 17 December 1955 investigations of the physical, chemical and biological oceanography of the Eastern Pacific Ocean in a region bounded approximately by 30° N. latitude, 9° S. latitude, 120° W. longitude and the mainland coast were conducted from the vessels *Horizon* and *Spencer F. Baird* of the Scripps Institution of Oceanography of the University of California. These were part of a cooperative operation, designated for convenience by the code name "Eastropic," in which a vessel of the U. S. Fish and Wildlife Service worked, during this same period, further west and a vessel of the Peruvian Navy worked further south, offshore from Peru. A vessel of the California State Fisheries Laboratory also conducted certain sub-surface tuna fishing operations and other studies in the same general region as the Scripps vessels.

In addition to carrying out a number of special studies related to particular oceanographic features, the Scripps vessels occupied a considerable number of hydrographic stations. The locations of these stations, at each of which were made net-hauls for zooplankton, are shown in Figure 4 and Tables 2 and 3. At some of the hydrographic stations, and in some places between stations, there were made from the *Spencer F. Baird* measurements of chlorophyll "a" and of primary production (by the C^{14} technique), both *in situ* and in a shipboard incubator. The purpose of this paper is to report on the results of these biological observations.

The authors wish to express their gratitude to Drs. Francis T. Haxo and William H. Thomas, and to Mr. Elmer Squier for advice and for help in building the shipboard incubator.

METHODS OF MEASUREMENT OF CHLOROPHYLL, PRIMARY PRODUCTION AND STANDING CROP OF ZOOPLANKTON

Chlorophyll "a"

Surface water samples for the determination of chlorophyll were collected with a plastic bucket both at hydrographic stations and while the vessel was underway. At stations, a lucite Van Dorn (1956) sampler was

---

[1] Contribution from the Scripps Institution of Oceanography, New Series No. 942. This paper represents, in part, results of research carried out by the University of California under contract with the Office of Naval Research.

[2] Scripps Institution of Oceanography.

[3] Inter-American Tropical Tuna Commission.

(563)

employed for the collection of sub-surface samples. The water sample (8.3 liters, or in some rich areas 4.1 l.) was filtered through either one or two 47-mm. type-HA Millipore filters after the addition of a small amount of magnesium carbonate to the water sample. The chlorophyll was extracted from each filter pad with 3 mls. of 90% acetone (reagent grade) in the cold (*ca.* 10° C.) and dark for approximately 10 hours. The extract from each sample was then centrifuged until clear and decanted into a 10-ml. volumetric flask. The remaining precipitate in the centrifuge tube was re-suspended in 3 mls. of 90% acetone, centrifuged, and the supernatant liquid combined with that obtained previously. The extract was then diluted to 10 mls. and its optical density measured in a 10 cm. semi-micro absorption cell at 750, 665, 645 and 635/mμ with a Beckman model DU spectrophotometer. Turbidity corrections were made on the basis of the transmission at 750mμ and the concentrations of chlorophyll "a" were calculated from the equation given by Richards with Thompson (1952), and are shown in Table 1.

Primary production

In this study, the C^{14} method was employed to determine the rate of carbon fixation by the phytoplankton. Following the precedent set by Ryther (1956b), we have considered the rate of C^{14} uptake to be synonymous with the term "primary production."

The C^{14} was prepared in the manner described by Steeman-Nielsen (1952) with the exception that glass-redistilled water instead of artificial sea water was used as the solvent for the $Na_2C^{14}0_3$. Two solutions were prepared: one containing approximately 100μC/ml. (which was employed from Stations 1 through 41), the other, 20μC/ml. (employed from Stations 45 through 57). One-ml. aliquots of these solutions were placed in one-ml. ampules, which were immediately sealed and autoclaved. The standardization technique was similar to that employed by Steeman-Nielsen (1952) with the exception that Millipore filters were employed instead of collodion filters.

The *in situ* studies were carried out in the following manner: A sample was collected at each desired depth with the lucite Van Dorn sampler shortly before daylight. The samples were transferred to 250 ml. Pyrex bottles. The C^{14} solution was carefully transferred from the ampule to the water sample with a hypodermic syringe and needle, each ampule being rinsed three times with water from the sample. The samples were re-suspended at dawn, at approximately the depth at which they were collected, on a weighted rope supported by a free-floating glass buoy, 14 inches in diameter, enclosed in cord netting and attached to a bamboo pole bearing a flag at its top, for ease in visual location. The "surface" sample was attached to the side of the buoy, just under the water surface, by tying the bottle to the netting in which the glass ball was enclosed. The incubation period was terminated at local noon. Immedicately after the incubation, the samples were filtered through 47-mm. type-HA (plain) Millipore filters. The filter pads were dried, fumed over concentrated HCI for 20 minutes, and re-dried with silica-gel before counting. Filter pad activity was measured using an ANTON 1001-T tube with a Nuclear-Chicago scalar (Mod. 182A).

The values for primary production (Table 1) were calculated from filter pad activity in the manner described by Steeman-Nielsen (1952). These data have not been corrected for any losses of carbon that would occur during the hours of darkness. Primary production in the *water column* (gC/m^2/day) was estimated by integration, with a planimeter, of the smoothed depth profiles (Figs. 6 to 11) for each station.

The samples placed in the shipboard incubator were collected and inoculated with C^{14} in the same manner as the samples utilized in the *in situ* studies. The temperature in the incubator was maintained within 1° C. of the sea surface temperature observed when the samples were collected. The light intensity to which the samples were exposed during a given 4-hour experiment was very nearly constant. At the beginning of the expedition the light intensity incident to the bottom of the reaction vessels was about 1100 foot candles; the light intensity decreased slowly as the daylight-type fluorescent lamps aged and as the reflector behind the lamps became tarnished. As a result, the last samples placed in the incubator received only 600 foot candles of incident illumination. In order to make the results of the different experiments comparable, we have reported the rate of carbon uptake in mgC/m^3/hr. at 1000 foot candles. 1000 foot candles was selected as a high light intensity believed to be below that which would cause saturation and yet still be on the linear portion of the curve relating photosynthesis to light intensity. The average intensity to which the plant population was subjected would be somewhat less than 1000 foot candles, because of the fall-off in intensity toward the neck of the bottle.

Where vertical series of observations were not made, primary surface *in situ* production was measured using samples dipped from the sea surface with a plastic bucket at or near sunrise. Samples were placed in Pyrex bottles, inoculated with C^{14}, and trailed astern of the vessel, just under the surface, until local noon. The subsequent treatment of the samples was identical with that described above for *in situ* vertical series. Results are reported as mgC/m^3/day in Table 1.

Samples collected for the measurement of primary production were seldom duplicated and no comprehensive study of variability due to sampling was attempted. However, at six stations (Nos. 6, 13, 19, 32-10, 45, and 55) two samples were collected from the same bucket of surface water and their C^{14}-uptakes measured after shipboard incubation. Two samples from the same bucket were also taken at Station 1 and these were incubated in bottles trailing astern of the vessel. In four out of the seven cases the duplicates agreed with one another to within ±10%, in one case they agreed to within ±20%, and in the remaining two cases agreement was poor (±100%). The values given in Table 1 and used throughout this paper represent the averages of the duplicates at these stations.

The reason for this variability is not understood. We have encountered similar variations in other areas, and Dr. W. H. Thomas of Scripps Institution of Oceanography in his studies off the Mississippi River Delta in the Gulf of Mexico has encountered similar variability (personal communication). It would seem that usually the C^{14} uptakes in duplicate samples agree well, but that occasionally disagreement between them is large; frequently the uptake of duplicate samples will disagree by a factor of two, three, or even four. These aberrancies may result from the experimental technique employed or may be due to real differences in the phytoplankton content of the two samples.

Zooplankton standing crop

Measurements were made of the standing crop of zooplankton by means of plankton net-hauls, using gear and techniques comparable to those presently employed by the California Cooperative Oceanic Fishery Investigations. At each station, an oblique tow was made with a one-meter (mouth diameter) plankton net made of 30XXX silk grit gauze in the body and 56XXX silk grit gauze in the rear section and cod-end bag. The net was lowered from the surface to a depth of approximately 300 meters (450 meters wire length) at a rate of 50 meter per minute while the vessel was slowly underway and retrieved at a rate of 20 meters per minute. The duration of a single haul, therefore, was about 32 minutes, on the average. An Atlas flow meter was mounted in the mouth of the net to record the volume of sea water filtered by the net. Flow meters were calibrated before and after the cruise. The details of all quantitative plankton hauls made from the vessels *Spencer F. Baird* and *Horizon* during Eastropic Expedition are given in Tables 2 and 3, respectively.

Zooplankton collections were preserved in 4 percent buffered formalin. Ashore, the collections were filtered and the total "wet" volumes of plankton obtained at each station were measured by displacement. The volume of water sampled by each haul was determined by a method described by the South Pacific Fishery Investigations of the U. S. Fish and Wildlife Service (1953) and the displacement volumes were then converted into terms of the volume of organisms, in cubic centimeters, collected from each 1000 cubic meters of sea water strained. The standardized values for each station are presented in the last 2 columns of Tables 2 and 3, first for the entire sample, and second, for the sample after removal of all organisms larger than 5 cubic centimeters volume.

RESULTS OF *IN SITU* MEASUREMENTS IN RELATION TO OCEANOGRAPHIC FEATURES

Surface observations

The values of surface chlorophyll "a," surface primary production *in situ*, and zooplankton volumes observed during the expedition are presented in Figures 2 to 4, while Figure 1 shows the current systems and water masses, based on a preliminary study of the hydrographic observations and current measurements made during the expedition.

In the water of the California Current and North Equatorial Current (Stations 1-10), well offshore from Baja California and Central Mexico, we find characteristically low concentrations of chlorophyll "a" (about 0.1 mg/m^3), very low surface primary production (about 0.40 mgC/m^3/day), and low zooplankton volumes (generally less than 50 cc/1000m^3).

Higher values of chlorophyll, primary production, and zooplankton volumes were found in the region of the northern boundary of the Equatorial Counter Current, and these values trend upward from west to east toward the coast of Central America. This seems to be related to the thermocline, which is elevated close to the surface as a ridge along this boundary, and which shoals from west to east. At Station 31-11 (Fig. 2), for example, at about 115° W. longitude, the mixed layer has a thickness of about 30 meters, while at Station 33 at about 90° W. longitude, it was only 18 meters thick. At the inshore end, this ridge appears to spread out into a broad "dome" off the Central American coast, the thermocline becoming slightly deeper again close inshore (e. g. Stations 35 and 39 had a mixed layer of some 25-30 meters thickness). In the region of this "dome" off Central America we find relatively high values of surface chlorophyll (0.2 to 0.3mg/m^3), surface primary production (about 25 mgC/m^3/day), and zooplankton volumes (200 cc/1000 m^3 and higher).

In the region of the northern boundary of the Peru Current, off northern South America and in the vicinity of the Galapagos Islands (Stations 50 to 59), we encounter high standing crops of phytoplankton (chlorophyll "a" up to 2.0 mg/m^3), and zooplankton (up to 600 cc/1000 m^3). The surface primary production at the two stations where measurements were made was also high, but not as high as off Central America. However, at Station 57 (Fig. 2), production in the water column as a whole exceeded the values obtained off Central America.

Quite high levels of chlorophyll "a," phytoplankton primary production, and zooplankton volumes were also observed in the South Equatorial Current (Stations 18 to 24) in the vicinity of the equator near 115° W. longitude. Hydrographic data from this and other cruises indicate the presence of upwelling along the equator (unpublished results).

High levels of chlorophyll and zooplankton volumes also appear in the sea areas just offshore from the coast of Mexico, from the Gulf of Tehuantepec to the vicinity of Cape Corrientes. Unfortunately, the supply of C^{14} had been used up by the time the expedition reached this area, so determinations of production were not possible.

Sub-surface observations

At seven stations observations of the chlorophyll "a" concentration and rate of primary production *in situ* were obtained at several depths down to 100 or 125 meters. These observations, together with the observed temperatures, salinity and oxygen concentrations are presented as functions of depth in Figures 5 to 11.

Stations 33, 35, 37, 39 located off Central America (Figs. 7 to 10) are generally similar as regards production and chlorophyll distributions, as well as physical characteristics. Stations 24 and 31-11 (Figs. 5 and 6) located in the far offshore waters of the Counter Current and South Equatorial Current are different with respect to both biological and physical properties.

The first group of stations is characterized by a well-defined, shallow, mixed layer within which most of the primary production occurs (90% or more, except at Station 35 where the ratio is about 67%). Gradients in chlorophyll "a" are small in the upper 40 meters, and an important fraction of the chlorophyll in the water column occurs below the thermocline and halocline. The maximum rate of primary production occurred at or very near the surface. Overcast conditions prevailed on the days on which these stations were occupied which presumably prevented light inhibition at the surface (see Steeman-Nielsen 1951 and 1952).

There also occurs at each of these stations (Figs. 7 to 10) an increase in the primary production just above the thermo and haloclines about which we can only speculate. It seems most improbable that the amount of photosynthetically active light could be greater at 10-20 meters than at some depth nearer the surface; thus it seems unlikely that light could be responsible for this increase. Similarly, the increase does not seem to be related to the quantity of chlorophyll "a" in the water, although it should be mentioned that the chlorophyll method employed does not distinguish between chlorophyll "a" and phaeophytin "a." If this observed increase is real, factors other than light and chlorophyll would seem to be responsible. Unfortunately, nutrient data are lacking at these stations. Such information might have been of value in explaining this apparent anomaly.

While the data from Stations 31-11 and 24 (Figs. 5 and 6) are not as complete nor as continuous as those off Central America, the few observations indicate a different type of situation. Here, an important fraction (about 50%) of total primary production is taking place below the mixed layer, and the primary production is relatively high at 70 meters depths. Only at Station 31-11 is there good correspondence between chlorophyll concentration and the rate of production. It may be noted that at Station 24 (Fig. 6), which is located in the region of equatorial upwelling, there is very little salinity gradient down to 100 meters and the thermocline is not sharply developed.

At Station 57 (Fig. 11) near the northern boundary of the Peru Current, the thermocline and halocline are much less sharp than at stations off Central America. At this station, the chlorophyll remains high down to a depth of 70 meters, while the primary production drops off to a negligible amount well above this.

The region off Central America is also characterized by the presence of a pronounced oxygen minimum in the upper layers (Figs. 7 to 10). The most rapid decrease in oxygen concentration generally occurs immediately below the mixed layer. It is hypothesized that the water of low oxygen content originates here, as a result of the oxygen demand of the phytoplankton below the compensation depth, through respiration of the phytoplankton and/or the bacterial activity associated with dead and dying phytoplankton. A similar explanation for the oxygen minimum south of the equator off Peru is likewise suggested by the data from Station 57 (Fig. 11).

CORRELATION OF SURFACE PRIMARY PRODUCTION AND ZOOPLANKTON VOLUMES WITH SURFACE CHLOROPHYLL

If all the available primary production and chlorophyll "a" data obtained in surface water are considered together (Fig. 12), there appears to be some correlation between these two variables, but with a fairly large scatter. The data reveal that, on the average, low primary production is associated with low chlorophyll "a" and that high production is associated with high chlorophyll. The points for most of the stations appear to fall about a vague line, with the production increasing faster than chlorophyll "a". The stations off Central America, however, particularly Stations 33, 35 and 37, indicate a relatively higher production per unit of chlorophyll than is shown by the rest of the data.

Edmondson (1955), working with populations, resulting from the enrichment of Woods Hole Harbor water, grown in concrete tanks, found that the relationship between production (as measured with the oxygen light-and-dark-bottle technique) and chlorophyll could be improved by taking into consideration variations in incident radiation. In order to see if such a relationship existed for our data, since no direct measurements of incident radiation were made, we obtained the average incident flux of radiation (direct plus diffuse) for a cloudless sky from the curves of Kimball (1928) for December and applied Kimball's (1928) correction for the degree of cloud cover observed. The surface *in situ* production was then calculated in terms of carbon uptake per cubic meter per day per unit of incident radiation and replotted against the surface chlorophyll concentration at the same stations. The resulting relationship was quite similar to that shown in Figure 12, with about the same degree of scatter.

If the *in situ* data in Figure 12 are viewed taking into account the geographic position of the sampling locations, we see that they isolate themselves into 3 groups, which possess different production/chlorophyll relationships. The offshore stations north of approximately 7° N. latitude (Stations 1, 6, 13, 32-10, 31-11, and 27), which are located in the North Equatorial Current and Equatorial Counter Current fall into one group, while the inshore stations off Central America (Stations 33, 35, 37, and 39) fall into another group. A third group is composed of the stations in the Peru Current, off Ecuador and Peru, and one considerably west of the Galapagos Islands on the equator in the South Equatorial Current (Stations 25, 45, 57, and 51).

We are uncertain about the meaning of these relationships. A possible explanation is suggested by the recent work of Rodhe (personal communication) who found a relationship between production and chlorophyll at a single station in Lake Erken. When his daily observations were grouped into monthly periods, they revealed, with a single exception, a good relationship between production and chlorophyll in any given month, but the relationship varied from month to month. He has suggested that these differing production/chlorophyll relationships may be the result of changes in the species composition of the phytoplankton standing crop. While the variations observed by Rodhe are temporal rather than spatial, considerable differences in the composition of the phytoplankton standing crop would also be expected to occur in the different water masses of the Eastern Tropical Pacific. While we have no data to support this postulated difference in phytoplankton composition, we believe that some of the observed variability in the observed production/chlorophyll "a" relationship may be attributed to it.

The existence of a general relationship between chlorophyll and production, with a rather high degree of variability, and some evidence of differences in widely separated areas, undoubtedly results from the interaction of a number of factors. Factors that may be important in causing variability are: differences in species composition, differences in rate of photosynthesis of each species depending upon the spectral distribution and energy of the sub-surface radiation, nutrient conditions, and, perhaps, differences in the rate of photosynthesis per unit of chlorophyll related to the position of various components of the population on their growth curves and to their past history.

Elucidation of the effects of these and other factors will require much more detailed studies. However, it appears that in a very general way the quantity of chlorophyll per unit volume of surface water provides a basis for estimating, albeit poorly, the rate of carbon fixation in the surface layer of the sea in the Eastern Tropical Pacific region. Low values of chlorophyll, less than about 0.2 mg/m^3, indicate very low productivity (i. e. less than about 2 $mgC/m^3/day$). At higher chlorophyll levels, however, the variability in observed rates of carbon fixation is so great from one water mass to another that the error of estimation becomes very large.

There is a fair general agreement between the geographical distribution of chlorophyll "a," primary production, and zooplankton volume (Fig. 2, 3, and 4). The relationship between surface chlorophyll and zooplankton volumes is even better illustrated in Figure 14. It appears that surface chlorophyll provides a useful basis of estimating the standing crop of zooplankton in the Eastern Tropical Pacific.

CARBON FOURTEEN UPTAKE OF SAMPLES INCUBATED ON SHIPBOARD

Surface samples for which production was measured *in vitro* under constant illumination at the temperature of the sea surface exhibit no clear relationship between chlorophyll concentration and primary production per unit of illumination (Fig. 13).

Ryther (1956b, Fig. 2) has found in his studies with cultures of marine phytoplankton that the rate of production (measured by the oxygen method) per unit of chlorophyll "a" at a constant light intensity is nearly constant for a number of species. The Eastropic data do not seem to support Ryther's conclusions. Admittedly the experiments made at sea were rather unsatisfactory in that the light intensity to which our samples were subjected varied from experiment to experiment, although the light intensity remained constant during any one experiment (see page 131). Nevertheless our intensities were presumably below those which would cause saturation (see Ryther 1956a, Steeman-Nielsen, 1952), so that we would expect, on the basis of Ryther's experiments, to find a positive correlation between chlorophyll and primary production per unit of illumination.

In seeking a possible explanation of our results in relation to Ryther's experiments, it may be noted that the range of concentrations of chlorophyll and of production in his cultures were very much greater than the range of chlorophyll concentrations and of rates of carbon fixation we encountered on "Eastropic." Indeed, the range of Ryther's values apparently far exceeded those normally encountered in the sea, even in northern latitudes.

Attempts to equate the radiocarbon uptake of surface samples incubated on shipboard with the uptake observed in surface samples incubated *in situ*, by taking into account variations in incident solar radiation, have not met with success. This may be the result of our inability to secure sufficiently precise estimations of radiation in the area from climatic charts, and our inadequate knowledge of the level of energy which causes the saturation of photosynthesis in natural populations. Similarly, the lack of submarine light measurements has prevented further analysis of results of incubator measurements of C^{14} uptake in samples taken from below the surface.

TIME VARIATION IN ZOOPLANKTON VOLUMES

Comparison between zooplankton volumes obtained during Shellback Expedition in 1952 (Fig. 15) and Eastropic in 1955 (Fig. 4) illustrates some of the variability that may occur in different seasons and years. The zooplankton volumes in the summer of 1952 were generally lower than in the fall of 1955. However, it is to be seen that certain areas of very high and very low standing crops appear in both years and in the same locations. Noteworthy are the area of high plankton volumes in the region of the Peru Current and along the equator, and the volumes off Central America. The paucity of organisms in the water some distance offshore from Baja California appears in both years. Inshore, along the Mexican coast, north of the Gulf of Tehuantepec, the zooplankton was poor in 1952 but rich in 1955.

COMPARISONS WITH OBSERVATIONS IN OTHER OCEANIC REGIONS

Steeman-Nielsen (1954) has reported on C^{14} productivity at a series of *Galathea* stations in the Pacific along a course from New Zealand to California. His values of production in the water column, per square meter of sea surface, were calculated from shipboard incubator determinations and light measurements at various depths in the sea. At the several stations along his section, lying between 140° and 180° W. longitude, he found production rates between 0.10 and 0.19 $gC/m^2/day$, except in the vicinity of the equator where a value of 0.5 $gC/m^2/day$ was recorded, and at a station somewhat north of the equator, which he believes was "influenced by the divergences produced by the Counter Current" at which 0.26 $gC/m^2/day$ was found. Our value of 0.51 $gC/m^2/day$ at Station 24, on the equator, corresponds well with Steeman-Nielsen's results at his station near the equator. Our *in situ* value of 0.012 $gC/m^2/day$ at Station 31-11 is, however, much lower than the *Galathea* results at the same latitude, further westward, and the C^{14} uptake in the *in vitro* samples was likewise very low. This very low value is somewhat anomalous, and requires verification on a future cruise, before accepting it as representative of the region in which Station 31-11 was located.

Steeman-Nielsen's data as to high production on the equator with somewhat lower rates to the north and south have been confirmed by M. Oguri (personal communication), who made *in vitro* determinations of C^{14} uptake of surface samples at a number of stations in the region between 110° and 140° W. longitude and between 5°N. and 5° S. latitude from the vessel *H. M. Smith* in the autumn of 1955, simultaneously with our studies further eastward. He found the C^{14} uptake in water samples from stations on the equator to be significantly higher than at 5° N. or 5° S. latitude.

Production found by us in the area of the "dome" off Central America (0.414-0.779 $gC/m^2/day$) is generally higher than anything encountered by Steeman-Nielsen in the Pacific, except in the coastal waters of New Zealand and the coastal waters off San Francisco. These rates of production in the area off Central America, and the even higher rate found by us at Station 57 near the north boundary of the Peru Current (1.02 $gC/m^2/day$) compare favorably with the most productive areas visited by the *Galathea,* in the southern part of the Benguela Current along the African coast, where Steeman-Nielsen has reported production rates of 0.46-2.5 $gC/m^2/day$.

The values of chlorophyll, zooplankton volumes, and surface primary production in the very poor area offshore from Baja California, indicate that this region is among the least productive of oceanic areas, being, probably, as poor as the Sargasso Sea. It is of interest to note that this area lies not very far offshore from the region along the coast of Baja California, which, on the basis of zooplankton volumes measured on other cruises, is known to be quite productive.

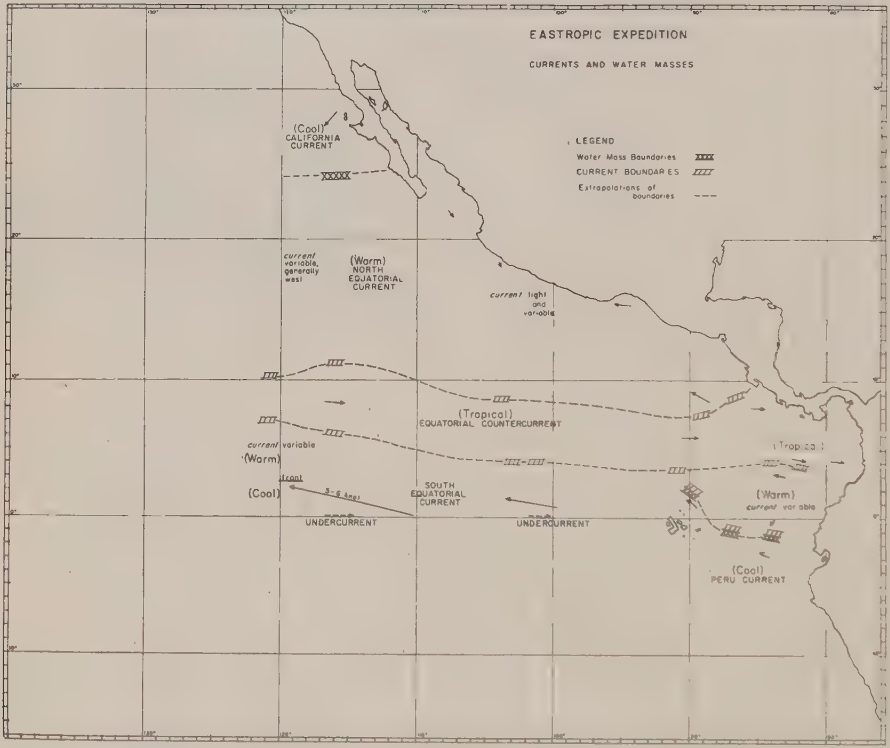
EASTROPIC EXPEDITION
CURRENTS AND WATER MASSES
LEGEND
Water Mass Boundaries XXXX
CURRENT BOUNDARIES ////
Extrapolations of boundaries ---
(Cool) CALIFORNIA CURRENT
current variable, generally west
(Warm) NORTH EQUATORIAL CURRENT
current light and variable
(Tropical) EQUATORIAL COUNTERCURRENT
current variable
(Warm)
front
(Cool)
3-6 knots
SOUTH EQUATORIAL CURRENT
UNDERCURRENT
UNDERCURRENT
(Tropical)
(Warm)
current variable
(Cool) PERU CURRENT
130°
120°
110°
100°
90°
80°
30°
20°
10°
0°
10°

Figure 1. Currents and water masses in the Eastern Tropical Pacific encountered on the "Eastropic" cruise.

Figura 1. Corrientes y masas de agua en el Pacífico Oriental Tropical, encontradas durante la Expedición Eastropic.

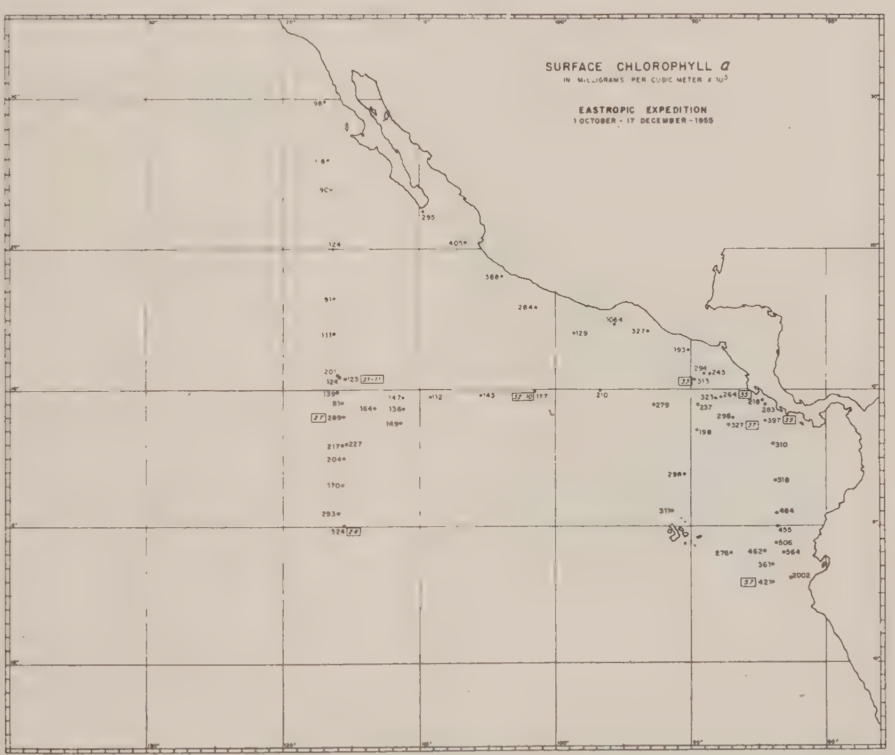
SURFACE CHLOROPHYLL a
IN MILLIGRAMS PER CUBIC METER x 10^3
EASTROPIC EXPEDITION
1 OCTOBER - 17 DECEMBER - 1955
98
90
295
124
405
388
91
284
129
1064
327
111
193
201
124
125
294
243
313
139
81
147
164
136
112
143
177
210
279
323
264
218
237
283
289
149
298
327
397
198
217
227
310
204
170
298
318
293
311
484
324
455
506
276
462
564
361
2002
421

Figure 2. Surface chlorophyll "a," in milligrams per 1000 m^3, at various locations, and positions of stations (station numbers in squares) at which were made sub-surface measurements of chlorophyll and C^{14} uptake.

Figura 2. Clorofila "a" de aguas superficiales, en miligramos por 1000 m^3, en varias localidades, y posición de las estaciones (cuyos números aparecen dentro de cuadrados) en donde se hicieron mediciones de la clorofila en aguas subsuperficiales y de la asimilación de C^{14}.

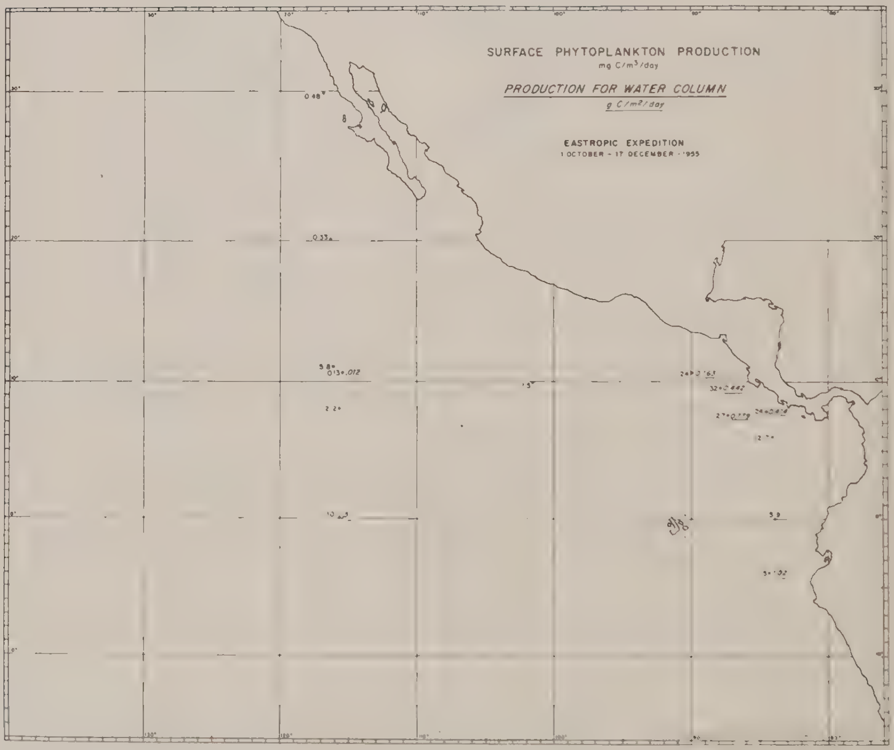
SURFACE PHYTOPLANKTON PRODUCTION
mg C/m³/day
PRODUCTION FOR WATER COLUMN
g C/m²/day
EASTROPIC EXPEDITION
1 OCTOBER - 17 DECEMBER - 1955
0.48
8
0.33
5.8
0.13 .012
2.2
5.9

Figure 3. Surface phytoplankton production in mgC/m³/day, and total production in water column in gC/m²/day (latter underlined).

Figura 3. Producción de fitoplancton en aguas superficiales, en mgC/m³/día, y producción total en la columna de agua en gC/m²/día (los valores de esta última son los subrayados).

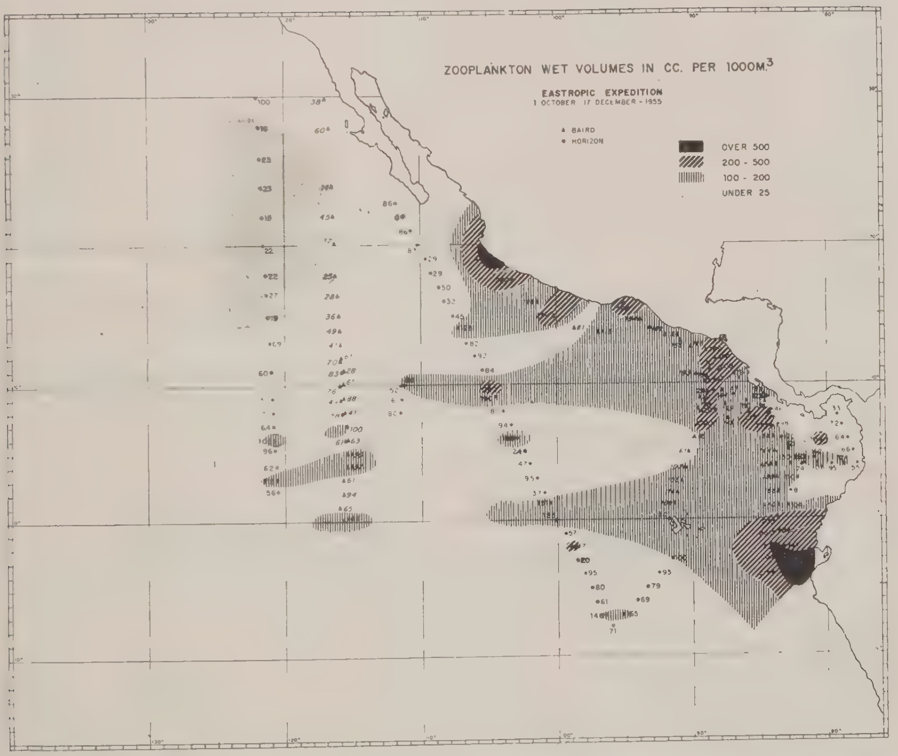
ZOOPLANKTON WET VOLUMES IN CC. PER 1000M.³
EASTROPIC EXPEDITION
1 OCTOBER - 17 DECEMBER - 1955
▲ BAIRD
● HORIZON
OVER 500
200 - 500
100 - 200
UNDER 25

Figure 4. Locations of hydrographic stations occupied by the vessels *Baird* and *Horizon*, with the zooplankton volumes at each. Contours drawn for high volumes (over 100 cc/1000 m^3) and low volumes (under 25 cc/1000 m^3). Unshaded region represents volumes between 25 and 100 cc/1000 m^3.

Figura 4. Localización de las estaciones hidrográficas establecidas por los barcos *Baird* y *Horizon*, con indicación de los volúmenes de zooplancton en cada una. Se han dibujado los contornos de los altos volúmenes (sobre 100 cc/1000 m^3) y de los bajos volúmenes (menos de 25 cc/1000 m^3). En la región no sombreada se encuentran los valores entre 25 y 100 cc/1000 m^3.

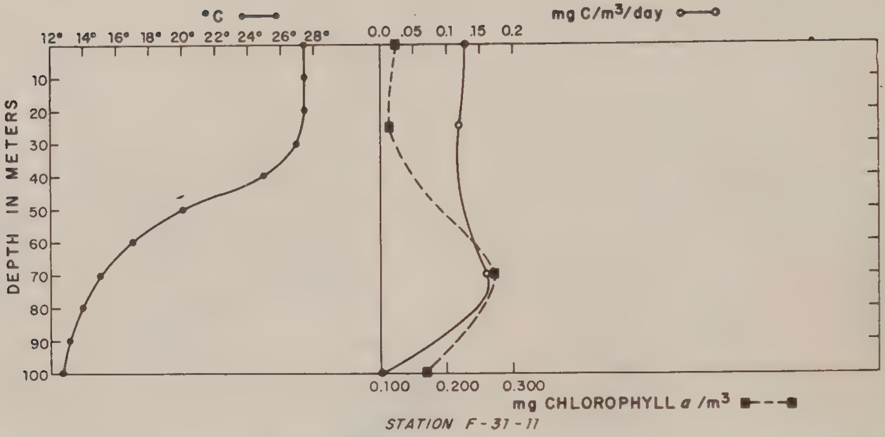

Figure 5. Vertical distributions of chlorophyll "a," C^{14} uptake, and temperature at Station F-31-11.

Figura 5. Distribuciones verticales de la clorofila "a", de la asimilación de C^{14} y de la temperatura en la Estación F-31-11.

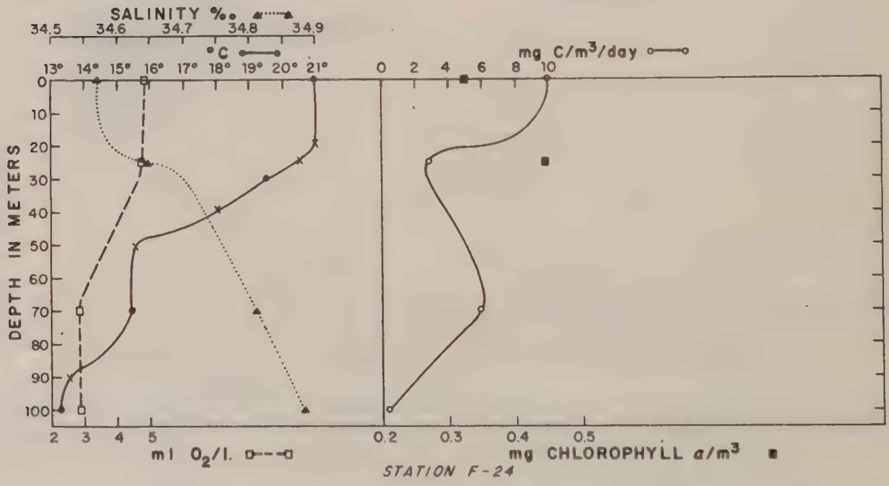

Figure 6. Vertical distributions of chlorophyll "a," C^{14} uptake, temperature, salinity, and oxygen at Station F-24.

Figure 6. Distribuciones verticales de la clorofila "a", de la asimilación de C^{14}, y de la temperatura, salinidad y oxígeno en la Estación F-24.

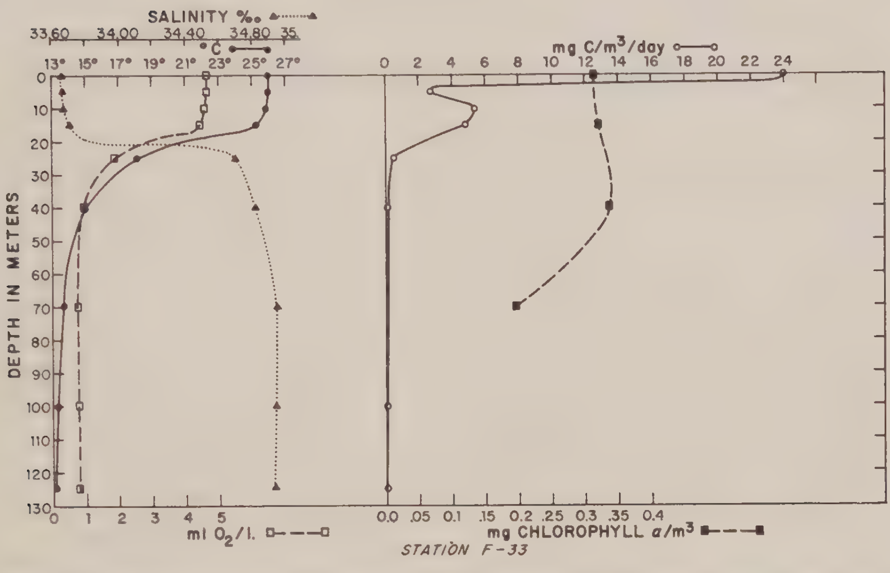

Figure 7. Vertical distributions of chlorophyll "a," C^{14} uptake, temperature, salinity, and oxygen at Station F-33.

Figura 7. Distribuciones verticales de la clorofila "a", de la asimilación de C^{14}, y de la temperatura, salinidad y oxígeno en la Estación F-33.

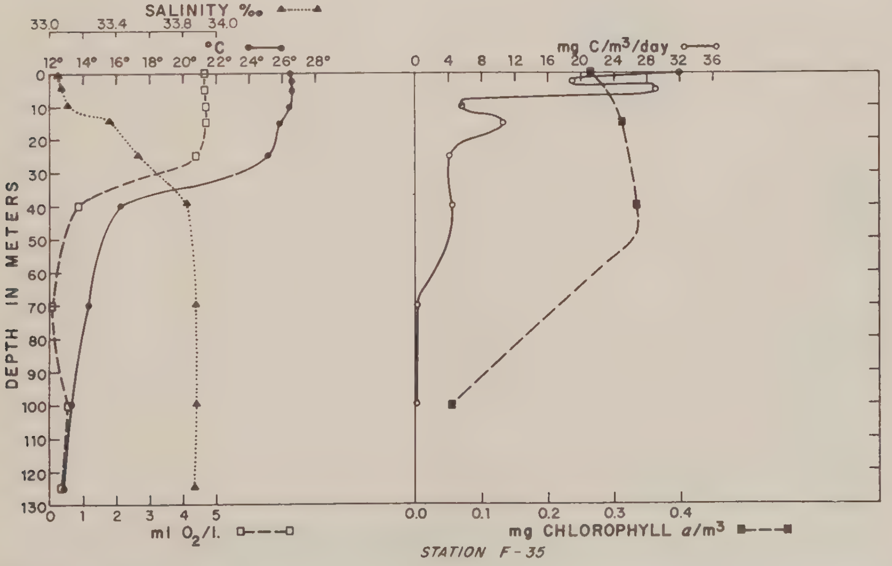

Figure 8. Vertical distributions of chlorophyll "a," C^{14} uptake, temperature, salinity, and oxygen at Station F-35.

Figura 8. Distribuciones verticales de la clorofila "a", de la asimilación de C^{14} y de la temperatura, salinidad y oxígeno en la Estación F-35.

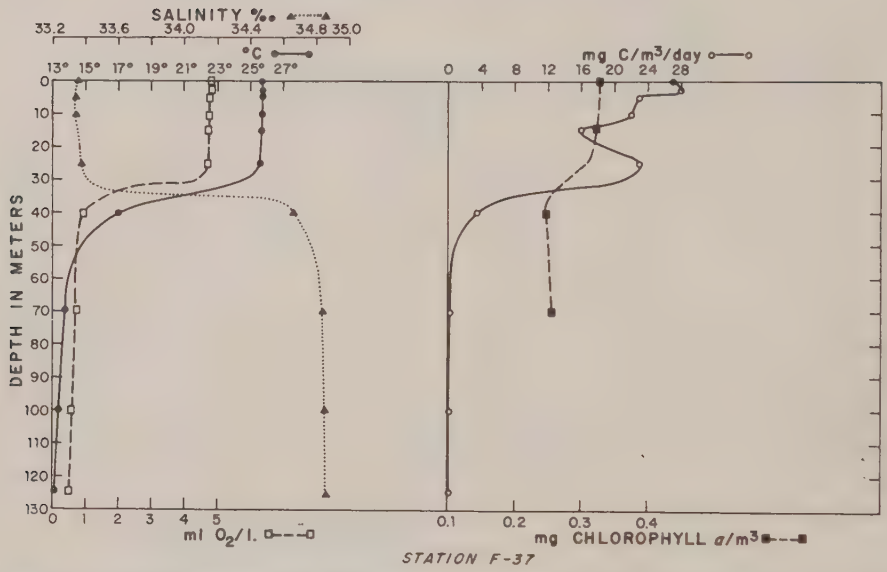

Figure 9. Vertical distributions of chlorophyll "a," C^{14} uptake, temperature, salinity, and oxygen at Station F-37.

Figura 9. Distribuciones verticales de la clorofila "a", de la asimilación de C^{14}, y de la temperatura, salinidad y oxígeno en la Estación F-37.

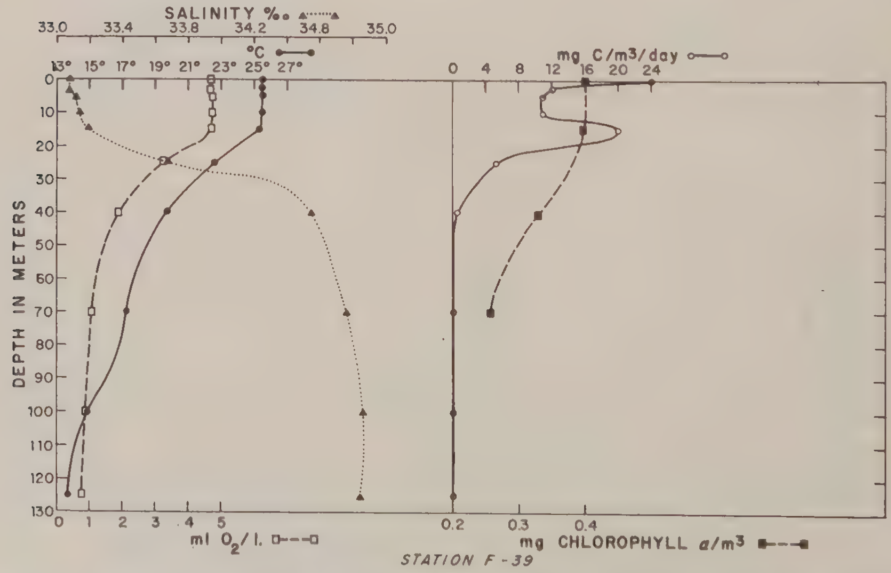

Figure 10. Vertical distributions of chlorophyll "a," C^{14} uptake, temperature, salinity, and oxygen at Station F-39.

Figura 10. Distribuciones verticales de la clorofila "a", de la asimilación de C^{14}, y de la temperatura, salinidad y oxígeno en la Estación F-39.

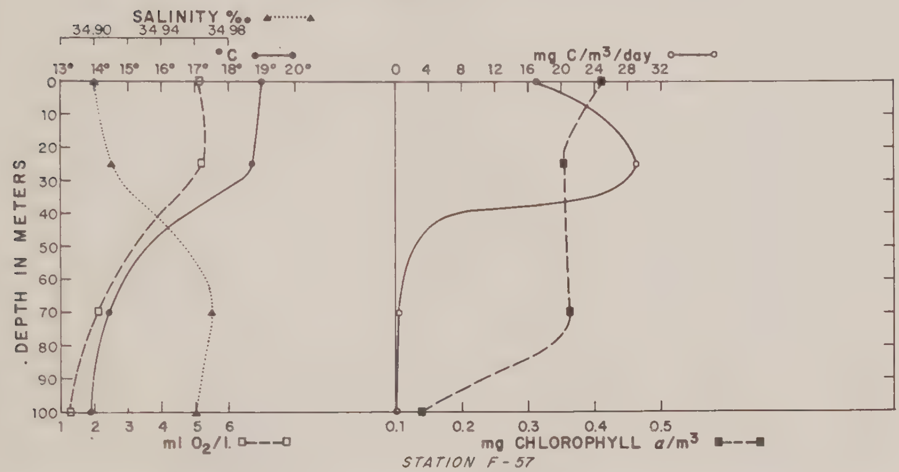

Figure 11. Vertical distributions of chlorophyll "a," C^{14} uptake, temperature, salinity, and oxygen at Station F-57.

Figura 11. Distribuciones verticales de la clorofila "a", de la asimilación de C^{14}, y de la temperatura, salinidad y oxígeno en la Estación F-57.

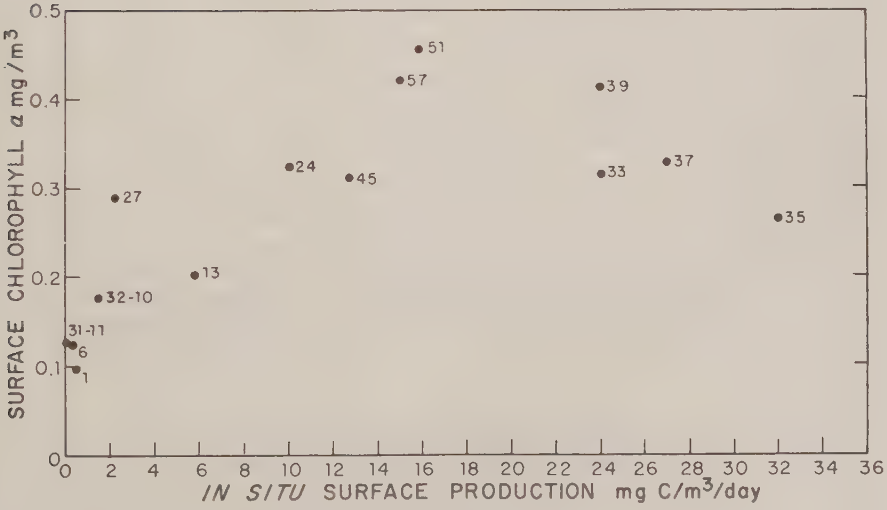

Figure 12. Relationship between *in situ* surface production and surface chlorophyll.

Figura 12. Relación entre la producción *in situ* y la clorofila, ambas de aguas superficiales.

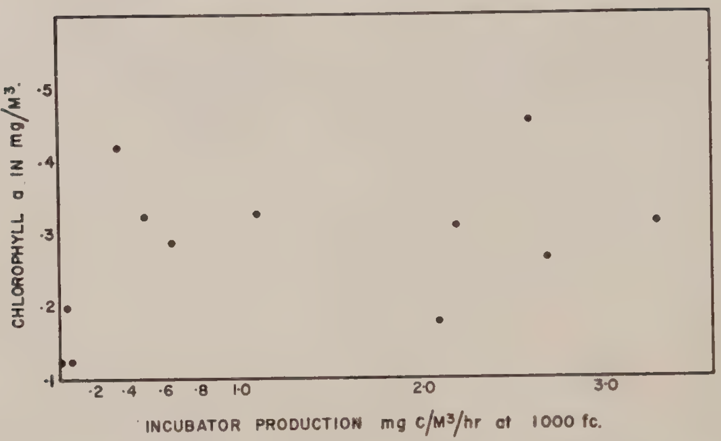

Figure 13. **Relationship between *in vitro* production of surface samples and surface chlorophyll.**

Figura 13. **Relación entre la producción *in vitro* de las muestras de agua superficial y la clorofila de superficie.**

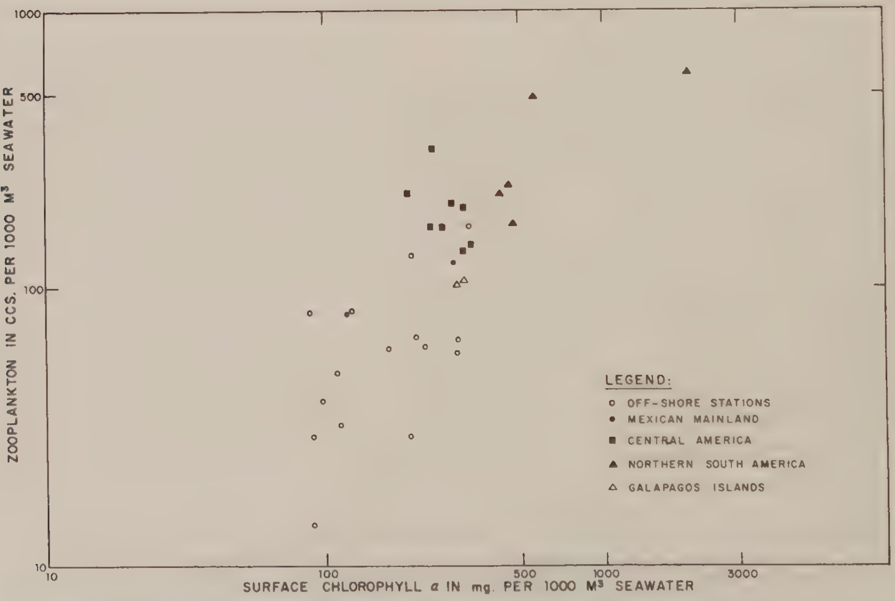

Figure 14. **Relationship between surface chlorophyll and zooplankton volume in water column.**

Figura 14. **Relación entre la clorofila de superficie y el volumen de zooplancton en la columna de agua.**

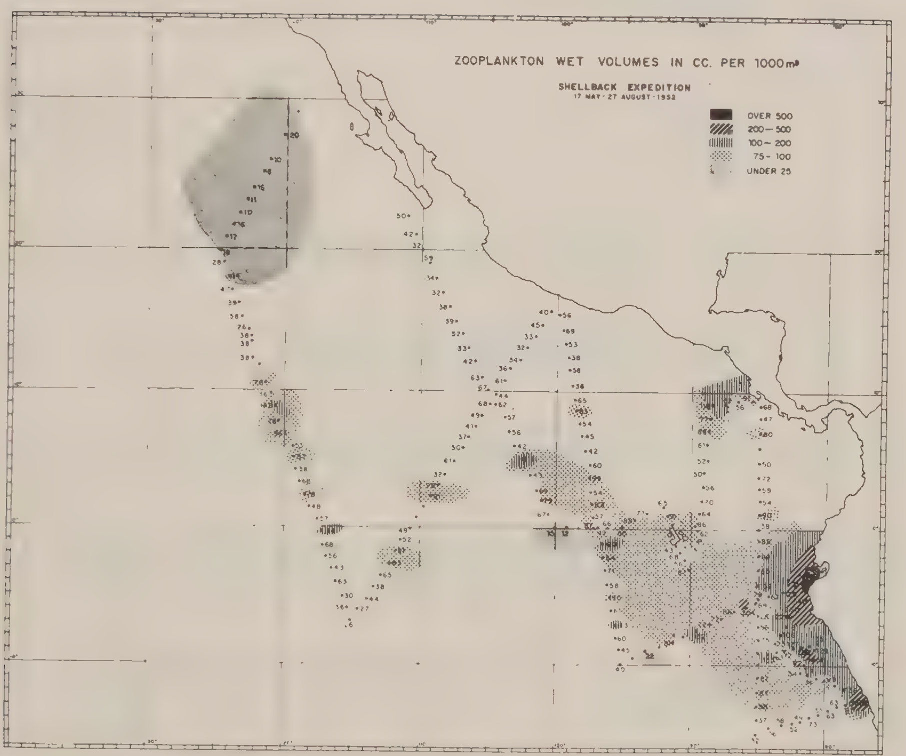
ZOOPLANKTON WET VOLUMES IN CC. PER 1000m³
SHELLBACK EXPEDITION
17 MAY - 27 AUGUST - 1952
OVER 500
200 — 500
100 — 200
75 - 100
UNDER 25

Figure 15. Zooplankton volumes measured by Shellback expedition in summer of 1952.

Figura 15. Volúmenes de zooplancton medidos durante la Expedición Shellback en el verano de 1952.

TABLE 1. Determinations of chlorophyll and primary production at stations of the Eastropic expedition, with related physical and chemical data.

TABLA 1. Determinaciones de la clorofila y de la producción primaria en las estaciones de la Expedición Eastropic, con datos sobre oceanografía física y química.

Station location		Date occupied 1955	Stat. No.	Depth in meters	Temp. °C	Salinity o/oo	Dissolved oxygen ml/l	Primary production in water column gC/m²/day	Primary *in situ* production. mgC/m³/day	Chloro-phyll a. mg/m³	Incubator production. mgC/m³/hr. at 1000 fc.
Localización de la estación		Fecha 1955	Número de la estación	Profundidad en metros	Temp. °C	Salinidad o/oo	Oxígeno disuelto ml/l	Producción primaria en la columna de agua gC/m²/día	Producción primaria *in situ* mgC/m³/día	Clorofila a mg/m³	Producción en la incubadora mgC/m³/hora a 1000 bp.
29°53′N	116°50′W	2 Oct.	1	Surface	19.32	33.65	5.51	......	0.48	0.0976	....
26°00′N	116°43′W	3 Oct.	3	Surface	20.75	33.71	5.29	......	....	0.118	....
24°02′N	116°31′W	4 Oct.	4	Surface	23.21	34.22	4.99	......	....	0.0899	....
20°09′N	116°16′W	5 Oct.	6	Surface	24.52	34.14	4.89	......	0.33	0.124	0.070
16°31′N	116°13′W	6 Oct.	8	Surface	26.90	34.44	4.84	......	....	0.0911	...
14°01′N	116°13′W	7 Oct.	10	Surface	27.07	33.70	4.75	......	....	0.111	....
11°02′N	116°05′W	8 Oct.	13	Surface	27.62	33.76	4.64	......	5.8	0.201	0.043
11°02′N	116°05′W	8 Oct.	13	40 m.	23.70	34.42	4.81	......	....		0.11
9°06′N	115°44′W	9 Oct.	15	Surface	26.69	33.65	4.70	......	....	0.0814	....
9°06′N	115°44′W	9 Oct.	15	40 m.	26.50	33.93	4.64	......	....	0.122	....
5°58′N	115°43′W	10 Oct.	18	Surface	25.89	34.56	4.89	......	....	0.217	....
5°00′N	115°36′W	10 Oct.	19	Surface	23.91	34.30	4.77	......	....	0.204	0.070
3°05′N	115°44′W	11 Oct.	21	Surface	23.61	34.33	4.87	......		0.170	....
0°58′N	116°03′W	12 Oct.	23	Surface	23.01	34.31	4.81	...	...	0.293	.
0°04′N	115°39′W	13 Oct.	24	Surface	20.97	34.57	4.86	0.51	10.	0.324	0.47
0°04′N	115°39′W	13 Oct.	24	25 m.	20.50	34.64	4.78	.....	2.8	0.445	0.47
0°04′N	115°39′W	13 Oct.	24	70 m.	15.40	34.81	2.83	......	5.9	....	1.2
0°04′N	115°39′W	13 Oct.	24	100 m.	13.29	34.88	2.97	...	0.36	....	0.055
6°00′N	115°24′W	17 Oct.	25	Surface	25.85	34.52	..	......		0.227	.
8°02′N	115°40′W	18 Oct.	27	Surface	26.25	33.52	....	......	2.2	0.289	0.62
8°02′N	115°40′W	18 Oct.	27	25 m.	26.4	......	......	......	....	0.178	....
8°02′N	115°40′W	18 Oct.	27	40 m.	26.5	......	......	......	....	0.199	0.0060
10°58′N	115°58′W	19 Oct.	30	Surface	27.30	33.47	......	......	....	0.124	...
9°50′N	115°56′W	20 Oct.	28-3	Surface	27.2	33.34	.	..	..	0.139	.
10°41′N	115°32′W	21 Oct.	31-11	Surface	27.4		.	0.012	0.13	0.125	0.015
10°41′N	115°32′W	21 Oct.	31-11	25 m.	27.2	......	......	......	0.12	0.114	0.017
10°41′N	115°32′W	21 Oct.	31-11	70 m.	15.6	......	......	......	0.16	0.273	0.030
10°41′N	115°32′W	21 Oct.	31-11	100 m.	12.9	......	......	.. .	0.02	0.169	0.0047
8°43′N	113°22′W	22 Oct.	31-22	Surface	26.7	33.16	......	......	....	0.164	....
7°36′N	111°21′W	23 Oct.	A-4	Surface	26.2	33.58	......	......	....	0.149	....
8°39′N	111°12′W	24 Oct.	A-5	Surface	26.5	......	......	......	....	0.136	..
9°29′N	111°12′W	25 Oct.	A-6	Surface	26.4	......	......	......	....	0.147	....
9°31′N	109°27′W	26 Oct.	31-50	Surface	26.4	33.30	......	......	....	0.112	....
9°35′N	105°35′W	27 Oct.		Surface	......	......	......	......	....	0.143	.. .
9°57′N	101°33′W	28 Oct.	32-10	Surface	26.6	33.38	......	......	1.5	0.177	2.1

TABLE 1 CONTINUED

Station location Localización de la estación		Date occupied 1955 Fecha 1955	Stat. No. Número de la estación	Depth in meters Profundidad en metros	Temp. °C Temp. °C	Salinity o/oo Salinidad o/oo	Dissolved oxygen ml/l Oxígeno disuel.o ml/l	Primary production in water column gC/m²/day Producción primaria en la columna de agua gC/m²/día	Primary *in situ* production. mgC/m³/day Producción primaria *in situ* mgC/m³/día	Chloro-phyll a. mg/m³ Clorofila a mg/m³	Incubator production. mgC/m³/hr. at 1000 fc. Producción en la incubadora mgC/m³/hora a 1000 bp.
9°57′N	101°33′W	28 Oct.	32-10	40 m.	18.2	......	......	......	....	0.394	
9°57′N	101°33′W	28 Oct.	32-10	70 m.	13.9	......	......	......	....	0.239	
9°56′N	96°45′W	29 Oct.	32-17	Surface	25.7	33.13	......	......	....	0.210	
8°53′N	92°38′W	30 Oct.	32-26	Surface	25.4	33.26	..	......	....	0.279	
11°05′N	88°58′W	31 Oct.	32-38	Surface	25.8	33.48	......	......	....	0.294	
7°54′N	87°01′W	1 Nov.	32-51	Surface	25.4	33.48	......	......	....	0.298	..
9°21′N	88°08′W	2 Nov.	32-62	Surface	25.7	33.54	.....		....	0.323	..
10°39′N	89°51′W	3 Nov.	33	Surface	26.01	33.66	4.68	0.163	24.	0.313	3.2
10°39′N	89°51′W	3 Nov.	33	2.5 m.	25.99	33.66	4.65	......	..	....	1.1
10°39′N	89°51′W	3 Nov.	33	5 m.	25.97	33.67	4.64	......	2.7	....	0.80
10°39′N	89°51′W	3 Nov.	33	10 m.	25.84	33.68	4.60	......	5.4	....	0.67
10°39′N	89°51′W	3 Nov.	33	15 m.	25.30	33.70	4.46	......	4.8	0.320	0.77
10°39′N	89°51′W	3 Nov.	33	25 m.	18.10	34.70	1.88	......	0.50		0.55
10°39′N	89°51′W	3 Nov.	33	40 m.	15.00	34.82	0.93	......	0.19	0.337	0.45
10°39′N	89°51′W	3 Nov.	33	70 m.	13.67	34.94	0.77	......	...	0.196	0.0065
10°39′N	89°51′W	3 Nov.	33	100 m.	13.33	34.94	0.78	......	0.08	....	0.0055
10°39′N	89°51′W	3 Nov.	33	125 m.	13.10	34.93	0.78	......	0.23	....	0.000
9°27′N	87°53′W	4 Nov.	35	Surface	26.53	33.04	4.68	0.442	32.	0.264	2.7
9°27′N	87°53′W	4 Nov.	35	2.5 m.	26.52	33.06	4.66	......	19.	....	1.3
9°27′N	87°53′W	4 Nov.	35	5 m.	26.51	33.08	4.67	......	29.	....	1.9
9°27′N	87°53′W	4 Nov.	35	10 m.	26.47	33.12	4.69	......	5.6	....	0.65
9°27′N	87°53′W	4 Nov.	35	15 m.	25.96	33.37	4.70	......	10.6	0.312	0.75
9°27′N	87°53′W	4 Nov.	35	25 m.	25.12	33.54	4.41	......,	4.1		0.080
9°27′N	87°53′W	4 Nov.	35	40 m.	16.32	34.82	0.88	......	4.4	0.332	0.75
9°27′N	87°53′W	4 Nov.	35	70 m.	14.18	34.88	0.09	......	0.13	....	0.030
9°27′N	87°53′W	4 Nov.	35	100 m.	13.38	34.89	0.57	......	0.08	0.0543	0.012
9°27′N	87°53′W	4 Nov.	35	125 m.	12.91	34.87	0.45		....		0.006
7°33′N	87°21′W	5 Nov.	37	Surface	25.76	33.35	4.81	0.779	27.	0.327	1.1
7°33′N	87°21′W	5 Nov.	37	2.5 m.	25.75	33.35	4.80	......	28.	....	1.5
7°33′N	87°21′W	5 Nov.	37	5 m.	25.74	33.34	4.78	......	23.	....	1.9
7°33′N	87°21′W	5 Nov.	37	10 m.	25.72	33.34	4.76	......	22.		0.70
7°33′N	87°21′W	5 Nov.	37	15 m.	25.67	33.35	4.77	......	16.	0.324	1.6
7°33′N	87°21′W	5 Nov.	37	25 m.	25.47	33.38	4.75	......	23.	....	1.6
7°33′N	87°21′W	5 Nov.	37	40 m.	16.98	34.66	0.98	......	3.3	0.249	0.72
7°33′N	87°21′W	5 Nov.	37	70 m.	13.69	34.84	0.70	....	0.16	0.256	0.023
7°33′N	87°21′W	5 Nov.	37	100 m.	13.31	34.85	0.58	......	0.056	....	0.017
7°33′N	87°21′W	5 Nov.	37	125 m.	13.07	34.86	0.54	......	0.040	....	0.000
7°51′N	84°34′W	6 Nov.	39	Surface	25.54	33.08	4.68	0.414	24.	0.397	...

TABLE 1 CONTINUED

Station location		Date occupied 1955	Stat. No.	Depth in meters	Temp. °C	Salinity o/oo	Dissolved oxygen ml/l	Primary production in water column gC/m²/day	Primary *in situ* production. mgC/m³/day	Chloro-phyll a. mg/m³	Incubator production. mgC/m³/hr. at 1000 fc.
Localización de la estación		Fecha 1955	Número de la estación	Profundidad en metros	Temp. °C	Salinidad o/oo	Oxígeno disuelto ml/l	Producción primaria en la columna de agua gC/m²/día	Producción primaria *in situ* mgC/m³/día	Clorofila a mg/m³	Producción en la incubadora mgC/m³/hora a 1000 bp.
7°51′N	84°34′W	6 Nov.	39	2.5 m.	25.54	33.08	4.70	......	12.	....	....
7°51′N	84°34′W	6 Nov.	39	5 m.	25.54	33.11	4.71	......	11.	....	....
7°51′N	84°34′W	6 Nov.	39	10 m.	25.53	33.14	4.74	......	11.	....	....
7°51′N	84°34′W	6 Nov.	39	15 m.	25.33	33.18	4.68	......	20.	0.396	....
7°51′N	84°34′W	6 Nov.	39	25 m.	22.65	33.68	3.28	......	5.3	....	....
7°51′N	84°34′W	6 Nov.	39	40 m.	19.70	34.55	1.90	......	0.41	0.329	....
7°51′N	84°34′W	6 Nov.	39	70 m.	17.30	34.76	1.08	......	0.037	0.258	....
7°51′N	84°34′W	6 Nov.	39	100 m.	14.90	34.86	0.86	......	0.028	....	....
7°51′N	84°34′W	6 Nov.	39	125 m.	13.72	34.84	0.74	......	0.000	....	....
9°13′N	84°51′W	7 Nov.	41	Surface	25.82	31.02	5.02	......	....	0.218	....
8°54′N	84°41′W	11 Nov.	42	Surface	26.23	30.89	4.83	......	....	0.283	....
6°04′N	84°09′W	12 Nov.	45	Surface	25.86	32.99	4.69	......	12.7	0.310	2.2
3°20′N	83°53′W	13 Nov.	47-2	Surface	24.8	33.52	......	......	....	0.318	....
0°57′N	83°49′W	14 Nov.	50	Surface	24.27	33.68	4.83	......	....	0.484	....
0°00′	83°47′W	15 Nov.	51	Surface	22.27	33.82	4.88	......	15.9	0.455	2.6
1°13′S	83°51′W	16 Nov.	52-1	Surface	17.7	34.83	......	......	....	0.506	....
3°42′S	83°06′W	17 Nov.	55	Surface	18.02	34.83	5.80	......	lost	2.00	18.
1°59′S	83°20′W	21 Nov.	56	Surface	20.35	33.90	4.97	......	....	0.564	....
2°48′S	84°12′W	21 Nov.	A-11	Surface	18.7	......	......	......	....	0.361	....
4°03′S	84°11′W	23 Nov.	57	Surface	18.98	34.90	5.11	1.02	15.	0.421	0.33
4°03′S	84°11′W	23 Nov.	57	25 m.	18.73	34.91	5.18	......	29.	0.354	4.0
4°03′S	84°11′W	23 Nov.	57	70 m.	14.40	34.97	2.10	......	0.40	0.361	0.081
4°03′S	84°11′W	23 Nov.	57	100 m.	13.89	34.96	1.26	......	0.047	0.142	0.019
1°48′S	84°46′W	23 Nov.	227	Surface	......	......	......	......	....	0.462	....
1°57′S	87°13′W	24 Nov.	W-1	Surface	......	......	......	......	....	0.276	....
1°06′N	91°31′W	28 Nov.	59	Surface	22.65	33.95	4.72	......	....	0.311	....
3°49′N	90°37′W	29 Nov.	62	Surface	25.66	33.43	4.75	......	....	0.298	....
7°01′N	89°39′W	30 Nov.	65	Surface	26.57	33.21	4.86	......	....	0.198	....
8°53′N	89°35′W	1 Dec.	67	Surface	24.96	33.94	4.22	......	....	0.237	....
11°02′N	88°46′W	2 Dec.	69	Surface	26.97	32.71	......	......	....	0.243	....
12°51′N	90°17′W	7 Dec.	77-1	Surface	27.6	33.28	......	......	....	0.193	....
14°11′N	93°15′W	8 Dec.	80-1	Surface	28.2	33.66	......	......	....	0.327	....
14°41′N	95°42′W	9 Dec.	....	Surface	......	......	......	......	....	1.06	....
14°02′N	98°42′W	10 Dec.	87	Surface	28.20	33.40	......	......	....	0.129	....
15°58′N	101°31′W	11 Dec.	89	Surface	27.31	33.89	......	......	....	0.284	....
18°07′N	104°03′W	12 Dec.	317	Surface	......	......	......	......	....	0.388	....
20°29′N	106°40′W	13 Dec.	91-4	Surface	24.2	......	......	......	....	0.405	....
22°40′N	109°41′W	14 Dec.	....	Surface	......	......	......	......	....	0.295	....

TABLE 2. Eastropic Expedition — *Spencer F. Baird* **Plankton collections.**

TABLA 2. Expedición Eastropic — Recolecciones de plancton del *Spencer F. Baird.*

Station	Position		Date 1955	Time (local)		Vol. water strained in m^3	Depth of haul in meters	Volume per 1000 M^3 strained	
	Latitude	W. Long.		Start	End			Total cc.	Small Org. cc.
Estación	Posición		Fecha 1955	Hora (local)		Volumen de agua colada en m^3	Profundidad del arrastre en metros	Volumen por cada 1000 m^3 de agua	
	Latitud	Long. O.		Emp.	Term.			Total en cc.	Pequeños org. en cc.
F- 1	29°50′N	116°55′	2 Oct.	1121	1154	1056	293	66	38
2	27°54′N	116°47′	3 "	0036	0108	916	330	306	60
4	24°02′N	116°31′	4 "	0921	0953	1053	305	14	14
5	22°00′N	116°23′	5 "	0021	0054	900	333	45	45
6	20°09′N	116°16′	5 "	1236	1308	952	330	32	32
7	17°56′N	116°12′	6 "	0231	0303	1000	317	197	25
8	16°31′N	116°13′	6 "	1351	1423	901	380	23	28
9	15°03′N	116°14′	7 "	0026	0058	978	312	36	36
10	14°01′N	116°13′	7 "	0851	0923	1026	291	215	49
11	13°00′N	116°11′	7 "	1806	1838	972	303	92	41
12	12°05′N	116°09′	8 "	0151	0232	902	308	61	61
13	11°02′N	116°05′	8 "	1221	1253	889	330	28	28
14	10°01′N	115°55′	8 "	1921	1953	926	310	82	76
15	9°06′N	115°44′	9 "	0501	0533	1029	308	97	88
16	8°00′N	115°37′	9 "	1351	1443	967	331	48	41
17	7°02′N	115°40′	9 "	2226	2259	1099	301	200	100
18	5°58′N	115°43′	10 "	0821	0853	1194	331	63	63
19	5°00′N	115°36′	10 "	1841	1913	960	325	153	130
20	4°04′N	115°35′	11 "	0851	0423	1392	194	137	137
21	3°05′N	115°44′	11 "	1236	1308	825	321	61	61
22	2°00′N	115°41′	11 "	2151	2223	904	299	94	94
23	0°58′N	116°03′	12 "	0706	0738	1488	168	239	65
24	0°04′N	115°39′	12 "	2221	2253	752	300	511	166
25	6°00′N	115°24′	17 "	1521	1553	990	322	61	61
27	8°02′N	115°40′	18 "	0751	0823	942	297	58	58
28	9°03′N	115°48′	18 "	1722	1754	1031	314	49	49
29	9°58′N	115°58′	19 "	0051	0123	978	325	61	61
30	10°58′N	115°58′	19 "	0822	0854	1032	308	126	83
31	11°41′N	115°59′	19 "	1451	1523	927	325	70	70
33	10°39′N	89°51′	3 Nov.	0951	1032	986	293	193	193
34	10°03′N	88°52′	3 "	2106	2138	1026	309	195	195
35	9°27′N	87°53′	4 "	1021	1053	948	323	164	164
36	8°24′N	87°37′	4 "	2321	2332	946	319	195	195
37	7°33′N	87°21′	5 "	0850	0923	980	307	161	143
38	7°47′N	85°45′	5 "	2221	2253	867	318	238	225
40	8°39′N	84°46′	6 "	2051	2123	1067	286	38	38
42	8°54′N	84°42′	11 "	0851	0922	957	296	199	199
43	7°53′N	84°32′	11 "	1651	1723	1120	254	246	246
44	6°54′N	84°21′	12 "	0121	0153	951	314	253	253
45	6°04′N	84°09′	12 "	0921	0952	919	314	136	136

TABLE 2 CONTINUED

	Position		Date 1955	Time (local)		Vol. water strained in m^3	Depth of haul in meters	Volume per 1000 M^3 strained	
Station	Latitude	W. Long.		Start	End			Total cc.	Small Org. cc.
	Posición		Fecha 1955	Hora (local)		Volumen de agua colada en m^3	Profundidad del arrastre en metros	Volumen por cada 1000 m^3 de agua	
Estación	Latitud	Long. O.		Emp.	Term.			Total en cc.	Pequeños org. en cc.
46	5°02′N	84°03′	12 Nov.	1821	1853	1007	298	144	144
47	4°02′N	83°56′	13 "	0306	0338	977	336	128	128
48	3°02′N	83°51′	13 "	1050	1123	941	306	159	159
49	1°59′N	83°50′	13 "	1851	1923	1085	267	166	166
50	0°58′N	83°49′	14 "	0221	0254	972	318	170	170
51	0°00′	83°47′	14 "	2011	2023	989	280	233	233
52	0°58′S	83°50′	16 "	0251	0323	753	312	302	292
53	2°02′S	83°52′	16 "	1151	1223	578	348	571	571
54	2°54′S	83°35′	16 "	2051	2123	811	314	554	554
55	3°42′S	83°06′	17 "	0521	0553	612	314	621	605
56	1°59′S	83°20′	20 "	2051	2123	772	293	486	486
57	4°03′S	84°11′	22 "	1721	1753	868	289	219	219
58	0°00′	91°41′	27 "	2206	2238	960	296	130	130
59	1°06′N	91°31′	28 "	0651	0723	1012	318	121	109
60	1°58′N	91°17′	28 "	1436	1508	1230	225	114	114
61	2°51′N	90°52′	28 "	2321	2353	953	293	105	105
62	3°49′N	90°37′	29 "	0736	0808	1018	274	103	103
63	5°00′N	90°20′	29 "	1621	1653	1235	300	82	61
64	6°05′N	89°57′	30 "	0251	0323	1018	306	95	95
65	7°02′N	89°39′	30 "	1051	1123	1221	292	220	220
66	8°03′N	89°43′	30 "	2206	2238	970	306	172	172
67	8°54′N	89°36′	1 Dec.	0851	0923	957	298	167	167
68	10°02′N	89°07′	1 "	1951	2023	972	298	463	463
69	11°02′N	88°46′	2 "	0621	0653	1068	263	314	314
70	11°48′N	88°25′	2 "	1836	1908	885	302	300	300
76	12°24′N	89°06′	6 "	2221	2353	986	302	305	289
77	12°44′N	90°01′	7 "	0521	0553	1016	297	128	128
78	13°05′N	90°54′	7 "	1306	1338	946	309	153	153
79	13°31′N	92°02′	7 "	2051	2123	896	363	141	134
80	14°05′N	93°05′	8 "	0521	0553	961	305	182	182
81	14°39′N	93°55′	8 "	1251	1323	979	301	209	194
82	15°48′N	95°03′	8 "	2255	2313	583	152	309	298
85	13°42′N	97°01′	9 "	1920	1938	1016	153	113	113
87	14°02′N	98°42′	10 "	1751	1823	991	292	81	81
88	14°58′N	100°14′	11 "	0051	0123	946	307	254	254
89	15°58′N	101°32′	11 "	1121	1153	993	298	126	126
90	17°27′N	103°19′	12 "	0321	0353	992	318	282	282
91	19°00′N	104°57′	12 "	1921	1953	990	293	515	515

TABLE 3. Eastropic Expedition — *Horizon* Plankton collections.

TABLA 3. Expedición Eastropic — Recoleciones de plancton del *Horizon*.

Station	Position		Date 1955	Time (local)		Vol. water strained in M³	Depth of Haul in Meters	Volume per 1000 m³ Strained	
	Latitude	W. Long.		Start	End			Total cc.	Small org. cc.
Estación	Posición		Fecha 1955	Hora (local)		Volumen de agua colada en M³	Profundidad del arrastre en metros	Volumen por cada 1000 M³ de agua	
	Latitud	Long. O.		Emp.	Term.			Total en cc.	Pequeños org. en cc.
H- 1	29°56′N	121°59′	2 Oct.	2111	2143	905	322	100	100
2	28°03′N	121°49′	3 "	0911	0943	903	311	348	16
3	25°58′N	121°48′	4 "	0051	0122	872	288	23	23
4	24°00′N	121°41′	4 "	1611	1643	870	320	23	23
5	22°00′N	121°35′	5 "	0621	0652	671	320	15	15
6	20°00′N	121°31′	5 "	2121	2153	907	324	22	22
7	17°57′N	121°26′	6 "	1141	1213	901	323	22	22
8	16°31′N	121°21′	6 "	2341	0014	738	330	27	27
9	14°58′N	121°15′	7 "	1121	1153	1061	312	19	19
11	13°02′N	121°03′	8 "	0242	0313	870	304	69	69
13	11°00′N	120°56′	8 "	2141	2213	835	305	88	60
15	9°00′N	120°48′	9 "	1321	1352	861	313	52	52
16	8°00′N	120°47′	9 "	2221	2253	720	309	77	77
17	7°00′N	120°46′	10 "	0841	0912	1020	322	64	64
18	6°01′N	120°46′	10 "	1701	1733	814	331	105	105
19	5°21′N	120°31′	11 "	0211	0252	833	307	127	96
20	4°01′N	120°40′	11 "	1331	1404	975	302	183	62
21	3°01′N	120°32′	12 "	0011	0043	891	329	218	112
22	2°10′N	120°32′	12 "	0901	0933	539	223	705	56
23	9°58′N	111°28′	23 "	1221	1254	1061	277	52	52
24	9°00N′	111°25′	23 "	2121	2153	907	295	61	61
25	8°00′N	111°33′	24 "	0911	0944	809	306	80	80
27	10°00′N	111°08′	25 "	2231	2303	866	292	129	116
29	7°54′N	89°15′	3 Nov.	1501	1533	880	280	205	205
30	9°29′N	88°25′	4 "	0521	0554	718	290	286	286
31	10°52′N	88°02′	4 "	1911	1944	1027	292	209	209
32	10°17′N	86°33′	5 "	1101	1123	1060	266	179	179
33	9°12′N	87°06′	5 "	2221	2254	885	295	147	147
34	8°41′N	86°00′	6 "	1651	1723	1192	281	189	191
35	9°01′N	84°32′	10 "	1521	1553	991	306	187	126
36	7°58′N	84°10′	10 "	2351	0023	1047	279	86	86
37	6°55′N	83°38′	11 "	011	1043	1070	260	145	98
38	5°55′N	83°26′	11 "	1801	1834	1045	281	120	120
39	5°07′N	82°52′	12 "	0250	0323	1031	320	121	121
40	4°02′N	82°48′	12 "	1131	1204	926	320	130	130
41	4°03′N	81°45′	12 "	2051	2124	1081	295	153	153
42	4°03′N	80°46′	13 "	0531	0604	1038	286	106	106
43	4°02′N	79°46′	13 "	1411	1443	1155	269	95	95
44	4°03′N	78°47′	13 "	2151	2223	809	329	124	124
45	4°05′N	77°45′	14 "	1000	1033	1279	228	55	55
46	5°00′N	78°09′	14 "	1811	1844	1144	302	66	66
47	5°49′N	78°31′	15 "	0641	0713	937	275	64	64
48	6°52′N	78°54′	15 "	1711	1744	1117	271	92	72
49	7°42′N	79°20′	16 "	0126	0143	888	130	130	33
52	5°43′N	80°31′	19 "	1436	1509	1068	258	225	225

TABLE 3 CONTINUED

Station	Position		Date 1955	Time (local)		Vol. water strained in M³	Depth of Haul in Meters	Volume per 1000 m³ Strained	
	Latitude	W. Long.		Start	End			Total cc.	Small org. cc.
Estación	Posición		Fecha 1955	Hora (local)		Volumen de agua colada en M³	Profundidad del arrastre en metros	Volumen por cada 1000 M³ de agua	
	Latitud	Long. O.		Emp.	Term.			Total en cc.	Pequeños org. en cc.
53	4°37′N	81°02′	20 Nov.	0201	0234	801	293	462	162
54	4°08′N	81°48′	20 "	1222	1253	946	296	74	74
55	3°01′N	82°15′	21 "	0022	0053	1003	242	110	110
56	2°03′N	82°45′	21 "	0931	1004	985	252	81	81
57	0°57′N	82°57′	21 "	1741	1813	1155	236	104	104
59	1°02′S	84°05′	22 "	0052	0123	913	276	261	261
61	2°56′S	91°32′	29 "	1021	1032	901	240	266	100
62	3°59′S	92°27′	29 "	1931	2003	698	324	3678	93
63	5°00′S	93°19′	30 "	0521	0553	726	281	258	79
64	6°00′S	94°13′	30 "	1521	1553	728	307	69	69
65	7°00′S	95°08′	1 Dec.	0131	0202	789	298	165	165
66	7°53′S	96°00′	1 "	1121	1153	637	313	71	71
67	7°00′S	96°33′	2 "	0311	0343	710	305	148	148
68	6°02′S	97°10′	2 "	1231	1305	822	366	61	61
69	5°00′S	97°30′	2 "	2001	2033	876	286	434	80
70	4°01′S	98°03′	3 "	0421	0453	788	281	95	95
71	3°00′S	98°37′	3 "	1232	1303	991	256	308	20
72	1°59′S	99°05′	3 "	2101	2134	808	298	4253	217
73	0°58′S	99°28′	4 "	0651	0723	788	307	953	57
74	0°00′	100°03′	4 "	1621	1653	811	306	142	123
75	1°14′N	100°34′	7 "	0011	0044	797	312	151	151
76	2°01′N	101°00′	7 "	0812	0844	958	307	37	37
77	3°03′N	101°35′	7 "	1851	1923	739	325	95	95
78	4°08′N	102°02′	8 "	0411	0444	847	283	47	47
79	5°05′N	102°26′	8 "	1142	1213	839	318	24	24
80	6°00′N	102°58′	8 "	2001	2034	799	291	250	188
81	6°59′N	103°25′	9 "	0441	0513	908	272	94	94
82	8°00′N	104°00′	9 "	1421	1452	812	293	80	80
83	9°03′N	104°34′	10 "	0001	0033	790	230	311	190
84	10°00′N	105°05′	10 "	0711	0744	763	277	242	242
85	10°59′N	105°35′	10 "	1514	1542	835	252	84	84
86	12°01′N	105°59′	10 "	2311	2343	818	310	92	92
87	13°00′N	106°38′	11 "	0831	0903	920	289	112	82
88	14°04′N	107°13′	11 "	1651	1724	875	272	268	126
89	14°58′N	107°37′	12 "	0052	0124	788	299	273	45
90	16°00′N	108°09′	12 "	0921	0953	929	241	32	32
91	17°00′N	108°38′	12 "	1721	1753	903	308	50	50
92	18°02′N	109°12′	13 "	0102	0132	875	243	29	29
93	19°01′N	109°40′	13 "	0851	0923	868	261	29	29
94	20°00′N	110°15′	13 "	1641	1713	787	285	128	83
95	21°00′N	110°38′	14 "	0121	0152	819	270	86	86
96	22°00′N	111°09′	14 "	0831	0903	729	296	357	0
97	22°56′N	111°43′	14 "	1631	1703	814	277	161	86

PRODUCCION PRIMARIA, CLOROFILA, Y VOLUMENES DEL ZOOPLANCTON EN LA ZONA TROPICAL DEL OCEANO PACIFICO ORIENTAL[1]

por

Robert W. Holmes[2], Milner B. Schaefer[2, 3], y Bell M. Shimada[3]

Entre el 1°. de octubre y el 17 de diciembre de 1955, a bordo de los barcos *Horizon* y *Spencer F. Baird,* de la Institución Scripps de Oceanografía de la Universidad de California, se hicieron investigaciones sobre la oceanografía física, química y biológica del Océano Pacífico Oriental, en una región limitada aproximadamente por los 30° N. de latitud, 9° S. de latitud, 120° O. de longitud y la costa continental. Estas investigaciones fueron parte de una operación que se realizó cooperativamente y a la que se convino darle el nombre codificado de "Eastropic". En ella, durante el mismo período, una embarcación del Servicio de Pesca y Vida Silvestre de los Estados Unidos (U. S. Fish and Wildlife Service) trabajó más hacia el oeste, y un barco de la armada peruana más hacia el sur, frente a la costa del Perú. También colaboró una nave del Laboratorio de Pesquerías del Estado de California (California State Fisheries Laboratory), realizando algunas operaciones de pesca de atún en aguas subsuperficiales, y otros estudios en la misma región general que recorrieron las embarcaciones de Scripps.

Además de efectuar estudios especiales relacionados con las características oceanográficas particulares de la región, las naves de Scripps establecieron un buen número de estaciones hidrográficas. La localización de estas estaciones se indica en la Figura 4 y en las Tablas 2 y 3; en cada una de ellas se hicieron rastreos con redes planctónicas para recoger muestras de zooplancton. En algunas de las estaciones hidrográficas, así como en algunos lugares entre estaciones, en el *Spencer F. Baird* se hicieron mediciones de la clorofila "a" y de la producción primaria (mediante la técnica del C^{14}), tanto *in situ* como en una incubadora instalada a bordo. El propósito del presente trabajo es dar a conocer los resultados de estas observaciones biológicas.

Los autores desean expresar su gratitud a los Drs. Francis T. Haxo y William H. Thomas y al Sr. Elmer Squier, por su asesoramiento y ayuda en la construcción de la incubadora que se instaló a bordo.

---

[1] Contribución de la Institución Scripps de Oceanografía, Nueva Serie No. 942. El presente estudio abarca, en parte, los resultados de la investigación efectuada por la Universidad de California bajo contrato con la Oficina de Investigación Naval.

[2] Institución Scripps de Oceanografía.

[3] Comisión Interamericana del Atún Tropical.

METODOS PARA LA DETERMINACION DE LA CLOROFILA, DE LA PRODUCCION PRIMARIA Y DE LA CANTIDAD DE ZOOPLANCTON

Clorofila "a"

Las muestras de agua de la superficie, para la determinación de la clorofila, fueron recolectadas con un cubo plástico tanto en las estaciones hidrográficas como durante la travesía. En las estaciones se usó un recipiente de lucite Van Dorn (1956) para la recolección de muestras subsuperficiales. El agua de las muestras (8.3 litros, y en algunas áreas ricas 4.1 l.) se filtró por uno o dos filtros Millipore de 47-mm., tipo HA, después de agregarle una pequeña cantidad de carbonato de magnesio. La clorofila fué extraída de cada filtro con 3 mls. de acetona al 90% (grado reactivo) al frío (*ca.* 10° C.) y en la obscuridad durante 10 horas aproximadamente. El material extraído de cada muestra fué entonces centrifugado hasta aclararlo y decantado en un frasco volumétrico de 10 ml. Con el precipitado que quedó en el tubo de la centrífuga se hizo una nueva suspensión en 3 mls. de acetona al 90%, la cual fué centrifugada otra vez y el líquido resultante se combinó con el obtenido previamente. El extracto fué diluído entonces a 10 mls., y su densidad óptica medida en una célula de semi-micro absorción de 10 cm., a 750, 665, 645 y 635 mμ, con un espectrofotómetro de Beckman modelo DU. Las correcciones de turbiedad se hicieron a base de la trasmisión a 750 mμ. y las concentraciones de clorofila "a" fueron calculadas por la ecuación de Richards y Thompson (1952) y aparecen en la Tabla 1.

Producción primaria

El método del C^{14} fué empleado en este estudio para determinar la proporción de la fijación del carbón por el fitoplancton. Siguiendo el precedente sentado por Ryther (1956b) hemos considerado la tasa de la asimilación de C^{14} como sinónimo del término "producción primaria".

La solución C^{14} fué preparada en la forma descrita por Steeman-Nielsen (1952), con la excepción de que se usó, como solvente para el $Na_2C^{14}0_3$, agua redestilada en aparatos de vidrio en vez de agua artificial de mar. Se prepararon dos soluciones: una conteniendo aproximadamente 100 μC/ml. (que se empleó en las Estaciones 1 a 41 inclusive), y la otra con 20 μC/ml. (usada en las Estaciones 45 a 57 inclusive). Alícuotas de 1 ml. de estas soluciones se envasaron en ampolletas de la misma medida (1 ml.), las cuales sin dilacion fueron selladas y cerradas herméticamente. La técnica de regularización aplicada fué la misma de Steeman-Nielsen (1952), pero se usaron filtros Millipore en vez de filtros de colodión.

Los estudios *in situ* se realizaron de la siguiente manera: se recogió una muestra de cada una de las profundidades deseadas por medio del cubo de lucite Van Dorn, poco tiempo antes de amanecer. Las muestras se envasaron en botellas Pyrex de 250 ml. La solución C^{14} fué pasada cuidadosamente de la ampolleta a la muestra de agua con una jeringa hipodérmica provista de aguja, siendo cada ampolleta enjuagada tres veces con el agua de la muestra. Las muestras fueron puestas en el mar otra vez al amanecer, aproximadamente a las mismas profundidades en que fueron recogidas, con la ayuda de una cuerda con pesos en su extremo, sostenida de una boya de cristal de libre flote, de 14 pulgadas de diámetro, forrada de tejido de cuerda y sujeta a una caña de bambú con un banderín en su extremo superior para facilitar su localización a simple vista. La muestra de "superficie" fué sujetada al lado de la boya, apenas debajo de la capa superficial del agua, mediante el amarre de la botella al tejido en que estaba forrada la bola de cristal. El período de incubación se terminó al mediodía. Inmediatamente despues de la incubación, las muestras se pasaron por filtros Millipore (simples) de 47 mm., tipo HA. Los filtros fueron secados exponiéndolos al vapor de HCl concentrado durante 20 minutos, y vueltos a secar con sílice gelatinosa antes de contar. La actividad del filtro fué medida usando un tubo ANTON 1001-T con un medidor Nuclear-Chicago (Mod. 182A).

Los valores de la producción primaria (Tabla 1) fueron calculados de acuerdo con la actividad del filtro, según el procedimiento indicado por Steeman-Nielsen (1952). Estos datos no han sufrido corrección por cualesquiera pérdidas de carbón que pudieran haber ocurrido durante las horas de obscuridad. La producción primaria en la *columna de agua* (gC/m^2/día) fué estimada por integración, con un planímetro, de los suavizados perfiles de producción a profundidad (Figuras 6 a 11), en cada estación.

Las muestras tratadas en la incubadora a bordo, fueron recogidas e inoculadas con C^{14} en la misma forma que las muestras utilizadas en los estudios *in situ*. La temperatura en la incubadora fué mantenida dentro de 1° C de diferencia de la que fué observada en la superficie del mar cuando se recogieron las muestras. La intensidad de la luz a que fueron expuestas las muestras durante un experimento de 4 horas fué casi constante. Al comienzo de la expedición, la intensidad de luz que iluminaba el fondo de los frascos de reacción fué de alrededor de 1100 bujías-pies; la intensidad decreció despaciosamente, conforme se desgastaban las lámparas fluorescentes del tipo de luz de día, y el reflector colocado detrás de las lámparas se tornaba opaco. En consecuencia, las últimas muestras colocadas en la incubadora recibieron una iluminación de sólo 600 bujías-pies. Con el objeto de hacer comparables los resultados de los diferentes experimentos, hemos dado la proporción de carbón alcanzada en términos de mgC/m^3/hr. a una intensidad de 1000 bujías-pies. Esta intensidad fué seleccionada como una alta luminosidad, que se consideró por debajo de la que podría causar saturación y que, sin embargo, se encuentra todavía en la porción linear de la curva en que la fotosíntesis está en relación con la intensidad de la luz. La intensidad promedio a que fué sometida la población vegetal fué algo menor de 1000 bujías-pies, si se toma en cuenta la disminución en intensidad hacia el cuello de la botella.

Cuando no se hicieron series verticales de observaciones, la producción primaria superficial *in situ* se determinó mediante las muestras sacadas de la superficie del mar con un cubo plástico a la salida del sol o pocos momentos antes. Las muestras fueron envasadas en botellas Pyrex, inoculadas con C^{14}, y remolcadas hasta mediodía por la popa del barco de modo que quedaran justamente bajo la superficie. El tratamiento posterior de las muestras fué idéntico al que se describió anteriormente con respecto a las series verticales *in situ.* Los resultados se dan a conocer como mgC/m^3/día, en la Tabla 1.

Las muestras recogidas para la determinación de la producción primaria fueron duplicadas muy pocas veces, y no se intentó un estudio completo de la variabilidad causada por el muestreo. Sin embargo, en seis estaciones (Nos. 6, 13, 19, 32-10, 45 y 55) se recogieron dos muestras del mismo cubo de agua superficial, y los resultados de su C^{14} determinación fueron medidos después de la incubación a bordo. También fueron tomadas dos muestras del mismo cubo en la Estación 1, las cuales fueron incubadas en botellas que se remolcaron por la popa de la embarcación. En cuatro de los siete casos, los duplicados concordaron entre sí dentro de ±10%; en un caso concordaron dentro de ±20%; y en los dos casos restantes el acuerdo fué muy pobre (±100%). Los valores que proporciona la Tabla 1, que se emplean en el curso de este estudio, representan los promedios de los duplicados en las mencionadas estaciones.

No se comprende la razón de esta variabilidad. Hemos encontrado variaciones similares en otras áreas, y el Dr. W. H. Thomas, de la Institución Scripps de Oceanografía, en sus estudios frente al Delta del Río Misisipí en el Golfo de México, ha podido apreciar también una variabilidad similar (comunicación personal). Pareciera que generalmente los resultados de la determinación del C^{14} concuerdan bastante bien en las muestras duplicadas, pero que ocasionalmente el desacuerdo entre ellas es grande; con frecuencia los resultados de las muestras duplicadas discrepan por uno, dos, tres, y aún cuatro factores. Estas aberrancias pueden resultar de la técnica empleada, o pueden ser debidas a diferencias reales en el contenido del fitoplancton de las dos muestras.

Cantidad de zooplancton

Se hicieron mediciones de la cantidad de zooplancton por medio de arrastres con mangas planctónicas, aplicando equipos y técnicas comparables a las empleadas por la entidad Investigaciones Cooperativas de la Pesquería Oceánica de California (California Cooperative Oceanic Fishery Investigations). En cada estación se hizo un recorrido oblicuo con una manga planctónica de un metro (diámetro de la boca) fabricada de gasa de seda de tejido "grano de arena" de 30XXX en el cuerpo de la red, y de 56XXX en la sección posterior y en la bolsa del extremo. La manga fué descendida desde la superficie hasta una profundidad de 300 metros aproximadamente (con

450 metros de línea) a una velocidad de 50 metros por minuto, en tanto que la embarcación seguía su camino despaciosamente y recuperaba a una velocidad de 20 metros por minuto. En consecuencia, la duración de cada arrastre oblicuo fué de 32 minutos, en promedio. Un medidor de paso de agua "Atlas" fué instalado en la boca de la red para registrar el volumen de agua de mar filtrada por la manga. Estos medidores de paso de agua fueron calibrados antes y después del crucero. Los detalles cuantitativos de todos los arrastres planctónicos hechos con los barcos *Spencer F. Baird* y *Horizon,* durante la Expedición Eastropic, aparecen en las Tables 2 y 3, respectivamente.

Las muestras de zooplancton fueron conservadas en formalina diluída al 4%. Ya en tierra, las recolecciones fueron filtradas y los volúmenes "húmedos" totales del plancton obtenido en cada estación fueron medidos por coladura. El volumen de agua muestreada en cada arrastre se determinó mediante el sistema descrito por la entidad Investigaciones de la Pesquería del Pacífico Sur del Servicio de Pesca y Vida Silvestre de los Estados Unidos (1953) (South Pacific Fishery Investigations of the U. S. Fish and Wildlife Service), y el volumen de plancton fué luego convertido en términos de volumen de organismos, en centímetros cúbicos, recogidos de cada 1000 metros cúbicos de agua de mar filtrada por la red. Los valores regularizados correspondientes a cada estación se indican en las dos últimas columnas de las Tablas 2 y 3, primero con respecto a la muestra completa y, segundo, respecto de la muestra una vez que fueron removidos todos los organismos de un volumen mayor de 5 centímetros cúbicos.

RESULTADOS DE LAS MEDICIONES *IN SITU* EN RELACION CON LAS CARACTERISTICAS OCEANOGRAFICAS

Observaciones de la superficie

Los valores de la clorofila "a" de las aguas superficiales, los de la producción primaria de estas mismas aguas, determinada *in situ,* y los volúmenes del zooplancton observados durante la expedición, aparecen en las Figuras 2 a 4; la Figura 1 muestra el sistema de corrientes y masas de agua, basado en un estudio preliminar de las observaciones hidrográficas y las mediciones de corrientes hechas durante el crucero.

En las aguas de la Corriente de California y la Corriente Ecuatorial del Norte (Estaciones 1-10), muy afuera de Baja California y de México Central, encontramos en general bajas concentraciones de clorofila "a" (alrededor de 0.1 mg/m^3), muy baja producción primaria de superficie (más o menos 0.40 mgC/m^3/día), y volúmenes pobres de zooplancton (generalmente menos de 50 cc/1000 m^3).

En la región fronteriza norte de la Contracorriente Ecuatorial se hallaron más altos valores de clorofila, producción primaria y volúmenes del zooplancton; estos valores tienden a subir de oeste a este, hacia la costa de América Central. Este fenémeno parece estar relacionado con la termoclina, que se eleva cerca de la superficie, como un cerro, a lo largo de esta frontera, y que disminuye de oeste a este. En la Estación 31-11 (Figura 2), por ejemplo, alrededor de los 115° de longitud oeste, el estrato de agua mezclada tiene un espesor de cerca de 30 metros, mientras que en la Estación 33, más o menos en los 90° de longitud oeste, solamente medía 18 metros. En el extremo de la costa, el cerro de agua parece convertirse en una ancha "cúpula" frente a la América Central, siendo de nuevo la termoclina ligeramente más profunda cerca de tierra (e.g. en las Estaciones 35 y 39, el estrato de agua mezclada tenía de 25 a 30 metros de espesor). En la región de esta "cúpula" frente a la América Central, encontramos en aguas superficiales, valores relativamente altos de clorofila (de 0.2 a 0.3 mg/m^3); de producción primaria (alrededor de 25 mgC/m^3/día) y de volúmenes del zooplancton (200 cc/1000 m^3 y más altos).

En la región fronteriza norte de la Corriente del Perú, frente a la parte septentrional de Sud América y en la vecindad de las Islas Galápagos (Estaciones 50 a 59), hallamos alta cantidad de fitoplancton (clorofila "a" hasta 2.0 mg/m^3) y zooplancton (hasta 600 cc/1000 m^3). La producción primaria de superficie, en las dos estaciones en que se midió, fué también alta, pero no tanto como frente a la América Central. Sin embargo, en la Estación 57 (Figura 2) la producción en la columna de agua, en su totalidad, excedió los valores obtenidos en la región de Centroamérica.

También se observaron niveles bastante altos de clorofila "a", producción primaria de fitoplancton y volúmenes del zooplancton en la Corriente Ecuatorial Sur (Estaciones 18 a 24(en la vecindad del ecuador, cerca de los 115° de longitud oeste. Los datos hidrográficos recogidos en este y otros cruceros indican la presencia de afloramiento a lo largo del ecuador (resultados sin publicar).

También se presentan altos niveles de clorofila y zooplancton en el área frente a la costa de México, desde el Golfo de Tehuantepec hasta las vecindades de Cabo Corrientes. Desgraciadamente la provisión de C^{14} se había terminado cuando la expedición llegó a esta área, de modo que no fué posible determinar la producción.

Observaciones en aguas subsuperficiales

En siete estaciones se efectuaron observaciones de la concentración de clorofila "a" y de la proporción de la producción primaria *in situ*, a diversas profundidades, hasta unos 100 ó 125 metros. Estas observaciones, junto con las temperaturas registradas y las concentraciones de salinidad y oxígeno, aparecen en las Figuras 5 a 11 inclusive, en función de profundidad.

Las Estaciones 33, 35, 37 y 39, situadas frente a la América Central. (Figuras 7 a 10), son generalmente similares en lo que se refiere a la distribución de la clorofila y de la producción primaria, lo mismo que a sus características físicas. Las Estaciones 24 y 33-11 (Figuras 5 y 6) situadas en aguas muy afuera en la Contracorriente y en la Corriente Ecuatorial Sur, son diferentes con respecto a sus propiedades biológicas y físicas.

El primer grupo de estaciones se caracteriza por una capa de agua mezclada bien definida y de poca profundidad, dentro de la cual se presenta la mejor parte de la producción primaria (90% o más, excepto en la Estación 35 en que la proporción es alrededor del 67%). Las gradientes en clorofila "a" son pequeñas en los 40 metros superiores, y un importante volumen de la clorofila en la columna de agua aparece debajo de la termoclina y la haloclina. El porcentaje máximo de producción primaria se presenta en la superficie o muy cerca de ella. Durante el tiempo en que se trabajó en estas estaciones, los días estuvieron muy nublados, lo que presumiblemente estorbó la inhibición de la luz en la superficie (ver Steeman-Nielsen 1951 y 1952).

También se observa en cada una de estas estaciones (Figuras 7 a 10 inclusive) un aumento de la producción primaria justamente sobre la termoclina y la haloclina; sobre ésto solamente podemos hacer especulaciones. Parece improbable que la cantidad de luz fotosintéticamente activa pudiera ser mayor en capas entre 10 y 20 metros, que en profundidades más cercanas a la superficie, de manera que no parece posible que la luz sea la causa de este aumento. De modo similar, el aumento no parece estar relacionado con la cantidad de clorofila "a" en el agua, aún cuando debe advertirse que el método para la determinación de esta sustancia no hace distinción entre la clorofila "a" y la faeofitina "a". Si el aumento observado es verdadero, otros factores que no son la luz y la clorofila, parecerían ser los causantes. Desafortunadamente, carecemos de datos sobre elementos nutritivos en estas estaciones. Una información de esta naturaleza podría haber sido valiosa para explicar esta aparente anomalía.

Aunque los datos correspondientes a las Estaciones 31-11 y 24 (Figuras 5 y 6) no son tan completos ni continuados como los de la zona frente a la América Central, las pocas observaciones que se han hecho indican una situación de tipo diferente. En este caso, una proporción importante de la totalidad de la producción primaria (más o menos 50%) se efectúa debajo de la capa de agua mezclada; dicha producción es relativamente alta en profundidades de 70 metros. Solamente en la Estación 31-11 se puede notar que existe una buena correspondencia entre la concentración de clorofila y la tasa de producción. En la Estación 24 (Figura 6), que se encuentra en la región del afloramiento ecuatorial, puede apreciarse que hay muy poco grado de aumento de salinidad hasta una profundidad de 100 metros y que la termoclina no está muy fuertemente desarrollada.

En la Estación 57 (Figura 11), cerca del borde norte de la Corriente del Perú, la termoclina y la haloclina están mucho menos marcadas que en las estaciones frente a Centroamérica. En dicha estación, la clorofila se mantiene alta hasta una profundidad de 70 metros, mientras que la producción primaria decae a una cantidad insignificante mucho más cerca de la superficie.

La región frente a la América Central se caracteriza también por un pronunciado mínimum de oxígeno en las capas superiores (Figuras 7 a 10). La disminución más rápida en la concentración de oxígeno se opera inmediatamente debajo de la capa mezclada. Existe la hipótesis de que el agua de pobre contenido de oxígeno se origina aquí, como un resultado de la necesidad que de éste tienen los organismos fitoplanctónicos debajo de la profundidad de compensación, a través de la respiración del fitoplancton y/o de la actividad de las bacterias, a lo que se suman los organismos muertos o al extinguirse. Del mismo modo, los datos recogidos en la Estación 57 (Figura 11) sugieren una explicación similar con respecto a la existencia de un mínimo de oxígeno al sur del ecuador, frente al Perú.

CORRELACION ENTRE LA PRODUCCION PRIMARIA Y LOS VOLUMENES DEL ZOOPLANCTON CON LA CLOROFILA DE AGUAS SUPERFICIALES

Si se consideran en conjunto los datos disponibles sobre producción primaria y clorofila "a", recogidos en aguas superficiales (Figura 12), parece que hubiera alguna correlación entre estas dos variables, pero con una dispersión bastante grande. Los datos revelan que, en promedio, la producción primaria baja se encuentra asociada a un punto bajo de clorofila "a", y que ésta es alta cuando la producción también lo es. Los puntos, en la mayoría de las estaciones, parecen localizarse a un lado y otro de una línea indefinida o vaga, con indicación de un aumento más rápido en la producción que en la clorofila "a". Sin embargo, las estaciones frente a la América Central, particularmente las números 33, 35 y 37, indican una producción relativamente más alta por unidad de clorofila que la que refleja el resto de los datos.

Edmondson (1955) al estudiar las poblaciones resultantes del enriquecimiento del agua de Woods Hole Harbor, cultivadas en tanques de concreto, encontró que la relación entre la producción (medida según la técnica del oxígeno en las botellas claras y obscuras) y la clorofila, podría mejorar si se toman en consideración las variaciones en la iluminación. A fin de examinar si existía tal relación en cuanto a nuestros datos, ya que no se habían hecho mediciones directas de la iluminación, obtuvimos el flujo promedio de radiación (directo más difuso) en un cielo sin nubes, mediante las curvas de Kimball (1928), por el mes de diciembre, y aplicamos la corrección del mismo Kimball (1928) con respecto al grado de sombra observado. La producción superficial *in situ* fué entonces calculada en términos del carbón obtenido por metro cúbico, por día, por unidad de iluminación, y la graficamos de nuevo en función de la concentración superficial de la clorofila en las mismas estaciones. La relación resultante fué muy similar a la que muestra la Figura 12, con el mismo grado de dispersión, aproximadamente.

Si los datos obtenidos *in situ* en la Figura 12 se estudian tomando en cuenta la posición geográfica de las localidades de muestreo, vemos que se separan en 3 grupos que presentan diferentes grados de relación entre la producción primaria y la clorofila. Las estaciones mar afuera, aproximadamente al norte de los 7° N. de latitud (Estaciones 1, 6, 13, 32-10, 31-11 y 27), que están situadas en la Corriente Ecuatorial Norte y en la Contracorriente Ecuatorial, se encuentran dentro de un grupo, mientras que las estaciones costeras frente a la América Central (Estaciones 33, 35, 37 y 39), forman otro grupo. Un tercer grupo está integrado por las estaciones situadas en la Corriente del Perú, frente al Ecuador y a la costa peruana, y por una que se halla bastante al oeste de las Islas Galápagos sobre el ecuador, en la Corriente Ecuatorial Sur (Estaciones 25, 45, 57 y 51).

Estamos dudosos acerca del significado de estas relaciones. Podrían tener una explicación en el reciente trabajo de Rodhe (según lo que nos ha comunicado personalmente), quien encontró una relación entre la producción primaria y la clorofila en una sola estación en Lago Erken. Al agrupar sus observaciones diarias en períodos mensuales, éstas le revelaron, con una sola excepción, que existía una buena relación entre la producción y la clorofila en cualquier mes, pero que esta relación variaba de un mes a otro. El sugiere que las diferencias apreciadas en las relaciones entre la producción y la clorofila pueden ser el resultado de cambios en la composición de las especies de la población de fitoplancton. Aún cuando las variaciones observadas por Rhode son en el tiempo y no en el espacio, sería de esperar que se presentaran diferencias considerables en la composición de la población de fitoplancton en las diversas masas de agua del Pacífico Oriental Tropical. En tanto no tengamos datos para respaldar esta postulada diferencia en la composición del fitoplancton, debemos creer que alguna de la variabilidad observada en la relación que se nota entre la producción primaria y la clorofila "a", debe ser atribuída a esta diferencia.

La existencia de una relación general entre la clorofila y la producción primaria, con un más bien alto grado de variabilidad y alguna evidencia de diferencias en áreas ampliamente separadas, resulta sin duda alguna de la interacción de diversos factores. Los factores que pueden tener importancia en esa variabilidad son los siguientes: diferencias en la composición de las especies; diferencias en el grado de la fotosíntesis de cada especie, que dependen de la distribución espectral y de la energía de la radiación en la subsuperficie; condiciones nutritivas y, tal vez, diferencias en el grado de la fotosíntesis por unidad de clorofila, relacionadas con la posición de los diversos componentes de la población en sus curvas de crecimiento y con su historia en el pasado.

La elucidación de los efectos de los factores que acabamos de apuntar y de otros factores necesitará de estudios mucho más detallados. Sin embargo, pareciera que, en forma muy general, la cantidad de clorofila por unidad de volumen de agua superficial proporciona una base para estimar, aunque deficientemente, el grado de fijación del carbón en la capa superficial del mar en la región tropical del Pacífico Oriental. Los bajos valores de clorofila, menos de unos 2 mg/m^3, indican muy baja productividad (i.e. menos de unos 2 mgC/m^3/día). Sin embargo, a niveles más altos de clorofila, la variabilidad en los grados de fijación del carbón entre una masa de agua y otra es tan grande que el error en la estimación viene a ser muy amplio.

En general, hay bastante concordancia entre la distribución geográfica de la clorofila "a", la producción primaria y los volumenes del zooplancton (Figuras 2, 3 y 4). La relación entre la clorofila de la superficie y los volúmenes del zooplancton está mejor ilustrada en la Figura 14. Se considera que la clorofila superficial proporciona una base útil para la estimación del volumen del zooplancton en el Pacífico Oriental Tropical.

ASIMILACION DE CARBON CATORCE EN MUESTRAS INCUBADAS A BORDO

Las muestras de aguas superficiales cuya producción fué medida *in vitro* bajo constante iluminación a la temperatura de la superficie del mar, no demostraron una relación clara entre la concentración de la clorofila y la producción primaria, por unidad de iluminación (Figura 13).

Ryther (1956b, Figura 2) ha encontrado en sus estudios con cultivos de fitoplancton marino, que el grado de la producción (medida por el método del oxígeno) por unidad de clorofila "a", a una intensidad invariable de luz, es casi constante en algunas especies. Los datos de la Expedición Eastropic no parecen apoyar las conclusiones de Ryther. Debemos admitir que los experimentos realizados a bordo fueron poco satisfactorios en cuanto a la intensidad de la luz a la que nuestras muestras fueron sometidas, ya que varió de un experimento a otro, a pesar de que esta intensidad se mantuvo constante durante cada experimento (ver página 159). A pesar de esto, los grados de intensidad empleados por nosotros se presume que estuvieron por debajo de los niveles que habrían causado saturación (ver Ryther 1956a, y Steemann-Nielsen, 1952), de modo que tendríamos que esperar, a base de los experimentos de Ryther, una positiva correlación entre la clorofila y la producción primaria por unidad de iluminación.

Tratando de encontrar una posible explicación de nuestros resultados en relación con los experimentos de Ryther, podemos observar que el radio de las concentraciones de clorofila y de la producción primaria, en sus cultivos, eran mucho mayores que el radio de las concentraciones de clorofila y de los grados de la fijación de carbón que encontramos en la Expedición Eastropic. En verdad, la escala de valores de Ryther ha excedido en mucho, aparentemente, a los encontrados normalmente en el mar, aún en latitudes nórdicas.

Los intentos para igualar la asimilación de carbón radioactivo de las muestras de aguas superficiales incubadas a bordo, con la observada en las muestras incubadas *in situ,* tomando en cuenta las variaciones en la iluminación solar, no han tenido buen éxito. Esto puede ser el resultado de la imposibilidad con que tropezamos para hacer estimaciones suficientemente precisas de la radiación en el área mediante mapas climáticos, y de nuestro conocimiento inadecuado del nivel de energía que causa la saturación de la fotosíntesis en las poblaciones naturales. De modo similar, la falta de mediciones de la luz submarina ha impedido un mayor análisis de los resultados de las medidas de la asimilación del C^{14} en la incubadora, realizadas con muestras tomadas debajo de la superficie del agua.

VARIACION EN EL TIEMPO EN LOS VOLUMENES DEL ZOOPLANCTON

La comparación entre los volúmenes del zooplancton estimados durante la Expedición Shellback en 1952 (Figura 15) y los de la Expedición Eastropic en 1955 (Figura 4) nos da alguna idea de la variabilidad que puede ocurrir en diferentes estaciones y años. Los volúmenes del zooplancton en el verano de 1952 fueron generalmente más bajos que en el otoño de 1955. Sin embargo, debe advertirse que ciertas áreas de muy altos y de muy bajos volúmenes aparecen en ambos años en las mismas localidades. Merecen citarse especialmente las áreas de la región de la Corriente del Perú y a lo largo del ecuador, con altos volúmenes de plancton, y frente a la América Central. La escasez de organismos en aguas a cierta distancia de Baja California se manifiesta en ambos años. En aguas cercanas a tierra, a lo largo de la costa mexicana al norte del Golfo de Tehuantepec, el zooplancton fué pobre en 1952 pero abundante en 1955.

COMPARACIONES CON OBSERVACIONES EN OTRAS REGIONES OCEANICAS

Steeman-Nielsen se refiere en un informe (1954) a la productividad de C^{14} en una serie de estaciones del *Galathea,* en el Pacífico, durante una travesía de Nueva Zelandia a California. Sus valores de producción en la columna de agua, por metro cuadrado de superficie, fueron calculados sobre la base de las determinaciones hechas en la incubadora de a bordo y de las mediciones de la luz a diferentes profundidades marinas. En las diversas estaciones a lo largo de la sección estudiada por él, situadas entre los 140° y 180° de longitud O. encontró que la proporción en la producción era entre 0.10 y 0.19 gC/m^2/día, excepto en la vecindad del ecuador, en donde se registró la cifra de 0.5 gC/m^2/día, y en una estación algo más al norte del ecuador, que él considera está "influída por las divergencias producidas por la Contracorriente", se anotó un valor de 0.26 gC/m^2/dia. Nuestro registro de 0.51 gC/m^2/día, en la Estación 24 sobre el ecuador, concuerda bien con los resultados que anota Steeman-Nielsen en su estación cerca del ecuador.

Sin embargo, nuestra cifra de 0.012 gC/m^2/día, *in situ,* en la Estación 31-11, es mucho más baja que lo que indican los resultados del barco *Galathea* en la misma latitud, más hacia el oeste, siendo también muy baja la asimilación de C^{14} en las muestras *in vitro.* Este valor tan bajo resulta en cierto modo anómalo, y es preciso confirmarlo en una futura expedición antes de ser aceptado como representativo de la zona en que la Estación 31-11 fué situada.

Los datos de Steeman-Nielsen sobre una alta producción en el ecuador, con valores algo más bajos al norte y al sur, han sido confirmados por M. Oguri (comunicación personal), quien hizo determinaciones *in vitro* de la asimilación de C^{14} en muestras de aguas superficiales en varias estaciones de la región entre los 110° y 140° de longitud O. y entre los 5° N. y 5° S. de latitud, con el barco *H. M. Smith* en el otoño de 1955, al mismo tiempo que nosotros hacíamos estudios más al este. Oguri encontró que la asimilación de C^{14} en las muestras de agua tomadas de las estaciones sobre el ecuador es significativamente más alta que en las situadas en los 5° N. ó 5° S. de latitud.

La producción que encontramos en el área de la "cúpula" frente a la América Central (0.414-0.779 gC/m^2/día), es generalmente más alta que cualquiera de las registradas por Steeman-Nielsen en el Pacífico, excepto en las aguas costeras de Nueva Zelandia y de San Francisco. Estas proporciones de la producción en el área de la América Central, y aún la de mayor nivel que hallamos en la Estación 57 cerca del borde norte de la Corriente del Perú (1.02 gC/m^2/día), compiten favorablemente con las áreas más productivas visitadas por el barco *Galathea* en la parte sur de la Corriente de Benguela, a lo largo de la costa africana, en donde Steeman-Nielsen ha registrado tasas de producción entre 0.46 y 2.5 gC/m^2/día.

Los valores de la clorofila, los volúmenes del zooplancton, y la producción primaria de las aguas superficiales en la muy pobre área mar afuera de Baja California, indican que esta región se halla entre las áreas oceánicas menos feraces, siendo probablemente tan pobre como la región del Mar de Sargaso. Es interesante observar que esta área no está muy lejana de la región que se encuentra a lo largo de Baja California que se conoce como muy rica en producción, a juzgar por los volúmenes de zooplancton medidos en otras expediciones.

LITERATURE CITED — BIBLIOGRAFIA CITADA

Edmondson, W. T.

1955 Factors affecting productivity in fertilized salt water. Papers in Mar. Biol. and Ocean., Deep Sea Research, supp. to Volume 3, pp. 451-464.

Kimball, Herbert

1928 Amount of solar radiation that reaches the surface of the earth on the land and on the sea, and methods by which it is measured. Monthly Weather Review, Vol. 56, pp. 393-399.

Richards, F. A., with Thompson, T. G.

1952 The estimation and characterization of plankton populations by pigment analyses. II. A spectrophotometric method for the estimation of plankton pigments.
Jour. Mar. Res., Vol. XI, No. 2, pp. 156-172.

Ryther, John C.

1956a Photosynthesis in the ocean as a function of light intensity. Limnology and Oceanography, Vol. I, No. 1, pp. 61-70.

1956b The measurement of primary production.
Limnology and Oceanography, Vol. 1, No. 2, pp. 72-84.

Steeman-Nielsen, E.

1951 The marine vegetation of the isefjord — a study on ecology and production.
Medd. Komm. Danmarks Havundersog, Serie plankton, Vol. V, No. 4, pp. 1-114.

1952 The use of radioactive carbon (C^{14}), for measuring organic production in the sea.
Jour. du Conseil, Vol. 18, No. 2, pp. 117-140.

1954 On organic production in the oceans.
Jour. du Conseil, Vol. 19, No. 3, pp. 309-328.

South Pacific Fishery Investigations, U. S. Fish and Wildlife Service

1953 Zooplankton volumes off the Pacific coast, 1952.
U. S. Fish and Wildlife Service, Spec. Sci. Rep., Fisheries, No. 100, 41 pp.

Van Dorn, William G.

1956 Large-volume water samplers.
Trans. Am. Geophisical Union, Vol. 37, No. 6, pp. 682-684.

Reprinted from TRANSACTIONS OF THE AMERICAN MICROSCOPICAL SOCIETY
Vol. LXXVI, No. 4, October, 1957
Reproduced by Permission

TWO NEW APPENDICULARIANS FROM THE EASTERN PACIFIC, WITH NOTES ON THE MORPHOLOGY OF *FRITILLARIA AEQUATORIALIS* AND *TECTILLARIA FERTILIS*[1]

TAKASI TOKIOKA[2]

During the examination of plankton samples collected by the Shellback Expedition carried out in 1952 by Scripps Institution of Oceanography in tropical and subtropical waters off the west coasts of North and South America, I found two strange appendicularians which upon a careful survey of the literature (Bückmann, 1923; Lohmann, 1892–1933; Lohmann & Bückmann, 1926; Vernières, 1934) prove to be new species. One of these species belongs to the genus *Fritillaria*. The other is closely related to *Althoffia tumida* Lohmann, but differs so remarkably that it is necessary to establish a new genus to receive the species. Thus the new genus *Sinisteroffia* is proposed in this paper.

Besides the discovery of these two new forms, I have had occasion to examine closely some excellently preserved specimens of *Fritillaria aequatorialis* Lohmann and some of *Tectillaria fertilis* (Lohmann) in a comparatively good condition. To my astonishment, both of these species have similar tails of a very characteristic type that has hitherto not been described. The significance of this similarity is not as yet quite clear, but it raises the question whether *Fritillaria aequatorialis* Lohmann and *Tectillaria fertilis* (Lohmann) might not actually belong in the same genus.

I wish to thank members of the Scripps Institution staff who have made this study possible and especially Professor Martin W. Johnson for his kindness in providing facilities and for critically reading the manuscript.

Sinisteroffia nov. gen.

The endostyle and spiracles are present. The alimentary canal consists in part of a thin oesophagus, a single-lobed stomach and an elongate intestine. The stomach is situated vertically just along the left lateral body wall in the posterior half of the body. The gonad is hermaphroditic.

REMARKS: Evidently this new genus is related closely to *Pelagopleura* and *Althoffia* in that (1) the stomach has only a single lobe, from the anterior part of which both the oesophagus and the intestine issue, and (2) in the arrangement of the gland cells on the tail. In *Pelagopleura*, which also occurred in the expedition samples, the stomach is situated vertically along the sagittal axis of the body, while in *Althoffia*, studied from samples collected on the Scripps Mid-Pacific Expedition, it is located horizontally above the level of the gonad. In this new genus, the stomach is situated vertically, but it is displaced strongly to the left side of the sagittal axis and here touches the left lateral wall of the body leaving a wide portion of the posterior half of the body nearly empty. At first, it was thought that such a strange position of the stomach might be a malformation. I have at hand three such individuals, however, one of which is somewhat younger than the others. Moreover, the position of the stomach within a notch in the anterior margin of the gonad is unique.

---

[1] Contribution from Scripps Institution of Oceanography, New Series No. 943. This work was supported in part by grants from the Rockefeller Foundation.

[2] Present address: Seto Marine Biological Laboratory, Kyoto University, Japan.

The generic name *Sinisteroffia* refers to the left position of the stomach and the resemblance of the gonad to that of *Althoffia*.

Type species: *Sinisteroffia scrippsi*.

Sinisteroffia scrippsi nov. sp.

(Figs. 1 and 2)

Three specimens are dealt with here, two of which were found in the sample from Station 125 off Peru (9° 52.5' S x 81° 32' W), whereas the other one was found together with specimens of *Pelagopleura* collected during the Shellback Expedition. The dimensions of these specimens are as follows:

Specimen Number	Trunk		Tail Length
	Length	Width	
1	1.69 mm.	0.98 mm.	5.41 mm. (injured)
2	1.3	0.65	6.18
3	1.3	0.43	5.85

TRUNK: The body is somewhat uniformly elongate in the younger specimen (No. 3), but in the two older specimens with fully matured gonads it is somewhat wider in the posterior half of the body. It is rather compressed dorso-ventrally, especially in the anterior half of the body, which is covered by the oikoplast-epithelium. The existence of a pair of Fol's cell groups (f.) is recognizable, although the number of cells can not be counted distinctly. Other cell groups are quite obscure, because the oikoplast-epithelium is not preserved perfectly in all specimens. The dorso-posterior margin of the epithelium (p.o.ep.) is divided into three narrow strands, one median and two lateral. The test on the oikoplast-epithelium is very soft. The area around the mouth (or.) is abruptly narrowed in dorsal view. The short endostyle (ed.) is situated near the mouth and there are no paired buccal glands. The spiracles (sp.) are situated near the anus (an.), slightly posterior to the middle of the anterior

---

EXPLANATION OF PLATE I

FIG. 1. *Sinisteroffia scrippsi* n. g., n. sp. A—Dorsal side of the 1.69 mm. long trunk. B—Left side of the same trunk. Abbreviations: an.—anus, c.—chorda, ed.—endostyle, ex.op.—external gill opening, f.—Fol's cell group, gl.—gland cell, gl.ap.—glandular appendage, gl.c.—large gland cell of stomach wall, hd.—hood, int.—intestine, m.—tail musculature, oe.—oesophagus, or.—mouth, ov.—ovary, ov'.—ovary?, pl.—plasma of gland cell, p.o.ep.—posterior margin of oikoplast-epithelium, pyl.—pyloric portion of intestine, r.—rectum, sp.—spiracle, st. stomach, t.—testis.

FIG. 2.—*Sinisteroffia scrippsi* n. g., n. sp. C—Posterior portion of tail of Sp. No. 1. D—left side of stomach of Sp. No. 2. E—Dorsal side of the 1.3 mm. long trunk (sp. No. 3). F—Left side of stomach of the same trunk. For abbreviations see Fig. 1.

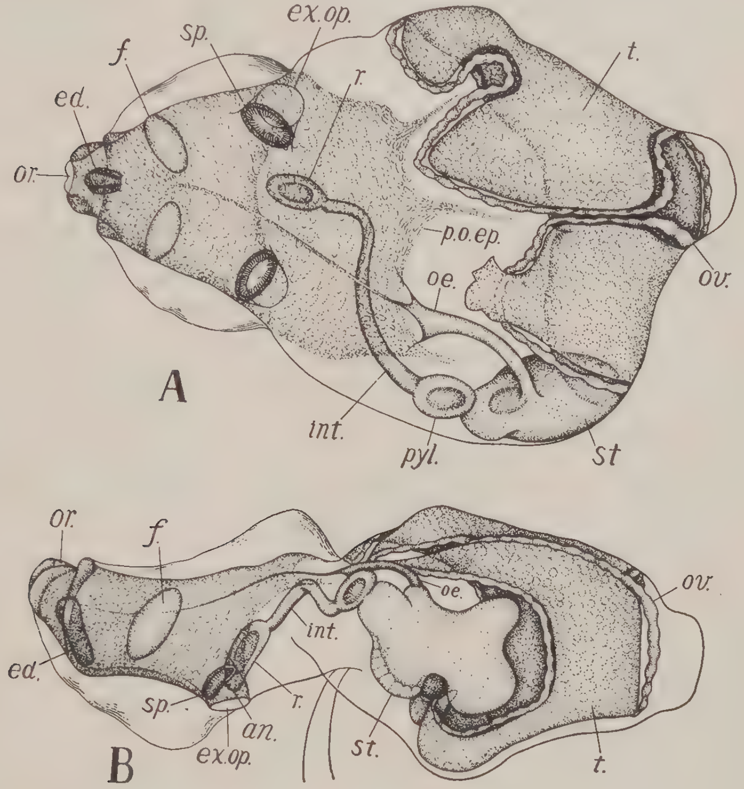
ex.op.
sp.
f.
ed.
or.
r.
t.
p.o.ep.
oe.
ov.
A
int.
pyl.
st
or.
f.
oe.
ov.
int.
ed.
sp.
r.
an.
ex.op.
st.
t.
B

1

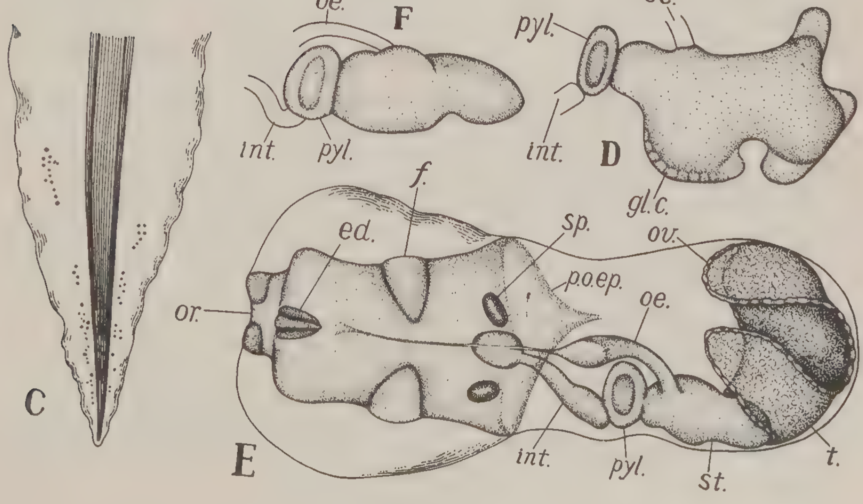
oe.
F
pyl.
oe.
int.
pyl.
int.
D
gl.c.
f.
ed.
sp.
ov.
p.o.ep.
oe.
or.
C
int.
pyl.
st.
t.
E

2

PLATE I

half of the body; the branchial canal between the spiracle and the external gill opening (ex.op.) is short. The right spiracle is situated nearer the anus than is the left one. The oesophagus (oe.) opens into the pharynx on the level of the tail insertion, near the middle of the body and opens into the stomach at about one third the stomach length from the cardiac end. It is narrow and comparatively long. The stomach (st.) is located vertically along the left lateral wall of the body in the anterior part of the posterior half of the body. In the younger specimen it is simple and elongate in outline (Fig. 2F), with a depression along the ventral margin. In the two older specimens, it is more complex in configuration (Figs. 1B and 2D). The cardiac portion is somewhat narrowed, the ventral margin is divided into anterior and posterior lobes by a deep depression and both the posterior margin and the dorsal margin posterior to the oesophagus are distinctly concave. There are large glandular cells (Fig. 2D, gl.c.) along the margin of the anterior ventral lobe. The intestine consists of a distinct pyloric division (pyl.), the intestine proper (int.) and the rectum (r.). The entire length may be twice that of the oesophagus in the older specimens, but it is not so long in the younger one. The pyloric portion of the intestine is comparatively larger in the younger specimen. The testis (t.) is a broad but thin, ribbon-like mass lying transversely on the inner surface of the ventral body wall of the posterior end of the body. In the adult, both edges are curled up dorsally so that they touch each other at the dorso-median line. The anterior margin of the testis has a distinct depression on each side, dorso-laterally on the right and laterally on the left side; and the stomach is situated in the left depression. In the younger specimen the right depression is also situated laterally. An incision is found on the anterior margin of the testis at the ventral mid-line in two older specimens, but it is missing in the younger one. The ovary (ov.) is a string-like tissue running along the whole margin of the testis. There may be a slight asymmetry in the genital region of the body even in the younger specimen and this asymmetry becomes very pronounced with the maturity of the gonad so that the posterior part of the body is strongly inclined to the right side and the posterior end may be pressed out by the gonad as shown in Figure 1A and the posterior half of the body is expanded laterally much more widely than in younger stages. The stomach and the oesophagus are displaced from the sagittal line of the body more and more and since the anus is fixed so tightly and immovably on the median line, the intestine becomes longer with the maturity of the gonad.

TAIL: The tail is preserved badly in specimens No. 2 and No. 3. In No. 1 it is severely injured near the middle and for this reason it is comparatively shorter in this specimen than in the other two. In specimen No. 1, the tail fin is rather wide, the greatest width of the tail musculature is 0.59 mm. and the width of the chorda/the width of the musculature is 0.44 at the position of the greatest width of the latter. The musculature is narrowed considerably in the posterior part of the tail. In the posterior one-fourth of the tail, there are many small gland cells arranged along both sides of the musculature. The number and the exact arrangement of these cells can not be given here, because this part of the tail is more or less shrunken in all specimens.

REMARKS: The large flattened testis fringed by a string-like ovary is a feature common to both this new species and *Althoffia tumida* Lohmann.

The gonad of *Althoffia tumida* has no depressions, however, as shown in the present species, and it is arranged quite differently against the stomach. The complex configuration of the stomach in the present species is also unique. The specific name is dedicated to E. W. Scripps, the founder of the celebrated oceanographic institution. All specimens are deposited in the U. S. Nat. Mus., Sp. No. 11375.

Fritiliaria taeniogona nov. sp.

(Figs. 3A and B)

Seven specimens were taken at Stations 60 (9° 53' N x 104° 28.5' W), 100 (7° 26' S x 89° 31' W), 112 (6° 21.5' S x 82° 23' W), 115 (8° 16' S x 83° 42' W) and 170 (9° 06' N x 88° 32' W); they are all, however, in part poorly preserved. Thus the following description is rather of a synthetic character, although the most important characteristic of the new species, the existence of a pair of double taenioid testes, is common to all specimens.

TRUNK: The body is elongate as in *Fritillaria haplostoma* Fol or *Fritillaria magna* Lohmann. The tail is usually inserted near the middle of the body, but the exact proportion of the posterior half of the body to the whole body length seems to differ considerably according to the degree of maturity of the gonad and also to the state of preservation. The anterior end of the hood (hd.) protrudes slightly beyond the mouth and is acute at the tip. The endostyle (ed.) is short and strongly curled. The oikoplast-epithelium occupies approximately the anterior half of the pharyngeal part of the body, but it may reach more posteriorly in some specimens (p.o.ep.). The oesophagus (oe.) is short; the stomach (st.) is roughly spherical in shape and has a nearly smooth surface, although a few low elevations may be observed in some specimens. A pair of glandular appendages (gl. ap.) are seen on the intestine (int.), but the exact position of the intestine can not be given here because in all specimens the intestine seems to have been more or less displaced from its natural position. A pair of long string-like testes (t.) are present; each of which is folded double into dorsal and ventral branches stretching anteriorly along the lateral wall of the body beyond the stomach so that both ends may reach nearly the posterior end of the oikoplast-epithelium. Usually, the testis is somewhat thickened at the point of flexure at the posterior end of the body and this thickened part is turned slightly dorsally. The ovary was not found in any specimen with certainty. In some specimens, a pair of small glandular masses (ov'.) are found, one on each side, near the posterior end of the oikoplast-epithelium. These glandular masses resemble somewhat a pair of ovaries, although they may be only fragments of the testes. In well-preserved specimens, however, the anterior ends of the testes usually terminate each in a rounded swelling which differ in appearance from the glandular mass. The dimensions of some of the specimens are given below:

Trunk Length	Tail Length
2.2 mm.	4.6 mm.
2.3 +	5.2
2.6	4.6
2.9	5.9

TAIL: The tail musculature is rather narrow, each muscular band is not so thick as in *Fritillaria magna* or *Fritillaria aberrans* Lohmann. The

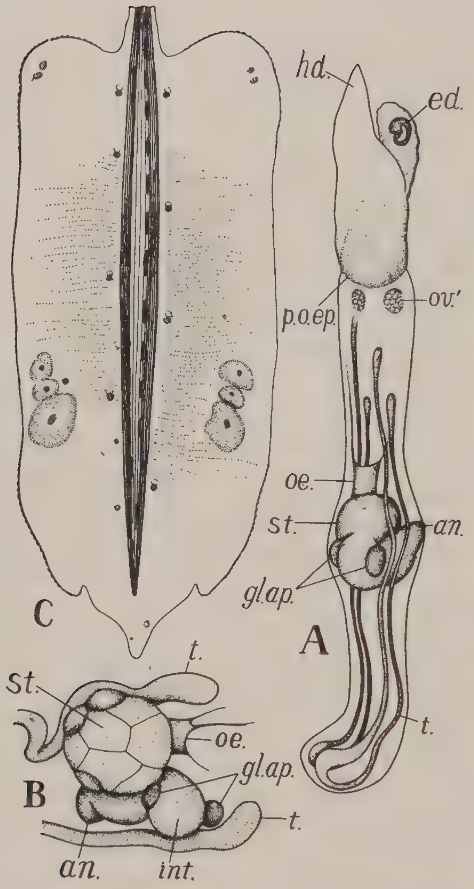

3

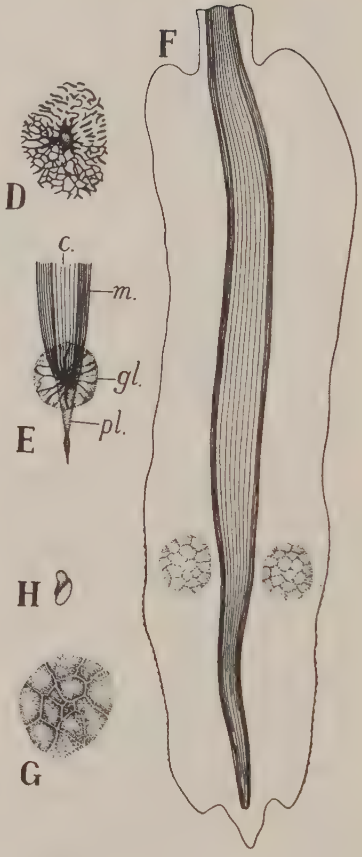

4

FIG. 3. *Fritillaria taeniogona* n. sp. (A and B) and tail of *Fritillaria aequatorialis* Lohmann (C). A—Right side of trunk. B—Dorsal side of alimentary organ. For abbreviations see Fig. 1.

FIG. 4. *Fritillaria aequatorialis* Lohmann (D and E) and *Tectillaria fertilis* (Lohmann) (F–H). D—One of large gland cells on tail fin, magnified. E—Posterior end of tail musculature. F—Entire tail. G—A gland cell group. H—A gland cell group in a young specimen.

width of the chorda/the width of the musculature is 0.46 in the basal half in an examined specimen. The posterior portion of the chorda does not protrude beyond the posterior margin of the musculature.

REMARKS: This new species is named for the unique appearance of the taenioid testes. Specimens are deposited in the U. S. Nat. Mus., Sp. No, 11376.

Fritillaria aequatorialis Lohmann 1896
(Figs. 3C, 4D and 4E)

TAIL: The fin is very wide; width/length is 0.38 in a perfectly preserved 2.3 mm. long tail. The anterior end of the fin forms shoulder-like angles. There is a pair of subterminal notches near the pointed posterior

610)

end of the fin, one on each side. Three pairs of large gland cells are found in the tail at a point approximately one-third from its distal end; the posterior-most pair of cells are the largest. These large gland cells are characteristic in their reticulated appearance (Fig. 4D). Besides, there are a considerable number of small gland cells arranged chiefly along both sides of the rather narrow musculature. The width of the chorda/the width of the musculature is 0.41 in a perfectly preserved 2.3 mm. long tail. The chorda does not extend beyond the posterior margin of the musculature. There is a comparatively large gland cell (Fig. 4E, gl.), however, at the posterior end of the musculature. A part of this cell (Fig. 4E, pl.) projects as a lancet pointed posteriorly. The appearance of the gland cell itself seems to differ considerably in individuals.

Tectillaria fertilis (Lohmann), 1896
(Figs. 4F–4H)

Tail: The fin is not so wide as in the preceding species. The anterior end of the fin forms shoulder-like angles. There is a pair of subterminal notches near the pointed posterior end of the fin as in *Fritillaria aequatorialis*. Two groups of gland cells (Fig. 4G) are found at approximately one-third the distance from the distal end of the tail; each group consists of about a dozen cells. This glandular cell group is observable even in young and small specimens, but in young specimens it may sometimes be represented by only a few cells (Fig. 4H). The musculature is narrow, extending laterally only slightly beyond the chorda. The chorda does not extend posteriorly beyond the posterior margin of the musculature.

Remarks: The existence of a pair of subterminal notches near the pointed posterior end of the fin in both *Fritillaria aequatorialis* and *Tectillaria fertilis* is unique. So far as I am aware, two types of the tail fin are recognizable in the Family Fritillaridae. In the type which is common to *Kowalevskaia* and the subgenus *Acrocercus* of *Fritillaria*, the fin tapers posteriorly into a simply-pointed end. In the other type which is common to Appendicularia and the subgenus *Eurycercus* of *Fritillaria*, the fin has a remarkable incision at the distal end. Thus, the type shared by *Fritillaria aequatorialis* and *Tectillaria fertilis* should be recognized as the third type of the tail fin.

Literature Cited

Bückmann, Ad. 1923. Bemerkungen über Appendicularien aus der Ausbeute der Deutschen Südpolar-Expedition. Zool. Anz., Bd. 59: 205-212.

Lohmann, H. 1892. Vorbericht über die Appendicularien der Plankton-Expedition. Ergebn. Plankton-Exped., Bd. I.

1896. Die Appendicularien der Plankton-Expedition. *Ibid.*, Bd. II, E c.

1914. Die Appendicularien der Valdivia-Expedition. Verhandl. Deutschen Zool. Gesell Jahrgang: 157-192.

1933. Appendicularien in: Handbuch d. Zoologie, Bd. V, Zweite Halfte, Liefs. 1–2.

Lohmann, H. and Buckmann, Ad. 1926. Die Appendicularien der Deutschen Südpolar-Expedition 1901 bis 1903. Ergebn. Deutschen Südpolar-Exped., Bd. 18 (Zool. Bd. 10).

Tokioka, T. 1955. General consideration on Japanese Appendicularian Fauna. Publ. Seto Mar. Biol. Lab., IV (2–3): 251-261.

Vernières, P. 1934. Les Appendicularies de la mer de Villefranche: *Pegalopleura haranti* n. sp. Bull. Soc. Zool. France, LIX: 160-163.

REPLY TO THE "DISCUSSION" OF A FABRIC AND PETROLOGIC STUDY OF THE PLEASANTVIEW SANDSTONE

BY

GENE A. RUSNAK

Reprinted from the Journal of Sedimentary Petrology for September, 1957

Reproduced by Permission

(613)

Journal of Sedimentary Petrology, Vol. 27, No. 3, pp. 346–350
Fig. 1, September, 1957

DISCUSSION

REPLY TO THE "DISCUSSION" OF A FABRIC AND PETROLOGIC STUDY OF THE PLEASANTVIEW SANDSTONE[1]

GENE A. RUSNAK
Scripps Institution of Oceanography, University of California, La Jolla, California

In the "Discussion" presented in the June, 1957, issue of the Journal of Sedimentary Petrology (v. 27, no. 2, p. 198–201) John E. Sanders has taken exception with several statements made by Rusnak in a paper entitled "A fabric and petrologic study of the Pleasantview Sandstone" (Rusnak, 1957). From this discussion it would appear that there have been some misunderstandings of the text and illustrations presented by Rusnak which require further clarification. Sanders objects in particular to (1) the comparison which was made of the Pleasantview depositional conditions with those prevailing in the Dutch Wadden Sea, and (2) Rusnak's use of the term "flow rolls." In order to reply to Sanders' first objection, it is necessary to restate the writer's reasons for suggesting a comparison with the Dutch Wadden Sea.

The Pleasantview Sandstone is the basal member of the Summum (Pennsylvanian) Cyclothem of western Illinois. This sandstone occupies deeply cut channels and can be conveniently described as two-phased; the thin (6–10 feet) non-channel phase, and the thick (up to 100 feet) channel phase. The non-channel phase is thin-bedded, wave-ripple marked, calcareous, slightly carbonaceous, and in apparent conformity with the underlying silty shales. The channel phase is massive to thin-bedded, cross-bedded, shaly, very carbonaceous, and contains a locally derived basal conglomerate and is uncomformable with the underlying channel-cut beds. A characteristic feature of the channel sandstone is the initial dip of the bedding, which dips towards the channel axis along the channel walls and assumes an essentially horizontal attitude in the central part of the channel. These relationships, along with the evidences of slump structures and scour marks within the channel, are considered by the writer as indications that the Pleasantview sandstone was deposited when both the channel and non-channel areas were submerged. The non-channel areas are thought to represent continuous gradational change of sedimentation from silty shale to sandstone and the channels represent areas of contemporaneous erosion and later filling.

Measurements made of the highly variable cross-bedding, indicated that the direction of sand transport (within the single channel studied) was up channel and contrary to the channel gradient. In addition, the studies of sand-grain orientation (in uncross-bedded units) indicated that some sand transport occurred across the channel axis. The sediment transport directions would seem, therefore, to indicate that the process of channel filling was largely independent of the process or processes which cut the channel.

An evaluation of the specific features in the Pleasantview Sandstone, in terms of a possible present day counterpart, lead the writer to believe that these features had many similarities with those reported from the tidal flats and tidal channels of the modern Wadden Sea off the northern coast of the Netherlands. Table 1 shows these similarities and includes some remarks on this comparison. The properties of the Wadden Sea deposits presented in this table are based on the published descriptions given by van Straaten (1951, 1952, 1954a, 1954b).

This comparison indicates that the apparent environment of deposition of the Pleasantview Sandstone is not greatly dissimilar from that of the Dutch Wadden Sea deposits. The greatest discrepancy in this comparison is the absence of marine fossils in the Pleasantview. Nonetheless, the writer suggests that the sedimentological

---

[1] Contribution from the Scripps Institution of Oceanography, New Series 944. Manuscript received June 26, 1957.

TABLE 1.—*Comparison of environment of deposition of Pleasantview Sandstone with the Dutch Wadden Sea*

Similarities	Remarks
1. Channels similar in shape and size	Sedimentation essentially continuous outside the channeled areas
2. Presence of locally derived mud-pebble basal conglomerate in the channels	These basal conglomerates are considered as lag deposits derived from the eroded walls of channel-cut sediments. The Wadden Sea conglomerates commonly consist of shell beds. No shells or evidence of organisms noted in the Pleasantview at the locality studied
3. General lithology and grain size	
4. Irregular cross-bedding	In the Wadden Sea the cross-bedding may be directed up channel in areas subjected mainly to flood tides and may be directed down channel in areas dominated by ebb tides
5. Presence of slump structures	
6. Wave and current ripple marks	Ripple marks in the Pleasantview are found in the non-channel areas, but are rare in the channels. They are common to both areas in the Wadden Sea
7. Great abundance of drifted plant debris in channels	
8. Irregular stratification	
9.	Although mud cracks are common to the Wadden Sea area; no mud cracks were noted in the Pleasantview
10. Inclined initial bedding along channel walls	The mechanism of forming the inclined bedding in the Wadden Sea channels is not the same as that of the Pleasantview

properties of the Pleasantview Sandstone can be explained best with an environment similar to the Wadden Sea tidal flats. Under such conditions the channel is first cut by tidal current action and then filled by a combination of lessened tidal currents sweeping sand up the channel and longshore current drifting of sand across the channel.

Sanders questions such a comparison with the Dutch Wadden Sea mainly on the basis of the structural relations of the channel-filled to channel-cut sediments. Figure 1 illustrates these relations in the Pleasantview and is a modification of the cross-section presented by Ekblaw (1931, fig. 4, p. 386). The figure used by Sanders (1957, fig. 1b) to illustrate this structure is a misapprehension of the description given by the writer (Rusnak, 1957, p. 43). However, the important thing to note is that the sandstone beds flanking the channel walls are inclined towards the channel axis, while near the center of the channel the bedding is essentially horizontal. This channel structure is similar to the smaller scale channel structures observed in the Wadden Sea by van Straaten (1951, 1952, 1954a, 1954b). However, although there is this structural similarity, the mechanism responsible for the inclined bedding along the Pleasantview channel is not comparable with that of the Wadden Sea channels. In this regard Sanders argues correctly against the application of the term "lateral sedimentation" to the inclined bedding along the Pleasantview channel. Nonetheless, without due regard to the numerous similarities between the Pleasantview Sandstone and the Wadden Sea deposits Sanders rejected the environmental comparison on the basis that the inclined beds of the Pleasantview are not due to "lateral sedimentation."[2]

---

[2] Sanders (1957, p. 198) implied that this comparison of environments by Rusnak (1957) was made solely on the basis of similarities in initial inclined bedding along channel walls. He states, "In view of this relationship, Rusnak compares the conditions of the Pennsylvanian Pleasantview

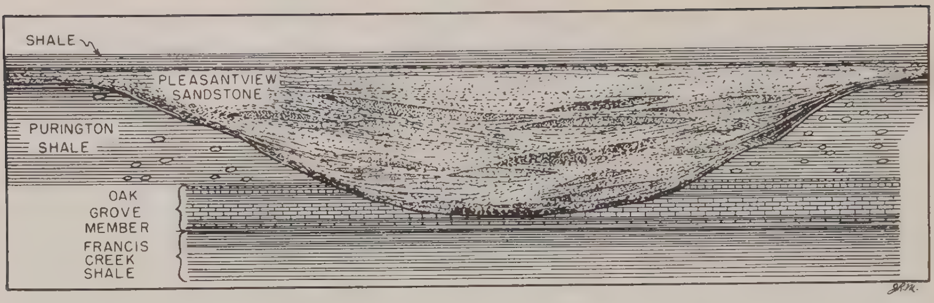

FIG. 1.—Generalized cross section of the Pleasantview channel exposed in outcrops along Coal Creek, Fulton County, Illinois (after the figure and interpretation by Ekblaw, 1931, fig. 4, p. 386). Depth of the channel in the central portion is about 50 to 55 feet. Vertical exaggeration ×33.

The term "lateral sedimentation" was used and defined first by van Straaten (1951, p. 236–238, 243; 1952, p. 500–502; 1954a, p. 26–27; 1954b, p. 7–8) for the specific mechanism associated with the development of inclined bedding in the Wadden Sea channel deposits. A detailed discussion of this mechanism and its resulting bedding need not be repeated here because this has already been elaborated upon by Sanders (1957). It is sufficient to say that the term can be applied only to inclined strata which are deposited laterally on point bars, such as those of tidal meanders, as Sanders rightly points out.

Lateral deposition could be only of minor importance in forming inclined bedding in the Pleasantview channel deposits. The great depth of this channel and the observed sand-grain orientation direction, which suggests deposition across the channel axis, would preclude such a process. The writer concluded, therefore, that the dominant mechanism which developed this inclined bedding consisted of a sweeping in of sediment from the surrounding area (Rusnak, 1957, p. 43, 52; for a generalization of other channel sandstones, see also Wanless and Shepard, 1936, p. 1202; and Weller, 1956, p. 29). It may well be, however, that some of the small-scale inclined bedding, associated with apparent meandering within the channel, is due to "lateral sedimentation."

Sanders further pursues his argument against a comparison with the Wadden Sea channels by suggesting four possible combinations of mechanisms to explain the origin and subsequent filling of the Pleasantview channels. These suggestions are:

> "1) tidal channels—littoral marine filling, perhapes indicating subsidence but no particular changes in geography; filling sediment of marine origin. 2) tidal channels—fluvial filling, indicating marine regression between cutting and filling; filling sediment non-marine. 3) fluvial channels—fluvial filling, indicating a change in stream regime from cutting to filling; filling sediment non-marine. 4) fluvial channels—littoral marine filling, indicating marine transgression; filling sediment should contain marine fossils."

Of these possible combinations, Sanders concludes, "As the basal channel sand of the cyclothem generally passes upward into coal deposits, the filling sediment is doubtless non-marine in most instances, though the channel could be of either tidal (alternative 2) or fluvial (alternative 3) origin." There are, however, several objections to these conclusions which can be resolved only by the first suggestion. Both suggestions 2 and 3 are based on the assumption that the channel deposits are of fluvial origin. This assumption arises from the fact that generally neither the channel sandstones[3] nor

---

Sandstone with those prevailing in the modern Wadden Sea off the northern coast of The Netherlands." That such an implication is in error, is demonstrated by the itemized list of comparable features from both areas listed under the heading "Comparison with the Dutch Wadden Sea" (Rusnak, 1957, p. 51) and amplified in the present paper (table 1).

[3] Ekblaw (1930) reports marine fossils from the Pleasantview sandstone in the area farther south than that which was studied by Rusnak (1957). This occurrence of marine fossils in the Pleasantview may represent another facies of the sandstone which was more favorable to marine organisms.

the overlying shales contain marine fossils. However, this assumption is not necessarily correct and is problematical. All investigators of the Pennsylvanian are not agreed that this assumption is valid (Wanless, 1950, p. 25). Indeed, Wanless (1952, p. 150–152) has suggested that the stratigraphically lower Seville Cyclothem channel (containing marine limestone) had been cut by streams or tidal currents and filled under deltaic of littoral conditions. Wanless has also suggested (with reservations) that the conditions of the Pleasantview were comparable (1952, p. 152). One should not, therefore, apply generalizations indiscriminately.

Perhaps the most serious objection to fluvial deposition of the Pleasantview lies in the observations of cross-bedding. These observations, although limited, indicate that the direction of sediment transport was in part up channel and contrary to the erosional gradient of the channel. It is difficult to conceive of a method whereby fluvial processes could form cross-bedding directed contrary to the bottom gradient since the water transport would have to follow the gradient. In the writer's opinion, this evidence alone precludes the possibility of fluvial channel filling. This apparent contradiction can be explained simply, however, by having tidal currents sweep sediments up the channel, as has been demonstrated by van Straaten (1950). Moreover, this mechanism may account for the variability of cross-bedding dip directions (see remarks in table 1).

The writer, furthermore, concluded that it is necessary to have two mechanisms operative during the channel filling stage in order to explain the initial dip along channel walls and the apparent discrepancy of grain-orientation direction from cross-bedding direction. For this purpose he proposed to explain the inclined bedding and grain-orientation direction as resulting from drifting of sand across the channel axis; while, the more nearly horizontal, massive and cross-bedded sandstone in the central section of the channel resulted from strong tidal currents sweeping sediment up the channel (Rusnak, 1957, p. 50, 52).

It was not the intent of the writer to solve regional problems of cyclothem channel cutting and filling with the very limited local study. He did try, however, to explain the observed phenomena from this single channel as best fitted the evidence. Whether the proposed mechanism of channel cutting and filling is valid and can be applied to more cyclothem channel systems remains to be seen. For the present, the writer rejects Sanders' suggestion of a fluvial origin for the Pleasantview channel filling, in the area investigated, and proposes instead to adhere to the original suggestion of a tidal flat environment similar to the Dutch Wadden Sea (Rusnak, 1957, p. 52).

Sanders' remarks concerning the use of the term "flow rolls" in Rusnak's paper (1957, p. 43) are in part correct. That is, not all "flow rolls" can be attributed to subaqueous scour. If the writer seemed to imply that Rich (1950, p. 727) attributed all "flow rolls" to scour, the implication was completely unintentional. Rich clearly stated that these markings can develop also by load flowage of unconsolidated sediments into underlying soft beds. The writer is fully aware of the distinction which Rich and Kuenen (1953, p. 23–25; and more recently 1957, p. 231–258) made of the causes of these markings. However, he believes that the marks described in the Pleasantview as "flow rolls" (and associated with channel walls) are scour casts rather than load casts. These features were examined in great detail in an effort to distinguish their mode of origin. In both the "groove casts" and the "flow rolls" there was no evidence to indicate structural deformation of the underlying surface. Furthermore, the casts were cut through on a diamond saw and examined for internal structure. No internal structure was observed and, hence, the writer concluded that these features were of the type described by Rich as scour markings.

Both load flowage and scour features are present in the Pleasantview as is obvious from the figures presented by Rusnak (1957). Where load flowage was clearly indicated by internal structure the features were described as such.

REFERENCES

Ekblaw, S. E., 1930, The stratigraphic relations of the Pleasantview Sandstone in western Illinois: Unpublished Master's Thesis, University of Illinois.

———, 1931, Channel deposits of the Pleasantview Sandstone in western Illinois: Illinois Acad. Sci. Trans. 23, p. 391–399.

Kuenen, Ph. H., 1953, Graded bedding, with observations on Lower Paleozoic rocks of Britain: Verh. Kon. Ned. Akad. Wetensch., Amsterdam, Afd. Nat., 1ste reeks, v. 20, no. 3, p. 1–47.

———, 1957, Sole markings of graded graywacke beds: Jour. Geology, v. 65, p. 231–258.

Rich, J. L., 1950, Flow markings, groovings, and intrastratal crumplings as criteria for recognition of slope deposits, with illustrations from Silurian rocks of Wales: Am. Assoc. Petroleum Geologists Bull., v. 34, p. 717–641.

Rusnak, G. A., 1957, A fabric and petrologic study of the Pleasantview Sandstone: Jour. Sedimentary Petrology, v. 27, p. 41–55.

Sanders, J. E., 1957, Discussion: A fabric and petrologic study of the Pleasantview Sandstone: Jour. Sedimentary Petrology, v. 27, p. 198–201.

Straaten, L. M. J. U. van, 1950, Giant ripples in tidal channels: Tidjschr. Kon. Nederl. Aardr. Gen., v. 67. p. 76–81.

———, 1951, Texture and genesis of Dutch Wadden Sea sediments: Third Int. Congress Sedimentology, Proc., Groningen Wageningen, p. 225–244.

———, 1952, Biogene textures and the formation of shell beds in the Dutch Wadden Sea: Kon. Ned. Akad. Wetensch., Amsterdam, Proc., Ser. B, v. 55, p. 500–516.

———, 1954a, Sedimentology of recent tidal flat deposits and the psammites du Condroz (Devonian): Geol. en Mijnbouw, Nw. ser., 16e Jaargang, p. 25–47.

———, 1954b, Composition and structure of recent marine sediments in the Netherlands: Leidse Geol. Med., v. 19, p. 1–110.

Wanless, H. R., 1950, Late Paleozoic cycles of sedimentation in the United States: Report of the Eighteenth Session, Great Britain 1948, International Geological Congress, Part IV, p. 17-28.

———, 1952, Studies of field relations of coal beds: Second Conference on the Origin and Constitution of Coal, Crystal Cliffs, Nova Scotia, June 1952, p. 148–175.

Wanless, H. R., and Shepard, F. P., 1936, Sea level and climatic changes related to Late Paleozoic cycles: Geol. Soc. America Bull., v. 47, p. 1177–1205.

Weller, J. M., 1956, Diastrophic control of late Paleozoic cyclothems: Am. Assoc. Petroleum Geologists Bull., v. 40, p. 17–50.

Reprinted from Bulletin of the American Association of Petroleum Geologists, Vol. 41, No. 9, 1957

MID-TERTIARY ROCK OUTCROP ON CONTINENTAL SHELF, NORTHWEST GULF OF MEXICO[1]

ROBERT R. LANKFORD[2] AND JOSEPH R. CURRAY[2]
La Jolla, California

In June, 1956, a field party from the Scripps Institution of Oceanography conducted a cruise on the continental shelf of the northwest Gulf of Mexico to sample the sediments and organisms on the shelf, including the banks and topographic highs. One of the banks studied (Fig. 1), for which the name Stetson Bank has been proposed in honor of the late Henry C. Stetson, was found to consist of bedrock of sandstone and claystone containing a mid-Tertiary microfauna. This topographic high is interpreted as the expression of a salt dome protruding through the unconsolidated sediment.

Description of area.—Stetson Bank lies at 28°09.8′ N. Lat., 94°17.7′ W. Long., rising from a surrounding depth of about 31 fathoms on the continental shelf, 73 nautical miles, 159° True from Galveston, Texas. The surface sediment on this part of the shelf is predominantly a silty sand high in shell content. The bottom is generally smooth, but may locally appear "broken" or irregular because of shell, coquina, and calcareous beachrock. The macro-organisms have been identified as

---

[1] Contribution from the Scripps Institution of Oceanography, New Series No. 945. This investigation was supported by a grant from the American Petroleum Institute, Project 51. Manuscript received, June 12, 1957.

[2] Scripps Institution of Oceanography, University of California.

Reproduced by Permission

predominantly old, shallow-water, or shoreline shells mixed with living organisms indigenous to the present water depth (R. H. Parker, personal communication).

Description of Stetson Bank.—The bathymetry of Stetson Bank is shown in Figure 1, which was prepared from the U. S. Coast and Geodetic Survey unpublished sounding chart No. 6291. The bank is about 2,800 feet long and 900 feet wide above the 25-fathom contour, with the long axis trending N. 65°E. Echo soundings indicate that the steepest flank slopes, up to 45° or more, occur between the depths of 17 to 24 fathoms. The bank is similar to some of the banks studied previously in that its top is relatively flat from 10½ to 13 fathoms, which approximates one of the preferred depths of bank tops in the northwest Gulf of Mexico (Parker and Curray, 1956). Terraces are lacking on the sides of the bank because the most common terrace depths on other banks are at or below the base of this bank.

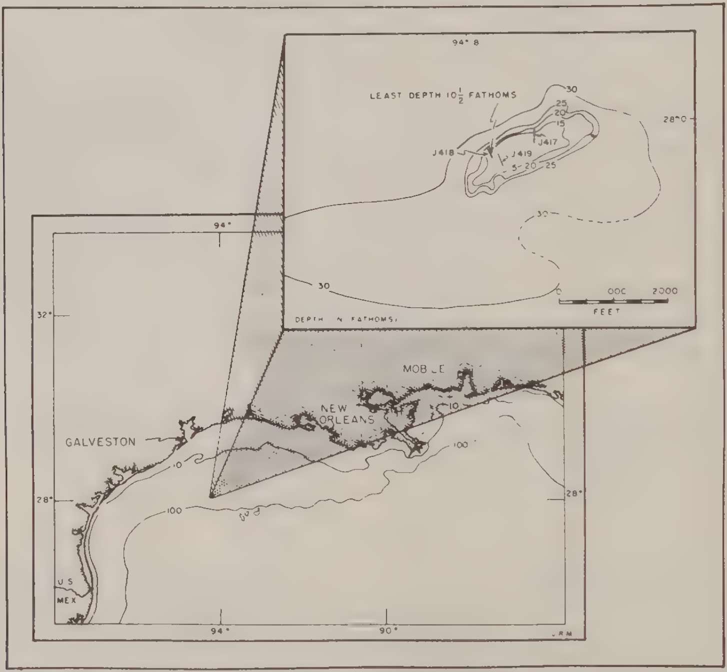

FIG. 1.—Location, bathymetry, and dredge stations on Stetson Bank.

Three dredge samples were taken on Stetson Bank in a steel box rock dredge at locations indicated on the chart in Figure 1. Each dredge haul contained fresh bedrock and living and dead biological specimens. The claystone contained abundant living rock-boring mollusks which may constitute a major agent of submarine erosion in areas of heavy infestation. At the time of sampling, diving operations could not be undertaken but the top of the bank could be seen through the clear water. Dark, elongate outcrops of rock gave the appearance of strike ridges trending about N. 45° E., or approximately parallel with the elongation of the bank.

Lithology.—The rock in each dredge haul consists of gray claystone and very fine-grained sandstone. The claystone is soft, non-fissile, generally massive, and light gray in color. Some pieces show extensive slickensides and fractures which cut across earlier thin veins of calcite less than 1 mm. thick. Crude laminations and bedding planes are present in some pieces but are rare. Sample J-418 contains iron-rich nodules up to 10 mm. in diameter. A size fractionation shows 0.5 per cent sand, 27.4 per cent silt, and 72.1 per cent clay. The approximate *weight* composition of the sand-size fraction is 44 per cent benthonic Foraminifera, 32 per cent planktonic Foraminifera, 17 per cent pyrite nodules, 6 per cent terrigenous sand (primarily quartz), and 1 per cent echinoid and other shell fragments. *Numerical* counts of only the Foraminifera, however, show about 53 per cent planktonic and 47 per cent benthonic species. Examination of other pieces of the claystone shows the presence of minor amounts of muscovite and trace quantities of glauconite. Results of these analyses are similar to those made of modern surface sediments near the edge of the present continental shelf or upper slope in the northwest Gulf of Mexico.

The sandstone is calcareous, silty, and very fine-grained. It is immature and near the borderline between subgraywacke and orthoquartzite according to the mineral composition and textural maturity terminology of Folk (1954). It is a hard, light gray, bedded sandstone, showing fine laminations in some beds. In places the laminations appear to be cross-bedded. The possibility that the sandstone might represent a Pleistocene sand deposited on top of the topographic high during lowered sea-level was ruled out by the presence of the same species of diagnostic Foraminifera in the sandstone as in the claystone. The approximate mineral composition of one thin section of the sandstone is quartz 40 per cent, chert 4 per cent, plagioclase 1 per cent, composite grains of strained quartz 2 per cent, mica 2 per cent, accessory minerals 1 per cent, matrix containing small amounts of silica cement 20 per cent, and crystalline calcite cement 30 per cent. Other thin sections show greater amounts of matrix and calcite cement replacing both matrix and grains.

Micropaleontology.—Most of the material from the three dredge samples contained Foraminifera. Preservation of the Foraminifera varies widely apparently due to recrystallization of calcite. Only in Sample J-417 was preservation sufficiently good to permit recognition of species of the easily destroyed discoasters.

Specimens from the three samples were sent to H. M. Bolli who very kindly identified a majority of the better preserved planktonic and benthonic Foraminifera. His identifications are summarized in Table I. The most striking feature of this assemblage is the similarity to faunas reported from the Caribbean and West Indian areas rather than to those described from the Gulf Coast. The Stetson Bank fauna is interpreted as representing a deeper-water facies than those de-

TABLE I

BENTHONIC FORAMINIFERA

Baggina sp.
Bathysiphon sp.
Bolivina spp.
Bulimina spp.
?Buliminella sp.
Chilostomella sp.
Cibicides matanzaensis (Hadley)
C. ?yaquensis Bermudez
C. spp.
Cyclammina sp.
?Dorothia nuttalli Cushman
Eggerella sp.
Eponides sp.
Gyroidina spp.
Hormosina sp.
Liebusella pozoensis Cushman and Renz var. *crassa* Cushman and Renz
Nonion pompilioides (Fichtel and Moll)
Plectofrondicularia ?mexicana (Cushman)
Pseudoclavulina chitinosa (Cushman and Jarvis)
Pseudoglandulina comatula (Cushman)
Pullenia bulloides (d'Orbigny)
?Pulvinulinella cultur (Parker and Jones)
Robulus formosus (Cushman)
R. ?occidentalis (Cushman) var. *torridus* (Cushman)
R. spp.
Saracenaria italica Defrance
S. senni Hedberg
Schenckiella cojimarensis (D. K. Palmer)
S. nodulosa (Cushman)

BENTHONIC FORAMINIFERA

Siphogenerina multicostata Cushman and Jarvis
S. transversa Cushman
S. sp.
Siphonina sp.
Sphaeroidina variabilis Reuss
Textularia excavata Cushman
Textulariella miocenica Cushman
Uvigerina carapitana Hedberg
U. mexicana Nuttall
U. rustica Cushman and Edwards
Vulvulina spinosa Cushman var. *miocenica* Cushman

PLANKTONIC FORAMINIFERA

?Globigerina foliata Bolli
G. cf. *rohri* Bolli
G. ?trilocularis d'Orbigny
G. venezuelana Hedberg
Globigerinoides triloba (Reuss)
G. triloba (Reuss) var. *immatura* Le Roy
G. triloba (Reuss) var. *sacculifera* (Brady)
?Globoquadrina altispira (Cushman and Jarvis)
?G. altispira (Cushman and Jarvis) var. *globosa* Bolli
G. dehiscens (Chapman, Parr, and Collins)
Globorotalia ?fohsi Cushman and Ellisor var. *barisanensis* Bolli
G. mayeri Cushman and Ellisor
G. obesa Bolli
Globorotaloides suteri Bolli
?Hasterigerina aequilateralis (Brady)
?Hasterigerinella bermudezi Bolli

scribed from the adjacent mainland. The foraminiferal fauna is believed to have accumulated in water depths equivalent to the modern upper continental slope, based on species of Foraminifera which are identical or closely related to forms living today. This interpretation is strengthened by absence of typical shallow-water genera and species and by the relative abundance of planktonic Foraminifera (53 per cent of the total population).

Considering the time-transgressive nature of many benthonic foraminiferal facies, the writers prefer to limit age considerations to the evidence derived from planktonic Foraminifera and discoasters. Based on the planktonic organisms, the several micropaleontologists who have examined the specimens generally agree on a mid-Tertiary age, probably middle Miocene. A more precise age determination is made more difficult by lack of agreement on how the American Tertiary is to be correlated with the European type section. Personal communications from various micropaleontologists are briefly summarized. In order to facilitate the age discussion, the stratigraphic divisions of the Miocene proposed by Akers and Drooger (1957) are used.

H. M. Bolli concludes that although the planktonic Foraminifera lack typical marker species, the assemblage strongly indicates that the fauna belongs either in the *Globigerinatella insueta* zone (Helvetian and Tortonian, middle Miocene) or is only slightly younger or older. W. H. Akers would assign the fauna to the Helvetian stage, middle Miocene, while Marcus A. Hanna considers the material to be no older than upper Tortonian (middle Miocene) and possibly considerably younger. Species of discoasters from Sample J-417 were examined by M. N. Bramlette, and although the assemblage was meager and poorly preserved, it appears to him to be middle Tertiary and not younger than middle Miocene.

INTERPRETATIONS

1. On the basis of Foraminifera, the Stetson Bank outcrops are believed to be mid-Tertiary, probably middle Miocene in age.
2. The environment of deposition is interpreted to have been equivalent to the water depths of the present upper continental slope (65–100 fathoms or even deeper).
3. In the general subsurface geologic section as it is now understood (Lowman, 1949; Houston Geological Society, 1951) a mid-Tertiary age would mean that the rock must have been pushed up from many thousands of feet to its present occurrence. It thus appears to be the surface expression of a salt-dome intrusion, as was previously suggested for some of these banks (Shepard, 1937).
4. The flat summit of this bank occurs in the depth range of one of the most frequent depths of bank tops in the northwest Gulf of Mexico (Parker and Curray, 1956). This suggests that Stetson Bank may have been in existence at the time sea-level stood 9–10 fathoms lower during the Pleistocene.

REFERENCES

AKERS, W. H., AND C. W. DROOGER, 1957, "Miogypsinids, Planktonic Foraminifera, and Gulf Coast Oligocene-Miocene Correlations," *Bull. Amer. Assoc. Petrol. Geol.*, Vol. 41, pp. 656–78.

FOLK, ROBERT L., 1954, "The Distinction between Grain Size and Mineral Composition in Sedimentary-Rock Nomenclature," *Jour. Geol.*, Vol. 62, pp. 344–59.

HOUSTON GEOL. SOCIETY, 1951, "Western Gulf Coast" in "Possible Future Petroleum Provinces of North America," *Bull. Amer. Assoc. Petrol. Geol.*, Vol. 35, pp. 385–92.

LOWMAN, S. W., 1949, "Sedimentary Facies in Gulf Coast," *ibid.*, Vol. 33, pp. 1939–97.

PARKER, ROBERT H., AND JOSEPH R. CURRAY, 1956, "Fauna and Bathymetry of Banks on Continental Shelf, Northwest Gulf of Mexico," *ibid.*, Vol. 40, pp. 2428–39.

RENZ, H. H., 1948, "Stratigraphy and Fauna of the Agua Salada Group, State of Falcon, Venezuela," *Geol. Soc. America Memoir 32.* 219 pp.

SHEPARD, FRANCIS P., 1937, "Salt Domes Related to Mississippi Submarine Trough," *Bull. Geol. Soc. America*, pp. 1349–62.

Geochimica et Cosmochimica Acta, 1957, Vol. 13, pp. 5 to 19. Pergamon Press Ltd., London

Reproduced by Permission

On the geochemistry of germanium*

SAYED A. EL WARDANI
Department of Oceanography, University of Washington

(*Received* 1 *April* 1957)

Abstract—Estimates of the abundance of germanium have been lowered to about 10 p.p.m. for its cosmic level and 1 p.p.m. for the earth's crust, as compared to GOLDSCHMIDT'S values of 55 p.p.m. and 7 p.p.m., respectively. Germanium in iron meteorites varied from less than 1 p.p.m. to 500 p.p.m.; chondrites were fairly uniform in their germanium content, which varied between 6 and 12 p.p.m. The concentration in granites, basalts and gabbros was consistently about 1 p.p.m. and thermal springs were found to be almost devoid of germanium. Germanium is classified among the less volatile elements when its escaping tendency is compared with that of other elements.

1. INTRODUCTION

EARLY estimates of the abundance of germanium in the earth's crust by CLARKE (1924) are of historical interest only, because they were not based on actual determinations of the element. Recent references to germanium abundance quote estimates by either the NODDACKS (NODDACK, 1930; 1931; 1934; 1939) or GOLDSCHMIDT (GOLDSCHMIDT, HAUPTMANN, and PETERS, 1933; GOLDSCHMIDT and PETERS, 1933; GOLDSCHMIDT, 1937). GOLDSCHMIDT found an average content of 4 p.p.m. for igneous rocks and 7 p.p.m. for sedimentary rocks (mostly from the analysis of shales), but he took 7 p.p.m. for the abundance of germanium in the earth's crust. GOLDSCHMIDT'S estimate for the cosmic abundance of germanium is 55 p.p.m. and is based on spectrographic determinations. The NODDACKS' estimate (1930) was based on the spectrographic analysis of some 1600 minerals and rocks, including a mixture of 110 eruptive rocks; however, the detailed results of few of their determinations were published. NODDACKS' average for igneous rocks is 1 p.p.m., and for the cosmic abundance is 31 p.p.m.

Since 1937 only a few determinations of germanium in igneous rocks have been made, spectrographically (PREUSS, 1941; and HARRIS, 1954) and colorimetrically (HYBBINETTE and SANDELL, 1942; SCHNEIDER and SANDELL, 1954). The range reported for this more recent work was from 0·8 p.p.m. to 3·0 p.p.m.

During the preparation of this manuscript, ONISHI (1956b) published the results of his germanium analyses for a number of geomaterials including some 18 chondrites. His findings are referred to in the appropriate sections of this paper and are compared with the data obtained by the present writer. Several of the samples were analysed independently by both ONISHI and the present author. In one way, the duplication was unfortunate; in another way, the two independent studies corroborate one another and the data are generally in excellent agreement.

The data prior to 1956 for the abundance of germanium are well summarized by ONISHI (1956b). The present paper provides data on the germanium content of chondrites, iron meteorites, common igneous rocks, sedimentary rocks, and thermal spring waters.

---

* Contribution No. 212 of the Department of Oceanography, University of Washington. Contribution No. 946, New Series, Scripps Institution of Oceanography.

2. ANALYTICAL METHOD

The procedure for determining germanium in geological material is being prepared by the author for publication. In brief, germanium is determined spectrophotometrically as the phenylfluorone-germanium complex. A Beckman Model DU Spectrophotometer is used and the absorbency is measured at 505μ. A 100-mesh powder of silicate rock (0·2–0·5 g) is put completely into solution by first treating with hydrofluoric acid in a platinum dish to remove the silica, and next fusing the residue with potassium pyrosulphate. Before converting the germanium into the phenylfluorone complex, the element is first separated by distilling as germanium tetrachloride from nearly-constant boiling point hydrochloric acid solution. For 1 p.p.m. of germanium the error is within 10 per cent, and for higher germanium concentrations it is proportionately less. Table 1 records the recovery of germanium from the complex matrix of pelagic clays to which known amounts have been added, and Table 2 gives the results of independent laboratory analyses for the same original material.

Table 1. Recovery of germanium from pelagic red clay
(Red clay Y2P-96, Lat. 20°50′ N., Long. 125°14·5′ W.)

Ge present* p.p.m.	Ge found p.p.m.
2·5	2·4
5·0	5·2
10·0	9·5
16·0	15·5
20·0	20·0
52·0	50·0

* The original germanium content of this sediment was 2·0 p.p.m., determined independently by the author's method and that of SCHNEIDER and SANDELL (1954). Germanium was then added to increase the content to the amounts indicated.

In the SCHNEIDER and SANDELL (1954) procedure, silicate rock powder is first treated with a mixture of nitric, sulphuric, and hydrofluoric acids. Germanium is then separated from interfering elements by taking up the residue in concentrated hydrochloric acid and extracting germanium tetrachloride with carbon tetrachloride. The element is next transferred to an aqueous solution by shaking the carbon tetrachloride solution with water. Subsequently, a photometric determination is made of the phenylfluorone complex. In spite of the differences in techniques used for decomposing the material and separating the element, the agreement between the author's results and those obtained by independent analysts using the SCHNEIDER–SANDELL (1954) procedure is striking. This agreement was also pointed out and discussed by ONISHI (1956a and b). These independent tests, made at different laboratories, give confidence in the values so obtained for the abundance of germanium.

Table 2. Independent laboratory analyses

Material	Present method p.p.m.	Other methods p.p.m.	Analyst and method
Pacific Red Clay Lat. 20°50′ N. Long. 125°14·5′ W.	2·0 2·1 2·1 2·0 1·95	2·0	A. Maxwell Geol. Surv. of Canada; Modified Schneider and Sandell colorimetric, technique (1954).
Average	2·0		
		1·5	Peter Zubovic, U.S. Geol. Survey, phenylfluorone colorimetric method, sensitivity 1 p.p.m.
		Not detected	Nola B. Sheffey, U.S. Geol. Survey, spectrographically,*
Pacific Red Clay Lat. 11°20′ S. Long. 142°25·5′ W.	1·0	Not detected	Nola B. Sheffey, U.S. Geol. Survey, spectrographically.*
		Not detected	Peter Zubovic, U.S. Geol. Survey, phenylfluorone colorimetric method, sensitivity 1 p.p.m.
Grand Marais diabase, Minn.†	1·4‡	1·4	Schneider and Sandell (1954).
Chondrite, composite of 7 meteorites §	10·6	10·0	Onishi and Sandell, personal correspondence; and later Onishi (1956a and b).

* Limit of sensitivity for germanium in the spectrographic technique used is reported to be 0·0002 per cent.

† Percentage composition; Si_2O 52·7, Al_2O_3 14·5, Fe_2O_3 7·4, FeO 5·6, MgO 3·7, CaO 8·0, Na_2O 3·2, K_2O 1·1, TiO_2 1·8, P_2O_5 0·25, MnO 0·24.

‡ Average of triplicate analyses of 1·4, 1·4, 1·4.

§ Arriba, Colo.; Beenham, N. Mex.; Cope, Colo.; Coterfield, Neb.; Morland, N. Mex.; Plainview, Texas; Roy, N. Mex.

3. Germanium in Meteorites

No analyses of meteorites for germanium are available since the early work of Goldschmidt and the Noddacks more than 20 years ago.* A summary of previous data and estimates of germanium in meteorites is given by Onishi (1956b).

Seven iron meteorites and eight chondrites (including two composites) were analysed for germanium. The results are shown in Tables 3 and 4 respectively. In Table 3 the nickel content of the iron meteorites is also given.

Onishi (1956b) reported the analyses of 18 individual chondrites and 2 com-

---

* While this manuscript was being prepared, Onishi (1956b) has published the results of the analysis of 18 individual chondrites and 2 composites.

Table 3. Germanium in iron meteorites

Meteorite	Description*	Ge, p.p.m.	Ni, per cent
Tlacotepec	Ataxite	<1·0	16·23
Duchesne	Fine octahedrite	<1·0	9·12
Edmonton	Fine to finest octahedrite	38·0	12·66
Toluca	Medium octahedrite	270·0	8·31
Henbury	Medium octahedrite	270·0	7·66
Canon Diablo	Coarse to coarsest octahedrite	350·0	7·18
Magura	Coarse octahedrite	520·0	7·08

* PRIOR and HEY (1953)

posites. All chondritic materials analysed by the present author were independently analysed by ONISHI. In spite of the differences in techniques used for decomposing the material and for separating of the element, and in the type of instrument used, the data are in good agreement. The author's range for the individual chondrites is 6·6*–12·0 p.p.m. with an average of 9·2 p.p.m. germanium as compared to a range of 9·0–12·4 p.p.m. and an average of 10·6 p.p.m. germanium obtained by ONISHI. ONISHI found 9·5, 10·0 p.p.m. (duplicate analyses) and 11·7, 10·9 (duplicate analyses) for composite I and II respectively. ONISHI's average for the two composites is 10·5 p.p.m. as compared to 10·0 p.p.m. for the present author. The average germanium content of all chondritic material analysed by ONISHI is 10·6 p.p.m. as compared to 9·4 p.p.m. found by the present author.

The grand average of both ONISHI's and the present author's germanium values for chondrites give 10 p.p.m. for the cosmic abundance of the element. This corresponds to less than one-fifth GOLDSCHMIDT'S 55 p.p.m. (GOLDSCHMIDT, 1954) and one third the NODDACKS' value of 31 p.p.m. (NODDACK, 1934) for the cosmic abundance of germanium.

Chondrites have fairly uniform germanium content. Such uniformity has been found for other trace elements such as molybdenum (KURODA and SANDELL, 1954), and gallium (ONISHI and SANDELL, 1956). Although some of the chondrites used in the present work are badly weathered, it does not appear that weathering has changed the germanium content significantly, inasmuch as the chondrites analysed show no apparent relationship between the germanium content and the degree of weathering.

If we adopt the UREY–CRAIG (1953) average for silicon in chondrites, namely 18 per cent, we obtain a weight ratio $Ge/Si = 10{\cdot}0/18 \times 10^4 = 5{\cdot}6 \times 10^{-5}$, as

---

* This represents the poorest agreement between the two workers. A single analysis by the present author gives 6·6 p.p.m. for the Ladder Creek chondrite as compared to 9·2, 9·2 p.p.m. (duplicate analyses) of the same chondrite by ONISHI.

Table 4. Germanium in chondrites

Chondrite	Description*	Ge, p.p.m.
Composite I:		10·3, 10·9
Arriba, Colo.	Polymict brecciated intermediate chondrite	
Beenham, N. Mex.	Veined grey hypersthene chondrite (Leard) or intermediate (Wahl)	
Cope, Colo.	No description	
Cotesfield, Nebr.	No description	
Morland, Kans.	Crystalline chondrite	
Plainview, Tex.	Polymict brecciated veined intermediate chondrite	
Roy, N. Mex.	Crystalline spherical bronzite chondrite	
Composite II:		9·4, 9·6
Alamogordo, N. Mex.	Crystalline spherical chondrite	
Estacado, Tex.	Crystalline bronzite chondrite	
Gladstone, N. Mex.	Black veined crystalline spherical chondrite	
Kingfisher, Okla.	Black chondrite	
Gruver, Tex.	No description	
Ladder Creek, Kans.	Crystalline spherical chondrite	
Melrose, N. Mex.	Hypersthene chondrite	
Arriba, Colo.	Polymict brecciated intermediate chondrite	9·2, 9·0
Ladder Creek, Kans.	Crystalline spherical chondrite	6·6
Melrose, N. Mex.	Hypersthene chondrite	9·3, 9·6
Plainview, Tex.	Polymict brecciated veined intermediate chondrite	12·0
Roy, N. Mex.	Crystalline spherical bronzite chondrite	8·8
	Average.......	9·4
	Component phases of chondrites	
Composite 11		
Magnetic fraction	38·8 per cent of the sample	29·0
Nonmagnetic fraction	61·2 per cent of the sample	2·5

* Prior and Hey (1953)

compared to a weight ratio $Ge/Si = 1{\cdot}0/2{\cdot}7 \times 10^5 = 0{\cdot}37 \times 10^{-5}$ for the earth's crust (based on the present work). The high germanium content of the magnetic fraction indicates the strong siderophilic nature of the element.

On comparing the germanium content of the chondrites with that of the iron meteorites, we find that the concentration is relatively uniform in chondrites with a maximum variation factor of 2. However, the iron meteorites show either a quantization of germanium, or a continuous distribution of meteoritic types and compositions with variation in the germanium content up to 500-fold or more.

Valid conclusions can scarcely be drawn from the few analyses of iron meteorites; nevertheless, two possibilities may be suggested:

(1) An inverse relationship possibly may exist between the germanium and nickel contents of iron meteorites.

(2) The germanium content of iron meteorites may be related to their structure, inasmuch as this content decreases from coarse octahedrites to fine octahedrites.

Additional analyses may reveal that iron meteorites possibly can be classified on the basis of their germanium and nickel contents.

While the Henbury meteorite, with a nickel content of 7·66 per cent, had 270 p.p.m. germanium, we find that the Magura meteorite, with an almost identical nickel content, has 520 p.p.m. germanium. The present data on germanium in meteorites reveal the complexity of the problem and suggest the need for more experimental studies before the physicochemical conditions associated with the formation of meteorites can be explained.

4. GERMANIUM IN ROCKS AND MINERALS

4.1. *Igneous rocks and their component minerals*

Both composites and individual samples have been analysed to obtain average concentrations of germanium in common rock types. According to DALY (1933), granitic rocks comprise at least 95 per cent of all intrusive rocks, and basalts about 98 per cent of the extrusive rocks. It is considered satisfactory for the present purpose to take the average germanium content of granites and basalts as representative of the germanium abundance of the earth's crust. The germanium content of igneous rocks analysed by the author is given in Table 5. Independent analyses by ONISHI (1956b) are in good agreement with the present data. ONISHI's averages for igneous rocks are reported in Table 6 for purposes of comparison.

The abundance of germanium is practically the same for granitic rocks, basalts, diabases, and gabbros. The average germanium content of the earth's crust, based on the samples analysed by this author, may be taken as 1·0 p.p.m. in comparison to 7 p.p.m. as estimated by GOLDSCHMIDT (1937). ONISHI (1956b) gives 1·5 ± 0·5 p.p.m. as the most reasonable figure for the germanium content of the lithosphere.

Based on the average chemical composition of igneous rocks (NOCKOLDS, 1954), the ratio of germanium to silicon for the common rock types analysed is as follows:

Rock type	Ge/Si (wt. ratio)
Granites	$3{\cdot}3 \times 10^{-6}$
Basalt and diabases	$5{\cdot}0 \times 10^{-6}$
Gabbros	$5{\cdot}0 \times 10^{-6}$

The present data and those of ONISHI (1956b) indicate that if there is any preferential enrichment of germanium relative to silicon in the silicate rock-forming

Table 5. Germanium in igneous rocks and their minerals

Sample	Ge, p.p.m.
Granitic rocks	
Porphyritic granite, Stearns Co., Minn.	1·1, 1·1
Hornblende granite, Freedhem, Minn.	0·9, 1·0
Porphyritic granite, Benton Co., Minn.	1·0
Quartz monzonite, Warman, Minn.	1·0, 1·1
Granite porphyry, Benton Co., Minn	1·2
Biotite granite (coarse grained), Benton Co., Minn.	0·9, 0·9
Biotite granite (fine grained), Benton Co., Minn.	1·1, 1·0
Granite "red," Benton Co., Minn.	1·4
Granite "red," Lower Falls, Snake River, Minn.	1·4, 1·5
Granite, near Pierz, Minn.	1·1, 1·2
Hornblende tonalite, Freedhem, Minn.	1·0, 0·9
Quartz monzonite, Rockville, Stearns Co., Minn.	0·9
Composite of 6 Central Texas granites (equal weights): Cassaday; Town Mtn.; Granite Mtn.; Llanite; Patrick Granite; Bear Mtn.	1·5
Composite of 5 granites (equal weights): Porphyritic granite, Stearns Co., Minn.; Hornblende granite, Freedhem, Minn.; Granite porphyry, Benton Co., Minn.; Biotite granite, Benton Co., Minn.; Granite "red", Benton Co., Minn.	1·2, 1·1
Composite, rhyolite, Cook Co., Minn (12 beach pebbles)	1·1, 1·0
Average	1·1

Sample	Ge, p.p.m.
Basic igneous rocks	
Diabase, Grand Marais, Minn.	1·4, 1·4*
Diabase, N.B.S., S.S. No. 4984	1·3, 1·2
Deccan Trap, N.B.S., S.S. No. 4978	1·3, 1·2
Basalt, N.B.S., S.S. No. 4978	1·2, 1·2
Basalt and diabase, composite of 8: Diabase, Grand Marais, Minn.; Diabase, Interstate Park, Wis.; Basalt, Douglas Creek, Wash.; Basalt, Columbia River; Diabase, S.S. No. 4984; Basalt, Deccan Trap; Basalt, St. Cloud, Minn; Diabase, porphyritic, Interstate Park, Wis.	1·3, 1·4
Basalt, composite of 8: Albert Lake, Oregon; Columbia Plateau; West of Madras; Devils Post Pile, Calif.; Keeler, Calif.; Blairsden, Calif.; Washington; S.S. No. 4985.	1·3, 1·2
Average	1·3

Table 5 (*continued*)

Gabbros	
Gabbro, composite of 6: Gabbro, Mora, Minn.; Gabbro, Lake Isabena, Minn.; Orthoclase Gabbro, Duluth, Minn.; Gabbro (above cement plant), Duluth, Minn.; Gabbro (S. Goldich sample), Duluth, Minn.; Gabbro, Duluth, Minn.	1·2, 1·3
Gabbro, Duluth, Minn.	1·1
Gabbro (S. Goldich sample), Duluth, Minn.	1·3, 1·5
Gabbro (above cement plant), Duluth, Minn	0·9, 0·8
Average	1·1
Average of all igneous rocks analysed = 1·1 p.p.m. Ge	
Minerals	
Quartz, extracted from manganese nodule, Pacific, lat. 19°49′ N., long. 121°43·5′ W.	0·0, 0·0
Quartz, pegmatitic, optical grade, Brazil	0·0, 0·0
Quartz, pegmatitic, Oak Grove, California	0·0
Quartz, locality and type not known	0·0
Feldspar, composite of 5: Pegmatitic microcline, Colo.; Pegmatitic orthoclase, Oak Grove, Calif.; Pegmatitic andesine, Hemet, Calif.; Anorthite; Oligoclase	0·9
Augite, Franklin, New Jersey	0·6
Augite, Danville, New Jersey	1·7
Hornblende, unknown location	2·0
Olivine, unknown location	1·6
Olivine, unknown location	2·1
Magnetite, unknown location	1·1
Magnetite, unknown location	0·9
Ilmenite, unknown location	1·0, 0·9
Hematite, unknown location	3·6, 3·4
Apatite, unknown location	0·0

* Independent analysis (SCHNEIDER and SANDELL, 1954) gives 1·4 p.p.m. germanium.

minerals, it is found in the least-linked silicate structures, substantiating the findings of HARRIS (1954), and in contrast to GOLDSCHMIDT–PETERS data suggesting an enrichment of germanium in silicic over subsilicic rocks.

In its distribution in igneous rocks and their component minerals, germanium does not appear to follow closely any one of the major constituents. Its absence in quartz and its presence in all the silicates analysed,* indicate that the element may frequently substitute for silicon in the silicates (GOLDSCHMIDT, 1926).

The principles governing the distribution of trace elements in minerals and rocks

---

* Zeolites (phillipsites) failed to give measurable germanium. The results of these analyses will be included in a separate paper on the marine geochemistry of germanium, being prepared by the author.

Table 6. Average germanium content of igneous rocks (Onishi, 1956b)

Rock (number of samples)	Range Ge, p.p.m.	Average Ge, p.p.m.
Granitic rocks (43)	0·7–1·8	1·3
Japanese (35)	0·7–1·8	1·3
U.S.A. (8)	0·9–1·8	1·2
Intermediate rocks (12)	0·9–2·0	1·5
Japanese (10)	1·3–1·7	1·5
Basalts and diabases (15)	1·0–1·7	1·3
Japanese (5)	1·0–1·7	1·5
Other localities (10)	1·1–1·6	1·3
Gabbros (20)	0·8–1·8	1·2
Japanese (12)	0·8–1·7	1·2
Other localities (8)	0·8–1·8	1·3
Ultramafic rocks (8)	0·7–1·6	1·0

were formulated by Goldschmidt (1937). The respective ionic radii (Ahrens, 1952) of Ge^{+4} and Si^{+4} are 0·53 Å and 0·42 Å. Although the ionic radii difference exceeds 15 per cent (the limit for isomorphous substitution), experimental evidence indicates that the two elements are similar geochemically in some compounds. The fairly uniform distribution of germanium among the common igneous rocks may be due to the ability of the element to replace a number of other elements in the rock-forming minerals. It is found in feldspars, amphibole, olivine, magnetite, and ilmenite, but is absent in quartz.

4.2. *Sediments of North America*

The germanium content of sediments and sedimentary rocks of North America is presented in Table 7. Analyses of reference clay minerals of the American Petroleum Institute are also included in the table. These analyses show that germanium is commonly present in shales and clays and their minerals, substantiating Goldschmidt's rules for the occurrence of germanium (Goldschmidt, 1926). Limestones, and dolomites contribute no germanium to the sediments, and sandstones most probably are similar to quartz in being devoid or possessing a fraction of a part per million of germanium.

Shales may show a strong variation in their germanium content depending on the type of shale and its organic content. Breger and Schopf (1955), by a semiquantitative spectrographic technique, were able to show that shales from the Chattanooga formation contain from 10-40 p.p.m. of germanium in the ash. A Chattanooga shale (IAB15B-3) received from Dr. I. A. Breger showed 16·6 p.p.m. germanium (or 25 p.p.m. in the ash) by the present method.

While the analysed shales give an average of 1·1 p.p.m. of germanium, similar

(633)

Table 7. Germanium in sediments of North America

Sample	Ge, p.p.m.
Shales	
Composite (3), St. Croix Falls, Wis.	0·8, 0·8
Shale, Glenwood, lower half, Minneapolis, Minn.	1·6, 1·5
Shale, Cambrian, St. Croix Falls, Wis.	1·5
Shale, pyritic, St. Croix Falls, Wis.	0·8
*Clays and clay minerals**	
Clay, cretaceous, Two Rivers, Minn.	1·0
Clay, residual, Redwood Falls, Minn., No. 27	1·1
Clay, cretaceous, Two Rivers, Minn., No. 17	1·0, 1·1
Illite, Morris, Ill.	1·2, 1·2
Illite, Fithian, Ill.	1·2
Kaolinite, Murfreesboro, Ark.	1·3, 1·4
Kaolinite, Macon, Ga.	1·3, 1·3
Kaolinite, Bath, S.C.	1·1, 1·1
Kaolinite, Mesa Alta, N. Mex.	1·0
Montmorillonite, marine, Polkville, Miss.	0·5
Montmorillonite, marine, Upton, Wyo.	0·5
Montmorillonite, marine, Little Rock, Ark.	0·5
Montmorillonite, non-marine, Otay, Calif.	2·3
Montmorillonite, non-marine, Chambers, Ariz.	12·0, 12·0
Montmorillonite, non-marine, Pioche, Nev.	0·0, 0·0
Montmorillonite, non-marine, Cameron, Ariz.	1·3, 1·2
Nontronite, non-marine, Spokane (Garfield); Wash.	0·0, 0·0
Glauconite, No. 28, (S.I.O. sample)	2·0, 2·0
Limestone and sandstone	
Limestone, Kasota, Minn.	0·0, 0·0
Dolomite, Platteville, Minneapolis, Minn.	0·0, 0·0
Dolomite, Red Wing, Minn.	0·0
Dolomite, Hastings, Minn.	0·0
Beach sand, washed with HCl, La Jolla, Calif.	0·5, 0·5
St. Peter sandstone, Minneapolis, Minn.	0·5, 0·5
Miscellaneous	
Gypsum, unknown locality	0·0
Barite, unknown locality	0·0
Zeolite, Natrolite, unknown locality	0·0, 0·0
Goethite, Pikes Peak, Colo.	16·0, 16·0

* All clay minerals analysed except glauconite No. 28 are Standard A.P.I. minerals.

to that for the average of igneous rocks, the wide variation of germanium content in shales makes it very difficult to arrive at an average figure for all shales. An average somewhat higher than that for igneous rocks is conceivable because of the scarcity of germanium in limestones and sandstones, because of the probable mobility of germanium, and because of its escape from magmas and its subsequent addition to the sea and the sediments. For the quantitative geochemical treatment at the present time, the average germanium content for all shales is estimated as twice that of the germanium content of igneous rocks, obtained by the present author.

A figure of 2·0 p.p.m. germanium is given by ONISHI (1956b) as the weighted average of 3 composites of 60 European and Japanese shales and his duplicate analyses of 4 Japanese shales gave a range of 0·8 to 1·7 p.p.m. with an average of 1·6 p.p.m. germanium. Our knowledge of the distribution of germanium in sedimentary rocks, particularly shales, is still fragmentary and analysis of larger numbers of samples is desirable.

4.3. *Shelf and deep-sea sediments*

Table 8 lists the number of samples analysed and the average germanium content of shelf and deep-sea sediments. The location and description of the samples analysed and their individual germanium content are being covered in a paper currently being prepared by the author on the marine geochemistry of germanium.

Table 8. Germanium in shelf and deep-sea sediments

Material	Number of samples	Ge, p.p.m.
Shelf and basin sediments	17	1·1
Pelagic clays (Pacific)	27	2·0
Globigerina ooze (Pacific)	4	0·0

5. CYCLE AND BALANCE OF GERMANIUM

Germanium finds its way to the ocean and into sediments most probably in association with clay minerals and detrital minerals. Doubtless some germanium is present in solution in ionic or molecular form. The germanium content of sea water was found by the author to be 5×10^{-5} p.p.m.; the total amount in the ocean waters, accordingly, is negligible compared to that in the sediments.

The problem of quantitative geochemistry has been studied by GOLDSCHMIDT (1933), KUENEN (1941; 1946; 1950), RANKAMA and SAHAMA (1950), and recently by WICKMAN (1954).

After complete weathering of an igneous rock, only the resistates such as quartz, ilmenite, and magnetite will be left. Elements which enter into solution are ultimately incorporated in limestone, dolomite, shales, and clays. Some elements remain in solution and are therefore found in sea water. The problem can be represented by the following equation: $i_x I = m_x M + s_x S$, where I = the total amount of weathered average igneous rocks; M = the total amount of sea water; S = the total amount of sediments formed from igneous rocks; i_x, m_x, s_x = the weight percentages of an element x in each type of material.

Since granites and basalts form at least 95 per cent and 98 per cent of the intrusive and extrusive rocks respectively (DALY, 1933), deep-sea and shelf sediments are assumed to have been formed from granite and basalt.

Opinions differ concerning the absolute amounts of the shelf and deep-sea sediments and their relative importance in contributing to the total amount of sediment. Furthermore, the proportion of shale, sandstone, and limestone in sediments of the continental shelf is open to question. The extent of contribution of deep-sea sediments to the total has been emphasized especially by KUENEN (1941; 1946; 1950). According to GOLDSCHMIDT (1933), weathered igneous rock amounts to $1{\cdot}6 \times 10^5$ g/cm² of the earth's surface.* If we assume that an equal weight of sediments resulted from the weathering of this amount of igneous rocks with the proportions 80 per cent shale and clay, 10 per cent sandstone, and 10 per cent limestone and dolomite (GOLDSCHMIDT's figures are 91 per cent clastics and 9 per cent limestone and dolomite), and if we take the germanium content of shales and clay as 2·0 p.p.m., and that of sandstone and limestone as 0·0 p.p.m., we then have:

$$\text{germanium from igneous rock} = 1{\cdot}6 \times 10^5 \times 1{\cdot}0 \times 10^{-6} = 0{\cdot}16 \text{ g/cm}^2$$

$$\text{germanium in sediments} = 1{\cdot}6 \times 10^5(0{\cdot}8 \times 2{\cdot}0 + 0{\cdot}2 \times 0{\cdot}0)10^{-6} = 0{\cdot}26 \text{ g/cm}^2.$$

The excess germanium amounts to 0·1 g/cm².

The physical and chemical properties of some germanium compounds suggest an appreciable mobility for the element germanium. Germanium tetrachloride and germanous oxide are volatile at moderately low temperatures. Germanium oxides are relatively soluble in water and the sulphides dissolve readily in alkalies and alkaline sulphide solutions, giving soluble thiosalts. There is evidence for the transport of some elements from deep sources to the surface, inasmuch as they are present in thermal waters (BRANNOCK *et al.*, 1948; WHITE and BRANNOCK, 1950). Seven hot-spring water samples from different localities were analysed for germanium. The results, given in Table 9, indicate that thermal spring waters may be practically devoid of germanium.

An attempt was made to compare the escaping tendency of germanium with that of a few elements which form volatile compounds. The relative escaping tendencies are obtained by taking the excess of element now in the atmosphere, hydrosphere, and sediments, and expressed in g/cm² of the earth's surface, and dividing by the amount of the element (g) found in the frustrum of a cone which has a 1 cm² base at the earth's surface and which extends downward 60 km through the granitic and basaltic shell. Although the absolute values of the ratios have little significance, the relative magnitudes may be used as a rough measure of the escaping tendencies and the behaviour of elements. The calculation of the escape ratios is represented by the following example for germanium: amount of

---

* WICKMAN (1954) gave $1{\cdot}94 \times 10^5$ g/cm² as the most probable amount of weathered igneous rock.

Table 9. Germanium content of thermal spring waters*

Sample	Location	Ge, p.p.m.
1233	Steamboat Springs, Nevada, Spring No. 50, February, 1955	0·04
599	Norris Basin, Yellowstone Park, Spring near Hurricane Vent, August, 1953	0·04
1278–28	Raudara', Reykjavik, Iceland	0·00
602	Punch Bowl Spring, Upper Basin, Yellowstone Park, Wyoming, August, 1953	0·00
587	Magnesia Spring, The Geysers, California, August, 1953	0·00
586	Devil's Range Spring, The Geysers, California, August, 1955	0·00
590	Large boiling pool, Sulphur Works, Lassen Park, California, August, 1953	0·00

* Samples were provided by DR. HARMON CRAIG of the Scripps Institution of Oceanography.

excess germanium = 0·1 g/cm²; amount of material from which this is assumed to be derived = $6 \times 10^6 \times 3 \times 1 = 1{\cdot}8 \times 10^7$ g/cm²; amount of germanium in this mass = $1{\cdot}8 \times 10^7 \times 1{\cdot}0 \times 10^{-6} = 18$ g/cm²; escape ratio of germanium = 0·1/18, approximately 0·005. The escape ratios for hydrogen, chlorine, arsenic, antimony, molybdenum, copper, and zinc are given in Table 10.

Table 10. Calculated escaping ratios for some elements

Element	Escape ratio	Source of data
Ge	0·005	Present Work
As	0·03	ONISHI and SANDELL (1955a)
Sb	0·03	ONISHI and SANDELL (1955b)
Cu	0·002	KURODA and SANDELL (1953)
Zn	0·002	KURODA and SANDELL (1953)
S	0·05	KURODA and SANDELL (1953)
Cl	2·0	KURODA and SANDELL (1953)
$H(H_2O)$	1·2	KURODA and SANDELL (1953)

The escaping tendency of germanium places the element among the less volatile ones, copper and zinc. The abundance of chloride in magmatic fluids and the volatility of germanium tetrachloride may suggest a possible relationship between the chlorine and the germanium contents of thermal waters of magmatic origin. On the other hand, the absence or presence of a fraction of a part per million of germanium in thermal waters may be due to the lithophilic, siderophilic, and chalcophilic nature of the element. During the crystallization of magma, germanium may enter the crystal lattice of the silicates and oxides by isomorphous substitution. Dilution of magmatic water by underground water may also bring about the precipitation of germanium. Chlorine, on the other hand, has little tendency for isomorphous substitution and escapes to the surface.

Acknowledgements—The author is indebted to Dr. E. B. SANDELL, who provided nearly all of the material analysed and who made invaluable comments through correspondence. Appreciation is expressed to Dr. GUSTAF ARRHENIUS, Dr. HARMON CRAIG, and Mr ROBERT REX for providing some of the samples, and for their help during the investigation; and to Dr. EARL INGERSON, Dr. MICHAEL FLEISCHER, and Dr. CLIFFORD BARNES who read and criticized the manuscript. The author is particularly grateful to Dr. NORRIS W. RAKESTRAW for his kind supervision and co-operation while this work was conducted at the Scripps Institution of Oceanography.

REFERENCES

AHRENS H. L. (1952) The use of ionization potentials, Part I. Ionic radii of the elements. *Geochim. et Cosmochim. Acta* **2,** 155–169.

BRANNOCK W. W., FIX P. F., GIANELLA V. P. and WHITE D. E. (1948) Preliminary geochemical results at Steamboat Springs, Nevada. *Trans. Amer. Geophys. Un.* **29,** 211–226.

BREGER I. A. and SCHOPF J. M. (1955) Germanium and uranium in coalified wood from upper Devonian black shale. *Geochim. et Cosmochim. Acta* **7,** 287–294.

CLARKE F. W. (1924) The data of geochemistry. (Fifth Edition) *U.S. Geol. Survey Bulletin* **770.**

DALY R. A. (1933) *Igneous rocks and the depths of the earth.* McGraw-Hill, New York.

GOLDSCHMIDT V. M. (1926) Uber das kristallochemische und geochemische Verhalten des Germaniums. *Naturwissenschaften* **14,** 295.

GOLDSCHMIDT V. M. (1933) Grundlagen der quantitativen Geochemie. *Fortschr. Min.* **17,** 112–156.

GOLDSCHMIDT V. M. (1937) The laws of the geochemical distribution of the elements. *J. Chem. Soc.* **1,** 655–675.

GOLDSCHMIDT V. M. (1954) *Geochemistry.* Clarendon Press, Oxford.

GOLDSCHMIDT V. M., HAUPTMANN H., and PETERS C. (1933) Ueber die Berucksichtigung "seltener" Elemente bei Gesteinsanalysen. *Naturwissenschaften* **21,** 362–365.

GOLDSCHMIDT V. M. and PETERS C. (1933) Zur Geochemie des Germaniums. *Nachr. Ges. Wiss. Göttingen* **111, 28,** iv; **31,** 141.

HARRIS P. G. (1954) Distribution of germanium among coexisting phases of partly glassy rocks. *Geochim. et Cosmochim. Acta* **5,** 185–195.

HYBBINETTE A. G. and SANDELL E. B. (1942) Determination of germanium in silicate rocks. *Industr. Engng. Chem. (Anal.)* **14,** 715.

KUENEN PH. H. (1941) Geochemical calculations concerning the total mass of sediments in the earth. *Amer. J. Sci.* **239,** 161–190.

KUENEN PH. H. (1946) Rate and mass of deep-sea sedimentation. *Amer. J. Sci.* **244,** 563–572.

KUENEN PH. H. (1950) *Marine geology.* John Wiley, New York.

KURODA P. K. and SANDELL E. B. (1953) Chlorine in igneous rocks. *Bull. Geol. Soc. Amer.* **64,** 879–986.

KURODA P. K. and SANDELL E. B. (1954) Geochemistry of molybdenum. *Geochim. et Cosmochim. Acta* **6,** 35–63.

NOCKOLDS S. R. (1954) Average chemical compositions of some igneous rocks. *Bull. Geol. Soc.* **65,** 1007–1032.

NODDACK I. and NODDACK W. (1930) Die Haufigkeit der chemischen Elemente. *Naturwissenschaften* **18,** 757–764.

NODDACK I. and NODDACK W. (1931) Die Geochemie des Rheniums. *Z. Phys. Chem.* **A154,** 207–244.

NODDACK I. and NODDACK W. (1934) Die geochemischen Verteilungs-Koefficienten der Elemente. *Svensk. Kem. Tidskr.* **64,** 173–201.

NODDACK I. and NODDACK W. (1939) Die Haufigkeiten des Schwermetalle in Meerestieren. *Ark. Zool.* **A32,** No. 4, 1–35.

ONISHI H. (1956a) Germanium in chondrites. *Kaga ku* **26,** 306; or *Chem. Abstr.* **50,** 15364.

ONISHI H. (1956b) Notes on the geochemistry of germanium. *Bull. Chem. Soc. Japan.* **29,** 686–694.

ONISHI H. and SANDELL E. B. (1955a) Geochemistry of arsenic. *Geochim. et Cosmochim. Acta* **7,** 1–33.

ONISHI H. and SANDELL E. B. (1955b) Notes on the geochemistry of antimony. *Geochim. et Cosmochim. Acta* **8,** 213–221.

ONISHI H. and SANDELL E. B. (1956) Gallium in chondrites. *Geochim. et Cosmochim. Acta* **9,** 78–82.

PREUSS E. (1941) Beitrage zur spektralanalytischem Methodik. II. Bestimmung von Zn. Cd, Hg, In, Ti, Ge, Sn, Pb, Sb, und Bi durch fraktionierte destillation. *Z. Angew. Mineral.* **3,** 8–20.

PRIOR G. T. and HEY M. H. (1953) *Catalogue of meteorites.* British Museum of Natural History, London.

RANKAMA K. and SAHAMA TH. G. (1950) *Geochemistry.* pp. 729–737. University Press, Chicago.

SCHNEIDER W., JR. and SANDELL E. B. (1954) Photometric determination of traces of germanium after carbon tetrachloride extraction. *Mikrochimica Acta* **2,** 263–268.

UREY H. C. and CRAIG H. (1953) The composition of the stone meteorites and the origin of the meteorites. *Geochim. et Cosmochim. Acta* **4,** 36–82.

WHITE D. E. and BRANNOCK W. W. (1950) The sources of heat and water supply of thermal springs, with particular reference to Steamboat Springs, Nevada. *Trans. Amer. Geophys. Un.* **31,** 566–574.

WICKMAN F. E. (1954) The total amount of sediments and the composition of the average igneous rocks. *Geochim. et Cosmochim. Acta* **5,** 97–110.

WAVE-GENERATED RIPPLES IN NEARSHORE SANDS

DEPARTMENT OF THE ARMY
CORPS OF ENGINEERS
TECHNICAL MEMORANDUM NO.100

OCTOBER 1957

FOREWORD

A study of the occurrence of sand ripples generated by wave action in the nearshore area has been made based on observations of swimmers equipped with self-contained underwater breathing apparatus. Such parameters as the symmetry of the ripples, and their wave length and crest length, were measured and are related to the sand size, and to the orbital velocity and displacement of the wave motion generating the ripples. It was felt that publication of this data would be of interest to workers in the coastal engineering and geology fields as presenting additional data to aid in the understanding of nearshore processes and the factors influencing longshore movement of material, in particular the mechanisms of ripple formation and growth. This report presents the results of this study.

In general the ripple size increased with an increase in sand size and, to a certain extent, with water depth. Ripples in more exposed areas were generally larger than those in sheltered bays. Ripples were always present when the orbital velocity was between about 0.3 and 3 feet per second.

This report was prepared at the Scripps Institution of Oceanography of the University of California in pursuance of contracts with the Beach Erosion Board and the Office of Naval Research. The author of the report, D. L. Inman, is a member of the staff of Scripps Institution of Oceanography.

Views and Conclusions expressed in this report are not necessarily those of the Beach Erosion Board or the Office of Naval Research.

This report is published under authority of Public Law 166, 79th Congress, approved July 31, 1945.

TABLE OF CONTENTS

Page

ABSTRACT ---------- 1

INTRODUCTION ---------- 1

METHOD ---------- 2
- Ripple Measurement ---------- 5
- Sediment Sampling ---------- 13
- Wave Measurement ---------- 14
- Expression of Hydraulic Conditions ---------- 14

INTERPRETATION ---------- 18
- Sand and Ripple Size ---------- 18
- Ripple Profiles ---------- 23
- Sorting ---------- 23
- Fine Sand Ripples, D-Range, La Jolla ---------- 27
  - Occurrence ---------- 31
  - Ripple Form ---------- 31
  - Variation in Form ---------- 37
- Comparison with Model Experiments ---------- 37

COMPLEX RIPPLES ---------- 38

ACKNOWLEDGMENTS ---------- 40

LITERATURE CITED ---------- 40

APPENDICES I through IV - Tables
- I - Ripple and wave parameters for coasts exposed to the open ocean, D-Range, La Jolla, California
- II - Ripple and wave parameters for coasts exposed to the open ocean, miscellaneous observations
- III - Ripple and wave parameters for lee and protected coasts of ocean islands
- IV - Ripple and wave parameters for areas of limited fetch; bays, models, etc.

APPENDIX V - Computation of Orbital Velocities and Displacements Near the Bottom

WAVE-GENERATED RIPPLES IN NEARSHORE SANDS*

by
Douglas L. Inman
University of California
Scripps Institution of Oceanography
La Jolla, California

ABSTRACT

A study of the formation and occurrence of sand ripples generated by oscillatory wave motion was made in coastal waters to gain a better understanding of the role ripples play in the sorting and transportation of sediments. The observations, which extend from the surf zone to depths of about 170 feet, were made by swimmers equipped with self-contained underwater breathing apparatus. The wave length, crest length, height and symmetry of the ripples were measured and these parameters compared with the size of the sand and with the orbital displacement and velocity of the wave motion generating the ripples.

Ripples were always present on sandy bottoms when the significant orbital velocity had a value between about 1/3 and 3 feet per second. The type of ripple was related to the size of the sand and the nature and rigor of wave motion. The ripple wave length ranged from 0.14 feet in fine sand to over 4 feet in very coarse sands. The heights of the ripples ranged from about one-fourth to one-sixteenth of the ripple wave length.

In areas of abundant sand, the largest and least dense material occurred on the ripple crests and the finest and heaviest in the trough. Over rocky bottoms where there was little sand, the relationship was frequently reversed. The ripple crest consisted of sand washed from among the rocks, while the coarse material remained in the trough.

INTRODUCTION

Ripples are generally subdivided into current ripples and oscillatory ripples, depending on whether the motion leading to their formation was that of a unidirectional current as in streams and eolian transport or an oscillatory current as in wave motion. This paper treats the oscillatory type of sand ripples, which are defined here as the systematic series of undulations or waves that form at the sand-water interface under the influence of surface gravity waves. Such ripples form

---

*Contribution from the Scripps Institution of Oceanography, New Series No. 947

Reproduced by Permission

when the fluid stress on the bottom is slightly in excess of that required to initiate movement of sediment particles, and disappear when there is general bed motion at somewhat higher fluid velocities.

There is extensive literature on ripple marks; earlier work is listed in a bibliography on the subject by Kindle and Edwards (1924), and more recent work is summarized in papers by van Straaten (1953) and Manohar (1955). However, most investigations and measurements of ripple characteristics have been restricted to ancient rocks or small scale laboratory studies, or to ripple impressions exposed at low water or observed from the surface in quiet water. The advent of self-contained underwater breathing apparatus, which allows swimmers to move about freely and to make measurements and observations under water, has provided the means for measuring and studying ripples in motion and under natural circumstances (figure 1). The purpose of this paper is to describe oscillatory ripples as they occur in nature, especially in oceanic coastal waters, and to discuss their occurrence and physical characteristics in relation to the waves generating them.

METHOD

Most ripple observations and measurements in the present study were made along the sandy shelf bordering the coast of southern California, although the field work included observations from the narrow shelf fringing the Hawaiian Islands and the shelves of other islands along the coast of Mexico and California. In addition to coasts exposed to the open ocean, observations were made in other environments including protected coasts, bays, bays behind barrier reefs, and one observation from a model wave tank. In all, about 1,000 ripples were measured during almost 200 observations which were made in waters ranging in depth from a fraction of a foot to 170 feet. The ripples measured had wave lengths from 0.14 to over 4 feet. Whenever possible, as in 102 cases, surface waves were recorded during the period of ripple observation.

In addition to a wide geographic distribution of observations, ripples from specific areas were studied over long periods of time and under various wave conditions. A series of four stations ranging in depth from 18 to 70 feet below mean lower low water were visited frequently during a period of several years. These stations are located on D range, which is on the shelf off La Jolla, California, where the sediments consist of a relatively uniform, fine quartz sand (figure 2). In addition, four areas were visited frequently on the shelf off Point La Jolla at depths of 30, 40, 55, and 85 feet. The sediments at these areas differ markedly from those on D range in that they occur in large patches separated by low rock outcrops. Sediments are coarser, somewhat more rounded, have more shell fragments, and in general do not grade from one type to another. The stations on D range were established in conjunction with a study of the changes in level of the sandy bottom.

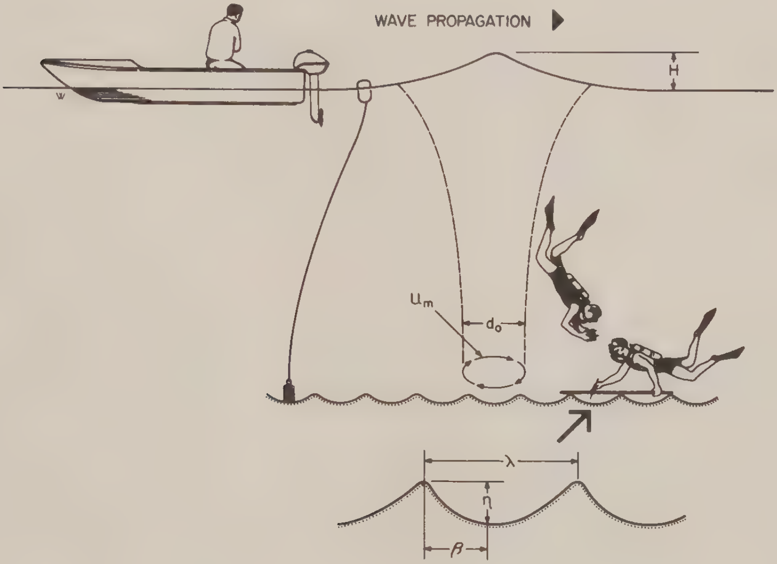

FIGURE I. SCHEMATIC DIAGRAM ILLUSTRATING THE TECHNIQUE USED IN MEASURING RIPPLES AND THE NOTATION FOR DESCRIBING WAVES AND RIPPLES. (u_m is the maximum horizontal orbital velocity of the waves, and d_0 is the orbital diameter near the bottom. λ is the ripple wave length, η the ripple height, and λ/η and β/λ are the ripple index and measure of symmetry respectively.)

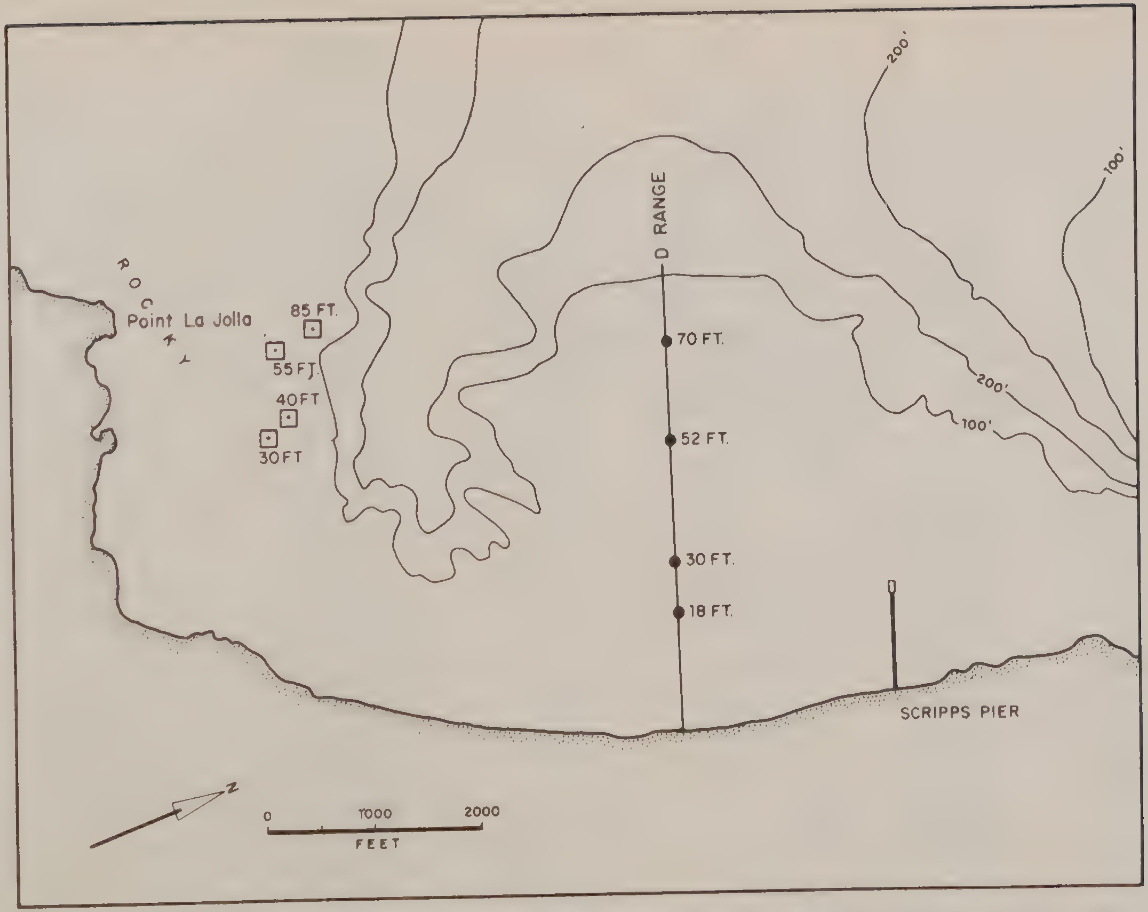
200'
100'
D RANGE
ROCKY
Point La Jolla
85 FT.
55 FT.
40 FT
30 FT
70 FT.
52 FT.
30 FT.
18 FT.
200'
100'
SCRIPPS PIER
N
0
1000
2000
FEET

FIGURE 2. INDEX CHART SHOWING LOCATION AND DEPTH OF STATIONS ON THE SHELF OFF LA JOLLA, CALIFORNIA. Observations from the four stations on D range are tabulated chronologically in Appendix I A–I D, and those from the stations off Point La Jolla, California are listed by depth in Appendix II A.

The changes in level between each ripple observation on this range are given by Inman and Rusnak (1956), and the description of the sediment characteristics and the hydrography of both areas is given by Inman (1953).

The collocation of all data was based primarily on the wave exposure of the area: observations from coasts exposed to the open ocean are tabulated in Appendices I and II; those from lee and protected coasts in Appendix III; and those from areas of limited fetch in Appendix IV. The most complete and systematic observations were made at the four stations on D range off La Jolla, and these are listed chronologivally by station in Appendix I. Observations from the four areas off Point La Jolla are listed under the appropriate depth in Appendix II-A.

Ripple Measurement

Various techniques were used in the measurement of ripples. The most convenient technique for smaller ripples was to mark the ripple dimensions on a transparent plastic strip which was placed on the bottom perpendicular to the ripple crests. The position of each ripple crest and trough and the height of the ripple were marked on the plastic with a grease pencil. After the diver returned to the surface, the markings on the plastic strip were measured and recorded. Three measures were obtained for each ripple: the wave length λ, which is the spacing between ripple crests; the ripple height η, which is the vertical distance from crest to trough; and the horizontal distance β, measured from the ripple crest to the deepest portion of the trough in the direction of propagation of the surface waves. These measurements are defined schematically in figure 1. λ and β for the smaller ripples were measured to the nearest hundredth of a foot and η to the nearest five thousandth of a foot. Since the positions of the ripple crests were usually quite sharp, λ is a reasonably accurate measure, while β, which depends on the lowest position of the concave ripple trough, is somewhat less accurate. η is the least accurate because it is the most difficult to measure and in fine sand the weight of the plastic strip tends to flatten the ripple crests.

The ratio of β to the wave length λ was used as a measure of ripple symmetry. Symmetrical ripples, insofar as the position of ripple crest and trough are concerned, have a value of β/λ equal to $\frac{1}{2}$. Values less or greater than $\frac{1}{2}$ indicate that the ripple has a tendency to be asymmetrical like a current ripple. If the ratio is less than $\frac{1}{2}$, the steep lee face of the ripple, faces in the direction of wave propagation, and if the value is greater than $\frac{1}{2}$ the opposite is true.

The ratio of ripple wave length to ripple height, λ/η, referred to as the "ripple index", is used in this study as a measure of ripple steepness. It is the inverse of the steepness measure commonly employed for wave phenomena.

(649)

The average values of ripple wave length λ, height η, and of the ratio λ/η and β/λ for each observation, together with the number of ripples measured are entered in the appendices. In cases where the data was inadequate to obtain numerical values of β, a notation was entered from the divers' observations indicating whether the ripples appear to be symmetrical, or if asymmetrical, whether they resembled current ripples resulting from onshore ($\beta/\lambda < \frac{1}{2}$) or offshore ($\beta/\lambda > \frac{1}{2}$) currents. In addition, if the ripple symmetry was observed to change with the passage of each wave crest and trough, the symmetry was recorded as "reversing".

A simple device was fabricated for more detailed measurement of the profile of large ripples. The device consisted of a series of parallel brass prongs welded at right angles to a metal bar so that the instrument has the appearance of a large comb (figure 3). The prongs were coated with grease so that when forced into the sand bottom, the imprint of the ripple profile was clearly marked in the grease. A spirit level was attached to the bar to permit the device to be leveled and thus give a profile of the ripple relative to a level datum. Representative profiles are shown in figure 4.

It became apparent during the study that ripple profiles could be broadly divided into two types: those with flat troughs separating the crests which, because of their resemblance to the analogous wave type were termed "solitary", and those with rounded troughs which were termed "trochoidal" (figures 5 and 6). In many cases, particularly for smaller ripples, it was not possible to measure the profiles accurately and the classification of solitary or trochoidal was determined from the visual observations of the diver. A "sawtooth" profile which is common in current ripples, was rarely observed in the oscillatory ripples.

Ripples were also classified as to pattern or plan, the basis of classification being the ratio of the average ripple crest length to wave length of the ripples. Long-crested ripples, that is, ripples with average crest lengths greater than 8 ripple wave lengths, were designated as pattern 1. Intermediate crested ripples, crest lengths between 3 and 8 λ, were designated as pattern 2, and short-crested ripples with crest lengths less than 3 λ as pattern 3 (see figures 6, 7 and 8). The limiting values of 3 and 8 λ were found to be most useful in dividing the ripples into three relatively discrete classes.

Whenever the water was clear, the ripples were photographed so that more leisurely study could be made in the laboratory. In this way the use of still photography accelerated the program by eliminating many of the intricacies of underwater observations and measurements. In addition, the mechanics of ripple movement, such as the change in ripple shape with time and the nature of the vortex formed in the ripple lee by each reversal in water motion were recorded and studied by motion pictures. Underwater motion pictures were made of ripples ranging in wave length from 0.2 to 3 feet.

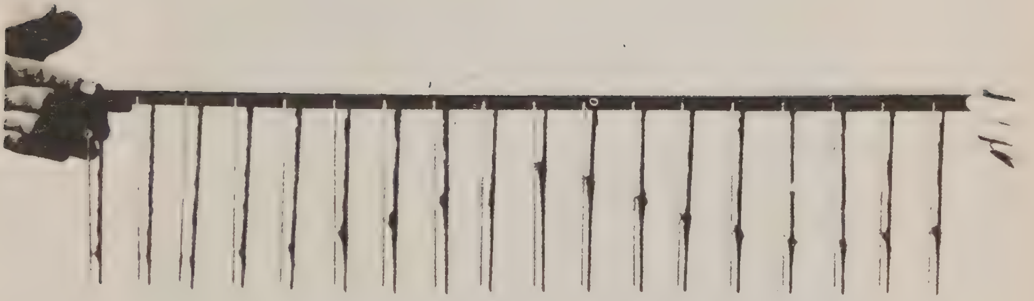

FIGURE 3. DEVICE USED FOR MEASURING RIPPLE PROFILE. (The prongs were coated with grease so that when forced into the sand bottom the imprint of the ripple profile is clearly marked in the grease. A spirit level (not shown) was attached to the bar to give a level datum. Typical profiles are shown in figure 4.)

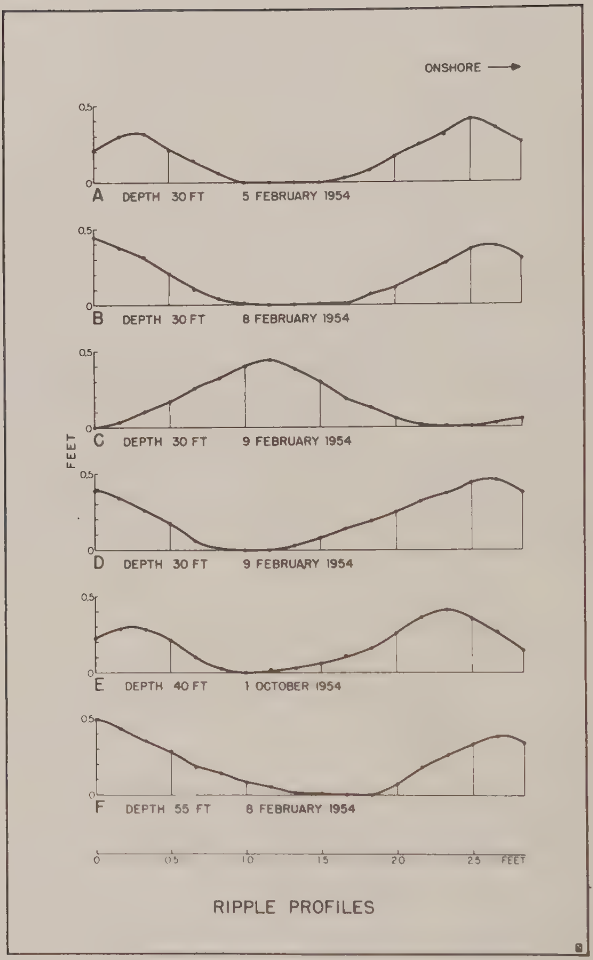

FIGURE 4. REPRESENTATIVE PROFILES OF LARGE RIPPLES FROM THREE STATIONS OFF POINT LA JOLLA, CALIFORNIA. Locations are shown by depths in figure 2, and complete descriptions are tabulated by depth and date in Appendix IIA.

(652)

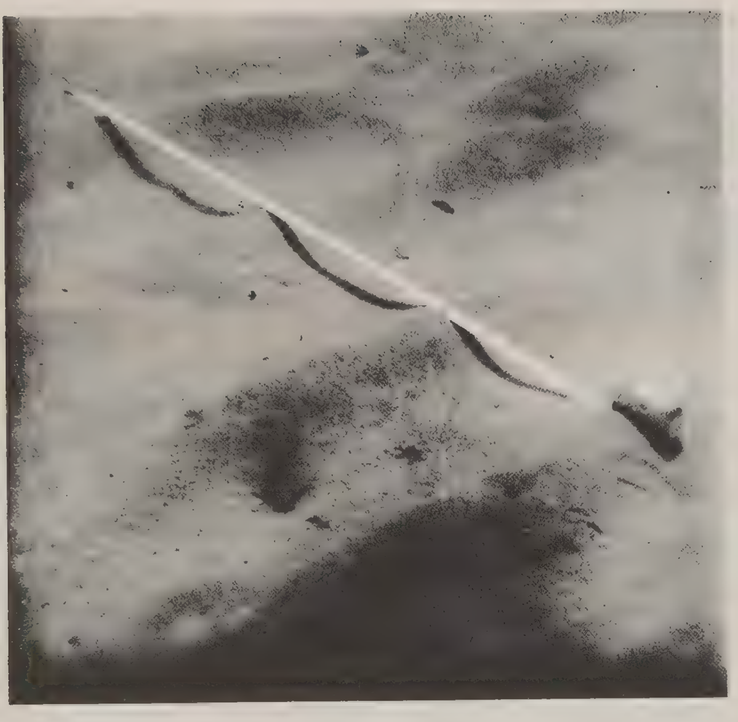

FIGURE 5. TROCHOIDAL RIPPLE PROFILE FROM THE PROTECTED SHELF OFF SAN CLEMENTE ISLAND, CALIFORNIA. Ripple wave length 0.67 ft., depth of water 21 ft. Sand on the ripple crest is slightly coarser than that in the trough. Complete description tabulated in Appendix III B

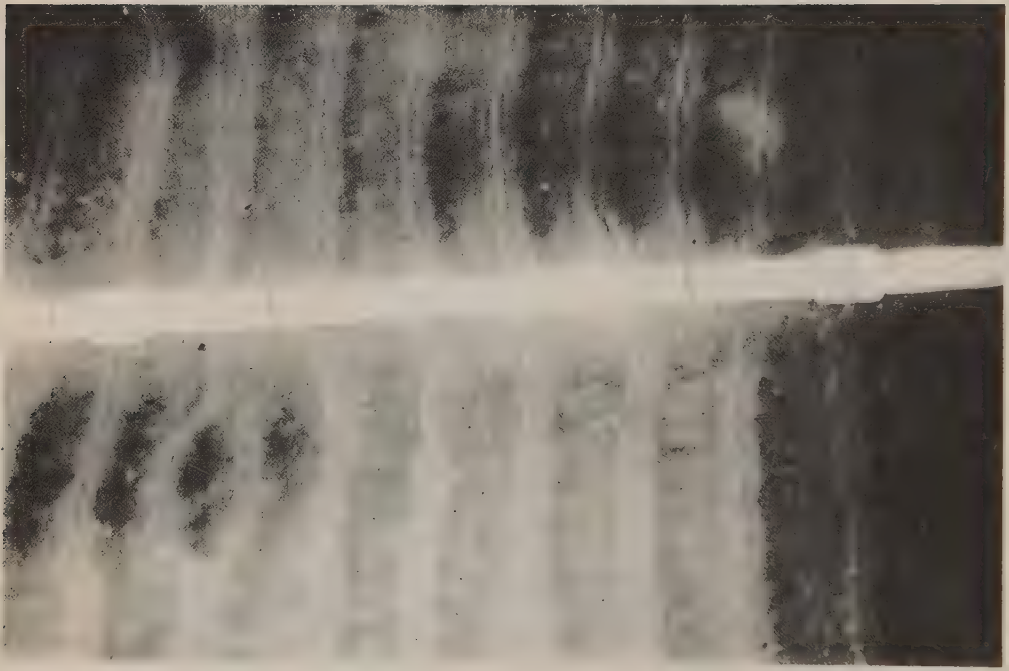

FIGURE 6. LONG-CRESTED RIPPLES (PATTERN I.) Ripples in fine sand at depth of 14 ft. on D range (Appendix I A, 2 August 1954). Ripple profile is "solitary" consisting of flat troughs separated by relatively sharp crests. Dark colored heavy minerals occur in the trough, light colored quartz sand in the crests, with a narrow line of dark mica at the apex of the crest. Each scale division is 0.1 ft.

(654)

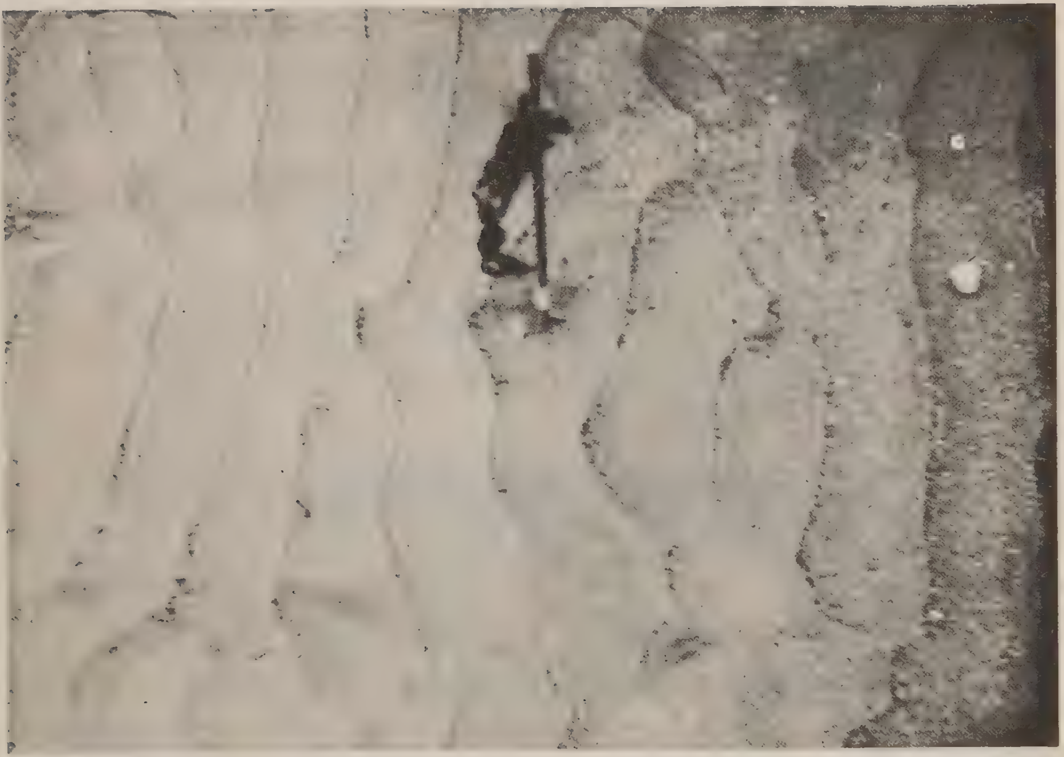

FIGURE 7. RIPPLES WITH INTERMEDIATE CREST LENGTHS (PATTERN 2). Ripples in fine sand at a depth of 30 ft. on D range (Appendix I B, 21 August 1953). Ripple profile is solitary and the average wave length is 0.22 ft. Reference rod is used for measuring changes in sand level (Inman and Rusnak, 1956).

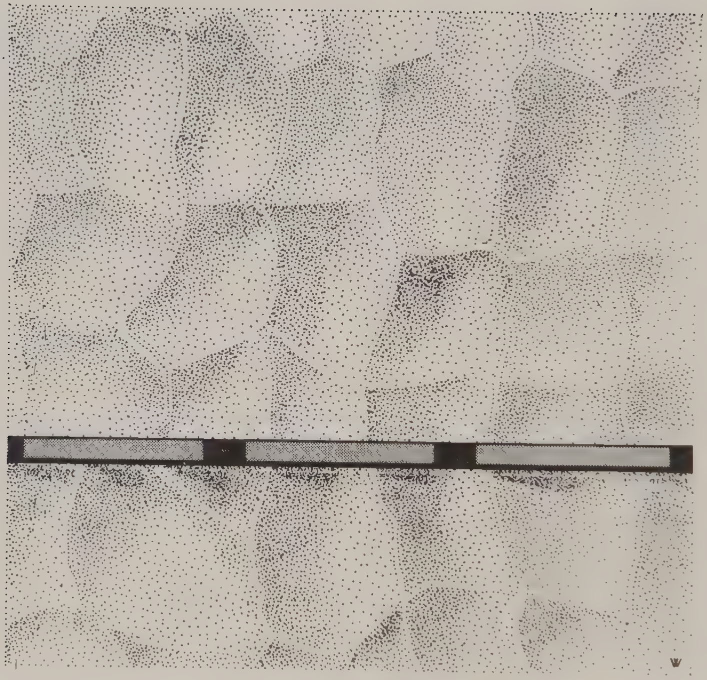

FIGURE 8. SHORT CRESTED RIPPLES (PATTERN 3). Ripples in fine sand at a depth of 52 ft. on D range. (Appendix I C, 23 November 1953). Ripple profile is trochoidal. Scale division 0.5 ft (Drawing of a photograph).

Sediment Sampling

During the ripple observations a sample of sand was obtained from the crests of the ripples, and in many cases from the ripple trough as well. The samples were labeled by date, number, and the letter C or T was appended to identify the sample with the ripple crest or trough. In addition to the routine sampling from the surface of the ripple crest and the trough, on two occasions examination of the structure of the sand under the crests and troughs was accomplished by lithifying a core of sand *in situ* with a polyester resin.

Because the study was concerned with water-transported sediments, hydraulic sizes, which are based on settling velocity were used in preference to sizes obtained by sieving. The sand-size fraction of the samples were analyzed with an Emery Settling Tube (Emery 1938, Poole et al. 1951). Material coarser than 1 millimeter was removed before the settling tube analysis, and then the weight percentage recombined after analysis into one cumulative frequency curve.

The particle-size distributions of the sediments were expressed in terms of phi measures (Inman, 1952) that serve as approximate graphic analogues to the moment measures commonly employed in statistics. The parameters used include the median diameter, a measure of standard deviation, and a measure of skewness. They are computed from three percentile diameters obtained from the cumulative size-frequency curve of the sediment and are defined as follows:

1) phi median diameter $Md_\phi = \phi_{50}$,

2) phi deviation measure $\sigma_\phi = 1/2\ (\phi_{84} - \phi_{16})$,

3) phi skewness measure $\alpha_\phi = \dfrac{M_\phi - Md_\phi}{\sigma_\phi}$,

where $\phi = -\log_2$ of the diameter in millimeters, $M_\phi = 1/2\ (\phi_{16} + \phi_{84})$ is the phi mean diameter, and ϕ_{16}, ϕ_{50}, and ϕ_{84} are the diameters in phi units corresponding to the 16th, 50th and 84th percentiles respectively of the cumulative weight-percent (coarser) curve. Since one phi unit is equivalent to one Wentworth division, the phi deviation measure gives the standard deviation of the sediment in terms of Wentworth units.

The graphic phi measures are tabulated in Appendix I through IV. For convenience in interpreting sand size, the median diameter is also tabulated in microns, using conversion tables compiled by Page (1955). The accuracy of measurement of the median diameter is about 0.02ϕ, which converts to about 2 microns for very fine sand and about 15 microns for coarse sand (Poole, et. al. 1951; Inman, 1953).

Wave Measurement

Wave height and period and the depth of water were measured from the boat during most ripple observations. Since it was not practical to use a conventional pressure type wave recorder, the trace from a recording fathometer was used in its place. A wave record of this type is reasonably accurate when used from small boats over flat bottoms. At times when fathograms were not available, visual observations of wave height and period were used, but reduction of this type of data was not attempted unless it appeared that a simple series of waves existed.

When available, a twenty-minute section of wave record was analyzed to obtain the wave period T, and the height H, of the significant wave, which is defined as the wave with the period and height of the average of the highest one-third waves. The significant wave period and height and the depth of water were used to compute the horizontal diameter of the orbit of a particle of water near the bottom, referred to hereafter as the orbital diameter d_o, and the maximum horizontal velocity, u_m*.

Although no great claim is made for accuracy in the wave computations, in general, it was found that the computed values for the wave period T, and the orbital diameter d_o, compared favorably with the period and orbital diameter observed near the bottom by the divers. Although it is difficult to measure velocity under water, the period of oscillation and the amount of displacement can be estimated with reasonable accuracy by a diver with a stop watch and a fixed point of reference.

Equations from the Airy wave theory were used in computing the orbital diameter and the maximum orbital velocity for observations well seaward of the surf zone. An adaptation of the solitary wave theory was used for orbital diameter and velocity computations when waves were near the surf zone. The conditions under which the Airy or solitary wave theory were used and the procedures for computing orbital diameter and velocity are described in detail in Appendix V.

Expression of Hydraulic Conditions

The work of Exner (1925) and von Karman (1947) indicated that the character of current ripples formed by unidirectional flow could be related to the velocity of flow. For shallow water, Anderson (1953) showed a correlation to exist between ripple wave length and the Froude number. Tsubaki, Kawasumi, and Yasutomi (1953) found that the dimensions of current ripples showed good correlation with Einstein's (1942) bed load function ψ , which is related to the ratio of the weight of a sediment particle to the lift force acting on the particle by the flow.

The practical application of hydrodynamic principles to ripples generated by oscillatory flow is more obscure. Bagnold (1946) in his

---

* It is realized that computations based on the significant surface wave do not necessarily give the "significant" orbital velocity and diameter at the bottom; however, under the conditions taken here this was not considered to be critical.

experiments on ripples generated on a movable bed, showed that ripples of shortest wave length were proportional to the horizontal amplitude of oscillation of the bed. Later, Manohar (1955) using somewhat similar apparatus showed that a modification of the ψ function could be used to predict the character of his model ripples.

Thus, general considerations indicated the need for a measure of the intensity of flow and, since the motion was oscillatory, for a measure of the particle displacement. However, the spectrum of ocean waves is often broad, so that the probable error of predicting mean values of velocity and orbital diameters may be in error by as much as 50%. Also, there is no satisfactory procedure for calculating the stress exerted on the bottom by wave motion. Because of these facts it was decided to base the characterization of the hydraulic conditions on simple dimensionless ratios that could be obtained at the time of ripple observation. The intensity of flow was characterized by the relative velocity u_m/u_1, where u_m is the computed maximum horizontal velocity near the bottom, and u_1 is the limiting value for initiating motion in sand of a given size. Since the relation between velocity and critical stress required to initiate motion was not clear, it was decided to arbitrarily use a value of $u_1 = 7u_*$ where u_* is the threshold or critical friction velocity (Inman 1949). The factor 7 was chosen because it gave a limiting velocity which was consistent although somewhat conservative in comparison with laboratory data of Menard (1950) and Manohar (1955). Their data and the relation of $u_1 = 7\,u_*$ is plotted against particle size in figure 9.

The displacement of a water particle relative to the ripples was obtained by the ratio of d_o/λ where d_o is the orbital diameter near the bottom computed for the significant waves and λ is the ripple wave length. A graph showing the relation of the relative velocity, u_m/u_1, to the relative displacement d_o/λ for all observations for which wave parameters were computed is shown in figure 10.

The hydraulic conditions were arbitrarily grouped into two general types on a basis of the relative velocity and the relative displacement (figure 10). Type I includes those conditions in which either or both ratios have a value less than 2, and type II includes those cases in which both ratios exceed a value of 2. Thus, type II indicates conditions in which the velocity is large compared to that required to initiate motion of the sand and the orbital diameter is large compared to the ripple wave length. On the other hand, the three types I indicate: Ic) conditions where the velocities are approximately the same order of magnitude as the limiting velocity for initiating sand movement, or Ib) that the orbital displacements are similar in magnitude to the ripple wave length, or Ia) both velocity and displacement are limiting. In addition, two extreme hydraulic conditions were noted: the condition in

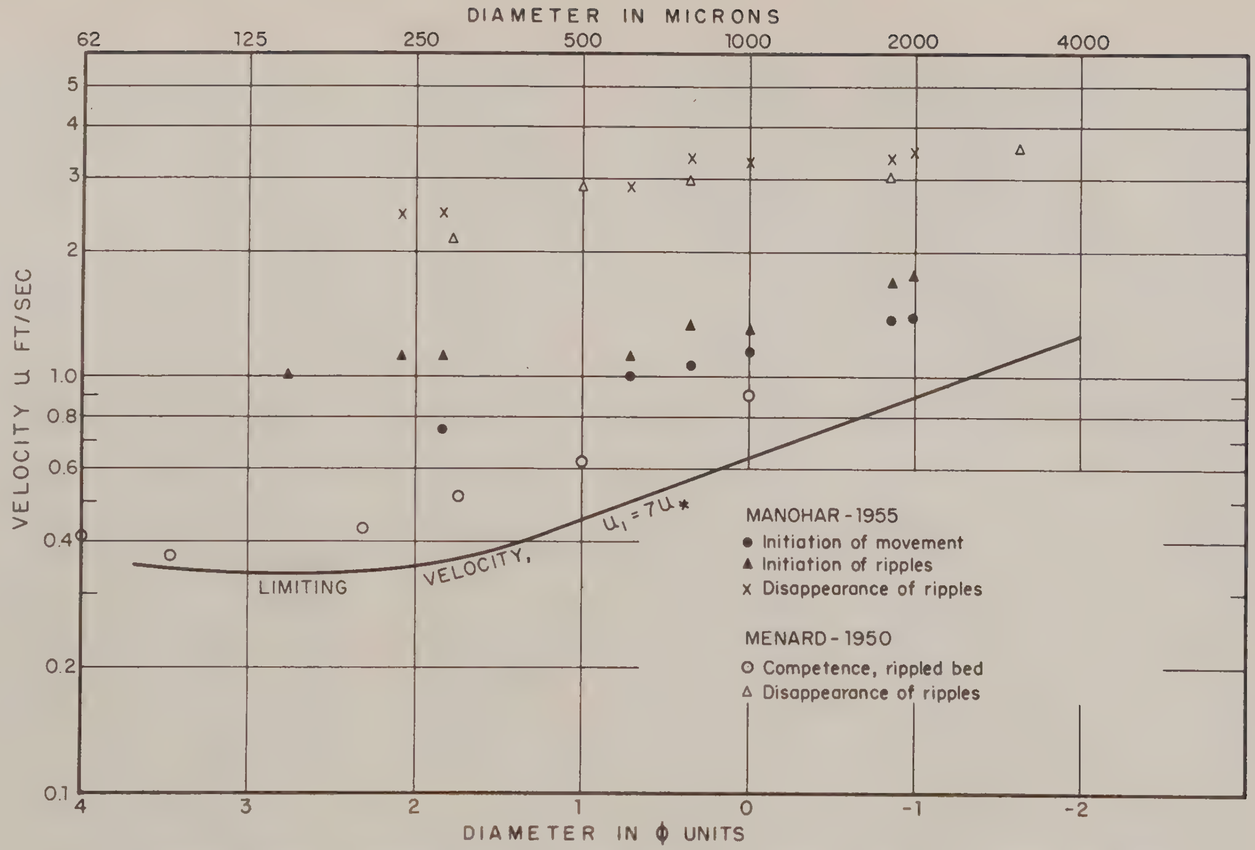

FIGURE 9. LIMITING OR MINIMUM VELOCITY FOR THE INITIATION OF MOTION OF SAND OF A GIVEN SIZE. Limiting velocity, arbitrarily defined as equal to $7u_*$, where u_* is the threshold or critical friction velocity (Inman, 1949). For unidirectional flow this relation would give a limiting velocity equivalent, for example, to the mean velocity measured 1 ft. above a bottom which has a roughness length of 2 cm. Field observations near the surf zone indicate that planation and disappearance of ripples does not occur unless the maximum velocity associated with the wave crest somewhat exceeds that listed by Menard and Manohar.

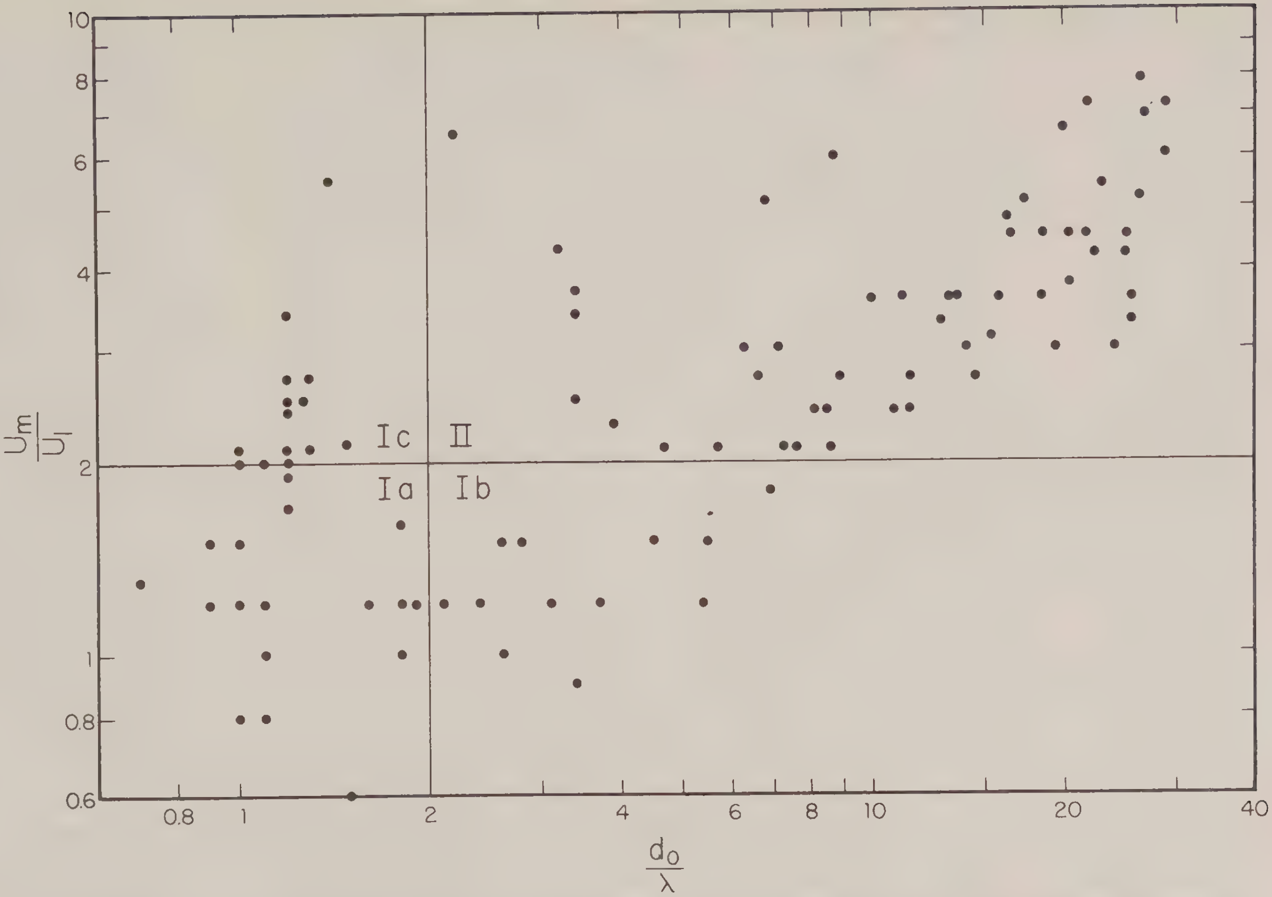

FIGURE 10. HYDRAULIC CONDITIONS EXPRESSED IN TERMS OF THE RELATIVE VELOCITY $^{U_m/U_l}$, AND THE RELATIVE ORBITAL DIAMETER (DISPLACEMENT) OF A WATER PARTICLE NEAR THE RIPPLE. Type II indicates conditions in which both the orbital velocities and diameters are relatively large, while types I pertain to conditions where either or both the velocities or orbital diameters are limiting. The notation is defined in figures 1 and 9.

which the velocity exceeded the upper limit for ripple formation and hence, the ripples were absent or "planed"; and the other extreme in which the water was still or "quiescent" and the ripple form was destroyed by burrowing organisms. The condition of planation was frequently observed near the surf zone while that of quiescence was more common in deeper water (figure 20).

INTERPRETATION

Sand ripples vary widely in size, shape, and duration. Some ripples are uniform with long parallel crests, others occur in various complex patterns such as rectangular, linguoid, and herringbone. Under some conditions ripples appear to change but little with time, while in others, especially near the surf zone, they are almost ephemeral in nature, changing with each wave surge. At times it appears that the ripples result from several factors, as for example when wave action is superimposed on tidal currents; at other times they appear to be in the process of modification from one form to another. Thus it becomes apparent that considerable care must be exercised in the collection of data if systemization is to be obtained from the various ripple forms, and the correlation of ripples and the forces generating them are to have significance. Therefore, care was taken to measure ripples in areas which were relatively far from bottom obstructions such as rocks, pier pilings, etc.

It is of course difficult in most cases to ascertain if the ripples measured were in fact formed by the waves present at the time of measurement. Many observers, dating back to Darwin (1883) and Forel (1895), have called attention to the fact that once formed, there is a tendency for the wave length of ripples to remain constant or to be but slowly modified, under changing conditions. In this regard, ripples in fine sand are more rapidly modified than ripples in coarse sand. A joint tabulation of ripple and wave characteristics was attempted only when it was considered that the ripples were in unison with the forces generating them. An exception to this undoubtedly occurred for measurements in coarse sand, as such ripples modify slowly and may only be in unison with generating forces under extreme wave conditions. Some aspects of complex ripples occurring near obstructions or in the process of modification are discussed briefly in a later section.

Sand and Ripple Size

The size of the sand is the single most important factor in determining the size of the ripple. A graph (figure 11) of the ripple wave length and the median diameter of the sand for all observations shows that in general, large ripples occur in coarse sand and smaller ripples in fine sand. It is also apparent from this graph that for equivalent sizes of sand, ripples from deeper water along exposed coasts tend to be larger than ripples in shallow water, and that ripples from areas such as bays and lakes where the wave fetch is limited have the shortest wave length

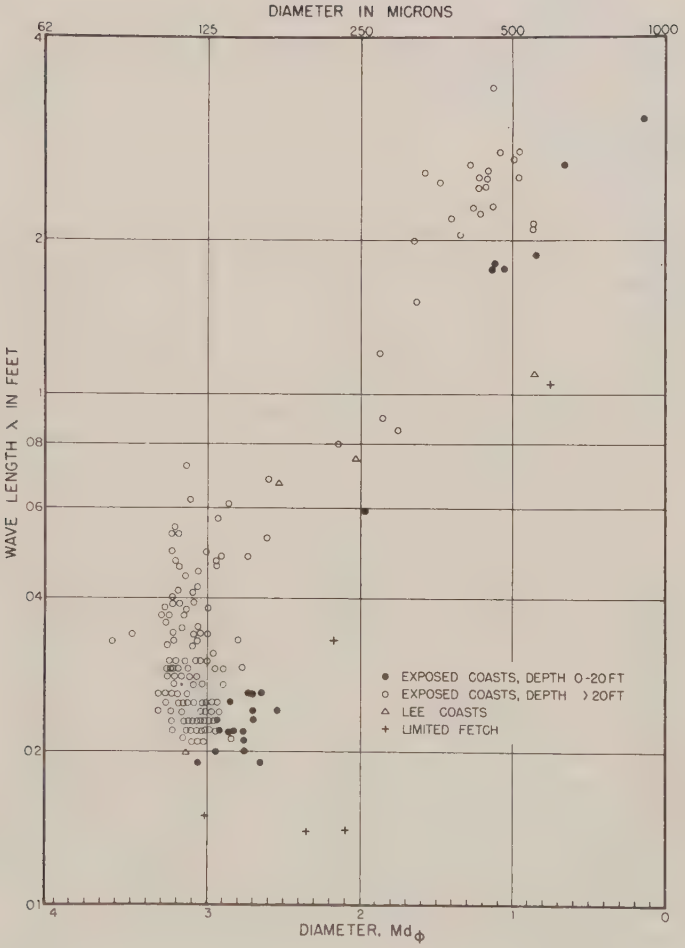

FIGURE 11. RIPPLE WAVE LENGTH AND SAND SIZE AT RIPPLE CREST. Includes all observations in which the median diameter of the sediment in the crest was 1000 microns or less. Tabulation of data is given in Appendix I through IV. Only data excluded is that for a ripple from a surge channel (Appendix II D), and for ripples generated by the re-formation of waves breaking over a barrier reef in the Hawaiian Islands (Appendix IV B, 8 December 1955).

of all. This general relation of ripple wave length to environment appears to result from the limitations on ripple size due to differences in orbital velocity and displacement. The wave length of ripples apparently cannot exceed the orbital diameter of the wave generating the ripple. Also, this study indicated that ripples generated by high velocities which approached the value of the upper limiting velocity (figure 9) tended to have shorter wave lengths even though the orbital diameter was large.

Thus, in general, ripples in the ocean tend to be large because the waves are long and consequently have large orbital diameters. Of these ocean ripples, those occurring near the surf zone are usually somewhat smaller because their size is affected by the higher orbital velocities. On the other hand, bays, lakes, and other areas of limited fetch tend to have small ripples because of the small orbital diameters associated with the short waves which occur there. The relation between the sand size and the ripple wave length for the special conditions where both the orbital diameter and velocity are relatively large, i.e. type II hydraulic condition, is shown in figure 12. The type II hydraulic condition is most typical of sandy areas along exposed coastlines just seaward of the surf zone.

The effect of orbital diameter and velocity on the wave length of ripples in three size ranges of sand is shown in figure 13. The maximum wave length for ripples in fine sand (125 microns) is about 3/4 foot. The ripple wave lengths are approximately equal to the orbital diameter, when the orbital diameter is less than the maximum wave length for the sand. As the orbital diameter increases beyond the maximum wave length of 3/4 foot., the ripple wave length gradually decreases to about 1/4 foot or less. The decrease in ripple wave length for large orbital displacement is attributed to the increase in orbital velocity rather than to the increase in displacement. If the wave period is constant, an increase in orbital displacement at the bottom results in a corresponding increase in the maximum velocity (Appendix V, equation 3). The tendency for the ripple wave length to decrease with increasing orbital velocity is not as apparent for the observations of large ripples in coarse sands. This may be because of the relative paucity of observations in coarse sands, or it may be due to factors associated with the wider range of hydraulic conditions and geographic location of the coarse sand stations. A tendency for ripple wave length to decrease near the upper critical velocity was not observed by Manohar (1955) in his laboratory studies of ripples generated on a movable bed.

Since the orbital diameter in shallow water is principally dependent on the wave height and period, on the average there exists a basic difference in wave length between ripples generated by wave action along oceanic coasts and those generated along the shores of water bodies with limited fetches such as small lakes. This dependence of ripples on the character of the waves generating them should be helpful in evaluating model studies of sand transport. It should also prove helpful in interpreting ancient environment from fossil ripple marks.

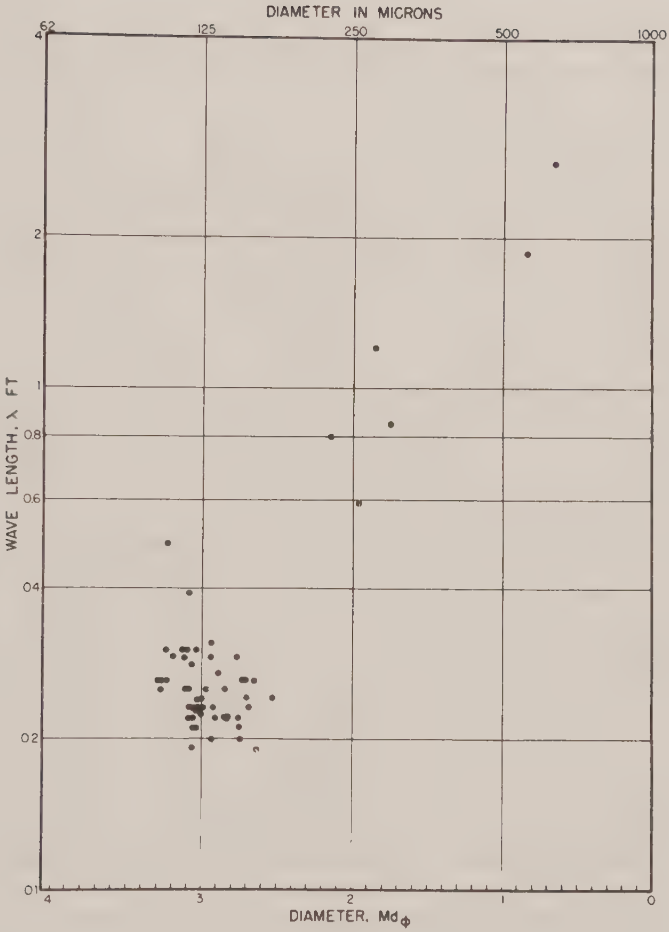

FIGURE 12. RIPPLE WAVE LENGTH AND SAND SIZE AT RIPPLE CREST. Includes observations where both orbital diameter and maximum velocity are large (Type II hydraulic condition). These conditions are most typical of sandy bottoms near the surf zone of ocean beaches. This data is also plotted in figure 11. Hydraulic Conditions are defined in figure 10.

(665)

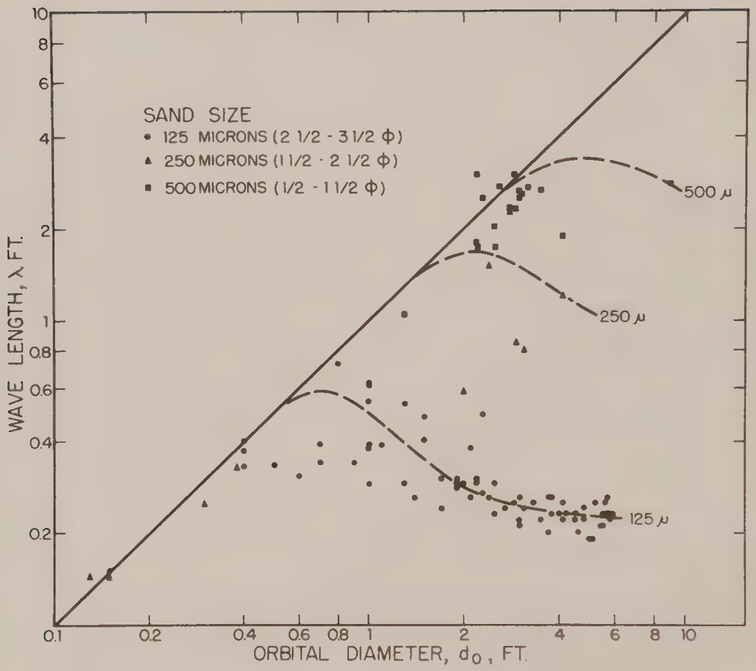

FIGURE 13. RELATION BETWEEN RIPPLE WAVE LENGTH AND THE ORBITAL DIAMETER OF WAVE MOTION FOR THREE RANGES OF SAND SIZE. The orbital diameter is a controlling factor in ripple wave length until the ripple reaches a maximum size. Increases in orbital diameter beyond the value of maximum wave length result in a decrease in ripple wave length, apparently because of the increase in the maximum orbital velocities. The orbital velocities for the 125-micron sand approach the disappearance or planation velocity at large orbital diameters (d_0 greater than about 4 ft.). Because of the paucity of points for the coarser sands the dashed lines are intended to be more schematic than best fit.

Ripple Profiles

The ripple index λ/η which is the inverse of the steepness, averaged between 8 and 10 for fine and very fine sands and about 6 for coarser sands. The variation in ripple index for fine sands was great, ranging from about 5 to 20, while in coarser sands it was relatively constant (figure 14). Even for small wave lengths the index for medium and coarse sands fell within a range of 4½ to 8. In part, the greater variability in fine sands results from the difficulties in measuring ripple heights discussed previously; however, there were sufficient observations to indicate that the difference is real and that the ripple index in fine sands can be much larger than in coarse sands. There is some correlation in fine sands between ripple index and the magnitude of the relative displacement at the bottom, d_o/λ, and relatively velocity u_m/u_1, which suggests that when the relative displacements and velocities are large, as near the surf zone, the ripples are less steep and thus have larger indices (figures 15 and 16). The plotted points in figure 16 for ripple index and relative velocity indicate a positive correlation for fine sand and little or no correlation for coarse sand.

The steepest ripples were commonly trochoidal in profile and were usually restricted to deeper water along exposed coasts and somewhat shallower water along lee and protected coasts (figure 5). The steep ripples are of the vortex type, the material on the ripple crest being lifted above the bottom and being moved an integral number of wave lengths with the passage of each wave crest and trough. Hydraulic condition Ia seems to be most conducive to the formation of ripples with steep trochoidal profiles. This condition occurs near the junction of the solid and dashed lines in figure 13 where the ripple wave lengths are greatest.

The solitary ripples which are most typical of fine sand in very shallow water tend to be less steep. The solitary ripples are formed when the wave trains are regular and the bottom velocities and the orbital diameters are relatively large, which is typically a Type II hydraulic condition. The higher velocities which are associated with the solitary profiles appear to place the material in a state of "sub-suspension" with the passage of each wave crest. In this case the bottom material is moved on and off shore as a thin but dense layer of suspended particles, and the discrete cloud of suspended particles which form at the crest of the trochoidal ripples appears to be absent. The thickness of the layer of "sub-suspension" although somewhat variable, is usually of the order of a few centimeters, and appears to depend on the size of the sand and on the orbital velocity and periodicity of the waves.

Sorting

The amount of sand available for transport was reflected in the relation between the size distribution of sand in the ripple crests and

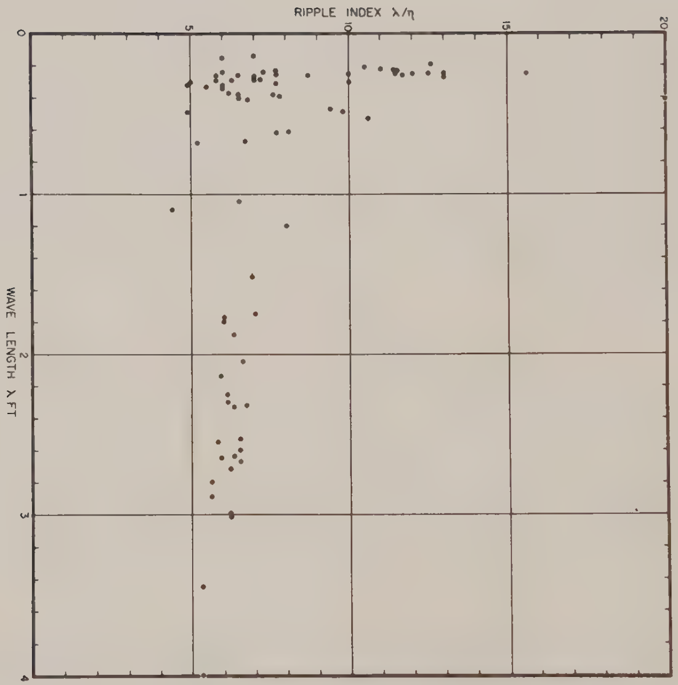

FIGURE 14. RELATION OF RIPPLE INDEX TO RIPPLE WAVE LENGTH FOR ALL OBSERVATIONS. (Ripple index is the inverse of ripple steepness.)

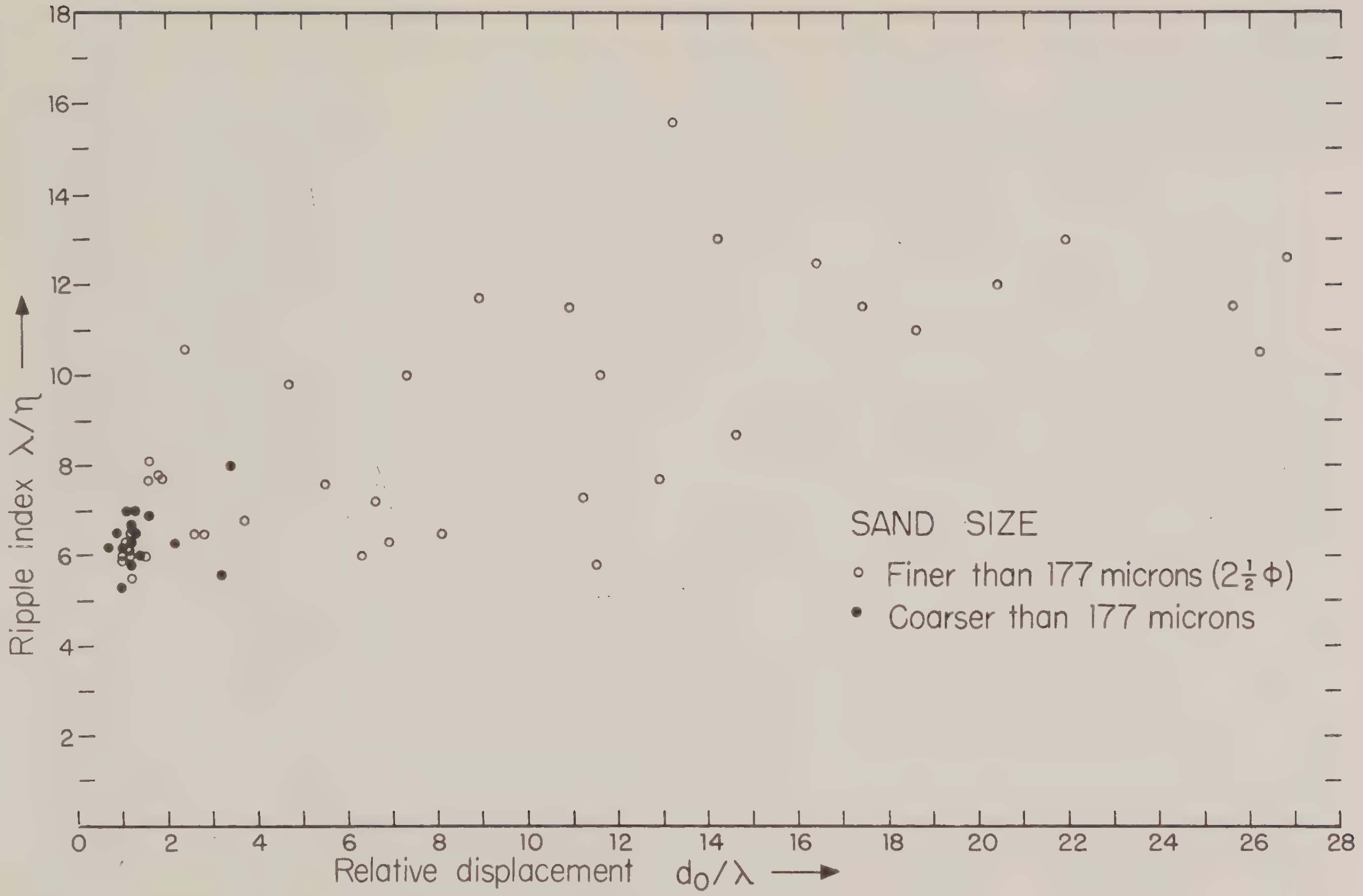

FIGURE 15. REATION BETWEEN RIPPLE INDEX AND RELATIVE DISPLACEMENT OF A WATER PARTICLE NEAR THE BOTTOM.

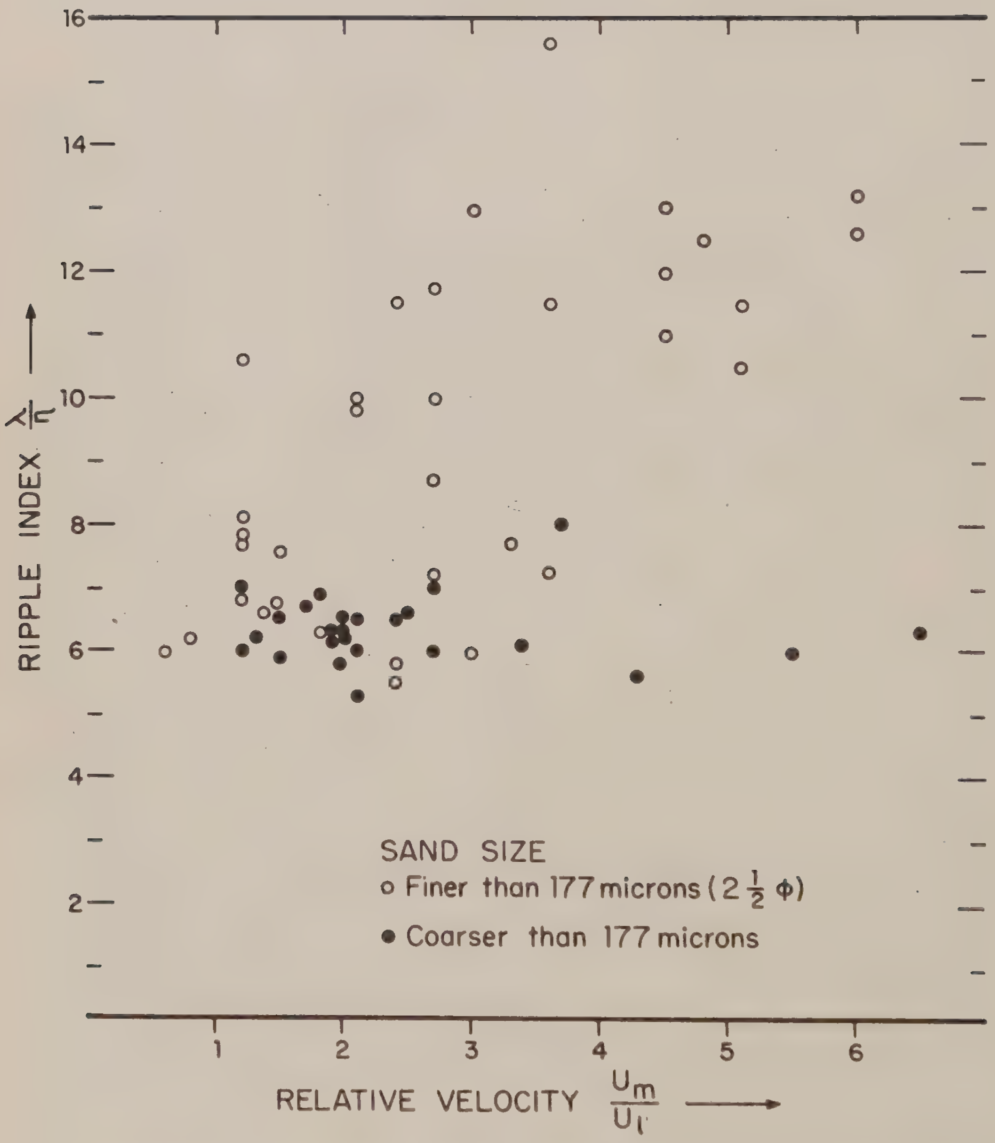

FIGURE 16. RELATION OF RIPPLE INDEX TO THE RELATIVE VELOCITY OF A WATER PARTICLE NEAR THE BOTTOM. A positive correlation is indicated for fine sands, while the index remains approximately constant for sands coarser than about 177 microns (2½ φ).

(670)

troughs. In general, if there was an abundance of sand available for transportation, the material of the largest size and least density was typically found on the ripple crests and the finest and heaviest material in the trough. If the source of sand was limited, a common condition along exposed rocky coasts, then the ripple crest consisted of sand sorted from the rocks and the trough material was essentially residual, which was frequently coarser than the material in the ripple crest (compare figures 5, 6 and 7 with 17). In either case it is the type of sand in the ripple crest which is influential in determining ripple properties, such as wave length and steepness.

The relation between the size distribution of sediments in the ripple crest and trough is shown in figures 18 and 19. Inspection of these figures shows that in general the sediments from the ripple crest tend to be coarser and have smaller distribution measures (i.e., be better sorted) than the sediments from the trough. Better sorting in the ripple crest was typical of all environments, as shown in the graph of figure 19 and illustrated by the ripple photograph in figure 17.

In only three cases was the material in the ripple trough found to be coarser than that in the crest (figure 18). In two of these, the samples were from rocky areas on exposed coasts where there was a very limited supply of sand, and the other was from a bay where the waves were relatively small.

Because turbulence and lift force are most intense at the crest of a ripple, only the coarsest of the transportable material is deposited there. Since coarser sand forms larger ripples, the ripple tends to grow in size commensurate with the coarsest material which the waves are capable of transporting. The capacity of a ripple to sort out and remove fine sand increases with ripple size, as the intensity of the vortex and lift forces increases with the length of the ripple. The fine material is placed in suspension by the vortex at the ripple crest, and either carried from the area or is deposited in the ripple trough.

It was found that boundaries between coarse and fine sand areas were sharp and well-defined. Apparently this is a natural result of the fact that large ripples grow at the expense of small ripples, and that once large ripples are formed, wave action tends to expel fine sand from the area. It was observed that the fineness of the trough sediment relative to the crest sediment could be used as an index of the proximity of fine sand areas. On the other hand, similarity in size of crest and trough material, or the occurrence of coarser material in the trough, indicated that the large ripples were more distant from fine sand areas.

Fine Sand Ripples, D-Range, La Jolla

The relatively large number of systematic observations at the four stations on D-range make it possible to describe the fine sand ripples

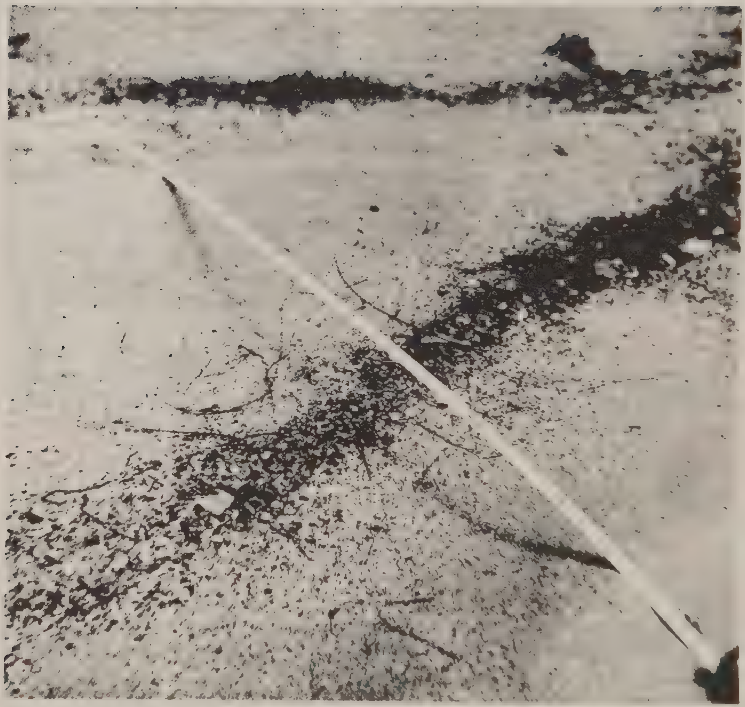

FIGURE 17. LARGE RIPPLE. Note coarse, poorly sorted debris in the trough and finer well sorted sand on the crest. Ripple is from a depth of 65 ft. off the rocky coast of Los Coronados Islands, Mexico, and has a wave length of 2.7 ft. Compare with ripple in figures 5, 6 and 7, which have coarsest sand on the ripple crests.

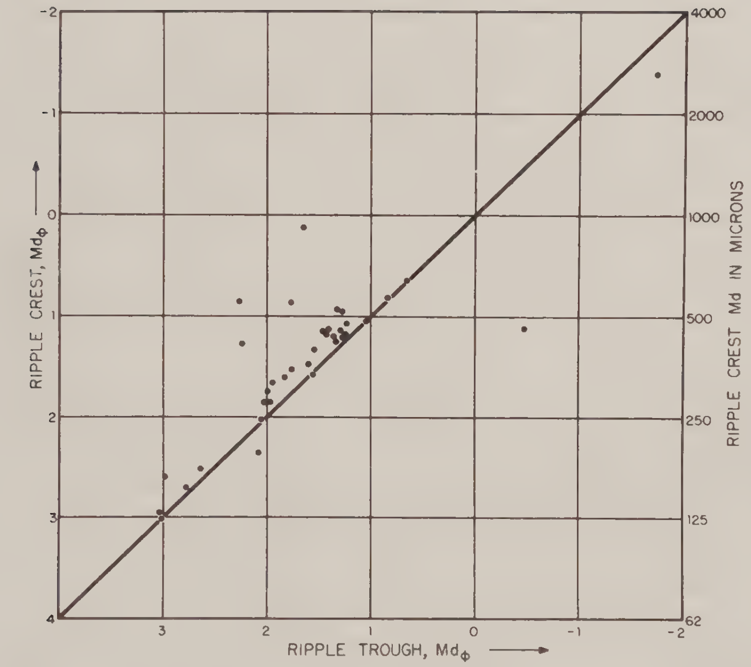

FIGURE 18. RELATION BETWEEN THE MEDIAN DIAMETER OF THE SEDIMENT IN THE RIPPLE CREST AND TROUGH. In general the crest sand is coarser than that in the trough. Exceptions occur in areas where the sand supply is limited and the sediment is relatively coarse compared with the ability of the waves to transport it. Two of the points below the line represent rocky areas with limited sand supply (Appendix II D, and III A, the other is from a small beach in Mission Bay (Appendix III A).

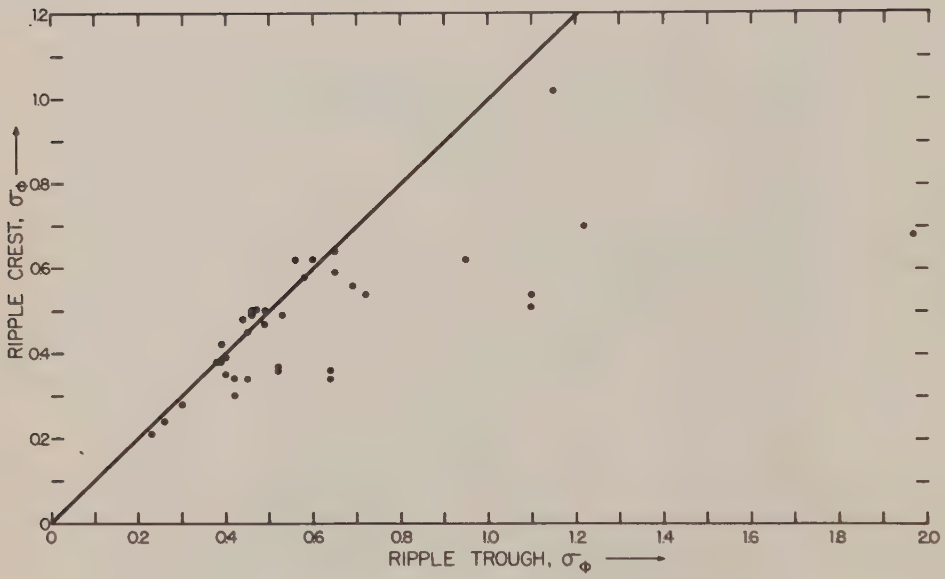

FIGURE 19. RELATION BETWEEN THE PHI DEVIATION MEASURE (SORTING) OF THE SEDIMENT IN THE RIPPLE CREST AND TROUGH. Sand from the crest was typically better sorted than that from the trough.

on this range in terms of depth and the frequency of occurrence of the various types of ripples. A complete presentation of these observations is given in Appendices I-a through I-D, and the data are summarized in tables 1 and 2, and presented graphically in figure 22.

Occurrence. Ripples were always present when the computed maximum orbital velocity was about 1/3 foot per second or greater. They were planed off and disappeared when the velocity exceeded about 2-1/2 feet per second. Because of high velocity, fine sand ripples were almost always absent in the breaker zone; they were frequently absent out to the depth of 18 feet, and occasionally at depths greater than 30 feet (Appendix I-B, 25 January 1955). Since orbital velocity decreases with increasing depth, the frequency of occurrence of periods during which the orbital velocity was insufficient to move sand was greater at the deeper stations. During these quiescent periods the ripple patterns were soon destroyed by burrowing organisms. Quiescent periods constituted 22% of the observations at a depth of 70 feet, and 5% at a depth of 50 feet (table 1). Although periods of quiescence certainly exist in shallow water as well, their occurrence is probably not statistically significant.

During quiescent periods, burrowing organisms and deposition of fine material from suspension give the bottom a very cluttered and dirty appearance as compared with the clean sand that appears when waves are actively forming ripples (compare figures 20 and 21). Within a matter of hours after sand ceases to move, the effect of bottom dwelling organisms in destroying ripples becomes apparent. Within a few days, as shown in figure 20, deposition of fine material causes the bottom to appear dirty and "rusty". Microscopic analyses of the film of "rusty" material covering the bottom on two occasions showed it to consist principally of siliceous planktonic diatoms.

The resumption of high orbital velocity following a period of quiescence soon causes the bottom to become rippled. The interaction of the wave motion and the ripples causes the fine material to be placed in suspension and the bottom soon appears to be composed of clean sand as shown in figure 21. The effective sorting action of the ripples must play an important role in removing silt- and clay-sized material from the bottom and in keeping it in suspension until it finds its way to deeper water.

Ripple Form. The patterns and profiles of the ripples varied systematically with depth (figure 22). In shallow water the fine sand ripples characteristically were long-crested (pattern 1), and were solitary in profile (figure 6). The only exceptions occurred in areas where the offshore flow of water in rip currents resulted in a confused water motion which caused the ripples to be intermediate or short-crested (patterns 2 and 3, illustrated in figures 7 and 8). Even in shallow water, short-crested ripples were more commonly associated with trochoidal rather than solitary profiles.

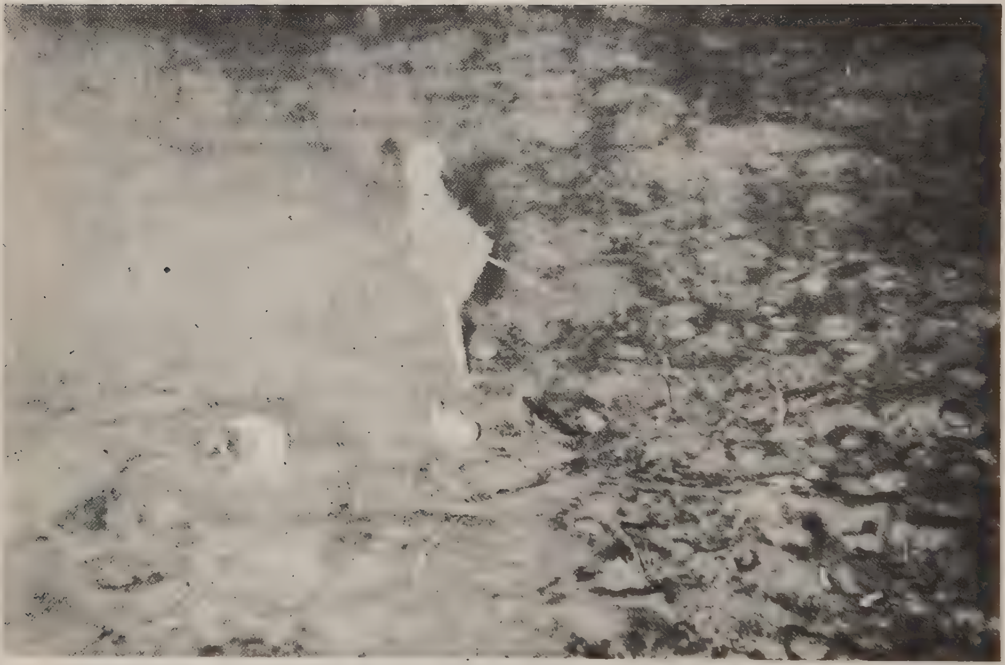

FIGURE 20. DEPOSITION OF MATERIAL FROM SUSPENSION AND DISRUPTION OF RIPPLE PATTERN BY BURROWING ORGANISMS DURING A QUIESCENT PERIOD ON D RANGE AT A 70 FT. DEPTH. (Appendix II D, 29 March 1954). Dark appearing material is principally deposition of planktonic diatoms. Compare with figure 21.

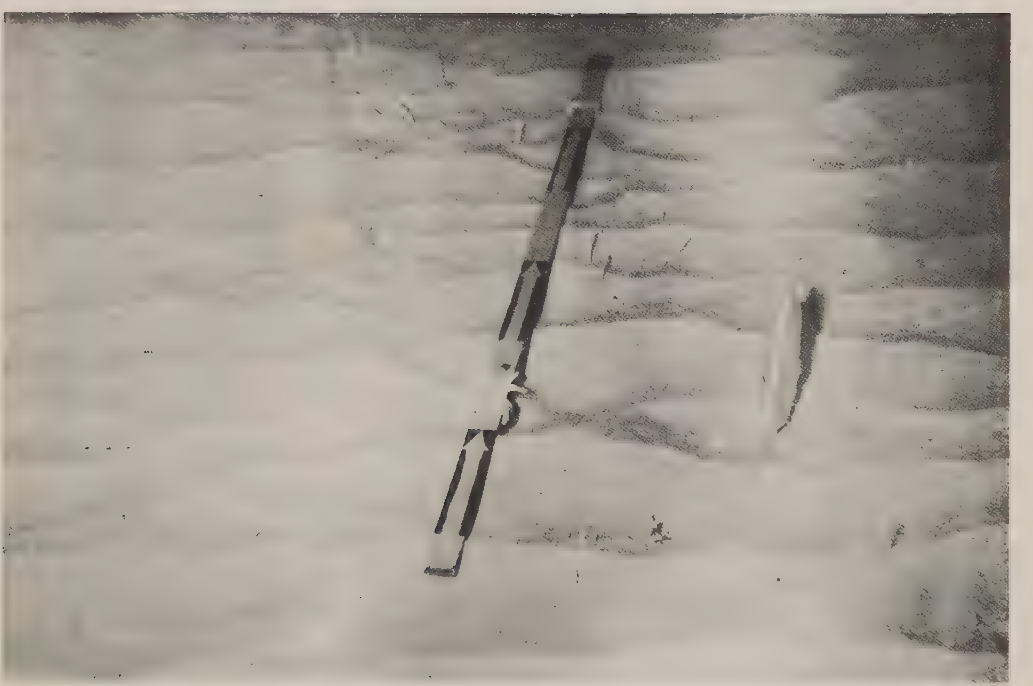

FIGURE 21. CLEAN RIPPLES GENERATED BY WAVE ACTION AT DEPTH OF 88 FT. ON D RANGE. Ripple profile is trochoidal and the wave length is 0.32 ft., (Appendix I D, 10 FEB. 54). Note burrowing organisms; sea pen (right) and distal ends of brittle stars (grass-like protrusions). Each black or white divison is ½ ft; arrows point towards shore. Compare with figure 20.

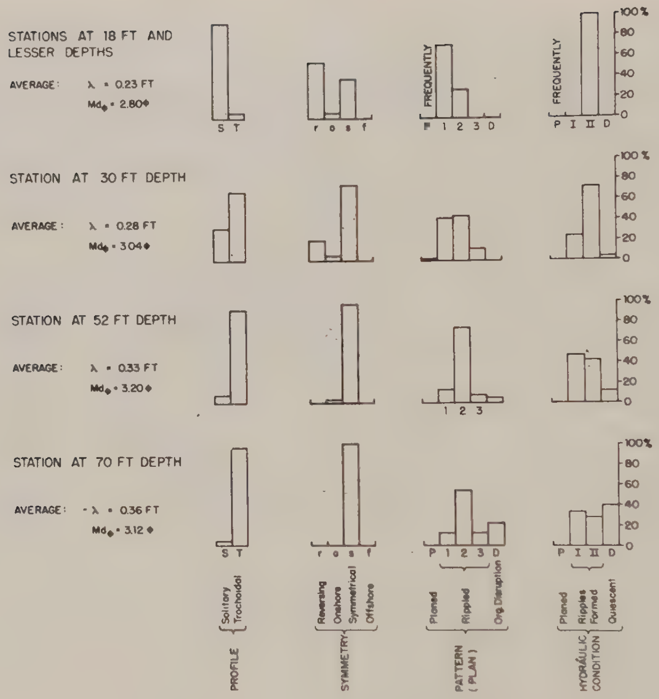

FIGURE 22. GRAPHIC SUMMARY OF RIPPLE PROPERTIES AT FOUR DEPTHS ON D RANGE, LA JOLLA, CALIFORNIA. Note that systematic difference occurs in the frequency of occurrence of all properties from shallow to deep water. Onshore and offshore symmetry pertains to asymmetrical profiles that resemble current ripples (lee face steep, stoss face gentle) formed by steady onshore or offshore flow respectively; reversing symmetry applies to conditions where ripple symmetry reverses with the passage of each wave crest and trough. Ripple patterns 1, 2, and 3 pertain to long, intermediate, and short crested ripples respectively, while planed refers to conditions where the orbital velocity was sufficiently great to cause ripples to disappear. Organic disruption of ripples occurs during quiescent conditions; other hydraulic conditions are defined in figure 10. Data are tabulated in Appendix I A through I D and are summarized in table I.

Table 1. Summary of ripple characteristics, D range, La Jolla. Individual observations are tabulated in Appendix 1A through 1D and the data are summarized graphically in figure 22.

STATION	18 ft. & lesser depths		30 ft. depth		52 ft. depth		70 ft. depth	
	No. of obs.	Value	No. of obs.	Value	No. of obs.	Value	No. of obs.	Value
RIPPLE WAVELENGTH								
Average	18	0.23 ft.	40	0.28 ft.	37	0.33 ft.	25	0.36 ft.
Maximum	1	.29 ft.	1	.21 ft.	1	.21 ft.	1	.22 ft.
Minimum	1	.19 ft.	1	.62 ft.	1	.72 ft.	1	.54 ft.
SAND SIZE								
Average Median Dia.	18	2.80 ϕ	40	3.04 ϕ	37	3.20 ϕ	25	3.12 ϕ
Coarsest " "		2.55 ϕ		2.80 ϕ		3.06 ϕ		3.28 ϕ
Finest " "		3.08 ϕ		3.28 ϕ		3.31 ϕ		2.90 ϕ
RIPPLE PROFILE								
Total Number Obs.	18		40		37		25	
Solitary	17	94%	13	32%	3	8%	1	4%
Trochoidal	1	6%	27	68%	34	92%	24	96%
RIPPLE SYMMETRY								
Total Number Obs.	18		40		37		24	
Reversing	10	55%	8	20%	0	0%	0	0%
Onshore $(\beta/\lambda < .45)$	1	6%	2	5%	1	3%	0	0%
Sym $(.45 < \beta/\lambda < .55)$	7	39%	30	75%	36	97%	24	100%
Offshore $(.55 < \beta/\lambda)$	0	0%	0	0%	0	0%	0	0%
RIPPLE PATTERN								
Total Number Obs.	18		41		39		32	
Planed P	Frequently		1	2%	0	0%	0	0%
Long crested 1	13	72%	17	42%	4	10%	4	12%
Intermed. " 2	5	28%	18	44%	30	77%	17	54%
Short " 3	0	0%	5	12%	3	8%	4	12%
Disrupted by organisms D	0	0%	0	0%	2	5%	7	22%
HYDRAULIC CONDITIONS								
Total Number Obs.	18		25		17		18	
Quiescent D	0	0%	0	0%	2	12%	7	39%
(Ia	0	0%	3	12%	4	23%	1	5%
Ripples (Ib	0	0%	3	12%	3	18%	5	28%
Formed (Ic	0	0%	0	0 %	1	6%	0	0%
(II	18	100%	18	72%	7	41%	5	28%
Planed P	Frequently		1	4%	0	0%	0	0%

Table 2. Representative ripple measurements, D range, La Jolla

Date and Station depth	Wavelength λ	Crest to trough β	Height η
21 Oct 53	0.25 ft	0.10 ft	0.02 ft
Station at 18 ft	.23	.09	.02
(Pattern 1)	.26	.09	.03
	.26	.09	.02
	.23	.08	.005
	.26	.12	.015
	.27	.10	.02
Mean	0.251	0.095	.019
C.V.*	8%	17%	55%
21 Oct 53	0.25 ft	0.12 ft	0.01 ft
Station at 30 ft	.23	.11	.015
(Pattern 1)	.24	—	.02
	.25	.11	.03
	.20	.10	.025
	.23	.12	.02
	.24	.12	.015
	.19	.09	.015
Mean	0.228	0.110	0.018
C.V.*	11%	9%	40%
20 Oct 53	0.28 ft	0.14 ft	0.02 ft
Station at 52 ft	.25	.12	.015
(Pattern 2)	.24	.11	.015
	.24	.11	.015
	.28	.11	.015
	.27	.14	.015
	.20	.10	.015
Mean	0.251	0.119	0.0157
C.V.*	11%	5%	13%
16 Nov 53	0.21 ft	0.09 ft	0.020 ft
Station at 52 ft	.24	.11	.015
(Pattern 2)	.23	.10	.010
	.19	.10	.025
	.36	.10	.020
	.34	.12	.045
Mean	0.261	0.103	0.0224
C.V.*	25%	10%	59%
19 Nov 53	0.23 ft	—	—
Station at 52 ft	.24	0.11 ft	0.015 ft
(Pattern 1)	.20	.11	.015
	.21	.13	.015
	.26	.12	.020
	.22	.10	.015
	.23	.09	.013
Mean	0.227	0.11	0.0155
C.V.*	9%	13%	14%
23 Nov 53	0.35 ft	0.16 ft	0.09 ft
Station at 52 ft	.25	.13	.06
(Pattern 3)	.30	.16	.03
	.27	.15	.04
	.29	.15	.02
	.27	.15	—
Mean	0.288	0.15	0.048
C.V.*	12%	7%	50%
28 Dec 53	0.21 ft	0.13 ft	0.070 ft
Station at 70 ft	.32	.12	.055
(Pattern 3)	.24	.12	.070
	.25	.18	.030
	.24	.11	.030
	.30	.12	.020
Mean	0.26	0.13	0.0458
C.V.*	14%	17%	44%

*Coefficient of variation is the ratio of the standard deviation to the mean, expressed in percent.

At progressively deeper stations there was a consistent change in ripple profile from solitary to trochoidal in pattern. At depths of 70 feet and greater, 65% of the ripple profiles were trochoidal and 66% of the ripple patterns were intermediate or short-crested.

Insofar as profile and pattern are concerned, the ripples tend to imitate in miniature the particular waves which generate them. In deeper water where orbital velocities are lower and the wave profile is approximately trochoidal, the ripples tend to be trochoidal. In shallow water where the velocities are higher and wave forms are solitary, the ripples tend to be solitary. In deeper water, the direction spectrum of waves is broader and the resulting variation in the direction of orbital motion is reflected in shorter crested ripples. In shallow water, because of refraction, the direction spectrum of the waves is narrow, resulting in a narrow spectrum of orbital velocities which produce long-crested ripples. On the other hand, the form of the ripple differs from that of the waves generating it in that the ripple wave length and steepness are greater in deeper water than in shallow water (figures 11 and 22). The average ripple wave length was 0.36 foot at depths greater than 70 feet, and 0.23 foot near the surface zone, even though the sand in the shallow water was slightly coarser.

Variation in Form. Measurements along D-range showed that ripple characteristics such as wave length, height, and symmetry were relatively uniform at any one time within the area of measurement (table 2). The variation in ripple wave length was considerably less, about 13%, than the variation in height, which was about 37%. The coherency of measurement was somewhat better for long-crested ripples (pattern 1) than for shorter crested ripples, although even short-crested ripples gave fairly consistent wave lengths as shown by comparison of figure 8 with the individual measurements listed in table 2. The relatively large variation in ripple height is due in part to the difficulties in making accurate measures of small ripples, as discussed previously.

The data in table 2 for the station at a depth of 52 feet on 16 November 1953 is representative of the least consistent data obtained. In this case the grouping of ripple wave lengths around values of 0.22 and 0.35 foot suggests that the ripples were not in complete unison with the waves generating them.

Comparison With Model Experiments

In many ways the findings from the laboratory and field are in agreement; however, there are significant differences which are illustrated by the following comparison of the field observations with the model experiments of Manohar (1955) and Bagnold (1946). The experiments by both Manohar and Bagnold were conducted in still water by subjecting the sediment bed to simple harmonic motion in a horizontal plane, a procedure adopted because the large bottom displacements and high orbital velocities typical of long waves in the ocean cannot be obtained in wave channels in the laboratory.

1) The maximum ripple wave length obtained in laboratory studies was somewhat less than that obtained in nature for the same size sand, even though the displacement of the movable bed exceeded the ripple wave length. For example, the maximum wave length obtained in quartz sand of about 1 mm diameter was approximately 0.7 foot in Bagnold's experiments, 1.0 foot in Manohar's work, and about 4 feet in the ocean.

2) For a given size sand, the longest ripple wave lengths in nature were observed in deeper water where the orbital velocities generating them were near the lower limit required for ripple formation. At higher velocities the wave lengths of natural ripples tended to decrease. In the laboratory investigations of Manohar, the longest ripples occurred at higher velocities just prior to the disappearance of ripples. Since these ripples were very low, it is possible that the occurrence of similar phenomena could not be detected in the field.

3) The ripple index for natural sands of all sizes ranged from about 5 to 20, while in medium and coarse sands the range was from 5 to 8. Bagnold's measurements compared favorably with the field observations. However, Manohar's observations which were made in medium and coarse sand had much larger indices, with an average value of about 20. The steepest ripples in Manohar's study had an index of 13.

COMPLEX RIPPLES

Ripples which form near obstructions such as rocks, pier pilings, and the like are frequently complex and do not always fall readily into the classifications used for the simple forms to which this paper is primarily devoted. It is also common to find that bottom dwelling animals may have an appreciable effect upon ripple form. This is particularly true of colonial animals such as sand dollars and polychaete worms like Owenia fusiformis.

A complex arrangement of ripples which has been observed near the end of Scripps Pier on several occasions will serve to emphasize the diversity of patterns possible in the vicinity of bottom obstructions (figure 23). The pattern observed apparently results from the superposition of two ripples systems. One system consists of the ordinary wave generated ripples which have wave lengths of about 1/4 foot, and ripple crests paralleling the wave crest. These are superimposed on large low ripples which form at angles of 30° to 60° with the long axis of the pier and have wave lengths of about 2-1/2 feet. Near the end of the pier where the water is deeper, the ordinary short ripples form

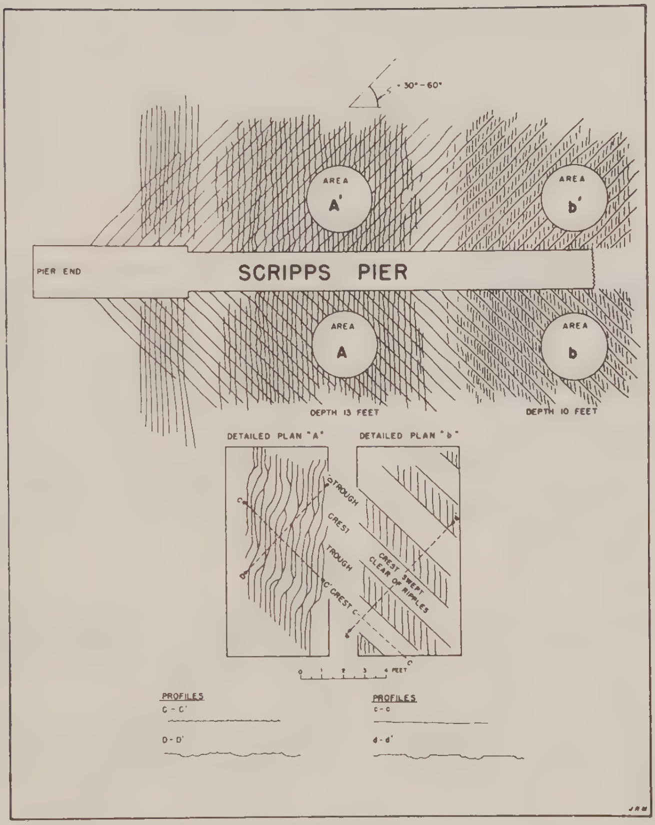
S = 30° – 60°
AREA
A'
AREA
b'
PIER END
SCRIPPS PIER
AREA
A
AREA
b
DEPTH 13 FEET
DEPTH 10 FEET
DETAILED PLAN "A"
DETAILED PLAN "b"
TROUGH
CREST
TROUGH
C' CREST
C
D
CREST SWEPT CLEAR OF RIPPLES
c
d
0 1 2 3 4 FEET
PROFILES
C - C'
D - D'
PROFILES
c - c
d - d'
JRM

FIGURE 23. COMPLEX RIPPLE PATTERN OBSERVED AT THE OCEAN PIER OF THE SCRIPPS INSTITUTION OF OCEANOGRAPHY ON 30 DECEMBER 1954. The position of area "b" was observed to move off and on shore with groups of high and low waves.

across the crests and troughs of the long ripple (area A, figure 23). In shallower water near the breaker zone, the ordinary ripples are planed from the crests of the large ripples by the high orbital velocities and are only found in the protective troughs of the large ripples (area b). The position of area b has been observed to move off and on shore with groups of higher and lower waves. On 30 December 1954, when the primary waves had a significant period of about 7 seconds and a direction of approach paralleling the axis of the pier, ripple patterns typical of area A were observed to occur in 10 feet of water when the waves were about two feet high, and to change to pattern b when the wave height increased to 3 or 4 feet.

ACKNOWLEDGMENTS

This paper represents in part results of research carried out by the University of California under contracts with the Beach Erosion Board and the Office of Naval Research. Field work was initiated in the summer of 1953 and the preliminary results were reported on briefly by Inman and Scott in 1954. The field phase of the study was largely the work of Earl Murray, who was in charge of the boat and took most of the underwater photographs and measurements. Assistance in analysis was given by Jean Short and Helene Flanders, and assistance with illustrations was given by Robert Winsett. Valuable suggestions and guidance during the study were contributed by Robert S. Arthur and Jeffery D. Frautschy.

LITERATURE CITED

Anderson, A. G.,1953. "Characteristics of sediment waves formed by flow in open channels", Proc. Third Midwestern Conference on Fluid Mechanics, University of Minnesota, pp. 379-95.

Bagnold, R. A. 1946. "Motion of waves in shallow water; interaction between waves and sand bottoms", Proc. Royal Soc. London, Vol.187, series A, pp. 1-15.

Bagnold, R. A. 1947. "Sand movement by waves: some small-scale experiments with sand of very low density", Jour. Inst. Civil Engineers, paper No. 5554, pp. 447-469.

Beach Erosion Board, 1954. "Shore protection planning and design", Corps of Engineers, Technical Report No. 4.

Darwin, G. H. 1883. "On the formation of ripple-marks in sand", Proceedings of the Royal Soc. of London, Vol. 36, pp. 18-43.

Einstein, H. A. 1942. "Formulas for transportation of bed load", Trans. Amer. Soc. Civil Engrs., Vol. 107, pp. 561-573.

Emery, K. O. 1938. "Rapid method of mechanical analysis of sands", Jour. Sed. Petrol. Vol. 8, pp. 105-111.

Exner, F. M. 1925. "Ueber die Wechselwirkung zwischen Wasser und Geschiebe in Flussen", Akad. d. Wiss., Wien, Sitzungsber, Math-Natur., Vol. 134:2a, pp. 165-203.

Forel, F. A. 1895. "Les rides de fond", Le Leman, Lausanne, Vol. 2, pp. 249-274.

Inman, D. L. 1949. "Sorting of sediments in the light of fluid mechanics", Jour. Sed. Petrol., Vol. 19, No. 2, pp. 51-70.

Inman, D. L. 1952. "Measures for describing the size distribution of sediments", Jour. Sed. Petrol., Vol. 22, pp. 125-145.

Inman, D. L. 1953. "Areal and seasonal variations in beach and near-shore sediments at La Jolla, California", Beach Erosion Board, Corps of Engineers, Tech. Memo. No. 39, 134 pp.

Inman, D. L. and N. Nasu. 1956. "Orbital velocity associated with wave action near the breaker zone", Beach Erosion Board, Corps of Engineers, Tech. Memo. No. 79, 43 pp.

Inman, D. L. and G. A. Rusnak. 1956. "Changes in sand level on the beach and shelf at La Jolla, California", Beach Erosion Board, Corps of Engineers, Tech. Memo No. 82, 30 pp.

Inman, D. L. and W. W. Scott. 1954. "Wave generated ripples in near-shore sands", Bull. Geol. Soc. Amer. Vol. 65, p. 1267.

Kindle, E. M. and E. M. Edwards. 1924. "Literature of ripplemarks", Pan-Amer. Geologist, Vol. 41, pp. 191-203.

Manohar, Madhav. 1955. "Mechanics of bottom sediment movement due to wave action", Beach Erosion Board, Corps of Engineers, Tech. Memo. No. 75, 121 pp.

Menard, H. W. 1950. "Sediment movement in relation to current velocity", Jour. Sed. Petrol., Vol. 20, pp. 148-160.

Munk, W. H. 1949. "The solitary wave theory and its application to surf problems", Ann. New York Acad. Sci., Vol. 51, Art. 3, pp. 376-424.

Page, H. G. 1955. "Phi-millimeter conversion table", Jour. Sed. Petrol., Vol. 25, pp. 285-292.

Poole, D. M., W. S. Butcher, and R. L. Fisher. 1951. "The use and accuracy of the Emery Settling Tube for sand analysis", Beach Erosion Board, Corps of Engineers, Tech. Memo. No. 23, 11 pp.

Tsubaki, T., T. Kawasumi, and T. Yasutomi. 1953. "On the influence of sand ripples upon sediment transport in open channels", Res. Inst. for Applied Mechanics, Kyushu Univ., Japan, Vol. 2, pp. 241-256.

van Straaten, L. M. J. U. 1953. "Rhythmic patterns on Dutch North Sea beaches", Overdruk uit Geologie en Mijnbouw, Nw. serie, Nr. 2, pp. 31-43.

von Karman, T. 1947. "Sand ripples in the desert", Amer. Technion Soc. Vol. 6, pp. 52-54.

Appendix IA - ID - Ripple and wave parameters for coasts exposed to the open ocean, D Range, La Jolla, California

1A - Stations at 18 ft. and lesser depths

1B - Station at 30 ft. depth

1C - Station at 50 ft. depth

1D - Stations at 70 ft. and greater depths

Appendix IIA - IID - Ripple and wave parameters for coasts exposed to the open ocean, miscellaneous observations.

IIA - Pt. La Jolla and San Diego Area, California

IIB - Pt. Dume, California

IIC - Guadalupe Island, Mexico

IID - Surge channel (special case)

Appendix IIIA - IIIC - Ripple and wave parameters for lee and protected coasts of ocean islands

IIIA - Santa Catalina Harbor, Santa Catalina, California

IIIB - San Clemente Island, California

IIIC - Los Coronados Islands, Mexico

Appendix IVA - IVC - Ripple and wave parameters for areas of limited fetch; bays, models, etc.

IVA - Mission Bay, California

IVB - Hawaiian Islands

IVC - Model Wave Tank (Beach Erosion Board)

Appendix V - Computation of Orbital Velocities and Displacements Near the Bottom

APPENDIX IA - Exposed Coast, D Range, La Jolla, 18 ft. and lesser depths

1) Sample Date-Number	Median Diameter in Microns	2) Sediment Size Distribution			Depth of Water ft	Ripple Characteristics							Waves			Hydraulic Condition		
		Md_ϕ	σ_ϕ	α_ϕ		Wave Length λ ft	Height η ft	Index $\frac{\lambda}{\eta}$	3) Symmetry β/λ	No. Meas.	4) Pattern	5) Profile	Period T sec	Orb. Diam. d_o ft	Orb. Veloc. u_m ft/sec	$\frac{d_o}{\lambda}$	$\frac{u_m}{u_1}$	6) Type
31 Aug 53-3	118	3.08	.41	-.12	10	.19	.015	12.6	r	5	1	S	10	5.1	2.0	26.8	6.0	II
7 Jul 54-1	130	2.94	.38	0	10	.23			r	7	1	S	10	5.5	2.4	23.9	7.2	II
7 Jul 54-2	132	2.92	.37	+.03	7	.22			r	6	1	S	10	5.8	2.6	26.3	7.8	II
27 Jul 54-1	136	2.88	.44	-.02	8	.22			r	11	1	S	10	4.8	2.4	21.8	7.2	II
27 Jul 54-2	129	2.95	.38	-.05	11	.20			r	8	1	S	10	4.6	1.8	23.0	5.4	II
27 Jul 54-3	145	2.79	.48	-.02	15	.22			r	7	2	S	10	4.5	1.4	20.5	4.2	II
2 Aug 54-1	171	2.55	.37	0	9	.24			r	14	1	S	10	4.8	2.2	20.0	6.6	II
2 Aug 54-2	139	2.85	.49	-.05	14	.22			r	15	1	S	10	3.0	1.2	13.6	3.6	II
2 Aug 54-3	157	2.67	.42	-.05	8	.19			r	15	1	S	10	5.0	2.3	26.3	6.9	II
17 Jul 53-1	153	2.71	.38	-.03	18	.24	.033	7.3	s	5	2	S	7	2.7	1.2	11.2	3.6	II

1) Samples from ripple trough designated by T, all others are from crest of ripple.

2) Size distribution expressed in graphic phi measures; Inman, 1952 (see text).

3) When not measured, symmetry determined by observation: r) reversing with each wave; s) symmetrical; o) asymmetrical, steep slope facing onshore; f) asymmetrical, steep slope facing offshore.

4) Pattern: 1) crest length greater than 8 λ; 2) crest length 3 λ to 8 λ; 3) crest length less than 3 λ.

5) Profile: S) solitary; T) trochoidal; SW) sawtooth.

6) Types I and II are defined in figure 10. P indicates surface of bottom smooth or planed because velocity exceeds upper critical limit for ripples; D refers to quiescent conditions where ripples were destroyed by burrowing organisms.

APPENDIX IA - Exposed Coast, D Range, La Jolla, 18 ft and lesser depths (cont.)

1) Sample Date-Number	Median Diameter in Microns	2) Sediment Size Distribution			Depth of Water ft	Ripple Characteristics							Waves			Hydraulic Condition		
		Md_ϕ	σ_ϕ	α_ϕ		Wave Length λ ft	Height η ft	Index $\frac{\lambda}{\eta}$	3) Symmetry $\frac{\beta}{\lambda}$	No. Meas.	4) Pattern	5) Profile	Period T sec	Orb. Diam. d_o ft	Orb. Veloc. u_m ft/sec	$\frac{d_o}{\lambda}$	$\frac{u_m}{u_1}$	6) Type
23 Jul 53-1	154	2.70	.38	-.05	18	.23	.02	11.5	s	12	1	S		4.0	1.7	17.4	5.1	II
-1T	146	2.78	.38	-.05														
12 Aug 53-1	146	2.78	.42	-.05	18	.20			o	13	1	S		3.7	1.2	18.5	3.6	II
14 Aug 53-1	145	2.79	.40	-.05	18	.29	.04	7.2	s	10	1	S	8	1.9	0.9	6.6	2.7	II
25 Aug 53-2	152	2.72	.45	0	18	.26	.04	6.5	.49	7	2	T	10	2.1	0.8	8.1	2.4	II
31 Aug 53-2	151	2.73	.42	-.07	18	.26	.02	13.0	s	8	2	S		3.7	1.0	14.2	3.0	II
11 Sep 53-2	147	2.77	.42	-.07	18	.21	.02	10.5	r	7	2	S	10	5.5	1.7	26.2	5.1	II
15 Oct 53-2	157	2.67	.38	-.03	18	.26	.02	13.0	.28	15	1	S	11	5.7	1.5	21.9	4.5	II
21 Oct 53-1	137	2.87	.45	-.09	18	.25	.02	12.5	.35	21	1	S	10	4.1	1.6	16.4	4.8	II

APPENDIX IB - Exposed Coast, D Range 30 ft

23 Jul 53-2	124	3.01	.46	-.06	30	.24	.03	7.7	o	10	1	S	9.2	3.1	1.1	12.9	3.3	II
27 Jul 53-1	117	3.09	.46	-.07	30	.28	.04	7.0	s	8	2	T	8	1.9	1.7	6.8	5.1	II
5 Aug 53-2	120	3.06	.47	-.11	30	.30	.05	6.0	s	7	3	T	6	1.9	1.0	6.3	3.0	II
12 Aug 53-2	117	3.10	.46	-.04	30	.39	.06	6.5	.58	6	2	T	6.2	1.1	0.5	2.8	1.5	Ib
21 Aug 53-2	118	3.08	.48	-.04	30	.22	.02	11.0	r	6	1	S	8.6	4.1	1.5	18.6	4.5	II

APPENDIX IB - Exposed Coast, D Range 30 ft (cont.)

1) Sample Date-Number	Median Diameter in Microns	2) Sediment Size Distribution			Depth of Water ft	Ripple Characteristics							Waves			Hydraulic condition		
		Md_ϕ	σ_ϕ	α_ϕ		Wave Length λ ft	Height η ft	Index $\frac{\lambda}{\eta}$	3) Symmetry $\frac{\beta}{\lambda}$	No. Meas.	4) Pattern	5) Profile	Period T sec	Orb. Diam. d_o ft	Orb. Veloc. u_m ft/sec	$\frac{d_o}{\lambda}$	$\frac{u_m}{u_1}$	6) Type
25 Aug 53-1	124	3.01	.48	-.02	30	.30	.03	10.0	.45	6	2	T	9.7	2.2	0.7	7.3	2.1	II
31 Aug 53-1	129	2.96	.47	-.04	30	.29	.045	6.3	.50	5	2½	T	10	2.0	0.6	6.9	1.8	Ib
15 Oct 53-1	126	2.99	.50	-.02	30	.25	.025	10.0	s	12	1	S	10.1	2.9	0.9	11.6	2.7	II
21 Oct 53-2	118	3.08	.48	-.17	30	.23	.02	11.5	.48	8	1	T	9.5	2.5	0.8	10.9	2.4	II
16 Nov 53-2	114	3.13	.47	-.17	30	.25	.02	12.0	r	7	1½	S	11.	5.1	1.5	20.4	4.5	II
28 Dec 53-2	117	3.10	.50	-.12	30	.23	.02	11.5	.50	8	1	T	13.	5.9	1.2	25.6	3.6	II
22 Jan 54-1	135	2.88	.47	-.02	30	.61	.075	8.1	.41	3	2	T	8.	1.0	0.4	1.6	1.2	Ia
2 Feb 54-1	124	3.01	.47	-.02	30	.25		10.0	r	6	1	S	13.	5.6	1.4	22.4	4.2	II
27 Apr 54-3	127	2.98	.51	-.06	30	.31	.04	7.7	s	6	2	T	5.	0.6	0.4	1.9	1.2	Ia
14 May 54-3	122	3.03	.45	-.07	30	.23			r	7	1	S	12.	5.8	1.5	25.2	4.5	II
18 Jun 54-3	121	3.05	.45	-.07	30	.23			s	7	1	S	8.	3.8	1.5	16.5	4.5	II
28 Jun 54-1	117	3.10	.51	0	30	.25			s	7	2	T						
26 Jul 54-1	117	3.10	.46	0	30	.34			s	5	3	T	5	0.7	0.4	2.1	1.2	Ib
16 Aug 54-1	121	3.05	.46	-.07	30	.30			s	6	3	T	7	1.7	0.7	5.7	2.1	II
26 Aug 54-1	115	3.12	.44	-.02	30	.28	.04	7.0	s	6	3	T						
1 Sep 54-1	118	3.08	.45	-.06	30	.42			s	4	3	T						
28 Sep 54-1	120	3.06	.45	0	30	.22			r	7	2	T						

APPENDIX IB - Exposed Coast, D Range 30 ft (cont.)

1) Sample Date-Number	Median Diameter in Microns	2) Sediment Size Distribution			Depth of Water ft	Ripple Characteristics							Waves			Hydraulic Condition		
		Md_ϕ	σ_ϕ	α_ϕ		Wave Length λ ft	Height η ft	Index $\frac{\lambda}{\eta}$	3) Symmetry $\frac{\beta}{\lambda}$	No. Meas.	4) Pattern	5) Profile	Period T sec	Orb. Diam. d_o ft	Orb. Veloc. u_m ft/sec	$\frac{d_o}{\lambda}$	$\frac{u_m}{u_1}$	6) Type
4 Oct 54-1	122	3.04	.47	-.10	30	.24			s	7	$1\frac{1}{2}$	S	6	1.7	1.0	7.1	3.0	II
15 Dec 54-3	118	3.08	.48	-.02	30	.21			s	7	2	T	10	3.0	1.0	14.3	3.0	II
20 Dec 54-1	138	2.86	.47	+.04	30	.22			s	13	1	S	15	4.5	1.0	20.4	3.0	II
21 Dec 54-4	125	3.00	.47	+.04	30	.23			s	6	1	S	11	4.2	1.2	18.3	3.6	II
25 Jan 55-3	103	3.28	.40	-.10	30	—	(bottom flat; strong surge)						16	10.2	2.4		7.2	P
15 Feb 55-3	115	3.12	.48	-.12	30	.23			r	8	1	S						
10 Mar 55-3	129	2.96	.42	-.11	30	.22			s	7	2	T						
22 Mar 55-3	115	3.12	.50	-.04	30	.62	.08	7.7	s	3	2	T	8	1.0	0.4	1.6	1.2	Ia
6 Apr 55-3	113	3.14	.45	-.30	30	.25			o	6	2	T						
29 Apr 55-3	125	3.00	.45	-.04	30	.23			s	5	2	T						
5 May 55-3	129	2.95	.44	-.02	30	.25			s	7	2	T	Moderate surge					
17 May 55-2	122	3.03	.45	-.07	30	.22			s	6	2	T						
8 Jun 55-3	115	3.12	.40	-.05	30	.22			s	7	2	T						
6 Jul 55-3	122	3.03	.41	-.10	30	.23			r	7	1	S	9	5.7	2.0	8.7	6.0	II
1 Aug 55-3	144	2.80	.45	0	30	.33			s	5	2	T						
12 Oct 55-3	125	3.00	.42	+.05	30	.24			s	7	1	T						
23 Nov 55-3	113	3.14	.45	-.22	30	.22			r	8	1	S						

APPENDIX IB - Exposed Coast, D Range 30 ft (cont.)

1)		2)				Ripple Characteristics							Waves			Hydraulic Condition		
Sample Date-Number	Median Diameter in Microns	Sediment Size Distribution Md_ϕ	σ_ϕ	α_ϕ	Depth of Water ft	Wave Length λ ft	Height η ft	Index $\frac{\lambda}{\eta}$	3) Symmetry β/λ	No. Meas.	4) Pattern	5) Profile	Period T sec	Orb. Diam. d_o ft	Orb. Veloc. u_m ft/sec	$\frac{d_o}{\lambda}$	$\frac{u_m}{u_1}$	6) Type
13 Jan 56-3	127	2.98	.50	-.04	30	.23			s	8	2	T						
30 Jan 56-3	109	3.20	.48	-.30	30	.25			s	6	1	T						

APPENDIX IC - Exposed Coast, D Range 52 ft

Sample Date-Number	Median Diameter in Microns	Md_ϕ	σ_ϕ	α_ϕ	Depth of Water ft	Wave Length λ ft	Height η ft	Index $\frac{\lambda}{\eta}$	Symmetry β/λ	No. Meas.	Pattern	Profile	Period T sec	Orb. Diam. d_o ft	Orb. Veloc. u_m ft/sec	$\frac{d_o}{\lambda}$	$\frac{u_m}{u_1}$	Type
10 Jul 53-1	106	3.24	.39	-.15	52	.39	.05	7.8	.55	7	2	T	6½	0.7	0.4	1.8	1.2	Ia
5 Aug 53-1	107	3.23	.42	-.12	52	.33	.06	5.5	.54	9	2	T	6	0.4	0.8	1.2	2.4	Ic
20 Oct 53-1	102	3.29	.38	-.13	52	.25	.016	15.6	.48	7	2	S	10.4	3.3	1.2	13.2	3.6	II
16 Nov 53-1	102	3.29	.38	-.08	52	.26	.022	11.7	.40	6	2	S	8.5	2.4	0.9	8.9	2.7	II
19 Nov 53-2	106	3.24	.38	-.05	52	.23	.02	11.5	.48	7	1	T						
23 Nov 53-1	103	3.28	.37	-.10	52	.29	.05	5.8	.51	6	3	T	(confused short crested)					
28 Dec 53-1	102	3.30	.36	-.17	52	.26	.03	8.7	s	7	2	T	13	3.8	0.9	14.6	2.7	II
14 Jan 54	105	3.25	.42	-.14	52	.24	.04	6.0	s	7	2	T						
28 Jan 54-2	106	3.24	.38	-.10	52	.53	.05	10.6	.51	3	2	T	9½	1.3	0.4	2.4	1.2	Ib
29 Mar 54-2	107	3.23	.41	-.10	52	.40			s	6	3	T	5	0.4	0.25	1.0	0.8	Ia
27 Apr 54-2	107	3.22	.40	-.05	52	.47	.05	9.4	s	4	2	T						
14 May 54-2	109	3.20	.40	-.05	52	.29			s	6	2	T	12	2.5	0.7	8.6	2.1	II
18 Jun 54-2	104	3.26	.38	-.10	52	.30			s	5	2	T	8	3.0	1.2	10.0	3.6	II

APPENDIX IC - Exposed Coast, D Range 52 ft (cont.)

1) Sample Date-Number	Median Diameter in Microns	2) Sediment Size Distribution			Depth of Water ft	Ripple Characteristics							Waves			Hydraulic Condition		
		Md_ϕ	σ_ϕ	α_ϕ		Wave Length λ ft	Height η ft	Index $\frac{\lambda}{\eta}$	3) Symmetry $\frac{\beta}{\lambda}$	No. Meas.	4) Pattern	5) Profile	Period T sec	Orb. Diam. d_o ft	Orb. Veloc. u_m ft/sec	$\frac{d_o}{\lambda}$	$\frac{u_m}{u_1}$	6) Type
28 Jun 54-2	107	3.23	.45	-.20	52	.22			s	7	2	T						
26 Jul 54-2	103	3.28	.39	-.10	52	.37	.06	6.2	s	4	2	T	5	0.4	0.25	1.1	0.8	Ia
16 Aug 54-2	107	3.23	.41	-.14	52	.29			s	5	2	T	8	1.3	0.5	4.5	1.5	Ib
26 Aug 54-2	107	3.22	.41	-.07	52	.28			s	5	3	T						
1 Sep 54-2	102	3.30	.40	-.15	52	.37			s	4	2	T						
28 Sep 54-2	108	3.21	.42	0	52	.28			s	6	2	T						
28 Sep 54-2	108	3.21	.42	0	52	.28			s	6	2	T						
4 Oct 54-2	101	3.31	.37	-.10	52	.24			s	7	2½	T						
15 Dec 54-2	109	3.20	.38	-.13	52	.26			s	6	2	T	10	1.4	0.4	5.4	1.2	Ib
25 Jan 55-2	120	3.06	.46	-.04	52	.21			s	5	1	S	16	5.4	1.1	25.7	3.3	II
15 Feb 55-2	113	3.14	.48	-.04	52	.23			s	8	2	T						
10 Mar 55-2	107	3.22	.43	-.11	52	.29			s	6	2	T						
22 Mar 55-2	112	3.16	.42	-.10	52	—							8	0.6	0.2		0.6	D
6 Apr 55-2	106	3.24	.36	-.36	52	.34			s	4	2	T						
29 Apr 55-2	109	3.20	.40	-.10	52	—												D
5 May 55-2	130	2.94	.54	0	52	.57			s	3	2	T	slight surge					

APPENDIX IC – Exposed Coast, D Range 52 ft (cont.)

1) Sample Date-Number	Median Diameter in Microns	2) Sediment Size Distribution			Depth of Water ft	Ripple Characteristics							Waves			Hydraulic Condition		
		Md_ϕ	σ_ϕ	α_ϕ		Wave Length λ ft	Height η ft	Index $\frac{\lambda}{\eta}$	3) Symmetry $\frac{\beta}{\lambda}$	No. Meas.	4) Pattern	5) Profile	Period T sec	Orb. Diam. d_o ft	Orb. Veloc. u_m ft/sec	$\frac{d_o}{\lambda}$	$\frac{u_m}{u_1}$	6) Type
17 May 55–1	117	3.09	.45	–.07	52	.33			s	5	2	T						
8 Jun 55–2	113	3.15	.38	–.03	52	.25			s	5	2	T						
6 Jul 55–2	117	3.10	.39	–.30	52	.22			s	7	1	T	9	3.5	1.2	15.9	3.6	II
1 Aug 55–2	110	3.19	.34	0	52	.24			s	7	2	T						
10 Sep 55–2	109	3.20	.34	–.12	52	.46			s	4	2	T						
3 Oct 55–2	113	3.15	.36	–.08	52	.72			o	4	2	T	7	0.8	0.35	1.1	1.0	Ia
12 Oct 55–2	102	3.29	.37	–.16	52	.36			s	5	2	T						
23 Nov 55–2	105	3.25	.38	–.13	52	.28			s	6	2	T						
13 Jan 56–2	118	3.08	.42	–.10	52	.45			s	4	1	T						
30 Jan 56–2	117	3.10	.36	–.08	52	.27			s	6	2	T						

APPENDIX ID – Exposed Coast, D Range 70 ft and greater depths

1) Sample Date-Number	Median Diameter in Microns	Md_ϕ	σ_ϕ	α_ϕ	Depth of Water ft	Wave Length λ ft	Height η ft	Index $\frac{\lambda}{\eta}$	3) Symmetry $\frac{\beta}{\lambda}$	No. Meas.	4) Pattern	5) Profile	Period T sec	Orb. Diam. d_o ft	Orb. Veloc. u_m ft/sec	$\frac{d_o}{\lambda}$	$\frac{u_m}{u_1}$	6) Type
22 Jul 53–1	109	3.20	.38	–.10	70	.39	.06	6.5	.53	7	$2\frac{1}{2}$	T	13	1.0	0.5	2.6	1.5	Ib
28 Dec 53–3	106	3.24	.39	–.08	70	.26	.045	5.8	.50	6	3	T	13	3.0	0.8	11.5	2.4	II
26 Jan 54–1	106	3.24	.38	–.13	70	.49	.05	9.8	.41	4	2	T	10	2.3	0.7	4.7	2.1	II
27 Jan 54–1	109	3.20	.44	–.05	70	.41	.06	6.8		4	2	T	12	1.5	0.4	3.7	1.2	Ib
28 Jan 54–1	107	3.23	.38	–.08	70	.54			s	4	2	T	$9\frac{1}{2}$	1.0	0.35	1.8	1.0	Ia

APPENDIX ID - Exposed Coast, D Range 70 ft and greater depths

1) Sample Date-Number	Median Diameter in Microns	2) Sediment Size Distribution			Depth of Water ft	Ripple Characteristics							Waves			Hydraulic Condition		
		Md_ϕ	σ_ϕ	α_ϕ		Wave Length λ ft	Height η ft	Index $\frac{\lambda}{\eta}$	3) Symmetry $\frac{\beta}{\lambda}$	No. Meas.	4) Pattern	5) Profile	Period T sec	Orb. Diam. d_o ft	Orb. Veloc. u_m ft/sec	$\frac{d_o}{\lambda}$	$\frac{u_m}{u_1}$	6) Type
29 Mar 54-1	111	3.17	.42	-.17	70	—							5	0.2	0.1		0.3	D
27 Apr 54-1	117	3.10	.42	-.10	70	.41	.02	20.0	s	9	2	T						
14 May 54-1	113	3.15	.41	-.02	70	.38	.05	7.6	s	5	2	T	12	2.1	0.5	5.5	1.5	Ib
18 Jun 54-1	114	3.13	.38	-.03	70	.29			s	5	1	T	8	2.2	0.7	7.6	2.1	II
26 Jul 54-3	109	3.20	.40	-.12	70	—							5	0	0			D
16 Aug 54-3	111	3.17	.34	+.03	70	—							8	still				D
26 Aug 54-3	112	3.16	.42	-.09	70	—								still				D
1 Sep 54-3	110	3.18	.40	-.05	70	—								still				D
4 Oct 54-3	111	3.17	.42	-.18	70	.37			s	5	2	T						
15 Dec 54-1	105	3.25	.42	-.07	70	.29			s	6	2	T	10	1.0	0.3	3.4	0.9	Ib
25 Jan 55-1	123	3.02	.46	-.06	70	.23			s	6	1½	S	16	4.5	1.0	19.5	3.0	II
15 Feb 55-1	103	3.28	.39	-.13	70	.38			s	4	2	T	12	1.0	0.3	2.6	0.9	Ib
10 Mar 55-1	113	3.15	.42	-.12	70	.22			s	7	3	T						
22 Mar 55-1	110	3.18	.37	-.10	70	—								still water				D
6 Apr 55-1	109	3.20	.36	-.16	70	.53			s	3	2	T						
20 Apr 55-1	110	3.18	.38	-.05	70	.35			s	5	2	T						
29 Apr 55-1	134	2.90	.25	-.20	70	.29			s	5	2	T						

APPENDIX ID - Exposed Coast, D Range 70 ft and greater depths

1) Sample Date-Number	Median Diameter in Microns	2) Sediment Size Distribution			Depth of Water ft	Ripple Characteristics							Waves			Hydraulic Condition		
		Md_ϕ	σ_ϕ	α_ϕ		Wave Length λ ft	Height η ft	Index $\frac{\lambda}{\eta}$	3) Symmetry $\frac{\beta}{\lambda}$	No. Meas.	4) Pattern	5) Profile	Period T sec	Orb. Diam. d_o ft	Orb. Veloc. u_m ft/sec	$\frac{d_o}{\lambda}$	$\frac{u_m}{u_1}$	6) Type
5 May 55-1	124	3.01	.42	-.07	70	—								still	water			D
16 May 55-1	117	3.10	.40	-.05	70	.32			s	4	2	T						
8 Jun 55-1	112	3.16	.36	-.06	70	.30			s	6	2	T						
6 Jul 55-1	134	2.90	.32	-.06	70	.27			s	5	3	T	9	2.3	0.8	8.5	2.4	II
1 Aug 55-1	129	2.95	.42	-.02	70	.46			s	4	2	T						
10 Sep 55-1	113	3.15	.37	+.03	70	.44			s	4	3	T						
12 Oct 55-1	119	3.07	.39	-.10	70	.35			s	5	2	T						
23 Nov 55-1	125	3.00	.40	-.05	70	.34			s	5	1	T						
13 Jan 56-1	125	3.00	.45	-.04	70	.38			s	5	2	T						
30 Jan 56-1	122	3.03	.38	-.18	70	.27			s	6	1½	T						
10 Feb 54-1	103	3.28	.40	-.08	88	.32	.065	4.9	.63	5	1½	T						
11 Feb 54-1	81	3.63	.39	-.03	110	.33	.055	6.0	.49	5	2½	T	9	0.5	0.2	1.5	0.6	Ia
30 Mar 56	no sample				170	Ripples observed but not measured												

APPENDIX IIA - Exposed coasts, Pt. La Jolla and San Diego Area

Sample Date-Number	Median Diameter in Microns	Md_ϕ	σ_ϕ	α_ϕ	Depth of Water ft	Wave Length λ ft	Height η ft	Index $\frac{\lambda}{\eta}$	Symmetry $\frac{\beta}{\lambda}$	No. Meas.	Pattern	Profile	Period T sec	Orb. Diam. d_o ft	Orb. Veloc. u_m ft/sec	$\frac{d_o}{\lambda}$	$\frac{u_m}{u_1}$	Type
2 Jul 54-2 -2T	556 555	.82 .85	.28 .30	-.07 -.13	8	1.88	.30	6.3	s	1	1	T	9	4.1	3.1	2.2	6.5	II
2 Jul 54-1 -1T	484 486	1.05 1.04	.24 .26	-.21 -.20	11	1.77	.30	6.0	s	2	1	T	9	2.5	2.4	1.4	5.5	Ic

APPENDIX IIA - Exposed coasts, Pt. La Jolla and San Diego Area (cont.)

1) Sample Date-Number	Median Diameter in Microns	2) Sediment Size Distribution			Depth of Water ft	Ripple Characteristics							Waves			Hydraulic Condition		
		Md_ϕ	σ_ϕ	α_ϕ		Wave Length λ ft	Height η ft	Index $\frac{\lambda}{\eta}$	3) Symmetry $\frac{\beta}{\lambda}$	No. Meas.	4) Pattern	5) Profile	Period T sec	Orb. Diam. d_o ft	Orb. Veloc. u_m ft/sec	$\frac{d_o}{\lambda}$	$\frac{u_m}{u_1}$	6) Type
4 Jul 56-1	637	.65	.21	-.05	19	2.80	0.5	5.6	s	1	1	T	15	9.0	2.2	3.2	4.3	II
-1T	633	.66	.23	-.13														
30 Nov 53-1	276	1.86	.50	-.22	30	1.20	.15	8.0	s	6	2½	T	9.7	4.1	1.3	3.4	3.7	II
-1T	257	1.96	.46	-.04														
15 Dec 53-2	325	1.62	.47	-.20	30	1.52	.22	6.9	.46	2	2	T	10.3	2.4	0.7	1.6	1.8	Ia
-2T	281	1.83	.49	-.02														
5 Jan 54-2	297	1.75	.48	-.19	30	.85			s	7	2	SW	10.0	2.9	0.9	3.4	2.5	II
-2T	254	1.98	.44	-.05														
14 Jan 54-2	457	1.13	.45	-.22	30	2.33	.37	6.3	s	4	1	S	10.0	2.8	0.8	1.2	1.9	Ia
-2T	379	1.40	.45	-.07														
2 Feb 54-3	415	1.27	.38	-.05	30	2.32	.35	6.7	.46	3	1	S	13	2.9	0.7	1.2	1.7	Ia
-3T	398	1.33	.39	-.13														
5 Feb 54-1	432	1.21	.42	-.12	30	2.25	.37	6.1	.44	1	1	S						
-1T	415	1.27	.39	-.03														
8 Feb 54-2	432	1.21	.34	-.06	30	2.67	.41	6.5	.49	1	1	S-T	12	3.5	0.9	1.3	2.1	Ia
-2T	392	1.35	.42	-.02														
9 Feb 54-1	441	1.18	.50	-.12	30	2.55	.44	5.8	.49	1	1	T	11	3.0	0.85	1.2	2.0	Ia
-1T	371	1.43	.46	-.02														
9 Feb 54-1	441	1.18	.50	-.12	30	2.64	.42	6.3	.42	1	1	T	11	3.0	0.85	1.1	2.0	Ia
-1T	371	1.43	.46	-.02														
9 Aug 54-1	514	0.96	.35	+.01	30	2.65	.45	5.9	o	1	1	S	12	2.6	0.7	1.0	1.5	Ia
-T	418	1.26	.40	-.02														
9 Aug 54-2	222	2.17	.92	0	40	.80				2	2	T	12	3.1	0.8	3.9	2.3	II

APPENDIX IIA - Exposed coasts, Pt. La Jolla and San Diego Area (cont.)

1) Sample Date-Number	Median Diameter in Microns	2) Sediment Size Distribution			Depth of Water ft	Ripple Characteristics							Waves			Hydraulic Condition		
		Md_ϕ	σ_ϕ	α_ϕ		Wave Length λ ft	Height η ft	Index $\frac{\lambda}{\eta}$	3) Symmetry $\frac{\beta}{\lambda}$	No. Meas.	4) Pattern	5) Profile	Period T sec	Orb. Diam. d_o ft	Orb. Veloc. u_m ft/sec	$\frac{d_o}{\lambda}$	$\frac{u_m}{u_1}$	6) Type
10 Aug 54-1 -1T	419 212	1.28 2.24	.34 .45	+.03 -.07	40	2.80				1	1	T			short per. complex			
10 Aug 54-2A -2AT	321 261	1.64 1.94	.54 .72	-.14 0	40	2.00				1	1	T						
10 Aug 54-2B -2BT	274 247	1.87 2.02	.56 .69	-.05 +.15	40	.90						T						
10 Aug 54-3 -3T	129 122	2.95 3.04	.64 .65	-.33 -.30	40	.47				6	2	T						
10 Aug 54-5	164	2.61	.98	-.80	40	.51				4	2½	T						
18 Aug 54 -1(0-1cm) -1(5-6cm) -1T	 398 287 342	 1.33 1.80 1.55	 .62 1.01 .95	 +.05 +.40 +.40	40	2.05	.31	6.6	s	1	1	T	8 short period superimposed	2.5	1.0	1.2	2.5	Ic
1 Oct 54-1 -1T	551 293	0.86 1.77	.51 1.10	+.05 +.30	40	2.14	.36	5.9	.36	1	1	T						
1 Aug 56-1 -1T	359 330	1.48 1.60	.30 .42	+.12 +.19	45	2.60	.40	6.5	o	1	1	T	11	3.1	0.8	1.2	2.0	Ia
30 Nov 53-2 -2T	470 426	1.09 1.23	.37 .52	-.14 +.17	55	3.00	.48	6.2	s	1	2	T	9.7	2.9	0.9	1.0	2.0	Ia
15 Dec 53-1 -1T	525 399	.93 1.33	.34 .64	-.03 +.17	55	3.00	.48	6.2	.54	4	1	S	10.3	2.2	0.6	0.7	1.3	Ia
16 Dec 53-1	501	.99	.28	+.04	55	2.89	.52	5.6	.48	4	1	S						
29 Jan 54-1 -1T	432 415	1.21 1.27	.36 .64	+.03 +.02	55	2.53	.39	6.5	s	2	1	S&T	11	2.3	.65	0.9	1.5	Ia

APPENDIX IIA - Exposed Coasts , Pt. La Jolla and San Diego Area (cont.)

1) Sample Date-Number	Median Diameter in Microns	2) Sediment Size Distribution			Depth of Water ft	Ripple Characteristics							Waves			Hydraulic Condition		
		Md_ϕ	σ_ϕ	α_ϕ		Wave Length λ ft	Height η ft	Index $\frac{\lambda}{\eta}$	3) Symmetry $\frac{\beta}{\lambda}$	No. Meas.	4) Pattern	5) Profile	Period T sec	Orb. Diam. d_o ft	Orb. Veloc. u_m ft/sec	$\frac{d_o}{\lambda}$	$\frac{u_m}{u_1}$	6) Type
8 Feb 54-1 -1T	448 412	1.16 1.28	.36 .52	+.11 -.04	55	2.72	.44	6.2	.66	1	1	S-T	12	3.2	0.8	1.2	1.9	Ia
28 Jul 54-1 -1T	124 124	3.01 3.01	.50 .49	-.34 -.35	85	.49	0.10	4.9	s	10	2	T						
3 Aug 54-1 -1T	165 127	2.60 2.98	.62 .56	-.25 -.30	85	.68	.13	5.2	s	2	2	T						
3 Aug 54-2 -2T	335 342	1.58 1.55	.59 .65	-.15 +.15	85	2.70			s	1	2	T						
31 Mar 54-1	88	3.50	.44	-.25	110	.34			s	5	2	T						
14 Jan 55-3	132	2.92	.50	-.12	120	.47			s	3	2	S						

APPENDIX IIB - Exposed Coast, Point Dume, Calif.

8 Sep 54-18 -18T	913 319	0.13 1.65	1.02 1.15	+.36 -.42	7	3.45	.65	5.3	o	1	1	T	13	3.5	1.3	1.0	2.1	Ic
8 Sep 54-14	254	1.98	.70	-.30	11	.59			s	2	2	T	13	2.0	1.2	3.4	3.4	II
9 Sep 54-27	120	3.06	.31	-.15	38	.34				3	2	T	8	.9	.35	2.6	1.0	Ib
8 Sep 54-10	149	2.75	.60	-.14	47	.48			s	2	2½	T	13	1.5	.4	3.1	1.2	Ib

APPENDIX IIC - Exposed Coast, Guadalupe Island, Mexico

15 Nov 54-6	122	3.04	.41	-.17	61	.25				6	1	T						

APPENDIX IIC - Exposed Coast, Guadalupe Island, Mexico (cont.)

1) Sample Date-Number	Median Diameter in Microns	2) Sediment Size Distribution Md_ϕ	σ_ϕ	α_ϕ	Depth of Water Ft	Ripple Characteristics: Wave Length λ ft	Height η ft	Index $\frac{\lambda}{\eta}$	3) Symmetry $\frac{\beta}{\lambda}$	No. Meas.	4) Pattern	5) Profile	Waves: Period T sec	Orb. Diam. d_o ft	Orb. Veloc. u_m ft/sec	Hydraulic Condition $\frac{d_o}{\lambda}$	$\frac{u_m}{u_1}$	6) Type
15 Nov 54-7	460	1.12	.84	-.14	61	4.00	.75	5.3	s	1	1	T						
15 Nov 54-8	379	1.40	.66	-.15	66	2.20			s	1	1	T						

APPENDIX IID - Surge Channel off Pt. Loma, San Diego, Calif. (special case).

1) Sample Date-Number	Median Diameter in Microns	Md_ϕ	σ_ϕ	α_ϕ	Depth of Water Ft	Wave Length λ ft	Height η ft	Index	Symmetry	No. Meas.	Pattern	Profile	Period T sec	Orb. Diam. d_o ft	Orb. Veloc. u_m ft/sec	$\frac{d_o}{\lambda}$	$\frac{u_m}{u_1}$	Type
14 Jan 55-1 -1T	2603 3317	-1.38 -1.73	.70 1.22	-.04 -.13	45	4.10												

APPENDIX IIIA - Protected Coast, Santa Catalina Harbor

1) Sample Date-Number	Median Diameter in Microns	Md_ϕ	σ_ϕ	α_ϕ	Depth of Water Ft	Wave Length λ ft	Height η ft	Index	Symmetry	No. Meas.	Pattern	Profile	Period T sec	Orb. Diam. d_o ft	Orb. Veloc. u_m ft/sec	$\frac{d_o}{\lambda}$	$\frac{u_m}{u_1}$	Type
10 Sep 54-5 -5T	460 1395	1.12 -0.48	.68 1.97	+.15 -.45	4½	1.80	.30	6.0	s	1	1	S	10	2.2	1.2	1.2	2.7	Ic
10 Sep 54-6	457	1.13	.80	-.45	4½	1.75	.25	7.0	s	1	1	S	10	2.2	1.2	1.3	2.7	Ic

APPENDIX IIIB - Protected Coast, Wilson Cove, San Clemente Island.

1) Sample Date-Number	Median Diameter in Microns	Md_ϕ	σ_ϕ	α_ϕ	Depth of Water Ft	Wave Length λ ft	Height η ft	Index	Symmetry	No. Meas.	Pattern	Profile	Period T sec	Orb. Diam. d_o ft	Orb. Veloc. u_m ft/sec	$\frac{d_o}{\lambda}$	$\frac{u_m}{u_1}$	Type
12 Jun 56-4 -4T	173 162	2.53 2.63	.58 .58	-.02 -.12	21	.67	.10	6.7	s	1	1	T		sheltered lee				

APPENDIX IIIC - Protected Coast, Los Coronados Islands, Mexico

1) Sample Date-Number	Median Diameter in Microns	Md_ϕ	σ_ϕ	α_ϕ	Depth of Water Ft	Wave Length λ ft	Height η ft	Index	Symmetry	No. Meas.	Pattern	Profile	Period T sec	Orb. Diam. d_o ft	Orb. Veloc. u_m ft/sec	$\frac{d_o}{\lambda}$	$\frac{u_m}{u_1}$	Type
9 Feb 56-1 -1T	245 242	2.03 2.05	.39 .40	-.18 -.17	35	.75			s	2	2	T		sheltered lee				
13 Jan 55-1	113	3.15	.38	-.05	65	.20				1	3	T		sheltered lee				
13 Jan 55-2	555	.85	.54	-.57	65	1.10	.25	4.4	s	1	2	T		sheltered lee				

APPENDIX IVA – Limited Fetch, Mission Bay, California

1) Sample Date–Number	Median Diameter in Microns	2) Sediment Size Distribution			Depth of Water ft	Ripple Characteristics							Waves			Hydraulic Condition		
		Md_ϕ	σ_ϕ	α_ϕ		Wave Length λ ft	Height η ft	Index $\frac{\lambda}{\eta}$	3) Symmetry $\frac{\beta}{\lambda}$	No. Meas.	4) Pattern	5) Profile	Period T sec	Orb. Diam. d_o ft	Orb. Veloc. u_m ft/sec	$\frac{d_o}{\lambda}$	$\frac{u_m}{u_1}$	6) Type
20 Jan 55–1	195	2.36	.49	–.14	0.16	.14	.020	7.0	s	5	1	T	0.7	0.15	0.4	1.1	1.2	Ia
–1T	237	2.08	.53	–.06														
20 Jan 55–2	123	3.02	.45	–.13	0.16	.15	.025	6.0	s	4	1	T	0.7	0.15	0.4	1.0	1.2	Ia
20 Jan 55–3	233	2.10	.45	+.04	0.11	.14			o	4	1	T	.45	.13	0.4	0.9	1.2	Ia

APPENDIX IVB – Hawaiian Islands (Lagoon Inside Reef)

8 Dec 55–62	344	1.54	.62	–.40	4.0	2.30	.38	6.1	o	1	1	T	$3\frac{1}{2}$	2.8	1.3	1.2	3.4	Ic
–62T	295	1.76	.60	–.50														
13 Dec 55–2	595	.75	.94	–.16	7	1.05	.16	6.5	s	1	1	T	$3\frac{1}{2}$	1.3	1.2	1.2	2.4	Ic

APPENDIX IVC – Beach Erosion Board, Model Wave Tank

	221	2.18			.40	.33	.055	6.0	.35	1		T	2.12	.38	.7	1.2	2.1	Ia

APPENDIX V

COMPUTATION OF ORBITAL VELOCITIES AND DISPLACEMENTS NEAR THE BOTTOM

There appears to be no single wave theory which is both capable of reliable prediction of the various wave properties from deep water into the surf zone, and which is in a practical form for their computation. For this reason it seemed expedient to use different techniques for computing orbital velocities and displacements near the surf zone from those used in deeper water. In general, the Airy theory for waves of small amplitude was used in deeper water, and an adaptation of solitary wave theory was used when waves were near the breaker zone. The two techniques are described below together with a criterion for their use.

AIRY WAVES

The classical theory of wave motion, attributed to Airy in 1845, is strictly applicable to waves of infinitely small height in water of any depth. The wave profile is sinusoidal and the particle orbits are closed circles in deep water and ellipses in shallow water. The orbital velocities and particle displacements vary as sine functions with time, and their maximum magnitudes in onshore and offshore directions are equal.

The instantaneous horizontal displacement, r, of a water particle from its equilibrium position for an Airy wave is:

$$r = -\frac{H}{2}\,\frac{\cosh 2\pi \frac{z}{L}}{\sinh 2\pi \frac{h}{L}}\,\sin \frac{2\pi}{L}(x - Ct) \qquad (1)$$

where L = CT is the wave length, h is the depth of water, C, T, and H, are the wave phase velocity, period, and height respectively, z is the vertical coordinate measured from the bottom upwards, and x and t are the horizontal distance and time measured from the wave crest. The total range of horizontal displacement, or orbital diameter d, is equal to twice the absolute maximum value of r. Near the bottom this reduces to

$$d_o = \frac{H}{\sinh 2\pi \frac{h}{L}} \qquad (2)$$

The maximum horizontal component of orbital velocity occurs at the instant of wave crest and trough passage, and near the bottom is given by

$$u_m = \frac{\pi d_o}{T} \qquad (3)$$

(703)

The computation of d_o and u_m is facilitated by tables of $\sinh 2\pi \frac{h}{L}$ as function of the depth and deepwater wave length (Beach Erosion Board Technical Report No. 4).

SOLITARY WAVE

In shallow water and near the breaker zone the continuous frequency characteristics commonly associated with waves in deep water are lost and individual waves tend to retain their identity and in many ways resemble the solitary wave of Scott-Russell. For this reason the solitary wave concept has been applied to waves near the breaker zone and has met with some degree of success. Munk (1949) summarized useful relations derived from solitary wave theory and made them accessible to numerical example and Inman and Nasu (1956) compared measurements of orbital velocity of ocean waves with theory. The later study suggests that a reasonable proximation to the horizontal orbital velocities of water particles near the bottom can be obtained from solitary theory.

According to solitary theory, water particles are essentially at rest at some distance in front of the wave crest. As the crest approaches they move forward and upward and attain their maximum velocity at the instant of crest passage. Following the passage of the crest the velocity of the particles decreases and they move downward, eventually reaching a new rest position a distance 2r in advance of their former rest position. Thus, when solitary waves travel through still water, particles undergo relatively flat trajectories with motion only in the direction of wave propagation. Closed or partially closed trajectories and orbital motion more nearly resembling that of shallow water waves in nature are obtained from the theory by superposing some sort of return flow on the solitary wave.

The condition of no return flow, or of solitary waves traveling through still water, leads to a maximum net particle displacement at the bottom with the passage of each wave crest. The net displacement decreases and the trajectory becomes more orbital in nature as the return flow increases. The net displacement becomes zero when the return flow, $\bar{v}$, is equal to the still water displacement, 2r, divided by the wave period. Although the condition of zero net particle displacement along the bottom is certainly not rigorously fulfilled in nature, on the whole such an assumption may give a reasonable approximation to conditions generally encountered in shallow water. However, applications of concepts of this type to conditions in nature are at best only approximate; and are subject among other things, to the limitation imposed by Bagnold (1947) and Munk (1949). An important limiting criterion, that the period of the waves must be equal to or greater than the effective period, is discussed later.

(704)

The particle displacement due to a solitary wave traveling through still water, and the orbital diameter of the particle trajectory for the special case in which there is no net particle displacement at the bottom are derived below, and graphs for their computation are given in Plates 1 and 2.

Solitary Wave in Still Water

Following approximately the dimensionless notation of Munk (1949, eq. 31), the McCowan equation for the horizontal component of orbital velocity along the bottom is

$$U = \frac{N}{1 + \cosh M X} \qquad (4)$$

where $u = CU$ is the horizontal component of orbital velocity, $x = hX$ is the horizontal distance measured from the wave crest, $C = \sqrt{g(h+H)}$ is the velocity of propagation of the wave crest, H is the wave height, h is the depth of water under the wave trough, M and N are functions of the relative wave height, $\gamma = H/h$, and are defined by the equations

$$\gamma = \frac{N}{M} \tan 1/2 \left[M(1 + \gamma)\right] \qquad (5)$$

$$N = 2/3 \sin^2 \left[M(1 + 2/3\,\gamma)\right] \qquad (6)$$

If r is the horizontal displacement of a water particle at time t relative to its position at the instant of passage of the wave crest, then (Munk, 1949, eq. 14)

$$r = \int_0^t u\,dt = \int_0^x \frac{u}{C-u}\,dx \qquad (7)$$

where $dx = (C-u)\,dt$. In dimensionless notation

$$R = \frac{r}{h} = \int_0^X \frac{U}{1 - U}\,dX \qquad (8)$$

Substituting the value of U from equation (4) and taking twice the value of the integral to include the displacement preceding the passage of the wave crest

$$2R = 2\,\frac{N}{M} \int_0^X \frac{dMX}{(1-N) + \cosh MX} = \left[4\,\frac{N}{M}\,k \csc \beta\right]_0^X \qquad (9)$$

where $\cos \beta = 1 - N$: $\tan k = \left[\tanh \frac{MX}{2}\right]\left[\tan \frac{\beta}{2}\right]$

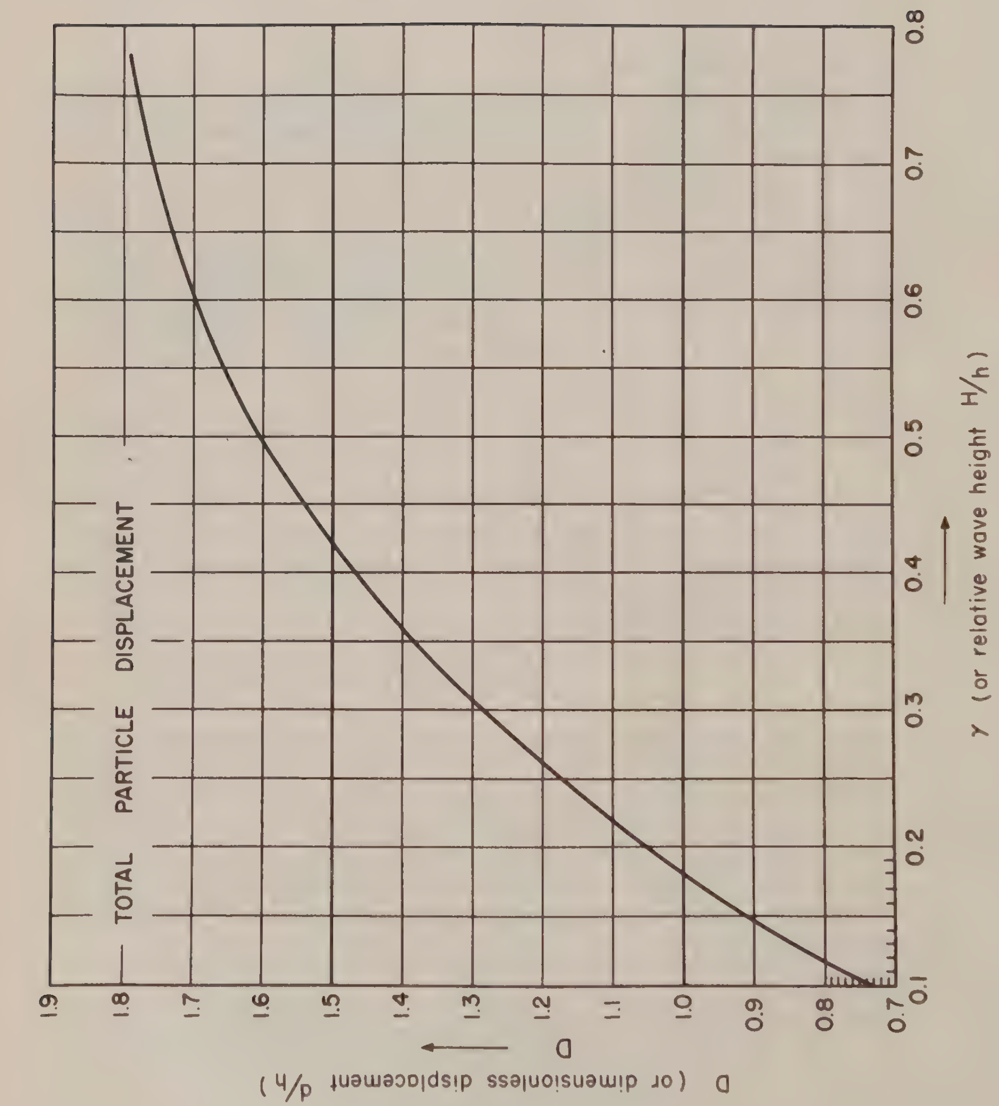

PLATE V-1. TOTAL PARTICLE DISPLACEMENT AT THE BOTTOM FOR A SOLITARY WAVE TRAVELING THROUGH STILL WATER; (EQUATION 10).

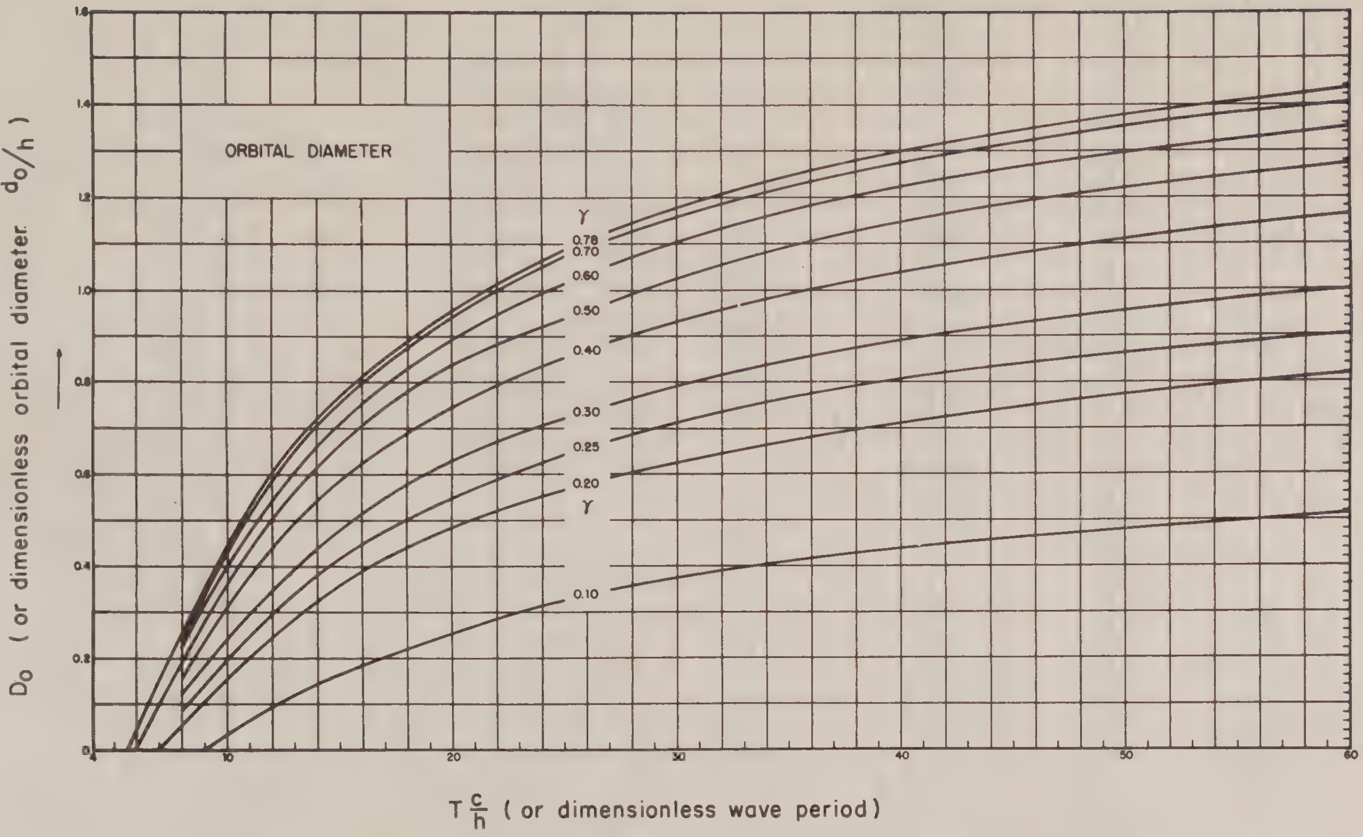

PLATE V-2. HORIZONTAL ORBITAL DIAMETER FOR THE CLOSED ORBIT TRAJECTORY OF A SOLITARY WAVE, (EQUATION 15).

For the case where X is taken to infinity, the total particle displacement is given by

$$D = 2R = \frac{2N}{M} \quad \beta \csc \beta \tag{10}$$

The dimensionless displacement D is graphed as a function of the relative wave height γ in Plate 1. To convert the displacement to conventional units it is necessary to multiply D by the depth of water, $d = hD$.

Closed Orbit Displacement

If it is assumed that there is no net displacement of a water particle along the bottom due to solitary wave motion, then a dimensionless return flow $\bar{V}$, opposed in direction to that of the wave propagation, is defined

$$\bar{V} = \frac{D}{T \frac{C}{h}} \tag{11}$$

where D is given by equation (10), T is the wave period, and $T \frac{C}{h}$ is the dimensionless wave period.

Under these conditions, and relative to a coordinate system moving with the wave crest, a water particle will move forward during the passage of a solitary wave crest a distance X_1 until the orbital velocity U decreases to the value of $\bar{V}$, at which time the particle will reach a maximum forward position in its trajectory. It will then move backward under the influence of the return flow, past its initial position to a position $-X_1$. The following wave crest will then cause the particle to move forward again when the orbital velocity exceeds the return flow, and the trajectory for the closed orbit will be completed. X is obtained from equation (4) by setting U equal to the return velocity V.

Relative to the moving coordinate system, the total displacement imparted to a water particle during the propagation of the wave crest from $-X_1$ to $+X_1$ is given by $2R$, in equation (9). It remains to evaluate the transit time, $2t_1$ of the particle between $-X_1$ and $+X_1$.

Since the wave crest is advancing with phase velocity C, relative to a fixed point on the bottom, the water particle will have advanced a distance r_1 and the wave crest will advance a distance $r_1 + x_1$ during time t_1. Thus in moving from $-x$ to $+x$ the water particle is acted on by the return flow $\bar{V}$ for a time.

$$2t_1 = \frac{2(r_1 + x_1)}{C} \tag{12}$$

or in dimensionless notation

$$2t_1 \frac{C}{h} = 2 (R_1 + X_1) \qquad (13)$$

In time $2t_1$ the water particle is moved backwards by the return flow $\bar{V}$ a total distance

$$2R_2 = 2 \bar{V} (R_1 + X_1) \qquad (14)$$

and during the same time the particle is carried forward by the orbital motion of the solitary wave a distance $2R_1$. Therefore, the total horizontal orbital diameter of the closed orbit trajectory becomes

$$D_o = 2(R_1 - R_2) \qquad (15)$$

The dimensionless orbital diameter D_o is graphed as a function of relative wave height γ and dimensionless wave period $T \frac{C}{h}$ in Plate 2. To convert the orbital diameter to conventional units it is necessary to multiply by the water depth h,

$$d_o = h D_o \qquad (16)$$

Closed Orbit Velocities

Under the assumption that the wave motion is solitary in nature and that the trajectories of water particles form closed orbits along the bottom, the maximum horizontal orbital velocities under wave crests and troughs can be computed from the above relations. If the wave length is very great compared to the depth of the water, the maximum backward velocity under the wave trough is simply equal to the net return flow defined in equation (11), which when converted to conventional notation is

$$u_t = \frac{hD}{T} \qquad (17)$$

Referring to equation (4), directly beneath the wave crest X is zero and the horizontal velocity along the bottom becomes, in conventional notation,

$$u = \frac{1}{2} NC \qquad (18)$$

This is the maximum horizontal velocity along the bottom for a solitary wave traveling through still water. The maximum horizontal velocity under the wave crest for the special case of a closed orbit trajectory then becomes

$$u_c = u - u_t \tag{19}$$

Values of u for various water depths and wave heights are graphed in Inman and Nasu (1956, Figure 27).

Field measurements of orbital velocity made just seaward of the breaker zone by Inman and Nasu (1956, table 2b) showed the ratio of the maximum crest to maximum trough velocity to range from about 1 to 4. If for practical purposes it is assumed that the ratio does not exceed 4, then as an upper limit the maximum crest velocity will not exceed 80% of the maximum still water velocity given by equation 18. Thus in regions where the solitary theory applies, the maximum horizontal orbital velocity under the wave crest, u_m, is arbitarily defined as being equal to u_c, but not to exceed $0.8^m u$.

$$u_m = u_c \leq 0.8\ u \tag{20}$$

Effective Wave Length and Period

Application of solitary theory to orbital velocities and displacements requires, among other things, that the wave crests be sufficiently far apart to permit the assumption that a water particle comes to rest following the passage of each wave crest when the solitary model is traveling in still water. An effective wave length $L_e = 2X$ can be defined where X is the distance from the wave crest necessary to reduce the orbital velocity to some acceptable fraction, f, of the maximum velocity under the wave crest. From equations (4) and (18) the dimensionless distance from the crest becomes

$$X = \frac{\cosh^{-1}\left(\frac{2}{f} - 1\right)}{M} \tag{21}$$

from which an effective wave period is obtained

$$T_e = \frac{2\ X\ h}{C} \tag{22}$$

If we assume that a reduction in orbital velocity to 2-1/2 percent of the maximum crest velocity is sufficient to permit application of solitary theory, then f = 1/40, and X equals approximately $\frac{5}{M}$, from which the effective period becomes

$$T_e = \frac{10}{M}\ \frac{h}{C}$$

This is not necessarily a conservative estimate for T_e because the reduction in wave velocity by the return flow is not considered in computing C. Therefore it was assumed that the solitary theory could apply only when the dimensionless wave period was somewhat greater than $\frac{10}{M}$,

$$T \frac{C}{h} > \frac{10}{M} \qquad (23)$$

This requirement is somewhat more conservative than the effective period defined by Bagnold (1947) and used by Munk (1949), $T_e = \frac{2\pi}{M}\sqrt{\frac{h}{g}}$.

SAMPLE COMPUTATION

Given

H, wave height	4 ft
h, water depth under wave trough .	8 ft
T, wave period	10 sec

Computation

γ, relative wave height H/h	0.5
M, and N (from Munk 1949, plate 5)	0.88 & 0.57
C, wave velocity $\sqrt{g\ (h + H)}$	19.6 ft/sec
Dimensionless wave period $T \frac{C}{h} > \frac{10}{M}$	24.5 > 11.4

∴ Solitary theory applies

* * * * * * * * * *

D, dimensionless particle displacement (still water) plate 1....	1.6
D_o, dimensionless orbital diameter (closed orbit) plate 2........	0.93
d_o, orbital diameter (closed orbit), hD_o	7.4 ft
u, maximum orbital velocity (still water), equation 18, or Inman and Nasu, 1956, figure 27	5.6 ft/sec
u_t, max. orbital velocity under trough (closed orbit), eq. 17 ...	1.3 ft/sec
u_c, max. orbital velocity under crest (closed orbit), $u - u_t$	4.3 ft/sec
u_m, practical max. orbital velocity equals $u_c < 0.8$ u, equation 20	4.3 ft/sec

Reprinted from METEOROLOGICAL MONOGRAPHS, Vol. 2, No. 10, June, 1957, pp. 32–45
Printed in U. S. A
Reproduced by Permission

DAY TO DAY VARIATION OF SEA LEVEL

By Gordon W. Groves

INTERACTION OF SEA AND ATMOSPHERE:

a group of contributions

by

A. C. Redfield, A. R. Miller;
G. W. Groves; D. L. Harris;
R. O. Reid;
W. Marks and J. Chase.

DAY TO DAY VARIATION OF SEA LEVEL[1]

By GORDON W. GROVES[2]

Scripps Institution of Oceanography

(Original manuscript received 26 September 1955; revised manuscript received 27 February 1956)

ABSTRACT

Tide gauge data are submitted to a special averaging process that eliminates the diurnal and higher species tides. The process has been applied to simultaneous data from many locations in order to obtain records of sea level. A typical value for the standard deviation of these records is 15 cm if attention is confined to a spectral window containing periods between two days and a month.

With this restriction in mind the observed tide activity is largely associated with variable atmospheric pressure and wind. The principal effect of the varying atmospheric pressure is direct and instantaneous. The sea level records have been adjusted for this direct pressure effect. The standard deviation is reduced by about 50 per cent on the average by this correction.

Comparisons among water density and wind data are made. The wind is, of course, one of the major factors in producing sea level variations. Changes of water density produce small but observable effects. Other factors are discussed.

1. Introduction

Tides usually present troublesome "high-frequency noise" in the study of long period fluctuations of sea level. In order to overcome this difficulty in the present work, hourly tidal heights were subjected to the special weighted average C_{51} [2]. The term C_{51} designates a particular set of weight factors by which the successive tidal heights are multiplied. The period response factor of C_{51} is shown in fig. 1.

The hourly tidal heights were punched onto punchcards and the numerical calculations were carried out by International Business Machines automatic computers. *Sea level*, the result of this process, was evaluated every 8 hr.

2. The sea-level records

It was desired to obtain an estimate, on a synoptic basis, of sea level fluctuations at many stations. For this reason, a three month interval of time was chosen, November and December 1952, and January 1953, for which the data from tide gauges at many places, mostly in the Pacific, were analyzed. The locations are listed in table 1.

Figure 2 shows the location of the tide gauges.

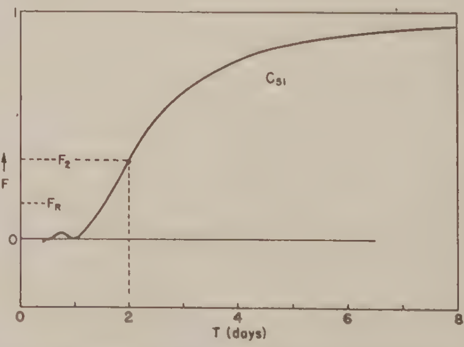

FIG. 1. Response factor of weighted average C_{51} as function of period. F_R indicates response factor for random errors in hourly values. F_2 indicates response for 2-day oscillation.

---

[1] Contribution from the Scripps Institution of Oceanography, New Series, No. 948. This paper represents in part results of research carried out by the University of California under contract with the Office of Naval Research. Reproduction in whole or in part is permitted for any purpose of the United States Government.

[2] Assistant Research Oceanographer, Scripps Institution of Oceanography, La Jolla, Calif.

TABLE 1. Tide gauge stations

Group 1	Group 2	Group 3	Group 4	Group 5	Group 6	Group 7
San Diego	Crescent City	Ketchikan	Seward	Hilo	Wake	La Habana
La Jolla	Astoria	Sitka	Kodiak	Honolulu	Eniwetok	Key West
Los Angeles	Port Townsend	Skagway	Dutch Harbor	Midway	Kwajalein	Cat Bay
Santa Monica	Seattle	Yakutat	Adak	Johnston	Canton Island	Charleston
Port Hueneme			Attu		Pago Pago	Bermuda
Avila						Atlantic City
San Francisco						

Figures 3a–3g show the sea level plots versus time for the above stations, grouped in the manner listed above. An attempt was made to have this grouping conform to geographical or environmental regions.

Several conclusions can be drawn by examination of the sea level curves of fig. 3a–3g:

1. The RMS (root mean square) departure from mean sea level varies widely from place to place. A good round figure to take for the average value might be 15 cm if the monthly drift is not considered. High latitude stations seem to be more active than low latitude stations.
2. The character of the records makes them appear similar to equivalent meteorological records *e.g.*, records of temperature, pressure, and humidity.
3. In many of the records, there appears to be a peak of spectral energy near periods of three or four days, with a possible trough near periods of a month. In addition, the plots vary during the three month interval shown. This month to month variation of mean sea level is associated with the seasonal variation [10].
4. There is coherence between adjacent stations which persists up to separation distances of several hundred kilometers.

A cursory comparison of the sea level records with daily sea level weather charts [11] showed a remarkable correlation between sea level and atmospheric pressure. A more detailed record of atmospheric pressure was obtained from the National Weather

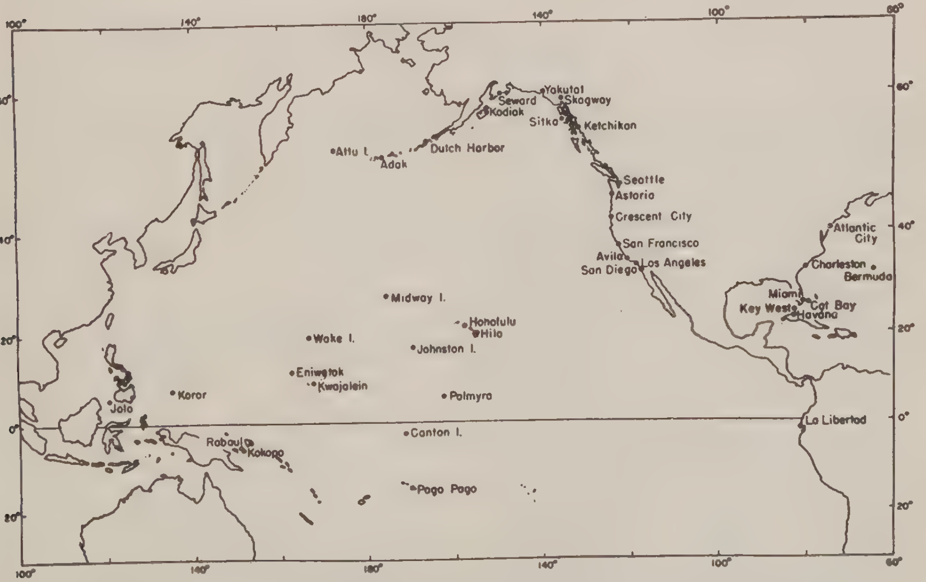
100°
140°
180°
140°
100°
60°
60°
40°
20°
0°
20°
Yakutat
Seward
Skagway
Kodiak
Sitka
Ketchikan
Attu I.
Adak
Dutch Harbor
Seattle
Astoria
Crescent City
San Francisco
Avila
San Diego
Los Angeles
Atlantic City
Charleston
Bermuda
Miami
Key West
Cat Bay
Havana
Midway I.
Honolulu
Hilo
Wake I.
Johnston I.
Eniwetok
Kwajalein
Koror
Jolo
Palmyra
Canton I.
Rabaul
Kokopo
Pago Pago
La Libertad

FIG. 2. Location of the tide gauges. *Solid dots:* Stations used in present study. (Two stations, Santa Monica and Port Hueneme, do not appear on map; they lie between Los Angeles and Avila.)

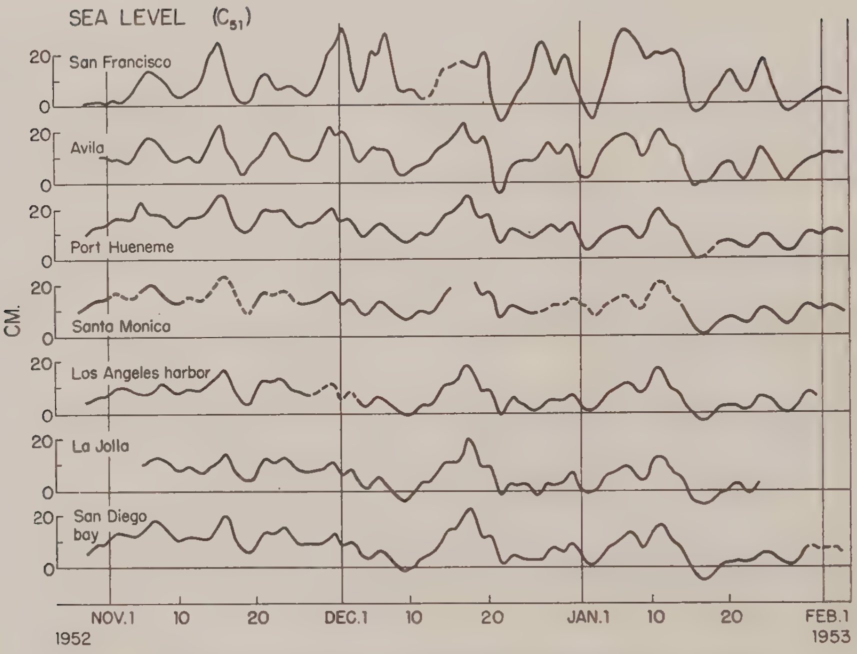

FIG. 3a. Simultaneous plots of sea level. *Dashed curve portions:* Values based on uncertain data. *Time scale:* Dates correspond to 0000, 120W meridian time.

Records Center, consisting of hourly values of corrected sea level pressure at nearby stations. These values were subjected to the same filtering scheme (C_{51}) as was used in the analysis of the hourly tidal heights in order to eliminate the diurnal pressure variation, and to permit immediate comparison with the sea level records (fig. 4). The response of the ocean to the variable atmospheric pressure seems to be direct and instantaneous for the spectral portion that will be considered here. An increase of air pressure by 1 mb produces a depression of the sea surface by 1 cm; *i.e.*, the sea acts as an "inverted barometer." This observation agrees with an idealized theory of a two layer model with linear friction [1].

3. The adjusted sea-level records

The plots of sea level have been adjusted for this pressure effect using the filtered (C_{51}) pressure data by taking

$$\text{(adjusted sea level)} = \text{(sea level)} + p_a/\rho g, \quad (1)$$

where p_a is atmospheric pressure, ρ is water density and g is the acceleration of gravity. The quantity

TABLE 2. Tide gauge and barometer locations

Group 1	Group 2	Group 3	Group 4	Group 5	Group 6	Group 7
San Diego	Crescent City	Kitchikan, Sitka	Kodiak	Hilo	Wake	Key West
La Jolla, San Diego	Port Townsend, Whidbey Island	Sitka	Dutch Harbor	Honolulu	Eniwetok	Bermuda
Los Angeles	Seattle	Skagway, Sitka	Adak	Midway	Kwajalein	Charleston
Santa Monica, Los Angeles		Skagway, Yakutat	Attu (daily pressure values taken from synoptic weather maps)	Johnston		Atlantic City
Avila, Santa Maria		Yakutat				
San Francisco						

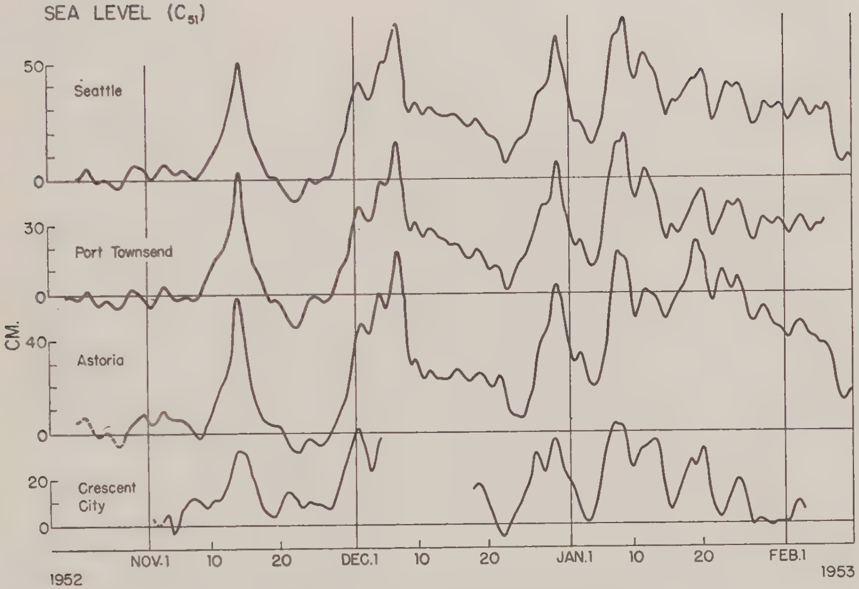

Fig. 3b. Simultaneous plots of sea level. *Dashed curve portions:* Values based on uncertain data. *Time scale:* Dates correspond to 0000, 120W meridian time.

$1/\rho g$ has been given the value 9.948×10^{-4} cm^2 sec^2 gm^{-1} in making the computations.

Weather stations are not always located near tide gauges; therefore it was impossible to apply the pressure correction to some of the sea level records. The combinations of tide gauge and barometer locations that were used are shown in table 2. If one location is given, both tide gauge and weather station are at that location. If two locations are given, the first refers to the tide gauge and the second to the weather station.

The plots of adjusted sea level versus time are shown in fig. 5a–5g. The locations of the tide gauges (TG) and the atmospheric pressure observations (AP) are indicated on each graph.

Several conclusions can be drawn by examination of the adjusted sea level curves:

1. The RMS departure from mean adjusted sea level varies widely from place to place, with a characteristic average value of perhaps half that of the uncorrected sea level plots, if monthly variation is not considered. Thus the direct effect of the atmospheric pressure variation accounts for about half the observed amplitude (on the average) of the sea level variation in the spectral range considered here.

2. The character of the records is about the same as that of the adjusted records, except that a fortnightly variation can be discerned at several stations (see Southern California stations and Adak). This variation is probably tidal, consisting mainly of the combined effect of the two constituents *Mf* and *MSf* (see section 3v.). Unfortunately, to the author's knowledge, the constants of these constituents have not been computed for any of the tide stations examined in this study.

3. The coherence between adjacent stations is obviously worsened when compared to that of the adjusted records, although coherence is still observed over separation distances of the order of hundreds of kilometers. This suggests that the observed coherence of (unadjusted) sea level is largely the coherence of atmospheric pressure, the "coherence length" being roughly the diameter of storms.

In comparing sea level to other variables, it is convenient to use the adjusted sea level records. The

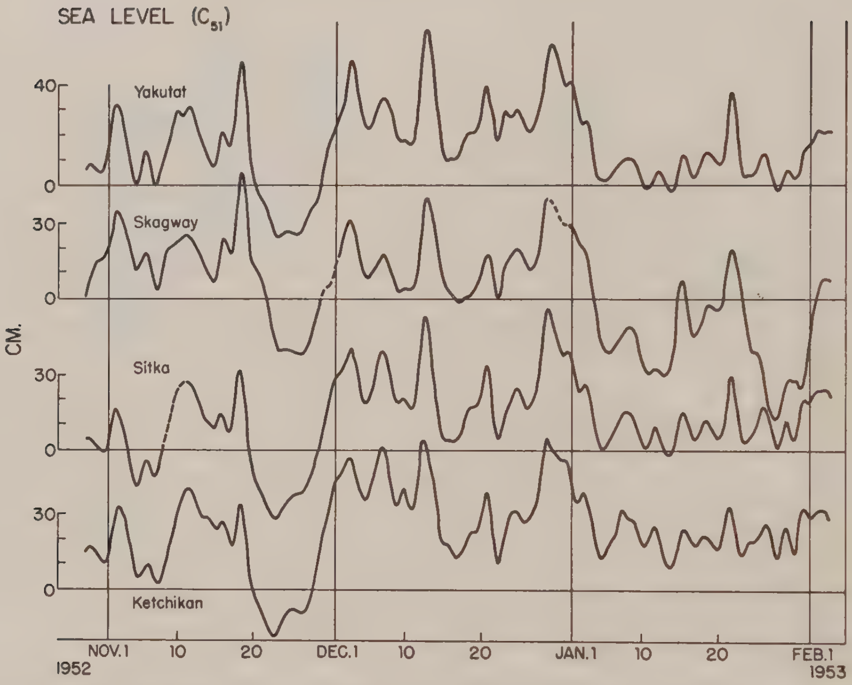

Fig. 3c. Simultaneous plots of sea level. *Dashed curve portions:* Values based on uncertain data. *Time scale:* Dates correspond to 0000, 120W meridian time.

principal agencies affecting the variations of adjusted sea level are discussed in the following sections:

i. *Transient pressure effects.* Consider first a sudden disturbance at time $t = 0$. Initially there will be a wave propagated away from the disturbance followed by an inertial oscillation, The initial wave will not have much spectral energy in periods longer than the time necessary for a gravity wave to travel across the horizontal extent of the pressure disturbance. The inertial oscillation will radiate very slowly and will probably persist until damped out by internal friction. In any case, these transients will probably have very little spectral energy for periods longer than two days.

ii. *Average pressure over entire ocean.* In order to make the adjustment for the direct effect of atmospheric pressure, the average pressure over the entire ocean is subtracted from the local pressure. Obviously, if the change of local pressure merely reflects a change in the average pressure over the ocean, no change in sea level would be expected except for a very small second order effect due to the compression of the sea water. However, nothing is known of the variation of average pressure over the entire ocean for periods as short as the ones considered here. Consequently, it is assumed that this average pressure remains constant. This assumption seems logical, although the direct atmospheric pressure effect is known to be large in the annual variation in sea level [10].

iii. *Surface tangential stress of the local wind.* It is difficult to define what is meant by the local wind effect. The wind itself is one of the primary agencies that causes ocean currents and redistribution of density within the ocean. This also takes place to some extent on a small local scale. As an example, consider an onshore wind that will raise the water level. If the vertical profile of density was computed from measurements taken in water of sufficient depth near the tide gauge, it might be found that a given mass of less dense surface water had been blown into the region by the wind, replacing an equal mass of more dense water. The resulting change in sea level

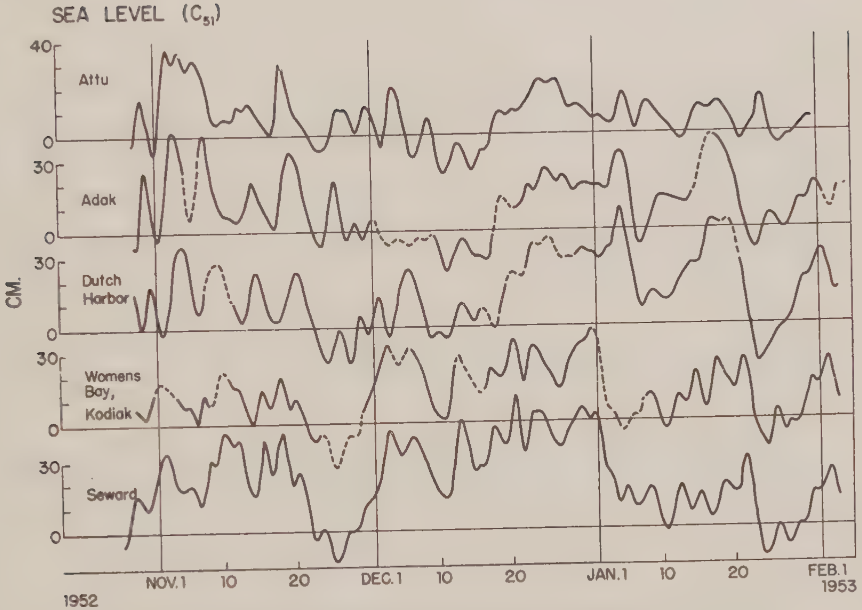

FIG. 3d. Simultaneous plots of sea level. *Dashed curve portions:* Values based on uncertain data. *Time scale:* Dates correspond to 0000, 165W meridian time.

near the shore, which occurs without change in mass, is conveniently referred to as a change in *steric level* (a term defined by Pattullo *et al* [10], essentially the same as the dynamic height). This change is known to occur [4]. The sea level measured at the tide gauge, therefore, is a combination of steric level change and the "strictly direct" effect of the local wind such that the mass of water in each

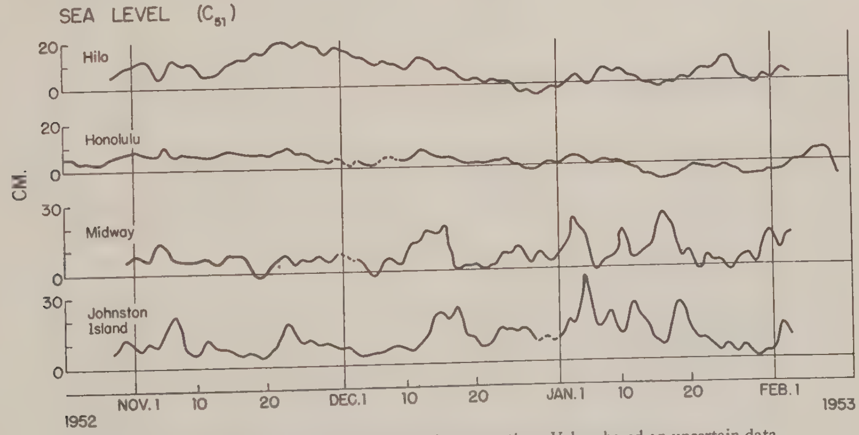

FIG. 3e. Simultaneous plots of sea level. *Dashed curve portions:* Values based on uncertain data. *Time scale:* Dates correspond to 0000, 150W meridian time.

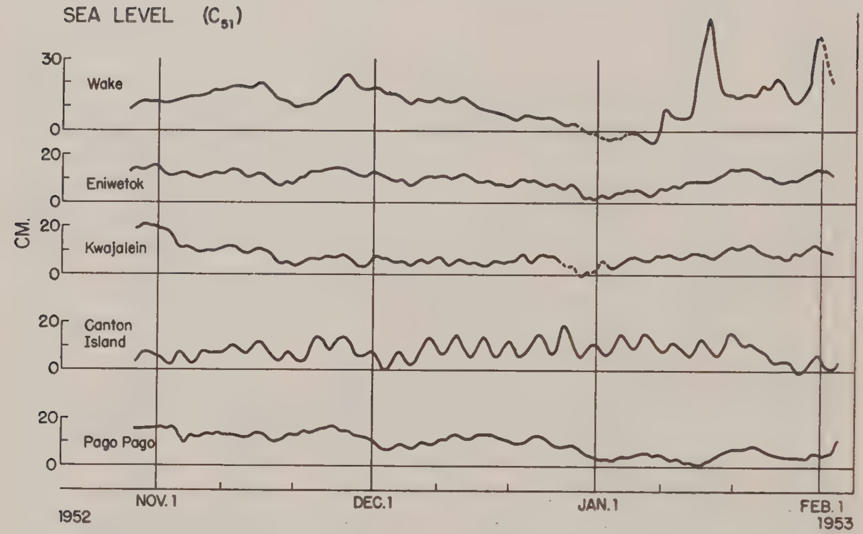

FIG. 3f. Simultaneous plots of sea level. *Dashed curve portions:* Values based on uncertain data. *Time scale:* Dates correspond to 0000, 180W meridian time.

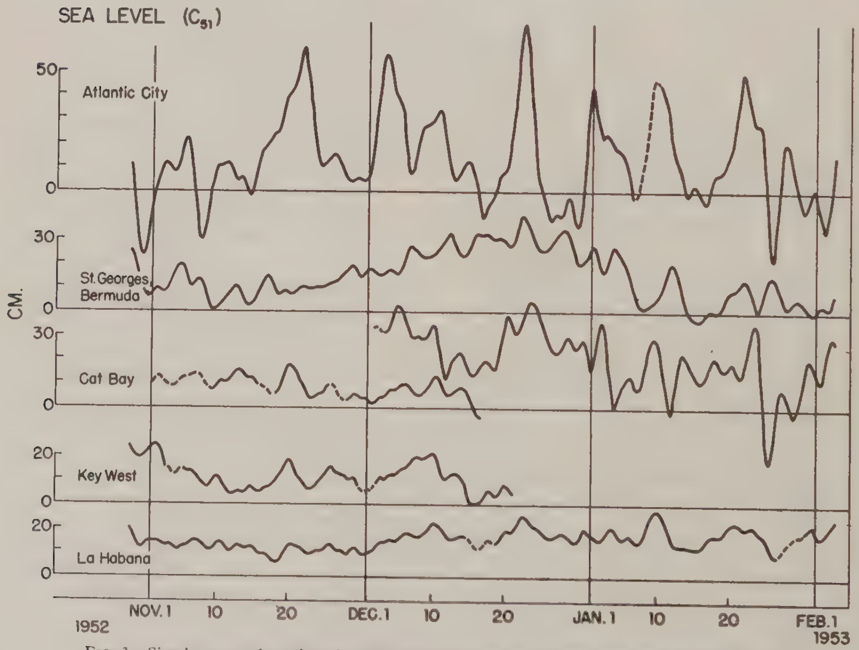

FIG. 3g. Simultaneous plots of sea level. *Dashed curve portions:* Values based on uncertain data. *Time scale:* Dates correspond to 0000, 75W meridian time.

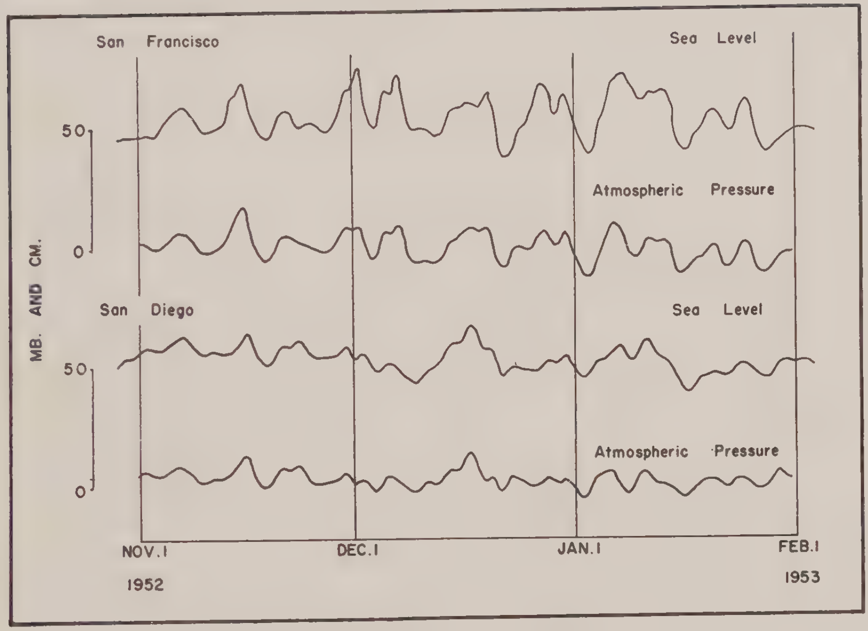

Fig. 4. Comparison of sea level and inverted atmospheric pressure at San Francisco and at San Diego.

vertical column near shore is actually increased. This combined effect will be called the *local wind effect.*

The effect of the local wind is most pronounced as follows: (1) where (or when) there are strong winds, (2) on the edge of continents, and (3) at stations where there is an extensive shoal region adjacent to the tide gauge. Condition (1) is obvious. Condition (2) follows from the fact that divergence of the horizontal wind-stress field is one of the most effective agencies in bringing about surface slopes. A coast line will act as a line of divergence if the wind is blowing across it. Condition (3) follows from the fact that the total horizontal force on a vertical column of water is independent of the water depth in the case of surface wind stress, although it is proportional to the depth in the case of the pressure gradient associated with a given surface slope. Thus, a greater wind stress is needed to balance a given slope in deeper water than in shallower water.

It is well known that winds blowing onshore, or alongshore with the land lying to the right of the wind vector, tend to raise the sea level at the shoreline (in the northern hemisphere). This fact is observed by comparing the adjusted sea level records of fig. 5a–5g with weather charts. The following facts seem to be borne out:

1. The small scale local topography seems to be unimportant. This is based on the similarity of the records from nearby stations in different topographical environments, such as La Jolla (open coast) and San Diego (within a very sheltered bay). Large scale topographical features are important. The coherence appears to be limited by the coherence of the wind pattern at least as much as by the coherence of the topography.
2. On the edge of continents the adjusted sea level at any instant appears not to be in equilibrium with the wind, but rather appears to reflect the time-integrated effect of the wind. That is, the adjusted sea level extremes tend to coincide in time with the wind reversals, and not to the wind extremes. There are two possible explanations for this: (a) The longshore component of the wind stress may be more important in changing the sea level than is the onshore component for these periods. According to an idealized theory [1] a sinusoidal onshore-offshore maximum wind, would give rise to a sea level maximum simultaneously with the onshore

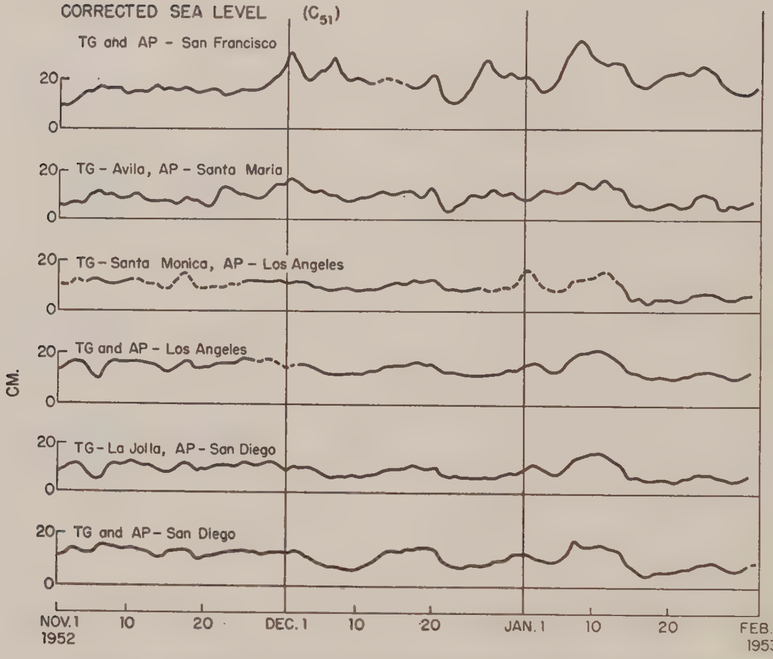

Fig. 5a. Simultaneous plots of adjusted sea level. *Dashed curve portions:* Values based on uncertain data. *Time scale:* Dates correspond to 0000, 120W meridian time.

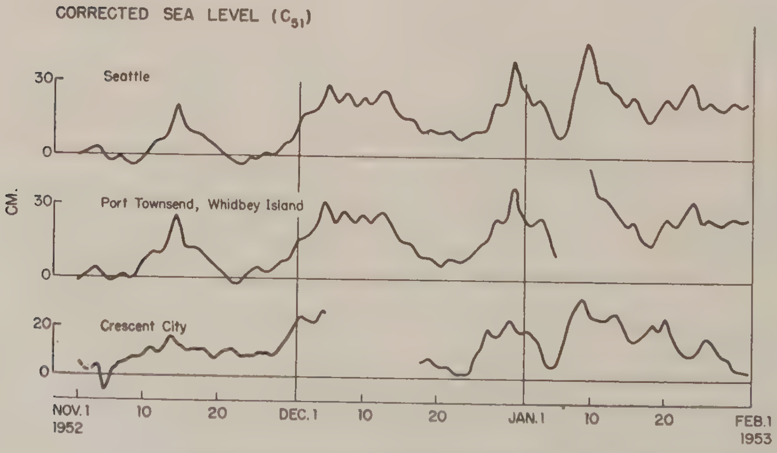

Fig. 5b. Simultaneous plots of adjusted sea level. *Dashed curve portions:* Values based on uncertain data. *Time scale:* Dates correspond to 0000, 120W meridian time.

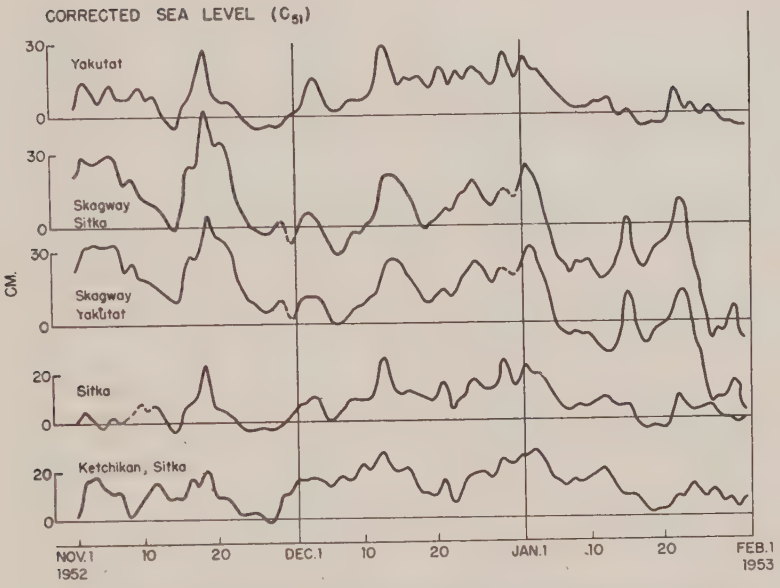

FIG. 5c. Simultaneous plots of adjusted sea level. *Dashed curve portions:* Values based on uncertain data. *Time scale:* Dates correspond to 0000, 120W meridian time.

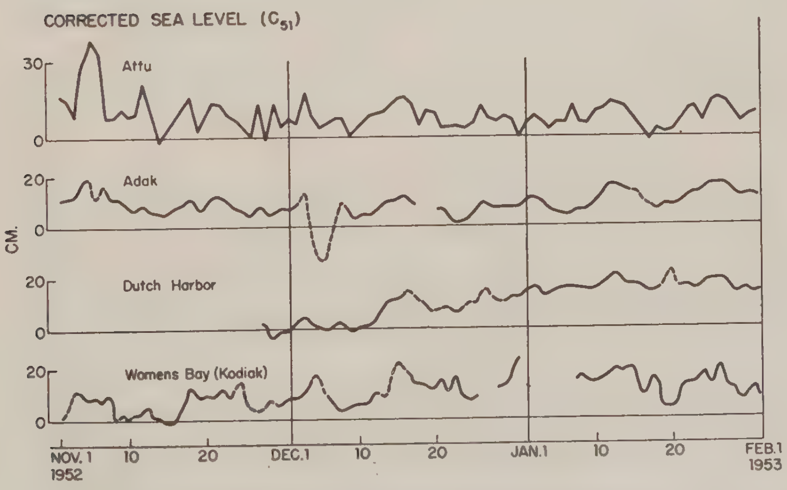

FIG. 5d. Simultaneous plots of adjusted sea level. *Dashed curve portions:* Values based on uncertain data. *Time scale:* Dates correspond to 0000, 165W meridian time.

maximum wind, whereas a sinusoidal longshore wind would be out of phase by $\pi/2$ with the sea level. (b) The sea level variation may be reflecting a redistribution of the density being brought about by the wind. This would take time, and the wind probably would not persist long enough for equilibrium to be reached. Mechanism (*a*) seems to be confirmed both by theory and by comparison of adjusted sea level records to weather maps.

3. The wind bears no immediately obvious relation to sea level at islands. There may be a simple relation between sea level and the field of divergence or curl of the wind stress, but these latter cannot be deduced from wind records from a single station.

iv. *Changes of the density of the water.* The variation of steric level (density changes) is known to be important in the annual variation of sea level [10]. It is very rare that vertical density profiles are measured often enough at one place to enable studying periods as short as the ones here considered. Figures 6a and 6b show the only two cases known to the

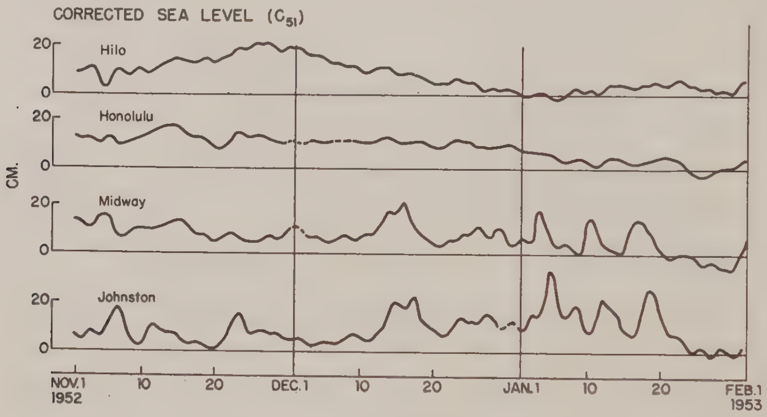

FIG. 5e. Simultaneous plots of adjusted sea level. *Dashed curve portions:* Values based on uncertain data. *Time scale:* Dates correspond to 0000, 150W meridian time.

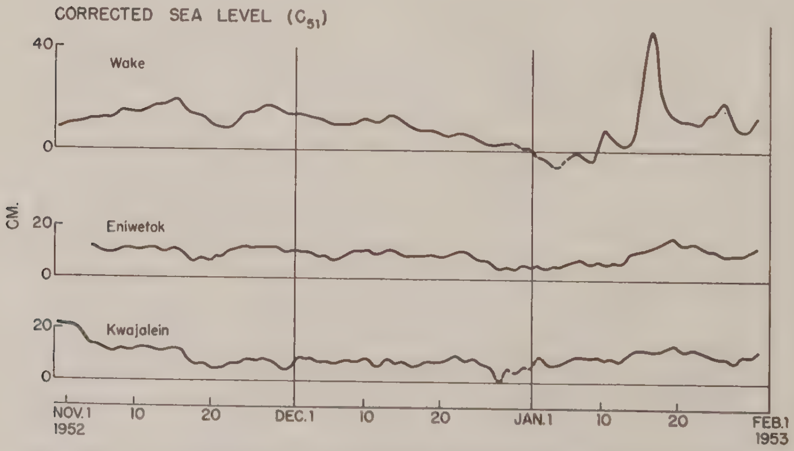

FIG. 5f. Simultaneous plots of adjusted sea level. *Dashed curve portions:* Values based on uncertain data. *Time scale:* Dates correspond to 0000, 180W meridian time.

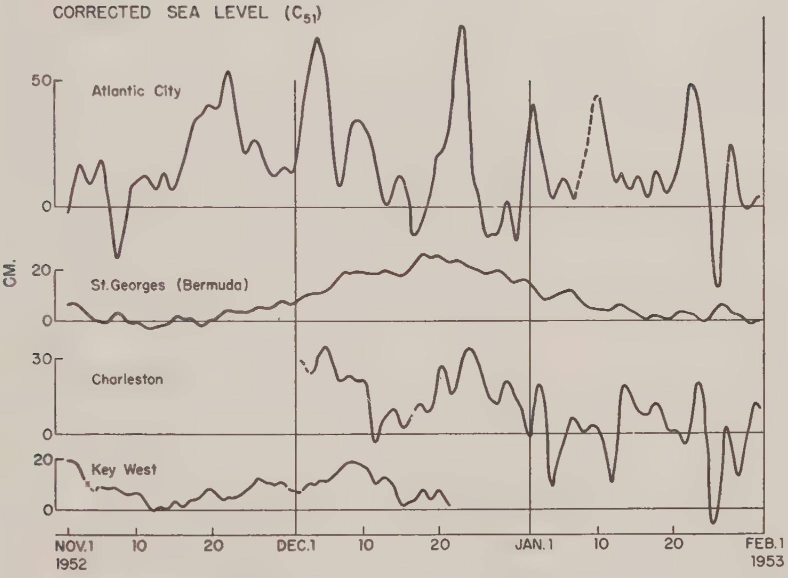

FIG. 5g. Simultaneous plots of adjusted sea level. *Dashed curve portions:* Values based on uncertain data. *Time scale:* Dates correspond to 0000, 75W meridian time.

author for which it was possible to make a satisfactory comparison of steric level to sea level. This meager evidence tends to indicate that changes of steric level are not the major cause of changes of sea level for the periods here considered, but that they are not negligible. Outflow of fresh water from rivers is a possible source of a variable steric level. Waldichuk[3] has evidence showing this to be an important factor in Puget Sound, at least for the month to month variation.

v. *Long period tides.* The tidal constituents *Mf* and *MSf* are the only ones of any importance in the day to day variation of sea level. Each has a period of about a fortnight. The constituent *Mf* is purely astronomical, arising from the variable declination of the moon. The constituent *MSf* results for the most part from nonlinear interaction between the M_2 and S_2 tides, although there is a weak astronomic tidal constituent having the same period. Typical amplitudes of 1 to 3 cm for both these constituents have been found wherever their constants have been evaluated.

A fortnightly variation can be discerned in many of the corrected sea level records. There is reason to believe that the fortnightly tide should be coherent over quite large distances, and this seems to be borne out. In fact, the fortnightly tide seems to be the most coherent part of the records.

The equilibrium *Mf* tide had its maxima (below 35N) on 12 and 25 November; 9 and 22 December; 5 and 19 January; and 1 February of the 1952–1953 period of sea level observations. It seems from fig. 5a–5g that these dates tend to correlate with low sea level.

vi. *Dynamic association with variable ocean currents.* If there are sea level changes associated with ocean currents, the most likely link between the two would be geostrophically balanced surface slopes. Since changes in steric level have been discussed under a different category, we are left only with slope currents (extending to the bottom and undetectable by measuring the density field of the water). The use of tide-gauge data in this manner may provide a useful way of getting at these slope currents. To balance the variable surface slope by other than geostrophic means would require extreme conditions to account for measurable sea level changes having the periods considered here. Consider an example where the surface slope balances the field acceleration of water in two dimensional flow (u and w velocity components

---

[3] Personal communication.

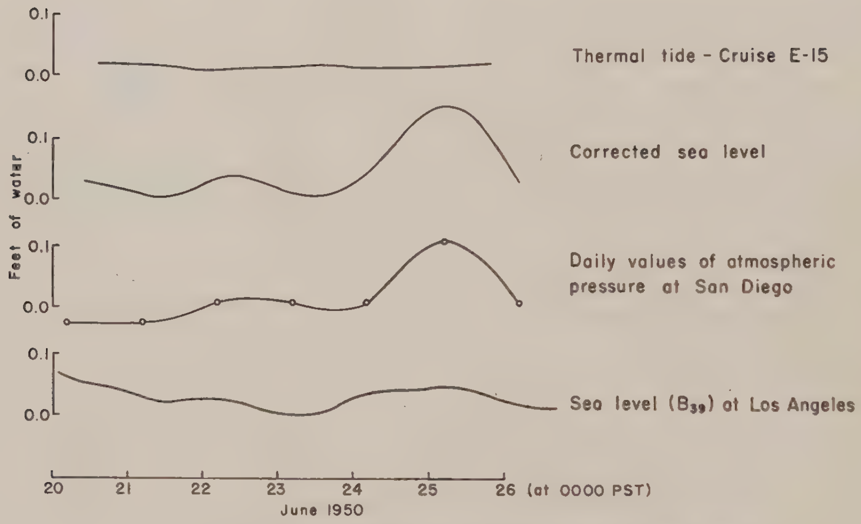

FIG. 6a. Comparison of sea level, atmospheric pressure, and steric level (thermal tide).

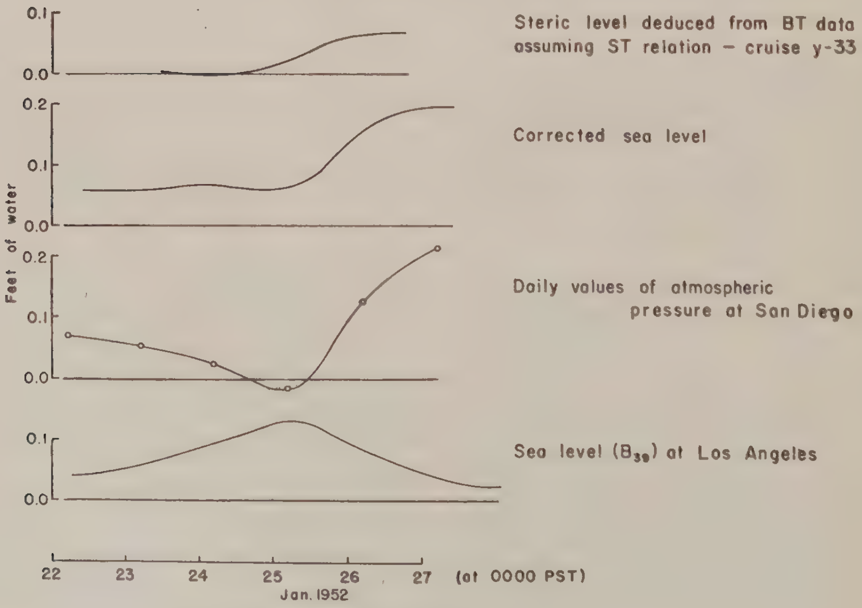

FIG. 6b. Comparison of sea level, atmospheric pressure, and steric level.

only). The surface elevation at the shore, relative to a position in the ocean where the RMS value of u is 1.5 kt, would only be about 6 cm.

vii. *Effect of swell.* The possible effect of surf or swell on sea level was suggested to the author by Col. Peter Ottosen. Munk [7] discusses this effect making use of solitary wave theory. The indication of Munk's theory is that this effect would be quite small under usual conditions. This effect, which has been called *surfbeat* [8], is known to produce variations of sea level having a period of about two minutes (equal to the period of the envelope of a swell) and an amplitude of several inches. It seems possible for this effect to give rise to periods of the order of days under certain special conditions, such as surf crashing over a sand bar into a semienclosed estuary. Certainly the swell envelope will commonly have spectral components of the order of days. In many localities surf is correlated with local wind, and it might be difficult to isolate this effect for study.

viii. *Some specific regions.* It is not intended to give a detailed description of the sea level records in this research at all the stations for which records were obtained; however, a few cases of interest will be discussed.

The extremely large variation at Atlantic City is the result of the local wind effect. This effect is enhanced by the large area of shallow water immediately offshore. Marmer [5] gives a brief discussion using daily averaged tide levels. More recently, Miller [6] has developed an empirical method for predicting the sea level at Atlantic City from the known wind.

Wake Island is in the midst of an extensive shoal region, and is therefore subject to a large local wind effect. The abnormally high sea level, which occurred there 17 and 18 January 1953 (fig. 3f and 5f), resulted from an extreme storm which inundated the island. Most of the other Pacific islands studied rise abruptly from great depths making the wind effect quite small.

There is a strong coherence between many of the Pacific islands for the long period components. This may be mostly the result of the fortnightly tide. This coherence of the fortnightly tide is more easily seen at "quiet" stations, and hence shows up well at these islands.

The records from Midway and Johnston show a remarkable correlation. In fact, there is a better correlation between these islands than between any other pair of islands studied, even though there are many pairs much closer together. The features on the Midway record seem to appear a day or two later on the Johnston record. So far, no explanation has been found for this correlation.

The remarkable periodicity, evident in the sea level record from Canton Island (fig. 3a–3g), is associated with equatorial waves in the easterly winds [9]. This curious oscillation is discussed more fully elsewhere [3].

Acknowledgments—The author wishes to thank Professor Walter Munk for his advice and encouragement in this study.

The numerical computations were carried out on International Business Machines automatic computers by the U. S. Navy Electronics Laboratory at San Diego. The author expresses his thanks to this facility, especially to Mrs. Dorothy Shumway of the IBM section.

The tide and weather data were furnished by the U. S. Coast and Geodetic Survey and by the National Weather Records Center, respectively. Acknowledgment is due both organizations for their cooperation. Under the direction of Mr. Leslie Smith, many computations were performed at the National Weather Records Center to process the atmospheric pressure data.

REFERENCES

1. Groves, G. W., 1954: Dynamic model of two-layer ocean under influence of atmosphere and coastal boundary. *Univ. of Calif., Scripps Institution of Oceanography*, Ref. no. 54–22. (Unpublished manuscript.)
2. ——, 1955: Numerical filters for discrimination against tidal periodicities. *Trans. Amer. geophys. Union*, **36**, no. 6, 1073–1084.
3. ——, 1956: Periodic variation of sea level induced by equatorial waves in the Easterlies. *J. deep sea Res.*, **3**, no. 4, 248–252.
4. Longard, J. R. and R. E. Banks, 1952: Wind-induced vertical movement of the water on an open coast. *Trans. Amer. geophys. Union*, **33**, no. 3, 377–380.
5. Marmer, H. A., 1951: Tidal datum planes. *U. S. Coast and Geodetic Survey*, Special publication no. 135.
6. Miller, A. R., 1957: The effect of steady winds on sea level at Atlantic City. *Meteor. Monogr.*, **2**, no. 10, 24–31.
7. Munk, W. H., 1949: The solitary wave theory and its application to surf problems. *Ann. N. Y. Acad. Sci.*, **51**, art. 3, 376–424.
8. ———: Surf beats. *Trans. Amer. geophys. Union*, **30**, no. 6, 849–854.
9. Palmer, Clarence E., 1952: Tropical meteorology. *Quart. J. roy. Meteor. Soc.*, **78**, no. 336, 126–164.
10. Pattullo, June, W. H. Munk, R. Revelle, and E. Strong, 1955: The seasonal oscillation in sea level. *J. mar. Res.*, **14**, no. 1, 88–155.
11. U. S. Weather Bureau, Daily Series, *Synoptic weather maps*, Part I, Northern Hemisphere Sea Level.

Reproduced by Permission

Reprinted from LIMNOLOGY AND OCEANOGRAPHY
Vol. II, No. 4, October, 1957
Printed in U.S.A.

The Euphausiid Crustaceans *Thysanopoda aequalis* Hansen and *Thysanopoda subaequalis* Boden, Their Taxonomy and Distribution in the Pacific[1]

BRIAN P. BODEN AND EDWARD BRINTON

Scripps Institution of Oceanography, La Jolla, Cal.

ABSTRACT

The original specific criteria given for *Thysanopoda subaequalis* are shown to be unreliable. However, on fresh morphological and distributional evidence it is decided that the species is valid. Its diagnosis is modified and the distribution of the species, in relation with *Thysanopoda aequalis*, is discussed.

Thysanopoda subaequalis[2] was established by Boden (1954) on specimens from the Straits of Mozambique. Its close relationship to *T. aequalis* was noted and it was pointed out that the frontal plate and first antennal peduncle of these species had points in common. The main criterion given at that time for separating *T. subaequalis* from *T. aequalis* was the presence of a spine-shaped process on the copulatory organ of the adult male of the former. *T. aequalis* was described as lacking this process (Hansen 1905).

Boden, Johnson, and Brinton (1955) indicated that the first antennal peduncle and spine-shaped process are unreliable as specific criteria and cannot be used to separate *T. subaequalis* from *T. aequalis*.

A critical examination of the copulatory organs has convinced us that the spine-shaped process is normal in both species. In those specimens where it is apparently lacking, there is a detectable scar indicating the insertion position of this process on the innermost margin of the inner lobe. We interpret this as evidence that the process has broken off. This mark is discernible in Hansen's (1910) figure of the copulatory organ of *T. aequalis*.

On the other hand, the frontal plate (Fig. 1) appears to be a more reliable specific character than was first suspected. This is true in both sexes. In neither species does the frontal plate reach beyond the eyes. In *T. subaequalis* (Fig. 1b, c) it appears fleshy and its anterior margin is thickened; there is no rostral process. The frontal plate of of *T. aequalis* (Fig. 1a) lacks this fleshy appearance and, in lateral view, the anterior margin tends to taper; in some specimens the rudiments of a rostral process can be discerned.

The endopodite of the third thoracic leg of the adult male of *T. subaequalis* is its most striking specific character. The propodal segment is greatly reduced, and the dactylus is modified as a long, naked spine (Fig. 2a, b). This modification was not mentioned when *T. aequalis* was described (Hansen 1905). It was described as a sexually dimorphic character of this species by Zimmer (1914) and Tattersall (1924), who did not realize that they were dealing with a separate species.

T. aequalis and *T. subaequalis* are similar, if not identical, in respect to the morphological characters which have heretofore been considered of primary importance in euphausiid taxonomy (*e.g.* eyes, male copulatory organ, antennal peduncle), indicating a possible subspecific relationship between them. The genetic basis for the diagnostic character described above could conceivably result in intergrades between *T. aequalis* and *T. subaequalis* being indistinguishable as such—an animal might either have the spine or not. However, while there is some overlap in the geographical ranges of the

---

[1] Contribution from the Scripps Institution of Oceanography, New Series, No. 949.

[2] British Museum (Natural History) type specimen registered no. 1951.IV.2.1. Additional specimens have been deposited at the U. S. National Museum and at the Scripps Institution of Oceanography (Division of Marine Biology).

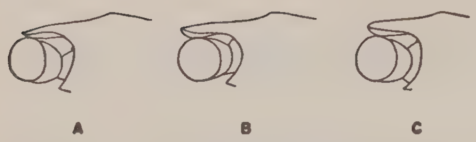

FIG. 1. Frontal plates in lateral aspect: *a*) *T. aequalis*; *b*) and *c*) *T. subaequalis*.

two forms (Fig. 3) we have no evidence regarding their possible reproductive isolation or compatibility, and we consider that they should be retained as distinct species.

The lateral aspect of the frontal plate has proved to be an almost invariably reliable means of separating the two species: only a few of the individuals examined have the third thoracic leg modified and the frontal plate tapered (Fig. 1b).

It has not been possible to distinguish between larval specimens of the two species, but on the basis of the distribution of the adults they may often be assigned with reasonable certainty to either *T. aequalis* or *T. subaequalis*.

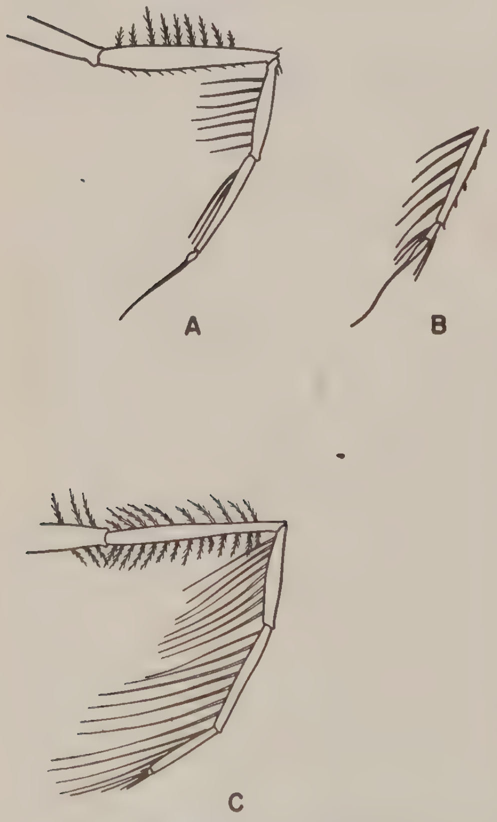

FIG. 2. Endopodite of third thoracic leg: *a*) *T. subequalis* (adult); *b*) *T. subaequalis* (12.5 mm young specimen); *c*) *T. aequalis*.

Immature individuals cannot be separated reliably. In *T. subaequalis* the dactylus of the third thoracic leg of the male is not modified until the onset of maturity, at a length of about 12.5 mm. Instars of this length carry the modified dactylus in addition to a number of normal setae on the reduced propodus (Fig. 2b). Specimens longer than 13 mm, which stage is probably attained with the succeeding ecdysis, bear only the naked terminal spine.

MATERIALS AND METHODS

The collections utilized in this study were made during a series of cruises carried out by the Scripps Institution of Oceanography from 1950 to 1956 as follows: "Mid-Pacific" Expedition (1950), east and southeast of the Hawaiian Islands; "Northern Holiday" Expedition (1951), Gulf of Alaska to 27°N, northeast of the Hawaiian Islands; "Shellback" Expedition (1952), eastern equatorial Pacific; "Capricorn" Expedition (1952–53), Equatorial Pacific, 170°E to 120°W; "Transpacific" Expedition (1953), northern Pacific, including Bering Sea, waters east and northeast of Japan, and the mid-central Pacific; "Troll" operation (1955), western equatorial Pacific; "Norpac" Expedition (1955), east of 150°W, between 49°N and 20°N; "Chinook" Expedition (1956), Aleutian to Hawaiian Islands; "Equapac" Expedition (1956), equatorial Pacific near 160°E, and 160–175°W. Material from a 1951 cruise to the mid-equatorial Pacific was kindly made available by the Pacific Oceanic Fishery Investigations of the U. S. Fish and Wildlife Service.

Net-tows were oblique, usually from depths of 140 or 300 meters. A one-meter plankton net of 0.5–0.6 mm mesh with an Atlas flow meter in the mouth (King and Demond 1953) was used. An opening and closing release mechanism (Leavitt 1935) was used for collections on which the vertical distribution pattern is based. A detailed discussion of collection methods and data

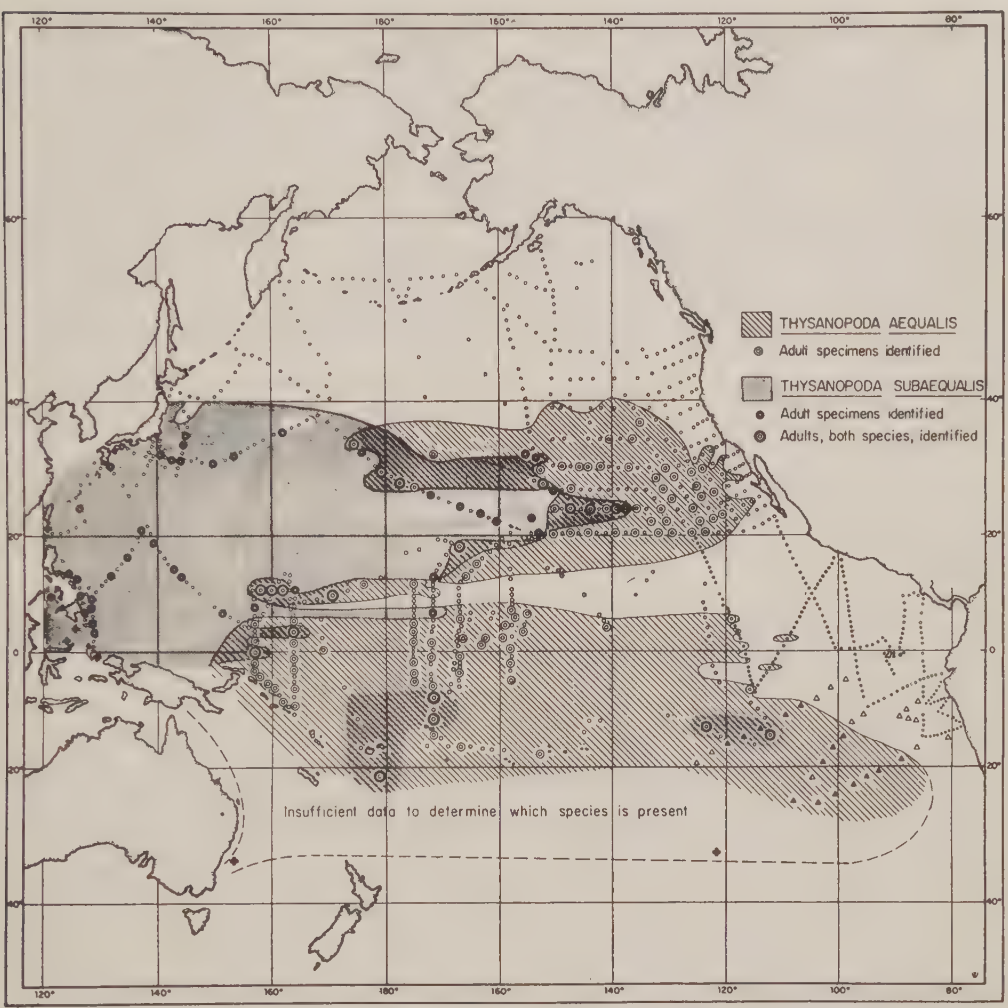
120°
140°
160°
180°
160°
140°
120°
100°
80°
60°
40°
20°
0
20°
40°
THYSANOPODA AEQUALIS
Adult specimens identified
THYSANOPODA SUBAEQUALIS
Adult specimens identified
Adults, both species, identified
Insufficient data to determine which species is present

FIG. 3. Horizontal distribution of *T. aequalis* and *T. subaequalis* in the Pacific based mainly upon Scripps Institution collections (see text). Small circles outside shaded or cross-hatched areas are stations at which no specimens of either species were taken. Similar circles within these areas represent stations at which immature or larval forms occurred. Triangles are "Albatross" stations (Hansen 1912). Solid triangles are positive *T. aequalis* records, while open triangles are negative. Crosses are records for *T. aequalis* from Hansen (1910, 1915, 1916) and Sheard (1953).

analysis will appear in a forthcoming paper on the distribution of Pacific euphausiids (Brinton, in preparation).

HORIZONTAL DISTRIBUTION

The composite range of *T. aequalis* and *T. subaequalis* (Fig. 3) extends from 40°N to at least 33°S in the eastern South Pacific (Hansen 1915) and to 34°S in the western South Pacific (Sheard 1955). Both species are missing from the eastern equatorial basin and from a tonguelike westward extension of equatorial waters reaching to at least 175°W, with an east-west axis at 9°–10°N. These species were lacking at a single station (8°N) on a north-south line of stations, at 164°E, occupied during "Equapac" Cruise, 1956. On the basis of this negative record, the area from which these species are apparently excluded is tentatively extended to

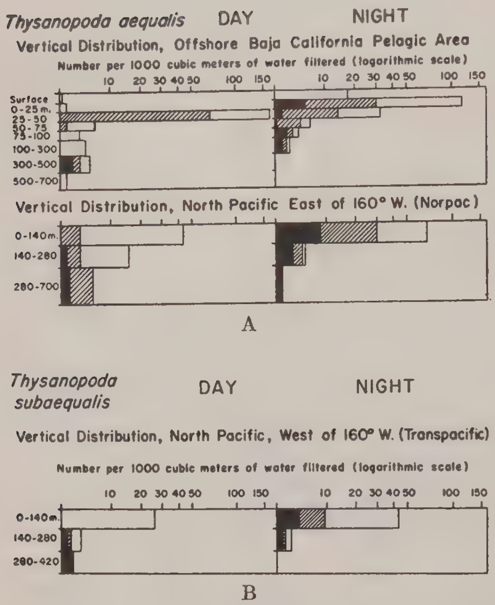

FIG. 4. *a*) Vertical distribution of *T. aequalis* in the Baja California Pelagic Area (a local area) in April, 1953, and in the larger "Norpac" area (see text) in 1955. *b*) Vertical distribution of *T. subaequalis* based on collections of the "Transpacific" Expedition (see text). In both *a*) and *b*) adults are indicated by the solid black bars, immature specimens by the cross-hatched bars, and furcilia larvae by the open bars. The number of specimens at each depth is the average collected at stations within the ranges of the two species on the above expeditions.

164°E (Fig. 3). The distribution of *T. subaequalis* is based upon identification of 300 adults in 58 collections; that of *T. aequalis* is based upon identification of 550 adults in 110 collections.

The 11° isotherm at 200 meters (Chart IV, Sverdrup, Johnson, and Fleming 1946) which follows the pattern of current flow in the central waters of the North Pacific, closely parallels the margin of the combined distribution of these species, and is associated with the tonguelike area of exclusion in the western equatorial Pacific. The temperature at 200 meters in the eastern equatorial basin south of 8°–10°N, including the Peru Current, is thus high enough to be within the postulated tolerance of *T. aequalis*. This species does, in fact, penetrate eastward to 110°W in the latitude of the equatorial countercurrent. However, the predominant direction of the currents is from east to west in the western equatorial region. The North Equatorial Current arises, in part, in the oxygen-poor waters off Mexico and Central America, while the South Equatorial Current derives some water from the colder part of the southern hemisphere via the Peru Current. The regions of origin of both of these currents appear to be unsuitable for these species, and to be outside their apparent geographic range.

T. aequalis is present in the cooler parts of the composite range in the North Pacific where the temperature of 200 meters approximates 11° to 16°C; *T. subaequalis* is predominant in a warmer western zone where the temperature at that depth is higher than 16°. *T. aequalis* occurs throughout the composite range of the two species in the South Pacific, whereas *T. subaequalis* appears to be limited to the warmer portion, approximately confined by the 21° isotherm at 200 meters.

VERTICAL DISTRIBUTION

The vertical ranges of these two species in the North Pacific appear to be the same (Figs. 4a and b). Furcilia larvae, which show no tendency to perform diurnal vertical migrations, occur above 280 meters. Adults are present below 140 meters during the day and move into the 0-280 meter layer at night. Most immature individuals are present above 140 meters at night.

REFERENCES

BODEN, B. P. 1954. The euphausiid crustaceans of southern African waters. Trans. Royal Soc. S. A., **34**(1): 181–243.

BODEN, B. P., M. W. JOHNSON, AND E. BRINTON. 1955. The Euphausiacea (Crustacea) of the North Pacific. Bull. Scripps Inst. Oceanogr. U. of Calif., **6**(8): 287–400.

HANSEN, H. J. 1905. Further notes on the Schizopoda. Bull. Mus. Oceanogr. Monaco, **42**: 1–32.

——— 1910. The Schizopoda of the Siboga Expedition. Siboga-Exped., **37**: 1–123.

——— 1912. The Schizopoda. Reports on Sci. Results Exped. to Tropical Pacific. U. S. Fish. Comm. Steamer "Albatross" XVI and XXVII. Mem. Mus. Comp. Zool., Harvard College, **35**: 173–296.

——— 1915. The Crustacea Euphausiacea of the United States Museum. Proc. U. S. Nat. Mus., **48**: 59–114.

——— 1916. The Euphausiacean Crustaceans of the "Albatross" Expedition to the Philippines. Sci. Results Phil. Cruise Fish. Steamer "Albatross" 1907–1910. No. 33, Proc. U. S. Nat. Mus., **49**: 635–654.

KING, J. E., AND J. DEMOND. 1953. Zooplankton abundance in the Central Pacific. Fishery Bull., U. S. Fish and Wildlife Service, **54**(82): 111–144.

LEAVITT, B. B. 1935. A quantitative study of the distribution of the larger zooplankton in deep water. Biol. Bull., **68**: 115–130.

SHEARD, K. 1955. Taxonomy, distribution and development of the Euphausiacea (Crustacea). B.A.N.Z. Antarctic Res. Exped. Series B, **8**(1): 1–72.

SVERDRUP, H. U., M. W. JOHNSON, AND R. H. FLEMING. 1942. The oceans, their physics, chemistry and general biology. New York, Prentice-Hall, Inc. 1,087 pp.

TATTERSALL, W. M. 1924. Euphausiacea. British Antarctic "Terra Nova" Exped. 1910. Nat. Hist. Rep. Zool. V., **13**(1), Crustacea, Pt. VIII, 1–36.

ZIMMER, E., 1914. Die Schizopoden der Deutschen Sudpolar-Expedition. Deutsche Sudpolar Exped. XV., Zool. VII: 379–445.

Chapter III

REMARKS ON THE OCEAN WAVE SPECTRUM

W. H. MUNK, M. J. TUCKER
AND F. E. SNODGRASS

Reprinted from

NAVAL HYDRODYNAMICS,
PUBLICATION 515
NATIONAL ACADEMY OF SCIENCES —
NATIONAL RESEARCH COUNCIL
1957 Reproduced by Permission

III

REMARKS ON THE OCEAN WAVE SPECTRUM *

W. H. Munk
Institute of Geophysics and Scripps Institution of Oceanography, University of California

M. J. Tucker
National Institute of Oceanography, Surrey, England

F. E. Snodgrass
Scripps Institution of Oceanography, University of California

ABSTRACT

A record of water level against time at a fixed point off La Jolla can be interpreted as the result of superposition from waves of all possible frequencies. A typical analysis into component frequencies shows five distinct bands of activity with frequencies higher than those of the tides: ripples around 20 c/s, ordinary gravity waves around 0.1 c/s, a narrow band of swell at 0.065 c/s, "surf beat" around 0.015 c/s (due to non-linear transformation of ordinary waves in shallow water), and surges with frequencies around 0.001 c/s. Quantitative estimates of energy density are given. The measurement of the directional properties of waves is discussed in some detail.

INTRODUCTION

"Remarkable progress would be attained if only naval architects and oceanographers would get together and study ship motion at sea." You may have come across statements like this; they frequently appear in the literature of the last hundred years. Offhand this sounds quite reasonable. But we doubt whether the proposed marriage of the two professions would have resulted in a healthy offspring if it had taken place prior to the last decade. The oceanographer simply could not offer an *adequate description* of the sea surface.

The latest and most successful of matchmakers is J. King Couper of the Bureau of Ships. We think his success is due, at least in part, to the circumstance that we are now more than halfway towards an adequate description of the surface in terms of the energy spectrum. The first step was to resolve the sea surface at a point in terms of elementary wave trains of various frequencies, but regardless of wave direction. This has been done. The next step is to obtain the directional pattern as well. Work on this problem is underway. When it has succeeded, an important goal will have been attained: the two-dimensional spectrum of the sea surface.

Two reviews have recently been published: Pierson (1955) emphasizes how much is known about what waves are like; and Ursell (1956) insists that nothing is known about how they are generated. Our remarks will be confined to a few selected topics: first a few basic (and well known) features of ocean wave spectra; then low frequency waves, because we find them interesting; and finally, the directional spectrum, because it is an urgent topic.

---

* Contributions from the Scripps Institution of Oceanography, New Series, No. 950.

DISCRETE AND CONTINUOUS SPECTRA

Suppose we were to convert the fluctuating water level above a point into a fluctuating voltage, pass this through a filter which responds fully to frequencies between $f - \frac{1}{2}\delta f$ and $f + \frac{1}{2}\delta f$ and not at all to others; then square the filter output and average. Designate the final output by $E(f)\ \delta f$. If the ocean waves consisted of one or several *discrete* frequencies, f_1, f_2, . . ., then we should expect a large output $E(f_1)\ E(f_2)$ . . . when the filter is tuned to these frequencies, and a very low output otherwise. What we find in fact is that $E(f)$ varies more or less smoothly with f, as if energy were distributed continuously among all possible frequencies. No matter how narrow we design the width δf of the filter, the result is the same. This leads us to suspect that the ocean wave spectrum is a continuous and not a discrete spectrum.

In practice we must always deal with records of finite length, T, and the best we can do is to analyze for harmonics of this record length. This means that we can sample only for frequencies separated by T^{-1}. But this discreteness in sampling has nothing whatever to do with whether the true spectrum is discrete or continuous. In the former case we would find that the energy content is insignificant except for just two or three lines in the immediate vicinity of the discrete frequencies present; in the latter case we would find individual energy values to be badly scattered, but if T is sufficiently long so that we can crowd (say) 10 or more values into the frequency range to be analyzed, $T = 10/\delta f$, then the average of these ten values is a meaningful measure of the energy density in this range.

The important thing is that all pertinent measurements of ocean waves with periods shorter than the tides have been in agreement with the expected results from continuous spectra, and none have given evidence for discrete spectral lines.

One observation all of us have made suffices to dispose of the idea that the ocean surface can be represented by a single-frequency, single-directional wave train. Consider sun glitter on the sea surface (Cox and Munk, 1956). The glitter pattern is composed of millions of tiny images of the sun, an image occurring wherever the sea surface has the slope (tilt and azimuth) required to reflect the sun's rays into the observer's eye. The radial grid lines in Fig. 1 give the required azimuth of tilt (to the right and left of the sun), the quasi-elliptical lines the required tilt, drawn for a solar elevation of 30°. Suppose the water pattern were represented by a train from a direction 60° to the right of the sun, with a maximum slope of 20°. The resulting glitter pattern is shown in the diagram on the left of Fig. 1. It lies entirely along the 60°

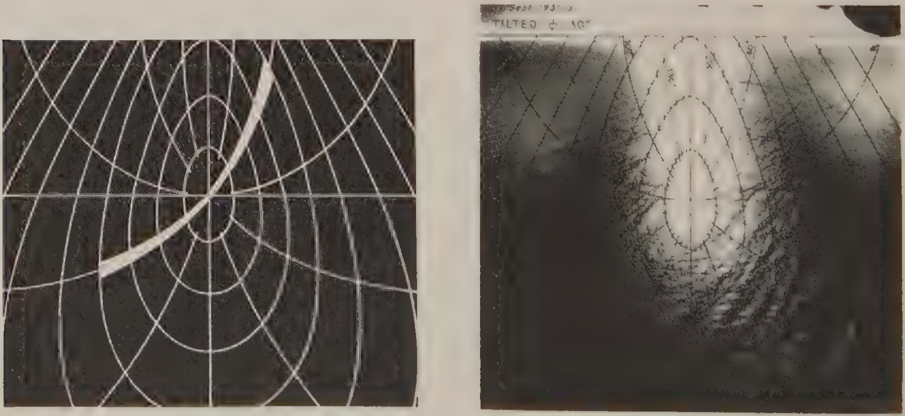

Figure 1. The glitter pattern due to a single sinusoidal wavetrain approaching from a direction 60° to the right of the sun, and a photograph of a real glitter pattern.

azimuth line. The glitter is brightest where the slope reaches the maximum values, these being the most probable slopes of a sinusoidal wave. Actual conditions are just the opposite. A real glitter pattern as shown in the photograph does not follow any particular azimuth line, and it is brightest in the center, where the required tilt is zero. The observed result is consistent with a continuous two-dimensional spectrum.

THE SPECTRUM FROM .2 to 200 C/KS

Most of our work deals with frequencies that are dismissed as D. C. by the radio engineer. For unit frequency we use cycles per 1000 sec., or c/Ks. Fig. 2 shows a typical La Jolla frequency spectrum (non-directional). The ordinate *E* in cm^2 per c/Ks is referred to as the "Energy density." The range between 50 and 200 c/Ks comprises the ordinary sea and swell spectrum, and has been extensively studied. The remaining part of the spectrum is based on recent work which has not been presented previously. The low frequency records were obtained by means of a sensitive pressure transducer, the Vibrotron. Some analyses have been performed with an analogue computer in England, others with a high speed digital computer in the United States.[1] It is encouraging that the results agree.

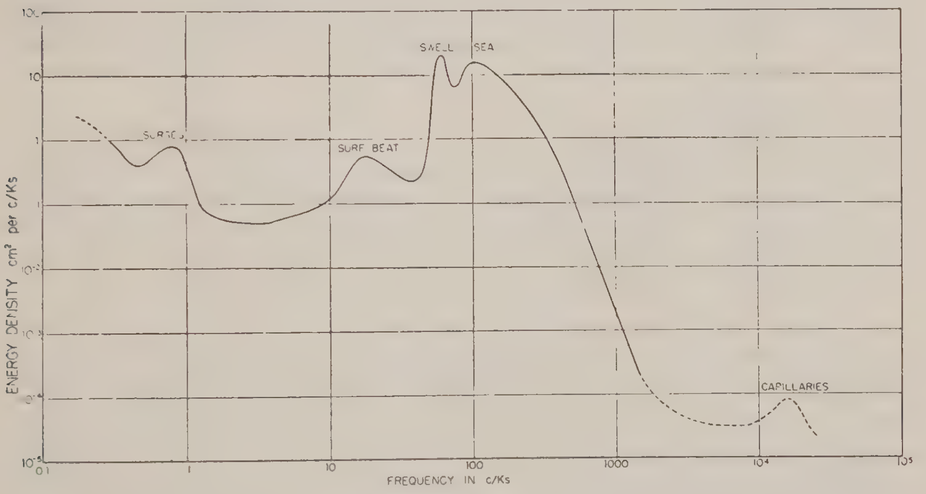

Figure 2. A typical frequency spectrum of the variations in the level of the sea surface above a fixed point at La Jolla, California.

Apparently there are five separate bands of high activity. This is a remarkably complex pattern. For comparison, the spectrum of sound background in the sea decreases monotonically between 10 c/s and 100,000 c/s by roughly 6 db per octave.

Of course, Fig. 2 is a description, not an explanation. But we have reasons to believe that each of the five peaks involves different physical factors, and that the resolution by frequency is a fruitful one. Also, that each of these bands is a factor in Naval Hydrodynamics when interpreted in its broadest sense.

The usefulness of the spectral representation has been limited largely to problems where each frequency could be considered as being independent of, and superimposed on, other frequencies; in other words, linear problems. The topic of ocean waves presents important non-linear problems, such as the breaking of ocean waves. The previous speaker, Dr. Lighthill, has been particularly successful in coming to grips with non-linear problems. But as far as we know, all such work has been confined to monochromatic, one-directional waves. What is the situation for a continuous spectrum? Not even the limits for the linear approximation have been stated explicitly. For the monochromatic case one simply assumes that the height-length and height-depth ratios must be small. Is the equivalent requirement that the rms slope must be small, or would infrequent occurrence of steep slopes change the situation materially. These remarks are in part directed at Professor Stoker, the chairman of this session. Is it safe to apply any of the work on the formation of bores to the actual ocean unless we understand more about the effect of non-linearity for continuous spectra?

---

[1] We are greatly indebted to B. Ferber, D. Shumway and M. Covher of CONVAIR, San Diego, for their part in analyzing many records.

RIPPLES

The tiny peak to the right of Fig. 2 represents enhanced activity for waves a mm or so in length. The result is preliminary, and numerical values of energy density are not yet available. It is based on work by Charles Cox. In this range of the spectrum, capillary forces are more important than gravity. Some of this activity must be related to tiny wavelets on the lee side (forward) of wave crests. An oil slick will wipe out this part of the spectrum.

It has been shown by Eckart (1953) and others that sound waves or electromagnetic waves impinging on the sea surface will be backscattered by ocean waves of about half the wavelength of the incident radiation. The problem of RADAR sea return and acoustic surface reverberation involves this high-frequency spectrum.

The visibility of objects beneath the surface from an observer above the surface also appears to be critically related to this part of the spectrum (Duntley, 1950).

SEA AND SWELL

This part of the spectrum is closely related to meteorologic activity. Sea is generated by local winds, swell by distant winds. In La Jolla we usually have a peak at about 65 c/Ks (period 15^s), presumably due to swell arriving from generating areas 5000 miles to the south. More often than not there is a second peak due to meteorologic activity in the Northern Hemisphere. Numerical values in the figure represent typical conditions. On occasion the energy might be 10 times higher or 10 times lower. The cutoff to the right is drawn as $E \propto f^{-6}$ in accordance with Neumann's proposed formula (Neumann, 1954) for the spectrum of a fully developed sea.

It is a strange, if you wish an unhappy circumstance, that this peak is associated with wave lengths of dimensions commensurate with those of ships. We shall return to this subject later.

SURF BEAT

This band was discovered several years ago by means of wave recorders tuned to low frequency (Munk, 1949; Tucker, 1950). At a depth of 20 to 30 feet the energy of the surf beat band is about 1 per cent of the sea-swell band; at greater depths and large distances offshore this band appears to be considerably reduced. The mechanism of generation is not clear, but some kind of non-linear interaction of the sloping bottom with the incoming groups of waves appears to be involved. Obviously our pressure mines, which are tuned to frequencies lower than the swell, must not be triggered by surf beat.

SURGES

These differ greatly from locality to locality, depending critically on offshore topography. Some of the activity is in the form of trapped modes, with the continental shelf acting as a wave guide (Munk, Snodgrass and Carrier, 1956). Crests and troughs are normal to shore, and the direction of propagation parallel to shore. Amplitudes decrease rapidly seaward, and are insensible at a distance of one wave length from shore. Such wave motion was theoretically described by Stokes more than one hundred years ago, and referred to as "edge waves." (see also Eckart, 1951; Ursell, 1952; Isaacs, Williams and Eckart, 1951.)

Edge wave activity is related to meteorologic activity, but not in the same sense as sea and swell. There is some indication that these waves are generated by traveling disturbances of atmospheric pressure, such as result from internal waves in the atmosphere. If so, they represent a curious coupling of the height and sharpness of the atmospheric inversion layer, on one hand, to the slope and width of the continental shelf on the other hand.

All our measurements so far have been confined to the continental shelf and borderland. One week from today we plan to occupy a station off the coast of Mexico and beyond the borderland to see whether such activity can be found also in the open sea If so, this would open up the possibility of an old dream; could deep sea surges, which travel at speeds of about 400 knots, serve as a storm warning?

SHIPS AND WAVES

The aspect of waves which is probably of greatest interest to the present gathering is their effect on ships. To a first order of accuracy, each degree of freedom of the ship may be regarded as an independent filter which responds in a prescribed way to the various wave components. For example, in its rolling motion a ship behaves rather like a pendulum and responds only to those components of the complex wave pattern which pass the ship with more-or-less the resonant frequency. It is obvious, however, that wave frequency is not the only factor since we all know that the rolling of a ship depends greatly on the direction of approach of the waves, usually being greatest when the waves approach from 2 or 3 points abaft the beam. The frequency at which the waves pass the ship will also depend on the ship's speed and its direction relative to the direction of wave travel.

If we regard the sea as being composed of a large number of simple sinusoidal, unidirectional wavetrains (see below), it is in principle possible to calculate the response of the ship to each of these, and the mean square response will be the sum of the mean square amplitudes of each individual wavetrain multiplied by the appropriate response factor. When generalized to a continuous spectrum, this is equivalent to regarding the ship as a filter with a two-dimensional filter function depending on the ship's geometry and velocity. The spectrum of the ship's motion is the integral of the appropriate product of this function with the two-dimensional spectrum of the waves, and can be calculated, at least in principle. From this, many useful statistical parameters can be calculated by methods developed by Rice (1944) for one-dimensional problems, and by Longuet-Higgins (1957) for two-dimensional problems. For example, r.m.s. amplitude, mean period, greatest expected amplitude during an hour's period of observation, number of times a given amplitude will be exceeded and whether the cook will be seasick can all be predicted. A convenient summary of these relationships is given by Cartwright and Rydill (1956).

A great deal of theoretical work has been done on the response of ships to waves, the effect of a simple sinusoidal wave train traveling in a single direction having received most attention, though more complicated wave patterns have recently been studied by St. Denis and Pierson (1953), by Cartwright and Rydill (1956) and others. (See, for example, several papers in Ships and Waves, 1954.) Considerable progress has been made in checking these theoretical results using models in tanks, but the acid test will be measurements using real ships in a real seaway. For these tests it will be necessary to measure the characteristics of the wave pattern in both frequency and direction of travel, and a knowledge of typical sea conditions based on such measurements is also necessary to enable the naval architect to design ships with the best performance in waves.

What is the present position with regard to the measurement of waves at sea? A shipborne wave recorder is available (Tucker, 1955) which enables the frequency composition and the mean direction of wave travel to be measured (Cartwright, 1956), but as far as the authors are aware no one has yet succeeded in measuring the complete wave characteristics in frequency and direction with anything approaching the necessary detail, and this remains one of the most important problems in wave studies. We shall now discuss the problem in more detail, and then some possible methods of measurement.

THE 2-DIMENSIONAL WAVE SPECTRUM

We have seen that the wave spectrum is continuous in direction. However, for most problems, both the conception and the mathematics become considerably simpler if we start by considering the sea as being made up of a large number of simple wavetrains, so that the elevation $\zeta\ (x,y,t)$ above a point in the mean sea surface with coordinates (x,y) is

$$\zeta(x,y,t) = \sum_n C_n \cos (\omega_n t - k_n x \cos \theta_n - k_n y \sin \theta_n + \epsilon_n) \tag{1}$$

where $k_n = 2\pi/\text{wavelength}$, $\omega_n = 2\pi f_n$ and ϵ_n is a phase angle which is assumed to be random and usually disappears when appropriate averages are taken. At some stage in the problem the expressions can be written in terms of $\frac{1}{2} C_n^2$, which is proportional to the energy per unit area of the sea surface associated with the n^{th} wavetrain. If the energy of all the wavetrains contained in an interval $\delta\theta$, δf is summed, then

$$\sum_{\delta\theta\delta n} \tfrac{1}{2}C_n^2 \simeq E(f,\theta)\delta\theta\delta f, \tag{2}$$

where $E(f,\theta)$ is the energy per unit frequency range and per unit angle. The number of elementary wavetrains can now be considered to be infinite, so $\delta\theta$ and δf to tend to zero, so that

$$\sum_n \tfrac{1}{2}C_n^2 \rightarrow \int E(f,\theta)d\theta df. \tag{3}$$

This process was used, for example, by Rice (1944) to solve one-dimensional problems. $E(f,\theta)$ is called the spectral density function, and is the characteristic of the waves which we desire to measure.

For a given f, $E(f,\theta)$ is periodic in θ with a period of 2π, and may therefore be represented as a Fourier series of harmonic components:

$$E(f,\theta) = a_0(f) + \sum_n [a_n(f) \cos n\theta + b_n(f) \sin n\theta] \tag{4}$$

where n has integral values from 1 to ∞, $a_n(f)$ and $b_n(f)$ define the n^{th} harmonic and are given by

$$a_n(f) = \frac{1}{\pi}\int_0^{2\pi} E(f,\theta) \cos n\theta d\theta \tag{5}$$

$$b_n(f) = \frac{1}{\pi}\int_0^{2\pi} E(f,\theta) \sin n\theta d\theta \tag{6}$$

Most methods for measuring $E(f,\theta)$ do not give a direct estimate of its value (smudged by the instrumental resolving power) but rather values of the individual

(762)

angular harmonics a_n, b_n. For example, pressure fluctuations at one point give a_0, the total energy; the shipborne wave recorder (see below) gives a_0, a_1 and b_1; a current meter and pressure recorder give a_0, a_1, b_1, a_2 and b_2. From a_0, a_1 and b_1 one could determine, at least in principle, three parameters of a wave pattern, such as energy, mean direction and angular spread (Longuet-Higgins, 1954). In practice these values are subject to instrumental and statistical uncertainties, and it will be difficult to distinguish between a narrow beam and a unidirectional beam.

The problem can be put in another way. A unidirectional wavetrain of unit energy has all its harmonics equal, so that if it comes from direction $\theta = 0$, an instru-

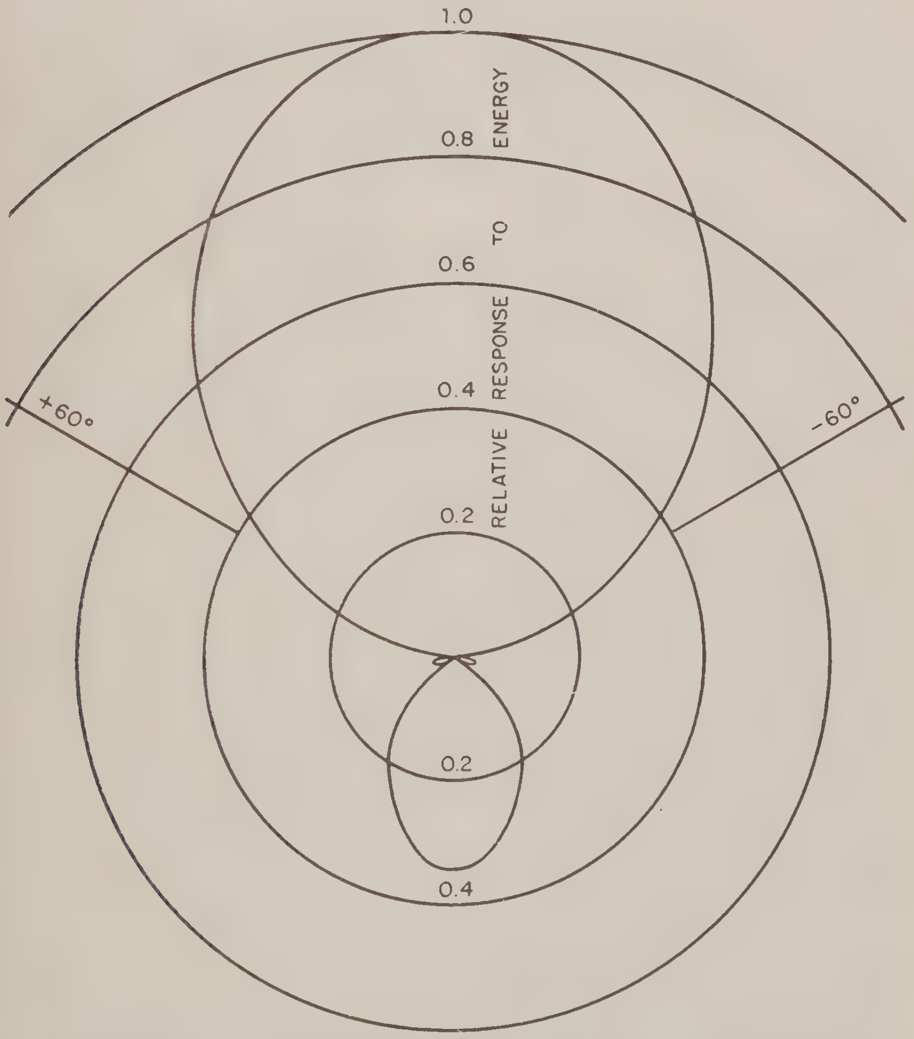

Figure 3. The directional sensitivity pattern of a device measuring the zero order and first two angular harmonics of the wave spectrum. The equation of the curve is $r = 1 + \cos\theta + \cos 2\theta$.

ment measuring the zero order and first two harmonics will show $a_0 = a_1 = a_2 = 1$, $b_1 = b_2 = 0$. Recombining these,

$$R(\theta) = 1 + \cos\theta + \cos 2\theta. \tag{7}$$

This is plotted in Fig. 3, and is the exact equivalent of the directional sensitivity pattern of a radio aerial or sound receiver. It shows a lobe covering approximately ±60°, and the accuracy of detecting mean direction and beam width of the waves is determined by this lobe. A beam width which is narrow compared to this lobe will be difficult to distinguish from a unidirectional beam.

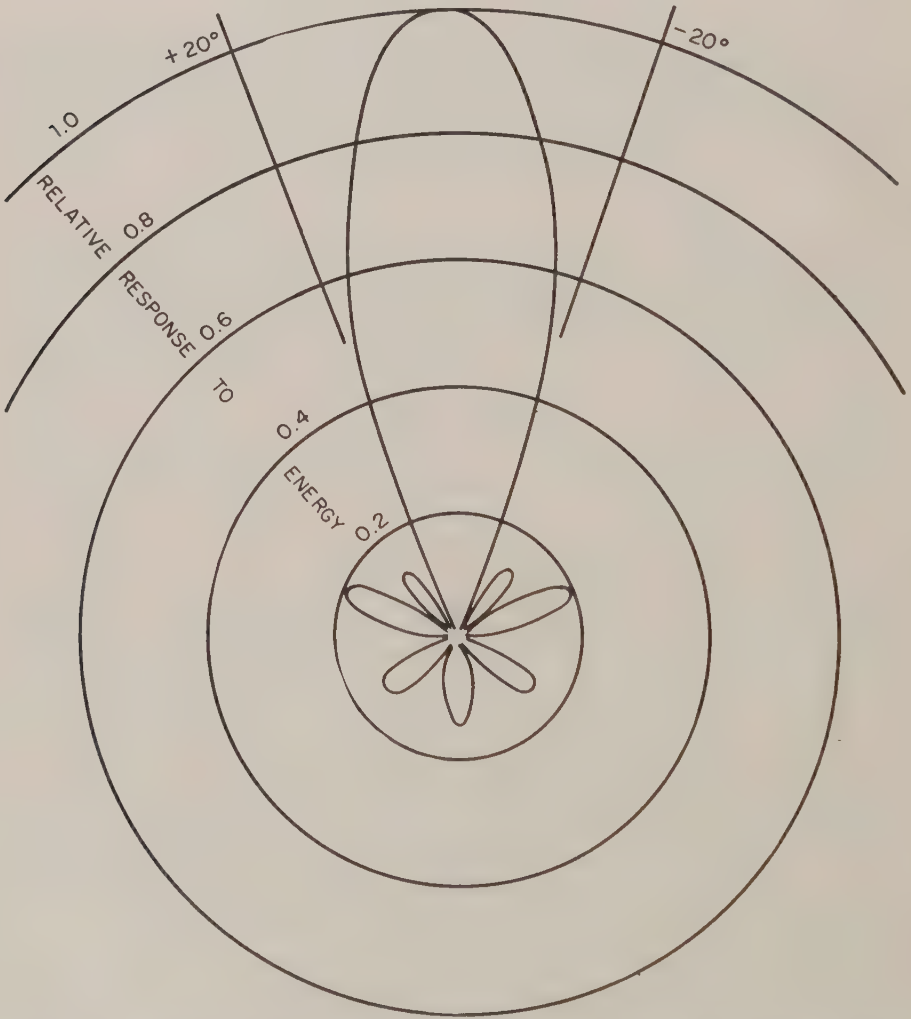

Figure 4. **The directional sensitivity pattern of a device measuring the zero order and first six angular harmonics of the wave spectrum. The equation of the curve is $r = 1 + \cos\theta + \cos 2\theta + \ldots + \cos 6\theta$.**

Instruments measuring higher harmonics have a narrower lobe. The directional sensitivity pattern for an instrument measuring the first 6 harmonics is shown in Fig. 4.

A locally generated sea is unlikely to contain important harmonics above the 5th or 6th, and an instrument giving the first six harmonics would therefore be adequate for measuring storm waves. Information approximately equivalent to this can be obtained for a limited range of frequencies using an array of six conventional wave recorders suitably spaced in an L-shaped pattern. The calculation of the spectrum from the recorder outputs requires a rather formidable amount of computation unless automatic equipment is used (see below).

Swell from a small distant storm may be a very narrow beam, and harmonics up to the 20th or 30th might be required to define it fully. For most purposes, however, a knowledge of the first 5 or 6 angular harmonics will be sufficient.

The first estimate of directional distribution was made by Arthur (1949). He observed that the high surf activity experienced during the landings in Sicily during World War II could not be accounted for if the wind-generated waves travelled only in the direction of the mean wind, but required that substantial energy be radiated up to 30° to each side of the mean wind direction.

PRACTICAL METHODS

At the present time the most practicable method of gaining some directional information is probably the shipborne wave recorder (Tucker, 1955; Cartwright, 1956), which is the basis of some very useful comparisons of ship and wave motion by Cartwright and Rydill (1956). This instrument may be regarded as measuring the height which the water surface would have near the center of the ship were the ship not there. The directional information is obtained by steaming the ship on a series of different courses (e.g., 12 courses at 30° spacings) and measuring the Doppler shifts of the various frequencies recorded. It is possible to measure only the first harmonic of the angular distribution integrated over all frequencies present, though in the special case where there are two or more separate bands of frequencies (e.g., long period swell and short period locally-generated sea), these can be studied separately. In principle more detail can be obtained, but impossibly long records are required to give sufficient statistical reliability.

Methods depending on the correlation of the outputs of various measuring devices are practicable with present techniques. The combination of a pressure measuring device with a current meter measuring the two horizontal componnts of orbital velocity gives a_0, a_1, b_1, a_2, b_2. The same information could be obtained by other similar methods, such as a free floating buoy measuring the three components of its acceleration (Barber, 1946). Barber (1954) has described a method for measuring the two-dimensional spectrum using a number of correctly spaced wave recorders and simple correlating equipment which works directly on the recorder outputs. Using three wave recorders in a limited fetch, Barber observed a "beam width" of ±45°. Barber and Doyle (1956) have described a simplified version of this which measures the mean direction of a narrow beam using just two measuring heads and which is suitable for measuring the direction of approach of swell.

Another series of methods depends on photography of the sea surface. Since these are instantaneous measurements, they all have a 180° ambiguity, and energy traveling in directions opposed by 180° is added together. Barber (1949) used a photograph of the sea surface as an optical diffraction grating. If the optical density at each point of the photograph were proportional to the elevation of the sea surface, the diffraction pattern would be a 2-dimensional analysis of the wave pattern, with the radius from the center of the pattern being proportional to 1/wavelength and the intensity being related to $E(\theta,f)$ in a simple manner. The difficulty is, of course, that the optical density of the photograph is a function of the slope of the surface, the angle of observation and of the distribution of the brightness over the sky. Cox (1955) has examined this problem in more detail, and finds that if a photograph of the sun's glitter pattern on the sea surface is taken, it is possible to deduce the angular distribution of the long wave components from diffration analyses of two small areas of the photograph. (In practice, two independent photographs of the required areas would be taken.) This technique has some theoretical and practical limitations, perhaps the most important being that it is only applicable to the long-wave part of the spectrum. It has not so far been applied to a practical example.

It is possible that Barber's simple diffration analysis could be applied to an artificial "photograph" of the sea surface prepared from stereoscopic photographs in such a way that the optical density is proportional to the corresponding surface elevation.

Pierson (brief remark in his 1955 reference) is analysing a number of stereoscopic photographs of the sea surface. Perhaps he will tell us later how he is analysing the measurements and something about the results. The first step is to convert the photograph into "maps" of the elevation of the sea surface. Marks (1954) has described one way in which these maps may be analysed by averaging surface elevations along a series of parallel lines to produce a one-dimensional record which contains contributions from components traveling in a known narrow range of directions. By altering the direction of the lines of averaging, a 2-dimensional analysis may be made. Methods using stereoscopic photographs are unlikely to become routine, since the labor of analysis is great.

A related method is based on recording surface profiles along different courses using an airborne radio altimeter. Perhaps Dr. Longuet-Higgins can inform us about the present status of this technique?

Cox and Munk (1954) have shown that it is possible to obtain some directional information from a simple photometric analysis of an out-of-focus photograph of the sun's glitter pattern (see Fig. 1). Their method gives only the second harmonic of the spectrum of the surface slopes integrated over all frequencies, and as such is of limited utility. (Their principal aim was to determine the statistical distribution of slopes.) They found a beam width of ±45°.

Another class of methods depends on the use of directional primary measurement. Eckart (1953) and Crombie (1955) have shown that if a beam of radio waves is directed at the sea surface at almost glancing incidence, the back-scattering is due to the component of the sea waves with half of wave-length of the incident radiation and which is traveling in the direction of the receiver. Since the sea-waves are moving, the back-scattered radiation has a Doppler shift in frequency which enables it to be separated from direct coupling between the transmitter and receiver and from back-scattering due to static objects. The range of directions included in the back-scattering depends on the beam-width of the transmitting aerial, and this can only be made small if the aerial is several wavelengths long. The method is therefore probably practical only for short waves.

Groves (private communication) is examining the possibility of using towed electrodes as a directional wave measuring device. The use of towed electrodes for measuring ocean currents is now a routine matter (Longuet-Higgins, Stern and Stommel, 1954). The average value of the recorded e.m.f. is due to the average motion of the cable in the Earth's magnetic field. Wave frequency oscillations, now smoothed, might give useful information. Groves finds that with normal electrode separations the results are rather difficult to interpret, particularly when the device is near the magnetic equator. If a cable with a length of several wavelengths is used the results become easier to interpret, but the device may then be impracticable. The cable has to be kept near the water surface and sufficiently slack to enable it to move with the water particles, but at the same time it must be kept in a straight line.

To sum up, through several ways of obtaining information about the direction of wave travel has been suggested, the more practicable methods give very limited information, and no satisfactory way of obtaining a detailed 2-dimensional spectrum is yet available.

(746)

REFERENCES

Arthur, R. S., 1949. Variability in direction of wave travel. *New York Academy of Sciences*, Vol. 51, p. 511.

Barber, N. F., 1946. Four theoretical notes on the estimation of sea conditions. *Admiralty Research Lab. Report*, No. 103-40/N3/W.

Barber, N. F., 1949. A diffraction analysis of a photograph of the sea. *Nature*, Vol. 164, p. 485.

Barber, N. F., 1956. Finding the direction of travel of sea waves, *Nature*, Vol. 174, p. 1048.

Barber, N. F., and Doyle D., 1956. A method of recording the direction of travel of ocean swell. *Deep-Sea Research*, Vol. 3, p. 206.

Cartwright, D. E., 1956. On determining the directions of waves from a ship at sea. *Proc. Roy. Soc. A*, Vol. 234, p. 382.

Cartwright, D. E. and Rydill, L. J., 1956. The rolling and pitching of a ship at sea. A direct comparison between calculated and recorded motions of a ship in sea waves. *Trans. Inst. Nav. Architects*, Vol. 99, p. 100.

Cox, C., 1955. Optical measurements of sea surface roughness, *Proc. First Conf. on Coastal Eng. Insts.*, Berkeley, California, Council on Ware Research, University of California, Richmond 4, Calif.

Cox, C. S., and Munk, W. H., 1954. Statistics of the sea surface derived from sun glitter, *Jour. Mar. Res.*, Vol. 13, No. 2, pp. 198-227.

Crombie, D. D., 1955. Doppler spectrum of sea echo at 13.56 Mc/s. *Nature*, Vol. 175, p. 681.

Duntley, S. Q., 150. The visibility of submerged objects. *ONR report* N5 ori-07831.

Eckart, C., 1951. Surface waves on water of variable depth. *Scripps Inst. Oceanography Ware report* 100, SIO reference 51-12.

Eckart, C., 1953. The scattering of sound from the sea surface. *Jour. Acoustic Soc. Amer.*, Vol. 25, p. 566.

Isaacs, J. D., Williams, E. A. and Eckart, C., 1951. Total reflection of surface waves by deep water. *Trans. Am. Geoph. Union*, Vol. 32, p. 37.

Longuet-Higgins, M. S., 1955. Bounds for the integral of a non-negative function in terms of its Fourier coefficients. *Proc. Camb. Phil. Soc.*, Vol. 51, p. 590.

Longuet-Higgins, M. S., 1957. Statistical analysis of a random moving surface. *Phil. Trans. Roy. Soc.* A, Vol. 249, p. 321.

Longuet-Higgins, M. S., Stern, M. E. and Stommel, H., 1954. The electrical field induced by ocean currents and waves, with applications to the method of towed electrodes. Pap. in *Phys. Oceanogr. and Met.*, Vol. 13, p. 1.

Marks, W., 1954. The use of a filter to sort out directions in a short-crested Gaussian sea surface. *Trans. Am. Geophys. Union*, Vol. 33, p. 758.

Munk, Walter H., 1949. Surf beats. *Trans. Amer. Geophys. Union*, Vol. 30, p. 849.

Munk, Walter H., 1955. The high frequency spectrum of ocean waves. *Jour. Mar. Res.*, Vol. 14, No. 4, pp. 302.

Munk, W. H., Snodgrass, F. and Carrier, G. F., 1956. Edge waves on the continental shelf. *Science*, Vol. 123, p. 484.

Neumann, G., 1954. Quoted by Pierson, 1955.

Pierson, W. J., 1955. Wind generated gravity waves. Chapter in *Advances in Geophysics*, Vol. II. Academic Press, New York.

Proceedings First Conf. on Ships and Waves, Hoboken, New Jersey, Oct. 1955. Council on Wave Research, University of California, Richmond 4, Calif.

Rice, S. O., 1944. Mathematical analysis of random noise. *Bell System Tech. Jour.*, Vol. 23, p. 282, Vol. 24, p. 26.

St. Denis, M., and Pierson, W. J., 1953. On the motions of ships in confused seas. *Trans. Soc. Nav. Archs. and Marine Engrs.*, p. 281.

Tucker, M. J., 1950. Surf beats: sea waves of 1 to 5 minutes period. *Proc. Roy. Soc. London A,* Vol. 202, p. 565.

Tucker, M. J., 1955. A shipborne wave recorder. *Proc. 1st Conf. Coastal Eng. Insts., Berkeley, Calif.,* Council on Wave Research, University of California, Richmond 4, Calif.

Ursell, F., 1952. Edge waves on a sloping beach. *Proc. Roy. Soc. London A,* Vol. 214, p. 79.

Ursell, F., 1956. Wave generation by wind. *Surveys in Mechanics,* p. 216. The University Press, Cambridge, England.

DISCUSSION

M. S. Longuet-Higgins

The paper presented by Dr. Munk has rightly stressed the importance of measuring the whole two-dimensional spectrum of the sea surface. I would like to describe to you more fully the method he has mentioned that we are developing at the National Institute of Oceanography, and to point out some of its advantages.

The principle of the method is as follows. Suppose the surface elevation is represented in the form

$$\zeta(x,y,t) = \sum_{n} C_n \cos\left(u_n x + v_n y + \sigma_n t + \epsilon_n\right), \tag{8}$$

where (x, y) are horizontal co-ordinates, and t is the time. The wave-numbers (u_n, v_n) are assumed to be distributed densely throughout the (u, v)-plane, and the frequency σ_n is a function only of the wavelength;

$$\sigma_n = \sigma(u_n^2 + v_n^2)^{1/2} \tag{9}$$

as in free gravity waves. The phases ϵ_n are randomly distributed between 0 and 2π and the amplitudes C_n are such that over any small interval of wave-number $du\, dv$

$$\sum_{du\,dv} \tfrac{1}{2} C_n^2 = E(u,v)du dv, \tag{10}$$

where $E(u, v)$ represents the spectrum of the surface. If, by some means, we take the intersection of the surface with a vertical plane $x \sin\theta = y \cos\theta$ then the resulting curve will have an autocorrelation function $\psi(R)$ given by

$$\psi(R) = \overline{\zeta(x,y,t)\zeta(x + X,y + Y,t)} = \int_{-\infty}^{+\infty}\int_{-\infty}^{+\infty} E(u,v) \cos\left(uX + vY\right)du dv, \tag{11}$$

where

$$X = R \cos\theta, \qquad Y = R \sin\theta \tag{12}$$

Assuming this function to be obtained for all directions θ and hence all values of X and Y, we may, by taking the cosine transform, obtain the function

$$\tfrac{1}{2}[E(u,v) + E(-u, -v)], \tag{13}$$

which is the even part of the energy spectrum.

Suppose also that we are able to measure $\partial\zeta/\partial t$ at all points along the plane section. Then from the relation

$$\overline{\frac{\partial\zeta}{\partial t}(x,y,t)\zeta(x + X,y + Y,t)} = -\int_{-\infty}^{+\infty}\int_{-\infty}^{+\infty} \sigma(u,v)E(u,v) \sin\left(uX + vY\right)du dv \tag{14}$$

we may find, by taking the sine-transform, the function

$$\tfrac{1}{2}[\sigma(u,v)E(u,v) - \sigma(-u,-v)E(-u,-v)] \tag{15}$$

But $\sigma(u, v)$ is known, even function. Thus on division we find

$$\tfrac{1}{2}[E(u,v) - E(-u,-v)] \tag{16}$$

and hence, by addition of (13) and (16), the spectrum $E(u, v)$ itself.

It is planned to measure $\zeta(x, y, t)$ along an arbitrary straight line $x \sin\theta = y \cos\theta$ by means of a radar altimeter mounted in an aircraft and directed vertically downwards to the sea surface. A second altimeter, mounted directly aft of the first, and therefore passing over the position occupied by the first a short time before, would provide a measure of $\partial\zeta/\partial t$ along the same path.

The method has certain advantages over stereophography. In the first place a large number of wavelengths may be included in each straight cross-section of the surface, so enabling a more accurate determination of the autocorrelation function to be made. In the second place the complete directional spectrum $E(u,v)$ is obtained, not merely its even part $\tfrac{1}{2}[E(u,v) + E(-u,-v)]$.

Even without performing the correlation analysis, the data may be made to yield some useful information. For example, it can be shown (see reference [1]) that the average number N_0 of zero-crossings of the surface $\zeta(x,y,t)$ along a plane section in direction θ is given by

$$N_0^2 = \frac{1}{\pi^2 m_{00}} (m_{20}\cos^2\theta + 2m_{11}\cos\theta\sin\theta + m_{02}\sin^2\theta), \tag{17}$$

where

$$m_{pq} = \int_{-\infty}^{+\infty}\int_{-\infty}^{+\infty} E(u,v)u^p v^q du dv. \tag{18}$$

Thus N_0 is a maximum and a minimum in two directions at right-angles. The ratio

$$\frac{N_{0\,\min}}{N_{0\,\max}} \tag{19}$$

is equal to the r.m.s. angular spread in direction of the energy about the mean direction, provided this is small (see reference [1]). So by measuring N_0 as a function of θ the r.m.s. spread in direction may be found.

Similarly, the number N_1 of crests and troughs per unit distance in the direction θ can be shown to be given by

$$N_1^2 = \frac{1}{\pi^4 N_0^2 m_{00}} (m_{40}\cos^4\theta + 4m_{31}\cos^3\theta\sin\theta + \cdots + m_{04}\sin^4\theta). \tag{20}$$

From this the moments $m_{40}, m_{31} \ldots m_{04}$ can be determined. If we write

$$\Delta_4 = \begin{vmatrix} m_{40} & m_{31} & m_{22} \\ m_{31} & m_{22} & m_{13} \\ m_{22} & m_{13} & m_{04} \end{vmatrix} \tag{21}$$

and

$$3H = m_{40}m_{04} - 4m_{31}m_{13} + 3m_{22}^2 \tag{22}$$

then it can be shown that the ratio

$$\frac{\Delta_4^2}{H^3} \tag{23}$$

vanishes only when the wave system consists of two intersecting systems of long-crested waves, and equals unity when the surface is isotropic. So this ratio is a measure of the "bimodality" of the spectrum with regard to direction. Upon the same parameter depend also the distribution of the "total" curvature of the surface and the number of maxima, minima and saddle-points per unit horizontal area.

Reference 1.

Longuet-Higgins, M. S. "The statistical analysis of a random, moving surface." Phil. Trans. Roy. Soc. A. *249*, p. 321 (1957).

R. W. L. Gawn

The determination of the frequency and amplitude of the complex undulations of the ocean surface is of fundamental importance to those who design ships, those who operate them and to those who plan operations.

Dr. Munk mentioned the importance of the information as regards ship motion but the designer's interest is much wider. The ship must stand up to all the hazards of rough weather and I would like to make a few remarks on the designer's problems in this connection. Gravity waves impose heavy stresses and slamming, objectionable motion and speed loss and further limit efficiency if operational positions, e.g. gun positions in a naval ship are exposed to water or spray.

In the past and that not far distant the information available on ocean waves was scanty and it is remarkable that the designer was able to achieve a good measure of success. He assumed for strength calculations that the height of an ocean wave was one twentieth the length, although later thanks to the observations of Vaughan Cornish and others he could accept a smaller ratio for longer waves.

Until a few years ago that was about all that was known of use to the designer and it is refreshing now to hear of the enterprising work and the ingenious and painstaking analysis which Dr. Munk and others are carrying out.

There is scope for a closer identification of the length or period of the wave and the related height with the probability of occurrence in different oceans. While height is the dominant term in the energy estimates mentioned in the paper, period or length is dominant for ship motion since it influences both the excitation and the magnification. The Authors mention that the gravity waves are centered around 10 seconds period or a length of about 500 feet. It is emphasized that the range of interest to the ship designer is really from about 100 to 1500 feet length or about 4 to 17 seconds period and it is hoped that the Authors' further investigations will include a detailed study of this particular field accordingly. It looks as though from the wonderful instruments described by Dr. Munk and the work of the last speaker this should be realized.

As regards instrumentation, one requirement is a handy apparatus that can be taken to a ship and dropped in the water as necessary. As a matter of fact thinking on these lines we have made a simple buoy at Haslar which transmits radio signals of its vertical movement. Whether it is effective or not I am not yet in a position to say but a preliminary trial was promising. I am hoping that it is at sea just about now so that we should soon know if it is at all promising.

J. D. Pierson

Before proceeding to a few comments on this excellent paper, I would like to bring a third party to the "marriage" of the oceanographers and ship builders. The designers of aircraft also have a great interest in the surface of the sea. Water-based aircraft are moving out of the bays and rivers further into the open sea.

Generally, aircraft are too fragile to operate in all sea conditions. The sea becomes too rough (both in a local and overall sense) once in a while, but on the other hand the hybrid nature of the water-based aircraft enables us to avoid the worst conditions. On the water, at rest or slowly taxiing, the seaplane experiences a long sequence of waves representing the full spectrum of the sea. However, in the transition conditions of landing and take-off, which are critical for the aircraft design, only a very small portion of the whole sea wave spectrum is encountered.

Thus, we may be looking for somewhat different information than ship designers. We are both concerned with the occurrence of high water loads and seaworthiness as they may be related to the energy spectrum for the seaways. Yet because of the short transient nature of the seaplane takoff and landing, a further analysis of the sea spectrum may be profitably employed.

For example, as the various components of the sea add to give the larger waves —do high crests generally follow immediately the deep troughs? The extent to which this may occur on a probability basis would be helpful in determining the conditions for which the hull loads should be obtained.

Another problem suggested by the type of operation of water-based aircraft is the description of the sea so that small areas at a time could be defined in terms of the overall spectrum existing at the time. Along this line we may be able to contribute through the measurement of the sea surface from the air. Although airborne direct wave measuring systems have not yet been satisfactorily demonstrated, there are several now under development which have considerable promise. Measurements of the sea roughness by aircraft will not only provide a tremendous increase in data over what can be obtained at fixed locations but also provide quick data for portions of the total sea spectrum for small transient areas.

W. J. Pierson, Jr.

I should like to add to Dr. Munk's remarks a very brief summary of Project SWOP (Stereo Wave Observation Project), a joint effort of the Office of Naval Research, U. S. Navy Hydrographic Office, Woods Hole Oceanographic Institution, and many operating arms of the Navy. A final report on the project is soon to appear under the title "The directional spectrum of a wind-generated sea as determined from data obtained by the Stereo Wave Observation Project."

The plan of the project was to take simultaneous stereo photographs and wave pole records of the sea surface. The directional spectrum could be computed from the stereo photographic data, and the frequency spectrum could be computed from the wave pole data. Theoretical considerations led to the conclusion that the total volume under the directional spectrum should equal the total area under the frequency spectrum and thus a check of the two methods would be obtained. After the computation of the directional spectrum and the wave pole spectrum, it was discovered that the two quantities given above did not agree. Several sources of discrepancy have been discovered and eliminated from the data. First of all, the wave pole spectrum did not have enough area under it to represent the true wave record. The spectral components for many important frequencies were attenuated because the wave pole had a tendency to move up under the crest of passing waves and move down in the troughs. A correction was derived for this effect, and brought the two results into closer agreement.

The stereo data unfortunately were obtained from topographic-base film instead of stereo-base film and there was some differential shrinkage in the record. The errors in the stereo data are due to this differential shrinkage, to a background curvature of the plane of the sea surface, and to spot height reading error. They all combine to make the volume under the directional spectrum quite a bit greater than the area under the frequency spectrum. The errors due to the spot height reading and to background curvature have been eliminated, and at the moment work is under way to eliminate the error due to differential shrinkage. The directional spectra have been computed and indications are that such a correction can be made and that the results of the wave pole observations and the stereo observations can be made consistent.

Some tentative conclusions can be made even with the data in their present form; and even if no further attempt were made in analyzing the data, many valuable conclusions could be drawn. The error due to differential shrinkage shows a definite pattern which can be removed qualitatively from the spectrum. The conclusions would then be that the theoretical Neumann spectrum is well verified by the corrected wave pole spectrum and that the directional spread of the spectrum is symmetric about the wind direction and falls to half power at ±30° to the wind direction.

Unfortunately none of the slides and drawings to accompany the final report are at present in a form ready for inclusion in this report. They need correction (in some cases) and further checking. Therefore the reader is requested to write for the forthcoming report which will describe this work in complete detail.

R. C. Vetter

It may be appropriate to add, to the various ingenious methods mentioned by Dr. Munk, one more method for determining some two-dimensional characteristics of ocean waves. If two identical transparent copies of a vertical photograph of the sea surface are super-imposed and illuminated by a beam of light, one may determine the correlation function of the density variations in the transparencies by recording the change in light intensity as one transparency is translated with respect to the other. The two dimensional power spectrum of the density patches in the transparencies can then be derived from this correlation function. This method is being used with some success by Dr. Uberoi of the University of Michigan in studies of turbulence in gases. Some of the same transparencies that were used in Project SWOP (see Dr. Willard Pierson's comments) have been sent to Dr. Uberoi for analysis. It seems highly unlikely that the two two-dimensional power spectra obtained from Dr. Pierson's SWOP Project and Dr. Uberoi's method of analysis will be alike since there is no simple relationship between the brightness of the sea surface and the height of waves. However, it will be interesting to see in what respects the two spectra are different or alike.

A tremendous effort has gone into the determination of a two-dimensional power spectrum by Project SWOP. I am sure that the results will justify this effort many times over. One wonders if an easier way can be found to give similar information. At present, none of the optical methods appear to be satisfactory. The value of more information about the two-dimensional characteristics of real ocean waves is considerable and I am sure that everyone, including Dr. Pierson, will thank the ingenious person who finds an easier way of getting it.

Walter H. Munk

Vetter's suggestion is closely related to Barber's diffraction method (PRACTICAL METHODS, p. 3 of our paper). In particular, the reference to Cox (1955) is pertinent.

Scripps Institution of Oceanography, New Series, No. 951

Reprinted, by permission, from the Quarterly
Journal of the Royal Meteorological Society,
v.83, no.358, 1957.

551.521.14

Exact reflectance under a cardioidal luminance distribution

By R. W. PREISENDORFER

Scripps Institution of Oceanography, University of California, La Jolla

(Manuscript received 11 June 1957)

SUMMARY

The *cardioidal luminance distribution* $B(\theta, k) = B(\pi/2, k)\,(1 + k\cos\theta),\ -1 \leqq k < \infty,\ 0 \leqq \theta \leqq \pi/2$ is the general empirical form of the luminance of overcast skies. It has been found empirically (Moon and Spencer 1942) and theoretically (Chandrasekhar 1946) that the value $k = 2$ represents most overcast skies. The purpose of this note is to obtain the exact algebraic expression for the reflectance $r(m, k)$ of a surface (between media of relative indices of refraction 1 and $m \geqq 1$) irradiated by an unpolarized cardioidal radiance distribution. In this way the classical reflectance formula of Walsh (1926) for the case $k = 0$ is generalized, and the approximately-obtained numerical results of Middleton (1952) for the case $k = 2$, $m = 4/3$ are extended. In addition it is found that the function $r(\cdot, k)$ is essentially linear over the range $1{\cdot}2 \leqq m \leqq 1{\cdot}9$ for each fixed value of k in the interval $0{\cdot}5 \leqq k < \infty$, and thus may be represented by the form : $r(m, k) = a(k)\,m + b(k)$. In particular $r(m, 2) = 0{\cdot}141965\,m - 0{\cdot}137709$ which has a maximum deviation of 3·2 per cent from the exact values of $r(m, 2)$ over the range $1{\cdot}2 \leqq m \leqq 1{\cdot}9$.

1. INTRODUCTION

The purpose of this note is to give an exact expression for the reflectance of a surface illuminated by a *cardioidal luminance distribution*, i.e., a luminance distribution of the form :

$$B(\theta, k) = B(\pi/2, k)\,(1 + k\cos\theta),\ -1 \leqq k < \infty,\ 0 \leqq \theta \leqq \pi/2 \quad . \qquad . \qquad (1)$$

The exact expression is used to obtain numerical values of the reflectance for a given set of values of k and the relative index of refraction m. In this way the classical exact expression for the case $k = 0$ given by Walsh (1926) is generalized (Eq. (14)), and certain results obtained by Middleton (1952) are extended (Table 1).

Before proceeding with the details, we observe that Eq. (1) with $k = 2$ is the empirical form for the luminance of an overcast sky, as reported by Moon and Spencer (1942) and recently confirmed by Hopkinson (1954). It is of interest to note that this empirical expression is in good agreement with the corresponding theoretical expression deduced by Chandrasekhar (1946).

2. THE REFLECTANCE $r(m, k)$

Let S be a surface between two optical media M and M' of relative indices of refraction (for a fixed wavelength λ) 1 and $m \geqq 1$ respectively. Let S be irradiated by an unpolarized radiance distribution coming from M of the form $N(\theta, k) = N(\pi/2, k)(1 + k\cos\theta)$ where θ is measured in radians from the normal to S in M and k is any fixed real number such that $-1 \leqq k < \infty$. Required to find the exact form of the spectral reflectance $r(m, k)$ of S with respect to $N(\cdot, k)$.

At a given point p of the surface S, the spectral reflectance r with respect to a radiance distribution N is defined as

$$r = W/H, \qquad (2)$$

where W is the radiant emittance of, and H is the irradiance on, S at p as induced by N. In the case of the distribution $N(\cdot, k)$, let $W(m, k)$ and $H(k)$ be the associated emittance and irradiance. Clearly

$$W(m, k) = 2\pi \int_0^{\pi/2} N(\theta, k)\, r'(\theta, m) \cos\theta \sin\theta \, d\theta, \qquad (3)$$

and

$$H(k) = 2\pi \int_0^{\pi/2} N(\theta, k) \cos\theta \sin\theta \, d\theta, \qquad (4)$$

where

$$r'(\theta, m) = \tfrac{1}{2}[\sin^2(\theta - \phi)\operatorname{cosec}^2(\theta + \phi) + \tan^2(\theta - \phi)\cot^2(\theta + \phi)] \qquad (5)$$

is the Fresnel reflectance formula in which θ and ϕ are related by Snell's Law : $\sin\theta = m\sin\phi$. Hence

$$r(m, k) = W(m, k)/H(k) = W'(m, k)/H'(k) \qquad (6)$$

where

$$W'(m, k) = W(m, k)/2\pi N(\pi/2, k), \quad H'(k) = H(k)/2\pi N(\pi/2, k) \, . \qquad (7)$$

It follows that

$$H'(k) = \int_0^{\pi/2} (1 + k\cos\theta)\cos\theta \sin\theta \, d\theta = \tfrac{1}{2} + k/3 \qquad (8)$$

Further, let $\theta' = \theta - \phi$, then r' may be written

$$r'(\theta', m) = [2m^2/(m^2 - 1)^2][(\cos\theta' - a)^2 + (\sec\theta' - a)^2] \qquad (9)$$

in which $a = (m^2 + 1)/2m$, and $0 \leqq \theta' \leqq \cos^{-1}(1/m)$. Letting $x = \cos\theta'$, $s = 1/m$, it follows that

$$W'(m, k) = \tfrac{1}{2}\int_1^s [1 + k(x - s)/(1 + s^2 - 2sx)^{\frac{1}{2}}]\{[(x - a)^2 + (1/x - a)^2]/(1 - s^2)^2\} \times \\ \times [(sx - 1)(x - s)/(x - a)^2]\, dx \qquad (10)$$

Clearly $W'(m, k)$ can be written in the form

$$W'(k, m) = A(m) + kB(m) \qquad (11)$$

where

$$A(m) = \tfrac{1}{2}\int_1^s \{[(x - a)^2 + (1/x - a)^2][(sx - 1)(x - s)]/(x - a)^2(1 - s^2)^2\}\, dx \, . \qquad (12)$$

and

$$B(m) = \tfrac{1}{2}\int_1^s \{[(x - a)^2 + (1/x - a)^2][(sx - 1)(x - s)^2]/(x - a)^2(1 - s^2)^2(1 + s^2 - 2sx)^{\frac{1}{2}}\}\, dx \, . \qquad (13)$$

So that

$$r(m, k) = 6[A(m) + kB(m)]/(3 + 2k) \qquad (14)$$

The classical expression considered by Walsh is

$$r(m, 0) = 2A(m) \qquad (15)$$

The evaluation of $A(m)$ is straightforward and yields :

$$\begin{aligned} 2A(m) = {} & \tfrac{1}{2} + (m - 1)(3m + 1)/6(m + 1)^2 - 2m^3(m^2 + 2m - 1)/(m^2 + 1)(m^4 - 1) \\ & + [8m^4(m^4 + 1)/(m^2 + 1)(m^4 - 1)^2]\ln m \\ & + [m^2(m^2 - 1)^2/(m^2 + 1)^3]\ln[(m - 1)/(m + 1)] \end{aligned} \qquad (16)$$

For $k \neq 0$, the new contribution is from the term $B(m)$. The most natural representation of $B(m)$ is:

$$B(m) = [m/2(m^2-1)^2]\left\{\sum_{i=1}^{4} B_{1i}(m) + m\left[\sum_{i=1}^{4} B_{2i}(m) - (a^2-1)\sum_{i=1}^{4} B_{3i}(m)\right]\right\} \tag{17}$$

where, with the abbreviations

$$p = m - 1, \quad q = m^2 - 1, \quad r = m^2 + 1, \tag{18}$$

$$B_{11} = (1/8m)\,[r^3(p - q^{\frac{1}{2}}) - r^2(p^3 - q^{\frac{3}{2}}) + (3r/5)(p^5 - q^{\frac{5}{2}}) - (1/7)(p^7 - q^{\frac{7}{2}})] \tag{19}$$

$$B_{12} = [(m^2+2)/2m]\,[(-r^2/2)(p - q^{\frac{1}{2}}) + (r/3)(p^3 - q^{\frac{3}{2}}) - (1/10)(p^5 - q^{\frac{5}{2}})] \tag{20}$$

$$B_{13} = [(2m^2+1)/2m]\,[r(p - q^{\frac{1}{2}}) - (1/3)(p^3 - q^{\frac{3}{2}})] \tag{21}$$

$$B_{14} = -m(p - q^{\frac{1}{2}}) \tag{22}$$

$$B_{21} = (r^2/8m^2)\,[r(p - q^{\frac{1}{2}}) - (1/3)(p^3 - q^{\frac{3}{2}})] \tag{23}$$

$$B_{22} = [-r(5m^2+1)/4m^2]\,(p - q^{\frac{1}{2}}) \tag{24}$$

$$B_{23} = [(2m^2+1)/r^{\frac{1}{2}}]\ln A, \quad A = (q^{\frac{1}{2}} - r^{\frac{1}{2}})(p + r^{\frac{1}{2}})/(q^{\frac{1}{2}} + r^{\frac{1}{2}})(p - r^{\frac{1}{2}}) \tag{25}$$

$$B_{24} = (-m/r)(p - mq^{\frac{1}{2}}) - (m^2/r^{\frac{1}{2}})\ln A \tag{26}$$

$$B_{31} = (r^2/2)\,[(p^{-1} - q^{-\frac{1}{2}}) - (r/3)(p^{-3} - q^{-\frac{3}{2}})] \tag{27}$$

$$B_{32} = [r(5m^2+1)/3]\,(p^{-3} - q^{-\frac{3}{2}}) \tag{28}$$

$$B_{33} = [4m^2(2m^2+1)/r]\,[(-2/r)(p^{-1} - q^{-\frac{1}{2}}) - (2/3)(p^{-3} - q^{-\frac{3}{2}}) + (1/r^{\frac{1}{2}})\ln A] \tag{29}$$

$$B_{34} = (40m^3/r^3)(p^{-1} - q^{-\frac{1}{2}}) + (40m^4/3r^2)(p^{-3} - q^{-\frac{3}{2}}) - (4m^3/r)(p^{-3} - mq^{-\frac{3}{2}}) - (20m^4/r^{\frac{3}{2}})\ln A \tag{30}$$

3. NUMERICAL RESULTS

Computations based on the exact expression for $r(m, k)$ over the ranges indicated below were carried out to nine places and rounded to six.

TABLE 1. THE REFLECTANCE $r(m, k)$

				k			
m	− 1·0	− 0·5	0	0·5	1·0	1·5	2·0
1·1	0·054315	0·032448	0·025159	0·021515	0·019328	0·017870	0·016829
1·2	0·088540	0·055346	0·044281	0·038749	0·035429	0·033216	0·031636
1·3	0·112699	0·074024	0·061132	0·054686	0·050819	0·048240	0·046399
4/3	0·119641	0·079754	0·066458	0·059811	0·055822	0·053163	0·051264
1·4	0·132357	0·090698	0·076811	0·069858	0·065702	0·062925	0·060941
1·5	0·149237	0·106143	0·091778	0·084595	0·080286	0·077413	0·075361
1·6	0·163601	0·120584	0·106245	0·099076	0·094774	0·091907	0·089858
1·7	0·177942	0·134726	0·120320	0·113117	0·108796	0·105915	0·103857
1·8	0·190639	0·148201	0·134055	0·126982	0·122738	0·119909	0·117888
1·9	0·202559	0·161246	0·147476	0·140590	0·136459	0·133705	0·131737
m	2·5	3·0	3·5	4·0	4·5	5·0	∞
1·1	0·016048	0·015440	0·014955	0·014557	0·014226	0·013945	0·010581
1·2	0·030450	0·029528	0·028790	0·028187	0·027684	0·027258	0·022152
1·3	0·045017	0·043943	0·043084	0·042380	0·041794	0·041299	0·035349
4/3	0·049839	0·048731	0·047845	0·047119	0·046515	0·046004	0·039867
1·4	0·059453	0·058296	0·057370	0·056613	0·055982	0·055448	0·049039
1·5	0·073822	0·072625	0·071667	0·070883	0·070230	0·069678	0·063048
1·6	0·088322	0·087127	0·086171	0·085389	0·084737	0·084186	0·077568
1·7	0·102313	0·101113	0·100152	0·099367	0·098712	0·098158	0·091509
1·8	0·116372	0·115193	0·114250	0·113479	0·112836	0·112292	0·105763
1·9	0·130262	0·129114	0·128196	0·127445	0·126819	0·126290	0·119934

4. APPROXIMATE FORMS FOR $r(m, k)$

A plot of the numerical results would show that $r(\cdot, k)$ is essentially a linear function for the ranges $1{\cdot}2 \leqq m \leqq 1{\cdot}9$, $\frac{1}{2} \leqq k \leqq \infty$. Hence over these ranges $r(m, k)$ can be represented by a form of the type $r(m, k) = a(k)\, m + b(k)$. The coefficients $a(k)$ and $b(k)$ have been evaluated for each of the k's in the range of linearity. Below is given the form which is perhaps of greatest immediate interest

$$r(m, 2) = 0{\cdot}141965\, m - 0{\cdot}137709 \quad . \quad . \quad . \quad (31)$$

When plotted, this function has a maximum deviation of 3·2 per cent from the exact curve for $r(m, 2)$. For example with $m = 4/3$, the above expression yields the value 0·051578. Rounded to 4 figures, this gives 0·0516 compared to 0·0513 for the exact reflectance, with a deviation of about 0·6 per cent.

In general a good rule of thumb for finding $r(m_2, k)$ if $r(m_1, k)$ is known is given by

$$r(m_2, k) = r(m_1, k) + 0{\cdot}142\,(m_2 - m_1),$$

$$\tfrac{1}{2} \leqq k < \infty, \quad 1{\cdot}2 \leqq m \leqq 1{\cdot}9. \quad . \quad . \quad . \quad . \quad (32)$$

The maximum errors of deviation in percentages over the range $1{\cdot}2 \leqq m \leqq 1{\cdot}9$ for each k is given by the following pairs of numbers (6·9 per cent, 0·5), (5·4 per cent, 1), (3·2 per cent, 2), (2·4 per cent, 2·5), (1·7 per cent, 3), (1·2 per cent, 3·5), (0·7 per cent, 4), (0·3 per cent, 4·5), (0·1 per cent, 5), (6·0 per cent, ∞).

ACKNOWLEDGMENTS

This paper represents results of research which has been supported by the Bureau of Ships, U.S. Navy. Careful checks of the integrations were made by Mr. James Bates, Miss Dolores Reinbold and Mrs. Margaret Rethwish. The numerical computations were performed by Mrs. Rethwish, Mrs. Alma Schaules and Mrs. Margaret Church.

REFERENCES

Chandrasekhar, S.	1946	*Astrophys. J.*, **103**, p. 165.
Hopkinson, R.	1954	*J. Opt. Soc. Amer.*, **44**, p. 455.
Middleton, W. E. K.	1952	*Quart. J. R. Met. Soc.*, **78**, p. 627.
Moon, P. and Spencer, D. E.	1942	*Illum. Engr.*, **37**, p. 707.
Walsh, J. W. T.	1926	*Illum. Res. Tech. Pap., D.S.I.R. (Brit.)*, **2**, p. 10.

Geochimica et Cosmochimica Acta, 1958, Vol. 13, pp. 153 to 212. Pergamon Press Ltd., London

Reproduced by Permission

Chemistry of Pacific pelagic sediments*

E. D. Goldberg and G. O. S. Arrhenius
Scripps Institution of Oceanography, La Jolla, Calif., U.S.A.

(*Received* 26 *July* 1957)

Abstract—The chemical and mineralogical composition of pelagic sediments from the East Pacific Ocean has been determined with the aim of defining the ultimate sources and the mechanisms of formation of the solid phases. The distribution of elements between sea-water, the pore solution and the various solid components of the sediments permits interpretations of the variations in time and space of the gross chemical composition of pelagic clays. For example, manganese, present in sea-water in a divalent form, is apparently oxidized at the sediment-water interface to tetravalent species which subsequently become a part of the group of ferromanganese oxide minerals which are found in the marine environment. It is suggested the rate of manganese accumulation in sediments is some function of the length of time the sediment surface is in contact with sea-water. The contribution of chemical species from the different geospheres is considered. The quantitative importance of pelagic clays in the major sedimentary cycle is studied on the basis of the distribution of the weathered igneous rock products between continental and pelagic deposits and sea-water. These analyses of a wide variety of pelagic clays allow a reformulation of the geochemical balance and it is concluded that pelagic clays account for approximately 13 per cent of the total mass of sediments produced over geologic time.

Contents

1. INTRODUCTION . . . 153
2. METHODS . . . 154
    2.1 Preparation of sediments . . . 154
    2.2 Separation of constitutuents . . . 155
        2.21 Dialysis . . . 155
        2.22 Ion exchange . . . 155
        2.23 Separation according to settling velocity . . . 155
        2.24 Separation according to density and magnetic susceptibility . . . 155
        2.25 Chelative dissolution . . . 158
    2.3 Elemental analysis . . . 161
3. THE NATURE OF DISSOLVED CHEMICAL SPECIES IN THE OCEAN . . . 162
4. DISTRIBUTION OF ELEMENTS IN THE DISSOLVED AND SORBED PHASES OF THE SEDIMENT . . . 166
5. DISTRIBUTION OF ELEMENTS IN THE SOLID PHASES . . . 169
    5.1 Silicon, aluminium and gallium . . . 172
    5.2 Sodium, potassium and lithium . . . 173
    5.3 Magnesium, calcium and strontium . . . 176
    5.4 Barium . . . 179
    5.5 Boron . . . 187
    5.6 The rare-earth elements, yttrium, scandium and thorium . . . 188
    5.7 Titanium . . . 188
    5.8 Zirconium . . . 191
    5.9 Vanadium . . . 192
    5.10 Chromium . . . 192
    5.11 Iron . . . 193
    5.12 Manganese, cobalt, nickel, lead and molybdenum . . . 193
    5.13 Copper . . . 200
6. COMPARATIVE CHEMISTRY OF PELAGIC SEDIMENTS IN SPACE AND TIME . . . 201
7. THE GEOCHEMICAL BALANCE . . . 203
REFERENCES . . . 209

---

* Contribution from the Scripps Institution of Oceanography New Series No. 952. The major portion of this work was performed under contract Nonr-233(17) between the University of California and the Office of Naval Research. Support was also received from the Institute of Geophysics, UCLA, and from the Geological Society of America.

1. INTRODUCTION

THE mineral components of pelagic sediments have their origin in all of the geospheres and in outer space. From the concentration and grouping of different elements in the minerals, inferences can be drawn regarding the sources of the solid phases. For example, the boron content of clay minerals crystallizing in the marine environment is approximately two orders of magnitude higher than the value for terrestrial clays (GOLDSCHMIDT and PETERS, 1932a, b). There are several indications that boron proxies for silicon in the tetrahedral sheets of the mineral structure. Hence, terrestrial clays could be detected in the pelagic environment by their low boron content, as a secondary exchange of the tetrahedral group probably is excluded for energetic reasons.

Changes in space and time of the contribution of minerals from different sources may be revealed by the proportions of the sedimentary components and by their structure and chemical composition. While in a number of clay cores from the Pacific Ocean, the stable proportions between marine hydrogenous and terrestrial detrital minerals indicate a relatively constant supply of both of these, other sequences bear witness of radical changes in the rate of accumulation of one or both of these components. A high manganese, phillipsite, and apatite content, and a large crystal size of phillipsite and barite, for example, characterize many of the Tertiary sediments of the north Pacific, in contrast to the overlying Quaternary deposits. An understanding of the processes responsible for such differences is of utmost importance in studies of the past history of the earth.

Finally, in geochemical balance computations of the type first used by JOLY (1899), the concentrations of elements in ocean sediments enter as important constants, influencing the final values for the proportions of different rock types making up the earth's crust. Two well-known balance computations (GOLDSCHMIDT, 1954; KUENEN, 1950) are in disagreement as to the total mass of pelagic clays produced in the major sedimentary cycle. KUENEN concludes that the pelagic clays represent 50 per cent of the total mass of sediments, while GOLDSCHMIDT considers pelagic clays quantitatively unimportant. Further evaluation of assumptions involved in geochemical balance computations, combined with additional data on the chemical and mineralogical composition of sediments, should reveal which, if either, of the two extremes is right.

This paper is an attempt to contribute to the knowledge of the localization of elements in the mineral phases of the pelagic sediments and to investigate the sources of the components of the deposits and their processes of formation. Further, upon the basis of new evidence, a modified geochemical balance is presented.

2. METHODS

2.1. *Preparation of sediments for analysis*

In general the sediments were treated as indicated by ARRHENIUS (1952, 4.1.) However, the sampling method was changed in order to smooth out gradients in the composition caused by the activity of benthonic animals, and in order to make possible stratigraphic summation without interpolation. Instead of cutting 1·5 cm thick sample slices every 10 cm, the entire length of the core was thus sampled in consecutive slices, each one 4 cm long.

Density and water content were determined in all samples. One segment of the sample slice was ground and used for chemical analysis, the other one was saved intact and used for the separation of different minerals or mineral groups which were subsequently analysed.

In the designation of the samples the first word refers to the name of the expedition, and the following number and symbols to the core number, the ship, and the type of core. The final number refers to the depth of the sample in cm below the sediment surface. A brief description of the samples is given in Table 1 (see also Fig. 1).

2.2. *Separation of constituents of the sediment*

In order to establish the distribution of different elements between the different constituents of the sediment, attempts were made to separate these. The separation processes include dialysis, exchange of sorbed ions, chelation, separation according to settling velocity, density, and magnetic properties. It should be noted that while bulk analyses of sediments reported in this paper include the sorbed solids, and the dissolved solids of the pore water, analyses of fractions of the sediment, given in the following, refer to material freed from interstitial salts and with exchange positions saturated with ammonium ion. The compositions of the interstitial solids and of the sorbates are given separately.

2.21. *Dialysis.* The wet sample was churned with distilled water, transferred to a thin-walled cellophane tube and dialysed in a volume of distilled water approximately five times the volume of the suspension. The water was changed every 6 hr and the first three dialysates combined and evaporated. The evaporate forms the sample referred to as the dialysate. Dialysis of the suspension was carried on until no chloride could be observed upon the addition of silver nitrate.

2.22. *Ion exchange.* In the samples Cap. 50 BP 812–817, and Cap. 33 BG, sorbed cations were exchanged by boiling the sample with 3 per cent LiOH. In the remaining samples the dialysis tubing with suspension was transferred to a beaker containing an approximately five times larger volume of N ammonium acetate. After heating to 80°C for 6 hr the solution was exchanged against distilled water. The resulting solution was separated after another 6 hr period, combined with the first solution, evaporated and ashed. The ash forms the sample.

2.23. *Separation according to settling velocity.* The mineral powders and the ammonium or lithium saturated sediment samples were suspended in 0·01 N ammonia, and successively finer grain size fractions were separated by repeated settling and decantation. The fractions so prepared had limiting equivalent diameters of spherical quartz grains of 32, 10, 3·2 and 1 μ. A CEPA continuous flow supercentrifuge with an electronic speed regulator, modified according to JASMUND (1948), was employed for the further subdivision of the sediment fractions with grain sizes smaller than 1 μ. The fractions thus obtained had the equivalent size limits 1, 0·32, 0·1 and 0·03 μ. For monomineralic suspensions the known density of the mineral in question was used for the computation of settling velocities; in the case of sediment suspensions a grain density of 2·60 was assumed.

2.24. *Separation according to density and magnetic susceptibility.* Mineral separation on the basis of differences in density and magnetic properties was

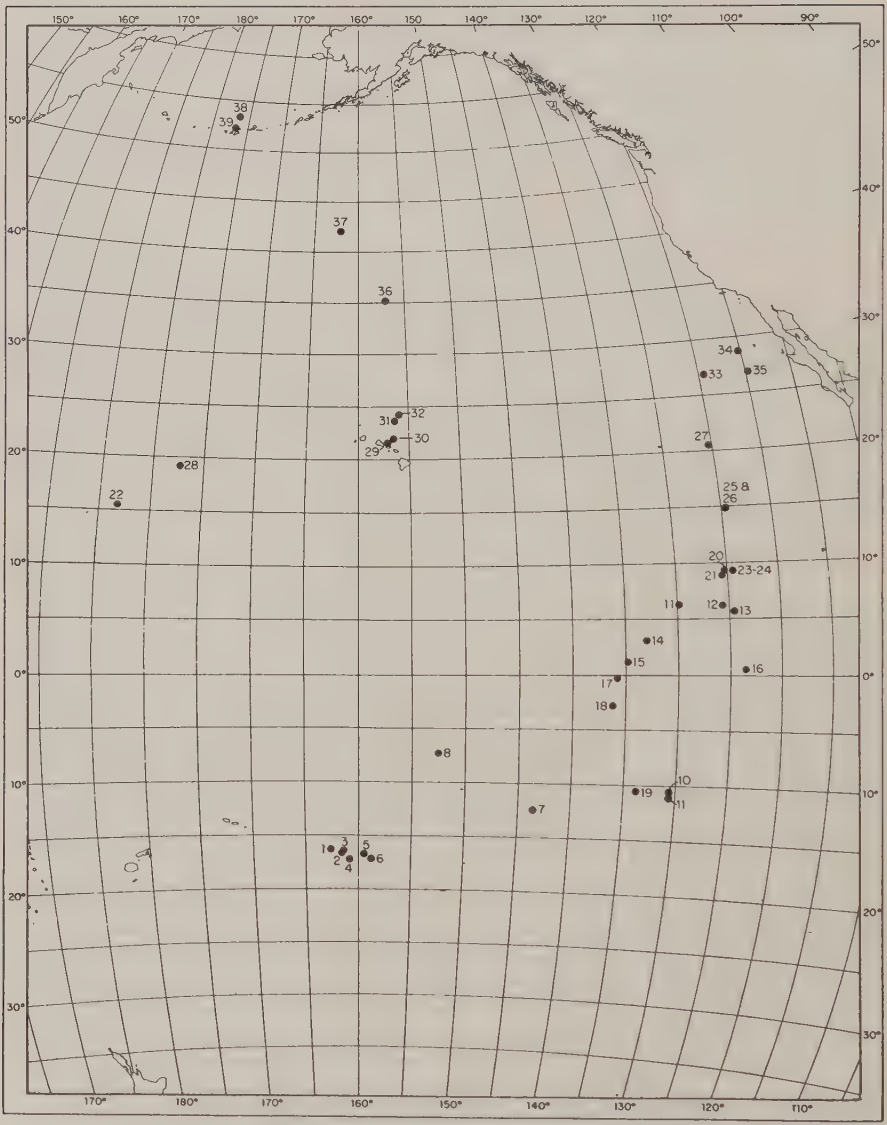
150°
160°
170°
180°
170°
160°
150
140°
130°
120°
110°
100°
90°
50°
40°
30°
20°
10°
0°
10°
20°
30°
38
39
37
36
34
33
35
32
31
30
29
27
28
22
25 &
26
20
21
23-24
11
12
13
14
15
16
17
18
8
10
19
11
7
1
2
3
4
5
6
170°
180°
170°
160°
150°
140°
130°
120°
110°

Fig. 1. Location of sediment samples used in the investigation.

Table 1. Description of samples

	South equatorial clays	
1	Capricorn 21 HG	Lat. 16°36′S, long. 162°43′W (NW of Cook Islands). Depth 5125 m. Dark brown clay with manganese micronodules, phillipsite and fish debris.
2	Capricorn 23 HG	Lat. 16°58·5′S, long. 161°35′W (NW of Cook Islands). Depth 5140 m. Dark brown clay as above.
3	Capricorn 24 HG	Lat. 16°44′S, long. 161°22′W (NW of Cook Islands). Depth 4685 m. Dark brown clay as above.
4	Capricorn 30 BG	Lat. 17°28′S, long. 160°59′W (N of Cook Islands). Depth 4710 m. Dark brown clay abundant in manganese nodules and phillipsite and with moderate amounts of fish debris, mica and quartz.
5	Capricorn 25 HG	Lat. 16°53′S, long. 159°8 W (N of Cook Islands). Depth 5040 m. Dark brown clay as Capricorn 31 BG.
6	Capricorn 31 BG	Lat. 17°29′S, long. 158°40′W (W of Society Islands). Depth 4890 m. Dark brown clay, abundant in manganese nodules, in augite, feldspar, and other igneous minerals, with moderate amounts of quartz and phillipsite and small amounts of fish debris.
7	Capricorn 33 BG	Lat. 12°46′S, long. 143°33′W (Tuamotu-Marquesas). Depth 4380 m. Similar in composition to Capricorn 30 BG.
8	Swedish Deep-sea Expedition 71	Lat. 7°38′S, long. 152°53′W (N of Society Islands). Depth 4990 m. Dark brown phillipsitic clay with radiolaria and fish debris.
	Calcareous oozes from the east Pacific rise	
9	Capricorn 32 HG	Lat. 11°00′S, long. 130°24′W (E of Marquesas Islands). Depth 4245 m. Foraminiferal ooze high in ferromanganese oxide minerals.
10	Capricorn 33 HG	Lat. 10°58′S, long. 130°30′W (E of Marquesas Islands). Depth 4040 m. Foraminiferal ooze high in ferromanganese oxide minerals.
	Equatorial calcareous-siliceous oozes and clays	
11	Swedish 58	Lat. 6°44′N, long. 129°28′W. Depth 4440 m (see further Arrhenius, 1952, 2·58).
12	Chubasco 23	Lat. 6°12′N, long. 125°27′W. Depth 4500 m.
13	Capricorn 48 BG1	Lat. 5°45′N, long. 124°02′W. Depth 4125 m.
14	Swedish 59	Lat. 3°05′N, long. 133°06′W. Depth 4370 m (*op. cit.*, 2·59).
15	Swedish 60	Lat. 1°35′N, long. 134°57′W. Depth 4540 m (*op. cit.*, 2·60).
16	Capricorn 47 BG	Lat. 0°40′N, long. 123°33′W. Depth 4230 m.
17	Swedish 61	Lat. 0°06′S, long. 135°58′W. Depth 4437 m (*op. cit.*, 2·61).
18	Swedish 62	Lat. 3°00′S, long. 136°26′W. Depth 4510 m (*op. cit.*, 2·62).
19	Capricorn 36 BG1	Lat. 10°45′S, long. 133°35′W. Depth 4490 m.
	Tertiary sediments	
20	Chubasco 15	Lat. 8°31′N, long. 125°25′W. Depth 4462 m. Tertiary clay.
21	Chubasco 40	Lat. 8°6′N, long. 125°26′W. Depth 4415 m. Tertiary coccolith ooze.
22	Mid-Pac. 40	Lat. 15°35′N, long. 177°30′E. Depth 4060 m. Tertiary coccolith ooze.
	North equatorial clays	
23	Capricorn 49 BG	Lat. 9°17′N, long. 124°9′W. Depth 4410 m. Buff siliceous clay with fine silt of quartz, feldspar and other detrital minerals, alternating with grey clay of similar composition but higher in manganese.
24	Capricorn 49 BP	Position and depth as 49 BG. Sediment as in 49 BG. Lower part of core grey from manganese micronodules. Sequence similar to core 54 of the Swedish Deep-Sea Expedition (Arrhenius, 1952 2·54).
25	Capricorn 50 BG2	Lat. 14°55′N, long. 124°12′W. Depth 4270 m. Sediment similar to Capricorn 49.

Table 1—*continued*

26	Capricorn 50 BP	Location and depth as Capricorn 50 BG2. Buff clay as in Capricorn 50 BG2, unconformally resting on dark reddish brown, partly phillipsite rich, Tertiary clay.
27	Yoyo 2P, 3G, 7P	Lat. 20°49·5′N, long. 125°15′W. Depth 4550 m. Brown, homogeneous clay with relatively high content of quartz, plagioclase, biotite and muscovite.
28	Mid-Pac. 38	Lat. 19°01′N, long. 177°19′W (foothills of Mid-Pacific Mountains). Depth 4774 m. Alternating dark and light brown clay.
	Hawaiian clays and volcanic mud	
29	NH (Navy-Hawaii) 9	Lat. 21°41·2′N, long. 157°28·5′W. Depth 3027 m. Globigerina ooze with abundant sand-silt sized pyroclastics.
30	NH 12	Lat. 22°49·0′N, long. 156°50·3′W. Depth 4484 m. Dark brown clay.
31	NH 13	Lat. 23°21·8′N, long. 156°28·7′W. Depth 4254 m. Dark brown clay.
32	NH 14	Lat. 24°07·5′N, long. 156°03·8′W. Depth 4466 m. Dark brown clay.
	Clays from Baja California Seamount Province	
33	Wigwam 5	Lat. 27°37·8′N, long. 124°25·7′W. Depth 4400 m. Dark brown, homogeneous clay.
34	NG (Navy-Guadelope) 2	Lat. 28°42′N, long. 120°12′W. Depth 3550 m. Dark brown, homogeneous clay.
35	NG 3	Lat. 27°09·N, long. 119°29′W. Depth 4100 m. Dark brown, homogeneous clay.
	North Pacific sediments	
36	Ck (Chinook) 2	Lat. 35°09′N, long. 157°17′W. Depth 5600 m. Brown clay alternating with dark brown clay.
37	Ck 4	Lat. 42°30′N, long. 162°08·2′W. Depth 5350 m. Brown clay, alternating with dark brown clay.
38	Ck 8	Lat. 53°01′N, long. 176°15′W. Depth 3660 m. Bering Sea. Diatomaceous sediment with volcanic ash layers.
39	Ck 9	Lat. 52°25′N, long. 176°24′W. Depth 3440 m. Bering Sea. Similar to Ck 8.

successfully undertaken on fractions with grain sizes larger than 3·2 μ. Tetrabromoethane was used as a heavy liquid and benzene as a diluent, in order to permit subsequent collection of the minerals on membrane filter pads (Millipore Type HA). The magnetic separation was carried out with a Franz Isodynamic Separator, using the normal feeding method along an inclined chute for grain size fractions larger than 32 μ. Magnetic separation of finer particles was achieved by settling of a dilute suspension through a glass tube, mounted vertically between the pole shoes of the separator.

2.25. *Chelative dissolution.* A separation method based on the preferential dissolution of oxyde-aquate minerals in solutions containing chelating agents was devised by TAMM (1932), who used oxalate ion as the complexing group.

In recent years water soluble chelating agents have been found (see, for example, MARTELL and CALVIN, 1952) with stability constants of the metal chelates, which are generally much larger than the stability constants of the corresponding oxalate metal chelates (Table 2).

In connection with investigations of the mineral chemistry of fine grained sediments where detrital igneous minerals are present together with authigenic phases, it is of interest to establish the partition of different elements between the sedimentary components. For this purpose the present authors attempted to use chelative dissolution with ethylene diamine tetra-acetate ion (EDTA) and a survey was made of the solubilities of a number of minerals in EDTA. The aim of the treatment of sediment samples with EDTA was to remove the readily soluble phases completely, leaving the rest of the minerals as intact as possible. To test to what an extent the latter aim was fulfilled, a series of experiments were performed, where the minerals, expected to be resistant to chelative dissolution were suspended in EDTA and their rate of dissolution determined. The conditions were such that non-resistant phases were completely dissolved. The soluble minerals present in the samples investigated were mainly the manganese oxide minerals (BUSER and GRÜTTER, 1956) and microcrystalline apatite (ARRHENIUS, BRAMLETTE, and PICCIOTTO, 1957).

Table 2. Stability constants for oxalate and EDTA chelates (from MARTELL and CALVIN, 1952)

Metal ion	Log K (oxalate)	Log K (EDTA)
Mg^{+2}	2·6	8·7
Ca^{+2}	3·0	10·6
Sr^{+2}	2·5	9·6
Ba^{+2}	2·3	7·8
Mn^{+2}	3·9	13·4
Fe^{+3}	10·0	25·1
Co^{+2}	4·7	16·1
Ni^{+2}	5·3	18·4
Cu^{+2}	8·3	18·3
Zn^{+2}	4·7	16·1

Five per cent EDTA buffered to a pH of 8 with ammonia was used as a standard solution for the dissolution experiment. The minerals were ground and samples prepared with a comparatively narrow grain size range by settling and decantation. The size range used was 3·2–10 μ equivalent diameter, except in the case of titanite, where the range was 1·0–3·2 μ. The surface area exposed to the solvent was therefore approximately known, and although varying shape factors involve a minor uncertainty, the results can at least roughly be expressed in mass dissolved per unit surface area and unit time. The mineral sample powder was suspended in the EDTA solution and kept at 100°C for 2 hr, agitated by a magnetic stirrer. After filtering and determination of the weight loss, the powder was again suspended and the dissolution experiment repeated in order to establish any change of the dissolution rate with time.

The results (Table 3) show that there is indeed a progressive decrease of the dissolution rate with time in most cases, probably due to the formation of structurally disturbed and therefore more easily soluble surface layers on the mineral grains at grinding. The formation, during the experiment, of a leached surface layer progressively slowing down diffusion of the solvent and the solute, may also contribute to this effect.

Arranged in approximate order of increasing rate of dissolution, the minerals investigated appear as follows: biotite, titanite, goethite, magnetite, rutile, hematite, lepidocrocite, nontronite, and augite. Calcite appears to have a still higher rate than the most rapidly soluble of these minerals, but was not investigated quantitatively. The very rapid dissolution occurring in the ferromanganese oxide minerals and microcrystalline apatite depends primarily on the large interior surface area of these minerals; this was found to be of the order 150–200 m^2g^{-1} both for the composite manganese nodule material as determined by Buser and Grütter (1956), employing gas adsorption technique, and for the apatite by Arrhenius, Bramlette, Picciotto, Chodos and Godijn (in preparation) from X-ray diffraction data. Due to the high rate of dissolution of these two minerals, accurate rate values could not be determined with the technique employed, but approximate values of 100–200 mg m^{-2} hr^{-1} were obtained, using the surface area data quoted above.

Table 3. Weight loss by dissolution in EDTA

Mineral or rock	Run No.	Weight loss (mg m^{-2} hr^{-1})
Titanite	1	39
	2	15
	3	11
Rutile	1	42
Augite No. 2 [a]	1	98
Augite No. 3 [b]	1	470
	2	340
Hematite	1	70
	2	46
Magnetite	1	36
	2	32
Lepidocrocite [c]	1	175
	2	90
Goethite [d]	1	25
	2	24
Biotite	1	17
	2	1
Nontronite A [e]	1	100
	2	62
Nontronite B [e]	1	100
	2	160
Balsaltic glass [f]	1	96
	2	112

[a] Hybia, Ont., U.S. Nat. Hist. Mus.
[b] Franklin, N.J., U.S. Nat. Hist. Mus.
[c] Princetown, Pa., U.S. Nat. Hist. Mus.
[d] Pikes Peak, Colo., U.S. Nat. Hist. Mus.
[e] API standard
[f] Douglas Creek, Wash., U.S. Nat. Hist. Mus.

In the study of the distribution of elements, reported in the following, chelative dissolution was used in some cases to indicate the localization of the elements in question in a mineral or in a group of minerals. The procedure is exemplified by the results given in Table 4. From this it is evident that the amount of insoluble magnesium, boron, copper, and vanadium increases with increasing content of clay minerals, and it is therefore assumed that most of the insoluble fractions of these elements are constituents of these minerals. Conversely, the soluble fractions of the same elements are believed to be the amounts sorbed to or structurally bonded in apatite, phillipsite, and in this case to a lesser extent, ferromanganese oxide minerals. Further references to similar interpretations are given in Section 5.

Table 4. Percentage loss of the total amount of individual elements at treatment with EDTA of fractions of sample Cap. 33 BG. The original percentage concentrations of the elements in the sample fractions are shown in the column marked "Orig."

Oxide	Grain size fraction							
	$>32\ \mu$		$10–32\ \mu$		$3–10\ \mu$		$1–3\ \mu$	
	Loss	Orig.	Loss	Orig.	Loss	Orig.	Loss	Orig.
MgO	100	0·8	45	0·9	35	2·2	30	4·6
SrO	100	0·14	100	0·11	83	0·08	57	0·08
B_2O_3	100	0·022	43	0·028	33	0·021	6	0·080
CuO	66	0·068	58	0·077	20	0·120	19	0·310
V_2O_5	50	0·026	25	0·015	15	0·020	7	0·054
					Amorphous ferric iron oxide–silicates, and clay minerals			
Most frequent minerals	Apatite Phillipsite (MnO_2)		Phillipsite Apatite (MnO_2)		Phillipsite Apatite (MnO_2)		Phillipsite (MnO_2)	

2.3. *Elemental analysis*

In order to obtain a maximal coverage of elements in a large number of samples, most of the analyses reported herein were made by emission spectrographic techniques. The methodology is fully described by HARVEY (1950), who carried out most of the analyses. Each sample was subjected to both an a.c. spark and d.c. arc analysis for the major and minor elements respectively. Some of the determinations of barium, titanium, and zinc required either greater accuracy or were outside of the limits of assay of the emission method. Such analyses were made by X-ray fluorescence analysis and the procedures and accuracy of measurement are given by LEWIS and GOLDBERG (1956). For the elemental analysis of microscopic crystals and aggregates the Castaing X-ray microanalyser was used (CASTAING, 1952).

Although the utmost in accuracy and reproducibility was sacrificed for a large number of analyses in using the emission spectrographic technique, the errors in the results have placed but minor limitations upon the interpretation of the data. A number of tests for the reproducibility of results were made to ascertain the differences in values from one series of runs to another which may have been several years apart. Two samples, 49 BP 120 and 50 BP 108, were analysed at intervals of over a year. The analyst was unaware that he was performing duplicate analyses. The results are given in Table 5. Only four elements showed variations in either of the samples by a factor of 2 (strontium, barium, boron, and zirconium) and the variations were in the same direction by essentially the same factor. The majority of elements show variations of under 25 per cent.

Table 5. Duplicate analyses of sediment samples by emission spectroscopy

	49 BP 120		50 BP 108	
	Series A	Series B	Series A	Series B
SiO_2	56	57	61	57
Al_2O_3	16·5	21	15	20
Fe_2O_3	5·7	6·4	6·6	7·0
TiO_2	0·63	0·65	0·72	0·60
MgO	2·6	3·3	2·1	2·9
CaO	2·6	2·3	1·5	2·2
Na_2O	5·9	5·5	3·5	5·1
K_2O	4·1	2·6	3·2	3·3
SrO	0·030	0·064	0·23	0·055
BaO	1·25	0·35	0·58	0·260
B_2O_3	0·046	0·110	0·05	0·120
MnO	0·20	0·16	0·91	0·69
Ga_2O_3	0·002	0·0037	0·0018	0·0027
NiO	0·019	0·017	0·023	0·020
CuO	0·19	0·15	0·14	0·14
Co_2O_3	0·006	0·007	0·015	0·013
Cr_2O_3	0·006	0·008	0·009	0·007
V_2O_5	0·016	0·028	0·025	0·023
ZrO_2	0·016	0·033	0·017	0·022
Y_2O_3	0·01	0·008	0·012	0·008

To test the accuracy of the measurements, thirty-two different glauconite samples were analysed by precision chemical techniques (the methods will be described elsewhere) and by emission spectrography. The data are presented in Fig. 2 and Table 6 and represent three separate series of analyses made over a 3 year period. The iron values are consistently low by 20 per cent, and this fact is reflected in the higher number of positive deviations from the true value of silicon, aluminium, calcium, and potassium. The magnesium values were low by an average of 25 per cent.

Wedepohl (personal communication) re-ran nine of our samples and found the average nickel contents of his precision spectrographic analyses to be similar to our average, while his average vanadium value was about one-half of the one reported herein. This discrepancy will be discussed in Section 5.9.

3. The Nature of the Dissolved Chemical Species in the Ocean

Studies on the types of dissolved chemical species of elements in marine waters can provide important criteria for the interpretation of the behaviour of elements in the major sedimentary cycle. Two elements that show a similar quantitative distribution of positively, negatively and uncharged species of the same type may have like geochemical paths. On the basis of available thermochemical data the nature of the dissolved chemical species of some of the metals can be described with confidence; on the other hand there is a nearly complete lack of data for the transition elements.

The basis of computing the speciation of elements in aqueous solutions depends upon the formation of complex ions and ionic associations (an excellent survey of our present knowledge of these phenomena may be found in Robinson and Stokes, 1955). Non-associated electrolytes exist in the form of simple anions and cations, probably solvated. The associated electrolytes include those solutes that exist as undissociated, covalent molecules as well as ions; and the ion-pair electrolytes in which association arises as a result of purely electrostatic attraction between oppositely charged ions.

Table 6. Accuracy of the spectrographic analysis of thirty-two different glauconite samples

Element	Positive deviations from true value			Negative deviations from true value	
	Av. wt.% in samples	No.	Average deviations in element percentage	No.	Average deviations in element percentage
Si	24	21	2·0	11	1·1
Al	5·5	26	1·7	6	0·5
Fe	17	0	—	32	3·7
Ti	0·10	26	0·03	6	0·03
Mg	2·8	4	0·3	27	0·7
Ca	1·0	25	0·42	5	0·61
Na	0·60	12	0·32	17	0·27
K	5·2	22	1·1	6	0·64

With respect to the major cations of marine waters, sodium, potassium, magnesium and calcium, it is of interest to consider the possible existence of associated electrolytes with the major anions, chloride and sulphate. Considerations on possible combinations of the alkali and alkaline earth metals with chloride ion may be neglected inasmuch as no evidence for such associations has been reported. Denney and Monk (1951) tabulate the dissociation constants of the associated electrolytes formed between the metals sodium, potassium, magnesium, and calcium and sulphate. Using these constants ($K_{Na_2SO_4} = 0{\cdot}19$ and $K_{K_2SO_4} = 0{\cdot}11$) and the values of the activity coefficients for uni-divalent salts from Latimer (1952, p. 354) of 0·4 for solutions with an ionic strength of 0·7, similar to that of sea-water, it is readily calculated that for the oceanic waters (Na = 0·45 M and $K = 0{\cdot}01$ M) much less than 1 per cent of either of these metals can be associated

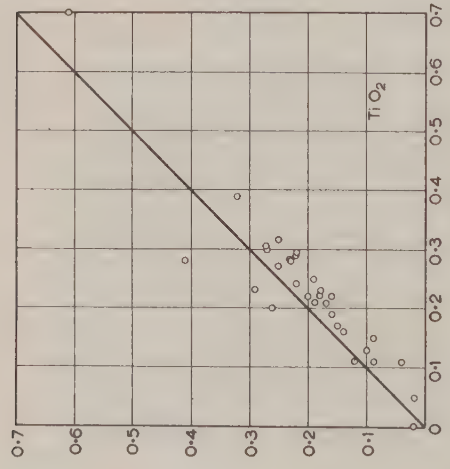

2(a)

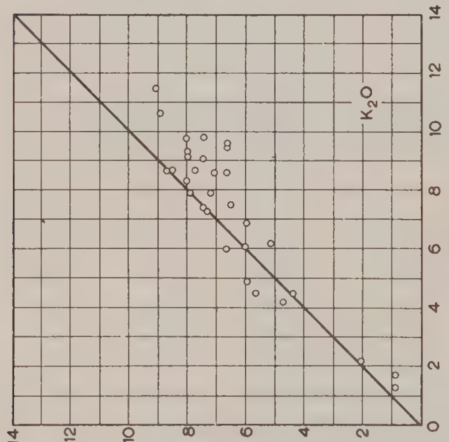

2(b)

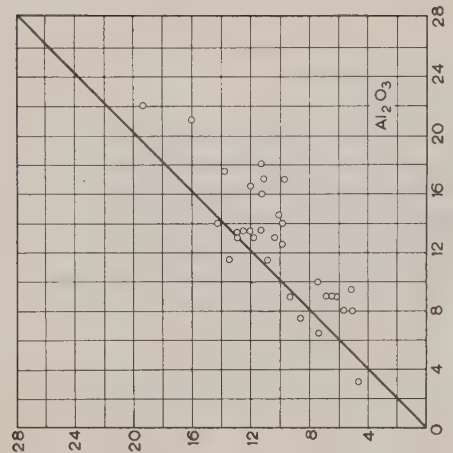

2(c)

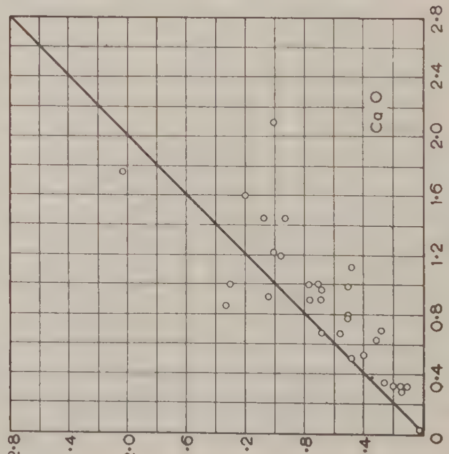

2(d)

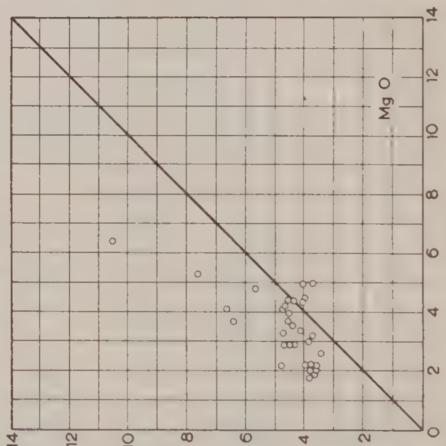

2(e)

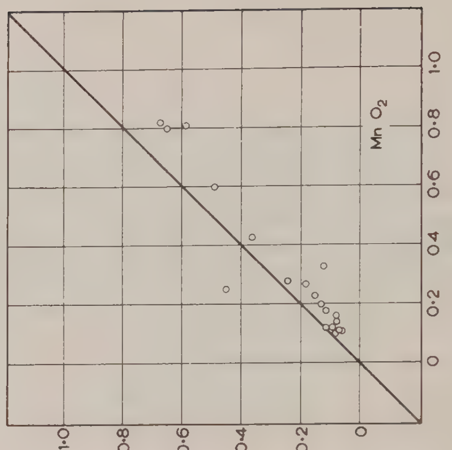

2(f)

(768)

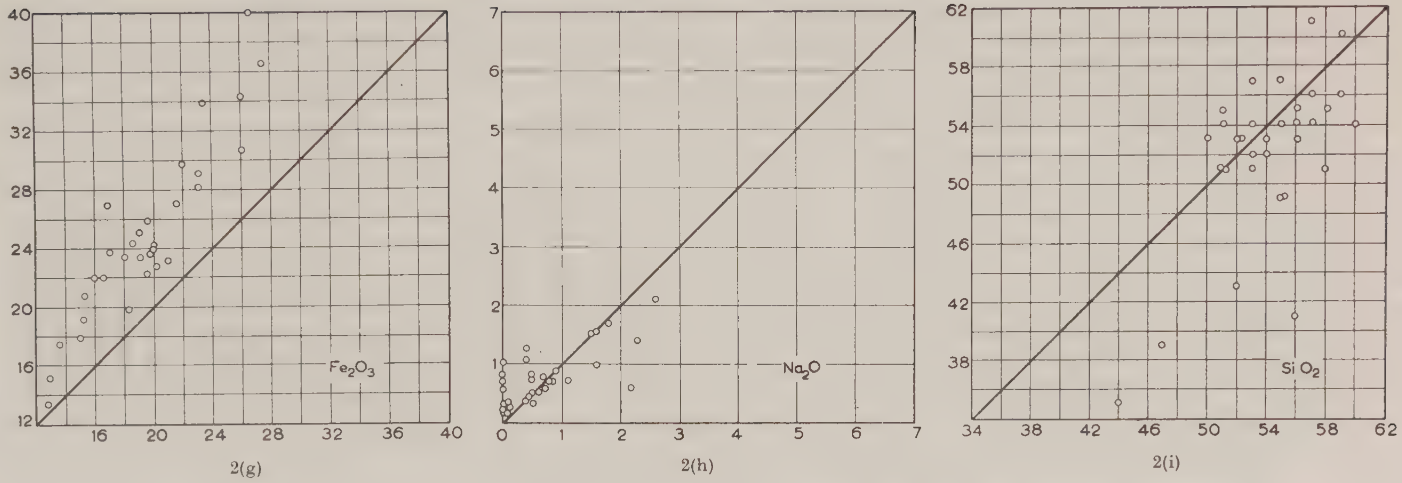

Fig. 2. Comparison of percentage yields obtained by spectrographic methods (abscissae) and colorimetric, volumetric, X-ray spectrometric or gravimetric methods (ordinates).

with sulphate ions. Further, the sulphate ion concentration (0·028 M) would not be significantly affected by such minor interactions.

Higher amounts of the alkaline earth sulphates probably exist in marine waters on the basis of such calculations. The dissociation constants of all divalent ions cluster about 0·005 for the sulphates (Robinson and Stokes, 1955, p. 405) and hence it appears justifiable to consider the magnesium and calcium as a single element for simplicity in calculations. Taking the sum of these ions in sea-water as 60 m moles/l., the sulphate concentration as 28 mM, and the activity coefficients for di-divalent salts as 0·12 (Latimer *op. cit.*), the amount of alkaline earth sulphates is 4 mM and accounts for about 7 per cent of the total content of these elements.

For the divalent group B metals such as nickel, copper, cobalt, and zinc, whose sea-water concentrations are of the order of 10^{-7}–10^{-8} M, approximately 10 per cent of the total amounts will be as associated sulphates. This observation complements those of Goldberg (1954) and Krauskopf (1956), who have emphasized the quantitative importance of the chloro-complexes of these elements. For copper, over 90 per cent of the non-sulphate associated forms would exist as the hydrated divalent ion or the $CuCl^+$ complex with but minor amounts of $CuCl_2$, $CuCl_3^-$, and $CuCl_4^{--}$. Similar speciation is expected for the other divalent group B metals whose hydrated ions have similar radii (Robinson and Stokes, 1955).

The work of Davies (1930) on the dissociation constant of $LaSO_4^+$ ($K = 2{\cdot}12 \times 10^{-4}$) suggests the existence of this pair and the corresponding ones for other rare earths in the marine environment. However, the absence of adequate concentration values of the rare earths in the oceans and of activity coefficients makes any computation unsatisfactory.

A second group of metals, including gold, silver, and mercury, probably occur principally as chloro-complex anions. Using the stability constant of Jonte and Martin (1952) for $AgCl_2^-$, a silver ion concentration in sea-water of 3×10^{-9} M, chloride ion concentration of 0·54 M, activity coefficients for silver and chloride ions of 0·7, it is readily calculated that over 99 per cent of the silver in sea-water exists as the di-chloro-complex. Similar calculations for mercury and gold suggest the dominance of the forms of $HgCl_4^{=}$ and $AuCl_4$ respectively (Lindgren, Johnson and Sillén, 1947; Bjerrum, 1948).

Other possible ion associations with the less abundant anionic species of sea-water as bromide, iodide, phosphate, bicarbonate, carbonate, hydroxide, and silicate could overshadow any of the above postulated species. However, at the present time dissociation constants are not available. Further, polynuclear complexes as described by Sillén (1954) may well exist in the marine environment. Mention should be made of possible organic complex and chelate formation. Again, we have no knowledge of the types of dissolved carbon compounds in the ocean, which exist at concentration of ca. 5 mg/l. of carbon.

4. DISTRIBUTION OF ELEMENTS IN THE DISSOLVED AND SORBED PHASES OF THE SEDIMENT

As pointed out in Section 2.21, dialysis of the sediment in distilled water probably changes the equilibrium between the pore solution and the surface of the solid, and the dialysate in this case therefore has to be regarded as representative of the sum of dissolved and weakly sorbed species. The composition of the dialysate from five sediment samples is compared with the composition of sea-water in Table 7. Concentrations are expressed in mg/kg of pore solution and sea-water respectively.

Due to the high concentration of sodium, this element could not be accurately assayed by the spectrochemical methods used, and is omitted from the table. The composition of the sorbate exchanged against ammonium acetate (Section 2.22) and subsequently separated by dialysis, is shown in Table 8 together with the exchangeable fraction of the total amount of each element.

Within the limits of analytical error and variability, potassium, magnesium, and calcium occur in the same concentration in the dialysate as in sea-salt.

As is evident from Table 8, the proportions of the alkali and alkaline earth elements are drastically different in the sorbed phase from those in sea-water and in the dialysate. Calcium is in the sorbate in excess over magnesium and potassium, and both of these ions are more abundant than, or in one case equally concentrated as, sodium. The reason for the preponderance of calcium over magnesium in the exchangeable phase, in spite of the more than three times higher concentration of magnesium in the sea-water and in the pore solution, may be explained by the greater tendency for fixation of magnesium, shown by the fact that there is about twice as much magnesium as calcium in the colloidal fraction (Fig. 5, Cap. 50 BP) of the sediment after ion exchange and chelative dissolution. The potassium/sodium ratio of the sorbate is especially high in Cap. 31 BG, undoubtedly due to the high content in this sample of the potassium zeolite phillipsite. An amount of aluminium, corresponding to about a hundred times the concentration in the open ocean, is present in the dialysate, but only small additional amounts are exchangeable against ammonium ion, and appear in the sorbate. A considerable fraction of the chromium in the sediment gel appears to be loosely bound, so that a thousandfold concentration above sea-water occurs in the dialysate, and an amount, varying between 0·1 and 5 per cent of the total chromium is exchangeable against alkali cations (Table 8).

Iron and manganese are concentrated fifty to a few hundred times above the sea-water contents in the dialysate. Only small additional amounts of iron are present as exchangeable ions on the solid surfaces, whereas in the case of manganese a tenth of a per cent to a few per cent of the total amount appear to be in alkali-exchangeable positions. More detailed and significant exchange experiments on manganese minerals have been carried out by BUSER and GRÜTTER (1957, in press), employing solutions of divalent radioactive manganese.

Copper shows a still higher concentration in the dialysate and a half of a per cent to a few per cent exchangeable from the mineral surfaces.

Of yttrium, scandium, and the rare-earth elements none has been detected in the dialysate, and only yttrium in the sorbate. This indicates that these elements do not occupy exchange positions. They may partly have become fixed as phosphates on the surface of the microcrystallites of the apatite and partly are relatively strongly bonded in the manganese minerals.

Titanium and vanadium also are below detectability in the pore solution, but at least a few tenths of a per cent of the total amount of these elements are exchangeable.

Table 7. Concentration (*c*) of elements in mg/kg of dialysate (dissolved and weakly bonded species) and in sea-water, and concentration ratio (*c*/*S*) between dialysate and sea-water

Sample	K		Mg		Ca		Sr		Ba		B	
	c	*c*/*S*	*c*	*c*/*S*	*c*	*c*/*S*	*c*	*c*/*S*	*c*	*c*/*S*	*c*	*c*/*S*
Cap. 31 BG	390	1·0	860	0·7	240	0·6	1·4	0·11	0·6	100	22	4·9
Cap. 21–25 HG	315	0·8	1400	1·1	550	1·4	2·9	0·22	0·3	50	15	3·3
Yoyo 7P	315	0·8	480	0·4	220	0·6	3·2	0·25	6·4	1700	11	2·4
Cap. 50 BP 0–30	520	1·4	820	0·6	270	0·7	1·7	0·13	2·7	450	20	4·4
Cap. 49 BP top	500	1·3	1600	1·3	410	1·0	2·6	0·20	0·9	150	17	3·8
Sea-water (*S*)	380	1	1300	1	400	1	13	1	0·006	1	4·5	1
	Si		Al		Cr		Fe		Mn		Cu	
Cap. 31 BG	40	10	0·45	45	0·05	1000	0·26	52	—	—	1·4	470
Cap. 21–25 HG	36	9	3·40	340	0·05	1000	1·4	280	0·21	105	1·1	340
Yoyo 7P	84	21	0·67	67	0·05	1000	0·24	48	—	—	0·6	200
Cap. 50 BP 0–30	40	10	0·72	72	—	—	0·24	48	0·13	65	1·4	470
Cap. 49 BP top	40	10	1·10	110	—	—	0·26	52	1·06	530	0·8	270
Sea-water (*S*)	4	1	0·01	1	0·00005	1	0·005	1	0·002	1	0·003	1

Table 8. Percentage concentration of elements in sorbate (*k*); and fraction (*q*) of element in sorbate in per cent of total amount of element in sample (solid + dissolved + sorbed phases)

Sample	Na		K		Mg		Ca		Sr		Ba		B	
	k	*q*	*k*	*q*	*k*	*q*	*k*	*q*	*k*	*q*	*k*	*q*	*k*	*q*
Cap. 31 BG	1·8	1·0	11	12	7	6·5	15	7·0	0·15	8·0	0·9	16	10·038	6·3
Yoyo 7P	1·7	1·1	8·7	5·0	9	11	14	21	0·25	5·3	16	63	0·016	1·1
Cap. 50 BP 0-30	6·4	4·1	6·5	4·5	5	7	10	17	0·10	5·0	6	20	0·036	4·5
Cap. 49 BP top	1·5	0·8	9·5	7·5	8	9	12	12	0·23	13	16	27	0·016	2·3
	Si		Al		Y		Ti		V		Cr		Fe	
Cap. 31 BG	1·0	0·09	0·003	0·0009	0·002	0·4	0·09	0·15	0·018	1·6	0·0012	0·22	0·019	0·006
Yoyo 7P	0·6	0·02	0·007	0·001	0·002	0·4	0·07	0·31	0·008	0·4	0·0055	2·2	0·017	0·007
Cap. 50 BP 0-30	2·1	0·08	0·003	0·0009	0·003	0·8	0·04	0·22	0·003	0·5	0·0006	0·1	0·013	0·005
Cap. 49 BP top	0·4	0·01	0·004	0·0007	0·009	1·5	0·08	0·42	0·018	3	0·0090	5	0·012	0·005
	Mn		Ni		Pb		Mo		Cu					
Cap. 31 BG	0·04	0·05	0·017	1·7	—	—	—	—	0·62	2·0				
Yoyo 7P	0·02	0·05	0·008	0·5	—	—	0·073	2·7	0·095	2·4				
Cap. 50 BP 0-30	0·45	1·9	0·023	2·8	—	—	—	—	0·062	1·0				
Cap. 49 BP top	0·12	0·13	0·007	0·4	0·007	1·2	0·018	2·2	0·036	0·4				

Nickel, lead, and molybdenum likewise are missing in the pore solution. Nickel was found in the sorbate in all four cases investigated, lead in one, and molybdenum in two. The exchangeable fraction of these metals appears to vary from half a per cent to a few per cent of the total amount in the sample.

Gallium, cobalt, silver and zirconium were detected neither in the dialysates nor in the sorbates.

Strontium is five to ten times depleted in the pore solution, and a rather large fraction of the total amount of this element is sorbed to the solid phases (Table 8).

The relatively large amounts of barium in the dialysate and in the sorbate may be explained at least partly as resulting from dissolution of microcrystalline barite during dialysis, when the sulphate ion concentration is decreased by a factor of 30–60, and during the ion exchange in ammonium acetate. A considerable fraction of the barium found in the sorbate (Table 8) is, however, certainly originally present as exchangeable cations sorbed in the zeolite structure (Section 5.4), and probably on the clay minerals, which in contact with barite are known to be able to retain enough barium to fill about 20 per cent of the exchange positions (BRADFIELD, 1932).

Boron shows a 2- to 5-fold excess in the dialysate over sea-water, and 1–7 per cent of the total amount originally present is removed from the solids at ion exchange.

Silicon as the univalent ion of monosilicic acid, or other species small enough to pass through the dialysis membrane, is ten to twenty times more concentrated in the dialysate than in sea-water. If the dissolved species are separated by centrifugation, and a less strict size limitation thus applied, still higher relative concentrations are obtained (of the order 200 mg/kg—ARRHENIUS and ROTSCHI unpublished). A steep gradient in the silicon content of the near bottom water was found by these authors at all South Pacific stations investigated, indicating a flow of dissolved silica from the bottom sediments back into the ocean.

5. DISTRIBUTION OF ELEMENTS IN THE SOLID PHASES

Table 9 gives the average chemical composition of 22 pelagic sediment cores from the eastern Pacific along with various igneous rock types and the average crustal composition of the earth. Cores Cap. 32 HG, 33 HG, NH 9, and MP 38 are calcareous oozes and the analyses are given both on a calcium carbonate-free basis and on the total material. The core descriptions and locations are presented in Table 1. Figs. 3 and 4 are a graphic representation of the data of Table 9. The ranges of the ratio of the concentration of the element in pelagic sediments to the concentration in igneous rocks are plotted for each element. The mode is noted by a small vertical line.

Fig. 5 shows some features of the chemical composition of sediment samples, which have been fractionated according to grain size, and to a limited extent according to density. Separation according to grain size corresponds to a rough fractionation of different minerals and mineral groups, and indications of the mineral localization of different elements can thus be obtained from analysis of these fractions. The details of the construction of the diagrams are given in the caption, and the conclusions drawn from the distributions are found in the paragraphs on different elements below.

Table 9. Chemical composition of

No.	Core	Si	Al	Fe	Ti	Mg	Ca	Na	K	Sr	Ba	B	Mn	Ga
1	Cap. 21 HG	21·3	10·8	6·2	0·78	1·8	3·3	4·5	2·6	0·050	0·069	0·029	1·5	0·0018
2	Cap. 23 HG	20·6	11·6	6·0	0·75	1·8	4·0	4·7	2·5	0·047	0·062	0·030	1·0	0·0018
3	Cap. 24 HG	21·4	10·3	6·2	0·84	1·9	4·7	3·8	2·4	0·055	0·093	0·030	1·2	0·0019
4	Cap. 30 BP	23·4	8·8	5·7	0·56	1·3	4·4	3·6	3·4	0·027	0·057	0·011	1·8	0·00097
5	Cap. 25 HG	22·9	8·7	6·8	1·44	2·3	3·1	3·9	2·2	0·063	0·128	0·033	1·3	0·0024
6	Cap. 31 BG	22·4	9·4	6·7	1·22	2·1	4·2	3·5	1·8	0·035	0·11	0·012	1·7	0·0014
7	Cap. 33 BG	22·0	7·8	6·2	0·36	1·9	5·9	4·4	2·2	0·041	0·26	0·0096	3·0	0·00097
8	Sw. 71	23·5	8·1	4·6	0·38	2·2	3·5	6·3	2·2	0·048	0·14	0·028	1·4	0·0016
9	Cap. 32 HG	12·0	4·4	9·2	0·39	1·5	16·3	3·7	—	0·072	0·69	0·022	2·2	—
	Cap. 32 HG ($CaCO_3$ free)	16·2	6·2	12·9	0·49	2·1	—	5·7	1·9	0·14	0·99	0·03	3·2	0·0009
10	Cap. 33 HG	3·6	1·0	3·7	0·05	0·60	3·2	2·4	—	0·076	0·30	0·012	1·2	—
	Cap. 33 HG ($CaCO_3$ free)	13·4	3·3	14·0	0·23	2·4	—	10·4	—	0·35	1·3	0·049	4·5	—
24	Cap. 49 BP	26·2	8·4	4·6	0·38	1·7	2·0	3·9	2·5	0·035	1·2	0·014	0·87	0·0017
26	Cap. 50 BP	27·5	8·0	5·0	0·43	1·5	1·1	3·1	2·9	0·021	0·60	0·016	0·48	0·0015
27	Y3G	25·8	9·9	4·9	0·50	1·8	1·1	2·6	3·5	0·038	0·37	0·034	0·58	0·0024
27	Y2P	25·7	9·4	4·6	0·45	1·6	1·3	3·2	3·5	0·047	0·51	0·030	0·82	0·0026
28	MP 38	28·7	10·3	3·5	0·43	2·4	5·8	4·1	3·1	0·061	0·16	0·031	1·6	0·0017
29	NH 9	8·1	3·9	5·0	1·06	1·6	23·9	1·5	0·71	0·093	0·078	0·032	0·12	0·0013
	NH 9 ($CaCO_3$ free)	18·7	9·0	11·6	2·5	4·3	—	3·5	1·6	0·23	0·17	0·076	0·27	0·0034
30	NH 12	22·1	11·9	6·4	1·1	2·0	3·1	3·1	1·7	0·043	0·19	0·031	0·30	0·0021
31	NH13	23·2	11·4	5·9	0·90	2·1	2·3	2·9	2·5	0·044	0·25	0·035	0·31	0·0022
32	NH 14	23·4	11·5	5·8	0·78	1·8	1·9	2·9	2·7	0·041	0·23	0·037	0·33	0·0022
33	WW 5	26·9	9·4	4·6	0·49	2·4	1·2	2·8	2·2	0·040	0·60	0·029	0·46	0·0022
34	NG 2	25·8	8·9	5·1	0·50	1·8	1·6	3·1	2·4	0·054	0·59	0·028	0·38	0·0019
35	NG 3	25·9	10·1	5·1	0·50	1·8	1·3	3·0	2·5	0·049	0·54	0·029	0·41	0·0021
36	Ck 2	24·7	7·8	5·7	0·44	2·2	2·1	2·6	2·9	0·030	0·11	0·032	1·6	0·0022
37	Ck 4	28·1	8·7	4·7	0·49	2·1	1·1	2·6	2·7	0·019	0·38	0·032	0·51	0·0031
38	Ck 8	31·2	6·0	4·0	0·33	2·3	2·9	2·6	1·1	0·036	0·10	0·014	0·14	0·0017
39	Ck 9	33·3	4·9	2·4	0·25	1·7	3·0	2·3	1·2	0·028	0·10	0·017	0·11	0·0016
1–35	Average	23·0	9·2	6·5	0·73	2·1	2·9	4·0	2·5	0·071	0·39	0·030	1·25	0·0019
	Pelagic Deposits$^{(m)}$	—	—	—	0·40	—	—	—	—	0·06	0·81	—	—	—
	Basalts	23·3$^{(a)}$	8·5$^{(a)}$	8·8$^{(a)}$	0·84$^{(a)}$	3·8$^{(a)}$	6·5$^{(a)}$	2·4$^{(a)}$	1·2$^{(a)}$	0·05$^{(b)}$	0·007$^{(c)}$	0·0005$^{(c)}$	0·15$^{(e)}$	0·0012$^{(d)}$
	Polynesian basalts$^{(n)}$	22·0	7·9	9·0	1·7	5·5	6·3	2·1	1·2	0·086	0·04	—	0·14	0·002
	Granites	33·1$^{(a)}$	7·7$^{(a)}$	2·5$^{(a)}$	0·25$^{(a)}$	0·54$^{(a)}$	1·4$^{(a)}$	2·6$^{(a)}$	3·4$^{(a)}$	0·02$^{(b)}$	0·048$^{(c)}$	0·001$^{(c)}$	0·1$^{(e)}$	0·0017$^{(d)}$
	Igneous rocks	27·0$^{(f)}$	8·0$^{(f)}$	—	0·5$^{(f)}$	2·0$^{(f)}$	3·5$^{(f)}$	2·8$^{(f)}$	2·5$^{(f)}$	0·03$^{(f)}$	0·025$^{(f)}$	0·003$^{(f)}$	0·1$^{(f)}$	0·0015$^{(d)}$
	Igneous rocks$^{(m)}$	—	—	—	0·44	—	—	—	—	0·022	0·099	—	—	—

(a) DALY (1933).
(b) TUREKIAN (1955).
(c) GOLDSCHMIDT (1954).
(d) SANDELL (1949).
(e) TUREKIAN (1956.
(f) SANDELL and GOLDICH (1943).
(g) SANDELL (1952).

(774)

pelagic sediments in weight per cent

Ni	Cu	Co	Cr	V	Pb	Be	Mo	Zr	Yb	Y	La	Sc
0·028	0·077	0·031	0·006	0·043	0·017	—	0·0065	0·020	0·0019	0·016	0·010	0·0018
0·034	0·063	0·023	0·008	0·047	0·016	—	0·0058	0·019	0·0021	0·024	0·014	0·0023
0·043	0·072	0·029	0·007	0·046	0·020	—	0·0066	0·020	0·0023	0·028	0·016	0·0022
0·031	0·068	0·019	0·0048	0·014	0·021	0·00036	0·0036	0·0096	0·0034	0·031	0·016	0·0049
0·030	0·071	0·023	0·014	0·060	0·017	—	0·0051	0·026	0·0017	0·016	0·012	0·0021
0·019	0·064	0·017	0·011	0·023	0·026	0·00061	0·0021	0·016	0·0014	0·013	0·0044	0·0026
0·039	0·14	0·024	0·014	0·020	0·021	0·00036	0·0008	0·013	0·0039	0·039	0·025	0·0044
0·047	0·011	0·027	0·002	0·042	0·011	—	0·0101	0·018	0·0029	0·039	0·024	0·0030
0·048	0·087	0·013	0·002	0·033	0·012	—	0·0087	0·019	0·0022	0·026	—	—
0·064	0·105	0·018	0·004	0·060	0·018	—	0·0107	0·026	0·0032	—	0·023	0·0019
0·016	0·010	0·005	0·0015	0·037	—	—	—	0·008	—	0·009	—	—
0·056	0·038	0·019	0·007	0·18	—	—	—	0·039	—	0·031	—	—
0·031	0·20	0·011	0·0037	0·012	0·012	0·0003	0·0017	0·012	0·0013	0·013	0·0040	0·0037
0·017	0·12	0·0098	0·0062	0·013	0·011	0·00036	0·0011	0·013	0·0011	0·0094	0·0029	0·0028
0·025	0·050	0·012	0·009	0·042	0·008	—	0·0044	0·018	0·0008	0·005	0·005	0·0017
0·035	0·077	0·019	0·005	0·043	0·009	—	0·0055	0·022	0·0012	0·010	0·008	0·0021
0·083	0·093	0·031	0·005	0·025	0·008	—	0·011	0·017	—	0·0038	0·033	0·0040
0·009	0·008	0·001	0·019	0·041	—	—	—	0·010	—	—	—	—
0·028	0·017	0·004	0·04	0·097	—	—	—	0·022	—	—	—	—
0·014	0·035	0·005	0·12	0·045	—	—	0·0022	0·016	—	0·003	—	0·0018
0·014	0·037	0·005	0·013	0·040	—	—	0·0021	0·017	—	0·003	—	0·0014
0·014	0·040	0·005	0·010	0·038	—	—	0·0021	0·017	—	0·003	—	0·0012
0·016	0·066	0·009	0·010	0·031	—	—	0·0037	0·018	—	0·005	—	0·0022
0·014	0·035	0·003	0·006	0·035	—	—	0·0024	0·014	—	0·002	—	0·0022
0·013	0·041	0·004	0·007	0·034	—	—	0·0028	0·014	—	0·002	—	0·0010
0·026	0·038	0·009	0·008	0·021	0·010	—	—	0·023	—	0·017	—	0·0028
0·016	0·027	0·006	0·010	0·012	0·005	—	—	0·020	—	0·004	—	0·0031
0·003	0·010	0·001	0·006	0·014	0·012	—	—	0·010	—	0·002	—	0·0020
0·002	0·009	0·001	0·004	0·012	0·012	—	—	0·010	—	0·002	—	0·0018
0·032	0·074	0·016	0·0093	0·045	0·015	—	0·0045	0·018	0·0021	0·015	0·014	0·0025
0·026	—	0·009	0·0082	0·015	—	—	—	0·013	—	—	0·022	0·0031
0·013(e)	0·0087(e)	0·0025(f)	0·0172(e)	0·02(c)	0·0006(l)	0·0001(g)	0·0001(h)	—	—	—	—	—
0·04	—	0·006	0·044	0·05	—	—	—	0·023	—	0·002	—	—
0·005(f)	0·003(f)	0·008(c)	0·001(c)	0·005(c)	0·0019(l)	0·0003(g)	0·0001(h)	—	—	—	—	—
0·004(k)	0·004(k)	0·002(i)	0·02(i)	0·015(i)	0·0015(l)	0·0002(g)	0·0001(h)	0·0156(h)	0·003(i)	0·003(i)	0·002(i)	0·0005(i)
0·0079	0·0020	—	0·010	0·02	—	—	—	—	—	—	0·0045	0·0020

(h) KURODA and SANDELL (1954).
(i) FLEISCHER (1953).
(j) DEGENHARDT (1957).
(k) MORITA (1955).
(l) WEDEPOHL (1956).
(m) YOUNG (1954).
(n) NOCKOLDS and ALLEN (1956).

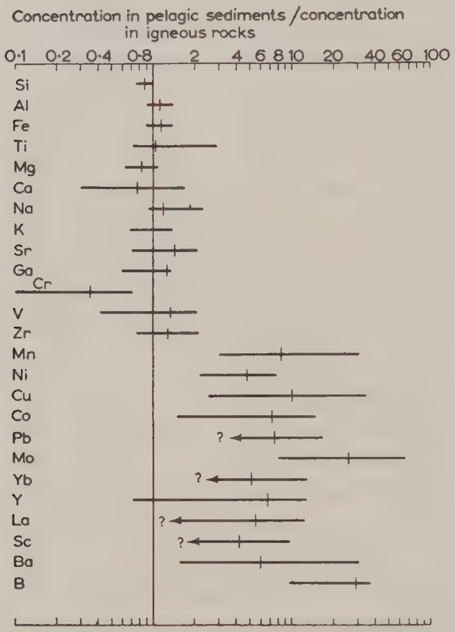

Fig. 3. Ratios of average elemental abundances in Pacific pelagic sediments and igneous rocks. Ranges are indicated by the lengths of the horizontal lines, and modes by a short vertical line.

5.1. *Silicon, aluminium, and gallium.* The overall range of silicon values is somewhat lower than in igneous rocks, and this probably results from a large portion of the silicon being incorporated into siliceous oozes and into continental sediments high in quartz. The silicon is mainly contained in the clay minerals and further in phillipsite in cores Cap. 31 BG; opal, quartz, and feldspar in Cap. 49 BP; quartz, feldspar, and opal in Cap. 50 BP; and quartz, feldspar, biotite, and muscovite in Y3G and Y2P. The quartz contents of some of these cores (49 BP, 50 BP, Y3P, NH 12, NH 13, and Wigwam 5) varies between 9 and 16 per cent. Both quartz and feldspar are on the average coarser in the north equatorial Pacific (cores Yoyo 7P and Cap. 50 BP), than further south and concentration of quartz is also higher in the northern area. More elaborate investigations upon the distribution and characteristics of detrital minerals have been carried out by REX and GOLDBERG (in preparation).

A proportionality is observed between average crystal size and concentration of phillipsite. This probably depends on the longer time available for individual crystals to grow in areas of a low rate of deposition, where high concentrations of phillipsite and other marine hydrogenous minerals are found.

The aluminium concentrations show a small variation about the igneous rock average. In the sediments, only a fraction of a per cent of the aluminium can be

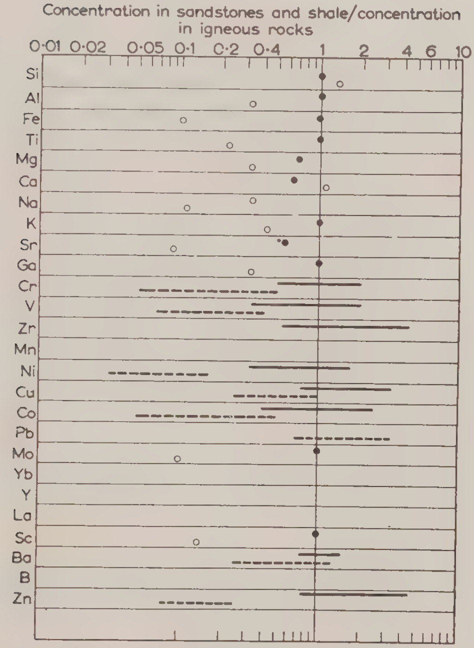

Fig. 4. Ratios of average elemental abundances in sand stones and igneous rocks (ranges marked by dashed lines, averages by open circles), and in shales and igneous rocks (solid lines and circles). Data for igneous rocks from FLEISCHER (1953) and for sandstones and shale from GOLDSCHMIDT (1954), RANKAMA and SAHAMA, (1949), and KRAUSKOPF (1956).

removed by chelative dissolution. The main occurrence of aluminium is in the aluminosilicates listed above.

A high organic productivity in the surface layer of the ocean should result in a high content of diatomaceous and radiolarian silica relative to inorganic constituents in the bottom deposit. This distribution has been verified in a north–south profile through the east equatorial Pacific (ARRHENIUS, 1952, 1.3), and is further illustrated by the data in Table 10, which presents the average ratio Si/Al in sediment cores as a function of latitude. The general increase of the ratio in the equatorial zone of high productivity is evident. Another area with high values for the ratio Si/Al is the sub-arctic productivity zone, where, in the absence of calcium carbonate, diatomaceous remains are the dominant component in the deposits (core Ck 8 and Ck 9, Table 10).

The gallium content of the clays is for all practical purposes constant and corresponds to the igneous rock value.

5.2. *Sodium, potassium and lithium.* Both sodium and potassium occur in concentrations comparable to those of igneous rocks. It should be emphasized that the unfractionated sediment samples contain the salts of the pore solution. The principal mineral group, the clays, contain the bulk of the potassium, and

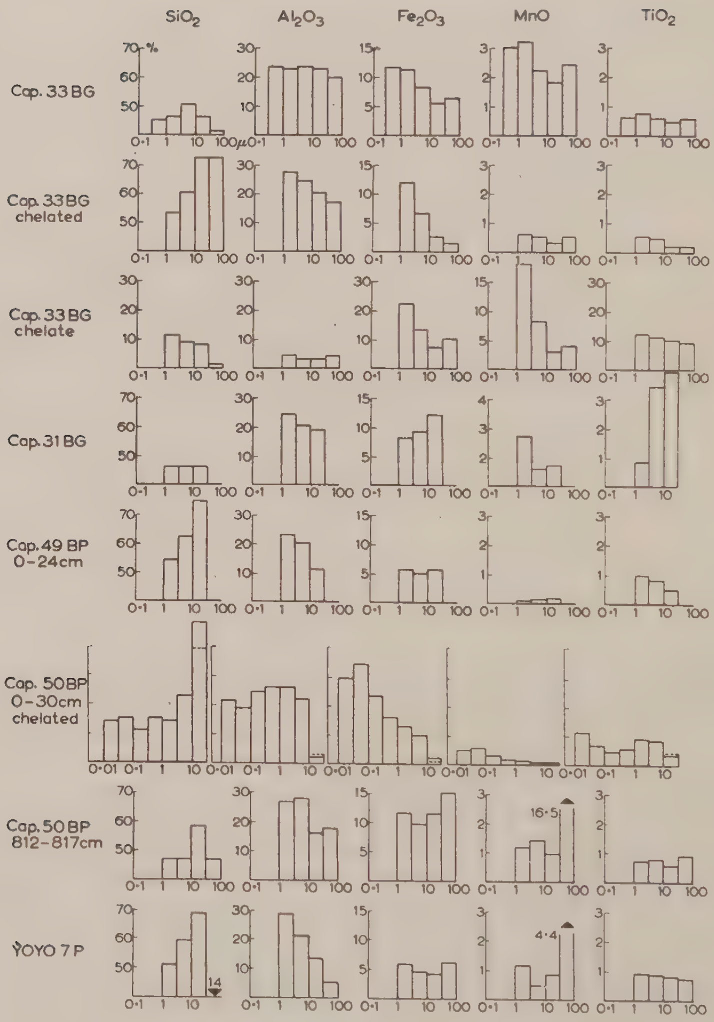

Fig. 5(a).

Fig. 5. Composition of grain size fractions of pelagic clay sediments. The different samples are grouped vertically, and the distributions of properties horizontally. Within the histograms concentrations of element oxides in percent, and size frequencies in percent, are represented by the ordinates. The particle size in μ, on a logarithmic scale, is indicated by the abscissae.

For location and type of samples, see Table 1. For explanation of the chelation procedure (see Section 2.25).

In the sample Cap. 50 BP 0–30 cm, the size fraction 10–32 μ has been subdivided into two density fractions, one mainly containing grains with a density less than 2·5 (full line in

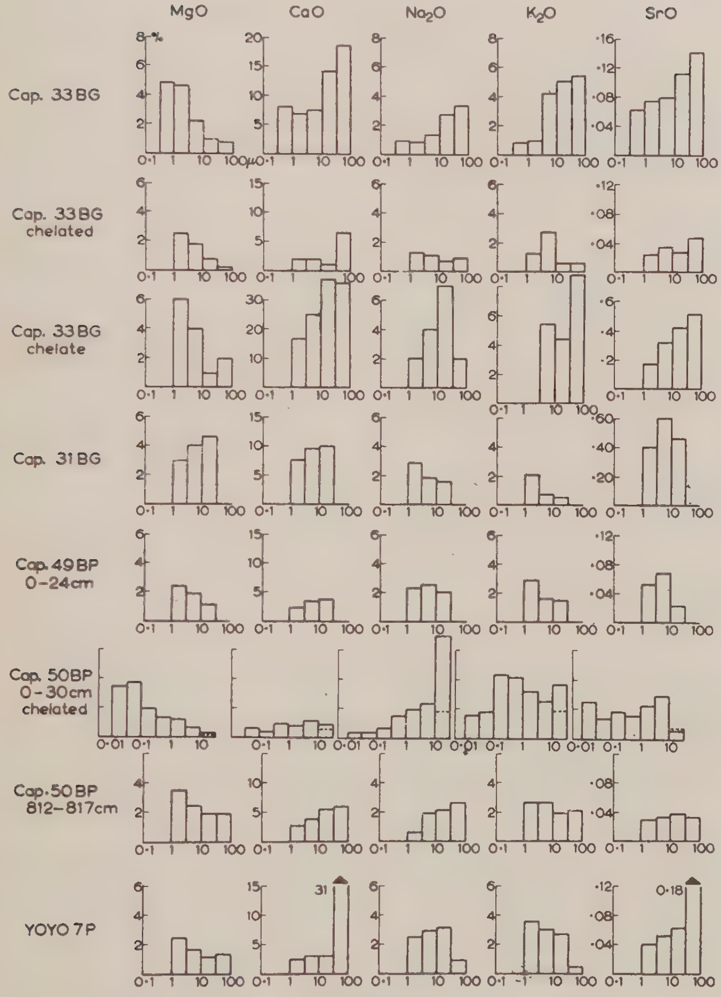

Fig. 5(b).

histograms), the other mainly with particles denser than 2·5 (dashed line in histograms). In this sample ordinate units have been omitted for space reasons. The ordinate scale is in this case always the same as in the corresponding histograms for the adjacent sample Cap. 50 BP, 812–817.

In cases where off-scale high concentrations occur, these have been indicated by a number drawn at the side of an open histogram rectangle, marked by an arrow, pointing upward (ex. BaO in Yoyo 7P, 32–100 μ).

Arrows pointing downward indicate concentrations below the sensitivity limit (ex. Co_2O_3 in Cap. 33 BG) or if a figure is simultaneously given, below the range of the scale (ex. SiO_2 in Yoyo 7P, 32–100 μ).

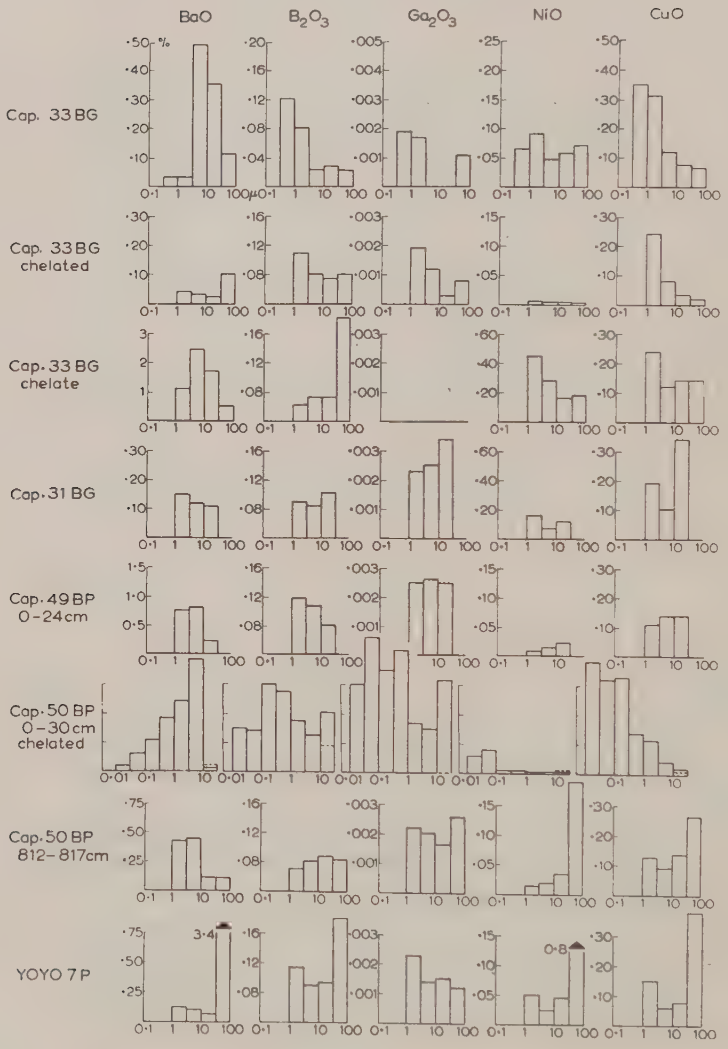

Fig. 5(c).

much of the sodium, yet individual minerals often show higher concentrations. Potassium appears concentrated in phillipsite,* and sodic feldspars contribute significantly to the total sodium content.

---

* The composition of a mixture of phillipsite and apatite is shown by the analysis of the coarse fraction of Cap. 33 BG (Fig. 5) which consists practically entirely of these two minerals. The difference in composition of apatite and phillipsite can be judged by comparing the above mentioned fractions with the 32–100 μ fraction of Yoyo 7P (Fig. 5), which in addition to the ferromanganese oxide minerals in the form of micronodules and barium-bearing pellets contains large amounts of apatite but no phillipsite.

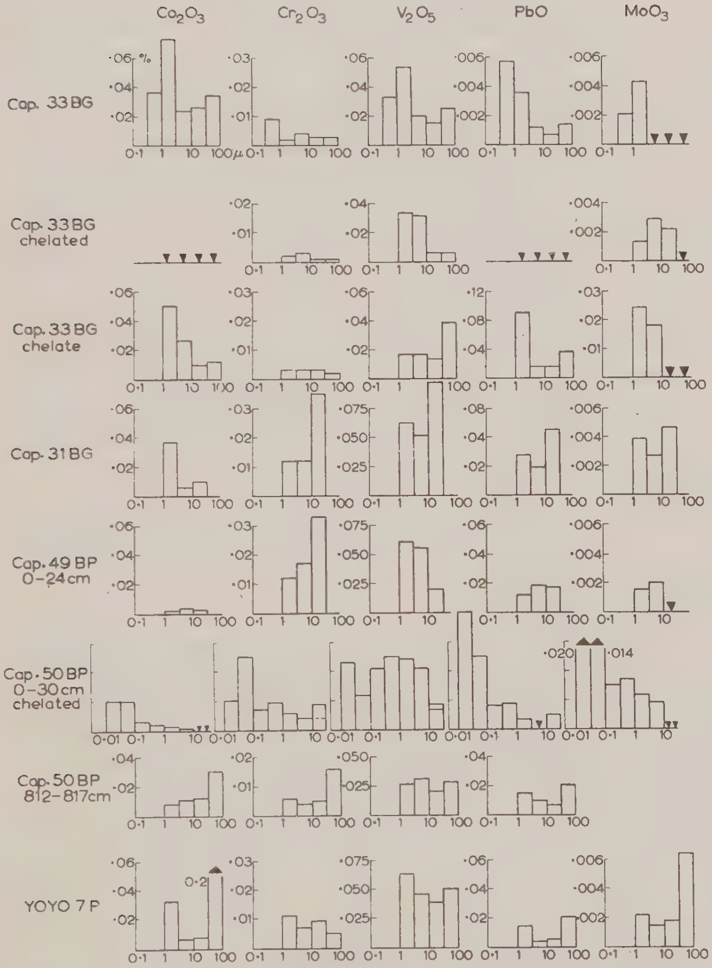

Fig. 5(d).

The lithium contents of a selected group of sediments (Table 11) fluctuate around the igneous rock value of 65 p.p.m. (Rankama and Sahama, 1950, p.143).

5.3. *Magnesium, calcium, and strontium.* The concentration of fixed magnesium increases with decreasing grain size, indicating that the main part of this element is bonded in the clay minerals. An exception is core 31, where large amounts of igneous ferromagnesian minerals occur.

In slowly depositing carbonate-free pelagic clays, comparatively large quantities of calcium (approximately 10 per cent) are stored in phillipsite and biogenous apatite. This calcium is largely removable by chelation. The amounts proxying

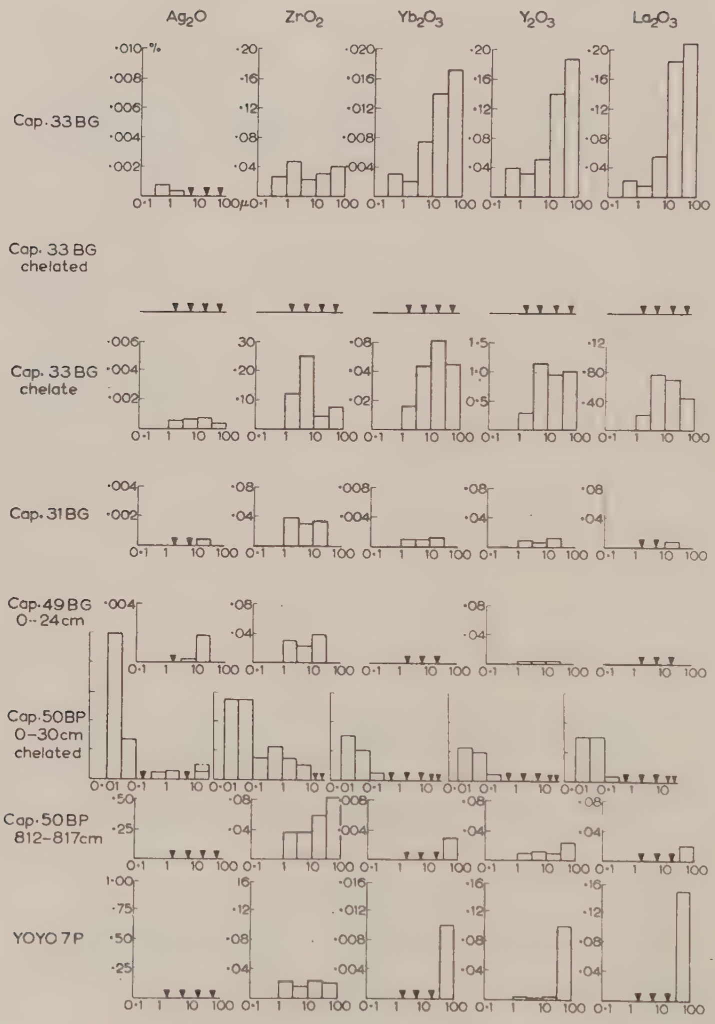

Fig. 5(e).

in ferromanganese oxide minerals are unknown, but may be important. A minor source of calcium is feldspar, whereas the clay minerals appear to be low in calcium. Pyroxenes contribute significantly in cores with a high content of pyroclastics.

The calcium/magnesium ratio is higher in the calcareous oozes than in clays as is evidenced by cores Cap. 32 HG and 33 HG. This is expected as magnesium is usually less abundant than calcium by an order of magnitude in calcareous tests (Clarke and Wheeler, 1922; Chave, 1954). The low values of both calcium

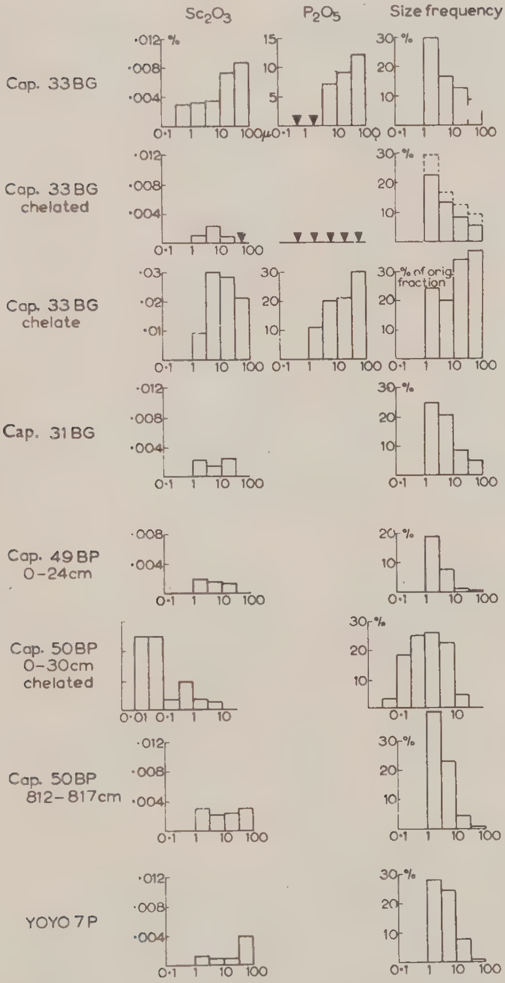

Fig. 5(f).

and magnesium in clays as compared to igneous rocks are compensated by the high concentrations of these elements in the calcareous oozes.

In the minerals, which are quantitatively important in the sediments investigated, high concentrations of strontium are found in the apatite phase of the fish debris (ARRHENIUS *et al.*, *op. cit.*) where it ranges between 0·2 and 0·7 per cent, and in calcite of pelagic planktonic fossils (0·1–0·2 per cent) (THOMPSON and CHOW, 1955). High concentrations might also be expected in phillipsite and in the ferromanganese oxide minerals, whereas the sediment fractions $<3{\cdot}2\ \mu$, which

Table 10. Silicon/aluminium ratios of Pacific sediments

Core	Lat.	Long.	Si/Al	Average ratio
Ck 8	53°02′N	176°15′W	5·2	6·0
Ck 9	52°25′N	176°25′W	6·8	
Wigwam 5	27°38′N	124°26′W	2·6	2·3
NH 14	24°08′N	156°04′W	2·0	
NH 13	23°22′N	156°29′W	1·9	
NH 12	22°49′N	156°50′W	1·9	
NH 9	21°41′N	157°29′W	2·1	
Y3G	20°49′N	125°15′W	2·6	
Y2P	20°49′N	125°15′W	2·7	
MP 38	19°01′N	177°19′W	2·8	
Cap. 50 BP	14°55′N	124°12′W	3·4	3·1
Cap. 49 BP	9°17′N	124°9′W	3·1	
Sw 71	7°38′S	152°53′W	2·9	
Cap. 33 HG	10°58′S	138°30′W	3·8	
Cap. 32 HG	11°00′S	130°24′W	2·7	
Cap. 33 BG	12°46′S	143°33′W	2·8	
Cap. 21 HG	16°36′S	162°43′W	2·0	2·3
Cap. 23 HG	16°58′S	161°35′W	1·8	
Cap. 25 HG	16°53′S	159°8′W	2·6	
Cap. 24 HG	16°44′S	161°35′W	2·1	
Cap. 30 BG	17°28′S	160°59′W	2·7	
Cap. 31 BG	17°29′S	158°40′W	2·4	

Table 11. Lithium concentrations in Pacific pelagic clays*

Sample	Li (p.p.m. by weight)
Cap. 31 BG 16	58
Cap. 50 BP 44	67
Cap. 50 BP 108	70
Cap. 50 BP 376	51
Cap. 50 BP 760	49

* These analyses were performed by precision emission spectrography by Mr. Arthur Chodos, California Institute of Technology.

consist mainly of clay minerals, have strontium contents of the order 0·05 per cent. The highest concentrations relative to aluminium consequently are found in calcareous oozes (Cap. 32 and 33 HG and NH 9, Table 9).

5.4. *Barium*. The high content of barium in the east equatorial Pacific sediments was first demonstrated by Steiger and Revelle (Revelle, 1944, pp. 66, 68). The correlation between calcium carbonate and barium concentrations was pointed out by the latter author (p. 68), who suggested that the barium in these sediments has been precipitated as the carbonate.

From previous results on the relation between the organic productivity in the surface layer of the ocean and the composition of the sediment below (Arrhenius, 1952, *loc. cit.*), it appeared probable that the rate of accumulation of barium, if this element is precipitated by organisms, would be a function of the rate of organic production in the euphotic zone. To check this assumption, the barium content of the surface layer of the sediment was determined by X-ray spectrometry (Section 2.3) in a meridional profile at approximately long. 125°W, extending from the north Pacific clay area over the zone of high productivity in the equatorial divergence (Arrhenius, 1952, Steeman-Nielsen, 1952) and into the south equatorial Pacific (Fig. 6). The amount of titanium per unit surface area is known to be practically constant within each time-rock unit of the Late Pleistocene-Recent series in the calcareous basin sediments of this profile (Arrhenius, 1952, 1.2.5) and an expression for the rate of accumulation of barium is therefore given by the ratio BaO/TiO_2, which is plotted as a function of latitude in Fig. 6. The corresponding data are also compiled in Table 12. As is seen from these, the rate of accumulation of barium is more than twenty times higher under the productivity zone of the equatorial divergence than outside the zone 10°N–10°S, and the increase toward the equator is remarkably regular.

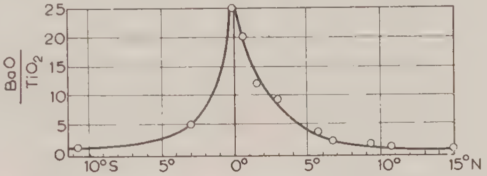

Fig. 6. Relative rate of accumulation of barium as a function of latitude, across the equatorial zone of high organic productivity. The rate is represented by the ratio BaO/TiO_2.

Table 12. Rate of accumulation of barium expressed as the ratio BaO/TiO_2 in a meridional profile through the Glacial and Postglacial strata under the equatorial zone of high productivity, and in a diatomaceous ooze from the Bering Sea

Core	Stratum (cm)	Lat.	Long.	BaO/TiO_2
Cap. 50 BG	0–30	14°58′N	124°12′W	0·8
Cap. 49 BG	0–30	9°17′N	124°9′W	1·5
Sw 58	0–30	6°44′N	129°28′W	2
Cap. 48 BG 1	0–50	5°45′N	124°2′W	3
Sw 59	0–80	3°05′N	133°6′W	9
Sw 60	0–150	1°35′N	134°57′W	11
Cap. 47 BG	0–80	0°40′N	123°33′W	20
Sw 61	190–200	0°6′S	135°48′W	25
Sw 62	0–56	3°0′S	136°26′W	5
Cap. 36 BG 1	9–108	10°45′S	133°35′W	1
Ck 8 (diatomaceous)	5–20	53°1′N	176°15′W	0·6

The relationship between the present productivity of the surface layer of the ocean and the recent rate of accumulation of barium on the ocean floor below, thus appears beyond doubt.

Marked variations in time of the organic productivity are inferred from the stratification of the sediments below and near the equatorial divergence (Arrhenius, *op. cit.*, 1.1.6, 1.9). A number of cores, displaying the typical alternation of calcareous and clayey strata, were therefore analysed for calcium carbonate, titanium, and barium. An example of the vertical distribution of these parameters is shown in Fig. 7. A relatively high barium/titanium ratio occurs only in the last productivity maximum (2). The penultimate productivity maximum, which, judging from paleotemperature distribution (Emiliani, 1955) and rate of accumulation of diatoms, coccoliths, and foraminifera (Arrhenius, *op. cit.*, 3.3.1, 3.4.2), was the highest of all, the increase in the Ba/Ti ratio is hardly noticeable, and in still older strata corresponding to ages of high productivity in the equatorial divergence, no increase whatsoever can be found in this ratio.

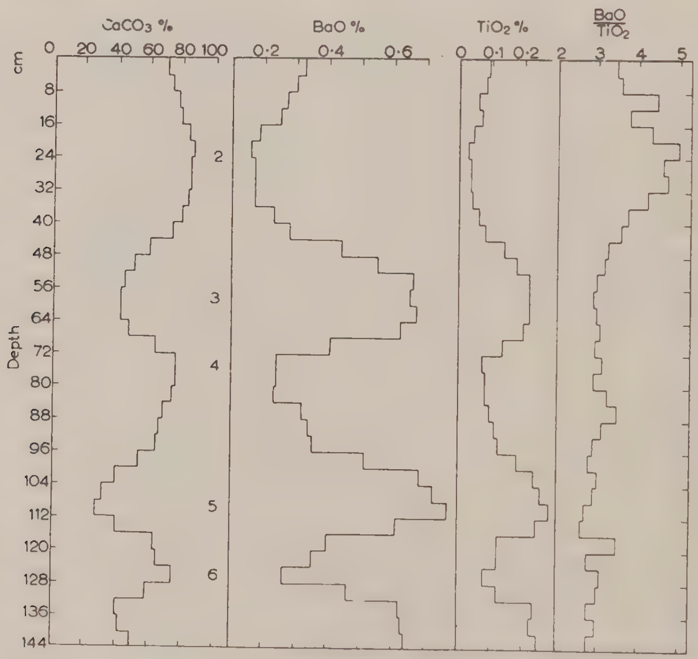

Fig. 7. Vertical distribution of calcium carbonate, titanium oxide and barium oxide, and the ratio BaO/TiO_2 in the core Cap. 48 BG1 (Table 12). The figures at the carbonate maxima and minima refer to the culmination of the stages earlier described (Arrhenius, 1952, 1.1.5.).

It appears from these results that a slow post-depositional migration of barium takes place in the sediments; this has completely levelled the original gradients of the Ba/Ti ratio in strata with an age of the order of 200,000 years or more. The relatively high mobility of barium in the deposit is further evidenced by the high content of alpha-active nuclides, presumably radium and its successors, in the microcrystals of the barium-bearing pellets (ARRHENIUS, BRAMLETTE and PICCIOTTO, 1957). These occur at such depths in the cores that the radium cannot have been taken up from sea-water but must have been released from adjacent ionium carrying minerals (cf. ARRHENIUS and GOLDBERG, 1955). The concentration of radium together with barium in the excreta of benthonic animals appears also to be reflected by the frequent concentration of alpha-activity to digging structures in the sediment (PICCIOTTO and ARRHENIUS, in preparation). The similarity in chemical behaviour of barium and radium emphasizes the importance of the chemistry and mineralogy of barium in pelagic sediments for the understanding of the final distribution of radium and its use for geochronological purposes.

The redistribution results in the smoothing out of the original gradients in the amount of barium per unit non-biogenous matter, represented by titanium, but leads to gradients steeper than the original ones, in the concentration of barium. This can readily be understood on the basis of the fact, evidenced below, that the clay minerals, the zeolites, and the ferromanganese oxide minerals, together constituting the bulk of the inorganic phases, have a high capacity to bond barium, in contrast to the calcite which cannot retain this element.

Analyses of diatomaceous oozes from the north Pacific and the Bering Sea (Ck 8, Table 12) indicate a low barium/titanium ratio in this environment, in spite of the supposedly high rate of organic production in the surface layer of the ocean. This may be explained either by assuming that barium is precipitated by an organism or a group of organisms abounding in the equatorial zone, or by assuming a larger contribution of titanium in the form of detrital and pyroclastic minerals in the sub-arctic areas, which are stratigraphically less known than the east equatorial Pacific. This latter explanation is suggested by the fact that the diatomaceous oozes investigated contain considerable amounts of glacial marine detritus and layers of volcanic ash.

It is not known whether the barium is concentrated from sea-water by planktonic or benthonic organisms in the areas in question. In littoral areas brown, red, and green algae are enriched in barium relative to calcium by factors of 16–78 (BOWEN, 1956). As is indicated by the results of WEDEPOHL (1955) and further shown below, the calcite of foraminifera and coccolithophoridae is practically free from barium, whereas the protoplast of live foraminifera appears to contain considerable amounts of this element (ARRHENIUS, BRADSHAW, CHODOS and WISNER, in preparation). The occurrence of the major part of barium in aggregates which probably are faecal pellets (see below) indicates that at least a mechanical concentration of barite is brought about by the benthonic animals.

In order to establish the mineral forms of barium in the sediments, material from the core Cap. 50 BP (Table 1) was divided into settling velocity fractions by decantation and centrifugation (cf. Section 2.2.3).

Analysis of the fractions (Fig. 5) demonstrated that the barium concentration is highest in the group with the velocity limits 85×10^{-5} and 85×10^{-4} cm/sec in water at 18°C (corresponding to diameters of 3·2 and 10 μ of spherical quartz grains). This fraction (sample 374) was selected for continued work and was further

Table 13. Distribution of barium in density fractions of fine pelagic silt (sample 374)

Fraction No.	Density	Mass percentage of total sample 374	BaO*%	TiO_2* Rel. units	Percentage of total Ba-content of sample 374	Major mineral components
1	<2·14	0·9	2·4	2	1·5	Opal, phillipsite, yellow aggregates (quartz, feldspar)
2	2·14–2·49	24·5	4·4	6	72·0	Opal, phillipsite, yellow aggregates, quartz feldspar
3	2·49–2·94	71·0	0·5	40	24·0	Quartz, feldspar, phillip site
4	>2·94	3·5	1·1	704	2·5	Augite, apatite, hornblende.
Total sample		100	1·7		100	

* By X-ray spectrometry.

subdivided in density groups by repeated centrifugation in tetrabromoethane, adjusted to the proper density with diethyllpthalate. The results of the analysis of the density fractions are shown in Table 13. The marked differentiation in mineral composition, which is also demonstrated by the titanium content, confirms that a satisfactory density separation was obtained, although quartz and feldspar still contaminate the light fractions.

Barium occurs in considerable concentration both in the light and the heavy minerals, especially in the former. As a result of the relatively high frequency of minerals in the density range 2·14–2·49 and their very high barium content, this fraction contains 72 per cent of the total amount of barium. Heavy minerals are responsible only for a small fraction of the barium present (2·5 per cent). In spite of this, it was regarded as a matter of interest to identify also the heavy components. For this purpose a larger quantity of mixed material from the core Cap. 49 BP (Table 14) was fractionated with regard to settling velocity of the grains in the same way as the sample from core Cap. 50 BP. The velocity group 85×10^{-5}–85×10^{-4} cm/sec was further split in two density groups, one heavier, the other lighter than 2·94. The heavy minerals were freed from manganese oxide minerals and manganite by chelative dissolution. The residue, constituting sample no. 564, was divided according to magnetic susceptibility into three fractions, one non-magnetic, one weakly and one strongly magnetic. The properties of these fractions are shown in Table 14.

Table 14. Properties of magnetic fractions and EDTA-soluble fraction of heavy minerals (Sample 564)

Fraction No.	Description	Mass mg	Ba Rel. units*	Ti Rel. units*	Major mineral components
1	Non-magnetic	19·5	270	3 2	Barite, apatite, quartz, pyroxene anatase
2	Weakly magnetic	29·7	68	n.d.	Pyroxene, hornblende, biotite, apatite, quartz, barite
3	Strongly magnetic	3·7	24	124	Pyroxene, hornblende, biotite
4	Residue of fraction 1 after acid treatment	9·0	0	336	Quartz, pyroxene, anatase
5	Acid soluble components of fraction 1 recovered by evaporation	10·5	54	10	(by difference) Barite, apatite
6	EDTA-soluble components of total sample 564 recovered by evaporation and ignition	65	160	63	Manganese oxide minerals

* By X-ray spectrometry.

The major part of the barium is concentrated in the non-magnetic and weakly magnetic fractions. It prevails as barite and to some extent in apatite (approx. 5 per cent, ARRHENIUS *et al.*, 1957) and is completely removed by boiling in concentrated HCl for 5 min. About twice as much barium is found among the components of the heavy mineral fraction soluble in EDTA. It appears reasonable to assume that this part of the barium is bound in the structure of the manganese oxide minerals.*

For the investigation of the quantitatively much more important barium-carrying minerals and aggregates with a low density, material was used from 165–170 cm depth in the core Ch 23 (Table 1), located in the equatorial high productivity zone, where the relative amount of barium in the sediment is high.

The barium content was determined by X-ray spectrometry. Table 15 shows the concentration in the original sample (no. 159), in the dialysate (no. 713), in the material exchanged and dissolved by N ammonium carbonate at 90°C during 2 hr (no. 714), and in different fossil groups, separated by size, density, and acid solubility† (nos. 159–1.1 to 2.6). From Table 15 it is seen that the barium contained in foraminiferal tests is negligible (sample 159–1.2) and that the amounts dissolved in the pore solution of the sediment or weakly sorbed (sample 713) or exchangeable against ammonium ion (sample 714) are relatively small.

---

* An experiment carried out with barite crystals of 3–10 μ size, demonstrated that less than 2 per cent of this mineral is dissolved in EDTA under the conditions indicated above.

† The calcareous components were dissolved in acetic acid, added dropwise to the sample suspension.

Table 15. Distribution of barium in a Pleistocene pelagic equatorial calcareous clay (Chubasco 23, 165–170 cm, sample 159) and in a Miocene pelagic coccolith ooze (MP 40, 34–45 cm, sample 569)

Sample No.	Description	Mass mg	% BaO	% Mass	Main constituents
159	Original	50,000	2·0	100	—
713	Dialysate from original	2475	0·005	—	—
714	Sorbate from original	1712	0·030	—	—
159–1.0	$>62\ \mu$, fraction of original	1640	0·080	3·3	Foraminifera radiolaria
159–1.1	$>62\ \mu$, residue after treatment with acetic acid	256	0·25	0·5	Radiolaria
159–1.2	$>62\ \mu$, components dissolved in acetic acid, recovered by evaporation and ignition	720	0·005	—	Foraminifera
159–2.0	3·2–62 μ, fraction of original	—	0·90	—	Unidentified calcareous fragm., coccoliths, foraminiferal fragm., diatoms, radiolaria
159–2.1	3·2–62 μ, residue after treatment with acetic acid	—	1·63	—	Diatoms, radiolaria, yellow aggregates (phillipsite)
159–2.2	3·2–62 μ, components dissolved in acetic acid, recovered by evaporation and ignition	—	0·12	—	Calcareous and phosphatic components of 159–2.0
159–2.3	3·2–62 μ, residue after acid treatment, density fraction $>2{\cdot}22$	—	1·25	30% of 2·1	Diatoms, radiolaria, yellow aggregates, phillipsite
159–2.4	3·2–62 μ, residue after acid treatment, density fraction $<2{\cdot}22$	—	1·97	70% of 2.1	Diatoms, radiolaria, yellow aggregates, phillipsite
159–2.5	Residue of sample 159–2.3 after 5 min treatment with boiling conc. HCl	—	0·24		Diatoms, radiolaria (degraded phillipsite)
159–2.6	Components dissolved from sample 159–2.5 recovered by evaporation	—	10	1·3% of 159–2.5	Yellow aggregates and part of phillipsite (by difference)
159–3	0·3–3·2 μ, fraction of original	—	1·26	—	—
159–4	$<0{\cdot}3\ \mu$, fraction of original	—	0·48	—	—
569–0	MP 40, 35–45 cm, coccolith ooze	—	0·020	99·5	Coccoliths
569–1	Residue of 569–0 after treatment with acetic acid	—	1·6	0·5	Siliceous remains
569–2	Components, soluble in acetic acid, recovered by evaporation and ignition	—	0·001	—	Dissolved coccoliths

Nor are any considerable quantities of barium found in that part of the 3–62 μ fraction which is soluble at pH 5–6 (sample 159–2.2) and which largely consists of carbonates, mainly in the form of coccoliths. The insoluble residue of the same size fraction, however, has a very high barium content (sample 159–2.1). This residue consists mainly of diatom frustules and other remains of siliceous organisms, with a minor amount of rounded, yellow aggregates. The heavier fraction of this material ($\rho > 2{\cdot}22$, sample 159–2.4) contains a larger amount of barium than the lighter fraction (sample 159–2.3).

After 5 min treatment with boiling conc. HCl, 80 per cent of the barium is removed from 159–2.5. As the yellow aggregates are simultaneously dissolved, a localization of barium in these is indicated. However, on the basis of the experimental evidence, the possibility could not be excluded that the barium is bonded in the opal or zeolite structure, and is removed by hydrochloric acid, although the opal is left intact and the phillipsite is only degraded to a certain extent. In order to check the distribution of barium between radiolarian and diatomaceous silica, the yellow aggregates and phillipsite in the barium-rich fractions of the sample 159, the sample was subjected to a particle by particle analysis* by means of the Castaing X-ray microanalyser, which has a resolution of 2 μ^2. The sample powder was distributed over a bright polished metal surface and coated with a 20 Å film of copper by condensation to make it electrically conducting. The spectrometer was set to the $L\alpha_1$ line in the barium spectrum, and the counter connected to a loudspeaker. During a preliminary scanning of the sample under visual control by the mirror microscope, the audible pulse-rate was used as a rough indication of the concentration of barium in each grain brought under the cross hair. A large number of grains were rapidly checked and it became evident that the aggregates were far higher in barium than were the other components. A number of quantitative measurements gave: for diatoms and radiolaria, 0–2 per cent; for phillipsite crystals, 3–15 per cent; and for the aggregates, 2–47 per cent BaO. Marked variations were noted in the concentration inside the aggregates, indicating that the barium is locally concentrated, probably in the highly refractive microcrystals occurring in varying amounts in the aggregates.

Additional experiments were carried out to check that the calcareous coccoliths lack importance as barium carriers. For this purpose was used the sample MP 40, 35–45 cm (Table 1), a coccolith ooze of high purity. The amount of the sediment soluble in weak acetic acid is 99·5 per cent, and the carbonate prevails almost entirely as coccoliths. The insoluble residue (0·5 per cent) consists mainly of siliceous fragments. As is seen from samples 569–0, 569–1, and 569–2 in Table 15, practically all the barium contained in the sample is retained in the residue, insoluble in weak acid.

The nature of the transparent, isotropic, greenish yellow or yellow matrix of the aggregates has not yet been revealed. The aggregates are rounded with a smooth or slightly irregular surface. They generally fall in a size range of 5–15 μ, although larger specimens have been observed in some north Pacific clays. Due to their low bulk density, the equivalent diameter of spherical quartz grains, which is used for a size scale in Fig. 5, is somewhat smaller (3–10 μ). The crystalline inclusions, which vary in size from barely visible under the microscope to a few micra, are highly refractive, and are therefore supposed to have a high density. The density of the matrix of the aggregates is therefore supposed to have a density well below 2·2. It appears reasonable on the basis of the evidence given above to assume that the crystalline inclusions consist of barite, and that the aggregates are faecal pellets of benthonic animals.

---

* This analysis was carried out by one of the present authors in the laboratories of the Office National d'Études et de Recherches Aéronautiques, Chatillon-sous-Bagneux (Seine), France.

Larger euhedral crystals of barite with an average length of 10–40 μ have been observed (Bramlette, personal communication) in a number of sequences of pelagic clays. Their occurrence appears to be limited to the surface of Tertiary outcrops, unconformities, and strata with extremely high contents of manganese, indicating a low total rate of deposition. These crystals may result from the decomposition of the aggregate matrix by degradation of organic matter at the sediment-water interface, and subsequent growth of the included barite microcrystals.

5.5. *Boron.* As has been suggested by Urey (1953), the high boron content of ocean water is explained by its introduction into the major sedimentary cycle as an "excess soluble". The high oceanic concentration of this element results in a correspondingly high content in marine sediments (several hundred p.p.m.), whereas in non-marine argillaceous sediments the boron content is generally at least one order of magnitude lower (Goldschmidt and Peters, 1932(a) and Landergren, 1945). The concentration of boron in marine sediments was assumed by Landergren (*op. cit.*) to be due to adsorption of the borate ion to detrital clay minerals. A closer examination of the bonding of this element in pelagic clay sediments, briefly reported on earlier (Arrhenius, 1954) indicates, however, that in this case only a minor fraction, roughly corresponding to the amount dissolved in the interstitial solution, is removed when the sediment is washed with distilled water. Less than 10 per cent of the remaining boron is removed at exchange of sorbed ions. The major part thus appears to be relatively strongly bonded in the authigenic minerals of the sediment. Upon chelative dissolution of the manganese and phosphate minerals, which are concentrated in the coarse grain size fractions (Fig. 5) a part of the remaining boron is released. Separate analyses of the phosphates (Arrhenius *et al.*, *op. cit.*) give low boron contents (0·003–0·01 per cent) for this material, which indicates that the main part of the boron released at solution in EDTA, occurs in the structure of the ferromanganese oxide minerals. The amount of this element which remains in the solid phases after this treatment, and which is quantitatively most important (Fig. 5, Cap. 33 BG chelated, and Cap. 50 BP 0–30 cm, chelated), resists dissolution at boiling 0·1 N hydrochloric acid, but is released at boiling in strong alkali. These results suggest that boron is proxying for silicon in the tetrahedral sheets of the clay minerals. If this is true, at least a fraction of these minerals appear to have formed from true solution of ionic species of boron, silicon and aluminium in sea-water (Arrhenius, 1954).

5.6. *Yttrium, scandium, thorium and the rare-earth elements.* All of these elements show a close similarity in their behaviour in the major sedimentary cycle, and appear to concentrate mainly in two groups of minerals, the ferromanganese oxide minerals (Goldberg, unpublished work; Goldberg and Picciotto, 1955) and the biogenous apatite (Arrhenius *et al.*, 1957). This distribution is illustrated by Fig. 5 where the very high concentrations of Yb, Y, La and Sc are shown in the coarse fractions of Cap. 33 BG and Yoyo 7P which are in the former case dominated by apatite and phillipsite, in the latter by apatite, ferromanganese oxide minerals and barium carrying aggregates. Separated samples of phillipsite showed the absence in this mineral of the elements in question in amounts above the sensitivity limit of the X-ray spectrometric method used (approx. 0·01 per cent). The manganese minerals previously investigated were derived from permanently exposed manganese nodules, where any apatite accumulating on the surface would have been redissolved. The ferromanganese oxide phases of such nodules could have inherited the heavy metals originally adsorbed to the apatite surface, in addition to the amount originally adsorbed directly from sea-water to the surface of the δ-MnO_2. Analyses of manganese micronodules from pelagic clays, and of apatite separated from the same sediment samples indicate a fractionation between the apatite and the manganese oxide phases with an excess of cerium in the latter (ARRHENIUS *et al.*, in press). A similar fractionation was obtained experimentally by ERÄMETSÄ *et al.* (1940) through differential adsorption of the carbonate complexes of the rare earths.

Beside the fraction of this group, which is localized in manganese oxide minerals and on the surface of the biogenous apatite, and which is completely removed by chelative dissolution (Fig. 5, Cap. 33 BG, chelated), quantitatively important amounts, insoluble in EDTA, are found in the colloidal fraction of the sediment (Fig. 5, Cap. 50 BP 0–30 cm). The nature of the host mineral is not known in this case.

5.7. *Titanium.* On the average the titanium content of the pelagic sediments investigated is similar to that of igneous rocks. High concentrations in the sediments are invariably due to the presence of basaltic pyroclastics. This is the case for example in Cap. 31 BG (Table 9) where the excess titanium occurs mainly in augite in the coarse mineral fraction (Fig. 5). The decreasing influence of basaltic pyroclastics with increasing distance from the source is illustrated by the decreasing titanium content of the sediment in a series of cores, extending northward from the Hawaiian Islands (Fig. 8 and Table 16). Similar distributions have been demonstrated in the Atlantic Ocean by CORRENS (1937, 1954).

A minor fraction of the titanium is readily soluble in EDTA, and probably prevails as colloidal oxyde aquate, dispersed through the manganese oxide minerals.

GOLDBERG's (1954, p. 255) investigations show a covariance between iron and

Table 16. Metal/aluminium ratios as a function of distance from Hawaiian Islands

Core	Number in Fig. 1	Normal distance from Island chain (naut. miles)	$1000\frac{Ti}{Al}$	$1000\frac{V}{Al}$	$1000\frac{Cr}{Al}$
NH 9	29	26	270	11	4·5
12	30	100	91	4·2	1·0
13	31	137	77	3·9	1·1
14	32	188	66	3·3	0·87
Y3G	27	1820	50	4·3	0·91

titanium in manganese nodules, with an average ratio Fe/Ti of about 18. It is not known if this titanium is a structural component of the ferric manganite, of the goethite, or of another iron mineral, or if it prevails as an independent phase, with a tendency to occur in high concentration under the same conditions as the iron minerals. It is interesting to note that the ferromanganese oxide minerals dispersed through the calcareous sediments of the east Pacific rise (cf. Section 5.11 and Revelle, 1944, Table 9) have considerably higher iron/titanium ratios than the manganese nodules referred to above, viz. of the order 30–100, as compared to 18 in the nodules.

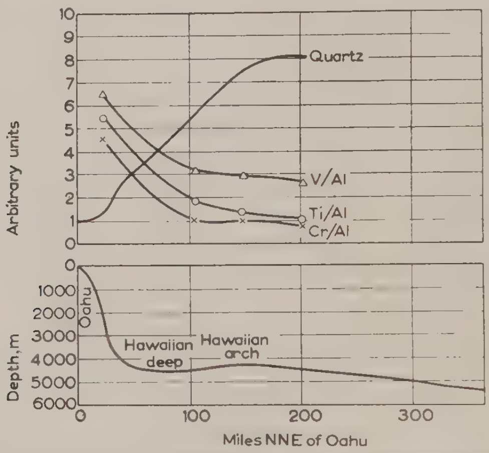

Fig. 8. Relative concentrations of titanium, vanadium and chromium and concentration of quartz in sediments off Hawaiian Islands (upper graph) compared with bottom topography (lower graph).

Flow along the bottom of sediments high in basaltic pyroclastics results in high concentrations of titanium, vanadium and chromium in the sediments of the apron around the islands and in the surrounding depression, the Hawaiian deep. The flow is efficiently stopped by the periferal rise, the Hawaiian Arch, and the pelagic sediments outside of the Arch contain only little of these elements in excess above the average for north Pacific pelagic clays, represented by Y3G in Table 16.

The content of eolian quartz silt is high in pelagic sediment of the lower and middle latitudes in the Northern Hemisphere, due to the vast arid areas in this zone. Near the islands, the concentration of quartz is lowered by the influx of detrital basaltic material.

The absolute concentrations and ratios of the three elements, given in arbitrary units in the figure, are found in Tables 16 and 9. Quartz data from Rex and Goldberg (in press). Topographic data from Dietz and Menard (1953).

Euhedral anatase and rutile appear to account for a large part of the approx. 0·8 per cent titanium occurring in such pelagic clays which do not have an appreciable pyroclastic contribution (Correns, 1954; Bramlette, personal communication; this paper, Table 14), and at least the anatase is certainly authigenic in the sediment. As pointed out by Correns (*loc. cit.*) the parent material of the authigenic titanium minerals may at least partly be weathering silicate minerals, glass and ilmenite.

The importance of formation of the hydrogenous titanium minerals from titanium in true solution in sea-water has been stressed by Goldberg (1954) on the basis of the association of titanium with hydrogenous iron minerals mentioned above and on GRIEL and ROBINSON's data (1952) for dissolved titanium in sea-water (approx. 1 μg/l.).

ARRHENIUS (1952) studied the distribution of titanium in sediment profiles from the east equatorial Pacific, and found only small variations in the titanium content of unit cross-section columns through the same time rock units of different latitudes. These results indicate uniformity in space of the accumulation of titanium in the sedimentary basins investigated. On the basis of the lack of stratification of adjacent Pleistocene clay sediments it was concluded that the accumulation had been uniform also in time through the major part of the Pleistocene, as any change in the proportions of the biogenous, hydrogenous and lithogenous contribution would be reflected by a corresponding change in composition of the sediment. The titanium content in core Cap. 49 BG, which includes the Recent and approximately the upper half of the Pleistocene, is shown in Table 17. The standard deviation, 7 per cent of the mean value, is close to the analytical error. The assumption of an approximate uniformity of the titanium accumulation during the corresponding time is thus not in disagreement with

Table 17. Concentration of TiO_2 as a function of depth; mean concentration and the standard deviation from the mean in the clay core Cap. 49 BG (Fig. and Table 1) adjacent to the equatorial area of carbonate sediments.

Depth below surface (cm)	$TiO_2 \times 10^4$	Depth below surface (cm)	$TiO_2 \times 10^4$
0–4	58	76–80	59
4–8	60	80–84	65
8–12	58	84–88	57
12–16	63	88–92	57
16–20	60	92–96	53
20–24	54	96–100	66
24–28	62	100–104	75
28–32	64	107–111	69
32–36	63	108–112	63
36–40	63	112–116	65
40–44	63	116–120	59
44–48	62	120–124	61
48–52	61	124–128	64
52–56	53	128–132	62
56–60	57	132–136	65
60–64	63	136–140	65
64–68	58	140–144	66
68–72	60	144–148	56
72–76	60	148–152	67
	$m = 61{\cdot}3$ $\sigma = \pm 4{\cdot}5 =$ $\pm 7{\cdot}3$ per cent		

m = mean concentration
σ = standard deviation

these results. However, if it is assumed that the genetic component group, in which the main part of the titanium falls is a very large proportion of the sediment, even relatively large changes in the rate of accumulation of this component would not markedly influence its absolute concentration in the sediment. That this might possibly be the case is suggested by the relatively large variations in concentration of manganese in core 49 BG (by a factor of 9) whereas the concentrations of iron and of quartz show the same invariability as titanium. Further experiments, preferably based on absolute age determinations from the ionium/thorium ratio, are needed before the variability in time of the accumulation rate of the inorganic components can be quantitatively determined.

Goldberg (1954, p. 259) indicated the possibility that biogenous titanium may form a considerable fraction of the total amount of this element in pelagic sediments. This suggestion was based on the observation (Collier, 1953) of concentration of titanium by planktonic dinoflagellates. The absence of an increase in the titanium/aluminium ratio in sediments with a large biogenous component like Cap. 32 and 33 HG (Table 9), however appears to rule out biogenous titanium as an important component, at least in the equatorial pelagic zone.

Correns (1954) pointed out, that the occurrence of microscopic authigenic anatase in the sediment requires the titanium to have prevailed in true solution, at least for a short time, and that the original distribution therefore might have been changed by migration. The maximum average mass transport by diffusion of titanium through the deposit can be estimated from Arrhenius' data (1952, 1.2.4, 1.2.5, Fig. 1.1.6.1) if it is assumed that the observed deviations from constancy in space of the titanium content of each time-rock unit is entirely due to this effect. Using the values $\overline{\Delta d} = 8{\cdot}5$ mg, $\overline{d}_0 = 13$ mg, and $\overline{a} = 16{\cdot}3$ cm for the cores 59, 60, 61 and 62 (Arrhenius *op. cit.*, Table 1.2.5) the maximum displacement of TiO_2 is 0·52 mg/cm^3 or 0·65 of the average titanium content of a stratum. The present authors believe, however, that convective displacement by benthonic animals, stratigraphic correlation errors, variations in the titanium content of the inorganic components of the sediment, and temporary, local variations in the rate of accumulation of titanium contribute to this effect at least as much as diffusive displacement.

5.8. *Zirconium.* This element occurs in the pelagic sediments investigated in concentrations which are on the average 0·8 of the average for crustal rocks. (Fig. 3, Table 9). This supports Goldschmidt's (1954, p. 426) opinion that the resistance of the zirconium minerals to weathering has been over-estimated and that considerable amounts of this element pass through the hydrosphere in true solution. Further evidence for this is provided by the results of Degenhardt on the distribution of zirconium in sediments (1957), and by the fact that a large part of the zirconium found in pelagic sediments appears to be localized in the authigenic ferromanganese minerals (Goldberg, 1954), and is soluble in EDTA (Cap. 33 BG, Fig. 5). Another appreciable part of the zirconium occurs in the colloidal fraction, and is resistant to chelative dissolution (Cap. 50 BP 0–30 cm, Fig. 5).

5.9. *Vanadium.* The average concentration of vanadium found in the sediments investigated is about $2\frac{1}{2}$ times the average for igneous rocks. However, the apparent discrepancy results from a systematic analytical error of a factor of 2 which was found by Wedepohl (personal communication) who made precision analyses of duplicate samples.

These vanadium contents in pelagic sediments are consistant with the observations of previous authors (Jost, 1932; Landergren, 1956; Goldschmidt, 1954) who found no marked enrichments or deficiencies of this element in marine deposits as compared to igneous rocks.

The relatively even distribution of vanadium through the sediment fractions (Fig. 5.) indicates its simultaneous occurrence in high concentration in several of the main mineral constituents. The reduction of the vanadium content in the coarse grain fractions of Cap. 33 BG (Fig. 5) through chelative dissolution indicates a localization of the element in either biogenous apatite or in phillipsite. The former alternative is excluded by the low contents found upon analyses of separated apatite and the accompanying organic phase (Arrhenius *et al.*, in press). Also inorganically precipitated marine apatites are shown by the same authors to be low in vanadium confirming the results of Jacob *et al.* (1933).

A large fraction of the vanadium found is resistant to chelative dissolution, and occurs throughout the finest grain size fractions of the sediments. Following the authors quoted above and Harder (1951), one might guess at a distribution of this fraction of the element between the clay minerals, the iron oxide minerals, and possibly the authigenic titanium minerals. A definite indication of a concentration in the iron oxide minerals is the high vanadium content of the carbonate-free fractions of cores Cap. 32 and 33 HG (Table 9).

Another important source of vanadium in the Pacific are igneous ferromagnesian minerals, magnetite and ilmenite, which are concentrated in core Cap. 31 BG and which probably are responsible for the high vanadium content of the fractions $>1\ \mu$ in this core. The decreasing influence of basaltic pyroclastics with increasing distance from the Hawaiian Islands is reflected by a decreasing content of vanadium in the series of cores NH 9–NH 14 (Fig. 8 and Table 16).

5.10. *Chromium.* Rankama and Sahama (1950, p. 620) point out that the igneous rock average values reported by various workers differ by an order of magnitude, the highest value being 530 p.p.m. (Hevesy, Merkel and Würstlin, 1934) and the lowest 35 p.p.m. (Lundegårdh, 1946). Shaw (1954) finds for shales and their metamorphic equivalents 59 to 190 p.p.m. and similar values have been reported for sandstones (Goldschmidt, 1937). An intermediate value for the average igneous rock concentration of chromium, 100 p.p.m. has been reported by Young (1954) without specification of the method of computation. The average found by us for Pacific pelagic sediments is close to this value by Young, which has been adopted as a basis for the computation in Figs. 3 and 4.

High chromium concentrations occur in sediments containing considerable amounts of basaltic pyroclastics (Cap. 25 HG, 31 BG, 33 BG, NH 9, in Table 9). The decreasing content of chromium bearing minerals with increasing distance from the Hawaiian Islands is illustrated by the falling chromium content in the series of Cores NH 9, NH 12, NH 13 and NH 14, ranging from latitude 21 to 24°N (Table 16 and Fig. 9). As is seen from Cap. 33 BG in Fig. 5, chromium, like titanium, vanadium, copper and magnesium is strongly concentrated in the 10–32 μ fraction, which is in this core dominated by ferromagnesian minerals, mainly augite. The distribution in Cap. 50 BP 0–30 indicates concentration of chromium also in the colloidal fraction, which is dominated by clay minerals. The lack of volcanic glass even in samples containing large amounts of ferromagnesian phenocrysts, and the high content of montmorillonite in such samples, indicate that basaltic glass is unstable in this environment, and decomposes to form montmorillonite. The colloidal chromium may be derived from the decomposed glass, and is probably present in the octahedral layers of the authigenic clay minerals.

The distribution of chromium suggests that an excess of this element above approximately 0·01 per cent in pelagic sediments, is a useful indication of the presence of altered or unaltered basaltic pyroclastics.

5.11. *Iron.* Largely due to the poor crystallinity of the authigenic iron minerals. little has been known about their character and relative distribution until the appearance of the recent work by Buser and Grütter (1956) and Grütter and Buser (1957). These workers demonstrated that the main iron-containing phases in manganese nodules are ferric manganite (see 5.12), goethite, and colloidal FeOOH. Goldberg (1954), on the basis of Cooper's (1948) and his previous (1952) results. pointed out that the primary phase deposited from the sea-water probably is colloidal iron oxide aquate. The present authors (section 5.12) interpret the information furnished by Buser and Grütter on the basis that the iron oxide aquate colloid, after discharge at the sediment-water interface, forms a highly active surface, which catalyses the oxidation of dissolved manganous ion to MnO_2. Upon precipitation as δ-MnO_2, part of this solid may combine with the catalyst, forming the double layer structure, described by Buser and Grütter as ferric manganite. Excess iron oxide aquate colloid may by ageing be transformed to goethite. In addition to these phases, nontronite has been observed on manganese nodules (Bramlette, personal communication).

It appears reasonable to assume that the same iron minerals are predominant also in other pelagic sediments; however, little is so far known about their relative proportions. Thus it is uncertain whether the very high iron concentrations in the colloidal fraction of pelagic clays (e.g. Cap. 50 BP 0–30 cm, Fig. 5) are due mainly to nontronite or goethite.

In sediments with a large pyroclastic contribution, considerable amounts of iron occurs as augite and hornblende, and further as magnetite and probably ilmenite, all concentrated in the coarse fraction (Fig. 5, Cap. 31 BG).

5.12. *Manganese, cobalt, nickel, lead and molybdenum.* These five elements display a similar behaviour in the marine part of the minor cycle (Goldberg, 1954). In sea-water they most probably prevail as dissolved species mainly as manganous, cobaltous, nickelous and plumbous ions, as either aquato- or chloro-complexes. In the solid phases precipitated from this solution a large part of the manganese occurs as δ-MnO_2* and as manganese and iron manganite, and much of the cobalt, nickel and lead is bound in the structure of these minerals, mainly in the disordered layer of the manganite (Buser and Grütter, 1956). The manganese, and associated metals, occurring in these ferromanganese oxide minerals, are readily soluble in EDTA, and can thus be separated from resistant phases. (cf. Fig. 5 and section 2.25). Another part of the manganese occurs together with iron, cobalt, nickel, copper. rare earths. zirconium and large amounts of lead, molybdenum and silver in the colloidal fraction of the sediment (Cap. 50 BP 0–30, Fig. 5), and is resistant to chelative dissolution. It is not known, what mineral carries this fraction of the manganese, which is quantitatively less important in sediments with a high manganese content, but approaches unity in manganese-poor strata of the buff clays from the north equatorial Pacific (Tables 1 and 9).

---

* δ-MnO_2 and manganite are throughout this work employed in the same sense as the one used by Buser and his co-workers, namely as a chemical term. A discussion of the proper mineral names for the species discovered by these workers will follow elsewhere.

The high concentration of manganese in many pelagic deposits has motivated a number of speculations as to the source and mechanisms of accumulation of this element. It is generally accepted that the manganese has been brought into solution by the weathering of igneous rocks, transported in solution to the site of deposition and precipitated there. However, there is a difference of opinion as to the location of the source rocks and the modes of transport and deposition of the dissolved manganese.

Although an obvious source of manganese is the crustal rocks of the continents, as first pointed out by RENARD (MURRAY and RENARD, 1891), MURRAY suggested volcanic debris on the ocean floor as more important. MURRAY was impressed by the association of manganese nodules and pyroclastics in many of the same samples of the Challenger Expedition. Confronted with the observation that the manganese/iron ratio in nodules is much higher than in the pyroclastics, he amended his ideas (MURRAY and IRVINE, 1894) by suggesting a diffusion of manganese from deeply buried strata of the decomposing rocks. The remnants of such weathered lavas, depleted in manganese, and approximately ten times the volume of the totality of the pelagic sediments, have never been found. In view of the obvious necessity of separating the source of the manganese from the deposits, the emphasis upon volcanic debris on the ocean bottom does not any longer seem to be needed.

Several processes bringing manganese to the sediment, other than oceanic mixing, have been proposed. Beside diffusion through the pore water of the sediments (MURRAY, *loc. cit.*), GÜMBEL (1878) suggested transport via submarine springs; in the latter two cases the source of the manganese is presumed to be below the sediment surface. CORRENS (1941) has indicated the possibility of a biological extraction of manganese from the sea-water into foraminiferal tests. At the partial dissolution of these after deposition, manganous ions are released in the pore water of the surface layer of the sediment. PETTERSSON (1945) has suggested the inability of this process to account for all the manganese in sediments. He pointed out that the necessary rates of accumulation of foraminifera and the subsequent rates of dissolution would be higher than is probable. A second criticism is based upon his belief that the relatively high manganese contents of the foraminifera, reported by CORRENS, are brought about after deposition. However, these values have been confirmed recently (ARRHENIUS, BRADSHAW, CHODOS and WISNER, in preparation) by analysis of planktonic foraminifera caught by tow-net. Thus it appears reasonable to accept CORRENS' suggestion as a contributing transport process. The outcome of all of these mechanisms is to increase the activity of manganous ion at the sediment-water interface.

The following processes of transfer of the manganese from dissolved to solid phases have been suggested: the deposition of manganous sulfide with subsequent oxidation (Buchanan, 1890); adsorbtion on volcanic glass particles (Pettersson, 1945); bacterial oxidation (Dieulafait, 1883; Dorff, 1935; Butkewitsch, 1928); and inorganic oxidation and precipitation (Murray and Renard, 1891; Boussingault, 1882; Kuenen, 1950). All of these hypotheses suffered at the time they were presented by inadequate knowledge of the nature of manganese in the ocean and in the solid phases of the sediment. It therefore appears worthwhile to consider some newer aspects of the geochemistry of manganese.

Table 18. Distribution of manganese between particulate and dissolved species on Trans-Pacific Station 129 (lat. 26°28·5′N, long. 170°23·0′W)

Depth in m	Dissolved manganese μg/l.	Particulate manganese μg/l.
0	2·8	0·22
200	4·7	0·08
1000	5·0	0·06
1500	2·0	0·05
2000	2·1	0·09
2500	1·2	0·02
3000	1·7	0·12
3500	0·4	0·07

The following lines of evidence point to the existence of manganese in the divalent state in sea water. Buser and Grütter's (1956) study of the mineral composition of manganese nodules indicates the main constituents to be δ-MnO_2 and manganites with double layer structures. The manganites contain, beside MnO_2, mainly divalent manganese 5–25 per cent, iron, calcium and sodium. It is difficult to conceive of a process of reduction of any tetravalent manganese in the oxidating environment where these concretions are found. Chemical analyses of manganese in Pacific Ocean waters indicate a distribution (Table 18) in which less than 10 per cent of the manganese occurred in phases that were retained by a molecular filter with a pore size of 0·5μ. Experiments with a filter of pore size of 5–10 millimicra yielded about the same amount of retained manganese, suggesting that 85 per cent or more of the element prevails in true solution. If one assumes that manganese is present as the divalent ion and that manganous carbonate rather than a silicate of manganese (for which data are lacking) is the least soluble compound that would form, the manganese is undersaturated by a factor of 200 ($K_{MnCO_3} = 8{\cdot}8 \times 10^{-11}$ [Latimer, 1952, p. 236]. CO_3^{--} and Mn^{++} in sea-water have respective concentrations of 5×10^{-4} M and 4×10^{-8} M and assumed activity coefficients of the divalent ions of 0·12).

The manganites described by Buser and Grütter (*op. cit.*), and Grütter and Buser (1957) consist of a double layer structure where layers of MnO_2 alternate with disordered layers of $Mn(OH)_2$-aquate in the case of manganous manganite, and of $Fe(OH)_3$-aquate in the case of the ferric manganite. Thus, the main part of the manganese prevails in the tetravalent form. The ions in the disordered layers appear to be exchangeable and at least minor amounts of other ions can proxy for the manganous, ferric, calcium and sodium ions. In the manganese nodules examined by GOLDBERG (1954) the iron/manganese ratio varied between 0·26 and 1·04. The lowest value reported for this ratio (0·018) is derived from a nodule from the Atlantic Ocean (BUSER and GRÜTTER *op. cit.*).

One of the results of the important work of BUSER and his collaborators was the observation of the large surface areas of the nodule materials. Values ranged between 6 and 190 $m^2 g^{-1}$, and the highest values are found in nodules with a large fraction of δ-MnO_2 or FeOOH. BUSER and GRÜTTER on the basis of these observations explain the high concentration of the accessory metals in manganese nodules. It is well known that such polyvalent ions with a high charge density as copper, the rare earths, zinc, lead, etc. more readily enter into sorption reactions than the alkali or alkaline earth metals (GOLDSCHMIDT, 1954, p. 67). The relative amounts of these metals in the ferromanganese oxide minerals probably reflect the activity in sea water of the corresponding ions. These activities may be enhanced at the sediment-water interface by the dissolution from the ocean floor of other phases high in the elements in question such as microcrystalline apatite (ARRHENIUS, BRAMLETTE and PICCIOTTO, 1957). Additional confirmation that these accessory metals are directly or indirectly derived from sea-water is given by the work of PATTERSON, GOLDBERG and INGHRAM (1953) on the isotopic composition of lead in manganese nodules.

Apparently the only non-biological agent in marine waters in appreciable concentrations that is capable of oxidizing manganese is oxygen. The reaction

$$2\,OH^- + Mn^{++} + \tfrac{1}{2}\,O_2 = MnO_2 + H_2O \qquad \Delta F^\circ = -38{\cdot}2 \text{ kcal}$$

has a free energy of $^-$9 kcal at 25°C at a pH of 8, a manganous ion concentration of 10^{-9} M and a partial pressure of oxygen of 0·25 atm (data from LATIMER, 1952).

The fact that the tetravalent manganese is not found in the sea-water but accretes at the sediment-water interface indicates that a surface is necessary for the reaction. The well known catalytic properties of iron oxides, coupled with the frequent presence of large amounts of iron in the manganese nodules, suggests that ferric oxides may provide the most important initial active surface. Assuming that the oxidation requires catalysis on the oxide surface, the amount of manganese deposited will be related to the length of exposure of a given surface to sea-water and to the rate of supply of ferric oxides. Thus, for high rates of accumulation of iron, the active surfaces will be continually replaced and high rates of manganese accumulation will be expected, although the mass concentration of manganese will be low.

Indirect indications, as well as direct measurements, point at a low total rate of accumulation in most localities where the manganese concentration of the sediment is high. The abundance of manganese nodules on topographic highs is greater than in sediments in adjacent depressions. Manganese nodules are commonly found accreting on top of outcrops of pre-Pleistocene sediments (Hamilton, 1956). The rate of accretion of manganese nodules has been estimated to be 1 mm/10^3 years* whereas the rates for Pacific clays and calcareous and siliceous oozes range from several mm to several cm in 1000 years (Arrhenius, 1952). Sedimentary components, which are diluted at high total rates of deposition, like fish debris, are highly concentrated to manganese sediments. The crystal size of authigenic minerals like barite and phillipsite tends to be large in sediments high in manganese (Bramlette and Arrhenius, in preparation).

In areas with a low total rate of deposition, and a high content of dissolved oxygen in the bottom water, oxidation of dissolved manganous ion at a suitable surface, and subsequent accretion of ferromanganese oxide minerals may thus become the dominant accumulation process. The forming δ-MnO_2 acts as a scavenger of high charge density ions in sea-water, which are probably accommodated in the disordered layers of the resultant manganite (Buser and Grütter, 1956).

Goldberg (1954) postulated that manganese nodules were formed by electrophoretic deposition of oceanic colloidal particles of iron and manganese. The iron colloids are known to be electropositive and the manganese colloids electronegative. The electro-potentials were attributed to the flow of ocean water, a good electrical conductor, through the earth's magnetic field. The natural electrodes would correspond to the nuclei about which manganese and iron accumulate such as pumice, clay aggregates, sharks' teeth or earbones of whales. Such electrodes must either possess a conductance greater than that of the surrounding sediment or project above the water-sediment interface. The positively charged iron particles and the negatively charged manganese particles would be electrophoretically deposited when the electrodes were negatively and positively charged respectively. Potential charge reversal could result if the water movement were tidal in nature. Since the majority of the manganese in sea-water has been observed to be in a dissolved state, such a mechanism appears unlikely for this element.

Some observations on a pair of recently dredged inshore nodules may be of interest from the point of view of deposition of iron from sea-water. Two nodules with metallic nuclei were obtained from dredge hauls taken in the San Clemente Basin (lat. 32·5°N; long. 118°W) at an approximate depth of 2000 m. The specimens consist of coatings of ferric oxides about pieces of steel and have gross features similar to manganese nodules. A section of one of the iron nodules is shown in Fig. 9. In the same figure, for the sake of comparison, is shown a cross-section of the Horizon manganese nodule, recovered from a depth of 5500 m at 40°14′N and 155°15′W.

The composition of the iron oxide coating appears to be indicative of its origin. The coating possesses, like the ferromanganese minerals of manganese nodules, such a low degree of crystallinity, that the structure could not be revealed with ordinary parafocusing methods of X-ray diffraction. A small amount of quartz

---

* This value from Pettersson (1943) and von Buttlar and Houtermans (1950) may in fact be much too high. It is based on the assumption that the radium in the nodules is unsupported, i.e. derived from sea-water. The unusually high amounts of thorium (Goldberg and Picciotto, 1955) which is directly or indirectly sorbed from the sea-water, suggest that the ionium in sea water, resulting from uranium decay, is collected by these concretions. If all of the radium is ionium supported, that is the extreme case, the rate of deposition given above is too high by a factor of 50, the ratio of ionium to radium half-lives.

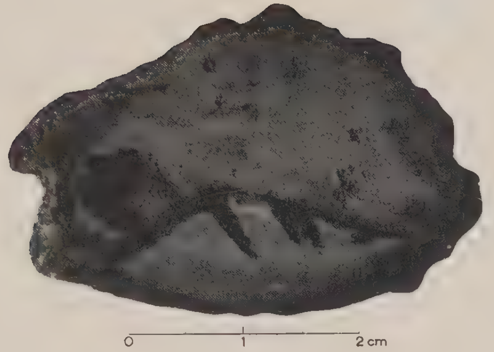

9 (a)

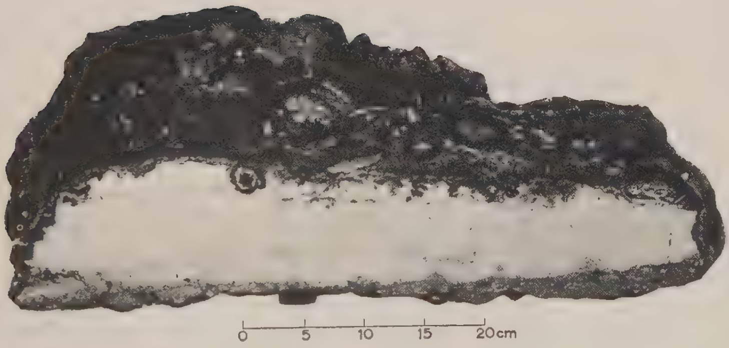
0
5
10
15
20 cm

9 (b)

Fig. 9. Sections through one of the San Clemente nodules (top) and the Horizon nodule (bottom).

is indicated by the diffraction pattern. The chemical composition of the oxide coating (Table 19) shows concentrations of zirconium and titanium, abundant elements in the hydrogenous ferromanganese oxide minerals (GOLDBERG, 1954; WISEMAN, 1956). The oxide coating also contains large amounts of magnesium, barium and boron, whereas the steel shows little or none of these elements. Conversely, the relatively high contents of manganese, chromium and vanadium in the steel core are not found in the coating, indicating that the metal was not the source material for the oxide accretion. Some oxidation of the steel fragment probably occurred during the initial period in which the metal lay at the sediment water interface but probably resulted only in a thin coating. The waters overlying the sediments in the San Clemente area contain around 2 ml of dissolved oxygen per litre of water (EMERY and RITTENBERG, 1952).

Table 19. Minor constituents in the San Clemente iron concretion and its metallic core

Element	Oxide phase	Metallic phase
	wt. %	wt. %
B	0·004	—
Ba	0·02	—
Ca	0·2	—
Co	0·005	0·01
Cr	0·002	0·01
Cu	0·05	0·05
Mg	0·5	—
Mn	0·1	1·0
Ni	0·02	0·1
Sn	—	0·005
Sr	0·002	0·005
Ti	0·02	—
V	—	0·005
Yb	0·0002	0·002
Zr	0·001	—

Any process, for example the rapid flow of ocean water through the earth's magnetic field, causing the steel to be cathodic with respect to sea-water would attract the positively charged iron colloidal particles from the sea-water. Such a precipitation has been produced in the laboratory with a potential difference of 0·5 V/cm in a colloidal solution containing a 100 μg of iron per l. of sea-water. Another precipitation mechanism could be the preferential discharging of the iron oxide colloid at conductive surfaces, where the stabilizing colloidal charge is readily dissipated to ground.

The steel nucleus appears to be a shell fragment and was probably deposited during the last 50 years when the San Clemente area was used as a U.S. Naval Target Range. Hence the rate of accumulation is at least of the order of mm per year. This high rate of accretion allows relatively short times for a given iron surface to be in contact with the sea-water containing the manganous iron. The iron content is 75 per cent and the manganese concentration 0·1 per cent. The iron-manganese ratio attains a value of 750.

In the more slowly accumulating pelagic clays (order of magnitude mm/1000 years) this ratio varies between 2 and 60. In the extreme case of pelagic manganese nodules, which accrete at a rate of 1 mm/1000 years or less, and where the iron oxide surfaces thus have time to attain a high degree of saturation with manganese oxide, the iron/manganese ratio accordingly reaches very low values, varying between 0·02 and 1.

The rate of accretion of manganese as expected appears to be highest in the San Clemente nodule, viz. a minimum of 200 μg cm^{-2} year^{-1} (assuming a total rate of growth of 100 cm in 1000 years). The average accretion rate is estimated to be 4 μg cm^{-2} year^{-1} in pelagic clays (assuming a manganese content of 1 per cent and a total rate of sediment growth of 2 mm in a thousand years). For manganese nodules with a content of 10 per cent manganese and rates of growth varying between 0·02 and 1·0 mm in 10^3 years, the computed accumulation rate of manganese ranges between 0·4 and 20 μg cm^{-2} year^{-1}.

The present interpretation of the mechanism of formation of nodules of manganese and iron oxide minerals in the ocean can be summarized as follows: Manganous ions brought to the sediment-water interface by oceanic mixing, by deposition and redissolution of organic remains, and possibly by other processes are oxidized to tetravalent manganese by the catalytic action of the discharged iron oxide colloid in the presence of oxygen. The tetravalent manganese oxide in the form of δ-MnO$_2$ associates with the catalyst, and to a smaller amount with divalent manganese oxyde-aquate to form the ferric and manganous manganites discovered by BUSER and GRÜTTER. The lower the total rate of accumulation the more complete is the utilization of the iron oxide as a structural element in the manganite. The concentration ratio between the free iron oxide left over in over in this process, on one hand, and tetravalent manganese in the nodules on the other, might therefore be indicative of the rate of growth of these polymineral aggregates.

Further, manganese and associated heavy metals occur in relatively large amounts in the most fine grained part of the sediment (Fig. 5) in a form that is resistant to dissolution in EDTA. The absence of a tendency to formation of soluble complexes, together with the fact that clay minerals are the only crystalline species which were found by X-ray diffraction technique in these fractions of the sediment, indicates that the insoluble manganese, nickel, copper, cobalt, lead, silver, zirconium, scandium, chromium and molybdenum in the colloidal range possibly proxy for the main cations in clay minerals. The amount of manganese and associated metals bound in this way is of the order of 0·1 per cent of the total sediment, whereas the amount present in ferromanganese oxide minerals varies between wide limits (approx. 0·1–25 per cent).

5.13. *Copper*. Copper prevails in sea-water as Cu^{++}, CuCl^{+} and CuSO$_4$, ionic species similar to those of the transition divalent metals. Like such elements as nickel, cobalt, lead and molybdenum it appears in δ-MnO$_2$ and manganite, 0·2–2 per cent (GOLDBERG, 1954; see further the covariance of copper and manganese in

Fig. 5), however, the relationship between copper and manganese is much less distinct than between nickel, cobalt, lead and molybdenum and manganese. This suggested other independent sources of copper.

The well known combination of copper with the organic molecules in the protein hemocyanin and the exceedingly strong ability of copper to complex with most organic functional groups (SCHUBERT, 1954) pointed to a biological origin. For a large number of organic complexes, containing bivalent metals, the order of stability is $Pd > Cu > Ni > Pb > Co > Zn > Cd \gg Mg; Ca > Sr > Ba > Ra$. The stability of the complex is apparently directly related to the basicity of the metal.

It is thus not surprising to find that copper appears in the organic phase of fish debris (ARRHENIUS, BRAMLETTE and PICCIOTTO, 1957; ARRHENIUS, BRAMLETTE, PICCIOTTO, CHODOS and GODIJN, in preparation) in amounts of 0·1–0·5 per cent of the mineral aggregate, and 2–10 per cent of the organic phase. That the concentration takes place after the death of the organism, is indicated by the fact that the skeletal ash of bathypelagic fish, caught alive, contains only one tenth of the amount of copper found in the skeletal remains of bathypelagic fish in the deposits.

Assuming both a biogenous and a hydrogenous source of copper in pelagic sediments, the total copper concentration can be expressed as the sum of these two components, with the hydrogenous copper equated to a constant times the manganese concentration. Such a computation was made by REVELLE *et al.* (1955) who found a remarkable covariance between the biogenous copper and barium, this latter element presumed to be dominantly associated with organic phases (see section 5.4).

Copper also occurs in igneous ferromagnesian minerals, abundant in Cap. 31 BG (Fig. 5). The pyroclastic material of the coarse fractions of this sediment which contain 0·2–0·3 per cent copper are high in augite, possibly indicating the proxying of copper for ferrous iron in this mineral as suggested by RAMDOHR (1940).

Finally, copper is found in the fine grained ($< 1\ \mu$) fractions of the sediment, in an unidentified form, resistant to chelative dissolution (Cap. 33 BG and 50 BP 0–30 cm, Fig 5). This copper occurs in concentrations of 0·2–0·4 per cent of the mass of the sediment fraction and may possibly be localized in the clay minerals.

6. COMPARATIVE CHEMISTRY OF PELAGIC SEDIMENTS IN SPACE AND TIME

Interpretations of the observed differences in the composition of pelagic deposits from different areas and of different ages may be proposed on the basis of the mechanics of formation of recent pelagic sediments in the Pacific.

A modest number of chemical analyses have been performed upon sediments from the Atlantic Ocean (WEDEPOHL, 1955; HUTCHINSON, BENOIT, COTTER and WANGERSKY, 1955; LANDERGREN, 1956; SMALES, MAPPER and WOOD, 1957) and these data have been collated in Fig. 10 together with the comparable elemental assays of Pacific clays and manganese nodules (GOLDBERG, 1954 and previously unpublished results).

The composition of the manganese nodules is characterized by high concentrations of the ferromanganese oxide minerals and by higher concentrations of manganese and other divalent transition elements than either the clay sediments from the Atlantic or Pacific Oceans. Accepting the assumption that the rate of deposition of marine deposits is inversely related to the manganese content (Section 5.12), it is apparent that accumulation rates in the Atlantic are higher than in the Pacific from Fig. 10. Seismic refraction studies of the thickness of the first layer encountered on the ocean floor, presumed to be a blanket of unconsolidated sediments, may be taken to support such an hypothesis. Raitt (1956) gives values for 37 stations in the central Pacific area ranging between zero and 2·12 km with a mode of 0·34 km and an average of 0·43 km. On the other hand, Worzel and Shurbet (1955) find a sedimentary layer of 1·0 km thick for a standard oceanic crustal section in the Atlantic.

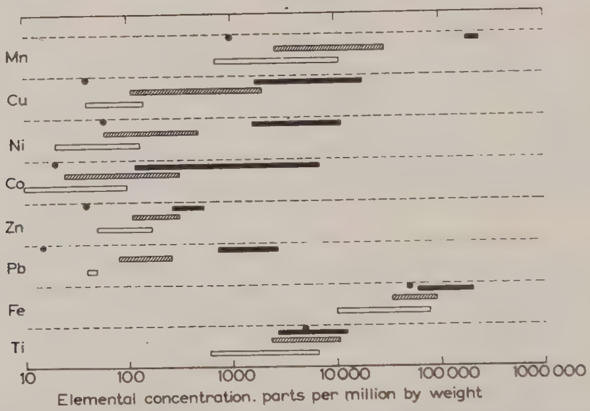

Fig. 10. Ranges of concentration of manganese and associated metals in manganese nodules (black rectangles), Pacific pelagic sediments stippled and Atlantic pelagic sediments (open). Filled circles represent igneous rock concentrations.

The observation that the rate of accumulation of sediments is higher in the Atlantic than in the Pacific is not suprising. Revelle *et al.* (1955) point out that the larger Pacific Ocean has a much smaller area of river drainage and a lower number of large rivers than the Atlantic. The sedimentation basins of the Pacific are to a great extent protected against turbidity transport of material from the continents by rises and trenches running parallel to the coast.

The more rapid decrease of calcium carbonate with increasing depth in the Pacific, compared to the Atlantic, might be explained by the lower rates of accumulation which would allow the carbonate to be in contact longer with the corrosive bottom waters.

In all of the cores from the north east Pacific Ocean that penetrate from Quaternary into Lower or Middle Tertiary strata, the quartz content rises markedly at the transition from the older to the younger system (Rex and Goldberg, in preparation). This has been interpreted by postulating either an increased rate of accumulation of quartz, which is presumed by the authors to be dominantly of eolian origin in the pelagic areas, or a decreased deposition of diluting materials during Quaternary as compared to Tertiary time. Further, in Quaternary clays from the south equatorial and equatorial Pacific, the quartz concentrations are much lower than in clays from the adjacent northern regions.

The changes in quartz content in the north equatorial Pacific deposits with depth are accompanied by changes in gross chemical and mineralogical composition.

Table 20. Ratios of chemical constituents between the Tertiary and Quaternary sections of a north equatorial Pacific core and between a recent south equatorial core and the north equatorial Quaternary section

	$\frac{\text{Cap. 50 BP}_{300-760\text{ cm}}}{\text{Cap. 50 BP}_{0-300\text{ cm}}}$	$\frac{\text{Cap. 33 BG}}{\text{Cap. 50 BP}_{0-300\text{ cm}}}$
SiO_2	0·97	0·80
Al_2O_3	0·83	0·98
Fe_2O_3	1·3	1·22
TiO_2	0·69	0·83
MgO	0·96	1·3
CaO	1·41	5·3
Na_2O	1·2	1·4
K_2O	0·89	0·77
SrO	1·6	1·9
BaO	1·5	0·43
B_2O_3	0·93	0·60
MnO	2·9	6·3
Ga_2O_3	0·70	0·65
NiO	1·2	2·4
CuO	1·1	1·1
Co_2O_3	0·50	2·4
Cr_2O_3	0·44	0·24
V_2O_5	1·1	1·5
PbO	1·3	1·9

REVELLE *et al.* (1955) found that the manganese/nickel and iron/titanium ratios in core Cap. 50 BP (Table 1) were markedly different in the Quaternary and Tertiary strata which are separated by a discontinuity. This observation is expanded in Table 20 which provides the ratios of the elemental abundances of the lower and upper parts of Cap. 50 BP, and for comparison the same ratio for the south equatorial Pacific core 33 BG and the upper part of Cap. 50 BP. Similar differences between Quaternary and Tertiary sediments have been observed in cores Cap. 49, Ck 2 and Ck 4 (Table 1). High manganese, calcium and sodium concentration in the Tertiary part of 50 BP and in the south equatorial deposits, as compared to the upper levels of 50 BP, result from the presence of ferromanganese oxide minerals and authigenic phillipsite, minerals indicative of low rates of accumulation.

It is tempting to relate these observed similarities to similar conditions in Tertiary times in the north central Pacific and at present in the south equatorial Pacific. The qualitative inference that the accumulation of solids was much less, appears grounded on the basis of both chemical and mineralogical evidence. However, it must be remembered that changes of other parameters directly or indirectly related to the total rate of accumulation may have contributed to the observed differences in properties of the sediments. The temperature of the deep and bottom water of the ocean is known to have decreased by 10–12°C since Early Tertiary (EMILIANI and EDWARDS, 1953), a change that may have markedly affected the rate of formation of authigenic minerals on the ocean floor directly, and in the case of ferromanganese oxide minerals indirectly through changes in the activities of the reactants.

Further, the solubility of calcium carbonate decreases with temperature. Any temperature change in the bottom waters could significantly influence the dissolution of calcium carbonate and concurrently the activity of calcium ion in the pore waters of the deposit. Other phenomena, as weathering and river influx, wind patterns and eolian transport, and possibly volcanism were quite different in extent between these two geological periods. Their influences upon the composition of the sediments can as yet not be definitively judged but future work may well reveal their significance.

7. THE GEOCHEMICAL BALANCE

The quantitative study of the changes of state of substances over the surface of the earth has attracted many contributions since the initial modern work of JOLY (1899). The goals of the calculations generally have been the determination of the total amounts of sediments formed and of the complementary amount of igneous rocks decomposed. The starting points are the tabulations of average elemental abundance in igneous rocks, in the various classes of sediments and in the oceans. These data are fed into a number of simultaneous equations relating the unknowns, the amount of weathered igneous materials and the amounts of sediments produced.

The general pattern for geochemical balance computations was set by CLARKE (1924) and GOLDSCHMIDT (1937) and was based to a large extent on the chemical composition of rock classes as given by CLARKE. Although modifications and attempts to increase the accuracy of the calculations have appeared (see for example CORRENS (1948) and WICKMAN (1954)), the basic conclusions initially reached have remained unaltered. There have been between 150 and 200 kg of igneous rocks weathered to produce a similar mass of sandstones and shales and around 15 kg of carbonate rocks for every cm^2 of earth's surface. These figures show marked differences from the relative percentages of sedimentary rocks from field measurements in which the sandstones and limestones are proportionally much higher. Such discrepancies are attributed to difficulties in respresentatively measuring and averaging sediments throughout the geological column on a worldwide basis and in determining the proportions of the basic constituents in mixed formations (PETTIJOHN, 1957, p. 11).

Although there is fundamental agreement as to the average composition of the earth's crust and of sea-water, there is no concurrence with respect to the relative proportions of the main types of sedimentary rocks. GOLDSCHMIDT (1954, p. 61) states "The regions of deposition of the great sedimentary masses are, as a rule, not the deep sea basins but chiefly those parts of the continental block which at the time happened to belong to the shelf region of the coastal sea". On this basis GOLDSCHMIDT considers the pelagic clays of negligible importance in his calculations and derives his average composition of sedimentary materials solely on the basis of shales, phyllites, mica schists and terrigenous mud (CLARKE's data from which the sea-salts were removed—see below). He arrives through his balance calculations at an average thickness of sediments of 638 m over the surface of the earth. Since one can assume a conservative minimal figure for the depth of pelagic sediments of 300 meters (WORZEL and SHURBET, 1955; RAITT, 1956) in both the Atlantic and Pacific Oceans, since red clays now cover about 28 per cent of the sea floor (KUENEN, 1950, p. 362) and the sea floor constitutes about 70 per cent of the earth's surface, the red clays account for at least 60 m or 10 per cent of GOLDSCHMIDT's figure. More important they would be the second most abundant sediment type inasmuch as shales and sandstones (according to GOLDSCHMIDT) have a thickness of 585 m while limestones and dolomites have computed depths of 38 and 15 m respectively.

KUENEN (op. cit., p. 364) on the other hand arrived at the conclusion that the ratio of red clay, blue mud and globigerina ooze is 3.2:1 and that the total mass of pelagic and hemipelagic sediments is three times the mass of the continental and epicontinental sediments. The mass of red clay is thus made to account for over 50 per cent of the mass of sediments. Although both authors arrive at not significantly different figures for the amounts of igneous rock weathered and sediments produced, the question of the proportion of pelagic deposits remains unresolved. Thus a closer scrutiny of both the assumptions involved in such balance computations and the validity of the data used appears warranted.

In order to ascertain the relative contribution of pelagic clays to the totality of sediments, general equations, based upon the principles of GOLDSCHMIDT and CLARKE, have been used in this work:

$$A_xX - B_xY - C_xZ - D_xS = M_x$$

where X, Y, Z and S are the total quantities of igneous rocks, pelagic clays, limestones and globigerina oozes, and shales and sandstones, expressed as kg/cm² of earth's surface. The coefficients A_x, B_x, C_x and D_x represent the per cent concentration of the element x in each respective class, while M_x is the amount of the element in sea-water in units of kg/cm² of earth's surface multiplied by 100.

The equations are most sensitive for products of the major sedimentary cycle whose chemical compositions show marked variations from those of igneous rocks. CORRENS (1954) has already discussed the minor changes observed in the results for modest alterations of the concentrations of elements in igneous rocks and sediments. The uncertainties inherent in the estimate of average elemental abundances in different rock types exert a great influence on the solution of the equations when the constants approach each other in magnitude, i.e. when the differentiation of elements between the different rock types is small. To obtain results of maximum significance, such elements must therefore be chosen which display a maximum differentiation between igneous rocks, the sedimentary rock types and sea-water. GOLDSCHMIDT considered in his primary calculations two major fractionations—the accumulation of calcium and magnesium in carbonates in which the enrichment of both elements is of one order of magnitude and the relative enrichment and depletion of the elements in the sea-water reservoir. In his computations, shales and sandstones were considered alike enough in composition not to warrant placing them initially in separate groups, and for the same reasons limestones and globigerina oozes were combined.

A third major fractionation occurs in the formation of the pelagic clays in which manganese and certain associated metals are enriched over their igneous rock values by factors of five to ten. Kuenen (1950, p. 390) noted in his balance sheet that the manganese contents of the red clays are far too high in relation to igneous rock values for a derivation of this element from magmatic source materials. He explained this discrepancy by stating that the slowly accumulating pelagic sediments are rich in manganese and such samples are overemphasized in the composite sample given in Clarke (1924).

The four elements used for the present computation were chosen with respect to the major fractionations: sodium and potassium because of the depletion of potassium relative to sodium in sea-water; calcium because of its concentration in carbonate sediments; and manganese due to its enrichment in pelagic sediments.

The igneous rock data are taken from Fleischer (1953); the data on shales and limestones from Clarke (1924); the data on pelagic clays from this paper; and the sea-water abundances from Sverdrup, Johnson and Fleming (1946). The manganese value in shales is Minami's average, quoted in Goldschmidt (1954, p. 652).

The data for pelagic clays include sorbed and interstitially dissolved solids and the assumption is made that these solids are a part of the sediments rather than a part of the hydrosphere. Clarke's data for red clays and terrigenous sediments refer to samples in which the sea-salts have been washed out (Clarke, *op. cit.* p. 517). Whether one considers the pore solution as a part of the hydrosphere or of the sediment may be simply a matter of definition, but both operationally and theoretically there are compelling reasons to include them as a part of the pelagic clays. First of all, there is no evidence to indicate that at least the water of the Cenozoic system has been returned to the major sedimentary cycle. Arrhenius (1952) has shown that even in the most advanced stage of diagenesis observed in indurated Tertiary pelagic clays, no marked expulsion of water has taken place. Secondly, the ion-exchange characteristics of the minerals of these clays make it very difficult by any washing technique to remove solely the sea-salts without altering the composition of the solids.

The so-called hemipelagic sediments are in the present paper regarded as a part of the shales due to the similarity in origin and composition.

As Kuenen has pointed out, the use of the arithmetic average of the manganese concentrations in pelagic clays introduces an error in the balance computation by overemphasis of the slowly accumulating deposits. It appears reasonable, in the absence of measured rates of accumulation for all samples involved, to assume that the manganese concentration is inversely related to the rate of accumulation. The use of the reciprocal average should under these conditions compensate for this over-representation. The reciprocal average of all Pacific clays reported herein is 0·77 per cent Mn whereas the arithmetic average is 0·95 per cent. Correns (1937) gives an arithmetic average of 0·25 per cent for the carbonate-free fraction of around 180 Atlantic sediment samples. This value has been reduced to 0·19 per cent such that the ratios of the arithmetic to reciprocal average are the same in both oceans. To obtain an average for all oceans these two values were combined with a weighting factor of one for the Atlantic Ocean and three for the Indo-Pacific oceanic area. The resulting average manganese content thus obtained is 0·4 per cent.

Even with due regard to the rate effect pointed out by KUENEN, the manganese content of pelagic clays is still significantly higher than that of igneous rocks. Further, a whole suite of heavy metals, including copper, nickel, cobalt and lead, display a similar concentration pattern such that the red clay values are much higher than those of the igneous rocks from which they were presumably derived. Therefore, either KUENEN's estimate of the amount of red clays must be too large, or there is another source of entry of manganese and associated heavy metals into the major sedimentary cycle.

The system of equations can be written as follows:

$$\begin{array}{ll}
\mathrm{Na} & 2{\cdot}8\,X - 3{\cdot}4\,Y - 0{\cdot}04\,Z - 0{\cdot}97\,S = 297{\cdot}5 \\
\mathrm{K} & 2{\cdot}5\,X - 2{\cdot}5\,Y - 0{\cdot}27\,Z - 2{\cdot}7\,S = 10{\cdot}7 \\
\mathrm{Ca} & 3{\cdot}5\,X - 2{\cdot}6\,Y - 30{\cdot}4\,Z - 2{\cdot}2\,S = 11{\cdot}3 \\
\mathrm{Mn} & 0{\cdot}1\,X - 0{\cdot}4\,Y - 0{\cdot}038\,Z - 0{\cdot}062\,S = 0
\end{array}$$

The solution of these equations gives: $X = 185$, $Y = 23$, $Z = 8{\cdot}5$ and $S = 145$ in units of kg/cm^7 of earth's surface. Thus, the contribution of pelagic clays appears to be approximately 13 per cent of the total amount of sediments and somewhat greater than that of the carbonates.

The importance of balance calculations of this kind lies not in sharply delimiting the amounts of each sediment class but rather in the elucidating the general features of the major sedimentary cycle. Too many assumptions of doubtful validity and uncertainties in the values for the composition of the geological domains deny a strictly quantitative interpretation of the results.

It is, for example, normally assumed that the ultimate source of pelagic sediments is the weathering products from the continents. A number of authors have pointed out that the pyroclastics and their subsequent weathering products may significantly contribute to pelagic clays. This point has been considered at great length by MURRAY in the case of submarine volcanism. Quantitative estimates of contributions of supramarine pyroclastics have been suggested by KUENEN (1941, p. 166). He took as the composition of the source material, one part of plutonic and one part of volcanic rocks, the latter with a composition of rhyolite: andesite: basalt as 1:2:4.

The values for pelagic sediments are obtained from the samples of the surface layer of the sedimentary carpet beneath the oceans. Most analyses are from columns extending less than 20 m into the deep-sea floor. Thus, the assumption that materials from the present pelagic sediment surface are representative of weathering processes and sedimentation throughout geologic time must be considered. Changes in the rate of deposition of several elements, amounting to one order of magnitude have been demonstrated to be common in the Tertiary and Quaternary of the east Pacific and the relative extent of calcareous sediments appears now to be considerably smaller than in Tertiary time (Arrhenius, 1952). The quartz content measured in a number of profiles shows a change between two geological periods by factors of three or four (Rex and Goldberg, in press). The amplitude in regional concentrations is also considerable (Revelle, 1944; Hutchinson, 1947; Goldberg, 1954) which makes it very difficult to decide upon an average compositional value for any element. Ocean to ocean variations in minor and trace elements have been clearly demonstrated (Fig. 10) and must be taken into account. Differences in the relative and absolute amounts of rock types exposed to weathering during geologic time are difficult to assess and present a further uncertainty in computations of a geochemical balance.

The residence times of elements in the ocean can be calculated on the basis of the values derived for the amounts of elements introduced into the major sedimentary cycle and for the rates of accumulation of pelagic clays.

Kuenen (1950, p. 362) gives the area of pelagic deposition as 268×10^{16} cm². Accepting an average accumulation rate of hydrogenous and lithogenous matter over this area of 0·1 cm/10^3 years and a density of the clay fraction of 2 with a water content of 50 per cent by weight, calculation of the total mass of pelagic clay accumulated in one year gives $26{\cdot}8 \times 10^{13}$ g. Division of this value with the fraction of pelagic clays in the totality of sediments (0·13), derived above, gives 2×10^{15} g/year as the amount of weathering products and pyroclastics. It is assumed in the present computation that practically all of this material enters the oceans.

If it is further assumed that the present chemical composition of the oceans represents a steady state system in which the amount of material introduced per unit time is compensated by an equal amount deposited as sediments, and that there is complete mixing of materials introduced into the oceans in times that are short with respect to the residence times. The residence time in years of an element in sea-water is then given by

$$T = \frac{A}{dA/dt}$$

where A is the total amount of the element in suspension or solution in the oceans and dA/dt is the amount introduced into the oceans per year. Values for the residence times of a selected group of elements are given in Table 21.

A remarkable agreement is observed between these values and those of Barth (1952), who made a similar set of calculations, using values for the rate of supply of elements to the ocean by rivers instead of the rate of removal from the ocean. Barth gives relatively few values, inasmuch as only a few elements have been adequately assayed in river water.

Although many independent assumptions are involved in the calculations, the absolute and relative values obtained for the residence times of the element appear reasonable. The element of longest residence, sodium, has a residence time within an order of magnitude of the age of the oceans, several billion years. The alkali and alkaline earth metals all have residence times in the range of 10^6–10^8

years. Manganese shows a remarkably low value in comparison to the metals associated with it in marine deposits such as zinc and nickel. This relation probably depends on the unique removal of manganese from solution in the oceans by oxidation (Section 5.12), a process that precedes the sorption which accounts for the deposition of the associated metals, and demands a larger amount of manganese than of the sorbed ions.

Silicon and aluminium are among the elements with the shortest residence times. Both are reactants in the formation of clay minerals and partly enter the oceans as rapidly settling suspended solids. Iron and titanium, which also pass rapidly through the hydrosphere, probably prevail as solid phases during the major part of their residence, even in the pelagic areas of the ocean. The absolute values for the residence times of these elements are somewhat tenuous as the assumption that these times are small in comparison with the mixing time is invalid in these cases. It may be worthwhile in the future, when values exist for the contribution of solid and dissolved phases of these elements to the total concentrations, to calculate more accurately the residence times of both of these components.

Table 21. Residence times of elements in the oceans

Element	Amount in oceans (g)	Residence time in years	
		This work	**Barth** (1952)
Na	$1\cdot47 \times 10^{22}$	$2\cdot6 \times 10^{8}$	$2\cdot1 \times 10^{8}$
Mg	$1\cdot8 \times 10^{21}$	$4\cdot5 \times 10^{7}$	$2\cdot2 \times 10^{7}$
Li	$2\cdot8 \times 10^{17}$	$2\cdot2 \times 10^{7}$	
Sr	$9\cdot8 \times 10^{18}$	$1\cdot6 \times 10^{7}$	
K	$5\cdot3 \times 10^{20}$	$1\cdot1 \times 10^{7}$	$1\cdot0 \times 10^{7}$
Ca	$5\cdot6 \times 10^{20}$	$8\cdot0 \times 10^{6}$	$1\cdot0 \times 10^{6}$
U	$5\cdot2 \times 10^{15}$	$6\cdot5 \times 10^{5}$	
Zn	$1\cdot4 \times 10^{16}$	$1\cdot8 \times 10^{5}$	
Cu	$5\cdot2 \times 10^{15}$	$6\cdot5 \times 10^{4}$	
Co	$7\cdot0 \times 10^{14}$	$1\cdot8 \times 10^{4}$	
Si	$5\cdot2 \times 10^{18}$	$1\cdot0 \times 10^{4}$	$3\cdot5 \times 10^{4}$*
Mn	$1\cdot4 \times 10^{15}$	$7\cdot0 \times 10^{3}$	
Fe	$1\cdot4 \times 10^{16}$	$1\cdot4 \times 10^{2}$	
Ti	$1\cdot4 \times 10^{15}$	$1\cdot6 \times 10^{2}$	
Al	$1\cdot4 \times 10^{16}$	$1\cdot0 \times 10^{2}$	

* This value was obtained from the influx value given by **Barth** (1952) and the amount of silicon in the oceans from this paper. **Barth** gives only an upper limit for this latter number.

Mention should be made of the importance of the residence time in predicting the increases in concentration of artificial radionuclides introduced into the oceans by nuclear detonations or as wastes from reactors. The isotopes of strontium and caesium, both hazardous to living organisms, would have residence times in the oceans which are very high relative to their half-lives. Hence, the great majority of radionuclides of these elements brought into the oceans would undergo radioactive decay there. Further, it is evident that the bulk of the radioisotopes introduced into the marine environment during the next few hundred years will build up to values of specific activity for each element that is principally a function of the decay constant of the isotope and the rate of entry, rather than of any sedimentary process.

Acknowledgements—The authors wish to express their gratitude to the sponsors of this research, and to those who gave their help in the work, viz. Dr. M. N. BRAMLETTE who continually contributed with suggestions, observations and criticism; Dr. HARRISON BROWN in whose institute the research under Section 5.5 was carried out; Dr. R. CASTAING, who took an active part in the X-ray microanalysis reported in Section 5.4; Dr. M. ROY and M. G. DE FAGET, who kindly put the facilities at the O.N.E.R.A. to disposal for this part of the investigation; Mr. C. HARVEY and Mr. A. CHODOS, who contributed to the optical spectrographic analysis; and Dr. F. A. PANETH, who gave help and constructive suggestions. The authors are further indebted to Drs. J. R. ARNOLD, O. ARRHENIUS, W. BUSER, C. W. CORRENS, H. CRAIG, G. DE HEVESY, M. FLEISCHER, E. INGERSON, PH. H. KUENEN, E. PICCIOTTO, R. REVELLE and K. H. WEDEPOHL, for their valuable criticism and comments.

REFERENCES

ARRHENIUS G. (1952) Sediment cores from the East Pacific. *Repts. Swed. Deep-Sea Exped.* No. 5.
ARRHENIUS G. (1954) *Bull. Geol. Soc. Amer.* **65**, 1228–1229.
ARRHENIUS G. and GOLDBERG E. D. (1955) *Tellus* **7**, 226–231.
ARRHENIUS G., BRAMLETTE M. N. and PICCIOTTO E. (1957) *Nature, Lond.* 180, 85–86.
BARTH T. W. (1952) *Theoretical Petrology*. John Wiley, New York.
BJERRUM N. (1948) *Bull. Soc. Chim. Belges* **57**, 432–495.
BOUSSINGAULT F. (1882) *Ann. Chim. Phys.* **27**, 289.
BOWEN H. J. M. (1956) *J. Mar. Biol. Ass. U.K.* **35**, 451–460.
BRADFIELD R. (1932) *J. Phys. Chem.* **36**, 340–347.
BUCHANAN J. Y. (1890) *Proc. Roy. Soc. Edinb.* **18**, 17–39.
BUSER W. and GRÜTTER A. (1956) *Schweiz. Min. Petrogr. Mitt.* **36**, 49–62.
BUSER W. and GRÜTTER A. (1957) Radiochemische Untersuchungen an Festkörpern IV.
BUTKEWITSCH W. S. (1928) *Ber. Wiss. Meeresinst. Moscow* **3**, 63–80.
VON BUTTLAR H. and HOUTERMANS F. G. (1950) *Naturwissenshaften* **37**, 400–401.
CASTAING R. (1952) *Office National d'Etudes et de Recherches Aéronautiques Publication Nr.* 55.
CHAVE K. (1954). *J. Geol.* **62**, 266–283.
CLARKE F. W. (1924) *U. S. Geol. Survey Bull.* 770.
CLARKE F. W. and WHEELER W. C. (1922) *U.S. Geol. Survey Prof. Paper* 124.
COLLIER A. (1953) *Science* **118**, 328.
COOPER L. H. N. (1948) *J. Marine Biol. Ass. U.K.* **25**, 279–313.
CORRENS C. W. (1937) *Wiss. Ergebn. Dtsch. Atlant. Exped. "Meteor"* 1925–1927 3, part 3.
CORRENS C. W. (1941) *Nachr. Ges. Wiss. Göttingen Math.-phys. Kl.* 5, 219.
CORRENS C. W. (1948) *Naturwissenschaften* **35**, 7–12.
CORRENS C. W. (1954) *Deep-Sea Res.* **1**, 78–85.
DALY R. A. (1933) *Igneous Rocks and the Depths of the Earth*. McGraw-Hill, New York.
DAVIES C. W. (1930) *J. Chem. Soc.* 1930 2421–2426.
DEGENHARDT H. (1957) *Geochim. et Cosmochim. Acta* **11**, 279–309.
DENNEY T. O. and MONK C. B. (1951) *Trans. Faraday Soc.* **47**, 992–8.
DIETZ R. S. and MENARD H. W. (1953) *J. Geol.* **61**, 99–113.
DIEULAFAIT L. (1883) *C. R. Acad. Sci., Paris* **96**, 718–721.
DORFF F. (1935) *Biologie des Eisens und Mangankreislaufes* Berlin.
EMERY K. O. and RITTENBERG S. C. (1952) *Bull. Amer. Ass. Petrol Geol.* **36**, 735–806.

EMILIANI C. (1955) *J. Geol.* **63**, 538–578.
EMILIANI C. and EDWARDS G. (1953) *Nature, Lond.* **171**, 887–889.
ERÄMETSÄ O., SAHAMA TH. and KANULA V. (1940) *Ann. Acad. Sci. Fenn. VLIIA* No. 3.
FLEISCHER M. (1953) *U.S. Geol. Survey Circular* 287.
GOLDBERG E. D. (1952) *Biol. Bull.* **102**, 243–248.
GOLDBERG E. D. (1954) *J. Geol.* **62**, 249–265.
GOLDBERG E. D. and PICCIOTTO E. (1955) *Science* 613–614.
GOLDSCHMIDT V. M. and PETERS C. (1932a) *Nachr. Ges. Wiss. Göttingen* **27**, 402.
GOLDSCHMIDT V. M. and PETERS C. (1932b) *Ibid.* **31**, 528.
GOLDSCHMIDT V. M. (1937) *J. Chem. Soc.* 1937, 655.
GOLDSCHMIDT V. M. (1954) *Geochemistry*. Oxford University Press, London.
GRIEL J. V. and ROBINSON R. J. (1952) *J. Mar. Res. Sears Foundation* **11**, 173–179.
GRÜTTER A. and BUSER W. (1957) *Chimia* **11**, 132–133.
VON GÜMBEL C. W. (1878) *S. B. Bayer. Akad. Wiss.* **8**, 189–209.
HAMILTON E. L. (1956) *Geol. Soc. Amer. Memoir* 64.
HARDER H. (1951) *Heidelberg. Beitr. Min.* **2**, 455–476.
HARVEY C. E. (1950) *Spectrochemical Procedures*. Applied Research Labs., Glendale, California.
VON HEVESY G., MERKEL A. and WÜRSTLIN K. (1934) *Z. Anorg. Chem.* **219**, 192.
HUTCHINSON G. E. (1947) *Ecol. Mon.* **17**, 299–315.
HUTCHINSON G. E., BENOIT R. J., COTTER W. B. and WANGERSKY P. J. (1955). *Proc. Nat. Acad. Sci. U.S.* **41**, 160–162.
JACOB K. D., HILL W. L. *et al.* (1933). *U.S. Dept. Agric. Tech. Bull.* 364.
JASMUND K. (1948) *Heidelberg. Beitr. Min.* **1**, 341–380.
JOLY J. (1899) *Trans. Roy. Dublin Soc.* **7**, 23.
JONTE J. H. and MARTIN D. S. (1952) *J. Amer. Chem. Soc.* **74**, 2052–2054.
JOST K. (1932) *Chem. d'Erde* **7**, 177.
KRAUSKOPF K. B. (1955) *Econ. Geol.* (*Fiftieth Anniv. Vol.*) 411–463.
KRAUSKOPF K. B. (1956) *Geochim. et Cosmochim. Acta* **9**, 1–33.
KUENEN PH. H. (1941) *Amer. J. Sci.* **239**, 161–190.
KUENEN PH. H. (1950) *Marine Geology*. John Wiley, New York.
KURODA P. K. and SANDELL E. B. (1954) *Geochim. et Cosmochim. Acta* **6**, 35–63.
LANDERGREN S. (1945) *Ark. Kemi. Min. Geol.* A **19**.
LANDERGREN S. (1956) *Repts. Swed. Deep-Sea Exped.* **7**, No. 2.
LATIMER W. M. (1952) *Oxidation Potentials* (Second Edition). Prentice-Hall, New York.
LEWIS G. J. and GOLDBERG E. D. (1956) *Analyt. Chem.* **28**, 1282–1285.
LINDGREN B., JOHNSON A. and SILLÉN L. (1947) *Acta Chem. Scand.* **1**, 479–88.
LUNDEGÅRDH P. H. (1946) *Ark. Kemi. Min. Geol.* A **23**, No. 9.
MARTELL A. E. and CALVIN M. (1952) *Chemistry of the Metal Chelate Compounds*. Prentice-Hall, New York.
MORITA Y. (1955) *J. Earth Sci. Nagoya Univ.* **3**, 33–57.
MURRAY J. and RENARD A. (1891) *Challenger Repts.* 525 pp.
MURRAY J. and IRVINE R. (1894) *Trans. Roy. Soc. Edinb.* **37**, 712–242.
NOCKOLDS S. R. and ALLEN R. (1956) *Geochim. et Cosmochim. Acta* **5**, 245–785.
PATTERSON C. C., GOLDBERG E. D. and INGRAM M. G. (1953). *Bull. Geol. Soc. Amer.* 1387–1388.
PETTERSSON H. (1943) *Medd. Oceanogr. Inst. Göteborg* B **2**. 1–39.
PETTERSSON H. (1945) *Ibid.* **3**, 1–37.
PETTIJOHN F. J. (1957) *Sedimentary Rocks* (Second Edition). Harper and Brothers, New York.
RAITT R. W. (1956) *Bull. Geol. Soc. Amer.* **67**, 1623–39.
RANKAMA K. and SAHAMA TH. (1950) *Geochemistry*. University of Chicago Press.
RAMDOHR P. (1940) *Abh. Preuss. Akad. Wiss.* No. 2.
REVELLE R. (1944) *Carnegie Inst. Wash. Publ. No.* 556.
REVELLE R., BRAMLETTE M., ARRHENIUS G. and GOLDBERG E. D. (1955) *Geol. Soc. Amer. Special Paper* 62, 221–236.
ROBINSON R. A. and STOKES R. H. (1955) *Electrolyte Solutions*. Butterworths, London.
SANDELL E. B. (1949) *Amer. J. Sci.* **247**, 40–48.

SANDELL E. B. (1952) *Geochim. et Cosmochim. Acta* **2,** 211–218.
SANDELL E. B. and GOLDICH S. S. (1943) *J. Geol.* **51,** 161–189.
SCHUBERT J. (1954) *Chemical Specificity in Biological Interactions* (Ed. F. R. N. GURD). Academic Press, New York.
SILLÉN L. G. (1954) *Acta. Chem. Scand.* **8,** 318–335.
SHAW M. (1954) *Bull. Geol. Soc. Amer.* **65,** 1151–1166.
SMALES A. A., MAPPER D. and WOOD A. J. (1957) *Analyst* **82,** 75–88.
STEEMAN-NIELSEN E. (1952) *J. Cons. Int. Explor. Mer.* 18, 117.
SVERDRUP H., JOHSON M. and FLEMING R. (1946) *The Oceans.* Prentice Hall, New York.
TAMM O. (1932) *Medd. Statens Skogsförsöksanst. Stockh.* **27,** 1–20.
THOMPSON T. G. and CHOW T. J. (1955) *Deep-Sea Res.* (Suppl. to Vol 3) 20–39.
TUREKIAN K. (1955) *Trans. Amer. Geophys. Un.* **36,** 523.
TUREKIAN K. (1956) *Ibid.* **37,** 361.
UREY H. C. (1953) *Proc. Roy. Soc.* **219,** 281–292.
WEDEPOHL K. (1955) *Nachr. Ges. Wiss. Göttingen Math. physik Kl.* 79–86.
WEDEPOHL K. (1956) *Geochim. et Cosmochim. Acta* **10,** 69–148
WICKMAN F. E. (1954) *Geochim. et Cosmochim. Acta* **5,** 97–110.
WISEMAN J. D. (1956). *Advanc. Sci., Lond.* **49,** 579–588.
WORZEL J. L. and SHURBET G. L. (1955) *Geol. Soc. Amer. Special Paper* 62, 87–100.
YOUNG E. J. (1954) *Bull. Geol. Soc. Amer.* **65,** 1329.

A Mathematical Foundation for Radiative Transfer Theory

R. W. PREISENDORFER

Communicated by E. Hopf

I. Introduction

Radiative transfer theory is the quantitative study, on a phenomenological level, of the transfer of radiant energy through media that absorb, scatter, or emit radiant energy. This paper* presents a set of physically motivated axioms phrased in the language of measure theory from which, as a special case, the salient features of radiative transfer theory may be rigorously deduced. The manifold problems of the theory are then subject to rigorous scrutiny by means of the powerful tools of modern analysis, notably measure theory and functional analysis, and thereby the gap between the pure and applied aspects of the mathematics of radiative transfer theory may be closed.

The need for a precise formulation of the notions of radiative transfer has become acute in the past several years. The ramification of the tenets of radiative transfer in particular to the problems of neutron transport theory has given rise to a flurry of mathematical work on the existence and structure of the solutions of the equation of transfer and notions such as group theory [19] and Hilbert space [13] have been pressed into use, all of which are directly transferable to the radiative transfer context. However, the foundations have remained untouched and the problem formulated by Hopf ([9], p. 101) over twenty years ago still stands: "The entire subject ought to be treated anew, and the fundamental equations be derived in a rigorous way, the main tool being the general theory of measure (in the sense of Lebesgue-Radon)."

A perusal of the long history of radiative transfer theory would reveal the enormous number of ramifications of the tenets of the theory and their connections with the foundations of physics from the early classical dynamics of gases to recent quantum theory, neutron diffusion theory, and probability theory. A sketch of the history and an extended bibliography may be found in [17]

---

* Scripps Contribution No. 953. This work has been supported by the Bureau of Ships of the U.S. Navy under contracts NObsr–43356 and NObs–72092.

Journal of Mathematics and Mechanics, Vol. 6, No. 6 (1957).
Reproduced by Permission

along with detailed heuristic discussions leading to the present axiomatic formulations.

In the interests of conceptual simplicity the present formulation will consider only the abstract counterpart to unpolarized radiant energy. It is to be noted, however, that the formal inclusion of the phenomenon of polarization introduces no essential modifications in the mathematical topography of the results (in the classical case, see, *e.g.*, [2], pp. 37–45). We will merely note here that when the notion of the Stokes vector is abstracted, and included in the present formalism, the discussions are elevated from the scalar to the vector level. As a consequence, certain close conceptual relationships may be shown to exist between $\mathcal{R}_\phi$ (the radiative process) and the Mueller phenomenological algebra for optics on both the *set* and *point* levels in the carrier space.

The mathematical core of present day radiative transfer theory rests in the integro-differential equation:

$$\frac{1}{v}\frac{DN}{Dt} = -\alpha N + \int_{\Xi} N\sigma \, d\Omega + N_\eta \,, \tag{1}$$

which is the *classical equation of transfer* for N. Values of the function N are called the *specific intensity*, or *radiance* of radiation: the time rate of change (the flow) of radiant energy across a unit area in a unit solid angle in a given direction normal to the area. It is customarily assumed that the basic carrier of the radiant energy is a photon. Nuclear physicists concerned with neutron transport theory view (1) as the linearized form of the Boltzmann equation [3], and the role of the photon is replaced by that of the neutron. Pure mathematicians concerned with the probability theory view (1) and related variants of (1) as a representation of certain Markoff processes [5]–[7], [10]. The domain of definition of N is some well defined subset of Φ of Euclidean 5-space E_5, where Φ is the Cartesian product $X \times \Xi$ of a given subset X of E_3 and the unit sphere Ξ in E_3. The functions α and σ are the *volume attenuation* and *volume scattering functions* respectively with domains on X and $X \times \Xi \times \Xi$ respectively. v is the *velocity function* with domain X. N_η is the *emission function* defined on Φ. All of these functions have as their range the subset of non-negative real numbers; it is implicitly understood that they are in addition dependent on wavelength and time. D/Dt is the *Lagrangian* (or *mobile*) *derivative operator* associated with Φ.

From the point of view of the mathematician radiative transfer takes place in the measure space $(\Phi, \boldsymbol{\Phi}, \nu)$, where $\boldsymbol{\Phi}$ is the family of Lebesgue measurable subsets of Φ and ν is the *clasical optical volume measure* on $\boldsymbol{\Phi}$ defined by $\nu = \int n^3 \, dp$, where p is the usual Lebesgue measure on $\boldsymbol{\Phi}$ and n is the (non-negative real-valued bounded) *index of refraction function* on X. It should be observed that p is the completed product measure of the *volume measure* V on $\mathbf{X}$ and the *solid angle measure* Ω on $\boldsymbol{\Xi}$, where $\mathbf{X}$ and $\boldsymbol{\Xi}$ are the families of Lebesgue measurable subsets of X and Ξ respectively. $(\Phi, \boldsymbol{\Phi}, \nu)$ is the *classical carrier space*. The *classical radiative measure* U on $\boldsymbol{\Phi}$ is defined by $U = \int (N/v) \, dp$, so that

$$U(X_0 \times \Xi) \equiv U(X_0) = \int_{X_0 \times \Xi} \left(\frac{N}{v}\right) dp$$

is the radiant energy content customarily associated with the subset X_0 of X. In measure-theoretic parlance, N/v is the Radon-Nikodym derivative of U with respect to p. The Radon-Nikodym derivative of U with respect to ν is denoted by G and is clearly related to N by the expression $G = N/n^2c\ [p]$, where c is the universal constant associated with the speed of light in a vacuum. G has the advantage of being invariant along the natural path of a stream of photons in a transparent isotropic optical medium and is related to the fundamental Straubel invariant [18].

The principal results of the paper may now be stated as follows:

(i) An explication, by means of measure-theoretic concepts, of the notions of *optical medium* (the carrier space axiom C_1, §1), *radiant energy* (the radiative measure axiom M_1, §2), the *evolution* of radiant energy in an optical medium (radiative process axiom R_1, §3), and the *transfer* of radiant energy in an optical medium (transfer process axiom T_1, §18).
(ii) The formal deduction from C_1, M_1, R_1, and T_1 of the existence and salient properties of G (and hence N) (§2), α and σ (§§13, 14), and v (§21).
(iii) A rigorous derivation of the most general homogeneous form of (1) in an arbitrary carrier space (§§15, 17) and necessary and sufficient conditions which yield as a special case the correct classical homogeneous form of (1) (§21).

Several intermediate results, mainly of mathematical interest, are obtained as the discussion is carried toward the principal goals, such as:

(iv) The *static transition relation* for relative radiative measures (§4) which is the most primitive form of the equation of transfer and which describes the radiative process in an arbitrary carrier space. It is the radiative transfer counterpart to the Chapman-Kolmogoroff transition relation for transition probabilities [10].
(v) The *dynamic transition relation* for relative measures (§12) which in the present formulations is the first recognizable counterpart to the classical equation of transfer on a set level.
(vi) The *static* (§9) and *dynamic* (§15) transition relations for certain densities g and γ which complement the general density G.

The measure-theoretic terminology and notation used in the sequel follows, wherever possible, that given in the standard treatise [8].

II. RADIATIVE PROCESSES

1. Carrier Space Axiom. Let X be a non-empty set and $\mathbf{S}$ a σ-algebra of subsets of X. Let ν be a totally σ-finite measure on $\mathbf{S}$ such that $\nu(X) > 0$. The measure space $(X, \mathbf{S}, \nu)$ will be referred to as the *carrier space*, and in the interests of brevity we will occasionally indulge in the customary symbolic confusion of X and the triple $(X, \mathbf{S}, \nu)$. The measure ν will be called the *carrier measure*. The elements of $\mathbf{S}$ are the *measurable sets* of X. The elements of X are the *points* of X.

C_1 : *There exists a carrier space* $(X, \mathbf{S}, \nu)$.

2. Radiative Measure Axiom. Let $(\Lambda, \mathbf{L}, l)$ denote the measure space consisting of the subset Λ of non-negative real numbers, the usual σ-algebra $\mathbf{L}$ of Lebesgue measurable subsets of Λ, and Lebesgue measure l. A point $\lambda \in \Lambda$ will be called the *wavelength* λ.

Let $(T, +, <)$ denote the additive semigroup consisting of the subset T of non-negative real numbers with the customary binary operation $+$ of addition and linear ordering $<$. Occasionally limit arguments involving elements of T will be required. These will be with respect to the order topology induced by $<$. A point $t \in T$ will be called the *time* t.

Suppose $\mathfrak{M}$ is the set of all measures on $\mathbf{S}$. $\mathfrak{M}$ is not empty since $\nu \in \mathfrak{M}$. Let $\mathfrak{M}_\nu$ denote the subset of $\mathfrak{M}$ consisting of all totally finite ν-continuous (*i.e.*, absolutely continuous with respect to ν) measures. $\mathfrak{M}_\nu$ is not empty since the zero measure is in $\mathfrak{M}_\nu$. The elements of $\mathfrak{M}$ will be referred to as the *radiative measures* on $\mathbf{S}$. We will say that a collection M of measures on $\mathbf{T}$ of a measurable space $(Y, \mathbf{T})$ forms a *non-negative cone* iff (if and only if) for any two m_1 , $m_2 \in M$ and for any two non-negative real numbers r_1 , r_2 , $r_1 m_1 + r_2 m_2 \in M$, where scalar multiplication and addition of elements of M are defined in the obvious way. $\mathfrak{M}_\nu$ forms a non-negative cone.

If m is a measure on $\mathbf{T}$ of a measurable space $(Y, \mathbf{T})$, we define for each $E \in \mathbf{T}$ the set function $\bar{m}_E$ on $\mathbf{T}$ by the relation $\bar{m}_E(F) = m(E \cap F)$ for $F \in \mathbf{T}$. Clearly $\bar{m}_E$ is a measure on $\mathbf{T}$. Finally, let $f(\cdot, \cdot)$ be a function defined on the product $X \times Y$ of two sets X and Y and with range in some set Z. If $x \in X$, the function $f(x, \cdot)$ defined on Y is an *X-section of f* determined by $x \in X$; similarly, if $y \in Y$, the function $f(\cdot, y)$ defined on X is a *Y-section of f* determined by $y \in Y$. For arbitrary but given $(x, y) \in X \times Y$ the two sections $f(x, \cdot)$, $f(\cdot, y)$ of f will be called *corresponding functions*.

M_1 : (i) *For every* $(t, \lambda) \in T \times \Lambda$, *there is a non-empty subset* $\mathfrak{M}_{\nu,t,\lambda} \subset \mathfrak{M}_\nu$ *which forms a non-negative cone.*

(ii) *If* $\mu \in \mathfrak{M}_\nu$ *and if for every* $E \in \mathbf{S}$ *there is a* $\mu_1 \in \mathfrak{M}_{\nu,t,\lambda}$ *and an* $E_1 \in \mathbf{S}$ *such that* $\mu(E) = \mu_1(E_1)$, *then* $\mu \in \mathfrak{M}_{\nu,t,\lambda}$.

(iii) *If* $\mu(t, \lambda, \cdot) \in \mathfrak{M}_{\nu,t,\lambda}$ *and t is fixed, the corresponding function* $\mu(t, \cdot, E)$, $E \in \mathbf{S}$, *is Lebesgue integrable on* Λ.

As an immediate consequence of (ii)M_1 , if $\mu \in \mathfrak{M}_{\nu,t,\lambda}$ and $F \in \mathbf{S}$, then $\bar{\mu}_F \in \mathfrak{M}_{\nu,t,\lambda}$. For $\bar{\mu}_F \in \mathfrak{M}_\nu$, and for every $E \in \mathbf{S}$, there is a $\mu_1 \in \mathfrak{M}_{\nu,t,\lambda}$, namely μ, and an $E_1 \in \mathbf{S}$, namely $E \cap F$, such that $\bar{\mu}_F(E) = \mu(E \cap F)$.

λ-convention: In the sequel, the wavelength $\lambda \in \Lambda$ will be considered arbitrary but fixed; the λ will be dropped from the notation.

Let $\mu \varepsilon \mathfrak{M}$, $E \varepsilon \mathrm{S}$. E is said to *support* μ (or is a *support for* μ) iff $\mu(E) > 0$. E is said to *fully support* μ (or is a *full support for* μ) iff $F \varepsilon \{G: G \varepsilon \mathrm{S}, \nu(E \cap G) > 0\}$ implies $\mu(E \cap F) > 0$. E is said to *maximally fully support* μ (or is a *maximal full support for* μ) iff (a) E is a full support for μ and (b) $F \varepsilon \mathrm{S}$ implies $\mu(F) \leqq \mu(E)$.

If $E \varepsilon \mathrm{S}$ supports $\mu \varepsilon \mathfrak{M}_\nu$, the set function μ_E on S defined by $\mu_E(F) = \mu(E \cap F)/\mu(E)$ is an element of $\mathfrak{M}_\nu$. We use the convention that $\mu_E \equiv 0$ on S if E does not support μ. μ_E will be referred to as a *relative (conditional) radiative measure*. Similarly, for $E \varepsilon \mathrm{S}$, $\mu \varepsilon \mathfrak{M}_\nu$, the set function $\bar{\mu}_E \varepsilon \mathfrak{M}_\nu$ will be called an *absolute (conditional) radiative measure.*

Theorem A. *Let $\mu \varepsilon \mathfrak{M}_\nu$. If X supports μ, then there exists a unique $[\nu]$ maximal full support for μ.*

Proof: Since $\mu \varepsilon \mathfrak{M}_\nu$, by the Radon-Nikodym theorem ([8], p. 128), there exists a finite-valued non-negative measurable function f on X unique $[\nu]$ such that $\mu(E) = \int_E f\, d\nu$ for every $E \varepsilon \mathrm{S}$. Define $F = \{x: f(x) > 0\}$. Since $\mu(X) > 0$, F is a set of positive ν-measure, is unique $[\nu]$, and $\int_X f\, d\nu = \int_F f\, d\nu$. If $E \varepsilon \mathrm{S}$ and $\nu(F \cap E) > 0$, then $\mu(F \cap E) = \int_{F \cap E} f\, d\nu > 0$, so that F fully supports μ. Finally, if $E \varepsilon \mathrm{S}$, then

$$\mu(E) = \int_E f\, d\nu \leqq \int_X f\, d\nu = \int_F f\, d\nu = \mu(F),$$

so that F is a maximal full support for μ. This completes the proof.

For any $\mu \varepsilon \mathfrak{M}_{\nu,t}$ the value $\mu(E)$ of μ at $E \varepsilon \mathrm{S}$ will be called the *radiant energy in E* (at $t \varepsilon T$ and at $\lambda \varepsilon \Lambda$). If the carrier space supports μ, the preceding theorem asserts that the radiant energy in X may be associated with a unique $[\nu]$ measurable set which maximally fully supports μ. The R-N (Radon-Nikodym) derivative of μ will be called the *general radiant density function on X associated with μ*, and its value at $x \varepsilon X$ the *general radiant density at x* (at $t \varepsilon T$ and at $\lambda \varepsilon \Lambda$). Paraphrasing the proof of the theorem, we may say that a radiative measure supported by the carrier space determines a unique $[\nu]$ general radiant density function on X. If the radiative measure is not supported by X, it is clear that the general radiant density function vanishes a.e. $[\nu]$ on X. We collect these observations in the following

Corollary. *Every radiative measure uniquely $[\nu]$ determines a general radiant density function on X.*

3. Radiative Process Axiom. If $\{\mu_n\}$ is a sequence of measures in $\mathfrak{M}$, the sequence will be said to *converge to the measure* $\mu \varepsilon \mathfrak{M}$, in symbols $\mu_n \to \mu \varepsilon \mathfrak{M}$, iff $\lim_n \mu_n(E) = \mu(E)$ for every $E \varepsilon \mathrm{S}$. If $\{\mu_n\}$ is a sequence of measures in $\mathfrak{M}$, which converges to $\mu \varepsilon \mathfrak{M}$, then $\mu \ll \nu$; for if $F \varepsilon \mathrm{S}$ and $\nu(F) = 0$, $0 = \lim_n \mu_n(F) = \mu(F)$. Let $\mathfrak{R}$ be the set of all linear transformations from the non-negative cone $\mathfrak{M}_\nu$ into $\mathfrak{M}_\nu$. $\mathfrak{R}$ is not empty: the identity transformation I_ϕ is an element of $\mathcal{R}$. The image of μ under $R \varepsilon \mathcal{R}$ will be written as μR. Let

$$D = \{(t_1, t_2) : (t_1, t_2) \varepsilon T \times T, t_2 \geqq t_1\}.$$

R_1 : *There exists a transformation* ϕ *from* D *into* $\mathcal{R}$ *such that* $\phi(D) \equiv \mathcal{R}_\phi$ *has the following properties. Let* $\phi[(t_1, t_2)] \equiv R_{t_1,t_2}$, $(t_1, t_2) \varepsilon D$, *then:*

(i) $\mu \varepsilon \mathfrak{M}_{\nu,t_1}$ *implies* $\mu R_{t_1,t_2} \varepsilon \mathfrak{M}_{\nu,t_2}$.
(ii) *If* t_1, t_2, t_3 *are elements of* T *and if* $t_1 \leqq t_2 \leqq t_3$, *then* $R_{t_1,t_3} = R_{t_1,t_2} R_{t_2,t_3}$.
(iii) *For every* $t \varepsilon T$, $R_{t,t} = I_\phi$.
(iv) *If* $\{\mu_n\}$ *is a sequence of measures in* $\mathfrak{M}_{\nu,t}$ *and* $\mu_n \to \mu \varepsilon \mathfrak{M}_{\nu,t}$, *then for every* $(t, t') \varepsilon D$, $\mu_n R_{t,t'} \to \mu R_{t,t'} \varepsilon \mathfrak{M}_{\nu,t'}$.
(v) *If* $\mu \varepsilon \mathfrak{M}_{\nu,t_1}$, $\mu R_{t_1,t_2}(X) \leqq \mu(X)$ *for every* $(t_1, t_2) \varepsilon D$.

The set $\mathcal{R}_\phi$ of linear transformations on $\mathfrak{M}_\nu$ will be called the *radiative process on the carrier space* (X, S, ν). The axioms C_1, M_1, and R_1 are the *structure axioms for* $\mathcal{R}_\phi$. Property (i) asserts the *radiative transition property of* $\mathcal{R}_\phi$ and reflects the classical radiative transfer of radiant energy under linear (integral) operators. Property (ii) asserts that the radiative transitions are uniquely determined by every given $(t_1, t_3) \varepsilon D$ and reflects the uniqueness of solutions of the classical equation of transfer which can be demonstrated under a rather wide set of conditions using the results of [12]. Property (ii) is the *unicity property of* $\mathcal{R}_\phi$. Property (iii) is the *identity property of* $\mathcal{R}_\phi$. Property (iv) is the *convergence property of* $\mathcal{R}_\phi$. Finally, (v) asserts the *contraction property of* $\mathcal{R}_\phi$ and reflects the physical situation on X when X is source-free, but by itself is not sufficient to insure that X is source-free. All the salient mechanisms of $\mathcal{R}_\phi$ can be studied using the contraction property (*e.g.*, the scattering and absorption mechanisms). The introduction of sources into X can be represented by the adjunction of an arbitrary general radiant density function onto the equation of transfer (Source Axiom S_1). The contraction property will not be used until the discussion of the measure attenuating functions (see lemma, §8; and (B, §11)).

4. Transition Relation for Radiative Measures. A *partition* of a measurable set E is a finite disjoint class of measurable sets whose union is E. If $\mu \varepsilon \mathfrak{M}$ and $\{F_j\}$ is a partition of X, then, for every $F \varepsilon \mathrm{S}$, $\bigcup_{j=1}^n (F \cap F_j) = F$, and

$$\mu(F) = \sum_{j=1}^{n} \mu(F \cap F_j) = \sum_{j=1}^{n} \mu(F_j)\mu_{F_j}(F),$$

that is, $\mu = \sum_{j=1}^n \mu(F_j)\mu_{F_j}$.

Let $\mu \varepsilon \mathfrak{M}_{\nu,t_1}$, $E \varepsilon \mathrm{S}$, and $R_{t_1,t_2} \varepsilon \mathcal{R}_\phi$. By (i)$M_1$ and (ii)M_1 we have $\mu_E \varepsilon \mathfrak{M}_{\nu,t_1}$, and, by (i)$R_1$, $\mu_E R_{t_1,t_2} \varepsilon \mathfrak{M}_{\nu,t_2}$. By the preceding discussion, if $\{F_j\}$ is a partition of X, then

$$\mu_E R_{t_1,t_2} = \sum_{j=1}^{n} \mu_E R_{t_1,t_2}(F_j) \cdot (\mu_E R_{t_1,t_2})_{F_j}.$$

For any $R_{t_1,t_3} \varepsilon \mathcal{R}_\phi$, by (ii)$R_1$,

$$\mu_E R_{t_1,t_3} = (\mu_E R_{t_1,t_2}) R_{t_2,t_3} = \sum_{j=1}^{n} \mu_E R_{t_1,t_2}(F_j)\cdot[(\mu_E R_{t_1,t_2})_{F_j}] R_{t_2,t_3} .$$

For simplicity we adopt the notation $\mu_E R_{t_1,t_2} \equiv \mu(t_1, E; t_2, \cdot)$, so that, for example, $\mu_E R_{t_1,t_2}(F) = \mu(t_1, E; t_2, F)$. We shall write $\bar{\mu}_E R_{t_1,t_2} \equiv \bar{\mu}(t_1, E; t_2, \cdot)$, and frequently the further abbreviation $\mu' \equiv \mu_E R_{t_1,t_2}$ will be used; it will always be clear from the context which triple $((t_1, t_2) \varepsilon D, \mu \varepsilon \mathfrak{M}_{\nu,t_1}, E \varepsilon \mathrm{S})$ is being considered. With these notational devices the above relation may be written as

$$\boxed{\mu(t_1, E; t_3, \cdot) = \sum_{j=1}^{n} \mu(t_1, E; t_2, F_j)\mu'(t_2, F_j; t_3, \cdot),}$$

where $t_1 \leqq t_2 \leqq t_3$, and $\{F_j\}$ is a partition of X. This is the *transition relation for relative radiative measures* and will be the starting point of the chain of arguments leading through the main features of the abstract radiative transfer theory.

There exists an alternative *transition relation for absolute radiative measures.* It may be obtained from the former by writing

$$\mu_E R_{t_1,t_2} = (1/\mu(E))\bar{\mu}_E R_{t_1,t_2}$$

and

$$\mu'(t_2, F_j; t_3, \cdot) = [\overline{(\bar{\mu}_E R_{t_1,t_2})_{F_j}} R_{t_2,t_3}]/\bar{\mu}(t_1, E; t_2, F_j),$$

so that

$$\bar{\mu}_E R_{t_1,t_3} = \sum_{j=1}^{n} \overline{(\bar{\mu}_E R_{t_1,t_2})_{F_j} R_{t_2,t_3}},$$

where $t_1 \leqq t_2 \leqq t_3$ and $\{F_j\}$ is a partition of X.

5. G- and g-densities. The $\mathcal{R}_\phi$-transforms of the relative radiative measures were used to obtain the fundamental transition relation for radiative measures. This relation may be considered as the necessary representation of a general radiative process $\mathcal{R}_\phi$ on a carrier space X. Its order of generality is such that it conveys little useful information except the single pleasant fact that the idea of a classical process can be extended to a carrier space which has a minimum of requisite structure, namely an arbitrary basic space X, a σ-algebra S of subsets of X, and a totally σ-finite measure on S. In fact, an examination of the derivation of the transition relations will show that it would indeed be permissible to employ an arbitrary measurable space and a "radiative process" which simply used some cone (not necessarily non-negative) of functions on S for its "radiative measures."

These observations show that the fundamental concepts of a classical radiative process can be pushed so far into the backwoods of abstraction that they become almost lost in the nebulous generalities of measure theory; and yet, despite this abstract character, the "radiative process" may still retain enough structure to yield a recognizable transition relation for the correspondingly abstract "radiative measures." As they stand now, the structure axioms are sufficiently detailed to allow a running start towards our goal of obtaining necessary characterizations of the radiative process in terms of abstract counterparts of the absorption and scattering functions in an integro-differential equation. The transition relation for radiative measures describes the radiative process on a set level (with respect to X). The purpose of this section is to prepare the ground for the description of the radiative process on a point level in X. This will require the consideration of various densities of elements of $\mathfrak{M}_\nu$.

Theorem A. *Let* $(t_1 , t_2) \in D$ *be arbitrary but fixed. Let* $\mu \in \mathfrak{M}_{\nu,t_1}$ *and* $E \in \mathrm{S}$; *then there exists a finite-valued non-negative measurable function* $G(t_1 , E; t_2 , \cdot)$ *on* X, *unique* $[\nu]$, *such that for every* $F \in \mathrm{S}$

$$\bar{\mu}(t_1 , E; t_2 , F) = \int_F G(t_1 , E; t_2 , \cdot)\, d\nu.$$

Proof: By hypothesis $\mu \in \mathfrak{M}_{\nu,t_1}$, so that, by (ii)M_1 , $\bar{\mu}_E \in \mathfrak{M}_{\nu,t_1}$, and, by (ii)R_1 and (i)M_1 , $\bar{\mu}_E R_{t_1,t_2} \in \mathfrak{M}_{\nu,t_2}$. Since $\bar{\mu}(t_1 , E; t_2 , \cdot) \ll \nu$, use of C_1 and a Radon-Nikodym argument completes the proof.

The elements of the collection of functions on X whose existence was demonstrated in the preceding theorem will be referred to as the *G-densities* (with respect to ν) *of radiative measures.* If X does not support $\bar{\mu}(t_1 , E; t_2 , \cdot)$, the ν-uniqueness of the associated G-density will permit the convention of defining $G(t_1 , E; t_2 , \cdot)$ as the zero function on X. On the other hand, if X supports $\bar{\mu}(t_1 , E; t_2 , \cdot)$, then by (A, §2) there is a unique $[\nu]$ maximal full support F for this radiative measure and we can establish the convention that $G(t_1 , E; t_2 , x) = 0$ for every $x \in F'$ (the complement of F).

Theorem B. *Let* $(t_1 , t_2) \in D$ *be arbitrary but fixed. Let* $\mu \in \mathfrak{M}_{\nu,t_1}$ *and* $F \in \mathrm{S}$; *then there exists a finite-valued non-negative measurable function* $g(t_1 , \cdot ; t_2 , F)$ *on* X, *unique* $[\nu]$, *such that, for every* $E \in \mathrm{S}$,

$$\bar{\mu}(t_1 , E; t_2 , F) = \int_E g(t_1 , \cdot ; t_2 , F)\, d\nu.$$

Proof: The set function $\bar{\mu}(t_1 , \cdot ; t_2 , F)$ is finite-valued and non-negative on S. If $E \in \mathrm{S}$ and $\nu(E) = 0$, then $\bar{\mu}_E \equiv 0$, so that, by the linear properties of the elements of $\mathcal{R}_\phi$, $\bar{\mu}(t_1 , E; t_2 , F) = 0$. Hence $\bar{\mu}(t_1 , \cdot ; t_2 , F) \ll \nu$. It remains to show that $\bar{\mu}(t_1 , \cdot ; t_2 , F)$ is countably additive on S. Let $\{E_i\}$ be any disjoint sequence of measurable sets in S. Let $E^{(n)} = \bigcup_{i=1}^{n} E_i$. Then $\{E^{(n)}\}$ is an increasing sequence of measurable sets such that $\lim_n E^{(n)} = E = \bigcup_{i=1}^{\infty} E_i \in \mathrm{S}$. The sequence $\{\bar{\mu}_{E^{(n)}}\}$ of elements in $\mathfrak{M}_{\nu,t_1}$ has the limit $\bar{\mu}_E \in \mathfrak{M}_{\nu,t_1}$; for

$$\lim_n \bar{\mu}_{E^{(n)}}(G) = \lim_n \sum_{i=1}^{n} \mu(E_i \cap G) = \sum_{i=1}^{\infty} \mu(E_i \cap G) = \mu(E \cap G) = \bar{\mu}_E(G)$$

for every $G \varepsilon \mathrm{S}$. By (iv)R_1 it follows that $\bar{\mu}_{E(n)}R_{t_1,t_2} \rightarrow \bar{\mu}_E R_{t_1,t_2}$. For every positive integer n, $\bar{\mu}_{E(n)}R_{t_1,t_2} = \sum_{j=1}^{n} \bar{\mu}_{E_j}R_{t_1,t_2} \varepsilon \mathfrak{M}_{\nu,t_1}$ by (i)M_1 and (i)R_1, hence

$$\lim_n \left(\sum_{j=1}^{n} \bar{\mu}_{E_j} R_{t_1,t_2} \right) = \sum_{j=1}^{\infty} \bar{\mu}_{E_j} R_{t_1,t_2} = \bar{\mu}_E R_{t_1,t_2}$$

implies that, for $F \varepsilon \mathrm{S}$, $\sum_{j=1}^{\infty} \bar{\mu}(t_1, E_j; t_2, F) = \bar{\mu}(t_1, E; t_2, F)$. It follows that $\bar{\mu}(t_1, \cdot; t_2, F)$ is a totally finite ν-continuous measure on S. An R-N argument yields the function $g(t_1, \cdot; t_2, F)$ on X satisfying all the requirements of the theorem.

The elements of the collection of functions on X whose existence was demonstrated in the preceding theorem will be referred to as the *g-densities* (with respect to ν) *of radiative measures*. We observe that the ν-continuous measure $\bar{\mu}(t_1, \cdot; t_2, F)$ is, by (ii)M_1, an element of $\mathfrak{M}_{\nu,t_1}$.

The set function $g(t_1, x; t_2, \cdot)$ which is the correspondent to $g(t_1, \cdot; t_2, F)$ is clearly non-negative and finite-valued on S. We will show that $g(t_1, x; t_2, \cdot)$ is almost a ν-continuous measure on S. The sense of "almost" will be made precise in the theorem which follows. The theorem and the subsequent discussion are designed to show certain limitations of the axioms C_1, M_1, and R_1 and to motivate the axiom R_2. The key to the following discussion lies in the observation that each $g(t_1, \cdot; t_2, F)$ is dependent upon $(t_1, t_2) \varepsilon D$ and $F \varepsilon \mathrm{S}$ so that the exceptional ν-null sets on which $g(t_1, \cdot; t_2, F)$ is perhaps undetermined depend upon $F \varepsilon \mathrm{S}$ for fixed $(t_1, t_2) \varepsilon D$. This is the reason which generally bars $g(t_1, x; t_2, \cdot)$ from being a measure for arbitrary $x \varepsilon X$. The removal of this restriction can be accomplished by considering special classes of radiative measures at the outset, or special classes of carrier spaces ([8], p 210).

Theorem C. *Let $(t_1, t_2) \varepsilon D$ be arbitrary but fixed. Let $\mu \varepsilon \mathfrak{M}_{\nu,t_1}$; then:*

(a) *For each fixed disjoint sequence $\{F_j\}$ of measurable sets*

$$g(t_1, x; t_2, \bigcup_{j=1}^{\infty} F_j) = \sum_{j=1}^{\infty} g(t_1, x; t_2, F_j) \; [\nu].$$

(b) *If $F_1, F_2 \varepsilon \mathrm{S}$, and $F_1 \subset F_2$, then $g(t_1, x; t_2, F_1) \leqq g(t_1, x; t_2, F_2)$ $[\nu]$.*

(c) *For each fixed decreasing sequence $\{F_j\}$ of measurable sets*

$$\lim_j g(t_1, x; t_2, F_j) = g(t_1, x; t_2, \bigcap_{j=1}^{\infty} F_j) \; [\nu].$$

(d) *If, for $F \varepsilon \mathrm{S}$, $\nu(F) = 0$, then $g(t_1, x; t_2, F) = 0$ $[\nu]$.*

Proof: (a) Let $F = \bigcup_{j=1}^{\infty} F_j$. Let the g-densities associated with $\bar{\mu}(t_1, \cdot; t_2, F_j)$ be designated by $g_j = g(t_1, \cdot; t_2, F_j)$, $j = 1, 2, 3, \cdots$, each being unique $[\nu]$. Then $\bar{\mu}(t_1, E; t_2, F_j) = \int_E g_j \, d\nu$ for every $E \varepsilon \mathrm{S}$. Since $\bar{\mu}(t_1, E; t_2, \cdot) \varepsilon \mathfrak{M}_{\nu,t_2}$,

$$\sum_{j=1}^{\infty} \bar{\mu}(t_1, E; t_2, F_j) = \bar{\mu}(t_1, E; t_2, F) < \infty,$$

and the series $\sum_{i=1}^{\infty} g_i(x)$ converges a.e. $[\nu]$ to a ν-integrable function g ([8], p. 114) such that

$$\int_E g\, d\nu = \sum_{i=1}^{\infty} \int_E g_i\, d\nu = \bar{\mu}(t_1, E; t_2, F)$$

for every $E \varepsilon$ S. Hence

$$g(t_1, x; t_2, \bigcup_{j=1}^{\infty} F_j) = \sum_{j=1}^{\infty} g(t_1, x; t_2, F_j)\ [\nu]$$

by the uniqueness of R-N derivatives.

(b) If $F_1, F_2 \varepsilon$ S, and $F_1 \subset F_2$, then, since $\bar{\mu}(t_1, E; t_2, \cdot) \varepsilon \mathfrak{M}_{\nu, t_2}$ for every $E \varepsilon$ S, $\bar{\mu}(t_1, E; t_2, F_1) \leqq \bar{\mu}(t_1, E; t_2, F_2)$ for every $E \varepsilon$ S, so that

$$\int_E g(t_1, \cdot; t_2, F_1)\, d\nu \leqq \int_E g(t_1, \cdot; t_2, F_2)\, d\nu$$

for every $E \varepsilon$ S, and the conclusion follows.

(c) If $\{F_j\}$ is a decreasing sequence of measurable sets, then, since $\bar{\mu}(t_1, E; t_2, \cdot) \varepsilon \mathfrak{M}_{\nu, t_2}$, we have for every $E \varepsilon$ S

$$\begin{aligned}\int_E \lim_n g(t_1, \cdot; t_2, F_n)\, d\nu &= \lim_n \int_E g(t_1, \cdot; t_2, F_n)\, d\nu \\ &= \int_E g\left(t_1, \cdot; t_2, \bigcap_{n=1}^{\infty} F_n\right) d\nu\end{aligned}$$

and the conclusion follows.

(d) If F is a ν-null set, then, since $\bar{\mu}(t_1, E; t_2, \cdot) \varepsilon \mathfrak{M}_{\nu, t_2}$, $\int_E g(t_1, \cdot; t_2, F)\, d\nu = 0$ for every $E \varepsilon$ S, and the conclusion follows. This completes the proof of the theorem.

Part (a) of the preceding theorem shows a restricted countable additivity property for $g(t_1, x; t_2, \cdot)$ and clearly limits the points $x \varepsilon X$ for which it holds to sets depending upon the given fixed sequence of measurable sets. Similarly, parts (b) and (c) in turn gather evidence for restricted types of monotonicity and continuity from above; and, finally, (d) asserts a restricted type of ν-continuity for $g(t_1, x; t_2, \cdot)$. These properties are reminiscent of the corresponding properties of densities of conditional measures on probability spaces ([8], pp. 206–211).

If the σ-ring S has at most an enumerable number of elements, the union of the exceptional ν-null sets of the elements of a chosen collection $\{g(t_1, \cdot; t_2, F): F \varepsilon \text{S}\}$ of g-densities would be a ν-null set, thereby allowing the definition of a set function $g(t_1, x; t_2, \cdot)$ for almost every $[\nu]$ $x \varepsilon X$ such that it is an element of $\mathfrak{M}_{\nu, t_2}$. Since a σ-ring cannot have an enumerably infinite number of distinct elements, this ruse will work only in the more trivial σ-rings.

6. Measurable Process Axiom. The corresponding set function $g(t_1, x; t_2, \cdot)$ to the g-density just misses being a radiative measure a.e. $[\nu]$ on X. Some ways of removing this restriction have been discussed or implied in the preceding section. Since ways and means do exist which will allow the g-density's correspondent to be a radiative measure a.e. $[\nu]$ we will postulate that this property is actually possessed by the correspondent without, however, making any commitment as to what route was taken. This is done by introducing the following measurable process axiom.

R_2 : *For each* $(t_1, t_2) \varepsilon D$, $\mu \varepsilon \mathfrak{M}_{\nu.t_1}$, *and* ν*-continuous measure* m *on* S *such that* $\mu \ll m$, *there exists a set function* $g(t_1, x; t_2, \cdot)$ *on* S *with the following properties:*

(i) $g(t_1, x; t_2, \cdot) \varepsilon \mathfrak{M}_{\nu.t_2}$ *for almost every* $[m]$ $x \varepsilon X$ *and has an R-N derivative with respect to* ν *which is the* X*-section, determined by* $x \varepsilon X$, *of a measurable function on the measurable space* $(X \times X, \mathsf{S} \times \mathsf{S})$.

(ii) *For each* $F \varepsilon \mathsf{S}$, *the corresponding function* $g(t_1, \cdot; t_2, F)$ *on* X *is a* g*-density with respect to* m *of* $\bar{\mu}(t_1, \cdot; t_2, F) \varepsilon \mathfrak{M}_{\nu.t_2}$.

This axiom will always allow the choice of a g-density whose correspondent is a radiative measure a.e. $[\nu]$. Henceforth the radiative process will be considered to obey R_2.

7. γ-density.

Theorem A. *For each* $(t_1, t_2) \varepsilon D$, $\mu \varepsilon \mathfrak{M}_{\nu.t_1}$, *there exists a finite-valued non-negative measurable function* $\gamma(t_1, \cdot; t_2, \cdot)$ *on* $(X \times X, \mathsf{S} \times \mathsf{S}, \nu \times \nu)$ *unique* $[\nu \times \nu]$ *such that:*

(a)
$$\bar{\mu}(t_1, E_1; t_2, E_2) = \int_{E_1} \int_{E_2} \gamma(t_1, x_1, t_2, x_2)\, d\nu(x_2)\, d\nu(x_1)$$

for every pair (E_1, E_2) *of measurable sets.*

(b)
$$g(t_1, x_1; t_2, E_2) = \int_{E_2} \gamma(t_1, x_1; t_2, x_2)\, d\nu(x_2)$$

for almost every $[\nu]$ $x_1 \varepsilon X$ *and all measurable sets* E_2, *and where* $g(t_1, \cdot; t_2, E_2)$ *is a* g*-density of* $\bar{\mu}(t_1, \cdot; t_2, E_2) \varepsilon \mathfrak{M}_{\nu.t_2}$.

(c)
$$G(t_1, E_1; t_2, x_2) = \int_{E_1} \gamma(t_1, x_1; t_2, x_2)\, d\nu(x_1)$$

for almost every $[\nu]$ $x_2 \varepsilon X$ *and all measurable sets* E_1, *and where* $G(t_1, E_1; t_2, \cdot)$ *is a* G*-density of* $\bar{\mu}(t_1, E_1; t_2, \cdot) \varepsilon \mathfrak{M}_{\nu.t_2}$.

Proof: In R_2 let m be the carrier measure. (i)R_2 then supplies a measurable function $\gamma(t_1, \cdot; t_2, \cdot)$ on $X \times X$ for each $(t_1, t_2) \varepsilon D$ such that it is non-negative, finite-valued and unique $[\nu \times \nu]$, and

$$g(t_1, x_1; t_2, E_2) = \int_{E_2} \gamma(t_1, x_1; t_2, x_2)\, d\nu(x_2)$$

for every $E_2 \varepsilon$ S and almost every $[\nu]$ $x_1 \varepsilon X$. By (ii)R$_2$, for each fixed $E_2 \varepsilon$ S, $g(t_1 , \cdot ; t_2 , E_2)$ is a g-density of $\bar{\mu}(t_1 , \cdot ; t_2 , E_2) \varepsilon \mathfrak{M}_{\nu,t_1}$, *i.e.*,

$$\bar{\mu}(t_1 , E_1 ; t_2 , E_2) = \int_{E_1} g(t_1 , x_1 ; t_2 , E_2) \, d\nu(x_1)$$

$$= \int_{E_1} \left\{ \int_{E_2} \gamma(t_1 , x_1 ; t_2 , x_2) \, d\nu(x_2) \right\} d\nu(x_1) < \infty$$

for each $E_1 , E_2 \varepsilon$ S. It follows ([8], p. 147) that $\gamma(t_1 , \cdot ; t_2 , \cdot)$ is in fact integrable on $X \times X$ for each $(t_1 , t_2) \varepsilon D$ and that

$$\bar{\mu}(t_1 , E_1 ; t_2 , E_2) = \int_{E_2} \int_{E_1} \gamma(t_1 , x_1 ; t_2 , x_2) \, d\nu(x_1) \, d\nu(x_2)$$

for every pair (E_2 , E_1) of measurable sets. Finally, by (A, §5) and the uniqueness of R-N derivatives,

$$G(t_1 , E_1 ; t_2 , x_2) = \int_{E_1} \gamma(t_1 , x_1 ; t_2 , x_2) \, d\nu(x_1)$$

for almost every $[\nu]$ $x_2 \varepsilon X$ and all measurable sets E_1 . This completes the proof.

The functions $\gamma(t_1 , \cdot ; t_2 , \cdot)$ discussed in the preceding theorem will be referred to as the γ-*densities* (with respect to ν) *of radiative measures.*

8. g′-density. We continue with the ground work which will lead to the transition relations for the G-, g-, and γ-densities. In this section we consider radiative measures which are specific images, under two successive applications of elements of $\mathcal{R}_\phi$, of given radiative measures. More precisely, let (t_1 , t_2), $(t_2 , t_3) \varepsilon D$ be arbitrary but fixed, and let $E_1 , E_2 \varepsilon$ S, and finally let $\mu \varepsilon \mathfrak{M}_{\nu,t_1}$. Then $\mu_{E_1} \varepsilon \mathfrak{M}_{\nu,t_1}$ and $\mu_{E_1}R_{t_1,t_2} \varepsilon \mathfrak{M}_{\nu,t_2}$ by (i), (ii)M$_1$, and (i)R$_1$ respectively. Using the abbreviated notation convention (§4) we have $\mu'_{E_2} \varepsilon \mathfrak{M}_{\nu,t_2}$ by the first two clauses of M$_1$. We can then write $\mu'(t_2 , E_2 ; t_3 , \cdot)$ for $\mu'_{E_2}R_{t_2,t_3} = (\mu_{E_1}R_{t_1,t_2})_{E_2}R_{t_2,t_3} \varepsilon \mathfrak{M}_{\nu,t_3}$. The absolute radiative measure $\overline{(\mu_{E_1}R_{t_1,t_2})_{E_2}}$ we may then designate, alternatively, by $\overline{\mu'_{E_2}}$. Hence

$$\mu'(t_2 , E_2 ; t_3 , \cdot) = \mu'_{E_2}R_{t_2,t_3} = \overline{\mu'_{E_2}}R_{t_2,t_3}/\mu'(E_2)$$

$$= \overline{\mu'}(t_2 , E_2 ; t_3 , \cdot)/\mu(t_1 , E_1 ; t_2 , E_2).$$

We observe that if $\mu \varepsilon \mathfrak{M}$ and $E \varepsilon$ S and r is a positive real number, then $r\mu \varepsilon \mathfrak{M}$ and $(r\mu)_E = \mu_E$; for if E supports μ, we have for every $F \varepsilon$ S

$$(r\mu)_E(F) = (r\mu)(E \cap F)/(r\mu)(E) = \mu_E(F).$$

On the other hand if E does not support μ neither does E support $r\mu$, so then once again $(r\mu)_E = \mu_E$ $(= 0)$. It follows, for example, that $(\bar{\mu}_{E_1}R_{t_1,t_2})_{E_2} = (\mu_{E_1}R_{t_1,t_2})_{E_2}$, *i.e.*, that μ'_{E_2} is independent of the choice of either the absolute or relative radiative measure associated with the pair (μ, E_1) where $\mu \varepsilon \mathfrak{M}_{\nu,t_1}$, $E_1 \varepsilon$ S, $\mu(E_1) > 0$.

Theorems A, B, and C of section 5 apply without qualification to $\mu' \varepsilon \mathfrak{M}_{\nu,t_2}$, so that we may speak of the G- and g-densities of μ'. Furthermore, by means of (A, §7) the existence of a γ-density connecting the G- and g-densities of μ' is asserted. Hence the results of the preceding sections on the three main types of densities may be carried over immediately to the transforms of μ'.

We now go on to consider certain properties which are peculiar to the specifically transformed radiative measures (*i.e.*, of the μ'-type).

Theorem A. *For arbitrary but fixed* (t_1, t_2), $(t_2, t_3) \varepsilon D$, $\mu \varepsilon \mathfrak{M}_{\nu,t_1}$, $E_1 \varepsilon$ S, *the corresponding set function* $\overline{\mu'}(t_2, \cdot; t_3, E_3)$, $E_3 \varepsilon$ S, *to* $\overline{\mu'}(t_2, E_2; t_3, \cdot) \varepsilon \mathfrak{M}_{\nu,t_3}$, $E_2 \varepsilon$ S, *is a* μ'-*continuous measure on* S. *There exists a finite valued non-negative measurable function* $g'(t_2, \cdot; t_3, E_3)$ *on* X *unique* $[\mu']$ *such that for every* $E_2 \varepsilon$ S

$$\overline{\mu'}(t_2, E_2; t_3, E_3) = \int_{E_2} g'(t_2, \cdot; t_3, E_3)\, d\mu'.$$

Proof: The proof of (B, §5) yields the fact that $\overline{\mu'}(t_2, \cdot; t_3, E_3)$ is a totally finite measure on S. The novel assertion of the theorem is that $\overline{\mu'}(t_2, \cdot; t_3, E_3)$ is μ'-continuous. If $F \varepsilon$ S and $\mu'(F) = 0$, then $\overline{\mu'_F} = 0$ (the zero measure) and so $\overline{\mu'_F} R_{t_2,t_3} = 0$, in particular

$$\overline{(\mu_{E_1} R_{t_1,t_2})_F R_{t_2,t_3}}(E_3) = \overline{\mu'}(t_2, F; t_3, E_3) = 0.$$

An R-N argument yields a finite-valued non-negative measurable function $g'(t_2, \cdot; t_3, E_3)$ unique $[\mu']$ which satisfies the remaining requirements of the theorem.

If we write $G(t_1, E_1; t_2, \cdot)$ for the R-N derivative $d(\mu(E_1)\mu')/d\nu$, then the real number $\overline{\mu'}(t_2, E_2; t_3, E_3)$ may always, by the preceding theorem and ([8], p. 134), be written as

$$\overline{\mu'}(t_2, E_2; t_3, E_3) = (1/\mu(E_1)) \int_{E_2} g'(t_2, \cdot; t_3, E_3) G(t_1, E_1; t_2, \cdot)\, d\nu.$$

If X supports μ' then by (A, §2) there is a unique $[\nu]$ maximal full support F for μ'. It follows that $G(t_1, E_1; t_2, x) > 0$ for every $x \varepsilon F$ except perhaps for a ν-null subset of F. In this case the restriction of the function $g'(t_2, \cdot; t_3, E_3)$ to F is unique $[\nu]$ since the only μ'-null subsets of F are the ν-null subsets of F. As before, we may write $G(t_1, E_1; t_2, x) = 0$ for every $x \varepsilon F'$. Since $g'(t_2, \cdot; t_3, E_3)$ is analytically linked to $G(t_1, E_1; t_2, \cdot)$ by means of the integral representation of $\overline{\mu'}(t_2, \cdot; t_3, E_3)$ defined above, and since $g'(t_2, \cdot; t_3, E_3)$ is in general unique $[\mu']$, it is permissible to adopt the following convention which will be used continually in the sequel: If X supports μ' and F is the unique $[\nu]$ maximal full support for μ', then $g'(t_2, x; t_3, E_3) = 0$ for every $x \varepsilon F'$ and for every $E_3 \varepsilon$ S. If X does not support μ', then $g'(t_2, x; t_3, E_3) = 0$ for every $x \varepsilon X$ and for every $E_3 \varepsilon$ S. We collect these observations and conventions in the

Corollary. $g'(t_2, \cdot; t_3, E_3)$, *the g-density with respect to* μ' *of the radiative measure* $\overline{\mu'}(t_2, \cdot; t_3, E_3)$, *is unique* $[\nu]$ *for every* $E_3 \varepsilon$ S.

Each of the following two theorems summarizes a property of g-densities with respect to μ', the latter being associated with the triple $((t_1, t_2) \varepsilon D, \mu \varepsilon \mathfrak{M}_{\nu,t_1}, E_1 \varepsilon \mathrm{S})$. These results properly belong to the present discussion, yet no immediate use will be made of them in the following section on the transition relations for the G-, g-, and γ-densities. Mention of this fact is made because the first of the following two theorems makes explicit use of clause (v) in R_1, yet this property of the radiative process is not required for the transition relations for the various densities.

Lemma. *For each* $(t_1, t_2) \varepsilon D$, $E \varepsilon \mathrm{S}$, $\mu \varepsilon \mathfrak{M}_{\nu,t_1}$, *and* $F \varepsilon \mathrm{S}$,

$$\bar{\mu}_E R_{t_1,t_2}(F) \leqq \mu(E).$$

Proof: By (v)R_1, $\mu R_{t_1,t_2}(X) \leqq \mu(X)$ for every $(t_1, t_2) \varepsilon D$. By (ii)M_1, $\bar{\mu}_E \varepsilon \mathfrak{M}_{\nu,t_1}$, so that, for every $F \varepsilon \mathrm{S}$,

$$\bar{\mu}_E R_{t_1,t_2}(F) \leqq \bar{\mu}_E R_{t_1,t_2}(X) \leqq \bar{\mu}_E(X) = \mu(E).$$

Theorem B. *If* $g'(t_2, \cdot; t_3, E_3)$ *is a g-density with respect to* μ' *of the radiative measure* $\bar{\mu}(t_2, \cdot; t_3, E_3)$, *then* $0 \leqq g'(t_2, x; t_3, E_3) \leqq 1$ *for almost every* $[\nu]$ $x \varepsilon X$.

Proof: If X does not support μ', $g'(t_2, \cdot; t_3, E_3) = 0$ (the zero function) on X. If X supports μ', then, if F is the unique $[\nu]$ maximal full support for μ', $g'(t_2, \cdot; t_3, E_3) = 0$ on F'. If G is a measurable subset of F with positive ν-measure on which $g'(t_2, x; t_3, E_3) > 1$ for every $x \varepsilon G$, then, since G fully supports μ',

$$\overline{\mu'}(t_2, G; t_3, E_3) = \int_G g'(t_2, \cdot; t_3, E_3)\, d\mu' > \int_G d\mu' = \mu'(G),$$

contrary to the conclusion of the lemma.

For every subset $E \subset X$, let χ_E denote the *characteristic function of* E, defined, as usual, by $\chi_E(x) = 1$ or 0 according as $x \varepsilon E$ or $x \varepsilon E'$ respectively.

Theorem C. *If* $g'(t_2, \cdot; t_3, E_3)$ *is a g-density with respect to* μ' *of the radiative measure* $\overline{\mu'}(t_2, \cdot; t_3, E_3)$ *and* (i) $t_2 = t_3 = t$, (ii) *F is the maximal full support for* μ', *then* $g'(t, \cdot; t, E_3) = \chi_{E_3 \cap F}$ $[\nu]$.

Proof: By (A, §8) we may represent $\overline{\mu'}(t_2, E; t_3, E_3)$ by

$$(1/\mu(E_1)) \int_E g'(t_2, \cdot; t_3, E_3) G(t_1, E_1; t_2; \cdot)\, d\nu$$

for every $E \varepsilon \mathrm{S}$, where $G(t_1, E_1; t_2, \cdot)$ is the R-N derivative introduced in §5. If (i) above holds, then, by (iii)R_1,

$$\overline{\mu'}(t_2, E; t_3, E_3) = \overline{\mu'_E} R_{t_2,t_3}(E_3) = \overline{\mu'_E} R_{t,t}(E_3) = \mu'(E \cap E_3 \cap F),$$

and using (A, §5) this may be written as

$$(1/\mu(E_1)) \int_{E \cap E_3 \cap F} G(t_1, E_1; t, \cdot)\, d\nu = (1/\mu(E_1)) \int_E \chi_{E_3 \cap F} G(t_1, E_1; t, \cdot)\, d\nu$$

for every $E \varepsilon \mathrm{S}$. Hence for case (i) the two integrals are equal for every $E \varepsilon \mathrm{S}$, so that

$$g'(t, \cdot; t, E_3)G(t_1, E_1; t, \cdot) = \chi_{E_3 \cap F} G(t_1, E_1; t, \cdot)[\nu]$$

by ([8], p. 105). If (ii) above holds, $G(t_1, E_1; t, x) > 0$ for almost every $[\nu]$ x in the maximal full support F for μ'; and $g'(t, x; t, E_3) = 0$ for every $x \varepsilon F'$. Hence if both (i) and (ii) hold, $g'(t, \cdot; t, E_3) = \chi_{E_3 \cap F}\ [\nu]$.

9. Transition Relations for Densities. Let $(t_1, t_2), (t_2, t_3) \varepsilon D$, $\mu \varepsilon \mathfrak{M}_{\nu, t_1}$, and $E_1 \varepsilon \mathrm{S}$ be arbitrary but fixed. Let $\{F_j\}$ be a partition of X; then using the notations of section 4 and the appropriate support conventions the transition relation for radiative measures may be written

$$\mu(t_1, E_1; t_3, E_3) = \sum_{j=1}^{n} \mu'(F_j)\mu'(t_2, F_j; t_3, E_3), \qquad E_3 \varepsilon \mathrm{S}.$$

By (A, §8) we may write

$$\begin{aligned} \mu(t_1, E_1; t_3, E_3) &= \sum_{j=1}^{n} \mu'(F_j)\left[(1/\mu'(F_j)) \int_{F_j} g'(t_2, \cdot; t_3, E_3)\, d\mu'\right] \\ &= \sum_{j=1}^{n} \int_{F_j} g'(t_2, \cdot; t_3, E_3)\, d\mu'. \end{aligned}$$

By (A, §5), ([8], p. 134), and the linearity of the radiative process,

$$(1/\mu(E_1))\bar{\mu}(t_1, E_1; t_3, E_3) =$$

$$(1/\mu(E_1)) \cdot \sum_{j=1}^{n} \int_{F_j} g'(t_2, \cdot; t_3, E_3)G(t_1, E_1; t_2, \cdot)\, d\nu.$$

Hence

$$\bar{\mu}(t_1, E_1; t_3, E_3) = \int_X g'(t_2, \cdot; t_3, E_3)G(t_1, E_1; t_2, \cdot)\, d\nu$$

holds for arbitrary $(t_1, t_2), (t_2, t_3) \varepsilon D$, $E_1, E_3 \varepsilon \mathrm{S}$. By ((c)A, §7) and (B, §5),

$$\begin{aligned} \bar{\mu}(t_1, E_1; t_3, E_3) &= \int_{E_1} g(t_1, x_1; t_3, E_3)\, d\nu(x_1) \\ &= \int_X g'(t_2, x_2; t_3, E_3)\left[\int_{E_1} \gamma(t_1, x_1; t_2, x_2)\, d\nu(x_1)\right] d\nu(x_2) \\ &= \int_X \int_{E_1} g'(t_2, x_2; t_3, E_3)\gamma(t_1, x_1; t_2, x_2)\, d\nu(x_1)\, d\nu(x_2) < \infty. \end{aligned}$$

By a Fubini argument and the fact that $E_1 \varepsilon \mathrm{S}$ is initially arbitrary we have

$$g(t_1, x_1; t_3, E_3) = \int_X g'(t_2, x_2; t_3, E_3)\gamma(t_1, x_1; t_2, x_2)\, d\nu(x_2)$$

for almost every $[\nu]$ $x_1 \varepsilon X$ and every $E_3 \varepsilon$ S. By ((b)A, §7) and ([8], p. 134)

$$\boxed{g(t_1, x_1; t_3, E_3) = \int_X g'(t_2, \cdot; t_3, E_3)\, dg(t_1, x_1; t_2, \cdot),}$$

for almost every $[\nu]$ $x_1 \varepsilon X$ and every $E_3 \varepsilon$ S, or in alternate notation (intended to be equivalent) for the radiative measure $g(t_1, x_1; t_2, \cdot)$

$$\boxed{g(t_1, x_1; t_3, E_3) = \int_X g(t_1, x_1; t_2, dx_2) g'(t_2, x_2; t_3, E_3).}$$

This is the *transition relation for g-densities.*

By R_2 (in which m is now μ') and the corollary of (A, §8), the g-density with respect to μ', $g'(t_2, \cdot; t_3, E_3)$, may for almost every $[\nu]$ $x_2 \varepsilon X$ and every $E_3 \varepsilon$ S be chosen as the corresponding function to $g'(t_2, x_2; t_3, \cdot) \varepsilon \mathcal{M}_{\nu, t_2}$; so that, by ((b)A, §7) and the previously cited measure-theoretical arguments, we have for every $E_3 \varepsilon$ S

$$\begin{aligned} \int_{E_3} \gamma(t_1, x_1; t_3, x_3)\, d\nu(x_3) \\ &= \int_X g(t_1, x_1; t_2, dx_2) \left[\int_{E_3} \gamma'(t_2, x_2; t_3, x_3)\, d\nu(x_3) \right] \\ &= \int_{E_3} \int_X \gamma(t_1, x_1; t_2, x_2) \gamma'(t_2, x_2; t_3, x_3)\, d\nu(x_2)\, d\nu(x_3), \end{aligned}$$

where $\gamma'(t_2, x_2; t_3, \cdot)$ is the R-N derivative with respect to ν of $g'(t_2, x_2; t_3, \cdot)$. It follows that

$$\boxed{\gamma(t_1, x_1; t_3, x_3) = \int_X \gamma(t_1, x_1; t_2, x_2) \gamma'(t_2, x_2; t_3, x_3)\, d\nu(x_2)}$$

for almost every $[\nu]$ $x_1 \varepsilon X$ and $x_3 \varepsilon X$. This is the *transition relation for* γ*-densities.*

Finally, for almost every $[\nu]$ $x_3 \varepsilon X$ and every $E_1 \varepsilon$ S, by ((c)A, §7) and the usual integration arguments,

$$\boxed{G(t_1, E_1; t_3, x_3) = \int_X G(t_1, E_1; t_2, x_2) G'(t_2, dx_2; t_3, x_3),}$$

where $G'(t_2, \cdot; t_3, x_3)$ has $\gamma'(t_2, \cdot; t_3, x_3)$ as an R-N derivative with respect to ν. In an alternative notation (intended to be equivalent) for the radiative measure $G'(t_2, \cdot; t_3, x_3)$,

$$\boxed{G(t_1, E_1; t_3, x_3) = \int_X G(t_1, E_1; t_2, \cdot)\, dG'(t_2, \cdot; t_3, x_3).}$$

This is the *transition relation for G-densities.*

The transition relation for G-densities is an abstract counterpart of the classical equation of transfer for the radiative process $\mathfrak{R}_\phi$ on a general carrier space (X, S, ν). Within the present axiomatic framework, it yields a symbolic description of the evolution of the general radiant density function $G(t_1, E_1; t_3, \cdot)$ associated with $\bar{\mu}(t_1, E_1; t_3, \cdot)$. That is, for fixed $t_1 \varepsilon T$ and $E_1 \varepsilon \mathrm{S}$ we have for each $\mu \varepsilon \mathfrak{M}_{\nu,t_1}$ the radiative measure $\bar{\mu}_{E_1} \varepsilon \mathfrak{M}_{\nu,t_1}$ which serves to yield a given initial condition by means of its associated general radiant density function on X at t_1. The transition relation for G-densities describes the values $G(t_1, E_1; t_3, x_3)$ of subsequent general radiant density functions in terms of the temporally intermediate densities of $\bar{\mu}(t_1, E_1; t_2, \cdot)$, $t_1 \leqq t_2 \leqq t_3$.

We may say that the transition relations for radiative measures and their various densities yield a *static* description of the evolution of the abstract radiation field; the next step in the line of development would be to consider a *dynamic* description: one which involves time derivatives of the measures and densities. The step from the static to the dynamic forms of the transition relations is considered in the following sections. In these sections we will study one example of just how much additional structure must be given the radiative process and its carrier space in order to make possible a rigorous derivation of the dynamical forms of the transition relations. The question of minimal required structure is not germane to the present goals and will be reserved for subsequent study. It turns out that relatively small concessions must be made in order to obtain the dynamical descriptions of the radiative process on both the set and point levels in X.

10. t-differentiable Process Axiom. We begin by motivating the choice of the present objects of study: the transforms of μ'-type measures and their g-densities with respect to μ'. Let $\mu \varepsilon \mathfrak{M}_{\nu,t_1}$, $(t_1, t_2) \varepsilon \dot{D}$, $E_1 \varepsilon \mathrm{S}$, and $\Delta \varepsilon T$, $\Delta > 0$. Let X support $\mu' = \mu_{E_1} R_{t_1,t_2} \varepsilon \mathfrak{M}_{\nu,t_2}$, and let F be the maximal full support for μ'. Then for every $E \varepsilon \mathrm{S}$, $E \subset F'$, $\bar{\mu}(t_1, E_1; t_2, E) = 0$. If $\bar{\mu}(t_1, \cdot; t_2, E)$ is the corresponding radiative measure, it follows that since $\bar{\mu}(t_1, E_1; t_2, E) = 0$ its g-density $g(t_1, \cdot; t_2, E)$ vanishes a.e. $[\nu]$ on E_1. Thus, by R_2, the corresponding measure $g(t_1, x_1; t_2, \cdot)$ vanishes on E for almost every $[\nu]$ $x_1 \varepsilon E_1$. From this and ((b)A, §7),

$$g(t_1, x_1; t_2, E_3) = \int_X \chi_{E_3}(x_2) g(t_1, x_1; t_2, dx_2)$$

$$= \int_X \chi_{E_3}(x_2)\chi_F(x_2) g(t_1, x_1; t_2, dx_2) = \int_X \chi_{E_3 \cap F}\, dg(t_1, x_1; t_2, \cdot)$$

for almost every $[\nu]$ $x_1 \varepsilon E_1$ and every $E_3 \varepsilon \mathrm{S}$.

The transition relation for g-densities may be written

$$g(t_1, x_1; t_2 + \Delta, E_3) = \int_X g'(t_2, x_2; t_2 + \Delta, E_3) g(t_1, x_1; t_2, dx_2),$$

so that a study of the quotient

$$[g(t_1, x_1; t_2 + \Delta, E_3) - g(t_1, x_1; t_2, E_3)]/\Delta$$

is equivalent to a study of

$$\int_X [(g'(t_2, x_2; t_2 + \Delta, E_3) - \chi_{E_3 \cap F}(x_2))/\Delta] g(t_1, x_1; t_2, dx_2)$$

in which we naturally choose to consider the quotients

$$[g'(t_2, x_2; t_2 + \Delta, E_3) - \chi_{E_3 \cap F}(x_2)]/\Delta,$$

and their μ'-integrals

$$\left(\int_{E_2} g'(t_2, \cdot; t_2 + \Delta, E_3)\, d\mu' - \int_{E_2} \chi_{E_3 \cap F}\, d\mu'\right)/\Delta, \qquad E_2 \in \mathrm{S},$$

which, by (A, §8) and the fact that F is the maximal full support for μ', may be written

$$\begin{aligned}(\overline{\mu'_F}(t_2, E_2; t_2 + \Delta, E_3) &- \overline{\mu'_F}(E_2 \cap E_3))/\Delta \\ &= (\overline{\mu'}(t_2, E_2; t_2 + \Delta, E_3) - \mu'(E_2 \cap E_3))/\Delta.\end{aligned}$$

Let $\{\Delta_n\}$ be a decreasing null sequence of positive elements in T. If (E_2, E_3) is an arbitrary pair of measurable sets it is then clear from the preceding sections that (C, §8) in general permits, but does not insure, the possibility that

$$\lim_n \, (g'(t_2, x_2; t_2 + \Delta_n, E_3) - \chi_{E_3 \cap F}(x_2))/\Delta_n$$

exists and is finite for almost every $[\nu]$ $x_2 \in X$. Finally, if X does not support μ', it is also clear that the above limit is zero for almost every $[\nu]$ $x_2 \in X$. This discussion indicates that, in the case of X supporting a radiative measure, the preceding set of axioms neither insures—but yet does not preclude—the possibility of the existence of finite limits of sequences of the kind exhibited above. Hence the preceding set of axioms will in general be independent of, but yet consistent with, the following regularity axiom.

R_3 : *Let* (t_1, t_2), $(t_2, t_3) \in D$, $\mu \in \mathfrak{M}_{\nu, t_1}$, *and* $E_1, E_3 \in \mathrm{S}$. *If* X *supports* $\mu' = \mu_{E_1} R_{t_1, t_2}$, *let* F *denote the maximal full support for* μ'. *If* $g'(t_2, \cdot; t_3, E_3)$ *is the g-density with respect to* μ' *of* $\bar{\mu}'(t_2, \cdot; t_3, E_3)$ *and* $\{\Delta_n\}$ *is any decreasing null sequence of positive elements in* T, *then:*

(i) *The sequence*

$$\{h'_{*n}(t_2, \cdot, E_3)\} = \{(\chi_{E_3 \cap F} - g'(t_2, \cdot; t_2 + \Delta_n, E_3))/\Delta_n\}$$

converges uniformly on X *to a unique* $[\nu]$ *essentially bounded function* $h'_*(t_2, \cdot, E_3)$.

(ii) *The corresponding function* $h'_*(t_2, x_2, \cdot)$ *is countably additive on* S *for almost* $[\nu]$ $x_2 \in X$

(iii)

$$\{\gamma_n\} = \{(\gamma(t_1\,, x_1\,; t_2 + \Delta_n\,, \cdot) - \gamma(t_1\,, x_1\,; t_2\,, \cdot))/\Delta_n\}$$

is fundamental in measure for almost every $[\nu]$ $x_1 \in X$.

(iv)

$$\{G_n\} = \{(G(t_1\,, E_1\,; t_2 + \Delta_n\,, \cdot) - G(t_1\,, E_1\,; t_2\,, \cdot))/\Delta_n\}$$

is fundamental in measure.

The references in R_3 to the concepts of essential boundedness and fundamentality in measure are, of course, with respect to the carrier measure. Clauses (iii) and (iv) will not be needed until section 15 at which time their motivation (which was not included in the preceding discussion) will be supplied. We observe that all three types of densities (G-, g-, and γ-densities) are represented in R_3. It turns out that in order to allow the present development of the foundations of radiative transfer theory to proceed rigorously, we require of the g-densities (in the form of g') the strongest, and of the G- and γ-densities the weakest, properties of convergence in general measure theory ([15], p. 237). However, it is worthwhile to observe that the attainment of the final goal of an abstract equation of transfer is possible on a *formal* level using only the three structure axioms C_1, M_1, and R_1, along with the final structure axiom T_1 introduced in section 18. Henceforth the radiative process $\mathcal{R}_\phi$ will be considered to obey R_3.

11. Measure Attenuating Functions.

Theorem A. *Let the hypothesis be as in* R_3. *If we write*

$$\int_{E_2} h'_{*n}(t_2\,, \cdot, E_3)\, d\mu' = \mathfrak{A}_{*n}(t_2\,, E_2\,, E_3), \qquad n = 1, 2, 3, \cdots,$$

and similarly

$$\int_{E_2} h'_{*}(t_2\,, \cdot, E_3)\, d\mu' = \mathfrak{A}_{*}(t_2\,, E_2\,, E_3), \quad \textit{for every } E_2 \in \mathsf{S},$$

then:

(a)

$$\lim_n \mathfrak{A}_{*n}(t_2\,, E_2\,, E_3) = \mathfrak{A}_{*}(t_2\,, E_2\,, E_3) < \infty.$$

(b) *The set function* $\mathfrak{A}_*(t_2\,, \cdot, E_3)$ *is a totally finite* μ'*-continuous signed measure on* S.

(c) *The set function* $\mathfrak{A}_*(t_2\,, E_2\,, \cdot)$ *is a totally finite* ν*-continuous signed measure on* S.

Proof: (a) By (i)R_3 the sequence $\{h'_{*n}(t_2\,, \cdot, E_3)\}$ converges uniformly on X to the function $h'_*(t_2\,, \cdot, E_3)$. For every $E_2 \in \mathsf{S}$, $\mu'(E_2) < \infty$ so that the sequence

$\{h'_{*n}(t_2, \cdot, E_3)\}$ converges in the mean ([8], p. 111) to the μ'-integrable function $h'_*(t_2, \cdot, E_3)$ on E_2, *i.e.*,

$$\int_{E_2} |h'_{*n}(t_2, \cdot, E_3) - h'_*(t_2, \cdot, E_3)|\, d\mu' \to 0 \quad \text{as} \quad n \to \infty,$$

which implies

$$\mathfrak{A}_{*n}(t_2, E_2, E_3) \to \mathfrak{A}_*(t_2, E_2, E_3) < \infty \quad \text{as} \quad n \to \infty.$$

(b) By definition $\mathfrak{A}_*(t_2, E_2, E_3) = \int_{E_2} h'_*(t_2, \cdot, E_3)\, d\mu'$, $t_2 \,\varepsilon\, T$ and $E_2, E_3 \,\varepsilon\, \mathbf{S}$. By (a), $h'_*(t_2, \cdot, E_3)$ is a μ'-integrable function so that in particular $\int_X h'_*(t_2, \cdot, E_3)\, d\mu' = \mathfrak{A}_*(t_2, X, E_3) < \infty$. In general ([8], p. 98) the indefinite integral of an integrable function is countably additive. Further, if $\mu'(E) = 0$, then $\int_E h'_*(t_2, \cdot, E_3)\, d\mu' = 0$ ([8], p. 104), *i.e.*, $\mathfrak{A}_*(t_2, E, E_3) = 0$.

(c) The finiteness of $\mathfrak{A}_*(t_2, E_2, \cdot)$ on $\mathbf{S}$ is implied by the μ'-integrability of $h'_*(t_2, \cdot, E_3)$ for every $E_3 \,\varepsilon\, \mathbf{S}$. If $\nu(E) = 0$, then, since $\overline{\mu}'(t_2, E_2; t_2 + \Delta_n, \cdot) \,\varepsilon\, \mathfrak{M}_{\nu, t_2+\Delta n}$, $n = 1, 2, 3, \cdots$, $g'(t_2, \cdot; t_2 + \Delta_n, E)$ vanishes almost everywhere $[\nu]$ on $E_2 \,\varepsilon\, \mathbf{S}$, so that $h'_{*n}(t_2, \cdot, E)$, $n = 1, 2, 3, \cdots$, vanishes almost everywhere $[\nu]$ on $E_2 \,\varepsilon\, \mathbf{S}$, which implies $\mathfrak{A}_*(t_2, E_2, E) = 0$. Let $\{D_n\}$ be a decreasing sequence of sets in $\mathbf{S}$ with $\lim_n D_n = 0 \,\varepsilon\, \mathbf{S}$. Now $h'_*(t_2, x, \cdot)$ vanishes at $0 \,\varepsilon\, \mathbf{S}$, is finite-valued and countably additive on $\mathbf{S}$ for almost every $[\nu]$ $x \,\varepsilon\, X$. $h'_*(t_2, x_2, \cdot)$ is therefore a signed measure on $\mathbf{S}$ and is continuous from above at $0 \,\varepsilon\, \mathbf{S}$ for almost every $x_2 \,\varepsilon\, X$. It follows that $\lim_n h'_*(t_2, x_2, D_n) = 0$ for almost every $[\nu]$ $x_2 \,\varepsilon\, X$ and that the sequence $\{\int_{E_2} h'_*(t_2, \cdot, D_n)\, d\mu'\}$ has the limit 0 for every $E_2 \,\varepsilon\, \mathbf{S}$. Therefore $\mathfrak{A}_*(t_2, E_2, \cdot)$, $E_2 \,\varepsilon\, \mathbf{S}$, is continuous from above at $0 \,\varepsilon\, \mathbf{S}$. Let $\{F_i\}$ be a disjoint sequence of measurable sets with union F''. Let $H_n = \bigcup_{i=1}^{n} F_i$ and $D_n = F'' - H_n$. By the finite additivity of $\mathfrak{A}_*(t_2, E_2, \cdot)$ we have

$$\mathfrak{A}_*(t_2, E_2, F'') = \sum_{i=1}^{n} \mathfrak{A}_*(t_2, E_2, F_i) + \mathfrak{A}_*(t_2, E_2, D_n)$$

$$= \lim_n \sum_{i=1}^{n} \mathfrak{A}_*(t_2, E_2, F_i) + \lim_n \mathfrak{A}_*(t_2, E_2, D_n) = \sum_{i=1}^{\infty} \mathfrak{A}_*(t_2, E_2, F_i),$$

which completes the proof of the theorem.

Letting $t_1 \,\varepsilon\, T$, $\mu \,\varepsilon\, \mathfrak{M}_{\nu, t_1}$, and $E_1 \,\varepsilon\, \mathbf{S}$ be arbitrary but fixed, the t-differentiable Process Axiom permits the definition of a real finite-valued function $\mathfrak{A}_*$ on the Cartesian product $T \times \mathbf{S} \times \mathbf{S}$. Some of its properties are summarized in Theorem A. In order to continue with the study of the dynamic aspects of the radiative process on X, we consider four restrictions of $\mathfrak{A}_*$ to certain subsets of $T \times \mathbf{S} \times \mathbf{S}$. These restrictions are as follows: Let $\mathbf{U} = \{(t_2, E_2, E_3) \,\varepsilon\, T \times \mathbf{S} \times \mathbf{S} : E_3 = X\}$. We will denote by A_* the restriction $\mathfrak{A}_*|\mathbf{U}$ of $\mathfrak{A}_*$ to $\mathbf{U}$ and write $(\mathfrak{A}_*|\mathbf{U})(t_2, E_2, X) = A_*(t_2, E_2)$ for every $(t_2, E_2, X) \,\varepsilon\, \mathbf{U}$. Let $T \times \mathbf{\Delta} = \{t_2, E_2, E_3) \,\varepsilon\, T \times \mathbf{S} \times \mathbf{S}$: $E_2 = E_3\}$. We will denote by $\mathfrak{a}_*$ the restriction $\mathfrak{A}_*|T \times \mathbf{\Delta}$ of $\mathfrak{A}_*$ to $T \times \mathbf{\Delta}$ and write $(\mathfrak{A}_*|T \times \mathbf{\Delta})(t_2, E_2, E_3) = \mathfrak{a}_*(t_2, E_2)$ for every $(t_2, E_2, E_3) \,\varepsilon\, T \times \mathbf{\Delta}$. Let $\mathbf{V} = \{(t_2, E_2, E_3) \,\varepsilon\, T \times \mathbf{S} \times \mathbf{S} : E_3 \subset E_2'\}$. We will denote by Σ_* the

(838)

restriction $\mathfrak{A}_*|\mathbf{V}$ of $\mathfrak{A}_*$ to $\mathbf{V}$ and write $(\mathfrak{A}_*|\mathbf{V})(t_2 , E_2 , E_3) = -\Sigma_*(t_2 , E_2 , E_3)$ for every $(t_2 , E_2 , E_3) \varepsilon \mathbf{V}$. Finally, it will be necessary specifically to consider the restriction of Σ_* to the subset $\mathbf{W}$ of $\mathbf{V}$, where $\mathbf{W} = \{(t_2 , E_2 , E_3) \varepsilon \mathbf{V} : E_2 = E_3'\}$. We will denote by S_* the restriction $\Sigma_*|\mathbf{W}$ of Σ_* to $\mathbf{W}$ and write $(\Sigma_*|\mathbf{W})(t_2 , E_2 , E_3) = S_*(t_2 , E_2)$ for every $(t_2 , E_2 , E_3) \varepsilon \mathbf{W}$.

The functions A_*, $\mathcal{A}_*$, Σ_*, and S_* will be referred to collectively as the *measure attenuating functions for* $\mathcal{R}_\phi$, where $\mathcal{R}_\phi$ is the radiative process on the carrier space X; they will be referred to individually as the *measure-absorption, -attenuation, -scattering,* and *total measure-scattering function* respectively. Further restrictions but of an obvious kind will be made of some of these functions. It will be clear from the context what the domains of the restrictions are in each case.

Theorem B. *Let the hypothesis be as in* R_3 , *then:*

(a) $A_*(t_2 , \cdot)$ *is a totally finite* μ'*-continuous measure on* $\mathbf{S}$.
(b) $\mathcal{A}_*(t_2 , \cdot)$ *is a finite-valued non-negative* μ'*-continuous function on* $\mathbf{S}$.
(c) $\Sigma_*(t_2 , \cdot, \cdot)$ *is a finite-valued non-negative function on* $\mathbf{S} \times \mathbf{S}$. *In particular, for fixed* $E_2 \varepsilon \mathbf{S}$, $\Sigma_*(t_2 , E_2 , \cdot)$ *is* ν*-continuous on* $\mathbf{S}$, *and if* $\{(t_2 , E_2 , F_j)\}$ *is a disjoint sequence in* $\mathbf{V}$,

$$\Sigma_*\left(t_2 , E_2 , \bigcup_{j=1}^{\infty} F_j\right) = \sum_{j=1}^{\infty} (\Sigma_*(t_2 , E_2 , F_j)).$$

On the other hand, for fixed $E_3 \varepsilon \mathbf{S}$, $\Sigma_*(t_2 , \cdot, E_3)$ *is* μ'*-continuous, and if* $\{(t_2 , F_j , E_3)\}$ *is a disjoint sequence in* $\mathbf{V}$,

$$\Sigma_*\left(t_2 , \bigcup_{j=1}^{\infty} F_j , E_3\right) = \sum_{j=1}^{\infty} (\Sigma_*(t_2 , F_j , E_3)).$$

(d) $\mathbf{S}_*(t_2 , \cdot)$ *is a finite-valued non-negative* μ'*-continuous function on* $\mathbf{S}$.

(e) $$\mathcal{A}_*(t_2 , \cdot) = A_*(t_2 , \cdot) + S_*(t_2 , \cdot).$$

Proof: (a) From (i)R_3 , the definition of A_* , and (a) of Theorem A we may write

$$A_*(t_2 , E_2) = \lim_n (\mu'(E_2) - \overline{\mu'}(t_2 , E_2 ; t_2 + \Delta_n , X))/\Delta_n$$

for every $E_2 \varepsilon \mathrm{S}$. With $E_3 = X$ in (b) of Theorem A, $A_*(t_2 , \cdot)$ is seen to be totally finite, μ'-continuous, and countably additive on S. From the lemma of §8 and the limit form above, $A_*(t_2 , \cdot)$ is non-negative on $\mathbf{S}$.

(b) From (i)R_3 , the definition of $\mathcal{A}_*$, and (a) of Theorem A we may write

$$\mathcal{A}_*(t_2 , E_2) = \lim_n (\mu'(E_2) - \overline{\mu'}(t_2 , E_2 ; t_2 + \Delta_n , E_2))/\Delta_n$$

for every $E_2 \varepsilon \mathrm{S}$. Hence $\mathcal{A}_*(t_2 , E_2) < \infty$ for every $E_2 \varepsilon \mathrm{S}$. Non-negativity follows from the limit form above and the lemma of §8. μ'-continuity follows from the limit form above.

(c) From (i)R_3, the definition of Σ_*, and (a) of Theorem A we may write

$$\Sigma_*(t_2\,,E_2\,,E_3) = \lim_n \overline{\mu'}(t_2\,,E_2\,;t_2+\Delta_n\,,E_3)/\Delta_n$$

for every $(t_2\,,E_2\,,E_3)\ \varepsilon\ \mathrm{V}$. Hence $0 \leqq \Sigma_*(t_2\,,E_2\,,E_3) < \infty$ for every $(t_2\,,E_2\,,E_3)\ \varepsilon\ \mathrm{V}$. For fixed $E_2\ \varepsilon\ \mathrm{S}$, the ν-continuity of $\Sigma_*(t_2\,,E_2\,,\cdot)$ is directly implied by the limit form above. If $\{(t_2\,,E_2\,,F_i)\}$ is a disjoint sequence in V, $\{F_i\}$ is a disjoint sequence in S ([8], p. 137). Hence for $x_2\ \varepsilon\ X \cap E_2 = E_2$, by (i)$R_3$,

$$-h'_{*n}(t_2\,,x_2\,,F_i) = g'(t_2\,,x_2\,;t_2+\Delta_n\,,F_i)/\Delta_n \geqq 0, \qquad n = 1, 2, 3, \cdots.$$

From (ii)R_3 it follows that on E_2, except perhaps for a ν-null subset, $\{\sum_{i=1}^{n} - h'_*(t_2\,,\cdot,F_i)\}$ is an increasing sequence of non-negative μ'-integrable functions with the limit $-h'_*(t,\cdot,\bigcup_{i=1}^{\infty} F_i)$. Hence ([8], p. 112)

$$\begin{aligned}\lim_n \int_{E_2}\left(\sum_{i=1}^{n} - h'_*(t_2\,,\cdot,F_i)\right)d\mu' &= \lim_n \sum_{i=1}^{n}(\Sigma_*(t_2\,,E_2\,,F_i))\\ &= \int_{E_2} - h'_*\left(t_2\,,\cdot,\bigcup_{i=1}^{\infty} F_i\right)d\mu' = \Sigma_*\left(t_2\,,E_2\,,\bigcup_{i=1}^{\infty} F_i\right).\end{aligned}$$

Finally, for fixed E_3 in S, μ'-continuity and countable additivity for $\Sigma_*(t_2\,,\cdot,E_3)$ (in the indicated sense) follow from (b) of Theorem A.

(d) From (i)R_3, the definition of S_*, and ((a) of Theorem A) we may write

$$S_*(t_2\,,E_2) = \lim_n \overline{\mu'}(t_2\,,E_2\,;t_2+\Delta_n\,,E'_2)/\Delta_n\,.$$

μ'-continuity follows from this form; finite-valuedness and non-negativity follow immediately from the fact that S_* is a restriction of Σ_*.

(e) From (c) of Theorem A,

$$\mathfrak{A}_*(t_2\,,E_2\,,X) = \mathfrak{A}_*(t_2\,,E_2\,,E_2) + \mathfrak{A}_*(t_2\,,E_2\,,E'_2)$$

which with the definitions of A^*, $\mathcal{A}_*$, and S_* yields the desired conclusion. This ends the proof.

12. Dynamic Transition Relation for Radiative Measures. The following heorem asserts the existence of the dynamic version of the transition relation for radiative measures and gives, on a set level, the first recognizable counterpart to the classical equation of transfer.

Theorem A. *Let* $(t_1\,,t_2)\ \varepsilon\ D$, $\mu\ \varepsilon\ \mathfrak{M}_{\nu,t_1}$, $E_1\ \varepsilon\ \mathrm{S}$ *be fixed. If* $E_2\ \varepsilon\ \mathrm{S}$ *and if* $\{\Delta_n\}$ *is any decreasing null sequence of positive elements in* T, *then:*

(a)
$$\lim_n (\mu(t_1\,,E_1\,;t_2+n,E_2) - \mu(t_1\,,E_1\,;t_2\,,E_2))/\Delta_n \equiv \partial^+\mu(t_1\,,E_1\,;t_2\,,E_2)/\partial t_2$$

exists and is finite.

(b) $\partial^+\mu(t_1, E_1; t_2, E_2)/\partial t_2 = -\mathfrak{A}_*(t_2, X, E_2) = -\mathcal{A}_*(t_2, E_2) + S_*(t_2, E_2')$.

Proof: Let $\{F_j\}$ be a partition of X. The appropriate support conventions being in force, we write the transition relation for radiative measures as follows:

$$\mu(t_1, E_1; t_2 + \Delta_n, E_2) = \sum_{j=1}^{m} \mu(t_1, E_1; t_2, F_j)\mu'(t_2, F_j; t_2 + \Delta_n, E_2),$$

for $n = 1, 2, 3, \cdots$. Using the μ'-notation, we have

$$\begin{aligned}\mu(t_1, E_1; t_2 + \Delta_n, E_2) &= \sum_{j=1}^{m} \mu'(F_j)\mu'(t_2, F_j; t_2 + \Delta_n, E_2)\\ &= \sum_{j=1}^{m} \overline{\mu'}(t_2, F_j; t_2 + \Delta_n, E).\end{aligned}$$

Further, $\mu(t_1, E_1; t_2, E_2) = \sum_{j=1}^{m} \mu'(F_j \cap E_2)$, so that

$$\begin{aligned}&\lim (\mu(t_1, E_1; t_2 + \Delta_n, E_2) - \mu(t_1, E_1; t_2, E_2))/\Delta_n\\ &\qquad = \sum_{j=1}^{m} [\lim_{n} (\overline{\mu'}(t_1, F_j; t_2 + \Delta_n, E_2) - \mu'(F_j \cap E_2))/\Delta_n]\\ &\qquad = \sum_{j=1}^{m} -\mathfrak{A}_*(t_2, F_j, E_2) = -\mathfrak{A}_*(t_2, X, E_2) < \infty,\end{aligned}$$

by ((b)A, §11). Hence $\partial^+\mu(t_1, E_1; t_2, E_2)/\partial t_2$ exists and is finite. Again by ((b)A, §11) and the definitions of the measure attenuating functions,

$$\begin{aligned}\partial^+\mu(t_1, E_1; t_2, E_2)/\partial t_2 &= -\mathfrak{A}_*(t_2, E_2, E_2) - \mathfrak{A}_*(t_2, E_2', E_2)\\ &= -\mathcal{A}_*(t_2, E_2) + S_*(t_2, E_2'),\end{aligned}$$

which proves (b).

We remark that the symbol $\partial^+\mu(t_1, E_1; t_2, E_2)/\partial t_2$ is to denote a right hand derivative with respect to t evaluated at t_2. Inasmuch as $\mu \varepsilon \mathfrak{M}_{\nu,t_1}$, $E_1 \varepsilon \mathrm{S}$, and $E_2 \varepsilon \mathrm{S}$ are arbitrary but fixed throughout the discussion, the right hand derivative is essentially a total derivative, t_1, E_1, and E_2 playing the roles of parameters. We observe that the form of the t-differentiability Axiom allows only derivatives of this kind. It should be evident after some reflection that t-differentiability of $\mathcal{R}_\phi$ in the other direction is, in general, too much to hope for. While such differentiability can actually be demanded in R_3 and resulting two-sided derivatives be obtained, this additional regularity condition adds nothing radically different to the present store of available techniques and will not materially affect the general symbolic structure of the subsequent theorems. For the present study we will continue with the adopted form of the radiative process.

For arbitrary $\mu \varepsilon \mathfrak{M}_{\nu,t}$ and $E \varepsilon \mathrm{S}$, the value $\mu(E)$ was defined earlier as the radiant energy in E (at $t \varepsilon T$ and $\lambda \varepsilon \Lambda$), μ by fiat being a ν-continuous totally finite measure on S. The set function $-\mathfrak{A}_*(t_2, X, \cdot)$ by ((c)A, §11) is a ν-continuous totally finite signed measure on S. Thus the properties of $-\mathfrak{A}_*(t_2, X, \cdot)$

parallel those of $\mu' = \overline{\mu'_X} \, \varepsilon \, \mathcal{M}_{\nu, t_2}$, and the value $\mu'(E_2)$ being the radiant energy in E_2 at t_2 (relative, in this case, to $\mu(E_1)$) has a counterpart in the value $-\mathfrak{A}_*(t_2, X, E_2)$ which we shall define as the *general radiant* (energy) *flux* into $E_2 \, \varepsilon \, \mathrm{S}$ at $t_2 \, \varepsilon \, T$ (and at $\lambda \, \varepsilon \, \Lambda$) for the radiative process $\mathcal{R}_\phi$. Thus while the radiant energy in a measurable set has been fixed as non-negative, its associated radiant flux (change in time) may well be negative. This fact is reflected formally in the *signed* character of the set function $-\mathfrak{A}_*(t_2, X, \cdot)$. We observe that the preceding theorem could have been proved using a much weaker form of R_3 (*e.g.*, using measures instead of functions on (points of) X and less stringent convergence requirements). However, since one of the central aims of this work is to develop a radiative transfer theory from a unified set of axioms, we retain the present form of R_3. Axiom R_3 will be used to its fullest extent somewhat later in the study.

Corollary. If $A_*(t_2, E_2) = 0$, *then*

$$\partial^+ \mu(t_1, E_1; t_2, E_2)/\partial t_2 = -S_*(t_2, E_2) + S_*(t_2, E_2').$$

This corollary indicates that if the measure absorption function vanishes for $E_2 \, \varepsilon \, \mathrm{S}$ at $t_2 \, \varepsilon \, T$, the phraseology of the definition of general radiant flux receives special justification. If, in addition, X has a topology commensurate with S (as is the case for the classical carrier space) it would be meaningful, as in the classical case, to say that the net rate of energy flow into E_2 takes place across the boundary of E_2. If $A_*(t_2, E_2) > 0$, then, in addition to the net flow of energy into E_2 across its boundary, there is a rate of loss of radiant energy in E_2 induced by a mechanism of $\mathcal{R}_\phi$ which we have summarized analytically by the function $A_*(t_2, \cdot)$ on S. This points up the nature of the *general* radiant flux into E_2 and attempts to draw an abstract parallel to the classical concept of absorption of radiant energy. It is clear from the definition of the measure absorption function that a sufficient condition that it vanish on S is that the contraction property of the radiative process exhibits an equality (*cf.* (v)R_1).

13. μ'-differentiable Process Axiom. In order to derive the dynamic transition relations for the various densities of radiative measures, we require further regularity properties of the radiative measures, the radiative process, and the carrier space. We now set about to motivate the μ'-differentiability Axiom, the last of the regularity axioms required for the development of the theory of radiative processes. We begin by proving a simple but important lemma.

Lemma. Let $(t_1, t_2) \, \varepsilon \, D$, $\mu \, \varepsilon \, \mathcal{M}_{\nu, t_1}$, *and* $E_1 \, \varepsilon \, \mathrm{S}$ *be arbitrary but fixed. If* $E_2, E_3 \, \varepsilon \, \mathrm{S}$, *then*

$$\begin{aligned} \mathfrak{A}_*(t_2, E_2, E_3) = {} & \mathcal{A}_*(t_2, E_2 \cap E_3) - \Sigma_*(t_2, E_2 \cap E_3, E_3 - E_2) \\ & - \Sigma_*(t_2, E_2 - E_3, E_3 - E_2) - \Sigma_*(t_2, E_2 - E_3, E_2 \cap E_3). \end{aligned}$$

Proof: By ((c)A, §11),

$$\mathfrak{A}_*(t_2, E_2, E_3) = \mathfrak{A}_*(t_2, E_2, E_3 - E_2) + \mathfrak{A}_*(t_2, E_2, E_2 \cap E_3).$$

By ((*b*)A, §11),

$$\mathfrak{A}_*(t_2\,, E_2\,, E_3 - E_2) = \mathfrak{A}_*(t_2\,, E_2 \cap E_3\,, E_3 - E_2) + \mathfrak{A}_*(t_2\,, E_2 - E_3\,, E_3 - E_2).$$

Similarly,

$$\mathfrak{A}_*(t_2\,, E_2\,, E_2 \cap E_3) = \mathfrak{A}_*(t_2\,, E_2 \cap E_3\,, E_2 \cap E_3) + \mathfrak{A}_*(t_2\,, E_2 - E_3\,, E_2 \cap E_3).$$

Since $(E_2 \cap E_3\,, E_3 - E_2)$, $(E_2 - E_3\,, E_3 - E_2)$, and $(E_2 - E_3\,, E_2 \cap E_3)$ are elements in the T-section of $\mathbf{V}$ determined by $t_2 \in T$ and $(t_2\,, E_2 \cap E_3\,, E_2 \cap E_3)$ is an element of $T \times \mathbf{\Delta}$, the lemma now follows from the definitions of $\mathcal{A}_*$ and Σ_*.

From (i)R_3 with given fixed E_3 and F,

$$\chi_{E_3 \cap F} - g'(t_2\,, \cdot\,; t_2 + \Delta_n\,, E_3) = h_*'(t_2\,, \cdot\,, E_3)\Delta_n + o(\Delta_n\,, \cdot)\ [\nu]$$

for every positive integer n. $o(\Delta_n\,, \cdot)$ is a μ'-integrable function on X for every positive integer n. Further, $o(\Delta_n\,, \cdot)/\Delta_n \to 0$ (the zero function) uniformly as $n \to \infty$. Hence

$$\mu'(E_2 \cap E_3) - \overline{\mu}'(t_2\,, E_2\,; t_2 + \Delta_n\,, E_3) = \mathfrak{A}_*(t_2\,, E_2\,, E_3)\Delta_n + \int_{E_2} o(\Delta_n\,, \cdot)\, d\mu',$$

$E_2 \in \mathrm{S}$, for $n = 1, 2, 3, \cdots$. By the preceding lemma this may be written as

$$\begin{aligned}\mu'(E_2 \cap E_3) - \overline{\mu}'(t_2\,, E_2\,; t_2 + \Delta_n\,, E_3) &= [\mathcal{A}_*(t_2\,, E_2 \cap E_3)\\ - \Sigma_*(t_2\,, E_2 \cap E_3\,, E_3 - E_2) &- \Sigma_*(t_2\,, E_2 - E_3\,, E_3 - E_2)\\ &- \Sigma_*(t_2\,, E_2 - E_3\,, E_2 \cap E_3)]\Delta_n + \int_{E_2} o(\Delta_n\,, \cdot)\, d\mu',\end{aligned}$$

$n = 1, 2, 3, \cdots$. In order to obtain the dynamic transition relations for the various densities it is clear from this equation that it must be possible to perform set differentiations on the indicated set functions. The ground work for these operations is prepared by the following discussion.

A *net* in X ([15], p. 296) is a countable class of disjoint measurable sets of finite ν-measure whose union is X. Since $(X\,, \mathrm{S}, \nu)$ is a totally σ-finite measure space, the collection of all nets in X is not empty. This is true also for the measure spaces (X, S, μ), $\mu \in \mathcal{M}_{\nu,t}$, $t \in T$. A sequence $\{\mathcal{N}_i\}$ of nets in X is *monotone* ([15], p. 296) if, for each positive integer n, every set of $\mathcal{N}_{n+1}$ is a subset of some set of $\mathcal{N}_n$. Let $\mu \in \mathcal{M}_{\nu,t}$ and let m be a μ-continuous set function on S. We define for each positive integer n the point function d_n on X by choosing for each $x \in X$ the (unique) set $F_n \in \mathcal{N}_n$ such that $x \in F_n$ and setting

$$d_n(x) = \begin{cases} \dfrac{m(F_n)}{\mu(F_n)} & \text{for} \quad \mu(F_n) > 0 \\ 0 & \text{for} \quad \mu(F_n) = 0. \end{cases}$$

(843)

The *upper and lower derivates of* m *with respect to* $\mathcal{N} = \{\mathcal{N}_i\}$ *and* μ will be denoted by

$$\overline{D}[\mathcal{N}, \mu]m(x) = \limsup_n d_n(x),$$

$$\underline{D}[\mathcal{N}, \mu]m(x) = \liminf_n d_n(x),$$

respectively. m is said to be *differentiable at* x *with respect to* $\mathcal{N}$ *and* μ if

$$-\infty < \underline{D}[\mathcal{N}, \mu]m(x) = \overline{D}[\mathcal{N}, \mu]m(x) < \infty,$$

and the common value will be the *derivative of* m *at* x *with respect to* $\mathcal{N}$ *and* μ and will be designated by $D[\mathcal{N}, \mu]m(x)$. The function d_n is clearly measurable, and so are $\overline{D}[\mathcal{N}, \mu]m$, $\underline{D}[\mathcal{N}, \mu]m$, and $D[\mathcal{N}, \mu]m$ ([8], p. 84). If $\mathcal{N}$ is a sequence of nets, let $\mathcal{N}_0 = \bigcup_{n=1}^{\infty} \mathcal{N}_n$. $\mathcal{N}$ is said to be *regular on* $E \varepsilon$ S *with respect to* μ ([15], p. 297) if, given $\epsilon > 0$, there is a sequence K of sets from $\mathcal{N}_0$ such that $\mu(E - \bigcup_{i=1}^{\infty} K_i) = 0$, $\mu(\bigcup_{i=1}^{\infty} K_i) \leqq \mu(E) + \epsilon$.

With these preliminaries in mind we return to consider the family of measure attenuating functions. By definition,

$$A_*(t_2, E_2) = \mathfrak{A}_*(t_2, E_2, X) = \int_{E_2} h_*'(t_2, \cdot, X)\, d\mu',$$

where μ' is defined by the fixed elements of the lemma. The set function $A_*(t_2, \cdot)$ is μ'-continuous, and if $\mathcal{N}$ is a monotone sequence of nets regular with respect to μ' on each measurable set then ([15], p. 299) $D[\mathcal{N}, \mu']A_*(t_2, \cdot) = h_*'(t_2, \cdot, X)$ $[\nu]$. (Clearly, by the source cited, there is equality $[\mu']$; however, on the maximal full support of μ' there is equality $[\nu]$ (§8), and, by earlier conventions, there is also equality $[\nu]$ on F'.) We write $a_*(t_2, \cdot) \equiv h_*'(t_2, \cdot, X)$. Again, by definition,

$$\begin{aligned} A_*(t_2, E_2 \cap E_3) &= \mathfrak{A}_*(t_2, E_2 \cap E_3, X) \\ &= \int_{E_2 \cap E_3} h_*'(t_2, \cdot, X)\, d\mu' = \int_{E_2} \chi_{E_3} h_*'(t_2, \cdot, X)\, d\mu', \end{aligned}$$

so that $A_*(t_2, E_3 \cap \cdot)$, the restriction of $A_*(t_2, \cdot)$ to $E_3 \varepsilon$ S, has the μ'-derivative

$$D[\mathcal{N}, \mu']A_*(t_2, E_3 \cap \cdot) = \chi_{E_3} a_*(t_2, \cdot)\ [\nu].$$

An examination of the set functions $\mathcal{A}_*(t_2, E_3 \cap \cdot)$, $\Sigma_*(t_2, E_3 \cap \cdot, E_3 \cap (\cdot)')$, $\Sigma_*(t_2, (E_3)' \cap \cdot, E_3 \cap (\cdot)')$, and $\Sigma_*(t_2, (E_3)' \cap \cdot, E_3 \cap \cdot)$ appearing in the decomposition of $\mathfrak{A}_*(t_2, \cdot, E_3)$ yields the realization that the use of the theorem (implicitly cited) above for obtaining the derivative of $A_*(t_2, E_3 \cap \cdot)$ with respect to $\mathcal{N}$ and μ' cannot be repeated. For example,

$$\begin{aligned} \mathcal{A}_*(t_2, E_2 \cap E_3) &= \mathfrak{A}_*(t_2, E_2 \cap E_3, E_2 \cap E_3) \\ &= \int_{E_2 \cap E_3} h_*'(t_2, \cdot, E_2 \cap E_3)\, d\mu', \end{aligned}$$

(844)

so that if $\mathcal{N}$ is a monotone sequence of nets regular with respect to μ' on each measurable set,

$$\lim_{n} \mathcal{A}_*(t_2\,, E_3 \cap F_n)/\mu'(F_n) = \lim_{n} \int_{F_n} \chi_{E_3} h_*'(t_2\,, \cdot, F_n \cap E_3)\, d\mu'/\mu'(F_n)$$

involves the elements of the members of the monotone sequence in the integrand. The μ'-continuity of the above set functions allows but does not insure the existence of derivatives with respect to $\mathcal{N}$ and μ'. We also observe that

$$\Sigma_*(t_2\,, E_3 \cap \cdot, E_3 \cap (\cdot)') + \Sigma_*(t_2\,, (E_3)' \cap \cdot, E_3 \cap (\cdot)') = \Sigma_*(t_2\,, \cdot, E_3 \cap (\cdot)'),$$

hence its corresponding function $\Sigma_*(t_2\,, E_2\,, (E_2)' \cap \cdot)$ by ((c)B, §11) is countably additive. It is desirable that the derivative of the latter set function retain this property. An examination of this situation would be analogous to that given in detail in (C, §5) for g-densities, and the conclusions would be similar. This hair's breadth gap between countable additivity almost everywhere $[\nu]$ and "almost countable additivity" is harmlessly bridged as before by axiomatic dictum. Finally, the property exhibited by the derivative of $A_*(t_2\,, E_3 \cap \cdot)$ is needed for the derivative of $S_*(t_2\,, E_3 \cap \cdot)$. Similar properties are also required for the Σ_* functions appearing in the decomposition of $\mathfrak{A}_*(t_2\,, \cdot, E_3)$. Such properties are generalizations of the properties possessed by metric densities in the (Euclidean) carrier spaces of the form E_n. With these preliminaries we state the following axiom.

R_4 : *Let* $(t_1\,, t_2) \in D$, $\mu \in \mathfrak{M}_{\nu, t_1}$, *and* $E_1 \in \mathbf{S}$ *be arbitrary but fixed.*

(i) *There exists a monotone sequence* $\mathcal{N}$ *of nets in* X *regular with respect to* μ' *on each measurable set.*

(ii) *Each of the following derivatives with respect to* $\mathcal{N}$ *and* μ' *exists and has an essential bound* $[\nu]$ *independent of* $E_3 \in \mathbf{S}$.

(a)
$$D[\mathcal{N}, \mu']S_*(t_2\,, \cdot) \equiv s_*(t_2\,, \cdot);$$
$$D[\mathcal{N}, \mu']S_*(t_2\,, E_3 \cap \cdot) = \chi_{E_3} s_*(t_2\,, \cdot)[\nu].$$

(b)
$$D[\mathcal{N}, \mu']\Sigma_*(t_2\,, E_3 \cap \cdot, E_3 \cap (\cdot)') \equiv {}^1\bar{\sigma}_*(t_2\,, \cdot, E_3)$$

and vanishes $[\nu]$ *on* E_3'.

(c)
$$D[\mathcal{N}, \mu']\Sigma_*(t_2\,, (E_3)' \cap \cdot, E_3 \cap (\cdot)') \equiv {}^2\bar{\sigma}_*(t_2\,, \cdot, E_3)$$

and vanishes $[\nu]$ *on* E_3.

(d)
$$D[\mathcal{N}, \mu']\Sigma_*(t_2\,, (E_3)' \cap \cdot, E_3 \cap \cdot) \equiv {}^3\bar{\sigma}_*(t_2\,, \cdot, E_3)$$

and vanishes $[\nu]$ *on* X.

(iii) *The corresponding set function* ${}^1\bar{\sigma}_*(t_2\,, x, \cdot) + {}^2\bar{\sigma}_*(t_2\,, x, \cdot)$ *is countably additive for almost every* $[\nu]$ $x \in X$.

Henceforth the process $\mathcal{R}_\phi$ will be considered to obey R_4. The derivatives in R_4 are unique $[\nu]$ ([15], p. 302). Since ((e)B, §11)

$$\mathcal{A}_*(t_2, E_3 \cap \cdot) = A_*(t_2, E_3 \cap \cdot) + S_*(t_2, E_3 \cap \cdot),$$

we have

$$D[\mathcal{N}, \mu']\mathcal{A}_*(t_2, E_3 \cap \cdot) = \chi_{E_3} a_*(t_2, \cdot) + \chi_{E_3} s_*(t_2, \cdot) \ [\nu].$$

Let $D[\mathcal{N}, \mu']\mathcal{A}_*(t_2, \cdot) \equiv \alpha_*(t_2, \cdot)$. Hence

$$\alpha_*(t_2, \cdot) = a_*(t_2, \cdot) + s_*(t_2, \cdot) \ [\nu].$$

The combination occurring in (iii)R_4 is to be used repeatedly. For brevity, we define

$$\bar{\sigma}_*(t_2, \cdot, E_3) \equiv {}^1\bar{\sigma}_*(t_2, \cdot, E_3) + {}^2\bar{\sigma}_*(t_2, \cdot, E_3).$$

The correspondent to this is the combination occurring in (iii)R_4. As an immediate consequence of this definition, we have

$$\bar{\sigma}_*(t_2, \cdot, X) = {}^1\bar{\sigma}_*(t_2, \cdot, X) = s_*(t_2, \cdot) \ [\nu].$$

14. Density Attenuating Functions. The functions $\bar{\sigma}_*(t, \cdot, E)$, $s_*(t, \cdot)$, $a_*(t, \cdot)$, and $\alpha_*(t, \cdot)$ will be referred to collectively as the *density attenuating functions for* $\mathcal{R}_\phi$, where $\mathcal{R}_\phi$ is the radiative process. $\bar{\sigma}_*(t, \cdot, E)$ is the *density scattering function into* $E \in \mathrm{S}$; $s_*(t, \cdot)$ is the *total density scattering function*; $a_*(t, \cdot)$ is the *density absorption function*; and $\alpha_*(t, \cdot)$ is the *density attenuation function.*

The non-negative, ν-continuous ((c)B, §11), countably additive ((iii)R_4), a.e. $[\nu]$ totally finite ((iii)R_4) set function $\bar{\sigma}_*(t, x, \cdot)$ has an R-N derivative $\sigma_*(t, x, \cdot)$ with respect to ν for almost every $x \in X$. We will call $\sigma_*(t, x, \cdot)$ the *density scattering function.* This function may be viewed as the X-section determined by $x \in X$ of the function $\sigma_*(t, \cdot, \cdot)$ defined on the measurable space $(X \times X, \mathrm{S} \times \mathrm{S})$. Further, by introducing the product measure $\nu \times \nu$, we observe that $\sigma_*(t, \cdot, \cdot)$ is determined uniquely $[\nu \times \nu]$; there is no general guarantee ([8], p. 142), however, that $\sigma_*(t, \cdot, \cdot)$ has the respectability of measurability on $(X \times X, \mathrm{S} \times \mathrm{S})$, and this indispensable property will be endowed by fiat, and considered in force in the sequel (*cf.* (i)R_2). Its formal announcement rightly belongs in (iii)R_4.

Since $\bar{\sigma}_*(t, x, E) = \int_E \sigma_*(t, x, \cdot)\, d\nu$, we see from the definitions above that the family of density attenuating functions is thus describable in terms of two functions: $\sigma_*(t, \cdot, \cdot)$ and $a_*(t, \cdot)$; one characterizes the scattering, the other the absorption phenomena of $\mathcal{R}_\phi$, respectively. We will consider $\sigma_*(t, \cdot, \cdot)$ a member of the family of density attenuating functions.

15. Dynamic Transition Relations for Densities.

Theorem A. *Let* $(t_1, t_2) \in D$, $\mu \in \mathfrak{M}_{\nu, t_1}$, *and* $E_1 \in \mathrm{S}$ *be arbitrary but fixed. Let* $\mu' = \mu_{E_1} R_{t_1, t_2}$, *and, for* $(t_2, t_3) \in D$, *let* $g(t_1, \cdot\,; t_3, E_2)$ *be the g-density associated* *with* $\overline{\mu'}(t_1\, , \cdot ; t_3\, , E_2)$, $E_2 \,\varepsilon\, \mathrm{S}$. *If* $\{\Delta_n\}$ *is any decreasing null sequence of positive elements in* T, *then:*

$$\text{(a)} \qquad \lim_n \,(g(t_1\, , x_1\, ; t_2 + \Delta_n\, , E_2) - g(t_1\, , x_1\, ; t_2\, , E_2))/\Delta_n$$
$$\equiv \partial^+ g(t_1\, , x_1\, ; t_2\, , E_2)/\partial t_2$$

exists and is finite for every $E_2 \,\varepsilon\, \mathrm{S}$ *and almost every* $[\nu]$ $x_1 \,\varepsilon\, X$.

$$\text{(b)} \qquad \partial^+ g(t_1\, , x_1\, ; t_2\, , E_2)/\partial t_2 = -\int_{E_2} \alpha_*(t_2\, , x_2) g(t_1\, , x_1\, ; t_2\, , dx_2)$$
$$+ \int_X \bar{\sigma}_*(t_2\, , x_2\, , E_2) g(t_1\, , x_1\, ; t_2\, , dx_2).$$

Proof: By (i)R_3 ,

$$\chi_{E_2 \cap F} - g'(t_2\, , \cdot ; t_2 + \Delta_n\, , E_2) = h_*'(t_2\, , \cdot, E_2)\Delta_n + o(\Delta_n\, , \cdot)\ [\mu]$$

for each positive integer n. For each n, $o(\Delta_n\, , \cdot)$ is a μ'-integrable function on X, and $o(\Delta_n\, , \cdot)/\Delta_n \rightarrow 0$ uniformly on X as $n \rightarrow \infty$. For each $E \,\varepsilon\, \mathrm{S}$ and positive integer n,

$$\mu'(E \cap E_2) - \overline{\mu'}\,(t_2\, , E ; t_2 + \Delta_n\, , E_2) = \mathfrak{A}_*(t_2\, , E, E_2)\Delta_n + \int_E o(\Delta_n\, , \cdot)\, d\mu'$$

which, by lemma §13, may be written

$$\mu'(E \cap E_2) - \overline{\mu'}(t_2\, , E ; t_2 + \Delta_n\, , E_2) = [\mathcal{A}_*(t_2\, , E, E_2)$$
$$- \Sigma_*(t_2\, , E \cap E_2\, , E_2 - E) - \Sigma_*(t_2\, , E - E_2\, , E_2 - E)$$
$$- \Sigma_*(t_2\, , E - E_2\, , E \cap E_2)]\Delta_n + \int_E o(\Delta_n\, , \cdot)\, d\mu'.$$

Using R_4 , ([15], p. 299), and the definitions of the density attenuating functions,

$$\chi_{E_2 \cap F} - g'(t_2\, , \cdot ; t_2 + \Delta_n\, , E_2) =$$
$$[\chi_{E_2}\alpha_*(t_2\, , \cdot) - \bar{\sigma}_*(t_2\, , \cdot, E_2)]\Delta_n + o(\Delta_n\, , \cdot)\ [\nu].$$

Hence

$$(\chi_{E_2 \cap F} - g'(t_2\, , \cdot ; t_2 + \Delta_n\, , E_2))/\Delta_n \rightarrow \chi_{E_2}\alpha_*(t_2\, , \cdot) - \bar{\sigma}_*(t_2\, , \cdot, E_2)$$

uniformly a.e. $[\nu]$ on X. Using the transition relations for g-densities and observing that $g(t_1\, , x_1\, ; t_2\, , X) < \infty$ for almost every $[\nu]$ $x_1 \,\varepsilon\, X$, we have

$$\lim_n \,(g(t_1\, , x_1\, ; t_2 + \Delta_n\, , E_2) - g(t_1\, , x_1\, ; t_2\, , E_2))/\Delta_n$$
$$= \lim_n \int_X [(g'(t_2\, , x_2\, ; t_2 + \Delta_n\, , E_2) - \chi_{E_2 \cap F}(x_2))/\Delta_n] g(t_1\, , x_1\, ; t_2\, , dx_2)$$
$$= \int_X [-\chi_{E_2}\alpha_*(t_2\, , x_2) + \bar{\sigma}_*(t_2\, , x_2\, , E_2)] g(t_1\, , x_1\, ; t_2\, , dx_2) < \infty$$

for almost every $[\nu]$ $x_1 \,\varepsilon\, X$. This ends the proof.

Theorem B. *Retaining the hypothesis of Theorem A, then:*

(a) $\lim_n (\gamma(t_1, x_1; t_2 + \Delta_n, \cdot) - \gamma(t_1, x_1; t_2, \cdot))/\Delta_n \equiv \partial^+\gamma(t_1, x_1; t_2, \cdot)/\partial t_2$

exists and is a.e. [ν] *finite for almost every* [ν] $x_1 \,\varepsilon\, X$.

(b) $$\partial^+\gamma(t_1, x_1; t_2, x_2)/\partial t_2 = -\alpha_*(t_2, x_2)\gamma(t_1, x_1; t_2, x_2) + \int_X \gamma(t_1, x_1; t_2, x')\sigma_*(t_2, x', x_2)\, d\nu(x')\ [\nu].$$

Proof: Let

$$\gamma_n = (\gamma(t_1, x_1; t_2 + \Delta_n, \cdot) - \gamma(t_1, x_1; t_2, \cdot))/\Delta_n .$$

By ((b)A, §7) and Theorem A, for almost every [ν] $x_1 \,\varepsilon\, X$

$$\lim_n \int_{E_2} \gamma_n\, d\nu = \int_{E_2} \alpha_*(t_2, x_2) g(t_1, x_1; t_2, dx_2) + \int_X \bar{\sigma}_*(t_2, x_2, E_2) g(t_1, x_1; t_2, dx_2) < \infty .$$

Thus the sequence $\{\int_{E_2} \gamma_n\, d\nu\}$ of real numbers is fundamental for almost every [ν] $x_1 \,\varepsilon\, X$ and every $E_2 \,\varepsilon\,$ S. By (iii)R_3, $\{\gamma_n\}$ is fundamental in measure for almost every [ν] $x_1 \,\varepsilon\, X$, so that ([15], p. 236) $\{\gamma_n\}$ is mean fundamental and there exists ([8], p. 107) a ν-integrable function $\gamma^+ \equiv \partial^+\gamma(t_1, x_1; t_2, \cdot)/\partial t_2$ to which $\{\gamma_n\}$ converges in the mean for almost every [ν] $x_1 \,\varepsilon\, X$. Hence, for every $E_2 \,\varepsilon\,$ S, by a Fubini argument,

$$\int_{E_2} \gamma^+(x_2)\, d\nu(x_2) = \int_{E_2} \left[-\alpha_*(t_2, x_2)\gamma(t_1, x_1; t_2, x_2) + \int_X \sigma_*(t_2, x', x_2)\gamma(t_1, x_1; t_2, x')\, d\nu(x') \right] d\nu(x_2).$$

An application of ([8], p. 105) yields (b) and completes the proof.

The result in part (b) of the preceding theorem is the *dynamic transition relation for γ-densities.* (b) of Theorem A gives the *dynamic transition relation for g-densities.* Part (b) of the following theorem gives the *dynamic transition relation for G-densities.*

Theorem C. *Retaining the hypothesis of Theorem A, then:*

(a)

$$\lim_n (G(t_1, E_1; t_2 + \Delta_n, \cdot) - G(t_1, E_1; t_2, \cdot))/\Delta_n \equiv \partial^+G(t_1, E_1; t_2, \cdot)/\partial t_2$$

exists, is a.e. [ν] *finite, and*

(b)

$$\partial^+ G(t_1, E_1; t_2, x_2)/\partial t_2 = -\alpha_*(t_2, x_2) G(t_1, E_1; t_2, x_2) + \int_X G(t_1, E_1; t_2, x')\sigma_*(t_2, x', x_2)\, d\nu(x')\ [\nu].$$

Proof: Let

$$g_n = (g(t_1, \cdot; t_2 + \Delta_n, E_2) - g(t_1, \cdot; t_2, E_2))/\Delta_n .$$

From the proof of Theorem A,

$$g_n(x_1) = \int_X [-\chi_{E_2}\alpha_*(t_2, x_2) + \bar{\sigma}_*(t_2, x_2, E_2)] g(t_1, x_1; t_2, dx_2) + \int_X (o(\Delta_n, x_2)/\Delta_n) g(t_1, x_1; t_2, dx_2)$$

for every positive integer n. For any given $\epsilon > 0$, there exists a positive integer n_0 such that for $n \geqq n_0$

$$\left|g_n(x_1) - \int_X [\ ] g(t_1, x_1; t_2, dx_2)\right| < \epsilon g(t_1, x_1; t_2, X) < \infty$$

for almost every $[\nu]$ $x_1 \varepsilon X$. Let

$$H_n(x_1) = g_n(x_1) - \int_X [\ ] g(t_1, x_1; t_2, dx_2), \qquad n = 1, 2, 3, \cdots .$$

Since each H_n and $g(t_1, \cdot; t_2, X)$ are ν-integrable, and since $H_n \to 0$ a.e. $[\nu]$, we conclude that $H_n \to 0$ in the mean by the Lebesgue bounded convergence theorem. That is, for $E_1 \varepsilon$ S,

$$\int_{E_1} g_n(x_1)\, d\nu(x_1) \to \int_{E_1} \left(\int_X [\ ] g(t_1, x_1; t_2, dx_2)\right) d\nu(x_1),$$

as $n \to \infty$. This limit is finite since $G(t_1, E_1; t_2, \cdot)$ is ν-integrable and the density attenuating functions are essentially bounded $[\nu]$. By (A, §7) we may write for arbitrary $E_2 \varepsilon$ S

$$\int_{E_1} g_n(x_1)\, d\nu(x_1) = \int_{E_2} G_n(x_2)\, d\nu(x_2),$$

where G_n is defined in (iv)R_3 for every positive integer n. By integrating the limit in (b) of Theorem A over $E_1 \varepsilon$ S and applying a Fubini argument, the result may be written as

$$-\int_{E_2} \alpha_*(t_2, x_2) G(t_1, E_1; t_2, x_2)\, d\nu(x_2) + \int_{E_2} \left(\int_X G(t_1, E_1; t_2, x')\sigma_*(t_2, x', x_2)\, d\nu(x')\right) d\nu(x_2) < \infty .$$

Since $\{G_n\}$ is fundamental in measure ((iv)R_3) and since, for every $E_2 \varepsilon$ S, $\{\int_{E_2} G_n \, d\nu\}$ is a fundamental sequence of real numbers, it follows that $\{G_n\}$ is mean fundamental and therefore converges in the mean to a ν-integrable function $G^+ \equiv \partial^+ G(t_1, E_1; t_2, \cdot)/\partial t_2$. (b) now follows by the same arguments as those used to conclude the proof of Theorem B.

16. Restricted Processes on General Carrier Spaces. Let (X, S, ν) be a carrier space. Let $\mathrm{S}_x = \{E : x \varepsilon E \varepsilon \mathrm{S}\}$ for every $x \varepsilon X$. The radiative process $\mathcal{R}_\phi$ is said to be *restricted at* $(t, x) \varepsilon T \times X$ iff $\bar{\sigma}_*(t, x, \cdot)$ is countably additive and $\bar{\sigma}_*(t, x, E') = 0$ for every $E \varepsilon \mathrm{S}_x$, otherwise it is *unrestricted at* (t, x). Since $\bar{\sigma}_*(t, x, E) + \bar{\sigma}_*(t, x, E') = s_*(t, x)$, the above condition may be replaced by $\bar{\sigma}_*(t, x, E) = s_*(t, x)$. $\mathcal{R}_\phi$ is said to be *restricted on* $(t, R) \varepsilon T \times \mathrm{S}$ iff it is restricted at (t, x) for almost every $x \varepsilon R$, otherwise it is *unrestricted on* (t, R).

Theorem A. Retaining the hypothesis of (A, §15), *let* $\mathcal{R}_\phi$ *be restricted on* $(t_2, R) \varepsilon T \times \mathrm{S}$; *then*

$$\partial^+ G(t_1, E_1; t_2, x_2)/\partial t_2 = -(a_*(t_2, x_2) + \chi_{R'}(x_2) s_*(t_2, x_2)) G(t_1, E_1; t_2, x_2) + \int_{R'} G(t_1, E_1; t_2, x') \sigma_*(t_2, x', x_2) \, d\nu(x') \ [\nu].$$

Proof: For every $E_2 \varepsilon$ S, we may write (proof, (C, §15))

$$\int_{E_2} G^+ \, d\nu = -\int_{E_2} \alpha_*(t_2, \cdot) G(t_1, E_1; t_2, \cdot) \, d\nu + \int_X G(t_1, E_1; t_2, \cdot) \bar{\sigma}_*(t_2, \cdot, E_2) \, d\nu < \infty.$$

Partitioning X so that

$$\int_X = \int_{R \cap E_2} + \int_{R \cap E_2'} + \int_{R'}$$

we observe that

$$(i) \quad \int_{E_2 \cap R} G\bar{\sigma}_* \, d\nu = \int_{E_2 \cap R} G s_* \, d\nu;$$

$$(ii) \quad \int_{R \cap E_2'} G\bar{\sigma}_* \, d\nu = 0;$$

$$(iii) \quad \int_{R'} G\bar{\sigma}_* \, d\nu = \int_{E_2} \left(\int_{R'} G\sigma_* \, d\nu \right) d\nu.$$

For (i), by the definition of restrictedness, $\bar{\sigma}_*(t_2, x, E_2) = s_*(t_2, x)$ for almost every $x \varepsilon E_2 \cap R$. For (ii), $\bar{\sigma}_*(t_2, x, E_2) = \bar{\sigma}_*(t_2, x, (E_2')') = 0$ for almost every $x \varepsilon E_2' \cap R$. (iii) follows by a Fubini argument using $\sigma_*(t, \cdot, \cdot)$ and the finiteness of $\int_{R'} G\bar{\sigma}_* \, d\nu$. Hence, for every $E_2 \varepsilon$ S, the integral over X may be written

$$\int_{E_2} \chi_R s_*(t_2\,,\,\cdot)G(t_1\,, E_1\,;\,t_2\,,\,\cdot)\,d\nu \\ + \int_{E_2}\left(\int_{R'} G(t_1\,, E_1\,;\,t_2\,, x')\sigma_*(t_2\,, x',\,\cdot)\,d\nu(x')\right)d\nu.$$

By ([8], p. 105), the identity $1 = \chi_E + \chi_{E'}$, $E \subset X$, and the decomposition of $\alpha_*(t_2\,,\,\cdot)$ given after R_4, the assertion of the theorem follows.

Analogous dynamic transition relations for γ- and g-densities may be derived, but we shall not carry out the details in this study. The G-density has been singled out for specific study mainly for the reasons cited in §9, and results obtained for it will be typical of the results obtainable for the other densities.

Corollary. (a) *If* $\mathcal{R}_\phi$ *is restricted on* $(t_2\,, R)$ *and* $\nu(R) = 0$, *then* ((b)C, §15) *holds.*

(b) *If* $\mathcal{R}_\phi$ *is restricted on* $(t_2\,, X)$, *then*

$$\partial^+ G(t_1\,, E_1\,;\,t_2\,, x_2)/\partial t_2 = -a_*(t_2\,, x_2)G(t_1\,, E_1\,;\,t_2\,, x_2)\ [\nu].$$

17. Restricted Processes on Product Carrier Spaces. Let $(X,\ \mathrm{S},\ \nu)$ be the Cartesian product of two carrier spaces $(X_i\,,\ \mathrm{S}_i\,,\ \nu_i)$, $i = 1, 2$, with M_1 valid on each. $\mathrm{S}_1 \times \mathrm{S}_2$ is the σ-algebra of subsets of $X = X_1 \times X_2$ generated by the class of all sets of the form $A_1 \times A_2\,,\ A_i \,\varepsilon\, \mathrm{S}_i\,,\ i = 1, 2$, which are the *measurable rectangles* in X. In addition, the product measure $\nu = \nu_1 \times \nu_2$ is totally σ-finite ([8], p. 144) with $\nu(X_1 \times X_2) = \nu_1(X_1)\nu_2(X_2) > 0$, so that $(X,\ \mathrm{S},\ \nu)$ is a carrier space. The collections of ν_i-continuous measures on $\mathrm{S}_i\,,\ i = 1, 2$, give rise to ν-continuous product measures on S ([8], p. 144) and the latter can be defined in a natural way so as to satisfy the conditions of M_1. A carrier space $(X,\ \mathrm{S},\ \nu)$ constructed in this way will be called a *product carrier space* and each coordinate space of $(X,\ \mathrm{S},\ \nu)$ a *coordinate carrier space.* It is clear that product carrier spaces can be compounded of an arbitrary finite number of coordinate carrier spaces to form finite dimensional carrier spaces of dimension greater than 2 with M_1 valid on the product.

Let $\mathcal{R}_\phi$ be a radiative process on the product carrier space $(X,\ \mathrm{S},\ \nu) = (X_1 \times X_2\,,\ \mathrm{S}_1 \times \mathrm{S}_2\,,\ \nu_1 \times \nu_2)$. The process $\mathcal{R}_\phi$ is said to be X_1*-restricted at* $(t,\ (x_1\,, x_2)) \,\varepsilon\, T \times X$ iff $\bar{\sigma}_*(t, x,\ \cdot)$ is countably additive and $\bar{\sigma}_*(t, x, E_1' \times E_2) = 0$ for every measurable rectangle $E_1 \times E_2 \,\varepsilon\, \mathrm{S}_x$, where $x = (x_1\,, x_2) \,\varepsilon\, X_1 \times X_2$. The process $\mathcal{R}_\phi$ is said to be X_2*-restricted at* $(t,\ (x_1\,, x_2)) \,\varepsilon\, T \times X$ iff $\bar{\sigma}_*(t, x,\ \cdot)$ is countably additive and $\bar{\sigma}_*(t, x, E_1 \times E_2') = 0$ for every measurable rectangle $E_1 \times E_2 \,\varepsilon\, \mathrm{S}_x$. $\mathcal{R}_\phi$ on X is X_i*-restricted on* $(t, R) \,\varepsilon\, T \times \mathrm{S}$ iff it is X_i-restricted at (t, x) for almost every $[\nu]\ x \,\varepsilon\, R$, $i = 1, 2$. The concepts on X_i-restrictedness of $\mathcal{R}_\phi$ on the coordinate carrier spaces are sufficient—when taken together—to characterize the concept of restrictedness of $\mathcal{R}_\phi$ on the product carrier space, as is proved in the following theorem.

Theorem A. *Let* $(X,\ \mathrm{S},\ \nu) = (X_1 \times X_2\,,\ \mathrm{S}_1 \times \mathrm{S}_2\,,\ \nu_1 \times \nu_2)$ *be a product carrier space with radiative process* $\mathcal{R}_\phi$. *Then the following two conditions are equivalent:*

(a) *$\mathcal{R}_\phi$ is restricted at $(t, x) \varepsilon T \times X$.*
(b) *$\mathcal{R}_\phi$ is both X_1-restricted and X_2-restricted at $(t, x) \varepsilon T \times X$.*

Proof: (a) $\Rightarrow$ (b). Only X_1-restrictedness will be demonstrated, the proof of X_2-restrictedness is similar. If $A \varepsilon \mathbf{S}_{x_1}$, $B \varepsilon \mathbf{S}_{x_2}$, $x = (x_1, x_2) \varepsilon X_1 \times X_2$, then $A \times B \varepsilon \mathbf{S}_x$, and the measurable set $(A \times B)' \supset A' \times B \varepsilon \mathbf{S}$. Hence

$$0 = \bar{\sigma}_*(t, x, (A \times B)') \geqq \bar{\sigma}_*(t, x, A' \times B) \geqq 0.$$

(b) $\Rightarrow$ (a). For any $x \varepsilon X$, $\mathbf{S}$ may be partitioned into $\mathbf{S}_x$ and its complement $\mathbf{S}_x'$, where $\mathbf{S}_x = \{E : x \varepsilon E \varepsilon \mathbf{S}\}$. Define

$$\mathbf{R}_x = \{E : E \varepsilon \mathbf{S}_x, \bar{\sigma}_*(t, x, E') = 0\}$$

and

$$\mathbf{T}_x = \{E : E \varepsilon \mathbf{S}_x', \bar{\sigma}_*(t, x, E) = 0\}.$$

Clearly $\mathbf{R}_x \subset \mathbf{S}_x$, $\mathbf{T}_x \subset \mathbf{S}_x'$, and $\mathbf{R}_x \cap \mathbf{T}_x = 0 \varepsilon \mathbf{S}$. The implication (b) $\Rightarrow$ (a) will be proved if the following three statements are shown to be true:

(i) $\mathbf{R}_x \cup \mathbf{T}_x$ contains all measurable rectangles in $\mathbf{S}$.
(ii) $\mathbf{R}_x \cup \mathbf{T}_x$ is a σ-algebra.
(iii) $\mathbf{R}_x \cup \mathbf{T}_x = \mathbf{S}$ iff $\mathcal{R}_\phi$ is restricted at (t, x).

By (i) and (ii), since $\mathbf{S}$ is by definition the smallest σ-algebra containing all measurable rectangles, the union of classes in (i) must contain $\mathbf{S}$, so that $\mathbf{R}_x \cup \mathbf{T}_x = \mathbf{S}$. (iii) would then complete the proof.

Proof of (i). First, if $A \times B \varepsilon \mathbf{S}_x$, $A \varepsilon \mathbf{S}_{x_1}$, $B \varepsilon \mathbf{S}_{x_2}$, then, since $(A \times B)' \subset (A' \times X_2) \cup (X_1 \times B')$,

$$0 \leqq \bar{\sigma}_*(t, x, (A \times B)') \leqq \bar{\sigma}_*(t, x, A' \times X_2) + \bar{\sigma}_*(t, x, X_1 \times B').$$

Each summand, by hypothesis (b), is zero, so that $A \times B \varepsilon \mathbf{R}_x$. Second, if $A \times B \varepsilon \mathbf{S}_x'$, then, $\{(A' \times B), (A \times B'), (A' \times B')\}$ being a partition of $(A \times B)' \varepsilon \mathbf{S}_x$, precisely one of the following three statements must hold: $A' \times B \varepsilon \mathbf{S}_x$, $A \times B' \varepsilon \mathbf{S}_x$, $A' \times B' \varepsilon \mathbf{S}_x$. If $A' \times B \varepsilon \mathbf{S}_x$, then, since $A \times B = (A')' \times B$, by the X_1-restrictedness of $\mathcal{R}_\phi$ at (t, x), $\bar{\sigma}_*(t, x, A \times B) = \bar{\sigma}_*(t, x, (A')' \times B) = 0$. If, on the other hand, $A \times B' \varepsilon \mathbf{S}_x$, $\bar{\sigma}_*(t, x, A \times B) = \bar{\sigma}_*(t, x, A \times (B')') = 0$ by the X_2-restrictedness of $\mathcal{R}_\phi$ at (t, x). Finally, if $A' \times B' \varepsilon \mathbf{S}_x$, then $(A' \times B')' \supset A \times B$, but by the first step above we conclude that $A' \times B' \varepsilon \mathbf{R}_x$. The monotonicity of $\bar{\sigma}_*(t, x, \cdot)$ then implies $\bar{\sigma}_*(t, x, A \times B) = 0$. In each case it follows that $A \times B \varepsilon \mathbf{T}_x$.

Proof of (ii). Clearly $X \varepsilon \mathbf{R}_x$, so that $\mathbf{R}_x \cup \mathbf{T}_x$ is not empty. If $E \varepsilon \mathbf{R}_x \cup \mathbf{T}_x$, and, in particular, $E \varepsilon \mathbf{R}_x$, then $E' \varepsilon \mathbf{S}_x'$ and $\bar{\sigma}_*(t, x, E') = 0$; hence $E' \varepsilon \mathbf{T}_x$. On the other hand, if $E \varepsilon \mathbf{T}_x$, then $E' \varepsilon \mathbf{S}_x$ and $\bar{\sigma}_*(t, x, (E')') = \bar{\sigma}_*(t, x, E) = 0$, so that $E' \varepsilon \mathbf{R}_x$. Thus we have shown that $\mathbf{R}_x \cup \mathbf{T}_x$ is closed under the operation of complementation. It remains to show that $\mathbf{R}_x \cup \mathbf{T}_x$ is closed under the operation of countable union. Since $0 \varepsilon \mathbf{T}_x$, we consider a non-empty countable subset

$\mathbf{Q}$ of $\mathbf{R}_x \cup \mathbf{T}_x$. $\{\mathbf{Q} \cap \mathbf{R}_x , \mathbf{Q} \cap \mathbf{T}_x\}$ is (in the extended sense) a partition of $\mathbf{Q}$. If $\mathbf{Q} \cap \mathbf{R}_x$ is not empty then $\bigcup (\mathbf{Q} \cap \mathbf{R}_x) \varepsilon \mathrm{S}_x$ and, since $(\bigcup (\mathbf{Q} \cap \mathbf{R}_x))' < Q_n'$ for some $Q_n \varepsilon \mathbf{Q} \cup \mathbf{R}_x$, we have

$$0 \leqq \bar{\sigma}_*(t, x, (\bigcup(\mathbf{Q} \cap \mathbf{R}_x))') \leqq \bar{\sigma}_*(t, x, Q_n') = 0,$$

so that $\cup(\mathbf{Q} \cap \mathbf{R}_x) \varepsilon \mathbf{R}_x$. If $\mathbf{Q} \cap \mathbf{R}_x$ is empty, $\mathbf{Q} \cap \mathbf{T}_x$ is not empty, and $\cup(\mathbf{Q} \cap \mathbf{T}_x)$ is an element of $\mathbf{S}_x'$. Further,

$$0 \leqq \bar{\sigma}_*(t, x, \bigcup(\mathbf{Q} \cap \mathbf{T}_x)) \leqq \Sigma_n \bar{\sigma}_*(t, x, Q_n) = 0,$$

where the summation is over all $Q_n \varepsilon \mathbf{Q} \cap \mathbf{T}_x$. Hence $\bigcup(\mathbf{Q} \cap \mathbf{T}_x) \varepsilon \mathbf{T}_x$. Thus, in any case,

$$\bigcup \mathbf{Q} = \bigcup(\mathbf{Q} \cap \mathbf{R}_x) \cup \bigcup(\mathbf{Q} \cap \mathbf{T}_x) \varepsilon \mathbf{R}_x \cup \mathbf{T}_x .$$

Proof of (iii). If $\mathcal{R}_\phi$ is restricted at (t, x), then, for every $E \varepsilon \mathrm{S}_x$, $\bar{\sigma}_*(t, x, E') = 0$, so that $\mathrm{S}_x \subset \mathbf{R}_x$. Hence $\mathrm{S}_x = \mathbf{R}_x$. Further, if $E \varepsilon \mathrm{S}_x'$, $E' \varepsilon \mathrm{S}_x$, so that $\bar{\sigma}_*(t, x, (E')') = 0$; thus $\mathrm{S}_x' \subset \mathbf{T}_x$. Hence $\mathrm{S}_x' = \mathbf{T}_x$. It follows that $\mathbf{R}_x \cup \mathbf{T}_x = \mathrm{S}$. Conversely, if $\mathbf{R}_x \cup \mathbf{T}_x = \mathrm{S} = \mathrm{S}_x \cup \mathrm{S}_x'$, then, in particular, $\mathbf{R}_x = \mathrm{S}_x$ which, by the definition, implies $\mathcal{R}_\phi$ is restricted at (t, x). This completes the proof of the theorem.

Let us say that a measurable space (X, S) is *discrete on* $Y \subset X$ iff $\{y\} \varepsilon \mathrm{S}$ for every $y \varepsilon Y$; and that (X, S) is *discrete* iff (X, S) is discrete on X. (b) of Theorem A cannot in general be weakened to have, say, X_1-restrictedness at (t, x) imply $\mathcal{R}_\phi$ restricted at (t, x). Since the definition of the three types of restrictedness are purely measure-theoretical and independent of the origin of the measure $\bar{\sigma}_*(t, x, \cdot)$, the following example will illustrate this fact.

Let $(X, \mathrm{S}) = (X_1 \times X_2 , \mathrm{S}_1 \times \mathrm{S}_2)$ be a measurable space formed from the discrete measurable spaces (X_1 , S_1) and (X_2 , S_2) such that $X_1 = \{x_{11} , x_{12} , x_{13}\}$, $X_2 = \{x_{21} , x_{22} , x_{23}\}$. For the point (x_{12} , x_{21}), let $\bar{\sigma}_*((x_{12} , x_{21}), \cdot)$ be an additive set function on $\mathrm{S}_1 \times \mathrm{S}_2$ such that

$$\bar{\sigma}_*((x_{12} , x_{21}), \{x_{1i}\} \times \{x_{2j}\}) = \begin{cases} 0 \begin{cases} i = 1, 3 \\ j = 1, 2, 3 \end{cases} \\ 1 \begin{cases} i = 2 \\ j = 1, 2, 3. \end{cases} \end{cases}$$

$\bar{\sigma}_*((x_{12} , x_{21}), \cdot)$ defined in this way is additive on S and satisfies the measure-theoretic requirements of the definition of X_1-restrictedness at (x_{12} , x_{21}) but not those of X_2-restrictedness or restrictedness at the given point.

An important two-way tie exists between the concept of restrictedness of $\mathcal{R}_\phi$ at (t, x) and the vanishing of $\sigma_*(t, x, \cdot)$ for carrier spaces which are discrete on $\{x\} \subset X$. This is given in the following theorem.

Theorem B. *If the carrier space (X, S, ν) is discrete on $\{x\} \subset X$ and $\nu(\{x\}) = 0$, then $\mathcal{R}_\phi$ is restricted at $(t, x) \varepsilon T \times X$ if and only if $\sigma_*(t, x, \cdot)$ vanishes a.e. $[\nu]$.*

Proof: If $\mathcal{R}_*$ is restricted at (t, x), then

$$\bar{\sigma}_*(t, x, X) = \bar{\sigma}_*(t, x, X - \{x\}) + \bar{\sigma}_*(t, x, X \cap \{x\})$$

so that, by hypothesis, the first and second summands vanish. Thus the R-N derivative $\sigma_*(t, x, \cdot)$ of $\bar{\sigma}_*(t, x, \cdot)$ must vanish a.e. $[\nu]$ ([8], p. 104). Conversely, if $E \,\varepsilon\, \mathrm{S}_x$, then in general $\bar{\sigma}_*(t, x, \cdot) = \int \sigma_*(t, x, \cdot)\, d\nu$ is countably additive, and, in particular, $\bar{\sigma}_*(t, x, E') = \int_{E'} \sigma_*(t, x, \cdot)\, d\nu = 0$. This completes the proof.

Observe that the "if" statement of the preceding theorem is valid without the two special provisos on the structure of the carrier space.

Product carrier spaces with variously restricted radiative processes, while still rather abstract, already possess features which allow the resulting dynamic relations for G-densities to be nearly indistinguishable (in form) from the classical equations of transfer. The groundwork will now be prepared for the theorem which is a precise statement of this assertion. This theorem will represent the culmination of the present study of radiative processes.

Lemma. *Let* $(X, \mathrm{S}, \nu) = (X_1 \times X_2, \mathrm{S}_1 \times \mathrm{S}_2, \nu_1 \times \nu_2)$ *be a product carrier space.*

(a) *If* $\mathcal{R}_\phi$ *is* X_1*-restricted on* $(t, R_1) \,\varepsilon\, T \times \mathrm{S}$, *then*

$$\bar{\sigma}_*(t, \cdot, A \times B) = \chi_{A \times X_2} \bar{\sigma}_*(t, \cdot, X_1 \times B)\ [\nu]$$

on R_1 *for every measurable rectangle* $A \times B \,\varepsilon\, \mathrm{S}$.

(b) *If* $\mathcal{R}_\phi$ *is* X_2*-restricted on* $(t, R_2) \,\varepsilon\, T \times \mathrm{S}$, *then*

$$\bar{\sigma}_*(t, \cdot, A \times B) = \chi_{X_1 \times B} \bar{\sigma}_*(t, \cdot, A \times X_2)\ [\nu]$$

on R_2 *for every measurable rectangle* $A \times B \,\varepsilon\, \mathrm{S}$.

Proof: Only (a) will be proved; the proof of (b) is similar. For every $A \times B \,\varepsilon\, \mathrm{S}$,

$$\bar{\sigma}_*(t, \cdot, A \times B) + \bar{\sigma}_*(t, \cdot, A' \times B) = \bar{\sigma}_*(t, \cdot, X_1 \times B)\ [\nu].$$

If $x \,\varepsilon\, (A \times X_2) \cap R_1$, then $\bar{\sigma}_*(t, x, A' \times B) = 0$. If $x \,\varepsilon\, (A \times X_2)' \cap R_1 = (A' \times X_2) \cap R_1$, then

$$\bar{\sigma}_*(t, x, (A')' \times B) = 0 = \chi_{A \times X_2}(x) \bar{\sigma}_*(t, x, X_1 \times B).$$

This completes the proof of (a).

The density scattering function was defined earlier (§14) by the relation $\int_E \sigma_*(t, x, \cdot)\, d\nu = \bar{\sigma}_*(t, x, E) < \infty$, $E \,\varepsilon\, \mathrm{S}$. If $X = X_1 \times X_2$ is a product carrier space, then, for each $t \,\varepsilon\, T$, $\sigma_*(t, \cdot, \cdot)$ has as its domain $X \times X = (X_1 \times X_2) \times (X_1 \times X_2)$. We will have occasion to work with certain iterated integrals of the multiple integral $\int_E \sigma_*(t, x, \cdot)\, d\nu$. If $E = A_1 \times X_2$,

$$\int_{A_1 \times X_2} \sigma_*(t, (x_1, x_2), (x_1', x_2'))\, d\nu((x_1', x_2'))$$

$$= \int_{A_1} d\nu_1(x_1') \int_{X_2} \sigma_*(t, (x_1, x_2), (x_1', x_2'))\, d\nu_2(x_2'),$$

and we will write $\sigma_*(t, (x_1, x_2), (\cdot, *))$ for the ν_1-integrable function

$$\int_{X_2} \sigma_*(t, (x_1, x_2), (\cdot, x_2')) \, d\nu_2(x_2').$$

If $E = X_1 \times A_2$, we will write $\sigma_*(t, (x_1, x_2), (*, \cdot))$ for the ν_2-integrable function

$$\int_{X_1} \sigma_*(t, (x_1, x_2), (x_1', \cdot)) \, d\nu_1(x_1').$$

Clearly

$$\begin{aligned} \int_{X_1} \sigma_*(t, (x_1, x_2), (\cdot, *)) \, d\nu_1 &= \int_{X_2} \sigma_*(t, (x_1, x_2), (*, \cdot)) \, d\nu_2 \\ &= s_*(t, (x_1, x_2)) \; [\nu]. \end{aligned}$$

Theorem C. *Retaining the hypothesis of* (A, §15), *Let* $(X, \mathrm{S}, \nu) = (X_1 \times X_2, \mathrm{S}_1 \times \mathrm{S}_2, \nu_1 \times \nu_2)$ *be a product carrier space. If a radiative process* $\mathfrak{R}_\phi$ *on* (X, S, ν) *is* X_1*-restricted on* $(t_2, R_1) \varepsilon T \times \mathrm{S}$ *and* X_2*-restricted on* $(t_2, R_2) \varepsilon T \times \mathrm{S}$, *then, for almost every* $[\nu]$ $(x_1, x_2) \varepsilon X_1 \times X_2$,

$$\boxed{\begin{aligned} &\partial^+ G(t_1, E_1; t_2, (x_1, x_2))/\partial t_2 = -(a_*(t_2, (x_1, x_2)) \\ &\quad + \chi_{(R_1 \cap R_2)'}((x_1, x_2)) s_*(t_2, (x_1, x_2))) G(t_1, E_1; t_2, (x_1, x_2)) \\ &\quad + \int_{X_2} \chi_{R_1 \cap R_2'}((x_1, x_2')) G(t_1, E_1; t_2, (x_1, x_2')) \sigma_*(t_2, (x_1, x_2'), (*, x_2)) \, d\nu_2(x_2') \\ &\quad + \int_{X_1} \chi_{R_1' \cap R_2}((x_1', x_2)) G(t_1, E_1; t_2, (x_1', x_2)) \sigma_*(t_2, (x_1', x_2), (x_1, *)) \, d\nu_1(x_1') \\ &\quad + \int_{(R_1 \cup R_2)'} G(t_1, E_1; t_2, (x_1', x_2')) \sigma_*(t_2, (x_1', x_2'), (x_1, x_2)) \, d\nu((x_1', x_2')). \end{aligned}}$$

Proof: From the proof of (C, §15), for every measurable rectangle

$$\begin{aligned} A_1 \times A_2 \varepsilon \mathrm{S}, \int_{A_1 \times A_2} G^+ \, d\nu = -\int_{A_1 \times A_2} \alpha_*(t_2, \cdot) G \, d\nu \\ + \int_{X_1 \times X_2} G \bar{\sigma}_*(t_2, \cdot, A_1 \times A_2) \, d\nu < \infty, \end{aligned}$$

where G is an abbreviation of $G(t_1, E_1; t_2, \cdot)$.

$$\{(R_1 \cap R_2), (R_1 \cap R_2'), (R_1' \cap R_2), (R_1 \cup R_2)'\}$$

is a partition of X. We examine each of the integrals over the first three elements of the partition. First,

$$\int_{R_1 \cap R_2} G \bar{\sigma}_*(t_2, \cdot, A_1 \times A_2) \, d\nu = \int_{A_1 \times A_2} \chi_{R_1 \cap R_2} G s_*(t_2, \cdot) \, d\nu$$

by applications of (a) and (b) of the preceding lemma and the relation $\bar{\sigma}_*(t_2, \cdot, X) = s_*(t_2, \cdot)$ $[\nu]$. Second

$$\infty > \int_{R_1 \cap R_2'} G\bar{\sigma}_* \, d\nu = \int_{A_1 \times X_2} \chi_{R_1 \cap R_2'} G\bar{\sigma}_* \, d\nu$$

$$= \int_{A_1 \times A_2} \left\{ \int_{X_2} \chi_{R_1 \cap R_2'}((x_1, x_2)) G(t_1, E_1; t_2, (x_1, x_2)) \right.$$

$$\left. \cdot \left[\int_{X_1} \sigma_*(t_2, (x_1, x_2), (x_1', x_2')) \, d\nu_1(x_1') \right] d\nu_2(x_2) \right\} d\nu_1(x_1) \, d\nu_2(x_2')$$

$$= \int_{A_1 \times A_2} \left\{ \int_{X_2} \chi_{R_1 \cap R_2'}((x_1, x_2')) G(t_1, E_1; t_2, (x_1, x_2')) \right.$$

$$\left. \cdot \sigma_*(t_2, (x_1, x_2'), (*, x_2)) \, d\nu_2(x_2') \right\} d\nu((x_1, x_2)).$$

The first equality above is obtained by using (a) of the preceding lemma; the second equality by a Fubini argument; the third by using the definition of $\sigma_*(t_2, (x_1, x_2), (*, x_2))$ and a change of dummy variable notation. Finally,

$$\infty > \int_{R_1' \cap R_2} G\bar{\sigma}_* \, d\nu = \int_{A_1 \times A_2} \left\{ \int_{X_1} \chi_{R_1' \cap R_2}((x_1', x_2)) G(t_1, E_1; t_2, (x_1', x_2)) \right.$$

$$\left. \cdot \sigma_*(t_2, (x_1', x_2), (x_1, *)) \, d\nu_1(x_1') \right\} d\nu((x_1, x_2)),$$

by an argument similar to that applied to the integral over $R_1 \cap R_2'$.

We observe that the integral over the fourth partition element can be cast into an iterated integral of the same general form as those over the second and third partition elements using a simple Fubini argument. We have shown that the integrated form (over $A_1 \times A_2$) of the relation given in the conclusion of the theorem's statement holds for every measurable rectangle in S. However, the non-empty subset $S_0 \subset S$ on which the ν-integrated relation holds is a σ-ring (an indefinite integral of an integrable function is countably additive) which must then contain the σ-ring generated by the measurable rectangles. An application of ([8], p. 105) completes the proof of the theorem.

If a radiative process $\mathcal{R}_\phi$ on $(X, S, \nu) = (X_1 \times X_2, S_1 \times S_2, \nu_1 \times \nu_2)$ is X_1-restricted on (t, X) and X_2-restricted on $(t, N) \in T \times S$ where $\nu(N) = 0$, then we will say that $\mathcal{R}_\phi$ is *1-factored on* (t, X) A similar definition may be made for a process $\mathcal{R}_\phi$ which is *2-factored on* (t, X). By (A, §17) and the subsequent discussion, an i-factored process ($i = 1$ or 2) $\mathcal{R}_\phi$ is in general unrestricted on (t, X). As an immediate consequence of the preceding theorem we have the important

Corollary. *If a radiative process* $\mathcal{R}_\phi$ *on the product carrier space is 1-factored, then*

$$\boxed{\begin{aligned} &\partial^+ G(t_1, E_1; t_2, (x_1, x_2))/\partial t_2 = -\alpha_*(t_2, (x_1, x_2))G(t_1, E_1; t_2, (x_1, x_2)) \\ &\qquad\qquad\qquad \int_{X_2} G(t_1, E_1; t_2, (x_1, x_2'))\sigma_*(t_2, (x_1, x_2'), (*, x_2))\, d\nu_2(x_2') \ [\nu]. \end{aligned}}$$

A similar expression holds for the case when $\mathcal{R}_\phi$ is 2-factored. i-factored radiative processes are the abstract generalizations of the classical radiative processes. We observe that if, in the preceding theorem, $R_1 = R_2$ $[\nu]$, then the conclusion reduces to that of (A, §16).

III. Radiative Transfer Processes

18. Transfer Process Axiom. This chapter is devoted to the introduction of the last important structure axiom. This axiom will be used in conjunction with the radiative process axiom to define what we will call call the radiative transfer process. The radiative transfer process will be shown to possess sufficient structure to yield a measure-theoretic foundation for the resulting classes of attenuating functions, and finally we show that the radiative transfer process on an abstract carrier space yields the desired generalization of the classical equation of transfer.

The transfer process axiom is an assertion about the existence of a set of measure preserving transformations with domain and range on the carrier space. The initial motivation for this axiom has been sketched in [17]. By way of introduction here we will show that the radiative processes of the preceding chapter possess features resembling some of those of a transfer process but fail to have all of the requisite structure to carry the present study to its proposed goal.

As shall be shown below, to complete the present study we require a certain set of one to one transformations T from $(X, \mathbf{S}, \nu)$ onto $(X, \mathbf{S}, \nu)$ such that T and T^{-1} are measurable transformations which preserve ν-measure. Do the elements of $\mathcal{R}_\phi$ have this property? Strictly speaking, no, for the domain of the elements of $\mathcal{R}_\phi$ is $\mathfrak{M}_\nu$. Yet the elements of $\mathcal{R}_\phi$ can be made to assign certain elements of $\mathbf{S}$ to other elements of $\mathbf{S}$ in the following way: Let E be a maximal full support for $\mu \varepsilon \mathfrak{M}_{\nu, t_1}$, hence E is determined uniquely up to a set of ν-measure zero. It is easy to show that, by (i)R_3, there exists a t_2 in T such that $t_2 > t_1$ and that $\mu R_{t_1, t_2} \varepsilon \mathfrak{M}_{\nu, t_2}$ is supported by X. Hence there exists a unique $[\nu]$ maximal full support F for $\mu R_{t_1, t_2}$. We may then say that, in this way, F is assigned to E by the element $R_{t_1, t_2} \varepsilon \mathcal{R}_\phi$. Conversely, if F is a maximal full support for $\mu_2 \varepsilon \mathfrak{M}_{\nu, t_2}$ such that $\mu_2 = \mu_1 R_{t_1, t_2}$, $\mu_1 \varepsilon \mathfrak{M}_{\nu, t_1}$, $(t_1, t_2) \varepsilon D$, then, since the elements of $\mathcal{R}_\phi$ are linear transformations on the non-negative cone $\mathfrak{M}_\nu$ of radiative measures, X must support μ_1, from which we deduce the existence of a unique $[\nu]$ maximal full support E for μ_1. Again, E is assigned to F by means of an element $R_{t_1, t_2} \varepsilon \mathcal{R}_\phi$. Since the important elements of $\mathbf{S}$ in this work are precisely those which fully support radiative measures, $\mathcal{R}_\phi$ can indeed supply a set of one to one transformations from the σ-algebra $\mathrm{S}(\nu)$ onto itself ([8], p. 167). If the carrier space is discrete (§17), the elements of $\mathcal{R}_\phi$ may then—in the above sense—have domain and range on X. However, for discrete spaces such that the singletons are assigned zero measure by ν (as is the state of affairs in the classical carrier space) there no longer is possible a unique assignation between $\{x\} = E \in \mathrm{S}$ and $\{y\} = F \in \mathrm{S}$ by means of the elements of $\mathcal{R}_\phi$, because singletons in this case cannot support radiative measures.

An examination of the source cited in the discussion in ([17], p. 13) would show that the idea of a radiative process (as summarized in R_1) has been abstracted from the linear properties of (and linear operations on) the classicial i.d.e. for specific intensity. The latter, however, is customarily derived with implicit help from the theory of geometrical optics which supplies the natural paths (rays) for photons in a transparent optical medium. It follows that radiative processes must have this geometrical feature packed away deep in their innards. The discussion in the preceding paragraph indicates that the classical radiative process has been abstracted to such an extent that this specific feature has been inextricably snarled up in the other properties of the elements of $\mathcal{R}_\phi$. In this light, it is then remarkable that the abstract radiative process was still sufficiently detailed to allow the development of its theory up to (C, §17) and its corollary.

With these remarks in mind, we add to the preceding three structure axioms, C_1, M_1, and R_1, the fourth and final structure axiom T_1. Let (X, S, ν) be a carrier space. Let $\mathfrak{T}$ be the (non-empty) set of all measure preserving transformations T from (X, S, ν) onto (X, S, ν). We will use the notation $T(x)$ and $T(A)$ to designate the images under $T \in \mathfrak{T}$ of $x \in X$ and $A \subset X$, respectively. I_x will denote the identity element in $\mathfrak{T}$. Henceforth, the unadorned symbol T will retain the meaning given it in §2.

T_1 : *There exists a transformation* ψ *from* D *into* $\mathfrak{T}$ *such that* $\psi(D) \equiv \mathfrak{T}_\psi$ *has the following properties. Let* $\psi[(t_1, t_2)] \equiv T_{t_1,t_2}$, $(t_1, t_2) \in D$; *then*

(i) *If* t_1, t_2, t_3 *are elements of* T *and if* $t_1 \leqq t_2 \leqq t_3$, *then* $T_{t_1,t_3} = T_{t_2,t_3} T_{t_1,t_2}$.

(ii) *For every* $t \in T$, $T_{t,t} = I_\psi$.

The set $\mathfrak{T}_\psi$ of measure preserving transformations will be called the *transfer process on the carrier space* (X, S, ν).

19. Radiative Transfer Processes. The pair $(\mathcal{R}_\phi, \mathfrak{T}_\psi)$ will be called the *radiative transfer process on the carrier space* (X, S, ν).[1] The axioms C_1, M_1, R_1, and T_1 are the *structure axioms* for the radiative transfer process. The elements of $\mathfrak{T}_\psi$ assign a function f to every function g on X; f is defined by $f(x) = g(T_0(x))$, $x \in X$, $T_0 \in \mathfrak{T}_\psi$. We will designate this correspondence in the usual way: $f = gT_0$. Similarly, the elements of $\mathfrak{T}_\psi$ assign a radiative measure m to every radiative measure $\mu \in \mathfrak{M}_\nu$; m is defined by $m(E) = \mu(T_0(E))$, $E \in \mathrm{S}$, and we will designate this correspondence by $m = \mu T_0$. The measure preserving character of the transformations is clearly needed in the latter correspondence; and the measurable character of the transformations is needed in the former correspondence in order to assure that the images of measurable functions on the carrier space are again measurable ([8], p. 162). If $\mu \varepsilon \mathfrak{M}_{\nu,t}$, $(t, t') \varepsilon D$, consider the radiative measure $\mu R_{t,t'} T_{t,t'} \varepsilon \mathfrak{M}_{\nu,t'}$ ((ii)M_1). The radiant energy $\mu R_{t,t'} T_{t,t'}(E)$ will be called the *residue at t' of $\mu(E)$*, $E \varepsilon$ S. This is a precise generalization of the notion of the Lagrangian residue of an ensemble of photons (*cf.* ([11], p. 4)). As an important example, consider $\mu \varepsilon \mathfrak{M}_{\nu,t_1}$, $E_1 \varepsilon$ S, $(t_1, t_2) \varepsilon D$, and $\Delta \varepsilon T$. Then $\bar{\mu}_{E_1} R_{t_1,t_2+\Delta} T_{t_2,t_2+\Delta} \varepsilon \mathfrak{M}_{\nu,t_2+\Delta}$. Using (ii)$R_1$, we see that the radiant energy $\bar{\mu}(t_1, E_1; t_2 + \Delta, T_{t_2,t_2+\Delta}(E_2))$ is the residue at $t_2 + \Delta$ of $\bar{\mu}(t_1, E_1; t_2, E_2)$. Further, if $G(t_1, E_1; t_2 + \Delta, \cdot)$ is the general radiant density function associated with $\bar{\mu}(t_1, E_1; t_2 + \Delta, \cdot)$, the radiant density

---

[1] Once RT_3 and RT_4 have been formulated, it will be understood that the pair $(\mathcal{R}_\phi, \mathfrak{T}_\psi)$ satisfies the requirements of all the appropriate axioms (see the diagram below).

$$[G(t_1, E_1; t_2 + \Delta, \cdot) T_{t_2,t_2+\Delta}](x) = G(t_1, E_1; t_2 + \Delta, T_{t_2,t_2+\Delta}(x))$$

will be called the *residue at $t_2 + \Delta$ of $G(t_1, E_1; t_2, x)$*, $x \varepsilon X$. Of course, this definition can be phrased generally as was done above for the case of μ. As should be expected, the following relation

$$\int_{E_2} [G(t_1, E_1; t_2 + \Delta, \cdot) T_{t_2,t_2+\Delta}]\, d\nu = (\bar{\mu}(t_1, E_1; t_2 + \Delta, \cdot) T_{t_2,t_2+\Delta})(E_2)$$

holds between the two residues. That this is true may be shown by using the measure preserving properties of the transformations $T_{t_2,t_2+\Delta}$, ([8], p. 163), and (A, §5). A similar discussion can be made for the γ-density $\gamma(t_1, x_1; t_2 + \Delta, \cdot)$.

20. Regularity Axioms for Radiative Transfer Processes. Consequences. The transfer process axiom may take its place, in the order of axioms, between R_1 and R_2. From this point on, a theory of radiative *transfer* processes may be developed along lines which very closely parallel those followed to develop the radiative process theory in Chapter II. An examination of the three regularity axioms R_2, R_3, and R_4 will show that: (a) R_2 need not be changed; (b) R_3 needs to be superficially modified to a form which makes use of the $\mathfrak{I}_\nu$-transforms of the various functions involved; (c) R_4 requires only token notational changes to be converted into a radiative transfer context. The burden of the conversion from radiative processes to radiative transfer processes is then placed on R_3 which we now modify.

RT_3: *Let $(t_1; t_2)$, $(t_2, t_3) \varepsilon D$, $\mu \varepsilon \mathfrak{M}_{\nu,t_1}$, and E_1, $E_3 \varepsilon$ S. If X supports $\mu' = \mu_{E_1} R_{t_1,t_2}$, let F denote the maximal full support for μ'. If $g'(t_2, \cdot; t_3, T_{t_2,t_3}(E_3))$ is the g-density with respect to μ' of $\overline{\mu}'(t_2, \cdot; t_3, T_{t_2,t_3}(E_3))$ and $\{\Delta_n\}$ is any decreasing null sequence of positive elements in T, then:*

(i) *The sequence*

$$\{h'_{0n}(t_2, \cdot, E_3)\} = \{(\chi_{E_3 \cap F} - g'(t_2, \cdot; t_2 + \Delta_n, T_{t_2,t_2+\Delta_n}(E_3)))/\Delta_n\}$$

converges uniformly on X to a unique $[\nu]$ essentially bounded function $h'_0(t_2, \cdot, E_3)$.

(ii) *The corresponding function* $h_0'(t_2, x_2, \cdot)$ *is countably additive on* **S** *for almost every* $[\nu]$ $x_2 \in X$.

(iii) $\{\gamma_n\} = \{(\gamma(t_1, x_1; t_2 + \Delta_n, \cdot)T_{t_2, t_2+\Delta_n} - \gamma(t_1, x_1; t_2, \cdot))/\Delta_n\}$ *is fundamental in measure for almost every* $[\nu]$ $x_1 \in X$.

(iv) $\{G_n\} = \{(G(t_1, E_1; t_2 + \Delta_n, \cdot)T_{t_2, t_2+\Delta_n} - G(t_1, E_1; t_2, \cdot))/\Delta_n\}$ *is fundamental in measure.*

To distinguish the new families of measure attenuating functions arising from RT_3, we replace the earlier asterisk subscript by the circle subscript. It follows that each theorem and definition between R_3 and R_1 has a precisely determinable analog which differs from the original by trivial changes in notation (asterisk to circle; E to $T_\circ(E)$; $\mathcal{R}_\phi$ references to $(\mathcal{R}_\phi, \mathfrak{I}_\psi)$ references). The μ'differentiability Axiom R_4 is now asserted for the density attenuating functions of the radiative *transfer* process and is assigned the signature RT_4; nothing is changed from the original except the obvious conversions from asterisk subscripts to circle subscripts and $\mathcal{R}_\phi$ references to $(\mathcal{R}_\phi, \mathfrak{I}_\psi)$ references. Again, it follows that each theorem following R_4 has an analog for the radiative transfer process. It is asserted that "nothing is changed" in this conversion from $\mathcal{R}_\phi$ to $(\mathcal{R}_\phi, \mathfrak{I}_\psi)$. Of course this phrase refers to the mathematical content of the definitions and theorems concerned. The physical consequences—with one notable exception—are profoundly altered: the $(\mathcal{R}_\phi, \mathfrak{I}_\psi)$ analogs of the theorems (A, §12), (A, §15), (B, §15), (C, §15), (A, §16), and (C, §17) now involve total (right hand) derivatives with respect to the time t_2, yielding the desired generalization of the classicial substantial (or Lagrangian) derivative. The one notable exception is the general definition of the measure (and hence also of the density) absorption function. This fact may be checked by an examination of the definitions of A_* and $A_\circ$. The concept of an absorption function (on **S** or on X) for either a radiative or a radiative transfer process appears to be unavoidably considered from an Eulerian point of view (*cf.*, *e.g.*, ([11], pp. 3–5)).

We summarize below the two axiom schemes for the foundations of radiative and radiative transfer processes as developed in this paper:

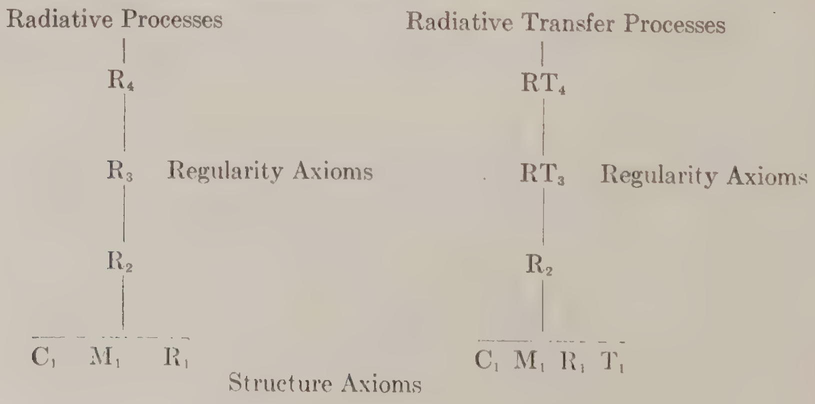

21. Conclusion. The purpose of this section is to exhibit the reduction of the general dynamic transition relation for G to the classical equation of transfer for N, thereby exhibiting a solution to the long standing problem of HOPF.

(a) *The velocity function.*

Let $\phi_0 = (\mathbf{x}_0, \xi_0) \in \Phi$, $\mathbf{x}_0 \in X$, $\xi_0 \in \Xi$. The transformation $T_{t_0,t'}$ determines a unique set $P(t_0, t)$ of points in Φ: the *light ray* between ϕ_0 and $\phi = T_{t_0,t}(\phi_0)$, that is,

$$P(t_0, t) = \{\phi' : \phi' = T_{t_0,t'}(\phi_0),\ t \leqq t' \leqq t\}.$$

Using the metric and algebraic structure of Φ, let $||P(t_0, t)||$ denote the length of $P(t_0, t)$ defined in the usual way. The limit

$$\lim_{t \to t_0} ||P(t_0, t)||/(t - t_0)$$

exists and is defined as the *speed* of light at $(t_0, \phi_0) \in T \times \Phi$ and is denoted by $v(t_0, \phi_0)$. The customary assumption of refractive isotropy is equivalent to the statement that, for arbitrary fixed $t \in T$, $v(t, \cdot)$ on Φ at each $(\mathbf{x}, \xi) \in \Phi$ is independent of ξ [14], and the value of v at time t at $(\mathbf{x}, \xi)$ may be written $v(t, \mathbf{x})$ to emphasize this independence. v is the *velocity function* on $T \times \Phi$. Within the present formalism, the speed of light in a "vacuum" may be defined by means of the corollary of (C, §17) in which $\alpha_* = 0$ on $T \times \Phi$, and (iv)RT$_3$. The resulting limit of the kind considered above is a constant function $[p]$ on $T \times \Phi$ and is denoted by c. The *index of refraction function* n on $T \times \Phi$ is then defined by the relation $n = c/v$.

(b) *The classical radiometric and attenuating functions.*

The following table exhibits the definitions of the classical radiometric and attenuating functions N, a, s, σ, and α on $T \times \Phi$ in terms of the precisely defined functions G, a_0, s_0, σ_0, and α_0 respectively. The columns marked [16] and [2] collate the abstract functions with their classical counterparts in the fields of geophysical and astrophysical optics respectively.

	[16]	[2]
(i) $N \equiv Gn^2c$	radiance function N	specific intensity function I_ν
(ii) $a \equiv a_0/v$	volume absorption function μ'	mass (true) absorption function $(\kappa_\nu - 4\pi\bar{\omega}_0\kappa_\nu)$
(iii) $s \equiv s_0/v$	volume total scattering function S'	mass scattering function $4\pi\bar{\omega}_0\kappa_\nu$
(iv) $\sigma \equiv \sigma_0/v$	volume scattering function σ	phase function p $(\int_{4\pi} p\, d\omega = 4\pi\bar{\omega}_0)$
(v) $\alpha \equiv \alpha_0/v$	volume attenuation function β'	mass absorption function κ_ν

The domains of these functions have already been defined in the introduction. We observe the following additional relations: from (§13), $\alpha = a + s$, and, from (§14), $s = \int_\Xi \sigma \, d\Omega$. Thus the basic pair of attenuating functions may be taken as (α, σ). An alternative pair would be (a, σ). The basic radiometric function is N in terms of which all other functions may be defined, as is well known.

(c) *The classical equation of transfer.*

From the corollary of (C, §17) now applied to the classical carrier space $(\Phi, \boldsymbol{\Phi}, \nu)$ we have

$$d^+G(t_1, E_1; t_2, (\mathbf{x}, \xi))/dt_2 = -\alpha_0(t_2, (\mathbf{x}, \xi))G(t_1, E_1; t_2, (\mathbf{x}, \xi)) + \int_\Xi G(t_1, E_1; t_2, (\mathbf{x}, \xi'))\sigma_0(t_2, \mathbf{x}, \xi', \xi) \, d\Omega(\xi'), \tag{1}$$

where the notational contraction $\sigma_0(t_2, (\mathbf{x}, \xi'), (*, \xi)) = \sigma_0(t_2, \mathbf{x}, \xi', \xi)$ has been made. (1) is understood to be the integro-differential representation of a radiative transfer process on $(\Phi, \boldsymbol{\Phi}, \nu)$. Using the identities $N \equiv Gn^2c$, $\alpha \equiv \alpha_0/v$, and $\sigma \equiv \sigma_0/v$, (1) may be written as

$$\boxed{(1/v) \, D(N/n^2)/Dt = -\alpha(N/n^2) + \int_\Xi (N/n^2)\sigma \, d\Omega,} \tag{2}$$

or

$$\boxed{(n^2/v) \, D(N/n^2)/Dt = -\alpha N + \int_\Xi N\sigma \, d\Omega,} \tag{3}$$

either of which is the correct homogeneous form of the classical equation of transfer. The notations d^+/dt and D/Dt are interchangeable symbols for the Lagrangian derivative operator. The function $\int_\Xi N\sigma \, d\Omega$ is known as the *path function* and is given the symbol N_*.

Continuing to descend the scale of generality by now supposing n to be locally constant on $T \times \Phi$, (3) may be written

$$(1/v) \, DN/Dt = -\alpha N + N_*, \tag{4}$$

which is the homogeneous form of equation (1) of the introductory chapter. Equation (4) and its minor variants are the usual starting points for most applications in the two main branches of radiative transfer: geophysical and astrophysical optics.

(d) *The local source axiom.*

The additive adjunction of an emission term to (1) or (3) can be justified within the present formalism by the inclusion of a properly phrased *local source* *axiom* S_1. This procedure is in keeping with the predominantly phenomenological outlook of the tenets of modern radiative transfer theory [20]. If N_η represents the *emission function* on $T \times \Phi$, then, under S_1, (3) would take the form:

$$\boxed{(n^2/v)\, D(N/n^2)/Dt = -\alpha N + N_* + N_\eta} \tag{5}$$

in which the duality of the pairs (aN, N_η) and (sN, N_*) may be disclosed by writing

$$(n^2/v)\, D(N/n^2)/Dt = (N_* - sN) + (N_\eta - aN). \tag{6}$$

The term $(N^* + N_\eta)/\alpha$ is the *Ergiebikeit* (the productivity) of the radiation field, a term due to SCHWARZSCHILD and used by HOPF. CHANDRASEKHAR has called the term the *source function.* The equation of transfer as written in (6) is of great generality. While we have in this discussion limited it to the radiative transfer context, our earlier observations have pointed out its roles in other branches of physics and mathematics. The form of (6) underscores its applicability to the study of any ensemble of entities whose space-time rate of change in numbers is subject to the generalized linear processes of immigration, emigration, birth, and death.

REFERENCES

[1] K. M. CASE, F. DE HOFFMAN & G. PLACZEK, *Introduction to the Theory of Neutron Diffusion,* Los Alamos Scientific Laboratory, Los Alamos, New Mexico, 1953, Vol. 1.
[2] S. CHANDRASEKHAR, *Radiative Transfer,* Clarendon Press, Oxford, 1950.
[3] B. DAVISON, *Neutron Transport Theory,* Clarendon Press, Oxford, 1957.
[4] S. GLASSTONE & M. C. EDLUND, *The Elements of Nuclear Reactor Theory,* D. Van Nostrand, New York, 1952.
[5] W. FELLER, Zur Theorie der Stochastischen Prozesse, *Math. Ann.* **113**, 113–160 (1937).
[6] ——— On the Integro-Differential Equations of Purely Discontinuous Markoff Processes, *Trans. Am. Math. Soc.* **48**, 488–515 (1940).
[7] ——— The General Diffusion Operator and Positivity Preserving Semi-Groups in One Dimension, *Ann. of Math.* **60**, 417–436 (1954).
[8] P. R. HALMOS, *Measure Theory,* D. Van Nostrand, New York, 1950.
[9] E. HOPF, *Mathematical Problems of Radiative Equilibrium,* Cambridge Tracts in Math. and Math. Phys. No. 31, University Press, Cambridge, 1934.
[10] A. KOLMOGOROFF, Über die Analytischen Methoden in der Wahrscheinlichkeitsrechnung, *Math. Ann.* **104**, 415–458 (1931).
[11] V. KOURGANOFF & I. W. BUSBRIDGE, *Basic Methods in Transfer Problems,* Clarendon Press, Oxford, 1952.
[12] R. KURTH, Das Anfangswertproblem der Stellardynamik, *Z. Astrophys.* **30**, 213–229 (1952).
[13] J. LEHNER & G. M. WING, Solution of the Linearized Boltzmann Transport Equation for the Slab Geometry, *Duke Math. J.* **23**, 125–142 (1956).
[14] R. K. LUNEBERG, *Mathematical Theory of Optics,* Lecture notes. Brown University Advanced Instruction and Research in Mechanics, Providence, R. I., Summer, 1944.
[15] M. E. MUNROE, *Introduction to Measure and Integration,* Addison-Wesley, Cambridge, Mass., 1953.

[16] R. W. Preisendorfer, *Lectures on Photometry, Hydrological Optics, Atmospheric Optics*, Lecture notes. Scripps Institution of Oceanography, La Jolla, Calif., Fall, 1953, Vol. 1.
[17] ——— *A Mathematical Foundation for Radiative Transfer Theory*, Dissertation, University of California at Los Angeles, May, 1956.
[18] R. Straubel, Über einen Allgemeinen Satz der Geometrischen Optik und einige Anwendung, *Physik. Z.* **4**, 114–117 (1902).
[19] E. P. Wigner, The Problem of Multiple Scattering, *Phys. Rev.* **94**, 17–25 (1954).
[20] R. Wildt, Radiative Transfer and Thermodynamics, *Astrophys. J.* **123**, 107–116 (1956).

Scripps Institution of Oceanography
University of California
La Jolla, California

BULLETIN OF THE GEOLOGICAL SOCIETY OF AMERICA
VOL. 69, PP. 121-126 Reproduced by Permission JANUARY 1958

SIGNIFICANCE OF COCCOLITHOPHORIDS IN CALCIUM-CARBONATE DEPOSITION

BY M. N. BRAMLETTE

Investigation of the living coccolithophorids by marine biologists is receiving increased attention as these forms constitute an important element of the oceanic plankton. Among the more important investigations are those of Braarud and associates at Oslo, Kamptner and predecessors at Vienna, and Deflandre in Paris. Even a brief review of present knowledge is not attempted in this paper, as this has been presented recently (Bramlette and Riedel, 1954, p. 385–386) and much more thoroughly considered by others (Deflandre, 1952, p. 439–470).

Coccolithophorids are minute beflagellate Protista that derive their food supply through photosynthesis and are usually classed as algae. The skeletal material consists of a number of coccoliths (about 2–20 microns) at or near the surface of a more or less globular body of protoplasm. The coccoliths are usually not well enough articulated to remain together in the sediments as complete skeletal remains (coccospheres), though these are found in some samples. X-ray-diffraction studies indicate that they consist of calcite in the bottom sediments, and if any originally form as aragonite these must be quickly dissolved or converted to calcite.

Studies on the stratigraphic distribution of coccolithophorids include preliminary examination of more than 1000 samples and indicate much promise for these neglected fossils in correlation and age assignments. The wide distribution of these planktonic organisms is strikingly evident in the many identical forms in strata assigned on other evidence to the middle Eocene of France, Louisiana, and California. Many samples must be examined before stratigraphic ranges are reasonably well established, but it now appears that their vertical ranges are comparable with other fossils, such as Foraminifera. For example, a peculiar and easily identified form, described by Deflandre from the upper Eocene of New Zealand, has now been found in the upper Eocene only of such widely separated regions as Australia, Trinidad, Alabama, and France.

Samples from the type Danian (generally considered uppermost Cretaceous) show an assemblage very different from that of the underlying Maestrichtian, and a closely comparable assemblage is found in the Midway of Alabama (usually assigned to the Paleocene) overlying an assemblage like that of the Maestrichtian. Though some discontinuity is evident between the type Danian and underlying Cretaceous, it does not seem to mark any very great time break, and the marked difference in the assemblages may prove to be largely due to some ecological difference such as change in surface-water temperatures. The coccoliths of both the Danian and Midway are more like those of the early Tertiary than like those of the underlying Cretaceous. This and other lines of evidence remain to be considered thoroughly, however, before an age equivalence between the Danian and Midway might be suggested.

A number of distinctive coccolithophorids seem to have developed near the end of the Oligocene or in the early Miocene, as interpreted from the sequences in Italy, Trinidad, and Indonesia. Some additional evidence may thus be available on the Aquitanian and equivalents elsewhere, including the E and F part of the lettered sequence used for the Tertiary of Indonesia.

The earliest known occurrence of well-preserved and definitely recognizable remains of coccolithophorids is in the Jurassic (Deflandre, 1952, p. 459–460), but they occur in great vari-

---

Contribution from the Scripps Institution of Oceanography, New Series, No. 954. This paper is based in part on results of research carried out by the University of California under contract with the Office of Naval Research.

(865)

TABLE 1.—RELATIVE IMPORTANCE OF COCCOLITHS, FORAMINIFERAL TESTS, AND OTHER CONSTITUENTS IN CALCAREOUS OOZE AND CHALK

(In per cent of total sample)

	Recent *Globigerina* ooze of deep Pacific Albatross 62 (56-60 cm)	Miocene calcareous ooze of deep Pacific Chubasco 24 (20-24 cm)	Oligocene (upper?) coccolith ooze of deep Pacific Chubasco 38 (10-12 cm)	Oligocene (middle?) coccolith ooze of deep Pacific Midpac 40 (130-140 cm)	Oligocene (lower?) coccolith ooze of deep Pacific Midpac 5-1 (50-60 cm)	Eocene (middle?) coccolith ooze of deep Pacific Midpac 25E (50-60 cm)	Cretaceous (Maestrichtian) chalk from Stevns Klint, Denmark	Cretaceous (Campanian) chalk from Travis County, Texas
Total calcium carbonate (from chemical analysis)	86	79	87	91	84	95	93	65
Coccoliths (including discoasters and related forms)	10	26	35	58	48	43	18	21
Foraminifera (including identifiable fragments)	55	25	30	5	15	32	23*	18*
Other calcareous skeletal debris	3	8	5	1	3	5	15	10
Indeterminate calcite particles	18	20	17	27	18	15	37	16
Radiolaria and diatoms	9	13	9	0	7	0	0	0
Inorganic non-calcareous residue	5	8	4	9	9	5	7	35

* In large part benthonic forms

ety and vast numbers in the Cretaceous chalk formations. They form an even greater part of the calcareous deep-sea deposits of the Tertiary, though they are of less importance in the late Tertiary and constitute only a minor part of most Recent calcareous ooze.

Table 1, showing the results of a careful examination of eight samples of calcareous pelagic deposits that appear to be fairly representative of many others examined less thoroughly, indicates the relative importance of the coccolithophorids, Foraminifera, and other significant constituents. An accurate determination of the percentages for a sample does not seem practicable, as any separation of the very small calcareous constituents is impossible. Most of the Foraminifera and siliceous shells are large enough for separation and fairly accurate weight determination. The indicated percentages of Foraminifera are nearly 100 per cent too high in the Cretaceous samples, however, because their chambers are filled with secondary calcite. A count of the finer constituents within fields under high magnification can give only approximations, as a size separation was unsatisfactory, and size ranges between about 1 and 20 microns had to be considered. Enough fields were examined, however, to indicate relative proportions. The accuracy of Table 1 is not determinable because of the great size differences. The percentages might, at least, be rounded off to the nearest 5 per cent. The percentages for the major constituent are even less precise, as they were adjusted so that the total of calcareous constituents agrees with the chemical determination of total calcium carbonate.

The distinctive interference patterns of coccoliths observed under crossed nicols (Kamptner, 1954, p. 1–51) are a considerable aid in determining their number in a field under the polarizing microscope. The percentages of indeterminate calcite particle doubtless include small fragments of the recognized groups and perhaps usually in about their same relative proportions. This is not the case, however, in the chalk sample from Denmark. As the later discussion indicates, this and many other Cretaceous chalk samples may consist largely of crystals of secondary calcite. Among noncalcareous skeletal components, only the Radiolaria and diatoms (together) are tabulated, and the "residue" consists largely of clay and other detrital minerals.

The Cretaceous chalk formations contain abundant coccoliths, though these are commonly not the dominant calcareous constituent and are not in the two samples in Table 1. No deep-sea pelagic deposits of Cretaceous age are now available, however, and these two samples represent relatively shallow epicontinental sea deposits with many benthonic Foraminifera and other fossil remains. One might expect that much of the tiny remains of coccolithophorids would be swept out into deeper water. Their abundance in the Cretaceous chalks as compared to deposits formed under comparable conditions in the Tertiary—when the coccoliths dominated the calcareous pelagic deposits—suggests that the coccolithophorids were at least as dominant in the calcareous plankton of the Cretaceous. This would be more strongly indicated if the loss of smaller coccoliths through dissolution and recrystallization is as important in the Cretaceous chalks as the following discussion suggests.

Some samples of Cretaceous chalk, such as one from the Selma Formation of Mississippi, obviously contain a greater percentage of coccoliths than do the two considered more or less representative. Some others, however, contain lower percentages of coccoliths, particularly those examined from England and Germany. These samples show much corrosion and secondary growth of the coccoliths. Their content of small calcite particles, higher than the 37 per cent tabulated for the Maestrichtian sample of Denmark, may represent a corresponding loss of coccoliths through recrystallization, with dissolution apparently accounting for the comparative sparsity of the normally abundant smallest coccoliths. The induration is generally greater in such samples, and commonly the chambers of Foraminifera have been filled with calcite. Less corrosion and recrystallization are usual in less permeable clayey chalks.

The many cores of Tertiary calcareous sediment obtained from the deep Pacific may be classed as coccolith ooze. Those of middle and early Tertiary age, particularly, show a consistent predominance in total mass of coccoliths over Foraminifera (largely planktonic), though in those of late Tertiary age this is less marked. In the post-Tertiary, however, Foraminifera (largely planktonic) greatly predominate. These more recent deposits have thus been commonly called *Globigerina* ooze, though this term is not entirely appropriate as the genus *Globigerina* does not everywhere predominate in pelagic foraminiferal ooze.

In much of the Atlantic Ocean, the percentage of coccoliths in the modern deposits seems to average even less than the 10 per cent shown in the recent sample from the Pacific (Table 1), but their dominance in the Tertiary seems to be comparable with that in the Pacific. Some cores of Tertiary age, collected from the Atlantic by Lamont Geological Observatory, were described (Ericson, Ewing, and Heezen, 1952, p. 504–507) as fine-grained chalk, and some of these samples examined by the writer contained a great abundance of coccoliths, though the samples were so small that relative percentages were not determined.

There is evidence that, during much of Tertiary time, ocean waters were warmer than at present, and oxygen-isotope data of Emiliani and Edwards (1953, p. 887) indicate that temperatures of the bottom waters may have averaged about 12° C. This would have lowered the solubility limits of calcareous deposits. The carbonate is dissolved, and little accumulates now below depths of about 4500 m in the Pacific Ocean and below somewhat greater depths in the Atlantic Ocean. Revelle has calculated (personal communication) from his graphs of the controlling variables (Revelle and Fairbridge, 1957) that the present critical depth of about 4500 m would correspond to about 6700 m for comparable solubility conditions with a Tertiary bottom-water temperature of 12°C. This would explain the occurrence of Tertiary calcareous ooze beneath "red clay" in some cores from areas where depths are too great for calcareous accumulation under present conditions. It does not seem that this solubility difference for different bottom temperatures could account for the relative proportions of coccoliths and Foraminifera in the Recent and Tertiary calcareous sediments, however, because even the smallest coccoliths are present in both, and they show little more susceptibility to dissolution than do the Foraminifera—as judged by their distribution with depth on present ocean bottoms. This is in peculiar contrast to the distinctly greater susceptibility of coccoliths to solution and recrystallization in the intrastratal waters of Cretaceous chalk formations.

The coccolithophorids thus have had a significant role in the geochemical cycle and balance of calcium carbonate in the ocean basins. An interesting and often-quoted suggestion by Twenhofel (1939, p. 327), later elaborated by Kuenen (1950, p. 392–394), was that *Globigerina* and other planktonic Foraminifera, which first appeared during the Cretaceous, have since greatly modified the major site of deposition of calcium carbonate and hence its whole geochemical cycle in sediments. The great amount of modern *Globigerina* ooze in the deep-ocean basins represents a loss to this cycle, in contrast with the great and presumed dominance of accumulation in shallow (perhaps epicontinental) seas of pre-Cretaceous time. Much of this earlier deposition in epicontinental or marginal seas must have been incorporated again into the continental masses and returned to the cycles of erosion and deposition. The large loss to the deep seas under modern conditions was calculated by Kuenen to indicate a potential calcium-carbonate "famine" in 100–150 million years. The lesser amount postulated as lost to the deep seas in earlier times would help account for the high proportion of limestones among older rocks of the continental areas.

Kuenen (1950, p. 393) also suggests that "the present relative scarcity of calcareous deposits in shallow waters, as compared to former periods," may be similarly explained. This scarcity seems questionable in island-atoll areas, however, and in shelf-sea areas seems more probably to reflect only a greater dilution with clastic sediments from rapid erosion of unusually great topographic relief in late geological time.

It is not yet apparent that the earlier dominance of coccolithophorids was due to a greater rate of production than at present, nor that there was a subsequent (post-middle Tertiary) increase in the rate of production of the pelagic Foraminifera. The latter possibility would help the budget problem of calcium carbonate in the oceans and seems to fit the meager data suggesting a greater-than-average rate of deep-sea deposition in Quaternary time. It is not too evident, however, that the rate of supply and consequent deposition of calcium carbonate has varied greatly, and perhaps only the relative importance of the two groups of calcareous plankton has changed. At least it seems evident that the rate of supply is the critical factor for much change in the rate of carbonate deposition. At present the oceans are about saturated with calcium carbonate, and the supply has been calculated to be sufficient to replace this total amount within roughly a million years (Revelle and Fairbridge, In press).

Though the coccolithophorids seem to have been more important than the pelagic Foraminifera before late Tertiary time, their importance is not demonstrable before the Cretaceous. Unless the coccolithophorids were important earlier, however, their dominance over the pelagic Foraminifera would not alter the significant conclusion of the hypothesis on calcium-carbonate loss to the deep-sea bottoms through pelagic accumulations since Cretaceous time. Kuenen's suggestion seemed particularly inviting because both the geochemical budget during later geologic time and the excess of calcium carbonate in known pre-Cretaceous rocks present a less serious problem if the present large loss to the deep sea is abnormal and most of the carbonate was deposited on or near continental blocks during much of geological time. Attractive as this hypothesis appears, it would have no basis if such organisms as coccolithophorids or an inorganic process could have segregated much calcium carbonate in the deep-ocean bottoms before the advent of pelagic Foraminifera; both possibilities seem to need consideration.

Very fine-grained limestones in especially thin sections under a high-power microscope show a fine mosaic texture similar to aplitic—or xenomorphic granular—texture in igneous rocks. The small (commonly only a few microns) interlocking crystals indicate a recrystallization of whatever small particles were originally present. One occurrence where these were evidently coccoliths will be described. Some may equally well have been like the tiny needles of aragonite now forming on the Bahama Banks, which have been called drewite. This drewite is considered here as probably of dominantly inorganic or at least nonskeletal origin. Though this has been questioned (Lowenstam, 1955, p. 270–272), its origin is not critical to this discussion. Such material has not been found in careful examination of many Recent and Tertiary deep-sea deposits. Drewite deposition would seem more probable in warm, shallow waters, and more certainly so if it should prove to be disintegrated debris of algae such as *Halimeda*, as suggested by Lowenstam.

The fine-grained Carmel limestone of Utah might well represent a deposit comparable to the drewite of the Bahama Banks. It is comparatively thin, occurs between nonmarine formations, and thus was probably formed in relatively shallow water. Thin sections of some parts also show small pellet forms like the oölites of the Bahama Banks deposits.

Very fine-grained limestones are common, however, and rather characteristic of some geosynclinal formations that seem to represent relatively deep-water accumulations. The Tithonian and other limestones of the sub-Alpine region of France are examples.

The requirements for inorganic precipitation of much calcium carbonate include warming of the water, or decrease of carbon dioxide, or increase of salinity through evaporation. In a former time without calcareous planktonic organisms, one or more of these requirements might have been maintained to a sufficient extent near the surface of relatively deep waters, despite some inevitable mixing with water from below the surface, and inorganic precipitation might have occurred here as well as in shallow water. Conceivably the fine-grained limestones of geosynclinal accumulations could have originated in this way. Assuming inorganic precipitation under these conditions, however, would make it equally possible in the open ocean and offers no support to the hypothesis of a change to a greater proportion of deep-ocean accumulation of calcium carbonate during Cretaceous and later time.

This hypothesis is not supported by evidence of greatly increased importance of calcareous plankton either unless forms such as the coccolithophorids were, like the pelagic Foraminifera, insignificant before about this time. The coccoliths actually are found in great abundance only with the earliest occurrences of chalk in the Cretaceous, but the following considerations suggest that earlier occurrences may be represented by some pre-Cretaceous fine-grained limestones. Thus the problem would remain regarding a geochemical balance for calcium carbonate.

The original absence or paucity of planktonic Foraminifera is evident in pre-Cretaceous limestones which show comparably robust microfossils preserved, despite the evident recrystallization of the much finer matrix particles inherent in lithification to a dense limestone. Though not recognizable, the original presence of the minute coccoliths is indicated in a Cretaceous limestone of Tunisia, and this example suggests that their preservation is not expectable in other fine-grained limestones, and especially in those of greater age.

The upper Cretaceous chalk formations in central Tunisia are represented by fine-grained limestones in the thick and folded geosynclinal sequence to the north. A thin section of the Maestrichtian part of the limestones shows Foraminifera (mostly pelagic) scattered in a matrix of interlocking calcite crystals which average a few microns—just as these Foraminifera are scattered in the abundant coccoliths of the less-deformed chalk equivalent to the south.

The thick section of geosynclincal deposits of the sub-Alpine region of France includes much very fine-grained limestone of Jurassic and Cretaceous age. Thin sections show that the interlocking grains of the dense Tithonian (upper Jurassic) limestone average little larger than the sizes of coccoliths which occur in a variety of forms in the somewhat older, though much less lithified, Oxfordian marl of northern France. The only common fossil recognizable in this Tithonian is a small form classed with the planktonic tintinnids. The skeleton of this *Calpionella* is considerably larger and more robust, and thus more apt to be preserved, than any of the coccolithophorids.

This little evidence obviously does not justify any generalizations about fine-grained limestones, but the possibility that geosynclinal ones, at least, were originally like the later coccolith chalks seems to offer fewer difficulties than does an inorganic (nonskeletal) origin. This would also explain an otherwise unrelated coincidence in the occurrence of coccoliths in abundance and great variety of forms along with the earliest occurrences of the relatively unlithified calcareous deposits known as chalk. The absence of the coccoliths and their progenitors in the older fine-grained limestones would be inevitable with the recrystallization that has evidently produced the aplitic texture and obliterated whatever form the small particles originally showed.

These considerations seem to indicate, at least, that no tacit assumption that these limestones represent a fine inorganic precipitate is justified, merely because no very small fossil remains are still recognizable. Geochemical studies may help the problem for any particular limestone, as the distribution of such minor elements as barium and strontium in inorganic and skeletal calcium carbonate becomes better understood; and the carbon and oxygen isotopes may offer some evidence despite the recrystallization.

References Cited

Bramlette, M. N., and Riedel, W. R., 1954, Stratigraphic value of discoasters and some other microfossils related to Recent coccolithophores: Jour. Paleontology, v. 28, p. 385–403

Deflandre, G., 1952, Traité de Zoologie, Grassé: Paris, Masson et Cie, Tome 1, p. 439–470

Emiliani, C., and Edwards, G., 1953, Tertiary ocean bottom temperatures: Nature, v. 171, p. 887–889

Ericson, D. B., Ewing, M., and Heezen, B. C., 1952, Turbidity currents and sediments in North Atlantic: Am. Assoc. Petroleum Geologists Bull., v. 36, p. 489–511

Kamptner, E., 1954, Untersuchungen über den Feinbau der Coccolithen: Archiv. f. Protistenkunde, Bd. 100, Heft 1, p. 1–90

Kuenen, P. H., 1950, Marine geology: New York, Wiley and Sons, Inc., 568 p.

Lowenstam, H. A., 1955, Aragonite needles secreted by algae and some sedimentary implications: Jour. Sedim. Petrology, v. 25, p. 270–272

Revelle, R., and Fairbridge, R., In press, Carbon dioxide and carbonates, Chapter 10 *in* Hedgpeth, J. W. H., *Editor*, Treatise on marine ecology and paleoecology, Volume 1: Geol. Soc. America Memoir 67

Twenhofel, W. H., 1939, Principles of sedimentation: New York, McGraw-Hill, 610 p.

SCRIPPS INST. OF OCEANOGRAPHY, LA JOLLA, CALIF.

MANUSCRIPT RECEIVED BY THE SECRETARY OF THE SOCIETY, FEBRUARY 14, 1957

Deep-Sea Research, 1957, Vol. 4, pp. 272 to 286. Pergamon Press Ltd., London
Reproduced by Permission

Measurements of southern swell at Guadalupe Island*

W. H. MUNK and F. E. SNODGRASS

(*Received* 24 *June* 1957)

Abstract—We have obtained some energy spectra of pressure fluctuations on the sea bottom at a depth of 60 fathoms off Guadalupe Island, Mexico. The spectra consist of peaks whose frequency increases by about 10 per cent per day ; sequences repeat once every three or four days. The waves come from the southwest quarter, and the distance of generation is estimated at 8000 nautical miles. The signals are attributed to cyclones in the storm belt of the Southern Hemisphere. The earliest arrivals are of the order of 1 mm high and 1 km long. They may have originated in the Indian Ocean and passed just east of New Zealand, or to the west through the Tasman Sea. Later arrivals were generated in the South Pacific. Measurements taken at many other occasions at various localities in the north-east Pacific indicate that this radiation from the Southern Hemisphere is present at all seasons. Apparently it constitutes the principal background in the ocean wave spectrum for the low frequencies under consideration.

A HISTORICAL NOTE

THE photograph shown in Fig. 1 was the first indication of southern swell reaching the coast of California. Allowing for refraction in shallow water the off-shore direction was computed to be south south-west, and it was inferred that the waves had originated in a storm area in the southern oceans (HYDROGRAPHIC OFFICE, 1944). The photographed wave pattern is remarkably regular; it looks almost like the single-frequency, long-crested train of sine waves used in elementary oceanographic texts and advanced mathematical treatises to portray ocean waves. A distant origin could account for the regularity. The wave direction would be nearly uniform (i.e. the waves are long-crested) inasmuch as a distant storm subtends a small angle, and the range of frequency would be small because of the sorting of frequencies by dispersion. Fig. 1 was the first of a long series of aerial photographs we took during the war, and it must be added that in no subsequent photograph did we observe quite as regular a wave pattern.

The problem of the propagation of ocean waves was not at all well understood until BARBER and URSELL (1948) succeeded in obtaining spectra of ocean waves. In nearly all of forty case histories they were able to trace prominent frequency bands to storms in the north Atlantic Ocean, but on at least two occasions they found unmistakable evidence that the swell had been generated in storms occurring beyond the limits of this ocean. In one case they first noted a spectral band peaked at a period of 21 sec at 1100 hr on 14 May 1946, and this period decreased uniformly (except for a frequency modulation by tidal currents, which confirmed the southern origin) to 15 sec on 19 May. We shall make references to the following quotation from BARBER and URSELL's (1948) paper :

"... there appears to be at least one significant discontinuity in the trend

---

*This paper represents results of research carried out by the University of California under contract with the Office of Naval Research and the Bureau of Ships of the Navy Department. Reproduction in whole or in part is permitted for any purpose of the United States Government.

> of maximum periods ; after 1700 hr on 16 May the spectra suggest that the frequency is widened by the arrival of swell whose maximum period is 2 to 3 sec longer than the mean maximum of the previous spectra. A second widening at the upper end of the frequency band possibly occurs at 1900 hr on 19 May when there is some, though not very reliable, indication of activity at periods up to 23 sec."

BARBER and URSELL compute the distance of origin from the observed frequency shift, and arrive at 6000–7000 nautical miles : " the storm must, therefore, be sought in the southern ocean, probably in the Falkland sector to which there is an open great circle course from Land's End". The meteorological evidence available was too scanty to be very helpful. The maximum height of the southern swell was 30 cm.

DONN (1949) has discussed wave spectra taken at Cuttyhunk and Bermuda. He notes that

> " The periodograms frequently show a unique wave signature exactly at the 15 sec mark. This group may show a range of from 14 to 18 sec, with occasional extensions slightly beyond these limits. From a study of many records it appears that this group is nearly always present, but at times may become too small to be detected, even by harmonic analysis."

Allowing for appropriate travel time, DONN has compared the Cuttyhunk and Bermuda spectra and concludes that the waves come from the south.

> " Assuming this southerly origin, weather maps of the belt of the westerlies of the Northern and Southern Hemispheres have been studied at length. No such swell source appears possible from transitory cyclones and anticyclones of either hemisphere. In addition the " window " of approach from possible storms in the South Atlantic is extremely restricted. The suggestion is thus offered here that this swell group is generated by the South-east trade winds. This seems to be the only source that would explain their constancy."

J. E. DINGER (personal communication) has remarked on a 15–16 sec hump in the spectra of waves at the Barbados. RUDNICK (1951) finds 15–20 sec bands in spectra of waves at Guam.

WIEGEL and KIMBERLEY (1950) obtained (without frequency analysis) the " significant " height and period of the predominant waves recorded at Camp Pendleton, California, and conclude that they originate in the area between 40° and 65°S and 120° and 160°W. The largest recorded period during a summer season was 22 sec.

OFF-SHORE RECORDING

For the last two years we have used a Vibrotron transducer (SNODGRASS, MUNK and TUCKER, in press) to record fluctuations in bottom pressure at depths varying from 80 to 300 m. Twenty-four stations have been occupied on the continental shelf and borderland off southern California. At *all* stations, regardless of season, we have noted a pronounced regular oscillation, such as shown in Fig. 2. The recorded periods (mean interval between crests) varies from 14 to 20 sec, wave heights (root mean square values corrected for depth) from 10 cm to 1 m. In the majority of cases the periods were between 15 and 16 sec.

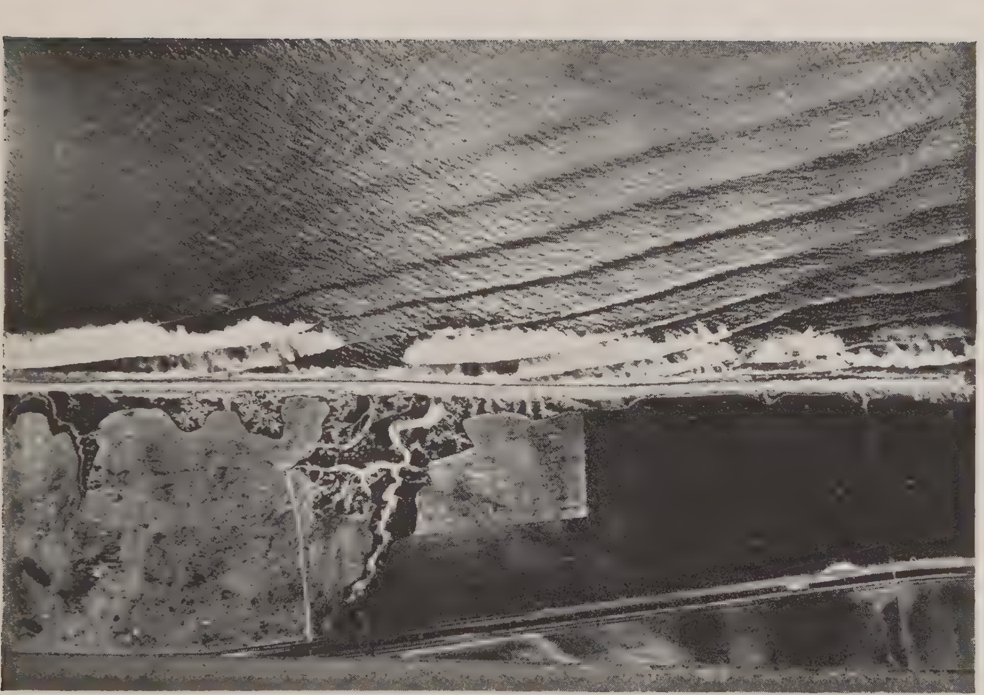

Fig. 1. Aerial photograph of waves at Camp Pendleton, California, on 16 January, 1944. The coast trends north-west – south-east.

(874)

Out first attempt to determine wave direction was by comparison with simultaneous visual observations conducted at Camp Pendleton (see Fig. 1) by Warrant Officer BOYD, U.S.M.C. The visual observations include breaker angle and littoral current ; these parameters are notoriously unreliable for determining off-shore wave direction, but they were the only means available. All that can be said is that on such days when the shore observations indicated waves from the south-west quarter, their height and period were consistent with the values recorded offshore.

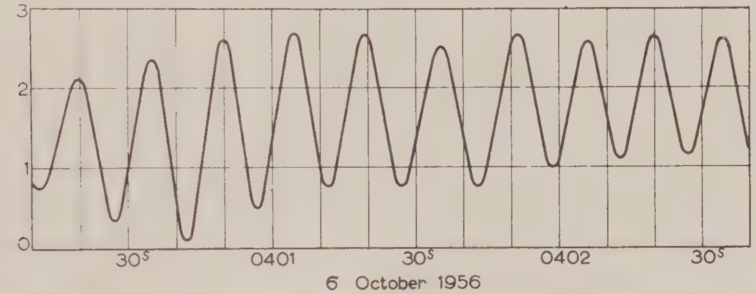

Fig. 2. Short section of Vibrotron record at the protected station of Guadalupe Island. The scale gives inches of water pressure on the sea bottom.

On 25–27 June we attempted to use the wave "shadow" behind San Clemente Island as a means of estimating wave direction. We first occupied a station at the north-west end of the island, which is exposed to waves from the south-west quarter, followed immediately by a station at the east side, which is protected from this quarter. The results were :

	June, 1954	*Period* (sec)	*Height* (cm)
San Clemente, West	25, 1300 hr	14·8	64
	25, 2300	14·4	59
	26, 0500	13·8	77
San Clemente, East	26, 1100	14·6	15
	27, 1400	14·1	10

On 3–8 October 1956 we occupied two stations at Guadalupe Island, 200 nautical miles off the coast of Mexico and well off the continental borderland. The first station was protected from the south-west quarter, the second station was not. At the exposed station the waves were four times higher.

The evidence, while not conclusive, points to a southern origin of the low-frequency signal. Our observations differ from previous work on account of the great depth at which they were taken. Depth acts as a low-pass filter ; local disturbances are of higher frequency, and attenuated accordingly. The result is that low frequency signals were prominent at all times in these filtered records, and at such times as we could check, a southern origin was indicated.

GUADALUPE SPECTRA

Fig. 3 shows seven successive spectra of the Guadalupe wave records. The following information is recorded :

Guadalupe Island, north station, 29°09′·30N, 118°16′·35W. Depth : 113 m

1956	m	N	f	95% limits
(1) 3 Oct., 2220 – 4, 0500	62	6000	194	0·82 – 1·24
(2) 4 Oct., 1020 – 4, 1700	62	6000	194	0·82 – 1·24
(3) 4 Oct., 2220 – 5, 0500	62	6000	194	0·82 – 1·24
(4) 5 Oct., 1020 – 5, 1700	62	6000	194	0·82 – 1·24
(5) 5 Oct., 2220 – 6, 0500	62	6000	194	0·82 – 1·24

Guadalupe Island, south station, 28° 50′·55N, 118°16′·45W. Depth : 109 m

(6) 7 Oct., 1236 – 7, 2142	62	8190	261	0·84 – 1·21
(7) 7 Oct., 2142 – 8, 0648	62	8190	261	0·84 – 1·21

Bottom pressure was recorded every 4 sec, and successive values were harmonically analysed on an electronic computer, following the method of Tukey (1949). We obtained $m = 62$ estimates of energy density, of which 25 values are plotted (without smoothing). The degrees of freedom $f - 2N/m$ determines the statistical reliability of the estimates. For spectra (1) to (4) there is only one chance in twenty that the true energy density is less than 0·82 or more than 1·24 times the computed value. Tides were removed prior to analysis by numerical high-pass filtering. The plotted curves are surface spectra ; the depth of the instrument has been allowed for according to hydrodynamic theory. The many details of the analysis have been described elsewhere (Munk, Snodgrass and Tucker, in press).

The characteristic feature of the spectra is the progressive shifts of individual peaks from low to high frequencies. The peaks emerge at about 50 cycles per kilosecond (period 20 sec) and their frequency increases by something like 7 per cent per day until they disappear in the locally generated spectrum. The energy of the peaks reaches a maximum around 65 c/ks. The history repeats itself at an interval of 3 to 4 days. This behaviour is in accord with the remarks by Barber and Ursell quoted earlier. There is a sharp increase in one of the peaks from record (4) to (5). We return to this later.

The essential point is that we have analysed records from 25 to 30 times longer than those previously used (except for two isolated analyses by Rudnick, 1951) and that the resolution is improved accordingly. Thus the spectrum between 40 and 90 c/ks is described by 25 estimates of energy density, rather than just a very few values of less reliability. The spectra available to Donn were of such poor resolution that progressive spectral peaks, if present, could not have been discerned, and the signals would appear as a steady " hum " at 15 sec. The observed steadiness has lead Donn (1949) to suggest generation by the steady south-east trades rather than by transitory storms to the south. The British results, and those obtained at Guadalupe, suggest that the Bermuda spectra could likewise reveal a fine structure of progressive peaks if the records were analysed with adequate resolution.

(876)

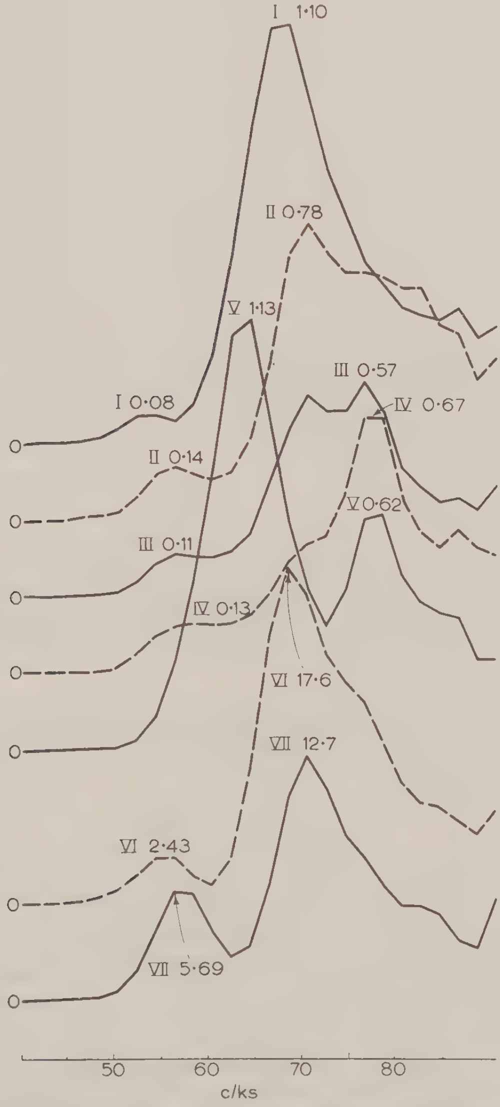

Fig. 3. Energy spectra of waves recorded at Guadalupe Island. The frequency scale is in cycles per kilosecond (or millicycles per second); the ordinate gives "energy" density in cm2 per c/ks on a sliding scale. Zeroes and peak values are indicated. The last two spectra are drawn to one-twentieth scale.

WAVES FROM A SINGLE IMPULSIVE SOURCE

A distance-time diagram is useful (Fig. 4, bottom). Suppose that at some distance r_0 from the recording station, and at some time t_0, a sudden concentrated disturbance generates waves over a broad band of frequencies. Any elementary wave train of frequency f, travelling at the appropriate group velocity $V = g/(4\pi f)$, is characterised by a " ray " in the r, t-diagram extending from the source (r_0, t_0) to the receiver (O, t) with slope $V(f)$, where

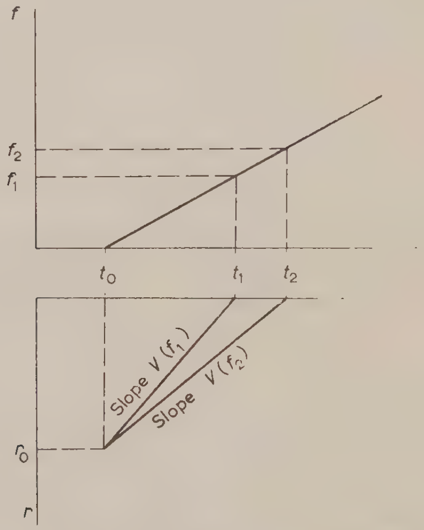

Fig. 4. Frequency-time and distance-time diagrams for an impulsive source at a distance r from the wave station, and time t_0. Two particular frequencies, f_1 and f_2, arriving at the station at times t_1 and t_2 respectively, are characterized by the rays of slope $V(f_1)$ and $V(f_2)$ on the r, t-diagram.

$$V = \frac{r_0}{t - t_0} = \frac{g}{4\pi f}. \tag{1}$$

The mathematical foundation of this simple geometric construction has been summarized by ECKART (1948). The requirement is that the different velocities of the Fourier components have dispersed the disturbance into a well-resolved spectrum.

BARBER and URSELL (1948) have constructed such " propagation diagrams " to locate the source of the recorded waves. Let the spectrum of waves arriving at time t_1 reveal a narrow band peaked at frequency f_1, and at a later time t_2 a peak at a higher frequency f_2. Then the rays drawn through the points 0, t_1 and 0, t_2 with the slopes V_1 and V_2 as given by equation (1) intersect at a point which determines the distance and time of the source. In one case five rays covering the interval 14–18 May 1946 give a good intersection for a point at a distance 6000 miles from the recording station, at a time 6 May 1946.

An equivalent construction has been used by MUNK (1947). Equation (1) can be written in the form

$$f = \frac{g}{4\pi r_0}(t - t_0) \tag{2}$$

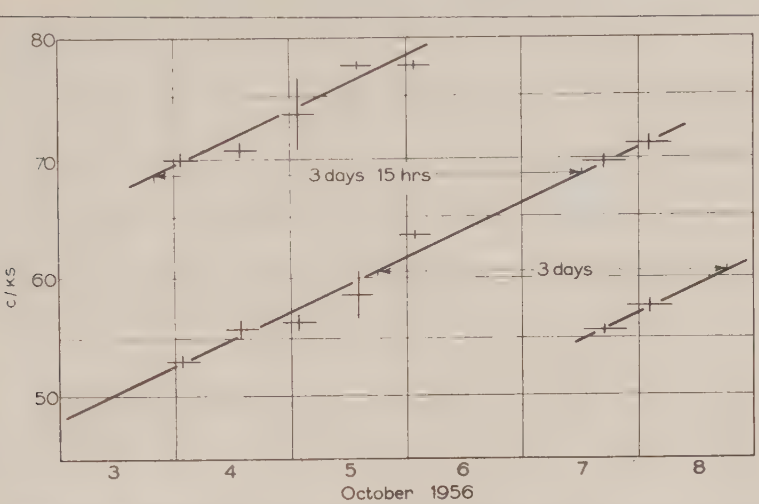

Fig. 5. Frequency-time diagram for the Guadalupe Spectral peaks, Fig. 3. Each frequency band is indicated by a cross. The vertical lines give a measure of the possible range of values of peak frequency; the horizontal lines give the duration of the analysed record.

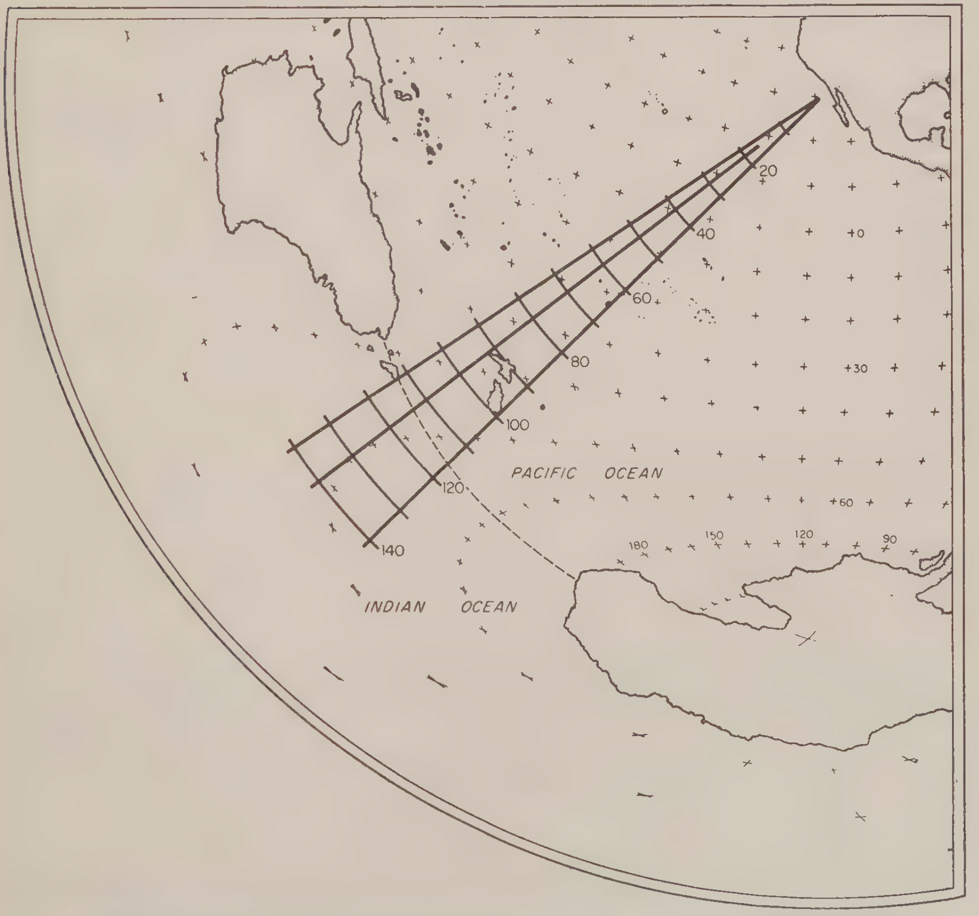
20
40
60
80
100
120
140
+0
+30
+60
PACIFIC OCEAN
180
150
120
90
INDIAN OCEAN

Fig. 6. Azimuthal-equidistant projection centred on San Diego. Distances from Guadalupe are given in units of degrees (1° equals 111 km).

so that the frequencies from a point source lie along a straight line in a frequency-time diagram (Fig. 4, top). The intercept determines t_0 and the slope gives r_0. The Guadalupe spectral peaks have been fitted by straight parallel lines on an f, t-diagram, (Fig. 5). There are three sequences, separated by 3 days 15 hr ; and by 3 days respectively. If we insist in fitting all sequences by parallel lines, we obtain a single value, $r_0 = 135°$ (15,000 km). This places the source in the Indian Ocean (Fig. 6) The values of t_0 are 18 Sept. 1956, 1900 hr ; 22 Sept., 1000 hr ; 25 Sept., 1000 hr. Conceivably we might ignore the last two values inasmuch as they were taken at another station, and draw a steeper line. The smallest value of r_0 is about 110°, and the t_0 times are later, but by no more than 1 day 17 hr.

But one is led immediately to question the validity of seeking an instantaneous point source. A travelling storm will be many days along an unobstructed path from the time it passes south of Australia. We are naturally led to generalize the construction.

WAVES FROM A MOVING POINT SOURCE

A storm is moving eastward at some constant rate W along colatitude c (Fig. 7). Then

$$\phi R \sin c = Wt \tag{3}$$

is the storm's distance from a point P just south of the station. R is the Earth's radius. The storm's longitude ϕ and the time t are taken as negative when the storm is west of the station, as shown in the figure. The great circle distance from storm to station* is rR, where

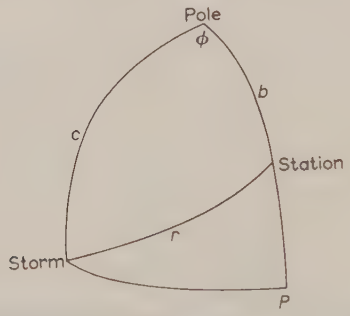

Fig. 7. b and c are polar angles of station and storm referred to the pole nearest the station. P is a point south of the station at co-latitude c.

$$\cos r = \cos b \cos c + \sin b \sin c \cos \phi. \tag{4}$$

It is convenient to interpret ϕ also as dimensionless time according to (3). Fig. 8 shows the storm track on an r, ϕ-diagram. The storm is nearest the station when $\phi = 0$ and furthest when $\phi = 180°$. The inflection point is of particular interest. Setting $d^2 r/d\phi^2 = 0$ gives two solutions :

$$\cos r_i = \frac{\cos b}{\cos c}, \qquad \cos \phi_i = \frac{\tan c}{\tan b}, \qquad \frac{dr}{dt} = \frac{W}{R}, \qquad \text{for } b + c > 180° \tag{5a}$$

---

*This presumes that waves travel along great circles. ECKART finds (personal communication) that because of the earth's rotation there will be an angular deflection of the order $(\text{wave period}/\tfrac{1}{2}\text{ day})^2$ or 10^{-7} for 20 sec waves. The deviation from the great circle route is then of the order of 1 m.

$$\cos r_t = \frac{\cos c}{\cos b}, \qquad \cos \phi_i = \frac{\tan b}{\tan c}, \qquad \frac{dr}{dt} = \frac{W \sin b}{R \sin c}, \qquad \text{for } b + c < 180° \tag{5b}$$

In the first case the wave station is no further north of the equator than the storm is south of the equator (or vice versa). There exists then a great circle route through the station and tangent to the storm's latitude. At the point of tangency the storm moves east with the same speed as it moves towards the station ; $R \cdot dr/dt = W$. In the second case the station is further north than the storm is south, and the rate of approach of the storm towards the station is always less than W.

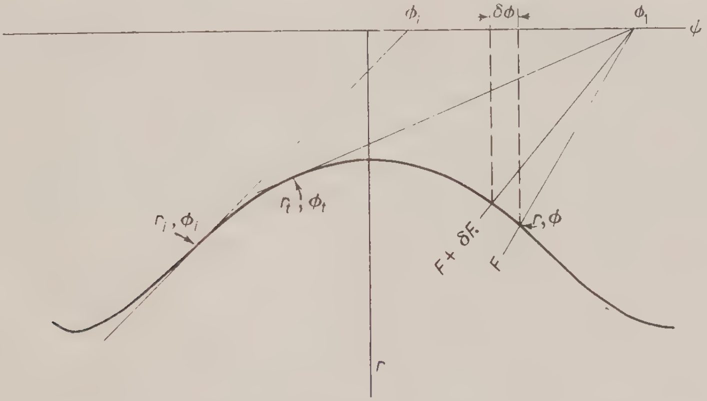

Fig. 8. A distance-time diagram for a moving point source.

Consider a " ray " from ϕ, r to ϕ_1, 0 (Fig. 8). This ray represents the travel of an elementary wave train having left the storm at time $t = (R \sin c/W)\,\phi$ and arrived at the station at $t_1 = (R \sin c/W)\,\phi_1$, thus having covered a distance rR with a group velocity

$$V = \frac{rR}{(R \sin c/W)\,(\phi_1 - \phi)}.$$

A convenient notation is $f_0 = g/4\pi\, W$ for the frequency corresponding to a group velocity W. In view of (1)

$$F = \frac{f}{f_0} = \frac{W}{V} = \frac{(\phi_1 - \phi) \sin c}{r}. \tag{6}$$

For any (dimensionless) frequency F recorded at time t_1 the distance and longitude of generation are determined by the intersect of the ray with the storm's track on the r, ϕ-diagram. There may be zero, one or three intersections. For the tangent ray (Fig. 8)

$$F_t = -\frac{\sin r_t}{\sin b \sin \phi_t} = \frac{(\phi_1 - \phi_t) \sin c}{r_t}. \tag{7}$$

Let $E(F)$ designate the " energy " spectrum of the wave record. The contribution to the mean square elevation from frequencies in the range F to $F + \delta F$ is denoted by $E(F)\,\delta F$. This contribution $E(F)\,\delta F$ comes from a segment of the storm track that is subtended by the rays associated with F and $F + \delta F$, respectively (Fig. 8).

Let $\delta\phi = [W/(R \sin c)]\, \delta t$ be the projection of this segment upon the ϕ-axis. The storm is presumed to radiate energy at a uniform rate*, and $E(F)\, \delta F$ is proportional to $|\delta t|$, and hence to $|\delta\phi| \sin c$; it also varies as the energy density $S(F)$ of the generation spectrum, inversely with r because of dispersion, and inversely with $\sin r$ because of angular spreading (see, for example, LAMB, 1932, pp. 432-433). Nothing is known about attenuation, and we neglect it. Hence

$$E(F)\, \delta f \sim S(F)\, |\delta\phi| \sin c/(r \sin r)$$

$$E(F) = \mu S(F), \qquad \mu = \frac{|\delta\phi/\delta F| \sin c}{r \sin r} \tag{8}$$

where $\mu(F)$ may be regarded as the energy amplification, operating on the generation spectrum $S(F)$ to give the recorded spectrum $E(F)$. The evaluation is a problem in differential geometry (see Appendix), but in general terms the result is evident from Fig. 8 : (1) For any given time t_1 (hence ϕ_1) μ is sharply peaked for the particular ray through r_t, ϕ_t tangent to the storm track ; (2) the tangent ray through the inflection point r_i, ϕ_i gives a peak of all such peak values. The foregoing argument is related to the method of stationary phase.

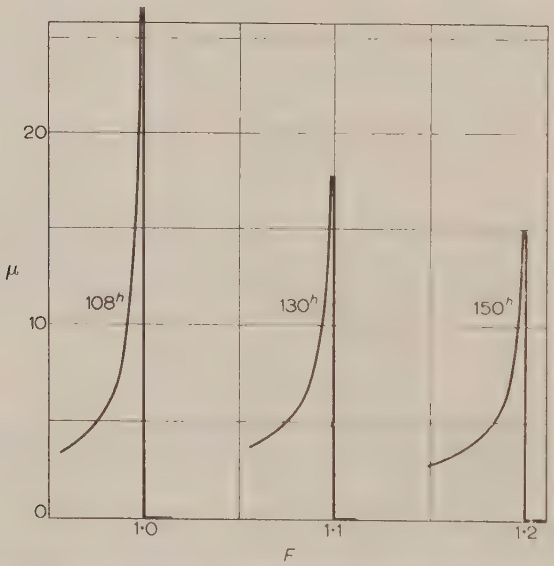

Fig. 9. The amplification factor at various times *after* the passage of the moving point source to the south of the station (point P, Fig. 7), the first " tangent arrival " through the inflection point is more amplified than successive tangent arrivals.

Fig. 9 has been drawn according to equation (15). Near the tangent ray μ approaches infinity as $(F - F_t)^{-\frac{1}{2}}$ except near the inflection point. Then $F_t = 1$, and μ $(= \mu_i)$ approaches infinity as $(F - 1)^{-\frac{2}{3}}$. Though the spikes are infinite, the area under the spikes is finite. If the generation spectrum $S(F)$ is a smooth function, estimates of the energy density in the frequency interval $F_t - \Delta F$ to F_t can be written

*One may think of the storm as a series of momentary disturbances, each sending out an identical dispersive train. The *number* of disturbances contributing to $E(F)\, \delta F$ is then proportional to $|\delta t|$.

$$\int_{F_t-\Delta F}^{F_t} E\mu\, dF = E\int_{F_t-\Delta F}^{F_t} \mu\, dF = 2h\,(\Delta F)^{\frac{1}{2}}\,E, \qquad \text{(tangent ray)}$$

$$= 3h_i\,(\Delta F)^{\frac{1}{3}}\,E \qquad \text{(inflection ray)}$$

as compared to something of the order $(\Delta F)\,E$ away from the spikes. The *recorded* peak amplifications

$$2h\,(\Delta F)^{-\frac{1}{2}}, \qquad 3h_i\,(\Delta F)^{-\frac{2}{3}} \tag{9}$$

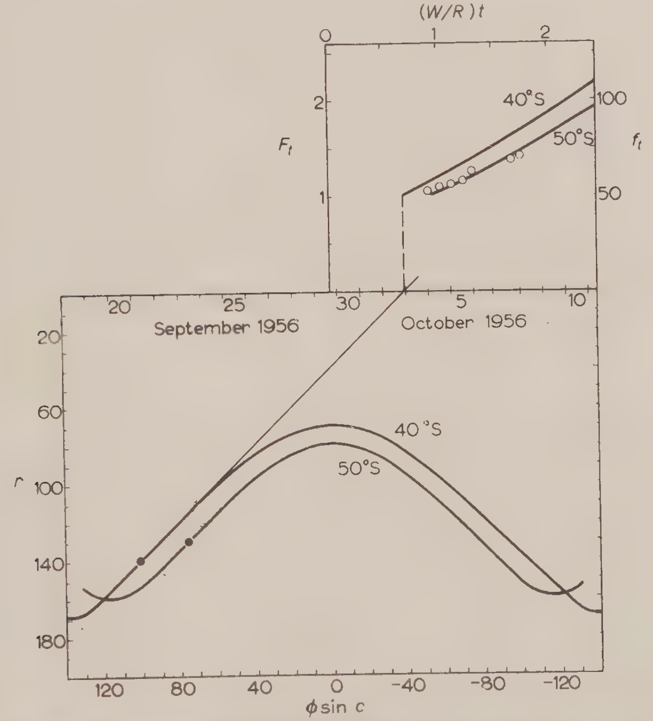

Fig. 10. The f_t, t- and r, t-diagrams for a spherical earth. The polar distance of the station is taken as $b = 61°$, corresponding to Guadalupe Island. The diagrams are drawn for the travelling point source at 40° and 50°S. The inflection points are marked and one of the tangents is drawn. The curves in the upper figure gives F_t against $(W/R)\,t$ for the two assumed latitudes of generation. The scales in real time and in frequency units c/ks have been drawn for $W = 30$ knots. The observed points are for the middle sequence of spectral peaks (Figs. 4 and 5).

depend upon the frequency *resolution* ΔF and will be large if the resolution is high, i.e. ΔF is small. In our work Δf is 4 c/ks, $f_0 = 50$ c/ks, hence $\Delta F = \Delta f/f_0 = 0{\cdot}08$ (equation (6)). Fig. 9 is drawn for $b = 61°$ (co-latitude of Guadalupe), $c = 140°$, $W = 30$ knots. For the tangent ray through the inflection point, and two subsequent tangent rays, we have

F_t	1·0	1·1	1·2
t_1	108^h	130^h	150^h
r_t	130°	107°	100°
ϕ_t	− 118°	− 82°	− 70°
h_i, h, h	0·41	0·78	0·64
Equation (9)	6·7	5·7	4·7

The conclusion is that at *any* time the energy density of the frequency corresponding to the tangent ray is amplified, but that the earliest of all possible tangent rays (the inflection point ray) is amplified more than subsequent tangent rays. We might then expect the observed spectral peaks to correspond to these tangent rays. In physical terms, the prominent waves are those whose group velocity equals the rate of approach of the storm toward the station somewhere along its path.* The existence of such a "group velocity peak" has been noted by ECKART (1953) for waves generated by a moving gust, and is implicit in his equation (35).

The constructions in Fig. 10 are for storms 40°S and 50°S and the wave station at 29°N. The computed f_t, t-curves in the upper figure are obtained by drawing tangents to the storm paths to where they intersect $r = 0$. The cotangent of the angle between $r = 0$ and the tangent line equals F_t at the time given by the intersection. The observed points correspond to the central sequence of spectral peaks. For a storm path along 50°S the storm was at the inflection point on 23 Sept., 0800 hr at a distance of 130°. The waves were recorded $4\frac{1}{2}$ days *after* the storm had passed to the south of the station. This is hardly synoptic information! The computed distance of generation is similar to that derived for an assumed point source. We conclude that according to the present hypothesis of a moving point source the earliest arrivals of swell observed off North America originated in the Indian Ocean at a distance of 120–140° (Fig. 6).

DISCUSSION

We have attempted to interpret the Guadalupe spectra on the basis of two hypotheses, both severely oversimplified: (1) generation by an instantaneous point source; (2) by a point source moving with constant speed along a fixed latitude. Both hypotheses lead to wave trains of gradually increasing frequency but for altogether different reasons. In the case of (1) the increase in frequency is due to dispersion; i.e. low frequencies travel faster than high frequencies, and arrive earlier. The essence of the moving-point hypothesis is that one frequency is amplified over all others: that frequency whose group velocity equals the rate at which the storm approaches the station (tangent rays on a distance-time graph).

The gravest observed frequency (from the first arrivals) are likewise determined by quite different considerations. In hypothesis (1) the limit is imposed by the generation spectrum: winds of velocity U cannot effectively generate waves whose *phase* velocity C exceeds U. In the latter case the *group* velocity $\frac{1}{2}C$ of the first arrivals is determined by the storm's rate of approach. In general this is less than the storm's rate of travel, W, unless the storm is moving along a great circle route towards the station. For an east-west movement there is a point where a great circle through the station is tangent to the storm's latitude circle, and the amplified frequency, $g/(4\pi W)$, is the gravest possible (the "inflection ray" on the distance-time graph). Suppose the storm is at 50°S; the great circle through the station can be drawn only if the station is south of 50°N. If it is north of 50°N then the gravest frequency is somewhat less than $g/(4\pi W)$ in accordance with equation (5b). Thus the gravest frequencies are of the order

$$g/(2\pi U) \text{ or } g/(4\pi W)$$

---

*OLIVER and EWING (1957) apply similar considerations to account for the observed increase in the frequency of waves and microseisms from hurricane Dolly. They refer to LAMB's discussion of the ship wake problem, being able to neglect the earth's curvature on account of the proximity of the storm.

according to the two hypothesis. Typical values for Antarctic cyclones are $U = 50$ knots, $W = 30$ knots. Both criteria lead to frequencies of the order of 1 cycle in 20 sec, as observed.

All of this discussion depends, of course, upon the existence of unobstructed great circle routes. One unobstructed great circle can be drawn from Guadalupe passing just east of New Zealand and tangent to 55°S at a point in the Indian Ocean 130°E longitude (see Fig. 6). Another great circle can be drawn through the Tasman Sea tangent to 50°S at a point in the Indian Ocean south of Western Australia. These regions are among the stormiest in existence. The window through the Tasman Sea is narrow, and the waves must be scattered by South Pacific islands. A storm moving eastward would be " seen " only briefly through the Tasman Sea window, and a proper hypothesis might be some combination of the instantaneous and moving source hypotheses. In all events, the observed frequency shift by less than 10 per cent per day is consistent only with very distant areas of generation, regardless of which of the two hypotheses is followed, and the estimated distance of 130° is consistent with either of the two routes. It is therefore tentatively suggested that the very low, long early arrivals came from the Indian Ocean. We are puzzled by the sharp increase in the spectral peak on the morning of November 6 (see Fig. 3), corresponding to the fifth point of the central sequence (Figs. 5 and 10). The corresponding tangent ray gives a distance 100° for the storm at 50°S. Could this represent an arrival of an unobstructed wave train from a storm passing over New Zealand into the Pacific Ocean ?

N. F. BARBER has kindly examined the weather maps drawn by the New Zealand Meteorological Office for the period in question. Unfortunately the meteorological situation was not clear-cut. The computed travel times are in doubt by, say ± 20 per cent or ± 2 days, and no definite correlations can be made. A 30–35 knot wind over a fetch of 500 nautical miles on 17 Sept. 1957 centred at 140°E is consistent with a route to the east of New Zealand, and may have been responsible for the central sequence. We prefer to postpone any detailed comparisons with meteorological data until the International Geophysical Year. For that purpose we are establishing a wave station west of San Clemente Island which will include a measure of wave direction and beam width in addition to the features discussed in this paper.

For the British records there is no unobstructed great circle corresponding to the inflection point arrival. Setting $b = 40°$, $c = 140°$, $\phi = -50°$ gives $r = 108°$,

$$(dr/dt)/W = \sin b \sin c \sin \phi = 0{\cdot}47$$

for the earliest unobstructed tangent arrivals. The corresponding frequencies of something like 100 c/ks are much higher than those observed for the first arrivals. In the case of the Bermuda records any unobstructed southern storm is east of the station, and receding from it. The tangent ray hypothesis is therefore inapplicable to the Atlantic records, and this detracts from its attractiveness. There is the possibility that reflection from ocean boundaries is an important factor, especially for the very long, low initial arrivals.

There has been no discussion as to why the spectral bands should reach their maximum development at frequencies of about 65 c/ks, or concerning the existence of a steady 15–16 sec "hum", if such a hum does in fact exist. In an average taken over many storms, the effect of the amplification spikes (Fig. 9) is erased, and an explanation must be sought along different lines. The generation spectrum is peaked at frequencies significantly higher than 65 c/ks, but it is possible that the shift toward lower frequencies resulting from selective attenuation may account for the observed values.

Acknowledgements—We are indebted to F. PETERSON, M. J. TUCKER and JOHN SWALLOW for their part in the Guadalupe measurements. DOROTHY SHUMWAY and MARGARET COVHER have been largely responsible for programming and carrying out the numerical analyses on the computer facilities at Convair, San Diego, and we are greatly indebted for the use of these facilities. CARL ECKART and MOHAMED HASSAN have given advice with regard to the problem treated in the appendix. We are also indebted to N. F. BARBER and C. PALMER for discussion and advice.

University of California
Scripps Institution of Oceanography, California

Contribution from the Scripps Institution of Oceanography, New Series No. 955

REFERENCES

BARBER N. F. and URSELL F. (1948) The generation and propagation of ocean waves and swell; I. Wave periods and velocities. *Phil. Trans. Roy. Soc.* A **240**, 527–560.

DONN W. L. (1949) Studies of waves and swell in the Western North Atlantic. *Trans. Amer. Geophys. Union* **30**, 507–516.

ECKART C. (1948) The approximate solution of one-dimensional wave equations. *Rev. Mod. Phys.* **20**, 399–417.

ECKART C. (1953) The generation of wind waves on a water surface. *J. Appl. Phys.* **24**, 1485–1494.

HYDROGRAPHIC OFFICE (1944) Breakers and surf, Principles in forecasting. *H. O. Pub.* 234.

LAMB H. (1932) *Hydrodynamics.* Dover Publications, New York.

MUNK W. H. (1947) Tracking storms by forerunners of swell. *J. Met.* **4**, No. 2, 45–57.

MUNK W. H., SNODGRASS F. E. and TUCKER M. J. (In press) Spectra of low frequency waves. *Bulletin of the Scripps Institution of Oceanography.*

OLIVER J. and EWING M. (1957) Microseisms in the 11- to 18-second period range. *Bull. Seism. Soc. Amer.* **47**, 111–127.

RUDNICK P. (1951) Correlograms for Pacific Ocean waves. *Proc. of the Second Berkeley Symposium on Mathematical Statistics and Probability* pp. 627–638.

SNODGRASS F., MUNK W. and TUCKER M. J. (In press) Offshore recording of low frequency ocean waves. *Trans. Amer. Geophys. Union.*

TUKEY J. W. (1949) The sampling theory of power spectrum estimates. *Symposium on Applications of Autocorrelation Analysis to Physical Problems* pp. 47–67. Woods Hole, Massachusetts.

WIEGEL R. L. and KIMBERLEY H. L. (1950) Southern swell observed at Oceanside, California. *Trans. Amer. Geophys. Union* **31**, 717–722.

APPENDIX

The problem is to evaluate

$$\mu(F) = \frac{\sin c}{r \sin r F'} \tag{10}$$

near the tangent ray

$$r_t' = r_t/x_t, \qquad x = \phi - \phi_1. \tag{11}$$

The accent denotes differentiation with respect to ϕ (or x), and the subscript " t " refers to evaluation at the tangent point. ϕ_1 and ϕ_t are constants. Differentiating $F = -x \sin c/r$ (equation (5)) and using $r_t' x_t = r_t$ leads to

$$F_t' = 0, \qquad F_t'' = x_t r_t^{-2} r_t'' \sin c, \qquad F_t''' = x_t r_t^{-2} r_t''' \sin c. \tag{12}$$

To evaluate F' we eliminate ξ from the Taylor expansions

$$F = F_t + \xi F_t' + \tfrac{1}{2}\xi^2 F_t'' + \tfrac{1}{6}\xi^3 F'''_t,$$

$$F' = F_t' + \xi F_t'' + \tfrac{1}{2}\xi^2 F_t'''.$$

For the ordinary tangent ray the last term for each series is dropped, and $F_t' = 0$. The result is

$$F' = [2(F - F_t) F_t'']^{\frac{1}{2}}. \tag{13}$$

But for the tangent ray through the inflection point $r_t'' = F_t'' = 0$. Eliminating ξ now gives

$$F' = (9/2)^{\frac{1}{3}} (F - F_t)^{\frac{2}{3}} (F_t''')^{\frac{1}{3}}. \tag{14}$$

The admittance factor μ can now be evaluated in terms of x and r making use of (12) :

$$\mu^{-2} = 2\sin^2 r_t (F - F_t)\, x_t\, r_t''/\sin c,$$

$$\mu_i^{-3} = (9/2)\sin^3 r_t (F - F_t)^2\, x_t\, r_t\, r_t'''/\sin^2 c.$$

Differentiating equation (4) and using (7) and (5a) leads to

$$r_t' = -\sin c/F_t$$

$$r_t'' = \sin b \sin c \operatorname{cosec}^2 r_t (\sin r_t \cos\phi_t - r_t' \cos r_t \sin\phi_t)$$

$$r_i''' = r_i'(r_i'^2 - 1), \qquad r_i' = \sin c,$$

so that finally

$$\mu = h(F - F_t)^{-\frac{1}{2}}, \qquad \mu_i = h_i(F - 1)^{-\frac{2}{3}} \tag{15}$$

where

$$h^{-2} = 2 r_t \sin b (\cos r_t \sin\phi_t + F_t \sin r_t \cos\phi_t/\sin c)$$

$$h_i^{-3} = (9/2)\cot^2 c\, r_i^2 \sin^3 r_i.$$

Printed in Great Britain by The Salisbury Press Ltd., Publicity House, Wilton Road, Salisbury, Wilts. (6904)

(888)

BULLETIN OF THE AMERICAN ASSOCIATION OF PETROLEUM GEOLOGISTS
VOL. 41, NO. 12 (DECEMBER, 1957), PP. 2723-2751, 16 FIGS.
Reproduced by Permission

MINOR INTERNAL STRUCTURES OF SOME RECENT UNCONSOLIDATED SEDIMENTS[1]

D. G. MOORE[2] AND P. C. SCRUTON[3]
San Diego, California, and Tulsa, Oklahoma

ABSTRACT

Widespread occurrence of several different minor sedimentary structures in shallow-water Gulf of Mexico sediments has been shown by more than 2,000 cores and bottom samples. Minor internal structures in two areas, one off the east side of the Mississippi River Delta and the other along the central Texas coast, were found to be similar. Deposits in these two areas were subdivided into those containing: (1) regular layers (thin beds or laminations), (2) irregular layers (rough or crude layers and lenses), (3) mottles (discontinuous lumps, tubes, and pockets), and (4) structureless homogeneous sediments, depending on the principal type that occurs.

Areal distributions of these different structures in the surficial sediments are mappable. Similar sedimentary structures and sequences of structures occur in the open gulf and in the bays and sounds. In the open gulf the structures occur in wide bands, and the sequences are developed through wide ranges of water depths; in the bays and sounds the bands generally are narrower, and the sequences are compressed into much smaller ranges of water depths.

The different types of structures are formed on or near the depositional surface, contemporaneous or nearly contemporaneous with deposition. The differences between depositional environments which produce the various structures are differences in: (1) sediment sources, (2) in physical processes and their intensities, and (3) rates of deposition. Regular layers are characteristic of areas of rapid deposition and/or relatively few bottom-living animals; they are either primary—formed by fluctuations of sediment, or secondary—formed by wave or current winnowing. Irregular layers and mottles are mostly secondary features, formed mainly by bottom-living animals altering existing sediments. Homogeneous deposits are either primary or secondary; they form by extremely rapid deposition, uniform deposition, or by complete secondary reworking. The appearance of many normal marine sediments is due in large measure to burrowing and crawling organisms.

Structures similar to those in presently forming sediments of the Gulf of Mexico apparently were developed in rocks of all ages when environmental conditions were proper. Knowledge of how these structures form, why they vary, and the relationships between them furnishes a valuable key for interpreting deposition of ancient rocks.

INTRODUCTION

Project 51 of the American Petroleum Institute, for the study of recent continental shelf and nearshore marine sediments in the northern Gulf of Mexico, has been active at the Scripps Institution of Oceanography since 1951. Two principal areas have been studied; one is on the east side of the active Mississippi River Delta, and the other is a region of protected bays, barrier islands, and open shelf on the central Texas coast near Rockport (Fig. 1, also Figs. 8 and 9 for detail). During the course of these studies more than 2,000 sediment samples have been collected, most of which were cores. Processing of these cores and other samples included visual study of their minor internal structures.[4]

---

[1] Contribution from the Scripps Institution of Oceanography by New Series No. 956. This investigation was supported by a grant from the American Petroleum Institute, Project 51. Manuscript received, August 9, 1957.

[2] U. S. Navy Electronics Laboratory.

Pan American Petroleum Corporation. *Acknowledgments*. Field work and preliminary composition of this study were done while the writers were associated with the Scripps Institution of Oceanography. They are indebted to the Navy Electronics Laboratory and to the Pan American Petroleum Corporation for time and facilities to complete the manuscript. Thanks also are due to F. P. Shepard for assistance in the Texas coast field work, to R. H. Parker for valuable help in the laboratory tank experiments, and to D. M. Poole who photographed many of the cores studied in this program. The manuscript was read and criticized by H. A. Bernard, P. A. Dickey, M. A. Hanna, N. A. Riley, and R. D. Russell of the A.P.I. 51 Advisory Committee and by F. P. Shepard and Tj. H. van Andel, Project 51 directors.

To many geologists, the small internal structures of sedimentary rocks, formed when the sediments were first deposited and still soft and plastic, are among their most interesting and puzzling features. One of the purposes of this paper is to describe those minor internal structures that occur in shallow-water deposits of the Gulf of Mexico and to discuss their distributions and origins. It is hoped this discussion will contribute to a better understanding of these structures in more ancient rocks. In addition, study of these sedimentary features has shown that their type and character are closely related to the sedimentary environments in which they are formed. These structures are of such widespread distribution and occurrence, both in recent sediments and in older rocks, as to deserve general attention in environmental interpretation.

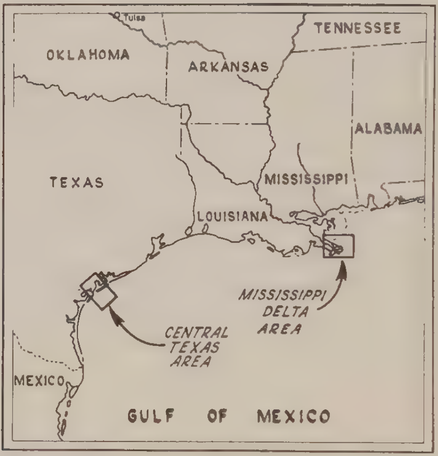

FIG. 1.—Map of northwest Gulf of Mexico, showing locations of study areas.

Some types of original sedimentary structures such as bedding, cross-bedding, ripple marks, animal tracks, shrinkage cracks, flow-casts, and features resulting from contemporaneous (wet) deformation are described and discussed in an extensive literature. Several of the minor structures discussed here also have been noted previously under various names, but they have not been discussed as extensively.

In the literature on minor structures such works as those of McKee (1939) and Thompson (1937) are noteworthy, because of the emphasis they laid on understanding of the processes that produce original structures, and the relationships these processes bear to the general sedimentary environment. Both these workers later were successful in applying their understanding of the processes that produce different structures to the interpretation of ancient rocks (McKee, 1954; Thompson, 1949). Recent work by other geologists also has emphasized the importance of describing minor sedimentary structures and determining the environmental processes that produce them. In studying sediments of the tidal flats of the Dutch Wadden Sea, van Straaten (1951) ascribed the minor structures within the sediments to processes of these depositional environments and used this as background for interpreting older (Devonian) rocks. Stewart (1956) described some minor contorted structures in exposed sand flats of a tidal delta and used laboratory experiments to demonstrate their formation by "air-heave." This is a mechanism active in only a few sedimentary environments.

---

[4] Minor internal structures and small original sedimentary structures are terms used here interchangeably to cover original lithologies or fabrics that are visible to the naked eye or with a hand lens. They may be of primary origin or developed secondarily, but in either case, they are formed *on* or *just beneath* the depositional surface. As these terms are used here, they exclude fabrics or structures of later, diagenetic, origin such as those produced by chemical alteration or reorientation of particles through compaction or tectonic forces.

Scruton (1955) has shown that depositional environments of the Mississippi River Delta differ from one to another because of variations between three fundamental factors. These factors are: (1) the sources of sediment, (2) the processes (physical and chemical) that occur in them and their intensities, and (3) the rate at which deposition occurs. These three basic factors are dynamic, and they interact with each other in a complicated way to govern the kinds and amounts of sediments deposited. Moore (1955) and Shepard and Moore (1955) have demonstrated that these same basic factors are responsible for variations in sediments in the central Texas coastal area. Rate of deposition in this area is much less variable than in the Mississippi Delta, however, and the fundamental importance of this environmental factor is therefore less striking.

DESCRIPTION

The minor structures that have been studied are visible in the sediments primarily because of textural variations, and secondarily because of differences in composition and color. The structures have been subdivided into four basic types depending on their appearance on the flat surface of a cut or of a longitudinally sectioned core. The four basic types are: (1) regular layers, (2) irregular layers, (3) mottles, and (4) homogeneous sediments (Fig. 2).

No attempt has been made to fit these features into any of the proposed size classifications of sedimentary structures (cf. Pettijohn, 1949, p. 120; McKee and Weir, 1953; Ingram, 1954; Gray, 1955). However, where amenable to such classification, they would be called medium, thin, or very thin beds following Gray (1955, p. 147), as they generally are less than 10 cm. in thickness.

LAYERS

Layered structures, as the name implies, are layers or bands of coarse- and fine-grained sediments (Fig. 2), which may alternate in any order. These structures are tabular or lenticular in three dimensions. Individual layers generally have sharp or relatively sharp contacts with adjacent material and therefore

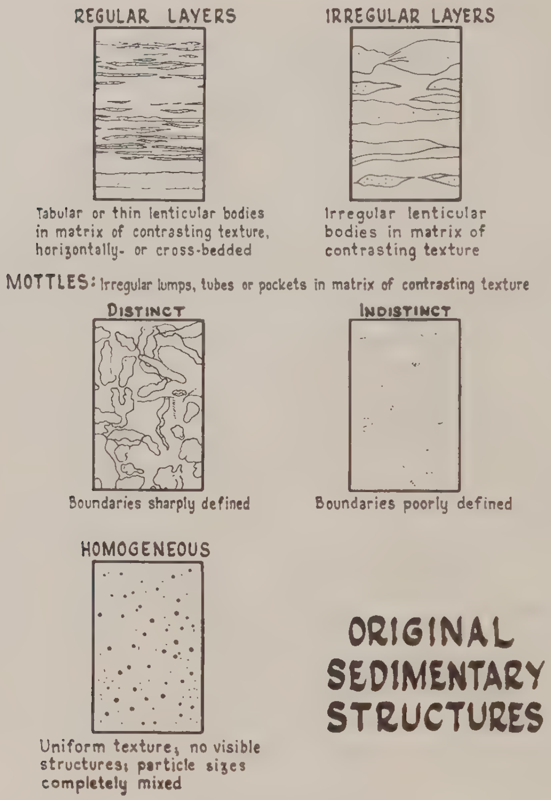
REGULAR LAYERS
Tabular or thin lenticular bodies in matrix of contrasting texture, horizontally- or cross-bedded
IRREGULAR LAYERS
Irregular lenticular bodies in matrix of contrasting texture
MOTTLES: Irregular lumps, tubes or pockets in matrix of contrasting texture
DISTINCT
Boundaries sharply defined
INDISTINCT
Boundaries poorly defined
HOMOGENEOUS
Uniform texture; no visible structures; particle sizes completely mixed
ORIGINAL SEDIMENTARY STRUCTURES

FIG. 2.—Basic types of minor internal structures.

stand out as distinct units from the general mass of sediment if it is uniform, or from adjacent layers if the sediment is variable. Two types of layered structures are recognized: (1) regular, and (2) irregular (Figs. 2–4).

REGULAR LAYERS

Regular layers have relatively uniform thickness in core section, and adjacent layers or sets of layers usually are nearly parallel. The layers are horizontal or inclined, and may be slightly curved. Thicknesses of individual layers generally range from a fraction of a millimeter to about 10 centimeters, and the thinnest ones usually lens or pinch out in core section. Regular layers may be relatively homogeneous in texture, but many coarse-grained layers, particularly the thicker ones, are thinly laminated or cross-laminated internally (Fig. 3). In general, regular layers present a neat, orderly, parallel or sub-parallel appearance, regardless of their thickness.

IRREGULAR LAYERS

In contrast to regular layers, irregular layers present a disorganized appearance. Thickness of irregular-layered structures is markedly non-uniform in core

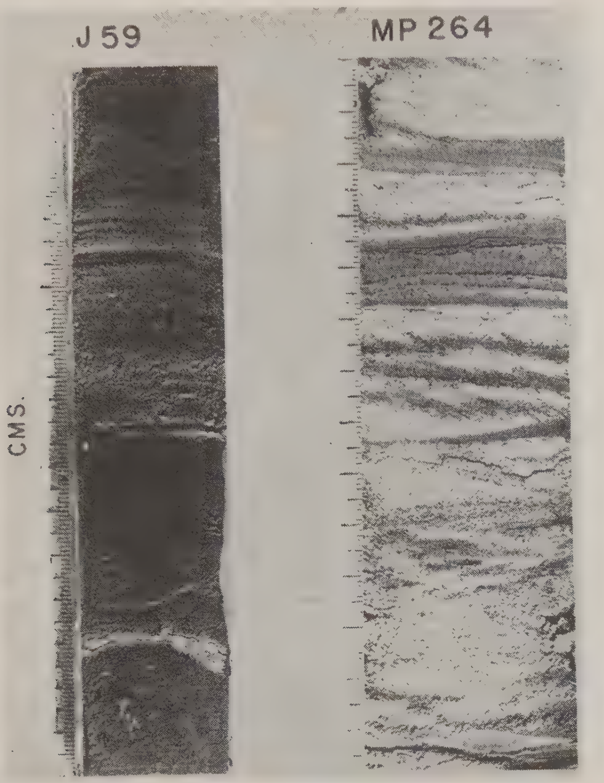

FIG. 3.—Regular layers. Cores showing general regularity of bedding; also cross-bedding in thicker coarse layers.

section, and individual layers or sets of layers may have little parallelism (Figs. 2, 4). They generally appear relatively jumbled and disorderly, but they have distinct elongation in a horizontal plane. They are equally irregular in three dimensions, but are crudely lenticular or tabular. Irregular layers usually are about $\frac{1}{2}$–3 centimeters thick; they have less range of thickness than regular layers, rarely are either very thin or very thick, and commonly wedge or lens out in core section. Normally irregular layers are relatively coarse in a finer-grained matrix, but they may be fine in a coarser matrix. Their internal texture usually is somewhat heterogeneous, rarely is uniform, and they seldom have internal lamination.

MOTTLED STRUCTURES

Mottled structures, or mottles, consist of peculiar, irregularly shaped lumps, lenses, pockets, tubes, or pods of sediment randomly enclosed in a matrix of contrasting texture (Figs. 2, 5). Color contrast alone, by this terminology, does not constitute a mottled structure. The contacts between contrasting textures generally are sinuous. Distributions of these bodies, as well as their shapes, are highly irregular, thereby imparting a mottled appearance to core sections. Mottled

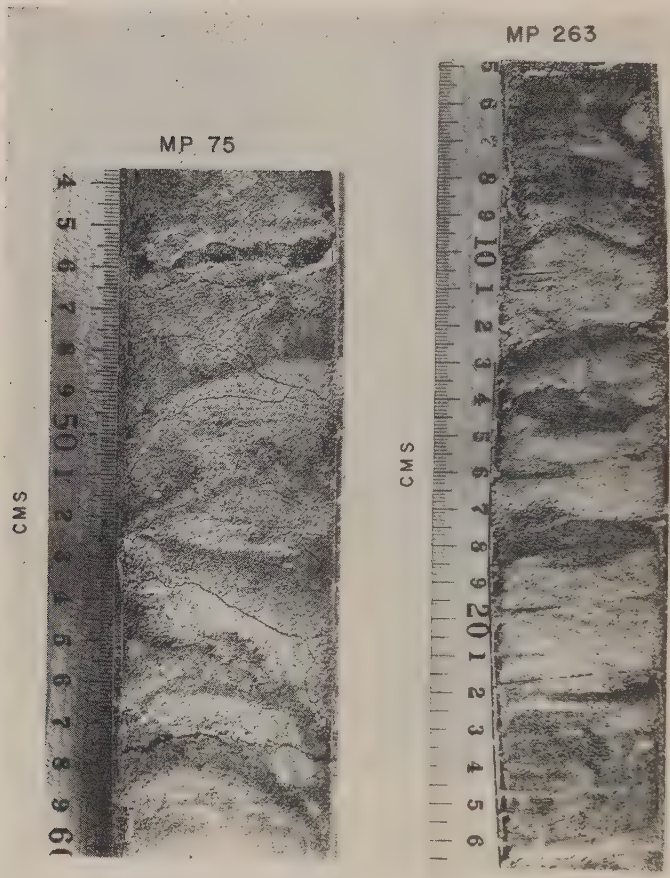

FIG. 4.—Irregular layers. Cores showing irregular shapes of layers and absence of cross-bedding.

structures commonly are a few millimeters to several centimeters in diameter. In cross section, individual lumps are ordinarily, but not necessarily, circular.

Texture of the irregular lumps, pods, tubes, and lenses may be either coarser or finer than the matrix, or there may be nearly equal distribution between coarse and fine lumps in the sediment. Examples of coarse lumps in a fine matrix and fine lumps in a coarse matrix are shown in Figure 5. Textures of individual structures range from clean sand in a fine matrix to poorly sorted sand in a matrix of silty clayey sand and from clay in a clean sand to sandy clay in poorly sorted sand. Shells and shell fragments generally are present but commonly are not.

There is no tendency toward horizontal alignment of typical mottles. In fact, the contrary ordinarily is the case, and there appears to be a preferred vertical orientation. Mottled structures become indistinguishable from irregular layers where there is some horizontal alignment and an increase in regularity.

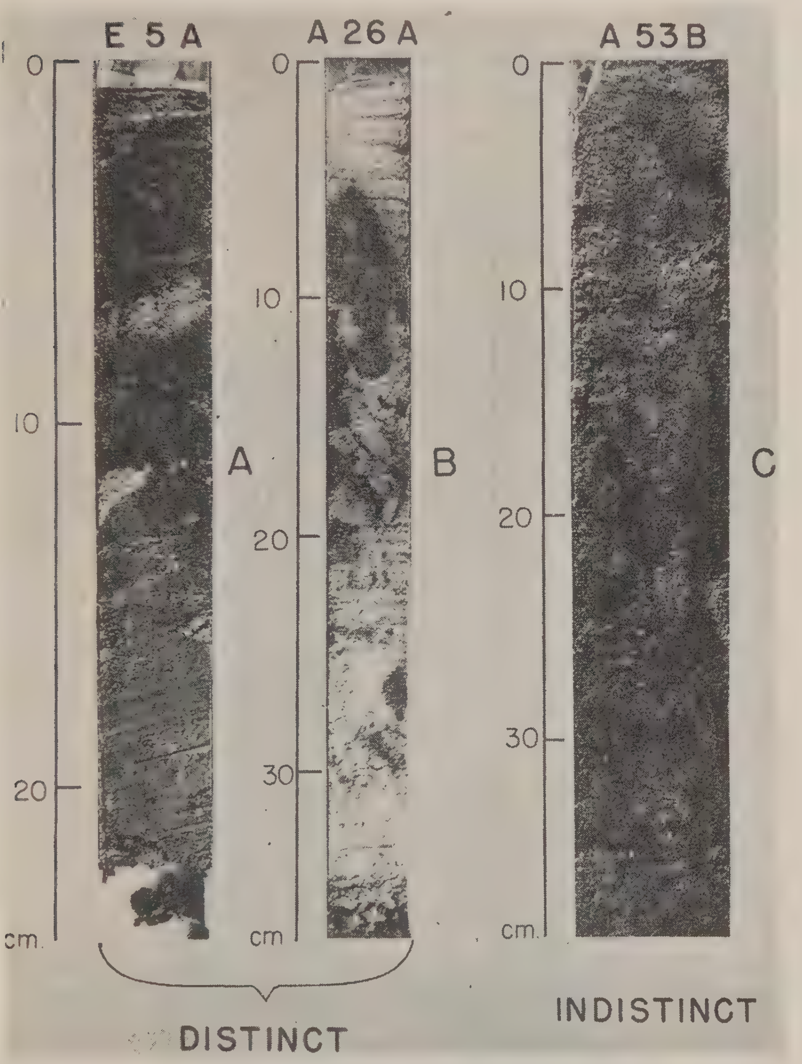

Fig. 5.—Mottled structures. Examples of coarse mottles in fine-grained matrix (A), fine-grained mottles in coarse matrix (B), and approximately equal distribution between coarse and fine sediments in mottles and matrix (C). Striations on E5A and A26A are knife marks.

True mottles are not produced by distortion of soft sediments in sampling. They have been found with all types of sampling equipment and are well developed where there is no question of the undisturbed nature of the sample.

Two types of mottled structures have been recognized: (a) those with distinct boundaries, and (b) those with indistinct boundaries (Figs. 2, 5). Their differentiation is based on the amount of textural gradation between lumps and matrix; there is no precise division between the types, and in places they constitute a continuous series. Sediments with indistinct mottling in turn grade into homogeneous sediments with further decrease in sharpness of contact and textural contrast between lumps and matrix.

HOMOGENEOUS SEDIMENTS

Sediments with no visible internal structures complete the list of types normally found in the unconsolidated shallow marine deposits of the two Gulf Coast areas. These sediments are massive, and their relatively uniform texture may be

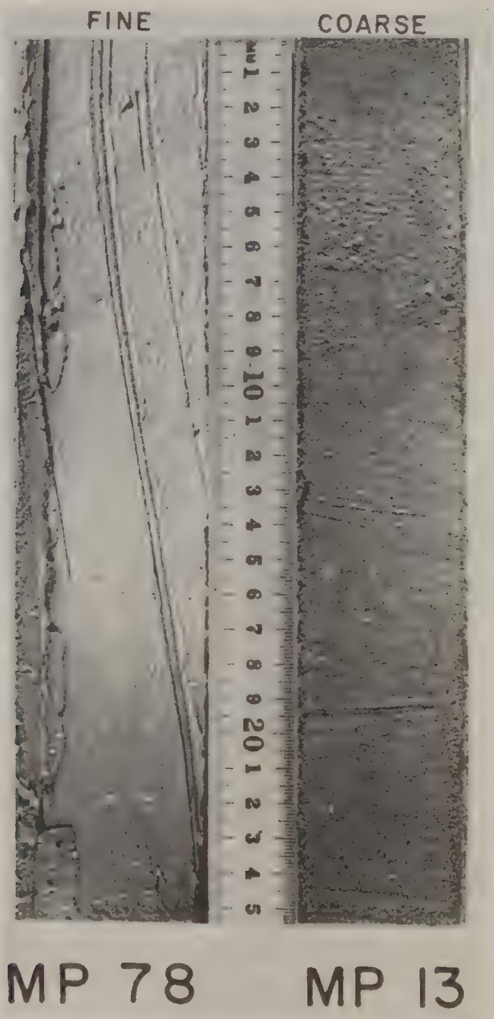

FIG. 6.—Homogeneous deposits. Clay and sand. Striations are knife marks.

fine-grained (clays and silty clays), coarse-grained (sands), or any intermediate texture (Figs. 3, 6). Homogeneous sediments approach "textural maturity" (Folk, 1951) in the petrographic sense as the proportion of coarse material increases.

LATERAL CONTINUITY

Duplicate and multiple cores between which layering might be traced were taken within small areas to determine the amount of lateral continuity in layered structures. Individual mottled structures by definition are discontinuous.

Short duplicate cores from 200 stations in San Antonio Bay, Texas, were compared by F. P. Shepard (1953) to determine continuity of sandy zones in that area. Generally the cores were collected only a few feet apart and at most only a few score feet. These observations showed that there is little tendency for irregular layers to persist laterally. Sixty of the 200 stations contained distinctive irregular layers, but in only nine instances were layers repeated at the same or approximately the same depth in the nearby duplicate core.

A double barrel, or bident, corer was used for collections in both the Mississippi Delta and Texas areas. Barrels of the bident corer were mounted 32 inches apart, giving samples with constant lateral separation. These samples showed that individual irregular layers, even though well developed in one core, could not be traced with certainty to the adjacent core. In most instances they also showed that the zones in which groups of irregular layers occurred could be traced from core to core, although in lower San Antonio Bay even zones could not be traced with certainty (Fig. 7).

To test the continuity of regular layers, multiple cores were taken in "delta-front silts and sands" and "pro-delta silty clays" of the Mississippi Delta (Scruton, 1955, Fig. 1). Sixteen of these cores were taken in a rectangular pattern 1 meter apart in the bay between Main Pass and Baptiste Collette Bayou. Some of the individual regular layers were recognizable in as many as 9 or 10 of the 16 cores. Some groups of layers or zones were traceable throughout all of the 16 cores. Continuity of the regular layers in these very shallow-water samples was greater than that of regular layers in bident samples from "pro-delta silty clays" that are forming farther seaward in deeper water. In the silty clays the thin, individual, regular layers rarely could be traced between bident cores, but zones or groups of layers usually extend from core to core.

Because the deposits are under water, trenching such as used by Thompson (1937) or McKee (1939) to test lateral development is not possible. However, methods other than coring were used in the continuity studies, and they have yielded similar results. A large van Veen sampler (2 cubic-foot clam shell) was used on the continental shelf offshore from the Texas barrier islands. These large samples are virtually undisturbed when taken in fine sediments, and many showed zones of discontinuous mottled structures traceable across the entire sample. Some samples contained large mottles of sand up to 4 or 5 inches in diameter which might be misinterpreted as thick layers in small-diameter cores.

Careful testing for small changes in bottom sediment was made in shallow water outside small distributaries of the Mississippi Delta. This was done by feeling the sediment with the hands, as it is impossible to see the bottom through the muddy water. It was found that thin, uniformly shaped, discontinuous lenses of more sandy material occurred on and below the sediment surface. These thin lenses ranged in diameter from a few inches to several yards.

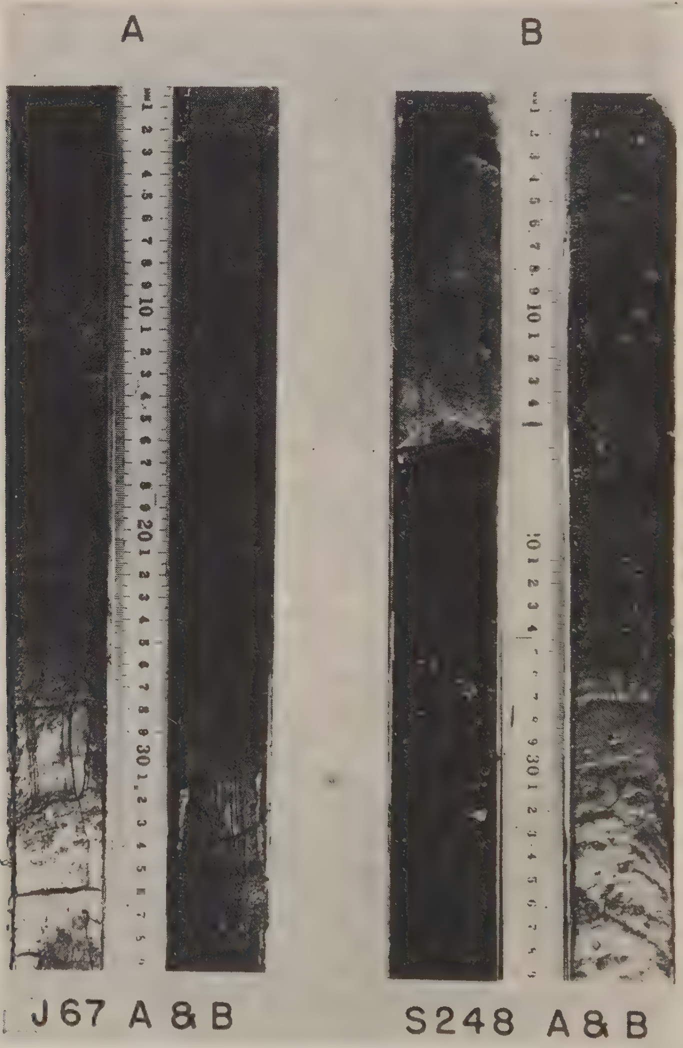

FIG. 7.—Bident cores. Pair A shows lateral continuity of zones; pair B shows lack of continuity.

In summary, it has been found that regular-layered structures may extend laterally for several feet, irregular layers generally are of small lateral extent (a few inches at most), and mottles have essentially no lateral continuity. Groups of these structures form zones which usually are traceable much farther than individual structures, commonly for 3 or 4 feet and exceptionally much farther.

OCCURRENCE OF MINOR INTERNAL STRUCTURES IN MISSISSIPPI DELTA AND TEXAS COASTAL AREAS

REGULAR LAYERS

Coarse regular layers are among the most prominent visible features in the beds surrounding the entire Mississippi Delta. They occur in a band about 2–8 miles wide that extends from the shoreline seaward into water depths of about 20 fathoms (Fig. 8). These structures are most abundant, thickest, coarsest, best sorted, most continuous, and contain most internal lamination and cross-lamination in water less than 6–8 feet deep. With increasing depth of water seaward they become progressively less abundant, finer-grained, more poorly sorted, thinner, and apparently have less lateral continuity. The zones into which coarse layers

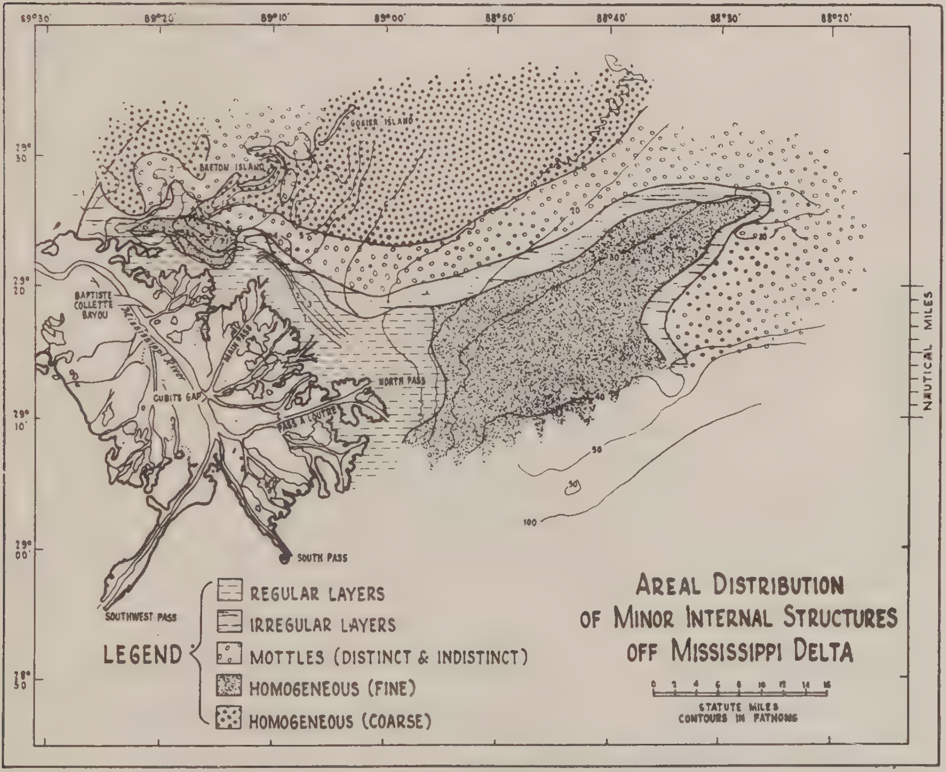
69°30'
89°20'
89°10'
89°00'
88°50'
88°40'
88°30'
88°20'
29° 30'
29° 20'
29° 10'
29° 00'
28° 50'
GOSIER ISLAND
BRETON ISLAND
BAPTISTE COLLETTE BAYOU
Mississippi River
MAIN PASS
CUBITS GAP
NORTH PASS
PASS A LOUTRE
SOUTH PASS
SOUTHWEST PASS
10
20
30
40
50
100
NAUTICAL MILES
LEGEND
REGULAR LAYERS
IRREGULAR LAYERS
MOTTLES (DISTINCT & INDISTINCT)
HOMOGENEOUS (FINE)
HOMOGENEOUS (COARSE)
AREAL DISTRIBUTION OF MINOR INTERNAL STRUCTURES OFF MISSISSIPPI DELTA
0 2 4 6 8 10 12 14 16
STATUTE MILES
CONTOURS IN FATHOMS

FIG. 8.—Distributions of minor structures north and east of Mississippi Delta.

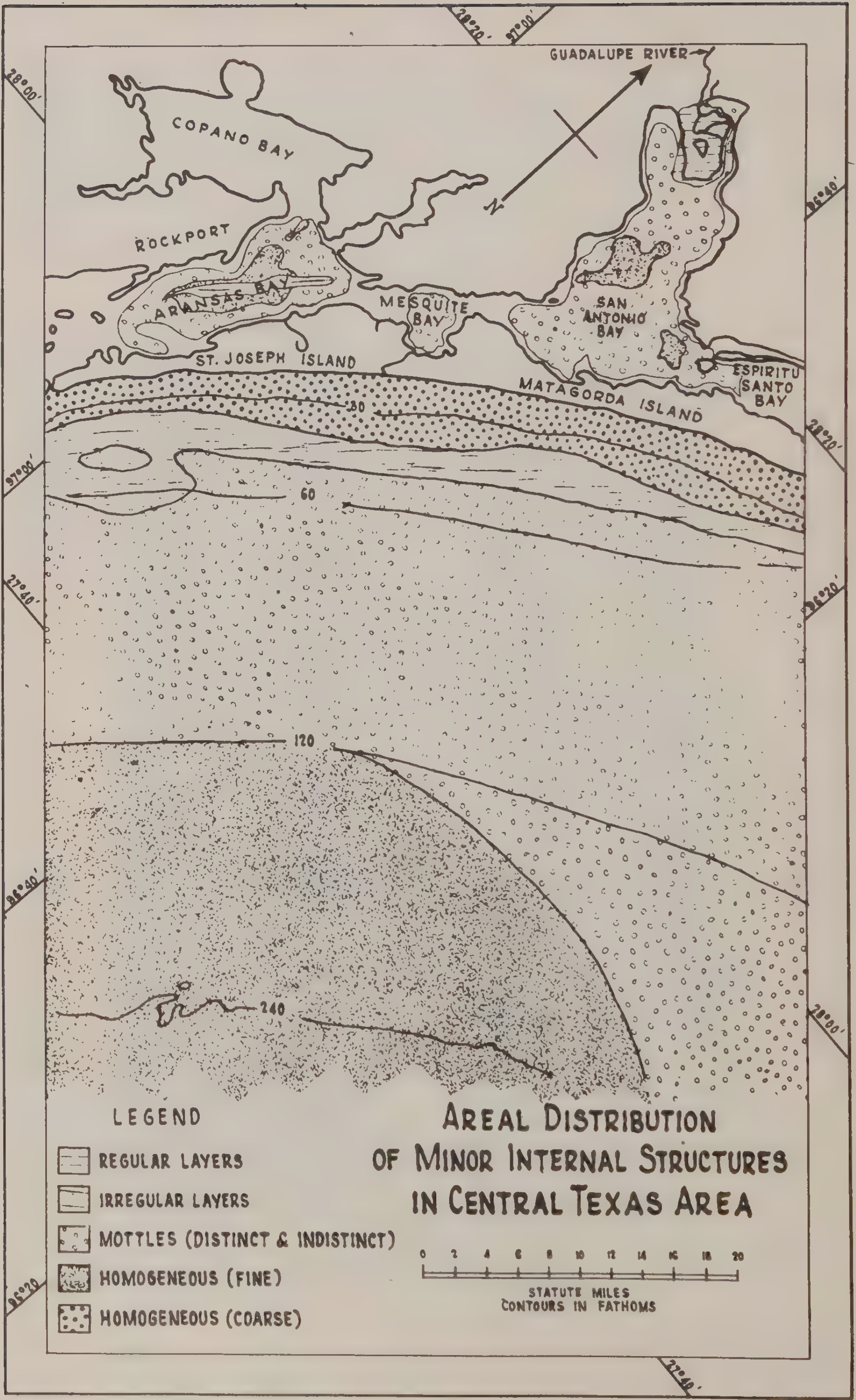
28°20'
97°00'
GUADALUPE RIVER
N
28°00'
COPANO BAY
ROCKPORT
ARANSAS BAY
MESQUITE BAY
SAN ANTONIO BAY
ESPIRITU SANTO BAY
ST. JOSEPH ISLAND
MATAGORDA ISLAND
96°40'
30
28°20'
97°00'
60
27°40'
96°20'
120
96°40'
240
28°00'
LEGEND
REGULAR LAYERS
IRREGULAR LAYERS
MOTTLES (DISTINCT & INDISTINCT)
HOMOGENEOUS (FINE)
HOMOGENEOUS (COARSE)
AREAL DISTRIBUTION OF MINOR INTERNAL STRUCTURES IN CENTRAL TEXAS AREA
0 2 4 6 8 10 12 14 16 18 20
STATUTE MILES
CONTOURS IN FATHOMS
96°20'
27°40'

FIG. 9.—Distributions of minor structures in central Texas bays, lagoons, and Gulf of Mexico.

cluster also become fewer and thinner seaward into deeper water. The gross sediment, therefore, becomes homogeneous seaward. Some regular coarse layers also occur in the deep water of lower Breton Sound just inside the shallow bar extending southwest from Breton Island (Fig. 8).

In the Texas area (Fig. 9) regular layered structures rarely occur on the inner shelf and are prominent only in the Guadalupe Delta of upper San Antonio Bay. Conditions there are similar to those of the Mississippi Delta but on a much smaller scale.

Coarse regular layers usually are similar in composition to a concentration from the adjacent finer sediments. Around the Mississippi Delta they consist mainly of silt with sand. In shallow water there also may be layers of woody material ("coffee grounds") some of which are up to 50 centimeters thick.

In lower Breton Sound the composition of coarse and fine layers reflects two sediment sources. The fine sediment comes from the river, but the coarse material is derived from the sandy bar nearby. In this area the coarse layers consist mostly of sand, silt, and usually some shell fragments.

IRREGULAR LAYERS

Around the Mississippi Delta irregular-layered structures occur most abundantly in a relatively narrow band encircling the fine-grained delta deposits (Fig 8; also Scruton, 1955). This narrow band merges in part with the seaward limit of abundant occurrence of regular-layered structures, but departs from the area of regular layers in deeper water on the shelf and continues out around the finer deposits. Irregular layers also occur in southern Breton Sound. The narrow band in which these structures are forming is more or less continuous in water depths from about 6 feet seaward to about 360 feet (Fig. 8).

Off the central Texas coast, typical irregular layers are found mainly seaward of the barrier islands on the open continental shelf (Fig. 9). They occur in a somewhat irregular zone roughly parallel with the coast in water depths ranging from about 30 to 65 feet. In central Aransas Bay, along the flanks of the intra-coastal waterway, irregular layered structures occur in a narrow band adjacent to the spoil-dumps. This occurrence is obviously related to the waterway. Similar structures also are found locally in San Antonio and Mesquite bays.

In both the Mississippi Delta and Rockport areas the composition of coarse irregular layers usually is similar to a concentrate of the adjacent finer deposits. They normally consist of sand and silt with tests of foraminifers, ostracods, and some shell fragments. Woody material also is commonly present.

MOTTLED STRUCTURES

Mottles are best developed in sediments of the Rockport, Texas, area; they are among the most prominent and characteristic visible features of these sediments. They occur both in the bays and seaward of the barrier islands (Fig. 9). In the bays these structures are found in water depths intermediate between the deepest and the shallowest (about 2–9 feet deep). As a general rule mottled structures in the deeper parts of the bays are distinct mottles, whereas those in the shallower water are of the indistinct type grading shoreward into coarse homogeneous sediments, as previously described. In the open gulf seaward of the barrier islands (Fig. 9) mottles are forming in a broad band roughly parallel with the coast in water depths greater than about 50 feet. This band is irregular in outline and extends seaward into water 120–300 feet deep.

In the Mississippi Delta area, mottles occur in sediments of both the sound and the open gulf (Fig. 8). In Breton Sound they are found predominantly in a belt just landward of the barrier islands. The depth of water ranges from about 4 to 20 feet. In the open gulf mottles occur in a band lying seaward of the band of irregular layers. The band of mottles also extends around the fine-grained delta deposits. On the landward side of this band the mottles are mostly distinct, and they grade into indistinct mottles on the seaward side away from the delta. Water depths in the open gulf where mottles are forming range from about 15 feet near Breton Island to about 350 feet on the outer shelf on the east.

HOMOGENEOUS SEDIMENTS

Homogeneous, structureless, fine-grained clays and silty clays are being deposited seaward from the Mississippi Delta in water depths greater than about 120 feet (Fig. 8). These fine homogeneous deposits occur as a large lobe on the shelf east of the delta. Fine-grained homogeneous beds also occur in the deepest parts of southern Breton Sound where water depths are between 18 and 27 feet. In the Texas area (Fig. 9) fine-grained homogeneous sediments are found only in the deepest parts of Aransas and San Antonio bays and in water deeper than about 120 feet in the open gulf.

Relatively coarse, virtually homogeneous sediments are forming short distances seaward of the mouths of North Pass, Pass a Loutre, and Southwest Pass of the Mississippi Delta. These sediments are mixtures of silt, clay, and sand, and they are being deposited at a very high rate.

Coarser-grained homogeneous sediments (sands or coarse mixtures of sand, silt, and clay) are found both landward and seaward of the barrier islands in each of the study areas. Coarse, homogeneous, texturally mature deposits extend from approximately the island shorelines seaward into about 75–90 feet of water east of Gosier and Breton islands and from near the shore seaward to depths of 30–45 feet off the Texas islands. The sands seaward of the barrier islands are coarsest and best sorted near shore; seaward they generally become progressively finer and more poorly sorted, and minor internal structures begin to occur. On the landward side of the barrier islands the sands are homogeneous in the shallowest water. In the Texas bays homogeneous sands fringe the narrow beaches, and they are found in the shallowest parts of Breton Sound.

SUMMARY OF DISTRIBUTION

Different areas of the sea and sound floors were found to contain different minor sedimentary structures. These structures are arranged in an order that is persistent within each study area and also between study areas where comparison is possible.

In a northerly or northeasterly direction from the Cubits Gap distributary system a definite succession of sedimentary structures is developed (Fig. 8). In shallow water around the delta shore there are abundant and complicated regular-layered structures. These structures become less abundant and less well developed in deeper water seaward. Farther offshore there is a band of mostly irregular-layered structures that grades outward into mottles. These mottled structures in turn become indistinctly mottled farther seaward and grade outward into coarse homogeneous sediments. Going eastward from the delta onto the continental shelf the outward succession is similar except that a broad area of homogeneous clays occurs between the regular and irregular layered bands. Toward the south in deep water of the gulf, there are no irregular layers or mottles—only fine-grained homogeneous clays. The outward sequence into deep water, grading from regular layers to homogeneous clays, is the same sequence Johnston

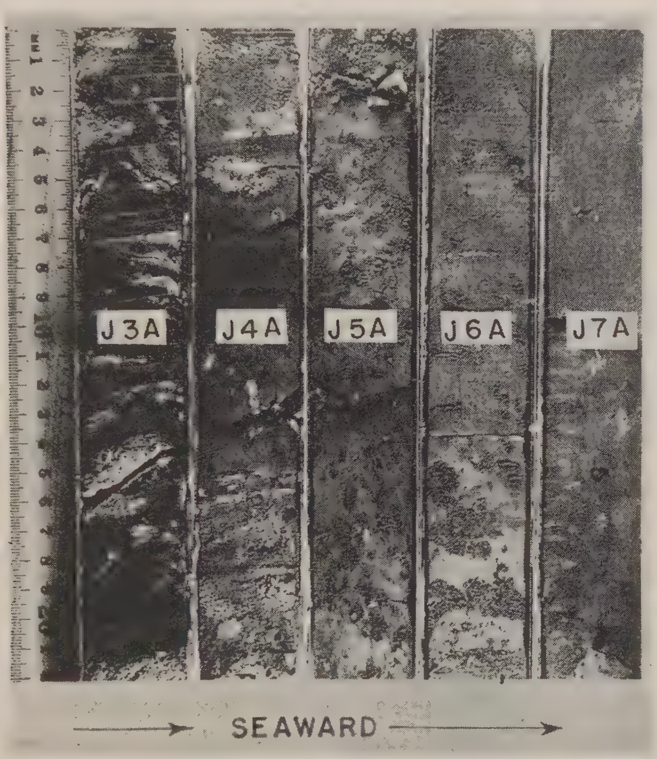

FIG. 10.—Series of cores from $3\frac{1}{2}$ to 8 miles offshore, showing seaward decrease in average grain size off part of central Texas coast expressed as decrease in abundance of coarse minor internal structures.

(1922) described off the delta of the Fraser River. From the Guadalupe Delta into upper San Antonio Bay there is a succession of sedimentary structures similar to this, but the zone of irregular layers is either poorly developed or poorly preserved.

Seaward from the Texas barrier islands (Fig. 9) there is a zone of homogeneous "mature" sands. In 30–40 feet of water a few irregular-layered structures begin to appear which increase seaward forming a zone of irregular-layered sediments. These, in turn, change gradually outward into sediments containing mottled structure. In still deeper water farther offshore, there is an area of homogeneous fine-grained sediments. Figure 10 shows how a part of this sequence of minor structures appears in cores. This simple outward sequence varies locally near secondary sources of shelf sand. Around these there is a small-scale repetition of the major outward sequence. A sequence of minor internal structures somewhat similar to that of the Texas area occurs eastward from the barrier islands north of the Mississippi Delta.

In the bays of the central Texas coast and in Breton Sound the sequence of sedimentary structures outward from the barrier island shore are similar to those just described in the open gulf, but the depth zonation is greatly compressed with the result that the irregular-layered zone is very narrow or missing. Coarse homogeneous sediments generally are found in the shallowest water near shore. They grade outward into mottled and irregularly layered sediments in deeper water. The deepest parts of the bays and sound contain fine-grained homogeneous sediments.

ORIGIN

Minor sedimentary structures—regular layers, irregular layers, mottles, or homogeneous sediments—may be either primary or secondary in origin. Primary minor structures are formed at the time of initial deposition by variations in amount and kinds of sediments from a single (simple) source or by alternating deposition of contrasting sediments from two or more (compound) sources. Sediments with primary regular layers and primary homogeneous sediments are common, whereas primary irregular layers or mottles apparently are uncommon and probably form only under specialized and unusual conditions.

Secondary minor structures are produced after initial deposition but before the sediment is buried beyond the reach of physical processes active on and just beneath the sea floor. They are formed both by partial or complete destruction of previously formed primary structures and by resorting or unmixing of homogeneous sediments. Secondary structures of all kinds are by far the most common sedimentary structures in both the Mississippi Delta and Rockport, Texas, areas.

Both primary and secondary structures may occur in the same local area. Provided contrasting sediments are available, the structure that forms depends on the processes that dominate the local sea floor at the time it is formed and on the local rate of deposition. Table I summarizes the processes that form most of the different structures.

TABLE I. PROCESSES THAT FORM MOST MINOR INTERNAL SEDIMENTARY STRUCTURES
(Capitalized methods are considered most important)

Type		*When Formed*	*Process of Formation*	
			If there is one major sediment source (simple source)	If there are two or more sediment sources (compound source)
REGULAR LAYERS		P*	FLUCTUATIONS IN SIZE OF MATERIAL TRANSPORTED AND DEPOSITED	TRANSPORTATION OF CONTRASTING MATERIAL FROM TWO OR MORE SOURCES
		S*	WINNOWING RESULTING FROM SUSPENSION BY CURRENTS (wave, tide, wind induced, etc.) Organic activity resuspending sediment with winnowing of fines	
IRREGULAR LAYERS		P	Fluctuations in size of material deposited on irregular bottom	Interrupted transport from both sources with deposition on irregular bottom
		S	ORGANIC ACTIVITY RESUSPENDING SEDIMENT WITH WINNOWING OF FINES. Local slump	
MOTTLES	Distinct	P	Open animal burrows or surface irregularities filled with contrasting material Mud pebbles eroded from stream bank; rarely formed	Dessication clasts from tidal flats and natural levees (clay galls); rarely formed
		S	BURROWING ORGANISMS DISTORTING LAYERED DEPOSITS OR CONCENTRATING MATERIAL COARSER OR FINER THAN MATRIX BY WINNOWING OR INGESTION. Local slump	
	Indistinct	P	Possibly by soft clay balls; rarely formed	Interstitial sedimentation of clay in sand; rarely formed
		S	PARTIAL DESTRUCTION OF EARLIER FORMED LAYERED OR DISTINCTLY MOTTLED STRUCTURES BY BURROWING AND CRAWLING ORGANISMS	
HOMOGENEOUS		P	DEPOSITION OF UNIFORM SEDIMENT or deposition at very high rate	DEPOSITION OF UNIFORM SEDIMENT
		S	TOTAL DESTRUCTION OF MINOR INTERNAL STRUCTURES BY BURROWING ORGANISMS WITH COMPLETE SEDIMENT MIXING	

P* Primary feature formed at time of initial deposition.
S* Secondary feature formed as alteration of initial deposit.

PRIMARY STRUCTURES

Primary regular layers in the two study areas form principally from fluctuations either in competence of transporting agent or in type of material off one major source of sediment. To a less but important extent they form as a result of interrupted transportation from more than one source of sediment.

In the shallow water surrounding river deltas primary regular layers are produced during unidirectional sediment transport through alternations in both volume of river discharge and character of river load. Variations in load are short term as well as seasonal. Where the currents which transport and distribute these sediments impinge directly on the bottom with sufficient velocity, regular coarse layers are produced. Finer material is deposited during periods when the currents cease to flow directly along the bottom or when the coarseness of river load decreases. Off river mouths the depths of water to which these primary layers extend depends on the discharge of the river or distributary. Off smaller distributaries of the Mississippi, for example, the depth is a maximum of 1½–2 feet, whereas it is at least 10 feet off the large undredged distributaries, such as North Pass.

Primary regular layers also are produced in environments which have more than one major sediment source. Deposition of river-borne silt and clay adjacent to a sandy barrier island, for example, may periodically be either interrupted by intermittent high winds, or its rate overbalanced by wind effects. These winds also create waves which vigorously stir nearby sandy bottoms and suspend some sand. The suspensions are transported laterally along and near the bottom by the wind and tidal currents, when some sand can settle rapidly onto river-derived silty clay. Later, when this sand is buried by resumption of silty clay deposition, it forms coarse, regular layers. An environment in which these events occur is in the deeper water of Breton Sound along the southwest flank of Breton Island (Fig. 8).

Primary regular layers may be contorted to a considerable extent and still be recognizable. Some forms of contortion such as local submarine slumping and the air-heave of sandy tidal flats described by Stewart (1956) cause much distortion but leave the lamination intact in many cases. However, extreme slumping or air-heave may result in alteration to irregular layers, or, conceivably, in the formation of homogeneous deposits.

Primary irregular layers have much the same genesis as do the regular layers, but they apparently form only if the surface of deposition is one of minor irregularities such as one covered with small ripple marks or the tracks of crawling organisms. Van Straaten (1951) describes some marsh sediments from the Wadden Sea which have layering that is irregular as a result of being deposited on a rough surface of marsh vegetation. This type of irregular layers seems to form only in environments which have intermittent periods of deposition. Intervening periods of non-deposition must be sufficient to allow the bottom surface to be roughened by currents, bottom organisms, or plants, so that the subsequent layer of sediment is discontinuous and irregular.

Primary mottles may form in environments having one or more major sediment source. However, in general, primary origin of mottles is uncommon, and like irregular layers, they are typically a secondary feature.

Perhaps the most usual origin of primary mottled structures is by filling of open animal burrows and borings with contrasting material after a period of non-deposition and reworking. Sharpness of the contacts between these fillings and their host matrix determines whether the mottles are distinct or indistinct; fine material deposited in burrows in porous sand may filter into the pores of the sand producing indistinct boundaries.

Primary mottles also may form from mud pebbles or balls dislodged from the banks of stream channels (Gardner, 1908). These are carried as bed load and deposited with normal river sediments. Dessication of layers of mud on tidal flats or natural levees forms mud curls or cylinders, which at higher water may be carried seaward and deposited as chips or rounded pebbles in sediment of contrasting texture When deposited as a chip or lenticule, these are known as clay galls (Burt, 1930). Although in some areas they may be important features, mud pebbles and clay galls were not positively identified in the cores of modern deposits of the two Gulf Coast study areas.

Structureless, homogeneous deposits often are primary. In the two study areas they are products either of a very high rate of deposition which reduces the time available for secondary alteration or of a moderate depositional rate where source materials do not contrast in texture or composition. The uniform, fine-grained clays lying offshore in deeper water east of the Mississippi Delta (Fig. 8) are the products of the latter type of environment.

SECONDARY STRUCTURES

Secondary regular layers form mainly by current action resuspending and sorting existing deposits. The orbital currents of ordinary wind waves probably accomplish resuspension most commonly, but tidal currents, wind currents, and semi-permanent currents also are active agents. The same agents also cause more or less lateral movement of the suspension. By means of this resuspension and transportation, poorly sorted sediments are unmixed and the different particle sizes are separated. Commonly only the finer particles of soft surficial sediment are suspended and moved, leaving a concentrate of the coarser particles on the

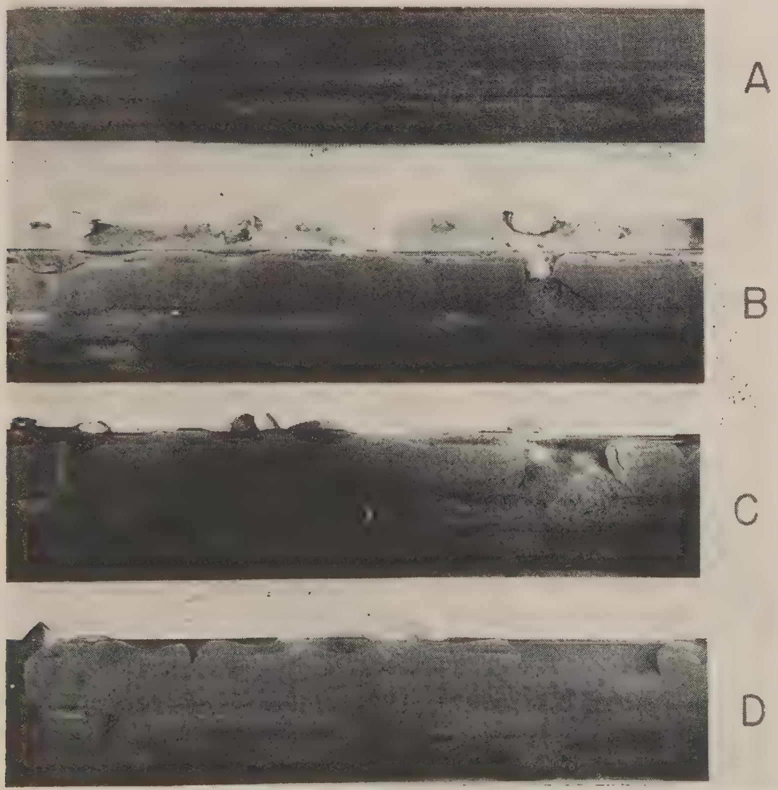

FIG. 11.—Effect of burrowing organisms on layered sediments. Progressive changes produced by burrowing animals in artificial-layered sediments. (A) original layering; (B) after 5 days; (C) after 10 days; (D) after 25 days.

sea floor. However, stronger current action frequently resuspends the entire surface layer. Later settling produces thin silt or sand beds which probably are graded laterally, because finer sediment is winnowed out. However, neither lateral grading or typical vertical grading have been observed. In either case the coarse concentrates form regular layers or bands when covered by later deposition of finer material. Locally the siphoning of some of the larger burrowing invertebrates may winnow fines and produce regular layers, but generally these are markedly lenticular and discontinuous.

Whichever their origin, regular layers are highly vulnerable to destruction. They are most likely to be preserved for lithification in environments which have rapid deposition or only few bottom-living organisms.

In the two study areas, formation of both irregular layers and mottles is almost entirely the work of bottom-living and -feeding animals. Off the Mississippi Delta and in the Texas bays and open gulf these secondary minor structures are extremely common. Their numbers increase directly with the numbers of mud-feeding, crawling, and burrowing animals and, in general, inversely with the rate of deposition.

In order to test these field observations, the effects of burrowing organisms on artificial sediments were studied in the laboratory. R. H. Parker, biologist for A.P.I. Project 51 at Scripps Institution, helped with this work. Specially constructed aquaria were used which contained sediments with different combinations of texture and stratification. Regular layers were deposited in the tanks. Organisms of a number of types were then introduced and photographs were taken at regular intervals. Figure 11 is a sequence of photographs of one of the tanks to show the way the organisms destroy primary structure and modify the sediment. Not only were the original layers locally disrupted to form irregular layers and mottles, but as the oblique view shows (Fig. 11-B), poorly sorted sand was transferred from beneath the surface and purified to form completely new lenses on the surface. These lenses would become irregular layers if they were buried.

All types of mud-feeders and burrowers made some changes, but the most active in modifying the sediment and forming irregular layers and mottles were the razor clam, *Tagelus*, the burrowing clam, *Zirfaea pilsbryi*, and the pink ghost shrimp, *Callianassa*. Much of the modification and alteration by such animals probably occurs within the upper 6 inches of sediment, and most of it occurs before the sediment has been buried more than about 2 feet below the sea floor. Experiments similar to this were done by Solowiew (1924). He had a tank of mud with a thin sand layer added above. On the second day after the addition of the worm *Tubifex tubifex* he noted that mud particles had been carried to the top of the sand and into its upper layers.

These observations show conclusively that irregular layers may be the result of animal activity. They form when the larger burrowers suspend the sediment in and about their burrows, winnowing the finer and concentrating the coarser materials. They also form when crawling and burrowing animals distort deposits initially containing regular layers. The same process forms most distinct and indistinct mottles, but disturbing action of the mud-eaters, grubbers, and crawlers is more nearly complete than in sediments with only irregular layers.

The fundamental relationships between the different types of minor structures and homogeneous deposits are illustrated in Figure 12. Alteration of existing sediments by organisms can proceed along either of two different courses. A regular-layered deposit attacked by bottom-dwellers can be converted first to irregular layers, and with continued disturbance, later to distinct mottles, still later to indistinct mottles, and finally to homogeneous deposits (Fig. 12, upper arrows). On the other hand, if initially the deposit is homogeneous and contains mixed particle sizes, a population of burrowers can form irregular layers, distinct or indistinct mottles, or complete the cycle to homogeneous deposits by syphoning and stirring (Fig. 12, lower arrows). The function of burrowing and crawling animals is both to create and to destroy minor internal structures. The extent to which these processes are carried out depends on the numbers of organisms and on the rate of deposition in the sedimentary environment.

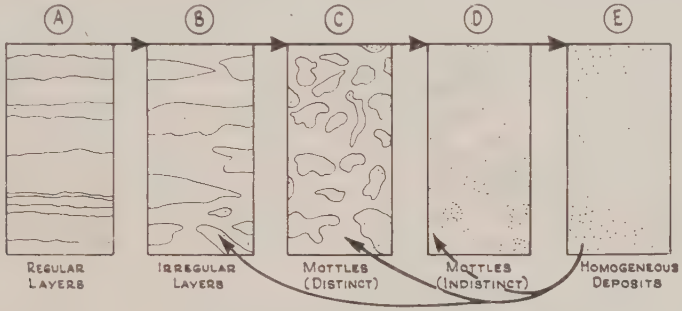

FIG. 12.—Progressive alteration of sediments by burrowing organisms. Sequences of minor internal structures formed by continuing action of burrowing animals. Top arrows indicate sequence formed by destruction of primary and secondary structures. Bottom arrows show how mottles or irregular layers may be created from homogeneous deposits.

Finally, since the existence of minor structures depends on the presence of contrasting sediments, the work of organisms may be altered or obliterated by long-continued wave and current sorting. Given sufficient time, the end product of reworking by organisms and current sorting is a coarse, structureless, homogeneous deposit that is texturally mature.

RELATIONS OF MINOR INTERNAL STRUCTURES TO SEDIMENTARY ENVIRONMENTS

The three fundamental factors which relate minor internal structures to their environments of formation are: (1) sources of sediment, the control of composition, texture, and quantity; (2) processes of primary sedimentation, and secondary alteration of deposits, together with their activities or intensities; and (3) rate of deposition, the time control on all processes of the water-sediment interface.

Regional climatic variations and regional or local physiographic variations may cause any one of these to assume a more prominent role. The relationships are shown graphically in Figures 13 and 14. For example, off the Mississippi River the tremendous volume of sediment introduced and locally deposited emphasizes the importance of rate of deposition as a basic factor in environmental control. The coarse, structureless, homogeneous deposits formed north of the delta at a slow rate grade shoreward into mottled deposits as deposition rate increases nearer the delta (Fig. 8). These in turn change shoreward into irregular layers and finally into regular layered beds or homogeneous beds of mixed sediments in the areas of fast deposition close to shore.

In Figure 13 the effect of processes on a unit volume of sediment is indicated schematically along the Y-axis. Rate of deposition is plotted along the X-axis, increasing from left to right. This diagram and Figure 14 are quantitative only in part, since there is no known way to measure all that has happened to a volume of sediment or the intensity of processes. Therefore, the curves are partly intuitive, but they show the *kinds* of relationships that must exist. Curve A of Figure 13 shows the decrease in effect of burrowing organisms with increasing depositional rate. On the north side of the Mississippi Delta, effects of burrowing organisms can not be recognized when the rate of deposition is greater than about 0.15 foot per year. In the same way curve B shows the changes in wave and current effects, and the total curve shows combined effects of A and B. In some places near those distributary mouths where sediments are deposited faster than 2–3 feet per year, wave and current effects are negligible, even though the

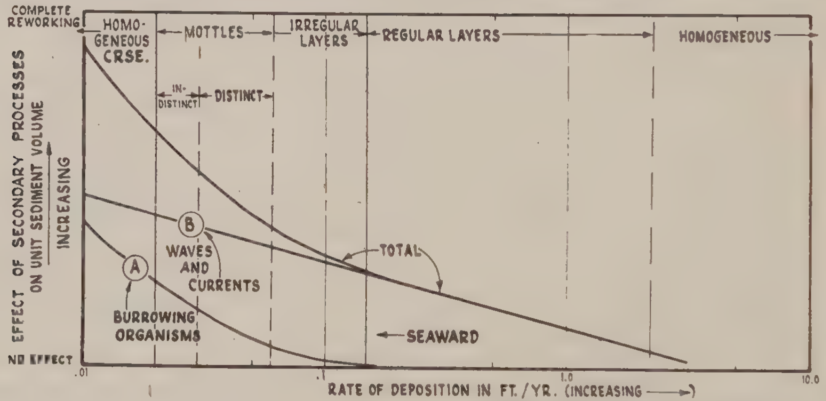

CURVE A: Intercepts and slopes depend on depositional rate and numbers and kinds of organisms (favorability of environments for life.)

CURVE B: Intercepts and slopes depend on depositional rate and (1) wave size and frequency, (2) water depths, (3) current strengths

FIG. 13.—Relations of minor internal structures to rate of deposition and processes off Mississippi Delta. Decreasing rate of deposition off Mississippi Delta causes effects of secondary processes to be greatest offshore in deeper water, although intensity of physical processes such as waves is greatest in shallow water nearshore.

water is shallow and waves and currents are very active. The sediments in these places contain no laminae or other secondary structures, but instead are essentially homogeneous as shown on the right side of Figure 13.

The time available for processes to work, although of great importance off the Mississippi Delta, is only one factor determining the variations in minor structures along this profile. The source of coarse sediment, necessary for contrasting texture in the area of slowly forming mottles and irregular layers, is the adjacent homogeneous deposit (Scruton, 1955). Amounts of this coarse material which are deposited decrease toward the areas of faster deposition nearer the delta, and the minor structures also reflect this changing source relationship.

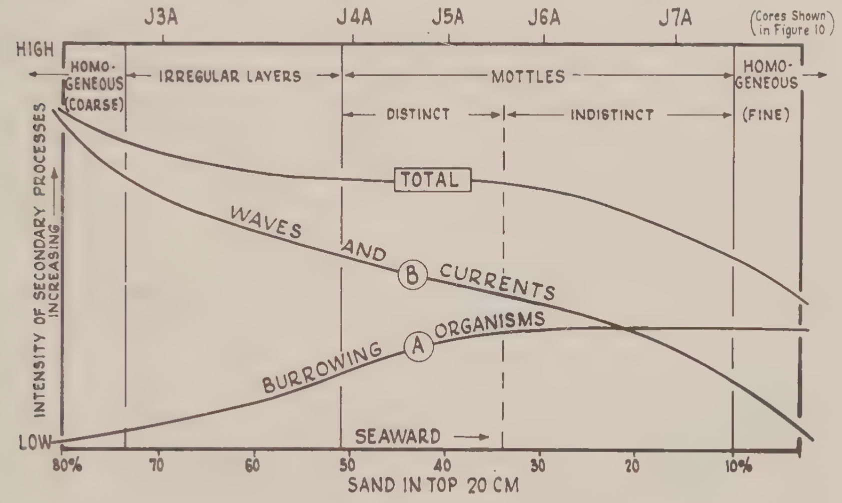

CURVE A : Intercepts and slopes depend on numbers and kinds of organisms (favorability of environments for life.)

CURVE B : Intercepts and slopes depend on (1) wave size and frequency, (2) water depths, (3) current strengths.

FIG. 14.—Relations of minor structures, sources of sand, and process intensities in Gulf of Mexico off central Texas coast. Relatively constant depositional rate.

In addition, the processes vary in their intensity. Parker (1956) showed that the area of irregular layers, mottles, and adjacent homogeneous deposits contains an abundant and varied fauna. This is in contrast to the area of regular layers nearer the delta where the fauna is more sparse. An abundant fauna is present because of favorable biological conditions (Parker, *op. cit.;* Scruton, 1956), and it is highly effective in reworking the sediments. Thus, curve A varies with the favorability of the environment for life which determines the numbers and kinds of organisms.

Similarly, curve B depends on the size and frequency of waves, the depth of water, and the strength of current. Scruton (1956) described these properties of the area in some detail. Along the profile of Figure 13 north of the delta, currents are most intense in the channel leading to Breton Sound, the area of irregular layers, mottles, and coarse, mature, homogeneous deposits. Waves of the open gulf and currents are both very active on the north in the area of homogeneous sands. Wave action is the predominant process near the delta shores where regular layers or homogeneous sediments of mixed texture occur.

In contrast to the Mississippi Delta, rates of deposition are relatively constant off the central Texas coast south of Rockport. For this reason the sources of sediments and the intensities of processes off Rockport are emphasized as the prominent controls. Figure 10 is a series of core photographs showing part of the changes that occur in minor structures going seaward from the barrier islands. Core J3A contains mostly irregular layers, whereas the rest are mostly mottled. Relative positions of the cores are shown in Figure 14. In the complete outward sequence, coarse, homogeneous, mature deposits which flank the barrier islands (St. Joseph and Matagorda) grade seaward into irregular-layered sediments, mottled deposits, and finally into fine-grained homogeneous deposits as the abundance of mottles decreases (Fig. 9).

In general the sediments in this area become homogeneous seaward because of a decrease in the sand content of the primary bulk sediment, not by an increase in secondary process effects. Figure 14 shows the relationships. The sand content, which is primarily a function of distance from the source of sand, is plotted on the X-axis. The intensity of secondary processes is indicated on the Y-axis. The total intensity of secondary processes is greatest in the area of coarse homogeneous sediments. In this zone, which extends a short distance seaward of the surf zone, secondary processes are overwhelmingly dominated by wave action (Shepard and Moore, 1955). Away from the effects of violent wave action, organism burrowing becomes an increasingly important post-depositional process. Secondary effects are most striking and easily detected in the intermediate region of mixed sediment sizes, where alterations result in the formation of minor internal structures. Thus, the structures change character seaward as the relation between the intensities of secondary processes changes, but they disappear where the sand content decreases to a low level.

Finally, comparison of Figures 13 and 14 shows the inverse nature of the effects of process intensity and depositional rate on internal structures and the relationships between these two fundamental factors. Internal structures or textural maturity, which generally are characteristic of slow deposition and moderate process intensity, may be produced by high process intensity under rapid depositional conditions. The reverse also may occur.

These examples have shown: (1) that the very existence of minor structures depends on the sediment sources, (2) that the types which form are a function of the processes, and (3) that the extent to which they develop is determined largely by depositional rate and process intensity. Because all of these factors are variable, absolute numerical values determined for one in any locality rarely if ever apply in another. However, similar sequences of structures may reflect similar environmental changes.

MINOR STRUCTURES IN ANCIENT ROCKS

Structures of regular type (layers, laminae, cross-lamination, etc.) and homogeneous (massive) beds are so commonly mentioned in descriptions of sedimentary rocks that they need no special comment. Mottles and irregular layers also have been described or figured from many different rocks but under a variety of names. For example, they are mentioned by Sherrill, Dickey, and Matteson (Sherrill *et al.*, 1941) from the Venango sands (Devonian) of Pennsylvania. These workers later described them (Dickey *et al.*, 1943, p. 31) as "a curious rock that is present in certain beds in all sands (that) consists of small lenses and lumps of sand in shale, in irregular positions as if kneaded. Small lenses and lumps of shale are frequently contained in the sands." These structures usually are described either as reworked or slump structures, as worm borings, or due to organisms, and they also have been figured by Minor and Hanna (1941, Pl. I, Figs. 1, 4) from the Cretaceous of Texas, by Fentress (1955, esp. Figs. 15B, 18A, B), and Curry and Curry (1954, Fig. 15) from the Cretaceous of the Rocky Mountains. These structures and their possible origin recently were described by Greensmith (1956) from the Carboniferous of England.

Despite the variety of names and descriptions, there seems to be little doubt that these authors are referring to the types of structures described here as mottles or mottled structures. Figure 15A–F shows other examples from the Eocene of Louisiana, the Pennsylvanian of Illinois, Oklahoma, and Missouri, and the Cretaceous of Wyoming. Figure 16 shows a series of photographs from a core of ancient rocks that is complete from regular layers through irregular layers to distinct and indistinct mottling into structureless, homogeneous deposits. This vertical series duplicates the sequence seaward from the Mississippi Delta. Undoubtedly this sequence has been duplicated many other times, and both mottles and irregular layers have been formed in rocks of all ages when depositional conditions were suitable.

Minor structures in ancient rocks can be studied particularly well in thin section. Sinuosity of contact between mottles and matrix and lack of textural organization in the mottles (also in the matrix) are especially apparent. In addition, gradations between the different types—distinct and indistinct mottles and coarse homogeneous sediments—can be seen well in thin section.

Because of mechanical diagenesis, mottling and irregular layers in ancient sediments are likely to appear somewhat different from those in modern sediments. As an example, compaction of silty clay with sand mottles can be cited. The silty clay matrix is more subject to compaction and deformation than the stronger sand lumps and pockets. Compaction of this sediment under overburden

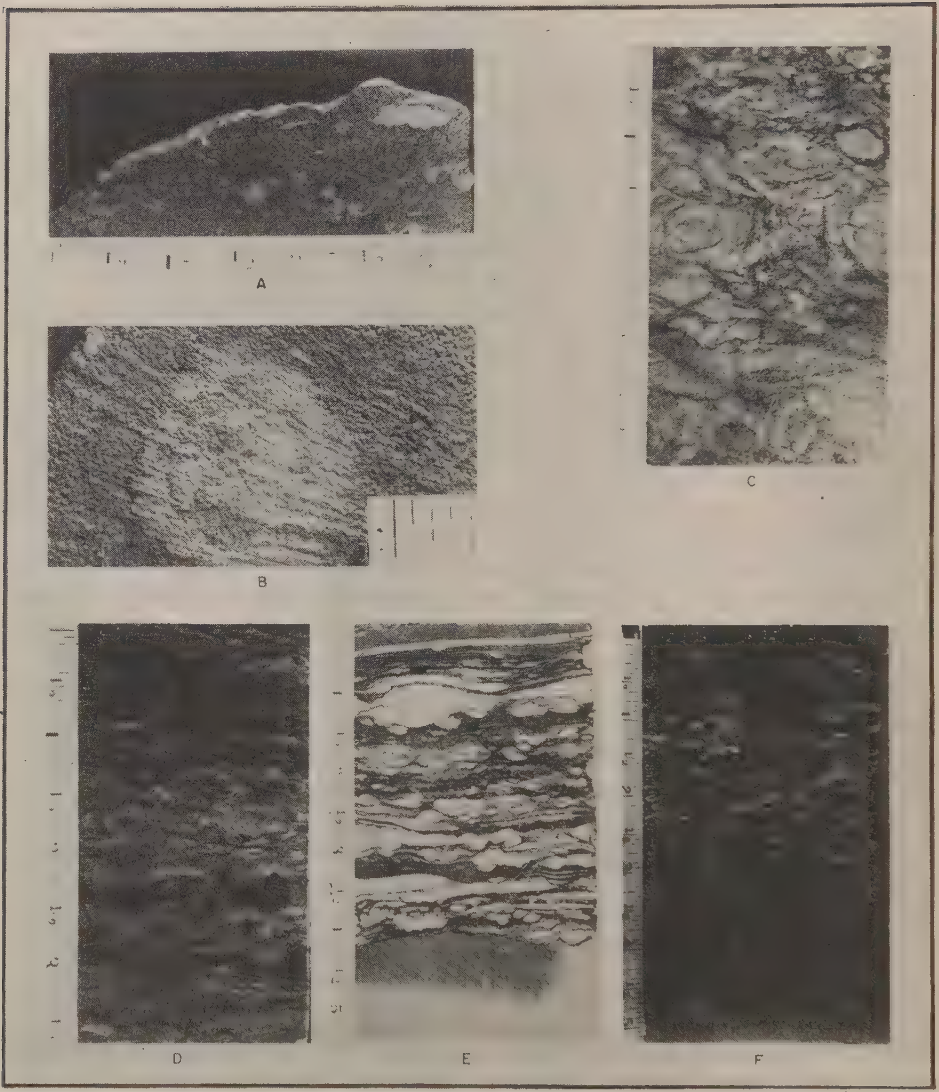

FIG. 15.—Mottles in ancient rocks. (A) Eocene of Louisiana; (B) Pennsylvanian of Illinois; (C) Pennsylvanian of Oklahoma; (D) Pennsylvanian of Missouri; (E, F) Cretaceous of Wyoming.

produces a tendency toward horizontal layering in the rock. Moreover, the volume occupied by the silty clay is reduced relative to the sand, making the rock appear sandier than would the original sediment.

Post-depositional chemical alteration is of great importance in some rock types and also may alter the original character and appearance of mottles or irregular layers. Osmond (1956) discusses mottled Middle Devonian limestones and dolomites in eastern Nevada and gives many references to similar rocks in

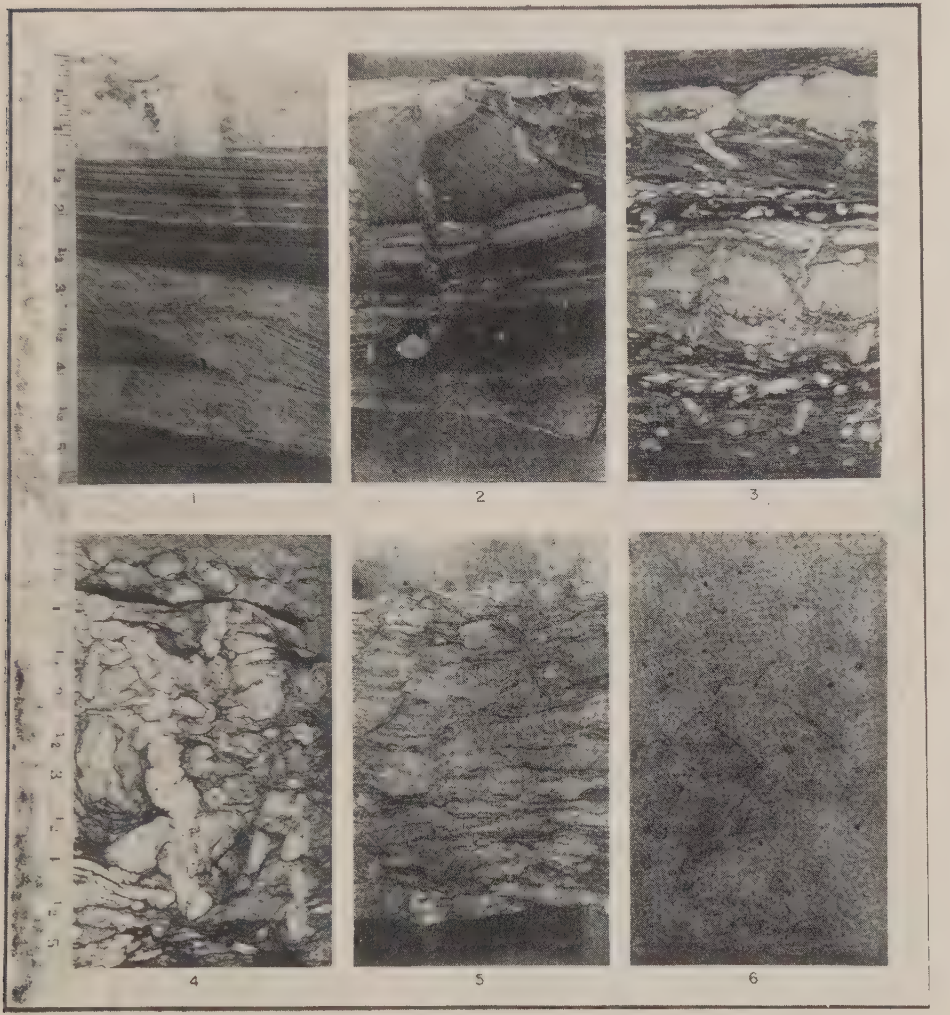

FIG. 16.—Complete sequence of minor structures in Cretaceous of Colorado. (1) Regular layers; (2) regular layers with some mottles; (3) irregular layers with mottles; (4) distinct mottles; (5) indistinct mottles; (6) homogeneous sands.

other carbonate sequences. He concludes (*op. cit.*, pp. 40–41): "The development of the mottled pattern is the result of incomplete or differential dolomitization which may follow a pattern established at the time of deposition," and attributes the original pattern to a number of processes operating under a moderate rate of deposition. The mottled rocks figured by Osmond (*op. cit.*, Figs. 1, 3–7) bear a remarkable resemblance to mottled and irregular-layered structures in the modern sediments of the Gulf Coast study areas, and burrowing animals may have established the pattern of dolomitization.

Osmond's work also provides a rare example of an areal distribution study of mottling in ancient sediments. His figure 2 (*op. cit.*, p. 37) is a map showing the variation of thickness in the Simonson dolomite of eastern Nevada between the lowest mottled stratum and the next lower stratigraphic marker. With respect to the lower marker, the mottled stratum systematically rises toward the east. Because of this, Osmond suggests that the mottled stratum may be a time-transgressive facies. However, in both of the Gulf Coast areas continuous beds of mottling are now forming through a wide range of water depths. This suggests as a second possibility that Osmond's lower mottled bed may be a time marker, with the eastward rise representing initial (primary) dip with respect to the underlying marker.

CONCLUSIONS

Extensive field studies and collections in the Gulf of Mexico off the Mississippi Delta and the central Texas coast have shown that minor internal sedimentary structures are extremely common in the nearshore sediments of both these regions. Regular-layered deposits (thinly bedded or laminated) are characteristic of areas of rapid deposition and relatively few bottom-dwelling organisms. When measured by areal distribution, these structures make up a relatively small part of the sediments of the study areas; however, by volume, they are very important because of the great thicknesses of deltaic deposits. Regular layers are both primary features, formed at the time of deposition by fluctuations in texture or composition of sediments deposited, and secondary, formed by wave and current winnowing.

Irregular-layered structures (roughly or crudely layered or lensed) and mottled structures (discontinuous tubes, lumps, and pockets) have a very wide areal distribution and are the most common types found in the surficial deposits of the Texas study area. These structures are largely secondary, formed by the burrowing and winnowing actions of bottom-living animals on existing sediments. Structureless homogeneous deposits are common in both areas and are both primary and secondary. They are produced either by extremely rapid deposition, uniform deposition, complete secondary mixing, or by complete winnowing.

The numbers and kinds of minor internal structures which occur within the sediments in any area depend fundamentally on the sources of sediment for deposition, the nature and intensity of physical processes within the environment, and the rate of deposition. This last factor is the basic time control on all processes of the water-sediment interface.

The importance of animals in forming the final fabric of shallow-water marine sediments can not be overstated. Were it not for burrowing and crawling organisms, the appearance of many of our marine sediments would be entirely different.

Sedimentary structures similar to those of the Gulf Coast study areas were formed in many ancient sediments. In all probability they reflect the same kinds of conditions as do the modern structures.

BIBLIOGRAPHY

BURT, F. A., 1930, "Origin and Significance of Clay-Galls," *Pan Amer. Geol.*, Vol. 53, pp. 105–10.

CURRY, W. H., JR., AND CURRY, W. H., III, 1954, "South Glenrock, a Wyoming Stratigraphic Oil Field," *Bull. Amer. Assoc. Petrol. Geol.*, Vol. 38, pp. 2119–56.

DICKEY, P. A., SHERRILL, R. E., AND MATTESON, L. S., 1943, "Oil and Gas Geology of the Oil City Quadrangle, Pennsylvania," *Pennsylvania Geol. Survey, 4th Ser., Bull. 25*, p. 31.

FENTRESS, G. H., 1955, "Little Beaver Field, Colorado, a Stratigraphic, Structural, and Sedimentation Problem," *Bull. Amer. Assoc. Petrol. Geol.*, Vol. 39, No. 2, pp. 155–88, Figs. 15B, 18A, B.

FOLK, R. L., 1951, "Stages of Textural Maturity in Sedimentary Rocks," *Jour. Sed. Petrology*, Vol. 21, pp. 127–30.

GARDNER, J. H., 1908, "The Physical Origin of Certain Concretions," *Jour. Geol.*, Vol. 16, pp. 452–58.

GRAY, H. H., 1955, "Thickness of Bedding and Parting in Sedimentary Rocks," *Bull. Geol. Soc. America*, Vol. 66, pp. 147–48.

GREENSMITH, J. T., 1956, "Sedimentary Structures in the Upper Carboniferous of North and Central Derbyshire, England," *Jour. Sed. Petrology*, Vol. 26, pp. 343–55.

INGRAM, R. L., 1954, "Terminology for the Thickness of Stratification and Parting Units in Sedimentary Rocks," *Bull. Geol. Soc. America*, Vol. 65, pp. 937–38.

JOHNSTON, W. H., 1922, "The Character of the Stratification of the Sediments in the Recent Delta of Fraser River, British Columbia, Canada," *Jour. Geol.*, Vol. 30, pp. 115–29.

MCKEE, E. D., 1939, "Some Types of Bedding in the Colorado River Delta," *ibid.*, Vol. 47, pp. 64–81.

———, 1954, "Stratigraphy and History of the Moenkopi Formation of Triassic Age," *Geol. Soc. America Memoir 61*. 133 pp.

———, AND WEIR, G. W., 1953, "Terminology for Stratification and Cross-Stratification in Sedimentary Rocks," *Bull. Geol. Soc. America*, Vol. 64, pp. 381–90.

MINOR, H. E., AND HANNA, M. A., 1941, "East Texas Oil Field, Rush, Cherokee, Smith, Gregg, and Upshur Counties, Texas," *Stratigraphic Type Oil Fields*, Amer. Assoc. Petrol. Geol., pp. 600–40, esp. Pl. I, Figs. 1, 4.

MOORE, D. G., 1955, "Rate of Deposition Shown by Relative Abundance of Foraminifera," *Bull. Amer. Assoc. Petrol. Geol.*, Vol. 39, pp. 1594–1600.

OSMOND, J. C., 1956, "Mottled Carbonate Rocks in the Middle Devonian of Eastern Nevada," *Jour. Sed. Petrology*, Vol. 26, No. 1, pp. 32–41.

PARKER, R. H., 1956, "Macro-Invertebrate Assemblages as Indicators of Sedimentary Environments in East Mississippi Delta Region," *Bull. Amer. Assoc. Petrol. Geol.*, Vol. 40, pp. 295–376.

PETTIJOHN, F. J., 1949, *Sedimentary Rocks*, pp. 120–28. Harper and Brothers, New York.

SCRUTON, P. C., 1955, "Sediments of the Eastern Mississippi Delta," in "Finding Ancient Shorelines," *Soc. Econ. Paleon. and Min. Spec. Pub. 3*, pp. 21–51.

———, 1956, "Oceanography of Mississippi Delta Sedimentary Environments," *Bull. Amer. Assoc. Petrol. Geol.*, Vol. 40, pp. 2864–2952.

SHEPARD, F. P., 1953, "Sand and Shell Lenses in Fine Sediments," *Amer. Petrol. Inst. Project 51, Rept. VI*, p. 5.

———, AND MOORE, D. G., 1955, "Central Texas Coast Sedimentation: Characteristics of Sedimentary Environment, Recent History and Diagenesis," *Bull. Amer. Assoc. Petrol. Geol.*, Vol. 39, No. 8, pp. 1463–1591.

SHERRILL, R. E., DICKEY, P. A., AND MATTESON, L. S., 1941, "Types of Stratigraphic Oil Pools in Venango Sands of Northwestern Pennsylvania," *Stratigraphic Type Oil Fields*, Amer. Assoc. Petrol. Geol., pp. 507–38.

SOLOWIEW, M. M., 1924, "The Influence of *Tubifex tubifex* in the Formation of Organic Mud," *Internat. Review Hydrobiology*, Vol. 12, p. 90.

STEWART, H. B., 1956, "Contorted Sediments in Modern Coastal Lagoon Explained by Laboratory Experiments," *Bull. Amer. Assoc. Petrol. Geol.*, Vol. 40, No. 1, pp. 153–61.

THOMPSON, W. O., 1937, "Original Structures of Beaches, Bars, and Dunes," *Bull. Geol. Soc. America*, Vol. 48, pp. 723–52.

———, 1949, "Lyons Sandstone of Colorado Front Range," *Bull. Amer. Assoc. Petrol. Geol.*, Vol. 33, No. 1, pp. 52–72.

VAN STRAATEN, L. M. J. V., 1951, "Texture and Genesis of Dutch Wadden Sea Sediments," *Proc. Third Internat. Cong. of Sedimentology*, Groningen-Wageningen, Netherlands, pp. 225–44.

SIZE ANALYSIS OF SAND BY A SEDIMENTATION TECHNIQUE

BY

DAVID M. POOLE

Reprinted from the Journal of Sedimentary Petrology for December, 1957

(919)

Reproduced by Permission

JOURNAL OF SEDIMENTARY PETROLOGY, VOL. 27, NO. 4, PP. 460–468
FIGS. 1–6, DECEMBER, 1957

SIZE ANALYSIS OF SAND BY A SEDIMENTATION TECHNIQUE[1]

DAVID M. POOLE
Scripps Institution of Oceanography,
University of California, La Jolla, California

ABSTRACT

The particle size distributions of sand-size material can be determined either directly by microscopic measurement, or indirectly by sieving or by sedimentation techniques. Routine size analyses by microscopic measurements are impractical because they are too time consuming, although other properties such as grain shape or roundness can be determined when making size analyses by this method. Sieve analyses, because of their convenience and resulting fractionation, have been most extensively used to determine the size frequency distribution of sands. However, since most sediments are deposited in fluid media, sedimentation size analyses are often desirable because they most nearly approach the hydrodynamic conditions of deposition. This paper discusses a sedimentation technique employed for the analysis of sand-size material, and demonstrates, by means of experiments with glass spheres, that single grain terminal settling velocities can be used as suitable approximations for fall rates of grain groups. The settling velocities for groups of grains are 10 to 15 percent faster than those for single grains of the same diameter. Comparative results of size analyses of the same sample indicate that sedimentation diameters generally were coarser than sieve diameters but finer than microscopically measured diameters.

INTRODUCTION

The Emery settling tube (Emery, 1938), which utilizes the principle of terminal settling velocities, is used at the Scripps Institution of Oceanography's sedimentation laboratory for the routine size analysis of "sand."[2] The simple method employed is rapid, and has a reproducibility which compares favorably with that of sieving (Poole, et al., 1951). Since it is a sedimentation method of size analysis, the settling tube technique more nearly approaches natural conditions of deposition and results in a better approximation of sediment particle behavior than either sieve or microscopic size analyses. The settling tube has been modified recently by the author (fig. 1) with the addition of a device[3] which makes the introduction of the sample more uniform.

The terminal fall velocities for sand-size materials have been determined experimentally (among others, Heywood, 1938; U. S. Engineers 1941, 1943) for single spherical grains. The use of single spheres in these experiments obviously simplifies theoretical and experimental considerations in determining fall velocities. However, the fact that the natural sand particles seldom approach a spherical shape led to the concept of the "sedimentation radius" defined by Wadell (1934) as "the radius of a sphere of the same specific gravity and of the same terminal uniform settling velocity as a given particle in the same sedimentation fluid." This definition presents a practical solution to the problem of expressing the "size" (radius or diameter) of particles which occur in nature. If, for the sake of convenience, the density of quartz is used as a reference, this definition serves adequately for expressing size in terms of a standard and is equivalent to the "hydraulic value" defined by Schöne (cited by Krumbein and Pettijohn, 1938, p. 94) as the diameter of a quartz sphere having the same settling velocity as a given particle in water. Moreover, since it is impractical to perform a routine sedimentation size analysis by dropping particles one at a time through a column of water to determine their settling velocities (hence size), many particles must be dropped. In such a case the settling velocities determined for single grains do not apply exactly. In a

---

[1] Contribution from the Scripps Institution of Oceanography, New Series No. 957. This investigation was supported by a grant from the American Petroleum Institute, Project 51. Manuscript received April 8, 1957.

Author's present address: The Ohio Oil Company, Denver Research Center, Littleton, Colorado.

[2] The term "sand" as used in this paper includes all particles with diameters between 1.0 mm and 0.0625 mm. This includes all the Wentworth sand size grades except very coarse sand (2.0 to 1.0 mm).

[3] This device was made by George S. Bien and is similar to the double cone device of Puri (1934).

settling tube analysis the grains fall as a group, and the grains have a higher initial settling velocity than they should because of the introduction of the sample as a unit.[4] In order to determine the effect that the introduction of the sample as a unit has on the settling velocities of particles, a series of tests were made using glass spheres. These were chosen because they were spherical, easy to obtain, and should give the same diameter whether measured by sieves, microscope, or sedimentation (using settling velocities for spheres with the density of glass).

The second part of this study consisted of making size analyses of four natural sands and a sample of glass spheres (with a "controlled" size distribution) by these three methods for the purpose of comparison.

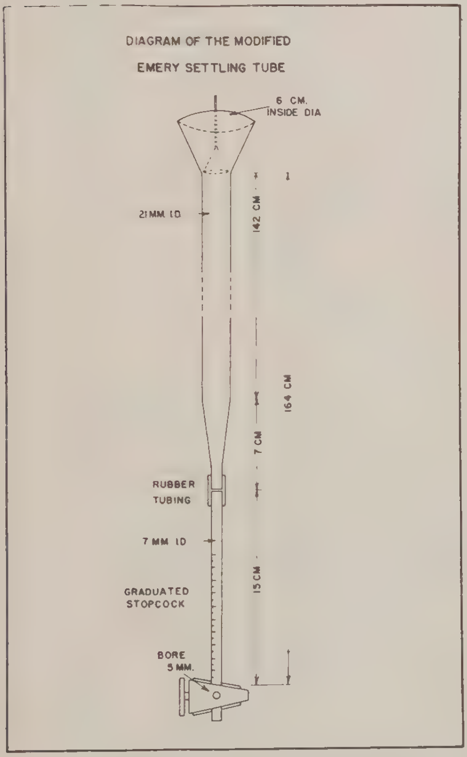

FIG. 1.—Diagram of the modified Emery settling tube showing the double-cone device for introducing the sample into the settling tube

METHODS OF STUDY

Only an outline of the methods used in preparing the glass spheres for the sedimentation tests will be given here, since complete details of the procedures followed can be found in U. S. Engineers Report #10, 1953. Irregularly shaped grains were eliminated by first sieving each size grade with a Ro-tap shaker, re-sieving lightly by hand, and assuming the material retained after hand sieving to be irregular in shape and discarding it. For large sizes, coarser than 1.50ϕ (0.351 mm), irregularly shaped grains were eliminated by rolling the grains down a narrow, inclined plate. The size distribution of each sieve fraction was determined by microscopically measuring the diameters of a random sample of 400 grains from each size grade. New Tyler Standard Screen Scale sieves with intervals based on the $\sqrt[4]{2}$ grade scale were used for the sieve analyses in this study. These sieves were calibrated by microscopically measured glass beads, and the difference between the mean diameters,

$$\left(\frac{\text{Coarser nominal sieve opening} + \text{finer nominal sieve opening}}{2}\right)$$

based on the nominal sieve openings[5] of each size fraction was generally slightly finer than the mean diameters based on measured glass spheres. From these microscopic measurements, percentages of grains larger and smaller than the nominal sieve openings were found, and the "controlled" size distribution of the sedimentation test samples could be obtained. The density of the beads in several size fractions was determined using distilled water and carbon tetrachloride in 25 ml pycnometers and 100 ml volumetric flasks. Densities of the larger beads averaged 2.47 gm/cc and were quite constant, but in the sizes finer than 3.25ϕ (0.105 mm) were much more variable. It was necessary to use heavy liquids to obtain grains with a uniform density (2.32 gm/cc) for use in determinations of the terminal fall velocity of single grains. The final step of preparation was to check the settling velocity of individual glass spheres from these samples of known size. This was done by dropping the grains down the settling tube, in distilled water held at a temperature of 24° C, and timing them during a measured distance of fall. The ratio of the largest particle diameter to the tube diameter was about 0.02 which eliminated any serious wall effects (McNown, et al , 1948). The settling velocities so determined were plotted against diameter on log-log paper and a smooth curve drawn. To render these data more useful for sedimentation studies, the curve was then transformed in the usual manner, by the use of Reynolds number R_e, and the coefficient of resistance, C_r (Krumbein and Pettijohn, 1938, p. 104), to one (fig. 2) for spheres with a density of quartz, 2.65 gm/cc. This resulting curve is almost identical with the curve shown for quartz spheres settling in distilled water at 25° C in the U. S. Engi-

---

[4] Emery's (1938) settling velocities were determined by the time of fall of sands sieved into Wentworth size grades, and are, therefore, closely related to sieve diameters rather than to sedimentation diameters.

[5] The nominal opening is the rated sieve opening, and the effective opening may be defined as the mean size of the grains that will pass through a sieve and be retained on the next smaller size sieve. These grain sizes are determined by the microscopic measurement of the intermediate diameters.

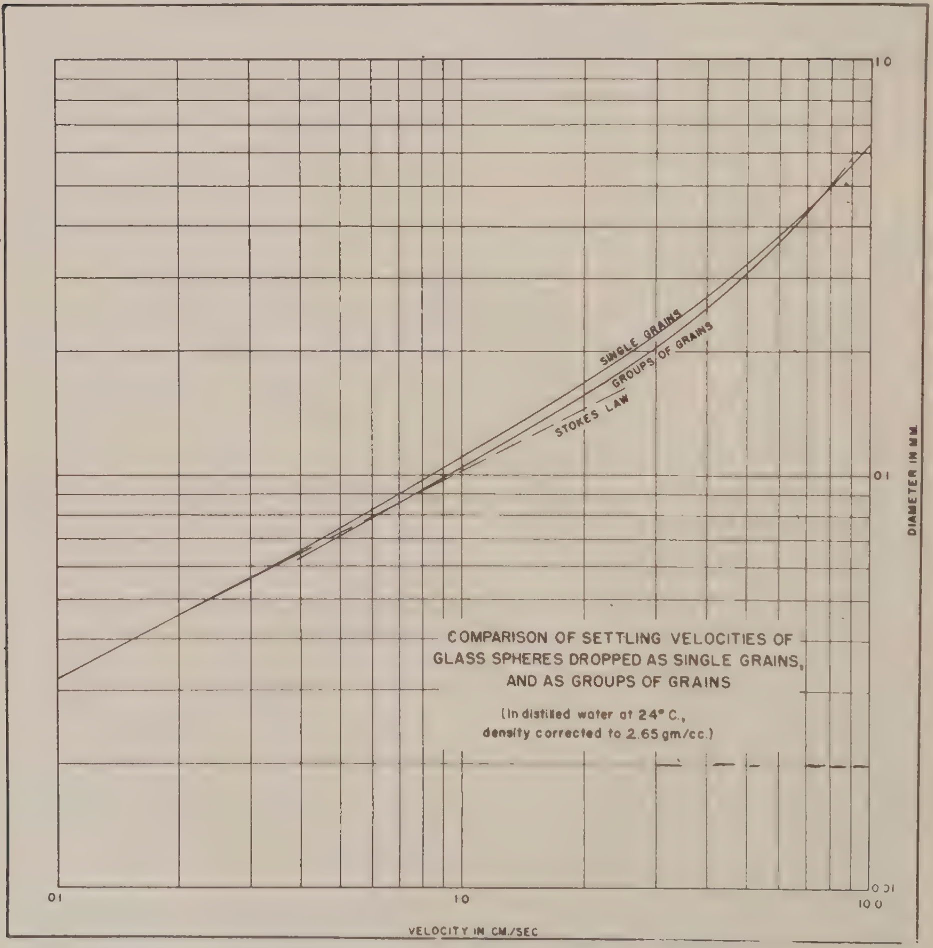

FIG. 2.—Comparison of settling velocities of single glass spheres and groups of glass spheres. The curves originally determined using glass spheres were transformed to curves for spheres with the density of quartz.

TABLE 1.—*Times for quartz spheres to fall 164 cm in distilled water at various temperatures (°C). From settling velocities determined by Heywood's (1938) method*

Diameters in		Settling times (Min.-sec.)					
φ	mm	18°	20°	22°	24°	26°	28°
0.00	1.000	11	10	10	10	10	10
0.50	0.71	15	15	15	14	14	14
0.75	0.59	18	18	18	17	17	17
1.00	0.50	22	21	21	21	20	20
1.25	0.42	27	26	26	25	25	24
1.50	0.354	32	32	31	30	30	29
1.75	0.297	40	39	37	37	36	35
2.00	0.250	49	48	47	46	45	44
2.25	0.210	1 03	1 01	1 00	58	56	54
2.50	0.177	1 23	1 20	1 17	1 15	1 12	1 10
2.75	0.149	1 51	1 46	1 41	1 37	1 34	1 31
3.00	0.125	2 28	2 23	2 17	2 11	2 06	2 02
3.25	0.105	3 21	3 13	3 04	2 56	2 50	2 44
3.50	0.088	4 34	4 23	4 11	4 03	3 52	3 45
3.75	0.074	6 16	6 00	5 45	5 31	5 20	5 08
4.00	0.0625	8 40	8 15	7 53	7 31	7 09	6 53
4.25	0.053	11 47	11 18	10 43	10 17	9 52	9 27
4.50	0.044	16 59	16 10	15 16	14 37	14 01	13 36

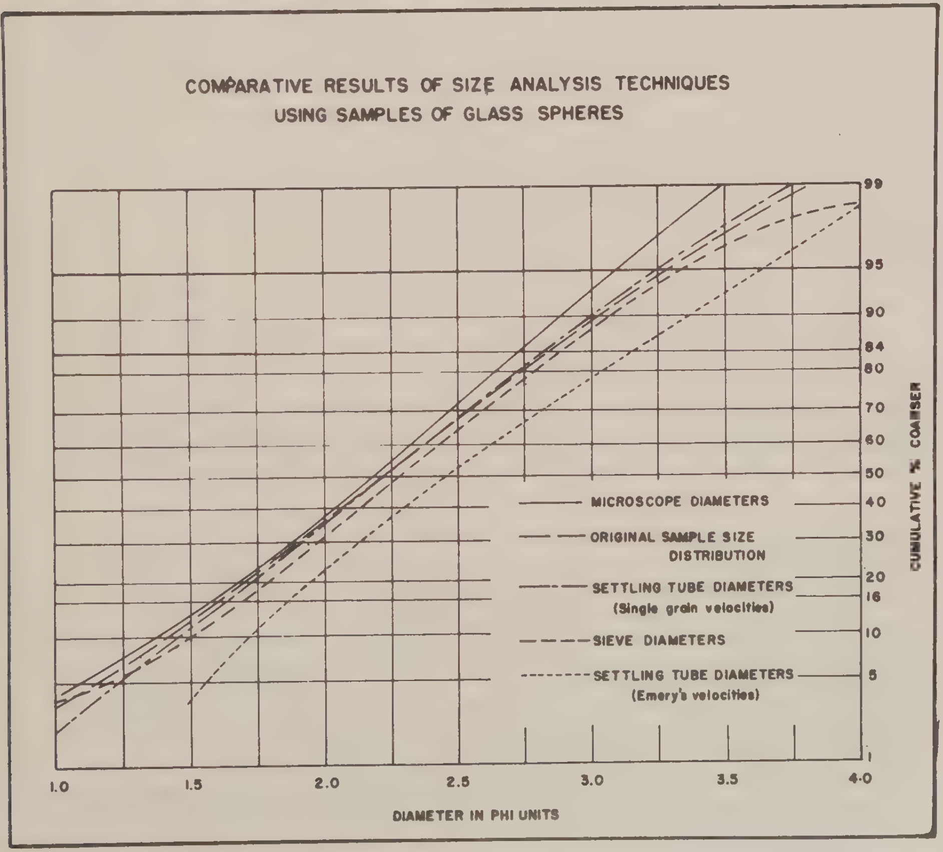

FIG. 3.—Comparison of several methods of size analysis of samples of glass spheres with a controlled size distribution. Settling velocities for the settling tube analyses were determined for spheres with the density of glass.

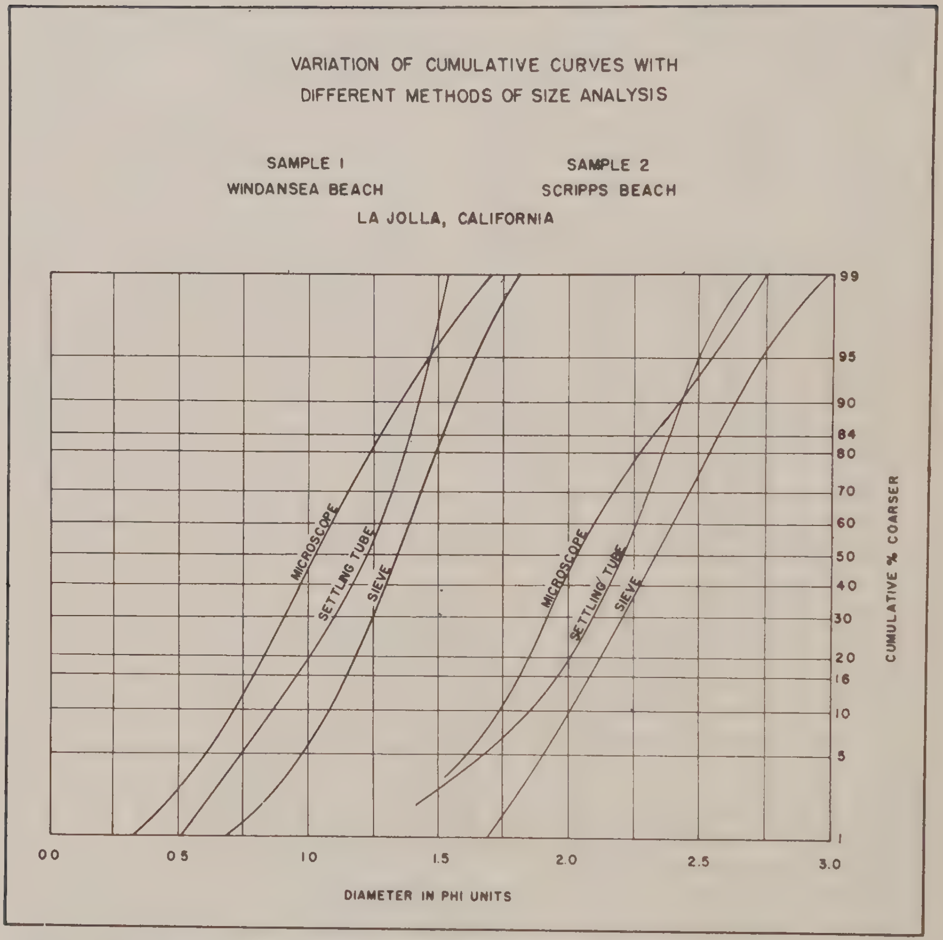

FIG. 4.—Comparison of cumulative curves of samples showing differences owing to the methods used for size analysis. Settling times determined by Heywood's method used for settling tube analyses. Diameters measured by microscope were converted to weight to make them comparable to sieve analyses.

neers Report #7, 1943, and extends smoothly into the Stokes' law curve.

To determine the effect on settling velocities caused by the introduction of the sample, using Puri's (1934) device, and fall of a group of grains in the settling tube, tests were run using samples of the glass spheres with controlled size distributions. Settling velocities were determined indirectly by a method similar to that of Emery (1938). The sample was dropped once to determine the total cumulative height in the graduated part of the tube, and from the known size distribution the cumulative height of each size fraction was noted on the graduations. The sample was dropped again and the time to reach each of the various cumulative heights was recorded and settling velocities calculated. Three test samples of 3.50 grams each were run in duplicate to avoid gross errors. Two of these samples contained between 40 and 60 percent material coarser than 2.0ϕ (0.246 mm) while the other contained about 70 percent material between 3.0ϕ (0.124 mm) and 4.0ϕ (0.061 mm). The settling velocities determined by

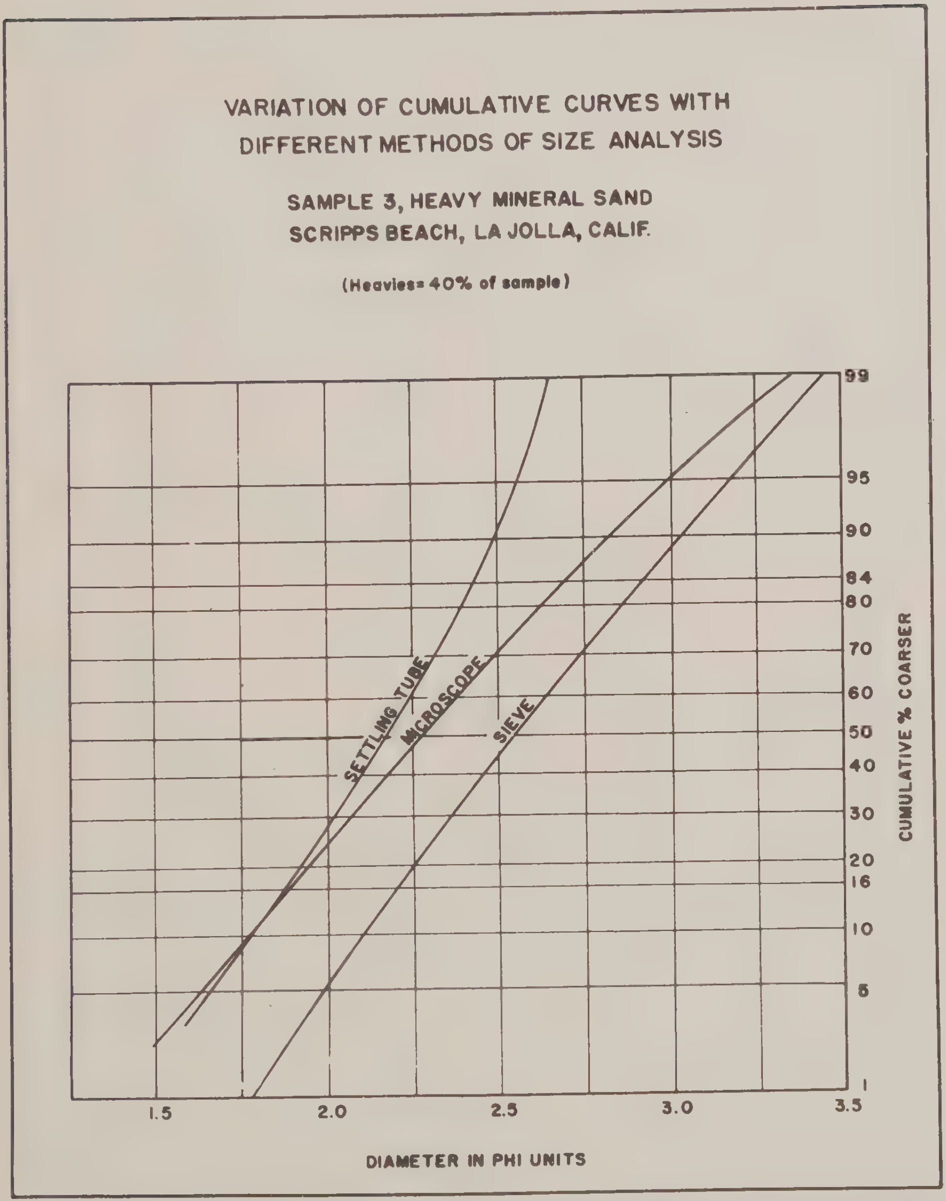

FIG. 5.—Comparison of cumulative curves of samples showing differences owing to the methods used for size analysis. Settling times determined by Heywood's method used for settling tube analyses. Diameters measured by microscope were converted to weight to make them comparable to sieve analyses.

group-grain tests were plotted against diameter and this curve was transformed, in the same manner as that for single grains, to one for spheres with a density of 2.65 gm/cc. It is apparent that the single grains fall about 10 to 15 percent more slowly than the group-dropped grains of the same diameter (fig. 2). Hence, the use of settling velocities based on the fall of single grains results in diameters about $\frac{1}{8}\phi$ unit coarser than the known diameters. The above is true only for the sample weight used, in this case 3.50 grams. McNown and Lin (1952), using homogeneous concentrations of uniformly sized material, have shown that large sample concentrations significantly reduced fall velocities. However, the effects of sample concentration on settling velocities for other than uniform and homogeneous (i.e., all particles of the same settling velocity distributed homogeneously through the column) samples are not known. In this study the effect on settling velocity of only three groups of samples with different particle size distributions, each weighing 3.50 grams, was evaluated. Therefore, because of unknown effects of concentration, it appears best to use settling velocities of single grains for routine size analyses, always remembering that the diameters obtained are probably somewhat larger (about $\frac{1}{8}\phi$ or less) than the actual diameters. Table 1 gives times of fall (for 164 cm—the length of the Emery settling tube) for quartz spheres in distilled water at various temperatures, using settling velocities determined by Heywood's (1938) method. These times of fall are useful for making up a settling tube data sheet, and were used in the settling tube analyses of the natural sands.

Size analyses of four sand samples (and a

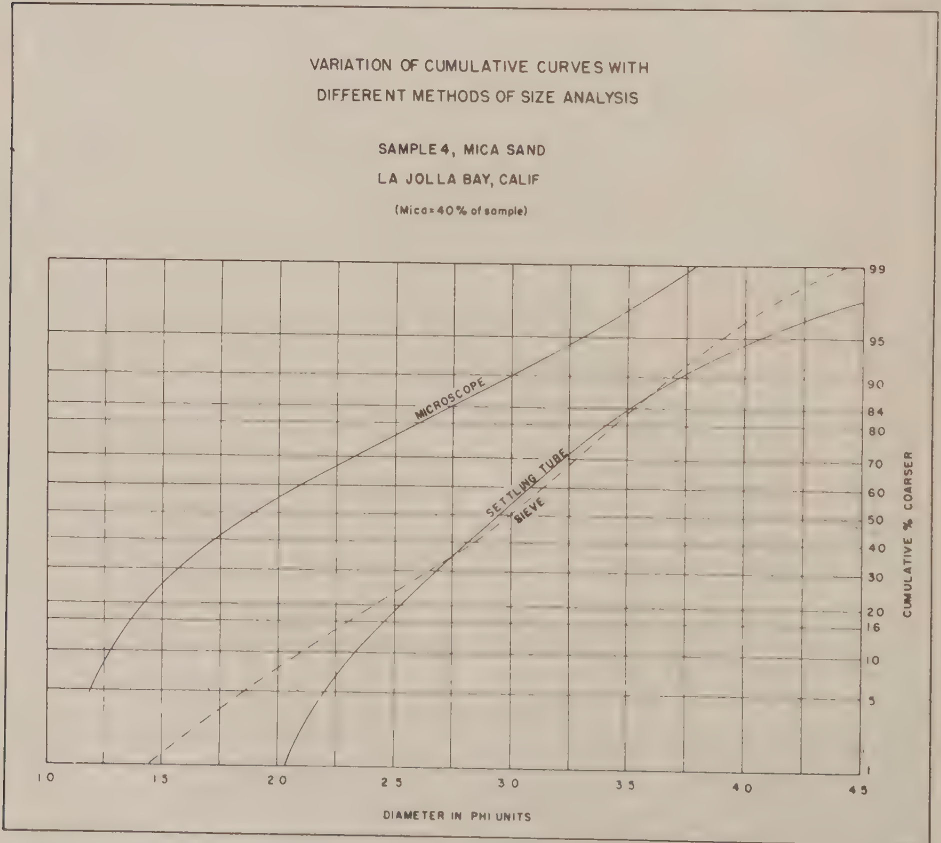

FIG. 6.—Comparison of cumulative curves of samples showing differences owing to the methods used for size analysis. Settling times determined by Heywood's method used for settling tube analyses. Diameters measured by microscope were converted to weight to make them comparable to sieve analyses.

TABLE 2.—*Summary of advantages and disadvantages of three methods of size analysis*

Method	Advantages	Disadvantages
Microscope	Factors such as shape and roundness can be measured while making size analysis. Size data expressed as a number frequency	Tedious and time consuming. Size distribution must be converted to weight to make it comparable to other methods, and this is shown to be inadequate
Settling Tube	Rapid and easy to use. Shape, volume, and density of particle are taken into account. May approach actual conditions of deposition	Sample on introduction tends to fall as a unit giving slightly erroneous settling velocities. Volume measurements rather than weight used
Sieve	Easy to use. Reliable. Most size analyses of sand-size material have been made by this method	Results adversely affected by particle shape. Density not taken into account. Rated sieve opening smaller than effective openings and change with usage

glass sphere sample with a controlled size distribution) were made by sieving, sedimentation, and microscope. Two of the samples were well-sorted sands with median diameters ranging from about 1.25ϕ (0.420 mm) to 2.25ϕ (0.210 mm), the third a sand with about 40 percent (by weight) heavy minerals (containing about 60 percent hornblende), and the fourth a sand with about 40 percent (by weight) mica. These samples were treated with 3 N HCl to free them from carbonates such as shell fragments, then were washed, soaked in a dispersing agent (0.025 N sodium hexametaphosphate, $Na_6(PO_3)_6$(?)), and stirred for 10 minutes in a malt-mixer. Any material finer than coarse silt (0.03125 mm) was decanted and the coarse material dried and saved. The dried portions were divided (by using the Otto microsplit) into fractions for the settling tube, sieve, and microscopic size analyses. A sample of glass spheres was made up with a controlled size distribution and was split into fractions for the three methods of size analysis.

The microscope size analyses were made by measuring the intermediate diameters, which were converted to weight in order to make them more comparable to sieve analyses (Krumbein and Pettijohn, 1938, p. 302). The microscopic size analyses were prepared by carefully splitting a sample to 300 or 400 grains, sprinkling them on a glass slide and then tapping the slide a few times so the grains would assume their most stable position. The most stable position is one in which the grains tend to lie on one of their larger surfaces, more or less parallel to the plane containing the largest and intermediate diameters (Wadell, 1935; Pettijohn and Ludahl, 1943). Only 300 to 400 grains were measured (using a micrometer eyepiece) according to the "rule of thumb" of Krumbein and Pettijohn (1938, p. 178), i.e., grains were measured until there was no great change in the size distribution.

RESULTS AND CONCLUSIONS

Results of the different methods of size analysis for a sample of glass spheres with a controlled size distribution are shown in figure 3. The microscope, settling tube (using single grain fall velocities), and sieve analyses fall close to the original (controlled) size distribution, while the settling tube analysis using Emery's velocities (corrected for the density of glass beads) gives a much finer distribution. This comparison shows that any of these methods of analysis are adequate to determine size distributions of spherical particles, but this is not true for natural sands where spherical shapes are rare.

The settling tube analyses, using fall velocities determined by Heywood's (1938) method, consistently gave coarser median diameters (about $\frac{1}{8}\phi$ coarser) than the sieve analyses in all the samples of natural sand (figs. 4–6). The greatest variation in median diameters occurred in the sand rich in heavy minerals. The heavies, which made up most of the finer fraction of the sand, settled with quartz grains of larger diameter and thus gave a much larger median diameter (about 0.5ϕ coarser) than the sieve analysis. In the mica-sand analyses the sieve and settling tube median diameters were similar but the tails of the distributions were quite different.

The mica grains which were in the coarsest fraction of the sample settled with finer quartz grains. The difference between settling tube and sieve diameters in these natural sands can be partially explained by the fact that effective diameters of the sieve are larger than the nominal diameters. Moreover, sieves give a size distribution dominated by particle shape (density is not a factor), whereas in a sedimentation analysis the shape, volume, and density of the grains determine their settling velocities and related size. Corrections of settling velocities for various particle shapes were attempted (Heywood, 1938), but the amount of labor involved and the inconsistencies of the results were too great to make them useful for routine size analyses. Consequently it was decided to use sedimentation diameters only as an expression of size.

In all except the heavy mineral sample, the median (intermediate) diameters determined by the microscope method were coarser than those of either the sieve or settling tube. In the microscopic size analyses shape is also dominant. If the grains were nearly all equi-dimensional (more like spheres), measurements of the intermediate diameters, converted to weight, would agree more closely with sieve and sedimentation analyses than if the grains were lath-shaped or disk-shaped.

From this study it is concluded that single grain settling velocities are most useful for settling tube analyses and until the effects of concentration and the introduction of the sample on settling velocities are adequately understood, the indiscriminate use of correction factors unnecessarily complicates results and reduces reproducibility among analysts. The advantages and disadvantages of the various methods of size analysis used here are summarized in table 2.

ACKNOWLEDGMENTS

The writer wishes to express his appreciation to G. A. Rusnak for his many valuable suggestions and critical reading of the manuscript. He would also like to thank F. P. Shepard, D. L. Inman, and J. R. Curray for their helpful suggestions and careful reading of the manuscript

REFERENCES

Emery, K. O., 1938, Rapid method of mechanical analysis of sands: Jour. Sedimentary Petrology, v. 8, p. 105–111.

Heywood, H., 1938, Measurement of the fineness of powdered material: Inst. Mechanical Engr., Proc., v. 140, p. 257–347.

Krumbein, W. C., and Pettijohn, F. J., 1938, Manual of Sedimentary Petrology. D. Appleton-Century Co., Inc., New York, 549 p.

McNown, J. S., Lee, H. M., McPherson, M. B., and Engez, S. M., 1948, Influence of boundary proximity on the drag of spheres: Proc. 7th. Inter. Congr. Applied Mechanics (London), p. 17-29.

McNown, J. S., and Lin, P. N., 1952, Sediment concentration and fall velocity: Proc. 2nd Midwestern Confr. Fluid Mechanics, Ohio State University, Columbus, p. 401–411.

Pettijohn, F. J., and Lundahl, A. C., 1943, Shape and roundness of Lake Erie beach sands: Jour. Sedimentary Petrology, v. 13, p. 69–78.

Poole, D. M., Butcher, W. S., and Fisher, R. L., 1951, The use and accuracy of the Emery settling tube for sand analysis: Beach Erosion Board, Corps of Engineers, Tech. Mem. No. 23, 11 p.

Puri, A. N., 1934, A siltometer for studying size distribution of silts and sands: Punjab Irrigation Research Inst., Research Publ., v. 2, no. 7.

U. S. Engineers, 1941, A study of methods used in measurement and analysis of sediment loads in streams. Rept. No. 4. Methods of analyzing sediment samples: Published at St. Paul, U. S. Engineer District Sub-Office, Hydraulic Lab., Univ. of Iowa, Iowa City.

U. S. Engineers, 1943, A study of methods used in measurement and analysis of sediment loads in streams. Rept. No. 7. A study of new methods of size analysis of suspended sediment samples: Published at St. Paul, U. S. Engineer District Sub-Office, Hydraulic Lab., Univ. of Iowa, Iowa City.

U. S. Engineers, 1953, A study of methods used in measurement and analysis of sediment loads in streams. Rept. No. 10. Accuracy of sediment size analyses made by the bottom withdrawal tube method: Published at St. Anthony Falls Hydraulic Lab., Minneapolis.

Wadell, H., 1934, Some new sedimentation formulas: Physics, v. 5, p. 281–291.

Wadell, H., 1935, Volume, shape, and roundness of quartz particles: Jour. Geology, v. 43, p. 250–280.

IS THE SPEAR OF ISTIOPHORID FISHES USED IN FEEDING?

Robert L. Wisner

Reprinted from PACIFIC SCIENCE, Vol. XII, No. 1, January, 1958,
Pages 60-70

Reproduced by Permission

Is the Spear of Istiophorid Fishes Used in Feeding?[1]

ROBERT L. WISNER[2]

THE SPORT OF ANGLING for spearfishes—the several marlins and sailfishes of the family Istiophoridae—has fostered many books and articles on the behavior of these large fishes. The swordfish, *Xiphius gladius* Linnaeus, comprising the family Xiphiidae, also commands a very considerable following among salt-water anglers and is the subject of an extensive literature. Certain beliefs have arisen concerning the behavior and habits of the fishes comprising these game fish families, particularly as to their methods of obtaining food. It seems worthwhile to attempt now an evaluation of the accumulated evidence. Only the true spearfishes, particularly the marlins, will be considered in detail. The broadbill swordfish will be mentioned only occasionally, and the conclusions reached do not necessarily pertain to this fish.

Angling lore is replete with reports of such fishes stunning prey and trolled fish baits with a blow of the spear before devouring them. The time-honored belief that the spearfishes possess their spears for the express purpose of striking or stabbing prey, however, may now be questioned. Recently accumulated evidence indicates that such fish can exist quite readily without a spear to aid in obtaining food. Other evidence has cast some doubt as to whether the spear is at all commonly employed in such a manner.

RECORDED OBSERVATIONS OF FISH WITHOUT SPEARS

Moore (1950) reported on a spearless black marlin, *Makaira mazara* (Jordan and Snyder), that was landed at a commercial fish market in Honolulu, Hawaii, without indicating the length of stub remaining. The nature of the wound indicated some time lapse since the loss. The specimen weighed 545 lbs. and was judged equal in physical condition to normal fish of the same species.

Mr. Vernon E. Brock, Director, Division of Fish and Game, Hawaii, in correspondence reports ". . . a spear removed from a marlin which has been broken with the remaining part that is spiraled like a corkscrew. The fish from which the spear was taken was, according to the fishermen, normal in all respects."

Morrow (1951) reported that a 172-lb. striped marlin, *Makaira mitsukurii* (Jordan and Snyder), taken with sporting tackle and trolled bait at Otehei Bay, New Zealand, had the spear broken off on a long slant reaching from several inches behind the mandible tip to within a few inches of the eye. The break had completely healed and was well covered with skin. The injury had affected the fish further in that the mouth was prevented from closing completely, one side remaining partly open. However, the fish appeared to have had no difficulty in taking the bait and gave a battle said to have been entirely normal for a fish of its weight.

Farrington (1942: 110) reported numbers of marlin with spears broken off. This observation was made at Guaymas, Sonora, Mexico. Grey (1926: 105) mentioned a marlin in New Zealand waters that had a broken spear. The region of the break is not indicated, nor is the amount missing. Grey states, "Deprived of his weapon of defense and for procuring food, this marlin might well have been expected to be thin, flat, in poor condition. Nevertheless, he was solid, fat, in splendid shape. He had been compelled to rely on his speed."

---

[1] Contributions from the Scripps Institution of Oceanography, New Series, No. 958. Manuscript received March 27, 1956.

[2] Scripps Institution of Oceanography, University of California, La Jolla, California.

In September, 1952, the author examined two spearless striped marlin at the Marlin Club dock at San Diego, California. Each was captured with sporting tackle and trolled bait. Each spear had been broken off at about the tip of the lower jaw, as in Figure 1. Since both stubs had healed completely and were well covered with skin, a considerable time must have elapsed since the injuries. The fish weighed, respectively, 149½ and 186 lbs. (official club weight). These fish were of at least average weight for their length (Fig. 3). Morphometric data obtained on both specimens when compared with those of normal fish of the same body length and weight disclosed no significant differences in body proportions.

The stomach contents of the smaller fish comprised the remains of 8 Pacific sauries, *Cololabis saira* (Brevoort), totalling 349 cc. The larger fish contained 5 small yellowfin croakers, *Umbrina roncador* Jordan and Gilbert, totalling 785 cc., a small halfmoon, *Medialuna californiensis* (Steindachner), 105 cc., and 1 trunk section of a Pacific saury, 23 cc. The first fish had eaten a main item in the diet of local marlin, as determined by Hubbs and Wisner (1953), but its stomach contents were of less than average volume. The second had eaten more than an average amount, but chiefly of a shore species not otherwise encountered in the food studies.

A third spearless striped marlin was landed at the San Diego Club on September 17, 1955. This fish was not examined by the author, but was reported to have been normal in all respects and fought strongly. The stub was reported to be smoothly healed and covered with skin. A fourth spearless fish, landed in September, 1956, also was reported to be quite normal despite its loss of spear. This fish also was not examined by the author.

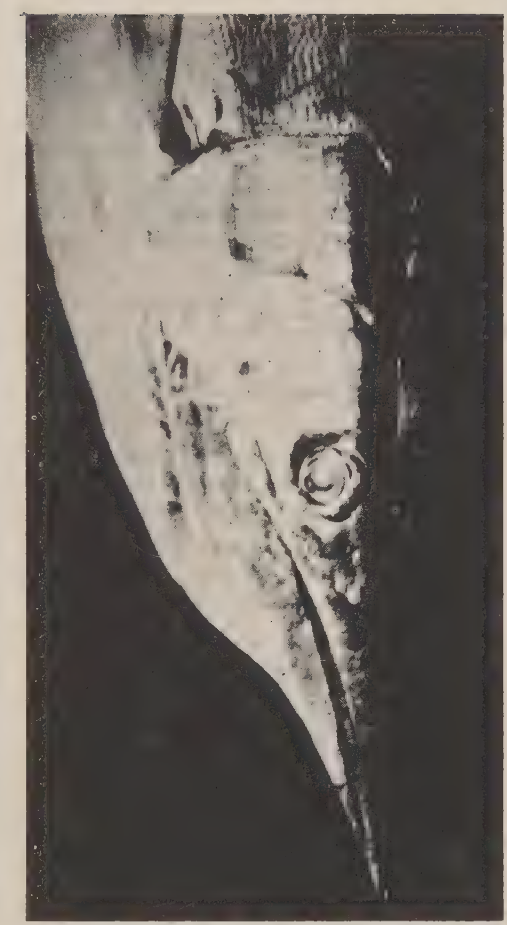

Fig. 1. Spearless striped marlin, weighing 149½ pounds. Photographed at the San Diego Marlin Club, Sept. 13, 1952, by R. Van Nostrand.

Gudger (1940) cited many examples of portions of spears having been broken off at a considerable period of time before capture. All these fish had apparently survived the wound and had flourished since. Unfortunately, most reports did not estimate the amount of spear missing. One account approaches the incredible. During the Michael Lerner Australian-New Zealand Expedition, Miles Conrad reported seeing a marlin with the spear sawed off, and yet the fish had survived. The spear had been removed by a square cut about midway between the tip of the lower jaw and the anterior edge of the eyes—the point generally selected for sawing off a spear trophy. The fish had evidently been caught by an angler, and, when the spear had been removed, had escaped to the ocean. The growth of skin that had formed over the stub still retained the rosy glow of healthy healing. The fish was reported to be thinner than a normal fish of its size. Without doubt a fish so injured as to leave the upper half of its mouth permanently open with but half an upper jaw would be seriously handicapped in feeding. The previously cited injuries had at least left the fish with mouths somewhat suited for grasping and holding prey.

As stated by Morrow (*op. cit.*), "It is obvious the spear is not absolutely essential to the well being of the spearfishes." The four specimens under the immediate cognizance of the author, as well as those reported by Moore, Morrow, Brock, and Gudger, had apparently existed in normal fashion despite the loss of the spear. None of those taken on sporting tackle had given any marked indication of weakness, or other abnormal behavior attributable to loss of the spear, while striking the trolled bait or during the ensuing battle.

RECORDED FEEDING AND BAIT-SEIZING HABITS

The fact that marlins can exist reasonably well without their spears reopens the question of how spearfish feed. Many anglers and authors of books on angling for the large game fishes have given accounts of spearfishes stunning their prey and trolled fish baits with a slashing blow, before turning to devour them. The angling methods for these fish have long involved a slack line arrangement to allow the bait to lie "dead" in the water following the initial rush or strike of the fish.

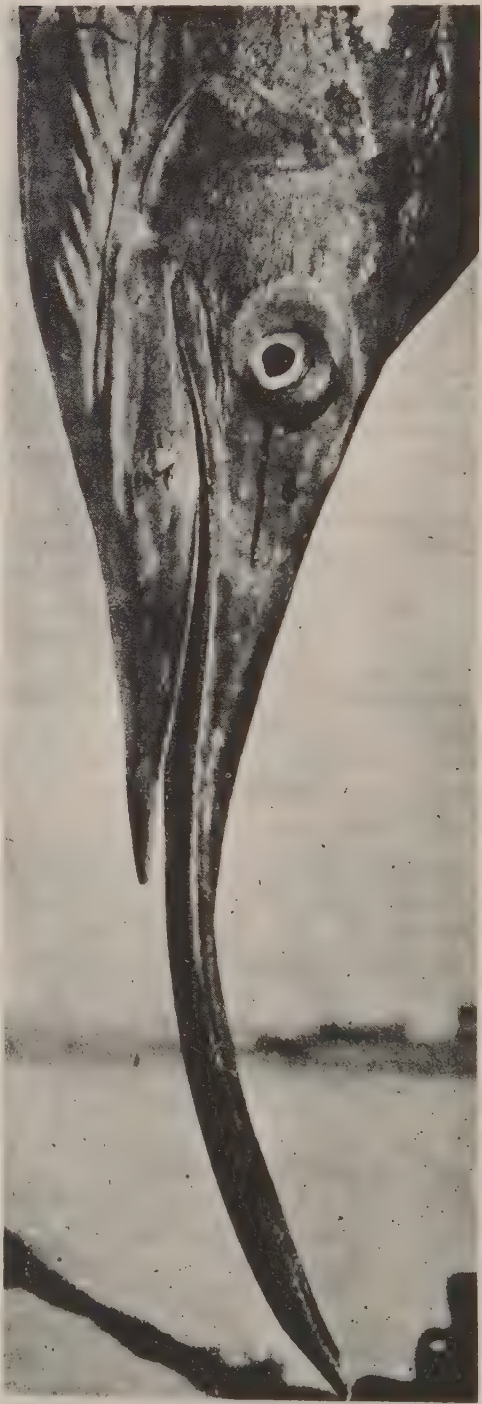

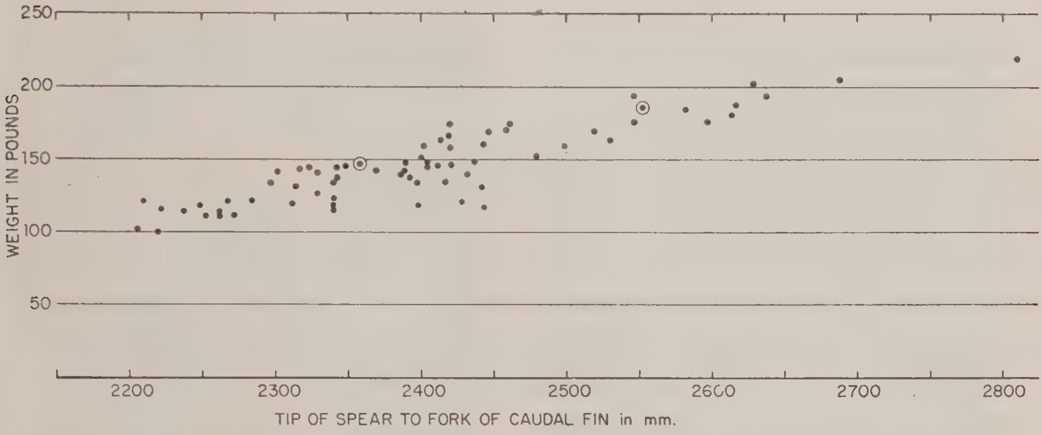

FIG. 3. Relation between weight and length from tip of spear to fork of caudal fin for striped marlin caught near San Diego in 1952. The two circled entries are for the two spearless fish caught that year. Their lengths are computed by adding the average length of spear from tip of mandible for other marlin of the same length behind tip of mandible. The two spearless fish are at least average weight.

According to Van Campen Heilner (1943: 108–109) almost no spearfish were taken in Florida waters before the discovery of this method by the famous Captain Bill Hatch of Miami, Florida, while experimenting with methods of taking sailfish. Heilner stated that Hatch, the father of the "Drop-back," came to the conclusion that, "When the sailfish first rushed the bait he struck it a blow with his spear to stun it and if it didn't collapse then and there, something was phoney. By immediately allowing a lot of line to run off the reel the sailfish was fooled into believing he had paralyzed his prey and would return to seize it." Prior to the use of this method the sailfish only mauled the fish being used as bait for kingfish and mackerel but could not be hooked, which may indicate that the sailfish were grasping the bait between their jaws rather than striking it with their spears and that the bait was pulled from their jaws or rejected before it could be swallowed.

It is known, of course, that marlin in particular do not always strike a blow before taking the bait. A fast rush and grab is most frequent. A hungry fish, of course, is much less apt to toy with a bait or prey than to make haste in consuming it. Thomas and Thomas (1930: 130) cited a fish that did not attempt to stun the bait with the spear. "The marlin changed direction in his rush and, just before he reached the lure he swerved to one side, as such fish nearly always do, and seizing his prey between his jaws, whirled, splashed a trifle, and, like a ray of light as he showed his gleaming underbody, turned downward and was away." In another connection (p. 122) these authors stated: "When marlin hit a troll they do not grab it in their mouths as do other fish; rather they seize it between their upper and lower bills before swallowing, and seem to approach the lure sideways, turning it before gulping it down." Bandini (1933) lent support to this opinion by stating, "A marlin seizes the bait crossways in his mouth and swims away with it."

In contrast to the foregoing testimony, Thomas and Thomas described the feeding habits of marlin as follows (p. 121): "They feed chiefly on anchovies, sauri [*sic*], sardines, flying fish, and other small fry, charging into schools of these unfortunates and slashing

FIG. 2. Striped marlin with a deformed spear. Photographed at Mazatlán, Sinaloa, México, Mar. 26, 1954, by R. L. Wisner.

right and left with their bills, before turning back and leisurely picking up those they have killed or crippled." Another report by these authors (p. 136) was that: "Marlin were everywhere, scattering bait and cutting the water with their fins and tails .... Terrified patches of bait skittered across the water endeavoring to elude their pursuers who slashed relentlessly."

Voss (1956) has contributed the following information. "How well the sailfish uses this weapon I discovered one calm winter day off Stuart, Florida, when we backed our boat into a school feeding on minnows. The sailfish circled slowly, sails half raised, herding their prey tighter and tighter. First one and then another broke from the circle and swam through the milling prey, thrashing right and left with their bills. Then the predators would submerge and lazily eat the dead and stunned minnows as they drifted down."

It is, of course, possible that a difference exists in the method of capturing trolled baits and free-swimming prey, even though the spearfishes may be facile in each method. One must give complete credence to such observations as made by Voss. It is evident that on occasion, abnormal though it may be, the spear is used to obtain food by thrashing. However, the mass of observations indicate this to be a rather infrequently employed method. The following observations from the field and from studies of stomach contents shed considerable light on the matter.

In examining the stomach contents of many marlin, the author has at times noted that the heads and pectoral regions of some of the less digested specimens had been severely damaged on both sides, presumably as a result of having been crushed between jaws. Along the same line Thomas and Thomas (*op. cit.*, p. 124) stated that "the bills [upper and lower jaws] of a marlin leave two distinct depressions on a small fish just behind the gills." These observations indicate that, at least at times, the struggling prey is seized so as to kill it, or to hold it firmly preparatory to swallowing it. The observations also indicate that in such situations the spear is not used to obtain food. If the prey had been killed or stunned or so injured as to prevent escape the marlin would not have needed to crush the prey before swallowing it.

That marlin can feed without the use of the spear is demonstrated by the following statement by Miss Francesca LaMonte of the International Game Fish Association (quoted by Hubbs and Wisner, 1953): "Dr. D. G. Maitland of Sydney, Australia, has recently written us as follows: 'It may interest you to know that I have actually watched a pair of Black Marlin feeding upon *Physalia*, like huge Rainbow Trout taking flies, and absolutely ignoring a most tempting looking mackerel bait drifting in front of their noses.' "

That prey much larger than the small coelenterate of the genus *Physalia* may be captured without obvious use of the spear is indicated by another observation. During preliminary studies of the food of striped marlin in the San Diego area in 1952, a young blue shark, *Prionace glauca* (Linnaeus), a little longer than 24 inches, was found in the stomach of a 205-pound marlin. This shark, which had been recently ingested bore no marks of a blow or thrust of the spear. A roughening of its skin over rather broad areas could have been produced by the sandpapery jaws of the marlin as it grasped and held the struggling shark. A blow, or blows, of sufficient force to kill or stun the notoriously hard-to-subdue shark would almost certainly have left identifiable marks on the body.

Still another indication of feeding that certainly would not call for use of the spear was encountered by the author while examining striped marlin stomach contents at Mazatlán, Sinaloa, México, in March, 1954. Both marlin and sailfish were feeding on a species of argonaut. Such a relatively slow-moving mollusk would be as easily captured as *Physalia* and would require not even the lightest tap from a spear.

Until very recently none of the studies of the food habits of marlin has disclosed any ingested fish that show the marks of having been slashed by or impaled on the spear. Hubbs and Wisner (1953), for example, found no evidence of fish having been damaged by the spear. A more definitive study of stomach contents for the 1952 and 1954 seasons in San Diego has substantiated these findings. Miss Francesca LaMonte (correspondence) states: "In no case have I ever seen anything that seemed to have been slashed by the spear or impaled upon it."

RECORDED USES OF THE SPEAR

The fact that the spear has been retained since possibly Upper Cretaceous, and certainly since Eocene times (Berg, 1940), indicates that it is much more of an aid than a hindrance to the fish. That the spear may, on occasion, be used to obtain food by stabbing, or as a weapon, is illustrated by the following observations. Anonymous writers (1955*a*, *b*) recorded that during a cruise into tropical waters south of Hawaii, "An interesting incident was the landing of a huge white marlin [*Istiompax marlina* (Jordan and Snyder)], estimated to have weighed around 1,500 pounds, which had in its stomach a freshly killed yellowfin tuna 5 feet in length and weighing 157 pounds. . . . The tuna had been speared clean through its body twice before being swallowed."

Another such observation from Hawaiian waters, again provided by Mr. Vernon E. Brock (correspondence), is as follows, ". . . the use of the spear to stab another fish does occasionally occur. One such observation by the skipper of the territorial research vessel was made off the Kona coast of Hawaii a number of years ago when a marlin was observed at the surface of the sea with its spear thrust through the body of a dolphin [*Coryphaena hippurus*]. The dolphin was struggling vigorously and the marlin would rear out of the water in an apparent attempt to prevent the flopping fish from working free of the spear."

Zane Grey (1926: 48) reported finding a snapper with a round hole in it in the stomach of a marlin caught in New Zealand waters. In Tahitian waters Grey (1931: 229) quoted Captain Mitchell, his fishing companion, as reporting his bonito bait rammed clear through by a marlin. Farrington (1937: 221) reported big dolphin "batted" into the air by marlin and that numbers of dolphin have been caught that had holes in them where marlin spears had pierced them.

This author has very recently studied a frigate mackerel, *Auxis* sp., and a sierra mackerel, *Scomberomorus sierra* Jordan and Starks, removed from marlin landed at Mazatlán, Sinaloa, México in March, 1954. These fish, respectively 300 and 430 mm. long, each bore the marks of a spear thrust through the midsection, respectively above and below the lateral lines. Each fish was removed by the author from undamaged, freshly caught striped marlin and wrapped and stored until studied. Unquestionably, the marks were made by spears as the holes were large and had been torn out through the dorsomedian flesh of the *Auxis*, and through the ventromedian flesh in the *Scomberomorus*. Several other fish of the same species groups and similar in body sizes bore no marks of the spear.

Gudger (*op. cit.*, pp. 271–274) cited several reports from reputable observers which indicate that battles occur between swordfish and spearfish, and between members of these two families and sharks. Broken spears have been found imbedded in the flesh of each, some obviously having been there for some time. Voss (*op. cit.*) reported catching a sailfish that had the broken bill of another sailfish projecting [through the body] on either side.

SPECULATION ON THE USES OF THE SPEAR

It seems probable that the spear is used both as an aid in food-getting and as a weapon. It is a rather moot question whether the cited stabbings and "battings" of larger fish resulted from pugnacity, playfulness, or a desire to obtain food. The 157-pound tuna could conceivably have been regarded as an enemy by even a 1,500-pound marlin. The big dolphin would not seem to fit the enemy category although the relative sizes of prey and predator were not given. If it may be assumed that marlin customarily charge their prey to engulf it, it is then possible that the stabbings were accidental. If a spearfish is able to overtake its prey with sufficient speed to impale it, such speed should be more than adequate to permit the prey to be seized. Accidental stabbings of the smaller prey seem quite plausible if one considers the almost phenomenal accuracy required of the predator to hit and penetrate even an unsuspecting prey. In line with this view, impaling an evasive prey appears to be governed by chance. The few observations of stabbing make it seem possible that the spear may be used against the larger fishes—those not readily captured by overtaking and seizing between jaws.

The preponderance of evidence indicates the spear is not commonly used as a means of getting food. The food content studies to date have all dealt primarily with smaller forage animals. Presumably few others have been found. One must conclude that these comprise the bulk of the food of the spearfishes. As stated earlier, few indications of stabbing and none of injury by blows have been found. The prey had evidently been overtaken and engulfed by the predators. Those spearfish found with the spears missing had almost certainly employed this method of getting food.

Examination of the spear and jaws indicates that the smaller forage fish and squid, the prime components of spearfish food, could not readily be stabbed. The spear is relatively dull at the tip and is covered by minute, sharp, backward-pointing nodules for its entire length. These nodules continue to each jaw, where they become a raspy band of teeth. The roughness of the spear covering is attested by fishermen who almost invariably wear gloves to avoid having their hands abraded while the fish are being boated. It would be difficult indeed for the dull tip to penetrate small fish. Certainly the soft, flexible body of a squid would be extremely difficult to be impaled or to be dealt a damaging blow with so blunt a weapon. The swordfish has a smooth, laterally flattened sword of proportionately greater length than that of the spearfishes, but it is equally blunt at the tip. It is better suited as a flail but no better suited for spearing small prey. A striped marlin poorly suited for stabbing prey was observed by the author at Mazatlán, México, 1954 (Fig. 2). The curve of its spear was such that a thrust would tend to slide off a relatively small fish.

Further evidence that the spearfishes do not commonly slash with their spears is found in their skeletal make-up. The construction is not suited to free and extensive sidewise motion. The istiophorids have heavy, flat, platelike neural and hemal spines rather than the common rodlike spines of other fishes. The neural processes are modified into broad platelike structures that extend far forward, almost reaching the middle of the preceding vertebra. The platelike hemal spines are firmly attached to the hemal processes of the neighboring vertebrae, as are the neural spines and processes. Such construction produces an exceptionally strong and inflexible, interlocking, bracing system. The vertebral column of the broadbill is less interlocked but is so fashioned as to resist greater shock from head-on encounters than is that of the spearfishes.

Nakamura (1938), who studied the skeletons of many spearfishes, concluded that "The vertebrae are most unsuited for precise movements, and sudden changes of direction are probably impossible." Furthermore, the deep and flat lateral surface of the anterior part of the body would require tremendous energy and leverage against the resistance of the water to accomplish a slashing movement sufficiently rapid to strike a small fish fleeing for its life. Such great expenditure of energy would detract from the forward speed of the spearfish, bringing it to a virtual standstill and allowing the prey to escape with but little damage.

It is more reasonable to assume that when a spearfish charges into a school of forage fish the slashing motion observed by many fishermen is really a slight changing of direction and a grasping for the fleeing prey, the head and body describing a relatively small arc. Such a grasping motion is not be to identified with any such deliberate slashing as Voss (*op. cit.*) reported for sailfish. In his observation the prey was herded into a tight school. The speed of the predators was not mentioned. They merely swam into the closely packed school, held together by the remaining sailfish (of unreported number), and thrashed with their spears. Presumably all energy could be utilized solely to kill fish rather than be expended in pursuit.

It must be assumed that spearfish are not always able to concentrate their prey in such fashion. In a less dense and guarded school of prey, and certainly in a very scattered school, it would not be advantageous to merely slash. It is entirely possible that the normal procedure is to charge into the school rapidly snapping the jaws and reaching, within physical limits, for as much prey as possible, with the result that many of the small fish are killed or wounded before the school scatters. Any effective striking with the spear that may occur is probably a secondary and fortuitous event. After the school has scattered the spearfish would likely see the wounded or killed fish and would return to ingest them.

These large fishes are obviously built more for forward speed than for marked agility. It is entirely within reason to assume that a spearfish can readily overtake any of the forage fishes or squid, which constitute the bulk of its food, and most of the larger fishes. A conservative estimate of their speed is at least 25 miles per hour and bursts of much greater speed are probable. A hooked sailfish was clocked at 100 yards in three seconds, or approximately 68 miles per hour (Walford, 1937).

The enormous speed and power of spearfish are dramatically attested by the puncturing of ship hulls. Gudger (1940) reported, with documentation and photographs, many spears found in wooden and copper-clad hulls of vessels. Some of these had penetrated fantastic thicknesses of timber and had broken off to furnish irrefutable evidence of speed and power. One remarkable example follows: "The spear was found to have penetrated through the copper sheathing, an inch board sheathing, a three inch hard wood plank, the solid white oak timber of the ship 12 in. thick, through another two and a half inch hard oak ceiling-plank, and lastly had perforated the head of an oil cask, where it remained immovably fixed so that not a single drop of oil had escaped." This total of 18.5 inches through hardwood, 14.5 of it through dense oak, was accomplished by a spearfish as the recovered spear was round, unlike the flattened blade of the broadbill swordfish.

San Diego based wooden-hulled fishing vessels have at times been placed in danger of sinking by these fish. The tuna vessel "Rose Ann" (San Diego Union, 24 Oct., 1946) was struck three feet below the water line off Punta Abreojos, Baja California, and was forced to use both bilge pumps constantly to remain afloat. Subsequent investigation revealed five inches of marlin spear projecting through the hull planking. Fishermen recalled that other vessels in 1942 and 1946 had suffered the same type of damage. Another recorded ramming occurred off Ecuador, involving the tuna vessel "Renown" (San Diego Union, 22 Aug., 1948). Pumps were operated continuously during the homeward voyage. When the hull was inspected 18 inches of marlin spear was found projected through the 3-inch hull planking, forming a crack an inch wide.

There are further indications of the speed and power of marlin, and possibly of their pugnacity. Morrow (1951) reported having seen on a beach in British East Africa a bale of crude rubber that held the broken spear of a black marlin imbedded 8 or 10 inches into rubber so tough a man could not drive a spike into it with a heavy hammer. Smith (1956) reported on floating rubber bales from the African coast. As many as four spears have been found in one bale. Another bale contained 24 inches of the spear of a large black marlin embedded to a depth of 13 inches. In one bale was found the sword of a broadbill swordfish, indicating that it also charges floating objects.

The reasons for these attacks are not completely understood. Some may be the result of sheer pugnacity. However, it has long been known that fish often lie beneath floating logs, debris, ship hulls or any fairly large, slowly moving object at or near the surface. The tuna live-bait fishermen make a practice of fishing, often with considerable success, close to such objects, including the large whale shark, *Rhineodon typus* Smith. The ramming of ship hulls may well be the result of excess speed and a lack of maneuverability of the attacker as it charges to engulf fish lying under such shelter.

Gudger (*op. cit.*) supported this view with an observation by F. D. Bennett (Narrative of a Whaling Voyage Round the Globe, 1833 to 1836, London, 1840). Bennett tells of albacore [*sic*], clustering in a dense shoal under the ship, that "swam with an appearance of trepidation and watchfullness. The cause of this unusual commotion was visible in a swordfish, lurking astern, awaiting a favourable opportunity to rush upon his prey when they should be unconscious of danger or away from the protection of the ship. . . . and in the course of the day we observed him make several dashes amongst the shoal with a velocity which produced a loud rushing sound in the sea. . . . It is probable, as a precaution against the attacks of this monster, that albacore, and some other tropical shoal fish, attach themselves to ships, . . . , the close vicinity of a large body being sufficient to deter the swordfish from making his usual impetuous thrusts amidst the shoal; the which, when rashly attempted, have given rise to the appearance of the broken rostra of these fish impacted in the planks of ships, . . . as is not unfrequently noticed." Although the name "swordfish" is used it may also have been a member of the round-speared Istiophoridae, as all were termed swordfish until recent years.

Certainly no flailing at prey could have resulted in such penetrations of hulls as recorded. The angle of incidence of spear and hull would either have deflected the spear or have caused only slight penetration. Also, if the spearfish had concentrated on a side-to-side motion, the greater portion of the total energy would have been expended in this action. The forward speed would have been correspondingly reduced, so as to lessen the depth of penetration, regardless of the angle of incidence. Only a straight-forward charge resulting from pugnacity or an attempt to capture prey could result in such penetrations.

The biological significance of the spear may well be an adaptation for the great speed and power of these large fish, as well as a weapon of defense or attack. I am indebted to John D. Isaacs and Carl L. Hubbs for the following suggestions. A terminally opening mouth would create enormous drag and would push in front a mass of water at a similar speed, so that a spurt of the intended prey would lead it to safety. If the mouth were terminal the common mode of ingestion by suction due to a sudden spreading of the gill covers as the mouth is opened would probably be difficult and perhaps dangerous at extreme speeds. On the other hand the projecting and tapered spear would scarcely impede the flow of water past the narrowly triangular mouth on the lower surface of the base of the beak. A sudden snapping of the sharply pointed inferior mandible would induce minimal drag and would be effective in grasping prey. If the spear is of use in feeding, it is probably of most value in permitting high speeds to be attained by the feeding fish.

It may be argued that the tunas and porpoises are also rapid swimmers yet have terminally opening mouths. However, they too are well streamlined and have relatively narrow snouts that no doubt induce minimal drag at high speeds. Indeed, their spearless heads may be considered analagous to those of spearfish without spears. There is little doubt but that the tunas and porpoises rely on speed to capture prey.

SUMMARY AND CONCLUSIONS

It is concluded that the spearfishes rely primarily on speed to overtake and engulf their food. This circumstance explains why spearless marlins are able to obtain food and to exist in competition with their undamaged fellows. The widely held belief that these fishes, marlins in particular, normally stun prey with a blow of the spear has presumably stemmed from fishermen watching fish turn slightly to grasp the bait between jaws or to engulf it, during which action the spear performs a lateral motion readily interpretable as a slash or blow. The several instances of stabbings of prey may well have resulted from the high speed of the predator and escape attempts of the prey, the spear point inadvertantly striking the prey. There is little to indicate that most stabbings are intentional. In the face of preponderant evidence that most of the prey is not stabbed, one must, for the present, accept the probability that such spear penetrations are quite accidental.

Further evidence that these fishes rely on speed to overtake prey are the numerous accounts of the ramming of ship hulls and floating objects. It seems logical to assume that many such rammings result when spearfishes charge prey lying under these vessels and either fail to see the hull or misjudge the distance between prey and hull. The depths of penetration strongly indicate that the spearfish was not using its spear as a flail to obtain food. Such penetrations of objects could have resulted only from a straight-forward charge, either to seize the prey lying underneath or to battle a fancied enemy.

The restrictions in rapid lateral movement imposed by the highly integrated and reinforced vertebral column render it highly improbable that such fishes normally kill or stun prey by slashing with their spears, particularly when in pursuit of fleeing prey. The roughened surface of the spear and its relatively blunt tip preclude the possibility of stabbing the smaller fishes and the squid, which comprise the major food items of the spearfishes.

In whatever way it is used, the spear presumably serves a hydrodynamic function, increasing the speed of these large fishes. In feeding it presumably does more. The form of the spear and of the adjacent parts of the head seem well fitted to avoid drag, escape of prey, and possible injury at high speeds when the mouth is opened. A rapid water flow is induced past the mouth region, and the mouth appears to be so formed as to present minimal resistance when closed and but slight resistance when opened to seize prey.

REFERENCES

Anonymous. 1955*a*. Pacific Oceanic Fishery Investigations. *Natl. Canners Assoc., Fishery Inform. Bul.*, 22 April, pp. 83–84. Washington.

Anonymous. 1955*b*. Feeding marlin uses its head. *Internatl. Oceanographic Found., Bul.* 1(3): 38, 39.

Bandini, Ralph. 1933. Swordfishing. *Calif. Fish and Game* 19(4): 241–248.

Berg, Leo S. 1947. *Classification of Fishes, Both Recent and Fossil.* J. W. Edwards, Ann Arbor, Michigan.

Farrington, S. Kip, Jr. 1937. *Atlantic Game Fishing*. New York. 298 pp.

——— 1942. *Pacific Game Fishing*. New York. 290 pp.

GREY, ZANE. 1926. *Tales of the Angler's Eldorado—New Zealand*. New York. 228 pp.

——— 1931. *Tales of Tahitian Waters*. New York. 303 pp.

GUDGER, E. W. 1940. The alleged pugnacity of the swordfish and the spearfishes as shown by their attacks on vessels. *Roy. Asiatic Soc., Bengal Branch, Mem.* xii(2): 215–315.

HEILNER, VAN CAMPEN. 1943. *Salt Water Fishing*. Alfred A. Knopf and Co., New York.

HUBBS, CARL L., and ROBERT L. WISNER. 1953. Food of marlin in 1951 off San Diego, California. *Calif. Fish and Game* 39 (1): 127–131.

MOORE, HARVEY L. 1950. The occurrence of a black marlin *Tetrapterus mazara* (Jordan and Snyder) without a spear. *Pacific Sci.* 4(2): 164.

MORROW, JAMES E. 1951. A striped marlin (*Makaira mitsukurii*) without a spear. *Copeia* 4: 303–304.

——— 1952. Food of the striped marlin, *Makaira mitsukurii*, from New Zealand. *Copeia* 3: 143–145.

NAKAMURA, HIROSHI. 1938. Report of an Investigation of the Spearfishes of Formosan Waters. *U. S. Fish and Wildlife Serv., Spec. Sci. Rpt., Fisheries* 153. 1955. 46 pp., 15 pls. Translation from the Japanese by W. G. Van Campen, Pacific Oceanic Fisheries Invest. U. S. Fish and Wildlife Serv. Honolulu.

SMITH, J. L. B. 1956. Pugnacity of marlins and swordfish. *Nature* 178: 1065.

THOMAS, GEORGE C., JR., and GEORGE C. THOMAS, III. 1930. *Game Fish of the Pacific, Southern California and Mexico*. J. B. Lippincott Company, London.

VOSS, GILBERT. 1956. Solving life secrets of the sailfish. *Natl. Geog. Mag.* CIX(6): 859–872.

WALFORD, LIONEL A. 1937. *Marine Game Fishes of the Pacific Coast, Alaska to the Equator*. University of California Press, Berkeley.

Reprinted from PACIFIC SCIENCE, *vol. XII, no. 1, January, 1958*

Reproduced by Permission

Oceanographic and Meteorological Aspects of the Gulf of California[1]

GUNNAR I. RODEN

THE PRIMARY OBJECT of the present paper is to give an adequate description of the climatic and oceanographic conditions in the Gulf as they are known today.

Only a few authors have discussed the Gulf (Sverdrup, 1940; Osorio Tafall, 1944) and only the geological work was described in detail (Anderson, 1950; Durham, 1950; Natland, 1950; Revelle, 1950; Shephard, 1950).

The data used in the present investigation are largely taken from the "E. W. Scripps" expeditions in 1939 (Sverdrup and staff, 1943) and from the publications of the Servicio Meteorológico Mexicano, the U. S. Coast and Geodetic Survey, and the U. S. Hydrographic Office.

The data for the Gulf are few and the conclusions that can be drawn from them are necessarily limited and should be taken only as a first approximation until more and better data are at hand.

The Gulf of California is of considerable interest both scientifically and economically, and it is expected that its importance will steadily increase in the future, especially as an additional food source for Mexico. A thorough knowledge of the physical and chemical changes taking place in the Gulf is essential to the understanding of its fisheries.

Moreover, the Gulf is interesting because it represents the only large evaporation basin of the Pacific Ocean and because it shows certain differences from other comparable evaporation basins. A final answer to all the different problems in the Gulf cannot be expected from the meager data available but it is the hope of the author that this paper may stimulate more research in this intriguing area.

ACKNOWLEDGEMENTS

The author is indebted to Dr. Warren S. Wooster and Dr. Robert S. Arthur for valuable help and suggestions that made this study possible, to Mr. Joseph L. Reid, Jr., Dr. F. Phleger, and Miss June G. Pattullo for reading the manuscript, to Mr. Townsend Cromwell for a discussion on a definition of a front, and to Sr. Enrique Avila for advice on the writing of Spanish place names and other terms. The author also wishes to express his thanks to those who have helped him to prepare the drawings.

---

[1] Contribution of the Scripps Institution of Oceanography, New Series, No. 960. The work reported on herein represents results of research sponsored in part by the Office of Naval Research under contract with the University of California. Manuscript received July 24, 1956.

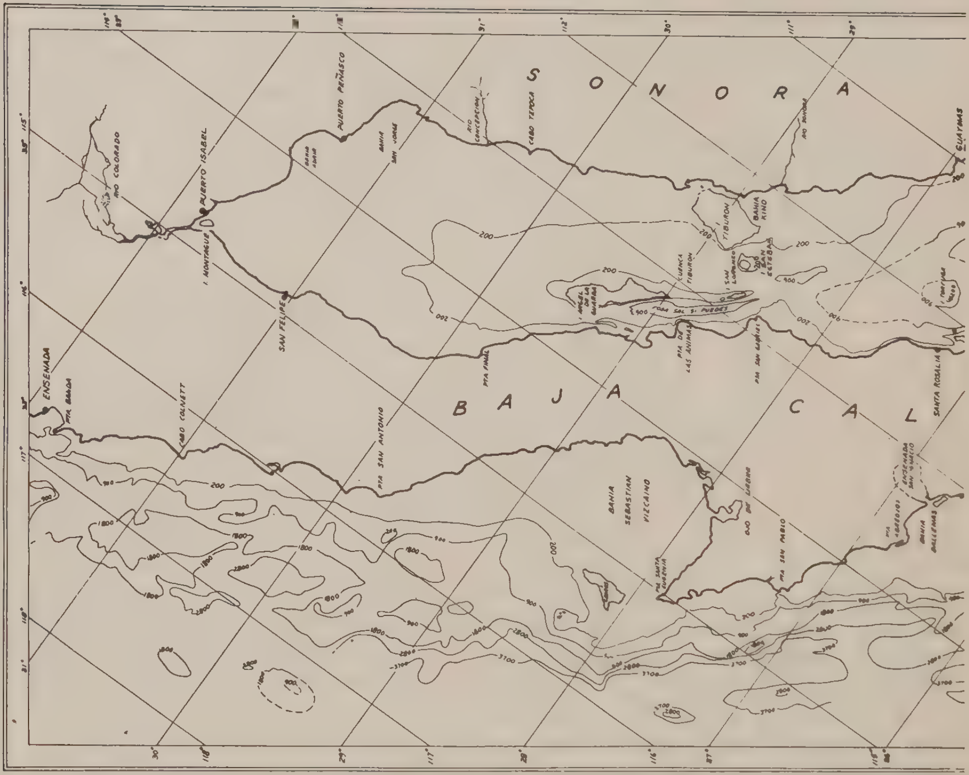
S O N O R A
B A J A C A L
RIO COLORADO
PUERTO ISABEL
I. MONTAGUE
PUERTO PEÑASCO
SAN FELIPE
BAHIA ADAIR
BAHIA SAN JORGE
RIO CONCEPCION
CABO TEPOCA
TIBURON
BAHIA KINO
GUAYMAS
SANTA ROSALIA
ENSENADA
PTA. BANDA
CABO COLNETT
PTA SAN ANTONIO
BAHIA SEBASTIAN VIZCAINO
PTA SAN PABLO
PTA DE LAS ANIMAS
SAL SI PUEDES
200
900
1800
2800
3700

FIG. 1. Bathymetric map of the Gulf of California.

GENERAL DESCRIPTION AND PREVIOUS INVESTIGATIONS

The Gulf of California is unique in many respects. Lying as it does in a predominantly arid region it comprises the only large evaporation basin of the Pacific Ocean. It is roughly rectangular in shape and lies between the Mexican states of Baja California to the west and of Sonora and Sinaloa to the east. At its southern end the Gulf is in open communication with the ocean. The length of the Gulf is about 1400 km. and the average width about 150 km., giving a total surface area of roughly 210,000 km.^{2}, if the southern boundary is taken along latitude 23°N. Between this latitude and a line joining Cabo San Lucas with Cabo Corrientes (Fig. 10) lies a transition region which occasionally is influenced by Gulf water (Schott, 1935). This region will be called the Gulf Entrance, and it has a total surface area of roughly 40,000 km.^{2}

Topographically the Gulf can be divided into a number of basins, separated from each other by transverse ridges. The deepest basins have a maximum depth of more than 3000 m. and a sill depth below 1500 m. (Geol. Soc. Amer., Mem., 1950). In the northern part of the Gulf isolated basins are found in which different hydrographic conditions prevail (Sverdrup, 1941). These basins seem to represent deep depressions in an otherwise quite narrow shelf and are completely isolated below 200 to 300 m. Their isolated character is quite sufficient to explain the hydrographic conditions found in them and it is not neces-

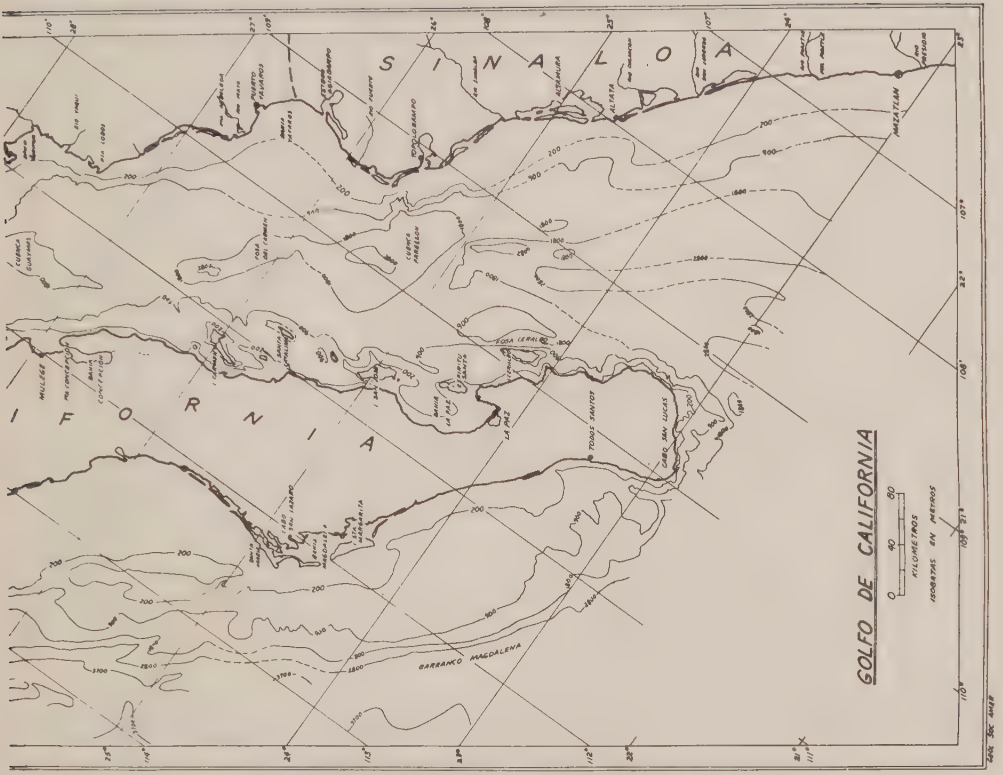
S I N A L O A
C A L I F O R N I A
GOLFO DE CALIFORNIA
0 40 80
KILOMETROS
ISOBATAS EN METROS
RIO YAQUI
RIO LOBOS
RIO MAYO
PUERTO YAVAROS
BAHIA YAVAROS
TOPOLOBAMPO
RIO FUERTE
ALTAMURA
ALTATA
MAZATLAN
RIO PRESIDIO
CUENCA GUAYMAS
FOSA DEL CARMEN
CUENCA FARELLON
FOSA CERALBO
MULEGE
BAHIA CONCEPCION
I. CARMEN
I. SAN JOSE
BAHIA LA PAZ
I. ESPIRITU SANTO
I. CERALBO
LA PAZ
TODOS SANTOS
CABO SAN LUCAS
BAHIA MAGDALENA
STA. MARGARITA
BARRANCO MAGDALENA
200
900
1800
2800
3700
110°
28°
27°
109°
26°
108°
25°
107°
24°
23°
22°
21°
111°
112°
113°
114°
GEOL. SOC. AMER.

FIG. 1. Bathymetric map of the Gulf of California (*continued*).

sary to assume the existence of a ridge running SSE between Angel de la Guarda and Tiburón to account for the differences (Sverdrup, 1941). There are two large islands in the Gulf—Angel de la Guarda and Tiburón—both with elevations exceeding 1500 m.

The coast along Baja California is very steep and flanked by numerous islands and rocks. Off Rio Colorado and northern Sonora the coast is less rugged and possesses a wide shelf. Along Sinaloa the shelf narrows again and disappears at Cabo Corrientes.

The Gulf remained scientifically unknown until fairly recent times. Prior to the coming of the conquistadores, the Gulf area was inhabited by different Indian tribes who lived by fishing and undoubtedly had some local knowledge of the currents and the general appearance of the water. Their observations are, however, lost because they had no written records.

With the coming of the Spaniards, trade developed between Gulf ports and the Far East (Hakluyt, 1598) and various captains entered the Gulf with lead and line. The first written records are therefore found in the ships' logs of the early seafarers. Scientific exploration began in 1889 when the U. S. Fish Commission steamer "Albatross" (Fig. 2) entered the Gulf to make a few hydrographic stations, especially in the northern part (Townsend, 1901). The data collected at these stations consisted of temperature and density determinations, the latter being made with a hydrometer. The results of the expedition (not previously published in this form) are shown in Figure 3.

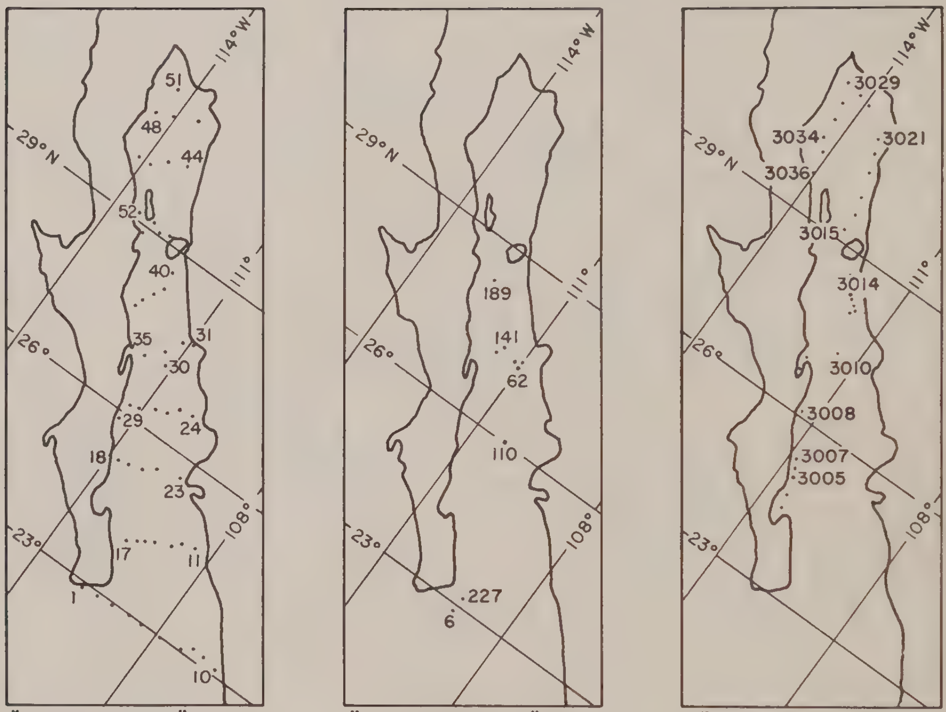

"E W SCRIPPS" 1939 "E W SCRIPPS" 1940 "ALBATROSS" 1889

FIG. 2. Stations occupied on previous expeditions.

Considerable warming and high salinity were found in shallow bays such as Bahia Guaymas and Bahia Concepcion. Upwelling was characteristic along the northern coast of Sonora where the temperature was about one degree lower and the salinity 0.4°/oo lower than in the neighborhood offshore. Near the mouth of Rio Colorado the salinity varied between 35.2 and 35.7°/oo, probably due to the admixture of fresh water. The bottom temperatures in the northern part everywhere exceeded 11°C. and the bottom salinity varied between 35.5 and 36.1°/oo.

The next important description of the Gulf of California was made by Thorade (1909) in a paper on the California Current. He examined a great number of ship logs over many years and was the first investigator to draw monthly surface temperature charts (Fig. 4) for the southern part of the Gulf and deduce from them the general circulation in the Gulf and to correlate the sea surface temperatures to the direction of the wind, the orientation of the shore line, and the special climatological conditions prevailing in the Gulf. His main conclusions were that the temperature of the Gulf is independent of the temperature in the adjacent ocean and that the low temperatures along the east coast in winter are the result of northerly winds that tend to transport surface water away from the coast and thus produce upwelling. He also observed correctly that during most of the year the circulation is counterclockwise in the Gulf and that the water enters the Gulf along the east coast and leaves it along the west coast. He mentioned that "manifold discontinuities are observed by a sudden change in tem-

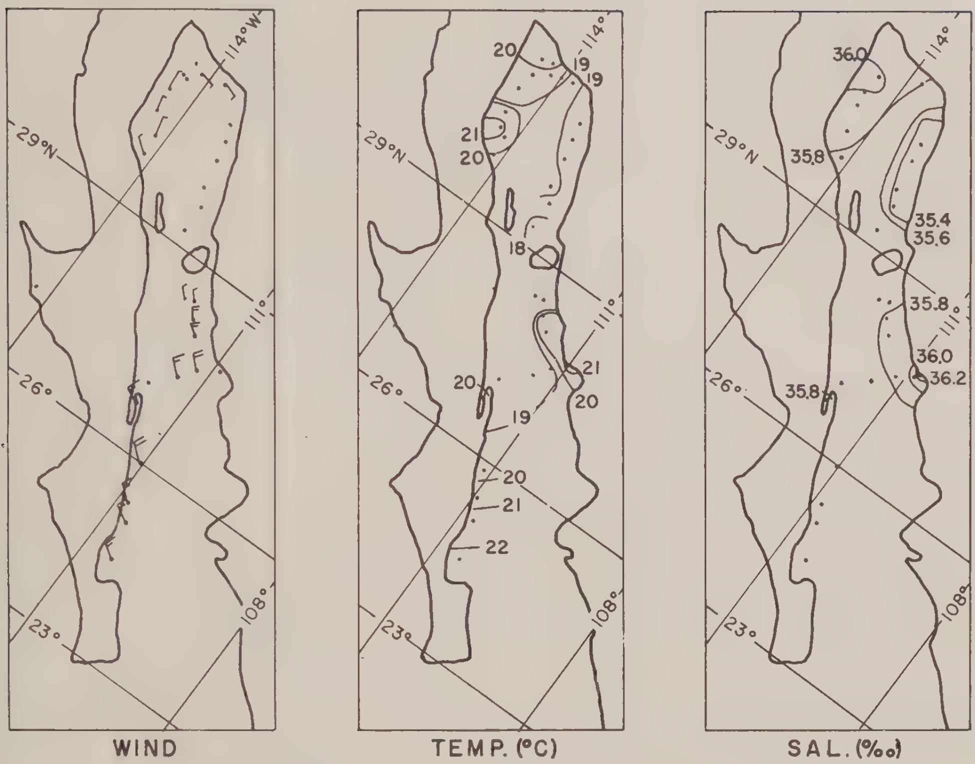

FIG. 3. Distribution of winds, temperature, and salinity in March, 1889.

perature" in the vicinity of Cabo San Lucas, which might well have been the first description of the San Lucas front.

Schott (1935: 208) described the Gulf of California as part of the Mexican region, a region defined roughly as lying between the Gulf of Tehuantepec and Cabo San Lucas and extending seaward between the California Current and the North Equatorial Current. The Mexican region is characterized by a very high surface temperature and very weak circulation. He briefly mentioned the temperature discontinuity near Cabo San Lucas and drew attention to the frequent hurricanes in that region.

In the spring of 1939 the Scripps Institution of Oceanography sent an expedition into the Gulf led by H. U. Sverdrup on the "E. W. Scripps." Fifty-three stations were made in the Gulf (Fig. 2) taking temperature, salinity, oxygen, calcium carbonate and plankton observations on each station from the surface to the bottom (Sverdrup and staff, 1943). These data are still the most complete ever taken in the Gulf. Sverdrup's main conclusions were that the Gulf can be subdivided into two parts, a northern part and a southern part, separated from each other by a submarine ridge which comes to within 200 m. below the surface. The water mass to the north is largely of local origin and formed by convective currents in winter, the water to the south is nearly the same as in the adjacent ocean and only modified slightly at the surface by extensive evaporation (Sverdrup, 1941).

In late fall of 1940 the "E. W. Scripps" made a second trip to the Gulf. The chief

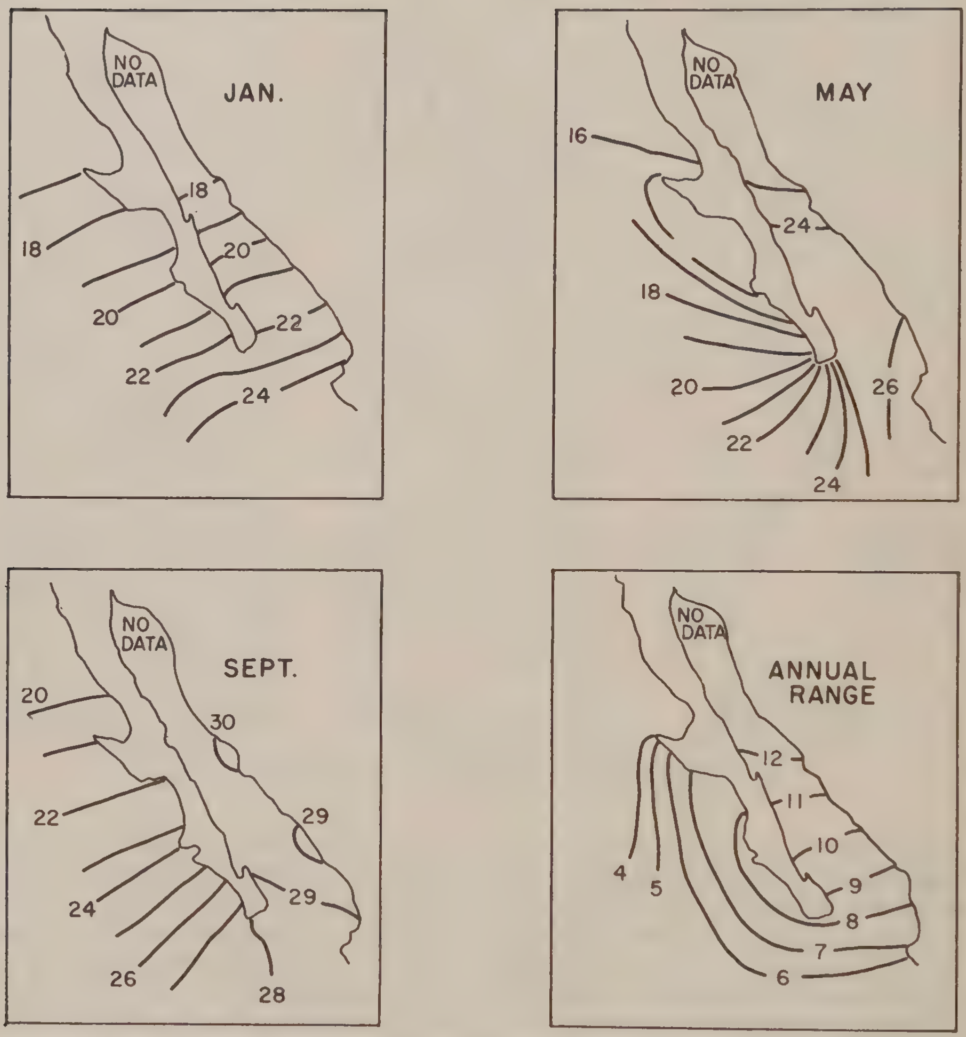
NO DATA
JAN.
18
18
20
20
22
22
24
NO DATA
MAY
16
24
18
20
26
22
24
NO DATA
SEPT.
20
30
22
29
24
29
26
28
NO DATA
ANNUAL RANGE
12
11
10
4
5
9
8
7
6

FIG. 4. Sea surface temperatures (°C.) in the Gulf of California. (After Thorade, 1909.)

aim was geological (Geol. Soc. Amer., Mem., 1950) but a few hydrographic stations were made (Fig. 2). Silicate and phosphate were measured for the first time in the Gulf, but the methods used in determining the concentrations do not warrant a detailed description of them. A brief account on the silicate distribution in the Gulf was given by Sverdrup (Sverdrup and staff, 1940). In 1944 the Mexican government sponsored a brief study of the Gulf in order to determine the feasibility of a minor guano industry (Osorio Tafall, 1944). The industry was never started. In 1956 the U. S. Fish and Wildlife Service has planned two expeditions into the Gulf to study the distribution of sardine eggs and larvae and to make frequent hydrographic stations, which undoubtedly will bring back new and valuable data for further scientific investigations.

CLIMATOLOGY

The great differences in climatic conditions observed in the Gulf as one proceeds from northwest to southeast, covering nearly nine degrees of latitude, and the differences that exist between the east side and the west side of the Gulf, are closely related to the atmospheric circulation and to the existence of mountain ranges that modify this circulation.

The influence of the Pacific Ocean upon the climate of the Gulf is greatly reduced by a nearly unbroken chain of mountains, 2000 to 3000 m. high, in Baja California. The considerable differences in temperatures and precipitation between the Pacific side and the Gulf side have already been mentioned by Thorade (1909) and are fully confirmed by data collected by the Servicio Meterologico Mexicano (Boletin Anual). Along the Pacific side of the peninsula the air temperatures are never excessively high and precipitation falls during the winter season in the northern part, and during the summer season in the southern part, with annual amounts around 200 mm. Along the Gulf side air temperatures are very high in summer and rather cool in winter. In the north all the precipitation falls in summer. The amount of rainfall (Table 1) varies between traces in the north and 200 mm. at the southern tip of Baja California, which is crossed by the Tropic of Cancer. The rainfall on the corresponding latitude on the eastern side of the Gulf amounts to 400 mm. per year.

On the average the west coast of the Gulf receives only half as much rain as the east coast. In Sonora the winter is cool and the summer hot. Precipitation falls from July to September, varying between traces in the northernmost part and 251 mm. in Guaymas. In Sinaloa the winter is warm and the summer less hot than in Sonora. Precipitation falls from August to October, with amounts between 300 mm. in the north and 850 mm. in Mazatlán (Table 1). From the discussion of the precipitation figures it becomes evident that the Gulf of California is far from being situated in a desertlike environment.[2] The vegetation in Baja California and Sonora is of

TABLE 1

MEAN MONTHLY AIR TEMPERATURE AND PRECIPITATION 1921–1935 (SERV. MET. MEX., BOLETIN ANUAL)

	WEST COAST (IN GULF)				EAST COAST (IN GULF)				EAST COAST (OUTSIDE GULF)			
	Mulege (26°53′N–112°00′W)		La Paz (24°10′N–110°18′W)		Guaymas (27°55′N–110°53′W)		Topolobampo (25°36′N–109°03′W)		Mazatlán (23°11′N–106°25′W)		Cabo Corrientes (20°24′N–105°43′W)	
	Temp. °C.	Prec. mm.	Temp. °C.	Prec. mm.	Temp. °C.	Prec. mm.	Temp. °C.	Prec. mm.	Temp. °C.	Prec. mm.	Temp. °C.	Prec. mm.
January	14.0	2.6	18.2	3.2	17.7	7.9	18.6	6.4	19.3	11.0	23.2	19.5
February	16.0	3.4	19.2	11.4	18.9	6.3	19.7	6.6	19.4	9.7	22.9	29.6
March	17.8	0.1	21.3	0.8	20.7	4.6	20.1	6.4	19.7	3.4	22.7	1.3
April	20.1	0.2	23.2	0.2	22.8	3.0	22.2	tr.	21.3	0.1	23.9	tr.
May	22.9	0.1	25.5	tr.	25.5	2.8	25.0	1.8	23.8	1.8	25.4	2.3
June	27.2	tr.	27.2	0.2	28.8	0.7	29.1	5.3	26.4	29.2	26.7	57.3
July	30.5	6.1	30.0	6.3	30.7	46.7	29.8	39.9	27.5	166.9	28.9	145.0
August	30.4	16.8	30.3	41.7	30.5	75.5	29.7	100.6	27.6	241.8	27.9	272.1
September	29.0	40.0	29.0	51.9	30.2	54.4	29.7	55.9	27.5	268.6	27.5	307.0
October	24.6	5.4	27.0	9.6	27.3	9.5	27.8	73.7	26.7	61.6	27.5	91.0
November	19.5	6.8	23.2	13.4	22.6	11.1	24.0	7.0	23.5	11.7	26.1	15.2
December	14.9	19.2	20.0	34.3	18.6	28.9	19.7	55.3	20.6	44.4	23.8	13.5
Year	22.2	101.1	24.4	173.0	24.5	251.4	24.6	358.9	23.6	850.2	25.5	953.8
Minimum	0.0	—	0.0	—	7.0	—	8.0	—	11.2	—	12.0	—
Maximum	41.9	—	40.5	—	47.0	—	41.1	—	33.4	—	43.8	—

---

[2] Most Americans call northern Sonora and Baja California a desert, though people from North Africa and South America would consider this region a dry steppe.

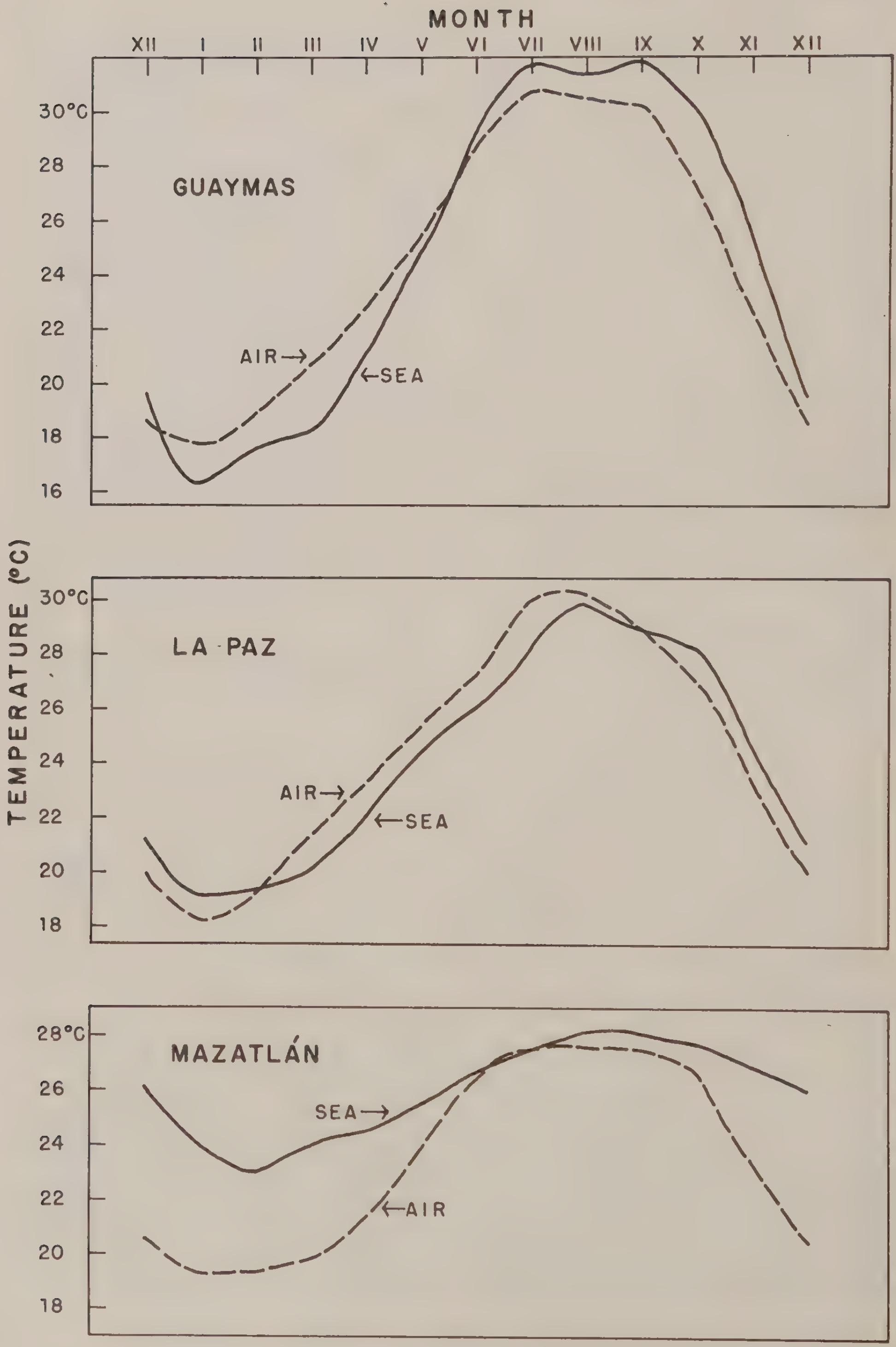

FIG. 5. Air and sea surface temperatures in Guaymas, La Paz, and Mazatlán.

(948)

the dry steppe type, and in southern Sinaloa it is tropical.

The distribution of air temperatures (Fig. 5) shows a temperature minimum in January and February and a maximum in August and September. The annual range in temperatures increases from south to north and is somewhat greater along the coast of Baja California than along Sonora and Sinaloa. The mean annual range at the entrance is around 10°C. and in the northernmost part about 20°C. The extreme annual range (Table 1) is approximately twice the average annual range (Serv. Met. Mex., Boletin Anual). In general the air is warmer than the sea during the first half of the year and cooler during the second, except for Mazatlán, where the air is always cooler than the sea (Fig. 5).

The distribution of winds (Table 2) shows that the monthly average wind velocities are quite low, lying between 1.5 m/sec and 6.1 m/sec. The higher values are found in winter and spring. The direction of winds varies with season and with distance from the entrance. During winter, northerly winds are predominant in the entire Gulf, but in summer the southern half of the Gulf is mostly influenced by southerly winds. In the northern half, southerly winds blow only one or two months of a year.

Winter gales of short duration, locally known as chubascos, are frequent and velocities may occasionally reach 30 m/sec.

Hurricanes are not as rare in the Gulf as is generally believed. Between 1910 and 1930 thirty-nine were registered (Schott, 1935: 280). These hurricanes, known as "El Cordonazo," may enter the Gulf any time between May and November, but are most frequent in September and October (Fig. 6).

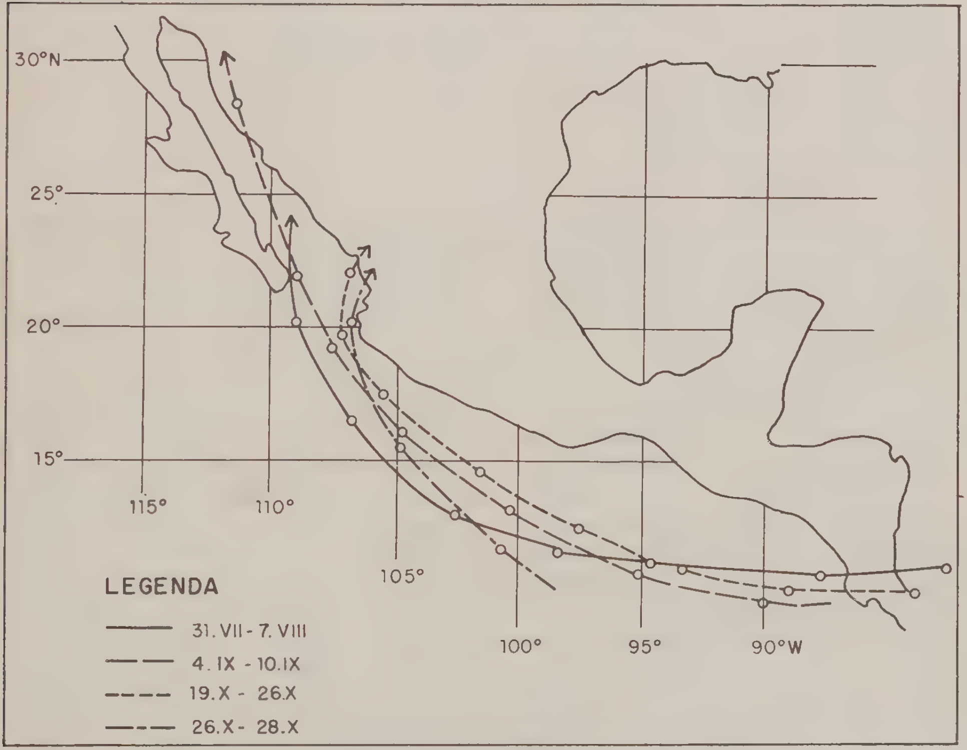

FIG. 6. Paths of hurricanes in 1936. (After Serv. Met. Mex., Boletin Anual, 1936.)

TABLE 2
MEAN MONTHLY WIND VELOCITY IN LA PAZ, GUAYMAS, AND MAZATLÁN
(Serv. Met. Mex., Boletin Anual)

	LA PAZ	GUAYMAS	MAZATLAN
	m/sec	*m/sec*	*m/sec*
January	2.6	4.8	6.1
February	2.4	4.2	5.9
March	2.2	5.3	5.5
April	2.3	5.1	5.0
May	2.1	4.6	4.8
June	2.4	4.3	4.6
July	2.0	3.5	4.3
August	2.0	3.6	4.9
September	1.5	4.4	5.0
October	1.8	4.8	5.1
November	2.3	4.6	4.1
December	2.3	4.9	5.5
Year	2.2	4.5	5.1

In La Paz winds are northerly from November until March and southerly from April until October.

In Guaymas winds are northerly from August until May and southerly in June and July only.

In Mazatlán winds are northerly from November until April and westerly from May until October.

They originate in the Caribbean Sea or off the coast of Central America and it takes them between five to seven days to reach the Gulf (Serv. Met. Mex., Boletin Anual).

If one compares the distribution of winds and the occurrence of the rainy season with the migrating low pressure system over western Mexico (Fig. 7) it is seen that northerly winds are found with the low pressure to the east, and southerly winds with the low pressure to the northwest. The beginning of the rainy season is connected with the appearance of southerly winds that carry moist air into the Gulf and give rise to uplift rain.

Evaporation is one of the most important factors in the Gulf and is responsible for the high salinity observed in the surface layers. The amount of evaporation has been determined from pan observations at a few shore stations (Serv. Met. Mex., Boletin Anual). These measurements show a main maximum in summer and a main minimum in winter. The amount of annual evaporation varies between 1800 mm. in La Paz and about 3000 mm. in Guaymas (Table 3). The values are consistent from year to year for each station and the deviations from the above values are generally less than 10 per cent (Serv. Met. Mex., Boletin Anual).

Since evaporation from pans is not strictly representative for evaporation from the sea surface, it is of interest to see how the observed evaporation from pans compares to evaporation derived from indirect methods.

The use of the energy budget method is restricted, because the advection term cannot be evaluated.

In the meteorological approach a straight line relationship between the evaporation, E, and the product of wind velocity, W, and vapor pressure difference, Δe, is assumed (Jacobs, 1951); the coeficient of proportionality depends upon the height where the wind velocity and the humidity has been measured, and upon the roughness of the sea surface. In the following the coeficient of proportionality will be taken as 4.26 (Jacobs, 1951) so that

$$E = 4.26\, W\Delta e$$

where E is in mm/month, W in m/sec, and Δe is in mb.

A comparison between the pan and computed evaporation for the year 1938 is shown in Table 3, and it is readily seen that notable differences exist. The computed evaporation is less than the observed evaporation (Fig. 8) for La Paz and Mazatlán. In La Paz the maximum evaporation occurs in summer and the minimum in winter; in Mazatlán the observed evaporation shows a winter minimum and a summer maximum, whereas the computed evaporation has a summer minimum and a fall maximum. The summer minimum is due to the low wind velocities observed during this season. Values for Guaymas are not strictly comparable because the pan observations were made on a nearby station farther inland; nevertheless it is interesting to note that there the total annual amount of evaporation is considerably higher than in La Paz or Mazatlán.

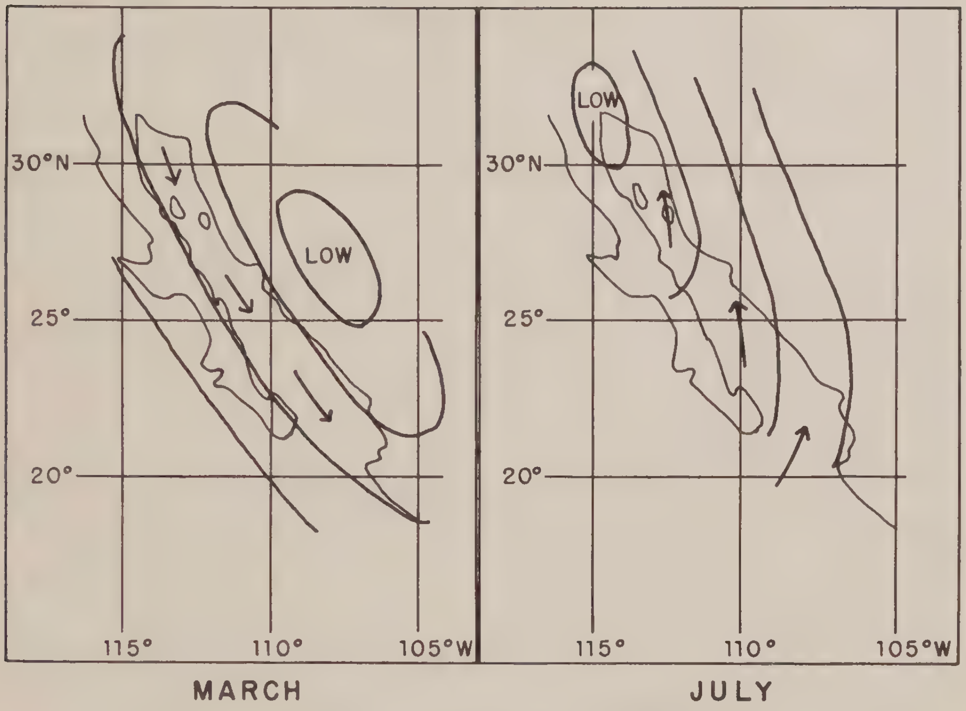

FIG. 7. Position of the low pressure in March and July, and resulting winds.

TABLE 3
Mean Monthly Evaporation
E_p = measured from pans, E_o = computed

	LA PAZ (1938)		GUAYMAS (1943)		MAZATLÁN (1938)	
	E_p	E_o	E_p	E_o	E_p	E_o
	mm.	mm.	mm.	mm.	mm.	mm.
January	139	76	139	174	185	172
February	120	41	206	216	213	194
March	129	81	286	269	148	129
April	119	98	351	276	205	133
May	146	127	446	337	210	163
June	166	126	420	299	211	130
July	174	172	294	280	230	123
August	197	156	246	239	289	181
September	150	82	198	266	202	190
October	159	180	162	337	210	245
November	158	98	148	178	162	196
December	154	57	92	288	140	196
Year	1809	1294	2958	3247	2492	2071
(E_o/E_p)year	0.72		(1.10)		0.83	

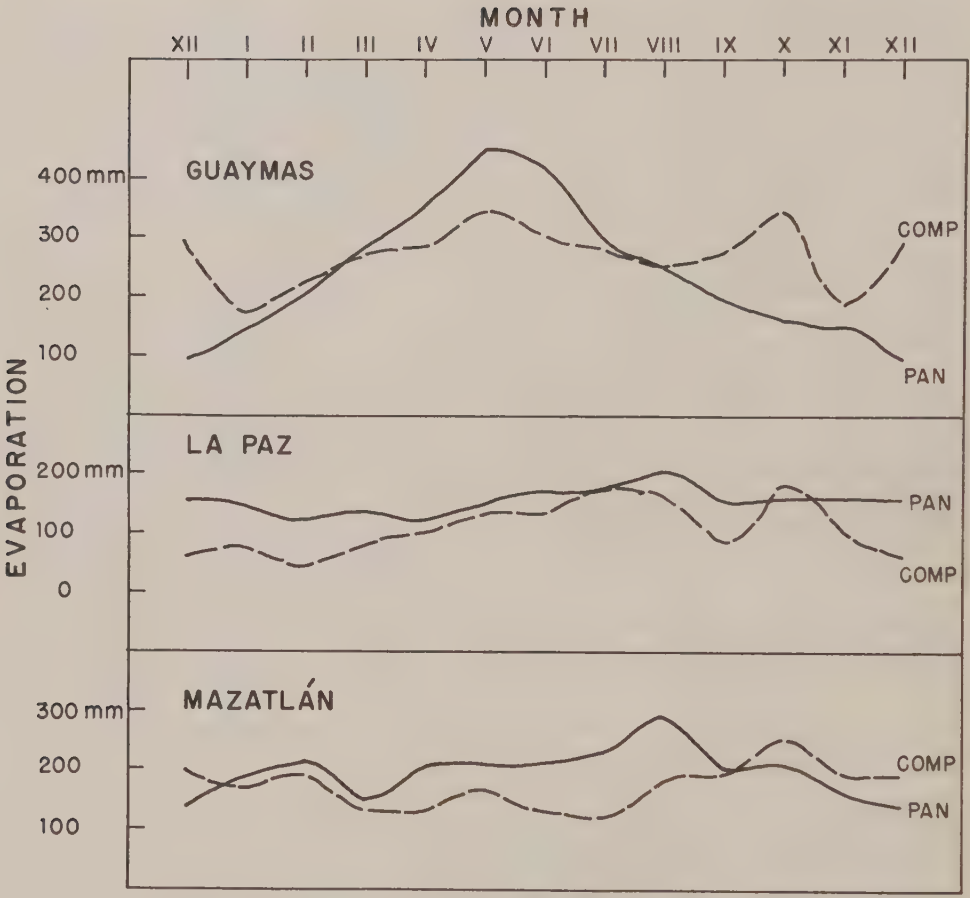

FIG. 8. Computed evaporation (E_o) and pan evaporation (E_p).

The difference, evaporation minus precipitation, has a maximum in early summer, a minimum during the rainy season, and a secondary maximum immediately after the rainy season. Except for Mazatlán during the peak of the rainy season, evaporation exceeds precipitation during all months of the year. The few available data indicate that the mean annual evaporation for the southern half of the Gulf lies between 1500 and 3000 mm. For the entire Gulf, considering the dry northern part, roughly 2500 mm. can be taken as a conservative estimate for the mean yearly evaporation. With this value the rate of evaporation over the entire surface of the Gulf becomes 5.25 x 10^{11}m^3/year or 1.7 x 10^4m^3/sec.

GENERAL CIRCULATION

The bulk of water in and near the Gulf of California is the same as in the equatorial Pacific, slightly modified at the surface by extensive evaporation and by the admixture with water brought south by the California Current. The influence of the latter is restricted to the vicinity of Cabo San Lucas.

The great similarity between the Gulf and Pacific Equatorial water, below the thermocline, is illustrated by the close agreement between the temperature-salinity relationships for either water mass (Fig. 9). Points for the Gulf were obtained from the "E. W. Scripps" expedition in 1939 (Sverdrup and staff, 1943). The solid curves represent the limits for typical Gulf water, the dashed curves show the limits for the equatorial Pacific (Sverdrup *et al.*, 1942: 741).

It is seen that a nearly straight line relationship exists between the points 16°C., 35.2‰ and 9°C., 34.6‰. The salinity minimum lies in both cases between 34.5 and 34.6‰ and has a corresponding temperature of between 5°C. and 7°C.

The circulation in the Gulf is rather complicated and not fully understood. In winter (Fig. 10) outflow takes place at the surface and inflow at greater depths, in summer (Fig. 11) the situation is reversed. Thorade (1909) mentioned one case of oppositely running currents at the surface and at 40 m. near the coast of central Baja California.

In the northern part of the Gulf cooling of high saline water in winter leads to the formation of a bottom water mass (Sverdrup, 1941), which is characterized by a temperature above 10°C. and a salinity above 34.9‰ and a relatively high oxygen content. This water fills the isolated basins of the northern shelf and moves southward along the coast of Baja California (Fig. 19).

Tidal currents are strong in the northern third of the Gulf and may obtain velocities of several knots in the narrows between the islands and near the mouth of Rio Colorado.

The exchange between the Gulf and the Pacific Ocean cannot be calculated accurately from the available data. It is, however, possible to get a rough estimate of the exchange of water and salt across latitude 23°N assuming conservation of these properties. If E denotes the rate of evaporation and if S_i, S_0 and Q_i, Q_0 represent the salinity and amount of the in- and outflowing water, respectively, the following equations hold (Sverdrup *et al.*, 1942: 148)

$$Q_i = \frac{S_0}{S_0 - S_i} E \qquad Q_0 = \frac{S_i}{S_0 - S_i} E.$$

Taking E as 1.7×10^4 m³/sec (see above), S_i as 34.6‰ and S_0 as 35.1‰ one gets:

$$Q_i = 1.19 \times 10^6 \text{ (m}^3\text{/sec)}$$
$$Q_0 = 1.17 \times 10^6 \text{ (m}^3\text{/sec).}$$

It is seen that evaporation plays only a negligible part in the general circulation of the Gulf, and that inflow very nearly balances outflow. If one assumes that the outflowing

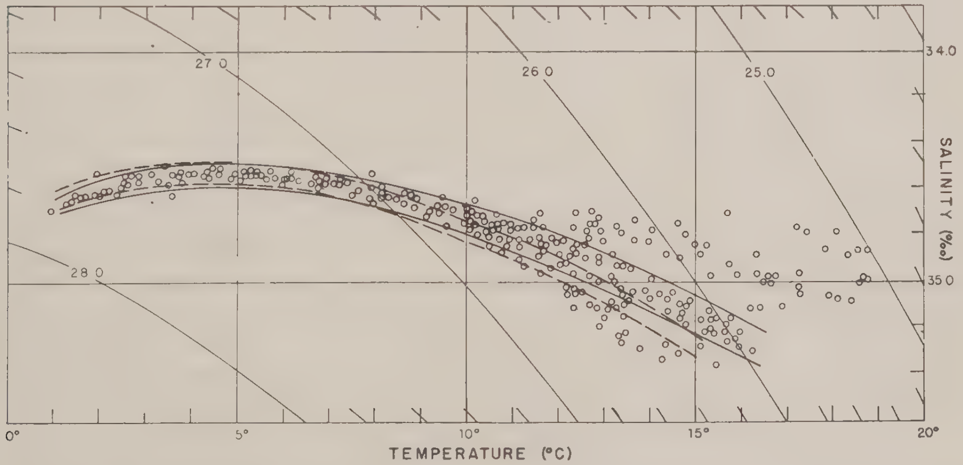

FIG. 9. Temperature-salinity diagram for the Gulf (solid lines) and for the equatorial Pacific (dashed lines).

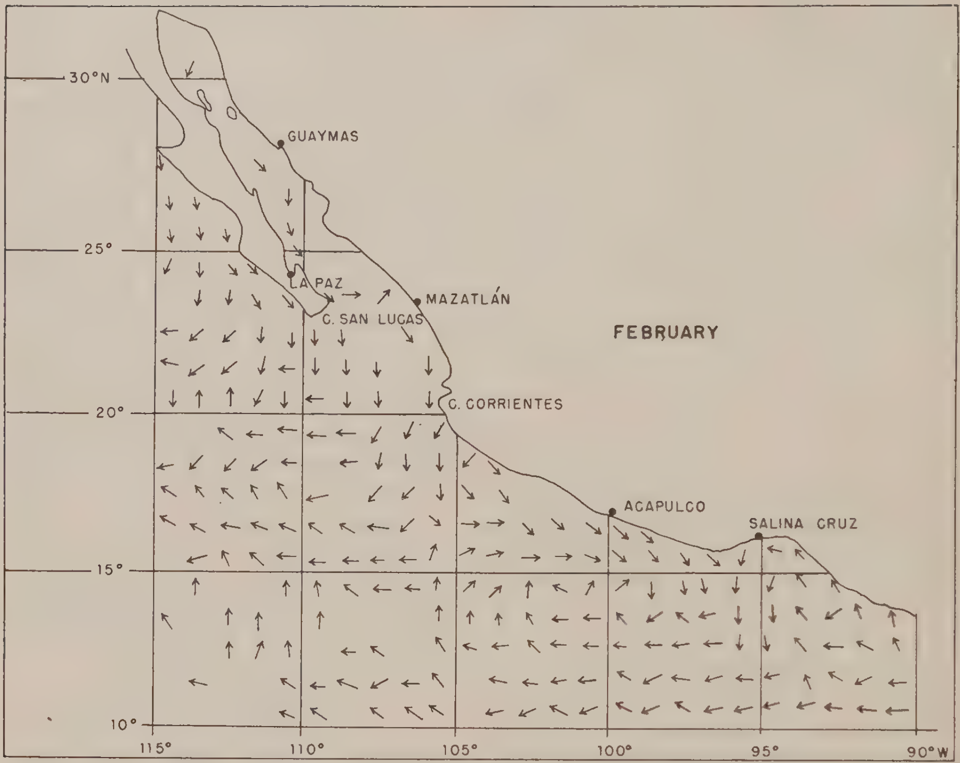

FIG. 10. Surface currents in February. (After U. S. Hydrog. Off., 1947.)

water extends over a depth range of 50 m. and inflowing over 1500 m., across latitude 23°N, the velocity of the outflowing water is 7 cm/sec and of the inflowing water 0.3 cm/sec. This calculation holds only for winter, when northerly winds are responsible for outflow at the surface.

The influence of the Gulf of California upon the adjacent Pacific Ocean is small (Sverdrup *et al.*, 1942: 732) and varies with season. The influence is greatest in winter when strong northerly winds drive the surface layers out of the Gulf and least in summer when southerly winds drive oceanic water into the Gulf. The exact distance seaward from the entrance of the Gulf that Gulf water can be detected (by its higher salinity) is not known.

The circulation in the vicinity of the Gulf of California is affected by the water carried south by the California Current and by the water found off Mexico and Central America. The former is characterized by a low temperature, a low salinity, and a rather high oxygen content, whereas the latter has a very high temperature at the surface and a very low oxygen content below the thermocline (Sverdrup *et al.*, 1942: 730). Between both lies a transition region which, 500 miles to the west, is found approximately between latitudes 17°N and 20°N (Wooster and Cromwell, verbal communication).

In February (Fig. 10) the coastal surface circulation (U. S. Hydrog. Off., 1947) is characterized by southward currents north of about latitude 20°N and by westward flowing currents south of this latitude. An interesting feature is a large gyre off the southern coast of Mexico which is maintained by strong

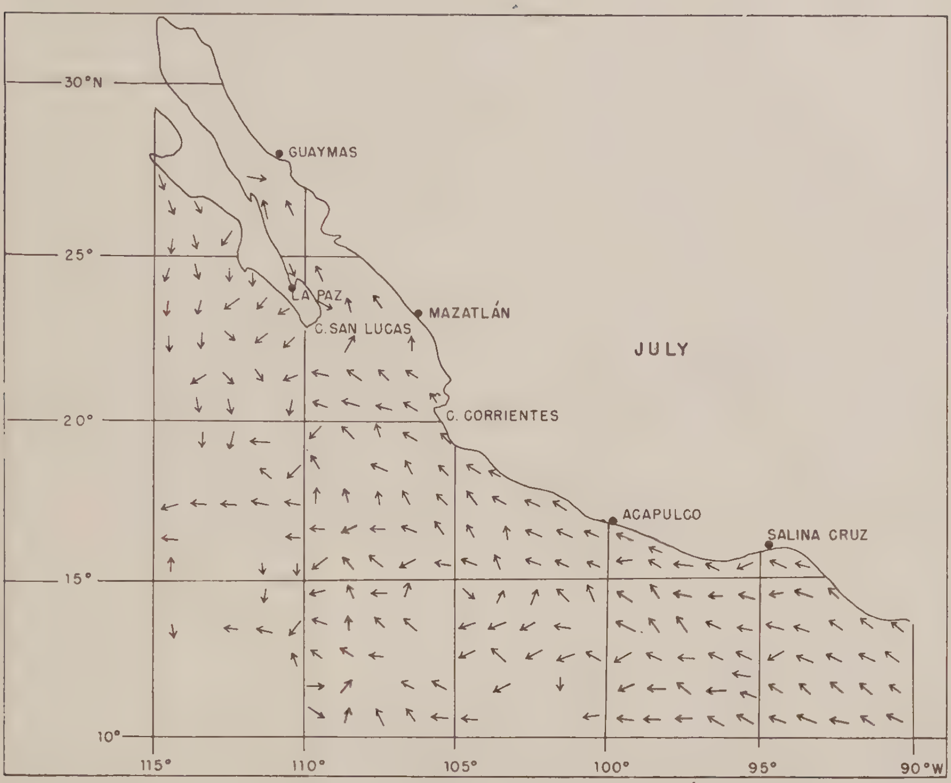

FIG. 11. Surface currents in July. (After U. S. Hydrog. Off., 1947.)

northerly winds blowing into the Gulf of Tehuantepec. This gyre is strictly a winter phenomenon and ceases as soon as the winds in the Gulf of Tehuantepec change their direction.

In July (Fig. 11) a current flows north along the coast of Mexico and enters the Gulf of California. The entire current pattern east of 110°W is characterized by a slowly west to northwest moving water mass. West of this longitude the current is toward the south north of latitude 20°N and toward the west south of this latitude.

The monthly average speeds of these currents are low and lie almost entirely within 5 cm/sec and 20 cm/sec.

FRONTS IN THE VICINITY OF THE GULF

In the following the term "front" will be used as suggested by Cromwell and Reid (1956), i.e., as a narrow band along the sea surface across which the density changes abruptly. The terms "temperature front" and "salinity front" will be used to describe the density front, since it is only from temperature and salinity measurements that the density can be adequately determined. The definite character of a front can only be established if continuous temperature and salinity records are available. Unfortunately there are no continuous records of salinity, for which reason a description of the fronts in the vicinity of the Gulf must be based on closely spaced stations rather than upon continuous records.

Two regions of rapid temperature and salinity transition have been found to exist in the Gulf Entrance, one off Cabo San Lucas and one off Cabo Corrientes (Fig. 12). The San

Lucas transition represents a very sharp boundary between warm and high-saline Gulf water, and cool, low-saline water from the California region. It was first described by Thorade (1909), who pointed out that the intensity of the front is seasonal in character and that the maximum intensity occurs in late spring when the temperature differences between the Gulf and California Current water are greatest.

The San Lucas front is illustrated in Figure 13 (unpublished data). It is seen that the front is marked by a narrow band across which the temperature decreases from 21° to 18°C. and the salinity from 34.6 to 34.1°/₀₀.

It is possible that when the more saline Gulf water is cooled rapidly some sinking of this water takes place at the front, but this feature has not been investigated. The temperature structure below the San Lucas front is shown in Figure 14. The bathythermograph section from Cabo Corrientes to Cabo San Lucas was prepared from hourly temperature observations made aboard the U. S. vessel "Golden Bear" and led to the discovery of another front in the vicinity of Cabo Corrientes. It is seen that the temperature differences across the front increase with increasing depth. The increase could be explained as the result of decreased mixing at greater depth, but the feature needs further investigation.

Since the winds were northerly in April, 1949, when the "Golden Bear" crossed the Gulf Entrance it can be assumed that an already warmed water mass was driven out of the Gulf and pushed the cooler water north

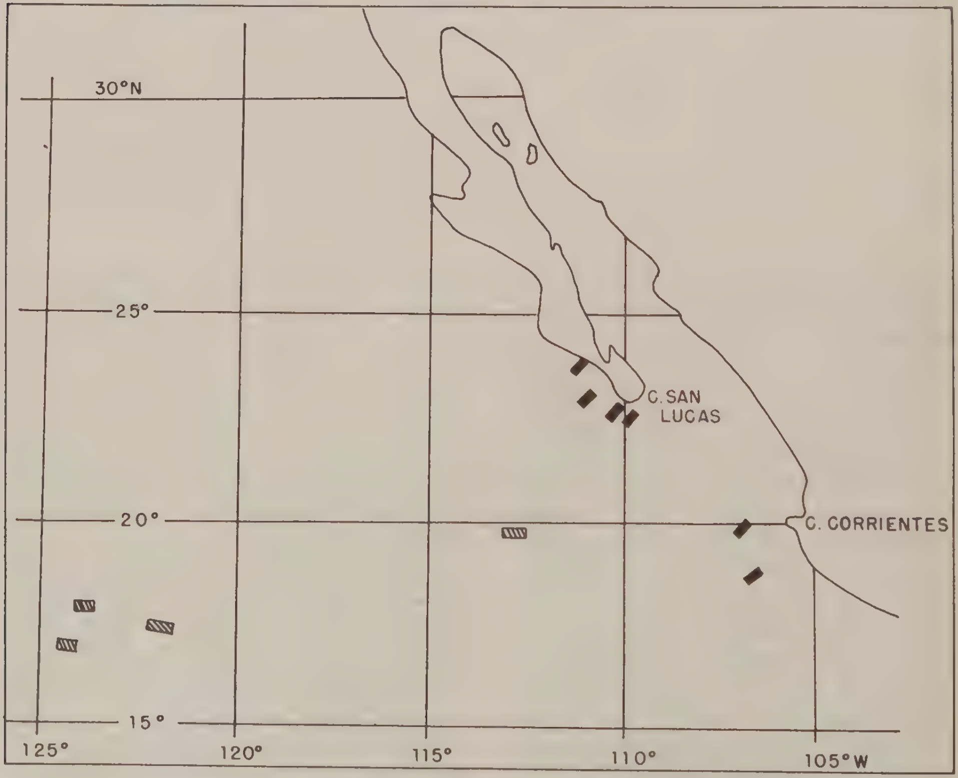

FIG. 12. Observed fronts (solid black) and transition regions (shaded) near the Gulf of California.

(956)

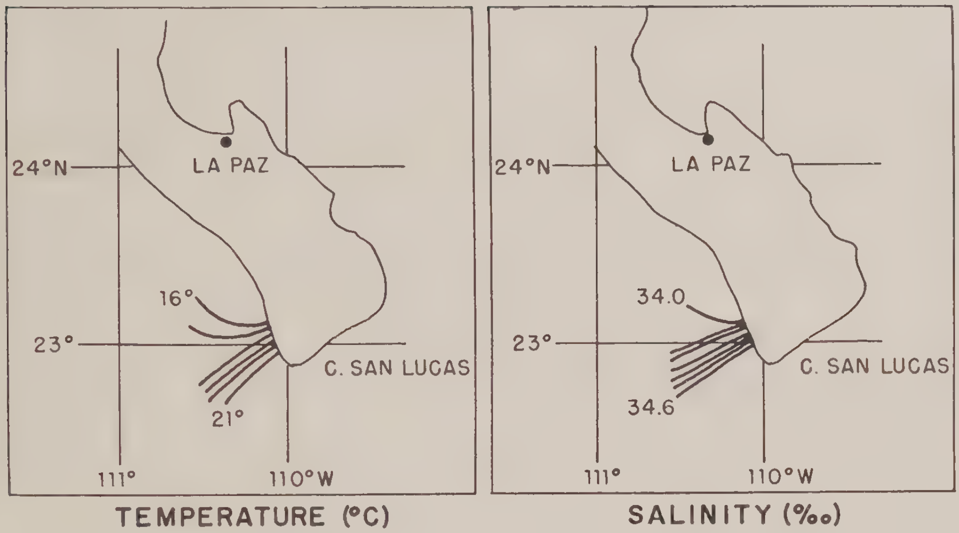
24°N
LA PAZ
16°
23°
C. SAN LUCAS
21°
111°
110°W
TEMPERATURE (°C)
24°N
LA PAZ
34.0
23°
C. SAN LUCAS
34.6
111°
110°W
SALINITY (‰)

FIG. 13. Surface appearance of the San Lucas front.

of Cabo San Lucas and south of Cabo Corrientes aside, thus giving rise to the fronts observed.

UPWELLING

Upwelling in the Gulf can be expected along the east coast with northerly winds and along the west coast with southerly winds. So far only upwelling along the east coast has been investigated (Allen, 1937).

The upwelled water is characterized by a low temperature and a low salinity when compared to the temperature and salinity of the surroundings. The surface oxygen content of the water is not necessarily a good indicator of upwelling, since it is strongly influenced by phytoplankton productivity, and by exchange with the atmosphere.

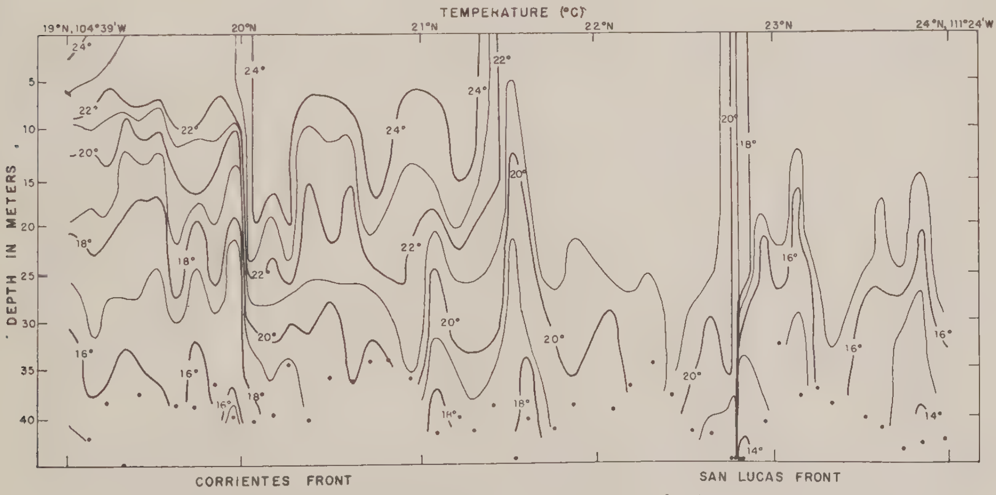

FIG. 14. Bathythermograph section from Cabo Corrientes to Cabo San Lucas, April, 1949.

Upwelling is not uniformly distributed along the east coast with northerly winds but seems rather to be confined to certain places. Such places are in the lee of Isla Tiburón, in Bahia Guaymas, in Bahia Yavaros and in the vicinity of Topolobampo (Allen, 1937). It is interesting to note that all these places are in the lee of islands or headlands, which suggests that upwelling is largely controlled by the irregularities of the coast line as well as by the winds.

Upwelling is important in the Gulf as a means of replenishing the depleted surface layers with plant nutrients from below. There are, unfortunately, no data on the concentration of plant nutrients available for the regions where upwelling occurs, and it is for the time being not possible to investigate the biological role of upwelling in a quantitative manner. The high concentration of phytoplankton in the upwelling areas in spring (Allen, 1937) is indicative, however, of a sufficient concentration in plant nutrients to support the large standing crop.

It should be pointed out that upwelling is not the only process to fertilize the surface layers with plant nutrients. Increased wind mixing and winter convection may be of equal importance. The latter process is effective in the northernmost part of the Gulf (Sverdrup, 1941) whereas the former is beneficial everywhere.

SEASONAL VARIATION OF TEMPERATURE AND SALINITY IN THE GULF

Information on the monthly variation of temperature and salinity at the sea surface in the Gulf is very scanty.

The first attempt to draw charts of monthly average sea surface temperatures was made by Thorade (1909). He collected data from ships' observations for many years and averaged them. These pre-World War I charts are still the only ones in existence (Fig. 3). Since the Second World War the U. S. Coast and Geodetic Survey has published sea surface temperatures from a few shore stations in the Gulf. These are given in Table 4. It is seen that the minimum temperatures occur in January and February and the maximum temperatures in August and September. The mean annual range lies between 23°C. and 28°C. in Mazatlán and between 16°C. and 32°C. in Guaymas. In the northern half of the Gulf the mean monthly temperatures are not known. The minimum in the northernmost part seems to be above 10°C. since this is the temperature of the bottom water found there (Sverdrup, 1941).

TABLE 4

MONTHLY VARIATION OF SEA WATER TEMPERATURE AND SALINITY FOR LA PAZ, GUAYMAS, AND MAZATLÁN (USCGS 1951, Schott, 1935)

	LA PAZ		GUAYMAS		MAZATLÁN	
	t°C.	S°/₀₀	t°C.	S°/₀₀	t°C.	S°/₀₀
January	19.1	35.5	16.3	36.2	24.0	34.8
February	19.3	35.8	17.6	36.0	23.0	34.9
March	20.0	36.4	18.2	35.8	24.0	35.0
April	22.0	36.6	21.0	36.2	24.5	35.1
May	24.4	36.6	24.8	36.4	25.5	35.5
June	26.0	36.4	29.3	37.0	26.7	35.8
July	28.2	36.6	31.7	37.1	27.5	34.8
August	29.8	36.2	31.4	36.3	28.2	34.6
September	29.0	36.2	31.9	36.3	28.0	32.8
October	28.3	36.2	30.0	36.7	27.8	34.5
November	24.7	35.9	25.4	36.2	26.9	35.1
December	21.2	35.7	19.6	36.2	26.1	35.0
Year	24.3	36.2	24.8	36.3	26.0	34.9
Minimum	17.8	34.1	11.0	31.4	—	11.1
Maximum	33.3	40.4	36.2	41.0	—	36.7

The mean annual surface temperature is quite high in the Gulf and lies around 24°C. (Table 4). In Mazatlán the mean annual temperature is very high (26.0) and the surface water there is probably of advective origin, because it is always warmer than the air above it (Fig. 5).

Mean monthly salinities (USCGS 1951) are listed in Table 4. The salinity (Fig. 15) has two maxima and two minima. The first maximum is found around June and is the result of excessive evaporation. With the coming of the rainy season the salinity of the surface water falls and reaches a minimum at the peak of the rainy season. In October increasing winds and rapidly decreasing air temperatures and the lack of large precipitation give rise to a second peak in net evaporation which is also reflected in the second salinity maximum. After the October maximum the salinity de-

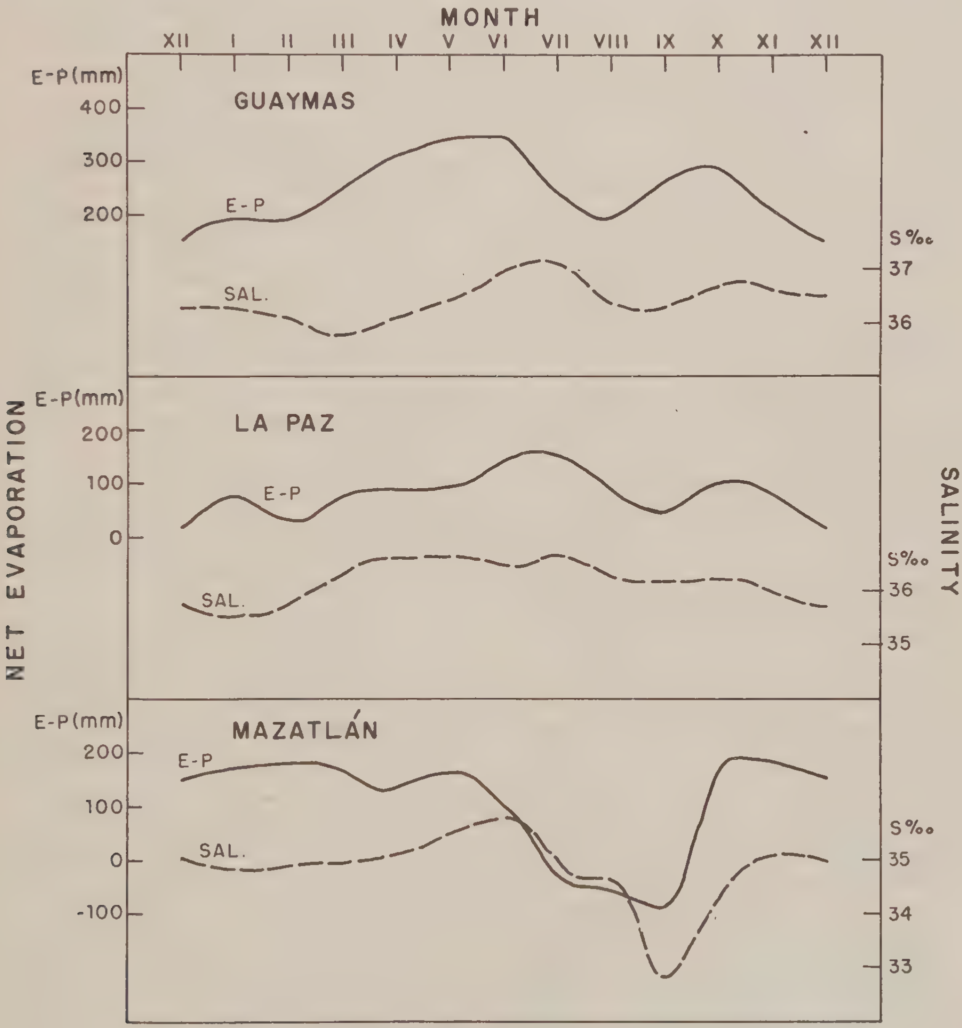

FIG. 15. Net evaporation and salinity for Guaymas, La Paz, and Mazatlán.

creases and reaches a second minimum around December. The salinity ranges between 35.5 and 36.5°/₀₀ in La Paz and between 35.8 and 37.1°/₀₀ in Guaymas. Both places are situated at the head of shallow bays where evaporation is extensive. These values are, therefore, not representative for the open Gulf.

In Mazatlán the salinity varies between 32.8 and 35.8°/₀₀. The very low value found in September (32.8°/₀₀) is possibly caused by extensive runoff from Rio Presidio during the rainy season.

Figure 15 illustrates that there is a very good agreement between net evaporation and salinity. The slight differences seen can be attributed to the different years in which the salinity was observed and for which the net evaporation was computed.

DISTRIBUTION OF PHYSICAL AND CHEMICAL PROPERTIES IN THE GULF

A preliminary discussion of the distribution of temperature, salinity, and oxygen in February and March, 1939, was published by Sverdrup (1941). A short report on the distribution of silicate and phosphate from October to December, 1940, was given by the same author (Sverdrup and staff, 1940). Here only a few conclusions will be drawn from the distribution of these properties. The distribution of phosphate and silicate in the Gulf can be discussed only qualitatively, because the measured data are such that they do not warrant a quantitative discussion.

Vertical Distribution

The Gulf can be divided vertically into a shallow upper layer (20 to 40 m. deep) where the distribution of properties is rather uniform due to wind stirring; a layer between roughly 50 and 150 m., varying with season, where the temperature, salinity and oxygen content decrease rapidly; and a deep layer, between the thermocline and the bottom, where the concentrations remain fairly constant from one season to another.

In the upper layer the concentrations vary considerably with time due to the amount of heating, cooling, stirring, evaporation, precipitation, runoff and various biological activities. Shallow and semi-enclosed bays show greater variations than the open Gulf. The layer of rapid density increase is generally closer to the surface during the warm season than during the cold season, but the available data are too few to give accurate depth ranges. Below the layer of rapid density increase the temperature decreases more or less slowly toward the bottom, but in a few deep basins, below 2000 m., a slight increase is observed due to the adiabatic effect.

The salinity shows a minimum (34.48–34.54°/₀₀) between 600 and 800 m. and increases slightly toward the bottom.

The amount of dissolved oxygen has a very pronounced minimum (less than 0.1 ml/l) between 300 and 700 m. and increases again toward the bottom.

The silicate content increases with depth and equals about 160 μg–at/l in the central part of the Gulf where the bottom deposits are largely diatomaceous oozes.

Horizontal Distribution

The horizontal distributions of temperature, salinity and oxygen in February and March, 1939, are illustrated in Figures 16, 17, 18 and 19.

At the surface (Figs. 16 and 17) the distribution of these properties is very complicated. The high oxygen values (more than 50 per cent supersaturated in places) are probably the result of extensive phytoplankton production. The southern half of the Gulf is slightly undersaturated with respect to oxygen. Upwelling as indicated by a low temperature (and salinity) can be seen to occur in Bahia Guaymas and Topolobampo.

At subsurface depths (Figs. 18 and 19) the two outstanding features are a tongue of warm, high saline and oxygen-rich water moving to the south along the coast of Baja California and a tongue of low saline, cool

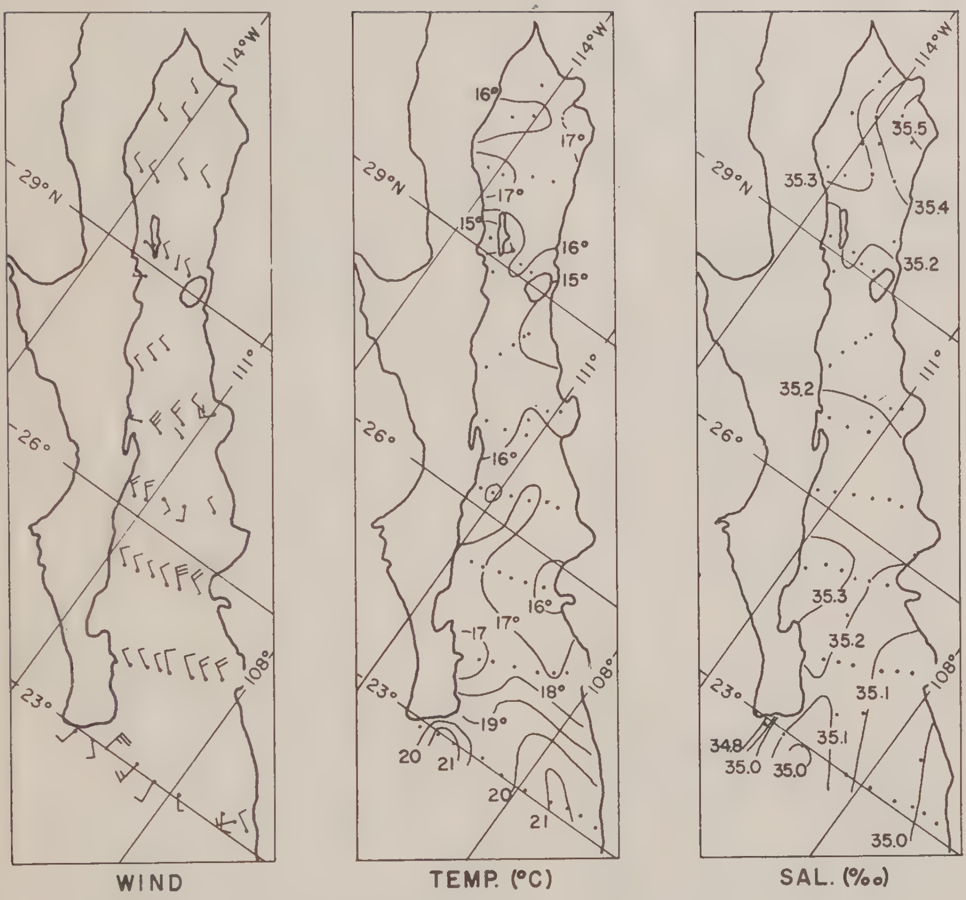

FIG. 16. Distribution of wind temperature and salinity at the sea surface in February and March, 1939.

and oxygen-poor water entering the Gulf from the south. The tongue along Baja California has possibly its origin in the northern part of the Gulf, because it is of nearly the same temperature, salinity and oxygen as the water of the northern area. The inflowing water mass shows the same characteritsics as the equatorial Pacific water (Fig. 9) and represents a compensation flow to replace the water lost by evaporation and wind drift out of the Gulf.

CONCLUSIONS

The Gulf of California remains oceanographically unknown to a great extent. The results that have been presented here are based on meager data and conclusions drawn from such data may have to be modified when more accurate and more complete data are available.

Conditions in the Gulf are dependent upon the conditions in the atmosphere and any changes that take place in the atmosphere will also be reflected in the Gulf. The submarine topography and the orientation of the shoreline also influence the circulation and hence the distribution of properties.

The bulk of the water found in the Gulf shows properties very similar to the Pacific Equatorial water mass. This water mass upon entering the Gulf is modified at the surface by extensive evaporation which increases its

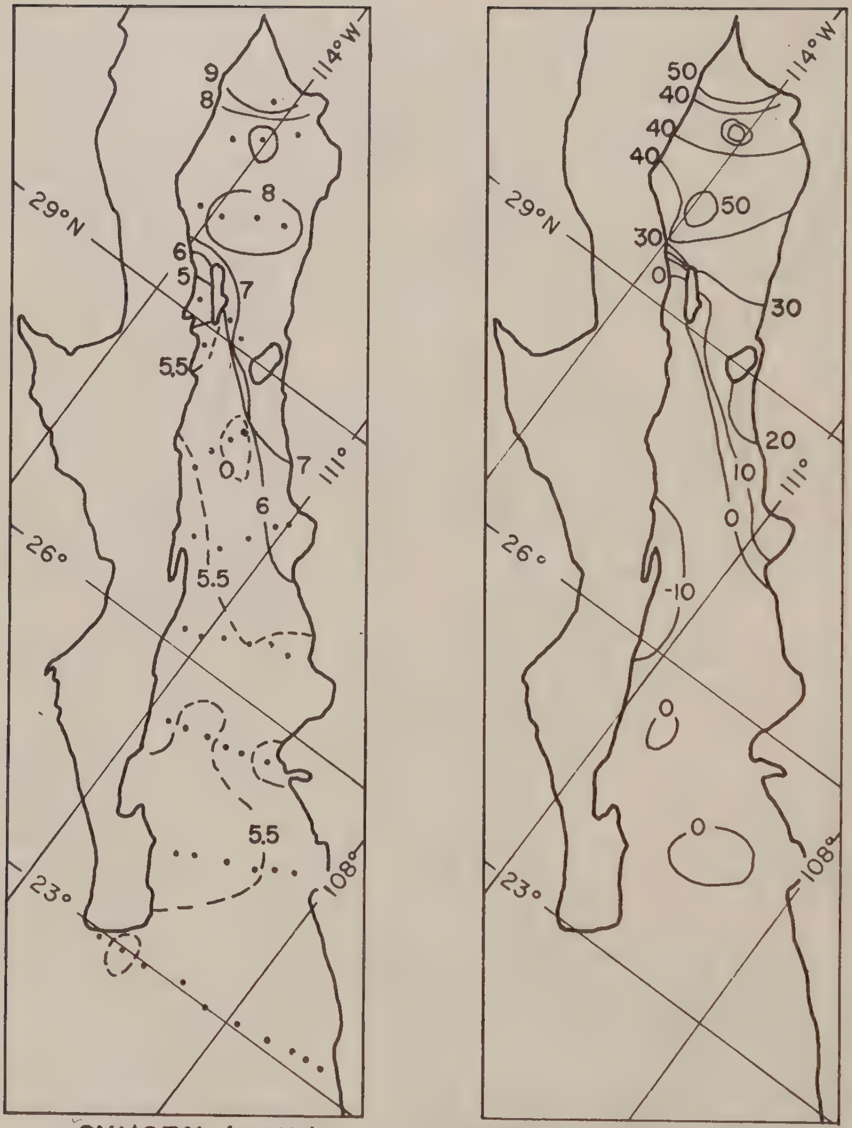
114°W
29°N
26°
23°
111°
108°
9
8
8
6
5
7
5.5
0
7
6
5.5
5.5
114°W
29°N
26°
23°
111°
108°
50
40
40
40
50
30
0
30
20
10
0
-10
0
0

OXYGEN (ml/L)

OXYGEN SUPERSATURATION (‰)

FIG. 17. Distribution of oxygen and oxygen saturation anomaly at the sea surface, in February and March, 1939.

salinity. The effect of evaporation increases as one proceeds toward the northwest.

The circulation in the surface layers is predominantly wind driven. Since the winds transport water of different origin towards the entrance of the Gulf, it is a transition region marked by the existence of fronts of which the San Lucas front is the best developed and best known.

In the Gulf, as elsewhere, upwelling, sink-

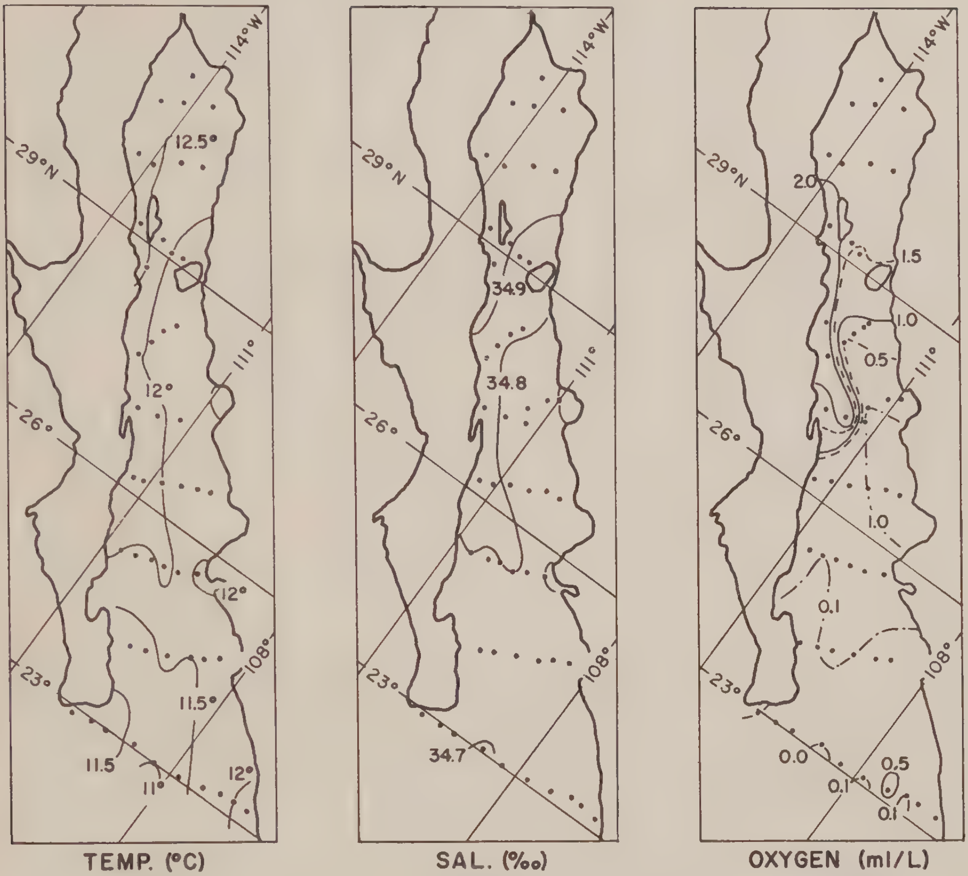

FIG. 18. Distribution of temperature, salinity, and oxygen at 200 m., in February and March, 1939.

ing, and convective overturn play important parts in determining the fertility of any given place. Convection is especially conspicuous north of Isla Tiburón and is responsible for the different hydrographic conditions there. Upwelling is largely found in the lee of headlands and islands, along the eastern coast with northerly winds, and along the western coast with southerly winds. Away from the shores the Gulf is fertile only in spring after considerable winter mixing has brought an adequate supply of phosphates and silicates to the surface. During the rest of the year the surface waters are relatively barren.

The field for investigations in the Gulf is nearly unlimited and it is the hope of the author that in the future increasing efforts will be directed towards the scientific exploration of one of the most fascinating seas in the Pacific, the Gulf of California.

REFERENCES

ALLEN, W. E. 1923. Observations on surface distribution of marine diatoms of Lower California in 1921. *Calif. Acad. Sci., Proc.* 12: 437–442.

——— 1937. Plankton diatoms of the Gulf of California obtained by the G. Allan Hancock Expedition of 1936. *The Hancock Pacific Expeditions, So. Calif. Univ. Pub.* 3: 47–59.

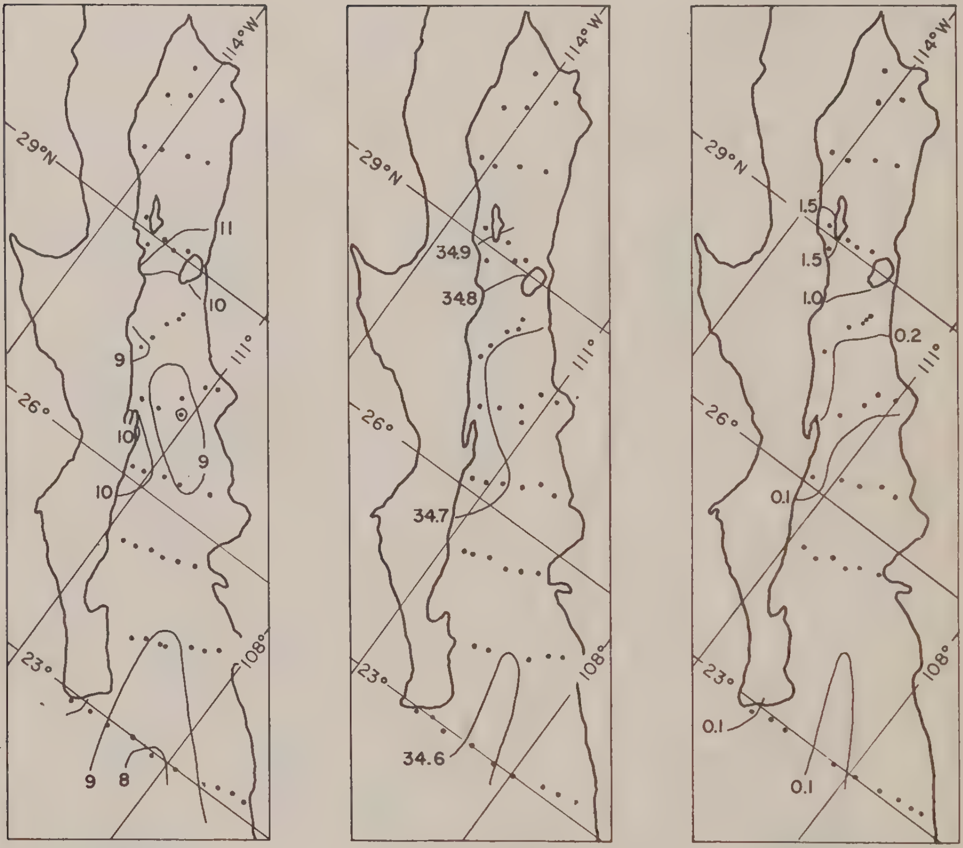

TEMP. (°C) SAL. (‰) OXYGEN (ml/L)

FIG. 19. Distribution of temperature, salinity, and oxygen at 400 m., in February and March, 1939.

——— 1938. The Templeton Crocker Expedition to the Gulf of California in 1935. The phytoplankton. *Amer. Micros. Soc. Trans.* 67: 328–335.

ANDERSON, C. A. 1950. 1940 "E. W. Scripps" cruise to the Gulf of California. Part I: Geology of islands and neighboring land areas. *Geol. Soc. Amer., Mem.* 43: 1–52.

ANDERSON, E. R. 1953. The exchange of energy between a body of water and the atmosphere with application in evaporation. *Scripps Institution of Oceanography, Calif. Univ., Dissertation.*

CROMWELL, T., and J. REID. 1956. A study of oceanic fronts. *Tellus.*

DURHAM, J. W. 1950. 1940 "E. W. Scripps" cruise to the Gulf of California. Part II: Megascopic paleontology and marine stratigraphy. *Geol. Soc. Amer., Mem.* 43: 1–216.

GILBERT, J. Y., and W. E. ALLEN. 1943. The phytoplankton of the Gulf of California obtained by the "E. W. Scripps" in 1939 and 1940. *Jour. Mar. Res.* 5: 89–110.

HAKLUYT, R. 1598. *The Principal Navigations, Voyages, Traffiques and Discoveries of the English Nation.* Vol. 3. 397 pp. J. Dent and Sons Ltd., London.

HOWARD, C. S. 1954. *Composition of the Colorado River.* Lake Mead Comprehensive Survey, 1948–1949. Vol. 2. 165 pp.

JACOBS, W. C. 1951. The energy exchange between sea and atmosphere and some of its consequences. *Scripps Institution of Oceanography, Bul.* 6: 27–122.

JOHNSTON, I. M. 1924. Expedition of the California Academy of Science to the Gulf in 1921. *Calif. Acad. Sci., Proc.* 12: 951–1218.

MUNK, W. H. 1941. Internal waves in the Gulf of California. *Jour. Mar. Res.* 4: 81–91.

NATLAND, M. L. 1950. 1940 "E. W. Scripps" Cruise to the Gulf of California. Part IV: Report on Pleistocene and Pliocene Foraminifera. *Geol. Soc. Amer., Mem.* 43: 1–55.

OSORIO-TAFALL, B. F. 1943. El Mar de Cortes y la productividad fitoplanctónica de sus aguas. *An. de la Esc. Natl. de Cien. Biol.* 3: 73–118.

——— 1944. La expeditión del M. N. "Gracioso" por aguas del extremo noroeste mexicano. *An. de la Esc. Natl. de Cien. Biol.* 3: 331–360.

PATTULLO, J., W. H. MUNK, and E. STRONG. 1955. The seasonal oscillation in sea level. *Jour. Mar. Res.* 14: 88–156.

REVELLE, R. 1939. Sediments of the Gulf of California. *Geol. Soc. Amer. Bul.* 50: 170, 171.

——— 1950. 1940 "E. W. Scripps" Cruise to the Gulf of California. Part V: Sedimentation and Oceanography. *Geol. Soc. Amer., Mem.* 43: 1–6.

SCHOTT, W. 1935. *Geographie des Indischen und Stillen Ozeans.* C. Boysen Ltd., Hamburg. 413 pp.

SHEPARD, F. P. 1950. 1940 "E. W. Scripps" Cruise to the Gulf of California. Part III: Submarine Topography of the Gulf of California. *Geol. Soc. Amer., Mem.* 43: 1–32.

SMITHSONIAN INSTITUTE. 1951. *Smithsonian Meteorological Tables.* Washington, D. C.

SVERDRUP, H. U. 1940. The Gulf of California. *Assoc. Ocean. Phys., Proc. Verb.* 3: 170, 171.

——— 1941. The Gulf of California: Preliminary discussion of the cruise of the "E. W. Scripps" in February and March, 1939. *6th Pacific Sci. Cong. Proc.* 3: 161–166.

SVERDRUP, H. U., M. W. JOHNSON, and R. H. FLEMING. 1942. *The Oceans.* Prentice Hall, Inc., New York. 1087 pp.

SVERDRUP, H. U., and STAFF. 1940. Research within physical oceanography and submarine geology at the Scripps Institution of Oceanography during April 1940 to April 1941. *Amer. Geophys. Soc., Trans.* 21: 490–495.

——— 1943. Oceanic observations of the Scripps Institution in 1939. *Scripps Institution of Oceanography, Records of Observations* 1: 65–160.

TANNER, F. L. 1889. Report on investigations of the U. S. Fish Commission Steamer "Albatross" for the year ending June 20, 1889. *U. S. Fish Comn. Rept. for 1888.* Pp. 395–512.

THORADE, H. 1909. Uber die Kalifornische Meeresströmung. *Hydrog. u. Marit. Met., Ann.* 37: 17–34, 63–76.

TOWNSEND, C. H. 1901. Dredging and other records of the U. S. Fish Commission Steamer "Albatross" with bibliography relative to the work of the vessel. *U. S. Fish Comn. Rept. for 1900.* Pp. 387–562.

U. S. COAST AND GEODETIC SURVEY. 1951. *Surface Water Temperatures at Tide Stations.* Spec. Pub. 280.

——— 1954. *Density of Sea-water of Tide Stations.* Spec. Pub. 281.

——— 1956. *Tide Tables: West Coast of South and North America.* Pub. 781.

U. S. GEOLOGICAL SURVEY. 1950. *Surface Water Supply of the United States. Part 9: Colorado River Basin.* Geol. Survey, Water Supply Paper 1179.

U. S. HYDROGRAPHIC OFFICE. 1947. *Atlas of Surface Currents: Northeastern Pacific Ocean.* Pub. 570.

——— 1951. *Sailing Directions: West Coast of Mexico and Central America.* Pub. 84. Charts 619, 620, 621, 622, 638, 639, 640, 800, 849, 850, 938, 1024, 1335, 1664, 1666, 1667, 2087, 2103, 2130, 2181, 2193, 5388.

U. S. WEATHER BUREAU. 1950–52. Climatological data. *National Summary* 1, 2, 3.

Reprinted from ARCHIVES OF BIOCHEMISTRY AND BIOPHYSICS, Volume 73, No. 1, January, 1958
Academic Press Inc. *Printed in U.S.A.*

ARCHIVES OF BIOCHEMISTRY AND BIOPHYSICS **73,** 207–219 (1958)

Comparative Biochemical Studies of the Phycobilins[1]

Colm Ó hEocha[2, 3]

From the Marine Botany Division, Scripps Institution of Oceanography, University of California, La Jolla, California

Received April 18, 1957

INTRODUCTION

The phycobilins are the prosthetic chromophoric groups of the algal proteins, phycoerythrins and phycocyanins (1, 2). The term originates from the similarity found by Lemberg (1–3) between the chromophores of these *biliproteins*[4] and the bile pigments of animals, the open-chain tetrapyrrole structure of which was established by Fischer in the early 1930s [cf. (5)].

The absorption spectra of phycoerythrins and phycocyanins can vary greatly, and such variations form the basis for Svedberg's nomenclature system for these chromoproteins (4). This might be attributable to the existence of many different phycobilins, but spectral variations are possible also in chromoproteins containing the same prosthetic group, as in the case of the various astaxanthin–protein complexes (6). In the present investigation a number of phycobilins were compared in an attempt to find the basis for the difference between their parent biliproteins.

Early attempts (7–9) to isolate the phycobilins were unsuccessful because of their lability and the tenacity of their attachment to the proteins. Lemberg (1–3) succeeded in obtaining a protein-free pigment from phycocyanin, but a phycoerythrin chromophore was not isolated in pure form (5).

Lemberg (3) differentiated *phycocyanobilin* (chromophore of phycocyanin) from *phycoerythrobilin* (chromophore of phycoerythrin). These

---

[1] Contribution from the Scripps Institution of Oceanography, New Series 962.

[2] Supported by an award from the Lalor Foundation.

[3] Present address: Chemistry Department, University College, Galway, Ireland.

[4] This term may be preferable, because of its brevity, to *bilichromoproteins* (4).

(967)

names refer specifically to what Lemberg considered to be the native prosthetic groups of C-phycocyanin and R-phycoerythrin, respectively. As a result of the present investigation, it is believed that the phycobilins isolated by Lemberg were artifacts formed during hydrolysis. It is proposed that the designations phycocyanobilin and phycoerythrobilin, as used in this communication, should more properly be applied to the newly isolated pigments, described below, which are thought to represent the native chromophores or very close derivatives of these.

The experiments of Lemberg and Bader (2) led them to believe that phycocyanobilin and phycoerythrobilin, obtained from the chromoproteins by acid hydrolysis, are identical with mesobiliviolin and mesobilirhodin (mesobilierythrin), respectively. These workers considered phycocyanobilin to be an oxidized form of phycoerythrobilin, but Siedel's (10) work indicated that synthetic mesobiliviolin and mesobilirhodin are prototropic isomers and Lemberg later assumed the same to be true of the phycobilins (5).

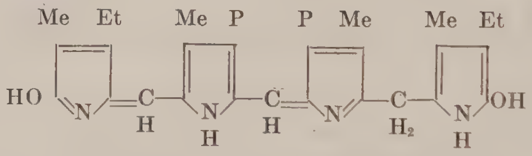

mesobiliviolin IXα [Siedel (10)]

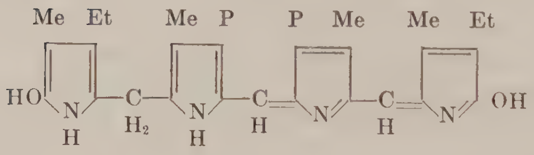

mesobilirhodin(?) [Siedel (10)]

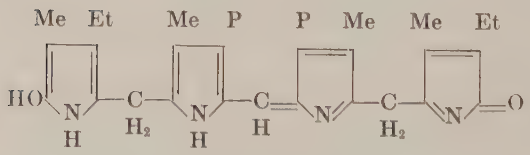

mesobilirhodin (?) [Lemberg and Legge (5)]

(Me: —CH_3; Et: —C_2H_5; P: —CH_2CH_2COOH)

Siedel's structure for mesobiliviolin is generally accepted, but neither of the formulas proposed for mesobilirhodin is considered satisfactory

(11). Mesobiliviolin IX α is the isomer obtained from C-phycocyanin (12), which contains about 4% of the tetrapyrrole.[5]

MATERIALS

The biliproteins were extracted into water from many of the algae employed by Haxo, Ó hEocha, and Norris (4). In addition, the blue–green *Arthrospira maxima* was collected as a thick scum floating in brackish water near Del Mar, California. The algae were extracted at 0–5°C. in the dark.

When spectral and chromatographic analyses indicated the presence in the aqueous algal extract of one biliprotein in very great preponderance, saturated ammonium sulfate was added to a concentration sufficient to precipitate the pigment. Mixtures of pigments were resolved by chromatography on tricalcium phosphate–Supercel (a purified diatomaceous earth) (4). The eluted individual chromoproteins were precipitated with ammonium sulfate or acetone and washed with acetone until the supernatant was no longer colored, thus removing fat-soluble pigments and associated fats. Denaturation of the proteins was completed by washing with ether. The precipitated biliproteins were then washed with distilled water on a Büchner filter to remove salts, and, finally, dried by washing with acetone and ether. Reagent-grade solvents were used throughout.

Dry cylinder nitrogen was purified by flowing over hot copper filings before being passed through all hydrolysis mixtures. Spectral readings were made on a Beckman DU spectrophotometer.

Isolation of the Phycobilins

In preliminary experiments, cleavage of C-phycocyanin was effected by the method of Lemberg (3), involving hydrolysis of the dried biliprotein in concentrated hydrochloric acid at 80–85°C. under nitrogen. Hydrolysis was discontinued after 20 min., the acid was diluted, and the pigment was then quickly but carefully extracted several times with small quantities of chloroform. The deep, indigo-blue chloroform solution of mesobiliviolin hydrochloride was purified by washing with 5% HCl. It was then washed several times with water; the hydrochloride was thus hydrolyzed, resulting in a color change from blue (absorption maximum at 608 mμ) to violet (maximum at 567 mμ) (see Fig. 1). Lemberg obtained the crystalline phycobilin from a solution in chloroform–benzene.

In the present investigation, the pigment was purified by chromatography under nitrogen on talc–Supercel (1:1). The main zone (mesobiliviolin), which was eluted with 0.01 *M* HCl in methanol was preceded by a narrow green zone, probably mesobiliverdin formed by oxidation of the mesobiliviolin.

Lemberg's method of hydrolyzing C-phycocyanin to yield mesobiliviolin, as described above, is now considered to alter the native chromophore; accordingly, the following less drastic method of hydrolysis was used in the course of the present investigation to prepare both phycocyanobilin and phycoerythrobilin. The dried, denatured biliprotein was placed in oxygen-free conc. HCl (*ca.* 0.1 g./10 ml. acid) in a large stoppered test tube with gas inlet and outlet. Nitrogen was bubbled through the mixture during hydolysis of the biliprotein at room temperature for 20–30 min.

---

[5] Clendenning, K. A., Ke, B., and Curry, T., unpublished studies, 1953–55.

It seemed from visual observation that phycoerythrins were hydrolyzed more rapidly and more completely than phycocyanins. However, as in the case of Lemberg's method (3)[5], hydrolysis was not complete after 20–30 min., but, due to secondary effects of acids on the liberated phycobilins, the reaction was not extended beyond this period. In order to terminate hydrolysis, the reaction mixture was diluted with three or four times its volume of boiled distilled water and then extracted by shaking gently and exhaustively with chloroform. All these operations were performed as expeditiously as possible in dim light. The lability of the recovered phycobilins necessitated the immediate determination of their spectral and chromatographic properties.

RESULTS

I. Phycocyanobilin

(*a*) *C-Phycocyanin.* C-phycocyanin from *Arthrospira maxima* was hydrolyzed under nitrogen with conc. HCl at room temperature for 30 min. as described above. The acid chloroform extract of the hydrolyzate

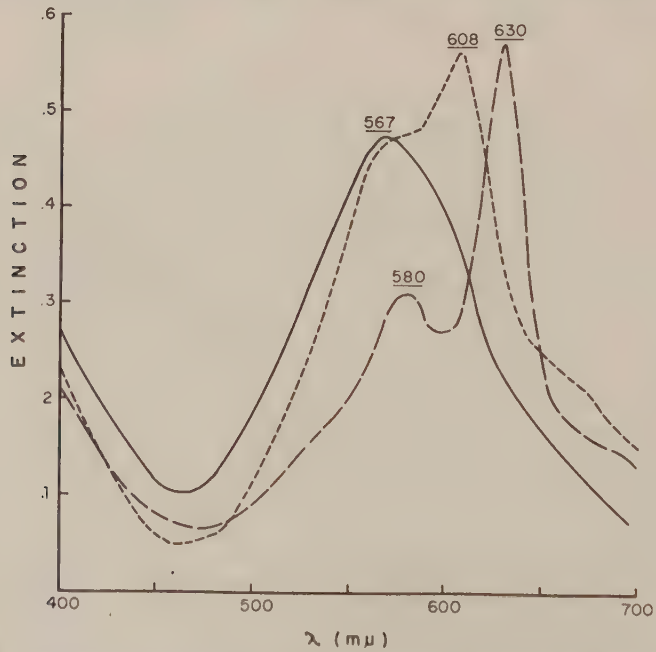

FIG. 1. Absorption spectra of a phycobilin and its derivatives, prepared from C-phycocyanin by the method of Lemberg (2). (All in chloroform.)
——— Phycocyanobilin (=mesobiliviolin) from C-phycocyanin
- - - - phycocyanobilin hydrochloride
— — — phycocyanobilin-zinc complex

absorbed broadly at 630 mμ (Fig 2.). Bile pigments normally form hydrochlorides in acid solutions and, consequently, this spectrum is assumed to represent phycocyanobilin hydrochloride. The acid chloroform solution was washed thoroughly with water and with 1% sodium bicarbonate solution in an attempt to form free phycocyanobilin. Both these treatments resulted in excessive loss of pigment without apparent alteration in spectral properties. On the addition of a few drops of alcoholic zinc acetate (Schlesinger reaction), a red fluorescence appeared, indicating the formation of a Zn complex of phycocyanobilin. On this basis the latter compound is considered to have a violin-type structure (13). The complex absorbs maximally at 630 mμ, as does the free chromophore. Attempts to purify phycocyanobilin by chromatography on talc–Supercel led to oxidation and possibly other alterations in the pigment (14).

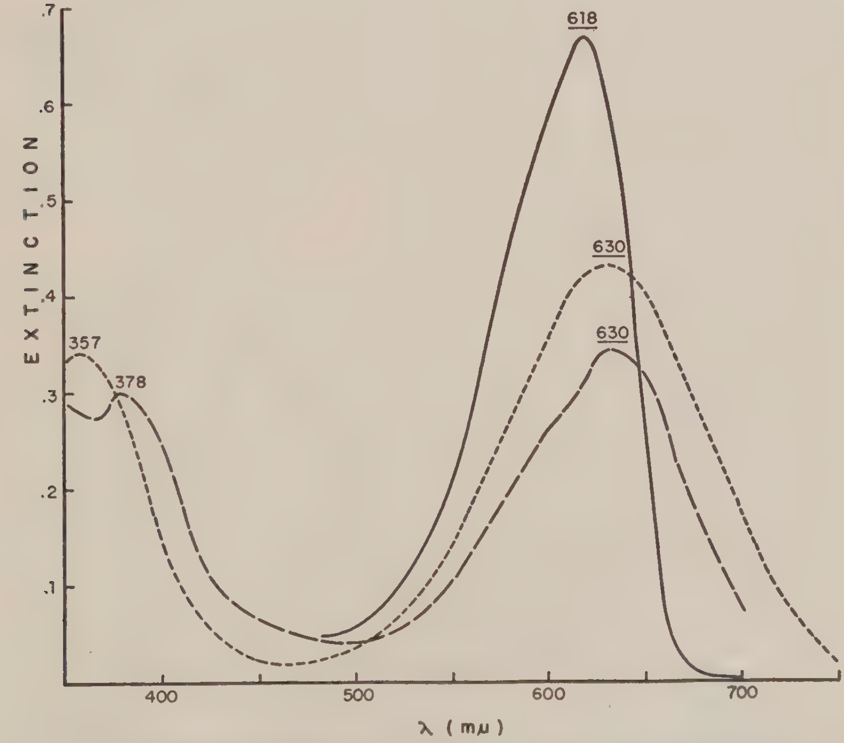

Fig. 2. Absorption spectra of C-phycocyanin and its chromophore.
——— C-phycocyanin from *Arthrospira* (in water, pH 6.0)
- - - - Phycocyanobilin of above (in acid chloroform)
— — — Phycocyanobilin Zn-complex (in chloroform)

The effect of conc. HCl on phycocyanobilin was followed spectrophotometrically. Aliquots of the C-phycocyanin hydrolyzate were removed at intervals and extracted with chloroform. Spectra of these extracts show that phycocyanobilin is sensitive to strong acid (Fig. 3). The substance formed after 7 hr. hydrolysis (maximum at 607 mμ) is probably mesobiliviolin hydrochloride (see Fig. 1); mesobiliviolin is therefore considered to be a product of acid treatment of phycocyanobilin.

(*b*) "*Allophycocyanin.*" The aqueous extracts of a number of red and blue–green algae contain, as a minor component, a light-blue colored protein which has been provisionally identified as allophycocyanin (4). Allophycocyanin from *Arthrospira maxima* was purified by chromatography and subjected to cold acid hydrolysis. The resulting phycocyanobilin, dissolved in acid chloroform, absorbed maximally in the red at

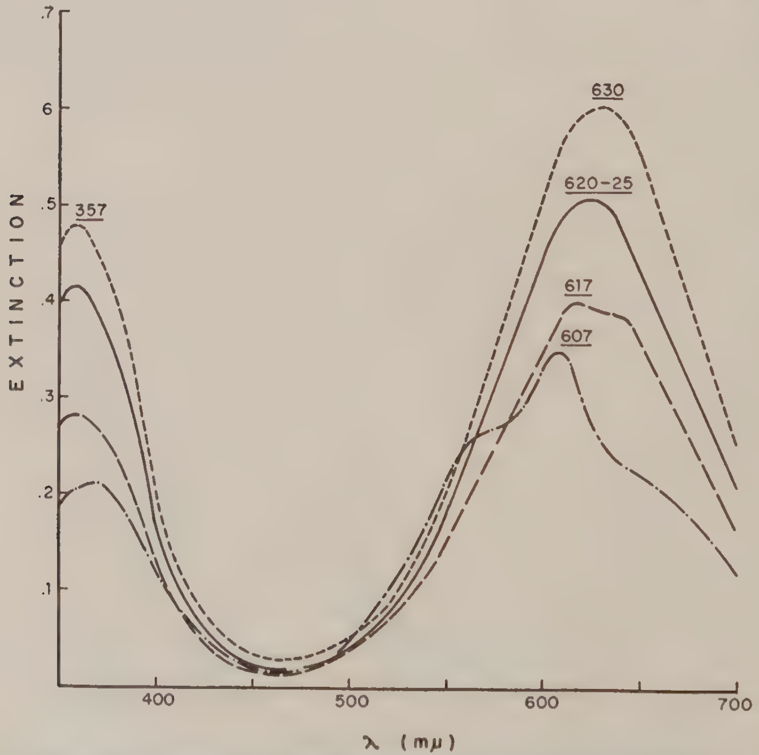

FIG. 3. Absorption spectra in acid chloroform of C-phycocyanobilin (top curve) and its breakdown products formed in concentrated hydrochloric acid.
- - - - C-phycocyanin hydrolyzed 30 minutes
——— C-phycocyanin hydrolyzed 60 minutes
— — — C-phycocyanin hydrolyzed 2 hours
—•—•—• C-phycocyanin hydrolyzed 7 hours

640 mμ (Fig. 4). Thus, it differs from the C-phycocyanin chromophore (max. at 630 mμ), but a close affinity between the two phycobilins is indicated by the fact that after 7 hr. acid hydrolysis at room temperature, or 20 min. at 82°C., allophycocyanin, like C-phycocyanin, yielded a blue pigment with absorption maximum at 607 mμ and a Zn complex with maxima at 580 mμ (slight) and 630 mμ, all reminiscent of mesobiliviolin hydrochloride.

The allophycocyanin chromophore forms a red-fluorescing Zn complex with an absorption maximum at 650 mμ in methanol. This complex, as well as that of C-phycocyanobilin, is oxidized by iodine to a green-fluorescing substance (absorption maximum at 510 mμ). Lemberg and Bader (2) reported that HCl hydrolysis of allophycocyanin at room temperature produced a substance absorbing maximally at 497 mμ; hydrolysis under more drastic conditions resulted in the appearance of two additional maxima. Spectral evidence (4) might indicate our chromoprotein to be identical with Lemberg's allophycocyanin, but this suggestion would seem to be contradicted by the apparent nonidentity of the chromophores of the two protein preparations, unless Lemberg's pigment was contaminated, possibly with phycoerythrin.

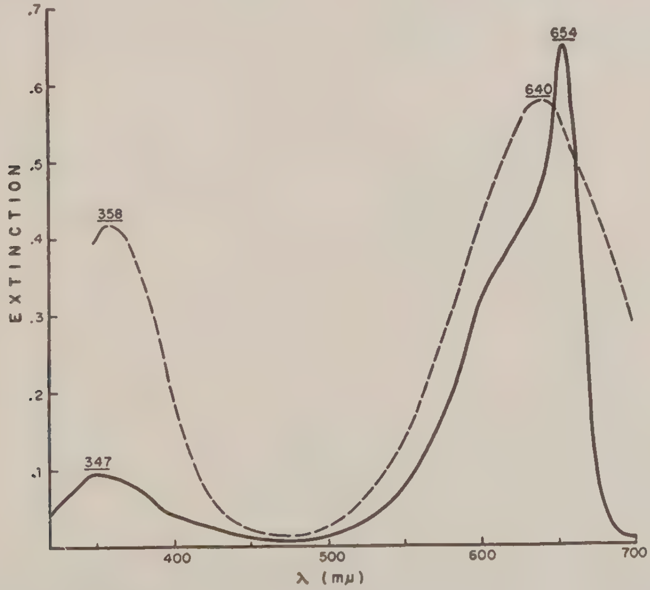

Fig. 4. Absorption spectra of "allophycocyanin" and its chromophore.
——— Allophycocyanin from *Arthrospira* (in phosphate buffer, pH 6.5)
— — — Its phycocyanobilin hydrochloride (in chloroform)

(*c*) *R-Phycocyanin.* The R-phycocyanins of both *Ceramium rubrum* and *Rhodymenia palmata* were found to be particularly resistant to acid hydrolysis. The blue, chloroform-soluble pigment which was obtained in low yields appears to differ from the other phycocyanobilins. There is some indication that phycoerythrobilin may also be present in these biliproteins. Lemberg (3) reported that R-phycocyanin contains both phycocyanobilin and phycoerythrobilin.

II. *Phycoerythrobilin*

Phycoerythrins differing greatly in absorption spectra were hydrolyzed and their chromophores compared on the basis of the spectra of the subsequent initial chloroform extracts. Minimal alteration in the natural prosthetic groups was involved in hydrolysis with concentrated HCl at room temperature for 20–30 min. (see C-phycocyanin section). Some spectral properties of the various phycoerythrobilins thus obtained are presented in Table I. Other properties of the chromophores were examined as permitted by the amounts of material available.

The phycoerythrobilin hydrochloride from *Porphyridium cruentum* absorbs maximally at 312 and 576 mμ in acid chloroform (Fig. 5). It is very labile; on careful washing of the acid chloroform solution with distilled water or dilute sodium bicarbonate solution considerable loss of color occurred and a blue substance (phycoerythrobilin?) with an

TABLE I

Spectral Characteristics of Phycoerythrobilins from Various Phycoerythrins

Algal source	Phycoerythrin abs. max. (mμ)	Phycoerythrobilin abs. max. (mμ)		
	In phosphate buffer pH 6.0–6.5	In acid $CHCl_3$	As Zn complex	
Porphyridium cruentum	545	575–77	583	(Orange–red fluorescence)
Phormidium persicinum[a]	543, 568	575–76	583	*Do.*
Phormidium fragile	563	576	—	*Do.*
Porphyra naiadum.	543, 560	574	—	*Do.*
Porphyra tenera	495, 563	577	583	*Do.*
Rhodochorton rothii	495, 540, 565	576	—	*Do.*
Plocamium pacificum	497, 540, 566	575	—	*Do.*

[a] The two-peaked phycoerythrin of *Phormidium persicinum* may be an artifact formed during extraction. The native biliprotein is probably C-phycoerythrin (max. *ca.* 560 mμ) (14).

absorption maximum at 593 mμ was formed. The phycoerythrobilin hydrochloride, on elution from a talc–Supercel chromatogram, absorbed maximally at 550 mμ in methanol–HCl and at 568 mμ in chloroform, and was seemingly altered by this attempt at purification.

Phycoerythrobilin formed a zinc complex, characterized by a brilliant orange–red fluorescence, and by maximal absorption at 583 mμ (Fig. 5). Oxidation of this complex with a few drops of iodine solution gave a green-fluorescing compound (absorption maximum at 510 mμ), which seems identical with that obtained from phycocyanobilin under the same conditions (see above). Phycoerythrobilin itself is oxidized by a drop of concentrated nitric acid, as indicated by a shift in absorption maximum to 500 mμ. The absorption maxima and green fluorescence of Lemberg's "phycoerythrobilin"–Zn complex, which led him to identify the phycobilin with mesobilirhodin, may have been due to such an oxidized compound, which, incidentally, is strongly reminiscent of Siedel and Möller's "oxo"–urobilin (15).

The spectral changes resulting from treatment of phycoerythrobilin with concentrated hydrochloric acid are plotted in Fig. 6. Nitrogen was continuously passed through the reaction mixture, although it was observed that contact with air did not materially alter the spectra. Prolongation of the hydrolysis beyond 20 min. resulted in a rapid decrease of the 576-mμ maximum of phycoerythrobilin, while new peaks appeared

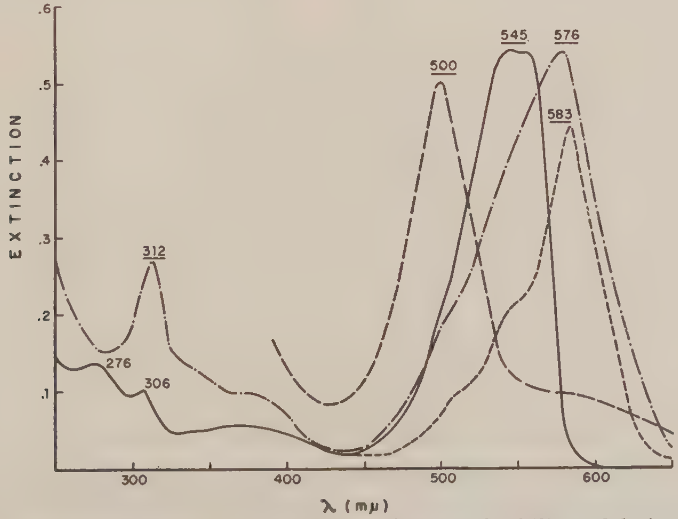

FIG. 5. Absorption spectra of *Porphyridium* phycoerythrobilin and derivatives.
——— Phycoerythrin from *Porphyridium* (in phosphate buffer, pH 6.5)
—•—•— Phycoerythrobilin from *Porphyridium* (in acid chloroform)
— — — Oxidized phycoerythrobilin (in chloroform)
- - - - Phycoerythrobilin Zn-complex (in chloroform)

at *ca.* 500 and 607 mμ in acid chloroform. These maxima were shifted to 500, 595, and 655 mμ in neutral chloroform. Three zones were formed by this neutral material on a talc–Supercel chromatogram which was developed with methanolic HCl: a blue–green zone was first eluted followed by a violet and a strongly adsorbed reddish brown one. The violet component, which was by far the largest, absorbed maximally at 578 mμ in neutral chloroform. It was not phycoerythrobilin, however, because its zinc complex (peaks at 637 and 590 mμ) differed from phycoerythrobilin–Zn (absorption maximum at 583 mμ). The reddish brown component resembled the oxidation product of phycoerythrobilin, with absorption maximum at 500 mμ.

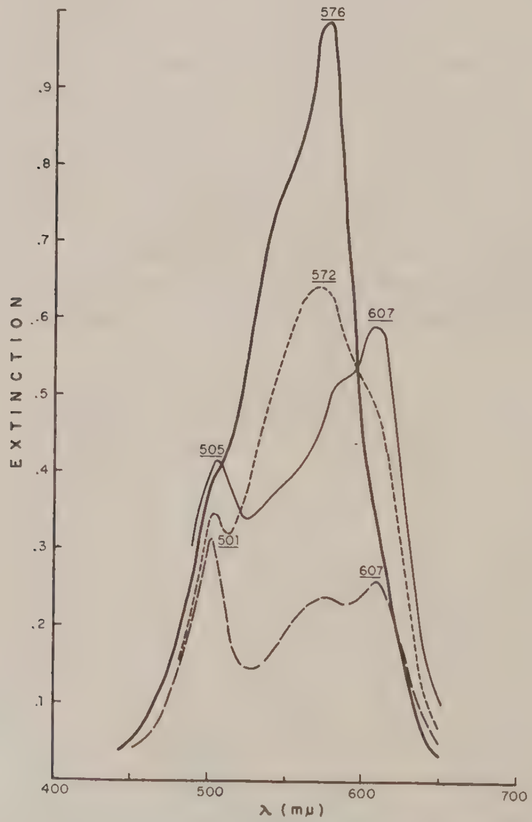

FIG. 6. Absorption spectra in acid chloroform of *Porphyridium* phycoerythrobilin (top curve) and its breakdown products formed in concentrated hydrochloric acid.

——— Phycoerythrin hydrolyzed 20 minutes
- - - - Phycoerythrin hydrolyzed 2 hours
——— Phycoerythrin hydrolyzed 5½ hours
— — — Phycoerythrin hydrolyzed 18 hours

Porphyridium phycoerythrobilin was subjected to descending paper chromatography with water-saturated 2,4-lutidine as the mobile phase. After a 12-hr. run no colored spots could be observed, but the phycoerythrobilin was identified by its reddish fluorescence in ultraviolet light (due possibly to complexing with metals in the paper). Its R_f was 0.80, while bilirubin on the same paper gave a value of 0.77. On lutidine chromatograms an inverse relationship exists between the R_f of tetrapyrroles and the number of their substituent carboxyl groups (16, 17). The values obtained suggest therefore that phycoerythrobilin, like bilirubin, has two carboxyl groups among its side chains.

This fact was indicated earlier by the isolation of mesobiliverdin from the alkaline hydrolyzate of R-phycoerythrin by Lemberg and Bader (2). We have found that under milder conditions of alkaline hydrolysis phycoerythrin yields, in addition to mesobiliverdin, a blue pigment (absorption maximum at 595 mμ) which is probably identical with neutral phycoerythrobilin as prepared from the acid hydrolyzate.

The different variants of R-phycoerythrin in *Plocamium pacificum*, *Rhodochorton rothii*, and *Porphyra tenera* all yielded a labile phycoerythrobilin, identical in its spectral properties with the *Porphyridium* pigment (Table I). Similar results were obtained with B-phycoerythrin (18) from *Porphyra naiadum* var. *australis* and C-phycoerythrin, as well as the two-peaked modification of the latter recovered under certain conditions from *Phormidium* spp. (4, 14).

DISCUSSION

A search of the bile pigment literature has not revealed any compounds identifiable with either phycocyanobilin or phycoerythrobilin.

The absorption spectrum of the phycocyanobilin hydrochloride is reminiscent of that of mesobiliverdin, but it differs from this oxidation product of mesobiliviolin in its chromatographic behavior, the absorption spectrum of its zinc derivative, and by its transformation by acid to a substance with a maximum at 607 mμ (probably mesobiliviolin hydrochloride).

The structural relationship of phycocyanobilin to mesobiliviolin is unclear; it may be a labile cyclic form of mesobiliviolin, possibly resembling verdohematin, a cyclic biliverdin–iron complex [see (5)]. It is probable that phycocyanobilin, as isolated, does not contain a metal atom, since it forms complexes readily with such ions as Zn^{++} and Cu^{++}. The lack of a shift in absorption maximum on forming such complexes may be evidence for the presence of a preformed tetrapyrrolic ring in phycocyanobilin.

Metal complexes of the phycobilins, if present in the native chromoproteins, would not be expected to survive acid-hydrolyzing conditions (5). However, it is assumed that the phycobilins are not complexed since Lemberg's purified R-phycoerythrin contained only traces of iron and magnesium and 0.25 % calcium, which was probably not associated with the chromophore (1).

The spectral evidence indicates that all the phycoerythrins examined contain one and the same chromophore. The nature of the products of its reaction with acid, corresponding to mesobiliviolin from phycocyanobilin, is unknown. No evidence has been obtained which would indicate a relationship between phycoerythrobilin and mesobilirhodin; it will be recalled that Lemberg proposed that these two compounds are identical. Neither is there any indication of the existence of any simple relationship between phycocyanobilin and phycoerythrobilin.

The finding that all phycoerythrobilins are probably identical prompts enquiries concerning possible differences in the globulin structures or in the protein–chromophore linkages which might account for the great spectral variations existing between the parent phycoerythrins. Lemberg (3) argued that the protein is attached to the phycobilin through labile linkages involving the pyrromethene grouping, in addition to primary peptide bonds. There are probably many chromophoric groups attached to a single protein—Lemberg and Legge (5) assume 16 in the case of C-phycocyanin, a figure which agrees with recent analytical[5] and physical (19) results—and it seems possible that the number of such groups attached by secondary linkages may vary according to the physical or chemical constitution of the protein, thus accounting for spectral variations among the biliproteins. However, this problem cannot yet be solved, since a few amino acid analyses (20–22) comprise the only knowledge of the proteins so far available.

ACKNOWLEDGMENTS

The author is greatly indebted to Dr. F. T. Haxo for his advice and criticism during the course of this work. Others who gave valued assistance were: Drs. L. R. Blinks, D. L. Fox, and T. A. Geissman; and Dr. A. A. Aleem, who identified the blue-green alga, *Arthrospira maxima*.

SUMMARY

The phycobilin chromophores of representative phycocyanins and phycoerythrins were examined after cleavage from the protein with concentrated HCl at room temperature for 20–30 min.

Both phycocyanobilin from C-phycocyanin and its red-fluorescing zinc complex absorbed maximally at 630 mμ in chloroform. When acid hydrolysis was conducted for a longer period or at elevated temperatures, phycocyanobilin was converted to mesobiliviolin. The chromophore of allophycocyanin differed in some spectral properties from C-phycocyanobilin.

A number of spectrally different phycoerythrins all yielded the same chloroform-soluble labile phycoerythrobilin. This bile-type pigment of unknown constitution absorbed maximally at 576 mμ in acid chloroform and at 583 mμ as an orange–red fluorescing zinc complex in chloroform.

REFERENCES

1. LEMBERG, R., *Ann.* **461,** 46 (1928).
2. LEMBERG, R., AND BADER, G., *Ann.* **505,** 151 (1933).
3. LEMBERG, R., *Ann.* **477,** 195 (1930).
4. HAXO, F. T., Ó HEOCHA, C., AND NORRIS, P., *Arch. Biochem. Biophys.* **54,** 162 (1955).
5. LEMBERG, R., AND LEGGE, J. W., "Hematin Compounds and Bile Pigments." Interscience Publ., New York, 1949.
6. FOX, D. L., "Animal Biochromes and Structural Colours." Cambridge University Press, Cambridge, 1953.
7. KYLIN, H., *Z. physiol. Chem.* **69,** 213 (1910).
8. KITASATO, Z., *Acta Phytochim.* (Japan) **2,** 75 (1925).
9. LEVENE, P. A., AND SCHORMÜLLER, A., *J. Biol. Chem.* **93,** 571 (1931).
10. SIEDEL, W., *Z. physiol. Chem.* **237,** 8 (1935).
11. RABINOWITCH, E. I., "Photosynthesis," Vol. II, part II. Interscience Publ., New York, 1956.
12. SIEDEL, W., *Ber.* **77A,** 21 (1944).
13. GRAY, C. H., "The Bile Pigments". Methuen, London, 1953.
14. Ó HEOCHA, C., Doctoral Thesis, University of California at Los Angeles, 1955.
15. SIEDEL, W., AND MÖLLER, H., *Z. physiol. Chem.* **264,** 64 (1940).
16. NICHOLAS, R. E. H., AND RIMINGTON, C., *Scand. J. Clin. & Lab. Invest.* **1,** 12 (1949).
17. TIXIER, R., *Mem. Mus. Nat. Hist. Nat.* **5,** *Ser. A*, 41 (1952).
18. BLINKS, L. R., *in* "Autotrophic Micro-organisms" (Fry, B. A., and Peel, J. L.). Cambridge University Press, Cambridge, 1954.
19. GOEDHEER, J. C., Doctoral Thesis, State University, Utrecht, 1957.
20. WASSINK, E. C., AND RAGETLI, H. W. J., *Koninkl. Ned. Akad. Wetenschap. Proc. Ser. C*, **55,** 462 (1952).
21. SISAKYAN, N. M., BEZINGER, E. N., AND KIVKUTSAN, F. R., *Doklady Akad. Nauk S.S.S.R.* **98,** 111 (1954).
22. FUJIWARA, T., *J. Biochem.* (Tokyo) **43,** 195 (1956).

(*Reprinted from Nature, Vol.* 180, *pp.* 1295–1296, *Dec.* 7, 1957)

Reproduced by Permission

Variability in Retention of Marine Phytoplankton by Membrane Filters

DURING a series of experiments designed to determine the relative sizes of tropical pelagic phytoplankton labelled with carbon-14, it was noted that the retentive capacity of '*AA* Millipore' membrane filters varied considerably in three experiments as shown by retention of passed material on a fine filter (Table 1). It seemed surprising that a membrane filter with a pore size of 0·8μ would pass significant amounts of carbon-14 activity, bound in phytoplankton.

Three experiments were performed in the laboratory to determine the retention of *Dunaliella primolecta*, a phytoflagellate grown in sea-water medium, by using membrane filters of different porosities. In each experiment a 40-ml. culture was inoculated with about 10 μc. (0·9 ml.) of NaH^{14}CO$_3$, *p*H 9·7. This was incubated at 22° C. over fluorescent bulbs of 545 foot-candles. The NaH^{14}CO$_3$ was prepared according to the method of Steemann Nielsen[1]. The initial experiment (*A*) was performed with a 25-day-old culture inoculated with carbon-14 twenty-two days before filtration, which may have become bacterized. A 10-ml. aliquot of the algal suspension was removed and filtered through an '*AA* Millipore' filter (pore size, 0·8 ± 0·05μ). (Porosity figures are those supplied by the manufacturers, Millipore Filter Corporation, Watertown, Mass., and Membranfilter, Göttingen.) The filtrate was then drawn through an *HA* (pore size, 0·45 ± 0·02μ) and a *PH* filter (pore size, 0·3 ± 0·02μ). All filter membranes were finally washed with approximately 75 ml. of *HA*-filtered sea water before drying by suction. The water thus filtered was combined with the original filtrate. The final filtrate was acidified with phosphoric acid to remove uncombined carbon-14, and an aliquot was air-dried for counting on a steel planchet. Each 'Millipore' filter was also air-dried. The activity of the filters and planchets was counted with a Nuclear Measurements Corporation proportional counter (Model *PC*–1). The results are presented in Table 1.

Experiment *B* (Table 2) differed in two respects from experiment *A*. (1) A four-day-old, bacteria-free culture was inoculated with carbon-14 five days before filtration; (2) a 3-ml. aliquot of the radioactive

Table 1. RETENTION OF PELAGIC PHYTOPLANKTON AND *Dunaliella primolecta* LABELLED WITH CARBON-14 BY MILLIPORE FILTERS AFTER SERIAL FILTRATION

Filter	Experiment 1 November 20, 1956 09° 15·5′ N., 89° 18·0′ W.		Experiment 2 December 2, 1956 05° 09·0′ N., 83° 34′ W.		Experiment 3 December 4, 1956 06° 46·0′ N., 89° 52·0′ W.		*Dunaliella primolecta* Experiment *A*	
	c./m.*	per cent of total	c./m.	per cent of total	c./m.	per cent of total	c./m.	per cent of total
'Millipore *HA*' (Control)	529	—	—	—	117	—	—	—
'Millipore *AA*'	298	55·5	1,464	91·6	71	55·5	123,271	59·6
'Millipore *HA*'	239	44·5	134	8·4	57	44·5	42,054	20·3
'Millipore *PH*'	—	—	—	—	—	—	16,482	8·0
Filtrate	—	—	—	—	—	—	25,115	12·1
Total	537	100	1,598	100	128	100	206,922	100

* c./m. = counts per minute

Table 2. RETENTION OF *D. primolecta* LABELLED WITH CARBON-14 BY MEMBRANE FILTERS

Filter	Experiment *B*—July 9, 1957						Experiment *C*—July 18, 1957	
	Series 1		Series 2		Series 3		Series 1	Series 2
	c./m.*	per cent *PH*	c./m.	per cent *PH*	c./m.	per cent *PH*	c./m.	c./m.
'*AA* Millipore'	37,819	79·2	36,846	87·0	33,970	90·0	47,116	45,574
'*HA* Millipore'	46,679	97·7	42,073	99·4	39,915	105·8	46,018	45,662
'*PH* Millipore'	47,744	—	42,326	—	37,721	—	46,176	43,438
Filtrate	0	—	0	—	0	—	—	3,264
					Coarse *MF*†		44,782	45,192
					Medium *MF*		45,982	44,338
					Dense *MF*		42,622	40,270
					Very dense *MF*		33,438	—
					Filtrate		—	4,840

* c./m. = counts per minute; † *MF*, 'Membranfilter'

algal suspension was filtered through each of the filters. The filtrates from the *PH* filters were analysed for activity. In experiment *C* (Table 2) an 18-day-old, bacteria-free culture was used and carbon-14 was added two days before filtration of the 3 ml. aliquots. Dry 'Membranfilters' (Göttingen) were also tested to compare their retention of *Dunaliella*. These are rated by the manufacturer as coarse (pore size, 3·0–0·75μ), medium (pore size, 0·75–0·5μ), dense (pore size, 0·5–0·2μ), and very dense (pore size, less than 0·2μ). Filtrates from a dense filter and a *PH* filter were tested for activity.

In Table 1, it can be seen that there may be considerable variability in retention by '*AA* Millipore' filters when used in the field. (Steemann Nielsen[1] found in two experiments that virtually all activity was retained by membrane filters with a pore size slightly in excess of 1μ.) In experiments *A* and *B*, a similar variability in retention of activity exists which seems to be associated with the age of the culture. We believe that this difference in retained activity is largely due to the fragility of the labelled cells. This seems to be borne out by the independent observation of Dr. W. Rohde (personal communication) who, by visual microscopy, noticed that many naked flagellates are destroyed beyond recognition on the surface of membrane filters after filtration. Presumably this is a result of mechanical destruction resulting from filtration. The loss of activity noted with dense and very dense filters may be due to prolonged filtration periods. Such a loss was not found by Steemann Nielsen[1].

Except in the last experiment, a significant portion of the algal-bound activity passed through the *AA* filters. In the case of the *Dunaliella* experiments, the cell-size ranged from 6 to 8μ and there was no evidence of cell debris in the culture medium prior to filtration. From these experiments it is concluded that it is advisable to employ filters with a porosity of at least 0·45μ and with relatively rapid flow characteristics, when sampling phytoplankton labelled with carbon-14.

REUBEN LASKER*
ROBERT W. HOLMES

Scripps Institution of Oceanography,
University of California,
La Jolla, California.

---

* Rockefeller Foundation Post-doctoral Fellow.

[1] Steemann Nielsen, E., *J. du Conseil*, **18**, 117 (1952).

Contributions from the Scripps Institution of Oceanography, New Series, No. 965

Printed in Great Britain by Fisher, Knight & Co., Ltd., St. Albans.

Reprinted from SCIENCE, December 27, 1957, Vol. 126, No. 3287, pages 1319–1323.

Reproduced by Permission

International Cooperation in Marine Sciences

Roger Revelle

World-wide cooperation among astronomers, meteorologists, and other geophysicists has long been taken for granted. For generations, in peace and war, astronomers have freely communicated their observations across national boundaries, and the international meteorological network has functioned continuously except under conditions of actual war. Such cooperation has lagged in studies of the ocean because of the lack of economic necessity, because of the wide differences in the level of development of marine sciences in different countries and different oceanic regions, and because of the great diversity of the scientific disciplines involved. Yet, like the atmosphere, the ocean cannot be separated into isolated parts; what happens in any part of the sea ultimately affects the waters everywhere. With the scientific resources that are now available, no one country can find out all it needs to know about the oceans except through the cooperative activity of many countries.

Although no part of the oceans has been well described, in certain areas our information is completely inadequate. Very little is known about the inshore waters off the coasts of the Indian Ocean, the east coast of Asia south of latitude 25°N, or the east and west coasts of South America. For any rational development of marine resources, simple but systematic observations are needed in all these coastal regions.

The Indian Ocean is the deep-sea area in which the deficiency of descriptive information is greatest. It is almost completely unexplored, from the scientific point of view. Not much more is known about the South Pacific. Knowledge of the South Atlantic is somewhat better, but more exploration is needed there, as well as in the Arctic Ocean and in the equatorial regions of both the Atlantic and Pacific.

In contrast to the need for elementary description in large oceanic areas, the most advanced methods and ideas of modern mathematics, physics, chemistry, and biology can be employed in studying some aspects of the marine sciences, with remarkable effectiveness. Development of these sciences throughout the world depends, in part, on enlisting the interest of workers in the basic sciences from many different countries in the problems of oceanic research.

On a regional basis, international cooperation in the marine sciences began some fifty years ago, when the countries bordering on the North Sea and the eastern North Atlantic formed the International Council for the Exploration of the Sea. Later the International Association of Physical Oceanography and the International Hydrographic Bureau began to deal with certain aspects of the subject—namely, the movements and properties of sea water and the problems of ocean surveys for navigational purposes. In more recent years, a series of international fisheries commissions has been established. These commissions have initiated cooperative research programs on the biological and environmental factors affecting a particular fishery or a particular part of the ocean. Such regional international organizations as the Pacific Science Association and the Pan American Institute of Geography and History have standing committees that compile and assimilate reports of oceanographic activities and arrange for exchanges of information. But, until the last two years, there has been no organization concerned with all the marine sciences on a world-wide basis, either from the standpoint of the fostering and coordinating of observations or from that of communication between workers in the different sciences of the sea.

The first world-wide attempt to make coordinated scientific observations in all the oceans is being carried out during the International Geophysical Year. Some seventy ships are taking part in an internationally planned program of observations, and many new shore stations are being operated, particularly on oceanic islands, to supplement the previously existing network of observatories.

The United Nations Educational, Scientific, and Cultural Organization, in its natural sciences program, has recently begun to place emphasis on the international development of the sciences of the sea, especially in regions where there has been little emphasis in the past. To guide this work, which is being carried out in cooperation with the Food and Agriculture Organization of the United Nations, UNESCO has established an International Advisory Committee on Marine Sciences. At the same time, the International Council of Scientific Unions, having in mind the successful planning of the IGY program, has established a Special Committee on Oceanic Research, with responsibility for developing an international cooperative program of fundamental research. Each of these committees has now had a formal meeting, and possibilities for the future have been to some extent clarified.

UNESCO's Marine Science Program

UNESCO's nine-man International Advisory Committee on Marine Sciences met in Lima, Peru, in October 1956 under the chairmanship of G. E. R. Deacon, director of the National Institute of Oceanography, near Godalming, England. Other members of the committee, selected to represent different regions and different marine science disciplines, are D. V. Bal (India); Anton F. Bruun (Denmark); Marc Eyries (France); Koji Hidaka (Japan); Luis Howell-Rivero (Cuba); R. Revelle (United States); D. J. Rochford (Aus-

---

Dr. Revelle is director of the Scripps Institution of Oceanography, University of California, La Jolla.

tralia); and Lev Zenkevitch (U.S.S.R.). Each member serves for three years. The meeting in Lima was preceded by a meeting of an interim committee, with virtually the same members, in Tokyo in October 1955.

The amount of funds available to UNESCO for promotion of scientific research is not comparable to the expenditure of any major country for this purpose. Consequently, its activities in the sciences must be very largely confined to the planning of international action, facilitation of the making of contacts among scientists of different countries, and exchange of ideas and information.

In accordance with the advice of the International Advisory Committee, the principal objective of UNESCO's marine sciences program is to encourage development of these sciences in regions where little is known about the oceans or the organisms that they contain and where there is economic and social need for increasing the harvest of food from the sea. Up to the present, UNESCO has taken steps toward the realization of this objective by providing (i) fellowships for advanced training of scientists from these regions at major centers of marine research; (ii) intensive training programs, lasting from a few weeks to a few months, for technicians and field workers within such a region; (iii) intraregional conferences that give local scientists opportunities to discuss their common problems; (iv) international symposia, conducted by scientists of wide reputation on general topics in the marine sciences, in countries or regions where these sciences have been little developed; and (v) funds to make possible the joint planning of cooperative observational programs. A modest start has been made in all these directions.

During 1956–57, grants were made for eight fellowships for advanced training, to Hong Kong, Japan, Mexico, Thailand, Argentina, Brazil, India, and the Philippines, respectively. A three-weeks' course in marine biology and taxonomy was held early in 1957 at the Oceanographic Institute at Nhatrang, Vietnam, and a course in research methods in marine biology and physical oceanography was given in São Paulo, Brazil, in 1955. Three meetings of South American marine biologists have been held; the meeting at Lima followed the third such conference, at the marine biology station of the University of Chile at Viña del Mar.

A Western Pacific oceanographic conference was held in Tokyo before the preliminary meeting of the interim committee, in 1955, and a symposium on problems in physical oceanography and biology in the Eastern Pacific, attended by scientists from the United States, Mexico, Peru, Chile, Brazil, Uruguay, and Argentina, in addition to members of the International Advisory Committee, was held prior to the Lima meeting. Travel funds have been provided to enable scientists from Australia, New Zealand, and New Caledonia to consult together concerning a joint study of the circulation of the Southeast Pacific Ocean and Tasman Sea.

The symposium at Lima centered around one of the most remarkable phenomena in the oceans, the Peru Current (the name applied to the north-flowing current along the west coast of South America). As is true of all currents along the eastern boundaries of oceans, this current is shallow, broad, and slow. But its waters are among the most productive on earth. It has been estimated that the guano birds of Peru annually harvest some 2½ million tons of pelagic fish, about 10 percent of the total annual catch of all the world's fisheries. This extraordinarily high fertility depends upon the upwelling of cold, nutrient-rich waters from intermediate depths, and these vertical movements are reflected also in tongues of comparatively cold water extending parallel to the coast. Because it depends upon the speed and direction of the southerly and southeasterly winds, upwelling off the coast of South America is an intermittent and highly variable process.

One of the striking facts brought out at the symposium was the considerable degree of asymmetry between the Peru Current and the corresponding California Current off the west coast of North America. As one looks northward toward the equator, from off the coast of Peru, the coastline trends northwestward, while off the coast of California and Mexico, as one looks southward, the coastline trends southeastward. In the comparatively low latitudes of Peru, the southeasterly trades blow nearly parallel to the coast and are much more intense than the winds to the south. This intensification of the winds accelerates the northwestward flow of the surface waters; consequently, vertical upward motion of the waters from mid-depths takes place on a large scale. Shifts in the wind system are apparently responsible for variations in the southgoing inshore countercurrent and in extreme cases produce the catastrophic series of atmospheric and oceanic events known as "El Niño" (because they occur at Christmas)—severe rainstorms and floods on land and mass mortalities of marine birds and fishes.

This model of the Peru Current and the associated inshore countercurrent is based on tenuous oceanographic observations, and it was clear from the discussions of the symposium that series of measurements very much more complete in time and area are required before a more satisfactory picture can be obtained. A new start is being made toward obtaining the necessary measurements through the recently organized Council for Hydrobiological Investigations of the Peruvian Government.

One of the most important proposals made by the International Advisory Committee has been that an international oceanographic ship should be commissioned and operated, either by UNESCO itself, under contract, or by a group of countries in accordance with the pattern for international operation of research facilities set by CERN (Comité Européen de Recherche Nucléaire). This ship would be used primarily in such a little-known area as the Indian Ocean and could serve both for obtaining scientific information and as a training ship for younger scientists in the bordering countries.

Members of the committee have advised against the establishment, in areas where the marine sciences have been little developed, of international laboratories supported with funds from governments of neighboring countries. But they have stated that new laboratories, endowed by foundations or other private sources (in order to give stability and ensure freedom for research), would be of great value. Marine biology might be emphasized at first, with expansion later into other fields as additional funds become available.

Financial Support

Financial support from UNESCO for scientific work in underdeveloped countries can be obtained in several ways. Under the technical assistance program of the United Nations, funds contributed by many different countries are used to support projects of direct economic benefit requested by the country in which the work is to be done. The Technical Assistance Board of the United Nations decides on the total yearly allocation for each beneficiary country and on the total amount of funds to be handled yearly by each operating agency (UNESCO, Food and Agriculture Organization, World Health Organization, and so on). In 1956, about $1 million was allocated to the Natural Sciences Department of UNESCO. Because the programs are established separately by the various countries that receive assistance, the technical assistance funds cannot be used as a means of developing an internationally coordinated scientific research program. They can be used to send experts, to provide 3- to 12-month fellowships, and to purchase equipment.

UNESCO, through the regular budget established every two years by its General Conference, can assist member states in carrying out educational, scientific, or cultural projects regardless of their immediate economic repercussion. Requests are submitted by the member states, but there is no priority allocation to the different countries, and the entire program is concentrated in particular fields of science or technology. During 1955–56 UNESCO spent about $100,000 for aid to member states for projects in natural sciences.

In both the technical assistance and the aid-to-member-states programs, the national commissions, advised by the UNESCO Science Cooperation Offices, play an important role in framing and choosing projects. Funds for regional conferences and training programs are provided from the budget of the Science Cooperation Offices.

In addition to the fellowships provided under technical assistance or aid-to-member-states activities, fellowships, generally for 12 months, are granted under the exchange-of-persons program of UNESCO. The number of fellowships for each particular field of activity is decided by UNESCO's General Conference, on the proposal of the director general.

In the field of research, small sums are assigned in the UNESCO budget to specific scientific programs (such as arid-zone and humid-tropics research and marine sciences). Part of these funds are used by UNESCO for research contracts with appropriate scientific institutions to encourage investigations of international scope. The total marine-sciences budget, however, is only $31,770 for 1957 and $22,170 for 1958, and only a small part of this sum is available for research contracts. This year the Geophysical Institute of Bergen, Norway, is being given financial assistance in order that it may participate in a multiple-ship current-measuring operation in the North Atlantic Ocean, to be undertaken jointly with the National Institute of Oceanography (United Kingdom) and the Woods Hole Oceanographic Institution (United States).

Subventions are granted by the General Conference of UNESCO to international scientific organizations for the support of international meetings, publications, and the planning of international activities. For example, the International Council of Scientific Unions received $360,000 in 1955–56 (out of a total of $448,000 granted to all international scientific organizations). The initial expenses of the Special Committee on Oceanic Research were paid from this subvention to the International Council of Scientific Unions.

The UNESCO marine sciences program has also directly supported certain advanced symposia organized by scientific bodies. The recent symposium in Bergen, Norway, held under the auspices of the International Council for the Exploration of the Sea, on the measurement of primary productivity in the sea, and the symposium on the circulation of the deep waters of the ocean, held at the meeting of the International Association of Physical Oceanography in Toronto, Ontario, in September 1957, were both partly financed by UNESCO.

A third area of activity has been that of furnishing scientific assistance to other United Nations organizations; for example, a report on sea and oceanic disposal of atomic wastes has been prepared, under the supervision of H. Charnock of the National Institute of Oceanography (United Kingdom), for the United Nations Scientific Committee on the Effects of Atomic Radiation. A report on scientific considerations related to the continental shelf has been completed by an international group of experts for use in the forthcoming United Nations conference on the Law of the Sea.

UNESCO, because of its broad educational and scientific responsibilities, can draw the attention of the governments of its member states to the importance of marine research without overemphasizing the prospects of immediate useful results. It can stress the longer-range possibilities and the value of the marine sciences as a means of introducing science for its own sake.

For example, at the Tokyo meeting, the interim committee recommended that in certain developed countries, such as Japan, Australia, the countries of Europe, and India, establishment of new national centers for fundamental research on the high seas, at least partly supported with government funds, would be highly desirable. Experience in Great Britain and North America shows that in such laboratories a diversity of disciplines should be represented, including applied mathematics, theoretical and experimental physics and geophysics, chemistry (geochemistry, biochemistry, and analytical chemistry), geology, meteorology, and biology (both experimental biology and natural history). A certain "critical mass" is essential—the scientific staff should number at least ten and preferably more, and these scientists must have adequate support in facilities and technically trained assistance. The research center should have an intimate relationship with one or more universities.

Finally, UNESCO, as an intergovernmental organization, can, by various means, encourage the member states to maintain policies favorable to international scientific work on the oceans. Examples are the facilitating of exchange of scientists between research vessels and laboratories of different countries in the face of political difficulties, the relaxing of customs regulations and of other barriers to the exchange of scientific instruments for use in international cooperative marine investigations, and the maintaining of freedom of scientific research on the continental shelf and offshore waters. Since 1949, the International Law Commission of the United Nations has been engaged in a study of the regimes of the high seas and territorial waters. An international conference of plenipotentiaries to examine the Law of the Sea has been called by the General Assembly of the United Nations, to be held in 1958. UNESCO's International Advisory Committee on Marine Sciences, although recognizing that each country has a right to protect its coastal waters from economic exploitation, and that there are also certain military considerations, has urged that there should be no restriction on scientific studies by research vessels of any nation, provided that the results are published and the work itself is open to exchange of scientists. This viewpoint has been supported by UNESCO's Advisory Committee on Research in the Natural Sciences. In April 1957 the latter committee adopted a resolution urging the director general of UNESCO "to present the International Conference on the Law of the Sea with proposals ensuring freedom of fundamental research on waters, sea bed and subsoil of the continental shelf carried out by any nation with open publication in the interest of all." This committee has further expressed serious concern about the possible consequences of Article 68 of the draft Articles of the Law of the Sea prepared by the International Law Commission, "which in its present form does not guarantee the freedom of scientific research on the physical characteristics, geology and biology of the sea bed and subsoil of the continental shelf."

Special Committee on Oceanic Research

The Special Committee on Oceanic Research of the International Council of Scientific Unions consists of 15 members. Six members were nominated by the International Council of Scientific Unions, four by the International Union of Geodesy and Geophysics, two by the International Union of Biological Sciences, and one each by the International Union of Pure and Applied Physics, the International Union of Pure and Applied Chemistry, and the International Geographical Union. This committee held its first meeting at the Woods Hole Oceanographic Institution from 28 to 30 Aug. 1957, under the chairmanship of director C. O'D. Iselin. Other members present at the meeting were A. F. Bruun (Denmark); G. Bohnecke (Germany);

L. R. A. Capurro (Argentina); G. E. R. Deacon (United Kingdom); M. N. Hill United Kingdom); N. B. Marshall (United Kingdom); Y. Miyake (Japan); H. Mosby (Norway); N. W. Rakestraw (United States); R. Revelle (United States); E. Steeman Nielsen (Denmark); and L. Zenkevitch (U.S.S.R.). Y. Le Grand of France and N. K. Pannikar of India were unable to attend.

The committee took as its first task that of defining the needs for further international scientific cooperation in the marine sciences. It is clear that, as in other sciences, a very large part of the pioneering research and new ideas concerning the oceans must come from individual scientists or small groups working independently. A broadly based international organization can be helpful, however, in several ways. It can serve as a sounding board to emphasize the economic and social importance of greater knowledge of the oceans and can thereby assist marine scientists in different countries to obtain support for their work. By arranging wide dissemination of ship operating schedules, it can help scientists to participate in cruises or to obtain desired data and collections. By pointing out areas where work is needed and the kinds of observations that should be made, it can encourage more efficient use of research vessels. It can facilitate the exchange of techniques, personnel, samples, and data. By sponsoring or encouraging discussions of problems of ocean research at national and international scientific meetings, it can help enlist scientists from other fields. It can arrange for coordinated work, by research vessels at sea and by shore observatories of different countries, in attacking problems where a wide network of observations is needed. It can serve as a mechanism for the standardization and intercalibration of techniques and instruments and can arrange for the introduction of techniques newly developed in one country or laboratory to other scientific groups elsewhere in the world.

The committee considered that its principal objective should be to encourage and coordinate an international program of observation and measurement in the deep ocean. One point of this program would involve an intensive effort to understand the relationships between the dynamics of the upper water layers and the plant and animal populations. Another would be the study of the region from below the thermocline down to the greatest depths of the sea and beneath the sea floor. Because so little is known about this region, its investigation will be, to a large extent, a task of widespread exploration. Such exploration must proceed hand-in-hand with theoretical studies and development of new techniques by individual scientists and must supplement rather than interfere with their work.

In making a decision to concentrate its program in the deep oceanic regions, the committee recognized that geophysical and geological studies of the earth beneath the sea are necessary for elucidating the structure and history of the earth. With regard to the waters and the organisms that they contain, it emphasized three long-range problems that may be critical to the future welfare of mankind.

Long-Range Problems

The first of the long-range problems concerns the use of the deep sea as a receptacle for the waste products of our industrial civilization. This may be a particularly important problem in the future, when very large quantities of poisonous radioactive wastes will be produced through the industrial use of atomic power. We need to know whether we can dispose of at least part of these wastes in the deep sea or whether the circulation of the ocean or the vertical movements of the fauna will result in a rapid transport of dangerous material to levels in the sea from which some of the world's food supplies are derived.

The second problem concerns the oceans as an important source of protein food for many of the world's peoples. With the growth of populations, man's need for food from the sea may be expected to increase rapidly. The living resources of the oceans are by no means infinite, and, like the land, the oceans differ widely in fertility in different parts. The fertile areas are those where nutrient trace substances, essential for plant life, are brought up from the deep waters. To obtain the maximum harvest, the processes by which this occurs must be elucidated.

The third problem is perhaps the least well understood of the three. It concerns the role of the oceans in climatic change. During the last 50 years the average temperature over eastern North America and northern Europe has increased markedly, while elsewhere prolonged droughts have destroyed the work of decades. Will this trend continue over the next 50 years, or will it be reversed? Because we do not have sufficient understanding of the processes that control climate, we are quite unable to make a forecast. Nevertheless, a prediction of future climate would be of inestimable value to society.

The waters of the oceans may play an important role in changing climates. For example, an excess of heat from the sun can be stored in the deep water and slowly released over many years, warming the air. Likewise, the amount of carbon dioxide in the air controls, at least to some extent, the average air temperature and the loss of heat from the earth. Any change in atmospheric carbon dioxide—for example, by addition from fossil fuel combustion—may be damped or modified by the absorption of carbon dioxide in the ocean waters.

New Techniques

For an understanding of each of these three problems, greater knowledge of the rate and character of the exchange between the deep and surface waters of the oceans is required. It is only within the last few years that we have been able to make an effective attempt to gain such knowledge, through theoretical analysis of the thermodynamics and hydrodynamics of the oceans, through laboratory and field experimentation, and through the development and field use of new techniques.

Among these new techniques are: (i) the use of radioactive substances that occur naturally in the water, such as radiocarbon and tritium, for tracing the paths of motion and the mixing of the waters; (ii) the making of direct measurements of the deep currents by using deep current meters or by following free-floating, neutrally buoyant buoys (for these it is necessary to maintain a fixed reference position; this can now be achieved by tautly anchoring a subsurface buoy to the sea bottom); (iii) the measurement, with a new degree of precision, of the salt content of the water and the tracing of the water movements by means of these data on salt content; (iv) the measurement of the heat flow from the interior of the earth into the deep water and use of data on the heating of the water as an index of the time of passage of the water over the bottom; (v) the possible introduction of relatively large amounts of artificially radioactive substances, of the order of tens of thousands of curies or more, into deep ocean areas and the measurement of the dispersion and transport of this material by the deep currents; (vi) detailed biological, chemical, and physical studies of the variations in the sediments of the deep-sea floor as a means of deciphering past changes in the water conditions; and (vii) utilization of new methods of high precision for determining carbon dioxide content in the water and the air.

Five-Year Program of Deep-Sea Research

Deep-sea exploration, because it involves the use of relatively large and heavily equipped ships for long periods, is the most expensive kind of oceanic research. An adequate program of exploration is beyond the resources of any one country. Moreover, the total cost will be minimized through planned international cooperation in the use of ships and facilities.

For the first two or three years the principal effort will be devoted to exchange and standardization of techniques, collection of samples for analysis and study by different laboratories, and exchange of data that can serve to guide further exploration. During this stage of development, effort will necessarily be concentrated in the North and South Atlantic and in the North and South Pacific oceans.

With adequate preparation during the first years, it should be possible, during the third or fourth years (provided that adequate funds and ships are made available), to make a combined assault on the largest unexplored area on earth, the Indian Ocean. This area is of special interest to physical oceanographers because seasonal reversals in wind direction that are not known elsewhere provide opportunity for studying the transient state in the wind-driven currents. Few scientific vessels have ever visited the Indian Ocean, and almost none of the new techniques have been applied there.

It would be anticipated that, in addition to scientists from the Northern Hemisphere, scientists and students from the countries bordering on the Indian Ocean would take part in this series of simultaneous expeditions. The expeditions would thus not only serve their primary purpose of exploration but would also have a lasting effect in encouraging and developing the marine sciences and fisheries in those countries.

It is estimated that at least 16 ships from 11 different countries could be enlisted. Each research vessel would spend approximately eight months at sea. The combined scientific party on all the ships would total about 125 persons; at least 25 of these might come from countries bordering on the Indian Ocean area, and it would be desirable to give many of the latter a year's prior training in centers of advanced oceanic research. At least 100 scientist-years would be required for working up the results.

During subsequent years, when the present extreme difficulties of making measurements at depths of several thousand meters and of obtaining accurate positions on the high seas have been sufficiently overcome, a tracer experiment, in which a large quantity of artificially radioactive material would be used, should be undertaken in some suitable deep-sea area. This will involve very careful international planning and coordination.

Organization and Budget

The Special Committee on Oceanic Research has set up five working groups, each consisting of five to seven active research workers in a particular field. These groups, with their conveners, are as follows: (i) group on the measurement of artificial radioactivity (Y. Miyake, Japan); (ii) group on the measurement of carbon dioxide in the air and the sea and its exchange rate (N. W. Rakestraw, United States); (iii) group on the measurement of standing crops of phytoplankton and zooplankton and the productivity of the sea (N. B. Marshall, United Kingdom); (iv) group on the measurement of the physical properties of sea water (H. Mosby, Norway); (v) group on exploration of the Indian Ocean (C. O'D. Iselin, United States).

Revelle, Deacon, and Bohnecke were nominated as chairman, vice chairman, and secretary, respectively, of the Special Committee on Oceanic Research. They will function as an executive committee responsible for the detailed administration of the committee's operations. Iselin and Zenkevitch were nominated as members of the finance committee to prepare the budget. These nominations have been confirmed by the International Council of Scientific Unions.

A program of international cooperation in deep-sea research cannot be carried out successfully without the enthusiastic support of existing international marine science organizations. Every effort will be made to utilize their facilities and procedures.

In organizing its scientific program, the Special Committee on Oceanic Research will also invite the cooperation of qualified academies or research councils of different countries, and each participating organization will be requested to designate a corresponding member to the Special Committee.

The total expenditures for the proposed year-long program of exploration of the Indian Ocean would be about $4 million, largely for ship costs. Half of this amount could come from the normal operating funds for ships and marine research laboratories of the participating countries, but additional sums totaling approximately $2 million must be raised. The Special Committee itself will need funds to establish a secretariat to maintain a flow of information about new methods, designs of instruments, and plans among the different countries; to pay for meetings of working groups of specialists who are developing and standardizing new techniques or planning expeditions; to make possible the transfer of key scientific personnel to the laboratories and ships where they can give training in, or learn from others, the use of specialized techniques and methods—for example, the seismic refraction methods of studying suboceanic structure that have been so successfully developed in the United States and England. An estimated annual budget of $45,500 a year for the next five years would cover these costs.

Note

This article is contribution No. 966, New Series, from the Scripps Institution of Oceanography.